



Journal which deals with research, Innovation and Originality



Table of Content

Topics	Page no
Chief Editor Board	3-4
Message From Associate Editor	5
Research Papers Collection	6-891

IJERGS

CHIEF EDITOR BOARD

- 1. Dr Chandrasekhar Putcha, Outstanding Professor, University Of California, USA**
- 2. Dr Shashi Kumar Gupta, , Professor, New Zealand**
- 3. Dr Kenneth Derucher, Professor and Former Dean, California State University, Chico, USA**
- 4. Dr Azim Houshyar, Professor, Western Michigan University, Kalamazoo, Michigan, USA**
- 5. Dr Sunil Saigal, Distinguished Professor, New Jersey Institute of Technology, Newark, USA**
- 6. Dr Hota GangaRao, Distinguished Professor and Director, Center for Integration of Composites into Infrastructure, West Virginia University, Morgantown, WV, USA**
- 7. Dr Bilal M. Ayyub, professor and Director, Center for Technology and Systems Management, University of Maryland College Park, Maryland, USA**
- 8. Dr Sarâh BENZIANE, University Of Oran, Associate Professor, Algeria**
- 9. Dr Mohamed Syed Fofanah, Head, Department of Industrial Technology & Director of Studies, Njala University, Sierra Leone**
- 10. Dr Radhakrishna Gopala Pillai, Honorary professor, Institute of Medical Sciences, Kirghistan**
- 11. Dr Ajaya Bhattarai, Tribhuwan University, Professor, Nepal**

ASSOCIATE EDITOR IN CHIEF

- 1. Er. Pragyan Bhattarai , Research Engineer and program co-ordinator, Nepal**

ADVISORY EDITORS

- 1. Mr Leela Mani Poudyal, Chief Secretary, Nepal government, Nepal**
- 2. Mr Sukdev Bhattarai Khattri, Secretary, Central Government, Nepal**
- 3. Mr Janak shah, Secretary, Central Government, Nepal**
- 4. Mr Mohodatta Timilsina, Executive Secretary, Central Government, Nepal**
- 5. Dr. Manjusha Kulkarni, Asso. Professor, Pune University, India**
- 6. Er. Ranipet Hafeez Basha (Phd Scholar), Vice President, Basha Research Corporation, Kumamoto, Japan**

Technical Members

- 1. Miss Rekha Ghimire, Research Microbiologist, Nepal section representative, Nepal**
- 2. Er. A.V. A Bharat Kumar, Research Engineer, India section representative and program co-ordinator, India**
- 3. Er. Amir Juma, Research Engineer ,Uganda section representative, program co-ordinator, Uganda**
- 4. Er. Maharshi Bhaswant, Research scholar(University of southern Queensland), Research Biologist, Australia**

IJERGS

Message from Associate Editor In Chief



Let me first of all take this opportunity to wish all our readers a very happy, peaceful and prosperous year ahead.

This is the Second Issue of the Fourth Volume of International Journal of Engineering Research and General Science. A total of 123 research articles are published and I sincerely hope that each one of these provides some significant stimulation to a reasonable segment of our community of readers.

In this issue, we have focused mainly on the innovative solutions for latest challenges. We also welcome more research oriented ideas in our upcoming Issues.

Author's response for this issue was really inspiring for us. We received many papers from many countries in this issue but our technical team and editor members accepted very less number of research papers for the publication. We have provided editors feedback for every rejected as well as accepted paper so that authors can work out in the weakness more and we shall accept the paper in near future. We apologize for the inconvenience caused for rejected Authors but I hope our editor's feedback helps you discover more horizons for your research work.

I would like to take this opportunity to thank each and every writer for their contribution and would like to thank entire International Journal of Engineering Research and General Science (IJERGS) technical team and editor member for their hard work for the development of research in the world through IJERGS.

Last, but not the least my special thanks and gratitude needs to go to all our fellow friends and supporters. Your help is greatly appreciated. I hope our reader will find our papers educational and entertaining as well. Our team have done good job however, this issue may possibly have some drawbacks, and therefore, constructive suggestions for further improvement shall be warmly welcomed.

Er. Pragyant Bhattarai,

Associate Editor-in-Chief, P&REC,

International Journal of Engineering Research and General Science

E-mail -Pragyant@ijergs.org

Suburbanization Case for Engineering as 1st Tier Government Industry Intrinsic Partner

Onyema K. N¹ (M.Sc. (Lagos), Highway and Transport, MNSE, COREN)

¹Department of Civil Engineering, Federal University of Technology, Adj. (IMSU), Owerri Nigeria
(kconyema@yahoo.com, 234-8063369743)

ABSTRACT- This paper presents a concept for a primary government industry character (intrinsic partner) on transportation layout management as engineering rules guided. The intrinsic is conceived as an aristocratic function in government industry, required to balance an exploratory partner. The intrinsic and explorer form a mutual government industry though exclusive in co-existence. These offer their unique governmental services on defined basis typical of their exclusive provisions and projects. In layouts as suggested, suburbanization is introduced as pivoting to rural and urban concepts of land use. Its aim being to introduce an engineering platform for connecting rural and urban land use challenges. Arguably, the suburban in concept is actually the locus of effective management of commuter transport flow. If viewed as such, a first tier government industry portfolio could act effectively as an engineership for a meaningful state-works promoting. By such it discourages pressure on arbitrary migration and leaves a lot of room for issues on functional coordinating of specific industries. This it does allowing specific facilitator of goals for this partner in government industry's transport-kind management portfolio (suburbanization roles) at the locals' basis, while incorporating first principles of life and motivations as engineership for living and active designing.

KEYWORDS: Commuter, Locus, Portfolio, Locals and Engineership

1.0 INTRODUCTION

The state of opinions that are decisive in the course of events is a gain through understanding troubled period of history. Perhaps by studying the achievements of leaders, we may be able to entrust the destiny of our nations to the hands of the right type of leaders in the future and not on failures of leaders. For a study of such sort to be meaningful it has to be situated within the context of events that happened at the time. Such context of events (**Osuntokun, 1987**) cover the life of the area (such as cloth weaving and dyeing), longevity (even at the age of seventy, Ibrahim was kept busy at the Shehu's palace as an adviser; his father never went anywhere without him particularly in the evening), leaving home (Kashim at six years old left the cosy comfort of his father's home for a better school), concept of school as new (Kashim had a happy life in school and always wanted to learn new things), new observation (pupils came from all over the North to attend this school and the subjects taught are listed), recreation observation (... the journey to Katsina, though long and time-consuming, was an enjoyable experience for the boys), tracing the roots and epitome of legacy (his success and attainment paved the way for a warm embrace of western education).

Osuntokun's book perceptions on Kashim Ibrahim and comments on his concepts, is a platform for a political titled intrinsic: Kashim's concept of political leadership is simple and straightforward ... and [he] believes that forms of government are for fools to debate 'the government that governs effectively in the long term interest of the people [such as] to appreciate the array of external forces that many African countries are faced with'. His concept is a subject for 'political design trend'. The nature of political design trend is characteristic of the issue to combat by the intrinsic government partner. This is as the case highlighted by Garba, who nevertheless dedicated his book to ... Hako, that vowed he would never attend the whiteman's school while Hako himself lived (**Garba, 1989**). As so, Kashim Ibrahim's life epitomises hybridisation of Western, Islamic culture and education. His success and attainment paved the way for a warm embrace of Western education by the aristocracy and the ulema of Borno of whom he was a representative (**Osuntokun, 1987**). Though there is fancy of 'new' in doctrinal challenge to combat, its benefit is aristocratic to define.

The challenges and conflict of heritage is the intrinsic partner's battle; which has a double weight unlike of the single weight of the explorer, who is much as a visitor-sightseeing. Explorers as new arrivals balance the intrinsic government character. The assumable state of the explorer is as the account of John Edward's political pursuit detailed by Andrew Young. He wrote a sermon by his father (**Young, 2010**) saying: 'the person who can give us hope is the one who knows the human condition and can encourage us to face the

realities of life'. Life inevitably brings change, loss and trauma to every-one. Growing up requires us to accept that people are deeply flawed sometimes and one just recovers his equilibrium in persevering time.

2.0 BACKGROUND

Sir Kashim as a typical intrinsic role player continues work duties at retirement who began life as a Borno patriot and Northern Nigerian defender to Nigerian nationalist – this is the way it should be and this is the way it had better be... (**Osuntokun, 1987**). Garba J M also is such a case as described. He recounted his growing up clichés (**Garba, 1989**), 'those were my grandfather's words of caution one evening being chased by some Kanuri boys of our village' exclaiming afuno.

The history of urbanism is largely the narration of the eras of town founders from the origins of the city down to contemporary new towns (**Carter, 1995**). The growth of urban expressways and 'circumferential limited-access highways' lead to the composing elements as 'float in space' rather than a structured relationship with the historic city. When planning a new or improved road or road system, it is necessary to know the distribution and performance of the traffic on existing roads. This is useful in predicting future traffic behaviour, determining justification for alterations and priorities for road improvement. In almost all planning studies, measurement of traffic flows and speeds are needed. In addition, measurement of stop times and their frequency are necessary. Traffic characteristics vary in cycles of hourly, daily, monthly/yearly patterns. Other characteristics are weather, directional distribution and traffic composition.

Garba description typifies suburban habitation platform as idealization, growth and living that is such is a worthy preference to be engineered. As he wrote 'our adventure left no part of our environment unexplored'. To us the children and to the adults as well, the village square served the combined functions of a club, school, dance-hall and a place of general congregation. On the sideline, the presence of so many horses in town was our opportunity. We knew where the best green grass was to be found and our reward was ample. At date Yerwa market had changed completely – a far cry from the days of the twenties. It is so completely different that it is like visiting a new place in a different country.

Further, he wrote, his grandfather did not hide disappointment and fears at seeing any apparent disintegration of the family. Why did he want to go to his father at Kano rather than remaining with his grandfather at Maisandari? 'It was simply because I wanted to escape from his severities'. Thus he with his company set out for Kano, the longest journey he undertook then. As soon as he got settled down in Kano, One Fatu wasted no time in utilising his idle hours and turning them to profitable ends. Working hard with good market, he sold more in a day. Life went on like this until a very close friend of his father, who was to completely change the direction of his whole life, appeared on the scene.

Garba's coming to age included lessons on cooking, superior mind state development from ability to associate with verities of persons (male, female, etc.), result-oriented intensive school and language(s) instructions, personal undivided attention to studies, interactions with senior heritage (layout-habiting) intrinsic workers and staff. As time went on he was considered experienced enough to give lectures on his own. The idea of deploying market-based original entrepreneurship efforts was to write about the plight of international issues from first-hand experience. Such becomes useful to developing first land owners to proffer solutions to the plight of international relations and the general being of greater importance. Such is the characteristic backing postings to improve education such as on agriculture, plantation businesses, and extra syllabic work-domain information. Such information includes general conservation needs, tours and personal plans making or development abilities. Such are necessary to establish a reputation of sound and effective agricultural-concept education. In addition to as describe, technological-kind educations require early report or letter writing experiences and leadership training abilities covering supervision, superintendent-ship, deputy-ship, industrial and manufacturing development, development of interviews, secretarial-ships and external affairs headship, correspondence-ship, concepts of regional and suburban designs, considerable experience places, quadrangle designs, occupational development, periodic alternative duties and placements, franchise and amorphous cases, artefacts designing (material and cultural), news and saddles, self grooming, religion and languages centres, and decisive role development. All these come as place focus for heritage approach to layout patterning.

The concepts of central, regional, neighbourhood and local market business value districts are 'commuter' laid-out. That is the concept of principal locus districts (central locus theory) with the idea of attached developments to central place theory ignored. Solving the interactions under a suburban concept will require a synergistic commuter zone development covering systematic business and

residential layout, all as business value of their kind. Associated with typical urban scenario traffic management are two basic concepts:

1. Provision of mass transit so that, as much as possible, private cars are removed,
2. Forbidding use of cars in the congested central areas.

There are two closely associated paradoxes which are immediately generated by an approach to transport in towns. The first is that the movement of people and goods is a consequence of the extension of land-uses but at the same time, it is the ease of movement which reinforces extension. Aside layout extension, transport as a (major) consumer of static space is a numeral issue with the argument that the ‘extent to which movement in the city should be a matter of private choice or public provision, hence the degree to which it is “class-based”’. The transport decision-planning scope covers consideration of trip generation, modal split, trip destination and route. In addition to the transport, it is necessary to consider the components of city development, solving the interactions of both market forces and planning. A strategy for reducing economic competition for land based on developing commuter zone areas (suburban areas) and converting existing cities to satellite cities will require the concept of radial expansion conceived as commuter movement, not as habitation limiting.

There are three principal types of major road patterns in the urban areas concept (O’Flaherty, 1974): gridiron, linear and radial. Gridiron is a pattern of rectangular layout system based on the ease of survey set out using straight lines and rectangular coordinates. Such produces monotonously long streets flanked by dull blocks of building. It may need tall buildings to break the effect of this monotony on the occupants. Nevertheless, it has considerable traffic-moving advantages, encouraging even spread of traffic over the grid and the consequence of the impact of a particular congested point is minimized. It facilitates the imposition of one-way street system. Introducing diagonal connect to this rectangular system to reduce the length of travel help to reduce the overall time increased by this system. However, this may affect the architectural development. Linear is a traffic flow pattern canalized into one major roadway. This type historically was developed as a result of topographic difficulties. Radial is a road system spreading out from a centre, idealized as connecting near towns. The radial system captures the required engineering for a central place theory in the form of ring road radius covering the CBD scope. In the simplest form there are five basic engineering options in a ring road plan thus (figure 2.1):

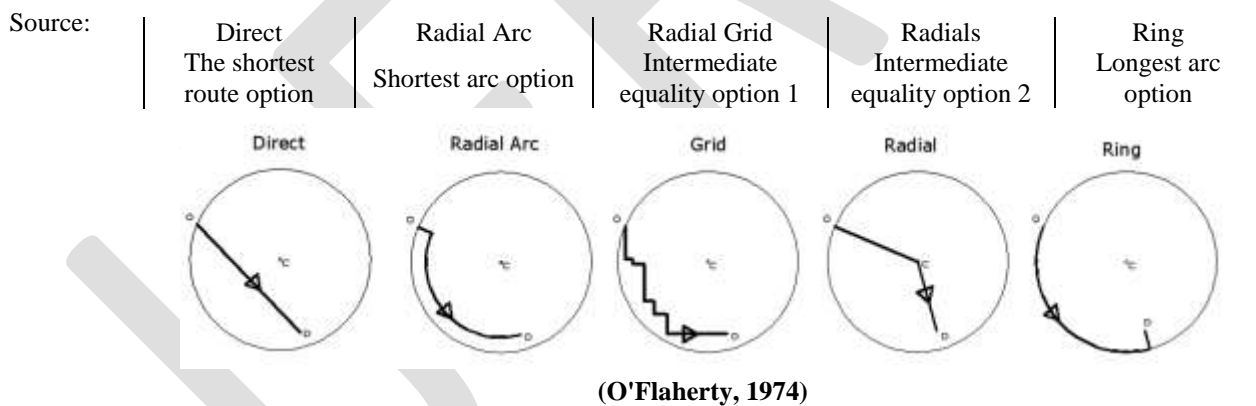


FIGURE 2.1: BASIC RING ROAD CONCEPTS

3.0 METHODOLOGY

Table 3.1 shows the mapping basis. It guides the layout designs to cover the planning stretch of A – E as shown.

TABLE 3.1 MAPPING BASIS OF COMMUTER LOCUS SUBURBANIZATION

Tag	(A) Objective Character	(B) Tech Character	(C) Route Implication	(D) Engineering Choice	(E) Balance
1	Ease of Movement	Line Direct	Shortest	Journey Extraction	Neighbourhood District
2	Private Cars Rerouting	Curve Connect	Average	Route Choice	Regional District

3	Land Use Extension	Network Grid	Longest	Modal Choice	Central District
4	Forbidding Cars in Congested Central Area	Time Jam	Divergence	Destination	Local Market District

The mapping basis is used as a projects' local suburban design, starting with tagging the preferred character features on the decisions slate (Appendix Table A.1).

Following the layout slate decisions, the strategic management operations are shared between the intrinsic and exploratory partners as co-role players in the activity of the government industry. The intrinsic player takes the lead on competence while the exploratory partner lags at daft issues (Table 3.2).

TABLE 3.2 THE MUTUAL INDUSTRY OPERATIONAL MODULE

Basis	Objective on Intrinsic Player	Objective on Exploratory Player	Inequality (Slack/Surplus)	Industry Size Limits
Establishments Slots	2 units of Time Size	1 unit of Time Size		Establishment Slots Value
$\text{Zeroed Incompetence} \geq \text{Zeroed Daft Competence}$				Objective Function

4.0 DISCUSSION AND CONCLUSION

Engineering is as much a science concept as science itself. However, engineering is not science (it has its own characteristic science). It leads to what is simply called 'problem solving'. Engineering in its simplest definition is designing, the designs are expected to be problem solutions (if not, science as standards or mathematics may just be sufficient for works). Much of the classroom study on engineering courses is the study of the sciences. However, in everyday science-applications, engineering as a concept or practice replaces science as an idea of natural laws of phenomenal characteristic responses. Engineering is the use of science. The nature of engineering decision steps are:

1. Area survey and case analysis
2. Basic solution option or process identification
3. Case competitions, specific to basic solution option or process
4. Definition of intrinsic basic solution and integrated competitions matrices on processes scope alternatives
5. Matrices mathematics, composite solutions and outcomes review
6. Solution parameters' Trajectory and Technical plans patterns
7. Standard-results communication extracting

REFERENCES:

1. **Carter, H. 1995.** *The Study of Urban Geography*. 4th. London : Arnold, 1995.
2. **Garba, J M. 1989.** *The Time Has Come...* . Ibadan : Spectrum books Limited, 1989. Reminiscences and Reflections of a Nigerian Pioneer Diplomat.
3. **O'Flaherty, C A. 1974.** *Highways: Highways and Traffic*. London : Edward Arnold, 1974. Vol. 1.
4. **Osuntokun, A. 1987.** *Power Broker*. Ibadan : Spectrum Books Ltd, 1987. A Biography of Sir Kashim Ibrahim.
5. **Young, A. 2010.** *The Politician*. St. Martins Griffin Edition. New York : Thomas Dunne Books, 2010.

APPENDIX

The following table A.1 is the decisions slate:

TABLE A.1 SUBURBANIZATION LAYOUT DECISIONS SLATE

S/N	Layout Projects	Description	Decisions Slate											
			Land Use: A, B, C				Travel: D				Route: E			
			1	2	3	4	1	2	3	4	1	2	3	4
1	Heritage Staff	Futures' view and professional analysis projects	√							√	√			
2	Conflict Mitigation	Early education and vernacular studies projects	√	√				√				√		
3	Growth's Build	Lectures, presentation and scouts projects												
4	Farms	First hand locus-agro districts. Agricultural projects												
5	Improvement & Reserves	Education and Improved focus relief projects												
6	Conservation & Reserves	Status quo and eco-balance projects												
7	Structures & Distinction	Instructive remarks and quality projects												
8	Naivety Bases	Guests and welcome back reputation and thesis projects												
9	Visits	Places upgrade and intermediate projects												
10	Pure Business	Supervisory projects of basic business plans and recommendations												
11	Superintendent-ship	Oversight and new business development projects												
12	Inspector-ship	New boss and market projects												
13	Industrial Development	Factory network and priority projects. Industry weather mitigation technique projects												
14	Interviews	Assessment duties and consulting set ups projects												
15	Headship/Positional	Liaison and local correspondence offices projects												
16	Correspondence Offices	Ambassadorial and international correspondence projects												
17	Reserves Design Districts	Vacation and casual leave projects												
18	Considerable Experience	Expatriate and emergency quarters projects												
19	City Designs	Quadrants design and mini-neighbourhood suburbs projects												
20	Occupational Development	Development plans framing and adapting projects												
21	Alternative/Similar Job Re-placements	New jobs and job expansion projects												
22	Franchise & Purposes	Affiliated institutions development projects												
23	Art, Languages & Anxiety	Economic gains stabilizations, art and symbolic structures projects												
24	News & Saddle	Local reports and development projects. Return to heritage												

S/N	Layout Projects	Description	Decisions Slate														
			Land Use: A, B, C				Travel: D				Route: E						
			1	2	3	4	1	2	3	4	1	2	3	4			
		projects															
25	Self Grooming	Intensive study and project-teaming projects															
26	Belief	Extractions of religio-works tenets, technology and development studies projects															
27	Decisive Role Development	Advanced quadrant designs on mini society and civil engineering cases or challenges															

ACKNOWLEDGEMENT

Prof. A. S. Adedimila (research), Prof. F. A. Falade (Input Engineering) with research by Dr. A. O. Olutaiwo and Engr Obaji. Others included are Prof. E. A. Mesida (Engineering Geology in Input Engineering) and Engr. Oribuyaku – Techgrade Consulting; with Asso. Prof. B. C. Okoro, Engr Dr. J. C. Osuagwu and Engr Dr L. Obi and school management cases (Imo State University) all on various units of supervision covering PhD work in progress.

Speaker Identification Based Home Automation System for Aging populations through Speech Recognition

Aamir Ali Malik¹, Fahad Raza Nizamani²

¹Department of Electrical Engineering, Sukkur Institute of Business Administration, Sukkur, Sindh, Pakistan

aamir.malik@iba-suk.edu.pk

²Department of Electronics Engineering, Hamdard University Karachi, Sindh, Pakistan

fahad.raza123@hotmail.com

Abstract— Old aged or disabled persons who can't walk are most sensitive persons and they must be served in a systematic, quick, sophisticated and efficient manner by very little effort. The problem is that there is no anybody who is always with them for 24 hours. Speech recognition can be used to serve the old aged or disable persons and to give a full control to them so that they may control all the appliances of home. Traditional home automation systems are not cost effective and they are not suitable for aging populations or disable persons. This paper presents an effective method to overcome these problems. We have designed and implemented a low-cost, reliable, efficient and secure speech operated system for home appliances especially for persons with disabilities to do their work at home. This system is both software and hardware designed using MATLAB R2009a. This system is divided into three main parts namely voice train process, voice recognition process and integration of hardware with MATLAB. This system used speaker dependent method. This proposed design is novel in the way that it is controlling loads by speech recognition using MATLAB to turn on/off loads via parallel port of a computer.

Keywords— Speaker Identification, Speech operated system, Home Automation system, Home Appliances, Aging populations, Speech Recognition, MATLAB Coding.

I. INTRODUCTION

Speech Recognition Systems have become so advanced and mainstream that business and health care professionals are turning to speech recognition solutions for everything from providing telephone support to writing medical reports [1, 2].

In many homes there are many people who are old aged or disabled and they can't walk. And there is no anybody who is always with them for 24 hours. There are people who look after them in periodic intervals. The problem is that when a people visits them then it is might not necessary that they needs them but the old aged or disabled person may need a person when he/she is not present with them. Hence home automation systems play a crucial role for elderly or disable persons, so that they can feel comfortable, independent and secure.

Voice activated technology is a rapidly developing area of the computer world. Today, many devices incorporate voice activation technology so certain functions of the device can be performed based on voice commands. For example, many home appliances are equipped with voice-activated technology as to allow a consumer to orally command, for example, a lighting system to power on by using voice commands. Such a feature is particularly advantageous when a person cannot manually activate a device because their hands are occupied or the device switch is in an inconvenient place. For example, one may be carrying groceries into a house and is unable to manually activate the light switch, consequently, if the lighting system in the house has voice activated technology therein, the person may simply say, for example, "lights on" to activate the lights [3].

Speech recognition is the process by which a computer (or other type of machine) identifies spoken words. Basically, it means talking to your computer, and having it correctly recognize what you are saying. This is the key to any speech related application. There are a number ways to do this but the basic principle is to somehow extract certain key features from the uttered speech and then treat those features as the key to recognizing the word when it is uttered again[4].

In this research paper, a low cost, reliable, efficient and secure Speaker identification based home automation system is presented which utilizes the use of biometric method such as human voice as a directive to activate any electrical appliances. This objective makes the human's voice as an input to the system and this system is speaker dependent that mean only the real or trained user and right command can activate the appliances. This produces and improves the security level of the system.

This research paper is based on 5 sections. Section II is based on literature review and reviews the common techniques and methods used for Home Automation systems. Section III is based on the methods and techniques which we have used for Speaker Identification based Home Automation system and describe our contribution as well. Section IV is based on results and discussions, and reflects the results obtained from research work. Section V is based on conclusions and future recommendations and concludes the research paper with the important suggestions and findings from the carried out research work.

II. LITERATURE REVIEW

Several techniques and methods are available for Home automation system. The common methods are given as:

1. Home Automation System using GSM Technology

Home Automation Systems are mostly developed by using microcontroller as a central controlling unit. The Central Control Unit is the hub and brain of a home automation system [5]. We consider three options for communication with GSM, namely SMS based, GPRS based and DTMF based Home Automation systems. Home appliance control system provides security on detection of intrusion via SMS using GSM technology [6]. In this system, user sends SMS from mobile phone to the GSM module connected with Microcontroller and on the basis of SMS various appliances in the home are turned on/off. This system provides mobility to user so that user can turn on/off appliances from anywhere in the world. However it is not possible to implement this system where the user is old aged or disabled with illness due to the main two reasons. The first main reason is that to use this system a user must know the use of mobile for sending SMS generally old aged person don't know much about creating and sending SMS and second is providing mobile phone to each old aged or disabled person is not cost effective. GPRS based technology uses a webcam to stream video and pictures of the home to its owner's mobile through GPRS. In GPRS based Home Automation system user has to monitor his/her phone constantly to successfully defend against intrusion detection. In DTMF based Home Automation system user calls a SIM number assigned to the home and presses the digits on their phone's keypad to control the home's devices by generating a DTMF tone. The tone is received and decoded by the GSM module at home using a DTMF decoder. The decoded instructions are passed to the microcontroller so that user commands can be implemented at home [7]. DTMF-based home security systems also have their security flaws. They are vulnerable to "fuzzing attacks," as described by R.Sasi [8]. This may cause whole home network to crash.

2. Home Automation System via Gesture Recognition System

Traditional input systems for interaction with machines include keyboards, joystick or the mouse. Those suffering from physical handicaps such as Carpel Tunnel Syndrome, Rheumatoid Arthritis or Quadriplegia may be unable to use such forms of input [9]. In that case Gesture recognition is used for Home Automation. Gesture recognition is not based on voice commands but, rather, allows a device to recognize certain gestures [3]. This approach does not require any technical knowledge (like in SMS based automation system). Old aged or disabled will use his/her hand to control appliances. By using a simple webcam the images will be taken and will be processed at Laptop in MATLAB software and once a particular gesture is recognized then the corresponding action will be performed [9]. Although it is a sophisticated solution but when Old aged or disabled person is not able to move hand and when they can only shake hand then hand detection may not accurately detected and the chance of false alarm is more in this approach and mostly the hand gesture recognition is done by detecting the human skin color and so because of this the background of the hand must be a non-skin color background with fixed distance between hand and the camera. Moreover for the smooth working of system there must be a proper arrangement of lighting always. Gesture recognition system can be used in various applications like Virtual reality, games and sign language. Sign language is an important case of communicative gestures [10, 11]. Sign language for the deaf (e.g. American Sign Language) is an example that has received significant attention in the gesture literature [12, 13, 14 and 15].

3. Home Automation System using Bluetooth, WIFI, WSN and Zigbee Technologies

Many Wireless Technologies like RF, Wi-Fi, Bluetooth and Zigbee have been developed and remote monitoring systems using these technologies are popular due to flexibility, low operating charges, etc [16]. Bluetooth looks like an attractive communication

technology for creating smart homes. It is cheap, easy, and quick to set up. People are already familiar with the technology; however Bluetooth communication should only be used on occasions where there is a need for quick short-lived network communication with little concern for security. Limitations include, they have maximum communication range of 100m in ideal conditions, and it has high power consumption [7]. It has serious security concerns such as eavesdropping and weak encryption as discussed by M.Ryan [17]. Other wireless technologies like WIFI, WSN and Zigbee have very high developing and deployment cost due to needs of motes, sensors, and radio transceivers etc, spread over a large area. Further it is difficult to upgrade existing conventional control system with remote control capabilities [16]. Moreover they are commonly used by mobile users, who want to monitor and control their home appliances remotely; hence these technologies are not suitable for aging populations.

III. DESIGN AND IMPLEMENTATION OF SPEAKER IDENTIFICATION BASED HOME AUTOMATION SYSTEM THROUGH SPEECH RECOGNITION

The block diagram of Speaker Identification based Home Automation system using speech recognition is shown in **figure 1**.

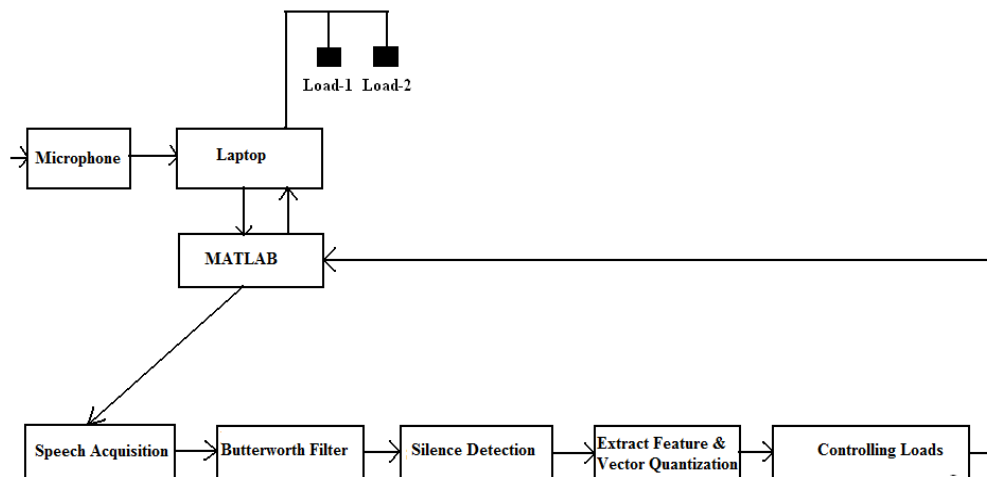


Figure 1 Block Diagram of Speech Operated System for Home Appliances

Speaker Identification based Home Automation system using speech recognition is a low-cost, reliable, efficient and secure method for Home Automation System.

As previously told paper is divided into three main parts which are Voice Training Process, Voice Testing Process and Integration of Hardware with the MATLAB. The system used is speaker dependant method that means user has to record his/her voice before using the system. Various steps involved in Speaker Identification based Home Automation system using speech recognition is shown in figure 1.

A. *Voice Training Process*

In voice training process the first step is acquisition of speech. Built in Microphone in laptop is utilized for Speech Acquisition, and then speech acquisition device is installed by simply Connecting the Microphone with laptop via sound card input port. In second step a function is created, which will record speech in MATLAB. In third step recorded speech is played on laptop based audio output device. Fourth step is to write acquired speech in MATLAB and .Wav file is created. In fifth step .wav file is loaded in MATLAB, in order to read the saved speech and in sixth step saved speech is acquired. In seventh step it is filtered out through the Butterworth band pass filter. Butterworth filter is used because it is the best compromise between attenuation and phase response. It has got no ripple in the pass band or the stop band. After that it is saved in the computer memory so that it can be matched with incoming utterance of speech. In this research work user has uttered two training voices to control the load. These uttered words are "CLOSE" and "YES". Now all above steps are applied to these uttered words. Silence detection or Voice Activity Detection (VAD) is used in speech processing, which is used to detect presence or absence of human speech. VAD is used here to deactivate some processes when there

is a silence or non-speech section in audio session. Short time Fourier transforms is performed successfully so that for each incoming speech, the part of containing high frequency component is extracted. Actually here in MATLAB coding 2500 samples per word are created for feature extraction.

B. Voice Testing Process

In voice testing process the user has uttered two different words each process. One word is same as which was trained in training phase was “CLOSE” and other one is “OPEN”. Then both uttered signals are further processed and analyzed by applying same steps which are already used in Voice Training Process. Like voice training process, 2500 samples per word are also created here for feature extraction. These testing signals are used to match with trained signals to authenticate the desired speech. There are various feature matching techniques used in MATLAB, from which Vector Quantization method is used in this research paper. Vector Quantization is a process of mapping vectors from a big vector space to a finite number of regions in that space. In the testing phase, a speaker-specific Vector Quantization codebook is generated for each known speaker by clustering his/her testing acoustic vectors.

C. Integration of Hardware with the MATLAB

Once all speech processing operations are completed now the final step is to perform a particular action related to the corresponding particular detected signal. There are two different loads that can be controlled via two different kinds of speeches. These loads are bulb and LED (light emitting diode). Loads can be different like fan, tube light, electronic room lock etc. Initially it was decided to use microcontroller for controlling loads based on speech recognition. As landline telephone can be used for controlling various home equipments. It was almost near to be implemented for the Speech Operated System but later on found that it was expensive and complex as compared to the approach which we have discussed in this research paper. In this approach parallel port (RS-232) of a computer is interfaced with the MATLAB and corresponding loads are turned on and off with the help of relays. This approach is simple and very less expensive as compared to other approaches. The block diagram of whole hardware design is shown in **figure 2**.

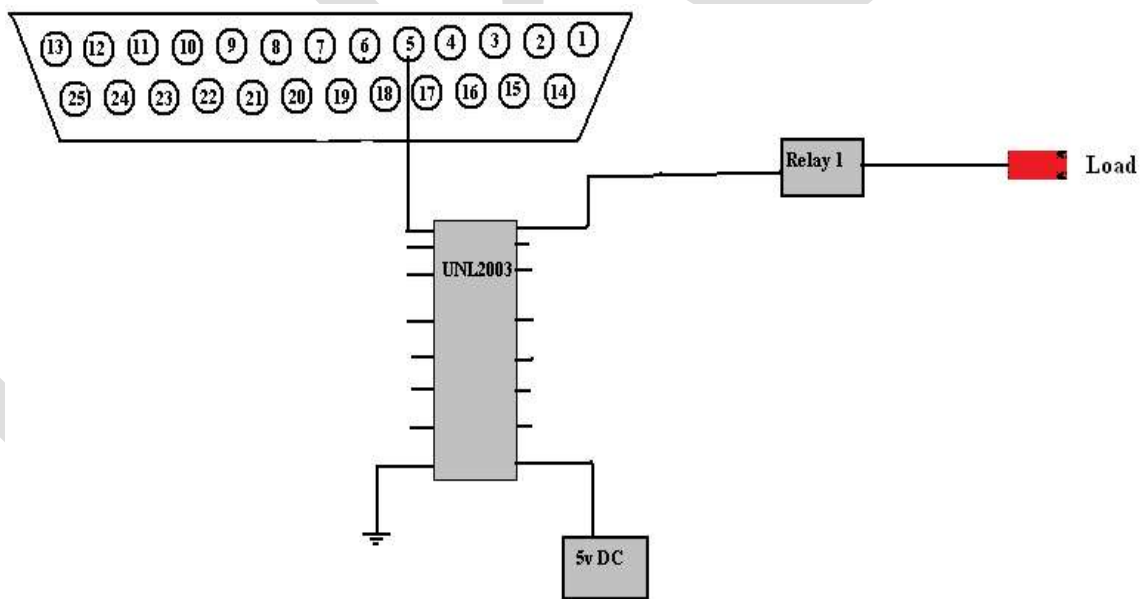
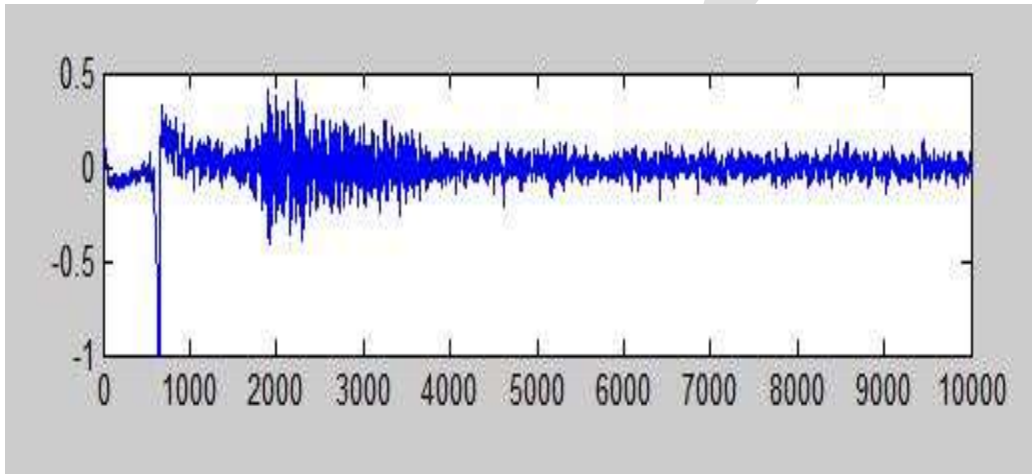


Figure 2 Block Diagram of whole Hardware Design

Figure 2 is showing over all hardware circuit of the project. A DC voltage of 3.2 volts will come out from the parallel port (RS-232) of a computer and this voltage will be input to the UNL2003 IC where this IC will generate 5 volts DC at the corresponding output pin and this 5 volts DC will be input for the relay so that relay should turn on and the corresponding load should also turn on.

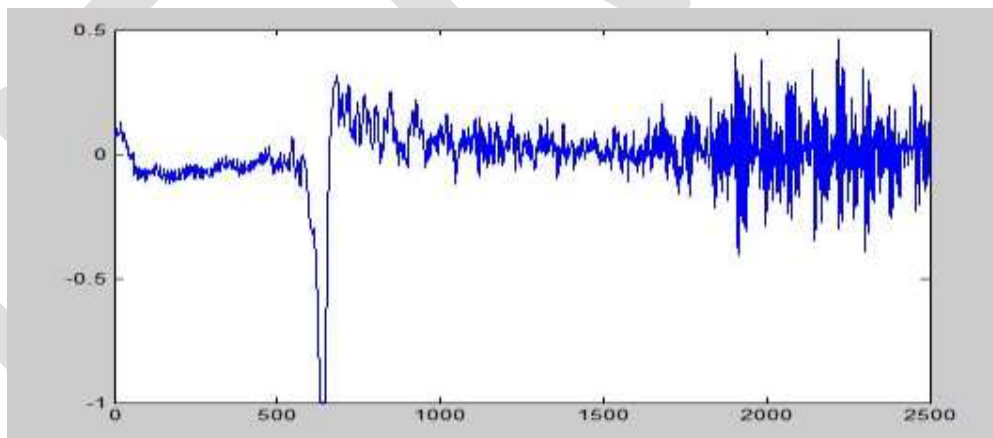
IV. RESULTS AND DISCUSSIONS

In this research work, we were able to successfully integrate hardware with the MATLAB software. In voice training and testing phase different words are uttered and correlation is performed between them to authenticate the trained user to control the different home appliances. In voice training phase user has uttered two different words ‘‘CLOSE’’ and ‘‘YES’’ in separate sections via using MATLAB. These uttered words are converted into .wav files and saved in computer memory. Short time Fourier transforms is applied and 2500 samples are created for each uttered word and features are extracted from them. The results obtained for Voice training phase are shown in **Figure 3(a) (b)** and **Figure 4(a) (b)** in form of graphs respectively.



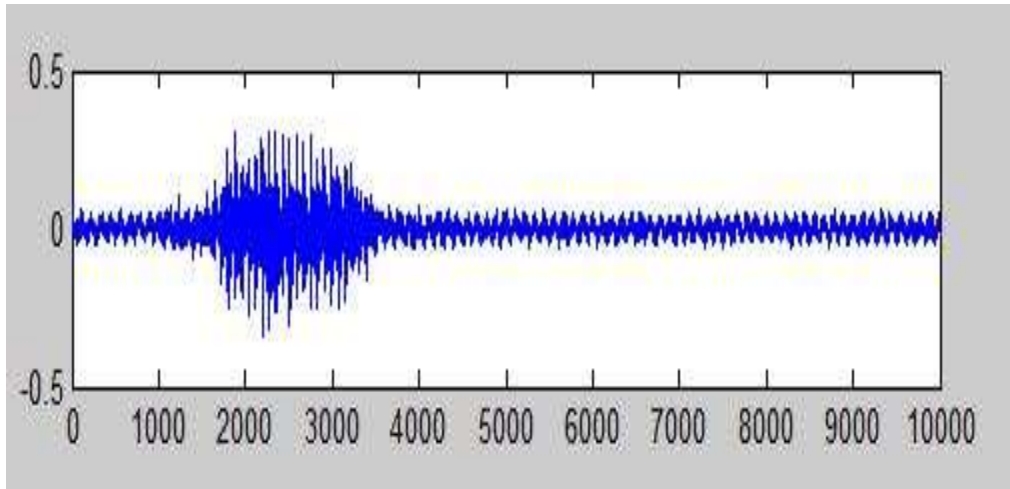
Time vs. Amplitude

Figure 3(a) Train Signal Uttered as ‘‘CLOSE’’



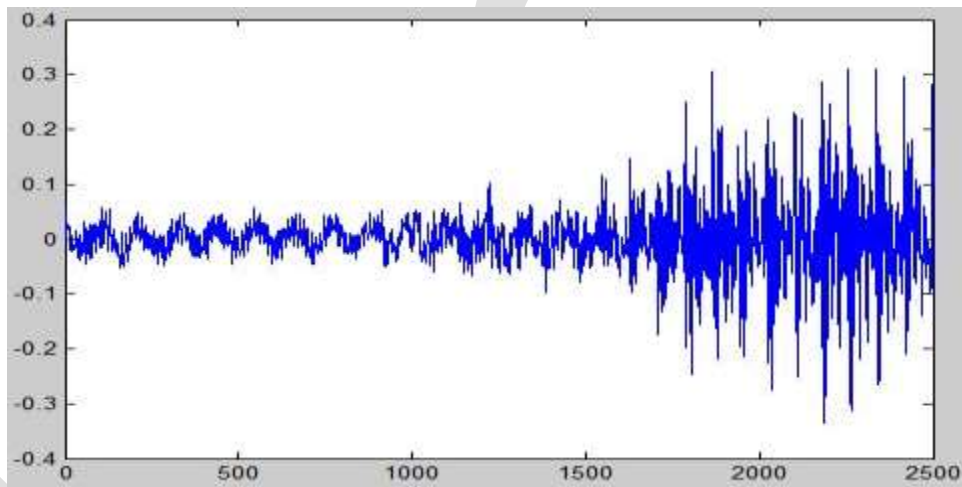
Samples vs. Amplitude (db)

Figure 3(b) Extracted 2500 Samples from Uttered Word ‘‘CLOSE’’



Time vs. Amplitude

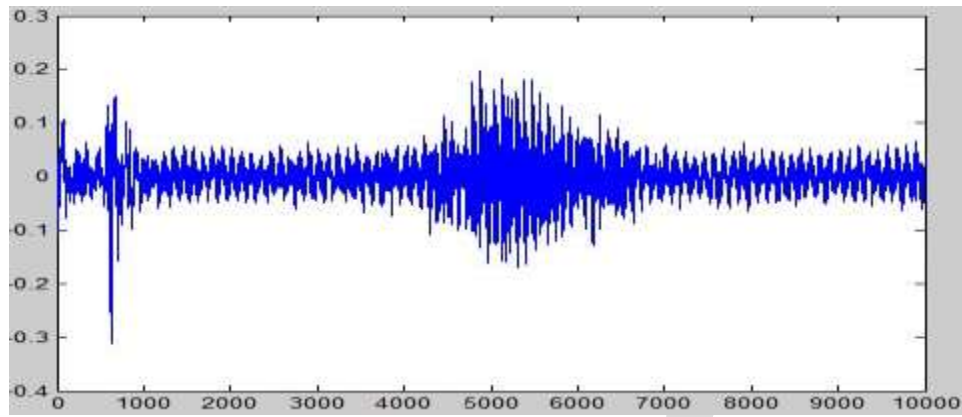
Figure 4(a) Trained Signal uttered as "YES"



Samples vs. Amplitude (db)

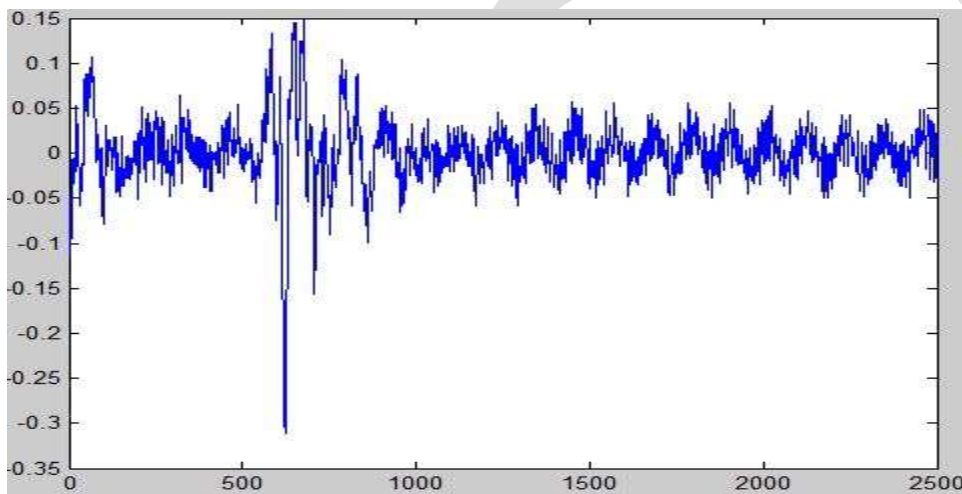
Figure 4(b) Extracted 2500 Samples from uttered word "YES"

Similarly for Voice testing process, user has uttered two different words each process. One word is same as which was trained in training phase was "CLOSE" and other one is "OPEN". Then both uttered signals are further processed and analyzed by repeating same steps which were used in Voice Training process. Finally correlation is performed between two phases by using Vector Quantization. The results of Voice Testing phase are shown in **Figure 5(a) (b)** and **Figure 6(a) (b)** in form of graphs respectively.



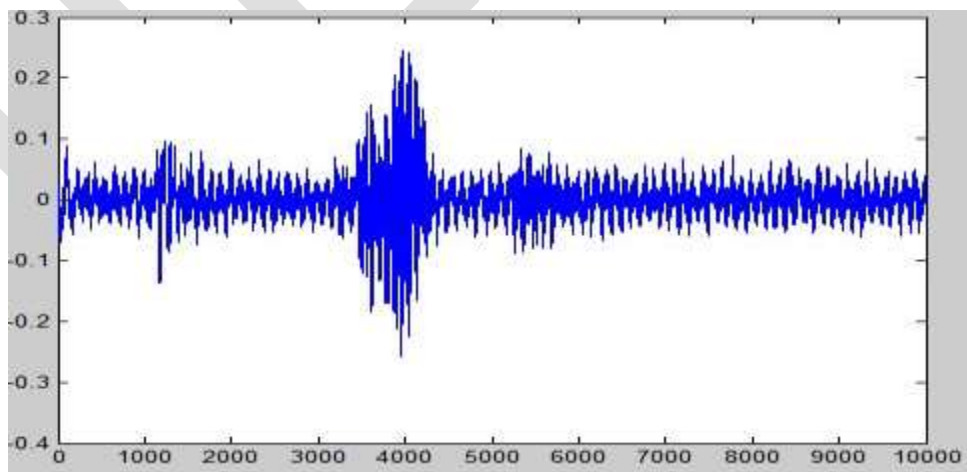
Time vs. Amplitude

Figure 5(a) Test Signal Uttered as "CLOSE"



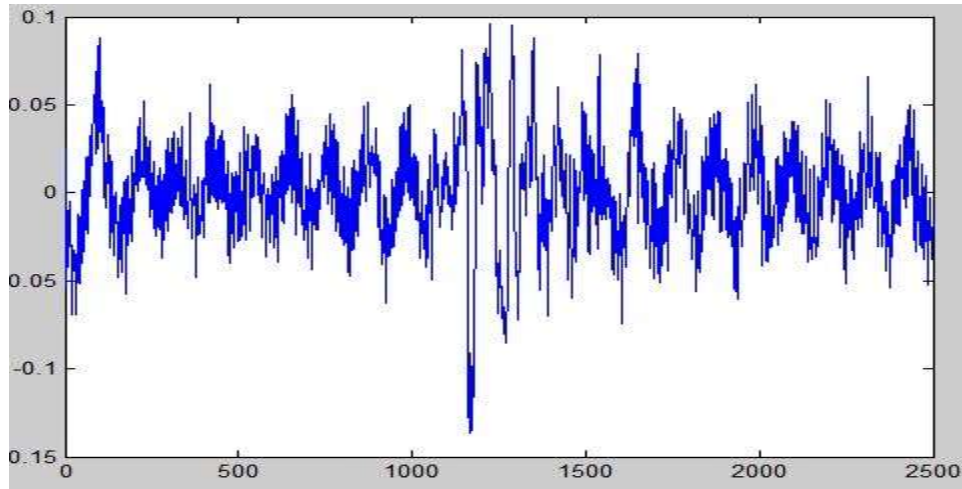
Samples vs. Amplitude (db)

Figure 5(b) Extracted 2500 Samples from Uttered Word "CLOSE"



Time vs. Amplitude

Figure 6(a) Test Signal Uttered as "OPEN"



Samples vs. Amplitude (db)

Figure 6(b) Extracted 2500 Samples from the Test Signal Uttered as “OPEN”

Now when user has uttered same word “CLOSE” in Testing Part then the load (LED) is turned “ON” as shown in **Figure 7(a)**.

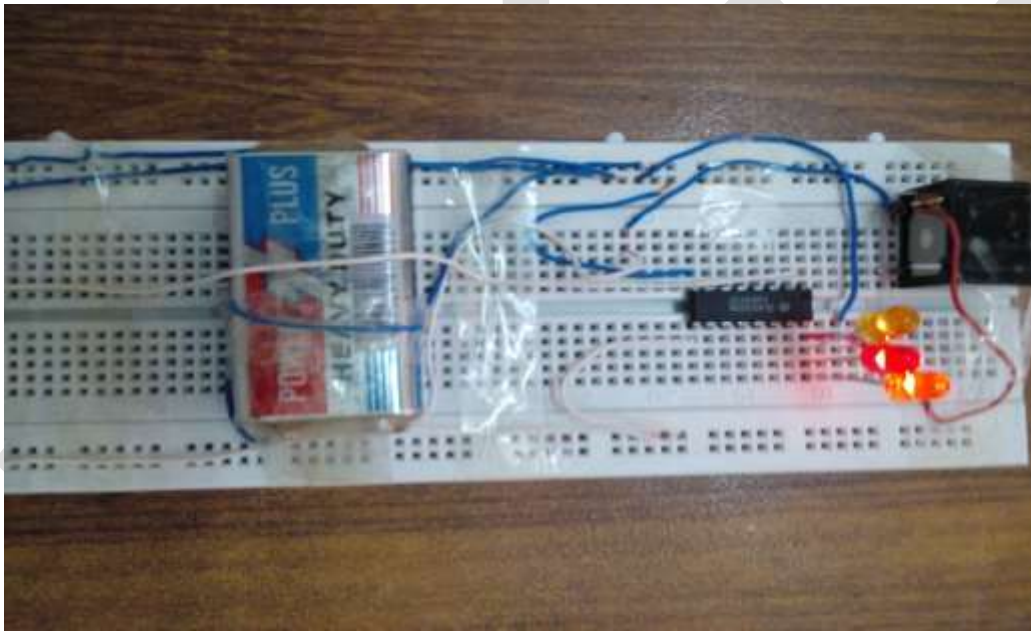


Figure 7(a) Load (LED) is turned ON when User has Uttered word “CLOSE”

As shown in **figure 7(a)**, Load(LED) is turned ON when user has uttered the word ‘‘CLOSE’’ in testing part, because this word is already recorded or trained in MATLAB program, in training phase and saved in computer memory. Now when user is again uttering or speaking the same word in testing part, then speaker identification is matched by MATLAB program and authentication is successful and Load (LED) is turned on for that user.

When user has uttered the word other than the trained word like “OPEN” then there is no any signal to load (LED) as shown in **Figure 7(b)**.

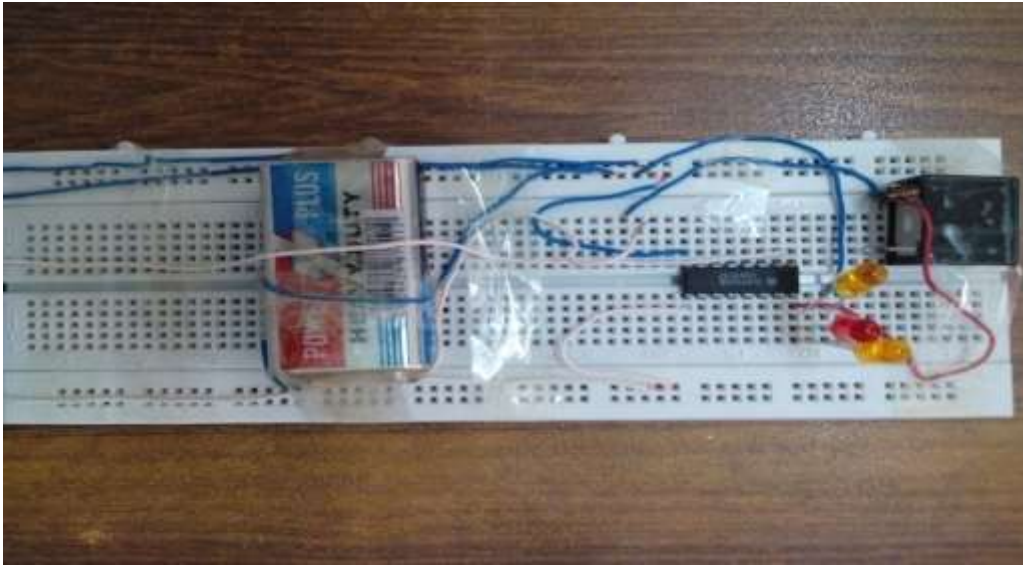


Figure 7(b) when user has uttered word other than the trained word

As shown in **figure 7(b)**, Load (LED) is not turned ON when user has uttered the word ‘‘OPEN’’ in testing part, because this word is not trained in MATLAB program, in training phase. Now when user is uttering or speaking the word ‘‘OPEN’’ in testing part, then speaker identification is not matched by MATLAB program and authentication is unsuccessful and Load (LED) is not turned on for that user.

This experiment shows that only the trained user and right command can activate the home appliances. It increases the security level of the system. For the smooth working of system there must be a proper arrangement of room always, there must be no any other noise. This is because speech operated system is very sensitive to noise. Noise can be of fan, other person speaking while in system’s process. The utterance of speaker must be very different like pitch, frequency and loudness. This is because the pitch, frequency and loudness each represent different information about the speech.

V. CONCLUSIONS AND FUTURE RECOMMENDATIONS

A successful experiment of Speaker Identification based Home Automation system is carried out in this research work. The designed Speech operated system is a low-cost, reliable, efficient and secure. The designed Speech Operated system can be used in various areas of application. In the area of Home security, the designed system can be used by using biometric system such as human voice to centrally monitor the doors, rooms, windows and other electrical home equipments. Moreover an intercom system can be integrated to the telephone or video door can be equipped with voice operated system, where old aged or disable person can remotely monitor the outdoor activity on the CCTV camera, this provides a remote surveillance of security. Speech operated system can be used in Ubiquitous transcripts to keep real-time transcripts during conversations. Speech operated system can also be used to answer computers in a hands-free environment, like when driving. Speech operated system can be used in tasks that require human-machine interface, for example automatic call processing in the telephone network and data query information systems. Smart Grid technology can also be integrated with Speaker Identification based home automation systems.

In future, a significant research can be carried out in the area of Speech Operated system for Home Appliances. Speaker Identification based Home Automation system with better efficiency can be developed which will also be operate able in noisy environment. Reliable and efficient Home Automation system can be designed in future which will be both speaker dependant as well as speaker independent with maximum efficiency, security and performance.

ACKNOWLEDGMENT

Our foremost thanks go to our Head of Department Professor Dr. Madad Ali Shah for his vital support and encouragement. Last but not least, we would like to express our appreciation to our beloved parents for their unconditional love and support that let us through the toughest days in our life.

REFERENCES:

- [1] B.H. Juang & Lawrence R. Rabiner, Automatic Speech Recognition – A Brief History of the Technology Development.
- [2] LumenVox Network, ‘History of Speech Recognition’, Web, <http://www.lumenvox.com/resources/tips/historyOfSpeechRecognition.aspx> , last visited on Dec 25, 2015.
- [3] LA Roberts, HT Nguyen, EM Silver, ‘Gesture Activated Home Appliance’- US Patent 6,937,742, 2005 - Google Patents
- [4] Coucopoulos, Andre; 2007, ‘Voice processing for home automation systems’, Network system design line, January 2007.
- [5] **Tushar Rastogi and Rahul Raj Sharma, Cypress Semiconductor, ‘Home automation system design: the basics’, June 11 2014, Web, <http://www.embedded.com/design/connectivity/4431025/Home-automation-system-design--the-basics> , Last visited on Dec 25, 2015**
- [6] Sikandar Malik Khiyal Hayat; Khan Aihab & Shehzadi Erum; 2009, ‘SMS based wireless home appliance control system (HACS) for automating appliances and Security’, Issues in information science and information technology, 2009, vol. 6.
- [7] Arun Cyril Jose and Reza Malekian; August 2015, ‘Smart Home Automation Security: A Literature Review’, Smart computing Review, August 2015, vol. 5.
- [8] R. Sasi, ‘How I DOS’ed My Bank,’ *Hack in the Box Security Conference (HITBSecConf2013)*, Oct. 2013.
- [9] Dand, D.; Mehta, S.; Sabesan, S.; Daftery, A., "Handicap Assistance Device for Appliance Control Using User-Defined Gestures," in *Machine Learning and Computing (ICMLC), 2010 Second International Conference*, pp.55-60, 9-11 Feb. 2010
- [10] Siddharth S. Rautaray, Anupam Agrawal, ‘Real Time Hand Gesture Recognition System for Dynamic Applications’, International Journal of UbiComp (IJU), Vol.3, No.1, January 2012
- [11] Liu, N., & Lovell, B. (2001), ‘Mmx-accelerated realtime hand tracking system’ In Proceedings of IVCNZ.
- [12] F. Chen, C. Fu, & C. Huang, 2003 , ‘Hand gesture recognition using a real-time tracking method and hidden Markov models’ Image and Vision Computing, pp. 745-758.
- [13] Lee, C. S., Ghyme, S. W., Park, C. J., Wohn, K., (1998) ‘The Control of avatar motion using hand gesture’, In Proceeding of Virtual Reality Software and technology (VRST), pp. 59-65.
- [14] Ahn, S. C., Lee, T. S., Kim, I. J., Kwon, Y. M., & Kim, H. G. (2004), ‘Computer Vision-Based Interactive Presentation System,’ Proceedings of Asian Conference for Computer Vision.
- [15] Moeslund, T. B., & Norgaard, L. (2002) ‘A brief overview of hand gestures used in wearable human computer interfaces’, Technical report, Aalborg University, Denmark
- [16] SHODHGANGA, ‘to design low cost intelligent embedded system based remote monitoring system using mobile/cell phone’, A Reservoir of Indian thesis, <http://shodhganga.inflibnet.ac.in> , last visited on Dec 27, 2015.
- [17] M. Ryan, ‘Bluetooth: With Low Energy comes Low Security,’ *WOOT'13 Proceedings of the 7th USENIX conference on Offensive Technologies*, pp. 4-4, 2013.

Plant classification with pollen characters using Neural Network : A Review

Ms.Shraddha Dasharathrao Gadge¹

Student of HVPM College of Engineering and Technology Amravati (India)
shraddha555gadge@gmail.com

Mr.Vijay L.Agrawal²

Associate Professor in Dept. (Electronic and Telecommunication) of HVPM'S
College of Engineering and Technology (India)

Abstract— Pollen grains are widely used as fingerprints of plants. Pollen grains play a vital role in the life of plants, animals and man. Pollen can tell us a lot about the world both past and present or even who may have committed a crime thus provide a biological and historical record of thousands years. Pollen can travel by transport of any form including insects, animals, birds, human and other transient materials such as planes, trains and boats; practically any moveable material. Many researcher, who uses Palynology as a primary research tool may have to spend up to 30 months of microscopic work for identifying and classifying the pollens. The aim of this purposed work is to develop an efficient classification algorithm based on computational intelligence approaches, with accuracy similar to that achieved by experienced palynologists.

Keywords— Signal & Image Processing, NeuralSolution(Neural Network), Transformed domain Technique, MATLAB ,Microsoft office excel , Statistic, SEM images.

INTRODUCTION

Pollen morphological characters are used for plant classification and identification of plants. The pollen grains are very typical and could provide very useful data for the delimitation of various genera and subsequently help to solve many stratigraphical and taxonomic problems (Sharma, 1968)[3]. Pollen can tell us a lot about the world both past and present. Polleng rains can tell us what plants were around thousands of years ago, how our ancestors used them, how plants have moved across the region, country and globe, what plants produced a certain variety of honey or even who may have committed a crime (Agashe, 2006). It is because pollen grains are so small, they can travel fast and be easily embedded in lake sediments, get preserved and thus provide a biological and historical record of thousands years.

Any researcher, who uses Palynology as a primary research tool may have to spend up to 30 months of microscopic work for identifying and classifying the pollens. Thus, automation of Palynology could lead to many advances: rapid results, larger data sets, objectivity, fine resolution sampling and possibly finer determinations (discriminations). Thus, in this research, the above problem was studied and an efficient algorithm which was a finite sequence of steps was used for image processing, feature extraction and design of CI based classifier which was reported as a final outcome of the study that will solve the problem of pollen classification. It is a list of well-defined instructions for completing the task of pollen classification.

The objective of the research is to develop an efficient classification based on computational intelligence approaches that provides the benefits of advances in engineering and technology to overcome the limitations of the present classification techniques giving precise classification accuracy of the sample pollen species of the pollen class.

Literature Review:

In the past, researchers in biology and Palynology were dependent on the traditional methods of pollen classification, which includes various skilled techniques that can only be performed by experts from the field of biology. Earlier interest in pollen classification was restricted to the image recognition and was hindered by slow computers with insufficient memory.

From the related work reported so far in the published literature, it is observed that some of the researchers employed neural network for pollen identification and classification.

Flenley (1968), was the first to identify the need to automate the process of classification of pollen grain. Langford et al. (1990) established a co-occurrence matrix of grey levels for each sample. Then texture measures were calculated and used as input to a classification programme. With a leave-one-out strategy and a variable selection procedure, the proportion of pollen grains correctly

identified increased to 94.30%. France et al. (2000) developed an automated system for identification, classification and counting of pollen grains.

The choice of the classification method is vital for satisfactory results. Simple discriminating algorithms, e.g. one nearest neighbor, have been used for clustering due to their easy implementation and sometimes, the low computational expense. For instance, Rodriguez-Damian et al. (2003) chose a minimum distance classifier. In order to select the most critical feature, a Floating Search Method (FSM) was performed, reducing the vector size from 14 to 5 in the optimal case. Boucher et al. (2002) reported also the minimum distance concept to assign probabilities to shape feature vectors. The class decision was made by confirming hypothesis probabilities by palynological features.

Rodriguez-Damian et al. (2004) presented a complete system for classification of pollen allergenic species of Urticaceae family. The images were taken by an optical microscope. A coarse border of pollen grain was estimated using Hough Transform. A set of shape measures was computed, which were used to discriminate between species. They considered 18 images per class, so that total number of images was 234. Similarly, Zhang et al. (2004) used IA texture and shape features to classify to 97% accuracy for 5 taxa of modern New Zealand pollen types. A workable set of features has been selected by Zhang (2004) and the study of image proposed by Hold away (2004) has paved usefully automates Palynology.

Li et al. (2004) used image analysis (IA) texture features coupled with ANN to correctly classify 100% of 13 taxa of modern pollen and spore types found in New Zealand. Flenley et al. (2004) demonstrated the first successful automated identification, with 100% accuracy. The technique involved a use of neural network classifier applied to surface texture data from LM images. Rodriguez-Damian et al. (2004) proposed brightness and shape descriptors for pollen classification. Zhang et al. (2004) employed a supervised multilayer perceptron to classify a 6-dimensional vector. Zhang et al. (2005) recommended a method of texture description using wavelet transforms in combination with concurrence matrices and neural network with a view to classify the extracted image features. Sixteen types of airborne pollen grains were used, and more than 91% images were correctly classified.

Weller et al. (2006) used pollen image analysis features including morphological, Fourier and textural descriptors, as well as geometric moments and color. To determine image clusters, unsupervised self-organized maps (a genre of artificial neural networks) were used. Using a SOM, major and minor clusters were identified. Kalva et al. (2007) used combination of neural network classifier with Naive Bayes classifier that uses features such as color, shape and texture. These features are extracted from web images giving meaningful improvement in the correct image classification rate relative to the results provided by simple neural network based image classifier, which does not use contextual information.

In a more sophisticated approach, Ronneberger et al. (2002) used a Support Vector Machine (SVM) technique together with one-versus-rest multi-class optimization to get the aforementioned classification results on high-dimensional vectors from 3D invariants. Hitherto, Neural Networks have become very popular due to its relative simple configuration, flexibility and favorable results. Hodgson et al. (2008) proposed the pollen recognition rate of the system, which is accomplished by including grey-level co-occurrence matrix. Carrion et al. (2008) proposed an improved classification of pollen texture images using SVM and MLP.

Baladal et al. (2010) suggested a computer vision as its artificial "eye" and an ANN as its artificial "brain". An automated image analysis procedure was used to extract gray-scale spectral values of pollen image and pollen classifier was designed based on 3-layer ANN and the gray-scale spectral values were used as input. Results showed that the automated procedure correctly classified pollen grains 78.7% of the time. Travieso et al. (2011) developed contour feature based classification, which was based on an HMM kernel. SVM was used as a classifier in that system. Ticay-Rivas et al. (2011) proposed the combination of features like shape and ornamentation that have been studied earlier and colour features over de-correlated stretched images for enhanced pollen classification by MLP NN based classifier. More standard characteristics like geometrical features and Fourier descriptors have been added to the pollen grain descriptions. Over this multiple feature vector, PCA has proven to increase the classification system performance.

Recently, Holt et al. (2011) used Neural Networks to classify the available pollen types. Holt et al. (2012) employed a system known as "classifynder" using robotics and image processing to locate, photograph and classify image fossil pollen on a conventionally prepared pollen slide and coupled it with a neural network based classifier to identify the pollen in captured images. Results justify that the accuracy of the neural network based classifier was quite variable, caused partly by misclassification of deformed or broken grains. However, final "classifynder" counts of the fossil samples matched very closely with the human counts.

Nguyen et al. (2013) proposed improved pollen classification with less training efforts by introducing a new selection criterion to obtain the most valuable training samples.

In view of the above reviewed work, the use of CI based neural classifier techniques is justified, in the light of the facts that the obtained classification accuracy is 100%, except for one pollen sample.

Research Methodology

Computational Intelligence techniques include the following well established techniques.

- i) Statistics
- ii) Signal & Image processing
- iii) Learning Machines such as neural network .
- iv) Transformed domain techniques such as FFT, WHT etc.

For choice of suitable classifier following configuration will be investigated.

- i) Multilayer perceptron Neural network.
- ii) Radial Basis function Neural network.

For each of the architecture, following parameters are verified until the best performance is obtained.

- i) Train-CV-Test data
- ii) Variable split ratios
- iii) Possibility different learning algorithms such as Standard Back-Propagation, Conjugate gradient algorithm , Quick propagation algorithm, Delta Bar Delta algorithm, Momentum etc.
- iv) Number of hidden layers
- v) Number of processing elements of neurons in each hidden layer.

After regions training of the classifier, it is cross validated & tested on the basis of the following performance matrix.

- i) Mean Square Error
- ii) Normalized Mean Square Error
- iii) Classification accuracy
- iv) Sensitivity
- v) Specificity

In order to carry out the proposed research work, Platforms/Software's such as Matlab, Neuro solutions, Microsoft Excel will be used.

Research Objectives

- To develop an efficient classification algorithm based on computational intelligence approaches, with accuracy similar to that achieved by experienced palynologists.
- To increase the classification accuracy for classification of Pollen grains of various plants

- To maintain the correctness & accuracy in the plant classification with Pollen characteristics even though the input images are contaminated by known or unknown noise.

ACKNOWLEDGMENT

We are grateful to our HVPM College Of Engineering and Technology to support and other faculty and associates of EXTC Department who are directly & indirectly helped me for this paper.

CONCLUSION

Use of the proposed Algorithm for Plant classification with pollen characters using Neural network will be result in more accurate and reliable.

REFERENCES:

1. Flenley J.R., The problem of pollen recognition. In: clowes M.B., Penny J.P.,(Eds.),Problems of picture Interpretation. C.S.I.R.O, Canberra, pp:141-145,1968
2. Roadriguez-damian M., cernadas, E., Formella,A., Sa-otero, R.: Pollen Clasification Using brightness-based and shape-based descriptor . in: Proceedings of the 17th International conference on Pattern recognition, ICPR 2004 , Agust 23-26,vol 2, pp.212-215(2004)
3. Sharma, B.D Contriubution to pollen morphology and plant taxonomy of the family Bombacaceae. Pakistan J.Rot. 36 (3): 175-191,1968
4. Aftab R. and Perveen A. (2006) A palynological studies ofsome cultivated trees from Karachi. Pak.J. Rot. 38 (1): 15-28.
5. Ahmad K., Khan M. A. and Shaheen N. Palyonological studies of the semi-desert plant species from Pakistan. African Journal of Biotechnology Vol. 9 (24): 3527-3535, 2010.
6. Arpaia P., Daponte D., Grimaldi D., Michaeli L., ANN-based error reduction for Experimentally modeled sensors, IEEE Transactions on Instrumentation and Measurement, 51: 23-29, 2002.
7. Baum E.B., On the capabilities of multilayer perceptrons, Journal of Complexity, 4:193- 215, 1988 .
8. Beevi H.and Nair, P.K.K. Pollen morphology of Coconut. Journal of Palynology Vol. 4: 1-118, 2006 .
9. Boucher, A., Thonnat, M.: Object recognition from 3D blurred images. In: Proceedings of 16th International Conference on Pattern Recognition, vol. 1, pp. 800-803 (2002).
10. Bradley, D. E. Some carbon replica techniques for the electron microscopy of small Specimens and fibers. Brit. J. appl. Phys. Vol. 8: 150, 1957.
11. Bricego, M., Murino, V.: Investigating Hidden Markov Models Capabilities in 2D Shape classification. IEEE Transactions on Pattern Analysis and Machine Intelligence 26(2), 281-286 (2004).
12. Brooks J and Shaw G., Chemical structure of the exine of pollen walls and a new function for carotenoids in nature. Nature 219:532-533,1968.
13. Chu Xiaowen, Li Bo, Zhang Zhensheng, A dynamic RWA algorithm in a wavelength-routed all optical network with wavelength converters, INFOCOM, 22nd Annual Joint Conference of the IEEE Computer and Communications, 3:1795-1804, 2003.

Fatigue Analysis of Alloy Wheel for Passenger Car under Radial Load

D.H.Burande¹, T.N. Kazi²

(1) Assistant Professor, Department of Mechanical Engg, Sinhgad College of Engineering, Pune (2) M.E. Mechanical (Automotive Engineering), Sinhgad College of Engineering, Pune, dhuburande.scoe@sinhgad.edu¹,taufikkazi031@gmail.com²

Abstract:-The alloy wheels of passenger cars are intended for better heat conduction and improved aesthetics appearance over steel wheels. The alloy wheels are lighter than steel wheels. In order to achieve better quality, the study of alloy wheel is necessary. The manufacturers carry out a number of wheel tests to ensure that the wheel meets the safety requirements and higher comfort level. Thus, simulations of alloy wheel were carried out for specific design through realistic loading conditions. Skoda Octiva passenger car alloy wheel was used for simulation. In this study, stress distribution of alloy wheel is evaluated by using finite element analysis. S-N curve was generated for aluminum alloy material. The radial fatigue test is carried on specimen according to industrial standards. The wheel was checked for fatigue life cycle and improvement in the material. An attempt has been made by conducting study to suggest a suitable safety for reliable fatigue life prediction.

Keywords: 1 finite element analysis technique 2. Radial fatigue test 3. Life cycle

1. INTRODUCTION

Alloy wheels were first developed in the last sixties to meet the demand of racetrack enthusiasts who were constantly looking for an edge in performance and styling. It was an unorganized industry then. Since its adoption by OEM's, the alloy wheel market has been steadily growing. Today, thanks to a more sophisticated and environmentally conscious consumer, the use of alloy wheels has become increasingly relevant. With this Increased demand came new developments in design, technology and manufacturing processes to produce a superior with a wide variety of designs. In the fatigue life evaluation of aluminium wheel design, the commonly accepted procedure for passenger car wheel manufacturing is to pass two durability tests, namely the radial fatigue test and cornering fatigue test. Since alloy wheels are designed for variation in style and have more complex shapes than regular steel wheels, it is difficult to assess fatigue life by using analytical methods. For this simulations of alloy wheel for specific design and improvement is carried out through realistic loading conditions.

i. Types of wheel (material)

Steel and light alloy are the foremost materials used in a wheel rim however some composite materials together with glass-fibre are being used for special wheels.

A. Wire spoke Wheel

Wire spoke wheel is an essential where the exterior edge part of the wheel rim and the axle mounting part are linked by numerous wires called spokes. Today's automobiles with their high horse power have made this type of wheel manufacture obsolete. This type of wheel is still used on classic vehicles.

B. Steel Disc Wheel

This is a rim which practices the steel made rim and the wheel into one by joining (welding), and it is used mainly for passenger vehicles especially original equipment tires.

C. Light Alloy wheel

These wheels are based on the use of light metals, such as aluminum and magnesium has come to be popular in the market. This wheel rapidly become standard for original equipment vehicle in Europe in 1960's and for the replacement tire in United States in 1970's. The advantages of each light alloy wheel are explained as below.

ii Aluminium Alloy Wheel

Aluminium is a metal with features of excellent lightness, thermal conductivity, physical characteristics of casting, low heat, machine processing and reutilizing, etc. This metal main advantage is decreased weight, high precision and design choices of the wheel.

iii) Magnesium alloy Wheel

Magnesium is about 30% lighter than aluminium and also admirable as for size stability and impact resistance. However its use is mainly restricted to racing, which needs the features of weightlessness and high strength. It is expansive when compared with aluminium

iv) Titanium alloy wheels

Titanium is an admirable metal for corrosion resistance and strength about 2.5 times compared with aluminium, but it is inferior due to machine processing, designing and more cost. It is still in developed stage.

v) Composite material wheel

The composite material wheel is different from the light alloy wheel, and it is developed mainly for low weight. However this wheel has inadequate consistency against heat and for best strength.

2. DESIGN AND FATIGUE ANALYSIS OF ALLOY WHEELS

After analysing the working condition of wheel, there are two major loads i.e. direct load (Radial load due to weight of vehicle) and tangential load (due acceleration torque or braking torque)

Table No 1: Material Properties

	Aluminium A356.2	Aluminium 7075-T6
Ultimate Tensile Strength (S_{ut})	250 MPa	570 MPa
Tensile Yield Strength (S_{yt})	230 MPa	503 MPa
Modulus of Elasticity or Young's Modulus (E)	72.4 GPa	71.7 GPa
Poisson's Ratio	0.33	0.33
Density (ρ)	2810 Kg/m ³	2700Kg/m ³

The wheels for passenger cars need satisfy two testing industrial standards. They are as follows

1. Bending Endurance Test
2. Radial Endurance Test

2.1 Bending Test

The bending moment to be imparted in test shall be in accordance to following formula

$$M = ((\mu * R) + d) * F * S(1)$$

According to the Japanese Industrial Standards (JID D 4103)

$$\mu = 0.7$$

$$d = 37 \text{ mm} = 0.037\text{m} \quad F = 4414.5 \text{ N}$$

$$\begin{aligned} \text{Bending Moment } M &= ((\mu * R) + d) * F * S \\ &= ((0.7 * 0.1904) + 0.037) * 4414.5 * 1.5 \\ M &= 1589 \text{ N-m} \end{aligned}$$

Table No 2. Loading Coefficient specified according to the Standards.

Division of wheel	Light alloy wheel	
	Coefficient S	Specified number of revolutions
Wheels under 100 mm in offset	1.8	10 ³
	1.5	10 ⁵
	1.35	25 x 10 ³
	1.33	10 ³
	1.26	10 ³
	1.1	10 ³

2.3 Radial Endurance Test

The radial load to be imparted in test shall be in accordance with following formula:

$$F_r = F * k$$

Angular Velocity

Angular Velocity is calculated by using the formula. From relation

$$V = r * \omega$$

Maximum Speed of the car is 80 km/hr = 22.22m/s

$$V = r * \omega$$

$$22.22 = 0.1904 * \omega$$

$$\omega = 116.70 \text{ rad/sec}$$

2.1 To find out Tensile Stress developed in rim

The Alloy wheel has Five Spokes,

$$2\alpha = \frac{2\pi}{5}$$

$$\alpha = 0.628 \text{ rad}$$

$$= 35.98^\circ$$

1. Mass of rim per mm of circumference (m)

Radius = 175 mm

Mass of rim per mm of circumference (m) = $Wt / \text{Circumference}$

$$(m) = \frac{2800 * 166 * 36}{1000 * 1000} = 0.016 \text{ Kg/m}$$

2. Evaluation of Tensile Stress

By using S Timoshenko's equations, We get

$$f_1(\alpha) = 0.7992$$

$$f_2(\alpha) = 0.00302$$

$$\sigma = 1.371 \text{ N/mm}^2$$

Table no.3 Alternating Stresses at Various Cycles for aluminium alloy A356.2

Cycles	Alternating Stresses (MPa)
10	468.01
20	419.16
50	362.32
100	324.50
200	290.63
2000	201.51
10000	156.00
20000	139.72
100000	108.16
200000	96.87
1000000	75

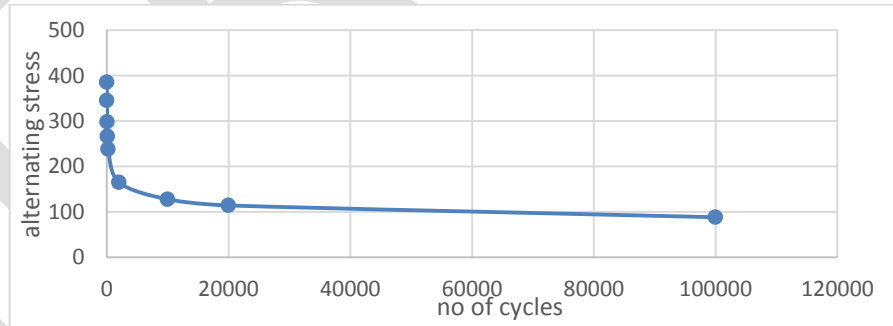


Figure 1 shows the graph of alternating stresses at various cycles for aluminium alloy A356.2.

It is obtained from Equation (5).

Table no.4 Alternating Stresses at Various Cycles for Aluminium 7075-T6

Cycles	Alternating Stresses (MPa)	Cycles	Alternating Stresses (MPa)
10	1067.08	10000	355.69
20	955.70	20000	318.56
50	826.00	100000	246.62
100	739.87	200000	220.88
200	662.64	1000000	171.00
2000	459.45		

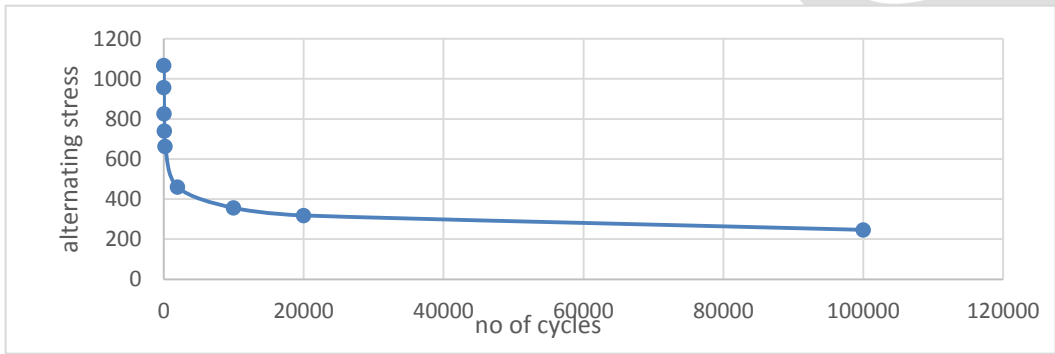


Figure 2 shows the graph of alternating stresses at various cycles Aluminium 7075-T6. It is obtained from equation (5)

3.1 MODELLING

Dimension of alloy wheel is take trough reverse engineering and by using the CMM technique. The CMM scanning was done by use Faro Scanning machine for complex part. The digital variner caliper is used measure the hole diameter and other dimension. Through CMM partially dimension recovered. The CMM scanning machine can generate rough geometry in unigraphics software and using this dimension model is built in Solidworks Software.



Figure 3 Cad model of alloy wheel

3.2 Meshing of alloy wheel

ANSYS is high performance finite element pre and processor for major finite element solvers. Which allows engineers to analyze design conditions in highly interactive and visual environment? ANSYS support the direct use of Cad geometry and existing finite element models, providing robust inter-operability and efficiency. Three-dimensional meshes created for finite element analysis consist of tetrahedral, pyramids, prisms or hexahedra. Advanced automation tools within ansys allow user to optimize meshes from a set of quality criteria change existing meshes through fine meshing. The total numbers of element formed are 62768 and total numbers of nodes formed are 112044. Table 5.2: Mesh information of Alloy wheel



Figure 4 Meshed model of alloy wheel

3.3 Applying of Boundary Conditions

Boundary Conditions:

1. Input Force: Radial force 9.93KN is applied on wheel
2. Pressure of 0.303MPa is applied to rim surface.
3. Rotational velocity of 116.7 rad/s is given.

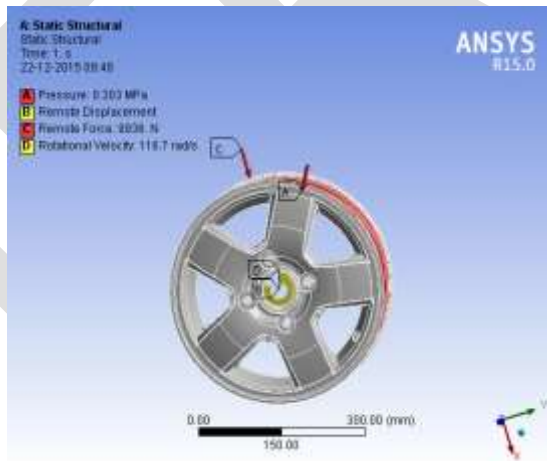
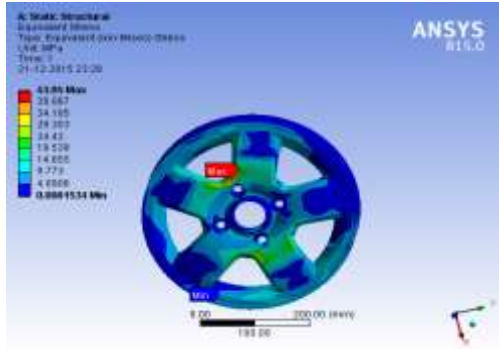


Figure 5 Constraining & Applying Boundary condition

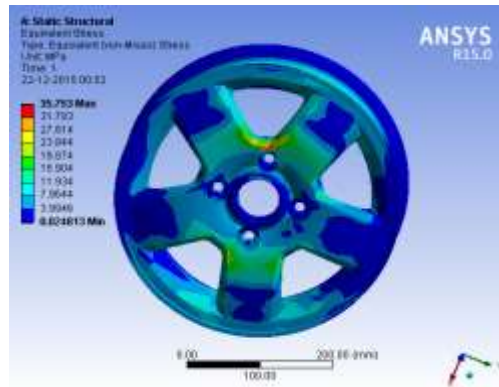
Table 5 Comparison of Simulation Results for A356.2 & 7075-T6 alloy Wheel

Aluminium A356.2 Alloy Wheel	Aluminium 7075-T6 Alloy Wheel
------------------------------	-------------------------------

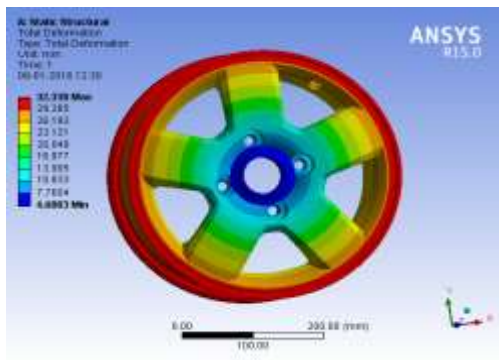
1. Equivalent stress



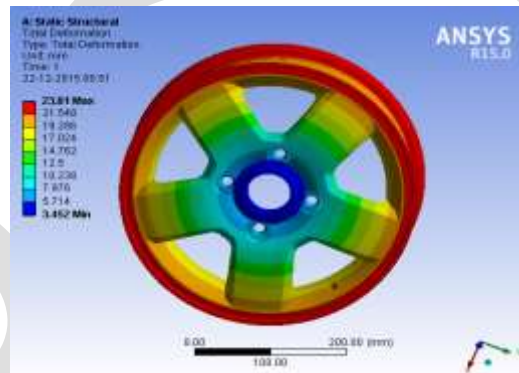
1. Equivalent stress



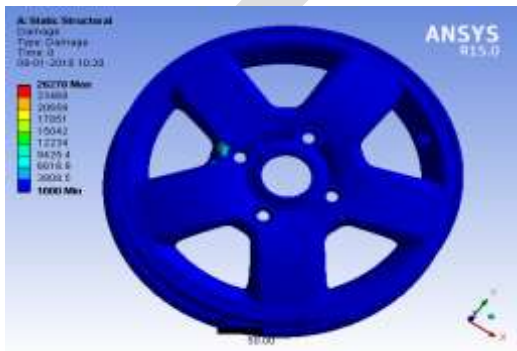
2. Deformation



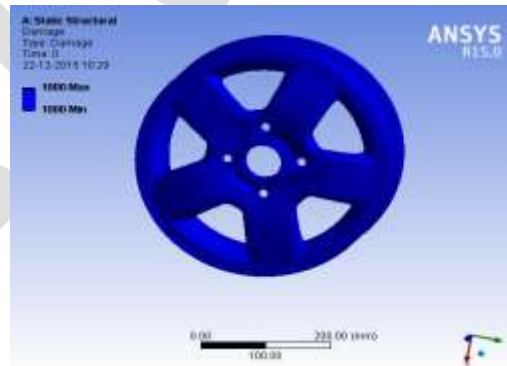
2. Deformation



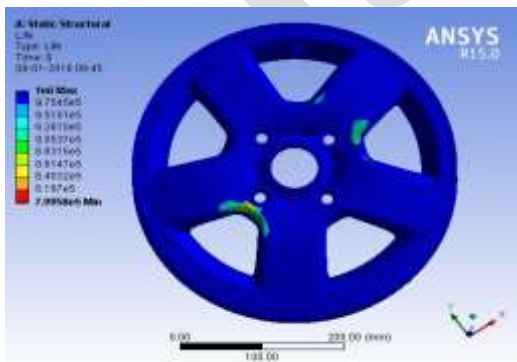
3. Damage Analysis



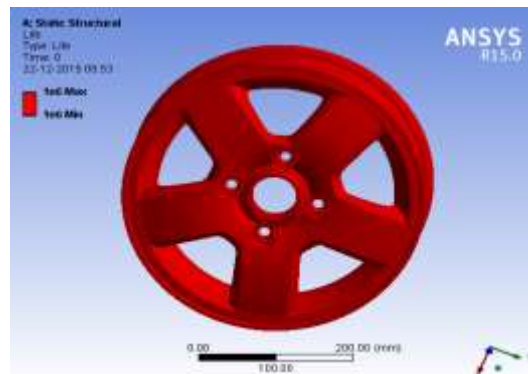
3. Damage Analysis



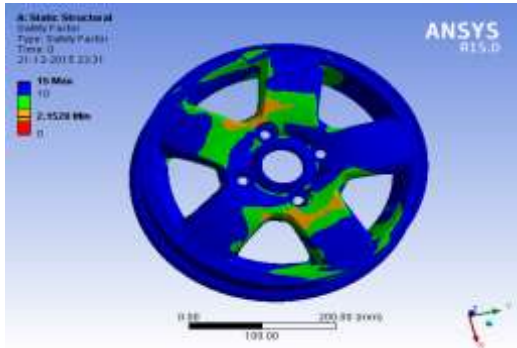
4. Fatigue Life Cycle



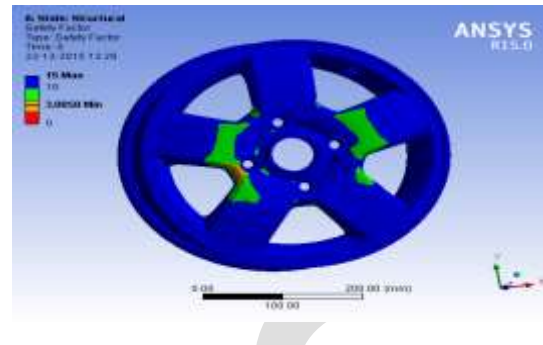
4. Fatigue Life Cycle



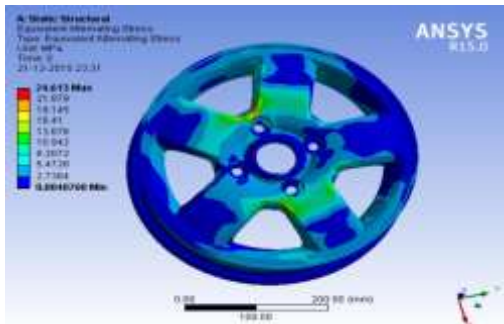
5. Factor of Safety



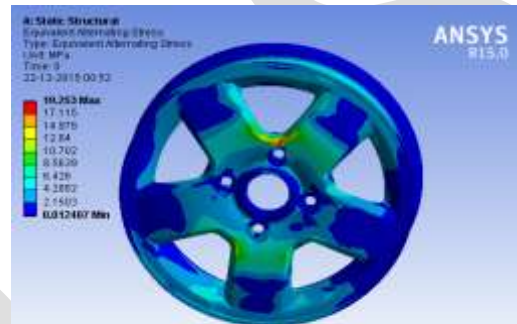
5. Factor of Safety



6. Alternating Stress



6. Alternating Stress



4. FATIGUE ANALYSIS OF ALLOY WHEEL BY EXPERIMENTAL METHOD

A typical test setup according to standard of the radial fatigue test is shown in the figure equipped with a driven Rotatable drum. The drum axis is parallel to the axis of the test wheel which presents smooth surface wider than the section width of the loaded test tyre section width. The test wheel and tyre provide loading normal to the surface of drum and in line radially with the centre of test wheel and the drum. The test wheel is fixed to the hub by nuts with a suitable torque specified by vehicle or wheel manufacturer. The total weight of a car is balanced with a vertical reaction force from the road through the tyre. This load constantly compresses the wheel radially while the car is running, the radial load becomes a cyclic load with the rotation of the wheel. Hence, the evaluation of wheel fatigue strength under radial load is an important performance characteristic for structural integrity.

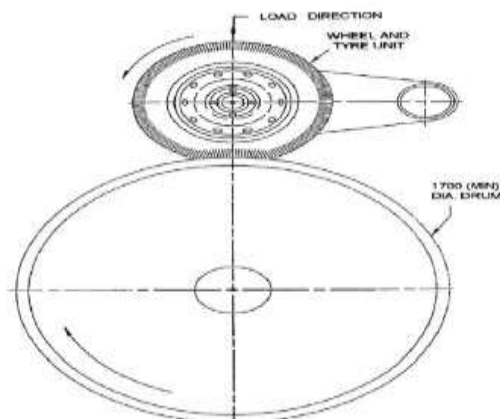


Fig 6 Layout of test setup radial fatigue test

Test Condition : The test condition shall be as follows:

Radial load The radial load shall be in accordance with the formula :

$$Fr = F \cdot K$$

Where, Fr : radial load (kN)

F the maximum value (generally in accordance with JIS D 4202) of maximum loads(10^5) of the tires applied to wheel.

Table No 6 Accelerated test factor for specified no of revolutions

Division of wheel	Light alloy wheel	
	Coefficient K	Specified number of revolutions 10^4
Wheels 17.5 or under in nominal rim diameter	2.25	50(10^4)
	2.2	10^3
	2.0	10^3
	1.8	10^3
	1.4	10^3

Test termination: -The test shall be terminated in either of the two following circumstances:

- a) Inability of wheel to sustain load
- b) Propagation of a cracks existing prior to test or new visible stress-caused cracks penetrating through a section of wheel

4.1 Radial fatigue Testing Machine.

The durability of the wheel is important for the safe operation of vehicle .Therefore, it is necessary to examine a wheel for both strength and fatigue life cycles. Fatigue test is carried for radial load. Figure 9 shows radial fatigue testing machine. The alloy wheel mounted on assembly, bolt are fixed. Then machine is started, initial radial load of 3.998KN is given. The Driver drum speed is setup for 80Kmph which makes alloy wheel to rotate. After minimum five lakh cycles the machine is stopped and checked for cracks and again its started.

According to JIS D4103 for Radial Fatigue Test

Radial Fatigue Test / No. of Cycles= 9932N/ 850000 cycles.

Wheel size = 14 inches

Flange shape = J

Rim width = 7 inches

Offset = 37mm

Weight= 9.8-10 kg



Figure 7 Radial Fatigue Testing Machine Setup

Table 7 .Experimental Fatigue test Results

Test RFT	
Test Load/ Weight(N)	9930.4
Nut torque (initial)	110 N-m
Test Cycles	8.5x 10 ⁵
D.P.T. result	Crack initiation from 8.15 lakh Cycles

5. RESULT AND DISCUSSION

Table 8 Results for Radial Fatigue Test

Parameters	Aluminum A356.2	Aluminum7075-T6
Von Mises Stresses	43.95 MPa	35.75MPa
Displacement	32.33mm	23.81mm
Factor of Safety	2.1528	3.085
Life of alloy wheel	7.995 x 10 ⁵	1x 10 ⁶

The Radial fatigue life cycle of alloy wheel was found out. A comparison is made for both Aluminium A356.2 and Aluminium 7075-T6 material used for alloy wheel. The existing components which are made of steel are slowly phased out by replacing with Aluminium alloys having comparable better properties. The maximum Equivalent stress (Von Mises stress) developed in Aluminium A356.2 alloy wheel is 43.95MPa and minimum stress was 0.008Mpa.For Aluminium 7075-T6Equivalent stress (Von Mises stress) developed are 35.75 MPa and minimum stress was 0.024MPa.The alloy wheel also needs to satisfy Automotive Industry Standard,According to AIS 073 (P1 &P2) maximum radial load given is 75kN and wheel size 12-24inch.The wheel passes minimum no of life cycle under radial load according to AIS 073 (P1 & P2) & IS9436.

Table No 9 Comparative Results A356.2 Alloy Wheel

Material A 356.2	Fatigue Life Cycle
Simulation results	Radial fatigue life 7.995 x 10 ⁵ cycles
Experimental results	Experimental found 8.15 x 10 ⁵ cycles

6 CONCLUSION

1. The Stress developed in alloy wheel for aluminium 7075-T6 less as compared to aluminium A356.2 alloy wheel. The maximum stress induced in the alloy wheel for aluminium A356.2 was 43.95 MPa and for aluminium 7075-T6 alloy wheel is 35.5 MPa.
2. The safety factor was higher in case of aluminium 7075-T6 as compared to Aluminium A356.2 alloy wheel.
3. The fatigue life alloy wheel of Aluminium A356.2 is 7.9985 x 10⁵cycles and that of Aluminium 7075-T6. alloy wheel is 1 x 10⁶ cycles.
4. Aluminium 7075- T6 grade are best suitable for alloy wheel

REFERENCES:

- [1] B. Satyanarayana (a), P. Ramamurty Raju (b), K. Suresh Babu (a), (a) Department of Mechanical Engineering, Sagi Rama Krishnam Raju Engineering College, Andhra Pradesh (b) Department of Mechanical Engineering, Andhra University,

- Vishakapatnam, Andhra Pradesh, India “*Evaluation of fatigue life of aluminium alloy wheels under radial loads*” Engineering Failure Analysis 14 (2007) 791–800.
- [2] Mehmet Firat (a), Recep Kozan (a), Murat Ozsoy (a), O. Hamdi Mete(a), (a) The University of Sakarya, Dept. of Mech. Engineering, Adapazari, Turkey “*Numerical modelling and simulation of wheel radial fatigue tests*” Engineering Failure Analysis 16 (2009) 1533–1541.
- [3] Xiaoge Zhang (a), Xiaofeng Wang (b), (a) Department of Automotive Engineering, Tsinghua University, Beijing ,china, (b) Dongfeng Automotive Wheel Co., Ltd., China, “*Simulation of dynamic cornering fatigue test of a steel passenger car wheel*” International Journal of Fatigue 32 (2010) 434–442.
- [4] Ch.Sambaiah (a),K. Ramji (a), (a) Department Of Mechanical Engineering, Nimra College of Engineering & Technology, Ibrahimpatnam, Vijayawada “*fatigue life of aluminium alloy wheels under radial loads*” International Journal of Mechanical and Industrial Engineering (IJMIE), ISSN No. 2231 –6477, Vol-2, Issue-1, 2012.
- [5] Chia-Lung Chang(a), Shao-Huei Yang(a), (a) Department of Mechanical Engineering, National Yunlin University of Science and Technology, Douliu, Yunlin 640, Taiwan, ROC “*Simulation of wheel impact test using finite element method*” Engineering Failure Analysis 16 (2009) 1711–1719.
- [6] U. Kocabicak,University of sakarya, faculty of Engineering, Esentepe kampusu, Adapazari, turkey, “*Numerical analysis of wheel cornering fatigue test Engineering*” Failure Analysis 8 (2009) 339–354.
- [7] Ricardo Coleville (a), Carloas Alberto Nunes (a), (a) Italy Speed AutomotiveLtd, “*Parametric Modelling of Steel Car Wheels for Finite Element Virtual Fatigue Tests,*” SAE Technical Paper 2001-01-4055.
- [8] P. V. Ravi Kumar (a), R. Satya Mehar (a), (a) Department of Mechanical Engineering, QIS College of Engineering college, Andhra Pradesh, “*Topology Optimization of Aluminium Alloy Wheel*”International Journal of Modern Engineering Research (IJMER) Vol. 3, Issue. 3, May.-June. 2013 pp-1548-1553, ISSN: 2249-6645.
- [9] Kublay Yay (a), I.Murat Ereke (a), (a) Department Mechanical of Engineering, Automotive Division, Technical university of Istanbul “*Fatigue strength of a rim model with FEM using a new Approximation technique*” SAE Technical Paper 2001-01-3339.
- [10] R.S. Khurmi and J.K. Gupta, Machine Design, 14th ed., Eurasia Publication House (Pvt.) Ltd., India, 2005, pp. 206, 220-224.
- [11] Thomas D. Gillespie, Fundamentals of Vehicle Dynamics, SAE, Warrendale, PA., 1992.
- [12] V.B. Bhandari, Design of machine elements, 3rd ed., Tata McGraw-Hill, India, 2010, pp. 749-760

LS- Sasakian Manifold with Semi-symmetric Non-metric F-connection

L K Pandey

D S Institute of Technology & Management, Ghaziabad, U.P. - 201007

dr.pandeylk@rediffmail.com

Abstract— Hayden [1] introduced the idea of metric connection with torsion tensor in a Riemannian manifold. In 1975, Golab [2] studied quarter-symmetric connection in a differentiable manifold. T.Imai [3] discussed on hypersurfaces of a Riemannian manifold with semi-symmetric metric connection. In 1980, R. S. Mishra and S. N. Pandey [4] discussed on quarter-symmetric metric F-connection and in 1970, K. Yano [9] studied on semi symmetric metric connections and their curvature tensors. In 1992, Nirmala S. Agashe and Mangala R. Chafle [5] studied semi-symmetric non-metric connection in a Riemannian manifold. Symmetric connections are also studied by K. Yano and T. Imai [10], A.Sharfuddin and S.I.Husain [8], R. N. Singh and S. K. Pandey [7] and many others. The purpose of this paper is to introduce a semi-symmetric non-metric F-connection in Lorentzian Special Sasakian manifold.

Keywords— Lorentzian Special Sasakian manifold, semi-symmetric non-metric F-connection, Nijenhuis tensor.

1. INTRODUCTION

An n-dimensional differentiable manifold M_n , on which there are defined a tensor field F of type $(1, 1)$, a vector field T , a 1-form A and a Lorentzian metric g , satisfying for arbitrary vector fields X, Y, Z, \dots

$$(1.1) \quad \bar{X} = -X - A(X)T,$$

$$(1.2) \quad A(T) = -1,$$

$$(1.3) \quad g(\bar{X}, \bar{Y}) = g(X, Y) + A(X)A(Y), \text{ where } A(X) = g(X, T), \quad \bar{X} \stackrel{\text{def}}{=} FX,$$

$$(1.4) \text{ (a) } (D_X F)(Y) + A(Y)\bar{X} - F(X, Y)T = 0 \Leftrightarrow$$

$$\text{(b) } (D_X F)(Y, Z) - A(Y)F(Z, X) - A(Z)F(X, Y) = 0, \text{ where } F(X, Y) \stackrel{\text{def}}{=} g(\bar{X}, Y)$$

$$(1.5) \quad D_X T = \bar{X},$$

Then M_n is called a Lorentzian special Sasakian manifold (an LS-Sasakian manifold).

In an LS-Sasakian manifold, it can be easily seen that

$$(1.6) \quad A(\bar{X}) = 0,$$

$$(1.7) \quad \text{rank } F = n - 1.$$

$$(1.8) \quad F(X, Y) = -F(Y, X),$$

$$(1.9) \text{ (a) } (D_X A)(\bar{Y}) = F(X, Y) \Leftrightarrow \text{(b) } (D_X A)(Y) = -g(\bar{X}, \bar{Y})$$

Nijenhuis tensor in an L-Contact manifold [6] is given by

$$(1.10) \quad N(X, Y, Z) = (D_{\bar{X}} F)(Y, Z) + (D_{\bar{Y}} F)(Z, X) + (D_X F)(Y, \bar{Z}) + (D_Y F)(\bar{Z}, X)$$

Where

$$N(X, Y, Z) \stackrel{\text{def}}{=} g(N(X, Y), Z)$$

2. SEMI-SYMMETRIC NON-METRIC F-CONNECTION IN AN LS-SASAKIAN MANIFOLD

An affine connection B is called non-metric connection, if

$$(2.1) \quad B_X g \neq 0$$

An affine connection B is called F-connection, if

$$(2.2) \quad B_X F = 0$$

Let us consider non-metric F-connection having torsion tensor S of the form

$$(2.3) \quad S(X, Y) = A(Y)X - A(X)Y,$$

Where S is the torsion tensor of the connection B .

Therefore,

Definition 2.1 A linear connection satisfying (2.1), (2.2) and (2.3) is called a semi-symmetric non-metric F-connection.

Theorem 2.1 In an LS-Sasakian manifold, the connection B defined by

$$(2.4) \quad B_X Y = D_X Y - A(Y)X + g(X, Y)T - 2A(X)Y$$

is a semi-symmetric non-metric connection, whose metric is given by

$$(2.5) \quad (B_X g)(Y, Z) = 4A(X)g(Y, Z)$$

Proof. Put

$$(2.6) \quad B_X Y = D_X Y + H(X, Y)$$

Where H is a tensor field of type (1, 2), given by

$$(2.7) \quad H(X, Y) = \alpha A(Y)X + \beta g(X, Y)T - 2A(X)Y,$$

Where α and β are constants to be determined.

From (2.6) and (2.7), we get

$$(2.8) \quad B_X Y = D_X Y + \alpha A(Y)X + \beta g(X, Y)T - 2A(X)Y$$

Then, torsion tensor of the connection B is given by

$$(2.9) \quad S(X, Y) = H(X, Y) - H(Y, X)$$

Therefore

$$(2.10) \quad \text{`}H(X, Y, Z) = \alpha A(Y)g(X, Z) + \beta A(Z)g(X, Y) - 2A(X)g(Y, Z) \text{ and}$$

$$(2.11) \quad \text{`}S(X, Y, Z) = \text{`}H(X, Y, Z) - \text{`}H(Y, X, Z)$$

Where

$$(2.12) \quad \text{`}H(X, Y, Z) \stackrel{\text{def}}{=} g(H(X, Y), Z)$$

$$(2.13) \quad \text{`}S(X, Y, Z) \stackrel{\text{def}}{=} g(S(X, Y), Z)$$

From (2.2) and (2.8), we get

$$(2.14) \quad (D_X F)(Y) - \alpha A(Y)\bar{X} - \beta F(X, Y)T = 0$$

In an LS-Sasakian manifold, we have

$$(2.15) \quad (D_X F)(Y) + A(Y) \bar{X} - F(X, Y)T = 0$$

From (2.14) and (2.15), we get, $\alpha = -1, \beta = 1$

Putting these values in (2.8), we obtain (2.4).

Also

$$(2.16) \quad X(g(Y, Z)) = (B_X g)(Y, Z) + g(B_X Y, Z) + g(Y, B_X Z) = g(D_X Y, Z) + g(Y, D_X Z)$$

Using (2.4) in (2.16), we get (2.5).

Theorem 2.2 In an LS-Sasakian manifold with semi-symmetric non-metric F-connection B , we have

$$(2.17) \quad (a) \quad B_X T = 2X + 2\bar{X}$$

$$(b) \quad (B_X A)(Y) = (D_X A)(Y) + g(X, Y) + 3A(X)A(Y)$$

$$(c) \quad (B_X F)(Y, Z) = (D_X F)(Y, Z) + 4A(X)F(Y, Z) - A(Y)F(Z, X) - A(Z)F(X, Y)$$

$$(d) \quad (B_X F)(\bar{Y}, \bar{Z}) - (B_X F)(\bar{Y}, \bar{Z}) = 8A(X)g(\bar{Y}, \bar{Z})$$

$$(e) \quad (B_X F)(\bar{Y}, \bar{Z}) + (B_X F)(\bar{Y}, \bar{Z}) = 8A(X)F(Y, Z)$$

Theorem 2.3 Nijenhuis tensor with semi-symmetric non-metric F-connection B is given by

$$(2.18) \quad N(X, Y, Z) = (B_{\bar{X}} F)(Y, Z) + (B_{\bar{Y}} F)(Z, X) + (B_X F)(Y, \bar{Z}) + (B_Y F)(\bar{Z}, X) - 4A(X)g(Y, Z) + 4A(Y)g(Z, X)$$

Proof. (2.18) follows from (1.10) and (2.17) (c).

Theorem 2.4 The connection induced on a submanifold of an LS- Sasakian manifold with a Semi-symmetric non-metric F-connection with respect to unit normal vectors M and N is also Semi- symmetric non-metric F-connection iff

$$(2.19) \quad (a) \quad h(\hat{X}, \hat{Y}) = p(\hat{X}, \hat{Y}) + \rho \tilde{g}(\hat{X}, \hat{Y})$$

$$(b) \quad k(\hat{X}, \hat{Y}) = q(\hat{X}, \hat{Y}) + \sigma \tilde{g}(\hat{X}, \hat{Y})$$

Proof. Let M_{2m-1} be submanifold of M_{2m+1} and let $c : M_{2m-1} \rightarrow M_{2m+1}$ be the inclusion map such that

$$d \in M_{2m-1} \rightarrow cd \in M_{2m+1},$$

Where c induces a Jacobian map (linear transformation) $J : T'_{2m-1} \rightarrow T'_{2m+1}$.

T'_{2m-1} is tangent space to M_{2m-1} at point d and T'_{2m+1} is tangent space to M_{2m+1} at point cd such that

$$\hat{X} \text{ in } M_{2m-1} \text{ at } d \rightarrow J\hat{X} \text{ in } M_{2m+1} \text{ at } cd$$

Let \tilde{g} be the induced metric tensor in M_{2m-1} , then

$$(2.20) \quad \tilde{g}(\hat{X}, \hat{Y}) = ((g(J\hat{X}, J\hat{Y}))b$$

Semi- symmetric non-metric F-connection B in an LS- Sasakian manifold M_n is given by

$$(2.21) \quad B_X Y = D_X Y - A(Y)X + g(X, Y)T - 2A(X)Y$$

Where X and Y are arbitrary vector fields of M_{2m+1} . Let

$$(2.22) \quad T = Jt - \rho M - \sigma N,$$

Where t is C^∞ vector fields in M_{2m-1} . M, N are unit normal vectors to M_{2m-1} .

Denoting by \tilde{D} the connection induced on the submanifold from D .

Put

$$(2.23) \quad D_{JX} J\hat{Y} = J(\tilde{D}_X \hat{Y}) - p(\hat{X}, \hat{Y})M - q(\hat{X}, \hat{Y})N$$

Where p and q are symmetric bilinear functions in M_{2m-1} . Also

$$(2.24) \quad B_{JX} J\hat{Y} = J(\tilde{B}_X \hat{Y}) - h(\hat{X}, \hat{Y})M - k(\hat{X}, \hat{Y})N,$$

Where \tilde{B} is the connection induced on the submanifold from B and h, k are symmetric bilinear functions in M_{2m-1} .

Inconsequence of (2.21), we have

$$(2.25) \quad B_{JX} J\hat{Y} = D_{JX} J\hat{Y} - A(J\hat{Y})J\hat{X} + g(J\hat{X}, J\hat{Y})T - 2A(J\hat{X})J\hat{Y}$$

Using (2.23), (2.24) and (2.25), we have

$$(2.26) \quad J(\tilde{B}_X \hat{Y}) - h(\hat{X}, \hat{Y})M - k(\hat{X}, \hat{Y})N = J(\tilde{D}_X \hat{Y}) - p(\hat{X}, \hat{Y})M - q(\hat{X}, \hat{Y})N - A(J\hat{Y})J\hat{X} + g(J\hat{X}, J\hat{Y})T - 2A(J\hat{X})J\hat{Y}$$

Using (2.22), we get

$$(2.27) \quad J(\tilde{B}_X \hat{Y}) - h(\hat{X}, \hat{Y})M - k(\hat{X}, \hat{Y})N = J(\tilde{D}_X \hat{Y}) - p(\hat{X}, \hat{Y})M - q(\hat{X}, \hat{Y})N - a(\hat{Y})J\hat{X} + (Jt - \rho M - \sigma N)\tilde{g}(\hat{X}, \hat{Y}) - 2a(\hat{X})J\hat{Y}$$

Where $\tilde{g}(\hat{Y}, t) \stackrel{\text{def}}{=} a(\hat{Y})$

Using (2.19) (a) and (2.19) (b), we get

$$(2.28) \quad \tilde{B}_X \hat{Y} = \tilde{D}_X \hat{Y} - a(\hat{Y})\hat{X} + \tilde{g}(\hat{X}, \hat{Y})t - 2a(\hat{X})\hat{Y}$$

This proves the theorem.

REFERENCES:

- [1] Hayden, H. A., "Subspaces of a space with torsion", Proc. London Math. Soc., 34, pp. 27-50, 1932.
- [2] Golab, S., "On semi-symmetric and quarter-symmetric linear connections", Tensor, N.S., 29, pp. 249-254, 1975.
- [3] Imai, T., "Hypersurfaces of a Riemannian manifold with semi-symmetric metric connection", Tensor N. S., 23, pp. 300-306, 1972.
- [4] Mishra, R. S. and Pandey, S. N., "On quarter-symmetric metric F-connection", Tensor, N.S., 34, pp. 1-7, 1980.
- [5] Nirmala S. Agashe and Mangala R. Chafle, "A Semi-symmetric non-metric connection on a Riemannian manifold", Indian J. pure appl. Math., 23(6), pp. 399-409, 1992.
- [6] Pandey, L.K., "Nijenhuis tensor in an L-contact manifold", International journal of Management, IT and engineering, vol.5, issue 12, 108-113, 2015.
- [7] Singh, R. N. and Pandey S. K., "On a quarter-symmetric metric connection in an LP-Sasakian Manifold", Thai J. of Mathematics, 12, pp. 357-371, 2014.
- [8] Sharfuddin, A. and Husain, S.I., "On a semi-symmetric connexion in almost contact manifolds", Progr. Math. (Allahabad), 12, No. 1-2, 101-113, 1978.
- [9] Yano, K., "On semi-symmetric metric connection", Rev. Roum. Math. pures et appl." tome XV, No 9,

Bucarest, pp. 1579-1584, 1970.

[10] Yano, K. and Imai, T., "Quarter-symmetric metric connections and their curvature tensors", Tensor, N. S., 38, pp. 13-18, 1982.

IJERGS

Artificial Bee Colony Based Content Adaptive Color Filter Array for Demosaicing

Ramandeep Kaur¹,

Ravneet Kaur Sidhu²

Department of Computer Science and Engineering

Department of Computer Science & Engineering

CT Institute of Technology and Research (CTITR),

CT Institute of Technology and Research (CTITR),

Maqsudan, Jalandhar, India

Maqsudan, Jalandhar, India

Email - ramandeep_wahla@yahoo.com

Jitenderpal Saini³

Department of Electronics and Communication Engineering

CT Institute of Management and Tehnology (CTIMT),

Jalandhar, India

Abstract—In the recent years, Digital cameras have become more dominant in the image capturing process. For low price digital cameras, concept of Bayer layer is more famous by the name, color filter array (CFA). An approach to produce full color image from the incomplete color sample output of a graphic sensor overlaid with a color filter array is called demosaicing. It can be called color reconstruction or CFA interpolation. Image demosaicing becomes major section of research in vision processing applications. A number of strategies have been developed like bilinear interpolation, constant hue based interpolation, edge adaptive interpolation etc. to produce full color image in demosaicing and the latest one is content adaptive CFA. The content adaptive strategy is simple as compared to the other interpolation strategies, but still there exist some limitations of this technique like static window size, large memory requirements. In this paper, we have proposed an algorithm: Artificial bee colony based content adaptive CFA for demosaicing which further will improve the working of content adaptive CFA. The proposed method has been developed to optimize the window size for each image and to overcome the limitations of the content adaptive strategy. This algorithm provides the best results on the behalf of MSE, PSNR, AD and RMSE parameters as compared to the other strategies.

Keywords—Demosaicing; interpolation; Color filter array; content classification; artificial bee colony; Average Difference.

1. INTRODUCTION

Digital image sensors have become the vital part of digital cameras. They are the light touching 'film' that records the image and enables to give a picture. A digital sensor is, in simple terms, composed of three different layers: **Sensor substrate, A Bayer Filter, microlens**. A Bayer filter has alternating red(R) and green (G) filters for odd rows and for even rows, alternating green (G) and blue (B) filters. The presence of green filters is in double amount as compared to red or blue ones, catering to the human eye's higher sensitivity to green light. Since every pixel of the sensor is behind a color (shade) filter, the result is a section of pixel values, each revealing a raw intensity of one of many three filter colors. Thus, an algorithm must estimate for every pixel along with levels of a number of color components, not a single part. A Bayer filtration mosaic is a color filter array for arranging RGB color filters on a square grid of photo-sensors. Particular layout of color filters has been used in most single-chip digital image sensors used in digital camera models, scanners and camcorders make a color image. The filter pattern is 50% green, 25% blue and 25% red, hence called RGBG, GRGB or RGG. The raw output of Bayer- filter cameras is known as a Bayer pattern image. Since each filtered pixel record only one of three shades, the info from each pixel cannot fully find color on its own. To get a full-color image, many demosaicing algorithms have been properly used to interpolate a couple of complete red, green, and blue values for each level. Fig. 1 represents the GRBG bayer pattern of color filter array.

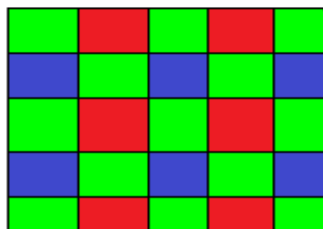


Fig. 1 Bayer Pattern array

Many research works have been proposed in the previous years for demosaicing. Different methods like bilinear interpolation, constant hue based interpolation, gradient based interpolation has been implemented and their comparison based on mean square error has been drawn by R. Ramanath in 2002 [10]. In 2003 R. Ramanath et al. have proposed a flexible demosaicing way in the concept of bilateral filtering. The bilateral selection gives an effective way to adaptively weight a pixel based on its location in the image. This process supplies a mean to denoise, sharpen and demosaicing the image simultaneously [11]. M. Zhao et al. have planned a technique for lowering the blocking artifacts in the decoded picture by applying adaptive filtration [12]. L. Shao et al. have planned an integrated resolution up-conversion and retention artifacts elimination algorithm. Regional picture design is classified into object details or code artifacts using the combination of structure information (ADRC) and the activity measure [13]. L. Shao et al. have introduced the classification-based least section trained filters on image quality improvement algorithms. For every algorithm, the working out method is exclusive and separately selected classification methods are proposed [15]. A. Jose et al. have presented the typical concepts of adaptive filtering and its individuals of formulas such as least-mean Square, data-reusing, and recursive least- sections (RLS) [16]. B. Leung et al. represented a luma–chroma demultiplexing algorithm utilizing a least-squares style strategy for the required bandpass filters [17]. L. Shao et al. have proposed a least squares solution that is self adaptive to the visible quality of the input sequence [19]. L. Shao et al. have planned a solution centered on classification and last section qualified filters to repair/patch low-quality video processing modules at the back end of a video chain [18]. L. Shao et al. have proposed a material adaptive demosaicing strategy utilising structure analysis and correlation between the red, green and blue planes [1].

All the above discussed techniques heavily rely on an edge detection mechanism except content adaptive CFA strategy. The content adaptive CFA technique is simple and there is no need of edge detection. The content adaptive strategy finds out least square window size and produces the results by using the filtering mechanism on all the images. There are two phases: offline and online. Offline training mechanism helps to identify the best window size and online phase is runtime phase. This strategy takes too much memory to maintain a lookup table. Look up table maintain the record of the location of the pixels in an image. In this paper, an algorithm named artificial bee colony based content adaptive color filter array has been proposed. The proposed algorithm will further improve the working of content adaptive CFA by optimizing the window size for each image using ABC optimization and produces high quality of the images compared to the content adaptive strategy.

2. METHODOLOGY

In the proposed method, Window size is being optimized by using the artificial bee colony (ABC) algorithm for every image further to improve the working of content adaptive CFA. Content adaptive demosaicing approach finds out the best window size, which is static for all images, by using two stages: training stage and testing stage. During the training phase, all training image patches are being classified by using adaptive range dynamic coding technique to define the texture of the images, and filter coefficient for each class is individually optimized with least square method and stored in a lookup table. Fig. 2 represents the working of the offline training stage:

A. Offline training stage:

Steps of the offline training stage are:

- 1.) Degrades each input image into the Bayer pattern. Mosaic image in the form of Bayer pattern is available as well as the original plan.
- 2.) Classification method ADRC is to be used to find the class index for every pixel place.
- 3.) Least square optimization is conducted to find out the coefficient of the different filters and optimized filter coefficient will be stored in a lookup table for use during demosaicing.

Least square optimization will find out the error between the original image and the filtered image by using the following equation

$$e^2 = \sum_{j=1}^{N_c} (F_{R,c}(J) - F_{F,c}(j))^2 \quad (1)$$

Where $F_{R,c}(J)$ the reference is image and $F_{F,c}(j)$ is the filtered image.

At the testing stage, the image will be demosaicised, same classification will be performed on the image and according to the class code filter coefficient will be retrieved from the lookup table. Fig. 3 describes the working of testing stage.

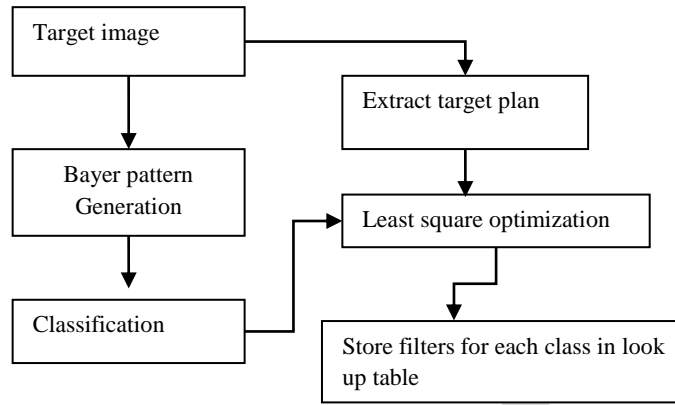


Fig. 2 Offline training procedure [1]

Furthermore strategy has been improved on the proposed method by applying the artificial bee colony optimization.

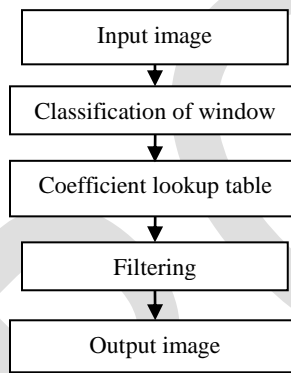


Fig. 3 Online procedure

The artificial bee colony algorithm will optimize the window size to produce better quality of an image. Here the window size is not static nature, its size will be dynamic, i.e. automatic and ABC will find out the optimum window size for every image. Here objective function is:

$$f(x) = \frac{1}{MSE} \quad (2)$$

The aim here is to maximize the objective function $f(x)$ to choose the best window by artificial bee colony. The proposed method will do the work under following methodology:

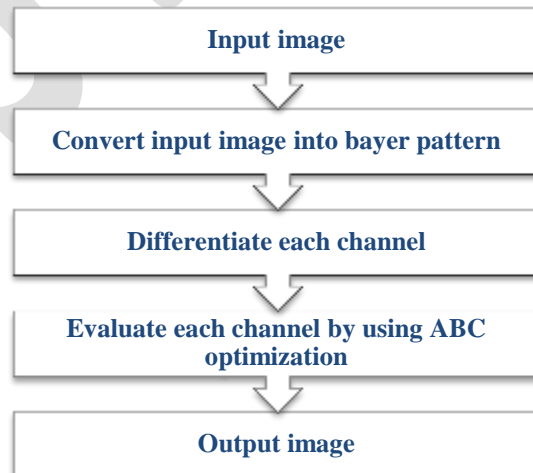


Fig. 4 Methodology

B. Artificial bee colony optimization

Optimization is the act of achieving the perfect result underneath the given circumstances to offer the utmost or the minimum value of an objective function. Two classes of optimization algorithms are: Evolutionary algorithms and Swarm intelligence based algorithms. Most prominent optimization algorithms are: ant colony optimization, particle swarm based optimization and artificial bee colony (ABC) optimization. In the proposed method, artificial bee colony optimization has been utilized because the major advantages which ABC holds over other optimization algorithms include its:

- Simplicity, flexibility and robustness.
- Use of less control parameters.
- Power to handle the objective cost with stochastic nature.
- Simple implementation with standard mathematical and logical operations.

The ABC meta-heuristic has been planned rather recently by Lucic and Teodorovic. It is a bottom-up method which acts partially alike, and partially differently from bee colonies in nature. Artificial bees will be the agents, which covers complicated combinatorial optimization problem. Here every artificial bee computes one means to the problem. There are two phases of the algorithm forward pass and backward pass. Initially in each ahead pass, every artificial bee is examining the search space. From a predefined number of moves it constructs or improves the Solution and also forms a new solution. After obtaining the new partial solution, the bees again go to the nest and move the next phase that is backward pass. In this all artificial bees share information about their solutions. In nature, bees perform a dancing ceremony, and signaled other bees about the quantity of food they have collected and the distance of the area

1.) Intialize population

For every bee do the forward pass

a) Set $k=1$

b) Evaluate all possible construct moves

c) Acc. To evaluation choose one move using route wheel

d) $K=k+1$;

If

{

$P \leq NC$

Goto step b

}

2) All bees are back to hive

3.) Sort bees by using objective function

$$\frac{1}{MSE}$$

4.) Every bee decides randomly whether to continue its own exploration and become a recruiter or to become a follower. (High function high change)

5.) For every follower choose a new solution for recruiter by wheel.

6.) If the stopping condition not met go to step 2.

7.) Choose the best solution.

In the proposed method, the working of three phases of the ABC algorithm with the combination of content adaptive CFA is as follows: The very first phase will be **employed bee phase**: population will be intialized ($p=1$) by randomly selected some pixel as the food sources. Employed bees exploit the food sources and generate the different solutions on the randomly selected food sources by making the iterations ($k=1$ to n), where n is the maximum number of cycles. The position of food source would be replaced with new one by $k+1$ to generate new solutions. If the previous existing solution has dominated value than the value of new one, then it will remain same otherwise it will be replaced by the new solution. In order to optimize the best solution image will pass through the second phase i.e. **onlooker bee phase**. Second phase check the probability of all the solutions by using the following equation:

$$p_i = \frac{fit_i}{\sum_{n=1}^{SN} fit_n} \quad (3)$$

Where fit_i is the fitness of the solution i which is proportioned to the nectar amount, i.e. in the proposed method, nectar amount will be the interpolated values of the pixels of the position i and SN is the food source that is to say number of pixels which is equal to the number of employed bees or onlooker bees. The third phase is onlooker phase: onlooker phase will find out the new pixels to find out the new solutions on the pixels of the selected image.

In this way these three phases help to optimize the best window size for each image of the selected dataset.

3. EXPERIMENTAL RESULTS

Kodak dataset image has been used for experimental results. Collected Kodak dataset images are shown in Fig. 5. We have totally collected 15 images from the Kodak dataset for experimental use.

Content adaptive strategy further will be improved by using an artificial bee colony algorithm. The artificial bee colony algorithm will find out the best solutions on the pixels of the image and help to optimize the best window size for each Kodak dataset image.

Fig. 6 shows the result images has been used by content adaptive CFA and Adaptive ABC strategies. Firstly, by performing processing operations on the image, the image has been converted into the GRBG pattern of the bayer filter. After that this image will be recovered by using content based CFA and Adaptive ABC optimization techniques.

The results of these images have been evaluated on the basis of PSNR, MSE, RMSE and AD.



Fig. 5 Kodak dataset images used for the experimental results

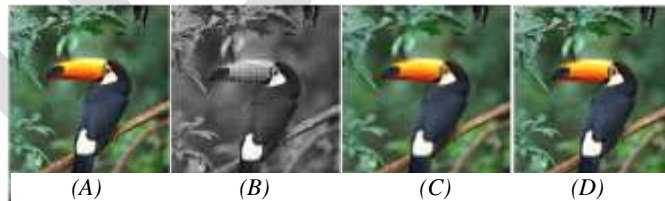


Fig. 6 (A) Input image (B) Bayer image (C) Content based CFA image (D) Adaptive ABC image

Adaptive ABC optimization result image will be of high quality as compared to the content based CFA based on these limit.

TABLE 1	Performance evaluations of MSE, RMSE, PSNR and AD of different channel R, G, B by using content adaptive CFA and adaptive ABC technique:				
	Method	Colours	MSE	RMSE	PSNR
Content based CFA	R	5	2.23	41.14	17.521
	G	5	2.23	41.14	16.196
	B	6	2.44	40.34	18.029
ABC	R	2	1.41	45.12	7.3862
	G	2	1.73	43.35	10.666
	B	3	1.41	45.12	8.4075

TABLE 1 Performance evaluations of MSE, RMSE, PSNR, and AD of R, G, B.

Table 1 represents the MSE, RMSE, PSNR, AD analysis based on different channels R, G, B by applying content based CFA and Adaptive ABC techniques on the image shown in Figure 4. The MSE values of different colors (R, G, B) by using content based CFA are R=5, G=5, B=6 and by using ABC are R=2, G=2, B=3. RMSE values of content based CFA are (R=2.23, G=2.23, B=2.44) and ABC based CFA is (R=1.41, G=1.73, B=1.41). PSNR values of content based CFA are (R=41.14, G=41.14, B=40.34) and ABC based CFA are (R=45.12, G=43.35, B=15.12). AD values of content based CFA are (R=17.521, G=16.196, B=18.029) and ABC based CFA are (R=7.3862, G=10.666, B=8.4075).

TABLE 2	Performance evaluations of MSE, RMSE, PSNR and AD by using content adaptive CFA and adaptive ABC techniques:			
	Method	MSE	RMSE	PSNR
Content based CFA	81	9	29.04	81.57
ABC	42	6.480	31.89	42.72

TABLE 2 Performance evaluations of MSE, RMSE, PSNR, and AD using content adaptive CFA and adaptive ABC techniques.

Table 2 shows that the results of ABC based CFA technique are better than the results of content based CFA.

In the similar way, an experiment has been performed on the dataset images based on the following parameters:

- **PSNR (Peak Signal to Noise Ratio)**

The term peak signal-to-noise ratio (PSNR) is an expression for the ratio between the largest possible value (power) of a signal and the power of distorting noise that affects the quality of its representation. PSNR is evaluated by

$$PSNR = 10 * \log(255 * 255 / MSE) / \log(10) \quad (4)$$

Where, 255 is the greatest power of the signal.

- **MSE (Mean Square Error)**

In this research $M \times N$ represents the size of the each image. Where M represents the number of rows and N represents the number of columns. The original image is represented by the function $f(i, j)$ at the location i, j and the filtered image, i.e. full color image is represented at location i, j by $\hat{f}(i, j)$. the mean square error between original image and demosaicised image is evaluated by using the following equation:

$$MSE = \frac{1}{MN} \sum_{i=1}^M \sum_{j=1}^N (f(i, j) - \hat{f}(i, j))^2 \quad (5)$$

- **RMSE (Root Mean Square Error)**

The RMSE represents the differences between predicted values and observed values of an input image. RMSE is a good measure of accuracy. The RMSE is the root of the mean square error and it is evaluated by using the following equation:

$$RMSE = \sqrt{MSE} \quad (6)$$

- **AD (Average Difference)**

The average difference represents the mean error between the original image and the filtered image. AD is evaluated by using the following equation:

$$AD = \frac{\sum_{i=1}^M \sum_{j=1}^N (f(i, j) - \hat{f}(i, j))}{MN} \quad (7)$$

On the behalf of these limits we have performed the experiment on the selected dataset. Experiment has been conducted in the proposed method on all the selected dataset images are shown in the Fig. 7.





Fig. 7 (A) Input image (B) Bayer image (C) Content based CFA image (D) Adaptive ABC image

In the figure 7, column A represents the input images, column B shows the bayer images, column C and D represents the recovered images by using content adaptive and ABC based CFA techniques.

TABLE 3 Performance evaluations of MSE using content adaptive CFA and adaptive ABC techniques.

TABLE 3	Performance evaluations of MSE by using content adaptive CFA and adaptive ABC technique	
	Content based CFA	ABC Optimization based content based CFA
	MSE	MSE
1	26	9
2	32	14
3	62	18
4	357	142
5	161	49
6	21	9
7	130	39
8	395	141
9	66	23
10	81	42
11	148	45
12	248	78
13	241	10
14	109	36
15	127	42
Average	146.9	46.46

TABLE 4 Performance evaluations of PSNR using content adaptive CFA and adaptive ABC techniques

TABLE 5	Performance evaluation of RMSE by using content adaptive CFA and ABC optimization based content adaptive CFA
----------------	---

TABLE 4	Performance evaluation of PSNR by using content adaptive CFA and ABC optimization based content adaptive CFA	
Image No.	Content based CFA	ABC Optimization based content based CFA
	PSNR	PSNR
1	33.98	38.58
2	33.07	36.66
3	30.20	35.57
4	22.60	26.60
5	26.06	31.22
6	34.90	38.58
7	26.99	32.22
8	22.16	26.63
9	29.63	34.51
10	29.04	31.89
11	26.42	31.59
12	24.18	29.20
13	34.32	38.13
14	27.75	32.56
15	27.09	31.89
Average	28.55	33.05

TABLE 5 Performance evaluations of RMSE using content adaptive CFA and adaptive ABC techniques

Image No.	Content based CFA	ABC Optimization based content based CFA
	RMSE	RMSE
1	5.099	3.000
2	5.656	3.741
3	7.874	4.242
4	18.89	11.91
5	12.68	7.000
6	4.580	3.000
7	11.40	6.245
8	19.87	11.87
9	8.120	4.790
10	9.000	6.480
11	12.16	6.708
12	15.74	8.831
13	4.899	3.162
14	10.44	6.000
15	11.26	6.480
Average	10.51	6.230

In table 3, the performance of both the techniques has been evaluated on the basis of Mean Square Error. The average of content based CFA technique based on MSE analysis is **146.9** and the average of ABC optimization based content based CFA is **46.46**. In table 4, the results of all the test images have been evaluated on the basis of PSNR. The average of peak signal to noise ratio of all the images by using ABC optimization based Content based CFA is **33.05** and the average of content based CFA **28.55**. In table 5, the performance of the images has been evaluated on the basis of RMSE. Root Mean Square Error is also a way to evaluate the error between the original image and output image. From the results of both the techniques, it's clear that the result of ABC optimization based technique is better. The average of ABC optimization based content based CFA is **6.230** and the average of content based CFA is **10.51**.

TABLE 6 Performance evaluations of AD using content adaptive CFA and adaptive ABC techniques

TABLE 6		
Performance evaluation of AD by using content adaptive CFA and ABC optimization based content adaptive CFA		
Image No.	Content based CFA	ABC Optimization based content based CFA
	AD	AD
1	26.30	9.811
2	32.70	14.19
3	62.10	18.83
4	357.6	142.1
5	161.5	49.55
6	21.21	9.772
7	130.4	39.85
8	395.8	141.1
9	66.59	23.30
10	81.57	42.72
11	148.6	45.24
12	248.9	78.86
13	24.20	10.79
14	109.8	36.19
15	127.0	42.31
Average	132.9	46.97

In the table 6, the results of the images have been evaluated based on the average difference. Here the average of all the dataset images based on AD by using ABC Optimization is **46.97** and the average of content based CFA is **132.9**. So it's clear that the results of ABC optimization technique are better than the content based CFA.

TABLE 7		Performance evaluation of MSE, RMSE, PSNR and AD of different R, G, B Channel by using content adaptive cfa and adaptive ABC technique of all the dataset images:							
Optimized adaptive ABC						Content based CFA			
Image No.	Colour	MSE	RMSE	PSNR	AD	MSE	RMSE	PSNR	AD
1	R	5	2.23	41.14	16.00	10	3.16	38.13	32.98
	G	6	2.44	40.34	18.71	10	3.16	38.13	30.42
	B	4	2.00	42.11	12.63	09	3.00	38.58	29.58
2	R	7	2.64	39.67	23.35	13	3.60	36.99	41.81
	G	9	3.00	38.58	27.55	13	3.60	36.99	39.64
	B	5	2.23	41.14	17.02	21	3.46	37.33	36.28
3	R	07	2.64	39.67	23.01	22	4.69	34.70	67.14
	G	13	3.60	36.99	39.34	24	4.89	34.32	72.51
	B	09	3.00	38.58	29.53	25	5.00	34.15	76.46
4	R	58	7.61	30.49	174.0	137	11.7	26.76	411.4
	G	86	9.27	28.78	260.0	131	11.7	26.95	393.5
	B	55	7.41	30.71	165.7	135	11.6	26.82	406.3
5	R	6	2.44	40.34	18.83	7	2.64	39.67	21.02
	G	7	2.64	39.67	22.89	11	3.31	37.71	33.69
	B	8	2.82	39.09	24.19	11	3.31	37.71	33.69
6	R	21	4.58	34.90	64.42	51	7.14	31.05	154.9
	G	24	4.89	34.32	74.82	46	6.78	31.50	139.5
	B	21	4.58	34.90	64.19	50	7.07	31.14	150.5
7	R	55	7.41	30.72	166.91	149	12.2	26.39	447.1
	G	93	9.64	28.44	279.53	144	12.0	26.54	443.4
	B	54	7.34	30.80	162.16	145	12.0	26.51	437.5
8	R	24	4.89	34.32	73.53	30	5.47	33.35	91.35
	G	24	4.89	34.32	74.66	33	5.74	33.94	100.8
	B	24	4.89	34.32	74.00	27	5.19	33.81	83.74
9	R	2	1.41	45.12	7.386	5	2.23	41.14	17.52
	G	3	1.73	43.35	10.66	5	2.23	41.14	16.19
	B	2	1.41	45.12	8.407	6	2.44	40.34	18.02
10	R	22	4.69	34.70	68.40	35	5.91	32.69	105.6
	G	27	5.19	33.81	82.55	35	5.91	32.69	105.6
	B	23	4.79	34.51	70.64	31	5.56	33.21	95.34
11	R	19	4.35	35.34	57.96	52	7.21	30.97	157.5
	G	32	5.65	33.07	97.48	56	7.48	30.64	170.9
	B	18	4.24	35.57	55.99	51	7.14	31.05	155.1
12	R	34	5.83	32.81	104.11	90	9.48	28.58	272.4
	G	54	7.34	30.80	164.93	94	9.69	28.39	284.3
	B	35	5.91	32.69	106.00	92	9.59	28.49	276.4
13	R	4	2.00	42.11	14.08	8	2.82	39.09	26.16
	G	7	2.64	39.67	21.26	10	3.16	36.13	30.65
	B	4	2	42.11	13.68	8	2.82	39.09	26.62
14	R	15	3.87	36.36	45.20	39	6.24	32.22	118.7
	G	25	5.00	34.15	77.01	42	6.48	31.89	126.4
	B	15	3.87	36.36	47.13	38	6.16	32.33	114.9
15	R	14	3.74	36.66	42.63	40	6.32	32.11	120.1
	G	30	5.47	33.35	92.95	52	7.21	30.97	157.6
	B	14	3.74	36.66	42.35	39	6.24	32.22	119.7
Average	RGB	22.7	4.31	36.41	69.72	46.26	6.105	33.43	139.7

From the above table 7, it is clear that the results of MSE, PSNR, RMSE, and AD of the adaptive ABC technique are better than the content adaptive strategy. In the adaptive ABC technique the average of MSE of all the images is **22.7** and the average of MSE of all the images of the content adaptive CFA is **46.26**. Similarly the average of RMSE, PSNR and AD of the adaptive ABC technique is 4.31, 36.41, 69.72 and the average of these parameters of the content adaptive CFA is 6.105, 33.43 and 139.7. So from the above results, it's clear that the Adaptive ABC technique provides better quality of images as compared to the content adaptive CFA technique.

4. CONCLUSION

The proposed work handles improving the content based color filter array further by using artificial bee colony in order to optimize the window size. These works have centered on reducing the color artifacts and maintain the quality of the images. The overall objective of the dissertation is to create and implement the artificial bee colony and content based color filter array. we have chosen ABC optimization because the major advantages which ABC holds over other optimization algorithms include its: Simplicity, flexibility and robustness, Use of fewer control parameters compared to many other search techniques, Ease of hybridization with other optimization algorithms, Ability to handle the objective cost with stochastic nature, Ease of implementation with basic mathematical and logical operations. The proposed methodology has taken a full color image as an input image and then converts this image into Bayer pattern. There are three channels presented into a bayer converted image and these channels are Red, Green and

Blue. Differentiate each channel and interpolate each channel by using optimized adaptive artificial bee colony algorithm. The comparison has clearly shown that the proposed over the available techniques.

REFERENCES:

- [1] S. Ling and R. Amin Ur, "Image Demosaicing using content and color-correlation analysis" Signal Processing, Elsevier, pp. 84-91, 2014.
- [2] k. Ryo, M. Ryo, K. Seisuke, S. Keiichiro and O. Masahiro, "Lossless/Near-Lossless color image coding by inversedemosaicing", IEEE International Conference on Acoustic Speech and Signal processing (ICASSP), pp. 2011-2014, 2014 .
- [3] Mohanbaabu, Vinothkumar and Ponvasanth, "A Modified Low power Color filter Array", International Conference on Communication and Signal Processing, pp. 011-015, April 3-5, 2014.
- [4] Z. Xingyu, S. Ming-Jing, F. Lu and Oscar C. AU, "Joint Demosaicing and Demosaicking of Noisy CFA Image based on Inter-color Correlation", IEEE International Conference on Acoustic, Speech and Signal Processing (ICASSP), pp. 5784-5788, 2014.
- [5] C. Xiangdong, H. Liwen, J. Gwanggil and J. Jechang, "Local Adaptive Directional Color Filter Array Interpolation based on Inter-channel Correaltion", Optic Communication, Elsevier, pp. 269-276, 2014.
- [6] P. ibrahim and A. Yucel, "Multiscale Gradients-Based Color Filter Array Interpolation", IEEE Transaction on Image Processing, Vol. 22, No. 1, pp. 157-165, January 2013.
- [7] W. Ting-Chum, L. Yi-Nung and Shao-Yichien, "A Color Filter Array Demosaicking using Self validation Framework", ICME, IEEE, pp. 604-609, 2012.
- [8] G. Jing Ming, L. Yun-Fu, L. Bo-Syun, W. Peng-Hua and L. Jiann-Der, "Classified-Filter-Based Compensation Interpolation for Color Filter Array Demosaicing", ICASSP, IEEE, pp. 921-924, 2012.
- [9] L. Dongjae , Byung J.B and K. Tae chan, "Two layer color filter array for high quality images", ICIP IEEE, pp. 345-348, 2012.
- [10] R. Rajeev, S. Wesley E. and B. Griff l, "Demosaicking methods for bayer color array", Journal of electronic imaging, pp. 306-315, 2002.
- [11] R. Rajeev and S. Wesley E., "Adaptive demosaicking", Journal of Electronic imaging, Vol. 12, pp. 633-642, 2003.
- [12] M. Zhao, R.E.J. Kneepkew, P.M. hofman, G. De Haan, "Content adaptive image deblocking", IEEE, pp. 299-304, 2004.
- [13] S. Ling, H. Hao, H. Gerard de, "Coding artifacts robust resolution Up-conversion", IEEE ICIP, pp. 409-412, 2007.
- [14] L. Olivier, M. Ludovic, Y. Yanqin, "Comparison of color demosaicing methods", Advances in imaging and electron physics, Elsevier, pp. 173-265, 2010.
- [15] S. Ling, Z. Hui, H. Gerard de, "An overview and performance evaluation of classification based least square trained filters", IEEE transaction on image processing, Vol. 17, pp. 1772-1782, 2008.
- [16] A. Jose Apolinario jr. and N. Sergio L., "Introduction to adaptive filters", Springer, pp. 23-49, 2009.
- [17] L. Brain, J. Gwanggil and W. Eeic, "Least Square luma-chroma demultiplexing algorithm for bayer demosaicking", IEEE Transaction on image processing, Vol. 20, pp. 1885-1894, 2011.
- [18] S. Ling, W. Jingnan, K. Ibor and H. Gerard de, "Quality adaptive least square trained filters for video compression artifacts removal using a no-reference block visibility metric", Vis. Commun. Image, Elsevier, pp. 23-32, (2011).
- [19] S. Ling, Z. Hui, W. Liang and W. Lijun, "Repairing imprefect video enhancement algorithms using classification based trained filters", SLVIP, Springer, pp. 307-313, 2011.
- [20] P. Ibrahim and A. Yucel, "Edge Strenght filter based color filter array interpolation", IEEE Transaction image processing, Vol. 21, pp. 393-397, 2012.
- [21] G. Zapryanov, "A new universal demosaicing pipeline Algorithm for RGB color filter array", ISSN Information technologies and control, pp. 2367-5357, 2012.
- [22] A. Robert Maschal, S. Jr. Susan young, P. Joseph Reynolds, K. Kerth, F. Jonathan and C. Ted, "New image quality assessment mlgorithm for CFA demosaicing", IEEE Sensor Journal, Vol. 13, pp. 371-378, 2013.
- [23] C. Nivedita and D. Avinash, "Analysis of image demosaicking algorithms", International journal of innovation research in computer and communication engineering, Vol. 2, pp. 4155-4164, 2014

IJERGS

A Review on Pipelined integer DCT architecture for HEVC

Mr. Rahul R. Bendale, Prof. Vijay L. Agrawal

HVPM COET, Amravati, Maharashtra, India, rahulbendale@gmail.com, 7758022401.

Abstract — Currently different types of transform techniques are used by different video codecs to achieve data compression during video frame transmission. Among them, Discrete cosine transform (DCT) is supported by most of modern video standards. The integer DCT is an approximation of DCT. It can be implemented exclusively with integer arithmetic. Integer DCT proves to be highly advantageous in cost and speed for hardware implementation. Implementation of an efficient discrete cosine transform with reduced complexity and number of multiplications. Pipelining technique is introduced to reduce the processing time. The full pipeline variable block size transform engine with the efficient hardware utilization is proposed to handle the DCT/IDCT. 2D-DCT is computed by combining two 1D-DCT that connected by a transpose buffer.

Keywords— Discrete cosine transform (DCT), HEVC, I-DCT, FPGA, VHDL, Video compression

INTRODUCTION

H.265/High Efficiency Video Coding (HEVC) is the successor codec to H.264, which, like H.264, is jointly developed by the ISO/IEC Moving Picture Experts Group and ITU-T Video Coding Experts Group (VCEG). To maximize compression capability and improve other characteristics such as data loss robustness, while considering the computational resources that were practical for use in products at the time of anticipated deployment of each standard. It is widely used for many applications, including broadcast of high definition (HD) TV signals over satellite, cable, and terrestrial transmission systems, video content acquisition and editing systems, camcorders, security applications, Internet and mobile network video, Blu-ray Discs, and real-time conversational applications such as video chat and video conferencing. However, an increasing diversity of services, the growing popularity of HD video, and the emergence of beyond-HD formats (e.g., 4k×2k or 8k×4k resolution) are creating even stronger needs for coding efficiency. Moreover, the traffic caused by video applications targeting mobile devices and tablet PCs, as well as the transmission needs for video-on-demand services, are imposing severe challenges on today's networks. An increased desire for higher quality and resolutions is also arising in mobile applications. HEVC has been designed to address essentially all existing applications of H.264/MPEG-4 AVC and to particularly focus on two key issues: increased video resolution and increased use of parallel processing architectures.

The 2D-DCT is computationally intensive and as such there is a great demand for high speed, high throughput and short latency computing architectures. Due to the high computation requirements, the 2D-DCT processor design has been concentrated on small non overlapping blocks (typical 8×8). Many 2D-DCT algorithms have been proposed to achieve reduction of computational complexity and thus increase the operational speed and throughput. The various algorithms and architectures for the 2D-DCT can be divided into two categories: The row-column decomposition methods and the non-row-column decomposition methods

Literature SURVEY:

- Gary J. Sullivan [1] introduces H.264/AVC video coding standard. The main goal is to enhance compression, performance. The advantage of this paper is that it explains the standardization process. The disadvantage of this paper is that the desired efficiency of video compression couldn't be achieved to that extent.
- Yunqing Ye and Shuying Cheng [3] Implement 2D-DCT Based on FPGA with Verilog HDL Discrete Cosine Transform is widely used in image compression. This paper describes the FPGA implementation of a two dimensional (8×8) point Discrete Cosine Transform (8×8 point 2D-DCT) processor with Verilog HDL for application of image processing. The row-column decomposition algorithm and pipelining are used to produce the high quality circuit design with the max clock frequency of 318MHz when implemented in a Xilinx VIRTEX-II PRO FPGA chip.
- Anas Hatim, S. Belkouch [5] Efficient hardware architecture for direct 2D DCT computation and its FPGA Implementation- In this paper, we propose a low complexity architecture for direct 2D-DCT computation. The architecture will transform the pixels from spatial to spectral domain with the required quality constraints of the compression standards. In our previous works we introduced a new fast 2D DCT with low computations: only 40 additions are used and no multiplications are needed. Based on that algorithm we developed in this work a new architecture to achieve the computations of the 2D DCT directly without using any transposition memory. We defined Sk functions blocks to build the 2D DCT architecture. The Sk

block perform 8 function depending on the control signals of the system. The number of additions/subtractions used is 63, but no multiplication or memory transposition is needed. The architecture is suitable for usage with statistical rules to predict the zero quantized coefficients, which can considerably reduce the number of computation. We implemented the design using an FPGA Cyclone 3. The design can reach up to 244 MHz and uses 1188 logic elements, and it respect the real time video requirements.

PROPOSED WORK :

1D DCT : The N-point DCT and inverse DCT (IDCT) of N-point sequence x(n) is defined as [1]:

$$X(k) = e(k) \sum_{n=0}^{N-1} x(n) \cos \left[\frac{(2n+1)k\pi}{2N} \right] \quad k = 0, 1, \dots, N-1$$

$$x(n) = \frac{2}{N} \sum_{k=0}^{N-1} e(k) X(k) \cos \left[\frac{(2n+1)k\pi}{2N} \right] \quad n = 0, 1, \dots, N-1$$

Where, $e(k) = \begin{cases} \frac{1}{\sqrt{2}} & \text{if } k = 0 \\ 1 & \text{otherwise} \end{cases}$

2D DCT : Mathematical representation of N x N point 2D DCT can be written as

$$X(k,l) = e(k)e(l) \sum_{m=0}^{N-1} \sum_{n=0}^{N-1} x(m,n) \cos \left[\frac{(2m+1)k\pi}{2N} \right] \cos \left[\frac{(2n+1)l\pi}{2N} \right]$$

Where, $e(k) = e(l) = \begin{cases} \frac{1}{\sqrt{2}} & \text{if } (k,l) = 0 \\ 1 & \text{otherwise} \end{cases}$

x(m,n) is 2D input data and X(k,l) is transformed DCT coefficients.

Equation for 2D-DCT can be written as follows:

$$X(k,l) = e(k)e(l) \sum_{m=0}^{N-1} \cos \left[\frac{(2m+1)k\pi}{2N} \right] \sum_{n=0}^{N-1} x(m,n) \cos \left[\frac{(2n+1)l\pi}{2N} \right]$$

In above equation

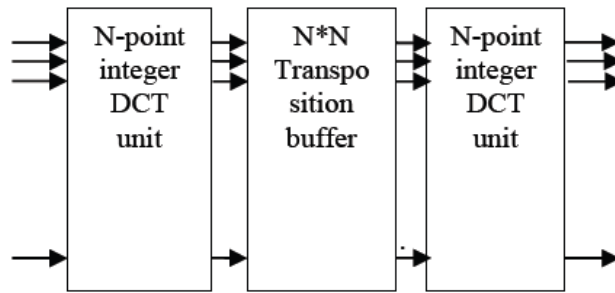
$$\sum_{n=0}^{N-1} x(m,n) \cos \left[\frac{(2n+1)l\pi}{2N} \right]$$

represent 1D

DCT of columns of x(m,n).

Therefore it is concluded that calculating 1D DCT of columns followed by 1D DCT of rows results in 2D DCT coefficients of 2D input data. Using the separability property of 2-D DCT/IDCT the 2-D transform can be carried out with two passes of 1-D transforms. allows the transform to be applied on one dimension (row) then on the other (column).

Parallel synthesizable implementation of 2D DCT in VHDL. By default it would work on 8 bit input data using 12 bit DCT coefficients (12-bit DCT output). Multiplier-less design, parallel distributed arithmetic with butterfly computation would be used. Implementation would be done as row-column decomposition, two 1D DCT units and transpose matrix between them (double buffered as ping-pong buffer for performance). Following is the probable block diagram for 2D DCT structure using two 1D DCT blocks; one for row and one for column.



To implement VHDL code in Xilinx Self-verifying testbench would be written which would include take matlab-converted image as input. Designed core would transform it to DCT coefficients and behavioral IDCT testbench code would reconstruct original image from it. PSNR would be computed between original and reconstructed image to find out error introduced by fixed point arithmetic.

In addition Matlab scripts would be written for computing floating point DCT/IDCT as reference for cross checking the DCT values calculated by our designed core. Also, scripts for converting 8 bit bitmap to txt format would be needed so that it becomes readable by testbench and vice versa.

Finally, designed core would be tested on Spartan 6 or Virtex 5 FPGA board as per decided by the memory required for our code. For reconfigurable structures so that it can work with 16, 32 bits etc, we have to just increase the ROM memory sizes and the input data feed line width. But it would take more latency in our parallel pipelined structure as the no. of bits increase.

CONCLUSION

In this paper we have proposed a very low complexity DCT approximation by the row column decomposition for computation of 2D-DCT. Parallel process causes latency in the system. Using the Row-Column decomposition algorithm, the number of calculations are logically reduced. The row column decomposition method reduces the hardware complexity as per the other methods.

REFERENCES:

- [1] Pramod Kumar Meher, Senior Member, IEEE, Sang Yoon Park, Member, IEEE, Basant Kumar Mohanty, Senior Member, IEEE, Khoon Seong Lim, and Chuohao Yeo, Member, IEEE 2013 IEEE "Efficient Integer DCT Architectures for HEVC" IEEE Transaction on circuits and systems for video technology.
- [2] Gary J. Sullivan, *Fellow, IEEE*, Jens-Rainer Ohm, *Member, IEEE*, Woo-Jin Han, *Member, IEEE*, and Thomas Wiegand, *Fellow, IEEE* "Overview of the High Efficiency Video Coding (HEVC) Standard", IEEE TRANSACTIONS ON CIRCUITS AND SYSTEMS FOR VIDEO TECHNOLOGY, VOL. 22, NO. 12, DECEMBER 2012
- [3] Yunqing Ye, Shuying Cheng "Implementation of 2D-DCT Based on FPGA with Verilog HDL". Electronics and Signal Processing, LNEE 97, pp.633-639.
- [4] Shivam Bindal, 2Udit Khanna, 3Manoj Sharma1 "Trends in Video Compression Technologies and Detailed Performance Comparison of H.264/MPEG-AVC and H.265/MPEGHEVC", Bharati Vidyapeeth's College of Engineering, New Delhi, India, International Journal of Engineering Research & Technology (IJERT) ISSN: 2278-0181
- [5] A. Hatim, S. Belkouch "Efficient hardware architecture for direct 2D DCT computation and its FPGA Implementation".-2013
- [6] R.Kamalakkannan. 2 Dr.S Ravi,3 V.Jayapradha 1SCSVMV University 2 Dr.MGR University 3 SCSVMV University "Reconfigurable Architecture for Video Codec Supporting Advanced Video Standard HEVC", International Journal of Engineering Research & Technology (IJERT) IJERTIJERT ISSN: 2278-0181 www.ijert.org Vol. 3 Issue 6, June – 2014
- [7] Yeshwanth. E, Shruthi. G, Department of Electronics and Communication Don Bosco Institute of Technology Bangalore, India, "Implementation of Reduced Area and Delay Integer DCT using Modified Transposition Buffer" International Journal of Engineering Research & Technology (IJERT) ISSN: 2278-0181 IJERTV4IS030882 www.ijert.org (This work is licensed under a Creative Commons Attribution 4.0 International License.) Vol. 4 Issue 03, March-2015

- [8] *E. Peixoto ,B. Macchiavello , E. M. Hung, A. Zagherro ,T. Shanableh , E. Izquierdo*
“AN H.264/AVC TO HEVC VIDEO TRANSCODER BASED ON MODE MAPPING”
,Universidade de Brasilia, Brazil,College of Engineering, American University of Sharjah, UAE.
School of Electronic Engineering and Computer Science, Queen Mary University of London, UK.
- [9] IEEE TRANSACTIONS ON CIRCUITS AND SYSTEMS FOR VIDEO TECHNOLOGY, VOL. 22, NO. 12, DECEMBER 2012,“HEVC Complexity and Implementation Analysis”
Frank Bossen, *Member, IEEE*, Benjamin Bross, *Student Member, IEEE*, Karsten S`uhring, and David Flynn
- [10] Jian-Liang Lin, Yi-Wen Chen, Yu-Wen Huang, and Shaw-Min Lei, *Fellow, IEEE* “Motion Vector Coding in the HEVC Standard”
- [11] Fatma Belghith*1, Hassen Loukil2, Nouri Masmoudi3 “Efficient Hardware Architecture of a Modified 2-D Transform for the HEVC Standard” University of Sfax, National Engineering School of Sfax, Electronics and Information Technology Laboratory BP W 3038 Sfax, TUNISIA, International Journal of Computer Science and Application (IJCSA) Volume 2 Issue 4, November 2013
- [12] D. Bugdayci Sansli, t K. Ugurt M.M Hannukselat, M. Gabbouj, “INTER VIEW MOTION VECTOR PREDICTION IN MULTIVIEW HEVC” Tampere University of Technology,Finland Nokia Research Center, Tampere, Finland

EFFLUENT TREATMENT PLANT USING PLC

Er. Ravinder Kumar, Sahil Jungral, Tavleen Singh, Ankit Gupta, Tanveer Hussain Khan

Assistant Professor, AE&IE, MBSCET, ravs17@gmail.com and 9419796100

Abstract— Water is basic necessity of life used for many purposes one of which is industrial use. Industries generally take water from rivers or lakes but they have to pay heavy taxes for that. So it's necessary for them to recycle that to reduce cost and also conserve it. Main function of Effluent Treatment Plant (ETP) is to clean industry effluent and recycle it for further use. Many manufacturing industries produce their products with using water. With their products industries produce wastewater, otherwise known as effluent, which can be removed with the help of an effluent treatment plant (ETP). Manufacturers face strict regulations on discharge and waste. Effluent from industries must meet the national effluent discharge quality standards (NEDQS) set by the Government. In this paper, we propose a few automated processes for a partial automation of the apartment which can be mostly used in residential areas and industries. It is developed using PLC. The main intent of the paper is to treat the waste water which can be in turn used for many other purposes and can be cost effective as well.

Keywords— PLC (Programmable Logic Controller), CV (Control Valve), ETP (Effluent Treatment Plant), Automation, pH, Sensor, Waste water Treatment

INTRODUCTION

Automation is basically the delegation of human control function to technical equipment. It uses controlled systems such as computers, PLCs, Microcontrollers to control machinery and processes to reduce the necessity of human involvement and mental requirements. Different types of controllers can be used to operate and control the equipment such as machinery, processes in factories, heat treating ovens and boilers, and other applications with minimal or reduced human intervention. Food/ Beverage, Chemical industries, Power, Machine Manufacturing, etc. are the few examples where we see the mechanization today. Most of the automation has been existing in industries from decades. But the shift for automation in home and apartments has popped in very recently. One can employ this kind of a system which enables an individual to supervise devices such as Lighting, Heating and ventilation, water pumping, gardening system, Overhead water flow control remotely or from any centralized location. Automatic systems are being preferred over manual system because they reduce individual's effort. Similarly talking about apartment automation, by use of PLCs everything seems to be more accurate, reliable and more efficient than the existing controllers.

As our paper is based on automation thus we can use both microcontroller and PLC. Microcontroller being an application oriented and can be programmed using C or Basic need some highly trained programmers to program it. Also microcontroller cannot withstand extreme conditions and cannot be reprogrammed. On the contrary, PLC is robust and can be programmed using ladder programming, structured text programming and functional block diagram programming which can be done easily and also it can be reprogrammed i.e. connections can be same but programming can be changed as per requirement. Thus comparing both of them, we found that there are more advantages of PLC than microcontroller except one fact that PLCs are costly. But on a long run, it works efficiently and its reliability is high. This is one of the factor due to which the cost can be neglected.

BLOCK DIAGRAM

The block diagram is shown in Fig.1 .The input action consists of a reservoir tank consisting of the waste water to be treated. The pump controlled by PLC pumps the water through a stainless steel mesh to filter macro particle macro particle like sand, stones etc. The next stage consists of the filter membrane which filter minute or dissolved particle present in the water. The system also allows the sedimentation to take place as the heavier particles settle at the bottom of the tank. The next stages consists of the flocculation, coagulation etc. as water treatment processes and the disinfection of water takes place by adding Alum, Sodium Bi sulphate and chlorine. The solenoid valves open and close according to the controlling action of PLC to allow the water treatment in different stages. Level sensors are applied in final tank to check the total amount or level of the waste water treated. The pH value of the treated water is checked if it lies in usable range the water is stored in the treated water tank and the untreated water i.e. the water which does not fulfil the pH criteria is pumped back to the waste water reservoir and the whole process for effluent treatment is repeated again. The components required are as follows:

Stainless steel mesh, Water Pump, Filter membrane, pH meter, Aluminum Sulphate (alum), Chlorine, Sodium Bisulphate, Level Sensors, Control Valves, PLC, LCD Display, PCB

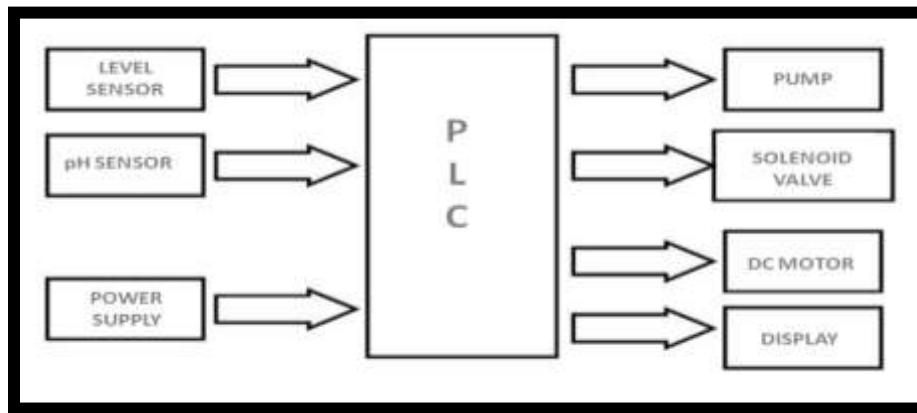


Fig.1 Block Diagram of PLC based ETP

Some of the components of the system are explained in brief below.

PLC: The programmable logic controller is defined as a digital electronic device that uses a programmable memory to store instructions and to implement functions such as logic, sequencing, timing, counting and arithmetic words to control machines and processes as shown in Fig.2. Here it is controlling the input parameters like pH sensor and Level sensor and output parameters like pump, solenoid valves, dc motor and display. The MicroLogix 1500 (Allen Bradley) Programmable Controller contains a power supply, input circuits, output circuits, and a processor. The controller is available in 24 I/O and 28 I/O configurations.

The hardware features of the controller are:

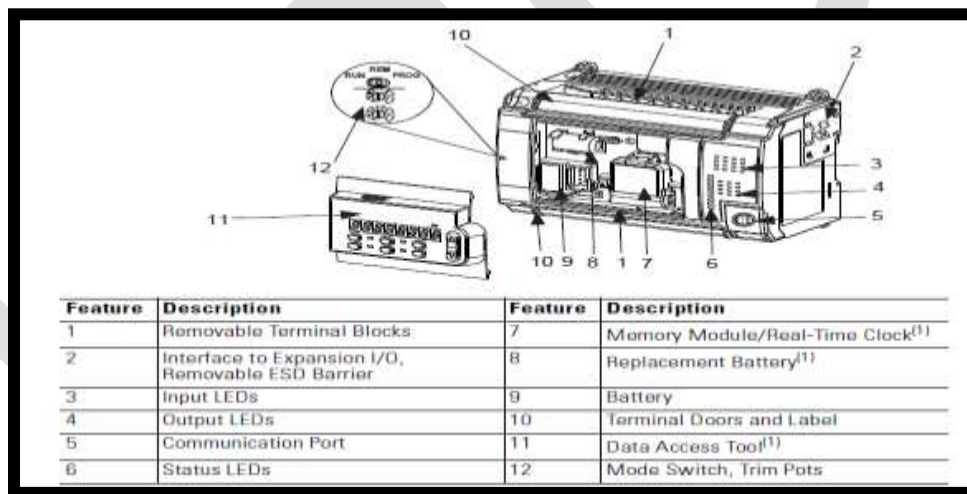


Fig.2 PLC MicroLogix 1500

pH sensor: It will sense the PH level of the waste water and is being controlled by PLC. A glass electrode is a type of ion-selective electrode made of a doped glass membrane that is sensitive to a specific ion. It is an important part of the instrumentation for chemical analysis and physio-chemical studies. In modern practice, widely used membranous ion-selective electrodes (ISE, including glasses) are part of a galvanic cell. The electric potential of the electrode system in solution is sensitive to changes in the content of certain type of ions, which is reflected in the dependence of the electromotive force (EMF) of galvanic element concentrations of these ions. It is shown in Fig.3.

A typical modern pH probe is a combination electrode, which combines both the glass and reference electrodes into one body. The combination electrode consists of the following parts (see the drawing):

1. A sensing part of electrode, a bulb made from a specific glass
2. Internal electrode, usually silver chloride electrode or calomel electrode
3. Internal solution, usually a pH=7 buffered solution of 0.1 mol/L KCl for pH electrodes or 0.1 mol/L MeCl for pMe electrodes
4. When using the silver chloride electrode, a small amount of AgCl can precipitate inside the glass electrode
5. Reference electrode, usually the same type as 2
6. Reference internal solution, usually 0.1 mol/L KCl
7. Junction with studied solution, usually made from ceramics or capillary with asbestos or quartz fiber.

8. Body of electrode, made from non-conductive glass or plastics.

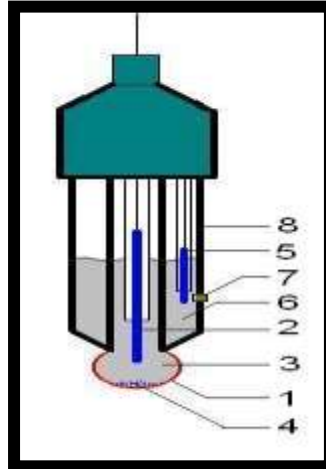


Fig.3 pH Electrode

The bottom of a pH electrode balloons out into a round thin glass bulb. The pH electrode is best thought of as a tube within a tube. The innermost tube (the inner tube) contains an unchanging 1×10^{-7} mol/L HCl solution. Also inside the inner tube is the cathode terminus of the reference probe. The anodic terminus wraps itself around the outside of the inner tube and ends with the same sort of reference probe as was on the inside of the inner tube. It is filled with a reference solution of 0.1 mol/L KCl and has contact with the solution on the outside of the pH probe by way of a porous plug that serves as a salt bridge.

Pump: It is acting as booster which will boost the flow of liquid through it. It is acting as an output parameter for PLC. It is shown in Fig.4.



Fig.4 Submersible Pump

Solenoid Valve: A solenoid valve or solenoid actuated valve is basically an electrical valve that controls the flow of media either open/closed or diverting my means of an electro magnet or solenoid. The principles are based around a thin copper wire wound around a bobbin or core (The solenoid) in such a way that when electrical energy is applied a sufficient magnetic field is generated to provide a lifting force to a ferromagnetic stainless steel armature within the solenoid valve armature assembly which in turn will directly or indirectly change the position of the valve. It is acting as an output parameter for PLC. A solenoid valve is an electromechanically operated valve. The valve is controlled by an electric current through a solenoid: in the case of a two-port valve the flow is switched on or off; in the case of a three-port valve, the outflow is switched between the two outlet ports. Multiple solenoid valves can be placed together on a manifold. Solenoid valves are the most frequently used control elements in fluidics. Their tasks are to shut off, release, dose, distribute or mix fluids. They are found in many application areas. Solenoids offer fast and safe switching, high reliability, long service life, good medium compatibility of the materials used, low control power and compact design. Besides the plunger-type actuator which is used most frequently, pivoted-armature actuators and rocker actuators are also used. It is shown in Fig.5.



Fig.5 Solenoid Valve

DC Motor: A dc motor is being controlled by PLC. It will operate the stirrer. A DC motor is any of a class of electrical machines that converts direct current electrical power into mechanical power. The most common types rely on the forces produced by magnetic fields. Nearly all types of DC motors have some internal mechanism, either electromechanical or electronic; to periodically change the direction of current flow in part of the motor. Most types produce rotary motion; a linear motor directly produces force and motion in a straight line. DC motors were the first type widely used, since they could be powered from existing direct-current lighting power distribution systems. A DC motor's speed can be controlled over a wide range, using either a variable supply voltage or by changing the strength of current in its field windings. Small DC motors are used in tools, toys, and appliances. The universal motor can operate on direct current but is a lightweight motor used for portable power tools and appliances. Larger DC motors are used in propulsion of electric vehicles, elevator and hoists, or in drives for steel rolling mills. The advent of power electronics has made replacement of DC motors with AC motors possible in many applications. It is shown in Fig.6.



Fig.6 DC Motor

LCD Display: It will display the parameters like pH value, level of liquid and project name. LCD stands for **Liquid Crystal Display**. It is shown in Fig.7. LCD is finding wide spread use replacing LEDs (seven segment LEDs or other multi segment LEDs) because of the following reasons:

- The declining prices of LCDs.
- The ability to display numbers, characters and graphics. This is in contrast to LEDs, which are limited to numbers and a few characters.
- Incorporation of a refreshing controller into the LCD, thereby relieving the CPU of the task of refreshing the LCD. In contrast, the LED must be refreshed by the CPU to keep displaying the data.
- Ease of programming for characters and graphics.

These components are “specialized” for being used with the microcontrollers, which means that they cannot be activated by standard IC circuits. They are used for writing different messages on a miniature LCD.



Fig.7 LCD Display

A model described here is for its low price and great possibilities most frequently used in practice. It is based on the HD44780 microcontroller (*Hitachi*) and can display messages in two lines with 16 characters each. It displays all the alphabets, Greek letters, punctuation marks, mathematical symbols etc. In addition, it is possible to display symbols that user makes up on its own.

General process diagram of PLC based ETP plant is:

PROCESS EXPLANATION

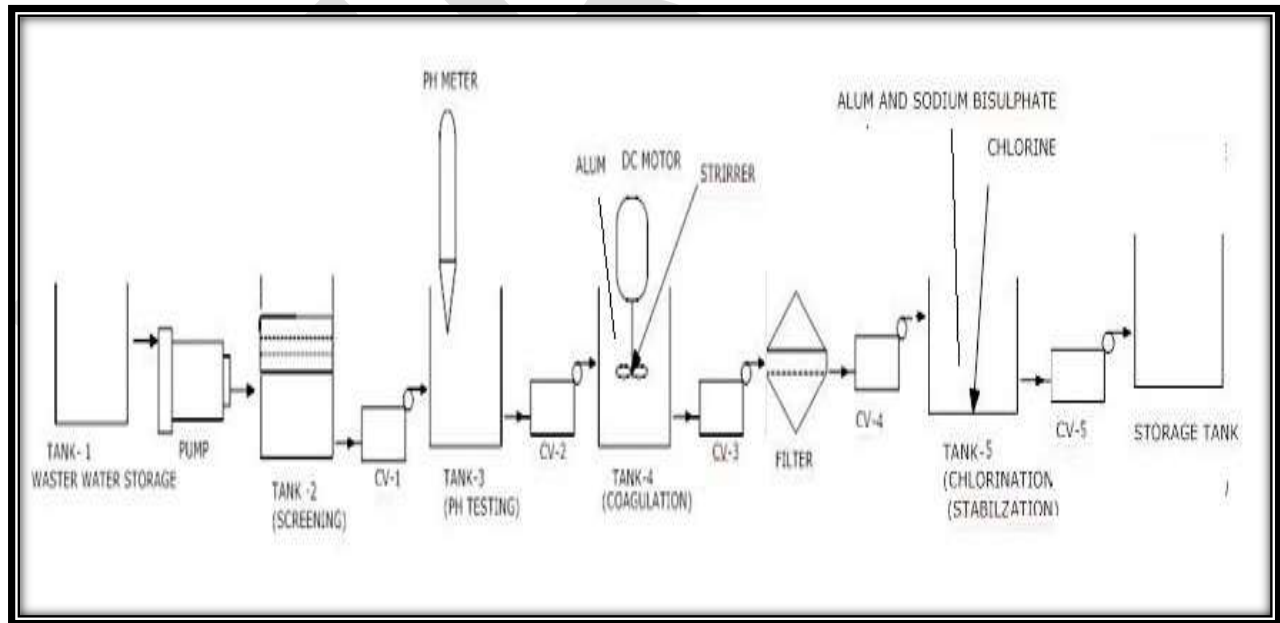


Fig.8 Process Diagram

The process of ETP mainly consists of four stages:

- preliminary
- primary
- secondary
- tertiary(advanced)

And treatment of three types

- physical
- chemical
- biological

In this diagram there are total six tanks including storage tank. Tank 1 contains waste water or untreated water or water containing effluents that has to be treated, is pumped to the tank 2 by the pump or dc motor.

In tank 2, the first stage takes place i.e. preliminary.

There are three processes in this stage i.e., screening, sedimentation and clarification.

- In screening process a screen with openings of uniform size is used to remove large solids such as plastics, cloth etc.. Maximum 10mm shall be used.
- Sedimentation process is a physical water treatment process using gravity to remove suspended solids from water.
- Filtration is a physical operation which is used for separation of solids from fluids.

All the above processes are physical in nature.

There is a valve CV-1 which allows the passage of treated water of first stage to tank3 for further treatment.

In tank 3, second stage takes place i.e. primary stage.

In this stage various floating and settable materials like suspended particles and organic materials are removed and pH value is maintained. In order to check the pH value, pH meter is used.

pH Control: It is necessary to adjust the pH in the treatment process to make the wastewater pH neutral. Various chemicals are used for pH control. For acidic wastes (low pH) sodium hydroxide, sodium carbonate, calcium carbonate or calcium hydroxide, may be added among other things. For alkali wastes (high pH) sulphuric acid or hydrochloric acid may be added. pH maintained water pass to the tank 4 through valve i.e. CV-2 in which process of coagulation takes place which is another process of primary stage.

Coagulation: Coagulation is a complex process but generally refers to collecting into a larger mass the minute solid particles dispersed in a liquid. Chemical coagulants such as aluminum sulphate (alum) or ferric sulphate may be added to wastewater to improve the attraction of fine particles so that they come together and form larger particles called flocs. Coagulation requires gentle mixing of particles which is done with the help of stirrer operated by dc motor.

The processes of primary stage are physical and chemical in nature.

Depending upon the possibility of the presence of biological wastes like bacteria or nature of the waste water, secondary stage treatment can be done in this stage also. If water consist waste like harmful bacteria and other biological effluents then water is treated under secondary treatment or biological treatment. The objective of biological treatment of industrial wastewater is to remove, or reduce the concentration of, organic and inorganic compounds. Biological treatment process can take many forms but all are based around microorganisms, mainly bacteria. Biological treatment plants must be carefully managed as they use live microorganisms to digest the pollutants. It consist two main processes i.e. Aerobic and Anaerobic. These processes are biological in nature. The treated water from tank 4 pass to the filter from third valve CV-3. Filter allows the water to pass to the tank 5 through valve CV-4 and in tank 5 final stage of treatment i.e. tertiary or advanced stage takes place.

- Tertiary treatment is the final cleaning process that improves wastewater quality before it is reused, recycled or discharged to the environment.
- The treatment re Tertiary moves remaining inorganic compounds, and substances, such as the nitrogen and phosphorus.
- Bacteria, viruses and parasites, which are harmful to public health, are also removed at this stage. Alum is used to help remove additional phosphorus particles and group the remaining solids together for easy removal in the filters.
- The chlorine contact tank disinfects the tertiary treated wastewater.
- Chlorine removes microorganisms in treated wastewater including bacteria, viruses and parasites.
- Any remaining chlorine is removed by adding sodium bisulphate just before it's discharged.

The process of this stage are physical, chemical and biological in nature. The water from tank 5 is completely treated water ready for discharge or further use can be collected in storage tank after passing through valve CV-5.

The figure 9 shows the flow diagram of the process.

First of all the waste water from the waste water tank is pumped to the screening section where all the solid waste are removed. Then after clearance control valve CV-1 is activated. This stage is the pH testing stage. There exists a condition if pH sensor detects that the pH value is greater than 7, then it is basic waste so for that CV-2 is activated and to neutralise the effect of basicity, some acid is added like HCl. In a similar context, if pH value is less than 7, being an acidic waste CV-3 is activated and base NaOH is added. In next stage, Stirrer is being driven by dc motor and coagulant alum is being added. After that control valve CV-4 is activated, in this stage filtration of water is done where flocs are removed after that control valve CV-5 is activated. Now stabilization and disinfection of water is done by adding alum, sodium bisulphate and chlorine. After this stage is over control valve CV-6 is activated and water is stored in the reservoir tank which is fitted with level sensor that will show the level water being treated.

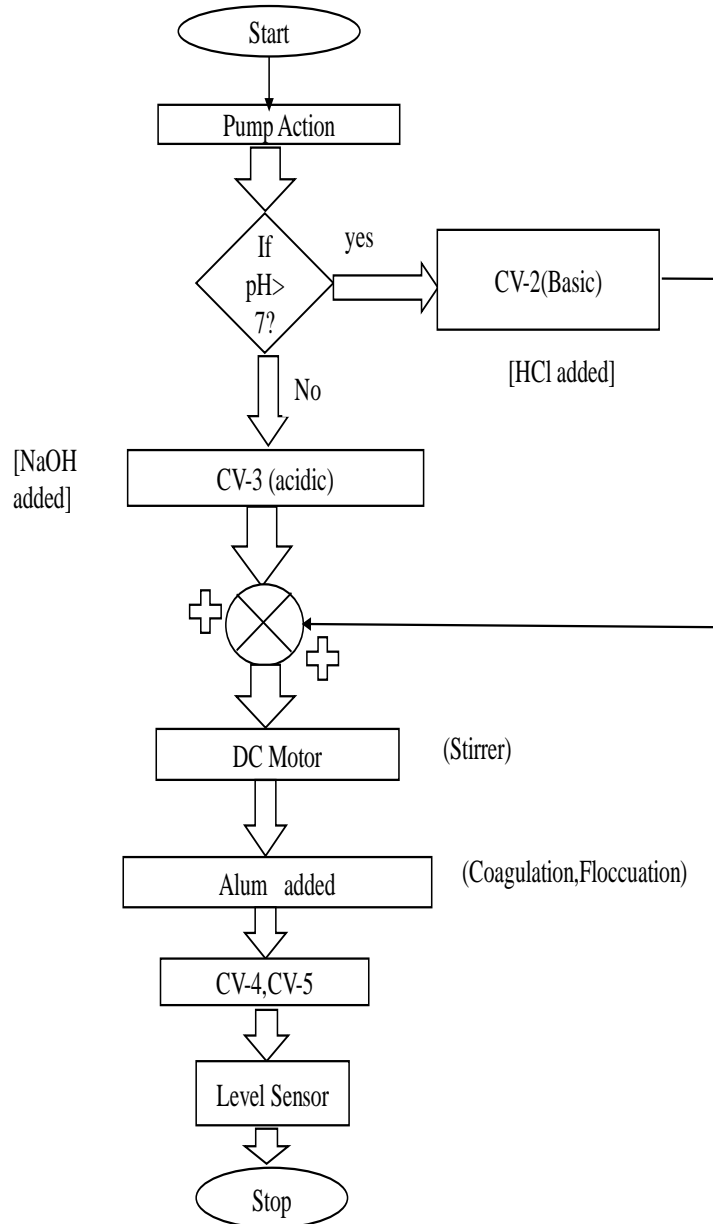


Fig.9 Flow Diagram of Process

CONCLUSION

The treatment of contaminated water can be done with the ETP, which is an effluent treatment plant that cleans up the industry effluents, polluted water from rivers, lakes, etc. So, they can be recycled for further use. Thus, water is recycled and stored. Water is one of the most important natural resources that is one of the basic necessities in human life. Water is used for a number of purposes, but it is used mainly for drinking. Apart from household uses, it is also used for several industrial purposes. Though water is found in abundance in nature, yet most of it is contaminated, and therefore it needs to be treated so that it can be recycled. The treatment of contaminated water can be done with the ETP, it is an effluent treatment plant that cleans the effluents from the industry, polluted water from rivers, lakes, etc. so that it can be recycled for further use. In this way, water is recycled and conserved. It is technically proven that any kind of pollutant can be removed from such effluent by the use of the water treatment plant. Again, the treatment of these effluents is treated depending on the type of industries.

The ETP has a great role to play in discharging the contaminated and polluted water before releasing it back to the environment. Without these water treatment plants, we would not be able to get clean water for domestic uses.

By using PLC, the cost-effective automation system for residences can be developed, and it is very user-friendly for the operator or control engineer to troubleshoot the process if any errors occur and can also be kept track of what is happening in the process.

This kind of implementation has many advantages. Some of them are:

- Increased level of comfort and time saving.
- Time and money saving during maintenance.
- Effective monitoring of the processes.
- Improved plant Reliability and life.
- Flexibility on change of building use.
- Remote monitoring of plants like water treatment plant or electrical supply, etc.
- Ease of storing reports of the systems.

By using PLC based automation in and around residences or apartments, we can lead to a better, comfortable life by reducing costs and improve the quality of life.

REFERENCES:

- [1] Beychok, Milton R. (December 1971). "Wastewater treatment". *Hydrocarbon Processing*: 109–112. ISSN 0818-8190.
- [2] Sadegh Vosough, Amir Vosough, "PLC and its Applications", *International Journal of Multidisciplinary Sciences and Engineering*, Vol. 2, No.8, November 2011.
- [3] Frank D. Petruzella, "Programmable Logic Controller", 3rd edition, Mc Graw Hill, pages:20-32, 2010.
- [4] Product Manual, "MicroLogix TM 1500 Programmable Controllers", Rockwell Automation, Allen- Bradley, pp.39-73, 1999.
- [5] Tchobanoglous, G., Burton, F.L., and Stensel, H.D. (2003). *Wastewater Engineering (Treatment Disposal Reuse) / Metcalf & Eddy, Inc. (4th ed.)*. McGraw-Hill Book Company. ISBN 0-07-041878-0.
- [6] <http://education.rec.ri.cmu.edu/content/electronics/boe/plc/1.html>.
- [7] www.sensorland.com/HowPage037pH.html.
- [8] www.solenoid-valve-info.com/solenoid-valve-basics.html.
- [9] https://en.wikipedia.org/wiki/DC_motor.
- [10] <http://www.merraim-webster.com/dictionary/lcd>.
- [11] <https://wastewatertreatmentplantsindia.wordpress.com/2015/04/21/importance-and-benefits-of-effluent-treatment-plant>.
- [12] www.science.uwaterloo.ca/~cchieh/cact/applychem/watertreatment.html.

Analysis and comparison of BER in cellular communication using Multi carrier-CDMA Technology

J.kameswararao
(M.Tech),SSCE,SRIKAKULAM
8096712159,sun.kameswararao@gmail.com

T.Manikyala Rao
Assoc prof.ECE.,SSCE,SRIKAKULAM
manik.me.au@gmail.com

D. Chiranjevulu
Asst prof.ECE.,SSCE,SRIKAKULAM
chiru.divvala@gmail.com

Abstract- In twenty first century mobile cellular communication is playing a vital role in our day to day life. The vast usage of mobile services has given birth to various security issues and errors in data communication. To sort out these issues it is essential to choose an effective coding technique to improve the Bit Error Rate and to provide timely security in 4G technology by performing various simulations. The main objective of this paper is to develop better codes to get one of the best BER Performances under the above mentioned conditions by performing various simulations. The performance of MC-CDM is to be evaluated using the best codes in Additive White Gaussian Noise (AWGN) and Rayleigh fading channel. The performance of MC-CDMA is evaluated by Computer simulation and control the bit error rate (BER) as a function of bit energy to noise density ratio (Eb/No).

Keywords- Multicarrier, BER, CDMA, Multipath Fading, Coding Techniques, Channel Noises.

I. INTRODUCTION

Future wireless communication systems must be able to accommodate a large number of users and at same time to provide the high data rates at the required quality of service. MC-CDMA is taking the advantage of two advanced technological concepts of wireless communications such as the code division multiple access (CDMA) and orthogonal frequency division multiplex(OFDM), especially in the multiple access capability, high spectral efficiency, robustness in the case of frequency selective channels, simple one-tap equalization, narrow-band interference rejection and high flexibility of the MC-CDMA. The outlined potential properties of the MC-CDMA represent the fundamental reasons, why MC-CDMA has been receiving a great attention over the last few days and has been considered a promising candidate for the future advanced wireless communication systems.

One of the major requirements are posed to the MC-CDMA is to reach the data rate at the acceptable complexity and acceptable bit error rate (BER) for the defined number of the active users. Mostly the Global System for Mobile telecommunications (GSM) technology is being applied to fixed wireless phone systems in rural areas or Australia. However, GSM uses time division multiple access (TDMA), it has a high symbol rate to prevent problems with multi path causing inter-symbol interference.

Multiple techniques are consideration for the feature generation of digital mobile systems, with the aim of improving cell capacity, multi path immunity, and flexibility. These include CDMA as well as OFDM. Both techniques could be used for rural areas to providing a fixed wireless system. Every technique as different properties, specific applications making it more suited. OFDM is currently being used in more new radio broadcast systems and the proposal for High Definition Digital Television (HDTV) and Digital Audio Broadcasting (DAB). However, small research has been done into the use of CDMA and OFDM as a transmitter and receiver for cellular mobile systems.

II. MULTIPLE ACCESS TECHNIQUES

Multiple access schemes are used to allow many simultaneous users to use the same fixed bandwidth radio spectrum. In any radio system, the bandwidth allocated is always limited. For mobile phone systems the total bandwidth is typically in MHz i.e., 50MHz, which is split in half to provide the forward and reverse links of the system. Sharing of the spectrum is required in order increase the user capacity of any wireless network [2]. TDMA, FDMA and CDMA are the three major methods of providing the available bandwidth in to multiple users in wireless system. However, an understanding of these methods we required for understanding of extensions to these methods.

A. Time Division Multiple Access:

Time Division Multiple Access (TDMA) divides the available spectrum into multiple slots divided with time, by giving a time slot in transmit or receive to each user. Figure 3 shows how the time slots are provided to users in a round robin fashion, with each user being allotted one time slot per frame.

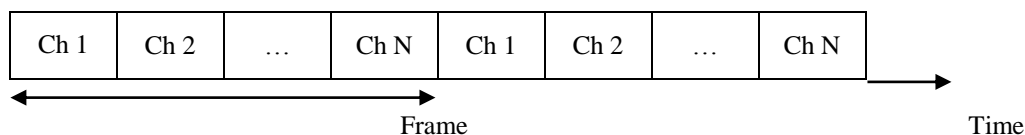


Fig.1. TDMA scheme where each user is allocated a small time slot

TDMA systems transmit data in a buffer method, so the transmission of each channel is non-continuous. The input data to be transmitted is buffered over the past frame and burst transmitted at a higher rate during the time slot for the channel shown fig.1.

Analog signals cannot send directly in TDMA because it required buffering, thus are only used for transmitting digital data. TDMA can suffer from multi path effects, as the transmission rate is generally very high. This leads the multi path signals causing inter-symbol interference.

This is used to reduce the effect of delay spread on the transmission. Several users can transmit of the one channel. This transmission technique is used by most second generation mobile phone systems.

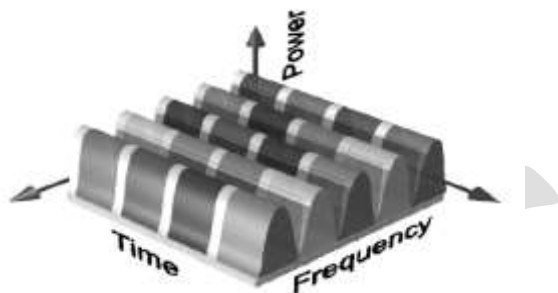


Fig.2. TDMA / FDMA hybrid, showing that the bandwidth is split Frequency Channels and time slots

B. Frequency Division Multiple Access:

The available total bandwidth is subdivided into a number of narrower band channels in Frequency Division Multiple Access (FDMA) and allocated a unique frequency band in transmit and receive to each user. No other user can use the same frequency band during a call. Each user is allocated a forward link channel (from the base station to the mobile) and a reverse channel (mobile to the base station), this are a single way link.

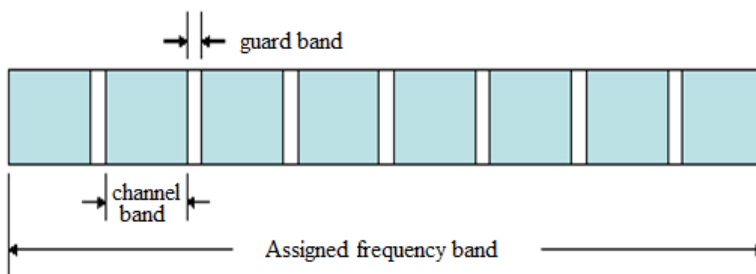


Fig.3. FDMA spectrum, where the available bandwidth is subdivided into narrower band channels

The bandwidths of FDMA channels are very low approximately 30 kHz and each channel only supports only one user. FDMA is used is used as part of most multi-channel systems [3]. Figure shows the allocation of the available bandwidth into several Channels explained in Fig.3.

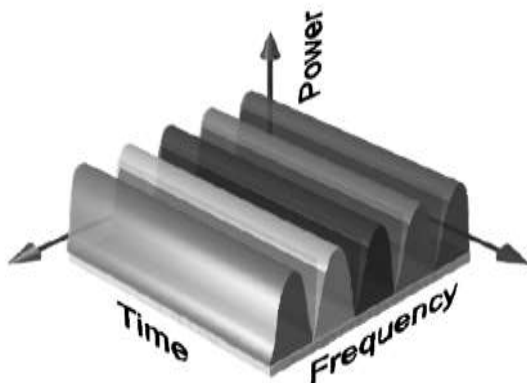


Fig.4. FDMA showing that the each narrow band channel is allocated to a single user

C. CDMA:

CDMA technology was originally developed by the military during World War II researches were spurred into communicating that can be secure and work in the presence of jamming [4]. A CDMA system is a multi-user spread spectrum system that eliminates the frequency reuse problem in cellular systems shown in Fig.5.

Unlike TDMA and FDMA systems, where user data never overlap in either the frequency domains or the time domains, respectively, a CDMA system allows transmissions at the same time while using the same frequency. For example, in the first

widespread commercial CDMA system, the mechanism separating the users in a CDMA system consists of assigning a unique code that modulates the signal from the each user. The unique codes in a CDMA are equal to the number of active users. The code modulating the user's signal is also called a spreading code, spreading sequence, or chip sequence.

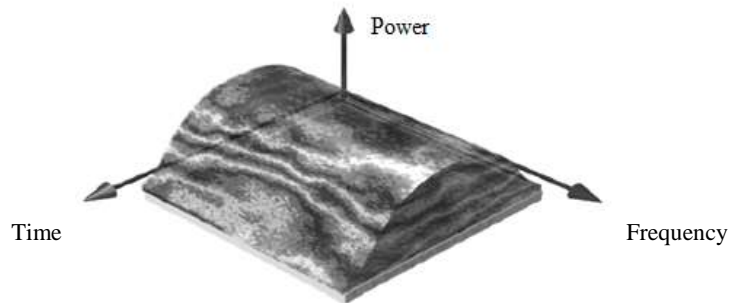


Fig.5. CDMA View

D. OFDMA:

The multicarrier transmission technique is OFDM, which divides the available spectrum into many carriers like Fig.6, each one being modulated by a low rate data stream. It has high popularity because of its capability to transmit effective data rate in a mobile environment, which makes a highly hostile radio channel. This method has been used in the implementation of (High Performance LAN (HIPERLAN/2), IEEE standard 802.16 and 802.11a.

OFDM is similar to FDMA the multiple user access is achieved by subdividing the total bandwidth into number of channels that are provided to users. OFDM more efficiently uses the total spectrum with closer spacing the channels together [6]. This is achieved by all the carriers orthogonal to one another by spacing them at integer multiples of the frequency. When the powers of the other subcarriers are null then the peak power of one subcarrier occurs, thereby countering any effect of interference.

The OFDM signal can be to represented as to generate OFDM successfully all the carriers must be controlled to maintain orthogonality of the carriers. This particulate reason, OFDM is generated by firstly choosing spectrum required, based on the input data, and modulation scheme used. Each carrier to be individually produced is assigned data to transmit.

The required phase and amplitude of the particular carrier is then calculated based on the modulation scheme (typically differential BPSK, QPSK, or QAM). The required spectrum is converted back to its actual time domain signal using an Inverse Fourier Transform. Present in most applications, an Inverse Fast Fourier Transform (IFFT) is also used. The IFFT performs transformation most efficiently, and provides a simple way of the carrier signals produced orthogonal.

OFDM Carriers Spectrum

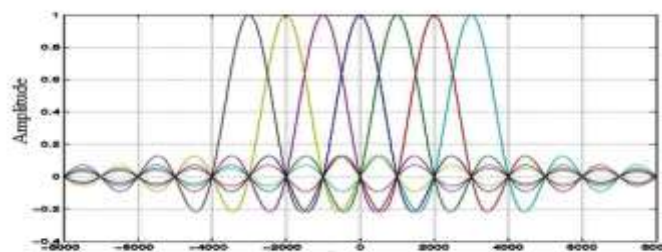


Fig.6. Model graph of OFDMA

The Fast Fourier Transform (FFT) is transforms a cyclic time domain signal into its equivalent frequency spectrum. This is done by finding its equivalent waveform, and it generated by a sum of orthogonal sinusoidal components. The amplitude and phase of the sinusoidal there components represent the frequency spectrum of the time domain signal. The IFFT performs the back process, converting a spectrum (phase and amplitude of each component) into a time domain signal. Number of complex data points converts by IFFT, of length that is a power of 2, into the time domain signal of the same number of points. For an FFT or IFFT each data point in frequency spectrum is used so it is called a bin.

E. OFDMA Transmitter and Receiver:

For the OFDM signal the orthogonal carriers required and it can be easily generated by setting the amplitude and phase of each frequency bin, then performing the IFFT. Each bin of an IFFT corresponds to the phase and amplitude of a set of orthogonal sinusoids, the reverse process guarantees that the carriers generated are orthogonal. OFDM is almost similar to FDMA in that the multiple user

access is achieved by subdividing the available total bandwidth into multiple channels that are then allocated to users. OFDM uses the spectrum more efficiently by spacing the channels very closer together. This is achieved by to make all the carriers orthogonal to one to other by spacing them at integer multiples of the symbol frequency

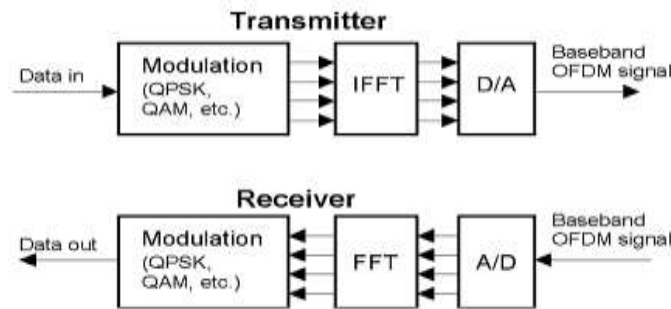


Fig.7. OFDMA Transmitter and Receiver

Thus, the peak power of one subcarrier occurs when the power of the other subcarriers are null, thereby countering any effect of interference. The Inter Symbol Interference (ISI) problem arising in OFDM can be removed by introducing certain guard bands between the subcarriers. This can be completely eliminated if the symbol is cyclically extended, by repeating the first part of the block at the end. The receiver can then operate on the part of the signal beyond the ISI with the only side effect a phase shift on each sub-carrier.

III. ADVANCED METHOD MC-CDMA

The MC-CDMA system has been considered as one of the possible candidates for the next generation of wireless communications. The MC-CDMA system divides the available bandwidth into a large number of narrow subchannels and spreads each data symbol in the frequency domain by transmitting all the chips of a spread symbol at the same time but in different orthogonal subchannels. One of the properties of multicarrier transmission is that the channel gain of each subchannel is different from the other. The inner product of different spreading codes will no longer be zero since the MC-CDMA systems spread transmitted symbols in a non-flat fading channel [7].

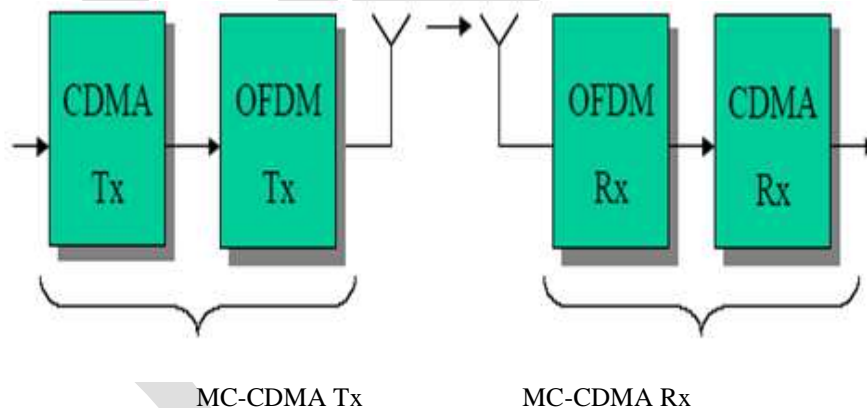


Fig.8. MC-CDMA block diagram

The internal blocks of MC-CDMA are transmitter and receiver. MC-CDMA transmitter section has CDMA, OFDM transmitters same as MC-CDMA receiver section has CDMA, OFDM receivers. In transmitter part encoder followed by mapper (QPSK or BPSK). The block of interleaving labelled in the presented scheme, multilevel sequence of complex numbers in M-array or BPSK modulation formats. The spread symbols are modulated by the multi-carrier modulation and it implemented by the Inverse Fast Fourier transformation operation (IFFT). After parallel-to-serial (P/S) conversion, the cyclic prefix (CP) is inserted in order to mitigate the inter-symbol interference (ISI) caused by the frequency-selective fading channel and The receiver consists of the serial-to-parallel converter (S/P), blocks of the Fast Fourier Transformation (FFT), channel equalization (EQ) using zero forcing method, CP removal Matched filters (MF), transformation, decision device, inverse block and finally decoding block.

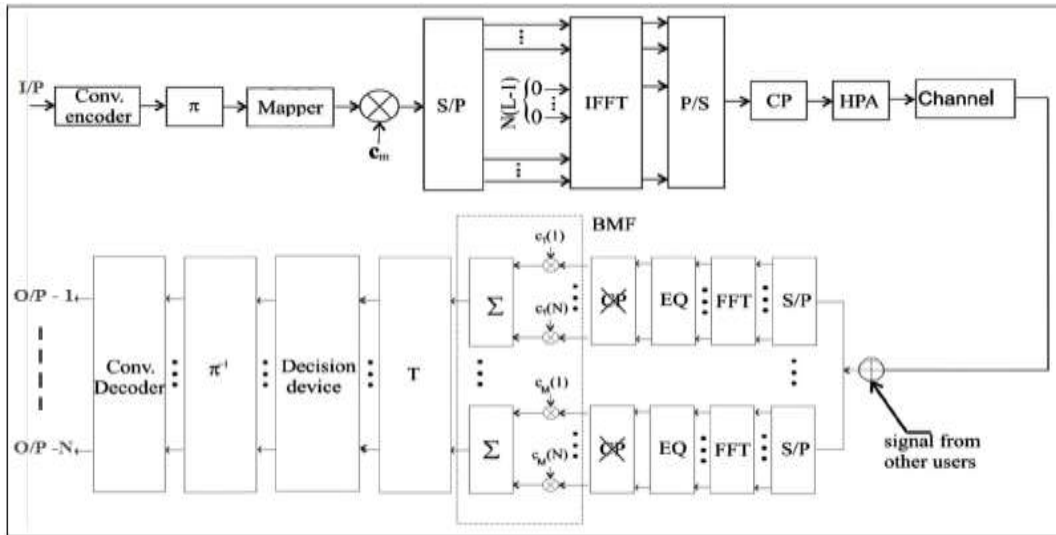


Fig.9. MC-CDMA internal block diagram

IV. NOISE IN COMMUNICATION CHANNEL

Within any communication channel, there is always noise present due to other surrounding radio signals. These noise can be white (colorless) or colored noise, and with interact differently with the transmitted user signal, for instance, the interaction can be additive, multiplicative or complex. In communication systems, the transmitting signal is much Vulnerable to noise especially with in the communication channel. Mostly in wireless channel considered AWGN and Rayleigh noise.

A. White Noise:

White noise is a type of noise that is often exists in communication channels. Compare to any other types of noise it is different, hence the fact that its Power Spectral Density (PSD) is independent of the operating frequency the word "White" is used in the sense that white Light contains all other visible light frequencies in the band of electromagnetic radiation.

B. Rayleigh noise:

The Rayleigh fading channel is mostly applied in case when there is no LOS between R_x and T_x. Mostly channel also adds AWGN noise to the signal samples after it suffers from Rayleigh fading. The Rayleigh probability density function is given by

Received signal $Y = hX + n$,

Where X is T_x signal, h is Rayleigh fading response and n is AWGN.

$$f(x) = \begin{cases} \frac{x}{\sigma^2} e^{-\frac{x^2}{2\sigma^2}} & x \geq 0 \\ 0 & x < 0 \end{cases} \tag{1}$$

Where σ^2 is known as the fading envelope of the Rayleigh distribution, in theoretical BER for BPSK Rayleigh fading

$$P_b = 1/2 \operatorname{erfc}(\sqrt{E_b/N_0}) \tag{2}$$

In theoretical BER for BPSK Rayleigh fading with AWGN channel

$$P_b = 1/2 (1 - \sqrt{(E_b/N_0)/(1 + (E_b/N_0))}) \tag{3}$$

Here we using spreading codes before IFFF process so, the spreading codes are Long PN sequence, Walsh coding and Gold code.

V. CODE GENERATORS:

A. Long PN sequence:

A Long PN sequence is uniquely assigned to each user and it is a periodic long code with Period $2^{42} - 1$. There are two reasons for using the long PN sequence.

1. Channelization the base station separates forward channel traffic by applying different Sequences to different subscribers
2. Privacy Each user uses different long codes, and due to the pseudorandom nature of the Codes, due to they are difficult to decode as different sequences are orthogonal to each other.

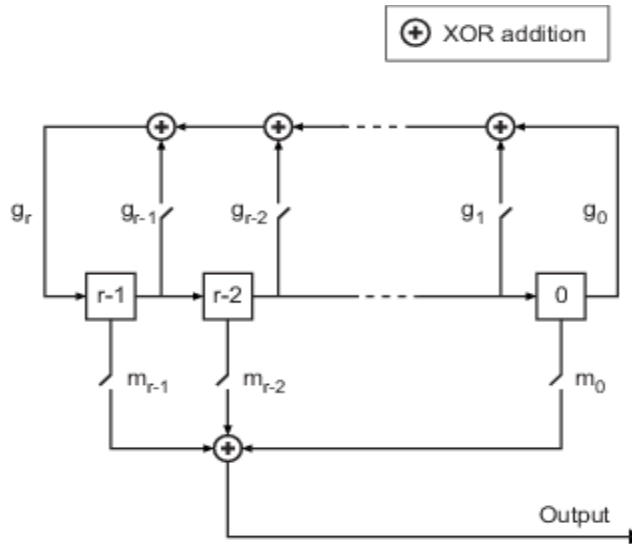


Fig.10. Generating PN sequences

Here are two ways for generating the long PN sequence. First technique uses the Electronic Serial Number (ESN) of the subscriber to generate the long PN sequence and is therefore publicly known if the ESN is known. Second technique generates the long PN sequence Using keys that are known only to the base station and subscriber unit, providing a level of Privacy and preventing simple de-spreading In is-95,it is derived from an M-sequence with $m = 42$ (shift register length). The greater polynomials are a Long Code Mask for generating long PN sequences is illustrated in Fig.10.

B. Orthogonal hadamard code:

Walsh coding is also called as Hadamard code. Walsh coding and it performed after data scrambling in the transmitter. Each data symbol coming Out of the scrambler is replaced by 64 sequence of Walsh chip. Each 64 Walsh chip sequence corresponds to a row of the 64 by 64 Walsh matrix (also called a Handmaid matrix).The Walsh matrix contain one row of all zeros, and the remaining Rows each have an equal number of ones and zeros and Figure3.5shows how a Walsh matrix is generated.

$$\begin{bmatrix} H & H \\ H & -H \end{bmatrix}$$

$$H_1 = \begin{bmatrix} 1 \\ 1 \end{bmatrix}; \text{ And}$$

$$H_2 = \begin{bmatrix} 1 & 1 \\ 1 & -1 \end{bmatrix},$$

$$H_{2^k} = \begin{bmatrix} H_{2^{k-1}} & H_{2^{k-1}} \\ H_{2^{k-1}} & -H_{2^{k-1}} \end{bmatrix} = H_2 \otimes H_{2^{k-1}}$$

Hadamard Matrix formation

Each subscriber is assigned a different row of 64 Walsh chips, depending on the channel Number which it is using, and each subscriber occupies a different channel. For example, if a Subscriber uses 23rd channel, each symbol of the subscriber's scrambled data symbol stream is processed using the 64 Walsh chips of the 23 row of the Walsh matrix. The symbol is simply replaced by the

23rd row Walsh chips when the scrambled data symbol is a 0. On the other hand if the data symbol is a 1, the symbol is replaced by the bit-inverted version of the 23 Row Walsh chips. As a result, Walsh coding increases the data rate from 19.2ksps to 1.2288Mps.

C. Gold code: The Gold Sequence Generator block uses two PN Sequence Generator blocks to generate the preferred pair of sequences, after those XORs to produce the output sequence as shown in Fig.11.

The Gold Sequence Generator block generates a Gold sequence. It forms a large class of sequences that have good periodic cross-correlation properties. The Gold sequences are defined using a specified pair of sequences u and v , of period $N = 2^n - 1$, called a *preferred pair*, and defined in Preferred Pairs of Sequences below.

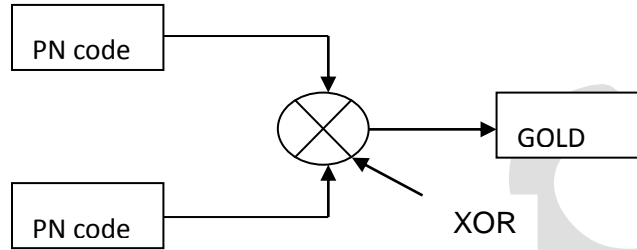


Fig.11. Gold code

The set $G(u, v)$ of Gold sequences is defined. Where T represents the operator that shifts vectors cyclically to the left by one place, and represents addition modulo 2. Note that $G(u,v)$ contains $N + 2$ sequences of period N . It is Generator block outputs one of these sequences according to the block's parameters. Gold sequences have the property that the cross correlation between any two, or in between shifted versions of them.

VI. SIMULATION RESULTS

The performance of MC-CDMA over AWGN channel using both orthogonal Hadamard as well as random codes can be seen in Fig. respectively. We can see that the MC-CDMA performance with orthogonal Hadamard codes does not degrade as the number of user increases, and it degrades with number of users when random codes are used. This is because of cross correlation between random codes increases with the number of users. We can expect when random codes are used over Rayleigh fading channel and AWGN channel, the performance of MC-CDMA will degrade more significantly because cross correlation between random codes will be affected by Rayleigh fading channel and AWGN channel

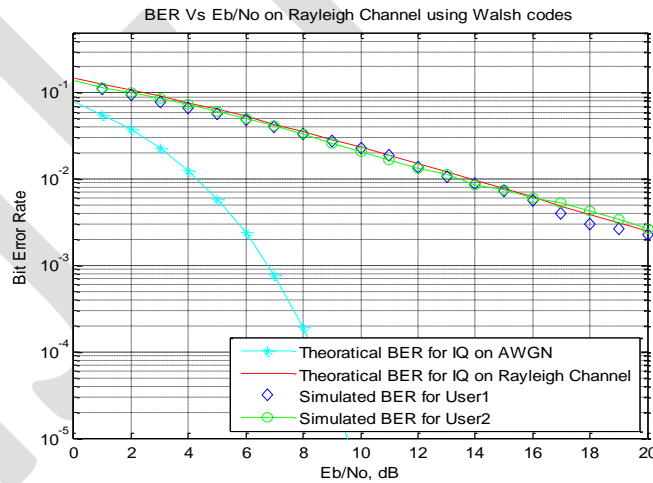


Fig.12. BER Vs Eb/No using Walsh code.

In Fig.12 specifies BER of detected user's with Walsh code.

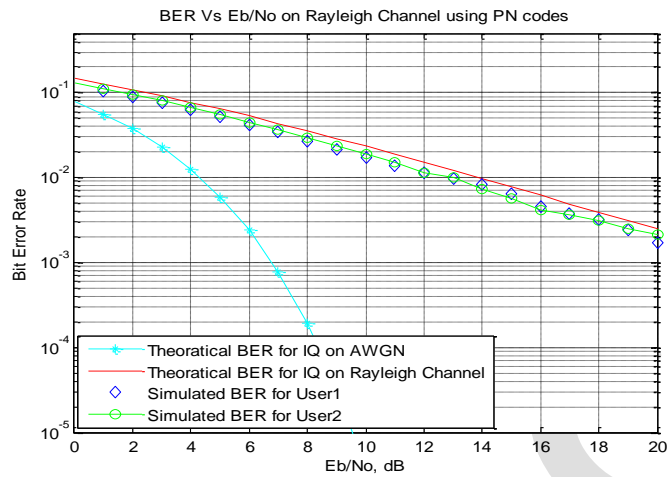


Fig.13.BER Vs Eb/No using PN code.

In Fig.13 specifies BER of detected user's with PN code.

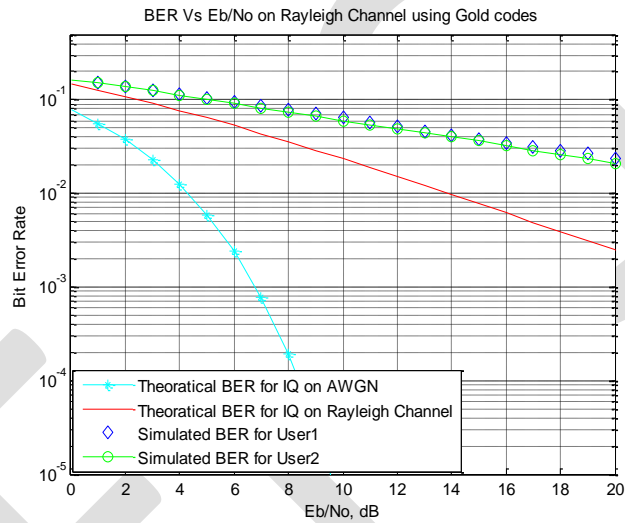


Fig.14.BER Vs Eb/No using Gold code.

In Fig.14 specifies BER of detected user's with Gold code.

VII. CONCLUSION

In MC-CDMA process both Additive White Gaussian Noise (AWGN) and Rayleigh fading channel noises are occur in cellular systems. These noises are evaluated by the performance of MC-CDMA with Long PN sequence, Gold code and Orthogonal Hadamard codes. Simulation is carried out to the performance of MC-CDMA as well as control the bit error rate (BER) as a function of bit energy to noise density ratio (E_b/N_0). Multicarrier CDMA needs more attention for future implementation on wireless data transmission systems. These codes are unique for each user so data reconstruction is much secured. MC-CDMA features are narrow-band interference rejection, high spectral efficiency, multiple accessing capability, frequency selective channels, simple one-tap equalization and flexibility. From the results Walsh (Hadamard) code has Good Bit Error Rate (BER) and Gold code has efficient E_b/N_0 .

REFERENCES:

- [1]. Adit Kurniawan School of Electrical Engineering and Informatics ITB, "Power controlled MC-CDMA in cellular communication systems", Bandung, Indonesia (TSSA) 978-1-4673-4550-7/12, IEEE, 2012.
- [2]. Hsiao-Hwa Chen and Wei-Xiao Meng, "A Survey on Complementary Coded MIMO CDMA Wireless", 1553-877X, 2013 IEEE.
- [3]. L.J.C.Jr. and Y. G. Li., "Orthogonal Frequency Division Multiplexing for Wireless Channels." GLOBECOM, Nov. 1998. Sydney, Australia.

- [4]. H. Bogucka, "Transmission and Reception of the Multicarrier CDMA Signals in the 3rd Generation Mobile Communication Systems," in IEEE Int. Conf. on Wireless Personal Communications, Feb. 1996. New delhi, India. pp. 319-322.
- [5]. Huan Cong Nguyen, Elisabeth de Carvalho and Ramjee Prasad, "Multi-User Interference Cancellation Schemes for Carrier Frequency Offset Compensation in Uplink OFDMA", IEEE Transactions On Wireless Communications, Vol. 13, No. 3, March 2014.
- [6]. Chang-Yi Yang And Bor-Sen Chen, " MC-CDMA Channel Tracking for FastTime -Varying Multipath Fading Channel", Fellow IEEE Transactions On Vehicular Technology, Vol. 59, No. 90018-9545, November 2010.
- [7]. Elisabeth de Carvalho, and Ramjee Prasad, " Statistical Precoder Design for Space-Time -Frequency Block Codes in Multiuser MISO-MC-CDMA Systems", 1932-8184, 2014 IEEE.
- [8]. Xiaoming Chen and Xiumin Wang "Space-Time-Frequency Block Codes in Multiuser MISO-MC-CDMA Systems", 2014 IEEE.
- [9]. Klein S. Gilhausen, "On the Capacity of a Cellular CDMA System Transactions On Vehicular Technology", Vol. 40, No. 2, May 1991 IEEE.

Neural Classifier for the diagnosis of Breast Cancer using Computational Intelligence Techniques

Miss. Sneha Badrinath Sanap

Student of HVPM's College of Engineering & Technology
Amravati (India)

Email Id: snehasanap25@gmail.com

Contact No: 9403399208

Mr. Vijay L. Agrawal

Associate Professor in Dept. (Electronic and Telecommunication)
of HVPM'S College of Engineering and Technology (India)

Abstract— Breast cancer is the most important cause of cancer death for women. Breast Cancer, the dreaded disease is one of the dominant causes of sufferings and death in modern world. Cancer is due to the uncontrolled proliferation of the body's cells resulting in an abnormal growth or disruption of the body's auto-regulation. Its cure rate and prognosis of the patient depends mainly on the early detection and diagnosis of the disease. Detection of Breast cancer in the body of the patient reveals through early symptoms in most of the cases. This study is aim to find out the feasibility of Breast cancer detection by systematic study of the risk factors. An expert system is developed based on supervisory neural network based learning approach, where in initially the input parameters and the output is mappable.

Keywords— Signal & Image processing, neural network, Transformed domain techniques, MATLAB, Microsoft Office Excel, CT scan images ,Different domain Technique like DCT,FFT etc.

INTRODUCTION

Breast Cancer disease is a new growth of tissue resulting from a continuous proliferation of abnormal cells that have the ability to invade and destroy other tissues. Cancer, which may arise from any type of cell and in any body tissue, is not a single disease but a large number of diseases classified according to the tissue and type of cell of origin. In the Indian scenario Breast Cancer disease has become a one of the vital cause of death for women's. Cancer deaths could be controlled to a large extent if this disease is diagnosed at an early stage and proper treatment is given to the patient. Knowledge-based expert systems, or expert systems, use human knowledge to solve problems that normally would require human intelligence. These expert systems represent the expertise knowledge as data or rules within the computer. These rules and data can be called upon when needed to solve problems. Mathematical models have been developed to predict output variable on the basis of input variable. The traditional approach involve simultaneous multiple linear regression analysis and backward elimination of variable to discriminate the most appropriate model. In contrast, new Artificial intelligence models, namely artificial neural networks, can solve problems of classification and estimation even in the presence of non-linear relationship between dependent and independent variable, or of a large database with numerous non-homogeneous variables, or both. The tumor is two types malignant and benign .A tumor does not invade the surrounding tissue called benign tumor. If tumor is invade and damage the surrounding of tumor called malignant tumor of cancer. Our objective was to develop a Computational Intelligence Techniques for distinguishing between benign and malignant pulmonary nodules by use of features extracted from CT Scan Images.

Here, The CT scan images of benign and malignant tumor.

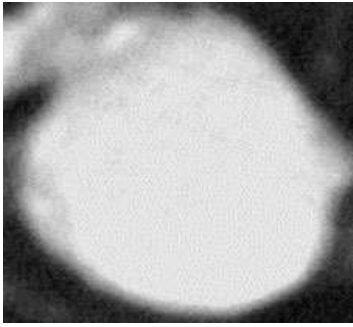


Figure a: Benign Tumor

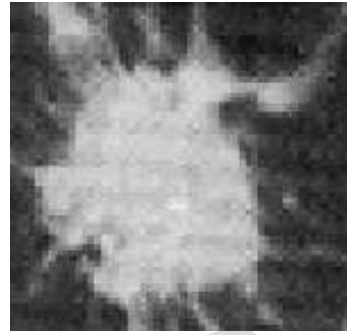


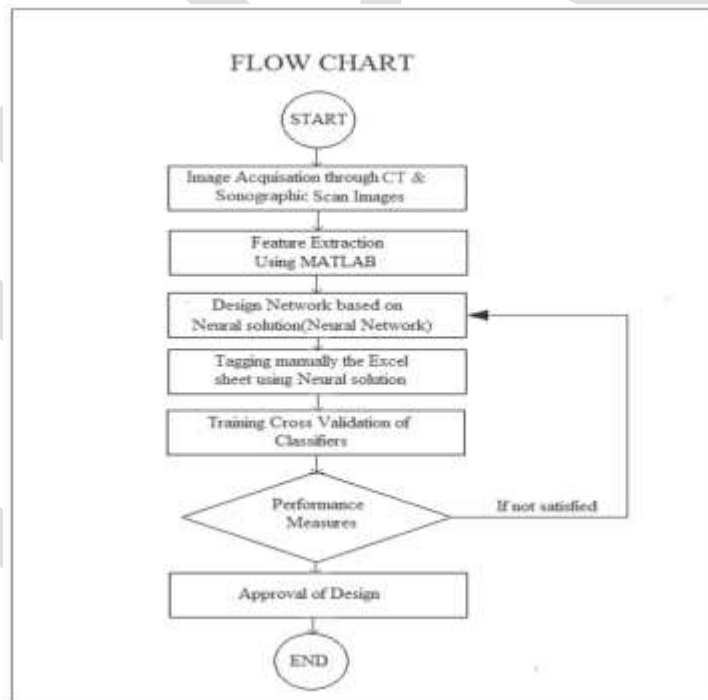
Figure b: malignant tumor

RESEARCH METHODELOGY

It is proposed to study Efficient Classification of Breast Tumor using Neural Classifier. Data acquisition for the proposed classifier designed for the diagnosis of Breast Cancer shall be in the form of CT Scanned and sonographic images. Image data will be collected from the different- different hospitals of the country .The most important uncorrelated features as well as coefficient from the images will be extracted .In order to extract features, statistical techniques, image processing techniques, transformed domain will be used.

For detection of Breast cancer following technique will be used

Statistics, Image processing, Transformed domain techniques. The research work Software's such as Matlab, Neuro solutions, XL Stat will be used.



RESEARCH OBJECTIVE

- 1] To maintain the correctness & accuracy in the diagnosis of Breast cancer.
- 2] To increase the accuracy for the diagnosis of Breast cancer.
- 3] To reduce confusion between of benign tumor, malignant tumor.

LITERATURE SURVEY

1] Artificial Neural Networks classifiers have been used in a variety of applications ranging from industrial automation to medical diagnosis. Because of its characteristics like fast learning, adaptability, fault tolerance, solving complex non linear problems efficiently, good recognition Neural Networks are being used in the medical domain to benefit the medical fraternity and patient's community alike, as opposed to the conventional methods. In the present paper we have conducted a survey which includes a detailed review of the various applications where Neural Networks have been used in Breast Cancer diagnosis in the recent years. Neural Networks classifiers have been used in a medical diagnosis because of its characteristics like fast learning.

2] A three-layer, feed-forward, artificial neural network with a back-propagation algorithm. And its outcome of research is this scheme has improved the diagnostic accuracy of radiologist who is differentiating benign from malignant pulmonary nodules on high-resolution CT.

3] Neural-digital computer intelligence technique system based on a parameterized two-level convolution neural network and on a special multi label output encoding procedure. In this Receiver Operating characteristic (ROC) method with area under the ROC(Az) as the performance index. And its outcome of research It is proven to be promising and to be extensible, problem-independent and applicable to other medical diagnostic task in 2-D image environment

ACKNOWLEDGMENT

We are very grateful to our HVPM College of Engineering and Technology to support and other faculty and associates of ENT department who are directly & indirectly helped me for these paper

CONCLUSION

Use of the proposed Efficient Classification of Breast Tumor using Neural Classifier and Computational Intelligence Techniques will be result in more accurate and reliable diagnosis of Breast cancer disease.

REFERENCES:

- [1] Brijesh Verma and John Zakos.: "A Computer-Aided Diagnosis System for Digital Mammograms Based on Fuzzy-Neural and Feature Extraction Techniques": IEEE TRANSACTIONS ON INFORMATION TECHNOLOGY IN BIOMEDICINE, VOL. 5, NO. 1, MARCH 2001.
- [2] Elise C. Fear, Xu Li, Susan C. Hagness, and Maria A. Stuchly.: "Confocal Microwave Imaging for Breast Cancer Detection: Localization of Tumors in Three Dimensions.: IEEE TRANSACTIONS ON BIOMEDICAL ENGINEERING, VOL. 49, NO. 8, AUGUST 2002.
- [3] Essex J. Bond, Susan C. Hagness, and Barry D. Van Veen.: Microwave Imaging via Space-Time Beamforming for Early Detection of Breast Cancer.: IEEE TRANSACTIONS ON ANTENNAS AND PROPAGATION, VOL. 51, NO. 8, AUGUST 2003.
- [4] Segyeong Joo, Yoon Seok Yang, Woo Kyung Moon, and Hee Chan Kim.: Computer-Aided Diagnosis of Solid Breast Nodules: Use of an Artificial Neural Network Based on Multiple Sonographic Features.: IEEE TRANSACTIONS ON MEDICAL IMAGING, VOL. 23, NO. 10, OCTOBER 2004
- [5] Mark Converse, Essex J. Bond, Barry D. Van Veen, F and Susan C. Hagness.: A Computational Study of Ultra-Wideband Versus Narrowband Microwave Hyperthermia for Breast Cancer Treatment.: IEEE TRANSACTIONS ON MICROWAVE THEORY AND TECHNIQUES, VOL. 54, NO. 5, MAY 2006.
- [6] Shivang Naik, Scott Doyle, Shannon Agner, Anant Madabhushi and Michael Feldman, +John Tomaszewski.: AUTOMATED GLAND AND NUCLEI SEGMENTATION FOR GRADING OF PROSTATE AND BREAST CANCER HISTOPATHOLOGY.: 978-1-4244-2003-2/08/\$25.00 ©2008 IEEE.
- [7] Jinshan Tang, S, Rangaraj M. Rangayyan, Jun Xu, Issam El Naqa, and Yongyi Yang.: Computer-Aided Detection and Diagnosis of Breast Cancer With Mammography: Recent Advances.: IEEE TRANSACTION ON INFORMATION TECHNOLOGY IN BIOMEDICAL VOL. 13, NO. 2, MARCH 2009.

- [8] Robert A. McLaughlin, Bryden C. Quirk, Andrea Curatolo, Rodney W. Kirk, Loretta Scolaro, Dirk Lorensen, Peter D. Robbins, Benjamin A. Wood, Christobel M. Saunders, and David D. Sampson.: Imaging of Breast Cancer With Optical Coherence Tomography Needle Probes: Feasibility and Initial Results.: IEEE JOURNAL OF SELECTED TOPICS IN QUANTUM ELECTRONICS, VOL. 18, NO. 3, MAY/JUNE 2012.
- [9] Karthikeyan Ganesan, U. Rajendra Acharya, Chua Kuang Chua, Lim Choo Min, K. Thomas Abraham, and Kwan-Hoong Ng.: Computer-Aided Breast Cancer Detection Using Mammograms: A Review: IEEE REVIEWS IN BIOMEDICAL ENGINEERING, VOL. 6, 2013.
- [10] Mitko Veta*, Josien P. W. Pluim, Paul J. van Diest, and Max A. Viergever "Breast Cancer Histopathology Image Analysis: A Review" IEEE TRANSACTIONS ON BIOMEDICAL ENGINEERING, VOL. 61, NO. 5, MAY 2014
- [11] D. Krag, D. Weaver, T. Ashikaga, F. Moffat, V. S. Klimberg, C. Shriver, S. Feldman, R. Kusminsky, M. Gadd, J. Kuhn, S. Harlow, and P. Beitsch, "The sentinel node in breast cancer: A multicenter validation study," N. Engl. J. Med., vol. 339, no. 14, pp. 941–946, 1998
- [12] S. A. Boppart, W. Luo, D. L. Marks, and K. W. Singletary, "Optical coherence tomography: Feasibility for basic research and image-guided surgery of breast cancer," Breast Cancer Res. Treat., vol. 84, pp. 85–97, 2004.
- [13] A. M. Zysk and S. A. Boppart, "Computational methods for analysis of human breast tumor tissue in optical coherence tomography images," J. Biomed. Opt., vol. 11, no. 5, pp. 054015-1–054015-7, 2006.
- [14] F. T. Nguyen, A. M. Zysk, E. J. Chaney, J. G. Kotynek, U. J. Oliphant, F. J. Bellafiore, K. M. Rowland, P. A. Johnson, and S. A. Boppart, "In- traoperative evaluation of breast tumor margins with optical coherence tomography," Cancer Res., vol. 69, no. 22, pp. 8790–8796, 2009.
- [15] C. Zhou, D. W. Cohen, Y. Wang, H.-C. Lee, A. E. Mondelblatt, T.-H. Tsai, A. D. Aguirre, J. G. Fujimoto, and J. L. Connolly, "Integrated optical coherence tomography and microscopy for ex vivo multiscale evaluation of human breast tissues," Cancer Res., vol. 70, no. 24, pp. 10071–10079, 2010.

An Effective Combined Cooling with Power Reduction for Refrigeration cum Air Conditioner, Air Cooler and Water Cooler: A Review

A. S. Dhunde¹, Prof. K. N. Wagh², Dr. P. V. Washimkar³

¹ M. Tech. Student, Mechanical Engineering Department, Guru Nanak Institute of Technology, Nagpur, India

Email:ashishdhunde@gmail.com, Mob No.08983273202

²Asst. Professor, Mechanical Engineering Department, Guru Nanak Institute of Technology, Nagpur, India

³Associate Professor and Head, Mechanical Engineering Department, Guru Nanak Institute of Technology, Nagpur, India

Abstract- In 21st century the world facing problem of electricity, to overcome this problem worldwide many researches going on. Many of the world's largest growing industries as well as electricity producers companies said that around 30% of electricity is consumption worldwide for the application of refrigeration and air conditioning. The manufacturers of refrigerants and refrigeration, air conditioning equipment, governmental agencies, and environmental groups continue working together toward the goal of reduced environmental impact via reduced emissions and improved energy efficiency. Examples of progress are presented for several sectors of refrigeration and air conditioning, followed by projections for further significant reductions. Although this paper will emphasize environmental impact for power reduction. Looking forward refrigeration has adverse effect on environment. Further cooler uses water so as to give cool air outside, for this application much more quantity of water has been used every year. Also to make this efficient woods product known as 'wood wool / khas' have been used which became a major reason of deforestation. To restrict all these, an attempt is made to have an optimized unit of refrigeration cum air conditioning which will overcome the problem of electricity required for running both the application so far and again help to save water and wood, also maintain an ecological balance between people and surrounding. Both the system will run on single cost of refrigerator so that the normal person can afford the system and will have pleasure to take a pleasant comfort.

Keywords: Refrigeration and Air conditioning, Optimized, Deforestation, Ecological Balance, Emphasize, Consumption, Pleasant

Introduction:

Cooling systems like air conditioning, Refrigerator, Air Coolers, Water Cooler systems are high electric power consumption's; these systems also have huge impacts on the ecosystem. A proper use or choice with an energy saving plan should be considered in order to make the development of ecosystem sustainable so that a harmony between people and environment could be formed. The best innovative work has done in 20th century was refrigeration where Refrigerator recognized and developed in earlier of 20th century and Air Conditioner is lately in that of 20th century. However it has become the prime necessity in 21st century. In over span of three decades, there is continuously increase in energy demand due to everlasting population increases in India. This has led to increase in pollution and power cost that cannot be afforded by normal person. The continuous cycling observed in those equipment's reduces their lifetime and increases power requirement. Worldwide acknowledge and said that refrigeration and air conditioning systems are responsible for roughly 30% of total energy consumption, therefore unquestionably with a major impact on energy demand. Researchers in many countries have been involved in developing refrigeration and air conditioning systems that deal with the drawbacks of conventional systems. The need of proper energy consumption is a worldwide concern and the big question arises for reducing energy wasting included proper used of energy and also how to lower power consumption. Instead of all these aim must be achieved without compromising comfort and other advantages brought by the use of energy, and with same efficiency and quality of installations. The concept of this project explores the possibility of combining four units i.e. Refrigerator and Air-Conditioner, Air-Cooler, Water Cooler into a single unit, such that the running cost should be reduced. This is how we are trying to make the environment and a common person comfortable. By this product a normal person could have a sound sleep so that his productivity for the next day increases.

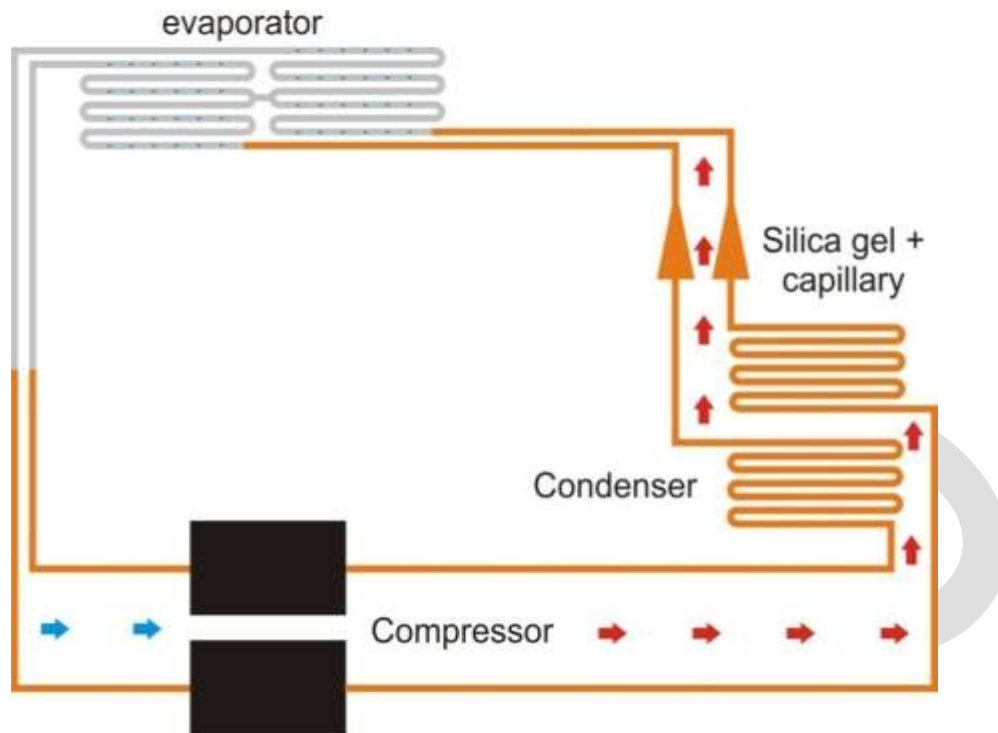


Fig. 1 Schematic diagram of Refrigeration Cycle (VCRS)

Literature Review:

L.O.S. Buzelina, S. C. Amicoa, [1] et.al (2005) discuss on an alternative solution to reduce energy consumption in industrial refrigeration systems is proposed and introduced. A typical industrial refrigeration system was conceived, built and modified in the laboratory, receiving a novel power law control system, which utilizes a frequency inverter. The operation and energy consumption of the system operating either with the new control system or with the traditional on-off control were compared to realistically quantify the obtained gains. In this manner, the measured temperature data acquired from several points of both systems and the energy consumption in kW h during a 24 h experimental run period are compared. From the experiment he concluded that the closed-loop power law controlled system shows a much smaller variation of the cold chamber internal temperature and electrical energy consumption economy of 35.24% in comparison with the traditional on-off system, under the same operating conditions.

U. V. Kongre, M. B. Salunkhe, [2] et.al (2013) discussed about the design contributions for evaporator, condenser and capillary tube. Based on conventional methodologies the design calculations were done. Further discusses the designed methods which are suitable for combined conventional air-conditioning and dispenser.

Tassou and Qureshi, [3] et.al (1994) showed that the use of a frequency inverter in refrigeration for compressor speed control may cause harmonic distortions in the systems and a power factor reduction which, in turn, increases energy consumption. However, benefits such as a better temperature control and a lower response time for abrupt thermal load changes were also mentioned.

M. Fande, A. M. Andhare [4] et.al (2015) discuss on the experimental investigation of the effect of HFC refrigerant R134a on a vapour compression refrigeration system by using two expansion devices with the conservation of energy by waste heat recovery system. He used two different evaporators for air cooling and water chilling respectively and a water cooled condenser is used to produce hot water. The existing system can be easily retrofitted as a waste heat recovery device and the existing R22 refrigerant can be replaced by R134a with minor modifications. After experimentation the maximum temperature achieved in water tank with 50 litre of water is 45 C during 3 to 4 working hour. After that performance of system decreases so it needs a regular use of that hot water which can be further used for household and industrial purposes.

Prof. S. K Gupta [5] et.al (2014) has discussed about the attempt he made to merge Domestic Refrigerator and Air conditioner into a combined system such that an ordinary man can have a sound sleep which automatically increases his working productivity for the next day. To fulfilled it in minimum construction, maintenance and running cost, he made an attempt which is quite useful for domestic purpose so that his ultimate aim of the project that is those who cannot afford an Air Conditioner can have the comfort of Air Conditioner could be completed.

S. A. Nada et.al [6] published a paper on“Performance analysis of proposed hybrid air conditioning humidification-dehumidification system for energy saving and water production in hot and dry climatic region” in which he discussed onThe objective behind the proposed system is energy saving and production of fresh water.

J. K. Dabas et.al [7] discuss about his study on the behavior of performance parameters of a simple vapour compression refrigeration system while its working under transient conditions occurred during cooling of a fixed mass of brine from initial room temperature to sub-zero refrigeration temperature. The effects of different lengths of capillary tube over these characteristics have also been examined. It was concluded that Larger capillary tube decreases the tendency of refilling of evaporator but offers less ‘evaporator temperature’ effective in lower range of refrigeration temperature. Shorter capillary tube ensures higher COP initially but which deteriorates at a faster rate in lower temperature range. Capillary tube length must be optimized for maximum overall average COP of the system for the complete specified cooling job.

Tarang Agarwal et.al [8] discussed in his paper about a cost-effective method to increase the COP and utility of a domestic refrigerator using R-134a refrigerant. In his experiment a cabin was installed on the top of a domestic refrigerator with condenser coils of refrigerator serving as heating coils inside the cabin. Known quantity of water was heated by the condenser coils thereby increasing the overall COP of the refrigerator. Further, the utility was increased since it can serve the purpose of cooking (oven), geysers etc. Besides, the refrigerator may be used as conventional refrigerator by keeping the cabin door open in case of absence of heat sink. He was concluded that one can increase the COP upto 11% just by using a cabin on the top of the refrigerator unit. Further increase in COP is possible; however enhancements will involve higher costs.

M.R. Abdelkader et.al [9] discuss on free cooling techniques can be used to substantially reduce energy costs. During cold weather, the outside ambient temp help in saving energy in refrigeration work. The minimum temperature of the ambient air supply enables free cooling technique to store fresh fruits and vegetables. This technique of energy-efficiency measure can save enough compressor electric power to pay for modulating damper installation costs in approximately one year. Free cooling has a kind of motorized damper that conducts the two flows of internal and external air. When the damper is open it takes the air necessary cooling directly from the exterior, excluding compressor operation. It starts the evaporator fan that takes external air if $T_{\text{external}} < T_{\text{internal}}$. A case study has been carried out for 17 Ton cooling load in a storage room and the COP can be reached to the only energy consumption is from the use of evaporative fans.

Raman Kumar Singh [10] (2015) discuss about the Human comfort conditions deal with the conditions of environment around us, viz. hot and cold. The control of temperature of air around us is done by controlling the output water from the water cooler. He made a novel idea to control air temperature around us by the incorporation of cooling system in a single unit. This unit would be an economic utility at all places to provide comfort conditions to the people. Faster, mightier & smaller is still the keyword for every invention and development he concentrate on the compactness and efficiency of every product. Accordingly he have designed and fabricate an economical and reliable unit known as —Water Cum Room Cooler(Three in one air conditioner).

Dr. U. V. Kongre, et.al [11] (2013) discuss about the multifunctional system he was built which gave output hot and cold water with hot and cold air . The paper introduced basic design principles and the test analysis performed in the laboratory also mentioned comfort conditions and suitable coefficient of performance with respect to atmospheric condition, without sacrificing the air conditioning output. The air-conditioner cum water dispenser was manufactured for air, water & air-water cycle combined. The air cycle provides good results with conventional optimum efficiency. The water cycle also predicts better results, but then water cycle alone is not useful. Hence the combine air conditioner cum dispenser by utilizing conventional air-conditioning. The dispenser gives required efficiency in terms of coefficient of performance.

K. Nagalakshmi et.al [12] (2014) discuss about the design and performance analysis of refrigeration system using R12 & R134a refrigerants.The purpose he mentioned behind his research is to investigate behavior of R134a refrigerant. This includes performance and efficiency variations when it replaces R12 in an existing system as well as changes involved in maintaining the system charged

with R134a. After demonstration on his project he found that, from the results and graphs that COP of R12 is little greater than COP of R134a. Even though COP of R12 is greater than R134a it must be replaced with R134a because R134a refrigerant is non-toxic and does not flare up within the whole range of operational temperatures, Ozone depletion potential ODP=0, global warming potential GWP=0.25 and Estimated Atmospheric life EAL=16. Again in high temperature refrigeration facilities, specific cold-productivity when operating on R134a is also a bit higher than that of R12. Further increasing of dehumidifying ability of filter dehydrators due to high hygroscopic property of R134a system-synthetic oil.

Vivek Sahu, Pooja Tiwari, et.al [13], (2013) has published a paper on “ Experimental Investigation of the Refrigerator Condenser by varying the fin spacing of the condenser”. This paper presents the experimental analysis of domestic refrigeration system by using wire operating parameters like heat transfer rate, condenser pressure and condenser temperature, refrigerating effect is increased by using wire-on-tube condenser comparatively power consumption remain same as with air cooled condenser in a domestic refrigeration system. Therefore wire-on-tube condenser can replace the ordinary air cooled condenser in a domestic refrigeration system and in this he mentioned that Discharge pressure with small fins spacing is highest than the larger fins spacing used in same project.

S. C. Walawade, B. R. Barve, et.al [14] has published a paper on “Design and Development of Waste Heat Recovery System for Domestic Refrigerator”. The main objective of this paper is to study “Waste Heat recovery system for domestic refrigerator”. An attempt has been made to utilize waste heat from condenser of refrigerator. This heat can be used for number of domestic and industrial purposes. The study has shown that such a system is technically feasible and economically viable also he made an attempt to recover the waste heat from 165 L refrigerator used for domestic purpose and from this he concluded that this combination of refrigerator and food warmer is efficient and it will help to conserve an enormous amount of energy.

Dr. A. G. Matani, Mukesh K. Agrawal [15] has published a paper on “Effect of capillary diameter on the power consumption of VCRS using different Refrigerants”. In which he discussed about experimental study he was conducted to observe the Power consumption of different environmental friendly refrigerant mixtures (HC mixture and R401a) and he observed the effect of working parameters like diameter of capillary tube, working pressures and inlet water temperatures, which affect the power consumption of vapour compression refrigeration system. It was observed that R401a consumed more power than HC mixture and R134a, but there is less mass quantity of HC mixture and R401a is required in the same system. So there is less effect in environment due to leakage further he analysed a system with the new refrigerant blend as substitute for R134a was made and concluded that Power consumption per ton of refrigeration of HC mixture (R290/R600a) was lower than other two refrigerants at all working pressure and inlet water temperature at capillary diameter 0.050 inch. So it can be used as Working medium in air conditioning system. also Power consumption per ton of refrigeration of R401a is always higher than other two refrigerants, so it is not efficient in use in general purpose.

Jala Chandramouli, Dr. E.V.Subbareddy [16] et.al (2015) has published a paper on “Design, Fabrication and Experimental Analysis of Vapour Compression Refrigeration System with Ellipse shaped Evaporator coil.” In this paper he discussed about objective his project is to increase the performance of the system by increasing the heat transfer rate through the evaporator. Heat transfer from the evaporator increased by the changing the shape of the evaporator and by extended surfaces. He used to conduct an experiment for the ellipse shaped design evaporator of a vapour compression refrigeration system used for a domestic refrigerator of 165 liter's capacity. By incorporating the ellipse shaped evaporator of the refrigeration system he concluded that the C.O.P enhance of by 1.5%, as a result of 1.5% increase in refrigeration effect and 1% reduction in compressor work and same in heat absorption. Further, system pressure is slightly increased, the ellipse shaped evaporator increases the C.O.P compared to existing evaporator, which is perhaps due to reduction in compressor work and increase in refrigeration effect.

P. Sarat Babu, Prof. N. Hari Babu, [17] (2013) has published a paper on “Experimental Study of A Domestic Refrigerator/Freezer Using Variable Condenser Length.” In which he used to optimize condenser length for domestic refrigerator of 165 litres capacity. It may give a chance to find a different length other than existing length will give better performance and concluded that the optimum length of coil is 7.01m also through his experimental investigation he found that the optimum length of coil is 7.01 m instead of standard value 6.1m.

S. B. Lokhande, Dr. S. B. Barve [18] (2014) has published a paper on “Design & Analysis of Waste Heat Recovery System for Domestic Refrigerator.” In which he discussed the objective of his paper is to study “Waste Heat recovery system for domestic

refrigerator". An attempt has been made to utilize waste heat from condenser of refrigerator. This heat can be used for number of domestic and industrial purposes. In minimum constructional, maintenance and running cost, this system is much useful for domestic purpose. It is valuable alternative approach to improve overall efficiency. From the results tabulated it can be concluded that with time the energy consumption of the refrigerator decreases for certain time and then it remain constant. The refrigerating effect keeps decreasing as the temperature difference between the refrigerant and article placed is decreased. The C.O.P. remains almost constant though it decreases a little bit. With hot case, as if we add up heating effect in desired effect, then the c.o.p. is increased.

Adrian Mota-Babiloni, Joaquin Navarro-Esbri, et.al [19] (2015) has published a paper on "Commercial refrigeration- An overview of current Status" in which he discussed about the most recent developments in commercial refrigeration available and also mentioned a good amount of results provided these systems, covering some advantages and disadvantages in systems and working fluids. He mentioned about latest researches which have objective of energy savings and to reduce CO₂ indirect emissions due to the burning of fossil fuels. He also discussed about system modifications trigeneration technologies and better evaporation conditions control. Further he concluded as his paper reviews the state-of art of recent developments and contains and covers important topics such as supermarket refrigeration system energy efficiency, GHG emission control regulations, HFC phase-out and low GWP alternatives. The important point mentioned here is energy consumption analysis of each supermarket is very important to identify the most beneficial energy saving techniques. From the analysis of supermarket he mentioned in paper, Among all Trigeration is an interesting option in supermarkets that produces great energy and CO₂ emission savings, especially when CO₂ is the working fluid selected. New GHG regulations impose strong GWP limitations that are going to phase out currently used HFC refrigerants in commercial refrigeration.

S. A. Nada, H. F. Elattar et.al [20] (2015) discussed about Performance of integrative air-conditioning (A/C) and humidification–dehumidification desalination systems proposed for hot and dry climatic regions. The proposed systems aim to energy saving and systems utilization in fresh water production. Four systems with evaporative cooler and heat recovery units located at different locations are proposed, analyzed and evaluated at different operating parameters. Other two basic systems are used as reference systems in proposed systems assessment. Fresh water production rate, A/C cooling capacity, A/C electrical power consumption, saving in power consumptions and total cost saving (TCS) parameters are used for systems evaluations and comparisons. After analyzing the system results show that the fresh water production rates of the proposed systems increase with increasing fresh air ratio, supply air temperature and outdoor wet bulb temperature, powers saving of the proposed systems increase with increasing fresh air ratio and supply air temperature and decreasing of the outdoor air wet bulb temperature, locating the evaporative cooling after the fresh air mixing remarkably increases water production rate, and incorporating heat recovery in the air conditioning systems with evaporative cooling may adversely affect both of the water production rate and the total cost saving of the system..

Kiyoshi Saito et.al [21] (2012) has published a paper on "Latest system simulation models for heating, refrigeration, and air-conditioning systems, and their Applications" in which he discussed about the simulation model they create for a heat pump, room air-conditioner, desiccant dehumidifier, indirect evaporative cooler, fuel cell, solar panel in order to reduce the energy consumption in the refrigeration and air conditioning. Again Paper describes high-accuracy simulation models for a CO₂ heat pump, absorption heat pump, and desiccant dehumidification system also discuss the simulator that they developed, based on those models for reducing energy consumption.

Chengchu Yan, Xue Xue, et.al. [22] (2015) has published a paper on " A novel air-conditioning system for proactive power demand response to smart grid." In which he discussed about a novel air conditioning system with proactive demand control for daily load shifting and real time power balance in the developing smart grid. This system consists of a chilled water storage system (CWS) and a temperature and humidity independent control (THIC) air-conditioning system, which can significantly reduce the storage volume of the chilled water tank and effectively enable a building with more flexibility in changing its electricity usage patterns. The power demand of the proposed air-conditioning system can be flexibly controlled as desired by implementing two types of demand response strategies: demand side bidding (DSB) strategy and demand as frequency controlled reserve (DFR) strategy, in respond to the day-ahead and hour-ahead power change requirements of the grid, respectively.

Conclusion:-

As per experimental study to reduce electricity consumption for refrigeration cum air conditioner, air cooler and water cooler, Also save water and forest which are affected a great impact to maintain an ecological balance and to make it cost effective, so normal person can offered this product. Environmental groups and governmental agencies have cooperated over the last two decades to bring about reductions in refrigeration and air conditioning systems energy consumption and refrigerant emissions.

The reductions have been possible through a combination of factors:

Increased environmental impact awareness, commitment of industry personnel, improved systems technology and operating/service procedures, and governmental regulations. These successes give us great confidence in continuing efforts for reduction of climate change impact of refrigeration and air conditioning system. HFC refrigerants have high societal value in providing safe and reliable refrigeration and air conditioning. At equivalent costs of other options, climate change impact from minimal refrigerant emissions can be more than offset by improved energy efficiency

REFERENCES:

- [1] L.O.S. Buzelina, S. C. Amicoa, (2005) 'Experimental development of an intelligent refrigeration system', International Journal of Refrigeration 28,165–175.
- [2] U. V. Kongre, M. B. Salunkhe, A. A. Pohekar, (2013) 'Design Methodologies of air-conditioner cum water dispenser', International Journal of scientific research and management (IJSRM) ,Volume1,Issue 1, Pages 18-22.
- [3] S. A. Tassou, T. Q. Qureshi, (1994) 'Performance of a variable-speed inverter motor drive for refrigeration applications, Compute Control Eng J 5 (4) 193–199.
- [4] M.Fande, A. M. Andhare, (2015) 'Experimental Investigation and Performance Evaluation of a Three in one Vapour Compression System using Refrigerant R134a', International Journal of Engineering Research & Technology, Volume 4, Issue 05, Pages 1109-1112.
- [5] Prof. S. K. Gupta, (2014) 'Feasibility Study and Development of Refrigerator cum Air Conditioner', International Journal of scientific and research publication, Volume4, Issue12.
- [6] S. A. Nada, (2015) 'Performance analysis of proposed hybrid air conditioning humidification-dehumidification system for energy saving and water production in hot and dry climatic region', Energy Conversion and Management, Volume 96, Page No. 208-227.
- [7] J. K. Dabas, A. K. Dodeja, (2011) 'Performance Characteristics of "Vapour Compression Refrigeration System" Under Real Transient Conditions', International Journal of Advancements in Technology, Vol. 2 No. 4.
- [8] Tarang Agarwal, (2014) 'Cost-Effective COP Enhancement of a Domestic Air Cooled Refrigerator using R-134a Refrigerant', International Journal of Emerging Technology and Advanced Engineering, Volume4, Issue11.
- [9] M. R. Abdelkader, (2010) 'Efficiency of Free Cooling Technique in Air Refrigeration Systems', Jordan Journal of Mechanical and Industrial Engineering, Volume4, Number6, Pages711–724.
- [10] Raman Kumar Singh, (2015) 'Design and Fabrication in one air conditioning', International Journal of Research in Computer Applications and Robotics, Vol. 3, Issue 6, Pages 8-14.
- [11] Dr.U. V. Kongre, (2013) 'Testing and Performance Analysis on Air Conditioner cum Water Dispenser', International Journal of Engineering Trends and Technology (IJETT), Volume4, Issue4.

- [12] K. Nagalakshmi, G. Marurhiprasad Yadav,(2014) 'The design and performance analysis of refrigeration system using R12 & R134a refrigerants', International Journal of Engineering Research and Applications, ISSN 2248-9622,Vol.4,Issue 2(Version 1), Page No. 638-643.
- [13] Vivek Sahu, Pooja Tiwari, K.K Jain and Abhishek Tiwari, (2013) 'Experimental Investigation of the Refrigerator Condenser by varying the fin spacing of the condenser', International Journal of Mechanical Engineering and Robotics, ISSN 2321-5747,Vol.-1,Issue-1.
- [14] S. C. Walawade, B. R. Barve, P.R. Kulkarni, 'Design and Development of Waste Heat Recovery System for Domestic Refrigerator', International Journal of Mechanical Engineering and Civil Engineering, ISSN 2278-1684, Page No.28-32.
- [15] Dr. A. G. Matani, Mukesh K. Agrawal,(2013) 'Effect of capillary diameter on the power consumption of VCRS using different Refrigerant', International Journal of Application or Innovation in Engineering & Management, ISSN 2319-4847, Volume 2, Issue 3.
- [16] Jala Chandramouli, C. Shreedhar, Dr.E.V.Subbareddy, (2015) 'Design, Fabrication and Experimental Analysis of Vapour Compression Refrigeration System with Ellipse shaped Evaporator coil', International Journal of Innovative Research in Science, Engineering And Technology, ISSN 2347-6710, VOL.4.
- [17] P. Sarat Babu, Prof. N. Hari Babu, (2013) 'Experimental Study of A Domestic Refrigerator/Freezer Using Variable Condenser Length', International Journal of Engineering Research And Technology, ISSN 2278-018,Vol.2,Issue12.
- [18] S. B. Lokhande, Dr. S. B. Barve, (2014) 'Design & Analysis of Waste Heat Recovery System for Domestic Refrigerator', International Journal of Modern Engineering Research, ISSN 2249-6645,Vol. 4, Issue 5.
- [19] Adrian Mota-Babiloni, Joaquin Navarro-Esbri, (2015)'Commercial refrigeration- An overview of current Status', International Journal of Refrigeration 57,186-196.
- [20] S.A. Nada, H.F. Elattar,(2015)'Performance analysis of proposed hybrid air conditioning and humidification dehumidification systems for energy saving and water production in hot and dry climatic regions', Energy Conversion and Management 96 , 208–227.
- [21] Kiyoshi Saito, (2012) 'Latest system simulation models for heating, refrigeration, and air-conditioning systems, and their Applications', International Journal of Air-Conditioning and Refrigeration, Vol. 20, No. 1 ,1230001 (13 pages).
- [22] Chengchu Yan, Xue Xue, (2015)'A novel air-conditioning system for proactive power demand response to smart grid', Energy Conversion and Management 102 239–246

IMPACT OF QUALITY DEGRADATIONS ON VIDEO FACE ANALYSIS

Manjunatha S B, Vineesh P, Bhaushi Aiyappa C

Coorg Institute of Technology, Ponnampet, Coorg-District, Karnataka, manjupuneeth99@gmail.com, 9611962024

Abstract— Compare to high-resolution analysis, the low-resolution face analysis suffers more significantly from quality degradations. In this work, we will investigate how some face analysis steps are influenced by low image quality and how this links to the low resolution. Effects of several quality degradations, namely low resolution, compression artifacts, motion blur and noise is analyzed. Depending on the condition, it becomes obvious that the low resolution is sometimes a minor degrading effect, outmatched by a single one or combination of the further effects. Typical counter measures are individual to one single effect, so when addressing real-world face recognition from surveillance data, the combination of the challenging effects is the biggest problem.

Keywords— Image resolution, compression artifacts, motion blur, noise.

[1] INTRODUCTION

Face analysis for low-quality data remains a challenge, while face analysis for high-quality material is a well studied topic. In spite of the increasing interest in the topic, the progress often remains behind the expectations of the potential users. This is mainly induced by the fact that no single effect is responsible for low data quality, but a variety in combination. Thus, approaches addressing one quality degrading effect have difficulties to prove their benefit in real world data, which always comprise a combination of several degradation effects. Apparently, the first effect that comes into mind is the low resolution. Even so, the effects of face resolution are usually only partially responsible for low quality with a lot of further effects contributing to it. Effects of some quality influencing effects, namely resolution, compression, motion blur and noise is analyzed. The selection represents our distinctive observations in the case of surveillance video footage and its forensic analysis. Our work is actuated by the application of surveillance video analysis, particularly in a forensic way. Face recognition is a useful tool in this domain to detect further occurrences of a criminal person in the data. Thus, the work we are faced with is low quality to low quality face comparison. Fundamentally, the processing involves five steps, face detection, face registration, face normalization, face feature extraction and face feature comparison. Face detection is probably the most robust step for low image quality, while the subsequent steps are still experiencing greater difficulties. While high-quality face recognition is able to bring out impressive results, even surpassing the human performance on particular data sets [06], low-quality face recognition faces several additional challenges. The biggest problems for low-resolution face recognition are misalignment, noise affection, lack of effective features and dimensional mismatch among probe and gallery [07]. This list addresses the quality problem only roughly by combining all quality faults under the term noise affection. Lack of effective features and Misalignment are consequences thereof and will be considered as such. Ultimately, dimensional mismatch is no major concern in our scenario which includes comparing low quality faces to further low quality faces. The effect, simulation of the effect, counter measures of several quality degradations namely low resolution, compression, motion blur and noise are discussed for face analysis.

[2] LITERATURE REVIEW

The recognition of human faces in video of low resolution is difficult. With the wide use of camera (surveillance etc.), solutions which solve such type of problems achieve more and more attention. The two main methods are Super Resolution (SR) and Multiple Resolution faces (MRF) approach. The former can be applied to compute high-resolution facial image from low-resolution ones. Even so, the disadvantage is that the multiple facial images that pertain to the same subject captured from same scene are needed. MRF [1] overcame such drawback; it increases the complexity and requires greater memory storage in face recognition system. Recently, researchers improved

existing methods of SR & MRF and proposed several new methods. In [2], color invariance was applied to face recognition. Their results demonstrated that color invariants do have substantial discriminative power and enhance the robustness and accuracy for low resolution facials. In [3], the author proposed an approach to provide a feature subspace to be directly compatible with arbitrarily changeable low-resolution of probe at testing/application stage and overcome dimension mismatch problem. In [4], the authors developed high-resolution frames from a video sequence by using both spatial and temporal information present in number of adjacent low-resolution ones. A new technique named face scoring was given by Tse-Wei Chen et al.[5]. The method included eight scoring functions based on feature extraction technique, integrated by a single layer neural network training system to get an optimal linear combination to select high-resolution faces.

[3] QUALITY DEGRADATIONS

Face analysis suffers from a broad range of quality degrading effects. Addressing them all would be beyond the scope of this work, thus, we limit ourselves to the impacts which are most present in low-resolution scenarios. These are the low resolution itself, video/image compression, motion blur and noise which are illustrated in figure 1.

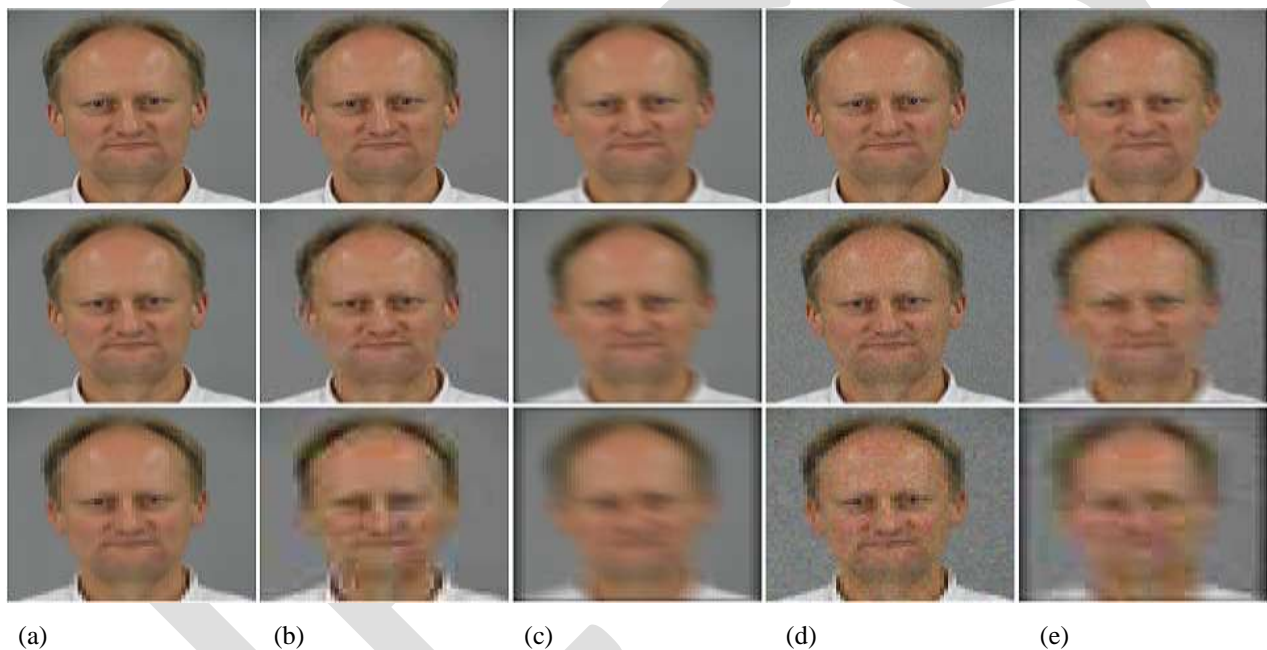


Figure 1: Impact of some image quality degradations: (a) resolution , (b) compression, (c) motion blur, (d) noise and (e) all combined. Severity increases with each row.

There exist a lot of further effects, but most of them, such as bad illumination (shadows, overexposure, low contrast) or harsh head poses, also relate to high-resolution applications and will consequently be omitted here.

[3.1] RESOLUTION

Effect: The resolution come into existence from the discrete sampling of the continuous image signal of a face. If the sampling is denser, the resulting resolution is higher, and the more information is included in the image and available for the processing.

Simulating the effect: For the investigation we need to simulate the particular effect in some severity steps for reproducible results.

In the case of face resolution this is unambiguous. Starting with a face width of W_0 pixels, further downsampled images with a face width W_0 are generated by

$$W_k = s^{-k} \cdot W_0 \quad (1)$$

Where $s > 1$ is the base for the scaling factor and $k = 0, 1, \dots$ the current severity step. Of course the same relation holds for the image height h_k . Suitable low-pass filtering is applied before downsampling to avoid aliasing. We will introduce the severity factor s^k in all further formulations of degradation effects, to set their severity in a similar manner to the reduction of the image resolution.

Counter measures: When matching low resolution to further low-resolution faces, adjustments of the used features are a common solution [11]. A popular approach to boost low resolution face recognition is to apply super-resolution to perform further analysis on the resulting high-resolution images [08], or incorporate super-resolution directly into face recognition [9]. This is particularly successful if the low-resolution probe faces should be compared to high resolution gallery faces [07, 10].

[3.2] COMPRESSION

Effect: Video data requires large space, so strategies to reduce this amount are employed in basically every video capturing system. Video compression formats such as H.264 are very common for movies, while surveillance systems with low frame rates use Motion-Jpeg compression quite often. There is large variety of compression algorithms and only a selection can be listed here. But fundamentally all popular compression algorithms work block based, which means to handle small regions of $n \times n$ pixels individually. Thus, the errors at the borders between the blocks grow stronger for high compression factors where each block can only be roughly approximated. And also, video compression is developed for the human visual sense, which is usually a suboptimal solution with respect to keeping the highest possible information density.

Simulating the effect: To simulate the compression artifacts, Jpeg-compression is a reasonable option. Jpeg-artifacts show the typical block-based pattern also eminent in video compression algorithms such as H.264. In addition, the quality can be effected by one single parameter which obviously simplifies things. This quality factor q ranges from 0 (worst) to $q_0 = 100$ (best) and can be adjusted by the same severity factor s^k as the resolution by

$$q_k = s^{-\alpha k} q_0, \quad (2)$$

where α adjusts the effect of the severity factor to result in a similar effect to image downscaling.

Counter measures: Each compression format leads to its own form of characteristic artifacts. This can be used to train matching blocks of low and high quality and substitute the low quality ones with the high quality counterpart [12]. However, this relies heavily on an according training database that comprises similar block patterns as the application domain and the knowledge what specific compression format was used. The General way to address the problem is to understand the effect as noise and employ according counter measures such as low-pass filtering.

[3.3] MOTION

Effect: Motion has a negative effect on image quality induced by the integration over time on image capturing. Motion blur can be formulated as a convolution of the image by a motion kernel that represents the relative motion of the camera to the object while capturing. We assumed that the object itself is static, leading to a constant motion kernel throughout the object. Mostly in dark and indoor environments, the effect becomes obvious in the presence of long exposure times. The sensitivity of face recognition to motion blur depends highly on the angle and the length of the effect [13]. Horizontal motion blur has a little effect on face recognition performance than vertical motion blur where the recognition rate dropped from 100 to 60 percent in their small scale experiment.

Simulating the effect: Synthetic motion blur can be developed by convolution of the image with a motion filter, the. In this case, we restrict the filter to linear motion which bring down it to two parameters, the angle φ of the motion in the image plane and the size

f characterizing the length and severity of the motion blur. We assume a random angle φ and a variable length

$$f_k = \beta s^k \quad (3)$$

that is characterized as a percentage of the face size W_0 . This forms the filter independent of the image resolution and relates instead to the motion and velocity of the face in front of the camera. The final filter length in pixels is given by

$$F_k = f_k \cdot W_0$$

Counter measures: Theoretically, motion blur can be mostly (except for zeros of the transfer function) removed by a deconvolution of the blurred image with the motion kernel (inverse filter). Nevertheless, the kernel is usually unknown and has to be estimated based on the blurred image itself. This is a hard task for low-resolution images where only little information is available. Known solutions commonly assume a fixed scene combined with camera motion, which is the typical case for snapshots taken by a digital camera in a shaking hand [14]. In the given scenario, the relation is vice versa; surveillance cameras are fixed installations and the scene in front of it is moving. Particularly, each object in the scene might move differently, leading to an individual motion kernel for each object. This way, only few pixels from each object are available as evidence for the motion, causing kernel estimation infeasible. In the of face recognition domain, the most promising strategies employ adapted features, that are insensitive to blur, e.g. local phase quantization (LPQ) [15]. However, one needs to keep in mind that LPQ assumes a symmetrical blur kernel, which basically never applies for motion kernels.

[3.4] Noise

Effect: Image noise is induced by the physical construction of the image sensor and its liability to quantum noise.

Simulating the effect: The noise can be simulated by additive Gaussian noise. Thus, the original image I_0 is degraded by Gaussian noise G as follows:

$$I_k = I_0 + y(s^k - 1) \cdot G, \quad G \sim N(0,1) \quad (4)$$

The Factor

$a = y(s^k - 1)$ denotes the standard deviation of the normal distribution the noise is sampled from. This influences the severity of the effect.

Counter measures: Best-shot face recognition strategy is the most common strategy to avoid noise issues. All images of a face sequence are examined with respect to the noise level and the one with the least amount of noise is selected for matching. This will fail if all images within one sequence shows a high noise level. Image noise can further be reduced by applying a low-pass filter to the image, reducing the high frequency noise components while preserving the low frequency image content.

4. CONCLUSION

Low quality face analysis remains a challenge and offers abundance opportunities for improvement. The effect, simulation of the effect, counter measures of some quality degradations namely low resolution, compression, motion blur and noise are discussed for face analysis. It was analyzed that the low resolution is only part of problem and several further effects have a significant impact on low-quality face analysis.

Finally, it is to say that the random mixture of effects causes the biggest challenges.

REFERENCES:

- [1] Y.Cheng, K.Liu, J.Yang, Y.Zhuang and N.Gu, "Human Face Recognition Method Based on the Statistical Model of Small Sample Size," in *Intelligent Robots and Computer Vision X: Algorithms and Techniques*, pp.85-95, 1991.
- [2] Arandjelovic O., Cipolla R., Colour invariants for machine face recognition, 8th IEEE International Conference on Automatic Face & Gesture Recognition, 2008. FG '08. pp: 1-8.
- [3] Jae Young Choi, Yong Man Ro, Konstantinos N. Plataniotis, Feature Subspace Determination in Video-based Mismatched Face Recognition, 8th IEEE International Conference on Automatic Face and Gesture Recognition (FG 2008).
- [4] Xiaoli Zhou; Bhanu B ,Human Recognition Based on Face Profiles in Video, IEEE Computer Society Conference on Computer Vision and Pattern Recognition - Workshops, 2005. CVPR Workshops. Pp:15.
- [5] Tse-Wei Chen, Shou-Chieh Hsu, Shao-Yi Chien, Feature-based Face Scoring in Surveillance Systems, Ninth IEEE International Symposium on Automatic Multimedia, 2007. pp: 139-146.
- [6] Y. Taigman, M. Yang, M. Ranzato, and L. Wolf. Deepface: Closing the gap to human-level performance in face verification. In *Computer Vision and Pattern Recognition*, pages 1701–1708, 2014.
- [7] Z. Wang, Z. Miao, Q. M. J. Wu, Y. Wan, and Z. Tang. Lowresolution face recognition: a review. *The Visual Computer*, 30(4):359–386, 2014.
- [8] X. Wang and X. Tang. Hallucinating face by eigentransformation. *Systems, Man, and Cybernetics, Part C: Applications and Reviews*, 35(3):425–434, Aug 2005.
- [9] P. H. Hennings-Yeomans, S. Baker, and B. V. Kumar. Simultaneous super-resolution and feature extraction for recognition of low-resolution faces. In *Computer Vision and Pattern Recognition*, pages 1–8, 2008.
- [10] C. Qu, H. Gao, E. Monari, J. Beyerer, and J.-P. Thiran. Towards Robust Cascaded Regression for Face Alignment in the Wild. In *Computer Vision and Pattern Recognition Workshops*, 2015.
- [11] C. Herrmann. Extending a local matching face recognition approach to low-resolution video. In *Advanced Video and Signal Based Surveillance*, 2013.
- [12] J. Z. Lai, Y.-C. Liaw, and W. Lo. Artifact reduction of JPEG coded images using mean-removed classified vector quantization. *Signal Processing*, 82(10):1375–1388, 2002.
- [13] A. Rajagopalan and R. Chellappa. *Motion Deblurring: Algorithms and Systems*. Cambridge University Press, 2014.
- [14] Q. Shan, J. Jia, and A. Agarwala. High-quality motion deblurring from a single image. In *ACM Transactions on Graphics*, volume 27, page 73. ACM, 2008.
- [15] V. Ojansivu and J. Heikkilä. Blur Insensitive Texture Classification Using Local Phase Quantization. In *Image and Signal Processing*, pages 236–243. Springer, 2008.

A Review on Design and Optimization with Structural Behavior Analysis of Central Drum in Mine Hoist

Sarang Mangalekar¹, Mr. Vaibhav Bankar², Mr. Pratik Chaphale³

¹M-Tech Student, Department of Mechanical Engineering, Vidarbha Institute of Technology, Nagpur

²Assistant Professor, Department of Mechanical Engineering, Vidarbha Institute of Technology, Nagpur

³Assistant Professor, Department of Mechanical Engineering, Vidarbha Institute of Technology, Nagpur

Sarang200252@gmail.com

Abstract— This work gives optimised solution to make feasible hoisting application in heavy lifting and passing in coal and minerals mines. Rotary drum to be optimised with putting same diameter as required. Design is planned with casting stiffening links patterned circularly in round drum to form complete hollow drum, its replacing side disc of drum to make lightweight, loading condition is put by considering maximum loads. Drum behaviour is analysed in ansys tool in variations of degree of rotation from 0 to 360 degree. Finally conclusion will be opting to make optimisation feasible or not. We form few variants in design and compare results with each other. Finally the best drum design is found and from results it's found feasible in working also in manufacturability.

Keywords Introduction— Mine hoist, Central hub, Weldment structure, manufacturability and installation feasibility.

INTRODUCTION

Hoist by definition means to haul or to raise an object to higher altitudes. Hoists are mechanical or electromechanical devices used to move an object from one point to another, which would be otherwise physically challenging. The object can be raised, lowered or moved depending on the necessity. The hoist work on the basic principle of balance of forces where an equal and opposite force is applied on the load force. The applied force can be reduced by using a pulley system.

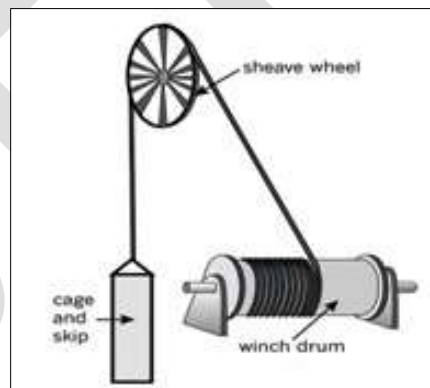


Fig.: - Mine Hoist

In underground mining a hoist or winder is used to raise and lower conveyances within the mine shaft. Modern hoists are normally powered using electric motors. Drum hoists are the most common type of hoist used. When using a drum hoist the hoisting cable is wound around the drum when the conveyance is lifted. Single-drum hoists can be used in smaller applications. Drum hoists are mounted on concrete within a hoist room, the hoisting ropes run from the drum, up to the top of the head frame, over a sheave wheel and down where they connect to the conveyance (cage or skip).

LITERATURE REVIEW

For this study, Observations are focused on existing system. The literature survey has been pioneered effort in this regard. Various machine design concepts and CAD/CAE concepts from literatures help to establish comparative study between existing and new experimentation. The terminologies referred from literatures for designing are discussed as follows:

WANG Jiu-feng, XU Gui-yun, ZHU Jia-zhou, YANG Yan-chu, in their paper named as, "*Parametric Design and Finite Element Analysis of Main Shaft of Hoister Based on Pro/E*", advanced parametric design method which realized in the process of modelling of main shaft of hoister was deal. Using the interface technology between Pro/E and ANSYS software, the simulation analysis of stress status of the main shaft of hoister designed in Pro/E under a certain load is made. The adoption of this method will dramatically shorten the development cycle and cut down the design costs. Otherwise the research method will reference value to gear model library development and to the optimization design of the main shaft of hoister^[1].

LUO Jiman, XING Yan, LIU Dajiang and YUAN Ye, in their paper, "*Modal Analysis of Mast of Builder's Hoist Based on ANSYS*", For the purpose of researching the factors which affect the dynamic characteristic of mast of builder's hoist and analyzing the impact of different factors over system security, the authors of the paper applied the finite element method to build the model and made the modal analysis for mast which was installed with various installation distances or under different working conditions^[2].

Yang Yuanfan, in the paper named as, "*The Study on Mechanical Reliability Design Method and Its Application*", Through the study on mechanical reliability design and combination with the structure of mine hoist, it is proposed that the crucial procedure of reliability design's application into mine hoist is as to ascertain the statistics of the relevant parameters, then to set up the failure mathematical model, and finally the reliability design can be operated^[3].

J.J. Taljaard and J.D. Stephenson, in the paper named as, "*State-of-art shaft system as applied to Palaborwa underground mining project*", The design of a 30,000 ton per day underground mine at Phalaborwa presented many and various challenges to the owner and the design team. Using modern best and proven practice, innovative engineering, extensive test work and verification by worldwide experts these challenges were met head on and overcome. The state-of-the-art system will be in operation by the end of the year 2000^[4].

Shuang Chen and Shen Guo, in their paper named as, "*Stress Analysis of the Mine Hoist Spindle Based on ANSYS*", In this paper, the three dimensional modeling of 2JK mine hoist spindle was established by using Pro/ E according to given data. Then the model was inputted into the finite element analysis in ANSYS, the stress distribution of the spindle was obtained, strength check of the dangerous section was made at the same time, which provides an accurate and reliable theoretical basis for improving the spindle structural design^[5].

HuYong and HuJiQuan, in their paper named as, "*Mechanical Analysis and Experimental Research of Parallel Grooved Drum Multi-layer Winding System*", in the present design criterion of multi-layer winding drum, multi-layer winding coefficient is chosen according to the number of wire rope layers. However, the actual wire rope arrangement on the drum and the elastic property of wire rope also play decisive roles in determining the multi-layer winding coefficient value. Analyzing the actual stress of the drum accurately is the precondition of ensuring the drums safety and reliability for meeting the lightweight design requirements^[6].

PROBLEM IDENTIFICATIONS: -

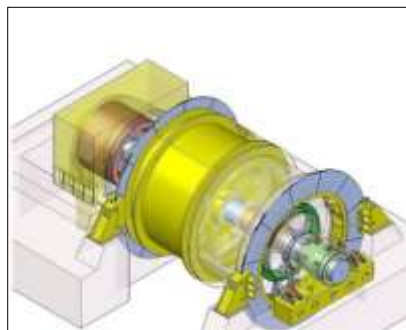
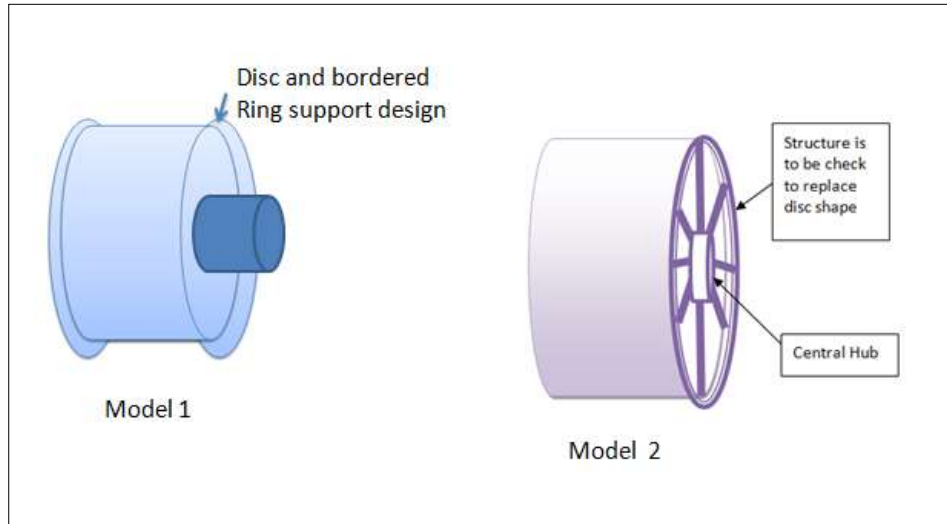


Fig.:- Closed Disc drum

1. Heavy drum difficult for commissioning and manufacturing in single body. Central hub is too heavy for making drive hold to rotate full body with loads.
2. Optimisation can be formed in drum structure to make it little lightweight without affecting its strength.

METHODOLOGY

Comparison in two models: -



Model 1: - Closed Disc Drum

Model 2: - Proposed Conceptual Model

INPUT: -

- Boundary conditions: Max. RPM 20
- Maximum Torque: 700 N-m
- Material: Cast iron / Carbon steel
- Technology of development: Weldment structure, Welding treatment, Sheet metal components.
- Optimized meshed drum body to be developed outer Dia. 1300 mm & Width =600 mm.

PARAMETERS FOR DESIGN CALCULATIONS

The shear stresses are induced in the shaft due to transmission of torque i.e. due to torsion loading. According to American Society of Mechanical Engineers (ASME) code for the design of transmission shaft the maximum permissible shear stress (τ) may be taken as 30% of the elastic limit (σ_{el}) in tension but not more than not more than 18% of ultimate tensile strength (σ_{ut})^[7]. In other words,

$$\tau = 0.3 \sigma_{el} \text{ or } 0.18 \sigma_{ut}$$

The shaft is subjected to twisting moment or torsion only, and then the diameter of the shaft may be obtained by using torsion equation.

$$\frac{T}{j} = \frac{\tau}{R} \dots\dots\dots (i)A$$

Where, T = torque acting on the shaft

j = polar moment of inertia

τ = torsion shear stress

R = Distance from neutral axis to outermost fibre

= D/2.... Where D is diameter of the shaft

We know that, for solid circular shaft, polar moment inertia (j) is given by,

$$j = \frac{\pi}{32} D^4$$

For rotating shafts, gradually applied or steady load, combined shock factor (K_s) and fatigue factor (K_m) are taken as 1^[8].

Also from torsion rigidity equation we have,

$$\theta = \frac{584TL}{GD^4} \dots\dots (ii)$$

Where, θ = angle of twist in degree

T = Torque, Nmm

L = length of shaft, mm

G = Modulus of rigidity, N/mm²

D = Diameter of shaft, mm

*Let the angle of twist for the shaft 1degree i.e. $\theta = 1^\circ$

ROPE SPECIFICATION

Rope construction: 6 x 26 RRL (right regular lay) rope

Safety factor of rope = (Minimum breaking load) / Load applied

DRUM CALCULATIONS

1. Diameter of drum

$$D_{\text{drum}} = (\text{ratio between 20 to 25}) \times d_{\text{rope}}$$

2. Groove radius,

$$r = 0.53 \times d$$

3. Groove diameter,

$$d = \text{groove radius} \times 2$$

4. Pitch diameter,

$$p = 2.065 \times \text{groove radius}$$

5. Groove depth

$$h = 0.374 \times d$$

6. Thickness

$$tx = P/kp$$

7. Drum grooved length, L3

$$L3 = (n - 1) \times P$$

8. Drum un-grooved length, L1=L2

$$L1 = L2 = 1/2 \text{ diameter of hook} + \text{radius of rope}$$

9. Factor of safety = 6

CAD Model

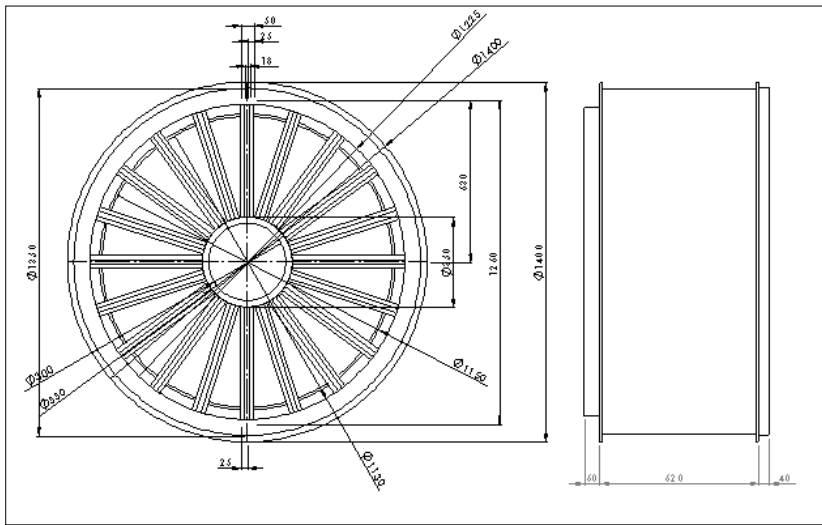


Fig.: - CAD Drawing

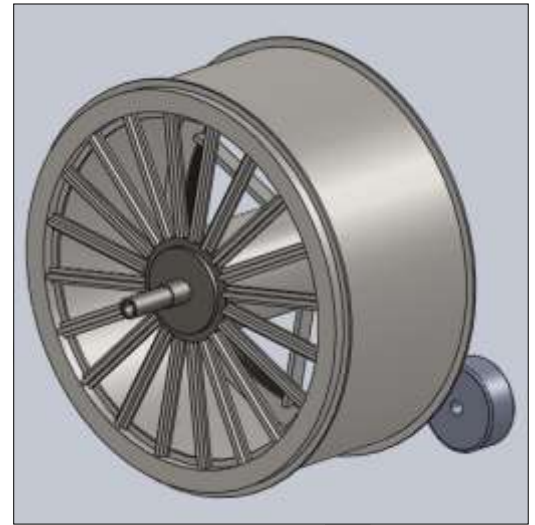


Fig.: - Axle Assembly

CAD Model is created by using Creo Parametric 2.0^{[9], [10]} on which we can perform engineering analysis like finite element analysis. Finite Element Analysis of structural behavior can be done by using Ansys by applying various boundary conditions. Meshing is done by using 20 noded Solid95 elements^{[11], [12]}.

VALIDATION STAGES

- Mathematical calculations with structural behavior loads
- Optimization with material weight and feasible manufacturability.
- Validation with comparing different variants results.
- Solution and selection of best design amongst all variants and their respective results

CONCLUSION

This paper reviews the studies of Design and Optimization with Structural Behavior Analysis of Central Drum in Mine Hoist. The review finds that, the central drum in mine hoist is large and too heavy for commissioning and manufacturing in single body and for making drive hold to rotate full body with loads. The design and optimization with structural behavior analysis can give the new design which can reduce the weight of central drum. Design is planned with casting stiffening links patterned circularly in round drum to form complete hollow drum its replacing side disc of drum, which can make the system little light in weight without affecting its strength. Because of the reducing the weight of central drum, we can make it feasible to manufacture and installation.

ACKNOWLEDGMENT

We would like to thanks to all the faculty members of Vidarbha Institute of Technology, Nagpur for their valuable guidance and for giving their valuable suggestions and time, which leded us to study hard and effectively.

We are also grateful to Mr. Ashish Dhakole (senior engineer Y.D.CORE Technology, Pune) for giving me great opportunity to work on this project.

Also thanks to all my colleagues for their significant contributions. Also thanks to all authors for giving me best past technical knowledge and reference about this topic.

Finally, our special thanks go to parent for their vast support for encouraging us, and great patience along the study.

REFERENCES:

- [1] WANG Jiu-feng, XU Gui-yun, ZHU Jia-zhou, YANG Yan-chu, "*Parametric Design and Finite Element Analysis of Main Shaft of Hoister Based on Pro/E*", (China University of Mining and Technology, Xuzhou 221008, China).
- [2] LUO Jiman, XING Yan, LIU Dajiang and YUAN Ye, "*Modal Analysis of Mast of Builder's Hoist Based on ANSYS*", (School of Traffic and Mechanical Engineering, Shenyang Jianzhu University, Shenyang China, 110168; 2. SIASUN Robot and Automation Co., Ltd., Shenyang China, 110016; 3. JIHUA 3523 Special Equipment Co., Ltd., Shenyang China, 110026).
- [3] Yang Yuanfan, "*The Study on Mechanical Reliability Design Method and Its Application*", International Conference on Future Electrical Power and Energy Systems, Energy Procedia 17 (2012) 467 – 472).
- [4] J.J. Taljaard and J.D. Stephenson, "*State-of-art shaft system as applied to Palaborwa underground mining project*", The South African Institute of Mining and Metallurgy, 2000. SA ISSN 0038-223X/3.00 + 0.00. First presented at the SAIMM conference Mine Hoisting 2000, Sept. 2000.
- [5] Shuang Chen and Shen Guo, "*Stress Analysis of the Mine Hoist Spindle Based on ANSYS*", Information and Computing (ICIC), Fourth International Conference, 2011.
- [6] HuYong and HuJiQuan, "*Mechanical Analysis and Experimental Research of Parallel Grooved Drum Multi-layer Winding System*", Wuhan University of Technology, 2013.
- [7] R. S. Khurmi and J. K. Gupta, "*A textbook of Machine Design*", S. Chand Publication, (14th edition).
- [8] N.G. Pandya and C.S. Shah, "*A textbook of Elements of Machine Design*", Charotar publishing house (10th edition).
- [9] Prof. Sham Tickoo and Prabhakar Singh, "*Pro/Engineer (Creo Parametric 2.0) for Engineers and Designers*", Dreamtech Press, Reprint Edition, 2014.
- [10] Ibrahim Zeid and R Sivasubramanian, "*CAD/CAM Theory and Practice*", McGraw-Hill Book Company, First edition, 2007.
- [11] Zeinkiewicz O.C, Taylor R.L. "*The Finite Element Method*", McGraw-Hill Book Company, 1989.
- [12] Chandrupatla T.R., "*Introduction to Finite Elements in Engineering*", Prentice –Hall, third edition (2001).

Experimental Investigation of Heat Transfer Enhancement Techniques in Two Phase Closed Thermosyphon

Mr. Sandipkumar B. Chauhan, Mr. Dr. M. Basavaraj and Mr. Prashant Walke

Student, M.Tech (Heat power Engg.),
Ballarpur Institute of Technology,
Chandrapur-442701, India

Email id- chauhansandipkumar@gmail.com

Mobile no- 08421889020

Abstract— The thermal performance of an inclined two phase closed thermosyphon with different working fluid has been investigated experimentally in this paper. Distilled water and Binary mixture of ethanol and methanol that has a positive gradient of surface tension with temperature are used as the working fluid. A copper thermosyphon with a length of 1000 mm long, an inner diameter of 20.5 mm and an outer diameter of 22.5 mm was employed. Thermosyphon was charged with 60% of the working fluid and was tested with an evaporator length of 300 mm and condenser length of 450 mm. The thermosyphon was tested for various inclinations of 45°, 60° and 90° to the horizontal. Flow rate of 4 Kg/hr, 12 Kg/hr and 20 Kg/hr and heat input of 40 W, 60 W and 80 W were taken as input parameters. The thermal performance of binary mixture charged two phase closed thermosyphon was out performed the distilled water in both heat transfer and temperature distribution.

Keywords: Two phase closed thermosyphon, Heat transfer limitations, Binary mixture, Heat load, Coolant flow rate, Inclination angle, Efficiency

I. INTRODUCTION

Energy is an important part of most aspects of daily life. The quality of life and even its substance depends on the availability of energy. Hence energy plays a vital role in day to day life as well as in heat transfer applications. Due to the human need for energy, a more efficient way of using it is a major challenge in the scientific community. The heat pipe and the thermosyphon specially designed by the engineers for transferring heat from a distance. The thermal performance of thermosyphon is one the most important part of these types of investigation in the field of heat transfer.

1.1. Heat Transfer Enhancement Techniques:

Heat transfer enhancement or augmentation techniques refer to the improvement of thermo hydraulic performance of heat exchangers. Existing enhancement techniques can be broadly classified into three different categories:

- Passive techniques
- Active techniques
- Compound techniques

1.1.1. Passive Techniques:

These techniques generally use surface or geometrical modifications to the flow channel by incorporating inserts or additional devices. They promote higher heat transfer coefficients by disturbing or altering the existing flow behaviour (except for extended surfaces) which also leads to increase in the pressure drop.

1.1.2. Active Techniques:

These techniques are more complex from the use and design point of view as the method requires some external power input to cause the desired flow modification and improvement in the rate of heat transfer, like mechanical aids, surface vibration, fluid vibration, suction, etc.

1.1.3. Compound Techniques:

A compound is the one where more than one of the above mentioned techniques is used in combination with the purpose of further improving the thermo- hydraulic performance of a heat exchanger.

1.2. Thermosyphon:

Thermosyphon is an enclosed two phase heat transfer devices. They make use of the highly efficient heat transport process of evaporation and condensation to maximize the thermal conductance between a heat source and a heat sink. They are often referred to as thermal superconductors because they can transfer large amounts of heat over relatively large distances with small temperature differences between the heat source and heat sink. The amount of heat that can be transported by these devices is usually several orders of magnitude greater than pure conduction through a solid metal. They are proven to be very effective, low cost and reliable heat transfer devices for applications in many thermal management and heat recovery systems. They are used in many applications including but not restricted to passive ground/road anti-freezing, baking ovens, heat exchangers in waste heat recovery applications,

water heaters and solar energy systems and are showing some promise in high-performance electronics thermal management for situations which are orientation specific.

1.3. Thermosyphon Geometry and Working Principle:

A cross section of a closed two-phase thermosyphon is illustrated in Fig. 1; the thermosyphon consists of an evacuated sealed tube that contains a small amount of liquid. The heat applied at the evaporator section is conducted across the pipe wall causing the liquid in the thermosyphon to boil in the liquid pool region and evaporate and/or boil in the film region. In this way the working fluid absorbs the applied heat load converting it to latent heat.

The vapour in the evaporator zone is at a higher pressure than in the condenser section causing the vapour to flow upward. In the cooler condenser region the vapour condenses and thus releasing the latent heat that was absorbed in the evaporator section. The heat then conducts across thin liquid film and exits the thermosyphon through the tube wall and into the external environment. Within the tube, the flow circuit is completed by the liquid being forced by gravity back to the evaporator section in the form of a thin liquid film. As the thermosyphon relies on gravity to pump the liquid back to the evaporator section, it cannot operate at inclinations close to the horizontal position.

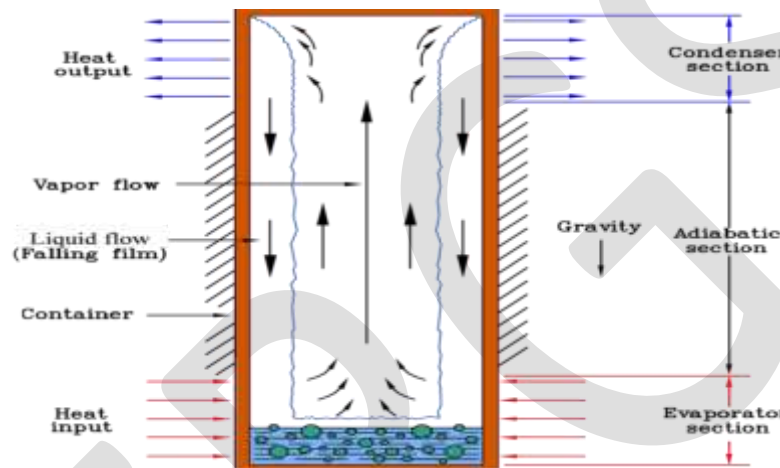


Fig.1: Two-phase closed thermosyphon working principle

1.4. Applications:

- Radiators
- Aerospace
- High tech electronics
- Solar system
- Satellite thermal control
- Waste heat recovery

1.5. Advantages:

- Passive heat exchange with no moving parts.
- Relatively space efficient.
- The cooling or heating equipment size can be reduced in some cases.
- The moisture removal capacity of existing cooling equipment can be improved.
- No cross contamination between streams.

II. REVIEW OF WORK CARRIED OUT

Many investigations were carried out in order to analyse and to enhance the thermal performance of thermosyphon. These are as follows.

Grover [1] (Los Alamos Laboratory, USA) introduced the term heat pipe in 1964. The two-phase closed thermosyphon used in this study is essentially a gravity-assisted wickless heat pipe, which is very efficient for the transport of heat with a small temperature difference via the phase change of the working fluid. It consists of an evacuated-closed tube filled with a certain amount of a suitable pure working fluid. The simple design, operation principle, and the high heat transport capabilities of two-phase closed thermosyphons

are the primary reasons for their wide use in many industrial and energy applications. Since there is no wick material, the thermosyphon is simpler in construction, smaller in thermal resistance, and wider in its operating limits than the wicked heat pipe.

Z. Q. Long, P. Zang [2] investigated the thermal performance of cryogenic thermosyphon charged with N₂-Ar binary mixture. They have discussed heat transfer of the binary mixture in the thermosyphon theoretically by considering the mass transfer of the components. They built an experimental setup for investigating the heat transfer performance of the cryogenic thermosyphon. They found that the N₂-Ar binary mixture can widen the operational temperature range of the cryogenic thermosyphon and it can work in the range of 64.0–150.0 K. The dry-out limit appears in the experiments for the cases with Ar fraction below 0.503. The heat transfer rate of the dry-out limit increases with the increase of Ar molar fraction until film boiling appears on the top of the condenser.

M. Karthikeyan, S. Vaidyanathan and B. Sivaraman [3] investigated the thermal performance of an inclined two phase closed thermosyphon with distilled water and aqueous solution of n-Butanol as a working fluid. They carried out the experiments for filling ratio of 60%. The thermosyphon was tested for various inclinations of 45°, 60° and 90° to the horizontal. Flow rate of 0.08Kg/min, 0.1 Kg/min and 0.12 Kg/min and heat input of 40 W, 60 W and 80 W. The thermosyphon was of a copper material with inside and outside diameter of 17mm and 19mm respectively. The overall length of thermosyphon was 1000mm (400mm-evaporator length, 450mm-condenser length). They obtained the result that the thermosyphon charged with aqueous solution has the maximum thermal performance than compared to thermosyphon charged with distilled water.

H. Z. Abou-Ziyan, A. Helali, M. Fatouh and M. M. Abo El - Nasr [4] investigated the thermal performance of two phase closed thermosyphon under stationary and vibratory conditions with water and R134a as a working fluid. They carried out the experiments for filling ratio of range (40% to 80%). The thermosyphon was tested for various adiabatic lengths of (275,325 and 350mm), vibration frequency (0.0-4.33Hz) and input heat flux (160-2800 kW/m²). They obtained the result that adiabatic length of 350mm and liquid filling ratio of 50% provide the highest heat flux.

Negishi and Sawada [5] made an experimental study on the heat transfer performance of an inclined two-phase closed thermosyphon. They used water and ethanol as working fluids. The highest heat transfer rate was obtained when the filling ratio (ratio of volume of working fluid to volume of evaporator section) was between 25% and 60% for water and between 40% and 75% for ethanol. The inclination angle was between 20° and 40° for water, and more than 5° for ethanol.

M. R. Sarmasti Emami, S. H. Noie and M. Khoshnoodi [6] made an experimental study on the effect of aspect ratio and filling ratio on the thermal performance of inclined two-phase closed thermosyphon under normal operating conditions. They used distilled water as a working fluid. They carried out the experiments for filling ratio of range (20% to 60%) and aspect ratio of 15, 20 and 30 for an inclination angle of range (15° to 90°). The thermosyphon was of a copper material with inside and outside diameter of 14mm and 16mm respectively. The overall length of thermosyphon is 1000mm. They obtained the following results that the maximum thermal performance at inclination angle of 60° for all three aspect ratios and filling ratio of 45%.

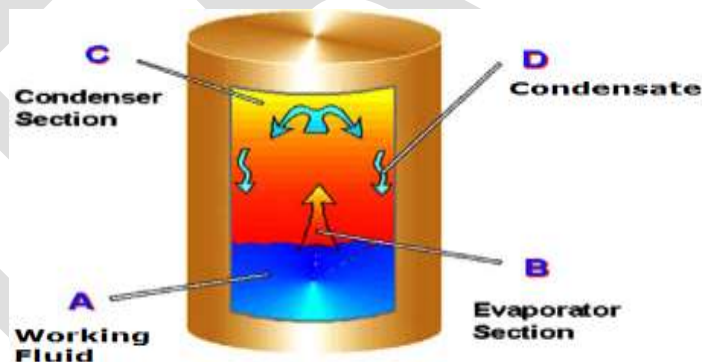


Fig.2: Schematic diagram of a two-phase closed thermosyphon

K.S. Ong and Md. Haider - E - Alahi [7] investigated performance of an R134a filled thermosyphon. They carried out the experiments to study the effects of temperature difference between bath and condenser section, fill ratio and coolant mass flow rate. The thermosyphon was of a copper material with inside and outside diameter of 25.5mm and 28.2mm respectively. The overall length of thermosyphon was 780mm (300mm-evaporator length, 300mm-condenser length). They obtained the results that the heat flux transferred increased with increasing coolant mass flow rate, fill ratio and temperature difference between bath and condenser section.

Sameer Khandekar, Yogesh M. Joshi and Balkrishna Mehta [8] investigated the thermal performance of closed two-phase thermosyphon using water and various water based nanofluids (of Al₂O₃, CuO and laponite clay) as a working fluid. They observed that all these nanofluids show inferior performance than pure water.

Gabriela Humnic, Angel Humnic, Ion Morjan and Florian Dumitrache [9] performed an experiment to measure the temperature distribution and compare the heat transfer rate of thermosyphon with diluted nanofluid (with 0%, 2% and 5.3% concentration) in DI-water and DI-water. The thermosyphon was a copper tube with internal and external diameter of 13.6mm and 15 respectively. The overall of length of thermosyphon was 2000mm (evaporator length-850mm, condenser length-850mm, adiabatic section-300). They

obtained the results that the addition of 5.3% (by volume) of iron oxide nanoparticles in water improved thermal performance of thermosyphon.

P. G. Anjankar and Dr. R. B. Yarasu [10] investigated the effect of condenser length, coolant flow rate and heat load on the performance of two-phase closed thermosyphon. The thermosyphon was a closed copper tube of length 1000mm (evaporator length-300mm, condenser length- 450mm/400mm/350mm) and internal and external diameter of 26 and 32mm respectively. They obtained the results that thermal performance of a thermosyphon was higher at flow rate 0.0027kg/s and heat input 500W with a condenser length of 450mm.

H. Mirshahi and M. Rahimi [11] investigated experimentally the effect of heat loads, fill ratio and extra volume on the performance of a partial-vacuumed thermosyphon. They obtained the results that the change in heat flux, fill ratio and employing different extra volumes has a significant effect on the performance of thermosyphon.

Masoud Rahimi, Kayvan Asgary and Simin Jesri [12] studied the effect of the condenser and evaporator resurfacing on overall performance of thermosyphon. They obtained the result that by making the evaporator more hydrophilic and the condenser more hydrophobic the thermal performance of thermosyphon increases by 15.27% and thermal resistance decreases by 2.35 times compared with plane one.

Asghar Alizadehdakhel, Masoud Rahimi and Ammar Abdulaziz Alsairafi [13] carried out experiments to investigate the effect of various heat loads and fill ratio on the performance of thermosyphon. They obtained the results that increasing the heat load up to certain limit increases the performance of thermosyphon further increase in heat load decreases the performance of thermosyphon. Also there is an optimum value of fill ratio for every energy input. Experimental results were compared with CFD modelling (FLUENT™ version 6.2) and there was a good agreement observed between CFD and experimental results.

S. R. Raja Balayanan, V. Velmurugan, R. Sudhakaran and N. Shenbagavinayaga Moorhy [14] have been carried out experimental and theoretical research to investigate the thermal performance of water to air thermosyphon heat pipe heat exchanger. They selected independent controllable process parameters heat input, water temperature and air velocity to carry out experimental work and correlation was developed for effectiveness of heat pipe heat exchanger. They developed mathematical model using regression coefficient method which is helpful in analyzing the performance of heat pipe heat exchanger.

III. CHARACTERISTIC OF THERMOSYPHON AND WORKING FLUID

As an effective heat conductor, thermosyphon can be used in situations when a heat source and a heat sink need to be placed apart, to aid heat conduction of a solid, or to aid heat spreading of a plane. However, not every thermosyphon heat pipe is suitable for all applications. For that reason and to develop an experimental model the following need to be considered while designing heat pipes.

A. Heat transfer limitations of the thermosyphon:

Thermosyphon heat pipe performance and operation are strongly dependent on shape, working fluid and wick structure. Certain heat pipes can be designed to carry a few watts or several kilowatts, depending on the application. The effective thermal conductivity of the heat pipe will be significantly reduced if heat pipe is driven beyond its capacity. Therefore, it is important to assure that the heat pipe is designed to transport the required heat load safely. But during steady state operation, the maximum heat transport capability of a heat pipe is governed by several limitations, which must be clearly known when designing a heat pipe. There are five primary heat pipe transport limitations.

• Viscous Limit:

At low operating temperatures, viscous forces may be dominant for the vapour moving flow down the heat pipe. For a long liquid-metal heat pipe, the vapour pressure at the condenser end may reduce to zero. The heat transport of the heat pipe may be limited under this condition. The vapour pressure limit (viscous limit) is encountered when a heat pipe operates at temperatures below its normal operating range, such as during start up from the frozen state. In this case, the vapour pressure is very small, with the condenser end cap pressure nearly zero.

• Sonic Limit:

The rate at which vapours travels from evaporator to condenser known as sonic limit. The evaporator and condenser sections of a thermosyphon represent a vapour flow channel with mass addition and extraction due to the evaporation and condensation, respectively. The vapour velocity increases along the evaporator and reaches a maximum at the end of the evaporator section. The limitation of such a flow system is similar to that of a converging-diverging nozzle with a constant mass flow rate, where the evaporator exit corresponds to the throat of the nozzle. Therefore, one expects that the vapour velocity at that point cannot exceed the local speed of sound. This choked flow condition is called the sonic limitation. The sonic limit usually occurs either during heat pipe start up or during steady state operation when the heat transfer coefficient at the condenser is high. The sonic limit is usually associated with liquid-metal heat pipes due to high vapour velocities and low densities. When the sonic limit is exceeded, it does not represent a serious failure. The sonic limitation corresponds to a given evaporator end cap temperature. Increasing the evaporator end cap temperature will increase this limit to a new higher sonic limit. The rate of heat transfer will not increase by decreasing the condenser temperature under the choked condition. Therefore, when the sonic limit is reached, further increases in the heat transfer rate can be realized only when the evaporator temperature increases. Operation of heat pipes with a heat rate close to or at the sonic limit results in a significant axial temperature drop along the heat pipe.

• Entrainment Limit:

This limit occurs due to the friction between working fluid and vapour which travel in opposite directions. A shear force exists at the liquid-vapour interface since the vapour and liquid move in opposite directions. At high relative velocities, droplets of liquid entrained into the vapour flowing toward the condenser section. If the entrainment becomes too great, the evaporator will dry out. The heat transfer rate at which this occurs is called the entrainment limit. Entrainment can be detected by the sounds made by droplets striking the condenser end of the heat pipe. The entrainment limit is often associated with low or moderate temperature heat pipes with small diameters, or high temperature heat pipes when the heat input at the evaporator is high.

• **Capillary Limit:**

It is the combination of gravitational, liquid and vapour flow and pressure drops exceeding the capillary pumping head of the heat pipe wick structure. The main cause is the heat pipe input power exceeds the design heat transport capacity of the heat pipe. The problem can be resolved by modifying the heat pipe wick structure design or reduce the power input.

• **Boiling Limit:**

The rate at which the working fluid vaporizes from the added heat. If the radial heat flux in the evaporator section becomes too high, the liquid in the evaporator section boils and the wall temperature becomes excessively high. The vapour bubbles that form near the pipe wall prevent the liquid from wetting the pipe wall, which causes hot spots, resulting in the rapid increase in evaporator wall temperature, which is defined as the boiling limit. However, under a low or moderate radial heat flux, low intensity stable boiling is possible without causing dry out. It should be noted that the boiling limitation is a radial heat flux limitation as compared to an axial heat flux limitation for the other heat pipe limits. However, since they are related through the evaporator surface area, the maximum radial heat flux limitation also specifies the maximum axial heat transport. The boiling limit is often associated with heat pipes of non-metallic working fluids. For liquid-metal heat pipes, the boiling limit is rarely seen.

B. Effect of Fluid Charge:

Filled ratio is the fraction (by volume) of the heat pipe which is initially filled with the liquid. There is two operational filled ratio limits. At 0% filled ratio, a heat pipe structure with only bare tubes and no working fluid, is pure conduction mode heat transfer device with a very high undesirable thermal resistance. A 100% fully filled heat pipe is identical in operation to a single phase thermosyphon. When the charge amount was smaller, there was more space to accommodate vapour and make the pressure inside heat pipe become relatively lower. It helped working fluids undergo vaporization and enhance its heat transfer performance. Therefore, the most proper filled ratio is between 40% and 60%.

C. Working Fluid:

• **Binary mixture:**

From the literature review, it is found that various researches has been done on various working fluid solutions like water, distilled water, butanol, ethanol, etc., refrigerant like R-12, R-22, R-134a, FC-72, FC-77, FC-84, etc. and nanoparticles such as Al₂O₃, Ag₂O₃ and Fe₂O₃, etc. In many investigation of thermosyphon, it is seen that water as a working fluid has a better performance than other solutions. But because of its high boiling point it cannot be used for cold temperature regions. By using other solutions as a working fluid does not get better thermal performance than water. So it is need of time to use binary mixture of various solutions to get better thermodynamic property for using working fluid in two phase closed thermosyphon .

• **Ethanol-Methanol Mixture:**

As far as selection of working fluid for thermosyphon is concerned, first go through various thermodynamic properties of ethanol and methanol.

Table.1: Properties of ethanol and methanol:

Property	Methanol CH ₃ OH	Ethanol C ₂ H ₅ OH
Molecular Weight	32	46
Boiling point (°C)	65	78
Melting point (°C)	-98	-144
Useful temperature range (°C)	10 to 130	0 to 130
Thermal Conductivity at 300K (W/m-K)	0.202	0.171
Latent heat of vaporization (kJ/kg)	1100	846

In this experiment we used ethanol and methanol ratio 60:40 (by volume) because at this ratio these two solutions are completely soluble with each other.

Table.2: Properties of ethanol-methanol mixture:

Property	Ethanol-Methanol Mixture
Boiling point (°C)	72.8
Melting point (°C)	-125.6
Useful temperature range (°C)	0 to 100
Thermal conductivity at 300 K (W/m-K)	0.1834
Latent heat of vaporization (kJ/kg)	947.6

These thermodynamic properties are useful for the thermosyphon as a working fluid in 0°C to 100°C temperature applications. Hence ethanol-methanol mixture was selected for the experimental assessment of the thermosyphon as a working fluid.

IV. EXPERIMENTAL SETUP DESCRIPTIONS

It consists of an enclosed evacuated copper tube having evaporator section at base and condenser section at the top. 9 thermocouples are attached on the copper tube at similar distances. Temperature indicator displays the temperature. The uniform heat flux wire type heater is fabricated from nickel-crome wire. This wire is connected in series with dimmer stat in order to supply the same amount of heat to nickel-crome wire. Nickel-crome coil heaters are attached to the evaporator section for heat supply and it is controlled by controlling the voltage and current. Condenser section is surrounded by concentric cylinder through with coolant flows. Flow of coolant is measured by rotameter and controlled by a valve. The range of rotameter is 0-20LPM. For initial evacuation of tube arrangement is made to attach vacuum pump at the top and also pressure gauge is attached to measure the pressure inside the tube.

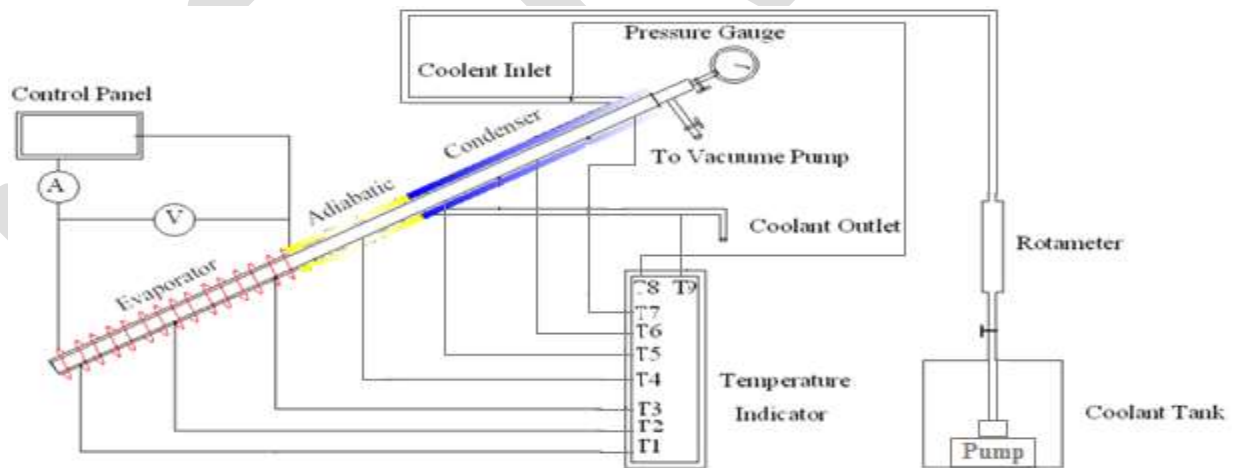


Fig.3: Schematic diagram of thermosyphon experimental setup

Following table shows the general configuration of experimental setup which may vary according to researchers requirement.

Table.3: Experimental Setup Description:

Tube Material		Copper
Diameter (mm)	Internal	20.5
	External	22.5
Dimensions (mm)	Total	1000
	Evaporator	300
	Condenser	450

	Adiabatic	250
Aspect Ratio (Le/Di)		14.63
Filling Ratio		60 %
Working Fluid	Mixture Of Methanol-Ethanol and Distilled Water	
Inclination Angle (°)		45, 60, 90
Heat Input (W)		40, 60, 80
Coolant Flow Rate (Kg/hr)		20, 12, 4

• **Factors for experimental analysis:**

Coolant flow rate:

It is also important parameter which affects the thermal performance of thermosyphon to large extent. Coolant used in this experimentation is water, because water has maximum ability to gain or lose the heat from the system. At the condenser part working fluid is condensed due to which heat is released to the atmosphere. For that purpose, condenser section is enclosed by another coaxial copper tube. Upper and lower ends of this external tube are perfectly closed. In this experimentation we have used various coolant flow rate which are 4kg/hr, 12 kg/hr, and 20 kg/hr. During experimentation it was found that at lower coolant flow rate, heat transfer efficiency of thermosyphon is maximum and at higher coolant flow rate, heat transfer efficiency was minimum. This is because at lower coolant flow rate, velocity of coolant is minimum inside the outer shell of the condenser due to which there is enough time to exchange heat from the working fluid to the coolant.

Inclination angle:

It is also important factor which affect thermal performance of thermosyphon to great extent. The lower end of the thermosyphon tube was heated causing the liquid to vaporise and the vapour to move to the cold end of the tube where it is condensed. The condensate is returned to the hot end by gravity. This is why thermosyphon is kept vertical i.e, 90° with horizontal. Experimentation also includes study at various inclination angles to evaluate thermal performance. At various inclination angles and at various heat loads thermal performance is varying. So after experimentation we got best configuration factor of inclination angle and heat load which is responsible for higher thermal performance.

Heat Load:

Heat load is given to the evaporator section of the thermosyphon. After applying heat, working fluid get vaporize in the evaporator. But heat load is dependent on working fluid. It defines boiling limit of the working fluid. If the boiling point of the working fluid is higher near about 100° C, then heat load can be applied from 100° C to the point where maximum fluid will evaporate. In this experimental model, we have used binary mixture of ethanol-methanol and distilled water as a working fluid. Thermodynamic properties of ethanol and methanol are shown in Table 2. Ethanol and methanol has lower boiling points than water and under vacuum mixture gain low boiling point. So for experimentation we have selected heat load range of 40W, 60W and 80 W.

• **Experimentation Parameters:**

Experimentation was carried on the two phase closed thermosyphon. Working fluid is important parameter in the experimentation. Ethanol-Methanol binary mixture and Distilled Water was used as a working fluid. Other parameters and its description as follows.

Table.4: Experimentation parameters

Parameter	Description
Heat load (W)	40, 60 and 80
Inclination angle with horizontal axis (°)	45, 60 and 90
Coolant flow rate (kg/hr)	4, 12 and 20
Aspect ratio	14.63
Filling ratio	60% (60% Ethanol and 40% Methanol) and 60% Distilled Water

V. RESULTS AND DISCUSSION

A. Temperature distribution along the thermosyphon:

Fig. 4 to 12 shows distance Vs surface temperature along the thermosyphon. When heat input increases, the surface temperature of distilled water and binary mixture used in the thermosyphon increases. The surface temperature of thermosyphon with binary mixture is lower than the distilled water.

B. Effect of thermosyphon efficiency:

Fig. 13 to 15 shows the heat input Vs efficiency of thermosyphon for various heat input and flow rates for both distilled water and binary mixture. The efficiency of thermosyphon gives better results for binary mixture than the distilled water all inclinations, heat input and flow rates. For vertical position of thermosyphon, the efficiency is higher than the other for inclination. The lower inclination reduces the efficiency due to the obstruction of vapour with condensate return from the condenser. The efficiency is higher for 80 W heat input than the 40 W and 60 W heat inputs.

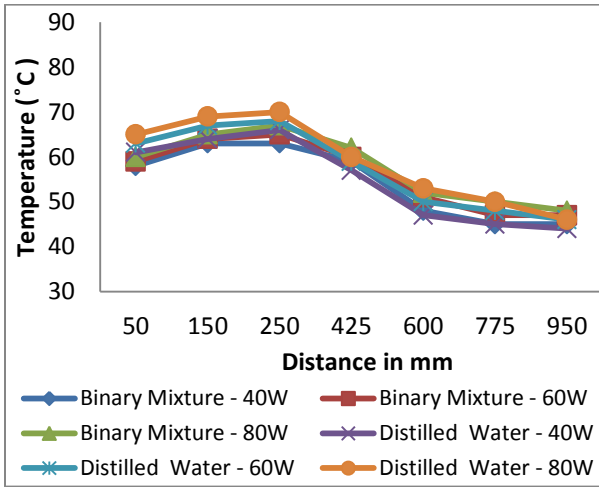


Fig.4: Flow rate 20Kg/hr inclination 90°

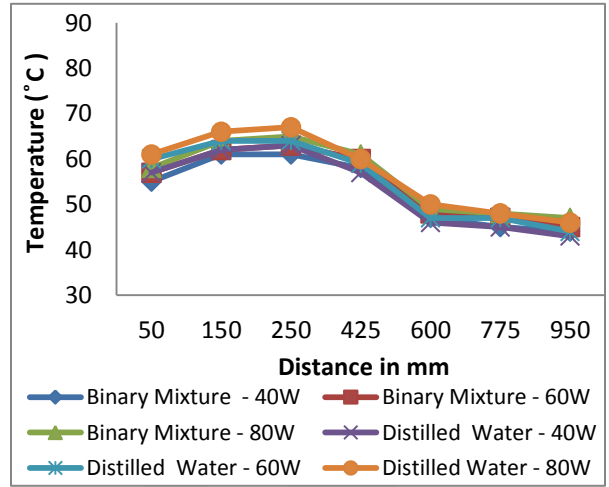


Fig.7: Flow rate 20Kg/hr and inclination 60°

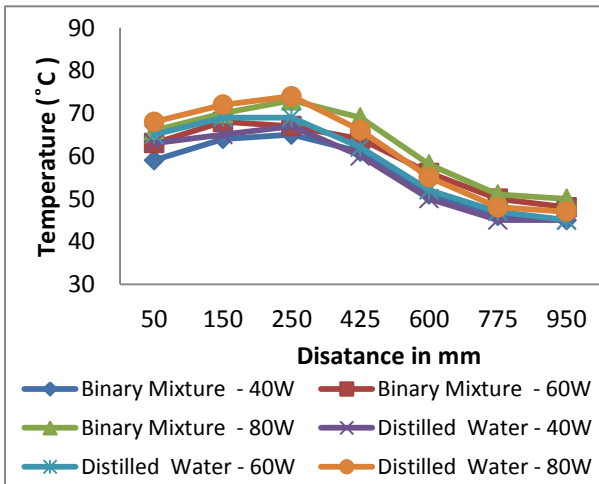


Fig.5: Flow rate 12Kg/hr and inclination 90°

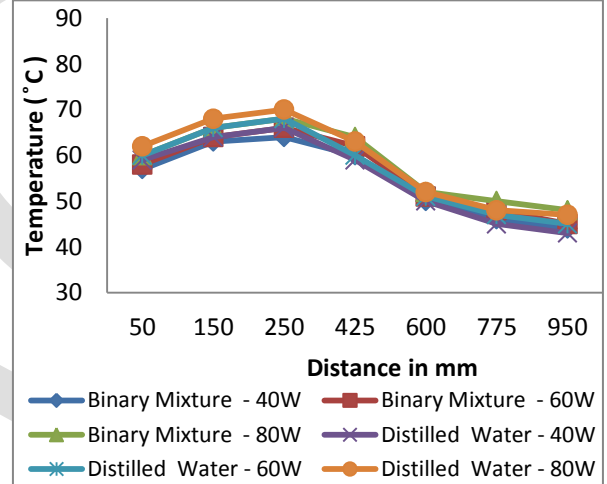


Fig.8: Flow rate 12Kg/hr and inclination 60°

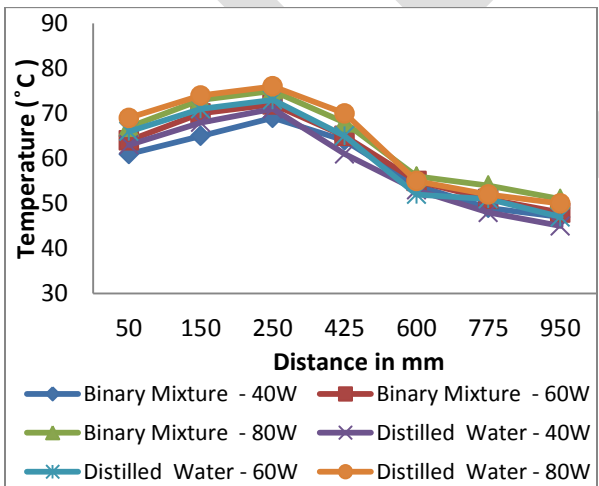


Fig.6: Flow rate 4Kg/hr and inclination 90°

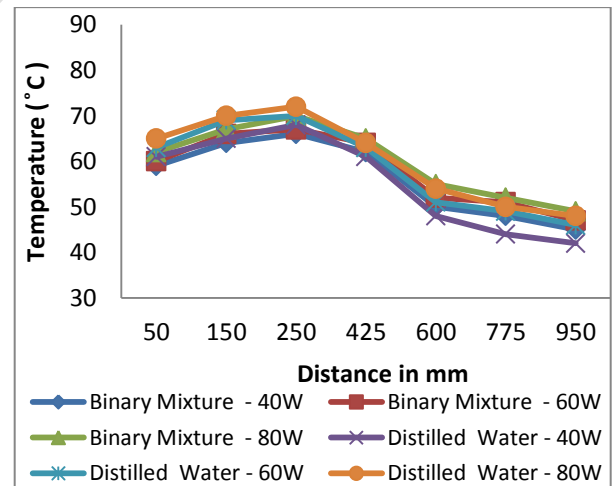


Fig.9: Flow rate 4Kg/hr and inclination 60°

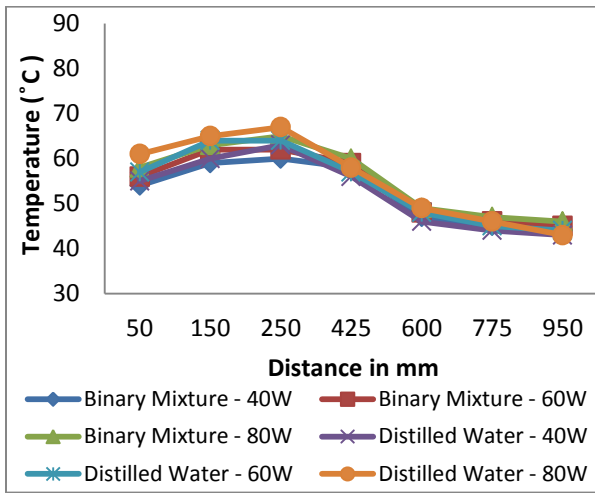


Fig.10: Flow rate 20Kg/hr and inclination 45°

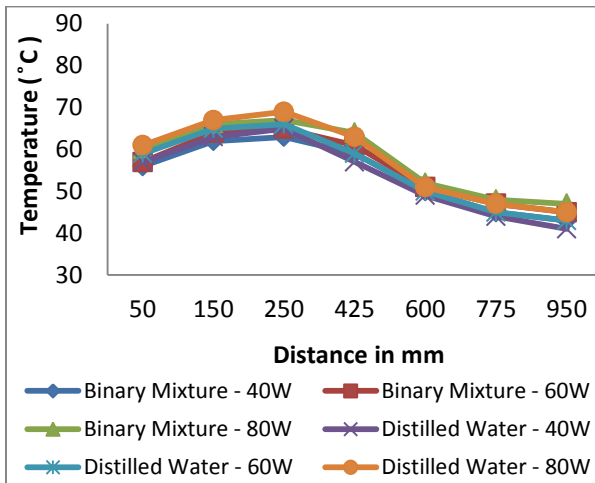


Fig.11: Flow rate 12Kg/hr and inclination 45°

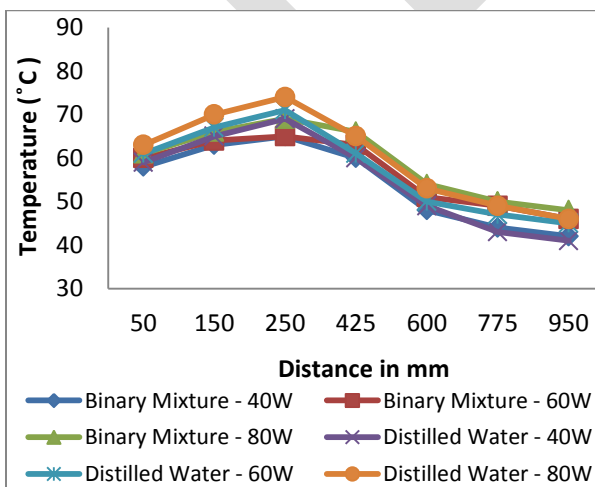


Fig.12: Flow rate 4Kg/hr and inclination 45°

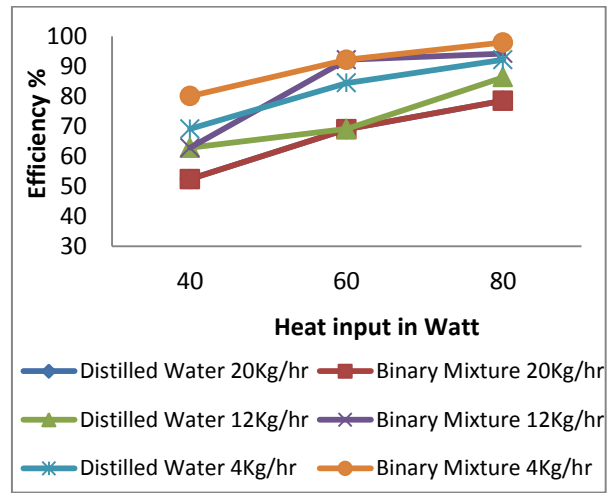


Fig.13: Efficiency for 90° inclination

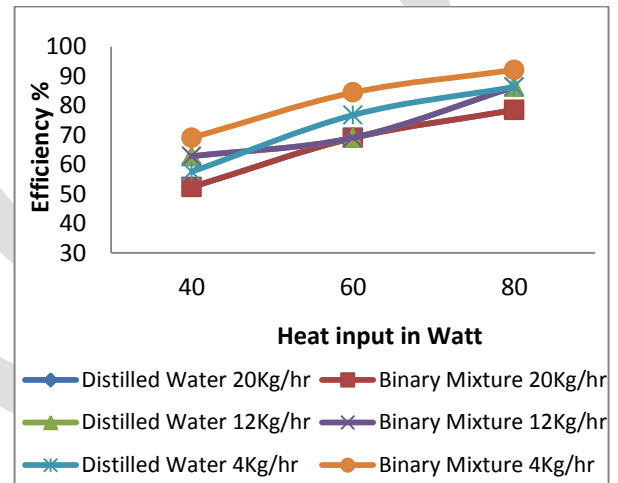


Fig.14: Efficiency for 60° inclination

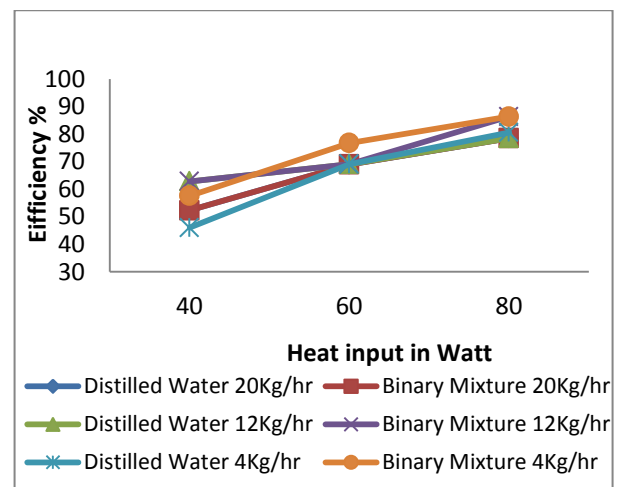


Fig.15: Efficiency for 45° inclination

VI. CONCLUSION

The experimental investigation was carried out on two phase closed thermosyphon charged with ethanol-methanol binary mixture and distilled water. The effect of inclination angle, coolant flow rate and heat load on the performance of thermosyphon was experimentally investigated. Coolant flow rate was varied from 4 kg/hr to 20 kg/hr along with inclination angle 40° to 90° with horizontal axis and heat load applied from 40 W to 80 W.

- Heat transfer efficiency is higher at coolant flow rate 4kg/hr. This is because at small cooling flow rate, coolant gets maximum time to exchange heat from condenser fluid and at larger cooling flow rate, that time span reduces because of high velocity. Therefore small flow rate coolant gets easily heated than larger one.
- Thermal performance of inclined thermosyphon with inclination angle 90° is better for coolant flow rate 4 kg/hr. This is because at vertical position condensate returns to evaporator at fast rate and there is restriction to appears flooding as well as entrainment limit.
- Based on the results, the thermosyphon charged with ethanol–methanol binary mixture has the maximum thermal performance than compared to thermosyphon charged with distilled water.

REFERENCES:

- [1] Grover, G. M. (1964). Evaporation-condensation heat transfer device. US Patent, No.3229759.
- [2] Z. Q. Long, P. Zang, (2013) "Heat Transfer Characteristics of Thermosyphon with N_2 -Ar Binary Mixture Working Fluid", *International journal of heat and mass transfer*, Vol. 63, pp 204–215.
- [3] M. Karthikeyan, S. Vaidyanathan and B. Sivaraman, (2010) "Thermal Performance of a Two Phase Closed Thermosyphon Using Aqueous Solution", *International Journal of Engineering Science and Technology*, Vol. 2(5), pp 913-918.
- [4] H. Z. Abou - Ziyen, A. Helali, M. Fatouh and M. M. Abo El - Nasr, (2001) "Performance of Stationary and Vibrated Thermosyphon Working With Water and R134a", *Applied thermal engineering*, Vol. 21, pp 813-830.
- [5] Negishi, K. & Sawada, T. (1983). Heat transfer performance of an ITPCT. *Int. J. Heat Mass Transfer*, Vol. 26, No. 8, pp. 1207-1213.
- [6] M. R. Sarmasti Emami, S. H. Noie and M. Khoshnoodi, (2008) "Effect of Aspect Ratio and Filling Ratio on Thermal Performance of an Inclined Two-Phase Closed Thermosyphon", *Iranian Journal of Science & Technology, Transaction B, Engineering*, Vol. 32, No. B1, pp 39-51.
- [7] K. S. Ong and Md. Haider – E - Alahi, (2003) "Performance of an R-134a Filled Thermosyphon", *Applied thermal engineering*, Vol. 23, pp 2373-2381.
- [8] S. Khandekar, Y. M. Joshi and B. Mehta, (2008) "Thermal Performance of Closed Two-Phase Thermosyphon Using Nanofluids", *International Journal of Thermal Science*, Vol. 47, pp 659-667.
- [9] G. Humnic, A. Humnic, I. Morjan and F. Dumitrache, (2011) "Experimental Study of the Thermal Performance of Thermosyphon Heat Pipe Using Iron Oxide Nanoparticles", *International Communications in Heat and Mass Transfer*, Vol. 54, pp 656–661.
- [10] P. G. Anjankar and Dr. R. B. Yarasu, (2012) "Experimental Analysis of Condenser Length Effect on the Performance of Thermosyphon", *International Journal of Emerging Technology and Advanced Engineering*, Vol. 2, Issue 3, pp 494-499.
- [11] H. Mirshahi and M. Rahimi, (2009) "Experimental Study on the Effect of Heat Loads, Fill Ratio and Extra Volume on Performance of a Partial-Vacuumed Thermosyphon", *Iranian Journal of Chemical Engineering*, Vol. 6, No. 4 (autumn), IChE.
- [12] M. Rahimi, K. Asgary and S. Jesri, (2010) "Thermal Characteristics of a Resurfaced Condenser and Evaporator Closed Two Phase Thermosyphon", *International Communications in Heat and Mass Transfer*, Vol. 37, pp 703–710.
- [13] Alizadehdakhel, M. Rahimi and A. A. Alsairafi, (2010) "CFD Modelling of Flow and Heat Transfer in a Thermosyphon", *International Communications in Heat and Mass Transfer* Vol. 37, pp 312–318.
- [14] S. R. Raja Balayanan, V. Velmurugan, R. Sudhakaran and N. S. Moorhy, (2011) "Optimization of Thermal Performance of Water to Air Thermosyphon Solar Heat Pipe Heat Exchanger using Response Surface Methodology", *European Journal of Scientific Research*, Vol. 59, pp 451-459.
- [15] S. H. Noie, "Heat Transfer Characteristics of a Two-Phase Closed Thermosyphon", *Applied Thermal Engineering*, 25, 2005, pp 495-506.

Face Recognition Using Eigen-Face Implemented On DSP Processor

Nawaf Hazim Barnouti

E-mail-nawafhazim1987@gmail.com, nawafhazim1987@yahoo.com

Abstract— This paper focus to develop an automatic face recognition using holistic features extracted that use the global features represented by low frequency data from face image. Holistic features are extracted using Eigen-face method where a linear projection technique such as PCA is used to capture the important information in the image. Euclidean distance is used for matching process. The propose method is tested using a benchmark ORL dataset that has 400 images of 40 persons. Euclidean distance classifier is tested using the TMS320C6713 digital signal processor (DSP). The computational time is less compared with the offline simulation using PC based. The best recognition rate is 95% when tested using 9 training images and 1 testing image represented with 35 PCA coefficients.

Keywords— Holistic features, Eigen-Face, PCA, Euclidean distance, ORL dataset, PCA coefficients, TMS320C6713

INTRODUCTION

Facial biometric is among the fastest growing biometric areas, but building an automated system for human face recognition is a challenge because humans are not well skilled in recognition numerous unknown faces. In recent years, much work has been carried out in face recognition, which has become successful in actual applications [5]. Face recognition can be divided into two main methods: two dimensional (2D) and three dimensional (3D). 2D and 3D refer to the actual dimension in a computer workspace. 2D is "flat", using the horizontal and vertical (X and Y) dimension, the image has only two dimensions. While 3D adds the depth (Z) dimension. This third dimension allows for rotation and visualization from multiple perspectives. Many face recognition methods including their modifications have been developed [3]. Identifying whether a face is known or unknown can be accomplished by comparing a person's face from a dataset of faces. Research interest in face recognition is rapidly increasing given the many laws and commercial applications of face recognition [8].

Face recognition has special advantages over their system characteristics because it is a non-contact process that can identify a person from a distance. People are not required to place their hands on a reader or their eyes in front of a scanner in a specific position [1]. Face recognition also aids in crime prevention because face images that are recorded and archived can later help identify a person. The advantage of face recognition is not the same based on all kind of methods. Different biometric indicators are appropriate for various kinds of identification applications because of the varying cost, intrusiveness, ease of sensing, and accuracy of these applications [4].

A face recognition classified into verification (one-to-one matting) and identification (one-to-many matching). Face verification will compare the face images against a template face images whose identity is being claimed. Face identification will compare a query face image against all images templates in a face dataset [7]. Figure 1 shows the process of face identification.

Face recognition methods can be divided into the following three categories:

1. Feature-based methods.
2. Appearance-based (Holistic) methods.
3. Hybrid methods.

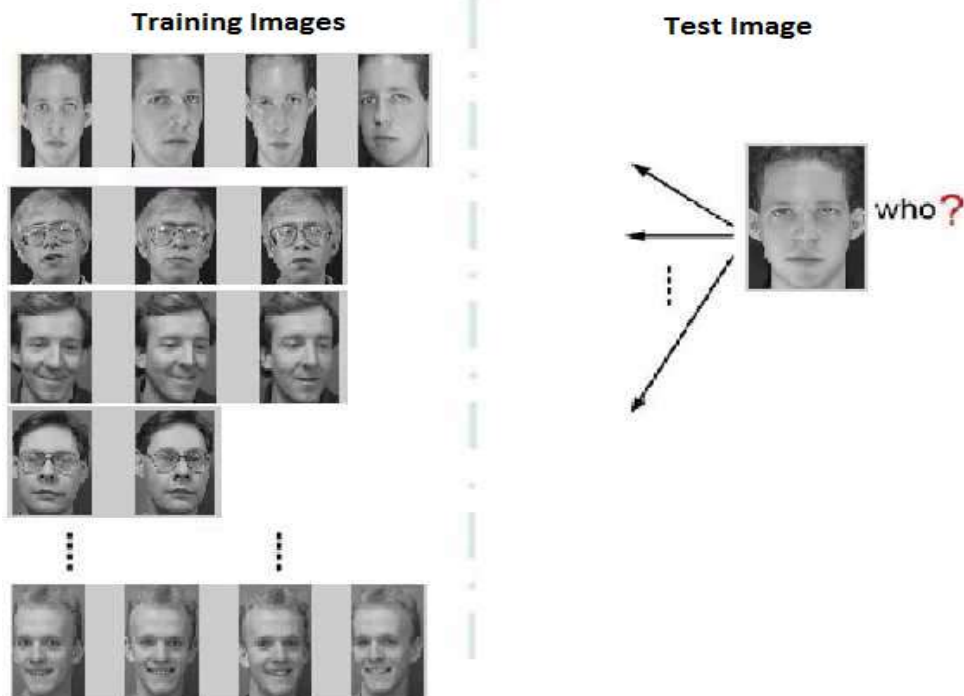


Figure 1: Face Identification Process.

Feature-based methods use a priori information or local facial features to select numerous features and the identify unique individuals. Local features include the eyes, nose, mouth, chin, and head outline, which are selected from face images. Appearance-based methods use global facial information for facial recognition. The features of holistic approaches represent optical variances in the pixel data of face images, which are used to identify one individual from another. Hybrid face recognition system combine both holistic and feature based methods. 3D images are used in hybrid methods [7] [8].

PRINCIPLE COMPONENT ANALYSIS

Numerous face recognition methods have been proposed, motivated by the increasing number of real world applications and by the curiosity on modeling human cognition. One of the most adaptable method for face images results from the statistical method called PCA. PCA is a feature extraction and dimensionality reduction method widely used for image recognition [7].

Covariance eigenvectors must be found to project the image to a lower dimensional feature space. The eigenvector corresponds to the original data directions of the principal components (PCs), and the statistical significance of the eigenvectors is provided by the corresponding eigenvalues. In PCA, the original data image is transformed into a subspace group of PCs [10]. PCA was initially offered by Kirby and Sirovich for face detection and identification. They showed that PCA is an optimal compression scheme the minimizes the mean squared error between original images and image reconstruction for any given compression level.

Applying PCA in face recognition is started by initially performing PCA on a set of training images of known human faces. A group of PCs is then computed from the covariance of the training sample image. Subsequently, the raw data in a high dimensional feature space are projected to a lower feature space through several eigenvectors with the highest eigenvalues. The classification is performed in a low dimensional feature space by using a simple classifier such Euclidean distance [2].

EIGEN-FACE APPROACH

Eigenfaces is a sufficient and efficient method for face recognition because of its learning capability, speed, and simplicity. In biometric recognition systems, the underlying facial information needs to be extracted and encoded efficiently, and one facial encoding is compared with similar information encrypted from the database. Eigenfaces is a projection technique derived from

eigenvectors when the raw image is projected to a new basis vector. It is an appearance-based method in face recognition which determines and captures the variation in a collection of face images, and then uses this information to encode and compare the images of human faces holistically. The idea behind extracting such type of information is to capture as many variations as possible from a group of training images [11].

Mathematically, the PCs of the feature distribution of faces can be found using the eigenfaces approach. First, the eigenvectors of the covariance matrix of the group of face images are located, and then the eigenvectors are sorted based on the corresponding eigenvalues [14]. Next, a threshold eigenvalue is determined. Finally, the eigenvectors with the most significant eigenvalue are selected. The original face images are then projected onto the significant eigenvectors to obtain a group called eigenfaces. Every face has a benefaction to the eigenfaces obtained. The perfect eigenfaces from a dimensional subspace is called face space [11].

The test image recognized is also projected onto the face space to obtain a low dimensional feature. Data distribution in the feature space are assumed to the Gaussian. Euclidean distance is used to determine a matching value with all the dataset templates. The matching value of all the training images can be also determined and stored in a distance matrix [2]. The matching value of the test image is then compared with the group of weights of the training images, and the most suitable match is located. The objective function for the decision is to determine the smallest distance value between the test image and the dataset template [12]. Figure 2 show the process of face recognition system.

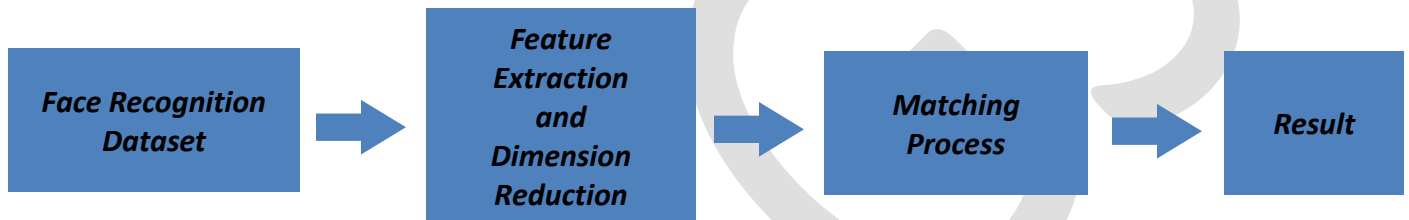


Figure 2: Face Recognition Process.

Training steps are as follows:

Step 1: Acquire an initial set of M number of face images (training images). ORL database with 400 images is used.

Step 2: More than one image $I(1), I(2), I(3), \dots, I(M)$ from M number is obtained, where each image has $w \times h$. The image is converted into a single vector and can be represented by the column vector of size $w \times h$. All images are represented as a column vector in this work as shown in Figure 3.

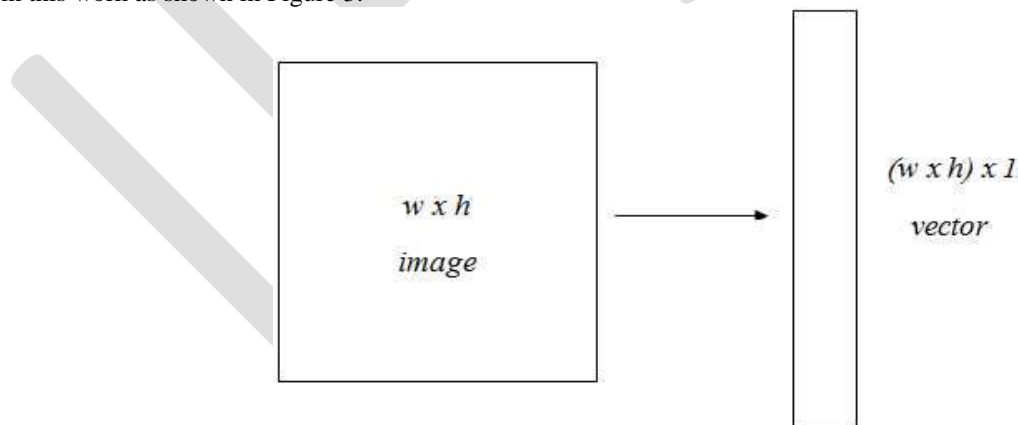


Figure 3: Image Representation.

Step 3: After the images are presented as column vector, the average of the M number of training images is given as follows:

$$av = \frac{1}{M} \sum_{n=1}^M I(n) \tag{1}$$

Where M is the total number of the training images.

Step 4: The original vector image is subtracted from the average image computed in the previous step. This process produces zero mean images and can be computed as follows:

$$A = I - av \quad (2)$$

Step 5: The total scatter matrix or covariance matrix is calculated from A , as shown in the equation below:

$$Covar = \frac{1}{M} \sum_{n=1}^M A(n) A^T(n) = A * A^T \quad (3)$$

Step 6: The eigenvalue and eigenvector of the covariance matrix need to be calculated.

Step 7: The diagonal of the eigenvalue matrix is sorted in decreasing order. The index of each sorted diagonal eigenvalue is sorted in a vector.

Step 8: The principle components is selected by calculating the eigenfaces from the training images. The M highest eigenvalue the belongs to a group of eigenvectors is chosen. These M eigenvectors describe the eigenfaces. Given that new faces are encountered, the eigenfaces can be updated or recalculated accordingly.

Step 9: The corresponding distribution in the M dimensional weight space is calculated for every known person by projecting the person's face image onto the face space.

Step 10: Each training sample is projected onto the eigenfaces space, and the projected features are obtained.

Step 11: When it is close, the weight patterns are classified as either a known person or an unknown person based on the Euclidean distance measured. When it is close enough, the recognition is then regarded as successful, and useful information about the recognized face is provided from the database that contain the face details. The Euclidean distance can be calculated from the equation below:

$$d(X, Y) = \sqrt{\sum_{i=1}^N (X_i + Y_i)} \quad (4)$$

Projection the test images are as follows:

Based on the procedure presented in the training phase, the testing phase projects the test image using the eigenvectors developed in the training phase. The testing sample is normalized and then the sample is projected onto the eigenfaces space. The projected test image is compared with the template stored in the dataset to determine the matching values. The training image that produces a minimum distance is assigned to a specific class or group.

HARDWARE IMPLEMENTATION

The goal of hardware implementation is to develop a prototype DSP platform. The purpose is to identify the individual or multiple faces and archive an acceptable recognition rate with less processing time [6].

In this experiment TMS320C6000 is used because its high performance and suitable for this types of problems. There are three distinct instruction set architectures as listed below:

1. High Performance TMS320C6000 DSP Platform.
2. Control Optimized TMS320C2000 DSP Platform.
3. Power Efficient TMS320C5000 DSP Platform.

TMS320C6713 DSP PROCESSOR

The C6713 DSK is a low cost standalone development platform that enables users to evaluate and develop applications for the TI C67xx DSP family [9]. The DSK comes with a full component of on-board drives that suit a wide variety of application environment. Key features are listed in Table 1.

Table 1: TMS320C6713 Key Features.

#	TMS320C6713
1	Operating at 225 MHz
2	16 Mbytes of synchronous DRAM
3	512 Kbytes of non-volatile flash memory
4	4 user accessible LED's and DIP switches
5	Software board configuration through registers implemented in CPLD
6	JTAG emulation through on-board JTAG emulator with USB host interface or external emulator
7	Single voltage power supply (+5v)

RESULT AND DISCUSSION

In this experiment, the ORL dataset is used to validate the proposed method. The images are organized in 40 directories (one for each subject), which have names in the *sn* form, where *n* indicates the subject number between 1 and 40. In each directory there are 10 different images of a person, whose name is in the form of *m.pgm*, where *m* is the image number between 1 and 10 for that person with each images 92 pixels x 112 pixels in size for a total of 10.304 pixels. The subjects comprise 4 females and 36 males. All the images are captured against a dark homogeneous background with the persons in an upright, frontal position, and with some allowance for side movement. Some variations occur in the facial expressions such as smiling/not smiling, open/closed eyes, and other facial details.

1. Analysis with different number of PCA Coefficient

In this analysis, the performance of their recognition system when using different number of PCA coefficient is tested. The number of eigenvectors is increased from 5 to 40, and the best recognition rates are examined in details. When the number of eigenvectors increases, many pieces of information are used during the classification. However, using too many eigenvectors produces less discriminative features because of the noise and redundant information in the feature space. Figure 4 shows the system performance by using different PCA coefficients on five training and five testing images. This analysis show that using 35 PCA coefficient produces results.

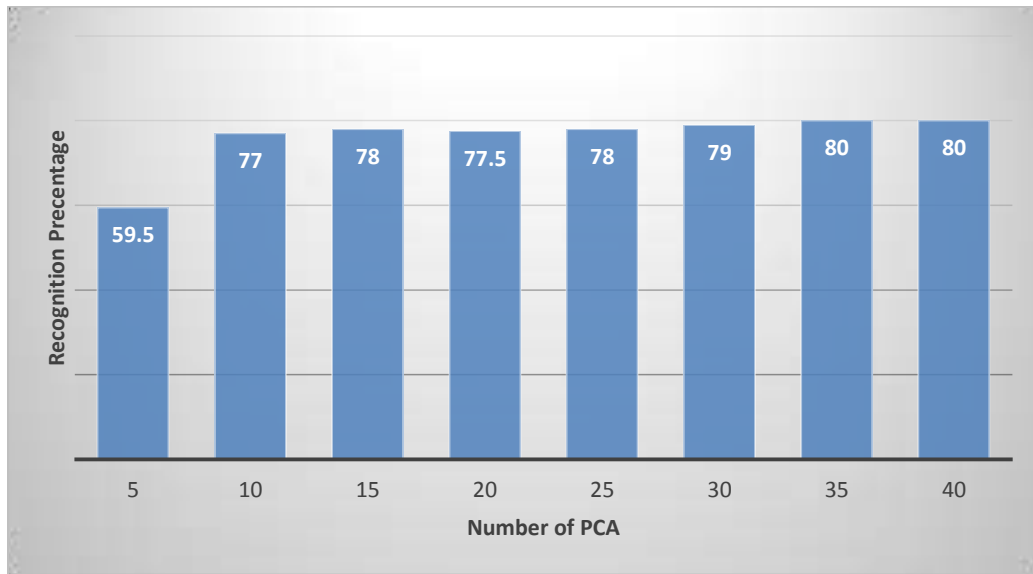


Figure 4: System Performance by Using Different PCA Coefficients

2. Analysis with different number of training and testing images

In this analysis, different number of training and tested images are used to examine the recognition rate. Table 2 shows that increasing the number of training images will increase the recognition rate.

Table 2: Recognition Rate Using Different Number of training and testing images.

No. of Testing Images	No. of Training Images	Recognition Rate
9	1	62.22 %
8	2	71.25 %
7	3	72.86 %
6	4	77.92 %
5	5	80 %
4	6	91.25 %
3	7	93.33 %
2	8	95 %
1	9	95 %

3. Comparison of Euclidean Distance Processing Time Using TMS320C6713 DSP Processor

In this analysis, the effectiveness of the Euclidean distance classifier when implemented using the TMS320C8713 digital signal processor (DSP) is tested. The computational time of the classification process is only examined because implementing the whole system in this board requires a large memory space for data storage. The TMS320 DSP family offers the most extensive selection of DSPs available in the market, with a balance of general purpose and application-specific processors to suit application needs. This processor has a floating point arithmetic logic unit, thus producing efficient computation accuracy. The output interface element, will communicate the decision of the face recognition system to the interfaced asset to enable access to the user. This can be a simple serial communication protocol like RS232, or a higher bandwidth USB protocol. It could also be the TCP/IP protocol via a wired medium. Classification using the TMS320 produces the same recognition rates, but with less processing time, as shown in Table 3. In this analysis, C language program is compiled and build, the PCA coefficient for the template and test image are pre-calculated and are located into the memory module on the DSP board.

Table 3: Processing Time Using TMS320 Compared with PC Based System.

Device	Time Required
PC Based System	5 Second
TMS320 DSP Processor	0.5 Second

CONCLUSION

Face recognition is a challenge because faces can change substantially in term of facial expression, detection, lighting and scale. This paper mainly focuses on the holistic face recognition method. The performance of the statistical PCA method is also investigated. PCA is used for the feature extraction and dimension reduction of given face images, whereas Euclidean distance is used for the matching process. The analysis using the ORL shows the significant performance achieved by this method, which has a 95% recognition rate. Using TMS320C6713 DSP Processor will reduce the time required for recognition process.

REFERENCES:

- [1] Singh, Prabhjot, and Anjana Sharma. "Face Recognition Using Principal Component Analysis in MATLAB." (2015).
- [2] Kadam, Kiran D. "Face Recognition using Principal Component Analysis with DCT." International Journal of Engineering Research and General Science, ISSN: 2091-2730 (2014).
- [3] Gawande, Mohit P., and Dhiraj G. Agrawal. "Face recognition using PCA and different distance classifiers." e-ISSN: 2278-2834,p- ISSN: 2278-8735. (2014).
- [4] Fan, ShaSha, Yang Du, Jia Zhao, Qiang Wang, and Fei Guo. "Comparative Research of PCA+ AdaBoost and PCA+ LDA for Face Recognition Technology." In 2015 International Industrial Informatics and Computer Engineering Conference. Atlantis Press, 2015.
- [5] Vig, Rekha. "A Gaussian Feature Adaptive Integrated PCA-ICA Approach for Facial Recognition." (2015).
- [6] Kumar, Neeraj, Sushree Mahapatro, and Sukanti Pal. "Implementation of Color Image Enhancement using DCT on TMS320C6713." ISSN -2277-1956
- [7] Shah, Deepali H., Dr JS Shah, and Dr Tejas V. Shah. "The Exploration of Face Recognition Techniques." International Journal of Application or Innovation in Engg. And Management (IJAIEM) Web Site: www. ijaiem. org Email: editor@ ijaiem. org, editorijaem@ gmail. com 3, no. 2 (2014).
- [8] Parmar, Divyarajsinh N., and Brijesh B. Mehta. "Face Recognition Methods & Applications." arXiv preprint arXiv:1403.0485 (2013).
- [9] Kumar, Mr P. Vijaya, and B. Swetha Reddy. "DSP Implementation of Gesture Recognition." (2010).
- [10] Abdullah, Manal, Majda Wazzan, and Sahar Bo-Saeed. "Optimizing Face Recognition Using PCA." arXiv preprint arXiv:1206.1515 (2012).
- [11] Slavković, Marijeta, and Dubravka Jevtić. "Face recognition using eigenface approach." Serbian Journal of Electrical Engineering 9, no. 1 (2012): 121-130.

Rapid Prototyping: A Review

¹Prof.N.U.Kakde,²Prof.V.J.Deshbhratar

Asstt. Professor, nagnath.kakde@gmail.com,DBACER,Nagpur.

Asstt. Professor,vishal.deshbhratar@gmail.com,itm,Nagpur.

Abstract— Rapid prototyping (RP) is one of the fastest developing manufacturing technologies in the world today. Rapid prototyping is a group of methods used to rapidly manufacture a scale model of a physical part or assembly using three-dimensional computer aided design (CAD), Computed Tomography (CT) and Magnetic Resonance Imaging (MRI) data. Construction of the part or assembly is usually done using 3D printing technology. Rapid prototyping techniques are often referred to solid free, computer automated manufacturing, form fabrication. The need of the hour is to bring together globally this fraternity to collaborate with each other.

Keywords— Rapid prototyping, STL File, SLA, LOM, SLS, FDM, 3D Jet Printing.

INTRODUCTION

To compete in today's industry environment, companies must keep up with the leading technologies and processes and also push the boundaries and develop new and improved products and processes. Shortening the lead-time for introducing a new product to the market has always been important to maximize profits and competitiveness. Recent developments in Computer Aided Design (CAD) technologies have significantly reduced the overall design cycle. However, the manufacturing process of the production mold still relies on slow and expensive machining processes. The Manufacturing Industry is an area where time, efficiency and accuracy are the major driving forces behind innovation and research. The most competitive companies are those who continually reduce process times, increase efficiency and improve accuracy. Rapid Prototyping is an area that has and is continuing to reduce production time and increase efficiency and accuracy in developing and manufacturing prototypes compared to traditional prototype manufacture. The research development of Rapid Prototyping (RP) is to give the Rapid manufacturing the needed confidence to go on to customized/tailor made product.

Investment casting is a combination of science, experience and art. Prior to final design and pattern construction, it is important to select an investment casting foundry and initiate communications. Typically, each foundry will have unique capabilities, processes and requirements. In addition, pattern specifications will vary with the selection of the metal alloy and the geometry of the part. If producing patterns for the foundry, it is critical that the foundry reviews the design so that it can recommend necessary design modifications to produce the highest quality part. The foundry can also make recommendations that reduce cost, time and weight, while improving cast ability and product performance. Additionally, FDM research is ongoing, so new process guidelines may evolve.

The goal of this research is to formulate a generalized Mathematical Model for Optimum temperature & time with given multiple choices of various Shell thickness & RP Part volume and find the optimal Model equation in project for the manufactured any complicated shape regular & non regular in confidence level by using Design of experiment technique.

All the RP techniques employ the same basic five step process. The steps are as follows:

- i. Create a CAD model of the design.
- ii. Convert the CAD model in to STL format.
- iii. Slice the STL model in to thin cross sectional layers.
- iv. Construct the model one layer atop another.
- v. Clean and finish the model.

a) CAD Model Creation

First the object to be built is modeled using a Computer added (CAD) software package. A large number of software packages are available in the market like PRO/ENGINEER. These tend to represent 3-D models more accurately than the wireframe modelers such as AutoCAD and hence produce very good results. The designer can create a new file expressly for prototyping or may use the existing CAD file. The process is same for all the RP build techniques.

b) Conversion to STL Format

The various CAD packages use a number of different algorithms to represent solid objects. To establish consistency, the STL (stereo lithography, the first RP technique) format has been adopted as the standard of the rapid prototyping industry. The second step, therefore, is to convert the CAD file into STL format. This format represents a three-dimensional surface as an assembly of planar triangles, "like the facets of a cut jewel. The file contains the coordinates of the vertices and the direction of the outward normal of each triangle. Because STL files use planar elements, they cannot represent curved surfaces exactly. Increasing the number of triangles improves the approximation, but at the cost of bigger files size. Large, complicated files require more time to pre-process and build, so the designer must balance accuracy with manageability to produce a useful STL file. Since the STL format is universal, this process is identical for all of the RP build techniques.

c) Slice the STL File

In the third step, a pre-processing program prepares the STL file to be built. Several programs are available, and most allow the user to adjust the size, location and orientation of the model. Build orientation is important for several reasons. First, properties of rapid prototypes vary from one coordinate direction to another. For example, prototypes are usually weaker and less accurate in the z (vertical) direction than in the x-y plane. In addition, part orientation partially determines the amount of time required to build the model. Placing the shortest dimension in the direction reduces the number of layers, thereby shortening build time. The pre-processing software slices the STL model into a number of layers from 0.01 mm to 0.7 mm thick, depending on the build technique. The program may also generate an auxiliary structure to support the model during the build. Supports are useful for delicate features such as overhangs, internal cavities, and thinwalled sections. Each PR machine manufacturer supplies their own proprietary pre-processing software.

d) Layer by Layer Construction

The fourth step is the actual construction of the part. Using one of several techniques (described in the next section) RP machines build one layer at a time from polymers, paper, or powdered metal. Most machines are fairly autonomous, needing little human intervention.

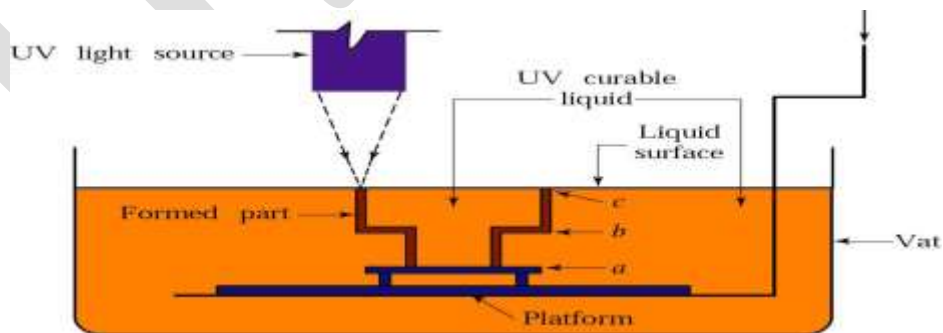
e) Clean and Finish

The final step is post-processing. This involves removing the prototype from the machine and detaching any supports. Some photosensitive materials need to be fully cured before use. Prototypes may also require minor cleaning and surface treatment. Sanding, sealing, and/or painting the model will improve its appearance and durability.

The six RP techniques available are as follows:

• Stereo Lithography (SLA).

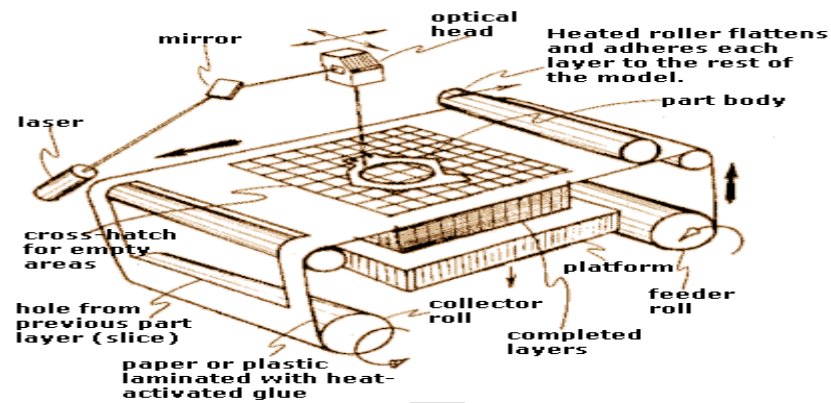
SLA RP technology has three main parts: a vat filled with ultraviolet (UV) curable photopolymer, a perforated build tray, and an UV laser. Due to the absorption and scattering of beam, the reaction only takes place near the surface and voxels of solid polymeric resin are formed. A SL machine consists of a build platform (substrate), which is mounted in a vat of resin and a UV Helium-Cadmium or Argon ion laser. A slice layer is cured on to the build tray with the UV laser. The pattern of the slice layer is "painted" with the UV laser with the control of the scanner system. Once the layer is cured, the tray lowers by a slice layer thickness allowing for uncured photopolymer covering the previously cured slice.



In new SL systems, a blade spreads resin on the part as the blade traverses the vat. This ensures smoother surface and reduced recoating time.

• Laminated Object Manufacture (LOM):-

The figure below shows the general arrangement of a Laminated Object Manufacturing (LOM™, registered trademark by Helisys of Torrance, California, USA) cell:



Material is usually a paper sheet laminated with adhesive on one side, but plastic and metal laminates are appearing.

1. Layer fabrication starts with sheet being adhered to substrate with the heated roller.
2. The laser then traces out the outline of the layer.
3. Non-part areas are cross-hatched to facilitate removal of waste material.
4. Once the laser cutting is complete, the platform moves down and out of the way so that fresh sheet material can be rolled into position.
5. Once new material is in position, the platform moves back up to one layer below its previous position.
6. The process can now be repeated.

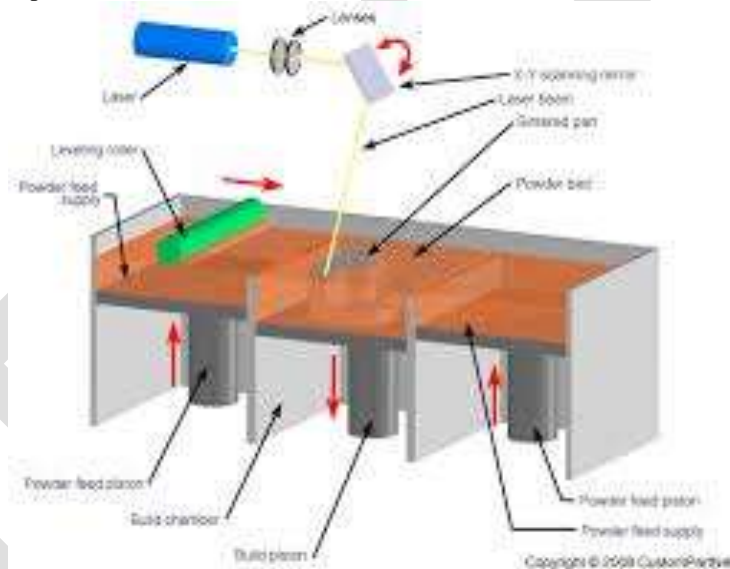
The excess material supports overhangs and other weak areas of the part during fabrication. The cross-hatching facilitates removal of the excess material. Once completed, the part has a wood-like texture composed of the paper layers. Moisture can be absorbed by the paper, which tends to expand and compromise the dimensional stability. Therefore, most models are sealed with a paint or lacquer to block moisture ingress.

The LOM™ developer continues to improve the process with sheets of stronger materials such as plastic and metal. Now available are sheets of powder metal (bound with adhesive) that can produce a "green" part. The part is then heat treated to sinter the material to its final state.

• **Selective Laser Sintering (SLS)**

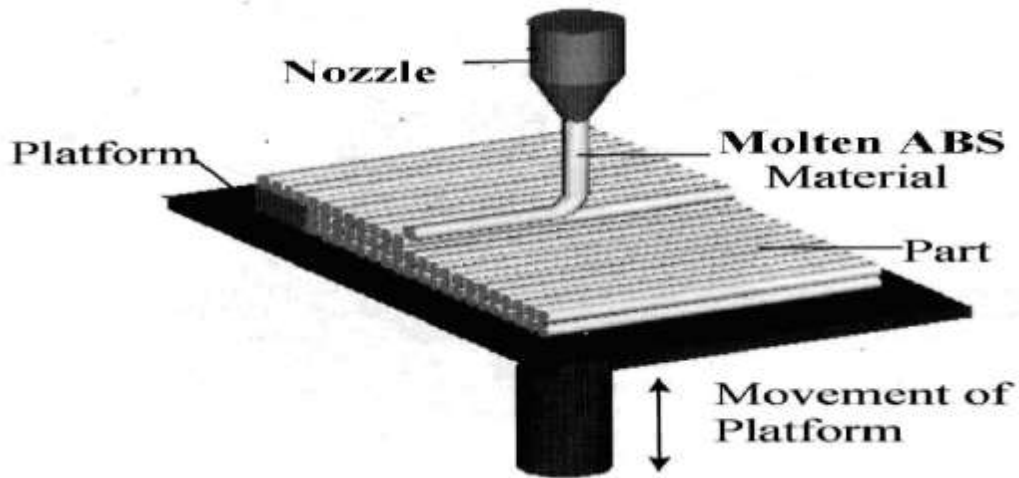
Selective Laser Sintering (SLS) is the rapid prototyping technology of choice for a range of functional prototype applications, including those with snap fits, living hinges and other mechanical joints. The ability of SLS to produce several pieces at one time also makes the process a good choice for Direct Digital Manufacturing (DDM) of products requiring strength and heat resistance.

Thermoplastic powder is spread by a roller over the surface of a build cylinder. The piston in the cylinder moves down one object layer thickness to accommodate the new layer of powder. A piston moves upward incrementally to supply a measured quantity of powder for each layer. A laser beam is traced over the surface of this tightly compacted powder to selectively melt and weld the grains together to form a layer of the object. The fabrication chamber is maintained at a temperature just below the melting point of the powder so that the laser elevates the temperature slightly to cause sintering - the grains are not entirely melted, just their outer surfaces - which greatly speeds up the process. The process is repeated, layer by layer, until the entire object is formed. After the object is fully formed, the piston is raised. Excess powder is simply brushed away and final manual finishing may be carried out. No supports are required with this method since overhangs and undercuts are supported by the solid powder bed. It takes a considerable cool-down time before the part can be removed from the machine. Large parts with thin sections may require as much as two days of cooling. SLS offers the key advantage of making large sized functional parts in essentially final materials. However, the system is mechanically more complex than stereolithography and most other technologies. A variety of thermoplastic materials such as nylon, glass filled nylon, and polystyrene are available. Surface finishes and accuracy are not as good as with stereolithography, but material properties can be quite close to those of the intrinsic materials. The method has also been extended to provide direct fabrication of metal and ceramic objects and tools. Since the objects are sintered they are porous. It may be necessary to infiltrate the part, especially metals, with another material to improve mechanical characteristics.



• **Fused deposition Modeling (FDM)**

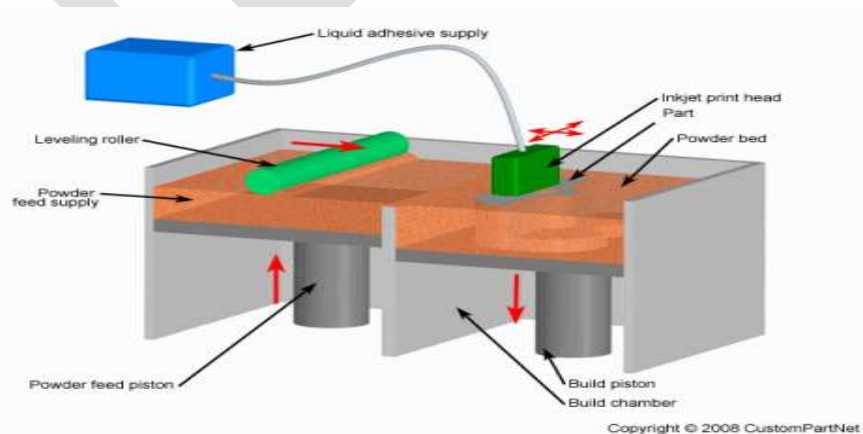
In Fused Deposition Modeling (FDM) process a movable (x-y movement) nozzle on to a substrate deposits thread of molten polymeric material. The build material is heated slightly above (approximately 0.5 C) its melting temperature so that it solidifies within a very short time (approximately 0.1 s) after extrusion and cold-welds to the previous layer as shown in figure. Various important factors need to be considered and are steady nozzle and material extrusion rates, addition of support structures for overhanging features and speed of the nozzle head, which affects the slice thickness. More recent FDM systems include two nozzles, one for part material and other for support material. The support material is relatively of poor quality and can be broken easily once the complete part is deposited and is removed from substrate. In more recent FDM technology, water-soluble support structure material is used. Support structure can be deposited with lesser density as compared to part density by providing air gaps between two consecutive roads.



• 3D Ink Jet Printing

Three Dimensional Printing (3DP) technology was developed at the Massachusetts Institute of Technology and licensed to several corporations. The process is similar to the Selective Laser Sintering (SLS) process, but instead of using a laser to sinter the material, an ink-jet printing head deposits a liquid adhesive that binds the material. Material options, which include metal or ceramic powders, are somewhat limited but are inexpensive relative to other additive processes. 3D Printing offers the advantage of fast build speeds, typically 2-4 layers per minute. However, the accuracy, surface finish, and part strength are not quite as good as some other additive processes. 3D Printing is typically used for the rapid prototyping of conceptual models (limited functional testing is possible).

The 3D printing process begins with the powder supply being raised by a piston and a leveling roller distributing a thin layer of powder to the top of the build chamber. A multi-channel ink-jet print head then deposits a liquid adhesive to targeted regions of the powder bed. These regions of powder are bonded together by the adhesive and form one layer of the part. The remaining free standing powder supports the part during the build. After a layer is built, the build platform is lowered and a new layer of powder added, leveled, and the printing repeated. After the part is completed, the loose supporting powder can be brushed away and the part removed. 3D printed parts are typically infiltrated with a sealant to improve strength and surface finish.



Copyright © 2008 CustomPartNet

CONCLUSION

This paper provides an overview of RP technology in brief and emphasizes on their ability to shorten the product design and development process. Classification of RP processes and details of few important processes is given. The description of various stages of data preparation and model building has been presented. An attempt has been made to include some important factors to be considered before starting part deposition for proper utilization of potentials of RP processes. Finally, the rise of rapid prototyping has spurred progress in traditional subtractive methods as well. Advances in computerized path planning, numeric control, and machine dynamics are increasing the speed and accuracy of machining. Modern CNC machining centers can have spindle speeds of up to 100,000 RPM, with correspondingly fast feed rates. Such high material removal rates translate into short build times. For certain applications, particularly metals, machining will continue to be a useful manufacturing process. Rapid prototyping will not make machining obsolete, but rather complement it.

REFERENCES:

- [1] Robert Bakker, Edwin Keijzers, and Hans van der Beek “Alternative Concepts and Technologies for Beneficial Utilization of Rice Straw” Wageningen UR Food & Biobased Research ,Number Food & Biobased Research number 1176 ,ISBN-number 978-90-8585-755-6,December 31st, 2009 [2] Ransom and Randolph – supplier of shell systems and other products to the IC industry
- [2] Schenectady Materials and Processes Laboratory, Inc & Biomet Inc.
- [3] Howmet Research Corporation, communication to Stratatsys, INC.-June 1998. ABS-P400 MSDS Sheet, November 4, 1994. EPA Handbook, Control Technologies for Hazardous Air Pollutants, June 1991.
- [4] Dilip Sahebrao Ingole; Abhay Madhusudan Kuthe, ”Rapid Prototyping –a Technology transfer approach for development of rapid tooling”; Rapid Prototyping Journal Vol.:15, No.:4, July 31,(2009),Pg 280-290.
- [5] Loose, K., Investigation of Optimum Process Parameters for Burnout of SLA Parts, Institute of Industrial Science, University of Tokyo.
- [6] Alain Bernard, Jean-Charles Delplace, Nicolas Perry and Serge Gabriel; “Integration of CAD and rapid manufacturing for sand casting optimization”; Rapid Prototyping Journal; Vol9, No.5, (2003), pp. 327–333
- [7] C. W. Lee, C. K. Chua, C. M. Cheah, L. H. Tan, C. Feng; “Rapid investment Casting: direct and indirect approaches via fused deposition modeling”; International Journal Adv Manufacturing Technology, (2004), vol23: pg 93–101.
- [8] S. Jones, C. Yuan; “Advances in shell molding for investment casting”; Journal of Materials Processing Technology; vol.135, (2003), pg 258–265.
- [9] W.L. Yao and Ming C. Leu; “Analysis of shell cracking in investment casting with laser stereolithography patterns”; Rapid Prototyping Journal; Volume 5, Number 1,(1999),pg 2–20. 109
- [10] D.K. Pal, Dr.B. Ravi; “Rapid tooling route selection and evaluation for sand and Investment casting”; Virtual and Physical Prototyping Journal; 2(4), pg197-207, (2007).
- [11] Rapid Prototyping (principles & applications)-Rafiq Noorani,Los Angeles, CA, Jhon wiley & sons, INC.
- [12] Rapid Prototyping & Manufacturing- Paul F. Jacobs, Mc graw-hill publishers.
- [13] Rapid Investment Casting via FDM Journal of advanced Manufacturing Technology C.lee, C.K.Chua Vol23,(2005),Pg 29-101.
- [14] Che Chung Wang, Shr-Shiung Hu; “Optimizing the rapid prototyping process by Integrating the Taguchi method with the Gray relational analysis”; Rapid Prototyping Journal; Vol 13,No.5, (2007), 304–315.
- [15] D. C. Montgomery, Design and Analysis of Experiments (second ed.), Wiley, New York, 1990.
- [16] Robert L. Mason, Richard F. Gunst, Dallas, Texas, James L. Hess. Statistical Design and Analysis of Experiments with Applications to Engineering and Science (Second Edition), A John Wiley & son’s publication, 2003
- [17] Minitab User Manual Release 14 MINITAB Inc, State College, PA, USA, 2003
- [18] Stratatsys material properties.

A Review On Gabor filters- An Optimal Filter For Corner Detection

Preeti Bala Sahu

Dept. Of Electronics & Telecommunication, Chouksey Engg. College, Bilaspur, Chhattisgarh

Chhattisgarh Swami Vivekananda Technical University, Bilai (Chhattisgarh)

495001, India

preeti.sahu62@gmail.com, 9074219475

Abstract— This study proposes a contour-based corner detector using the magnitude responses of the imaginary part of the Gabor filters on contours. The proposed corner detector combines the pixels of the edge contours and their corresponding grey-variation information. Firstly, edge contours are extracted from the original image using Canny edge detector. Secondly, the imaginary parts of the Gabor filters are used to smooth the pixels on the edge contours. At each edge pixel, the magnitude responses at each direction are normalised by their values and the sum of the normalized magnitude response at each direction is used to extract corners from edge contours. Thirdly, both the magnitude response threshold and the angle threshold are used to remove the weak or false corners. Finally, the proposed detector is compared with five state-of-the-art detectors on some grey-level images. The results from the experiment reveal that the proposed detector is more competitive with respect to detection accuracy, localisation accuracy, affine transforms and noise-robustness.

Keywords— contours, pixels, normalized, localisation, affine transforms, grey-variation, noise-robustness

INTRODUCTION

Corner detection is an important task in computer vision and image processing systems. There are many applications based upon the successful detection of corners, including object tracking, three-dimensional scene reconstruction [1–3]. The existing corner detectors can be broadly classified into two groups: intensity-based [4–12] and contour-based [13–17] methods.

Intensity-based methods indicate the corners directly on the grey-level image. Moravec [4] observed the intensity variation between the adjacent pixels of an edge or a uniform region of an image is small. However, the intensity variation is large in all the directions at the corner. Harris and Stephens [5] developed Moravec's idea into the Harris algorithm, applying the local auto-correlation matrix's eigen values to detect corners. This method has good repeatability under rotation and affine transforms. However, it is sensitive to noise and suffers from delocalisation problem, because the Gaussian filtering is not adapted to the image structure [6]. Later, the wavelet [7], the Gabor wavelet [8] and the Log-Gabor wavelet [9] were used to detect corners in the framework of Harris algorithm, which extract fine local multi-scale and multi-direction intensity variations information, construct the second moment matrix and take the eigen values as the corner measurement. There are many other algorithms [10–12] that examines image patches to fit predefined corner models, which have good or better corner localisation and noise robustness than those previously mentioned algorithms.

Contour-based methods first extract input image's edge contour by some edge detector and then analyse contours' shape to detect corners. The curvature scale space (CSS) technique is widely used in the contour-based methods [13–17]. Mokhtarian and Suomela [13] proposed CSS algorithm by computing the edge contours' absolute curvature at different scales and tracking curvature from high to low scale. CSS detector performs well in corner detection but suffers from two main problems [14]. Curvature estimation technique is sensitive to the local variation or noise on the contour, and it is difficult to choose appropriate Gaussian scales to smooth edge contour. Large Gaussian scale suppress noise well while degrades corner localisation, and small Gaussian scale preserves the corner localisation well while fails in noise suppression. Therefore some algorithms are developed to alleviate these problems. He & Yung [15] modified the CSS detector by using the dynamic region of support (ROS). Awrangjeb et al. [14] proposed multi-chord corner detector based upon the chord-to-point distance accumulation (CPDA) [16] technique. Hu et al. [17] proposed a corner detector by searching the contour for the tangent point in the direction of the angle bisector. In a way, the above mentioned detectors have improved CSS detectors' performance, while the analysis of the contour shape without considering the grey information of the edge contour.

It was proved [18] that the Gabor filters are suitable to be used as the model of human visual system. Shen and Bai [19] demonstrated Gabor filters are the optimal filters to extract local feature for various applications, such as face recognition [20] and edge detection [21]. Inspired by the definition that corner is the point with low self-similarity in all directions [12], as well as the work of contour-based corner detectors [13–17], we use the imaginary part of Gabor filters (IPGFs) to smooth the pixels of edge contours and extract the fine grey variation information. The sum of the normalised magnitude response at each direction (SNMRED) is embedded into the framework of the contour-based methods to develop a new corner detector. Here, the SNMRED is defined as a new corner measure to detect corners from edge contours, which also confirms the corner's definition [12].

Compared with the traditional contour- based detectors, the new corner measure uses not only the contours' geometric features well but also the directional grey-variation information of the pixels of contours completely. The proposed detector is compared with the five state-of-the-art corner detectors [5, 10, 13–15] based upon detection accuracy, localisation accuracy, repeatability under image affine transform and noise-robustness. The experimental results show our approach is more competitive.

This paper is organised as follows. In Section 2, characteristics of the IPGFs are introduced. The new corner measure on contours and proposed algorithm are presented in Section 3. The new detector is compared with the five state-of-the-art detectors, and performance analysis is described in Section 4. Finally, a conclusion is given.

IPGFs for corners detection

Pellegrino et al. [22] analysed IPGFs can provide fine directional intensity variation information around a pixel which motivates us to develop a new corner detector. In this section, we briefly introduce the property of IPGFs for corner detection.

In the spatial domain, two-dimensional (2D) Gabor is an elliptical Gaussian function in any rotation modulated by a sinusoidal plane wave. The corresponding IPGF [23] is

$$\Psi(x,y;f;\theta) = \frac{f \cdot f}{\pi \gamma \eta} \exp\left(-\frac{(f \cdot f)x' \cdot x' + (f \cdot f)y' \cdot y'}{2\pi f x'}\right) \sin(2\pi f x')$$

$$x' = x \cos \theta + y \sin \theta$$

$$y' = -x \sin \theta + y \cos \theta \quad (1)$$

where γ and η are the sharpness along the major and minor axis, respectively, which control the filter's sharpness; f is the central frequency of the filter, θ is the anticlockwise rotation angle of the Gaussian major and the plane wave. For an input image $I(x, y)$, IPGFs response can be calculated at any location (x, y) with the convolution

$$\zeta(x, y; f, \theta) = I(x, y) \psi(x, y; f, \theta)$$

$$= \int_{-\infty}^{\infty} \int_{-\infty}^{\infty} I(x - x_r, y - y_r) \psi(x, y; f, \theta) dx_r dy_r \quad (2)$$

The input images are 2D discrete signals in the integer lattice

To extract local intensity variation information around a pixel, various filters along different orientations need to be used. Given a central frequency f , the width of the major axis γ and minor axis η , the discrete IPGFs are derived by sampling the function in (1)

$$\Psi(m,n;f,k) = \frac{f \cdot f}{\pi \gamma \eta} \exp\left(-\frac{(f \cdot f)u \cdot u + (f \cdot f)v \cdot v}{2\pi f u}\right) \sin(2\pi f u)$$

$$u = m \cos \theta_k + n \sin \theta_k, \quad v = -m \sin \theta_k + n \cos \theta_k$$

$$\theta_k = \frac{2\pi k}{K}, \quad k = 0, 1, \dots, K-1 \quad (3)$$

where K is the number of orientations, θ_k is the k th orientation. Fig. 1 shows the IPGFs at eight orientations.

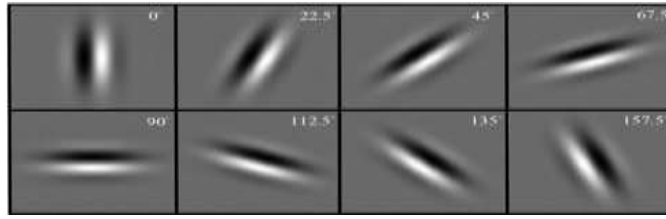


Fig. 1 A set of IPGFs at eight orientations, $f = 0.2$, $\gamma = 1$, $\eta = 2$

In this way, for an input discrete image $I(m, n)$, the magnitude response of the discrete IPGFs along the orientation θ_k is calculated by the convolution operator

$$\zeta(m, n; f, k) = I(m, n) * \psi(m, n; f, k)$$

$$= \sum \sum I(m - mx, n - ny) \Psi(m, n; f, k) \quad (4)$$

The magnitude response of the IPGFs along the orientation θ_k reflects the intensity variation of the input image along the orientation $\theta_k + \pi/2$. As a result, a set of the IPGFs along the different orientations can reflect the intensity variation around the edge pixels or corners completely. For a step edge, L-type corner, Y-junction, X-junction and star-like junction, the magnitude responses of the IPGFs are shown in Fig. 2.

Corner measure on contours and new corner detector

In this section, we propose a new corner measure and detection algorithm using the IPGFs on contours to detect corners, which combines the shape of the edge contours and the grey-variation information of pixels on the edge contours.

New corner measure using IPGFs on contours

The contour-based methods[13–17] are popular in corner detection that include three steps: extract edge contour by some edge detectors (such as Canny detector [24]), smooth edge contour by single- or multi-scale Gaussian function and compute their corresponding curvatures, the local curvature maxima points are selected for corner decision. These methods only consider the shape of the edge contours, with lack of intensity-variation information bringing two problems: Gaussian smoothing degrades the localisation accuracy and it is sensitive to local variation or noise on the contour. To overcome the above mentioned problems, we propose a new corner measure using the IPGFs on the edge contours.

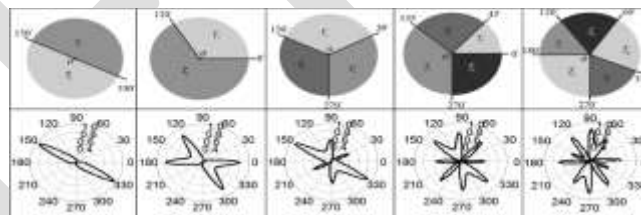


Fig. 2 Magnitude responses of the IPGFs of a step edge, L-type corner, T-junction, X-junction, and star-like junction

After the edge contours are extracted by the Canny edge detector, IPGFs smooth the pixels on the contours. In [4], corner is defined as the intensity variation is large in all directions, but small otherwise. However, we found image may be polluted by the noise or discretisation errors, it causes some non-corner pixels have large value of intensity variation at one or several orientations and leads to the increase of the probability of the false or missing detection. To enhance the detection accuracy and alleviate the noise or local variation's effect, the new corner measure is constructed by the SNMRED. In addition, normalisation makes the feature also illumination invariant. For each pixel on the contour, the SNMRED is defined by

$$\psi(m, n; f, k) = \frac{|\zeta(m, n; f, k)|}{\max_k \{|\zeta(m, n; f, k)|\}}$$

$$k \quad (5)$$

$$\text{SNMRED}(m, n; f) = \frac{1}{k} \sum \psi(m, n; f, k) \cdot m, n; f, k$$

K k=1

Whether a pixel is a corner point depends upon the pixel itself and its neighbouring pixels. In this sense, only if the orientation angle sampling interval in (5) is close enough, each pixel on the contour and its neighbouring pixels' relation information can be fully derived, which will be helpful to construct a robust corner detector.

An example of the new corner measure and its corresponding comparison results with He & Yung [15] corner measure is given in Fig. 3. The test image 'Block', one contour of the test image (extracted by Canny edge detector) and its corresponding 13 real corners are shown in Figs. 3a and b, respectively.

Fig. 3c shows the corner measure of He and Yung detects a false corner (marked by '□') and some false local maxima (marked by 'o'), which may increase the probability of the false detection. The reason is that the CSS curvature estimation technique involves the second derivative computation. The higher-order derivatives cause instability and errors in results. The local variation or noise on the contour degrades the detection performance. To alleviate the noise influence, He and Yung algorithm applies a Gaussian function to smooth the contour. The large scale Gaussian function removes noise well while degrades the localisation performance; and vice versa. Fig. 3d shows the result of the proposed corner measure. With the observation of SNMRED change, the SNMRED of the 13 real corners are all large which can easily be detected, and the SNMRED of edge pixels are all relatively small. The reason is that the proposed corner measure uses not only the edge pixels' shape information but also the edge pixels and their neighbouring pixels' fine intensity-variation information.

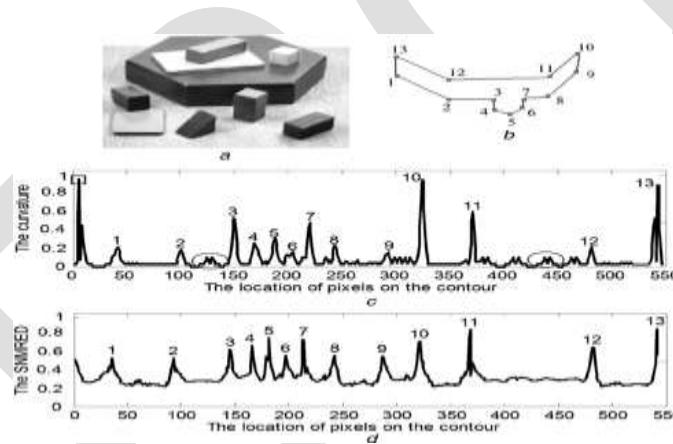


Fig. 3 Comparison of the two corner measures on a contour

- a 'Block' image b Edge contour with 13 corners
- c He and Yung [16] corner measure, and
- d Proposed corner measure

Some local variation or noise effect can be effectively reduced by the normalised sum of the magnitude responses. In this context, the new corner measure can reduce the probability of false or missing corner detection.

Candidate corner set refinement

After the computation of the corner measure, the local maximum SNMRED points are collected as candidate corners. A local maximum is either a true corner or a weak corner or a false corner. The latter two are because of the noise impact, and Canny edge detector may cause some edge contours deviating from true position.

To alleviate this problem, angle-threshold decision is used. If the estimated angle at each candidate corner is larger than the angle-threshold δ , the candidate corner is removed from the candidate corner set. The angle calculation technique [13] is applied as shown in Fig. 4.

As for a candidate corner C, the corresponding angle $\angle C$ is calculated by using the two tangents TDl and TD_r on both sides of the corner C. The ROS of point C is defined by the two nearest points D and E on both sides of the corner C. The two points D and E could be the candidate corners or the end points. To calculate the tangent angle β_{TDl} , $0 \leq \beta_{TDl} \leq 2\pi$, three points (C, the mid-point M and E) are selected; then, a simple three-point method is employed to fit a circle approximately on the left arm of ROS (from C to D). If the three points are collinear, the tangent direction on the left side of C is from C to E. Otherwise, the centre of circle C_o is calculated by the three points C, M, and D. ϑ is used to represent the direction from C to M and ϕ is used to represent direction from C to C_o. Then, the left tangent angle β_{TDl} is calculated as follows

$$\beta_{TDl} = \phi + \text{sign}(\sin(\vartheta - \phi))\pi/2 \quad (6)$$

where sign is a signum function. Similarly, the tangent angle β_{TDr} , $0 \leq \beta_{TDr} \leq 2\pi$, on the right arm of CE is determined.

Hence, the angle $\angle C$ can be obtained

$$\angle C = \begin{cases} |\beta_{TDl} - \beta_{TDr}|, & \text{if } |\beta_{TDl} - \beta_{TDr}| < \pi \\ 2\pi - |\beta_{TDl} - \beta_{TDr}|, & \text{otherwise} \end{cases} \quad (7)$$

Finally, the candidate corner C is a true corner if $\angle C$ satisfies

$$\angle C \leq \delta \quad (8)$$

where δ is the angle threshold.

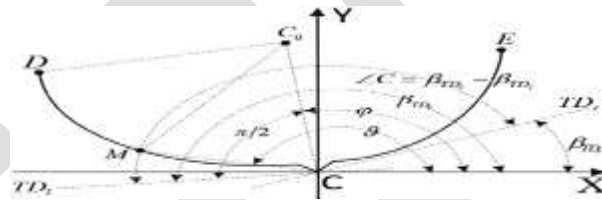


Fig. 4 Angle calculation on the candidate corner C

Proposed SNMRED corner detector

The proposed method first detects binary edge map by Canny edge detector and extracts edge contour. IPGFs are used to smooth the edge pixels on the contours, and the magnitudes at every pixel along different directions are obtained. Then the SNMRED is computed as the corner measure. The outline of the proposed algorithm is

1. Extract a binary edge map from the input image by Canny edge detector.
2. Extract edge contours from the edge map, fill gaps if they are within a range.
3. Smooth the pixels on the edge contours using IPGFs, compute SNMRED for each pixel on the contours.
4. For each edge contour, apply non-maximum suppression to the result obtained in the step 3. If the SNMRED of one pixel is a local maximum, the pixel is marked as a candidate corner; otherwise, it would be set to zero.
5. To remove weak corners, compare the candidate corners obtained in step 4 with a threshold Th.
6. Calculate angle at each candidate corner obtained in step 5 and compare with the angle-threshold δ to remove false corners.

EXPERIMENTAL RESULTS AND DISCUSSION

Summary of the proposed parameter setting

The parameters setting of the proposed detector are: $f = 0.2$, $\gamma = 1$, $\eta = 2$, $K = 90$, $Th = 0.52$ and $\delta = 168^\circ$. According to the Nyquist sampling theory, the upper and low central frequency f for a 2D image is 0.5 and 0 cycles/pixel, respectively. As [25] mentioned implementation of filters with high central frequency (e.g. above 0.2 cycles/pixel) requires the filters to be sampled more densely than

the available grid, which increases the difficulty of filter design; whereas the low central frequency may degrades the feature localisation accuracy. Then the central frequency is 0.2. The selection of the parameters $\gamma = 1$ and $\eta = 2$ conform to the physiology findings [18], which help the Gabor filters to extract the image structure information effectively and economically. The parameter values of K , Th , and δ are decided by experiments. Two commonly-used grey-scale images with GTs, 'Block' and 'Lab', are used in the experiments of parameters selection. Fig. 5 shows the two images and their GTs, which have 59 and 249 GTs, respectively. The criteria [15] of detection accuracy and localization error are as follows: CDET and CREF represent the detected corners set by a particular detector and the reference corners set, respectively. For a detected corner in the CDET set, its corresponding minimal distance from the CREF set is found. If the minimal distance is less than the predefined distance D_{max} ($D_{max} = 4$), then the detected corner is marked as a true corner; otherwise, it is labelled as a missed corner. The localisation error is defined as the average distance on all the matched pairs.

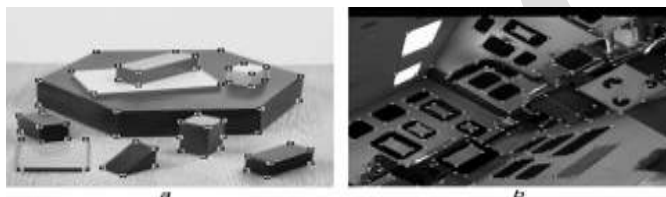


Fig. 5 Test image a 'Block' with GTs b 'Lab' with GTs

Let $\{(CREF_i, CDETi), i = 1, 2, \dots, Nr\}$ be the matched corner pairs in the reference and detected corners set, respectively. Then, the localisation error [14] is calculated by

$$Le = \sqrt{\frac{1}{Nr} \sum_{i=1}^{Nr} \|CREF_i - CDETi\|^2} \quad (9)$$

where Nr is the number of the repeated corners between them.

The values of K , Th and δ affect the detection accuracy, and only the orientation numbers K affects the localisation. Provided that the orientation sampling interval is close enough, the effect of two variables Th and δ change on the proposed method is shown in Fig. 6a. When both the two variables were set small, the average missed corners were relatively small, but its average false corners were high.

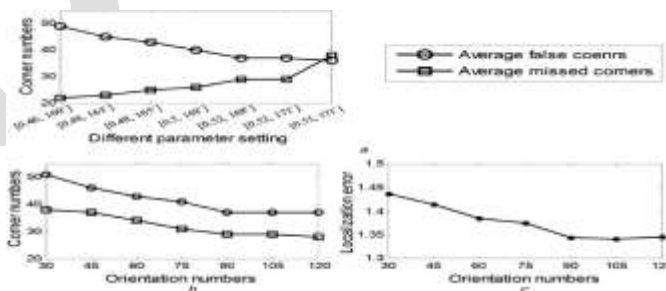


Fig. 6 Effect of the parameters change on the proposed detector

a Different parameter setting

b Orientation numbers

c Orientation numbers

However, when the two variables were increased above $Th = 0.52$ and $\delta = 168^\circ$, the average missed corners became large, whereas the average false corners remained constant. Therefore we chose the two thresholds $Th = 0.52$ and $\delta = 168^\circ$. Figs. 6b and c show the effect of the orientation numbers change on the proposed detector. With the reduction of the orientations, all the average of missed corners, the average of false corners, and the localization error increase. The reason is that small orientations cannot extract enough grey-variation information. However, when the orientation was above 90, both the detection accuracy and localisation error remain stable. In this way, the orientation number is set to 90.

Performance evaluation using GT images

In this subsection, 'Block' and 'Lab' are used in the performance evaluation using GTs. The detection results in the noise-free cases are shown in Figs. 7 and 8, respectively. The results are summarised in Table 1. For the two test images, the Harris and SUSAN detect the more number of false corners than the four contour-based corner detectors and the localisation errors are the worst. The reason is that the two methods are single-scale detectors and only work well if the image has similar-size features [15], but ineffective otherwise; and the accuracy of localisation degrades for the same reason. The CSS has the third largest number of the false corners and the third worst localisation. It is because of the CSS depends on the choice of Gaussian smoothing-scale, which results in the corner localisation deviates from the really position; meanwhile, the inappropriate smoothing scale results in some true corners missing detected and some false corners detected. The CPDA performs the best in the index of false corners and the second best in localisation error. However, the CPDA performs the worst in the index of missed corners. The reason is that multi-chord product in the CPDA measure depends upon the chord choice. Only if the three curvatures of the corner are all strong, then the corner be distinguished. Otherwise, if two curvatures of three are large, one is small, or one is large and two are small, the multi-product may be small, which results in missing many true corners. By contrast, He and Yung and the proposed method achieve better performance, which have smaller number of missing corners, false corners and amount of localisation error relatively.

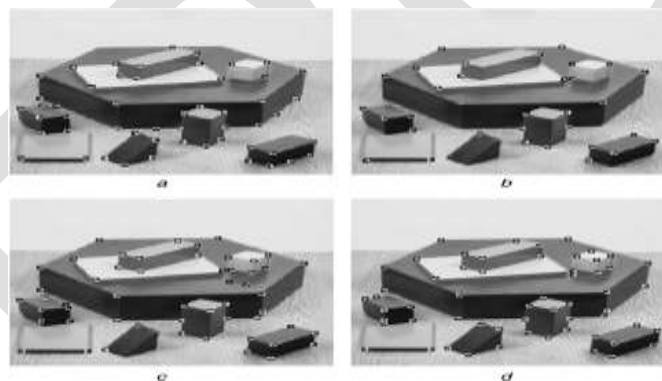


Fig. 7 Detection results on the 'Block' image

- a Harris
- b CPDA
- c He and Yung
- d Proposed method

As for a test image, missing a true corner and detecting a false corner yield the same loss in detection performance, the ratio of the number of missed and false corners to the number of GTs is used to evaluate the detection performance of a detector quantitatively. For the test image 'Block', the ratios of the six detectors are 19/59, 34/59, 21/59, 29/59, 18/59 and 12/59, respectively. For the test image 'Lab', the ratios of the six detectors are 195/249, 166/249, 146/249, 138/249, 128/249 and 119/249, respectively. It can be seen that the proposed method achieves the best detection performance in the noise-free case. Meanwhile, it is shown in Table 1 that the proposed method achieves the smallest localisation error, CSS, CPDA and He and Yung are moderate, the Harris and SUSAN are the poorest.

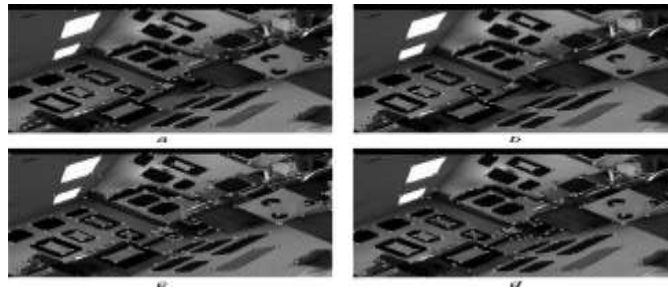


Fig. 8 Detection results on the 'Lab' image:

a Harris b CPDA c He and Yung d Proposed method

Table 1 Evaluation results for the noise-free images

Detectors	Missed corners	False corners	Localisation
'block' image			
Harris [5]	13	6	1.8484
SUSAN [10]	15	19	1.7626
CSS [13]	4	17	1.7545
CPDA [14]	28	1	1.4011
He and Yung[15]	12	6	1.4802
Proposed	5	6	1.4008
'Lab' image			
Harris	67	128	1.5011
SUSAN	69	97	1.4981
CSS	58	88	1.5097
CPDA	124	14	1.3206
He and Yung	51	77	1.3926
Proposed	52	67	1.2884

Repeatability under image affine transform

In this subsection, performance evaluation of corner detection based upon average repeatability under affine transform [14] is adopted, which avoids the traditional evaluation technique based upon the human judgment and can be used with any size of database. Twenty-eight different common images, including 'Lena', 'Leaf', 'Lab' and 'Block' are used to evaluate the average repeatability. The transformed images were obtained by applying the following six different types of transforms on each original image:

† Rotations: 18 different angles θ in $[-90^\circ, 90^\circ]$ at 10° apart, excluding 0° .

† Uniform scaling transforms: scale factors $s_x = s_y$ in $[0.5, 2.0]$ at 0.1 apart, excluding 1.0.

† Non-uniform scaling transforms: scale factor $s_x = 1$ and s_y in $[0.5, 1.9]$ at 0.1 apart, excluding 1.0.

† Gaussian noise: zero mean white Gaussian noise at 15 standard deviation in $[1, 15]$ at 1 apart.

The average repeatability R_{avg} measures the average number of repeated corners between original and affine transformed images. It is defined as

$$R_{avg} = \frac{N_r (N_o + N_t)}{2 N_o N_t} \quad (10)$$

where N_o and N_t represent the number of detected corners in the original and transformed images by one detector, and N_r is

the number of repeated corners between them. It is noted that a corner point p_i is detected in original image and its corresponding position is point p_j after image geometric transform. If a point is detected in geometric transformed image, which is in the neighbourhood of p_j (within 4 pixels), then a repeated corner is achieved.

The results of the average repeatability under the six transforms are shown in Fig. 9. As the Figs. 9a and b shown, the six detectors preserve high repeatability under rotation and uniform scaling. The reason is the six detectors are robust to image rotation and uniform scaling in the continuous form. However, the resampling of the transform images mainly affects the corner detection performance of the three transforms. Fig. 9c shows the repeatability of non-uniform of the six detectors is low. The reason is that six detectors are sensitive to image non-uniform in continuous form. For Gaussian noise, the six detectors' robustness decreased with the increase of the noise variance, as shown in Fig. 9d. It is shown the proposed method achieves the largest repeatability for rotation, uniform scaling transformation. For the other two indices, the proposed method is the second best. It can be seen the six detectors are different in detection performance, localisation accuracy, affine transforms and noise-robustness. Fully compared the performance of the detectors at these four aspects, the proposed detector is better in overall performance. This owes to the fact the pixels' intensity variation of the edge contour is realizable utilised in contour-based detection frame.

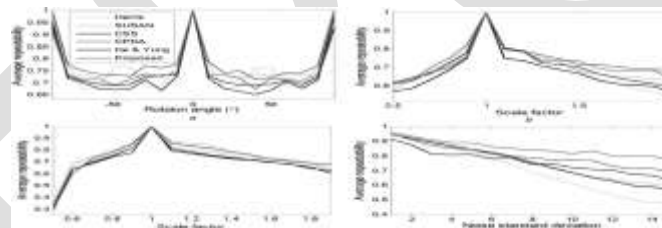


Fig. 9 Average repeatability results under rotation, uniform scaling, non-uniform scaling and Gaussian noise

a Rotation transformation b Uniform scaling transformation c Non-uniform scaling transformation d Gaussian noise

ACKNOWLEDGMENT

The author will be very thankful to the reviewers and the editors for their valuable suggestions to improve the paper and professor for their valuable assistance.

CONCLUSION

The main contribution of the paper is the consideration of the edge contours and their corresponding grey-variation information in the corner detection. The IPGFs are used to smooth the edge pixels and the sum of the normalized magnitude responses are used to identify corners, which can enhance the detection accuracy and suppresses the false or missing detection. The proposed detector outperforms the five state-of-the-art corner detectors in terms of the detection accuracy, localisation accuracy, noise robustness and the repeatability under image affine transforms. However, it has been observed from some of the experimental results that the proposed detector also detects some false corners. This is because of the fact that the single centre frequency is used to tune the IPGFs, thus ignoring some special corner features present within other bands. This suggests the use of multi-frequencies for the construction of IPGFs and the detection of corners. Moreover, the use of 90 orientations of IPGFs to detect corners increases the computational complexity. The future work is to use the simplified Gabor filters [21] to detect corners, which may keep the similar performance of the proposed method, but it requires a significantly smaller amount of computation.

REFERENCES:

- [1] Dutta, A., Kar, A., Chatleri, B.N.: 'A new approach to corner matching from image sequence using fuzzy similarity index', Pattern Recognit. Lett, pp. 712–720, 32, (5), 2011
- [2] Yang, F., Lu, H., Zhang, W., Yang, G.: 'Visual tracking via bag of features', IET Image Process, pp. 115–128, 6, (2), 2012
- [3] Mikolajczyk, K., Schmid, C.: 'Scale & affine invariant interest point detectors', Int. J. Comput. Vis, pp. 63–86, 60, (1), 2004
- [4] Moravec, H.P.: 'Towards automatic visual obstacle avoidance'. Proc. 5th Int. Joint Conf. on Artificial Intelligence, MA, pp. 584, 1977
- [5] Harris, C., Stephens, M.: 'A combined corner and edge detector'. Proc. 4th Alvey Vision Conf., pp. 147–151, 1988
- [6] Kim, B., Choi, J., Park, Y., Sohn, K.: 'Robust corner detection based on image structure', Circuits Syst. Signal Process, pp. 1443–1457, 31, (2), 2012
- [7] Yeh, C.-H.: 'Wavelet-based corner detection using eigenvectors of covariance matrices', Pattern Recognit. Lett, pp. 2797–2806, , 24, (15), 2003
- [8] Panning, A., Al-Hamadi, A., Michaelis, B.: 'Facial feature point detection using simplified Gabor wavelets and confidence-based grouping' (IEEE SMC, Seoul,), pp. 2687–2692, 2012
- [9] Gao, X.-T., Sattar, F., Venkateswarlu, R.: 'Multiscale corner detection of gray level images based on log-Gabor wavelet transform', IEEE Trans. Circuits Syst. Video Technol., pp. 868–875, 17, (7), 2007
- [10] Smith, S.M., Brady, J.M.: 'SUSAN-A new approach to low level image processing', Int. J. Comput. Vis., pp. 45–78, 23, (1), 1997
- [11] Sinzinger, E.D.: 'A model-based approach to junction detection using radial energy', Pattern Recognit., , pp. 494–505, 41, (2), 2012
- [12] Edward, R., Reid, P., Tom, D.: 'Faster and better: A machine learning approach to corner detection', IEEE Trans. Pattern Anal. Mach. Intell., pp. 105–119, 32, (1), 2010
- [13] Mokhtarian, F., Suomela, R.: 'Robust image corner detection through curvature scale space', IEEE Trans. Pattern Anal. Mach. Intell., pp. 1376–1381, 20, (12), 1998
- [14] Awrangjeb, M., Lu, G.: 'Robust image corner detection based on the chord-to-point distance accumulation technique', IEEE Trans. Multimedia, pp. 1059–1072, 10, (6), 2008
- [15] He, X.C., Yung, H.C.: 'Corner detector based on global local curvature properties', Opt. Eng pp. 057008–0, 47, (5), 2008
- [16] Han, J.H., Poston, T.T.: 'Chord-to-point distance accumulation and planar curvature: a new approach to discrete curvature', Pattern Recognit. Lett., pp. 1133–1144, 22, (10), 2001
- [17] Hu, H., Lin, X., Zhang, X., Feng, y.: 'Detection of local invariant features using contour', IET Image Process., pp. 364–372, 7, (4), 2013
- [18] Daugman, J.G.: 'Uncertainty relation for resolution in space, spatial frequency and orientation optimized by two-dimensional visual cortical filters', J. Opt. Soc. Am. A, pp. 1160–1169, 2, (7), 1985
- [19] Shen, L., bai, L.: 'A review on Gabor wavelets for face recognition', Pattern Anal. Appl., pp. 273–292, 9, 2006
- [20] Liu, C., Wechsler, H.: 'Gabor feature based classification using the enhanced fisher linear discriminant model for face recognition', IEEE Trans. Image Process., pp. 467–476, 11, (4), 2002
- [21] Jiang, W., Lam, K.-M., Shen, T.-Z.: 'Efficient edge detection using simplified Gabor wavelets', IEEE Trans. Syst. Man Cybern. Part B: Cybern., pp. 1036–1047, 39, (4), 2009
- [22] Pellegrino, F., Vanzella, W., Torre, V.: 'Edge detection revisited', IEEE Trans. Syst. Man Cybern., pp. 1500–1518, 34, (3), 2004

[23] Kamarainen, J.-K., Kyrki, V., Kalviainen, H.: '*Invariance properties of Gabor filter-based features-overview and applications*', IEEE Trans. Image Process., pp. 1088–1099, 15, (5), 2006

[24] Canny, J.: '*A computational approach to edge detection*', IEEE Trans. Pattern Anal. Mach. Intell., pp. 679–698, 8, (6), 1986

[25] Bovik, A.C., Clark, M., Geisler, W.S.: '*Multichannel texture analysis using localized spatial filters*', IEEE Trans. Pattern Anal. Mach. Intell., pp. 55–73, 12, (1), 1990

[26] The Image Database [Online]. Available: <http://figment.csee.usf.edu/edge/roc>

IJERGS

Estimation of Software Reliability on the Basis of Bits for Embedded System

Sanjay Kumar Chauhan¹ Rajesh Mishra² Rajendra Bahadur Singh³

Gautam Buddha University, Noida, Uttar Pradesh, India
sanjay_itm07@hotmail.com, contact No.- +918005246558

Abstract - As software in an embedded system has taken responsibility for controlling both software, and hardware components, the importance of estimating more accurate reliability for such software has been increased. To estimate the reliability of software, we use software which is a collection of bits so while analyzing of system the software reliability in terms of bit it gives better result comparison to software reliability in terms of time analysis. The software is the collection of bits and during the execution bits are processed and it defines the level of execution. While we analyze the bit we justify the performance of system and estimate the reliability in a better way. However, many researchers have developed software reliability models assuming that software failures are caused by only software faults, which might lead to inaccurate reliability estimation.

In this paper a Software Reliability model is proposed in which the performance of the existing reliability model is improved.

Keywords – Software Reliability, Embedded Software Reliability, Embedded System, Bit-rate, Clock speed, TPT, BSC.

INTRODUCTION

Software is safety-critical if a failure can directly cause loss of human life or have other catastrophic consequences [1], examples include systems that control aircraft, nuclear reactors, and medical devices. Clearly the reliability and correctness of such software needs to be demonstrated with high assurance, and regulatory agencies in safety-critical industries typically require system providers to meet stringent certification requirements [2]-[4].

Software reliability is defined as the probability of the failure-free operation of a software system for a specified period of time in a specified environment [4]. For mission critical systems, redundancy techniques are commonly applied to achieve high reliability. For embedded systems consisting of software and hardware components, redundancy can be achieved by applying extra copies of these components (in parallel) to handle the system workloads [5]-[7]. Various software reliability growth models (SRGMs) exist to estimate the expected number of total defects (or failures) or the expected number of remaining defects (or failures). Some well known SRGMs are Goel model (1985), Goel and Okumoto model (1979), Kececioglu model (1991), Musa and Ackerman model (1989), Musa et al. Model (1987), Yamada et al. Models (1983, 1985, 1986) etc [8]-[18]. These models have some limitations. Each model can provide good result for a particular data set, but no model is good for all data sets [19]-[28].

In this paper we present a software reliability model which is successfully used to solve the reliability modeling problem according to embedded software size and its execution rate, that are having limited number of bits.

1. EMBEDDED SOFTWARE RELIABILITY

Software is a set of instruction that have several bits to elaborate the bits (0/1). Embedded software are basically design for a specific task for example press, air-condition, aircraft etc. that have a specific length, and can be countable in bits, or during execution we can justify each and every clock cycle for its bits involved. According to clock speed we can also define its reliability of instructions per cycle execution, if we justify the probability of failure free operation then we can easily estimate the reliability problem.

Reliability is the function of time and probability in hardware reliability calculation but software is not having the wear out time so we can say that a software may not fully depend upon time so estimation of software reliability is quite crucial in terms of time. While we consider bit rate and probability of its failure then we can easily derive the reliability in form of total probability theorem and Bernoulli Trials. So the reliability model with respect to bits can be processed data for failure free operation per clock, and estimate the failure per cycle until the whole execution completes.

1.1 SOFTWARE RELIABILITY IN PER CYCLE EXECUTION

Let a system that have 'n' bits that execute in one clock cycle and each bit having its own failure probability, where P_f is failure probability per bit and R is reliability. According to the reliability theory reliability is compliment of probability of failure occurred, so reliability occurrences per bit in each cycle is:

$$R(n) = 1 - P_f(n) \tag{1}$$

The above expression shows the reliability per bit, where $R(n)$ is the reliability of n^{th} bit, $P_f(n)$ is the probability of failure of n^{th} bit, n is the number of bit per cycle. In case of over-all reliability of n bits in a clock cycle, the execution fails if any bit is missing in the clock. The over-all reliability of 'n' bit's is:

$$F(R_n) = R(1)UR(2)...UR(n) \tag{2}$$

The above expression shows that the over-all reliability is the union of the all individual bit reliability.

1.2 SOFTWARE RELIABILITY IN TERM OF TOTAL PROBABILITY THEOREM (TPT)

Let a system clock cycle execute 8 bits data (it can have 'n' bits), and all bits having its own failure probability ($B_1, B_2, B_3, B_4, B_5, B_6, B_7, B_8$), and the shaded portion shows the probability of failure for clock.

See figure 1.

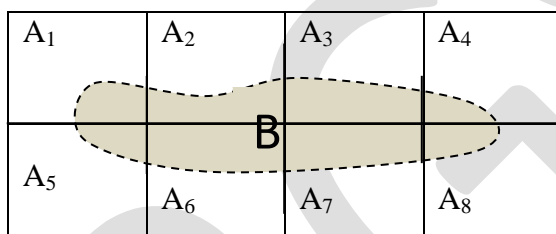


Figure 1:- A system clock having 8 bit.

The shaded portion represents 'B', and $B = B_1 + B_2 + B_3 + B_4 + B_5 + B_6 + B_7 + B_8$. Where $B_1, B_2, B_3, B_4, B_5, B_6, B_7, B_8$ is the failure probability of each bits in clock and A_1 to A_8 are mutually exclusive or disjoint event (that bits are process) of clock 'C'. So $C = A_1 + A_2 + A_3 + A_4 + A_5 + A_6 + A_7 + A_8$.

The total probability theorem let us to compute the probability of an event occurring by enumerating all the different condition that can occur which gives the probability of failure that occurs in the cycle execution ' P_{fc} '.

So , $P_{fc} = P(B \cap C) \tag{3}$

$$P_{fc} = P(B \cap (A_1 \cup A_2 \dots \cup A_8))$$

$$P_{fc} = P((B \cap A_1) \cup (B \cap A_2) \dots \cup (B \cap A_8))$$

$$P_{fc} = \sum_i^8 P(B \cap A_i)$$

$$P_{fc} = \sum_i^8 P(B | A_i) P(A_i) \tag{4}$$

This give the failure probability occurs in clock execution.

1.3 RELIABILITY IN TERM OF BERNOULLI TRIALS

For 'n' bits, data are processed in per clock cycle, and having failure probability ' P_e ' for each bits, so the probability of successes is:

$$Q = 1 - P_e \tag{5}$$

Failure probability in term of Bernoulli Trials is the probability of achieving exactly k failure in n trials.

Let the probability for 'k' failure in 'n' bits data process, and ' p_c ' is the failure probability of clock cycle.

$$P_c = \binom{n}{k} P_e^k (Q)^{n-k} \tag{6}$$

$$P_c = \binom{n}{k} P_e^k (1 - P_e)^{n-k}$$

$$P_c = \frac{n!}{k!(n-k)!} P_e^k (1 - P_e)^{n-k} \tag{7}$$

Bernoulli trials in term of binary symmetric channel (BSC), Lets probability for error per bit is P_e

$$P(0|1) = P(1|0) = P_e \quad (\text{red}) \quad \longrightarrow$$

$$P(0|0) = P(1|1) = 1 - P_e \quad (\text{green}) \quad \longrightarrow$$

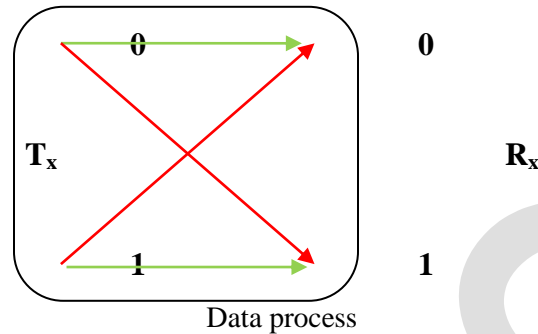


Figure 2: Binary Symmetric channel

According to Bernoulli trials P_e is the define for 'n' bit clock size having 'k' errors. But if any one bit may miss, that cause failure. That minces for failure free operation 'k' have the minimum value '1'. So for 'k = 1' P_c will be.

$$P_c = \binom{n}{1} P_e^1 (1 - P_e)^{n-1} \quad (8)$$

For reliability R_c of a clock if there failure occurrence is P_c then according to reliability theorem.

$$R_c = 1 - P_c \quad (9)$$

So,

$$R_c = 1 - \binom{n}{1} P_e^1 (1 - P_e)^{n-1} \quad (10)$$

2. RELATIONSHIP BETWEEN RELIABILITY AND CLOCK SPEED

The clock cycle is the time between two adjacent pulses of the [oscillator](#) that sets the tempo of the computer processor. The number of these pulses per second is known as the [clock speed](#), which is generally measured in [Mhz](#) (megahertz, or millions of pulses per second) and even in [Ghz](#) (gigahertz, or billions of pulses per second).

A system may provide variable response while we are varying the clock speed, this may affect the reliability of the system in different terms (ex.- In term of failure, in term of utility, in term of cost or optimization).

A clock speed may cause failure in execution of the bits. If the clock speed is higher than the band limit of the system then due to internal capacitance a system can't operate beyond the clock speed (ex. ARM TDMI 7 operation is crucial above 30MHz). If the frequency is beyond its range then due to extra attenuation (the cutoff frequency at which the current gain drops by 3 decibels (70% amplitude)) the bits can be missed and failure occur in the system, while increasing the frequency we observe that the fault rate will increases.

When a system operate at low frequency, then it can't provide optimum work due to low speed, there cost utility factor is effective which reduces the reliability as a cost effective function (ex. below 1 MHz operation is better to use other low operating frequency microcontroller then ARM TDMI 7, it increase the product manufacturing cost, ultimately it reduces the reliability in term of cost and speed).

For maximum reliability a system may operate at its desire operating range (ex. ARM TDMI 7 provide optimum response in 1 MHz to 30MHz). In the desire range current gain drops is less then 3 decibels (amplitude grater then 70%).

The above discussion gives a relative graph in between reliability and clock cycle.

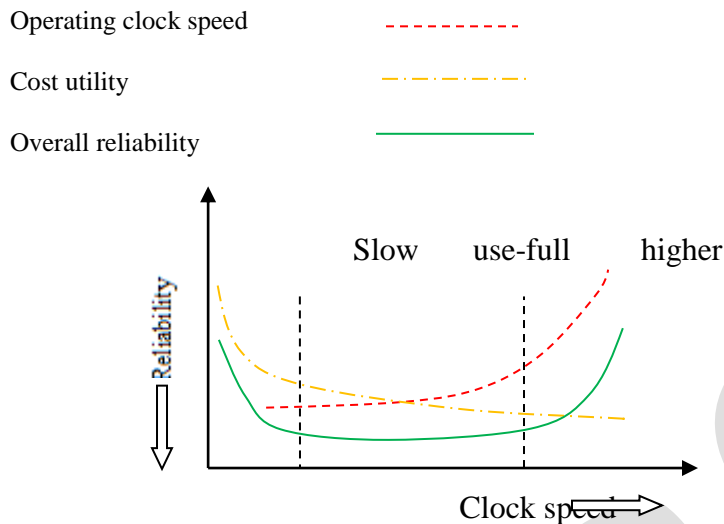


Figure 3: Reliability versus clock speed graph

ACKNOWLEDGMENT

First of all, I would like to thank **Dr. Rajesh Mishra (HOD)**, and **Mr. Rajendra Bahadur Singh, Faculty Associate**, School of Information & Communication Technology, Gautam Buddha University for giving me support and courage to reach here. I would like to take the opportunity to express my gratitude to people who have played an important role in the completion of this paper. I wish to express my deep sense of gratitude to my supervisor for his valuable guidance and useful suggestions, which helped me in completing the work.

CONCLUSION

In this paper we present a software reliability model in terms of bits which is more efficient to estimate the software reliability. A hardware reliability is fully depend upon time so its reliability versus time graph is much suitable to demonstrate in bath tub curve while a software reliability can't because software does not have wear out time. In case of clock speed versus reliability graph, the bath tub curve achieves better reliability in comparison to the time versus failure/reliability graph. Due to fully dependency of software on bits we can easily demonstrate reliability in terms of bits and it gives a better estimation for software reliability.

REFERENCES:

- [1] N. G. Leveson, *Software system safety and computers*, Addison Wesley, ISBN : 0-201-11972-2, Año de publicación, 2001.
- [2] M Handbook, *Reliability Test Methods, Plans and Environments*, MIL-HDBK-781 14 July 1987 MILITARY HANDBOOK Reliability Test Methods, Plans, and Environments for Engineering Development, Qualification US Department of Defense, Washington, 1996.
- [3] L. Michael, *Handbook of Software Reliability Engineering*, McGraw Hill and IEEE Society Press, 1996.
- [4] Zhidong Qin, Hui Chen, Youqun Shi, *Reliability Demonstration Testing Method For Safety –Critical Embedded Application Software*, ICESS2008 IEEE.
- [5] J.-C. Laprie, J. Arlat, C. Beounes, and K. Kanoun, "Definition and analysis of hardware- and software-fault-tolerant architectures," *IEEE Computer*, pp. 39–51, July 1990.
- [6] M. R. Lyu, Ed., *Handbook of Software Reliability Engineering*: Mc-Graw-Hill, IEEE Computer Society Press, 1996, ch. 1–3, and 14.
- [7] R. K. Scott, J. W. Gault, and D. F. McAllister, "Fault-tolerant software reliability modeling," *IEEE Trans. Software Engineering*, vol. SE-13, pp. 582–592, 1987.
- [8] Kazuhira Okumoto, — *A Statistical Method for Software Quality Control*, IEEE Transactions On Software Engineering, Vol. Se-1L, No. 12, December 1985
- [9] Chin-Yu Huang, Michael R. Lyu & Sy-Yen Kuo, — *A Unified Scheme of Some Non-homogenous Poisson Process Models for Software Reliability Estimation*, IEEE Transactions On Software Engineering, Vol. 29, No. 3, Page 261-270, March 2003
- [10] Qiuying Li and Jian Wang—*Determination of Software Reliability Demonstration Testing Effort Based on Importance Sampling and Prior Information*, Springer Berlin Heidelberg, Print ISBN 978-3-642-25907-4, Online ISBN 978-3-642-25908-1, Page 247-255, 2012.

- [11] Hoang Pham, —*An Imperfect-debugging Fault-detection Dependent-parameter Software*, *International Journal of Automation and Computing*, 04(4), October 2007, 325-328, DOI: 10.1007/s11633-007-0325-8
- [12] Xuemei Zhang, Xiaolin Teng, & Hoang Pham, —*Considering Fault Removal Efficiency in Software Reliability Assessment*, *IEEE Transactions On Systems, Man, And Cybernetics—Part A: Systems And Humans*, Vol. 33, No. 1, January 2003
- [13] Anthony Iannin et al., —*Criteria for Software Reliability Model Comparisons*, *IEEE Transactions On Software Engineering*, Vol Se-10, No. 6, Page 687-692, November 1984
- [14] Chin-Yu Huang and Michael R. Lyu, —*Estimation and Analysis of Some Generalized Multiple Change-Point Software Reliability Models*, *IEEE Transactions On Reliability*, Vol. 60, No. 2, Page 498-515, June 2011
- [15] Katerina Go'seva-Popstojanova and Kishor S. Trivedi, —*Failure Correlation in Software Reliability Models*, *IEEE Transactions On Reliability*, Vol. 49, No. 1, Page 37-49, March 2000
- [16] Shinji Inoue and Shigeru Yamada, —*Generalized Discrete Software Reliability Modeling With Effect of Program Size*, *IEEE Transactions On Systems, Man, And Cybernetics—Part A: Systems And Humans*, Vol. 37, No. 2, Page 170-180, March 2007
- [17] Kazuya Shibata, Koichiro Rinsaka and Tadashi Dohi, —*Metrics-Based Software Reliability Models Using Non-homogeneous Poisson Processes*, 17th International Symposium on Software Reliability Engineering (ISSRE'06)
- [18] Hoang Pham and Xuemei Zhang, —*NHPP software reliability and cost models with testing coverage*, *European Journal of Operational Research* 145 (2003) 443–454
- [19] Michael R. Lyu, Sampath Rangarajan and Aad P. A. van Moorsel, —*Optimal Allocation of Test Resources for Software Reliability Growth Modeling in Software Development*, *IEEE Transactions On Reliability*, Vol. 51, No. 2, Page 183-193, June 2002
- [20] K.B.P.L.M. Kelani Bandara et al., —*Optimal Selection of Failure Data for Reliability Estimation Based on a Standard Deviation Method*, Second International Conference on Industrial and Information Systems, ICIIS 2007, 8 – 11 August 2007, Sri Lanka
- [21] RajPal Garg, Kapil Sharma, Rajive Kumar, and R. K. Garg, —*Performance Analysis of Software Reliability Models using Matrix Method*, *World Academy of Science, Engineering and Technology* July, 2010
- [22] Sultan Aljahdali and Alaa F. Sheta, —*Predicting the Reliability of Software Systems Using Fuzzy Logic*, 2011 Eighth International Conference on Information Technology: New Generations
- [23][23] Ralf H. Reussner, Heinz W. Schmidt and Iman H. Poernomo, —*Reliability prediction for component-based software architectures*, *The Journal of Systems and Software* 66 (2003) 241–252
- [24] Kapil Sharma, Rakesh Garg, C. K. Nagpal, and R. K. Garg, —*Selection of Optimal Software Reliability Growth Models Using a Distance Based Approach*, *IEEE Transactions On Reliability*, Vol. 59, No. 2, Page 266-277, June 2010
- [25] Norman F. Schneidewind, —*Software Reliability Model with Optimal Selection of Failure Data*, *IEEE Transactions On Software Engineering*, Vol. 19, No. 11, Page 1095-1105, November 1993
- [26] Dr. Ajay Gupta, Dr. Digvijay Choudhary and Dr. Suneet Saxena, —*Software Reliability Estimation using Yamada Delayed S Shaped Model under Imperfect Debugging and Time Lag*, *International Journal of Computer Applications* (0975-8887) Volume 23– No.7, June 2011
- [27] Shaik.Mohammad Rafi et al., —*Software Reliability Growth Model with Logistic-Exponential Test-Effort Function and Analysis of Software Release Policy*, (IJCSSE) *International Journal on Computer Science and Engineering* Vol. 02, No. 02, 2010, 387-399
- [28] Mohd. Anjum, Md. Asrafal Haque, Nesar Ahmad, —*Analysis and Ranking of Software Reliability Models Based on Weighted Criteria Value*, *MICS I.J. Information Technology and Computer Science*, 2013, 02, 1-14

A Review on Design and Analysis of Work Holding Fixture

Shivaji Mengawade¹, Vaibhav Bankar², Pratik P Chaphale³

M Tech Student, Department of Mechanical Engineering, VIT, Nagpur.

Ass.Prof, Department of Mechanical Engineering, VIT Nagpur.

Ass.Prof, , Department of Mechanical Engineering, VIT Nagpur.

shivajimengawade@gmail.com

yhbankar@gmail.com

chaphale.pratik@gmail.com

Abstract—The design of a fixture is a highly complex and intuitive process, which require knowledge. Fixture design plays an important role at the setup planning phase. Proper fixture design is crucial for developing product quality in different terms of accuracy, surface finish and precision of the machined parts. In existing design the fixture set up is done manually, so the aim of this project is to replace with fixture to save time for loading and unloading of component. fixture provides the manufacturer for flexibility in holding forces and to optimize design for machine operation as well as process function ability.

Keywords— Fixture, product Quality, Quick holding ability, Firmly Locating work piece, Improve Accuracy, Save time

INTRODUCTION

Fixtures are the tool used to locate and hold the work piece in position during the manufacturing process. Fixtures are used to hold the parts firmly which are to be machined, it is used to produce the duplicate parts accurately. In order to produce parts with required accuracy and dimensions the parts must be firmly and accurately fixed to the fixtures. To do this, a fixture is designed and built to hold, support and locate the work piece to ensure that each work piece is machined within the specified limits. Set blocks, feeler or thickness gauges are used in the fixture to refer the work piece with the cutter tool.

A fixture should be securely fastened to the table of the machine upon which the work is to be done. Though largely used on milling machines, fixtures are also designed to hold the work for various operations on most of the standard machine tools. Fixtures vary in design based on the use of relatively simple tools to expensive or complicated devices. Fixture helps to simplify metalworking operations performed on special equipments.

The fixture is a special tool for holding a work piece in proper position during manufacturing operation. For supporting and clamping the work piece, device is provided. Frequent checking, positioning, individual marking and non-uniform quality in manufacturing process is eliminated by fixture. This increase productivity and reduce operation time. Fixture is widely used in the industry practical production because of feature and advantages. To locate and immobilize workpieces for machining, inspection, assembly and other operations fixtures are used. A fixture consists of a set of locators and clamps. Locators are used to determine the position and orientation of a workpiece, whereas clamps exert clamping forces so that the workpiece is pressed firmly against locators. Clamping has to be appropriately planned at the stage of machining fixture design.

LITERATURE REVIEW

Chen Luo, LiMinZhu, Han Ding[1] In his paper Two-Sided Quadratic Model for Work piece Fixturing Analysis, 2011 proposed that presents a novel model for work piece positioning analysis. Existing fixturing models may under estimate the positioning error due to neglect of the curvature of one or both contacting bodies.

S. Kashyap W.R. DeVries[2] In their paper Finite element analysis and optimization in fixture, proposed with minimizing deformation of the work piece due to machining loads about fixturing support positions, especially in thin castings.

Y. Zheng& Y. Rong& Z. Hou[3] Intheir paper, A finite element analysis for stiffness of fixture units, proposed a systematic finite element model to predict the fixture unit stiffness by introducing nonlinear contact elements on the contact surface between fixture components.

M. Y. Dakhole, Prof. P.G. Mehar, Prof. V.N. Mujbaile[4]In their paper, Design And Analysis Of Dedicated Fixture With Chain Conveyor, gives a feasible solution on conventional roller chain conveyerised arrangement with dedicated moving fixture with conveyor for the tractor components like rear axle career, bull gear and shaft of a tractor model.

J. C. Trappey and C. R. Liu [5]This paper gives a review of fixture-design research, most of it done in the 1980s. the major topics of the review are the fixturing principals (supporting ,locating and clamping), automated fixtures design (configuration, assembly and verification) and fixtures hardware design (delicated, modular and electric /magnetic type).

Shrikant.V.Peshatwar, L.P Raut [6] This paper present a fixture design system of eccentric shaft for ginning machine.. Fixture is required in various industries according to their application .Designer design fixture according to dimension required by industry to fulfill our production tar gate. In traditional manufacturing process performing operation on eccentric shaft is critical. so holding a work piece in proper position during a manufacturing operation fixture is very necessary and important. Because the shaft is eccentric so for this requirement of manufacturing process Designer design proper fixture for eccentric shaft. Fixtures reduce operation time and increases productivity and high quality of operation is possible

IDENTIFIED GAPS IN THE LITERATURE

In existing design the fixture set up is done manually, so the aim of this project is to replace with fixture to save time for loading and unloading of component. Fixture provides the manufacturer for flexibility in holding forces and to optimize design for machine operation as well as process function ability.

PROBLEM FORMULATION

Workpiece is hold in to workpiece holder and this all attachment fix in to the fixture plate. A rigid positioning of the workpiece with least time takes place. Springs are design such a way to carry the pressure don't allow to deflect the work piece, Cam is used for mounting and un-mounting purpose. Cam is fixed into frames slot. Base plate for rigid support to fixture .two mesh bull gear are fitted to rotating purpose to take the advantages of rotation and increase the application of fixture. Fixed plate with center attachment is provided to locking purpose. When fixture in use center push in to the fixed plate hole so hole attachment is getting fixed.

This fixture used in vertical milling machine. Different electrode profiles are easily manufactured by using this fixture. Mounting, un-mounting and locating of workpiece is very easy and 1 than this electrode is used on electro discharge machine to manufacture molds. Complicated mold profile are done with this process. Grafite or Cooper material is used to manufacture electrode.

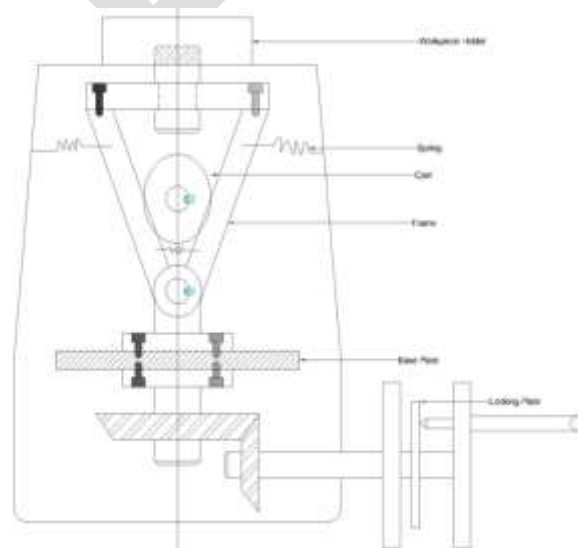


Fig1 Concept design of Work holding Fixture

CONCLUSION

It reduces or sometimes eliminates the efforts of marking, measuring and setting of workpiece on a machine and maintains the accuracy of performance. The workpiece and tool are relatively located at their exact positions before the operation automatically within negligible time. So it reduces product cycle time. Variability of dimension in mass production is very low so manufacturing processes supported by use of jigs and fixtures maintain a consistent quality. Due to low variability in dimension assembly operation becomes easy, low rejection due to less defective production is observed. It reduces the production cycle time so increases production capacity. Simultaneously working by more than one tool on the same workpiece is possible. The operating conditions like speed, feed rate and depth of cut can be set to higher values due to rigidity of clamping of work piece by fixtures. Operators working become comfortable as his efforts in setting the work piece can be eliminated. Semi-skilled operators can be assigned the work so it saves the cost of manpower also. There is no need to examine the quality of produce provided that quality of employed fixtures is ensured

REFERENCES:

- [1]. Melkote, S. N. "Optimal fixture design accounting for the effect of workpiece dynamics," International Journal of Advanced Manufacturing Technology, Vol. 18, pp. 701-707, 2001.
- [2]. Michael Stampfer "Automated setup and fixture planning system for box-shaped Parts" International Journal of Advance Manufacturing Technology 45:540–552 DOI 10.1007/s00170-009-1983-1, 2008.
- [3]. DjordjeVukelic, UrosZuperl&JankoHodolic "Complex system for fixture selection, modification, and design" Int J AdvManufTechnol 45:731–748 DOI 10.1007/s00170-009-2014-y, 2009
- [4]. WeifangChen ,Lijun Ni &JianbinXue "Deformation control through fixture layout design and clamping force optimization" Int J AdvManufTechnol 38:860–867 DOI 10.1007/s00170-007-1153-2,2008
- [5]. J. Cecil "A Clamping Design Approach for Automated Fixture Design" Int J AdvManufTechnol 18:784–789,2008
- [6]. Nicholas Amaral · Joseph J. Rencis · Yiming (Kevin) Rong "Development of a finite element analysis tool for fixture design integrity verification and optimization" Int J AdvManufTechnol 25: 409–419, 2005
- [7]. Y. Wang, X. Chen. N, Gindy "Surface error decomposition for fixture development" Int J AdvManufTechnol DOI 10.1007/s00170-005-0270-z, 2007
- [8]. Shrikant.V.Peshatwar, L.P Raut "Design and development of Fixture for eccentric shaft: A Review" International Journal of Engineering Research and Applications (IJERA) ISSN: 2248-9622 Vol. 3, Issue 1, February 2013.
- [9]Asada, H. and A.B. By. Kinematic Analysis of Work part Fixture for Flexible Assembly with Automatically Reconfigurable Fixtures, IEEE Journal of Robotics and Automation, Vol.1(2), pp. 86-94. 1985.
- [10]Cogun, C. The Importance of the Application Sequence of Clamping Forces. ASME Journal of Engineering for Industry, Vol. 114, pp. 539-543. 1992.
- [11]Daimon, M., Yoshida, T., Kojima, N., Yamamoto, H., Komatsu, and Hoshi, T. "Study for designing fixture considering dynamics of thinwalled plate and box-like workpieces," Annals of the CIRP, Vol. 34, No. 1, pp. 319-324, 1985.
- [12] Deb, K. "An introduction to genetic algorithms," Sadhana Journal, Vol. 24, pp. 293-315, 1999.
- [13]Deiab, I. M., Veldhuis, S. C. and Dumitrescu, M. "Dynamic modeling of face milling process including the effect of fixture dynamics," Transactions of NAMRI/SME, Vol. 30, pp. 461-468, 2002.
- [14]Fang, B., DeVor, R. E. and Kapoor, S. G. "An elastodynamic model of frictional contact and its influence on the dynamics of a workpiecefixture system," ASME J. Manuf. Sci. Eng., Vol. 123, pp. 481-489, 2001.
- [15]Hockenberger, M. J. and DeMeter, E. C. "The effect of machining fixture design parameters on workpiece displacement," ASME, Manufacturing Review, Vol. 8, No. 1, pp. 22-32, 1995.

- [16] Haiyan Deng, "Analysis and synthesis of fixturing dynamic stability in machining accounting for material removal effect," Ph.D. thesis, Georgia Institute of Technology Atlanta, Georgia, 2006,
- [17] Hurtado, J. F. and Melkote, S. N. "A model for the prediction of reaction forces in a 3-2-1 machining fixture," Transactions of the North American Research Institution of SME, pp. 335-340, 1998.
- [18] Kang Y., Rong Y. and Yang J.A. "Geometric and kinetic model based computer-aided fixture design verification," ASME Journal of Computing and Information Science in Engg., Vol.3, pp.187-199, 2003.
- [19] Kulankara, K., Satyanarayana, S. and Melkote, S. N. "Iterative fixture layout and clamping force optimization using the Genetic Algorithm," Journal of Manufacturing Science and Engineering, Transactions of the ASME, Vol. 124, No. 1, pp.119-125, 2002.
- [20] Lai, X. M., Luo, L. J. and Lin, Z. Q. "Flexible assembly fixture layout modeling and optimization based on genetic algorithm," Chin. J. Mech. Eng., Vol. 1, pp. 89-92, 2004.

Scalable and Competent Audit Service for Storage Data in Clouds Retaining IHT

Vinoth kumar.R¹, R.Latha²

PG Scholar¹, Assistant Professor², Veltech High tech Dr.Rangarajan Dr.Sakunthala Engineering College, Avadi, Chennai.
vinoth061093@gmail.com, 8015220510

ABSTRACT- In cloud, the shield subject in outsourced storage space data is the tough challenge. To vanquish the setback, established way industrialized vibrant audit ability for verifying the respect of an untreated and outsourced storage space. Appraisal capability is crafted established on the methods, fragment construction, casual sampling, and index-hash table, keeping provable updates to outsourced data and timely anomaly discovery. The method conventional on probabilistic query and periodic confirmation for enhancing the presentation of audit services. The audit ability is given by TPA monitoring. From time to time the TPA could have chances to obscure anomaly features to cloud users. To conquer the drawback, counsel vibrant audit ability in the cloud. By the method it can vibrantly audit the anomaly and dispatch intimation to cloud user. So that it can safeguard the cloud storage space data.

Keywords: fragment construction, casual sampling, index-hash table, probabilistic query and periodic confirmation.

I. INTRODUCTION

The cloud storage space ability (CSS) relieves the weight for storage space connection and safeguarding. Though, if such a vital ability is vulnerable to aggressions or wrecks, it should hold irretrievable defeats to the users because their data or records are stored in a tentative storage space pool beyond the enterprises. Reliable than confidential computing mechanisms, but they are yet susceptible to inner menaces and external menaces that can damage data honor; subsequent, for the profit of rights, there carry on mixed motivations for cloud ability providers to behave adulterously in the direction of the cloud users; besides, arguments sporadically tolerate from the lack of belief on CSP because the data change could not be timely recognized by the cloud users, even if these arguments could consequence from the users' own unacceptable operations. It is imperative for CSP to tender an effectual audit facility to check the respect and potential of stored data.

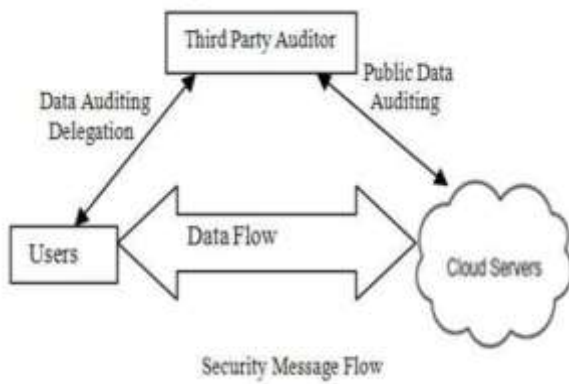
Keywords: concerning four key words alienated by commas

RELATED WORK

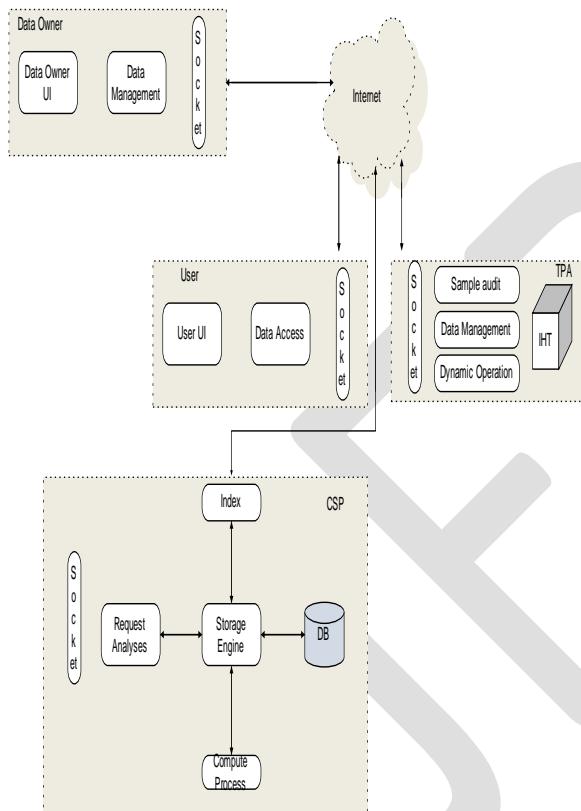
Vibrant audit ability for respect verification of untreated and outsourced storage spaces. Twisted on interactive facts arrangement (IPS) in conjunction with the zero vision property, our audit ability can furnish area auditability lacking downloading rare statistics and guard isolation of the statistics. The audit arrangement can prop vibrant data procedures and timely anomaly detection alongside the aid of countless competent methods, fragment construction, it additionally industrialized an effectual way established on probabilistic query and periodic verification for enhancing the presentation of audit services... The experimental aftermath not merely validate the effectiveness of our ways, but additionally display that our arrangement does not craft each momentous computation price and need less supplementary storage space for respect verification. The method additionally has one drawback that is shouted as TPA monitoring.

DISADVANTAGES

- It has to needs exterior TPA monitoring
- Nope protected

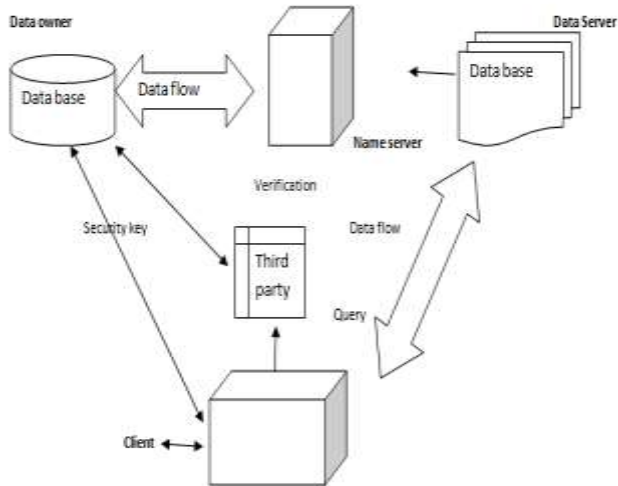


SYSTEM ARCHITECTURE



SYSTEM MODEL

The audit ability is given by TPA monitoring. From time to time the TPA could have chances to obscure anomaly features to cloud users. To vanquish this drawback, counsel vibrant audit ability in the cloud. In this method user dispatched query appeal to attendant and that attendant matches the user reservation and keyword if it is match, user can tolerate the procedure or else, the user is automatically marked as untreated and sends intimation concerning anomaly detection to cloud user. So that it can maintain the cloud storeroom information.



ADVANTAGES

- No demand exterior TPA
- Safeguard & Effective.

MODULES

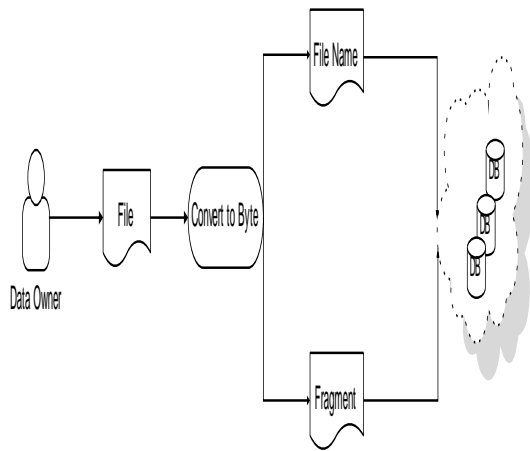
- certification
- Fragment Structure and Sheltered Tags
- Periodic Sampling Audit
- protection Notification
- Presentation & Evaluation

A. CERTIFICATION

Approval is the procedure of providing user consent to do or have something. Accepting that someone has logged in to a computer working arrangement or request, the arrangement or request could desire to recognize what resources the user can be given across this session. Thus, approval is from time to time perceived as both the preliminary setting up of permissions by an arrangement administrator and the actual checking of the consent profit that include set up after a abuser is suitable access. Qualifications are the procedure of ascertaining whether rather is, in fact, who or what it is uttered to be. In confidential and area computer webs (including the Internet), certification is usually completed across the utilize of logon passwords. Visualization of the password is consented to promise that the abuser is valid. Every solo abuser lists primarily (or is registered by someone else), employing an allocated or self-declared password.

B. FRAGMENT STRUCTURE AND SHELTERED TAGS

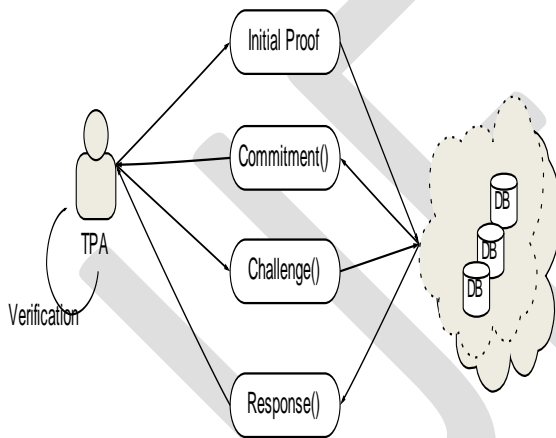
To maximize the storage effectiveness and audit performance, our audit system introduces a general fragment structure for outsourced storages.



An outsourced file F is dividing into n blocks $\{M_1, M_2, \dots, M_n\}$, and every block m_i is divide into s sectors $\{M_{i,1}, M_{i,2}, \dots, M_{i,s}\}$. The section structure consists of n block-tag join up (M_i, σ_i) , where σ_i is a signature tag of a block m_i generated by some secrets $\tau = (\tau_1, \tau_2, \dots, \tau_s)$. Use such tags and matching data to construct a reply in conditions of the TPA's challenges in the confirmation procedure, such that this reply can be verified without rare data. If a tag is un-forgable by anyone apart from the original signer, we call it a sheltered tag.

C. PERIODIC SAMPLING AUDIT

In periodic sampling with “complete” inspection, random “example” checking deeply reduces the workload of audit services, while still realizes a successful detection of misbehaviors. The probabilistic audit on instance checking is preferable to understand the indiscretion revealing in a timely manner.



D. PROTECTION NOTIFICATION

Detection and notification mentions to automatic detection of adjustments made to User pages and notification to interested users by Cloud Server or supplementary means. Whereas find engines are projected to find User pages, detection and notification arrangements are projected to monitor adjustments to User pages. Effectual and competent change detection and notification is hindered by the fact that most servers do not precisely trail content adjustments across Modified.

E. PRESENTATION AND EVALUATION

To notice anomalies in a low-overhead and timely manner, we endeavor to optimize the audit presentation from two aspects: Presentation valuation of probabilistic queries and arranging of episodic verification. Our frank believed is to uphold a tradeoff amid overhead and accuracy, which helps us enhance the presentation of audit systems.

1. PRIVACY-PRESERVING AREA AUDITING FOR SAFEGUARD CLOUD STORAGE SPACE EMPLOYING CLOUD STORAGE SPACE

Users can remotely accumulate their records and appreciate the on require lofty feature requests and services from a public pool of configurable computing resources, lacking the burden of innate data storage space and maintenance. Though, the fact those users no longer have physical ownership of the outsourced data makes the data respect shield in Cloud Calculating a formidable task, exceptionally for users alongside constrained computing resources. Moreover, users brought to be competent to immediately use the cloud storage space as if it is innate, lacking fretting concerning the demand to confirm its honor. Enabling region auditability for cloud storage space is of dangerous consequence so that users can remedy to a third party auditor to ensure the esteem of outsourced statistics and be unstressed. To securely familiarize a competent TPA, the auditing procedure ought to hold in no new vulnerabilities towards user data privacy, and familiarize no supplementary online burden to user. It counsels a safeguard cloud storage space arrangement upholding privacy-preserving area auditing. Comprehensive shield and presentation scrutiny display the counseled schemes are provably safeguard and exceedingly efficient. To address these setbacks, work utilizes the method of area key established homomorphic linear authenticator (or HLA for short), that enables TPA to present the auditing lacking demanding the innate duplicate of data and therefore drastically reduces the contact and computation overhead as contrasted to the frank data auditing approaches. By incorporating the HLA alongside random masking, our protocol guarantees that the TPA might not discover each vision concerning the data content stored in the cloud server diagonally the proficient auditing development.

2. BAF: AN EFFICIENT OPENLY VERIFIABLE SAFEGUARD APPRAISAL LOGGING FORMAT FOR DISTRIBUTED SYSTEMS

Audit logs, bestowing data concerning the present and past states of provision, are solitary of the majority crucial portions of in attendance computer systems. Bestowing shield for audit logs on an untreated contraption in a colossal distributed arrangement is a challenging task, exceptionally in the attendance of alert adversaries. In such a arrangement, it is critical to have onward shield such that after an antagonist compromises a contraption, she cannot adjust or forge the log entries amassed beforehand the compromise. Unfortunately, continuing safeguard audit logging schemes have significant limitations that make them impractical for real-life applications: Continuing Area Key Cryptography (PKC) established schemes are computationally luxurious for logging in task intensive or resource-constrained arrangements, as continuing symmetric schemes are not openly Verifiable and incur significant storage space and contact overheads. Counsel a novel onward safeguard and aggregate logging scheme shouted Blind-Aggregate-Forward (BAF) logging scheme, which is suitable for colossal distributed systems. BAF can produce openly Verifiable onward safeguard and aggregate signatures alongside near-zero computational, storage space, and contact prices for the loggers, lacking needing each online (TTP) support. Clarify that BAF is safeguard below appropriate computational assumptions, and clarify that BAF is significant extra efficient and scalable than the preceding schemes. Therefore, BAF is a flawless resolution for safeguard logging in both tasks intensive and resource-constrained systems. To address the above setbacks, a set of cryptographic countermeasures have been counseled to enable safeguard logging on untreated mechanisms, lacking consenting a tamper-resistant hardware or constant real-time log verifiers In order to fully this necessity, we counsel a novel onward maintain and aggregate logging scheme for safeguard audit logging in distributed arrangements, BAF can address all the aforementioned limitations of the continuing ways simultaneously.

3. VIBRANT PROVABLE DATA POSSESSION

As storage space-outsourcing services and resource- allocating webs have come to be accepted, the setback of efficiently clarifying the respect of data stored at untreated servers has consented increased attention. In the provable data ownership (PDP) ideal, the user preprocesses the data and next sends it to an untreated server for storage space, as keeping a tiny number of Meta data. The user afterward asks the server to illuminate that the stored data have not be tampered alongside or deleted (without downloading the actual data). Definitional framework and efficient constructions for vibrant provable data ownership (DPDP) that extends the PDP ideal to prop provable updates to stored data. Authenticated lexicons established on locale information. The worth of vibrant updates is a presentation change from $O(1)$ to $O(\log n)$ (or $O(n \log n)$), for a fields encompassing of n blocks, as maintaining the alike probability of naughtiness exposure. Our examinations display that this slowdown is extremely low in exercise. Additionally display how to apply our DPDP scheme to outsourced fields arrangements and edition manipulation arrangements deliver a definitional framework and efficient constructions for vibrant provable data ownership (DPDP) that extends the PDP ideal to prop provable updates on the stored data. Given a fields F encompassing of n blocks, define a notify as whichever insertion of a new block or modification of a continuing chunk, or removal of each block. Consequently our notify procedure describes the most finished form of modification a user could desire to present on a fields. Our DPDP resolution is established on a new variant of authenticated lexicons, whereas we use locale

data to coordinate lexicon entries. Therefore to prop efficient authenticated procedures on fields at the block level, such as authenticated insert and delete. It clarifies the shield of our constructions employing average assumptions.

4. SCALABLE AND EFFECTUAL PROVABLE DATA

Possession Storage space outsourcing is a rising trend that prompts a number of interesting shield subjects, countless of that have been widely investigated in the past. Though, Provable Data Ownership (PDP) is a case that has merely presently materialized in the scrutiny literature. The main subject is how to oftentimes, efficiently and securely confirm that a storage space server is devotedly storing its user's (potentially extremely large) outsourced data. The storage space server is consented to be untreated in words of both shield and reliability. (In supplementary words, it could maliciously or unintentionally remove hosted data; it could additionally relegate it to sluggish or off-line storage space.) The setback is exacerbated by the user being a tiny computing mechanism alongside manipulated resources. Prior work has addressed this setback employing whichever area key cryptography or needing the user to outsource its data in encrypted form. Craft an extremely efficient and provably maintain PDP method established completely on symmetric key cryptography, as not needing each bulk encryption. Also, in difference alongside its predecessors, our PDP method permits outsourcing of vibrant data.

5. OBLIGING PROVABLE DATA OWNERSHIP FOR RESPECT VERIFICATION IN MULTI-CLOUD STORAGE SPACE

Provable data ownership (PDP) is a method for safeguarding the respect of data in storage space outsourcing. In this paper, we address the assembly of an effectual PDP scheme for distributed cloud storage space to prop the scalability of ability and data migration, in that we ponder the attendance of several cloud ability providers to obligingly store and uphold the users' data. Present an obliging PDP (CPDP) scheme established on homomorphic verifiable reply and hash index hierarchy. We clarify the shield of our scheme established on multi-prover zero-knowledge facts arrangement, which can gratify completeness, vision soundness, and zero-knowledge properties. In supplement, we articulate presentation optimization mechanisms for our method, and in exacting here an effectual method for selecting optimal parameter benefits to minimize the computation prices of users and storage space ability providers. Our examinations display that our resolution introduces lower computation and contact overheads in analogy alongside non-cooperative ways to check the potential and respect of outsourced data in cloud storage spaces, researchers have counseled two frank ways shouted Provable Data Ownership and Proofs of Retrievability. Early counseled the PDP ideal for safeguarding ownership of files on untreated storage spaces and endowed an RSA-based design for a fixed case that achieve the contact cost. They additionally counseled an openly verifiable edition that permits anybody, not just the proprietor, to trial the server for data possession. They counseled a handy PDP scheme established on cryptographic hash purpose and symmetric key encryption, but the servers can mislead the proprietors by employing previous Meta data due to the lack of unpredictability in the brave. The numbers of updates and valiant are manipulated and fixed in advance and users cannot present block insertions anywhere.

6. EFFICIENT AUDIT SERVICE OUTSOURCING FOR DATA RESPECT IN CLOUDS

Cloud-based outsourced storage space relieves the user's trouble for storage space association and maintenance by bestowing a comparably cut-rate scalable, location-independent proposal. That users no longer have physical rights of data indicates that they are confronting a potentially terrible chance for missing data. To get around the shield dangers, audit services are grave to safeguard the value and possible of outsourced data and to realize digital forensics and sincerity on cloud computing. Provable data ownership (PDP), that is a cryptographic scheme for verifying the value of data deficient reclaiming it at an unprocessed server, can be utilized to understand audit services. In this profiting from the interactive zero-knowledge specifics collection, address the assembly of an interactive PDP protocol to stop the dishonesty of prover and the leakage of confirmed data. Additionally counsel an effectual mechanism alongside respect to probabilistic queries and periodic verification to cut the audit prices each confirmation and apply a usual detection timely. In supplement, we present an effectual method for selecting an finest parameter worth to diminish computational overheads of cloud audit services.

7. IDENTITY-BASED ENCRYPTION FROM THE WEIL PAIRING

It counsel a fully useful identity-based encryption scheme (IBE). The scheme has selected cipher text shield in the random oracle ideal consenting an elliptic camber alternate of the computational Difi Hellman trouble. Our arrangement is established on the well pairing. We give precise definitions for safeguard individuality established encryption schemes and give countless requests for such systems Shamir's early motivation for identity- established encryption was to elucidate certificate association in e-mail systems. To counsel a

fully useful identity-based encryption scheme. The presentation of our arrangement is comparable to the presentation of ElGamal encryption in F. Instituted on this assumption that displays that the new arrangement has selected cipher text shield in the random oracle model. Employing average methods from threshold cryptography the PKG in our system can be spread so that the master key is not ever accessible in a private location.

8. TAUT PROOFS FOR SIGNATURE SCHEMES LACKING RANDOM ORACLES

It present the early taut shield proofs for two finished classes of forceful RSA established signature schemes. As the representation of agents in prime order bilinear clusters is far tinier than in RSA clusters, additionally present two bilinear variants of our cross classes that yield petite signatures. Comparable to beforehand and able to display that the sevariants have taut shield facts sunder the forceful Hellman (SDH) assumption. Central to our aftermath is new facts method that permits the simulator to circumvent estimating that of the attacker's cross queries will be reuse in the phony. In difference to preceding proofs, our shield reduction does not lose a factor of q here. In a comparable method, to familiarize a subsequent finished class of signature schemes shouted 'chameleon hash scheme' that can be considered as a oversimplification of the Cramer-Shoup cross plot. Next joining signature scheme and the chameleon hash scheme to be tautly safeguarded below the SRSA assumption after instantiated alongside each safeguard joining purpose, suitably chameleon hash function.

9. ENABLING AREA VARIABILITY AND DATA DYNAMICS FOR STORAGE SPACE SHIELD IN CLOUD COMPUTING

Cloud Calculating has been envisioned as the subsequent conception design of IT Enterprise. It moves the request multimedia and databases to the centralized colossal data centers, whereas the association of the data and services could not be fully trustworthy. This exceptional paradigm brings concerning countless new assurances valiant, which have not been well understood. This work studies the setback of safeguarding the respect of data storage space in Cloud Computing. The task of permitting a third party auditor (TPA), on behalf of the cloud user, to confirm the respect of the vibrant data stored in the cloud. The introduction of TPA eliminates the involvement of user across the auditing of whether his data stored in the cloud is indeed finish, which can be vital in accomplished economies of scale for Cloud Computing. The prop for data dynamics via the most finished forms of data procedure, such as block medication, insertion and deletion, is additionally a significant pace to practicality, as services in Cloud Calculating are not manipulated to record or backup data only. As prior works on safeguarding remote data respect frequently needs the prop vibrant data operations. Early recognize the difficulties and possible shield setbacks of manage expansions alongside fully vibrant data updates from prior works and next display how to craft a graceful friction scheme for seamless combination of these two leading facial exterior in our protocol propose. In particular, to accomplish antique data dynamics, the Evidence of Irretrievability ideal by affecting the vintage Merle Hash Tree (MHT) assembly for block tags certification. Comprehensive shield and presentation scrutiny display that the counseled scheme is exceedingly effectual and provably secure.

10. SAFEGUARDING DATA STORAGE SPACE SHIELD IN CLOUD CALCULATING

Cloud computing has been envisioned as the subsequent creation design of IT enterprise. In difference to established resolutions, whereas the IT services are below proper physical, logical and workers controls, cloud computing moves the request multimedia and databases to the colossal data centers, whereas the association of the data and services could not be fully trustworthy. This exceptional attribute, though, poses countless new shields valiant that have not been well understood. In cloud data storage space shield, that has always been a vital aspect of quality of service? To safeguard the correctness of users' data in the cloud, so counsel a competent and flexible distributed scheme alongside two salient features, opposite to its predecessors. By employing the homomorphic indication next to spread confirmation of erasure-coded statistics, our scheme achieves the integration of storage space precision assurance and statistics fault localization. Unlike most prior works, the new scheme more supports safeguard and effectual vibrant procedures on data blocks, including: data notify, delete and append. Comprehensive shield and presentation scrutiny displays that the counseled scheme is exceedingly effectual and resilient opposing convoluted wreck, hateful data change aggression and even server scheme attacks.

CONCLUSION

An encounter of vibrant audit services for entrusted and outsourced storage spaces. Additionally provided an effectual method for periodic sampling audit to enhance the presentation of TPAs and storage space skill providers. Our examinations displayed that our resolution has a puny, stable number of overhead, which minimizes computation and link costs.

REFERENCES:

- [1] Amazon Web Services, "Amazon S3 Availability Event: July 20, 2008," <http://status.aws.amazon.com/s3-20080720.html>, July 2008.
- [2] A. Juels and B.S. Kaliski Jr., "PORs: Proofs of Retrievability for Large Files," Proc. ACM Conf. Computer and Communications Security (CCS '07), pp. 584-597, 2007.
- [3] M. Mowbray, "The Fog over the Grimpen Mire: Cloud Computing and the Law," Technical Report HPL-2009-99, HP Lab., 2009.
- [4] A.A. Yavuz and P. Ning, "BAF: An Efficient Publicly Verifiable Secure Audit Logging Scheme for Distributed Systems," Proc. Ann. Computer Security Applications Conf. (ACSAC), pp. 219-228, 2009.
- [5] G. Ateniese, R.C. Burns, R. Curtmola, J. Herring, L. Kissner, Z.N.J. Peterson, and D.X. Song, "Provable Data Possession at Untrusted Stores," Proc. 14th ACM Conf. Computer and Comm. Security, pp. 598-609, 2007.
- [6] G. Ateniese, R.D. Pietro, L.V. Mancini, and G. Tsudik, "Scalable and Efficient Provable Data Possession," Proc. Fourth Int'l Conf. Security and Privacy in Comm. Networks (SecureComm), pp. 1-10, 2008.
- [7] C.C. Erway, A. Kuzuno, C. Papamanthou, and R. Tamassia, "Dynamic Provable Data Possession," Proc. 16th ACM Conf. Computer and Comm. Security, pp. 213-222, 2009.
- [8] H. Shacham and B. Waters, "Compact Proofs of Retrievability," Proc. 14th Int'l Conf. Theory and Application of Cryptology and Information Security: Advances in Cryptology Advances in Cryptology (ASIACRYPT '08), J. Pieprzyk, ed., pp. 90-107, 2008.
- [9] H.-C. Hsiao, Y.-H. Lin, A. Studer, C. Studer, K.-H. Wang, H. Kikuchi, A. Perrig, H.-M. Sun, and B.-Y. Yang, "A Study of User-Friendly Hash Comparison Schemes," Proc. Ann. Computer Security Applications Conf. (ACSAC), pp. 105-114, 2009.
- [10] A.R. Yumerefendi and J.S. Chase, "Strong Accountability for Network Storage," Proc. Sixth USENIX Conf. File and Storage Technologies (FAST), pp. 77-92, 2007.
- [11] Y. Zhu, H. Wang, Z. Hu, G.-J. Ahn, H. Hu, and S.S. Yau, "Efficient Provable Data Possession for Hybrid Clouds," Proc. 17th ACM Conf. Computer and Comm. Security, pp. 756-758, 2010.
- [12] M. Xie, H. Wang, J. Yin, and X. Meng, "Integrity Auditing of Outsourced Data," Proc. 33rd Int'l Conf. Very Large Databases (VLDB), pp. 782-793, 2007.
- [13] C. Wang, Q. Wang, K. Ren, and W. Lou, "Privacy-Preserving Public Auditing for Data Storage Security in Cloud Computing," Proc. IEEE INFOCOM, pp. 1-9, 2010.
- [14] B. Sotomayor, R.S. Montero, I.M. Llorente, and I.T. Foster, "Virtual Infrastructure Management in Private and Hybrid Clouds," IEEE Internet Computing, vol. 13, no. 5, pp. 14-22, Sept./Oct. 2009

Effect of T6 type heat treatment on dry sliding wear behaviour of LM6/SiCp using Taguchi and ANOVA

Yadavalli Basavaraj¹, Pvan Kumar B.K², Mallikarjuna G³,

¹Professor & Head, Department of Mechanical Engineering,
Ballari Institute of Technology and Management, Ballari, Karnataka, India

²Assistant Professor, Department of Mechanical Engineering,
Ballari Institute of Technology and Management, Ballari, Karnataka, India

³M.Tech Student, Department of Mechanical Engineering,
Ballari Institute of Technology and Management, Ballari, Karnataka, mallig30967@gmail.com, 9035973559, India

Abstract- In this study, the effects of T6 type heat treatment of LM6 reinforced with SiCp were prepared by stir casting techniques. The LM6 composite reinforced with 5 wt% and 15 wt% of SiCp. Dry sliding wear test is conducted using pin-on-disc testing machine. L9 orthogonal array was selected for the experimental run. The optimum process parameters were determined by using signal-to-noise ratio. S/N ratio and ANOVA were used to investigate the influence of process parameters on the wear rate. The regression analysis employed to find the optimal process parameters levels and to analyze the effect of process parameters on LM6/SiCp.

Keywords: ANOVA, composites, Heat treatment, smaller-the-better, Taguchi Technique.

I. INTRODUCTION

Amid the previous couple of years, materials plan has moved accentuation to pursue light weight, environment friendliness, ease, quality, and performance. Parallel to present trend, metal-matrix composites (MMCs) are attracting growing interest. The requirement for cutting edge engineering materials within the areas of aerospace and automotive industries had led to a fast development of metal matrix composites (MMC)[1-4]. The utilization of various metal matrix composites (MMCs) is continually since they have better physical, mechanical and tribological properties compared to the matrix materials. Aluminium matrix composites (AMCs) reinforced with ceramic particles are gaining wide spread popularity in several technological fields owing to their improved mechanical properties when compared with conventional aluminum alloys[4-10]. They exhibit higher mechanical properties than the unreinforced aluminium alloys and are used as tribological components in some vehicles for years thanks to their high specific strength and better wear resistance[10-15]. Rajashekhar et.al[16] Studied on Effect of Heat Treatment on Mechanical Properties of Hybrid Aluminum Matrix Composites hybrid composite materials developed with soft and hard reinforcements subjected to heat treatment for further enhancement of their mechanical properties have shown keen interest in the last few decades. Sridhar Bhat et.al investigated Effect of Heat Treatment on Microstructure and Mechanical Properties of Al-FA-SiC Hybrid MMCS. In this investigation Preheated silicon carbide (SiC) And Fly Ash(FA) was used as the reinforcements, produced by stir casting process. Cut pieces of alloy Al6061 were preheated at 450 °C for 1h before melting. Firstly SiC and Fly Ash particles were heated at 8000C for 2 hrs. before adding preheated SiC and Fly Ash particles in to Al6061 melt, 1Wt% of Mg is added to melt to improve the wettability between matrix and reinforcement. Daljeet Singh et.al investigated Mechanical behavior of Aluminum by adding SiC and Alumina. This work is focused to study the change in behavior of aluminum by adding different %age amount of 'SiC' and 'Al2O3' composites. Vijay Kumar S Maga et.al[17] studied on Mechanical Properties of Aluminium Alloy (Lm6) Reinforced With Fly Ash, Redmud and Silicon Carbide. This deals with fabricating or producing aluminium based metal matrix composite and then studying its microstructure and mechanical properties such as tensile strength, impact strength and wear behavior of produced test specimen. Satpal Kundu et.al[18] investigated of hybrid metal matrix composites with SiC, Al2O3 and graphite reinforced aluminium alloy (Al 6061T6) composites samples, processed by stir casting route are reported. The aluminium alloy was reinforced with 10 wt. % (SiC, Al2O3) and 5 wt. % of graphite to mixture the hybrid composite. Dry Sliding Wear of the hybrid composite were tested it was found that when the wear resistance of the hybrid composites can be increased when compared to Al6061 T6 alloy. The parameters such as load, sliding speed and sliding distance were identified will affecting wear rate.

Hence, Present work is focused on the effect of T6 type heat treatment on the tribological wear behavior of LM6 /SiCp MMC.

II. EXPERIMENTAL METHOD

A. Fabrication Process

Stir casting set up as shown in the Fig.1 consisted of resistance furnace and a stirrer assembly was used to synthesize the composite.



Fig 1: shows the graphical representation of Stir casting and Resistance Furnace

The matrix material used for the present study is LM6 Al-SiC alloy. The chemical composition of matrix material is as shown in Table 1 determined using Atomic Absorption Spectrophotometer (model AA-670, Varian, The Netherlands). SiC particles with size of 150 μ m and with varying amounts of 0, 5 and 15 wt% are being used as reinforcing material in the preparation of composites. Stir casting technique has been used for the preparation of composites. Initially calculated amount of LM6-alloy was charged into Gr crucible and superheated to a temperature of 750 $^{\circ}$ C in an electrical resistance furnace.

The furnace temperature was controlled to an accuracy of $\pm 50^{\circ}$ C using a digital temperature controller. Sliding wear test specimens were machined from as-cast samples, to obtain cylindrical pins of diameter 10 mm and length 24 mm. then the samples were subjected to heat treatment (T6 type), where composites have been subjected to solutionizing treatment at 530 $^{\circ}$ C for 1 h followed by quenching in water. The quenched samples again subjected to artificial aging at 170 $^{\circ}$ C for 6 h followed by air cooled.

Table1: Composition of LM6 alloy

Elements	Percentage (%)
Si	10-13.0
Cu	0.1
Mg	0.1
Fe	0.6
Mn	0.5
Ni	0.1
Zn	0.1
Pb	0.1
Sb	0.05
Ti	0.2
Al	Remaining

B. Wear test

Dry sliding wear tests for different number of specimens was conducted by using a pin-on-disc machine (Model: Wear & Friction Monitor TR-20) supplied by DUCOM, was shown in Figure.2.

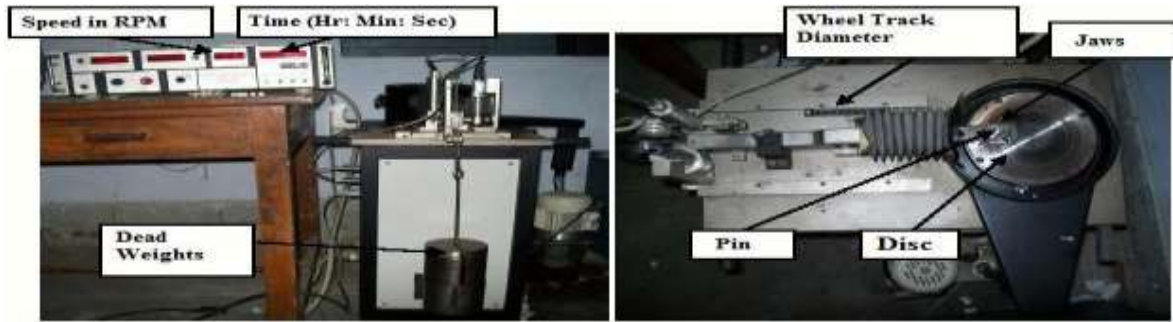


Fig. 2:- Showing Wear Testing Machine

The pin was held against the counter face of a rotating disc (EN32 steel disc)

with wear track diameter 80mm. The pin was loaded against the disc through a dead weight loading system. The wear test for all specimens was conducted under the normal load of 1,3 & 5 kg . Wear tests were carried out for a total sliding distance of approximately 1000m under similar conditions as discussed above. The pin samples were 24 mm in length and 8 mm in diameter. The surfaces of the pin samples was slides using emery paper (80 grit size) prior to test in ordered to ensure effective contact of fresh and flat surface with the steel disc. The samples and wear track were cleaned with acetone and weighed (up to an accuracy of 0.0001 gm using microbalance) prior to and after each test. The wear rate was calculated from the weight loss technique and expressed in terms of wear volume loss per unit sliding distance.

C. Taguchi Method

The taguchi method was developed by Dr.Genichi Taguchi. He developed a method for designing experiments to investigate how different parameters affect the mean and variance of a process performance characteristic. The experimental design proposed by Taguchi involves using orthogonal arrays to organize the parameters affecting the process and the levels. This technique is carried out in a three stages approach such as system design, parameter design and tolerance design. System design reveals the usage of scientific and engineering information required for producing a part. Parameter design is used to obtain the optimum levels of process parameters for developing the quality characteristics and to determine the product parameter values. Tolerance deign is used to determine and analyze tolerance about the optimum combination suggested by parameter design.

Table 2: Control and Noise Factors

Sl.No.	Process Parameters	Level 1	Level 2	Level 3
1	SiCp (wt%),A	0	5	15
2	Normal Pressure (MPa),B	0.19	0.59	0.990
3	Sliding Speed (m/s.), C	1	3	5

D. Design of Experiment

The experimental plan was formulated considering three parameters (variables) and three levels based on the Taguchi technique. % of SiCp (A), Normal Pressure (B) and Sliding Speed (C), these are process parameters are considered for the study. Process parameters setting with the highest S/N ratio always yield the optimum quality with minimum variance. The levels of these variables chosen for experimentation are given in the Table 2.

In the present investigation an L9 orthogonal array was chosen as shown in table 3. The selected of the orthogonal array is based on the condition that the degrees of freedom for the orthogonal array should be greater than, or equal to, the sum of the variables. The experiments were conducted based on the run order generated by Taguchi model and the results were obtained. This analysis includes the rank based on the delta statistics, which compares the relative value of the effects. S/N ratio is a response which consolidates repetitions and the effect of noise levels into one data point. The experimental results were transformed into signal-to-noise ratio (S/N)

ratios. An S/N ratio is defined as the ratio of the mean of the signal to the standard deviation of the noise. The S/N ratio indicates the degree of the predictable performance of a product or process in the presence of noise factors. The S/N ratio for the wear rate and coefficient of friction using ‘smaller the better’ characteristics, which can be calculated as logarithmic transformation of the loss function is given as

$$S/N = -10 \log_{10} (MSD) \quad \text{----- (1)}$$

Where MSD = Mean Square Deviation

For the smaller the better characteristic,

$$MSD = (Y_1^2 + Y_2^2 + Y_3^2 + \dots) \times 1/n$$

Where Y1, Y2, Y3 are the responses and ‘n’ is the number of tests in a trial.

Table 3: L9 Orthogonal Array

	(OA)		
SI No.	A	B	C
1	1	1	1
2	1	2	2
3	1	3	3
4	2	1	2
5	2	2	3
6	2	3	1
7	3	1	3
8	3	2	1
9	3	3	2

Table 4: Combination of parameters in (L9) Orthogonal Array

Expt Run	Process Parameters			Volumetric Wear rate (mm ³ /m)	S/N ratio for Vol. Wear rate (db)	COF (N)	S/N ratio for COF (db)
	% of SiCp	Nr. Pressure (MPa)	Sliding speed (m/s)				
01	0	0.19	1	8.92857E-5	80.9844	0.34659	9.2037
02	0	0.59	3	4.01786E-4	67.9201	0.35338	9.0352
03	0	0.990	5	6.69643E-4	63.4831	0.4159	7.6202
04	5	0.19	3	2.67857E-4	71.4419	0.22426	12.9850
05	5	0.59	5	4.91071E-5	86.1771	0.49269	6.1485
06	5	0.990	1	9.375E-4	60.5606	0.33843	9.4106
07	15	0.19	5	2.23214E-4	73.0256	0.42813	7.3685
08	15	0.59	1	5.35714E-5	85.4213	0.36697	8.7074
09	15	0.990	2	9.82143E-4	60.1565	0.58308	4.6854

III. RESULTS AND DISCUSSION

The experiments were conducted as per the orthogonal array and the volumetric wear rate for various combinations of process parameters. The experimental values were remodelled into S/N quantitative measuring for measure the standard characteristics using MINITAB 16.

A. Analysis of S/N Ratio

In Taguchi method, the term ‘signal’ represents the desirable value (mean) for the output characteristics and the term ‘noise’ represents the undesirable value for the output characteristics. Taguchi uses S/N ratio to measure the quality characteristics deviating from the desired value. The volumetric wear rate and COF readings are shown in Table 4. The influence of control parameters such as Normal pressure, Sliding speed and wt% of reinforcement content has been analyzed and the rank of involved factors like wear rate of composite materials which supports S/N ratio response is given in the table 5 & 6 and for COF is given in the table 7 & 8. It is evident from the table that among these process parameters, normal pressure is a dominant factor on the wear rate. The influence of controlled process parameters on wear rate are graphically represented in figures 3 and 4 and for COF are graphically represented in figures 5 and 6. The response tables 3, 4 and 5, 6 shows the average value of each response characteristics (S/N ratios, means) for each level of each factor for volumetric wear rate and COF of LM6-SiCp composites. The table indicates ranks based on Delta statistics, which compare the relative magnitude of effects of all the parameters. The Delta statistic is the highest minus the lowest average of S/N ratio and mean for each factor. Minitab 16 assigns ranks based on Delta values; rank 1 indicates highest Delta value, rank 2 second highest, and so on.

Table 5: Response Table of volumetric wear rate for S/N Ratio Smaller is better

Level	% of SiCp	Nr. Pressure	Sliding speed
1	70.80	75.15	75.66
2	72.73	79.84	66.51
3	72.87	61.40	74.23
Delta	2.07	18.44	9.15
Rank	3	1	2

Table 6: Response Table of volumetric wear rate for mean

Level	% of SiCp	Nr. Pressure	Sliding speed
1	0.000387	0.000193	0.000360
2	0.000418	0.000168	0.000551
3	0.000420	0.000863	0.000314
Delta	0.000033	0.000695	0.000237
Rank	3	1	2

Table 7: Response Table of COF for S/N Ratio (Smaller is better)

Level	% of SiCp	Nr. Pressure	Sliding speed
1	8.620	9.852	9.107
2	9.515	7.964	8.902
3	6.920	7.239	7.046
Delta	2.594	2.614	2.061
Rank	2	1	3

Table 8: Response Table of COF for mean

Level	% of SiCp	Nr. Pressure	Sliding Speed
1	0.3720	0.3330	0.3507
2	0.3518	0.4043	0.3869
3	0.4594	0.4458	0.4456
Delta	0.1076	0.1128	0.0949
Rank	2	1	3

In the experimental run our goal was to minimize the volumetric wear rate and COF of LM6-SiCp composites. In Taguchi experiments, we always want to maximize the S/N ratio. The S/N ratios with high values in the response tables 5 and 7 shows that the S/N ratios can be maximized at these levels and wear can be minimized at these levels.

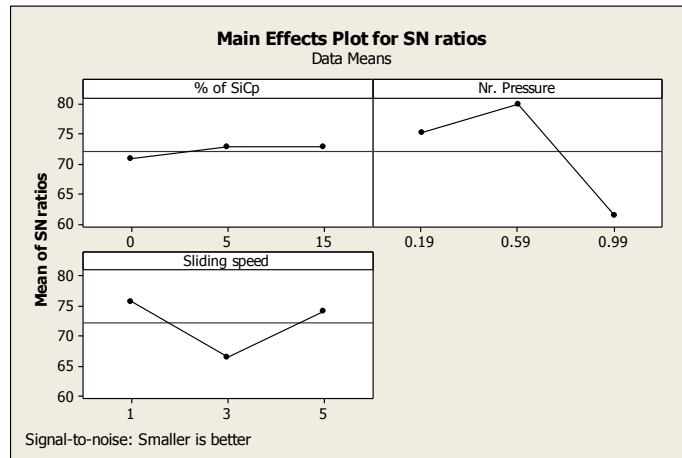


Fig 3: Main Effects Plot for SN ratios – volumetric wear rate

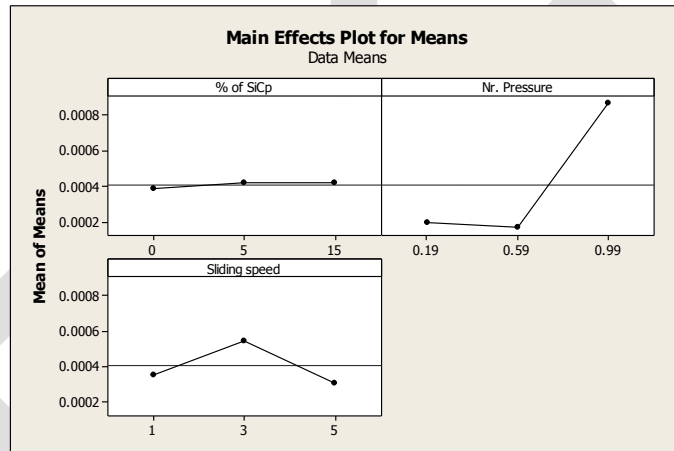


Fig 4: Main Effects Plot for Means- volumetric wear rate

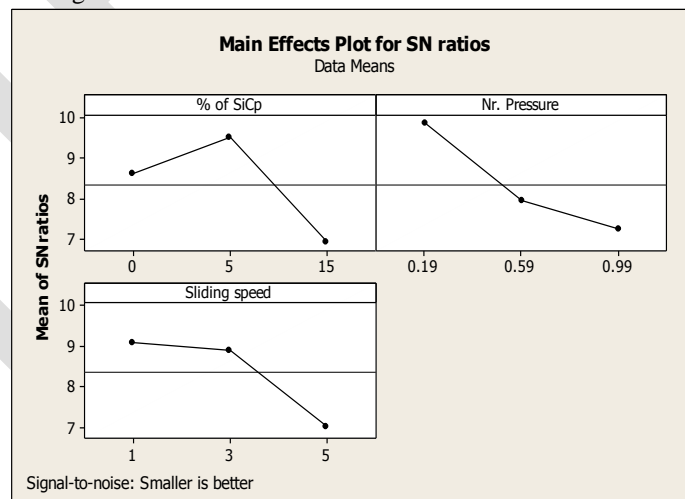


Fig 5: Main Effects Plot for SN ratios – COF

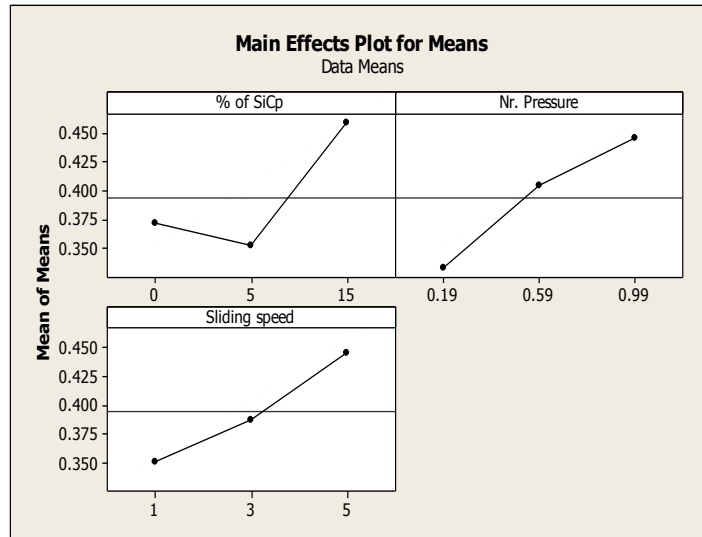


Fig 6: Main Effects Plot for Means- COF

Main effects plot is a plot of the means at each level of a factor. One can use these plots to compare the magnitudes of the various main effects and compare the relative strength of the effects across factors. However it is important to be sure to evaluate significance by looking at the effects in the analysis of variable table.

Analysis of the influence of each control factor (A, B and C) on the friction characteristics is obtained from the response table of mean S/N ratio. When % of SiCp is 15, Nr. Pressure 0.59 MPa and sliding speed is 1m/s for LM6-SiCp composite the volumetric wear is minimum. Similarly, when % of SiCp is 10, Nr. Pressure 0.19 MPa and sliding speed is 1m/s for LM6-SiCp composite the COF is minimum. Examining the main effects plots and interaction plots confirms the above results.

B. Analysis of variance

Analysis of variance (ANOVA) was introduced by Sir Ronald Fisher. This analysis was carried out for a level of significance of 5%, i.e., for 95% level of confidence. The purpose of ANOVA is to investigate the percentage of contribution of variance over the response parameter and to find the influence of wear parameters. The ANOVA is also needed for estimating the error of variance and variance of the prediction error. The table 4.6 shows analysis of variance for volumetric wear rate of the composite material. From the table 9, it is observed that the normal pressure, sliding speed and wt% of reinforcement have the influence on wear of composite material. The last column of the table 9 indicates the percentage contribution of each other on the total variation indicating their degree of influence on the result. It can be observed from the ANOVA table that the normal pressure (75.01) was the most significant parameter on the dry sliding wear of composites followed by sliding speed (08.33) and SiCp wt% (08.33). It can be observed from the ANOVA Table 10 that the SiCp wt% (23.46) was the most significant parameter on the COF of composites followed by Nr. pressure (23.35) and sliding speed (16.44). When the P-value for this model was less than 0.05, then the parameter can be considered as statistically significant. The pooled error associated in the ANOVA table was approximately about 08.33% for volumetric wear rate and 36.75% for COF. This approach gives the variation of means and variance to absolute values considered in the experiment and not the unit value of the variable.

Table 9: Analysis of Variance for volumetric wear rate (mm³/m)

Source	DF	Seq SS	Adj SS	Adj MS	F	P	% of contribution
% of SiCp	2	0.0000001	0.0000001	0.0000001	0.03	0.967	08.33
Nr. Pressure	2	0.0000009	0.0000009	0.0000005	15.57	0.060	75.01
Sliding speed	2	0.0000001	0.0000001	0.0000000	1.58	0.388	08.33
Error	2	0.0000001	0.0000001	0.0000000			08.33

Total	8	0.0000012					100
-------	---	-----------	--	--	--	--	-----

Table 10: Analysis of Variance for COF

Source	DF	Seq SS	Adj SS	Adj MS	F	P	% of contribution
% of SiCp	2	0.01963	0.01963	0.00981	0.64	0.610	23.46
Nr. Pressure	2	0.01954	0.01954	0.00977	0.64	0.611	23.35
Sliding speed	2	0.01376	0.01376	0.00688	0.45	0.691	16.44
Error	2	0.03073	0.03073	0.01537			36.75
Total	8	0.08366					100

C. Multiple Linear Regression Models

Statistical software MINITAB R16 is used for developing a multiple linear regression equation. This developed model gives the relationship between independent/predictor variable and a response variable using by fitting a linear equation to the measured data.

The regression equation developed for volumetric wear rate is,

$$\text{Volumetric Wear rate} = -6.36427e-005 + 1.892e-006 \% \text{ of SiCp} + 0.000837054 \text{ Nr. Pressure} - 1.15327e-005 \text{ Sliding speed} \quad \text{----- (2)}$$

R-Sq = 94.50%

The regression equation developed for COF is,

Regression Equation

$$\text{COF} = 0.196444 + 0.00653352 \% \text{ of SiCp} + 0.141013 \text{ Nr. Pressure} + 0.0237275 \text{ Sliding speed} \quad \text{----- (3)}$$

R-Sq = 63.26%

IV. CONCLUSION

LM6/SiCp composites can be made in an open atmosphere by stir casting using fabrication scheme derived from the literature review and mentioned in the experimental.

Based on the above analysis the following conclusions are drawn from the present study.

1. In this study, hardness and analysis of mechanical characteristics of Al-SiC reinforced with 0, 5 and 15 wt% of SiC was examined with and without heat treatment. With the increase in reinforcement ratio, the impact strength and hardness of the aluminium silicon carbide metal matrix composite material is increased.
2. Taguchi method provides a systematic and efficient methodology for the design and optimization of volumetric wear rate parameters with far less effort than would be required for most optimization techniques.
3. For LM6-SiCp the optimal tribological testing combination for minimum volumetric wear rate is found to be when % of SiCp is 15, Nr. Pressure 0.59 MPa and sliding speed is 1m/s and minimum COF is found to be when % of SiCp is 5, Nr. Pressure 0.19 MPa and sliding speed is 1m/. All the factors % of SiC (A), Nr. Pressure (B) and sliding speed(C) are found to affect the friction significantly.
4. The analysis of variance shows that the Normal pressure (75.01%) is the wear factor that has the highest statistical influence on the dry sliding wear of composites followed by sliding speed (8.33%) and reinforcement (8.33%) and and reinforcement (23.46%) is the COF that has the highest statistical influence on the dry sliding wear of composites followed by sliding speed (16.44%) and Normal pressure (23.35%).
5. The pooled error associated with the ANOVA analysis was 8.33% for wear rate and 36.75% for COF for the factors and the correlation between the wear parameters was obtained by multiple linear regression models.

REFERENCES:

- [1] Alpas AT, Zhang J. Effect of SiC particulate reinforcement on the dry sliding wear of Aluminium-silicon alloys (A356). *Wear* 1992; 155:83-104
- [2] Seo YH, Kang CG (1999) *Compo Sci Techno* 59:643
- [3] Skolianos S (1996) *Mater Sci Eng A* 210:76
- [4] Kang CG, Yoon JH Seo YH (1997) *J Mater Proc Technol* 66: 30
- [5] Yunsheng X, Chung DDL (1998) *J Mater Sci* 33:5303
- [6] Seo YH Kang CG (1995) *J Mater Proc Techno* 55:370
- [7] Zhang S, Cao F, Chen Y Li, Q, Jiang Z (1998) *Acta Mater* 45:5303
- [8] Bar J, Klubmann HG, Gudlat HJ (1993) *Scripta Metal Mater*; 29:787
- [9] Gui MC, Wang DB, Wu, JJ, Yuan GJ Li CG (2000) *Mater Sci tech*; 16:556
- [10] Skolianos, Skattamis TZ Tribological Properties of SiCp reinforced Al- 4.5% Cu-1.5% Mg alloy composites *Mater Sci Eng A* 1993; 163:107-12
- [11] Veerabhadrapppa Algur, Balaraj V, Kori Nagaraj, "Effect of T6 type heat treatment on the Mechanical characterization of Al6061-Al₂O₃ particulate composites", *International Journal of Emerging Trends in Engineering and Development*, Issue 5, Vol. 3 (April-May. 2015), ISSN 2249-6149, Pp-309-319.
- [12] Surappa MK, Prasad SC, Rohatgi PK. Wear and abrasion of cast Al-Alumina particle composites.
- [13] Veerabhadrapppa Algur, Lakshmana Naik T K, Ravi B Chikmeti, Akhil Sohan A, Golla Sunil, Mohan and Karoor Shekappa, "Dry Sliding Wear Behaviour Of Aluminium Alloy Reinforced With Sic Metal Matrix Composites Using Taguchi Method", Vol. 3, No. 4, October 2014, pp. 49-57.
- [14] Shouvik Ghosh, *Prasanta Sahoo, Goutam Sutradhar, Wear Behaviour of Al-SiCp Metal Matrix Composites and Optimization Using Taguchi Method and Grey Relational Analysis, *Journal of Minerals and Materials Characterization and Engineering*, 2012, 11, 1085-1094.
- [15] N. Chawla et.al, "Tensile and fatigue fracture of discontinuously Reinforced Aluminium", D. *Advances in Fracture Research*, (2001), pp. 1-6.
- [16] Rajashekhar et al, "Studies on Effect of Heat Treatment on Mechanical Properties of Hybrid Aluminum Matrix Composites", *International Journal of Innovative Research in Science, Engineering and Technology* Vol. 2, Issue 11, November 2013.
- [17] Vijay Kumar S Maga et al, "A Study on Mechanical Properties of Aluminium Alloy (Lm6) Reinforced With Fly Ash, Redmud and Silicon Carbide" *IOSR Journal of Mechanical and Civil Engineering (IOSR-JMCE)* e-ISSN: 2278-1684, p-ISSN: 2320-334X, Volume 11, Issue 5 Ver. III (Sep- Oct. 2014), PP 07-16
- [18] Satpal Kundu et al, "Study of Dry Sliding Wear Behaviour of Aluminium/SiC/Al₂O₃/Graphite Hybrid Metal Matrix Composite Using Taguchi Technique" *International Journal of Scientific and Research Publications*, Volume 3, Issue 8, August 2013 1 ISSN 2250-3153.

Strength and Workability Properties of GGBS and Rice husk Ash

Divya BhavanaTadepalli, Madhavi Etaveni, Syed Eashan Adil
Assistant professors, Department of Civil engineering
Aurora engineering college , Hyderabad, India

Abstract— Sustainable development is mandatory to protect our environment .In agriculture and other industries waste materials are released which are organic and inorganic materials and can be an alternate material for cement . Rice husk ash which reduces the emission of carbon and produces green effect in environment .GGBS a slag material which also be an alternate to the cement. In this research the experimental investigations carried out in three phase M30 mix grade concrete is used with RHA in proportions of 0%,5%,10%and 15% .In second phase GGBS in various proportions of 10%,20%and 30% were tested . In third phase combination of GGBS and rice husk ash were tested .From this research the results are much better as compare to conventional concrete.

Keyword: Rice husk ash (RHA),Ground granular blast furnace slag (GGBS),compressive strength,split tensile strength,conventional concrete,workability.

INTRODUCTION

Concrete has been the major in construction for providing stable and reliable infrastructure since the days of Greek and roman civilization. Concrete is the most world widely used in construction material. The increase in demand of concrete more the new method and materials are being developed for production of concrete. Concrete is a mixture of cement, water, and aggregates with or without chemical admixtures. The most important part of concrete is the cement. Use of cement alone as a binder material produces large heat of hydration. Since the production of this raw material produces lot of CO₂ emission. The carbon dioxide emission from the cement raw material is very harmful to the environmental changes. Nowadays many researchers have been carried out to reduce the CO₂.The effective way of reducing CO₂ is using rice husk ash which is an agricultural residue accounts for 20%of 649.7 million tons of rice produced annually worldwide. The produced partially burnt husk from the milling plants when used as a fuel also contributes to pollution and efforts are being made to overcome this environmental issue by utilizing this material as a supplementary cementing material.

MATERIALS USED

Cement

The ordinary Portland cement of 53 grade conforming to IS 12269: 2013 was used. The specific gravity of cement was 3.11.

Rice husk ash

Rice husk ash is a pozzolanic material .A residual obtained from open field burning .In this investigation specific gravity for RHA is 2.3

GGBS

GGBS has been used in construction industry for years as replacement of ordinary Portland cement when molten iron slag is quenched in steam or water, a glassy product is obtained. It is then dried and made into powder. In this investigation specific gravity for GGBS is 3.09

Fine aggregates

Natural river sand was used as a fine aggregate conforming to grading zone I of IS: 383 1970 was used. Its specific gravity was 2.6.

Coarse aggregate

Coarse aggregate obtained from local quarry units has been used for this study. Maximum size of aggregate used is 20mm with specific gravity of 2.67.

Water

In this experimental investigation portable water which is free from organic substances is used for mixing and curing.

EXPERIMENTAL INVESTIGATION

In present study M30 grade concrete were designed as per IS: 10262-2009

A. Workability

Freshly mixed concrete were tested for workability by slump test. In this investigation, M30 mix concrete the test by-weight basis by replacing cement by 0%,10%,20%,30% with RHA and 10%,20%,30% with GGBS and 30% combine effect of RHA and GGBS are carried out.

B. Compressive strength

In this investigation, M30 mix concrete is considered to perform the test by-weight basis with 0%,10%,20% and 30% of cement replaced by RHA and 10%,20%,30% of cement by GGBS and combination of both RHA and GGBS. A 150x150 mm concrete cube was used as test specimens to determine the compressive strength of concrete cubes. The ingredients of concrete were thoroughly mixed till uniform consistency was achieved. The cubes were properly compacted. All the concrete cubes were de-moulded within 24 hours after casting. The de-moulded test specimens were properly cured in water available in the laboratory at an age of 28 days. Compression test was conducted on a 2000KN capacity universal testing machine. The load was applied uniformly until the failure of the specimen occurs. The specimen was placed horizontally between the loading surfaces of the compression testing machine and the load was applied without shock until the failure of the specimen occurred.

C. Split tensile strength

In this investigation, M30 mix concrete is considered to perform the test by-weight basis by replacing 0%,10%,20% and 30% of cement replaced by RHA and 10%,20%,30% of cement by GGBS and combination of both RHA and GGBS and combination of both quarry dust and GGBS. Cylinders of 150 mm diameter and 300 mm length were used as test specimens to determine the split tensile strength of concrete. The ingredients of concrete were thoroughly mixed till uniform consistency was achieved. The cylinders were properly compacted. All the cylinders were de-moulded within 24 hours after casting. The de-moulded test specimens were properly cured in water available in the laboratory for an age of 28 days. The split tensile strength was conducted as per IS 5816-1976. The specimen was placed horizontally between the loading surfaces of the compression testing machine and the load was applied without shock until the failure of the specimen occurred.

RESULTS AND DISCUSSIONS

A. WORKABILITY

Slump test of various mix proportions of RHA and GGBS in concrete are shown below

Table1: Slump values with various proportions of Rice husk ash and GGBS replacing cement in M30 grade concrete

S.No	RHA Content	Slump
1	0%	96
2	5%	90
3	10%	85
4	15%	79

S.No	GGBS content	slump
1	0%	96
2	10%	97
3	20%	98
4	30%	99

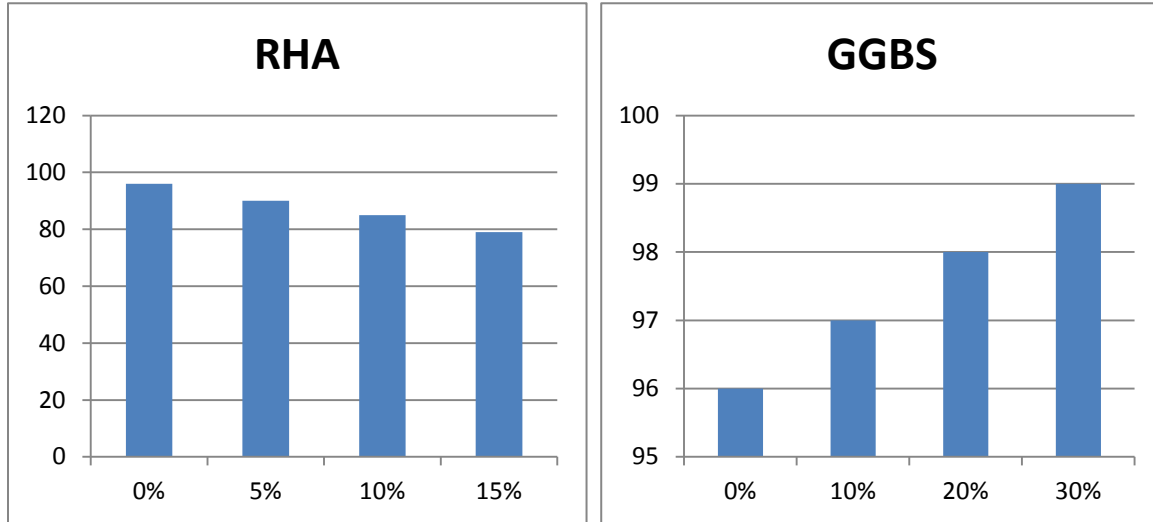


Fig 1: slump values when replacement of cement by RHA and GGBS

B. Compressive Strength Test

The compressive strength of concrete was achieved in 28 days of various proportions and presented below. The specimens were cast and tested as per IS: 516-1959.

Table 2: Compression test at 28 day with various Proportions of RHA and GGBS replacing cement in M30 grade concrete

S.No	RHA Content	Compressive strength N/mm ²
1	0%	32
2	5%	33.44
3	10%	35.8
4	15%	30.4

S.No	GGBS Content	Compressive strength N/mm ²
1	0%	32
2	10%	36.44
3	20%	39.55
4	30%	23.55

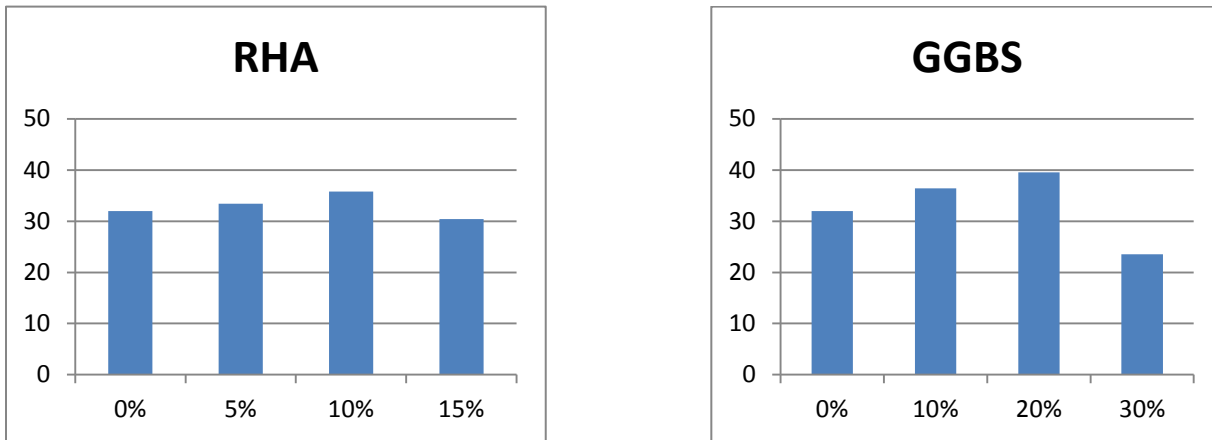
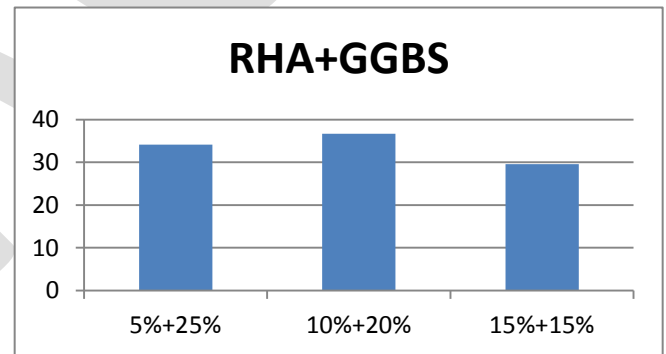


Fig 2: Compressive Strength when replacement of Cement by RHA and GGBS

From the figure 2 and table 2 it is observed that 10% Rice husk ash (RHA) and 20% GGBS achieved maximum strength in comparison to normal concrete.

Table 3 and Fig 3: Compression test at 28 day with various Proportions of GGBS and RHA replacing cement in M30 grade concrete

S.No	RHA and GGBS content	Compressive strength N/mm ²
1	5% RHA +25% GGBS	34.11
2	10% RHA+20%GGBS	36.7
3	15% RHA+ 15%GGBS	29.6



From the figure 3 and table 3 it is observed that combine 5% RHA and 20% GGBS achieved maximum strength in comparison to normal concrete.

c. Split Tensile Test

The tensile strength of concrete with 28 days curing period for various proportions and presented below. The specimens were cast and tested as per IS: 516-1959.

Table 4: Split tensile test at 28 day with various Proportions of RHA and GGBS replacing cement in M30 grade concrete

S.No	RHA Content	Split tensile strength N/mm ²
1	0%	3.56
2	5%	3.57
3	10%	3.6
4	15%	3.4

S.No	GGBS Content	Split tensile strength N/mm ²
1	0%	3.56
2	10%	3.58
3	20%	3.65
4	30%	3.01

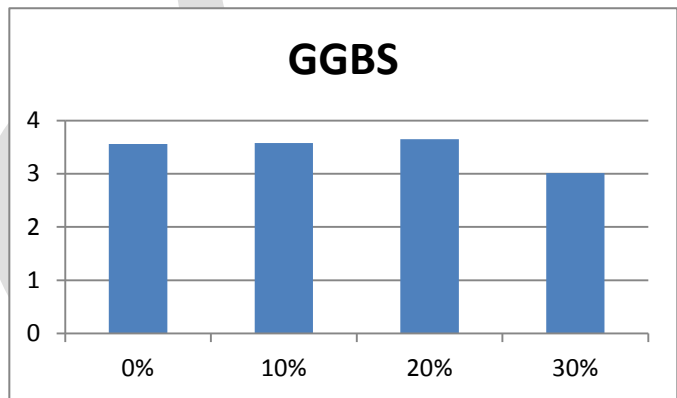
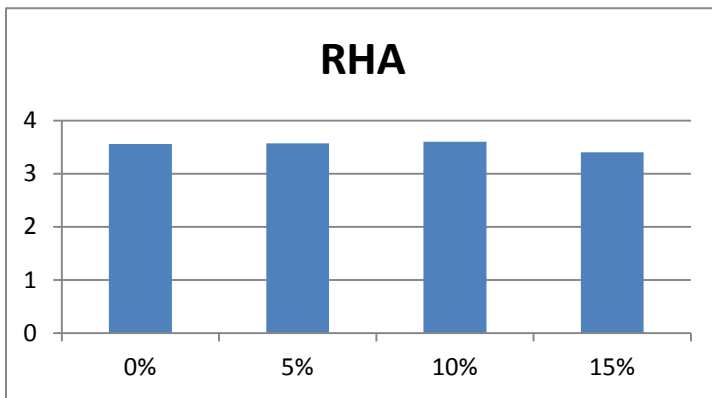
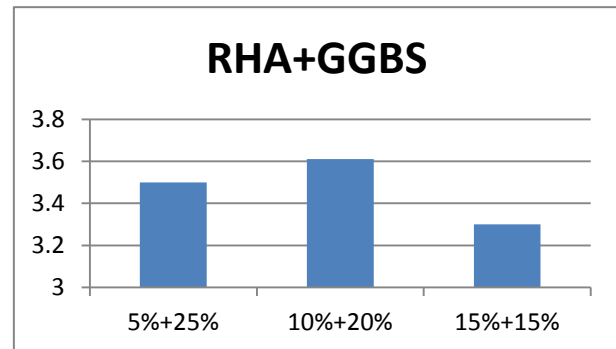


Fig 4: split tensile Strength when replacement of Cement by RHA and GGBS

From the figure 4 and table 4 it is observed that 10% Rice husk ash (RHA) and 20% GGBS achieved maximum strength in comparison to normal concrete.

Table 5 and Fig 5: Split tensile test at 28 day with various Proportions of RHA and GGBS replacing cement in M30 grade concrete

S.No	RHA and GGBS content	Split tensile strength N/mm ²
1	5% RHA +25% GGBS	3.5
2	10% RHA+20%GGBS	3.61
3	15% RHA+ 15%GGBS	3.3



From the figure 5 and table 5 it is observed that 10% Rice husk ash (RHA) and 20% GGBS achieves maximum strength in comparison to normal concrete

CONCLUSION

Based on the experimental investigations the following conclusions are drawn:

- As cement is very costlier and use of cement creates an environmental problem, need to find alternative material. Rice husk ash is a waste material which is obtained from rice mills, it is a suitable substitute for cement at very low cost.
- By adopting critical mix and replacing the cement by rice husk ash fine, it is found that by increasing the percentage of rice husk ash workability decreases because of its increased water absorption and strength decreases gradually.
- Similarly replacing cement with GGBS increases the workability
- From the above compressive strength results, it is observed that rice husk ash based concretes have achieved an increase in strength for 10% replacement of cement and 20% replacement of cement by GGBS and combine 10% RHA and 20% GGBS at the age of 28 days when compared to conventional concrete.
- From the above split tensile strength results, it is observed that rice husk ash based concretes have achieved an increase in strength for 10% replacement of cement and 20% replacement of cement by GGBS and combine 10% RHA and 20% GGBS at the age of 28 days when compared to conventional concrete.
- From the above experimental investigation rice husk ash (RHA) can be used as alternate material to cement up to 10%, 20% GGBS and 10% and 20% combine effect of RHA and GGBS.

ACKNOWLEDGMENT

The author T.Divya Bhavana wish to thank S.k Chandra sir Associate professor and aurora engineering college for their kind support, valuable guidance and providing all facilities for conducting this experiment on replacement of RHA and GGBS in concrete.

REFERENCES :

- [1]. Satish H.Sathawane and Vikrant S.Varigade "Combine Effect of Rice Husk Ash and Fly Ash on Concrete by 30% Cement Replacement".
- [2]. B. N. Sangeetha "Effect of Rice Husk Ash and GGBS on Performance of Concrete".
- [3]. Prasanna Venkatesan Ramani, Pazhani Kandukalpatti Chinnaraj, "Geopolymer concrete with ground granulated blast furnace slag and black rice husk ash"
- [4]. Sonali K. Gadpalliwar¹, R. S. Deotale², Abhijeet R. Narde To Study the Partial Replacement of Cement by GGBS & RHA and Natural Sand by Quarry Sand In Concrete".
- [5]. IS 2386: Part 3: "Methods of Test for Aggregates for concrete" Part 3, 1963.
- [6] IS 4031: Part 4: "Methods for physical test for hydraulic cements", Bureau of Indian standards, New Delhi, 1988.
- [7] IS 516:1959, "Method of Test for Strength of Concrete", Reaffirmed 2004, Bureau of Indian standards, New Delhi
- [8] IS 10262 -2009 "IS Method of Mix Design", Bureau of Indian Standards, New

Design and Development of Clamping Fixture for Drilling of Boiler Tube Plate

Amit V. Patil¹, Sanjivani R. Bhosale¹, Sunny N. Shahane¹, Neha S. Shirodkar¹, Prof. Amol D. Lokhande²

¹Students, Savitribai Phule Pune University, MIT College of Engineering, Pune

²Assistant Professor, Savitribai Phule Pune University, MIT College of Engineering, Pune

Email ID:- amitpatil050@gmail.com (8275749450)

Abstract— Present invention provides special design of clamping fixture for drilling of boiler tube plate. This clamping fixture is necessary in order to self Centre the boiler tube plate. This self-centering can be done by using rack and pinion mechanism. This fixture was designed and built to hold, support and locate fire tube boiler plate to ensure that it is drilled with accuracy. The fixture set up for component is done manually. For that more cycle time required for loading and unloading the material so, there was a need to develop a system which can help in improving productivity and time. Fixtures reduce operation time and increase productivity and high quality of operation is possible.

Keywords— Boiler Tube Plate, Self Centering, Rack and Pinion, Hydraulic Clampers, Simulation in solidworks, Shaft,

INTRODUCTION

The present scenario is that for the purpose of drilling of fire tube boiler plate manual clamping method is used. This consumes more time and due to which production rate affects. Hence clamping and declamping requires high manpower. Also during drilling vibrations are induced. To remove that the conventional method of setting blocks is used. These blocks may obstruct the path of tool and require constant relocating of the blocks. Fixture design plays an important role at the setup planning phase. Proper fixture design is crucial for developing product quality in different terms of accuracy, surface finish and precision of the machined parts. In existing design the fixture set up is done manually, so the aim of this project is to replace with hydraulic fixture to save time for loading and unloading of component. Hydraulic fixture provides the manufacturer for flexibility in holding forces and to optimize design for machine operation as well as process functionality.

Steps for Fixture Design

Successful fixture designs begin with a logical and systematic plan. With a complete analysis of the fixture's functional requirements, very few design problems occur. The following is a detailed analysis of each step.

- Step 1: Define Requirements
- Step 2: Collect/Analyze Information
- Step 3: Develop Several Options
- Step 4: Choose the Best Option
- Step 5: Implement the Design

Consideration Parameters

Designing of fixtures depends upon so many factors. These factors are analyzed to get design inputs for fixtures. The list of such factors are mentioned below:

1. Study of work piece and finished component size and geometry.
2. Type and capacity of the machine, its extent of automation.
3. Provision of locating devices in the machine.
4. Available clamping arrangements in the machine.
5. Available indexing devices, their accuracy.
6. Evaluation of variability in the performance results of the machine.
7. Rigidity and of the machine tool under consideration.
8. Study of ejecting devices, safety devices, etc.
9. Required level of the accuracy in the work and quality to be produced

Fixture Design

To meet all design criteria for work holder is impossible, compromise is inevitable. The most important hint of optimal design objectives is positioning, holding& supporting functions that fixtures must fulfill.

1. Position: Fixture must above all else hold the work piece, precisely in place to prevent 12 degrees of freedom, linear movement in the either direction about each axis.
2. Repeatability: Identical work piece specimens should be located by work holder in precisely the same space on repeated loading & unloading cycles. It should be impossible to hold the work piece incorrectly.
3. Adequate clamping forces: The work holder must hold the work piece immobile against the forces of gravity. Centrifugal force, inertia force, wetting force, milling & the design must calculate these machines forces against the fixture holding capacity. The device must be rigid: clamping forces must be maintained.
4. Care during loading cycles: As the work holders usually receive more punishment during the loading & unloading cycle than during the machining operation. The device must endure impact & aberration for at least the life of the job.

Literature Survey

Shailesh S. Pachbhai, Laukik P. Raut (2014) have described that in machining fixtures, minimizing work piece deformation due to clamping and cutting forces is essential to maintain the machining accuracy. This can be achieved by selecting the optimal location of fixturing elements such as locators and clamps. The fixture set up for component is done manually. For that more cycle time required for loading and unloading the material. So, there is need to develop system which can help in improving productivity and time.

T. Papastathisa, O. Bakker , S. Ratcheva, A. Popova (2012) have described that instead of using passive fixture element use active fixture element because it reduce the dynamic deformation of the work piece by 84.2%.

Chetankumar M. Patel, Dr. G. D. Acharya (2014) have discussed that Paper proves utility of hydraulics in fixture design in three different ways: (i) reduces cycle time, (ii) reduces operator fatigue and increases productivity and (iii) reduces wear and tear of fixture components.

CENTERING OF TUBE PLATE

Initially centering of the plate is done manually. Perpendicular diameters are drawn approximately and center is plotted. Now the plate is loosely clamped and tool is allowed to move from one end point of diameter towards the other and then the tool moves half of the distance backward to obtain the center. If this center matches with the manually obtained center then machining is done by tightening the clamping or else procedure is repeated unless and until exact center is obtained. During the drilling operation vibrations are induced in the plate. Hence to overcome this presently 100*100 mm blocks are placed below plate to support it.

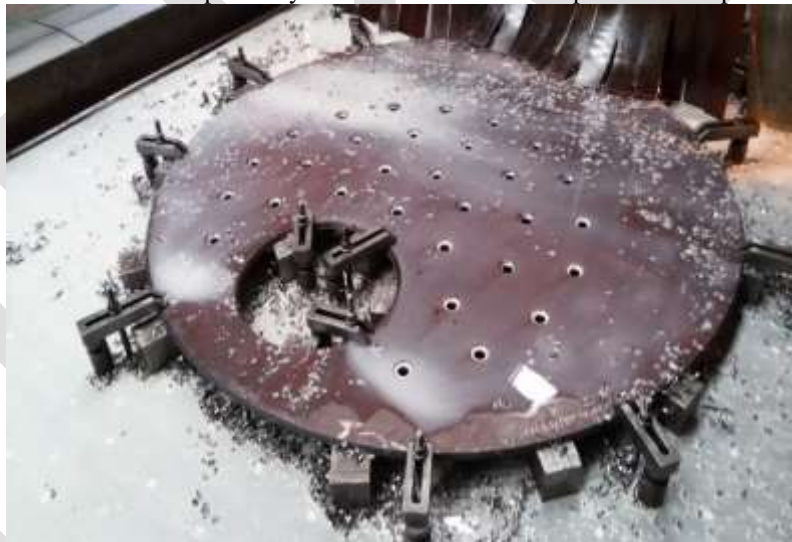


Figure 1. Actual Mounting of Plate



Figure 2. Manually adjusted Clamps

MAJOR PARTS OF THE SYSTEM

The following major parts are used in this system

1. Rack and Pinion
2. Shaft
3. Bearing
4. Coupling
5. Stand
6. Base plate
7. Clampers

DESIGN PROCEDURE

1. Design of Rack and Pinion: [7]

We have the standard rack and pinion pair available from ATALANTA RACK AND PINION Company.

Selection criteria are as follow:

Force required to pull the plate = weight of 2m diameter plate

$$W = \text{volume} \times \text{density} \times 9.81$$

$$W = \pi r^2 \times 7850 \times 9.81 = 5320 \text{ N}$$

- Step 1: Determining the Tangential Force

$$a = \frac{v}{t} \text{ [m/s}^2\text{]}$$

$$F = ((m \times g \times \mu) + (m \times a)) \text{ N}$$

- Step 2: From the given force select the standard rack and pinion pair and calculate F_{perm} .

$$F_{perm} = \frac{F_{(tab)}}{K_A \cdot S_B \cdot f_n \cdot L_{KHB}}$$

The Condition $F < F_{perm}$. Must be fulfilled.

- Step 3: Selection of load Factor K_A :

Drive	Type of load from the machines to be driven		
	Uniform	Medium Shocks	Heavy Shocks
Uniform	1	1.25	1.75
Medium Shocks	1.25	1.5	2.00
Heavy Shocks	1.5	1.75	2.25

Table 1. Shock Load Factor

Step 4: Safety Coefficient S_B :

The safety coefficient should be taken as 1.1 to 1.4
 ($S_B = 1.1$ to 1.4).

Step 5: Life-Time Factor (f_n):

Considering the peripheral speed of the pinion and lubrication.

Lubrication Peripheral Speed of Gearing m/sec	Continuous	Daily	Monthly
0.5	0.85	0.95	3 to 10
1.0	0.95	1.10	
1.5	1.00	1.20	
2.0	1.05	1.30	
3.0	1.10	1.50	
5.0	1.25	1.90	

Table 2. Life time factor

Step 6: Selection of Linear Load Distribution Factor L_{KHB} :

The linear load distribution factor considers the contact stress, while it describes unintegrated load distribution over the tool width

$L_{KHB} = 1.1$ for counter bearing, e.g. Torque Supporter.

= 1.2 for preloaded bearings on the output shaft e.g. ATLANTA HT, HP and E servo-worm gear unit, BG bevel-gear unit.

= 1.5 for unpreloaded bearings on the output shaft e.g. ATLANTA B servo-worm gear unit.

Calculations:

Mass to be Moved (m) = 550 kg

Speed (v) = 0.05 m/s

Acceleration Time (t_b) = 1 s

Acceleration Due to Gravity (g) = 9.81 m/s²

Coefficient of Friction (μ) = 0.23

Load Factor (K_a) = 1.25

Life-Time Factor (f_n) = 0.85

Safety Coefficient (S_B) = 1.4

Linear Load Distribution Factor (L_{KHB}) = 1.5

$$a = \frac{v}{t} = 0.05 \text{ m/s}^2$$

$$F_u = ((m \times g \times \mu) + (m \times a))$$

$$F_u = ((550 \times 9.81 \times 0.23) + (550 \times 0.05))$$

$$F_u = 1.268 \text{ KN}$$

Assumed feed force:

Rack C45, ind. hardened, straight tooth, and module 3.

Pinion 16MnCr5, case hardened, 40 teeth,

With $F_{tab} = 16.5 \text{ KN}$

$$F_{perm} = \frac{F_{(tab)}}{K_a \cdot S_B \cdot f_n \cdot L_{KHB}}$$

$$F_{perm} = \frac{16.5}{1.25 \times 1.4 \times 0.85 \times 1.5}$$

$$F_{perm} = 7.39 \text{ KN}$$

Condition

$$F_{perm} > F_u;$$

$$1.268 \text{ KN} > 7.39 \text{ KN} = > \text{fulfilled}$$

Result:

Rack 27 30 1001

Pinion 24 35 240 (case hardened). [4]

2. Design of Shaft

The shaft is designed using ASME code. According to this code, the permissible shear stress T_{max} for the shaft without keyways is taken as 30% of yield strength in tension or 18% of the ultimate tensile strength of the material, whichever is minimum. If keyways are present, the above are reduced by 25%. Also, the bending and torsional moments are to be multiplied by factors K_b and K_t respectively, to account for shock and fatigue.

Thus,

$$T_{max} = \frac{16Te}{\pi d^3} \sqrt{[(K_B \times M)^2 + (K_t \times T)^2]}$$

Where,

K_b = combined shock and fatigue factor applied to bending moment

K_t = combined shock and fatigue factor applied to torsional moment

Step 1: Selection of material for shaft.

The material selected for the shaft is C40 [7]

The values of the ultimate tensile strength and yield strength are as follows:

$$S_{ut} = 640 \text{ N/mm}^2$$

$$S_{yt} = 380 \text{ N/mm}^2$$

Step 2: Calculation of permissible shear stress

$$\begin{aligned} \text{Allowable stress} &= .75 \times .3 \times S_{yt} \text{ or } .75 \times .18 \times S_{ut} \\ &= 85.5 \text{ N/mm}^2 \text{ or } 86.4 \text{ N/mm}^2 \end{aligned}$$

Hence, permissible shear stress is 85.5 N/mm² Minimum value is taken.

Step 3: Calculation for maximum bending moment

Force acting on pinion is $F=1.25 \text{ kN}$

This force is resolved into two components as follows:

a) Tangential component acting in the direction of motion of pinion.

$$\begin{aligned} F_t &= F \cos(\alpha) \\ &= 1.25 \times \cos(20) \quad \dots 20^\circ \text{ pressure angle of pinion} \\ &= 1.17 \text{ KN} \end{aligned}$$

b) Radial component acting away from the Centre of the pinion.

$$\begin{aligned} F_r &= F_t \tan(\alpha) \\ &= 1.17 \times \tan(20) \\ &= 0.427 \text{ KN} \end{aligned}$$

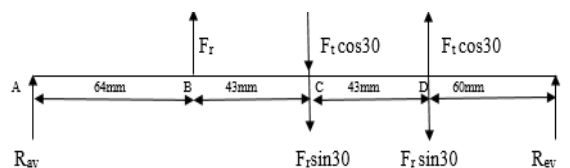


Figure 3. Vertical force diagram

$$\sum F_y = 0$$

Therefore, from vertical force diagram,

$$F_r - F_r \sin 30 - F_r \sin 30 + F_r \cos 30 - F_r \cos 30 + R_{AV} + R_{EV} = 0$$

$$0.427 - 2 \times (0.427) \times \sin 30 + R_{AV} + R_{EV} = 0$$

$$R_{AV} + R_{EV} = 0 \quad \dots (1)$$

Consider the moments about 'A'.

$$\sum M_a = 0$$

$$F_r \times 64 - (F_r \cos 30 + F_r \sin 30) \times 107 + (F_r \cos 30 - F_r \sin 30) \times 150 + R_{EV} \times 210 = 0$$

Thus,

$$R_{EV} = -0.076 \text{ kN}$$

$$R_{AV} = 0.076 \text{ kN}$$

Bending moments at different points are as follows:

$$M_{BV} = R_{AV} \times 64$$

$$= 4.864 \text{ kN-mm}$$

$$M_{CV} = R_{AV} \times 107 + F_r \times 43$$

$$= 26.514 \text{ kN-mm}$$

$$M_{DV} = R_{EV} \times 60$$

$$= -4.595 \text{ kN-mm}$$

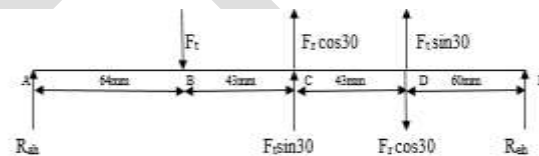


Figure 4. Horizontal force diagram

$$\sum F_y = 0$$

Therefore, from horizontal force diagram,

$$-F_t + F_r \cos 30 + F_r \sin 30 + F_r \sin 30 - F_r \cos 30 + R_{AH} + R_{EH} = 0$$

$$-1.17 - 2 \times (1.17) \times \sin 30 + R_{AH} + R_{EH} = 0$$

$$R_{AH} + R_{EH} = 0 \quad \dots (1)$$

Consider the moments about 'A'.

$$\sum M_a = 0$$

$$-F_t \times 64 + (F_r \cos 30 + F_r \sin 30) \times 107 + (F_r \sin 30 - F_r \cos 30) \times 150 + R_{EH} \times 210 = 0$$

Thus,

$$R_{EH} = -0.28 \text{ KN}$$

$$R_{AH} = 0.28 \text{ KN}$$

Bending moments at different points are as follows:

$$M_{BH} = R_{AH} \times 64$$

$$= 17.92 \text{ kN-mm}$$

$$M_{CH} = R_{AH} \times 107 - F_t \times 43$$

$$= -20.35 \text{ kN-mm}$$

$$M_{DH} = R_{EH} \times 60$$

$$= -16.8 \text{ kN-mm}$$

Resultant bending moments

$$M_B = \sqrt{[(M_{BH})^2 + (M_{BV})^2]}$$

$$= 1.856 \text{ kN-mm}$$

$$M_C = \sqrt{[(M_{CH})^2 + (M_{CV})^2]}$$

$$= 33.42 \text{ kN-mm}$$

$$M_D = \sqrt{[(M_{DH})^2 + (M_{DV})^2]}$$

$$= 17.41 \text{ kN-mm}$$

Therefore the highest total bending moment is occurring at point 'C'.

$$\text{Hence } M = 33.42 \text{ kN-mm}$$

Step 4: Calculation of torsional moment

Torque acting on the shaft is

$$T = F_t \times r$$

$$= 0.0702 \times 10^3 \text{ KN-mm}$$

Step 5: Calculation of equivalent torsional moment

For gradually loaded rotating shaft

$$K_b = 1.5 \text{ and } K_t = 1 \dots \text{ V. B. Bhandari Pg. No.334}$$

Thus the equivalent torque is

$$T_e = \sqrt{[(K_b \times M)^2 + (K_t \times T)^2]}$$

$$= 86.26 \text{ kN-mm}$$

Step 6: Verification of safety of shaft

The allowable torsional stress is given as

$$\begin{aligned}\tau_{\text{all}} &= \frac{16T_e}{\pi d^3} \\ &= 10.24 \text{ N/mm}^2 > 85.5\end{aligned}$$

Therefore design is safe.

3. Design of key

Step 1: Selection of material

C50 is selected as material for key

$$S_{\text{ut}} = 520 \text{ N/mm}^2$$

$$S_{\text{yt}} = 340 \text{ N/mm}^2$$

Step 2: Determination of dimensions of the key

For diameter of 35mm, the dimensions of keys are 10mm × 8 mm. [8]

Step 3: Permissible compressive and shear stresses

$$\begin{aligned}\sigma_c &= \frac{S_{yc}}{f_s} \\ &= 340/3 \\ &= 113.33 \text{ N/mm}^2\end{aligned}$$

According to maximum shear stress theory of failure,

$$\begin{aligned}S_{sy} &= 0.5 S_{yt} \\ &= 0.5 \times 340 \\ &= 170 \text{ N/mm}^2\end{aligned}$$

$$\begin{aligned}\tau &= \frac{S_{sy}}{f_s} \\ &= 170/3 \\ &= 56.67 \text{ N/mm}^2\end{aligned}$$

Step 4: Determination of induced compressive and shear stress

$$\begin{aligned}\sigma_c &= \frac{4 \cdot T}{d \cdot h \cdot l} \\ &= \frac{4 \cdot 70.2 \cdot 1000}{35 \cdot 8 \cdot 30} \\ &= 33.42 \text{ N/mm}^2 < 113.33 \text{ N/mm}^2\end{aligned}$$

$$\begin{aligned}\tau &= \frac{2 \cdot T}{d \cdot b \cdot l} \\ &= \frac{2 \cdot 70.2 \cdot 1000}{35 \cdot 10 \cdot 30} \\ &= 13.37 \text{ N/mm}^2 < 56.67 \text{ N/mm}^2\end{aligned}$$

Hence, the design of key is safe.

4. Design of Bearings:

Procedure for selection of bearing from manufacturing catalogue

Step 1:

Calculate i) radial (f_r) and axial forces (f_a) acting on the bearings

ii) Diameter of shaft (d)

iii) Speed of shaft (n)

Step 2:

Select the type of bearing for the given application.

Step 3:

Calculate the values of X and Y, the radial and thrust factors, from the catalogue. These values depend upon ratios, (f_a/f_r) and (f_a/C_0). The selection therefore, done by trial and error method.

To begin with, a bearing of light series, such as 60, is selected for the given diameter of the shaft and the values of C_0 is found from the catalogue.

Step 4:

Calculate the equivalent dynamic load from the equation.

$$P = X \times f_r + Y \times f_a$$

Step 5:

Make a decision about the expected bearing life and express the life L_{10} in million revolutions.

$$L_{10} = \frac{60 \times n \times L_{10h}}{10^6}$$

$$L_{10} = \frac{60 \times 10 \times 30000}{10^6}$$

$$= 18 \text{ millions}$$

Step 6:

$$C = P \times (L_{10})^{1/a}$$

$$a = 3 \text{ (ball bearing)}$$

$$C = 360.49 \times (18)^{1/3}$$

$$= 944.7525 \text{ N}$$

$$C_r = 19613.3$$

$$\text{So, } C_r > C$$

So selected bearing is safe

Step 7:

Referring the SKF manufacturing catalogue the selected bearing no is 6207[6]

Dimensions of the bearing

Inner diameter of shaft = 35mm

Outer diameter of shaft = 72mm

Thickness of bearing =17mm

5. Design of coupling:[7]

The basic procedure for finding out the dimensions of the rigid flange coupling consists of the following steps:

Shaft diameter: Calculate the shaft diameter

Dimensions of flanges: Calculate the dimensions of the flange by the following empirical equations:

$$d_h = 2d$$

$$L_h = 1.5 d$$

$$D = 3 d$$

$$t = .5 d$$

$$t_1 = .25 d$$

$$d_r = 1.5 d$$

$$D_o = (4d + 2t_1)$$

The torsional shear stress in the hub can be calculated by considering it as a hollow shaft subjected to torsional moment M_t .

The inner and outer diameters of the hub are d and d_h respectively. The torsional shear stress in the hub is given by,

$$\tau = \frac{T \times r}{J}$$

$$J = \frac{\pi}{32} (d_h^4 - d^4)$$

$$r = d_h/2$$

Shaft diameter = 35 mm

Dimensions of flange are given by following empirical equations:

$$d_h = 2d = 70\text{mm}$$

$$L_h = 1.5 d = 52.5\text{mm}$$

$$D = 3 d = 105\text{mm}$$

$$t = .5 d = 17.5 \text{ mm}$$

$$t_1 = .25 d = 8.75 \text{ mm}$$

$$d_r = 1.5 d = 52.5 \text{ mm}$$

$$D_o = (4d + 2t_1) = 157.5 \text{ mm}$$

For $d < 40\text{mm}$, $N = 3$

6. Design of hydraulic clampers [8]

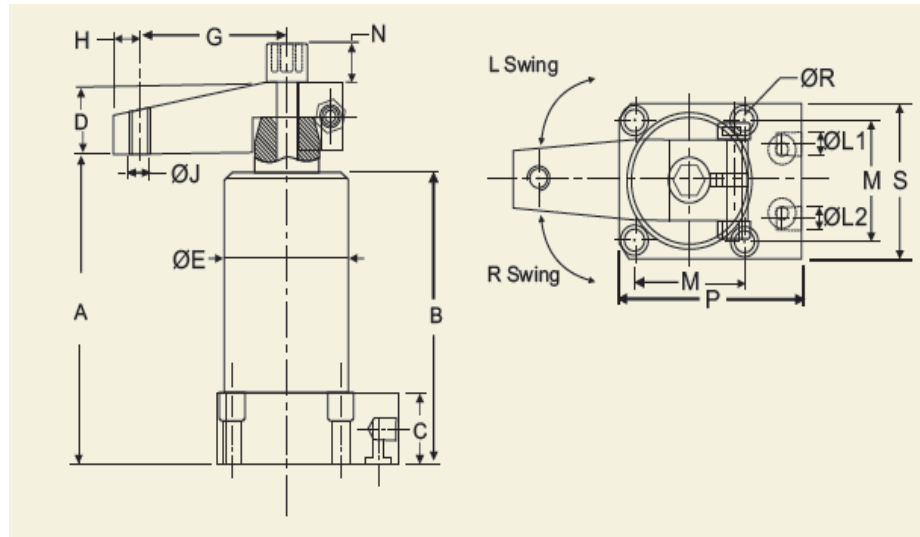


Figure 5. Design of hydraulic clampers

Model	A unclamp position	B	C	D	E	G	H	J	INLETS L1 & L2
030- 92- R/L	126	102	25	25	47.8	45	11	M10	G1/4

M	N	P	R	S	Bore dia.	Swing stroke	Clamping stroke	Clamping force(kg)
42	14.5	70.1	6.9	54	32	10	12	550

Table 3. Clamper Specifications

RESULT TABLE

Sr. No.	Component	Dimensions
1.	Rack and Pinion	Rack 27 30 1001 Pinion 24 35 240
2.	Shaft	φ35mm
3.	Bearing	6207 ID = 35mm OD = 72mm

		Thickness=17mm
4.	Coupling	dh=70mm,Lh=52.5mm D=105mm,t=17.5 mm t1 = 8.75 mm
5.	Stand	15mm

Table 4. Component Specification

ACTUAL MODEL



Figure 6. Self-Centering Mechanism without plate



Figure 7. Self-Centering Mechanism with plate

CONCLUSIONS

1. This automation reduced the human effort and hence don't need a person to adjust the plate for drilling.
2. This design also enabled vibration free operation which increased the quality of drill to the plate.
3. It increased the productivity and reduced the cycle time of 1 hour to 15 minutes.

REFERENCES:

- [1] Shailesh S .Pachbhai, Laukik P. Raut (2014) "A Review on Design of Fixtures" International Journal of Engineering Research and General Science Volume 2, Issue 2, Feb-Mar 2014.
- [2] T. Papastathisa , O. Bakker , S. Ratcheva , A. Popova, Design Methodology for Mechatronic Active Fixtures with Movable Clamps , 45th CIRP Conference on Manufacturing Systems 2012
- [3] Chetankumar M. Patel, Dr. G. D Acharya, Design and manufacturing of 8 cylinder hydraulic fixture for boring yoke on VMC – 1050, 2nd International Conference on Innovations in Automation and Mechatronics Engineering, ICIAME 2014
- [4] Atlanta Rack and pinion drive manufacturer's catalogue
- [5] Tool Fast Work holding Specification Catalogue 2015 for hydraulic clampers
- [6] SKF bearing manufacturer's catalogue
- [7] V. B. Bhandari 'Design of Machine Element' Tata McGraw-Hill Education, 2010 - Machine design
- [8] Tool Fast Work holding Specification Catalogue 2015 for hydraulic clampers

STRUCTURAL STATIC ANALYSIS OF KNUCKLE JOINT

Sangamesh B. Herakal, Ranganath Avadhani, Dr.S.Chakradhar Goud

Asst.Prof Dept. of Mechanical Engineering, Holy Mary Institute of Technology and Science, sachin.herakal@gmail.com, 7842915795

Abstract— The rapid growth of technology in recent decades has led to the reduction of cost and weight of materials. The aim of the present paper is to study calculate the stresses in Knuckle joint using analytical method. Further study in this direction can made by using various directions of the pin and the capacity to withstand load. The present work is concentrating on which type of meshing is preferable for components. Here knuckle joint is modeled by making use of catia, later on that model is imported in Hypermesh and carried out both mesh those are hexahedral and tetra mesh. This model is solved by using Abacus software. The FEA results are compared with analytical results.

Keywords— Knuckle joint, FEA, hexahedral, tetrahedral, abaqus, hypermesh, axial load.

INTRODUCTION

A Knuckle joint is used to connect two rods under tensile load. This joint permits angular misalignment of the rods and may take compressive load if it is guided. These joints are used for different types of connections i.e. tie rods, tension links in bridge structure. In this, one of the rods as an eye at the rod end and other end is forked with eyes at the both the legs. A pin (knuckle pin) is inserted through the rod-end and fork end eyes and is secured by collar and a split pin. Normally, empirical relations are available to find different dimensions of the joint and they are safe from design point of view. The proportions are given in the figure.

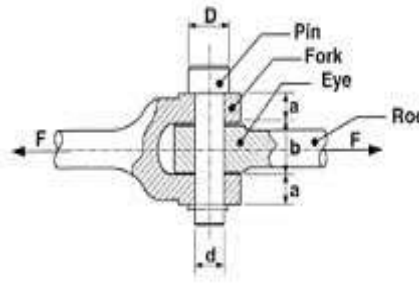


Fig 1 2D model of knuckle joint

MAJOR COMPONENTS OF KNUCKLE JOINTS:

- Single eye end
- Double eye end
- Knuckle pin
- Collar
- Taper pin / Split pin

GEOMETRIC MODELING

Early cad systems were basically automated drafting board systems which displayed a two dimensional representation of the object being designed. Operations could use these graphics systems to develop the line drawing the way they wanted it and then obtain a very high quality paper plot of the drawing. By using these systems, the drafting process could be accomplished in less time, and the productivity of the designers could be improved. Although they were able to reproduce high quality engineering drawing efficiently and quickly, these systems stored in their data files a two dimensional record of the drawing. The drawing usually of three-dimensional objects and it was left to the human being who read these drawing to interpret the three dimensional shape from the two dimensional representation. The major drawback of the early CAD systems was that they were not capable of interpreting the three dimensionality of the object.

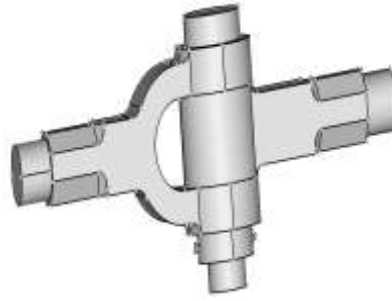
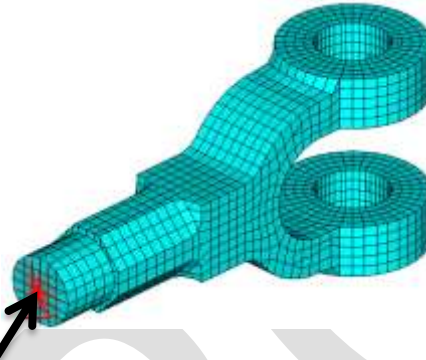
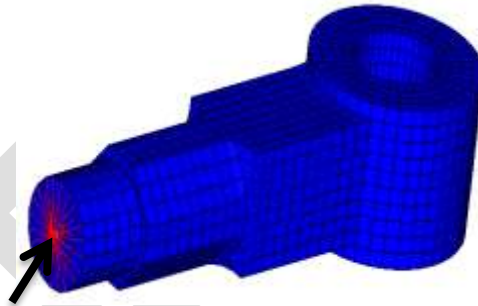


Fig 2. 3D model of knuckle joint

BOUNDARY CONDITION



Knuckle joint is hinged by the end surface of fork.



Tension force is applied on the end surface of eye

Table 1: Dimensions of knuckle joint

Sl no.	Parameters	Values
1	Diameter of rod	30mm
2	Diameter of pin	30mm
3	Diameter of pin head and collar	60mm
4	Thickness of eye	45mm
5	Thickness of fork	35mm
6	Thickness of eye end	36mm
7	Thickness of fork end	45mm
8	Thickness of collar	22.5mm
9	Thickness of pin head	15mm

Table 2: Material properties for steel

Mechanical property	Value	Unit
Density	7850	Kg/m ³
Coefficient of thermal expansion	1.7e ⁻⁰⁰⁵	
Specific heat	480	J/Kg/C
Thermal conductivity	15.1	W/m/C
Resistivity	7.7e ⁻⁰⁰⁷	Ohm
Compressive yield strength	2.07e008	Pa
Tensile yield strength	2.07e008	Pa
Tensile ultimate strength	5.86e ⁰⁰⁸	Pa
Reference Temperature	22	C
Young's modulus	21000	Pa
Poisson's ratio	0.31	
Bulk modulus	1.693e ⁰¹¹	Pa

RESULTS AND DISCUSSION

A.Stress values of Hex mesh

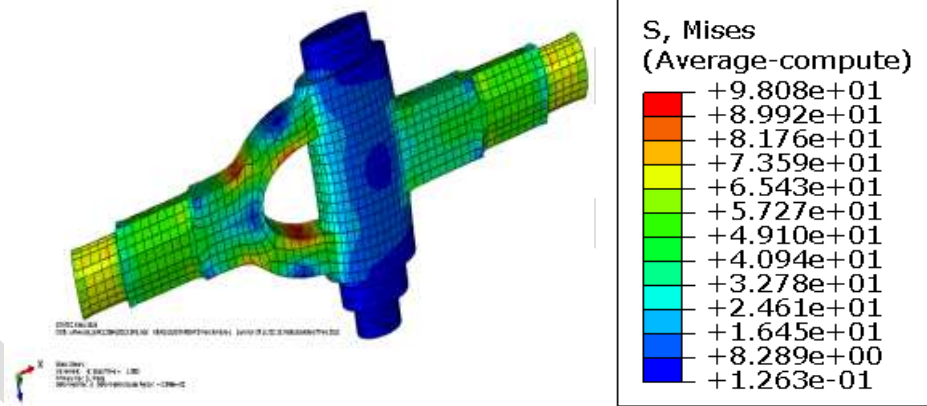


Fig 3: Stress values of hex mesh

B.Stress values for tetra mesh

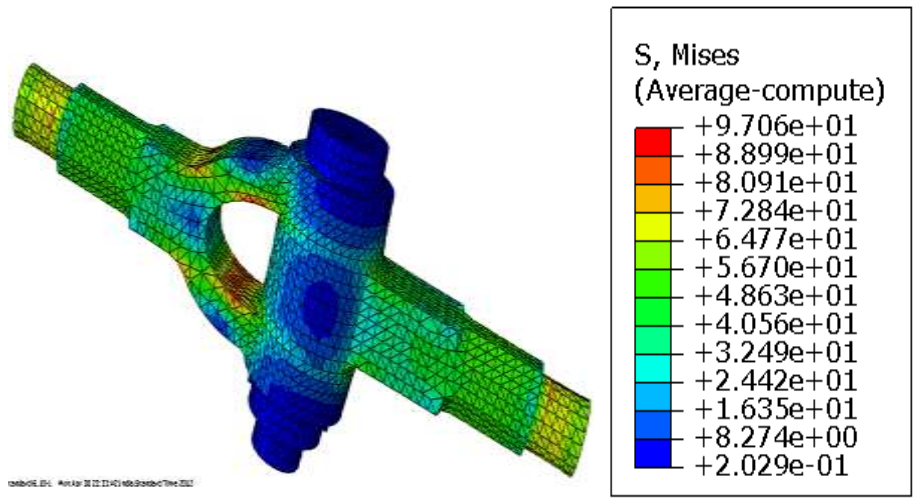


Fig 4: Stress values for tetra mesh

C.Strain values for hex mesh

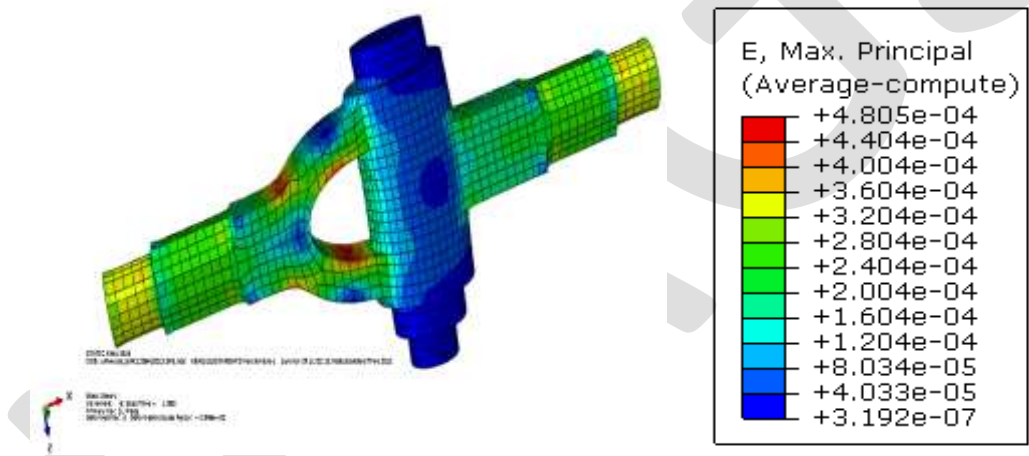


Fig 5: Strain values for hex mesh

D.Strain values for tetra mesh

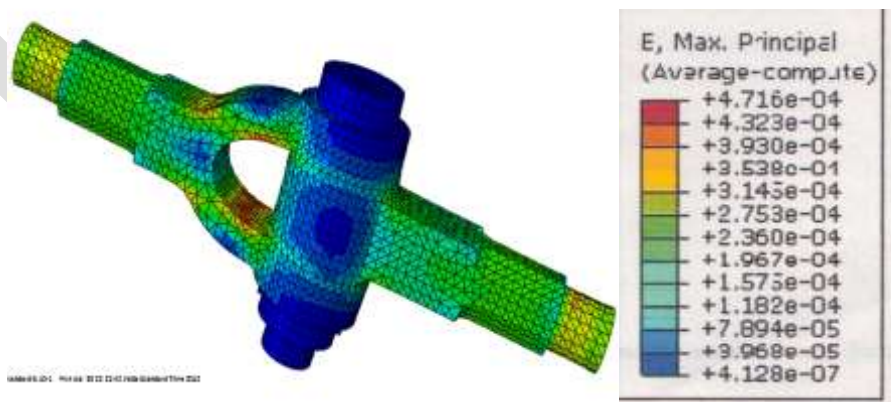


Fig 6: Strain values for tetra mesh

ANALYTICAL RESULTS

Theoretical calculation for maximum stress

Let, applied load=50kn

But the fork is considered as plate which is subjected to abrupt changes in cross sectional area therefore stress concentration factor should be required to determine max stress.

We know that,

$$K_t = \frac{\sigma_{max}}{\sigma_{nom}} \quad (1)$$

K=stress concentration factor.

σ_{max} = maximum stress

σ_{nom} = nominal stress

$$\sigma_{nom} = \frac{\text{force}}{\text{area}} \quad (2)$$

$$\begin{aligned} \text{Area} &= (w-d) \times h \\ &= (90-36) \times 35 \\ &= 1890 \text{mm}^2 \end{aligned}$$

$$\text{Therefore } \sigma_{nom} = \frac{50,000}{1890} = 26.45 \text{ N/mm}^2$$

Also we have that, fork is subjected to abrupt changes in two major sections and hence we get

$$K_t = (K_1 + K_2)$$

K₁=stress concentration factor for plate with hole

$$\text{i.e.} = 2.23 \text{ for } \frac{d}{w} = \frac{36}{90}$$

From DDHB V1 by Dr.LINGAIAH

K₂=stress concentration factor for filleted flat bar in tension

$$\text{i.e.} = 1.6 \text{ for } \frac{r}{d} = 0.28 \text{ and } \frac{w}{d} = 2.5$$

$$K_t = (2.23 + 1.65) = 3.88$$

$$\sigma_{max} = K_t \times \sigma_{nom}$$

$$= 3.88 \times 26.45$$

$$\sigma_{max} = 102.6 \text{ N/mm}^2$$

Theoretical calculation for maximum stress

$$\text{Youngs modules}(E) = \frac{\text{stress}}{\text{strain}}$$

$$\mu = \frac{\sigma}{E}$$

$$= (102.6/210000)$$

$$\text{Strain} = 4.84 \times 10^{-4}$$

Table 3: Comparison of stress values as measured by theoretical in component and as predicted using the finite element analysis for hex & tetra mesh on knuckle joint

S.no	Types of mesh	The,value	Exp,value	%Error
1.	HEX	102.6N/mm ²	98.08	4.41%
2.	TETRA	102.6Nmm ²	97.06	5.39%

Table 4: Comparison of strain values as measured by theoretical in component and as predicted using the finite element analysis for hex & tetra mesh on knuckle joint

S.NO	Types of mesh	The, value	Exp, value	%Error
1.	HEX	4.88×10^{-4}	4.80×10^{-4}	1.64%
2.	TETRA	4.88×10^{-4}	4.71×10^{-4}	3.48%

CONCLUSIONS

Fork is analyzed for stress for the tensile load 50kn for the both mesh viz hex and tetra mesh and compared with theoretical value.

1. The conclusion is drawn from work are as follows:
2. The results show that the fork takes higher stress and eye takes less stress under loading condition.
3. The induced stress in the fork is higher than allowable stress hence the design is out of safe for that diameter of rod of knuckle joint needed to be varied.
4. The error between theoretical value and hex meshed analyzed value has less than that of between theoretical and tetra meshed analyzed value and hence hex mesh is better than the tetra mesh.

REFERENCES:

- [1] Dominick Rosato and Donald Rosato, *Plastics Engineered Product Design*, ELSEVIER
- [2] R.J. Crawford, BSc, PhD, DSC, FEng, FIMechE, FIM_Butterworth Heinemann. *PLASTICS ENGINEERING_ Third Edition_*
- [3] K.I.Narayan, P, kannaiyah, K.Venkata reddy, *Machine drawing*
- [4] H. Gradin Jr. Macmillan, New York, Xvi + 528pp, 1986, *Fundamental of FEM*,
- [5] Irvin L. Rubin (1990). *Dry-as Molded/Moisturized*, Adapted from: *Handbook of Plastic Materials and Technology*
- [6] SAE J328 Revised 1994: *knuckle joint of car and truck performance requirements and test procedures*.
- [7] Khurmi R.S., (2007), *Machine design*, S Chand Publishers, Delhi.
- [8] Stuart B. H.: *Tribological studies of composite material*. *Tribology International*, 31, 647-651(1998).
- [9] Yijun Liiu., *Introduction to the finite element method*.
- [10] *Mechanical and structural properties of Ductile Cast Iron-* M.A.Kenaawy, A.M. Abdel Fattah, N. Okasha and M.EL-Gazery, *Egypt. Sol*, vol. (24), No. (2), 2001
- [11] Rajeev Sakunthala Rajendran, Subash Sudalaimuthu and Mohamed Sixth "Knuckle Development Process with the Help of Optimization Techniques" *Altair Technology Conference, India,2013*

[12] S. Kilian, U. Zander, F.E. Talke “Suspension modeling and optimization using finite element analysis” Tribology International 36 (2003) 317–324

[13] Sonia Calvel and Marcel Mongeau “Black-box structural optimization of a mechanical component “Computers & Industrial Engineering 53 (2007) 514–530.

IJERGS

Comparative study of Image processing techniques used for Scene text detection and extraction

Akhilesh Panchal, Shrugal Varde, Dr.Prof.M.S.Panse

V.J.T.I. Mumbai, akhileshp31@gmail.com

Abstract— In recent years, wide variety of research has been done on Text detection and Extraction from Scene images. These techniques are used for large number of applications like aid for visually impaired people, Document analysis, Vehicle license plate recognition, etc. Text Extraction plays a major role in finding vital and valuable information from captured image. With rapid development in Multimedia Technology and growing requirement for information, identification, indexing and retrieval, several image processing techniques have been developed for extracting text. Each technique has its pros and cons depending on various conditions like Speed, Accuracy, Complexity, Processing time, etc. Hence, only single method is insufficient for overall text detection and extraction system. To achieve better performance, it is necessary to combine these techniques. So, we need to have adequate knowledge of various techniques proposed worldwide. On this background, this article discusses various schemes proposed earlier for extracting the text from an image. This paper also provides the performance comparison of several existing methods proposed by researchers in extracting the text from an image.

Keywords— Text detection, Image Enhancement, Image Preprocessing, Localization, Text extraction, Text Recognition.

I. INTRODUCTION

Text data is particularly interesting, because text describes the contents of an image. Text embedded in images is mainly classified as Caption/Artificial text and Scene/Natural text [9]. Caption text is laid over the image during editing e.g. score of match whereas Scene text is actual part of the scene e.g. street signs, name plates. The problem of Text detection in printed document has been focused for many years and has already reached high recognition rates made it the most successful applications of Compute vision and Machine learning techniques. However, characters recognition from scene images is still a challenging task due to complex background, non-uniform lighting condition, font size, styles, perspective distortion multilingual environment or blurring effects of natural images and active subject for many researchers nowadays [6] [9]. Hence, this paper focuses on extraction of text from Scene image. In order to overcome these problems in scene images, many preprocessing, image enhancement and extraction techniques are proposed and they are used in particular conditions. So, it is essential to study these techniques for employing simple, robust, high performance and cost effective system for Scene text recognition. To achieve this goal, current paper surveys most of the image processing techniques used for text detection and extraction in Scene images. The purpose of the survey is to compare text extraction techniques for selecting proper technique according to applications and conditions.

II. BACKGROUND

Typically, Text extraction consists of various steps like Preprocessing, Text detection, Localization, Binarization and Thresholding, Extraction, Enhancement and Recognition. Order may vary according to application and convenience. The methods cited in this paper are based on morphological operators, wavelet transform, Feature Learning algorithm, artificial neural network, edge detection algorithm, histogram technique etc.

Earlier methods consider only 2-D image or B&W image but nowadays 3-D or Color images are also taken into consideration. They used mainly the image datasets such as ICDAR competitions and Chars 74k for experimentation which is shown in figure 1. Software used for simulation in most of the researches is MATLAB as it is simple to use and easily available image processing tool. It has various inbuilt commands for image processing. Also, Mathscript built on MATLAB can be used on different platforms. Lots of research work has been done to improve accuracy and performance of text extracting techniques. Recently, researchers have explored approaches that prove effective for text captured in various configurations, in particular, incidental text in complex backgrounds. Such approaches typically stem from advanced machine learning and



Figure 1: Examples of Scene images

unsupervised feature learning ,convolutional neural networks (CNN), deformable part-based models (DPMs) , belief propagation and conditional random fields (CRF) [10] [14].

III. LITERATURE SURVEY

For convenience, we break the system into three stages: 1. Pre-processing stage 2. Processing stage 3. Post processing stage. Pre-processing stage use some enhancement algorithms to eliminate challenges created by noise, blurring effect and uneven lighting whereas Processing stage includes Text Detection, Extraction, Segmentation and Localization which uses sophisticated methods. Third stage is Text recognition stage which is applied after processing stage.

A) IMAGE ENHANCEMENT / PREPROCESSING

Before proceeding to text detection and extraction methods used, we have to first consider Scene image can be mixed with noise like Salt and pepper noise, Impulse noise etc. or it can be blurred due motion of camera. For that purpose, we should use some image preprocessing/enhancement Techniques. De-blurring techniques like Lucy Richardson algorithm, Blind de-convolution algorithm, Wiener de blurring techniques are generally used [17]. Out of them, Wiener filter is selected which is a natural extension of the inverse filter when noises are present. Figure 2 illustrates how de-blurring is achieved using Wiener filter on MATLAB. From figure, it is observed that binarization after wiener filtering produces better result which will be effective for further processing.



Figure 2: De-blurring of an image using Wiener filter. (a) Blurred image; (b) Binarized image without filtering; (c) Binarization after De-blurring

Salt and pepper noise is one type of impulse noise which can corrupt the image, where the noisy pixels can take only the maximum and minimum values in the dynamic range i.e. black dot on white background (pepper) and white dot on black background (salt) which degrades the text extraction performance of system [19]. Since, linear filtering techniques are not effective, standard median filter (SMF), which is a non-linear filter used to remove such noise due to its good denoising power and computational efficiency. However, when noise level is more than 50%, edge details of the original image will not be preserved by the median filter as shown in Figure 3. So, It is recommended that during the filtering (restoration) process the edge details have to be preserved without losing the high frequency components of the image edges.

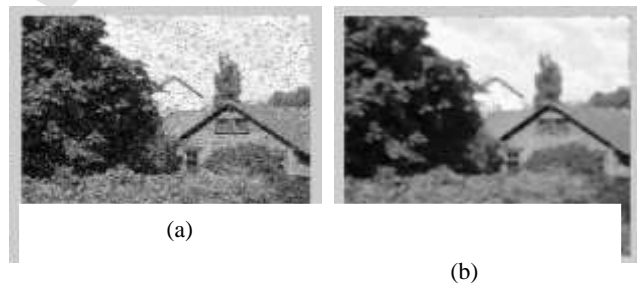


Figure 3: Salt and pepper noise removal using Median

Sometimes, image is captured in dark or uneven lighting for which Text extraction becomes difficult. So, application of contrast enhancement is necessary. Histogram Equalization method is mostly used for Contrast enhancement. Figure 4 shows how contrast enhancement done using Histogram Equalization. Hence, this leads to overcome Uneven lighting, Blurring and noise degradation problems which would adversely affect system performance.



Figure 4: Contrast Enhancement using Histogram equalization.

B) PROCESSING STAGE:

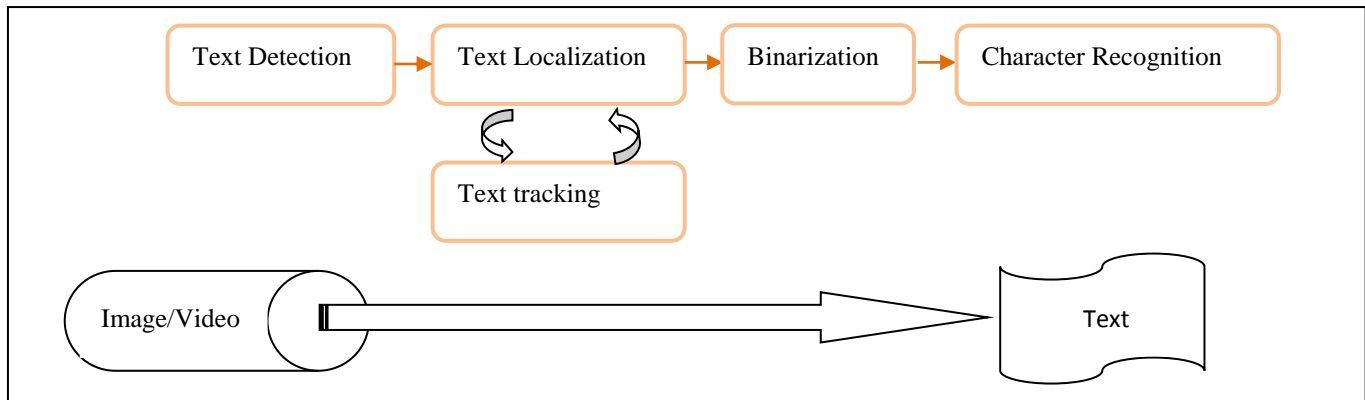


Figure 5: Architecture of Text Detection & recognition System

Text Detection phase takes enhanced image or video frame as input and decides it contains text or not. It also identifies the text regions in an image whereas *Text Localization* merges the text regions to formulate the text objects and define the tight bounds around the text objects. Figure 5 shows Architecture of Processing stage. Text detection, localization and tracking modules are closely related to each other and it is the most challenging and difficult part of extraction process as it feeds to character recognition system [11].

Text Tracking: This phase is applied to video data only. For the readability purpose, text embedded in the video appears in more than thirty consecutive frames. This phase exploits temporal occurrences of the same text object in multiple consecutive frames. It can be used to rectify the results of text detection and localization stage. It is also used to speed up the text extraction process by not applying the binarization and recognition step to every detected object [11].

Text Binarization: This step is a part of image segmentation, used to segment the text object from the background in the bounded text objects. The output of text binarization is the binary image, where text pixels and background pixels appear in two different binary levels like white text on dark background or vice versa. Many times Binarization can be applied before localization step.

For Text Detection, connected component analysis (CCA) and sliding window classification are two widely used methods, and color, edges, strokes, and texture are typically used as features [10]. CCA which is a graph algorithm, where subsets of connected components are uniquely labeled based on heuristics about features, i.e. color similarity and spatial layout. The use of statistical models in CCA significantly improves its adaptivity. In the sliding window classification method, multi-scale image windows that are classified into positives are further grouped into text regions with morphological operations, CRF [13] or graph methods. For text localization, color, edge and texture features were conventionally used, and stroke, point, region and character appearance features have recently been explored [10]. M. Swamy Das et.al [8] provides detail analysis of detection techniques such as Connected component based, edge based and Texture based method. From this article, it is observed that Texture based method is more efficient compared to that of the performance obtained with edge based method and connected component based method. But for better performance it is always advisable to combine this techniques.

C) POST PROCESSING STAGE:

Character Recognition: The last stage is the character recognition. This module converts the binary text object into the ASCII text. There are various sophisticated tools already developed which are used for recognition like OCR, Snooper text [22] etc. Figure 6 shows how 'hello' word wrapped in image gets recognized through Text Extraction process.

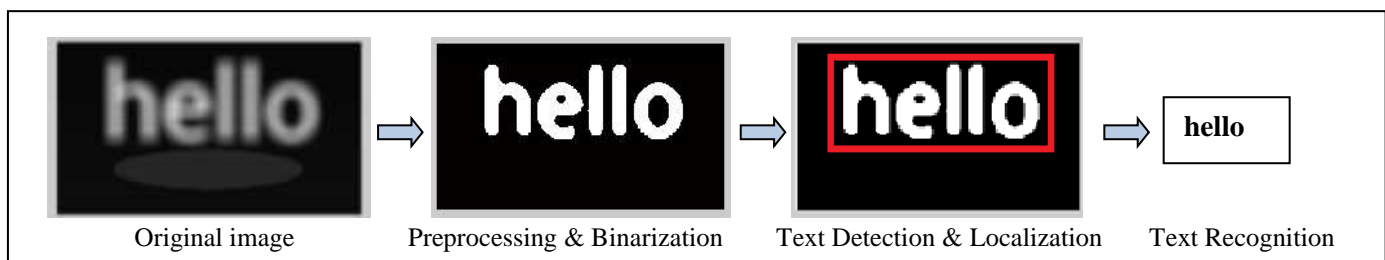


Figure 6: Text Extraction process on image

IV. ANALYSIS

The performance of each algorithm mostly evaluated based on parameters like precision rate, recall rate, average run time etc. The Precision and recall rates are calculated as

$$\text{Precision} = \frac{\text{Correctly detected}}{\text{Correctly detected} + \text{False positives}} \times 100\% \quad \text{Recall} = \frac{\text{Correctly detected}}{\text{Correctly detected} + \text{False negatives}} \times 100\%$$

Where, False positives are the non-text regions in the image and have been detected by the algorithm as text regions and False negatives are the text regions in the image and have not been detected by the algorithm [8]. Both precision and recall rates are useful to determine the accuracy of each algorithm in eliminating the non-text regions and locating the correct text regions. Higher accuracy and Less run time is preferred for any application which requires text extraction from an image. Performance analysis based on such parameters on some of surveyed papers is given in Table 1 as shown below.

Table 1: Performance Analysis of Text Extraction methods

SR. NO.	AUTHOR	YEAR	METHOD/S USED	ACCURACY	ADVANTAGES	DISADVANTAGES
1.	Wahyono, et.al [27]	2015	Canny edge detector, Fast Stroke Width Transform (FSWT)	61% (Precision), 63% (Recall)	Fast (0.18 sec.) So, it can be used in real time. Also used for Multi Language text detection.	Complex in Design
2.	Hrishav raj, et.al [7]	2014	Binarization, Connected Components (CC), Morphological operations, Canny Edge detection	72.8% (Precision), 74.2% (Recall)	Independent of Font Size, Style and directions.	Trained only for extracting Devanagari Text from image
3.	C.P. Sumathi et.al [4]	2013	Wavelet transformation, Morphological operation, Feature extraction, Neural Network classifier	87.0%	Low fragmentation, low error rate, Tolerance to noise. Works on Video frames	Slow and Complex to design.
4.	Ho Vu, et.al [1]	2012	Feature learning method with Orthogonal matching pursuit for training & sparse coding as a mapping-function.	83.8%	Less affected by the categorization of images	Takes long time while extracting feature vectors.
5.	Huizhong Chen et.al [10]	2011	CC based Edge-enhanced Maximally Stable Extremal Regions (MSER), Stroke width Transform (SWT)	73% (Precision), 60% (Recall)	Simple & efficient, can be combined with visual search systems without further computational load	Detection fails due to excessive blur and out of focus as no preprocessing
6.	Andrej Ikica, et.al[20]	2011	Edge profile based detection with Canny edge map, Heuristic rules	70.9% (Precision), 55.2% (Recall)	Simple, fast and efficient	Sometimes Non Text areas get detected leads to low accuracy.
7.	Huang et.al [25]	2010	Stroke Map, Connected component analysis, Harris Corner Detection	90.2%	Robust to detect and locate video scene text with variation of text size, Good speed	Not suitable in low contrast background
8.	Pan et. al [13]	2009	Combination of CC & region based approach includes Conditional Random Field(CRF) model, Minimum classification error (MCE) learning, Graph cuts inference, Minimum spanning tree	67% (Precision), 71% (Recall)	Robust and accurately Localize texts	Takes More time and Complex

9.	Nobuo Ezaki et.al [18]	2004	Sobel edge detection, Otsu binarization, connected-component extraction, rule-based connected-component selection	48% (Precision), 76% (Recall)	Easy to design, Combination of these methods gives good overall performance	Low detection accuracy for small text in images
10.	Gllavata et.al [5]	2003	Color reduction technique, Edge detection, and localization of text regions using projection profile and geometrical properties	83.9% (Precision), 88.7% (Recall)	Works well in Grayscale as well as Color image.	Low quality images makes detection complex.

V. CONCLUSION

This paper covers detail analysis of the text detection, localization and tracking techniques. After comparison study of recent researches on Text extraction in scene images, it is observed that each proposed method has its own advantages depending on various conditions which are mentioned before. Some papers have modified the techniques while some invent new techniques. It is necessary to first preprocess the image before applying Text Extraction algorithms cause it can produce false detection and hence less accuracy. Accuracy and speed are important factors while considering performance and there is trade-off between two factors. So, keeping this in mind proper technique should be selected.

Recent methods developed using neural network, Fuzzy logic, DCT, Wavelet transforms are complex but produce good results rather than conventional methods. Connected component based, Edge detection based methods are comparatively easy to develop but are less accurate than modern techniques. Hence, to achieve good performance, System needs to be design by combining these techniques as per user's requirement.

REFERENCES:

- [1] Ho Vu, Duongl and Quoc Ngoc, 'A Feature Learning Method for Scene Text Recognition', *IEEE International Symposium on Signal Processing and Information Technology (ISSPIT)*, pp. 176 - 180, 2012.
- [2] Jun Ohya, Akio Shio, and Shigeru Akamatsu, 'Recognizing Characters in Scene Images', *IEEE Transactions on Pattern Analysis And Machine Intelligence*. Vol. 16, No. 2, February 1994.
- [3] Linlin Li, Chew Lim Tan, 'Character Recognition under Severe Perspective Distortion', *IEEE 19th International Conference on Pattern Recognition(ICPR)*, pp.1-4, 2008.
- [4] C.P. Sumathi, N. Priya, 'Analysis of an Automatic Text Content Extraction Approach in Noisy Video Images', *International Journal of Computer Applications (0975 – 8887) Volume 69– No.4, May 2013*
- [5] Julinda Gllavata, Ralph Ewerth and Bemd Freisleben, 'A Robust Algorithm for Text Detection in Images', *IEEE Proceedings of the 3rd International Symposium on Image and Signal Processing and Analysis (ISPA)*, Volume 2, pp.611 – 616, 2003.
- [6] Roberto Manduchi and James Coughlan, 'Computer Vision Without Sight', *Communications of the ACM*, Vol.55, no.1, January 2012.
- [7] Hrishav raj, Rajib Ghosh, 'Devanagari Text Extraction from Natural Scene Images', *IEEE International Conference on Advances in Computing, Communications and Informatics (ICACCI)*, pp.513-517, 2014.
- [8] M. Swamy Das, B. Hima Bindhu, A. Govardhan, 'Evaluation of Text Detection and Localization Methods in Natural Images', *International Journal of Emerging Technology and Advanced Engineering*, ISSN 2250-2459, Volume 2, Issue 6, pp.277-282, 2012.
- [9] Qixiang Ye and David Doermann, 'Text Detection and Recognition in Imagery: A Survey', *IEEE Transactions on Pattern Analysis and Machine Intelligence*, Vol.37, No.7, July 2015.
- [10] Huizhong Chen, Sam S. Tsai, Georg Schroth, David M. Chen, Radek Grzeszczuk and Bernd Girod, 'Robust Text Detection In Natural Images with Edge-Enhanced Maximally Stable Extremal Region', *Image Processing (ICIP)*, 18th IEEE conference on Image Processing, 2011.
- [11] G. Gayathri Devi, T. Santhanam and C.P. Sumathi, 'A Survey On Various Approaches of Text Extraction in Images', *International Journal of Computer Science & Engineering Survey (IJCSSES) Vol.3, No.4, August 2012*.
- [12] Shyama Prosad Chowdhury, Soumyadeep Dhar, Karen Rafferty, Bhabatosh Chanda, 'Robust Extraction Of Text From Camera Images

- Using Colour And Spatial Information Simultaneously', *Journal Of Universal Computer Science*, Vol. 15, No.18, pp.3325- 3342, 2009.
- [13] Y. Pan, X. Hou, and C. L. Liu, 'Text Localization in Natural Scene Images based on Conditional Random Field', *Proc. IEEE International Conf. Doc. Anal. Recognition*, pp. 6-10, 2009.
- [14] Michael R. Lyu, Jiqiang Song and Min Cai, 'A Comprehensive Method for Multilingual Video Text Detection, Localization, and Extraction', *IEEE Transactions on Circuits And Systems For Video Technology*, Vol. 15, No. 2, pp.243-255, February 2005.
- [15] Ananta Singh, Dishant Khosla, 'Text Localization and Recognition in Real-Time Scene Images', *International Journal of Scientific Engineering and Research (IJSER)*, Volume 3 Issue 5, pp. 123-125, May 2015.
- [16] Adesh Kumar, Pankil Ahuja, Rohit Seth, 'Text Extraction and Recognition from an Image Using Image Processing In Matlab', *Conference on Advances in Communication and Control Systems (CAC2S)*, pp. 429-433, 2013.
- [17] Sonia George, Noopa Jagdeesh , 'A Survey on Text Detection and Recognition from Blurred Images', *International Journal of Advanced Research Trends in Engineering and Technology(IJARTET)*, Vol. II, Special Issue X, pp. 1180-1184, March 2015.
- [18] Nobuo Ezaki, Marius Bulacu, and Lambert Schomaker, 'Text Detection from Natural Scene Images: Towards a System for Visually Impaired Persons', *Proc. of 17th Int. Conf. on Pattern Recognition (ICPR)*, IEEE Computer Society, pp. 683-686, vol. II, 23-26 August, Cambridge, UK, 2004.
- [19] Madhu S. Nair, K. Revathy, and Rao Tataavarti, 'Removal of Salt-and Pepper Noise in Images: A New Decision-Based Algorithm', *Proceedings of the International Multi-Conference of Engineers and Computer Scientists IMECS, Hong Kong, Volume I, March 2008*.
- [20] Andrej Ilic, Peter Peer, 'An improved edge profile based method for text detection in images of natural scenes', *IEEE EUROCON - International Conference on Computer as a Tool (EUROCON)*, pp. 1-4, 2011.
- [21] Lukas Neumann, Jiri Matas, 'Real-Time Scene Text Localization and Recognition', *25th IEEE Conference on Computer Vision and Pattern Recognition, CVPR, Providence, RI, USA, June 16-21, 2012*.
- [22] Rodrigo Minetto, Nicolas Thome, Matthieu Cord, Neucimar J. Leite, Jorge Stolfi, 'Snooper Text: A text detection system for automatic indexing of urban scene', *Computer Vision and Image Understanding*, journal homepage: www.elsevier.com/locate/cviu, 2013.
- [23] Xiaoqian Liu, Weiqiang Wang, "Extracting Captions From Videos Using Temporal Feature", *Proceedings Of The International Conference On Acm Multimedia*, pp.843-846, 2010.
- [24] Liang Wu, Palaiahnakote Shivakumara, Tong Lu, and Chew Lim Tan 'A New Technique for Multi-Oriented Scene Text Line Detection and Tracking in Video', *IEEE Transactions on Multimedia*, Vol. 17, No. 8, pp.1137-1152, August 2015
- [25] Xiaodong Huang, Huadong Ma, 'Automatic Detection and Localization of Natural Scene Text in Video', *International Conference on Pattern Recognition (ICPR 2010)*, IEEE Computer Society, pp.3216-3219, 2010.
- [26] N. Senthilkumaran and R. Rajesh, 'Edge Detection Techniques for Image Segmentation – A Survey of Soft Computing Approaches' *International Journal of Recent Trends in Engineering*, Vol. 1, No. 2, pp.250-254, May 2009.
- [27] Wahyono, Munho Jeong and Kang-Hyun Jo, 'Multi Language Text Detection Using Fast Stroke Width Transform', *IEEE 21st Korea-Japan Joint Workshop on Frontiers of Computer Vision (FCV)*, pp.1-4, 2015.
- [28] Miriam Leon, Veronica Vilaplana, Antoni Gasull, Ferran Marques , 'Caption Text Extraction For Indexing Purposes Using A Hierarchical Region-Based Image Model', *Proceedings Of The 16th IEEE International Conference On Image Processing*, pp.1869-1872, 2009.
- [29] Guowei Yang, Fengchang Xu, 'Research and analysis of Image edge detection algorithm Based on the MATLAB', *Elsevier Ltd., Procedia Engineering 15*, pp.1313-1318, 2011.

A Review on Design, Analysis and Optimization of Plate bending Machine

AkashGurve¹, Vaibhav Bankar²

M Tech Student, Department of Mechanical Engineering ,VIT ,Nagpur.

Ass.Prof, Department of Mechanical Engineering, VIT Nagpur.

adgurve43@gmail.com

vhbankar@gmail.com

Abstract— In these types of presses, press-body is of C Shaped. When free space required from three sides of press table to work for loading and unloading of pressed component then this type of presses are designed. As main cylinder placed eccentric to central axis of press-body, it applies eccentric load on press-body hence heavier press body is required as compared to same capacity of other type of press. These types of presses are also called as single press.

Keywords—Press table,cylinder, Central axis, Press-body, heavier body.

INTRODUCTION

Sheet metal fabrication plays an important role in the metal manufacturing world (Cloutier, 2000). Sheet metal is used in the production of materials ranging from tools, to hinges, automobiles etc. Sheet metal fabrication ranges from deep drawing, stamping, forming, and hydro forming, to high-energy-rate forming (HERF) to create desired shapes (Cloutier, 2000). Fascinating and elegant shapes may be folded from a single plane sheet of material without stretching, tearing or cutting, if one incorporates curved folds into the design (Martin et al., 2008). Shape rolling of sheet metal is the bending continually of the piece along a linear axis.

In Plate bending machine, the force generation, transmission and amplification are achieved using fluid under pressure. The liquid system exhibits the characteristics of a solid and provides a very positive and rigid medium of power transmission and amplification. In a simple application, a smaller piston transfers fluid under high pressure to a cylinder having a larger piston area, thus amplifying the force. There is easy transmissibility of large amount of energy with practically unlimited force amplification. It has also a very low inertia effect.



LITERATURE REVIEW

Muni Prabakaran and V.Amarnath [1] Structural optimization tools and computer simulations have gained the paramount importance in industrial applications as a result of innovative designs, reduced weight and cost effective products. Especially, in aircraft and automobile industries, topology optimization has become an integral part of the product design process. In this project, topology optimization has been applied on various components of scrap baling press and 5Ton hydraulic press using NASTRAN WORKBENCH software. Suitable loads and constraints are applied on the initial design space of the components. An integrated approach has also been developed to verify the structural performance by using NASTRAN software. At the end, shape optimized design model is compared with the actual part that is being manufactured for the press. It is inferred that topology optimization results in a better and innovative product design. In this project, we showed 26.26 percent cost reduction in scrap baling press. And we fabricated 5ton hydraulic press with cost reduction of 24.54 percent.

B.PARTHIBAN1 , P.EAZHUMALI 2 , S.KARTHI 2 , P.KALIMUTHU [2]A hydraulic press is a machine using a hydraulic cylinder to generate a compressive force. Frame and cylinder are the main components of the hydraulic press. In this project press frame and cylinder are designed by the design procedure. Press frame and cylinder are analyzed to improve its performance and quality for press working operation. Structural analysis has become an integral part of the product design. The frame and cylinder are modeled by using modeling software CATIA. Structural analysis has been applied on C frame hydraulic press structure and cylinder by using analysing software NASTRAN. An integrated approach has been developed to verify the structural performance and stress strain distributions are plotted by using NASTRAN software. According to the structural values the dimensions of the frame and cylinder are modified to perform the functions satisfactory.

Ankit H Parmar, Kinnarraj P Zala, Ankit R Patel [3] The goal of structure optimization is to decrease total mass of hydraulic press while assuring adequate stiffness. Structural optimization tools and computer simulations have gained the paramount importance in industrial applications as a result of innovative designs, reduced weight and cost effective products. A method of structure optimization for hydraulic press is proposed in order to reduce mass while assuring adequate stiffness. Key geometric parameters of plates which have relatively larger impacts on mass and stiffness are extracted as design variables. In order to research relationship between stiffness, mass and design variables, common batch file is built by SOLIDWORKS and analysis is done in NASTRAN. Top plate, movable plate and column design and analysis done.

IDENTIFIED GAPS IN THE LITERATURE

In hydraulic press, the force generation, transmission and amplification are achieved using fluid under pressure. The liquid system exhibits the characteristics of a solid and provides a very positive and rigid medium of power transmission and amplification. In a simple application, a smaller piston transfers fluid under high pressure to a cylinder having a larger piston area, thus amplifying the force. There is easy transmissibility of large amount of energy with practically unlimited force amplification. It has also a very low inertia effect. Main objective of project is to modify major component of one cylinder four post hydraulic press so that rigidity and strength of the components are increase by using optimum material. The function of the major component like frame, bottom plate, bed, top box are to absorb forces, to provide precise slide guidance and to support the drive system and other auxiliary units. The structural design of the component depends on the pressing force this determines the required rigidity. The current machine does not have high rigidity and needs to be redesigned.

CONCLUSION

The aim of the project is to modify major component of one cylinder four post hydraulic plate bending machine so that the rigidity and strength of the machine is increased.

REFERENCES:

- [1] Muni Prabakaran and V.Amarnath, "Structural Optimization of 5Ton Hydraulic Press and Scrap Baling Press for Cost Reduction by Topology"International Journal of Modeling and Optimization, Vol. 1, No. 3, Pg-185-190, August 2011
- [2] B.Parthiban, P.Eazumali, S.Karthi, P.Kalimuthu, "Design and analysis of c type hydraulic press structure and cylinder" International Journal Of Research In Aeronautical And Mechanical Engineering, Vol.2 Issue.3, March 2014. Pgs: 47-56.

- [3] Ankit H Parmar, Kinnarraj P Zala, Ankit R Patel, "Design and Modification of Foremost Element of Hydraulic Press Machine" International Journal of Advanced Scientific and Technical Research, Issue 4 volume 3, May-June 2014, ISSN 2249-9954, Pg. 658-667.
- [4] WaqasSaleem, Fan Yuqing, Wang Yunqiao "Application of Topology Optimization and Manufacturing Simulations - A new trend in design of Aircraft components", Proceedings of the International Multi Conference of Engineers and Computer Scientists 2008 Vol II IMECS 2008, 19-21 March, 2008, Hong Kong.
- [5] Smith & Associates, "Hydraulic Presses", 530 Hollywood Drive, Monroe, Michigan 48162-2943, Dec 1999.
- [6] Lars Krog, Alastair Tucker, Gerrit Rollema, "Application of topology, sizing and shape optimization methods to optimal design of aircraft, components", Airbus UK Ltd, Altair Engineering Ltd., 2002.
- [7] Gerd Schuhmacher, Martin Stettner, Rainer Zotemantel, O. Owen Leary, Markus Wagner, "Optimization assisted structural design of a new military transport aircraft", EADS Military Aircraft, Munich, Germany, 2004, [10th AIAA/ISSMO Multidisciplinary Analysis and Optimization Conference, Albany, New York]
- [8] Müller, O; Albers, A; Sauter, J; Allinger, P. "Topology Optimization of Large Real World Structures, NAFEMS World Congress 1999", 26.-28. April 1999, Newport (Rhode Island), USA.
- [9] Malachy Sumaila and Akii Okonigbon Akaehomen Ibhaddode, "Design and Manufacture of a 30-ton Hydraulic Press" Mechanical Engineering Department, Federal University of Technology Yola, Adamawa State, Nigeria, Jan 2011.
- [10] V. D. Lee, "Configuration Development Of A Hydraulic Press For Preloading the Toroidal Field Coils of the Compact Ignition Tokamak", Fusion Engineering Design Center and McDonnell Douglas Astronautics Company, 1998.
- [11] Bambhania, M.P. and Chauhan, H.N. (2013) 'Design & analysis of frame of 63 ton power press machine by using finite element method', Vol.3, pp.285-288.
- [12] Amarnath, V. and Muni prabakaran (2011) 'Structural Optimization of 5Ton Hydraulic Press and Scrap Baling Press for Cost Reduction by Topology', Vol.1, pp.1-6.
- [13] Malachy Sumaila and Akii Okonigbon Akaehomen Ibhaddode. (2011) 'Design and manufacture of a 30-ton hydraulic press', Vol.14, pp.196-200.
- [14] Drake, K.R. Fone, D. and Smith, T.W.P. (2012) 'A simple hydraulic model for the hydrodynamic loading on a heaving horizontal cylinder with a small damage opening at its keel', pp 15-19.
- [15] Bednarek, T. Jakubczak, H. Marczewska, I. Marczewski, A. Rojek, J. and Sosnowski, W. (2006) 'Practical fatigue analysis of hydraulic cylinder and some design recommendations', pp. 1739-1751.
- [16] Fulland, M. Kullmer, G. Richard, H.A and Sander, M. (2008) 'Analysis of fatigue crack propagation in the frame of a hydraulic press', pp. 892-900.

Design and Analysis of M.S Roller in Sheet Metal Rolling Machine

Pramod Vishwakarma¹, Vaibhav Bankar²
M Tech Student, Department of Mechanical Engineering, VIT, Nagpur.
Assist.Prof, Department of Mechanical Engineering, VIT Nagpur.
pramodvishwakarma201@gmail.com

yhbankar@gmail.com

Abstract-Sheet metal rolling machine is a process of turning the flat sheet metal of appropriate length into a desired curvature as the manufacturer wants or into a complete hollow cylinder. This metal rolling machine is used largely in industry of pharmaceutical machine manufacturing company. Rolling machine has an application in manufacturing of heat exchanger, pressure vessel, octagonal blender etc. The metal sheet is fed continuously between upper lower and two lower roller. The lower roller revolve freely in the circular hole at the both support end. The upper roller is an adjustable roller which slide upward and downward direction normal to the roller. In this project, the objective is to analyse the contact stress analysis on the end support of the rolling machine and the lifting force on handle of the rolling machine which result in slip due to the crushing stress.

Keyword - Contact stress, Crushing stress, Metal Rolling, Support end, Improved Strength, Reduce maintenance cost.

1. INTRODUCTION

Three roller sheet metal rolling machine is a process of converting metal sheet of varying thickness into curve sheet at required circumference or into complete hollow cylinder at required radius. The factors on which the sheet metal rolling machine is designed includes maximum thickness of sheet to be used, minimum and maximum diameter of hollow sheet cylinder which the company want from rolling machine,

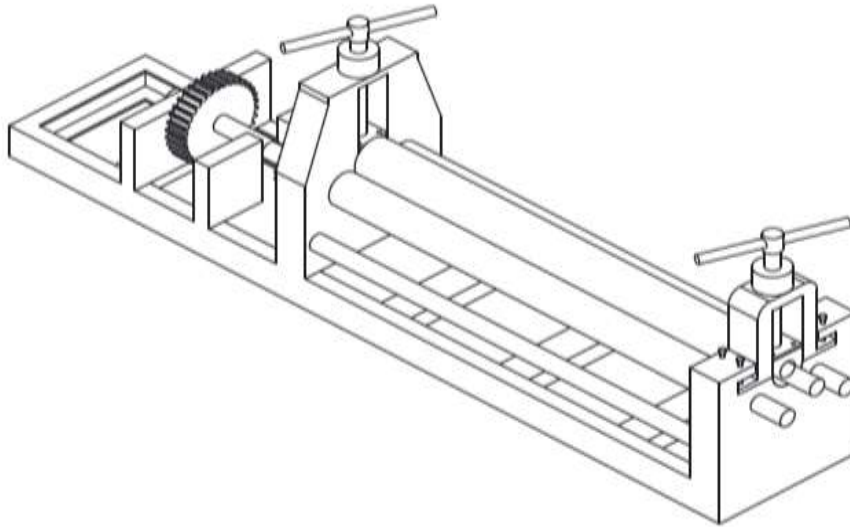
The sheet metal rolling machine include several component:-

Base- The base on the sheet metal rolling machine is formed by used standard channel of 80X100 on which the entire weight of the metal rolling machine is acted.

Roller:-The metal rolling machine has two lower roller and one upper roller between which the sheet metal is feeded. The material of the roller used in mild steel

Support end:-The rolling has two a support end on both side of the roller. One support has a single complete assembly and the other end can be splitted into two. The upper half support end can be removed completely so that the after the end of metal rolling process the hollow cylindrical sheet can be removed. The material of the support end is mild steel.

Manually operated handle:- The handle of the roller carries the upper roller such that its can be moved up and down normal to the roller so that sheet feeding between upper and lower lower roller can be done. V- threaded handle is used.



when the metal sheet is feed into the roller this causes vertical upward force acting on upward roller. This load causes a crushing stress in the teeth of the v-threaded handle. The upper and lower rollers have a support at both the ends, when the sheet passes between the rollers the support of rollers causes a frictional wear. Wear in friction material result in eccentric motion of in rolling shaft. The more the wear, the lead to dissatisfaction and disturbance in the company manufacturing process who need to send the machine for maintenance.

2. LITERATURE REVIEW

Ahmed Ktari:-In his paper he has done Modeling and computation of the three-roller bending process of steel sheets. This experiment consists of two-dimensional finite element model of this process was built under the Abaqus /Explicit environment based on the solution of several key techniques, such as contact boundary condition treatment, material property definition, meshing technique, and so on.

Jong GyeShin:-In their paper he has done the experiment on Mechanics-Based Determination of the Center Roller Displacement in Three-Roll Bending for Smoothly Curved Rectangular Plates. The objective of this paper is to develop a logical procedure to determine the center roller displacement, in the three-roll bending process, which is required in the fabrication of curved rectangular plates with a desired curvature.

M K Chudasama:-In their paper he has done the experiment on Analytical Model for Prediction of Force during 3-Roller Multi-pass Conical Bending. In this paper, the total deflection of the top roller required is divided in steps to get the multi pass bending

M. B. Bassett, and W. Johnson :-In their paper, The bending of plate using a three roll pyramid type plate bending machine, J. strain Analysis Process manual, maintenance manual, machine capacity chart and technical specification of rolling machine, M/s Larsen & Toubro Ltd, Hazira, Surat, India.

Dr. C. C. Handa et. al :-This paper gives a review and Discussed about the productivity analysis of manually and power operated sheet bending machine considering time required to complete one pipe, total expenditure required to manufacture one pipe, number of operators and labors required during both operations, etc. Limitations of the manually operated sheet bending process over power operated sheet bending machine is also discussed.

P.G. Mehar:- In his M. Tech Thesis studied the manually operated and power operated sheet bending machine. Experimentations were conducted on sheet in order to measure actual no. of passes, time required to complete bending process etc. Also, productivity of sheet bending process is analyzed in depth. Design of various components of power operated sheet bending machine considering various theories of failure in elastic region and values for bending force, power required, spring back radius etc. for different diameters, thicknesses and width of sheet metal has been determined.

3. IDENTIFIED GAPS IN THE LITERATURE

Normal practice of the roller bending still heavily depends upon the experience and skill of the operator, so the aim of this project, the objective is to analyse the frictional wear on the end support of the roller and the lifting force on handle of the rolling machine which result in slip due to bending force.

4. PROBLEM FORMULATION

- To study & simulate the frictional wear on the support of rolling shaft and thread of handle.
- To compare static contact stress on various conditions.
- To suggest the new material and change of thread design to overcome existing problem.
- Fabrication of the change in design with minimum costing.

5. CONCLUSION

The new change in the design will reduce the crushing stress in the handle of the rolling machine on which the upper roller is mounted. The addition in the change of material will reduce the contact stress in the support end where the roller rolls which result in frictional wear. Thus, the rolling machine will have a less maintenance which will directly reduce the maintenance cost.

REFERENCES:

- [1] Mr. Nitin P. Padghan, "Force Analysis of Metal Sheet in Bending Operation on Sheet Bending Machine"
- [2] Himanshu V. Gajjar, Anish H. Gandhi, Tanvir A Jafri, and Harit K. Raval "Bendability Analysis for Bending of C-Mn Steel Plates on Heavy Duty 3-Roller Bending Machine"
- [3] Y. H. Lin, M. Hua, "Mechanical analysis of edge bending mode for four-roll plate bending process", Computational Mechanics, Springer-Verlag 1999, pp 396-407
- [4] P. S. Thakare¹, P. G. Mehar, "PRODUCTIVITY ANALYSIS OF MANUALLY OPERATED AND POWER OPERATED SHEET BENDING MACHINE : A COMPARATIVE STUDY"
- [5] K. L. Elkins, R. H. Sturges, "Spring back analysis in Air bending", Tran, ASME, J. Manufacturing science and engineering, 121, Nov. 1999, PP. 679-688
- [6] Aniruddha Kulkarni Mangesh Pawa "SHEET METAL BENDING MACHINE" VOLUME 2, ISSUE 3, March.-2015
- [7] Jong Gye Shin, Tac Joon Park & Hyunjune Yim — Roll Bending, Tran, ASME, J. Mechanical Design, 123 May 2001, PP 284-290
- [8] Yiljep, T. P. 1999. Characterization of major Agricultural Tools manufacturing Artisans in Northern Nigeria. Journal of agric. Eng. & Tech. 7: 45-52.
- [9] George, L. 1983. The theory and practice of metal work. 3rd edition. PTF low price edition. Longman, London
- [10] R. S. Bello "Development and evaluation of metal rolling machine for small-scale manufacturers" Vol. 15, No.3
- [11] M.B. Bassett, and W. Johnson — Design of machine elements, Tata mc-Graw Hill Publication

- [12] Gandhi, A. A. Shaikh & H. K. Raval, "Formulation of springback and machine setting parameters for multipass three-roller cone frustum bending with change of flexural modulus", Springer/ESAFORM 2009, pp 45-57

IJERGS

Comparison of Hybrid Composites with Different Filler Material

Madhusudhan T¹, Senthil Kumar M²,

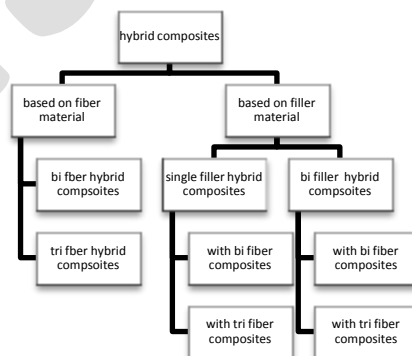
¹Research Scholar, PRIST University, Thanjavur, Tamil Nadu,
Email : t.madhusudan50@gmail.com, +919844106203

Abstract- Hybrid composites are those composites that are fabricated by combining different reinforcement materials to the combination of matrix material present in the reinforcement, sometimes may be filler or fibers or both. In the present study an effort is made to understand the behavior of different combination filler material to the epoxy resin matrix and test results are compared. The test results reveal that the hybrid composites with 2 different fiber materials and tungsten carbide as the filler material has higher tensile strength and hardness when compared to the material with 3 fiber material and Silicon carbide as the filler material. On the other side the hybrid composites with 3 fibers and Silicon carbide as the filler material showed higher strength than hybrid composites with 2 fibers and tungsten carbide in case of flexural strength and impact strength. Same trend is followed for the cold treated specimen also. Irrespective the material combination the cold treatment has reduced the strength of the material for tensile, flexural and impact strength but hardness of the material found to be increasing

Keywords— Impact, Flexural, Hybrid, Filler, Composites, Hardness, 2fiber hybrid, 3 fiber hybrid

INTRODUCTION

It is known that the combinations of several different materials have enhanced the mechanical properties in composites. This has led to the formation of Hybrid composites. The behavior of composites has improved characteristics than individual components or the composites with normal combination. The strength or performance of hybrid composites is always a sum of the strengths of individual components in which the weight due to their sum is compensated by their strength. The strength of one component can be used for overcoming the weakness of the other components. Hybrid composites have feather of less costly when compared to other composites with same strength and application. The different forms of hybrid composites are formed based on their combination. Metal matrix composites with different material combination and fiber are called metal matrix composites. With added fiber and filler material, they are called hybrid composites. In other different combination, the metal matrix composites are combined with 2 or more filler material to form hybrid composites. In case of polymer matrix composites hybrid composites are formed by combining two different fibers with filler material as bi fiber hybrid polymer composites. When three different fiber materials are used as the reinforcement with filler material, it is called as tri fiber hybrid polymer composites. The hybrid composites can be classified based on their matrix material, fiber present and filler used in it.



Generally composites are fabricated by using hand layup technique as it is most suitable and cheapest mode of fabrication and easily available. In this method the laminates are placed one above the other to obtain the desired thickness. The stacking sequence is sometimes varied in orientation so the strength in all direction remains same. In the present study the woven fabric is used as the reinforcement to bind the matrix, therefore the strength of the lamination in both directions is same. As the strength remains same in both directions the orientation angle need not be varied. The minimum required thickness of the hybrid composites can be obtained by just placing one laminate over the other in same order. The hybrid composites fabricated in present study are having fiber and matrix in the ratio of 60%: 40% of the weight ratio. The stacking sequence used for the two hybrid polymer composites fabricated in the present study is as follow for bi (two- fiber) hybrid composites the sequence is (G-A-G-A-G-A-G-A) where G- glass fiber and A is aramid fiber is used the reinforcement in of the laminates along with epoxy resin and tungsten carbide (WC) as the filler miller in proportion of (0, 5%, 7.5%&10) weight ratio. The other tri fiber hybrid composites the stacking order is (G-C-A-G-C-A-G-C-A) where C-carbon fiber is used the reinforcement in of the laminates along with epoxy resin and Silicon carbide (SiC) as the filler miller in proportion of (0, 5%, 7.5%&10) weight ratio.

REMAINING CONTENTS

Material testing

The different material testing conducted for the materials fabricated are tensile test flexural or 3 point bending test, impact test, hardness test for the specimen at normal temperature and cold treated specimen(cold treatment was done for -30°C for 24 hours).

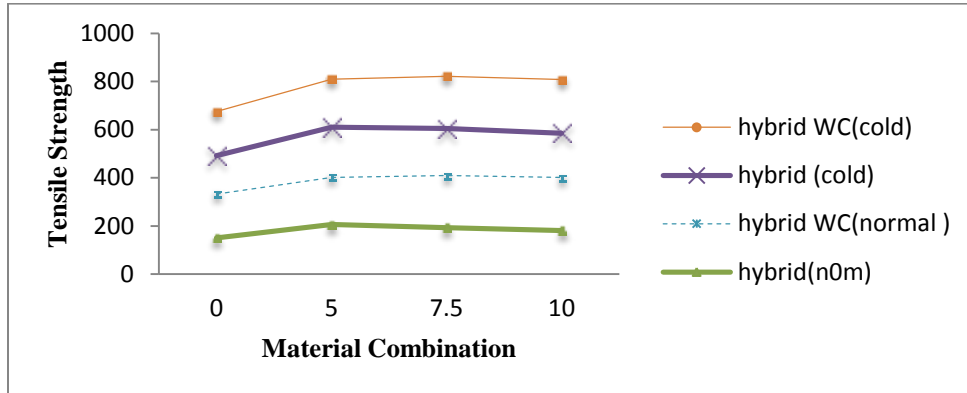
Tensile test

Tensile test is conducted according to the ASTM standard D3039 with the dimension of 250mm of length, 25.4mm of width and 3mm thickness.

Material composition	Tensile strength (MPa)	
	Normal	cold
Aramid-G-E	180.73	182.56
5WC-Aramid-G-E	196.26	199.35
7.5WC-Aramid-G-E	215.79	217.48
10WC-Aramid-G-E	220.36	222.89

Material composition	Tensile strength (MPa)	
	Normal	cold
Aramid-G-carbon -E	151.259	160.250
5SiC-Aramid-G-carbon-E	206.05	207.52
7.5SiC-Aramid-G-carbon-E	193.56	195.18
10SiC-Aramid-G-carbon-E	181.2	183.466

Plots of tensile stress



From comparison of tensile test result is evident that the tensile strength of the aramid glass fiber with tungsten carbide as the filler material shows increase in strength as the percentage of filler material increases. 10 % tungsten carbide filled aramid –glass composite shows higher strength for both normal and cold treated specimen. In case of SiC carbide filled aramid-glass-carbon fiber polymer composites shows increase in tensile strength up to 5% SiC. Any further increase in filler material, the strength found to be decreased but it was higher than the unfilled hybrid composites. When compared to both the hybrid polymer composites the glass – aramid hybrid composite filled with tungsten carbide shows higher strength.

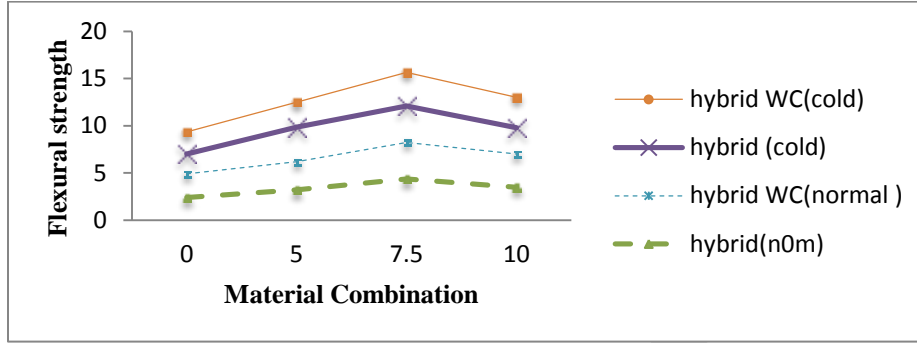
Flexural Test or 3- Point Bending Test

Flexural test is conducted according to the ASTM standard D790 of having the dimension of 125mm of length, 12.7mm of width and 3.2mm thickness

Material composition	Flexural strength (MPa)	
	Normal	cold
Aramid-G-E	9.32	9.07
5WC-Aramid-G-E	11.76	11.16
7.5WC-Aramid-G-E	13.91	12.98
10WC-Aramid-G-E	15.73	15.25

Material composition	Flexural strength (MPa)	
	Normal	cold
Aramid-G-carbon -E	10.2907	9.72
5SiC-Aramid-G-carbon-E	15.1074	11.43
7.5SiC-Aramid-G-carbon-E	12.36	10.24
10SiC-Aramid-G-carbon-E	9.7707	8.6328

Plots of Flexural Stress



From comparison of flexural test result is evident that the tensile strength of the aramid glass fiber with tungsten carbide as the filler material shows increase in its strength as the percentage of filler material increase and 10 % WC filled aramid –glass composite shows higher strength for both normal and cold treated specimen. In case of SiC carbide filled aramid-glass-carbon fiber polymer composites show the increase in flexural strength up to 5% SiC filled and any further increase in filled material the strength found to be decreased but it was even lesser than the unfilled hybrid composites. The flexural strength of the composite material will increases with the increasing tungsten carbide quantity. The increasing of filler material should be stopped where the flexural strength of the composite material start to decreases. The flexural strength of the given composite material cannot withstand the large amount of the filler/resin mixture. A right percentage of the filler material is decided earlier to get the maximum flexural strength of the composite material. The cold treated specimen will lose their flexural quality due to the hardness of the material after the cold treatment. So the cold treatment in case of flexural strength is not recommended.

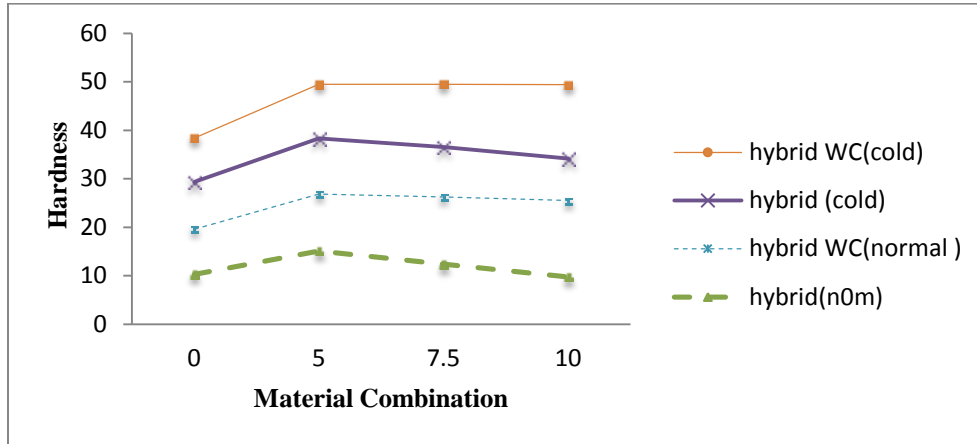
Hardness Test

To determine the hardness of the composites Rockwell hardness tester was used for both normal and cold treated specimen. The dimension of the components tested was 25*25mm with 3 mm thickness it does not have any standard dimension for harness test for convenience it is chosen as 25*25mm

Material composition	Hardness	
	Normal	cold
Aramid-G-E	59	62
5WC-Aramid-G-E	62	66
7.5WC-Aramid-G-E	65	68
10WC-Aramid-G-E	69	73

Material composition	Hardness	
	Normal	cold
Aramid-G-carbon -E	54	56
5SiC-Aramid-G-carbon-E	57	58
7.5SiC-Aramid-G-carbon-E	58	60
10SiC-Aramid-G-carbon-E	60	62

Plots of hardness



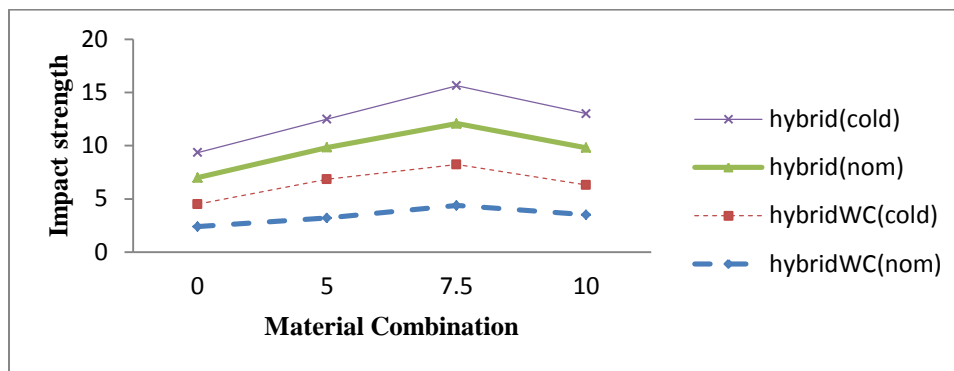
From comparison of hardness of both the composition components it is found that with increase in filler material percentage the hardness of the components was found to be increased and the material filled with 10 % filler showed higher hardness both in case of normal and cold treated specimen. The cold treatment has enhanced the hardness of the material irrespective of the filler used. Also it is observed that cold treatment has increased the brittleness of the composites. This may also be the one of the factor for higher hardness of the cold treated specimen.

Impact strength

Impact test is conducted according to the ASTM standard D256 of having the dimension of 69mm of length, 12.7mm of width and 3mm thickness

Material composition	Hardness	
	Normal	cold
Aramid-G-E	2.5	2.35
5WC-Aramid-G-E	2.99	2.65
7.5WC-Aramid-G-E	3.85	3.56
10WC-Aramid-G-E	3.5	3.2

Material composition	Hardness	
	Normal	cold
Aramid-G-carbon -E	2.40	2.1
5SiC-Aramid-G-carbon-E	3.2	3.65
7.5SiC-Aramid-G-carbon-E	4.38	3.85
10SiC-Aramid-G-carbon-E	3.5	2.8



From comparison of impact test of the given specimen shows the impact strength of the composites increased till 7.5% usage of filler material any further increase in the filler material has depleted the impact strength, for both normal and cold treated specimen. As compared to Aramid- glass fiber with WC, Aramid-glass and carbon fiber with SiC shows higher impact strength both in case of normal and cold treated specimens.

ACKNOWLEDGMENT

If acknowledgement is there wishing thanks to the people who helped in work than it must come before the conclusion and must be same as other section like introduction and other sub section.

CONCLUSION

From the above result it is confirmed that material with two fiber and tungsten carbide filler shows higher strength when compared with a polymer composites with 3 fiber and SiC carbide as the filler material. The cold treatment has degraded material strength in all the mechanical characteristics except the hardness. The bonding between the materials may be the reason for decrease in the strength. Cold treatment has increased only the hardness of the material. This may due to increased brittleness. The hybrid material with aramid-glass-carbon fibers filled with SiC has showed higher strength than hybrid material with aramid and glass fiber filled with WC. This may be due to the resistance of the fibers or may be due to incorporation of SiC filler material.

REFERENCES:

1. RogérioLago Mazur São Paulo State University Guaratinguetá-Brazil Michelle Leali Costa São Paulo State University Guaratinguetá-Brazil. Journal of Aerospace Technology and Management dec-2009.
2. Zahra Riahi MASC in Earthquake Engineering, Energy and Infrastructure Division, Sandwell Engineering INC, Vancouver, BC. FarzadFaridafshin MASC in Structural Engineering, Concept and Technology Department, Aker Solutions, Bergen, Norway.
3. Arpitha G R*, Sanjay M R, B Yogesha, Department of Mechanical Engineering, Malnad College of Engineering, Hassan - 573202, Karnataka, India.
4. Manoj Singla1 Department of Mechanical Engineering, R.I.E.I.T., Railmajra, Distt. Nawanshahr (Pb.)-144533, INDIA. VikasChawla Department of Materials & Metallurgical Engineering, I.I.T. Roorkee (Uttaranchal), INDIA.
5. Critiane M. Becker,TeoA.Dick et al universidade do riogrande do sul, Department of materials and chemistry department brazil.

6. GaoGuangfaa,b,c, Li Yongchic, Jing Zhengc, Yuan Shujiea,b a Key Laboratory of Integrated Coal Exploitation and Gas Extraction , Huainan, 232001 , China b School of Energy and Safety, Anhui University of Science and Technology, Huainan□232001, China c CAS Key Laboratory of Mechanical Behavior and Design of Materials □Hefei,230027, China.
7. Yu-Chung TSENG¹a Chih-Yu KUO²b .1,2Department of Aviation Mechanical Engineering, China University of Science and Technology, Taiwan R.O.C.
8. Rim Ben Toumia,b, Jacques Renard a, Martine Monin b , PongsakNimdum a Centre des Matériaux Pierre-Marie Fourt, Ecole des Mines de Paris, BP 87, 91003 EvryCedex, France. b PSA Peugeot-Citroën, Centre technique La Garenne, 18 rue des Fauvelles, 92250 LA GARENNE-COLOMBES Cedex, France.
9. R. Murugana, R. Rameshb, K. Padmanabhanc. A Research Scholar, Sri Venkateswara College of Engineering, Sriperumbudur-602117, India. B Professor, Sri Venkateswara College of Engineering, Sriperumbudur-602117, India. C Professor, School of Mechanical and Building Sciences, VIT University, Vellore 632014, India.
10. Ramesh K. Nayak a*, AlinaDasha and B.C.Ray b. A School of Mechanical Engineering, KIIT University, Bhubaneswar, 751024, India. B Department of Metallurgical and Materials Engineering, National Institute of Technology, Rourkela, 769008, India
11. R.Panneerdhassa , A.Gnanavelbabub*, K.Rajkumarc,Mechanical Properties of Luffa Fiber and Ground nut Reinforced Epoxy Polymer Hybrid Composites.
12. B.M.Girish^{1,*}, Basawaraj B. R.¹, B.M.Satish¹, D.R.Somashekar² ¹R&D Center, Department of Mechanical Engineering, East Point College of Engineering and Technology, Bangalore, Karnataka, 560095, India ²Department of Mechanical Engineering, Rungta College of Engineering and Technology,Nandanvan, Raipur, Chattisgarh, 492019, India.

PHASE CHANGE MATERIAL REVIEW

¹AKSHAY R HEDAOO ²ASHWIN HEDAOO

8149219397

7387185840

^{1,2}STUDENT OF MECHANICAL DEPARTMENT

KDKCE

NAGPUR, MAHARASHTRA, INDIA

AKSHAYHEDAOO11@GMAIL.COM

Abstract: Thermal energy storage has gained increasing interest in past decade. While the storage of heat as sensible heat is established in many applications, the storage of heat as latent heat is not yet as wide spread. The storage of heat as latent heat using the phase change solid-liquid promises high storage density in small temperature range around the melting point. Due to its low cost, high storage capacity, and suitable melting temperature for applications, water is by far the most commonly used PCM for cooling applications. They range from cooling food and beverages to space cooling and process cooling. As a short survey shows, the globally installed storage capacity in large ice storage is quite significant. Application of other PCM have by far not reached a comparative market penetration. However, they promise better efficiency in many cooling as well as heating applications. To develop this potential, current R&D focuses, among other things, on improving the technical properties and performance of these PCM.

Keywords: thermal energy storage, phase change materials (PCM), organic PCM, inorganic PCM, advantages, eutectics applications

Introduction:

Energy storage is a key issue to be addressed to allow intermittent energy sources, typically renewable sources, to match energy supply with demand. There are numerous storage technologies that are capable of storing energy in various forms including kinetic energy, chemical solutions, magnetic fields, or other novel approaches. PCM is substance with a high heat of fusion which, melting and solidifying at certain temperature, is capable of storing and releasing large amounts of energy. Heat is absorbed or released when the material changes from solid to liquid and vice versa. Phase change material or PCM have the capacity to store and release large amount of energy that energy is called latent heat. Each PCM has specific melting and crystallisation temperature and a specific latent heat storage capacity.

PHASE CHANGE MATERIAL (PCM):

Phase change materials are a class of material that use a phase transition to store energy. A phase transition occurs when a material changes from one state of matter to another without changing its chemical composition, for example from liquid to solid or from solid to gas. Although transitions involving gas have very large enthalpies of transition, containing a large mass of gas is very difficult, requiring expensive and potentially dangerous pressure vessels. Therefore almost all practical PCMs will have solid-liquid transition [1]. There are some materials that exhibit solid-solid transitions; these have a much lower enthalpy of transition. Solid-solid transition involve a change in the crystal structure of the material, for example iron changes from body-centred cubic to face-centred cubic at 1185K[2]. Solid-solid transitions are advantageous from the perspective that they do not require containment the way solid-solid material do [3] [4].

SELECTION CRITERIA OF PCM

A good PCM must meet certain criteria and possess certain material characteristics. These have been listed in a number of reviews by various authors and they are summarised below:-[1] [5] [6] [7] [8] [9]

A. Thermodynamic criteria:-

1. The material should have a large enthalpy of transition, i.e. latent heat ΔH .
2. Material should have a high heat capacity in both the liquid and solid phase.
3. The PCMs should have an appropriate melting point.
4. High thermal conductivity

B. Kinetic criteria:-

1. PCM should exhibits a small amount of super cooling, which occurs when a material fails to crystallize at its melting temperature.
2. The crystal growth rate of the material must also be high.

C. Other criteria:-

3. PCM must have long term chemical stability.
4. PCM should have be non-
5. Corrosive.
6. PCM should have be non-flammable and non-toxic.
7. Cost of PCM must be low.
8. PCM should not contain any rare element.
9. Material should be eco-friendly.

No single material can possibly fulfil all of these stringent requirements, and engineering solutions must be made to accommodate any shortfalls.

TYPES OF PCM:-

Largely through the work of Lane a few broad categories of potential PCMs were delineated [10] [11]. Lane sorted through tens of thousands of materials to find candidates that could be good PCMs. There are two main type that naturally form, inorganic and organic, which are broken up into several major subtypes. In the organic group there are metals, salts hydrates, water, and salts. Organic PCMs includes paraffin waxes, which are long chain hydrocarbons; fatty acids and esters; sugar alcohols; and other miscellaneous organic compounds. Additionally there are mixture of the above categories both in eutectic and non-eutectic mixture.

ORGANIC PCMs:

1. Paraffin

Paraffin of type C_nH_{2n+2} are a group of saturated hydrocarbons with very similar properties. Paraffin between C_5 and C_{15} are liquids and the rest are waxy solids. Paraffin wax is one of the most popular organic heat storage PCM for commercial applications. It consists of a straight chain hydrocarbons having melting temperature between 23°C and 67°C [12]. Paraffin are available in large temperature range, Paraffin have no tendencies to super cool. Paraffin are chemically stable. Paraffin waxes show high heats of fusion. Paraffin waxes don't segregate. Paraffin waxes are safe. Paraffin are non-corrosive. [12][13] Paraffin has Low thermal

conductivity. High volume change between the solid and liquid phases. Commercial paraffin do not sharp exact melting point Paraffin are flammable. Pure paraffin are expensive. [12][13]

2. Non-Paraffin:

The non-paraffin organic are most numerous of the PCMs with highly varied properties. Non-paraffin organic PCMs are characterised by their varied properties. Each of these materials will have its own properties unlike the paraffin's, which have very similar properties. Abhat et al [14], Buddhi and Sawhney [15] have conducted an extensive survey and recognised a number of esters, fatty acids, alcohols, and glycols suitable for thermal energy storage. These organic materials are subdivided into fatty acids and other non-paraffin organic [13]. These materials are flammable and should not be exposed to excessively high temperature, flames or oxidizing agents. Following are some features of non-paraffin [13]. Non-paraffin has High heat of fusion. Non-paraffin has Low thermal conductivity, Low flash points. Non-paraffin are Inflammable. Non-paraffin has Instability at high temperature. Varying level of toxicity.

- Fatty acids

General formula for all the fatty acid is given by $\text{CH}_3(\text{CH}_2)_{2n} \times \text{COOH}$. Fatty acids have the same characteristic as paraffin and have high values of latent heat of fusion compared to paraffin. Fatty acids have the ability of many cycling of melting and freezing with no super cooling, and they are characterised by sharper phase temperature than technical grade paraffin. The major drawback of fatty acids is their high cost that is 2-2.5 times greater than that of the technical grade paraffin. Additionally they are mild corrosive. [13]

INORGANIC PCMs:

Inorganic phase change materials are classified as salt hydrates and metallic. These phase change materials do not supercool appreciably and their heats of fusion do not degrade with cycling.

1) Salt hydrates

Salt hydrates consist of a salt and water that combine in crystalline matrix when the material solidifies. There are many different salt hydrates having melting temperature ranges between 15°C - 117°C . Salt hydrate are considered as the most important group of PCMs that have been studied for application in latent thermal energy storage system. [12] Salt hydrates has High latent heat of fusion per unit mass of volume (higher than paraffin) It has High thermal conductivity (compared to paraffin) And Have sharp phase change temperature. Salt hydrates has Small volume changes during melting. It has High availability And Low cost. Segregation is the formation of other hydrates or dehydrated salts that settle and reduce the volume that is available for thermal energy storage. Salt hydrate show super cooling because they are unable to start crystallization at the freezing temperature. This problem can be avoided by using nucleating agents. Salt hydrates causes corrosion in metal container, whereas metal containers are common containers used in thermal energy storage system.

2) Metallic

Metallic include the low melting metals and metal eutectics. Metallic have not been strongly studied as PCM for latent heat storage because of their heavy weights. For the applications that weight is not important issue while volume is an important parameter, metallic are attractive because of their high heat of fusion per unit volume. [13] Some features of these materials are: It has Low heat

of fusion per unit weight, High heat of fusion per unit volume and High thermal conductivity. Metallic has Low specific heat and relatively low vapour pressure.

3) Eutectics

The eutectic consist of two or more components where each of them melts and freezes congruently forming mixture of a component that crystals during crystallization process. Usually eutectic melt and freeze without segregation. During melting process, both components liquefy at the same without possibility of separation.

ENERGY STORAGE:

Thermal energy storage can have a positive impact in the form of increasing the reliability of the system, improving the functioning of the power plants and energy system, reducing energy purchase costs by shifting energy surplus from period of lower to period of higher demand. During day time when solar energy collection takes place and terminates with complete melting of the PCM, charging of the store does not terminate with complete melting of the PCM if the inlet fluid temperature is above the melt temperature, charging of sensible heat continues. Heat transfer fluid exit temperature is time dependent because the rate of the solidification of the PCM varies with time. This mode terminates with complete solidification of the PCM. Latent heat storage system have many advantages like large heat storage capacity in a unit volume and their isothermal behaviour during the charging and discharging process. Al-Jandal and Sayigh [16] studied the thermal performance characteristics of a solar tube collector (STC) system with phase change storage analytically and experimentally. STC performance during charging is studied and it is concluded that fin structure are strongly affecting the melting process. Mehling et al [17] concluded that placing PCM module at the top the water tank in TES (thermal energy storage) has given higher storage density and compensated the heat loss at the top surface by doing both numerical and experimental investigation.

APPLICATIONS OF PHASE CHANGE MATERIALS INCLUDE, BUT ARE NOT LIMITED TO:

1. Thermal energy storage
2. Conditioning of buildings, such as 'ice-storage'
3. Cooling of heat and electrical engines
4. Cooling: food, beverages, coffee, wine, milk products, green houses
5. Medical applications: transportation of blood, operating tables, hot-cold therapies, treatment of birth asphyxia
6. Human body cooling under bulky clothing or costumes.
7. Waste heat recovery
8. Off-peak power utilization: Heating hot water and Cooling
9. Heat pump systems
10. Passive storage in bioclimatic building/architecture (HDPE, paraffin)
11. Smoothing exothermic temperature peaks in chemical reactions
12. Solar power plants
13. Spacecraft thermal systems
14. Thermal comfort in vehicles
15. Thermal protection of electronic devices
16. Thermal protection of food: transport, hotel trade, ice-cream, etc.

17. Textiles used in clothing
18. Computer cooling
19. Turbine Inlet Chilling with thermal energy storage

Telecom shelters in tropical regions. They protect the high-value equipment in the shelter by keeping the indoor air temperature below the maximum permissible by absorbing heat generated by power-hungry equipment such as a Base Station Subsystem. In case of a power failure to conventional cooling systems, PCMs minimize use of diesel generators, and this can translate into enormous savings across thousands of telecom sites in tropics.

CONCLUSION:

1. From the review it is seen that the energy stored time can be reduce with the use of phase change material
2. It provide greater advantage towards meeting of energy storing needs, compactness and energy supply at constant temperature.
3. The use of PCM is beneficial towards storing the waste heat with its low cost advantages.

REFERENCES:

1. Belton, G. and Ajami, F. Thermochemistry of salt hydrates Technical Report NSF/RANN/SE/GI27976/TR/73/4 University of Pennsylvania (1973).
2. Haynes, W., Lide, D., and Bruno, T. (2012) CRC Handbook of Chemistry and Physics, CRC Press, Cleveland, Ohio <http://hbcnetbase.com/>.
3. Hong, Y. and Xin-shi, G. (2000) Solar Energy Materials and Solar Cells 64(1), 37 – 44.
4. Zhang, L.-J., Di, Y.-Y., Tan, Z.-C., and Dou, J.-M. (2012) Solar Energy Materials and Solar Cells 101(0), 79 – 86.
5. Zalba, B., Marín, J. M., Cabeza, L. F., and Mehling, H. (2003) Applied Thermal Engineering 23(3), 251 – 283.
6. Sharma, A., Tyagi, V., Chen, C., and Buddhi, D. (2009) Renewable and Sustainable Energy Reviews 13(2), 318 – 345.
7. Abhat, A. (1983) Solar Energy 30(4), 313–332.
8. Agyenim, F., Hewitt, N., Eames, P., and Smyth, M. (2010) Renewable and Sustainable Energy Reviews 14(2), 615 – 628.
9. Tyagi, V. V. and Buddhi, D. (2007) Renewable and Sustainable Energy Reviews 11(6), 1146 – 1166.
10. Lane, G. A. (1983) Solar Heat Storage: Background and Scientific Principles, CRC Press, Boca Baton, Florida.
11. Lane, G. A. (1986) solar heat storage: Latent Heat Materials, CRC Press, Boca Baton, Florida.
12. Sharma Someshower Dutt, Kitano Hiroaki, and Sagara Kazunobu, “Phase Change Materials for Low Temperature Solar Thermal Applications”, Res. Rep. Fac. Eng. Mie Univ., Vol. 29, pp. 31-64, 2004.
13. Sharma Atul, Tyagi V.V., Chen C.R., and BuddhiD., “Review on Thermal Energy Storage with Phase Change Materials and Applications”, Renewable and Sustainable Energy Reviews, Vol. 13, pp. 318–345, 2009.
14. Abhat A, et al., “Development of a Modular heat Exchanger with an Integrated Latent heat Storage”, Report no. BMFT FBT 8 -050, German Ministry of Science and Technology, Bonn, 1981
15. Farid Mohammed M., Khudhair Amar M., Razack Siddique Ali K., and Al-Hallaj Said, “A Review on Phase Change Energy Storage: Materials and Applications”, Energy Conversion and Management, Vol. 45, pp. 1597–1615, 2004.

16. S. Al-Jandal and A. A. M. Sayigh, Thermal performance Characteristics of STC system with phase change storage, Renewable Energy, 5 (1994), 390–399. S. S. Al-Jandal and A. A. M. Sayigh, Thermal performance Characteristics of STC system with phase change storage, Renewable Energy, 5 (1994), 390–399.
17. H. Mehling, L. F. Cabeza, S. Hippeli, and S. Hiebler, PCMmodule To improve hot water heat stores with stratification, Renewable Energy, 28 (2003), 699–711

IJERGS

An Intelligent System Control Using Speech Recognition

Girish. S, Anoopal. K. S

Abstract— Speech recognition technology has refashioned the way people with disabilities to use computers. This raising technology accelerates more opportunities for medical prescriptions, education, employment etc. Speech recognition is an alternative to typing on a keyboard. Just talk to the computer and our words appear on the screen. The software has been developed to administer a fast approach of writing onto a computer and can help people with a variety of disabilities. It is useful for people with physically challenged who often find typing difficult, painful or impossible. Voice recognition software further help those who with spelling adversity, including dyslexic users, because recognized words are always correctly spelled.

Speech recognition technology helps people with disabilities to interact with computers more easily and support doctors to make prescription easily. Using this speech recognition we create a system which acts according to the voice commands given by the user. People with motor limitations, which cannot use a standard keyboard and mouse, can use their voices to navigate the computer and create documents. The technology is further convenient to people with learning disabilities that experience dilemma with spelling and writing. Some individuals with speech impairments may practice speech recognition as a therapeutic tool to progress vocal quality. Speech recognition technology has great potential to provide people with disabilities greater access to computers and a world of opportunities.

Keywords — Speech recognition; Intelligent System.

INTRODUCTION

Research in automatic speech recognition by machine has been done for almost five decades. It is worthwhile to briefly review some research highlights. The earliest attempts to devise systems for automatic speech recognition by machine were made in the 1950s, when various researchers tried to exploit the fundamental ideas of acoustic-phonetics. In 1952, at Bell Laboratories, Davis, Biddulph and Balashek built a system for isolated digit recognition for a single speaker [1]. The system relied heavily on measuring spectral resonances during the vowel region of each digit. In an independent effort at RCA Laboratories in 1956, Olson and Belar tried to recognize 10 distinct syllables of a single talker, as embodied in 10 monosyllabic words [2].

The system again relied on spectral measurements (as provided by an analog filter bank) primarily during vowel regions. In 1959, at University College in England, Fry and Denes tried to build a phoneme recognizer to recognize four vowels and nine constants [3]. They used a spectrum analyzer and pattern matcher to make the recognition decision. A novel aspect of this research was the use of statistical information about allowable sequences of phonemes in English (a rudimentary form of language syntax) to improve overall phoneme accuracy for words consisting of two or more phonemes. Another effort of note in this period was the vowel recognizer of Forgie and Forgie, constructed at MIT Lincoln Laboratories in 1959, in which 10 vowels embedded in a/b/-vowel-/t/ format were recognized in speaker independent manner [4]. Again a filter bank analyzer was used to provide spectral information, and a time varying estimate of the vocal tract resonances was made to decide which vowel was spoken.

In the 1960s several fundamental ideas in speech recognition surfaced and were published. However, the decade started with several Japanese laboratories entering the recognition arena and building special purpose hardware as part of their systems. One early Japanese system, described by Suzuki and Nakata of the Radio Research Lab in Tokyo [5], was a hardware vowel recognizer. An elaborate filter bank spectrum analyzer was used along with logic that connected the outputs of each channel of the spectrum analyzer (in a weighted manner) to a vowel-decision circuit, and a majority decision logic scheme was used to choose the spoken vowel. Another hardware effort in Japan was the work of Sakai and Doshita of Kyoto University in 1962, who built a hardware phoneme recognizer [6]. A hardware speech segmented was used along with a zero crossing analysis of different regions of the spoken input to provide the recognition output. A third Japanese effort was the digit recognizer hardware of Nagata and coworkers at NEC Laboratories in 1963 [7]. This effort was perhaps most notable as the initial attempt at speech recognition at NEC and led to a long and highly productive research program.

In the 1960s three key research projects were initiated that have had major implications on the research and development of speech recognition for the past 20 years. The first of these projects was the efforts of Martin and his colleagues at RCA Laboratories, beginning in the late 1960s, to develop realistic solutions to the problems associated with non-uniformity of time scales in speech

events. Martin developed a set of elementary Time-normalization methods, based on the ability to reliably detect speech starts and ends that significantly reduced the variability of the recognition scores [8]. Martin ultimately developed the method and founded one of the first companies, Threshold Technology, which built, marketed, and sold speech-recognition products. At about the same time in the Soviet Union, Vintsyuk proposed the use of dynamic programming methods for time aligning a pair of speech utterances[9]. Although the essence of the concepts of dynamic time warping, as well as rudimentary versions of the algorithms for connected word recognition, were embodied in Vintsyuk's work, it was largely unknown in the West and did not come to light until the early 1980s; this was long after the more formal methods were proposed and implemented by others. A final achievement of note in the 1960s was the pioneering research of Reddy in the field of continuous speech recognition by dynamic tracking of phonemes [10], Reddy's research eventually spawned a long and highly successful speech-recognition research program at Carnegie Mellon University (to which Reddy moved in the late 1960s) which, to this day, remains a world leader in continuous-speech-recognition systems.

In the 1970s speech-recognition research achieved a number of significant milestones. First the area of isolated word or discrete utterance recognition became a viable and usable technology based on fundamental studies by Velichko and Zagoruyko in Russia [11], Sakoe and Chiba in Japan [12], and Itakura in the United States [13]. The Russian studies helped advance the use of pattern-recognition ideas in speech recognition. The Japanese research showed how dynamic programming methods could be successfully applied; and Itakura's research showed how the ideas of linear predictive coding (LPC), which had already been successfully used in low-bit-rate speech coding, could be extended to speech recognition systems through the use of an appropriate distance measure based on LPC spectral parameters. Another milestone of the 1970s was the beginning of a longstanding, highly successful, group effort in large vocabulary speech recognition at IBM in which researchers studied three distinct tasks over a period of almost two decades, namely the New Raleigh language [14] for simple database queries, the laser patent text language [15] for transcribing laser patents, and the office correspondence task, called Tangora [16], for dictation of simple memos. Finally, at AT&T Bell Labs, researchers began a series of experiments aimed at making speech-recognition systems that were truly speaker independent [17]. To achieve this goal a wide range of sophisticated clustering algorithms were used to determine the number of distinct patterns required to represent all variations of different words across a wide user population. This research has been refined over a decade so that the techniques for creating speaker-independent patterns are now well understood and widely used.

Just as isolated word recognition was a key focus of research in the 1970s, the problem of connected word recognition was a focus of research in the 1980s. Here the goal was to create a robust system capable of recognizing a fluently spoken string of words (e.g. Digits) based on matching a concatenated pattern of individual words. A wide variety of connected word-recognition algorithms were formulated and implemented, including the two-level dynamic programming approach of Sakoe at Nippon Electric Corporation (NEC) [18], the one-pass method of Bridle and Brown at Joint Speech Research Unit (JSRU) in England [19], the level building approach of Myers and Rabiners at Bell Labs [20], and the frame synchronous level building approach of Lee and Rabiner at Bell Labs [21]. Each of these "optimal" matching procedures had its own implementation advantages, which were exploited for a wide range of tasks. Speech research in the 1980s was characterized by a shift in technology from template-based approaches to statistical modeling methods-especially the hidden Markov model approach [22, 23]. Although the methodology of Hidden Markov Modeling (HMM) was well known and understood in a few laboratories (primarily IBM, Institute for Defense Analyses (IDA), and Dragon Systems), it was not until widespread publications of the methods and theory of HMMs, in the mid-1980, that the technique became widely applied in virtually every speech-recognition research laboratory in the world.

Another "new" technology that was reintroduced in the late 1980s was the idea of applying neural networks to problems in speech recognition. Neural networks were first introduced in the 1950s, but they did not prove useful initially because they had many practical problems. In the 1980s, however, a deeper understanding of the strengths and limitations of the technology was obtained, as well as the relationships of the technology to classical signal classification methods. Several new ways of implementing systems were also proposed [24, 25]. Finally, the 1980s was a decade in which a major impetus was given to large vocabulary, continuous-speech-recognition systems by the Defense Advanced Research Projects Agency (DARPA) community, which sponsored a large research program aimed at achieving high word accuracy for 1000-words, continuous-speech-recognition, and database management task. Major research contributions resulted from efforts at CMU (Notably the well-known SPHINX system) [26], BBN with the BYBLOS system [27], Lincoln Labs [28], SRI [29], MIT [30], and AT&T Bell Labs. The DARPA program has continued into the 1990s, with emphasis shifting to natural language front ends to the recognizer, and the task shifting to retrieval of air travel information. At the same time, speech-recognition technology has been increasingly used within telephone networks to automate as well as enhance operator services.

SPEECH RECOGNITION

The primary objective of this paper is to allow the user to interact with the computer through voice commands and let the user to control computer functions and dictate text by voice. For example, a person can scroll down the web page with a voice command, such as "Scroll down" control application functions, also performing various operations such as opening programs, web browser, notepad, search, documents, run, help, undo, etc. and also perform cut, copy and paste operations. Now doctors have to write prescription in capital letters so speech recognition supports doctors for medical prescription easily. More and more people with special needs are considering speech recognition as an alternate method for computer access because speech recognition products are more affordable and user-friendly than ever before and these applications needs less initial training than their predecessors and typically offers much improved accuracy. The system operations are to be performed according to the voice commands given by the user and it is created as an agent. This agent gets the voice commands from the user and performs the system functions. I.e. the agent acts as an interface between the user and the system. The commands which will be given by the user are separately stored in an xml file. This file helps the new user to understand the commands that he can execute in the system.

Speech recognition software has to be trained to recognize and understand the user's voice. The user has to train the software by reading a selection of paragraphs to the computer. By analyzing the voice, the computer creates a unique voice file for that particular user. For successful voice recognition, an appropriate training of the system is necessary. For this purpose we have used the software tool SDK 5.1 which converts voice to text and also add a vocabulary to the system to match or correct spellings while reading. A speech-enabled application and an SR engine (speech recognition engine) do not directly communicate with each other-all communications are done by using SAPI (Speech Application Programming Interface). Controlling audio input, from a microphone, or from other sources, converting audio data in to a valid engine format, loading grammar files, resolving grammar imports and grammar editing, compiling standard SAPI XML grammar format, conversion of custom grammar formats, parsing semantic tags in results, sharing of recognition across multiple applications, marshaling between engine and applications are done by SAPI. SAPI also manage other aspects like feedback the results and other information to the application, storing audio and serializing results for later analysis. SAPI ensures that applications do not cause errors, prevents applications from calling the engine with invalid parameters and further dealing with crashing of applications. The SR engine Performs recognition, uses SAPI grammar interfaces, loads dictation, generates, recognition and other events to provide information to the application.

FUNCTIONAL OVERVIEW

Most speech recognition software arrives bundled with noise canceling microphone. Placing an appropriate and consistent positioning of the microphone is indispensable for good recognition. It is also helpful to adjust the audio levels before each session to accommodate for everyday fluctuation in environmental cacophony and divergence in microphone positioning. The sound card is a critical factor of a speech recognition system. Recognition problems may be the result of low quality sound card performance or incompatibility between the soundcard and the voice recognition software. Generally speech recognition programs contain a utility program that assesses the quality of the soundcard. If the computer's soundcard is deficient, the intended user will need to get a vendor-approved soundcard. Voice recognition software vendors commonly provide a permitted list of soundcard's with their technical specifications. Laptop computer noise may interfere with quality sound processing using a USB microphone, which bypasses the internal soundcard, may resolve this issue.

Speak in a consistent level emphasis, speaking too vehemently or too tenderly makes it laborious for the computer to recognize what you've said. Practice a consistent rate, without speeding up and slowing down. Speak without pausing between words; a phrase is easier for the computer to interpret than just one word. For example, the computer has a hard time understanding phrases such as, "This (pause) is (pause) another (pause) example (pause) sentence". Start by working in a quiet environment so that the computer hears you instead of the sounds around you, and use a good quality microphone. Try to keep the microphone in the same position do not change once it is adjusted or use microphone head set. Train your computer to recognize your voice by reading clearly the prepared training text in the Voice Training Wizard. Additional training increases speech recognition accuracy. As you dictate, do not be anxious if you do not rapidly examine your words on the screen. Continue speaking and pause at the end of your thought. The computer will display the recognized text on the screen after it finishes processing your voice. Pronounce words clearly, but do not separate each syllable in a word. For example, sounding out each syllable in "e-nun-chi-ate," will make it harder for the computer to recognize what you've said.

Our paper aims at creating an agent which acts as an interface between user and the system. The system operations are performed according to the voice commands given by the user. An agent is used in order to make the user aware of what commands he will be

giving. The commands which will be given by the user are separately stored in an xml file. Using this store of commands new user comes to know about the commands which he can execute in the system. Speech recognition software is “speaker dependent,” which means that it must be trained to recognize and understand the user’s voice. The user trains the software by reading a selection of paragraphs to the computer and computer analyzes the voice data then creates a unique voice file for each particular user. Thorough training of the system is very important stage for successful voice recognition. Most speech recognition systems require the user to complete an initial training session so that the software can learn the user’s vocal style and speech patterns. However, additional training is usually necessary to improve recognition accuracy to a satisfactory level. Some people with disabilities require customized training, set up and technical support. There may be technical difficulties with the software or hardware. In the case of system failure, an alternative method should be readily available for use. Local voice recognition vendors may provide training and technical support packages for additional cost.

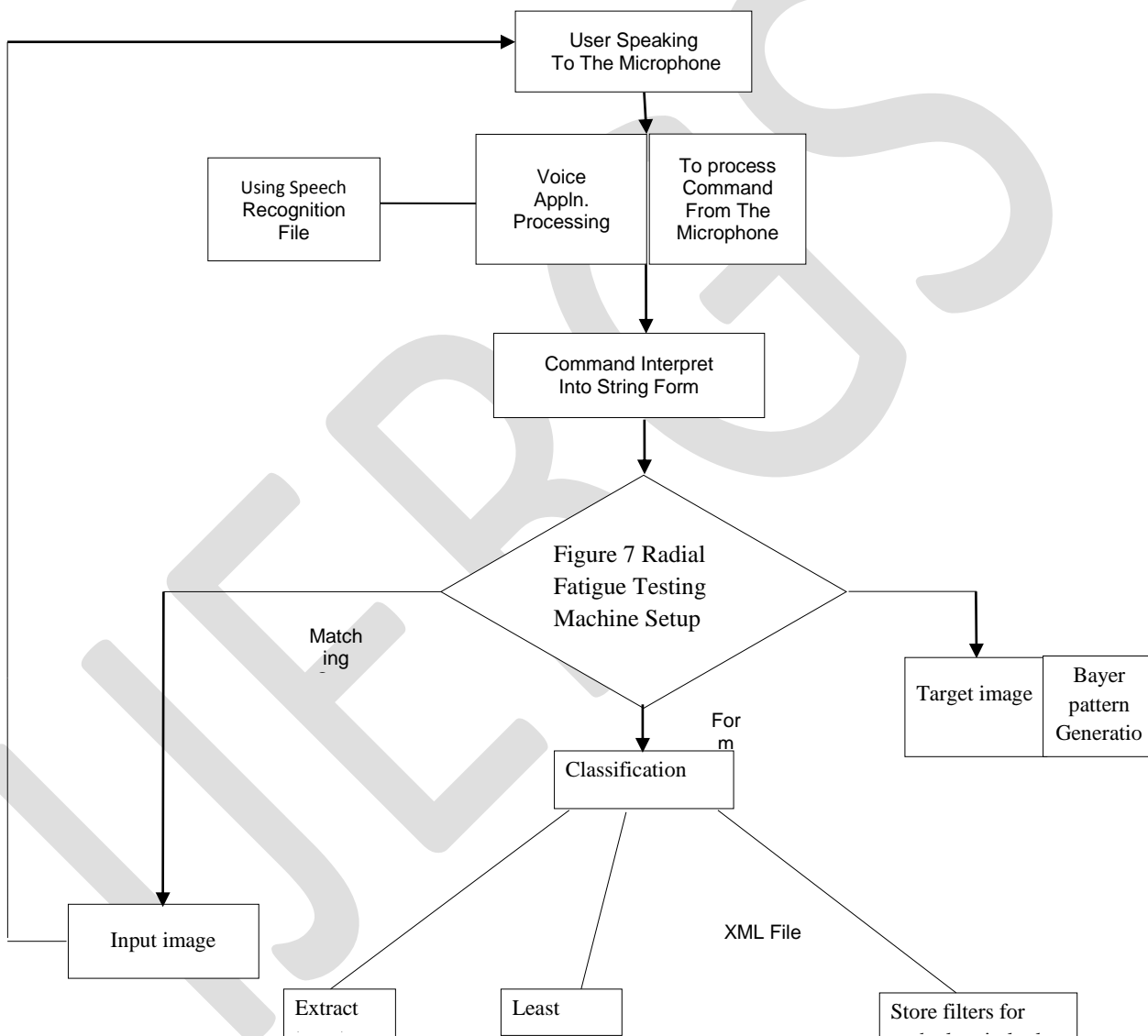
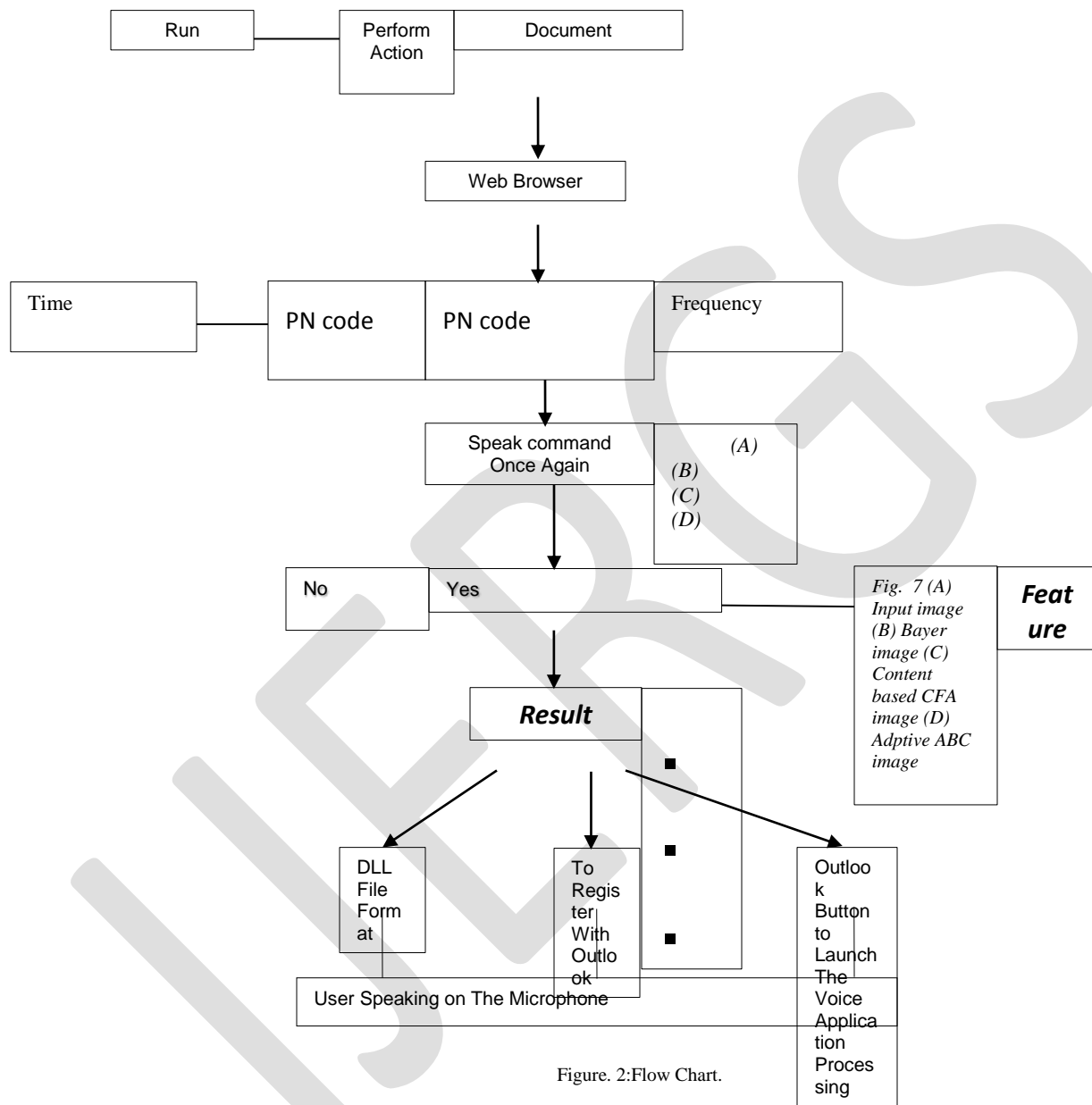


Figure. 1: General Approach of Speech Recognition.

IMPLEMENTATION

Here we proposed to write code by using a .NET-compatible language such as C Sharp. C Sharp can be used to create applications that will run in the .NET platform. We created various forms like formabout, formprofilechange, formaccuracychange, formfavorites, formaddfavorites, and formcommands in C sharp.net. Also we created various xml files like xmlactivate, xmlstart, xmldeactivate,

xmlstickykeys, xmlabout, xmlalphabeticstate, and xmlnumericstate. XML schema describes the SAPI 5.0 SR Command and Control grammar format which is based on the XML framework. The schema is included in the speech grammar compiler tool (gramcomp.exe or gc.exe). We can use the SDK components and redistributable SAPI/engine run-time to build applications that incorporate speech recognition and speech synthesis. Using this speech recognition we create a system which acts according to the voice commands given by the user.



Feat ure
 Fig. 7 (A) Input image
 (B) Bayer image (C) Content based CFA image (D) Adptive ABC image

formAccuracychange.cs: This form allows setting the accuracy with which user should speak. This form contains labels like accuracy limit, accuracy percent, a list box which helps to set the accuracy percent and buttons like ok which helps to accept the selected accuracy percent and cancel to close this form.

formAddfavorites.cs: Whenever user gives the command “Add favorites” this form will be loaded. This form allows user to add various applications into favorites form which can be opened with a single command. Here we are adding the program names along with the phrases which are used to open those programs. Here two list boxes namely program and phrase are used which contain the list of programs with corresponding phrases which can be opened. To add a new program with corresponding phrase two textboxes are used. Upon entering the new program and phrase name into the textbox, Add button helps to update the list boxes with newly entered program and phrase. Delete button is used to delete a program from the list box with the phrase. Browse button is used to add the

program to list box from various locations. Save button is used to update code for added or deleted program. Close button is used to close this form.

formCommands.cs: In this form the various commands for which this project works are included. Tree view of visual studio .NET to design this form. By this form user gets knowledge about commands which he can work with.

formFavorites.cs: Whenever user gives the command “form favorites” this form will be loaded. This form allows user to know about various applications which can be opened with a single command. Here two list boxes namely program and phrase are used which contain the list of programs with corresponding phrases which can be opened. Here user can open any program specified in the list boxes with the corresponding phrase as the voice command.

BIOGRAPHIES

¹ **Mr. Girish. S** received B. E. in Electronics & Communication Engineering from VTU, Belagavi and M.Tech Degree in Networking & Internet Engineering from JNNCE, Shimoga. He is currently working as Assistant Professor in Computer Science & Engineering Department at Sahyadri College of Engineering & Management Mangaluru, India-575007. Email – giriait@gmail.com.

² **Mr. Anooplal. K. S** received B. E. Degree in Information Science & Engineering (ISE) from VTU, Belagavi and M.Tech Degree in Computer Science & Engineering (CSE) from Sahyadri College of Engineering & Management Mangaluru, India, affiliated to Visvesvaraya Technological University (VTU) Belgavi. Email – anooplalks@gamil.com.

CONCLUSION

As an improving technology, not all developers are intimate with speech technology. While the essential accretions of this speech synthesis and speech recognition take only minutes to figure out, there are subtle and powerful capabilities provided by computerized speech.

An effective speech application is one that uses speech to enhance a user's performance of task or enable an activity. Designing an application with speech in mind from the outset is a key success factor. In future it may replace the keyboard and other peripherals.

Most importantly, speech technology does not consistently meet the immense assumptions of users familiar with formal human to human speech communication. Understanding the limitations—as well as the strengths—is important for effective use of speech input and output in a user interface. So here we present in our project a provision for user to open various applications such as Microsoft Word, Microsoft Excel, and Notepad just by saying a word. We can also open calculator and perform various operations in it.

REFERENCES:

- 1) K. H. Davis, R. Biddulph, and S. Balashek “Automatic Recognition of Spoken Digits”, J. Acoust. Soc. Am. 24 (6):637-642, 1952.
- 2) H. F. Olson and H. Belar, “Phonetic Type writer”, J. Acoust. Soc. Am, 28(6):1072-1081, 1956.
- 3) B. Fry, “Theoretical Aspects of Mechanical Speech Recognition”; and P. Denes, “The Design and Operation of the Mechanical Speech Recognizer at University College London,” J. British Inst. Radio Engr., 19: 4, 211-229, 1959.
- 4) J. W. Forgie and C. D. Forgie, “Results Obtained From a Vowel Recognition Computer Program,” J. Acoust. Soc. Am., 31(11): 1480-1489, 1959.
- 5) J. Suzuki and K. Nakata, “Recognition of Japanese Vowels-Preliminary to the Recognition of Speech,” J. Radio Res. Lab, 37(8): 193-212, 1961.
- 6) T. Sakai and S. Doshita, “The Phonetic Typewriter, Information Processing 1962,” Proc. IFIP Congress, Munich, 1962.
- 7) K. Nagata, Y. Kato, and S. Chiba, “Spoken Digit Recognizer for Japanese Language,” NEC Res. Develop., No6, 1963.
- 8) T. B. Martin, A.L. Nelson, and H. J. Zadell, “Speech Recognition by Feature Abstraction Techniques,” Tech. Report ALT-TDR-64-176, Air Force Avionics Lab 1964.
- 9) T. K. Vintsyuk, “Speech Discrimination by Dynamic Programming,” Kibernetika, 4(2); 81-88, Jan-Feb 1968.
- 10) R. Reddy, “An Approach to Computer Speech Recognition by Direct Analysis of the Speech Wave,” Tech. Reprint No. C549, Computer Science Dept., Stanford Univ., September 1966.
- 11) M. Velichko and N. G. Zagoruyko “Automatic Recognition of 200 words”, Int. J. Man-Machine Studies, 2:223, June 1970.
- 12) H. Sakoe and S. Chiba, “Dynamic Programming Algorithm Optimization for Spoken word Recognition,” IEEE Trans. Acoustics, Speech, Signal Proc., and ASSP-26 (1): 43-49, February 1978.
- 13) Itakura “Minimum Prediction Residual Applied to Speech Recognition”, IEEE Trans. Acoustics, Speech, Signal Proc., ASSP-23(1):67-72, February 1975.

- 14) C. Tappert, N. R. Dixon, A. S. Rabinowitz, and W. D. Chapman, "Automatic Recognition Of Continuous Speech Utilizing Dynamic Segmentation, Dual Classification, Sequential Decoding and Error Recovery," Rome Air Dev. Cen, Rome, NY, Tech. Report TR-71-146, 1971.
- 15) Jelinek, L. R. Bahl, and R. L. Mercer, "Design of a Linguistic Statistical Decoder for the Recognition of Continuous Speech", IEEE Trans. Information Theory, IT-21: 250-256, 1975.
- 16) Jelinek, "The Development of an Experimental Discrete Dictation Recognizer", Proc. IEEE, 73(11):1616-1624, 1985.
- 17) L. R. Rabiner, S. E. Levinson, A. E. Rosenberg, and J. G. Wilpon, "Speaker Independent Recognition of Isolated Words Using Clustering Techniques", IEEE Trans. Acoustics, Speech, Signal Proc., ASSP-27:336-349, August 1979.
- 18) Sakoe, "Two Level DP Matching -A Dynamic Programming Based Pattern Matching Algorithm for Connected Word Recognition," IEEE Trans. Acoustics, Speech, Signal Proc., ASSP-27:588-595, December 1979.
- 19) S. Bridle and M.D. Brown, "Connected Word Recognition Using Whole Word Templates," Proc. Inst. Acoust. Automn Conf., 25-28, November 1979.
- 20) S. Myers and L. R. Rabiner, "A Level Building Dynamic Time Warping Algorithm For Connected Word Recognition," IEEE Trans. Acoustics, Speech, Signal Proc., ASSP-29:284-297, April 1981.
- 21) H. Lee and L. R. Rabiner, "A Frame Synchronous Network Search Algorithm for connected Word Recognition," IEEE Trans. Acoustics, Speech, Signal Proc., 37(11): 1649-1658, November 1989.
- 22) Ferguson, Ed., Hidden Markov Models for Speech, IDA, Princeton, NJ, 1980.
- 23) R. Rabiner, "A Tutorial on Hidden Markov Models and Selected Applications in Speech Recognition", Proc. IEEE, 77(2):257-286, February 1989.
- 24) R. P. Lippmann, "An Introduction to Computing with Neural Nets," IEEE ASSP Mag., 4 (2):4-22, April 1987.
 - a. Weibel, T. Hanazawa, G. Hinton, K. Shikano, and K. Lang, "Phoneme Recognition Using Time-Delay Neural Networks" IEEE Trans. Acoustics, Speech, Signal Proc., 37:393-404, 1989.
- 25) F. Lee, H. W. Hon, and D. R. Reddy, "An Overview of the SPHNX Speech Recognition System," IEEE Trans. Acoustics, Speech, Signal Proc., 38:600-610, 1990.
- 26) Y. L. Chow, M. O. Dunham, O. A. Kimball, M. A. Krasner, G. F. Kubala, J. Makhoul, S. Roucos, and R. M. Schwartz, "BBYLOS: The BBN Continuous Speech Recognition System," Proc. ICASSP 87, 89-92, April 1987.
- 27) B. Paul, "The Lincoln Robust Continuous Speech Recognizer," Proc. ICASSP 89, Glasgow, Scotland, 449-452, May 1989.
- 28) Weintraub et al., "Linguistic Constraints in Hidden Markov Model Based Speech Recognition," Proc. ICASSP 89, Glasgow, Scotland, 699-702, May 1989.
- 29) Zue, J. Glass, M. Phillips, and S. Seneff, "The MIT Summit Speech Recognition System: A Progress Report," Proc. DARPA Speech and Natural Language Workshop, 179-189, February 1989.

Hardware architecture of a Real Time Operating System

Shweta Ohri

Jagannath International Management School,

Vasant Kunj, New Delhi-70

Emails: shweta.ohri@jagannath.org

Abstract- In this paper we discuss prescribed design of a real time operating system. A real-time operating system provides a platform for the design and implementation of a wide range of applications in real-time systems, embedded systems, and mission-critical systems. The conceptual model of the real time operating system is introduced as the initial requirements for the system. Our main focus on this paper is to explain some fundamental processes of real time operating system like The CPU Scheduling Process, The System Initialization Process, The System Clock Process, and The System Event Capture Process in brief.

Keywords:

The Real Time Operating System, The CPU Scheduling Process, The Memory Management Process, The Device Management Process, The File Management Process, UPMS for process management in real time operating system, UPMs for System Management in real time operating system.

1. Introduction

As we know that An operating system is a set of integrated system software that organizes, manages, and controls the resources and computing power of a computer or a computer network. It also provides users a logical interface for accessing the physical machine in order to run applications. A general-purpose operating system may be perceived as an agent between the hardware and resources of a computer and the applications and users. An operating system may be divided into three subsystems known as those of the kernel or system management, the resource management, and the process management. The kernel of an operating system is a set of central components for computing, including CPU scheduling and process management. The resource management subsystem is a set of supporting functions for various system resources and user interfaces. The process management subsystem is a set of transition manipulation mechanisms for processes and threads interacting with the system kernel and resources.

A real-time operating system (RTOS) is an operating system that supports and guarantees timely responses to external and internal events of real-time systems. An RTOS monitors, responds to, and controls an external environment, which is connected to the computer system through sensors, actuators, or other input-output (I/O) devices. In a real-time system in general and an RTOS in particular, the correctness of system behaviors depends not only on the logical results of computation but also on the time point at which the results are obtained. Real-time systems can be divided into hard and soft real-time systems. In the former, a failure to meet timing constraints will be of serious consequences, while in the latter, a timing failure may not significantly affect the functioning of the system.

A great variety of real-time operating system has been developed in the last decades. The existing real-time operating system is characterized as target-machine-specific, implementation-dependent, and not formally modeled. Therefore, they are usually not portable as a generic real-time operating system to be seamlessly incorporated into real-time or embedded system implementations. Problems often faced by real-time operating system are CPU and tasks scheduling, time/event management, and resource management. Efficient and precise methodologies and notations for describing solutions to these problems are critical in RTOS design and implementation. Generally, real-time operating system requires multitasking, process threads, and a sufficient number of interrupt levels to deal with the random interrupt mechanisms in real-time systems. In modern real-time operating system, multitasking is a technique used for enabling multiple tasks to share a single processor. A thread is individual execution of a process in order to handle concurrent tasks. In addition, an interrupt is a request of an external device or internal process that causes the operating system to suspend the execution of a current low priority task, serve the interrupt, and hand control back to the interrupted process.

This paper develops a comprehensive design paradigm of the formal real-time operating system in a top-down approach. In the remaining of this paper, there are five more sections. In Section 2, we provide a succinct thought about the CPU scheduling process.

Also, the memory management process, the device management process and the file management process are discussed in section 3, 4 and 5. Finally, conclusions and references are provided in Section 6 and 7.

2. The CPU Scheduling Process

CPU scheduling is the most inner kernel process of a real-time operating system to maximize CPU utilization. Real time operating system adopts multiprocess and multithread techniques to keep the CPU running different processes or threads of multiple processes on a time-sharing basis with a predetermined scheduling interval. The CPU scheduler selects which process in the ready queue should be run next based on a predefined scheduling algorithm or strategy. The CPU scheduler switches control of the CPU to the process selected for a certain time interval.

In real-time operating system, every ten time-intervals (10ms) forms a cycle to run all ready processes in the ReadyQHST (maximum 6) and ReadyQLST (maximum 4) as specified in the design of the system control block SCBST. The CPU scheduler process of real-time operating system, CPUSchedulerPC, dispatches a maximum of ten processes in both ready queues ReadyQHST and ReadyQLST within a low interrupt period 10ms, where each of them will be dispatched for running for 1ms scheduled by the high interrupt period. In the peak CPU load period of real-time operating system, 6 tasks from ReadyQHST and 4 from ReadyQLST will be scheduled, respectively, in a series of ten 1ms time intervals. However, during low CPU load period, any combination of high/low tasks may be scheduled including a series of multiple threads of the same process. In case there is a current task in the CPU but no other task in the ReadyQHST and ReadyQLST, the currently scheduled task may continue to run for at least another 1ms interval until the statuses of the ready queues are changed. Except the above two special conditions, the current process will be swapped out of the CPU as a delayed process. Instead, a new qualified process in the front of ReadyQHST or ReadyQLST will be scheduled into CPU for running.

3. The Memory Management Process

Memory management is one of the key functions of operating systems because memory is both the working space and storage of data and files. real-time operating system adopts a flexible segmentation method for system memory management with variable sizes of memory blocks for different events and processes. MemoryManagementPC supports dynamic and absolute physical memory manipulations that are necessary for real-time operating systems and real-time applications.

The process AllocateMemoryPC deals with dynamic memory allocations in real-time operating system. When a request for memory from a process is identified by the system, AllocateMemoryPC searches for a suitable sized memory block that is free. When a suitable memory block is identified by a given memory block number (MBN), AllocateMemoryPC sets its status as in-use.

The process ReleaseMemoryPC deals with dynamic memory release requests of the system when a process terminates and the memory allocated to it is no longer required. ReleaseMemoryPC operates on the memory control block when it is invoked. It gets the memory block number associated to the process that requests to release the memory. Then, it sets the status of the given memory block to free.

4. The Device Management Process

Devices as well as their I/O ports are directly manipulated by the processes DeviceManagementPC in real-time operating system. DeviceManagementPC encompasses both GetDevicePC and ReleaseDevicePC processes. Additional plug-in device drivers may also be incorporated via the same interface mechanisms by the adding device and deleting device processes.

The process GetDevicePC handles device allocations in real-time operating system. When a request for a device from a process is identified by the system, GetDevicePC searches for a suitable type of device that is free. When a suitable device is found, GetDevicePC sets its status as seized. Then, the associate process required the device is registered in the device control block. If there is no free and/or suitable device available in the system, a feedback status, &DeviceAllocatedBL:= F, will be generated.

The process ReleaseDevicePC handles device release requests for the system when a process terminates the use of a device. ReleaseDevicePC operates on the device control block when it is invoked. It first gets the device number (DNN) to be released associated to the process. Then, it sets the status of the given device in DCBST as free and disconnects the link between the device and the previously associated process.

5. The File Management Process

On the basis of the architectural model of the file system FilesST, the behaviors of the file management subsystem of real-time operating system, FileManagementPC, are modeled by a set of 14 behavioral processes in the categories of file system administrations and file manipulations. .

UPMS for Process Management in Real Time Operating System

A process is a basic unit of system function that represents an execution of a program on a computer under the support of an operating system. A process can be a system process or a user process. The former executes system code, and the latter runs an application. Processes may be executed sequentially or concurrently depending on the type of operating systems.

A thread is an important concept of process management in operating systems. A thread is a basic unit of CPU utilization, or a flow of control within a process, supported by a PCBST, a program counter, a set of registers, and a stack. Conventional operating systems are single thread systems. Multithreaded systems enable a process to control a number of execution threads. The benefits of multithreaded operating system are responsiveness, resource sharing, implementation efficiency, and utilization of multiprocessor architectures of modern computers.

According to the high level specifications of the static behaviors of real-time operating system, the process management subsystem of real-time operating system encompasses a set of nine task handling processes corresponding to the states of behavioral processes for the entire task lifecycle of process manipulating.

The Static Behavioral Models of the Real Time Operating System

According to the RTPA methodology, a static behavior is an encapsulated function of a given system that can be determined before run-time. On the basis of the system architecture specifications and with the UDMs of system architectural components developed in the preceding section, the operational components of the given real-time operating system system and their behaviors can be specified as a set of UPMs as behavioral processes operating on the UDMs.

The basic functions of operating systems can be classified as system management, resources management, and processes management. The high-level static behaviors of real-time operating system StaticBehaviorsPC, encompasses three process subsystems such as SystemManagementPC, ResourcesManagementPC, and ProcessesManagementPC in parallel.

The following subsections describe how the real time operating system static behaviors in the three subsystems are modeled and refined using the denotation mathematical notations and methodologies of RTPA.

UPMs for System Management in Real-Time Operating System

According to the high level specifications of the static behaviors of real time operating system, the system management subsystem of real time operating system encompasses a set of five behavioral processes such as system initialization, system clock manipulation, system event capture, Device interrupt handling, and the CPU scheduler.

6. Conclusion

The design of real-time operating systems has been recognized as a comprehensive and complex system design paradigm in computing, software engineering, and information system design. This paper has demonstrated that the real time operating system (RTOS), including its architecture, static behaviors, and dynamic behaviors, can be essentially and sufficiently described by real time process algebra. On the basis of the formal specifications of real time process algebra (RTPA) by the coherent set of unified data models (UDMs) and unified process models (UPMs) in RTPA, the architectural and behavioral consistency and run-time integrity of an RTOS have been significantly enhanced. It has been identified that RTOS can be applied not only as a formal design paradigm of RTOS's, but also a support framework for a wide range of applications in design and implementation of real-time and embedded systems. The RTOS model may have also provided a test bench for the expressive power and modeling.

With a stepwise specification and refinement methodology for describing both system architectural and operational components, the formal model of the RTOS system has provided a foundation for implementation of a derived real-time operating system in multiple programming languages and on different operating platforms. It has also improved the controllability, reliability, maintainability, and quality of the design and implementation in real-time software engineering. The formal models of RTOS have been adopted as part of the supporting environment for the implementation of the RTPA-based software code generator (RTPA-CG). On the basis of the formal and rigorous models of the RTOS, code can be automatically generated by RTPA-CG or be manually transferred from the formal models.

A series of formal design models of real-world and real-time applications in RTPA have been developed using RTPA notations and methodologies in the formal design engineering approach, such as the telephone switching system, the lift dispatching system, the automated teller machine (ATM), the real-time operating system, the air traffic control system, the railway dispatching system, and the intelligent traffic lights control system. Further studies have demonstrated that RTPA is not only useful as a generic notation and

methodology for software engineering, but also good at modeling human cognitive processes in cognitive informatics and computational intelligence as reported.

REFERENCES:

- [1] Anderson, T. E., Lazowska, E. D., & Levy, H. M. (1989). The Performance Implications of Thread Management Alternatives for Shared-Memory Multiprocessors. *IEEE Transactions on Computers*, 38(12), 1631–1644. doi:10.1109/12.40843
- [2] Bollella, G. (2002). *The Real-Time Specification for Java*. Reading, MA: Addison Wesley.
- [3] Brinch-Hansen, P. (1971). Short-Term Scheduling in Multiprogramming Systems. In *Proceedings of the Third ACM Symposium on Operating Systems Principles* (pp. 103-105).
- [4] Deitel, H. M., & Kogan, M. S. (1992). *The Design of OS/2*. Reading, MA: Addison-Wesley.
- [5] Dijkstra, E. W. (1968). The Structure of the Multiprogramming System. *Communications of the ACM*, 11(5), 341–346. doi:10.1145/363095.363143
- [6] ETTX. (2009, February). In *Proceedings of the First European TinyOS Technology Exchange*, Cork, Ireland.
- [7] Ford, B., Back, G., Benson, G., Lepreau, J., Lin, A., & Shivers, O. (1997). The Flux OSKit: a Substrate for OS and Language Research. In *Proceedings of the 16th ACM Symposium on Operating Systems Principles*, Saint Malo, France.
- [8] ISO/IEC 9945-1. (1996). *ISO/IEC Standard 9945-1: Information Technology-Portable Operating System Interface (POSIX) - Part 1: System Application Program Interface (API) [C Language]*. Geneva, Switzerland: ISO/IEC.
- [9] Kreuzinger, J., Brinkschult, U. S., & Ungerer, T. (2002). *Real-Time Event Handling and Scheduling on a Multithread Java Microcontroller*. Dordrecht, The Netherlands: Elsevier Science Publications.
- [10] Labrosse, J. J. (1999). *MicroC/OS-II, The Real-Time Kernel* (2nd ed.). Gilroy, CA: R&D Books.
- [11] Lamie, E. L. (2008). *Real-Time Embedded Multithreading using ThreadX and MIPS*.
- [12] Laplante, P. A. (1977). *Real-Time Systems Design and Analysis* (2nd ed.). Washington, DC: IEEE Press.
- [13] Lewis, B., & Berg, D. (1998). *Multithreaded Programming with Pthreads*. Upper Saddle River, NJ: Sun Microsystems Press.
- [14] Liu, C., & Layland, J. (1973). Scheduling Algorithms for Multiprogramming in Hard-Real-Time Environments. *Journal of the Association for Computing Machinery*, 20(1), 46–56.
- [15] McDermid, J. (Ed.). (1991). *Software Engineer's Reference Book*. Oxford, UK: Butterworth Heinemann Ltd.
- [16] Ngolah, C. F., & Wang, Y. (2009). Tool Support for Software Development based on Formal Specifications in RTPA. *International Journal of Software Engineering and Its Applications*, 3(3), 71–88.
- [17] Ngolah, C. F., Wang, Y., & Tan, X. (2004). The Real-Time Task Scheduling Algorithm of RTOS+. *IEEE Canadian Journal of Electrical and Computer Engineering*, 29(4), 237–243.
- [18] Peterson, J. L., & Silberschultz, A. (1985). *Operating System Concepts*. Reading, MA: Addison-Wesley.
- [19] Rivas, M. A., & Harbour, M. G. (2001). MaRTE OS: An Ada Kernel for Real-Time Embedded Applications. In *Proceedings of Ada-Europe 2001*, Leuven, Belgium.
- [20] Sha, L., Rajkumar, R., & Lehoczky, J. P. (1990). Priority Inheritance Protocols: An Approach to Real-Time Synchronization. *IEEE Transactions on Computers*, 39(12), 1175. doi:10.1109/12.57058
- [21] Silberschatz, A., Galvin, P., & Gagne, G. (2003). *Applied Operating System Concepts* (1st ed.). New York: John Wiley & Sons, Inc.
- [22] Tanenbaum, A. S. (1994). *Distributed Operating Systems*. Upper Saddle River, NJ: Prentice Hall Inc.
- [23] Viscarola, P. G., & Mason, W. A. (2001). *Windows NT Device Driver Development*. New York: Macmillan.
- [24] Wang, Y. (2002). The Real-Time Process Algebra (RTPA). *Annals of Software Engineering: An International Journal*, 14, 235–274. doi:10.1023/A:1020561826073
- [25] Wang, Y. (2004). *Operating Systems*. In Dorf, R. (Ed.), *The Engineering Handbook* (2nd ed.). Boca Raton, FL: CRC Press.
- [26] Wang, Y. (2007). *Software Engineering Foundations: A Software Science Perspective*. In *Software Engineering*, Vol. II. New York: Auerbach Publications.
- [27] Wang, Y. (2008a). RTPA: A Denotational Mathematics for Manipulating Intelligent and Computational Behaviors. *International Journal of Cognitive Informatics and Natural Intelligence*, 2(2), 44–62.
- [28] Wang, Y. (2008b). Mathematical Laws of Software. *Transactions of Computational Science*, 2, 46–83. doi:10.1007/978-3-540-87563-5_4
- [29] Wang, Y. (2008c). Deductive Semantics of RTPA. *International Journal of Cognitive Informatics and Natural Intelligence*, 2(2), 95–121.
- [30] Wang, Y. (2008d). On Contemporary Denotational Mathematics for Computational Intelligence. *Transactions of Computational Science*, 2, 6–29. doi:10.1007/978-3-540-87563-5_2
- [31] Wang, Y. (2009a). Paradigms of Denotational Mathematics for Cognitive Informatics and Cognitive Computing. *Fundamenta Informaticae*, 90(3), 282–303.
- [32] Wang, Y. (2009b). The Formal Design Model of a Telephone Switching System (TSS). *International Journal of Software Science and Computational Intelligence*, 1(3), 92–116.

- [33] Wang, Y., & Chiew, V. (2010). On the Cognitive Process of Human Problem Solving. *Cognitive Systems Research: An International Journal*, 11(1), 81–92. doi:10.1016/j.cogsys.2008.08.003
- [34] Wang, Y., & Huang, J. (2008). Formal Modeling and Specification of Design Patterns Using RTPA. *International Journal of Cognitive Informatics and Natural Intelligence*, 2(1), 100–111.
- [35] Wang, Y., Ngolah, C. F., Ahmadi, H., Sheu, P. C. Y., & Ying, S. (2009). The Formal Design Model of a Lift Dispatching System (LDS). *International Journal of Software Science and Computational Intelligence*, 1(4), 98–122.
- [36] Wang, Y., Ngolah, C. F., Zeng, G., Sheu, P. C. Y., Choy, C. P., & Tian, Y. (2010c). The Formal Design Model of a Real-Time Operating System (RTOS+): Conceptual and Architectural Frameworks. *International Journal of Software Science and Computational Intelligence*, 2(2), 107–124.
- [37] Wang, Y., & Ruhe, G. (2007). The Cognitive Process of Decision Making. *International Journal of Cognitive Informatics and Natural Intelligence*, 1(2), 73–85.
- [38] Wang, Y., Tan, X., & Ngolah, C. F. (2010b). Design and Implementation of an Autonomic Code Generator based on RTPA. *International Journal of Software Science and Computational Intelligence*, 2(2), 44–67

Variance of atmospheric radio wave refractivities across Nigeria – from the Savannah to the mangrove

Amajama Joseph, Iniobong Prosper Etim

University of Calabar-Nigeria, joeamajama2014@yahoo.com, +2347036357493

Abstract— The variance of atmospheric radio wave refractivities across the different vegetative climatic belts in Nigeria has been examined. Data abstracted from Weather API (Weather2), Yr. no and NIMET (Nigeria meteorological agency) websites has been analyzed. Generally, there was an increase in the average atmospheric radio wave refractivities as one confronts the coastline of the Atlantic Ocean and in the reverse, there was a decrease in the average atmospheric radio wave refractivities as one travels towards the borderline of the Sahara desert. This indicates that, gradually radio wave propagation worsens towards the Atlantic Ocean and reversely; step by step, the radio wave propagation betters towards the Sahara desert. The correlation between the average atmospheric radio wave refractivities and the perpendicular distances away from the coastline of the Atlantic Ocean was 0.84 with an approximate model of $y = -0.125x + 388.9$. Similarly, the correlation between the average atmospheric radio wave refractivities and the perpendicular distances away from the Sahara desert was 0.84 with an approximate model of $y = 0.122x + 267.2$. The correlations were not absolute because of the non-uniformity of the weather or climate patterns across the country. Reliefs and rivers account for some of the anomalies in the non-uniform trends. In addition, isotherms and isohyets in the weather map are non-linear and can cut across the vegetative climatic zones. By and large, results registered that the Sahel savannah will favour radio signal propagation through the troposphere better than any other belt and the mangrove was the least, but on the contrary, the mangrove will record better signal stability than any other belt and the Sahel savannah will register the least due to high variance in the weather pattern in the former than the latter belt. Finally, the dry will favour radio signal propagation through the troposphere better than the wet due to reduction in mean monthly relative humidities.

Keywords— Variance, Atmospheric radio wave refractivity, Vegetative climatic belts, Savannah, Rainforest, Mangrove and Radio signal strength.

INTRODUCTION

Radio wave is a member of the electromagnetic wave. It is an essential element required for communications. The range of their frequencies is from 300GHz to as low as 3Hz and their proportionate wave lengths span 1 millimeter to 100 kilometers [11]. The atmosphere is an indispensable channel for the propagation of radio waves, most especially communications that employ tropospheric propagation mode [9]. The condition of the atmosphere has a force on propagating radio waves through it.

Refractivity or refraction is the bending of electromagnetic waves away from a particular path due to difference in the composition of the medium(s) which they travel through [7]. The difference in medium(s) is observed as an obstacle, especially if the composition of the new medium(s) is denser. It alters the speed and direction of propagation of the radio wave.

In the atmosphere, radio wave refractivity is the variation of radio waves from a straight path as it propagates through the atmosphere due to variation in the density of air as a function of altitude [1] [5]. Radio wave refractivity in the atmosphere is due to the velocity of radio waves through air decreasing (or increasing) with increasing (or decreasing) density (this is, increasing or decreasing index of refraction) [6]. The afore-mentioned is true, since the index of atmospheric radio wave refractivity is the ratio of the speed of radio wave in free space to that of the radio wave in the atmosphere. The speed of the radio wave is a function of the density of the medium which it is travelling through [10].

Without atmospheric radio wave refractivity, it will be near impossible for radio waves or signals to travel round the globe [9]. The atmosphere as a channel bends the radio wave back to the earth after being transmitted into space from an earth station. However, study has shown that refractivity has a negative force on radio waves together with the weather components [1].

The weather of a place is the state of its atmosphere at a particular time [2], while the climate of a place is the general weather conditions prevailing in a place over a very long period [3]. Weather components, atmospheric pressure, temperature, humidity bear negatively on radio waves, invariably radio signals [1]. Also depending on the direction of wind, the atmosphere has an impact on radio waves. Mathematically, radio wave refractivity is a function of atmospheric pressure and temperature and relative humidity.

Nigeria is divided into several climatic belts depending on their vegetations. The vegetation of a place is a mirror of the state of the atmosphere of that place and invariably the weather or climate of that place. The different vegetative climatic belts in Nigeria are: Sahel savannah, Sudan savannah, Guinea savannah, Rainforest, Mangrove (freshwater and saltwater types) and Montane [4].

Nigeria falls on the tropical plate of Africa and lies between longitudes $4^{\circ}00'00''$ E and $14^{\circ}00'00''$ E and latitudes $3^{\circ}00'00''$ N and $14^{\circ}00'00''$ N respectively [4]: a location slightly above the equator.

The focus of this research narrows on the variance of the atmospheric radio wave refractivities across Nigeria; from the savannah belts to the rainforest belt, through to the mangrove belt and the relatively striking montane belts. Also, the relevance of the work is to establish the best belt(s) suitable for radio wave propagation and the worse. More so, it intends to probe and draw a verdict on which atmospheric or climatic conditions are favourable for radio wave propagation, since Nigeria has predominantly two seasons: the wet and the dry and both have characteristic different atmospheric conditions.

A REVIEW OF THE CLIMATE OF SELECTED CITIES ON THE DIFFERENT VEGETATIVE CLIMATIC BELTS

In this research, data from eighteen cities (18) in Nigeria was analyzed. The cities are situated on different belts. The cities captured are: Kano, Maiduguri, Minna, Akure, Aba, Onitsha, Makurdi Abuja, Enugu, Calabar, Lagos, Jos, Sokoto, Obudu, Lokoja, Warri, Kaduna and Ibadan. Below is a review of the climates of the different cities.

Kano – This is a city formerly in the Sudan savannah but presently in the Sahel savannah in view of the Nigerian satellite images and global climatic changes due to undue warming of the globe. It is situated in longitude and latitude $8^{\circ}31'0.12''$ E and $12^{\circ}00'00''$ N respectively in Northern Nigeria [50]. Kano shows monthly average minimum and maximum humidities of 25.00 % in August and 80.00 % in March respectively and an overall monthly mean humidity of 51.42 % [47]. Also, it shows monthly mean minimum and maximum temperatures of 71.60°F in February and March and 89.60°F in April with a gross monthly mean temperature of 79.40°F [28].

Maiduguri – This is a city in the Sahel savannah. It is situated in longitude and latitude $13^{\circ}9'35''$ E and $11^{\circ}50'42''$ N respectively [48]. It is in the northern segment of Nigeria. It records monthly average minimum and maximum humidities of 28.00 % in March and 82.00 % in August respectively and an overall monthly mean humidity of 53 % [46]. Also, it records monthly mean minimum and maximum temperatures of 71.60°F in December and January and 90.50°F in May with a gross monthly mean temperature of 81.05°F [27].

Abuja – It is situated in the heart of Nigeria. It sits on the Guinea savannah belt with a longitude and latitude of $7^{\circ}10'50''$ E and $9^{\circ}10'32''$ N in that order [51]. It shows monthly mean minimum and maximum humidities of 30.00 % in December and 84.00 % in July respectively and an overall monthly mean humidity of 60.50 % [41]. Also, it shows monthly mean minimum and maximum temperatures of 77.18°F in July and 86.36°F in March with a gross monthly mean temperature of 87.14°F [13].

Enugu – It is situated in the east of the southern segment of Nigeria. The longitude and latitude of the city is $6^{\circ}26'24.71''$ E and $7^{\circ}29'39.47''$ N in that order [62]. It is in the rainforest belt with a derived savannah and it is located on an escarpment in-between the Cross River basin and Benue trough [12]. Enugu registers monthly mean minimum and maximum humidities of 83.00 % in February and March and 92.00 % in August respectively and an overall monthly mean humidity of 86.75 % [31]. Also, it registers monthly mean minimum and maximum temperatures of 78.88°F in August and 84.74°F in March with a gross monthly mean temperature of 81.20°F [16].

Calabar – This is a city in the shadow of the Atlantic Ocean. It is planted in the southern-most region of Nigeria with longitude and latitude of $8^{\circ}20'49.92''$ E and $4^{\circ}58'33.67''$ N in the sequence [60]. It is in the saltwater Mangrove belt. It shows monthly mean minimum and maximum humidities of 83.00 % in February and March and 92.00 % in August respectively and an overall monthly mean humidity of 86.75 % [32]. Also, it shows monthly mean minimum and maximum temperatures of 76.10°F in August and 83.30°F in February and with a gross monthly mean temperature of 80.27°F [17].

Lagos – This is a city whose outstretched arm hugs the Atlantic Ocean. It stands on the west of southern Nigeria. Its longitude is $3^{\circ}23'44.98''$ E with a latitude of $6^{\circ}27'11.01''$ N. It shares the saltwater Mangrove belt with other cities in the neighbourhood of the Atlantic Ocean [57]. It records monthly mean minimum and maximum humidities of 81.00 % in February and April and 88.00 % in June through October respectively and an overall monthly mean humidity of 84.83 % [37]. Also, it records monthly mean minimum and maximum temperatures of 77.18°F in August and 83.30°F in February and March with a gross monthly mean temperature of 80.25°F [18].

Jos – It is a city in the Northern half of Nigeria. Even though it is located in the Guinea savannah area with a longitude of $8^{\circ}53'31''$ E and a latitude of $9^{\circ}55'42''$ N, it sits on the montane belt. It is embraced by mountains [61]. It registers monthly mean minimum and maximum humidities of 26.00 % in April and 72.00 % in August respectively and an overall monthly mean humidity of 40.80 % [43]. Also, it registers monthly mean minimum and maximum temperatures of 68.00°F in January and 75.74°F in April with a gross monthly mean temperature of 71.11°F [14].

Sokoto – This is a city situated at the northern-most axis of Nigeria with a longitude of $5^{\circ}13'53''$ E and a latitude of $13^{\circ}3'5''$ N [49]. It is in the region just after the borderline of the Sahara desert and lies in the Sahel savannah belt. Sokoto shows monthly mean minimum and maximum humidities of 18.00 % in March and 69.00 % in September respectively and an overall monthly mean humidity of 40.67 % [45]. Also, it shows monthly mean minimum and maximum temperatures of 23.60°F in January and 92.66°F in May with a gross monthly mean temperature of 83.87°F [29].

Obudu – She strikingly sits in the borderland of the Guinea savannah and Rainforest belts and stands on a montane belt. Her longitude and latitude are $9^{\circ}10'0''$ E and $6^{\circ}40'0''$ N in sequence [55]. It is located in the south-eastern region of Nigeria. Obudu records monthly mean minimum and maximum humidities of 57.00 % in February and 90.00 % in August respectively and an overall

monthly mean humidity of 72.82 %. Also, it records monthly mean minimum and maximum temperatures of 77.72 °F in August and 82.20 °F in March with a gross monthly average temperature of 79.52 °F [23].

Lokoja – This city shores the confluence of the rivers Niger and Benue in the borderland of the North and South halves of Nigeria. It is in the Guinea savannah belt with longitude and latitude of 6° 44' 0" E and 7° 48' 0" N in that order. [53]. Lagos registers monthly mean minimum and maximum humidities of 49.00 % in January and 84.00 % in August and September respectively and an overall monthly mean humidity of 71.08 % [40]. Also, it registers monthly mean minimum and maximum temperatures of 78.62 °F in July and 84.74 °F in March with a gross monthly mean temperature of 81.02 °F [25].

Warri – This is a deltaic city, deep down south of Nigeria. Its longitude and latitude are respectively 5° 45' 0" E and 5° 31' 0" N. As a deltaic city, it shores so many freshwater rivers: hence it is classified as a Freshwater mangrove [59]. It shows monthly mean minimum and maximum humidities of 78.00 % in January and 86.00 % July through September respectively and an overall monthly mean humidity of 82.67 % [36]. Also, it shows monthly mean minimum and maximum temperatures of 77.90 °F in July and 83.30 in April and May °F with a gross monthly mean temperature of 80.42 °F [24].

Kaduna – The city is located in the Sudan savannah belt in the north west of Nigeria. Its geographical coordinates are 7° 26' 25" E and 10° 31' 23" N [63]. Kaduna is located on the southern end of the high plains of Northern Nigeria [68]. It is made up of undulating plateau and hills [69]. Kaduna records monthly mean minimum and maximum humidities of 19.00 % in March and 72.00 % in August respectively and an overall monthly mean humidity of 40.08 % [44]. Also, it records monthly mean minimum and maximum temperatures of 76.82 °F in September and 86.36 °F in March with a gross monthly mean temperature of 40.08 °F [15].

Ibadan – It is a city in the western region of southern Nigeria with geographical coordinates of 3° 53' 48.9" E and 7° 23' 16" N [64]. It has a rainforest vegetation. It registers monthly mean minimum and maximum humidities of 70.00 % in February and 90.00 % in August respectively and an overall monthly mean humidity of 82.00 % [38]. Also, it registers monthly mean minimum and maximum temperatures of 75.00 °F in August and September and 80.00 °F in December and April with a gross monthly mean temperature of 78.42 °F [20].

Minna – It is situated in the northern segment of Nigeria. It is located on the Guinea savannah belt with longitude and latitude of 6° 33' 25" E and 9° 36' 50" N in that order [65]. It shows monthly mean minimum and maximum humidities of 15.00 % in February and 82.00 % in August respectively and an overall monthly mean humidity of 46.00 % [42]. Also, it shows monthly mean minimum and maximum temperatures of 82.00 °F in August and 88.00 °F in March with a gross monthly mean temperature of 82.37 °F [26].

Aba – This is a city positioned in the south eastern sector of Nigeria. It has longitude and latitude of 8° 10' 0" E and 7° 21' 0" N in the sequence [56]. It is in the rainforest belt. Aba records monthly mean minimum and maximum humidities of 83.00 % in February and March and 92.00 % in August respectively and an overall monthly mean humidity of 86.75 % similar to her neighbouring city, Calabar [33]. Also, it records monthly mean minimum and maximum temperatures of 77.90 °F in July and 82.40 °F in March and with a gross monthly mean temperature of 86.75 °F [21].

Akure – It is a city in the western segment of southern Nigeria with geographical coordinates of 5° 12' 00" E and 7° 15' 00" N [58]. It has rainforest vegetation. Akure registers monthly mean minimum and maximum humidities of 84.00 % in August and September and 49.00 % in January respectively and an overall monthly mean humidity of 70.50 % [35]. Also, it registers monthly mean minimum and maximum temperatures of 84.00 °F in August and 85.00 °F in March with a gross monthly mean temperature of 80.42 °F [19].

Makurdi – This city embraces the river Benue and it is in the neighbourhood of the Northern and Southern borderline of Nigeria. It is in the Guinea savannah belt with longitude and latitude of 8° 32' 00" E and 7° 44' 00" N [52]. Makurdi shows monthly mean minimum and maximum humidities of 83.00 % in February and March and 92.00 % in August respectively and an overall monthly mean humidity of 86.75 % [39]. Also, it shows monthly mean minimum and maximum temperatures of 78.44 °F in December and 89.80 °F in March with a gross monthly mean temperature of 81.97 °F [30].

Onitsha – It is situated in the east of the southern sphere of Nigeria. The longitude and latitude of the city are 6° 47' 00" E and 6° 10' 00" N in that order [54]. It is in the rainforest belt. Onitsha records monthly mean minimum and maximum humidities of 83.00 % in February and March and 92.00 % in August respectively and an overall monthly mean humidity of 86.75 % [34]. Also, it records monthly average minimum and maximum temperatures of 78.62 °F in July and 84.74 °F in March with a gross monthly mean temperature of 80.98 °F [22].

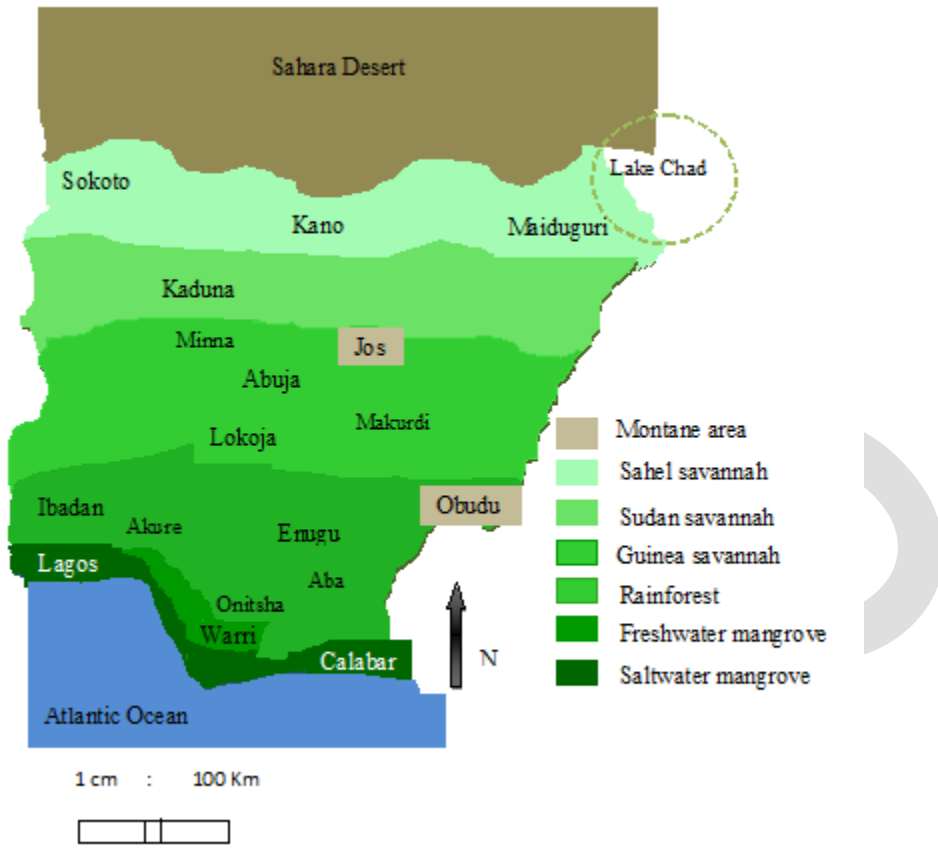


Fig. 1 The locations of the various cities on their respective vegetative climatic belts.

MATERIALS AND METHODS

Relevant data for mean monthly weather parameters was accessed from Yr. no, Weather2 and NIMET (Nigeria Meteorological Agency) websites. The atmospheric radio wave refractivity was computed using the Eqn. 1 below [1].

$$N = K \times P^2 \times \sqrt{T} \times \sqrt[3]{H} \tag{1}$$

Where K = Constant = 0.01064097915

P = Atmospheric pressure in inHg

T = Atmospheric temperature in ⁰F

H = Relative humidity in %

N = Radio refractivity [(inHg)² ⁰F^{1/2} %^{1/3}]

The above formulation has an accuracy of +-5 in comparison with the existing International Telecommunication Union (ITU) expression for calculating Radio refractivity. The ITU expression may be used for all radio frequencies: for frequencies up to 100 GHz, the error is less than 0.5 % [8].

RESULTS AND ANALYSIS

The Figs. 2, 3, 4, 5, 6, 7, 8, 9, 10 show the comparison between the average monthly atmospheric radio wave refractivities of all cities; comparison between average monthly atmospheric radio wave refractivities of the cities in the wet; comparison between the

average monthly atmospheric radio wave refractivities of the cities in the dry; comparison between the average monthly atmospheric radio wave refractivities of the savannah cities; comparison between the average monthly atmospheric radio wave refractivities of the rainforest and mangrove cities; relationship between perpendicular distances away from the Atlantic Ocean and average atmospheric radio wave refractivities; line of best fit between perpendicular distances away from the Atlantic Ocean and average atmospheric radio wave refractivities; relationship between perpendicular distances away from the Sahara desert and average atmospheric radio wave refractivities and line of best fit between perpendicular distances away from the Sahara desert and average atmospheric radio wave refractivities respectively. The legend series of the cities in the figure below is in order of increasing magnitude of average atmospheric radio wave refractivity.

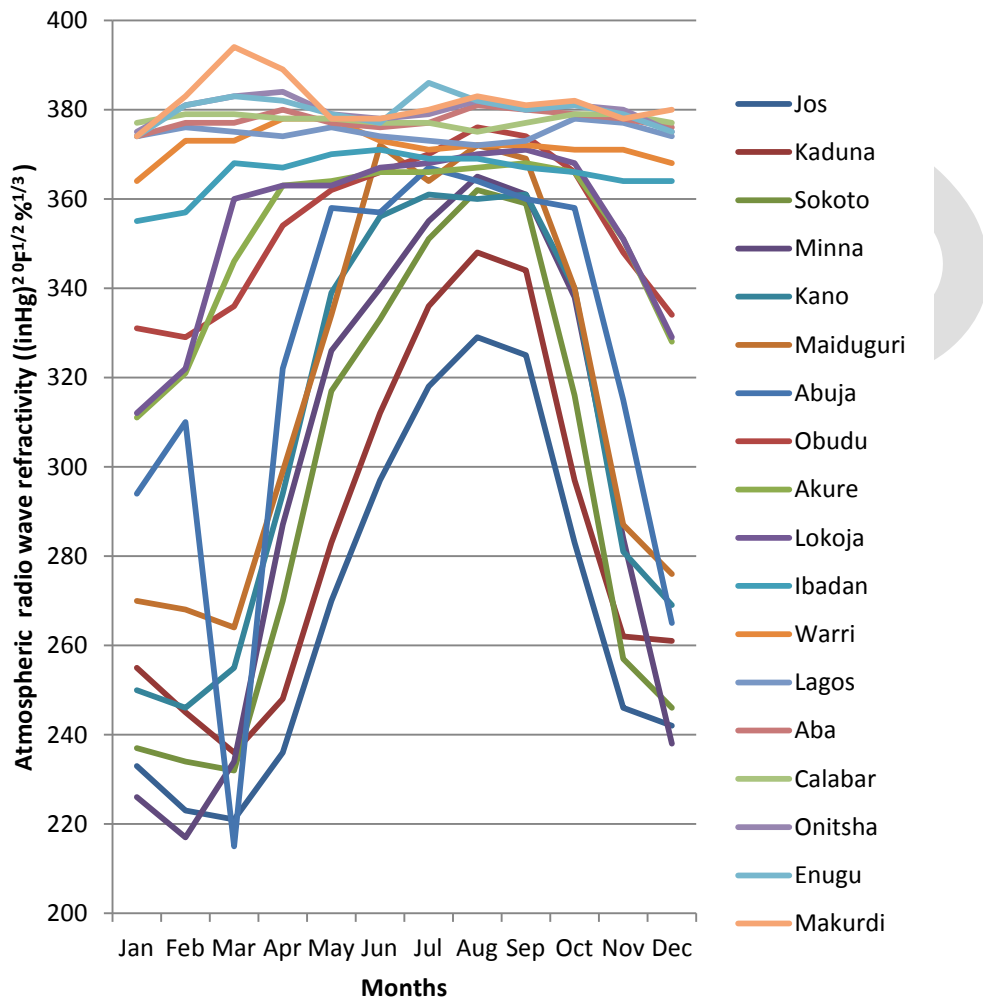


Fig. 2: Comparison between the average monthly atmospheric radio wave refractivities of all cities

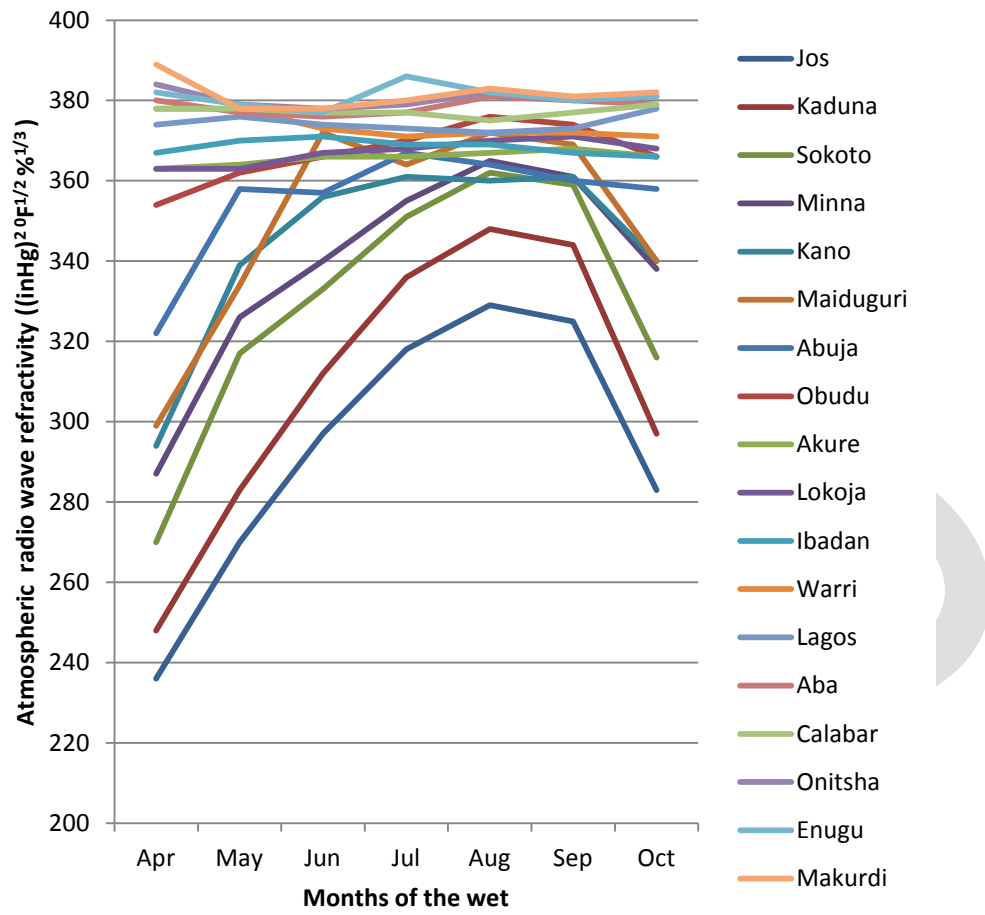


Fig. 3: Comparison between average monthly atmospheric radio wave refractivities of the cities in the wet

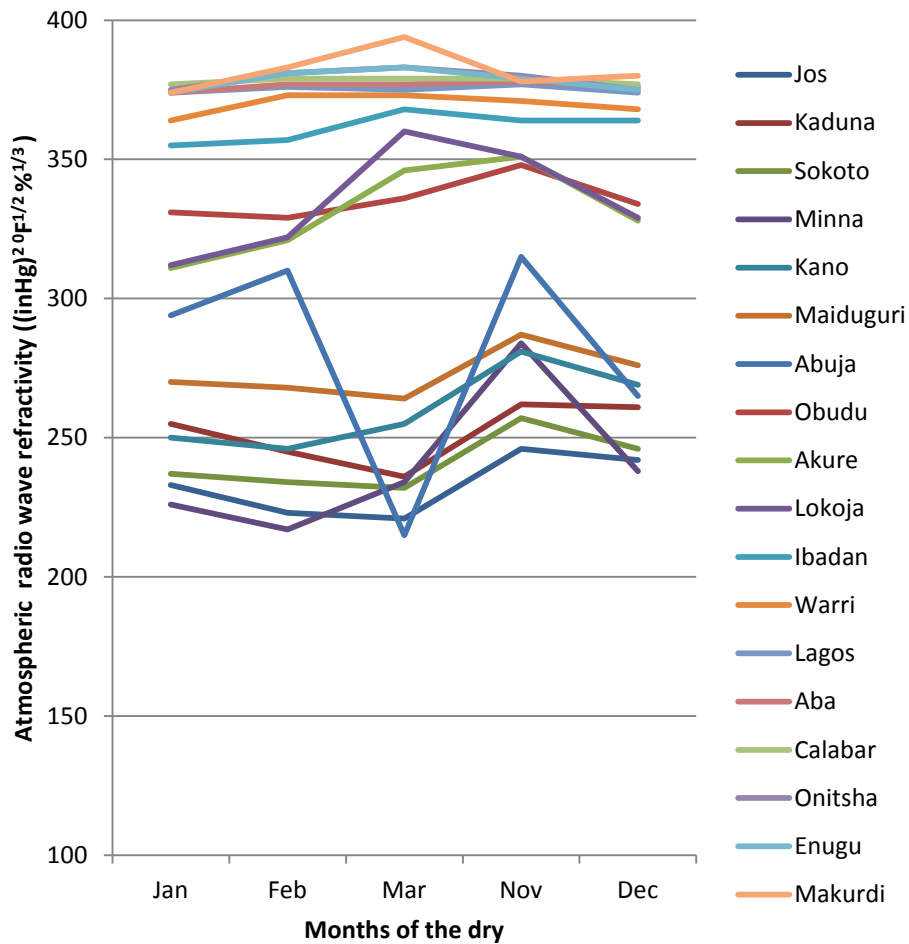


Fig. 4: Comparison between the average monthly atmospheric radio wave refractivities of the cities in the dry

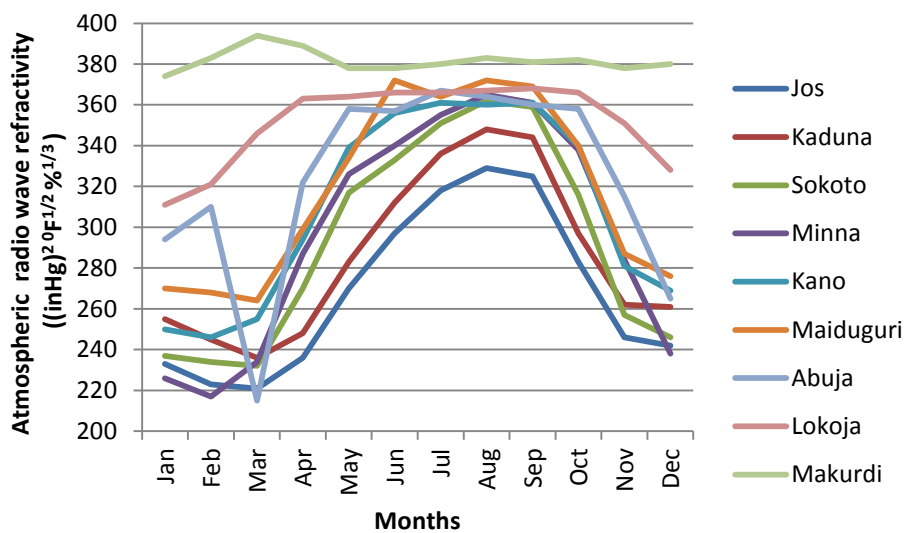


Fig. 5: Comparison between the average monthly atmospheric radio wave refractivities of the savannah cities

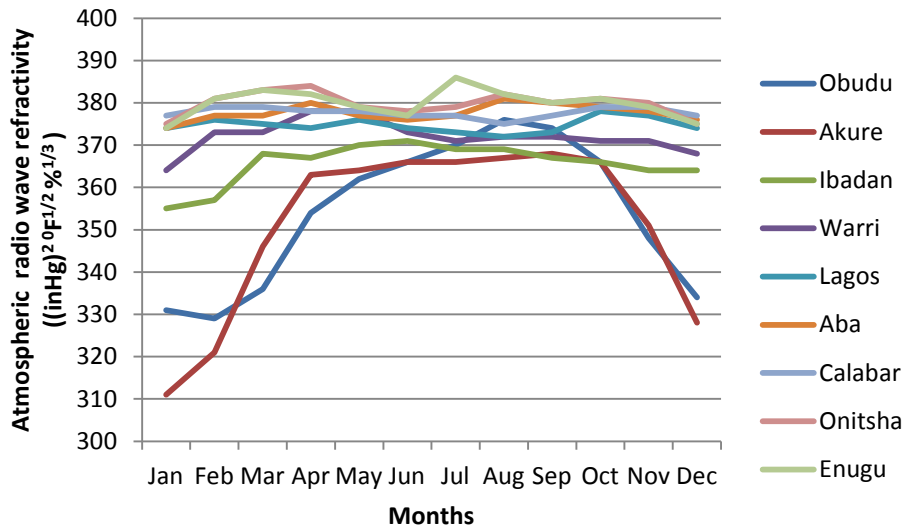


Fig. 6: Comparison between average monthly atmospheric radio wave refractivities of the rainforest and mangrove cities

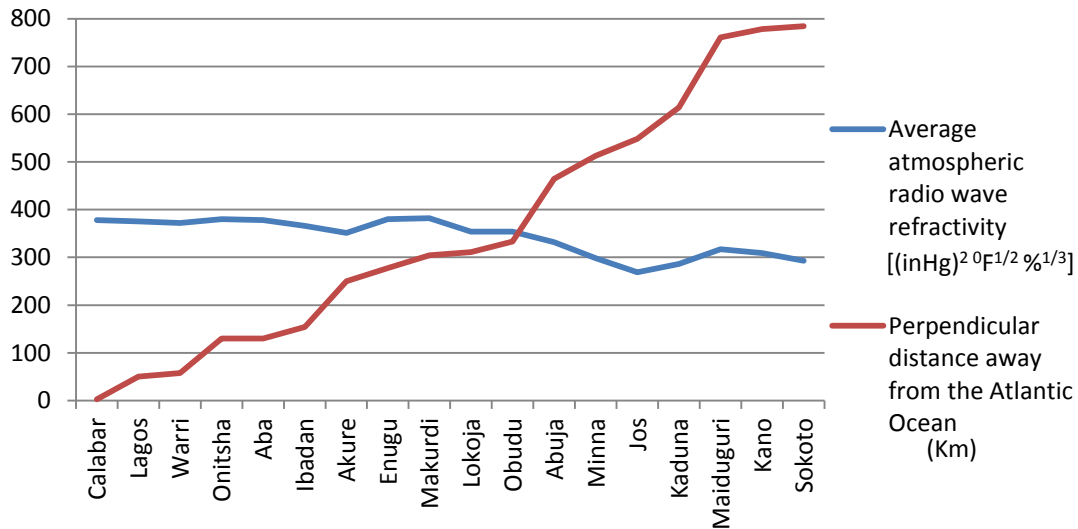


Fig. 7: Relationship between perpendicular distances away from the Atlantic Ocean and average atmospheric radio wave refractivities

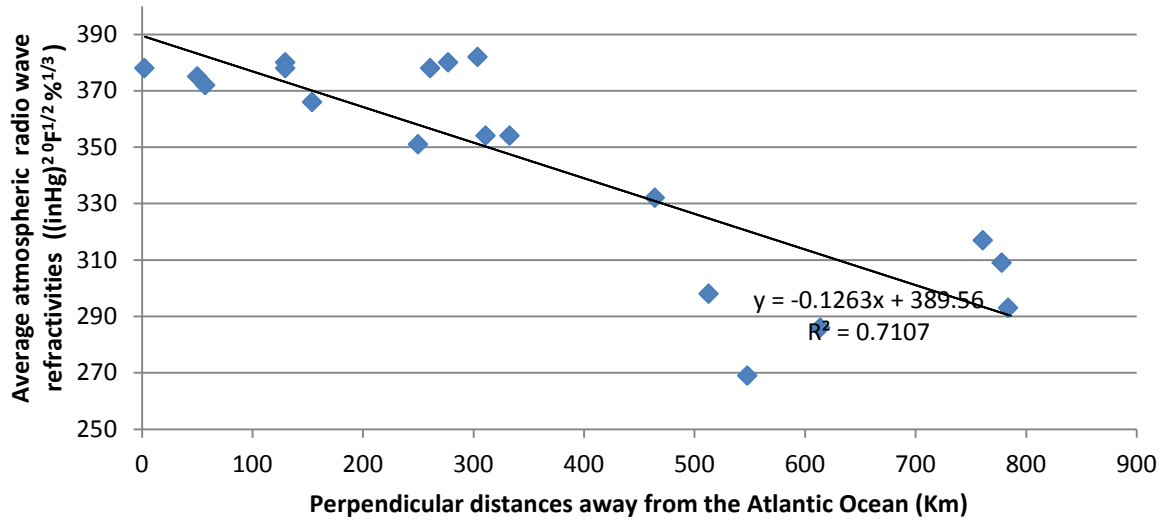


Fig. 8: Line of best fit between perpendicular distances away from the Atlantic Ocean and average atmospheric radio wave refractivities

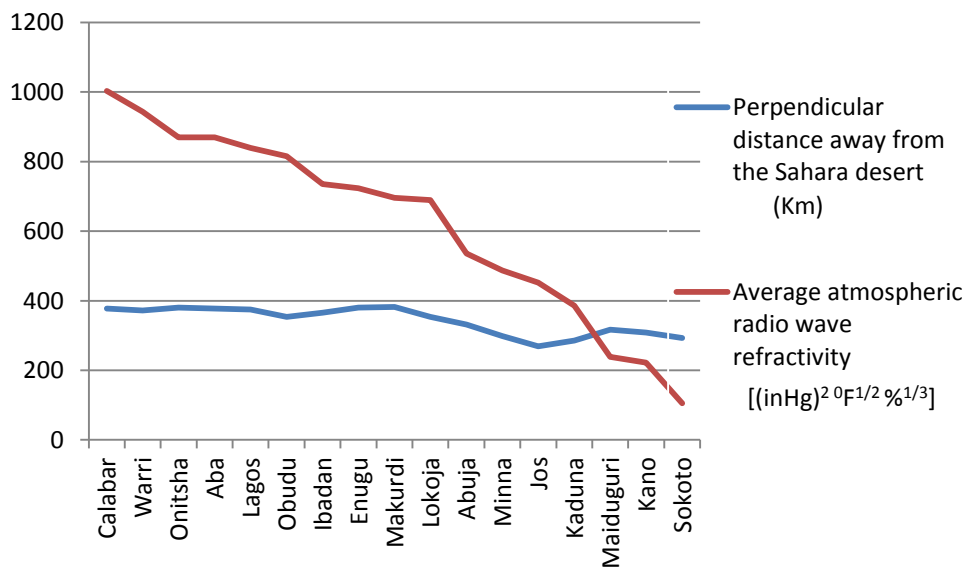


Fig. 9: Relationship between perpendicular distances away from the Sahara desert and average atmospheric radio wave refractivities

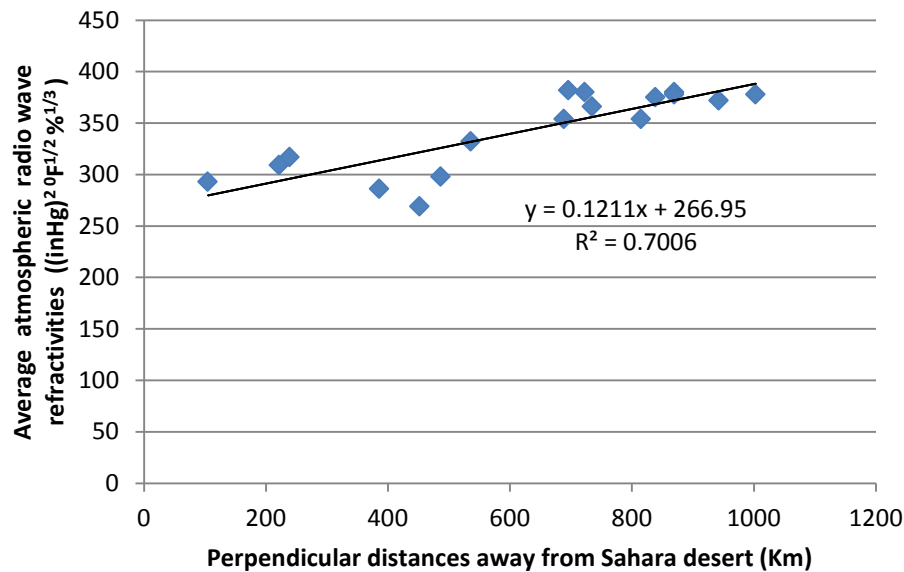


Fig. 10: Line of best fit between perpendicular distances away from the Sahara desert and average atmospheric radio wave refractivities

In a peck order of increasing magnitude of average atmospheric radio wave refractivities, the cities are arranged thus: Jos, Kaduna, Sokoto, Minna, Kano, Maiduguri, Abuja, Obudu, Akure, Lokoja, Ibadan, Warri, Lagos, Aba, Calabar, Onitsha, Enugu and Makurdi.

In fig. 1, observe that the refractivities of the rainforest and mangrove cities are higher than those of the savannah cities with the exception of Makurdi. This is owing to the fact that the relative humidities of the former cities are very high compared to that of the latter cities. Even though the highest temperatures are registered in the savannah cities, it is counterbalanced by the lowest temperatures also registered there, since the monthly mean temperatures were considered. More so, relative humidity has a higher weight in deciding the magnitude of refractivity than the other two atmospheric parameters: temperature and pressure. Generally, the mean monthly atmospheric pressure on the average throughout the country was near even. Hence the atmospheric pressure contributed near negligible number in the differences read in the atmospheric radio wave refractivities above. The exception shown in Makurdi results from the fact that the city hugs the river Benue and in consequence, accounts for the near steady and high mean monthly relative humidities. Also, the city is in the Guinea Savannah, which accounts for high mean monthly temperatures that is brought to bear in radio wave refractivity. To buttress this, Lokoja also in the Guinea savannah has very high average atmospheric radio wave refractivity, consequent upon the fact that it is a town lying next to the confluence of the Benue and Niger rivers with higher mean monthly relative humidities than its counterpart cities in the Guinea savannah. However, Makurdi is further down south than Lokoja and is closer to the rainforest and Atlantic Ocean; in regard to their coordinates. This suggests the higher average atmospheric radio wave refractivity in the former than the latter, since its mean monthly relative humidities are higher.

In figs. 3 and 4, the refractivities of the rainforest and mangrove cities were to a vast degree stable, this due to fact that the mean monthly humidities and temperatures are relatively stable, unlike the savannah cities where high mean monthly humidities and temperatures are registered during the wet and in the contrary, very low mean monthly humidities and temperatures are recorded in the dry. Even though, the highest temperatures are registered in the savannah during the dry, on the average it is low because of the very low night temperatures.

Study has shown that atmospheric radio wave refractivity has a negative bearing on signals [1]. Hence, to a very large extent, propagations of signals are better in the northern sphere of Nigeria than the southern sphere for communications that employ the tropospheric propagation mode, since low refractivity favours propagation of radio waves through the atmosphere.

Also in figs. 3 and 4, notice that Jos recorded the least mean monthly atmospheric radio wave refractivity, both in the wet and dry in Nigeria. This entails that for tropospheric propagation mode, the best quality of signal propagation will be recorded here. Even though it sits in the Sudan savannah belt, its montane climates strikingly differentiates it from other cities on the selfsame belt. Throughout Nigeria, it records the lowest mean monthly temperatures and comparatively low mean monthly relative humidities: since on the average; the atmospheric pressure that has a minimal effect on atmospheric radio wave refractivity is near uniform in Nigeria.

More so in figs. 3 and 4, Makurdi registered the highest mean monthly atmospheric radio wave refractivity throughout the year followed by Enugu, this is both in the wet and dry. As earlier highlighted, Makurdi hugs the river Benue. This accounts for its high mean monthly humidities in comparison with other Guinea savannah cities but shows similar mean monthly temperatures with these sister cities in the Guinea savannah: hence the very higher mean monthly radio wave refractivities relative to its sisters. This city's higher average refractivity than those of the coastal cities of Atlanta is in regard to the comparable high mean monthly relative humidities with these Atlantic coastal cities, but distinctly higher mean monthly temperatures. Similarly Enugu shares similar mean

monthly relative humidities as her twin rainforest cities – Ibadan and Akure, but differs in higher mean temperatures, since from its coordinates it is farther away from the Atlantic Ocean. Its climate is a hybrid of the rainforest and mangrove in view of mean monthly temperatures and mean monthly relative humidities respectively. This is true because, Calabar and Lagos that are in the shadow of the Atlantic Ocean, share similar mean monthly relative humidities as Enugu, but Enugu records a higher mean temperature than the aforementioned twin: Calabar and Lagos which equates to higher average atmospheric radio wave refractivity. The above weather pattern may be attributed to the fact that Enugu has a derived savannah, even though it is located in the rainforest and it lies at the foot of an escarpment of the Udi hill with a lake (Nike Lake) [12]. In communications wordings, this spells that Makurdi followed by Enugu will have the least propagation quality of signals for communication that utilize tropospheric propagation mode because a high refractivity bears negatively on radio wave propagation and invariably radio signals.

Strikingly, in fig. 5, Kaduna has the second lowest average atmospheric radio wave refractivity. This is because it is located in the borderland between the Sahel and Guinea savannah: that is in the Sudan savannah. Here, there is a characteristic lower mean monthly temperatures than the cities in the Sahel savannah, but shears similar temperatures with the Guinea savannah cities like Abuja. In other words, Kaduna has lower mean monthly relative humidities than that of its brothers in the Sudan savannah, but comparable to that of the Sahel savannah. In short words, its weather is a hybrid of the Sahel and Guinea savannah. This may be owed to the fact that Kaduna stands on the southern end of the high plains of northern Nigeria with a quasi-montane climate. It shares similar mean monthly relative humidities with Jos that posses a montane climate. That is, Kaduna and Jos sit on the same isohyets.

In fig. 5, Sokoto has the lowest average atmospheric radio wave refractivity and invariably the lowest mean monthly relative humidities and highest mean monthly temperatures in Nigeria. Even though, Sokoto, Kano and Maiduguri are located on the same belt, the coordinates of Kano and Maiduguri show that these cities are farther away from the Sahara desert than Sokoto. Similarly the coordinates of Maiduguri show it is farther away from the Sahara desert than that of Kano. This is responsible for the higher average atmospheric radio wave refractivity registered in Maiduguri relative to its counterparts in the Sahel savannah, since there is a gradual decrease in mean monthly temperatures and relative humidities as one drifts away from the Sahara desert. Also, the Maiduguri is close to the Lake Chad. This has a significant effect in the comparatively higher average relative humidities and consequently average atmospheric radio wave refractivity. This entails in communication that in the Sahel savannah, radio signals will propagate better as we move towards the Sahara desert due to decrease in humidity which favours radio wave propagation through the troposphere, even though there is are slight variations in temperatures. Recapitulating, relative humidity has a higher force in determining the weight of atmospheric radio wave refractivity.

Also, in fig. 5, Lokoja amongst the cities in the Savannah has the highest atmospheric radio wave refractivity because it is located close to a confluence. This accounts for its high mean monthly relative humidities and invariably high average atmospheric radio wave refractivity compared to the other cities in the savannah belt. It also has a stable refractivity to a very huge extent, unlike the other savannah cities which have varying refractivities with relatively very low refractivities during the dry and higher refractivities during the wet. Hence radio signal propagation quality will be worse where there is a huge water body since it has a bearing on its refractivity. Lokoja will impede radio signal through the atmosphere more than any other savannah city. Also notice that amongst the Sahel savannah cities, Maiduguri has higher mean monthly relative humidities in view of the fact that it sits close to the Lake chad as earlier accentuated.

In fig. 6, Lagos and Calabar have the highest atmospheric radio wave refractivities than Ibadan and Warri in the southern segment of Nigeria (that is, in the rainforest and mangrove). Calabar's average refractivity is higher than that of Lagos by virtue of the fact that Calabar is further down the south into the Atlantic Ocean and in a sequel has a higher relative humidity than Lagos even though they shear similar mean monthly temperatures. Warri trails the twin cities mentioned above (Calabar and Lagos) because it is farther from the Atlantic Ocean, even though it is a deltaic city with many fresh waters, it has a lower mean relative humidity compared to the above duo: Lagos and Calabar. Ibadan trails Warri in the increasing peck order of average atmospheric radio wave refractivity because it is farther away from the Atlantic Ocean with lower mean monthly relative humidities, but with similar mean monthly temperatures compared to the cities in the rainforest and mangrove. In few words, there was a gradual increase in the refractivity of the cities in the rainforest and mangrove belts as one heads down the Atlantic Ocean with the exception of Enugu that has a higher temperature than the coastal cities but shares similar relative humidity with these coastal cities. In communications tune, signal will propagate better as you move away from the Atlantic Ocean in the rainforest and mangrove, because of the decrease in relative humidity as one heads away from the Ocean, even though there are slight variances in temperatures.

Also, in fig. 6, notice that Obudu has the least average atmospheric radio wave refractivity compared to the other cities in Southern Nigeria. Even though she stands in the Guinea savannah, she lies on a montane belt with strikingly low mean monthly temperatures compared to the other cities in the south but has comparative mean monthly relative humidities in the wet. Consequently in the southern cities (that is, cities in the rainforest and mangrove), signals will propagate far better than any other in Obudu through the atmosphere.

In fig. 7, generally; there is a gradual increase in the average atmospheric radio wave refractivity down the Atlantic Ocean coast. This means, there will be worse propagation of radio wave or signal through the atmosphere as one heads towards the Atlantic Ocean.

In fig. 8, the correlation between the perpendicular distances away from the coastline of the Atlantic Ocean and the average atmospheric radio wave refractivities is 0.84. The approximate model of average atmospheric radio wave refractivity away from the Atlantic Ocean coast is $y = -0.125x + 388.9$. The above correlation was not absolute because of the non-uniformity of the weather patterns across the country. The relief (mountains and hills) and rivers (very large water bodies) mainly is responsible for some of these anomalies: for example; Jos recorded the least average atmospheric radio wave refractivity in the North, while Obudu registered

the least in the South, by virtue of their montane climate. Also Lokoja and Makurdi registered the highest average radio wave refractivity in the Savannah by virtue of the large river bodies embracing them. Strikingly there was a shift in the pattern of the atmospheric radio wave refractivity in Kaduna and Enugu. Both cities are located in the Sudan savannah and Rainforest belts respectively. Kaduna shares similar mean monthly temperatures with cities in the Guinea savannah but has common relative humidity with Jos on a montane area in the Guinea savannah. Similarly Enugu shares the same monthly average temperatures with cities in the mangrove but records higher mean temperatures than those cities. Here also: isotherm and isohyets but not isobars (since mean monthly air pressure was near uniform in the country) were brought into consideration for the anomalies, because these lines are non-linear and can cut across the vegetative climatic zones. This accounts as well for the deviation of the correlation from absoluteness.

In fig. 9, mostly; there was a gradual decrease in average atmospheric radio wave refractivities up the Sahara desert border. This entails that there will be better propagation of radio wave or signal through the atmosphere as one moves towards the Sahara desert.

In fig. 10, the correlation between the perpendicular distances away from the borderline of the Sahara desert and the average atmospheric radio wave refractivities is 0.83. The approximate model of average atmospheric radio wave refractivity away from the Sahara desert borderline is $y = 0.122x + 267.2$. The above correlation was not absolute because of the non-uniformity of the weather patterns across the country as earlier captured.

CONCLUSION

Generally, there was an increase in the average atmospheric radio wave refractivities as one confronts the coastline of the Atlantic Ocean and in the reverse, there was a decrease in the average atmospheric radio wave refractivities as one heads towards the borderline of the Sahara desert. Hence radio wave propagation through the troposphere gradually worsens towards the Atlantic Ocean and reversely the radio wave propagation via the troposphere step by step, betters towards the Sahara desert.

The correlation between the perpendicular distances away from the coastline of the Atlantic Ocean and the average atmospheric radio wave refractivities is 0.84. The approximate model of average atmospheric radio wave refractivity away from the Atlantic Ocean coastline is $y = -0.125x + 388.9$: where y is the average atmospheric radio wave refractivity and x is the perpendicular distance away from the Atlantic Ocean coastline. Similarly, the correlation between the perpendicular distances away from the borderline of the Sahara desert and the average atmospheric radio wave refractivities is 0.84. Also, the approximate model of average atmospheric radio wave refractivity away from the Sahara desert borderline is $y = 0.122x + 267.2$: where y is the average atmospheric radio wave refractivity and x is the perpendicular distance away from the Sahara desert borderline. The above correlations were not absolute because of the non-uniformity of the weather or climate patterns across the country. The reliefs and rivers account for some of the anomalies in the non-uniform trend down the ocean coastline or up the desert borderline. In addition, isotherm and isohyets but not isobars were brought into consideration because these lines are non-linear and can cut across the vegetative climatic zones, for example is Enugu that sits in the rainforests, shares similar mean monthly temperatures as other cities in this belt; but has common mean monthly humidities with cities in the mangrove. Also, Kaduna shares similar mean monthly temperatures with cities in the Sudan savannah but has common mean monthly humidities as Jos in the Guinea savannah and a montane climate.

By and large, the most favourable belt for radio signal propagation through the troposphere is the Sahel savannah belt with low mean monthly relative humidities, while the least favourable belt for radio signal propagation through the troposphere is the Mangrove belt with very high mean monthly relative humidities, in view of the fact that, the variance in mean monthly temperatures between the two belts is not comparable to their relative humidities and the variance in the mean monthly atmospheric pressure is near uniform. A point of note is that: relative humidity bears more weight in the expression for calculating radio wave refractivity, seconded by atmospheric temperature and the least is the atmospheric pressure [1]. This is due to their ranges of variations.

With the exception of winds and may be rainfall that affect communications [66] [67], radio signal propagation through the troposphere in the Savanna will be less stable than the rainforest and mangrove owing to the fact that there is less variance in the atmospheric parameters, that is atmospheric temperature, pressure and humidity in the latter belts than the former belt.

Finally, radio signal propagation will generally propagate better throughout the country in the troposphere during the dry than the wet. This is on the account that the mean monthly relative humidities generally falls during the dry, but rises in the wet.

REFERENCES:

- [1] Amajama J. (2015). Relationship between radio refractivity and its meteorological components with a new linear equation to calculate radio refractivity. *International Journal of Innovative Science, Engineering and Technology*, 2(12), 953 – 957.
- [2] Weather. (n.d.). *Concise English Oxford Dictionary* (11th ed.). (2004). Oxford: Oxford University Press
- [3] Climate. (n.d.). *Concise English Oxford Dictionary* (11th ed.). (2004). Oxford: Oxford University Press.
- [4] About Nigeria (n.d.). Retrieved January 10, 2016 from <http://www.nigeriahc.org.uk/about> Nigeria.
- [5] Atmospheric refraction (2015). In Wikipedia. Retrieved November 10, 2015, from http://en.wikipedia.org/wiki/Atmospheric_refraction.
- [6] Barclay, L. W., Hall, M. P. M. and Hewitt, M. T. (Eds.) (1996). *Propagation of radio waves*. IEE. ISBN 0 85296 8191.
- [7] Mike W. (2015). Refraction. Retrieved November 10, 2015, from <http://www.mike-wills.com/Tutorial/refraction.htm>.

- [8] Recommendation ITU-R (2003). The radio refractive index: its formula and refractivity data. Retrieved November 10, 2015, from <http://www.itu.int/rec/R-REC-P.453-9-200304>.
- [9] Tropospheric propagation (2015). In Wikipedia. Retrieved April 5, 2015, from http://en.wikipedia.org/wiki/tropospheric_propagation.
- [10] The effects of the earth's atmosphere on radio waves (2015). Introduction to wave propagation, Transmission lines and Antennas. Hwy - Port Richey: Integrated Publishing, Inc. Retrieved April 5, 2015, from www.tpub.com/neets/book10/40c.htm.
- [11] Dell, W. R., Groman, J. & Timms, H. (1994). *The worldbook encyclopedia*. Chicago: World Book Incorporated.
- [12] Enugu (n.d.). Wikipedia: the free encyclopaedia. Retrieved 10 January, 2016 from <https://en.m.wikipedia.org/wiki/Enugu>
- [13] Weather statistics for Abuja (Nigeria) (2015). Retrieved 1 January, 2016 from <http://m.yr.no/place/Nigeria/Abuja/Abuja/statistics.html>
- [14] Weather statistics for Jos, Plateau (Nigeria) (2015). Retrieved 1 January, 2016 from <http://m.yr.no/place/Nigeria/Plateau/Jos/statistics.html>
- [15] Weather statistics for Kaduna (Nigeria) (2015). Retrieved 1 January, 2016 from <http://m.yr.no/place/Nigeria/Kaduna/Kaduna/statistics.html>
- [16] Weather statistics for Enugu (Nigeria) (2015). Retrieved 1 January, 2016 from <http://m.yr.no/place/Nigeria/Enugu/Enugu/statistics.html>
- [17] Weather statistics for Calabar, Cross River (Nigeria) (2015). Retrieved 1 January, 2016 from http://www.yr.no/place/Nigeria/Cross_River/Calabar/statistics.html
- [18] Weather statistics for Lagos (Nigeria) (2015). Retrieved 1 January, 2016 from <http://m.yr.no/place/Nigeria/Lagos/Lagos/statistics.html>
- [19] Weather statistics for Akure, Ondo (Nigeria) (2015). Retrieved 1 January, 2016 from <http://m.yr.no/place/Nigeria/Ondo/Akure/statistics.html>
- [20] Weather statistics for Ibadan, Oyo (Nigeria) (2015). Retrieved 1 January, 2016 from <http://m.yr.no/place/Nigeria/Oyo/Ibadan/statistics.html>
- [21] Weather statistics for Aba, Abia (Nigeria) (2015). Retrieved 1 January, 2016 from <http://m.yr.no/place/Nigeria/Abia/Aba/statistics.html>
- [22] Weather statistics for Onitsha, Anambara (Nigeria) (2015). Retrieved 1 January, 2016 from <http://m.yr.no/place/Nigeria/Anambara/Onitsha/statistics.html>
- [23] Weather statistics for Obudu, Cross River (Nigeria) (2015). Retrieved 1 January, 2016 from http://m.yr.no/place/Nigeria/Cross_River/Obudu/statistics.html
- [24] Weather statistics for Warri, Delta (Nigeria) (2015). Retrieved 1 January, 2016 from <http://m.yr.no/place/Nigeria/Delta/Warri/statistics.html>
- [25] Weather statistics for Lokoja, Kogi (Nigeria) (2015). Retrieved 1 January, 2016 from <http://m.yr.no/place/Nigeria/Kogi/Lokoja/statistics.html>
- [26] Weather statistics for Minna, Niger (Nigeria) (2015). Retrieved 1 January, 2016 from <http://m.yr.no/place/Nigeria/Niger/Minna/statistics.html>
- [27] Weather statistics for Maiduguri, Borno (Nigeria) (2015). Retrieved 1 January, 2016 from <http://m.yr.no/place/Nigeria/Borno/Maiduguri/statistics.html>
- [28] Weather statistics for Kano (Nigeria) (2015). Retrieved 1 January, 2016 from <http://m.yr.no/place/Nigeria/Kano/Kano/statistics.html>
- [29] Weather statistics for Sokoto (Nigeria) (2015). Retrieved 1 January, 2016 from <http://m.yr.no/place/Nigeria/Sokoto/Sokoto/statistics.html>
- [30] Weather statistics for Makurdi, Benue (Nigeria) (2015). Retrieved 1 January, 2016 from <http://m.yr.no/place/Nigeria/Benue/Makurdi/statistics.html>
- [31] Enugu climate history (2015). Retrieved 1 January, 2016 from <http://www.myweather2.com/City-Town/Nigeria/Enugu/climate-profile.aspx>
- [32] Calabar climate history (2015). Retrieved 1 January, 2016 from <http://www.myweather2.com/CityTown/Nigeria/Calabar/climate-profile.aspx>
- [33] Aba climate history (2015). Retrieved 1 January, 2016 from <http://www.myweather2.com/City-Town/Nigeria/Aba/climate-profile.aspx>

- [34] Onitsha climate history (2015). Retrieved 1 January, 2016 from <http://www.myweather2.com/City-Town/Nigeria/Onitsha/climate-profile.aspx>
- [35] Akure climate history (2015). Retrieved 1 January, 2016 from <http://www.myweather2.com/City-Town/Nigeria/Akure/climate-profile.aspx>
- [36] Warri climate history (2015). Retrieved 1 January, 2016 from <http://www.myweather2.com/City-Town/Nigeria/Warri/climate-profile.aspx>
- [37] Lagos climate history (2015). Retrieved 1 January, 2016 from <http://www.myweather2.com/City-Town/Nigeria/Lagos/climate-profile.aspx>
- [38] Ibadan climate history (2015). Retrieved 1 January, 2016 from <http://www.myweather2.com/City-Town/Nigeria/Ibadan/climate-profile.aspx>
- [39] Makurdi climate history (2015). Retrieved 1 January, 2016 from <http://www.myweather2.com/City-Town/Nigeria/Makurdi/climate-profile.aspx>
- [40] Lokoja climate history (2015). Retrieved 1 January, 2016 from <http://www.myweather2.com/City-Town/Nigeria/Lokoja/climate-profile.aspx>
- [41] Abuja climate history (2015). Retrieved 1 January, 2016 from <http://www.myweather2.com/City-Town/Nigeria/Abuja/climate-profile.aspx>
- [42] Minna climate history (2015). Retrieved 1 January, 2016 from <http://www.myweather2.com/City-Town/Nigeria/Minna/climate-profile.aspx>
- [43] Jos climate history (2015). Retrieved 1 January, 2016 from <http://www.myweather2.com/City-Town/Nigeria/Jos/climate-profile.aspx>
- [44] Kaduna climate history (2015). Retrieved 1 January, 2016 from <http://www.myweather2.com/City-Town/Nigeria/Kaduna/climate-profile.aspx>
- [45] Sokoto climate history (2015). Retrieved 1 January, 2016 from <http://www.myweather2.com/City-Town/Nigeria/Sokoto/climate-profile.aspx>
- [46] Maiduguri climate history (2015). Retrieved 1 January, 2016 from <http://www.myweather2.com/City-Town/Nigeria/Maiduguri/climate-profile.aspx>
- [47] Kano climate history (2015). Retrieved 1 January, 2016 from <http://www.myweather2.com/City-Town/Nigeria/Kano/climate-profile.aspx>
- [48] Latitude and Longitude of Maidugari (n.d.). Retrieved 5 January, 2016 from <http://www.newstrackindia.com/informations/locations/Nigeria/1642826-city-maidugari.htm>.
- [49] Latitude and Longitude of Sokoto (n.d.). Retrieved 5 January, 2016 from <http://www.newstrackindia.com/informations/locations/Nigeria/1651045-city-sokoto.htm>.
- [50] Latitude and Longitude of Kano (n.d.). Retrieved 5 January, 2016 from <http://www.newstrackindia.com/informations/locations/Nigeria/1639346-city-kano.htm>.
- [51] Latitude and Longitude of Abuja (n.d.). Retrieved 5 January, 2016 from <http://www.newstrackindia.com/informations/locations/Nigeria/1622291-city-abuja.htm>.
- [52] Latitude and Longitude of Makurdi (n.d.). Retrieved 5 January, 2016 from <http://www.newstrackindia.com/informations/locations/Nigeria/1643115-city-makurdi.htm>.
- [53] Latitude and Longitude of Lokoja (n.d.). Retrieved 5 January, 2016 from <http://www.newstrackindia.com/informations/locations/Nigeria/1642358-city-lokoja.htm>.
- [54] Latitude and Longitude of Onitsha (n.d.). Retrieved 5 January, 2016 from <http://www.newstrackindia.com/informations/locations/Nigeria/1648048-city-onitsha.htm>.
- [55] Latitude and Longitude of Obudu (n.d.). Retrieved 5 January, 2016 from <http://www.newstrackindia.com/informations/locations/Nigeria/164590-city-obudu.htm>.
- [56] Latitude and Longitude of Aba (n.d.). Retrieved 5 January, 2016 from <http://www.newstrackindia.com/worldinfo/latitudelongitude/CountryCities/Nigeria/city-aba-1621916.htm>.
- [57] Latitude and Longitude of Lagos (n.d.). Retrieved 5 January, 2016 from <http://www.newstrackindia.com/worldinfo/latitudelongitude/CountryCities/Nigeria/city-lagos-1645071.htm>
- [58] Akure □ geographic coordinates, longitude and latitude of Akure, Federal Republic of Nigeria (n.d.). Retrieved 5 January, 2016 from <http://www.wemakemaps.com/coordinates/Akure.2350841/>
- [59] Latitude and Longitude of Warri (n.d.). Retrieved 5 January, 2016 from <http://www.newstrackindia.com/worldinfo/latitudelongitude/CountryCities/Nigeria/city-warri-1654745.htm>.

- [60] Latitude and Longitude of Calabar (n.d.). Retrieved 5 January, 2016 from <http://www.newstrackindia.com/worldinfo/latitudelongitude/CountryCities/Nigeria/city-calabar-1628567.htm>.
- [61] Latitude and Longitude of Jos (n.d.). Retrieved 5 January, 2016 from <http://www.newstrackindia.com/worldinfo/latitudelongitude/CountryCities/Nigeria/city-jos-1638664.htm>
- [62] Latitude and Longitude of Enugu (n.d.). Retrieved 5 January, 2016 from <http://www.newstrackindia.com/worldinfo/latitudelongitude/CountryCities/Nigeria/city-enugu-1631383.htm>
- [63] Latitude and Longitude of Kaduna (n.d.). Retrieved 5 January, 2016 from <http://www.newstrackindia.com/worldinfo/latitudelongitude/CountryCities/Nigeria/city-kaduna-1638872.htm>
- [64] Ibadan □ geographic coordinates Latitude and Longitude of Ibadan, Federal republic of Nigeria (n.d.). Retrieved 5 January, 2016 from <http://www.wemakemaps.com/coordinates/Ibadan.2339354/>
- [65] Minna Nigeria (General) Geography population map cities coordinates' location. Retrieved 10 January, 2016 from www.tageo.com/index-e-ni-v-00-d-m2808445.htm
- [66] Amajama J. & Oku E. D. (2016). Wind versus (UHF) radio signal. International Journal of Science, Engineering and Technology Research, vol 5 (2).
- [67] Meng, Y. S., Lee, Y. H. & Ng, B. C. (2013). The effects of tropical weather on radio wave propagation over foliage channel. IEEE transaction on vehicular technology, 58(8), 4023 – 4030.
- [68] Nigeria: Physical setting – Kaduna state (2015). Retrieved 12 December, 2015 from www.onlinenigeria.com/links/Kadunaadv.asp?blurb=294
- [69] Kaduna – NigerianWiki (2015). Retrieved 1 December, 2015 from <http://nigerianwiki.com/wiki/kaduna>

Development and Evaluation of Various Properties of Crystalline Silica-Aluminium Metal Based Composites

Sourav Debnath¹, Akshay Kumar Pramanick²

Senior Research Fellow¹, Associate Professor², Department Of Metallurgical and Material Engineering, Jadavpur University, Jadavpur, Kolkata-700032, West Bengal, India

Email: souravdebnath262@gmail.com¹, akshay99.ju@gmail.com²

Contact no.- (0) 9903336810

Abstract— Aluminium based metal composites have been developed due to its superior properties and performance. The aim of this study is to develop aluminium metal based composites with crystalline silica as reinforcement. Aluminium metal based composites with 5, 10, 15, 20, 30 Wt. % crystalline silica were developed through powder metallurgy techniques and characterized by XRD, EDX, Microstructure, and SEM. Physical properties like density, porosity and mechanical property like hardness have been observed. It has been seen that addition of 30 Wt. % crystalline silica was able to increase the hardness nearly two times than pure aluminium. It has been observed density decreases while both apparent porosity and hardness increases with silica content. This study also involves the effect of adding silica particulates on corrosion behavior of Silica-Aluminium metal based composite in 3.5% NaCl solution at room temperature using polarization method at scan rate 3 mV/sec. The result obtained from the potentiodynamic polarization test shows that corrosion rate decreases due to increase of crystalline silica particulate on aluminium matrix.

Keywords— Aluminium matrix, Crystalline silica particulate, Powder metallurgy, XRD, EDX, Microstructure, SEM, Density, Porosity, Micro hardness, Corrosion.

INTRODUCTION

Modern technology requires materials with unusual combination of properties that could not be met by conventional metal alloys, ceramic and polymeric materials. In practice, metal matrix composites are preferred for greater strength, stiffness and low weight compared to metal and alloys [1-4] and can withstand higher temperature than polymer matrix composites. Metal matrix also exhibit good fracture toughness. In metal matrix composite (MMC), fibrous or particulate phase is distributed in metal matrix. Metal matrix composite reinforced with ceramic particulate have shown improved sliding wear resistance [5, 6].

Aluminium based metal composite is preferable and widely used as a substitute material in transport sector especially in aerospace, aeronautics and automobile applications for making engine parts due to its good casting abilities, high corrosion resistance, low thermal expansion, wear resistant, and low density [7-11].

On the other hands low strength and low melting point are the problems for using pure aluminium and its alloys [12]. These problems can be solved by reinforcing SiO₂, Al₂O₃, SiC in whiskers or particulate form in aluminium matrix [12]. The reinforcing phase is selected depending on the application of developed material and compatibility between matrix and second phase. Load transfer capability between matrix and reinforcement depends on the matrix composition, the nature of the reinforcement, the fabrication method, and the sintering temperature of the composite. Strong interface protect crack propagation across both matrix and second phase. SiC, Al₂O₃, TiC, Ti-Aluminide, B₄C, Si are the commonly used particulates for reinforcement on aluminium based metal matrix [7, 13-18] but the use of silica as reinforcement on pure aluminium matrix is rare.

This paper describes about the development methods of Silica-Aluminium metal based composite and various physical, mechanical, and also chemical property in various environment.

EXPERIMENTAL PROCEDURE

2.1 Development of Silica-Aluminium Metal Based Composite by Powder Metallurgy Technique

The matrix material used in the present study was aluminium powder (99.7 %) and crystalline silica (SiO₂) powder, obtained from natural sand. Crystalline silica was prepared with heating natural sand at 1150^oC for one hour in muffle furnace at open atmosphere. Mixture of silica-aluminium powder with composition of 0%, 5%, 10%, 15%, 20%, and 30% crystalline silica (based on Wt. % of SiO₂) were mixed in hand driven ceramic bowls with ceramic pressing hammer until very fine powder was produced, mesh size -200

μm . Then the compact powder was pressed and sintered at 600°C for 1 hour duration using hot press. Figure 1 shows the step wise development of silica-aluminium metal matrix composite.

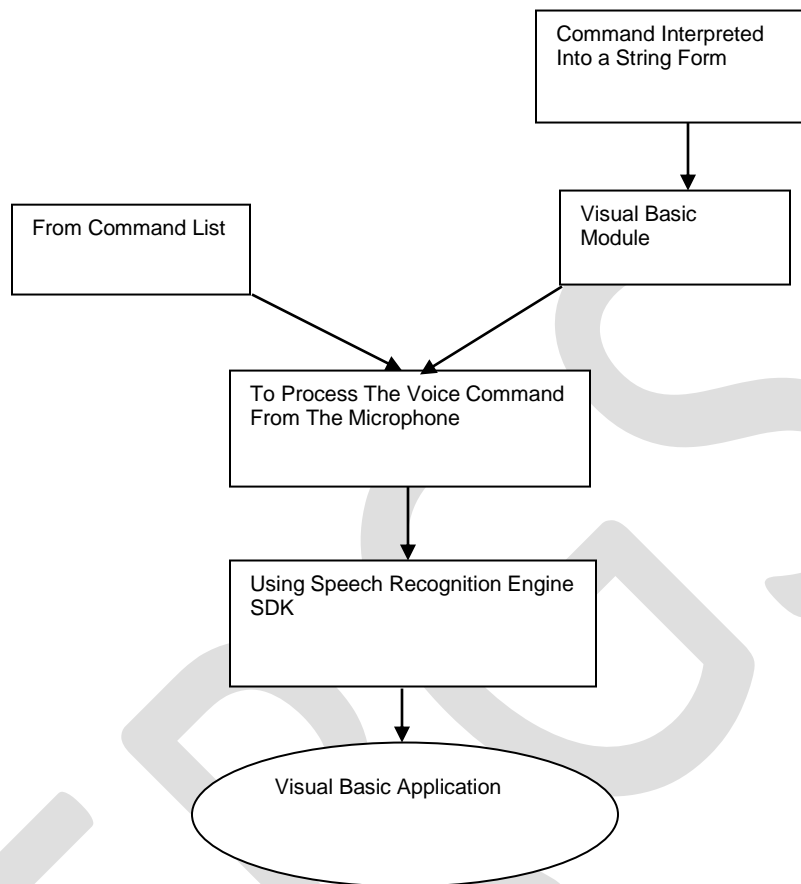


Fig. 1. Flowchart for development of crystalline silica-aluminium metal based composite

2.2 Testing and Characterization

2.2.1 XRD Analysis

X-ray diffraction (XRD) patterns were obtained for silica-aluminium composites using Rigaku Ultima III analytical diffractometer (with $\text{Cu-K}\alpha$ radiation, $\lambda = 1.54059 \text{ \AA}$) at 40 kV and 30 mA. Intensity (% abundance) data were recorded by the step-counting method (step 0.05 and a time per step of 0.6 second) between 10° and 80° (2θ) for each sample. Various phases were identified by comparing with standard JCPDS files.

2.2.2 Microstructure

For observing microstructure the surfaces were mirror polished by the emery paper 1/0 and 2/0 grade and then wheel cloth. After polishing, the samples were etched by Keller's solution and microstructures were observed at 20 X magnification by LEICA Optical Microscopy model no DM-2700M Image Analyzer.

2.2.4 SEM/EDX Analysis

SEM/EDX was carried out for each sample using JEOL MAKE SEM model JSM 6360, operated by PCSEM software.

2.2.5 Density and Apparent Porosity Measurement

Weight and dimension were measured for each sample to determine the density of the final composite product. Apparent Porosity was measured by the universal porosity measurement technique.

2.2.6 Micro-hardness

Micro-hardness survey was carried out on the same metallographic specimen of bead –on– plate sample at different positions by using 100 gf loads with 10 sec dwell time. The hardness was taken simultaneously in three different positions and finally averages them for more accuracy using Leco Micro Hardness tester (Model LM248SAT).

3. RESULTS AND DISCURSION

3.1 XRD Analysis

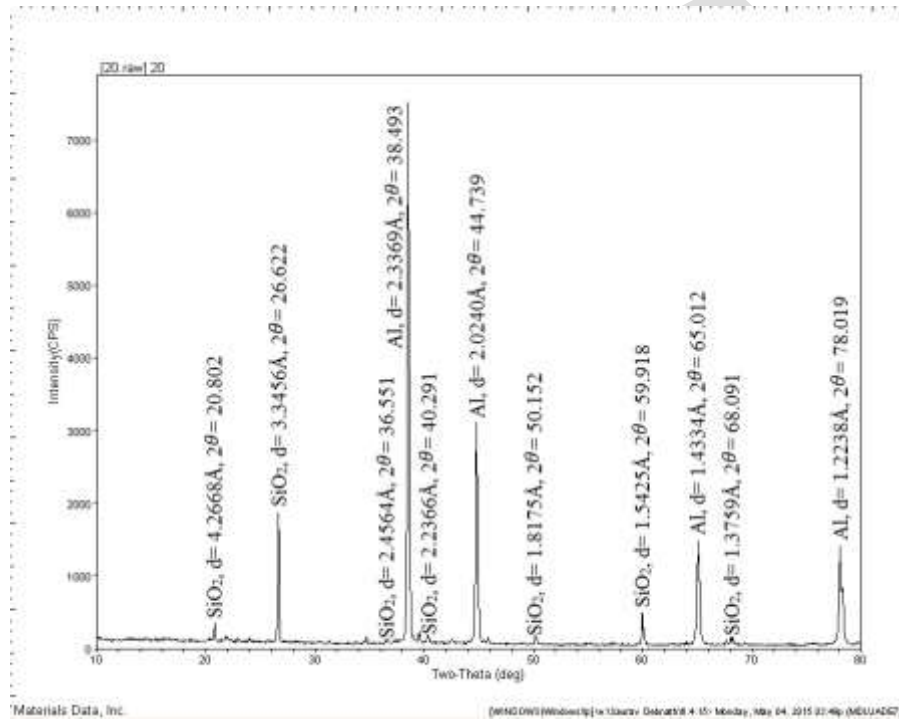


Fig. 2. XRD of 20 Wt. % crystalline silica-aluminium blended powder

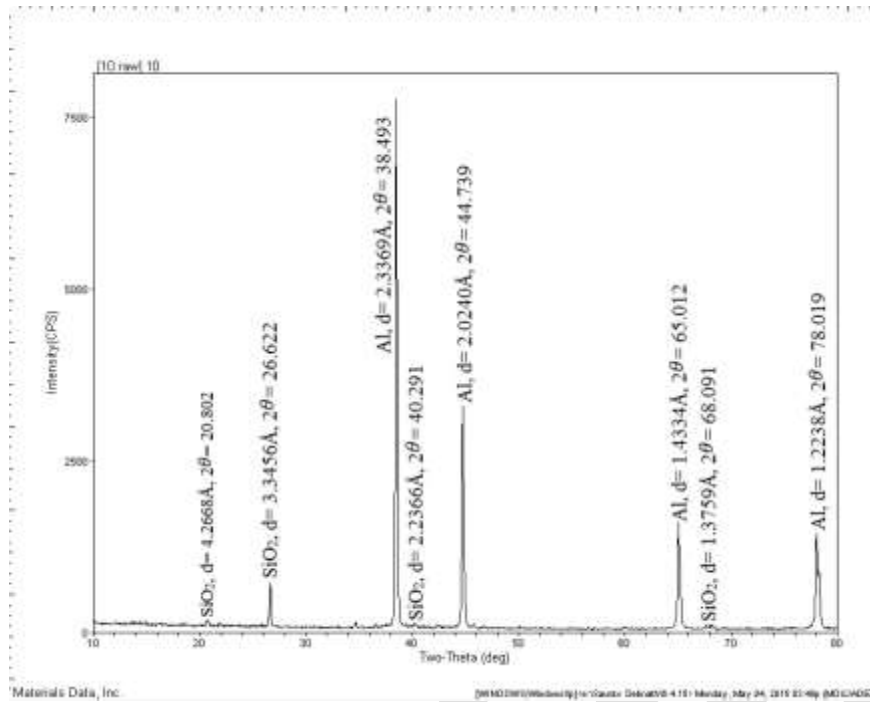


Fig. 3. XRD of 20 Wt. % crystalline silica-aluminium composite

XRD analysis before sintering was conducted for checking the purity of the crystalline silica- aluminium compact powder as crystalline silica was obtained from natural sand. Figure 2 and 3 shows the presence of only crystalline silica and aluminium before and after sintering.

3.2 Microstructure

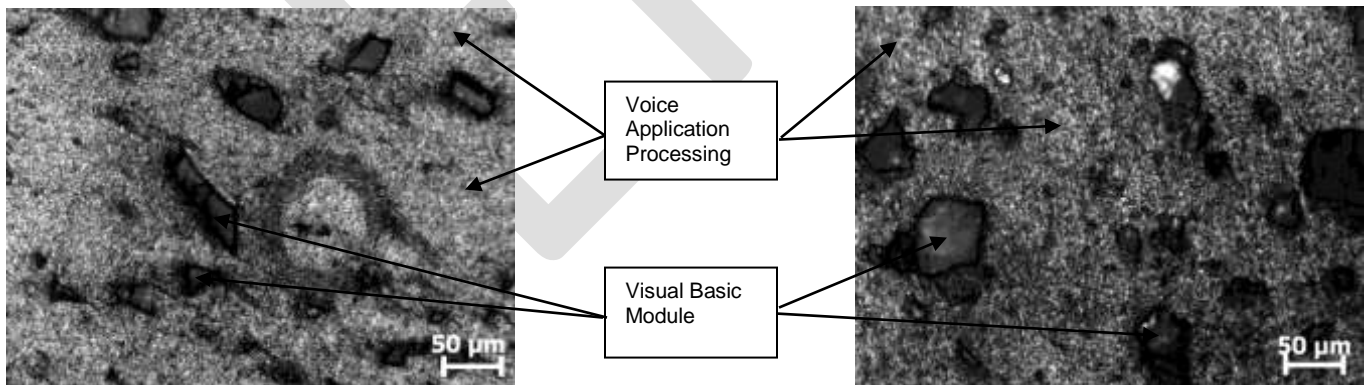
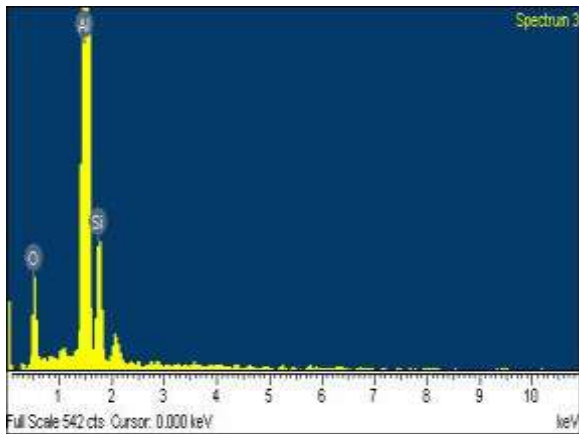


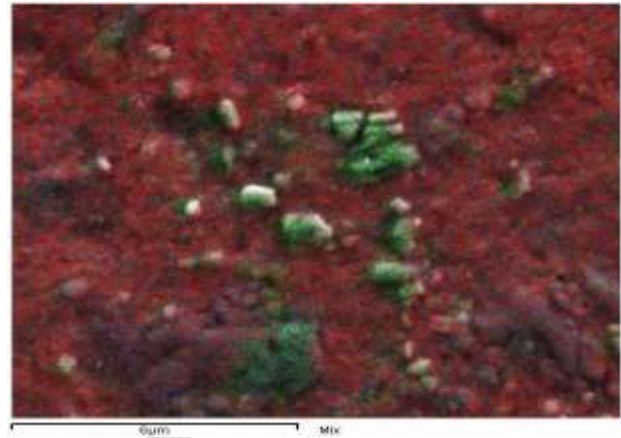
Fig. 4. Microstructure by optical microscopy at 20X magnification for (a) 5 Wt. % and (b) 10 Wt. % crystalline silica-aluminium composite

In figure 4, black portion indicates silica particles and white portion indicates aluminium matrix. Crystalline silica particulates are well distributed throughout entire aluminium matrix.

4.3 EDX Analysis



(a)



(b)

Fig. 5. EDX Analysis (a) EDX analysis (b) MAPPING on EDX

From EDX, there was 82.04 Wt. % Aluminium, shown by the highest peak in figure 5 (a). Corresponding mapping of EDX is shown in figure 5 (b) where red indicates aluminium (Al), green indicates silicon (Si) and white indicates oxygen (O). Actually, EDX analysis after sintering was done for known the elemental composition of the developed composite after sintering, precisely for understanding more clearly about the reaction between aluminium matrix and crystalline silica particulates. Result shows that there was no other element produced other than Si, O, and Al.

4.4 SEM Analysis

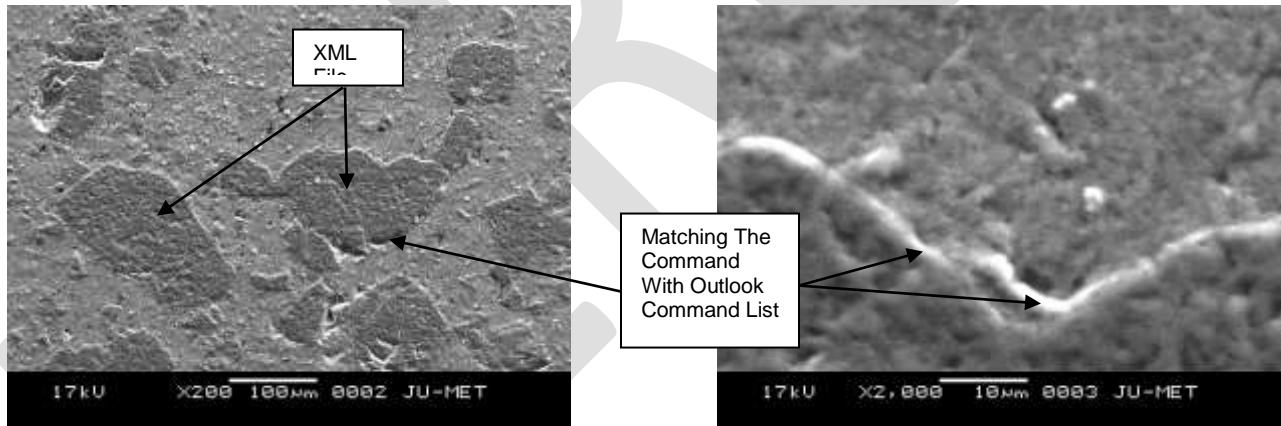


Fig. 6. SEM image of 20 Wt. % crystalline silica-aluminium composite (a) distributions of silica on aluminium matrix, (b) interface between silica particulates and aluminium matrix

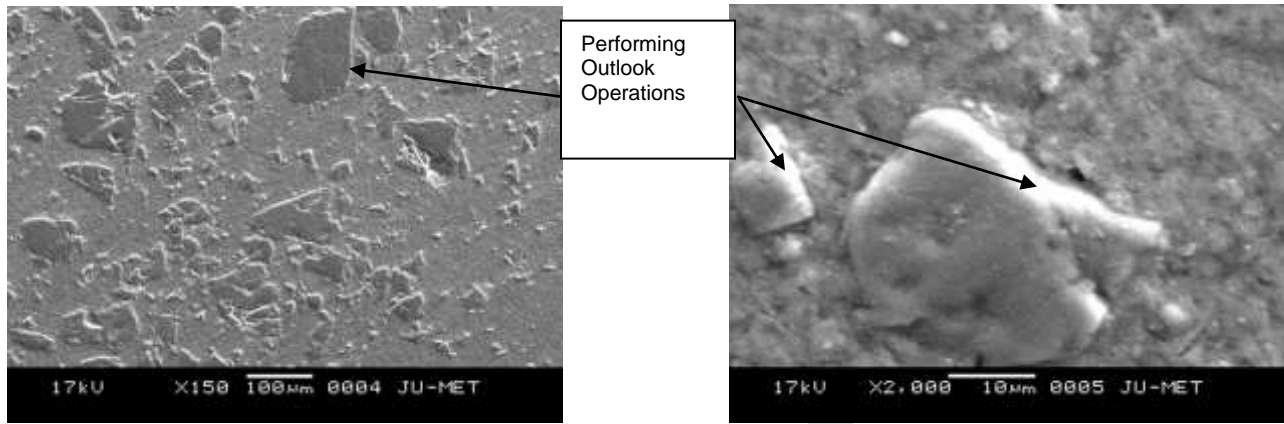


Fig. 7. SEM image of 20 Wt. % crystalline silica-aluminium composite (a) distributions of silica on aluminium matrix, (b) interface between silica particulates and aluminium matrix

SEM analysis was carried out to identify morphology, distribution of crystalline silica particulate in aluminium matrix and bonding quality between ceramic and metal matrix. Figure 6 (b) and 7 (b) shows the interface and bonding between aluminium matrix and crystalline silica particulate which indicates that crystalline silica particulate in aluminium matrix reduce the mobility of aluminium grain boundaries and better adhesion between matrix and reinforcement.

4.5 Density Measurement

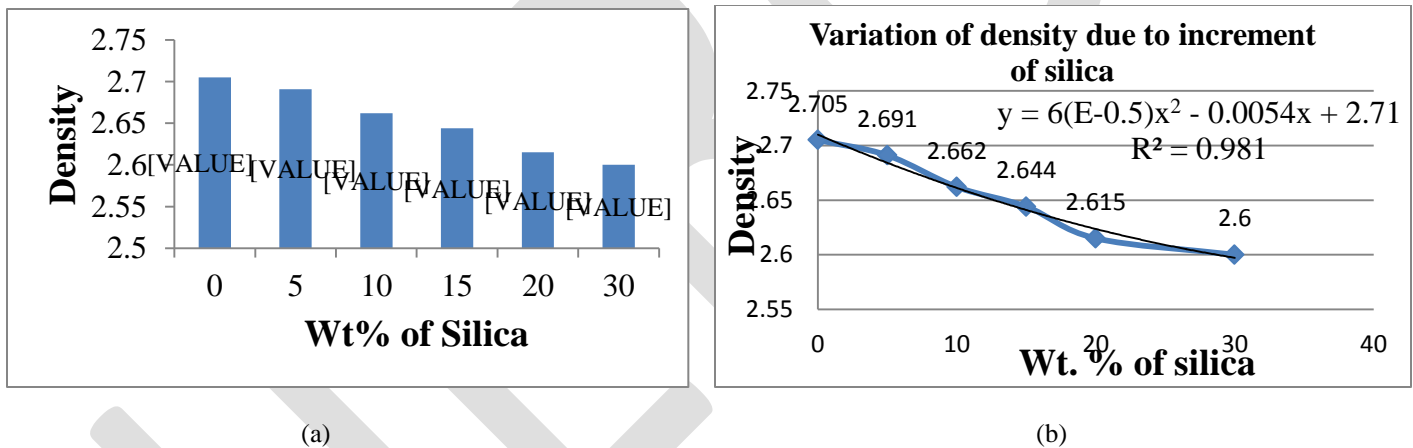


Fig. 8. Density- (a) individual density, (b) Variation of density due to increment of crystalline silica

Figure 8 shows that density, hence weight of the composite material, decreases with increment of crystalline silica particulates in aluminium matrix.

4.6 Apparent Porosity

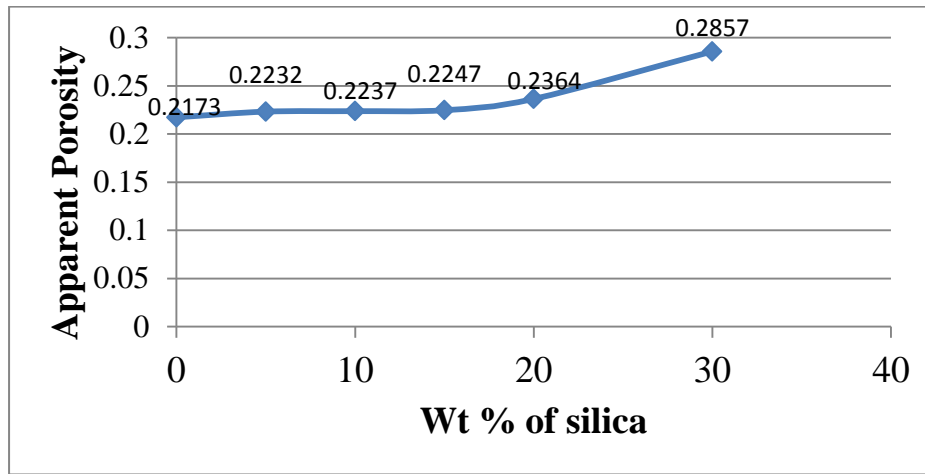


Fig. 9. Variation of apparent porosity due to increment of silica

Figure 9 implies that porosity is very low and vary only 0.2173% to 0.2857 % which is slightly increased due to increment of crystalline silica.

4.7 Hardness

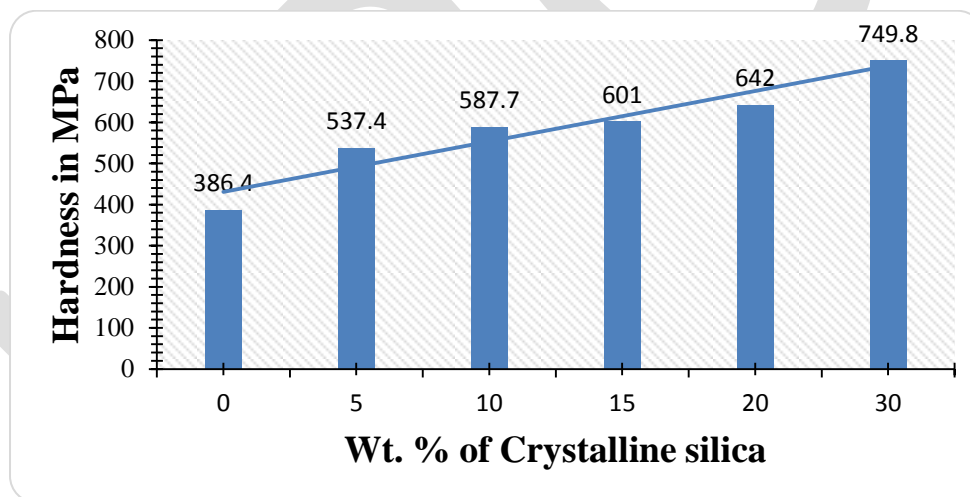


Fig.-10, Variation of hardness due to increment of crystalline silica

Figure 10 suggest that hardness values were increased gradually with increment of crystalline silica particulates in aluminium matrix. The maximum hardness value observed based on Vickers micro hardness was 749.8 MPa for 30 Wt. % of crystalline silica particulate addition while pure aluminium shows hardness value 386.4 MPa.

4.8 Potentiodynamic polarization

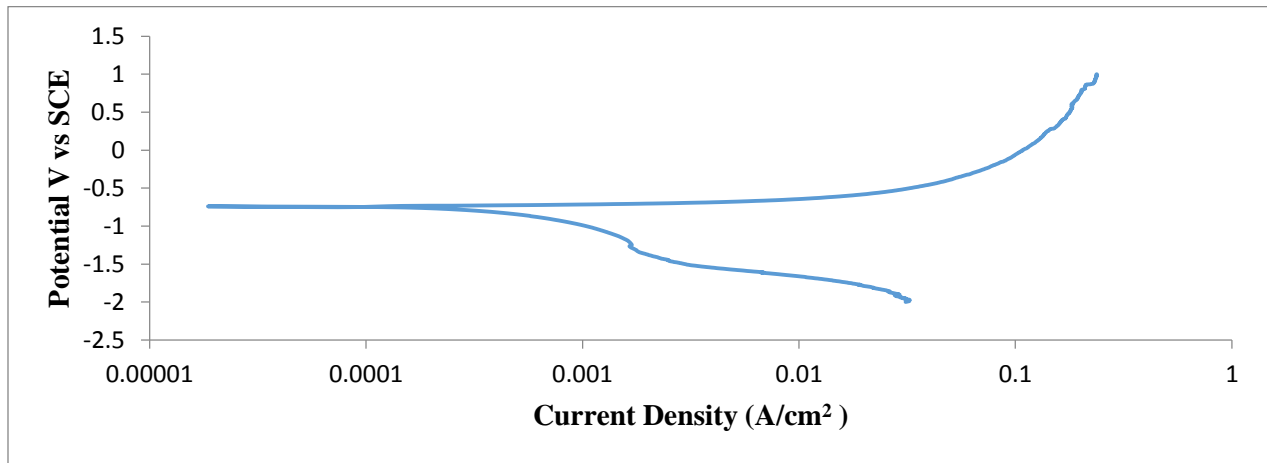


Fig. 11. Potentiodynamic polarization of pure aluminium in sea water solution

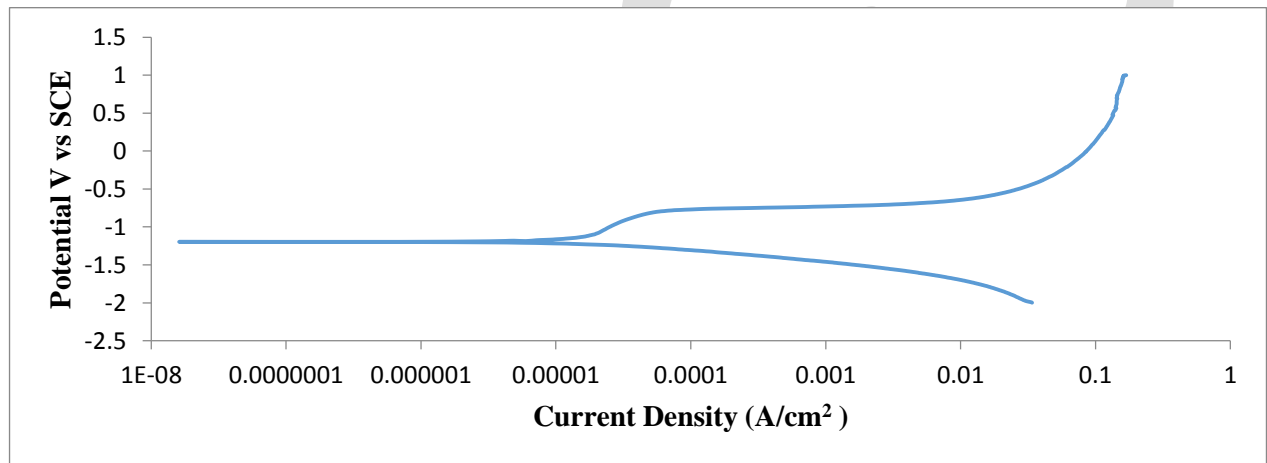


Fig. 12, Potentiodynamic polarization after adding 20 Wt. % silica particulates on aluminium matrix in sea water solution

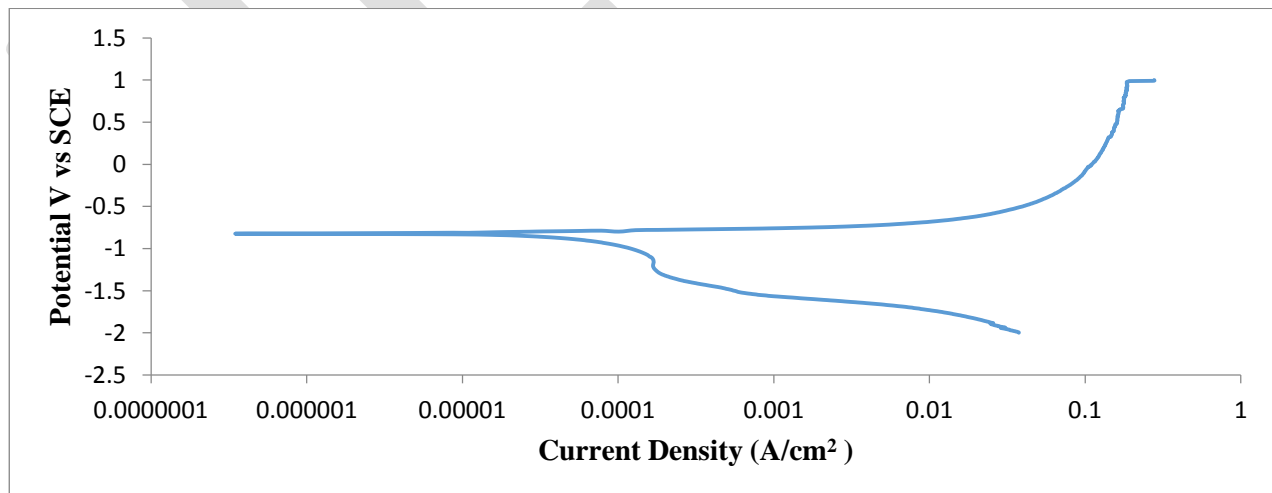


Figure 13, Potentiodynamic polarization after adding 30 Wt. % silica particulates on aluminium matrix in sea water solution

Figure 11 represents the potentiodynamic polarization for pure aluminium in 3.5% NaCl solution. After addition of 20 Wt. % and 30 Wt. % crystalline silica particulates on aluminium matrix, potentiodynamic polarization changes as shown in figure 12 and figure

13 respectively, in seawater solution. The corrosion current density i_{corr} for pure aluminium is 0.0017 A/cm^2 while after addition of 20 Wt. % and 30 Wt. % crystalline silica particulates, i_{corr} changes from 0.0005 A/cm^2 to 0.00045 A/cm^2 . Clearly corrosion current density i_{corr} , hence corrosion rate, decreases with increasing weight percent addition of silica particulates on aluminium matrix. This result shows the role of crystalline silica particulates on aluminium matrix to increase corrosion resistance with covering the anodic sites and enhancing the passivity of surface and finally reduces the dissolution of aluminium; hence increase the life span of the material.

CONCLUSION

The significant conclusions of the studies on crystalline silica- aluminium composites are as follows:

- Crystalline silica-aluminium composites were developed successfully using powder metallurgy technique.
- The experiments showed that an extruded mixture of crystalline silica and commercial powder aluminium heated at 600°C for one hour using hot press promote no reaction between matrix and reinforcement.
- Morphology obtained from optical microscope and SEM was found to the uniform distribution of crystalline silica in aluminium matrix.
- The density of crystalline silica-aluminium composites were decreased slightly with the increased of silica content. Soft aluminium matrix reinforcement with crystalline silica particles, were able to improve mechanical property like Vickers micro-hardness significantly with the increment of crystalline silica content.
- Corrosion resistance, more accurately pitting corrosion of silica-aluminium composite was enhanced in sea water environment with the addition of crystalline silica particulates in aluminium matrix.

REFERENCES:

- [1] Bharath; V Nagaral; M; Auradi; V., "Preparation of 6061Al-Al₂O₃ metal matrix composite by stir casting and evaluation of mechanical properties", International Journal of Metallurgical & Materials Science and Engineering, Vol.2, Issue 3, ISSN(Print)- 2278-2516; ISSN(Online)- 2278-2524; pp. 22-31, 2012.
- [2] Kleme; S.A; Reponen; P.K.; Liimatainen; J.; Hellman; J; Hannula; S.P., "Abrasive wear properties of metal matrix composites produced by hot isostatic pressing", Proc. Estonian Acad. Sci. Eng., vol. 12, Issue no.4, ISSN- 1406-0175, pp 445-454, 2006.
- [3] Toptan, F.; A. Karaaslan; A.; Cigdem; M; Kerti, "Processing and microstructural characterization of AA 1070 and AA 6063 matrix B4Cp reinforced composites", Materials and Design 31, ISSN- 0264-1275, pp.87-91, 2009.
- [4] Chawla, N. and Chawla, K. K., "Metal Matrix Composites in ground transportation," Springer-Verlag, New York, ISSN (Print)- 895-4852, ISSN (Online)- 1936-4709, pp- 401, 2006.
- [5] Sannino, A. P. and Rack, H. J., "Dry Sliding Wear of Discontinuously Reinforced Aluminium Composites: Review and Discussion," Wear, 189, 1-2, 1995, 1-19, 1995.
- [6] Sinclair, I. and Gregson, P. J., "Structural Performance of Discontinuous Metal Matrix Composites," Material Science and Technology, Print ISSN- 0267-0836, Online ISSN- 1743-2847, 13, 9, 709-726, 1997.
- [7] S.V Prasad and R.Asthana, 'Aluminium metal matrix composites for automotive applications; Tribological Considerations', Tribology Letters, ISSN: 1023-8883 (Print) 1573-2711 (Online), Vol. 17, No.3 October 2004
- [8] Z.RazaviHesabi, A.Simchi and S.M. Syed Raihani, 'Structural evolution during mechanical milling of nanometric and micrometric Al₂O₃ reinforced Al matrix composites', Materials Science and Engineering, ISSN: 0921-5093, A428, 2006
- [9] X.C.Tong and A.K.Ghosh, "Fabrication of in situ TiC reinforced Aluminum matrix composites", Journal of Materials Science, ISSN: 0022-2461 (Print) 1573-4803 (Online), 36, 4059-4069, 2001
- [10] M.Magesh,L. John Baruch, D. George Oliver, "Microstructure and Hardness of Aluminium Alloy- Fused Silica Particulate Composite", International Journal of Innovative Research in Advanced Engineering (IJRAE), ISSN: 2349-2163, Volume 1 Issue 5, 2014
- [11] A.M.S. Hamouda; S. Sulaiman ; T.R Vijayaram ; M. Sayuti; M.H.M. Ahmad., "Processing and characterization of particulate reinforced aluminium silicon matrix composite", Journal of Achievements in Materials and Manufacturing Engineering, ISSN: 2249-6645, Volume 25, Issue 2, 2007.
- [12] A. M. Usman, A. Raji, N. H. Waziri and M. A. Hassan, "Production and Characterization of Aluminium Alloy - Bagasse Ash Composites", IOSR Journal of Mechanical and Civil Engineering (IOSR-JMCE) e-ISSN: 2278-1684, p-ISSN: 2320-334X, Volume 11,

Issue 4 Ver. III (Jul- Aug. 2014), PP 38-44, 2014

- [13] M. M. Dave, K. D. Kothari, "Composite Material-Aluminium Silicon Alloy: A Review", Volume- 2, Issue : 3, ISSN- 2250-1991, 2013
- [14] X.C.Tong and A.K.Ghosh, 'Fabrication of in situ TiC reinforced Aluminum matrix composites', Journal of Materials Science, ISSN: 0022-2461 (Print) 1573-4803 (Online), 36, 4059-4069, 2001
- [15] S.ghosh et al., 'Preparation of Ti-Aluminide reinforced in situ Aluminum matrix composites by Reactive Hot Pressing', Journal of Alloys and Compounds doi: 10.1016/j.jallcom.2006.07.017, ISSN: 0925-8388, 2006
- [16] M.J.Flonas-Zamora et al., 'Aluminum-Graphite composite produced by mechanical milling and hot extrusion', Journal of Alloys and Compounds doi: 10.1016/j.allcom.2006.08.145, ISSN: 0925-8388, 2006
- [17] H.Huo et al., 'In situ synthesis of Al₂O₃ particulate reinforced Al matrix composite by low temperature sintering', Journal of Materials Science, ISSN: 0022-2461 (Print) 1573-4803 (Online), 41, 3249-3253, 2006
- [18] Zhongliang Shi, 'The oxidation Of SiC Particles and its interfacial characteristics in Al-Matrix composite', Journal Of Materials Science, ISSN: 0022-2461 (Print) 1573-4803 (Online), 36, 2441 – 2449, 2001

Designing of an efficient image encryption-compression system using a New Haar and Coiflet with Daubchies and Symlet wavelet transforms

Savita Devi, Astha Gautam(Assistant Professor)

Department of CSE, LRIET Solan,savitasharma.b@gmail.com

Abstract - The security of multimedia becomes more important, since multimedia data are transmitted over open networks more frequently. In this modern world, hidden information concept are very important and play a significant role to reducing the space in the memory as well as on disk drives. Compression of the encrypted information has taken more attention due to security reasons from last few years. If encryption and compression of the information works properly then it results to high speed computation. According to practical scenario encryption should be performed before the compression of information. Because unencrypted information have more chances of stealing. And now a day's data hacker becomes too intelligent to break the encrypted images to get the original contents, so many systems are designed to combine the encryption and compression in single module to provide greater security. Therefore we have proposed system where encryption is done prior to the image compression by random permutation method and after that we can efficiently compress the encrypted image. In this paper, we study a new approach is named as ECNHCDST (Encryption-Compression using New Haar and Coiflet with Symlet and Daubchies wavelet transform).

Keywords –Encryption, Compression, ETC, Haar, Coiflet, Symlet, Daubchies, CR, MSE, PSNR.

1. INTRODUCTION

The security of multimedia becomes more important, since multimedia data are transmitted over open networks more frequently. Typically, reliable security is necessary to content protection of digital images and videos [2]. Encryption and compression schemes for multimedia data need to be specifically designed to protect multimedia content and fulfill the security requirements for a particular multimedia application. Image Encryption means that convert an image to unreadable format so that it can be transmitted over the network safely. Image Decryption means to convert the unreadable format of an image to original image. This is used to protect the secrets of corporate as well as government's offices. [1].

Compression: It is done in order to save storage space or transmission time. The purpose of compression is reduction in size. The main objective behind compressing an image is to reduce the unimportant and redundant data, so as to store or transmit data in more efficient way. The applications of data compression in diverse areas re as follows:

- Satellite imagery
- Mini discs
- MP3technology
- Modems
- Digital cameras
- Database Design
- Storage and transmission of data
- Distributing Software
- Data Transmission

Image compression addresses the problem of reducing the amount of data required to represent a digital image. It is a process intended to yield a compact representation of an image, thereby reducing the image storage/transmission requirements [3]. Compression is achieved by the removal of one or more of the three basic data redundancies:

- Coding Redundancy
- Interpixel Redundancy
- Psychovisual Redundancy

The image compression techniques are broadly classified into two categories depending whether or not an exact replica of the original image could be reconstructed using the compressed image.

These are:

- Lossless technique
- Lossy technique

Lossless compression technique

In lossless compression techniques, the original image can be perfectly recovered from the compressed (encoded) image. These are also called noiseless since they do not add noise to the signal (image). It is also known as entropy coding since it use

statistics/decomposition techniques to eliminate/minimize redundancy. Lossless compression is used only for a few applications with stringent requirements such as medical imaging.

Lossy compression technique

Lossy schemes provide much higher compression ratio than lossless schemes. Lossy schemes are widely used since the quality of the reconstructed images is adequate for most applications. By this scheme, the decompressed image is not identical to the original image, but reasonably close to it.

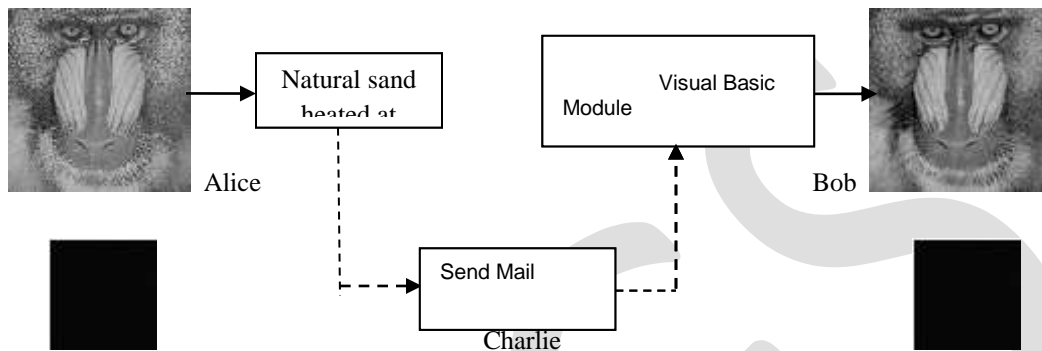


Fig. 1. Encryption-Then-Compression System

2. WAVELET

A mathematical function which cut up data into different frequency components, and then study each component with a resolution matched to its scale is known as Wavelet. In analyzing physical situations where the signal contains discontinuities and sharp spikes. Wavelet method has many advantages over the traditional Fourier methods. These are the functions which satisfy certain mathematical requirements and are used in representing data or other functions. This idea is not new; since the early 1800's, approximation using superposition of functions has existed when Joseph Fourier discovered that he could superpose sines and cosines to represent other functions. However, in wavelet analysis, the scale that we use to look at data plays a special role. At a determination interpreted information can then be sorted which matches its scale. The procedure of wavelet analysis is to adopt a wavelet prototype function, known as an analyzing wavelet or mother wavelet. There are two types of analysis i.e. temporal analysis and frequency analysis. Temporal analysis is performed with a contracted, high-frequency version of the prototype wavelet, whereas frequency analysis is performed with a dilated, low-frequency version of the same wavelet.

2.1 Discrete Haar Wavelet Transform (DHWT)

An outstanding property of the Haar functions is that except function Haar (0, t), the i^{th} Haar function can be generated by the restriction of the $(j - 1)^{th}$ function to be half of the interval where it is different from zero, by multiplication with $\sqrt{2}$ and scaling over the interval [0, 1]. These properties give considerable interest of the Haar function, since they closely relate them to the wavelet theory. In this setting, the first two Haar functions are called the global functions, while all the others are denoted as the local functions. Hence, the Haar function, which is an odd rectangular pulse pair, is the simplest and oldest wavelet. The motivation for using the discrete wavelet transform is to obtain information that is more discriminating by providing a different resolution at different parts of the time–frequency plane. The wavelet transforms allow the partitioning of the time-frequency domain into non-uniform tiles in connection with the time–spectral contents of the signal. The wavelet methods are strongly connected with classical basis of the Haar functions; scaling and dilation of a basic wavelet can generate the basis Haar functions.

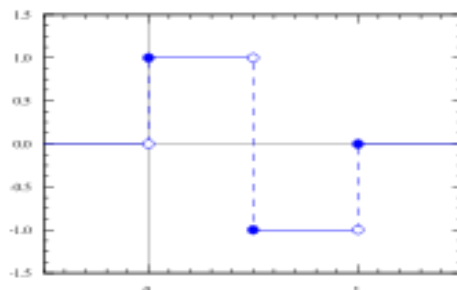


Fig. 2. Haar function on real line [2]

The Haar wavelet operates on data by calculating the sums and differences of adjacent elements. The Haar wavelet operates first on adjacent horizontal elements and then on adjacent vertical elements. Then it operated transformation coding and then encoding steps take place. For the retrieval of original image inverse process needs to follow so that the reconstruction of image can take place.

2.2 Coiflet Wavelet

Coiflets are discrete wavelets designed by Ingrid Daubchies, at the request of Ronald Coifman, to have scaling functions with vanishing moments. The wavelet is near symmetric; their wavelet functions have $N/3$ vanishing moments and scaling functions $N/3 - 1$, and have been used in many applications using Calderón-Zygmund Operators.

Both the scaling function (low-pass filter) and the wavelet function (High-Pass Filter) must be normalized by a factor $1/\sqrt{2}$. Below are the coefficients for the scaling functions for C6-30. The wavelet coefficients are derived by reversing the order of the scaling function coefficients and then reversing the sign of every second one (i.e. C6 wavelet = $\{-0.022140543057, 0.102859456942, 0.544281086116, -1.205718913884, 0.477859456942, 0.102859456942\}$). Mathematically, this looks like $\mathbf{B}_k = (-1)^k \mathbf{C}_{N-1}$ where k is the coefficient index; B is a wavelet coefficient and C a scaling function coefficient. N is the wavelet index, i.e. 6 for C6. A biorthogonal wavelet is a wavelet where the associated wavelet transform is invertible but not necessarily orthogonal. Designing biorthogonal wavelets allows more degrees of freedom than orthogonal wavelets. One additional degree of freedom is the possibility

to construct symmetric wavelet functions. In the biorthogonal case, there are two scaling functions $\phi, \tilde{\phi}$, which may generate different multi resolution analyses, and accordingly two different wavelet functions $\psi, \tilde{\psi}$. So the numbers M and N of coefficients in the scaling sequences a, \tilde{a} may differ. The scaling sequences must satisfy the following biorthogonality condition

$$\sum_{n \in \mathbb{Z}} a_n \tilde{a}_{n+2m} = 2 \cdot \delta_{m,0}$$

Then the wavelet sequences can be determined as

$$b_n = (-1)^n \tilde{a}_{M-1-n} \quad (n = 0, \dots, N-1)$$

$$\tilde{b}_n = (-1)^n a_{M-1-n} \quad (n = 0, \dots, N-1). \text{ In } \textit{coif}N, N \text{ is the order.}$$

Coiflet wavelets are discrete wavelet outlined by Ingrid Daubechies, on the requisition of Ronald Coifman, to have scaling operations with vanishing time period. The wavelet is closing symmetric and their wavelet operation has $N/3$ vanishing time period and the scaling operation is $N/3-1$. They have been utilized in numerous applications by the use of Calderón-Zygmund Operators. Both the scaling operation and the wavelet operation must be normalized by a consideration $1/\sqrt{2}$. The following are the coefficients for the scaling operations for C6-30. The wavelet coefficients are demonstrate by switching the request of the scaling capacity coefficients and after that turning around the indication of each second one (i.e. C6 wavelet = $\{-0.022140543057, 0.102859456942, 0.544281086116, -1.205718913884, 0.477859456942, 0.102859456942\}$).

Scientifically, where k is the coefficient file and B is a wavelet coefficient and C a scaling capacity coefficient and N is the wavelet.

2.3 Symlet Wavelet

Symlet wavelets are a family of wavelets. They are a modified version of Daubchies wavelets with increased symmetry. In $\textit{sym}N$, N is the order. Some authors use $2N$ instead of N . Symlets are only near symmetric; consequently some authors do not call them symlets. More about symlets can be found in [Dau92], pages 194, 254-257. By typing `waveinfo('sym')` at the MATLAB command prompt, you can obtain a survey of the main properties of this family [11].

2.4 Daubchies

Daubchies proposes modifications of her wavelets that increase their symmetry can be increased while retaining great simplicity.

The idea consists of reusing the function m_0 introduced in the dbN , considering the $|m_0(\omega)|^2$ as a function W of $z = e^{i\omega}$.

Then we can factor W in several different ways in the form of $W(z) = U(z) \overline{U(\frac{1}{z})}$ because the roots of W with modulus not equal to 1 go in pairs. If one of the root is z_1 , then $\frac{1}{z_1}$ is also a root.

- By selecting U such that the modulus of all its roots is strictly less than 1, we build Daubchies wavelets dbN . The U filter is a "minimum phase filter."
- By making another choice, we obtain more symmetrical filters; these are symlets.

The symlets have other properties similar to those of the $dbNs$.

2.5 ETC SYSTEM

The scheme includes the details of the three key components in modified ETC system, first is image encryption control by Alice, and second is image compression control by Charlie and then bob controlled the logical order decryption and decompression. Encryption

is the process in which plain text is converted into unreadable form to provide the high level of security. To decrypt or decode the text, the receiver use that key which is used for encrypting the text [7]. Encryption method is used of securing the data which is very important and confidential for the military and the government operations. Now a day it is also used by the civilian's in day-to-day life. There are various applications like in the online transactions of banks and the data transfer via networks and exchange of vital personal information etc. All these require the application of encryption from the aspects of reliability and security. The work which is done earlier only addressed the compression of bi-level images and binary i.e. black and white images with asymmetric probabilities of black and white pixels. The growth of lossless compression of the encrypted images has been recently signified by relying on the comparison with source coding and the side information at the decoder. Bob aims to retrieve the original I image I after receiving the compressed and encrypted bit stream B. A multimedia technology used for hiding information which provides the authentication and copyright protection.

3. ARITHMETIC CODING

It is most often used when we have to code binary symbols or bits. Each bit begins the coding process. The arithmetic codes generate non-block codes; that is a correspondence between source symbols and code words does not exist. Instead, an entire sequence of source bits is allocated to a single code word which defines an interval of real numbers between 0 and 1.

As the number of symbols or bits in the message increases, the interval used to represent it becomes smaller and the number of bits needed to represent the interval becomes larger. Each symbol in the message reduces the size of the interval according to its probability of occurrence. Since the symbols are not coded one at a time, this technique can achieve the highest possible coding efficiency.

4. METHODOLOGY

Encryption-Compression using New Haar, Coiflet, Symlet and Daubchies wavelet transform (ECNHCSNDWT)

The input image has been considered as 'I', encryption over 'I' has been implemented using random permutation method. The obtained result after encryption has been considered as 'I_e', and then a new Haar, Coiflet, Symlet and Daubchies wavelet technique has been used for compression. The output after compression has been stored as image 'B'. Then the image 'B' has been decrypted after decompression. [1]

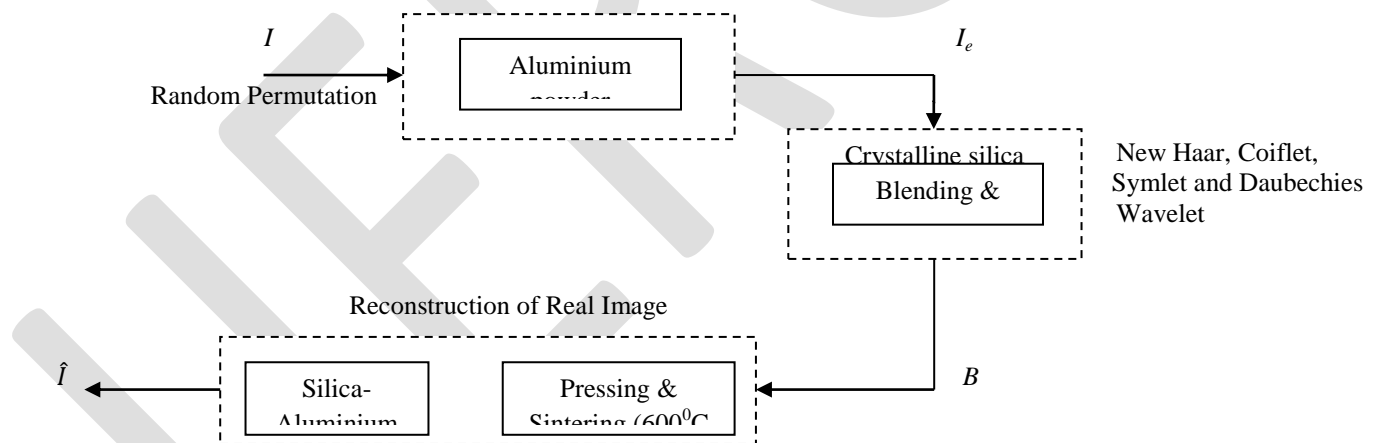


Fig. 3. Proposed Model for Encryption-Compression System

As shown in Fig. 3. Encryption-Compression system is proposed. The resultant image \hat{I} is evaluated using various parameters like CR, MSE and PSNR to check the efficiency and to compare it with the result of existing system. We can also represent the proposed schema with the help of flowchart. Fig.4. Shows the flowchart that represents the procedure flow of various steps. Half of the flowchart represents the encryption steps and rest represents the compression steps. Then inverse process to retrieve the real image and then calculation steps to check the efficiency.

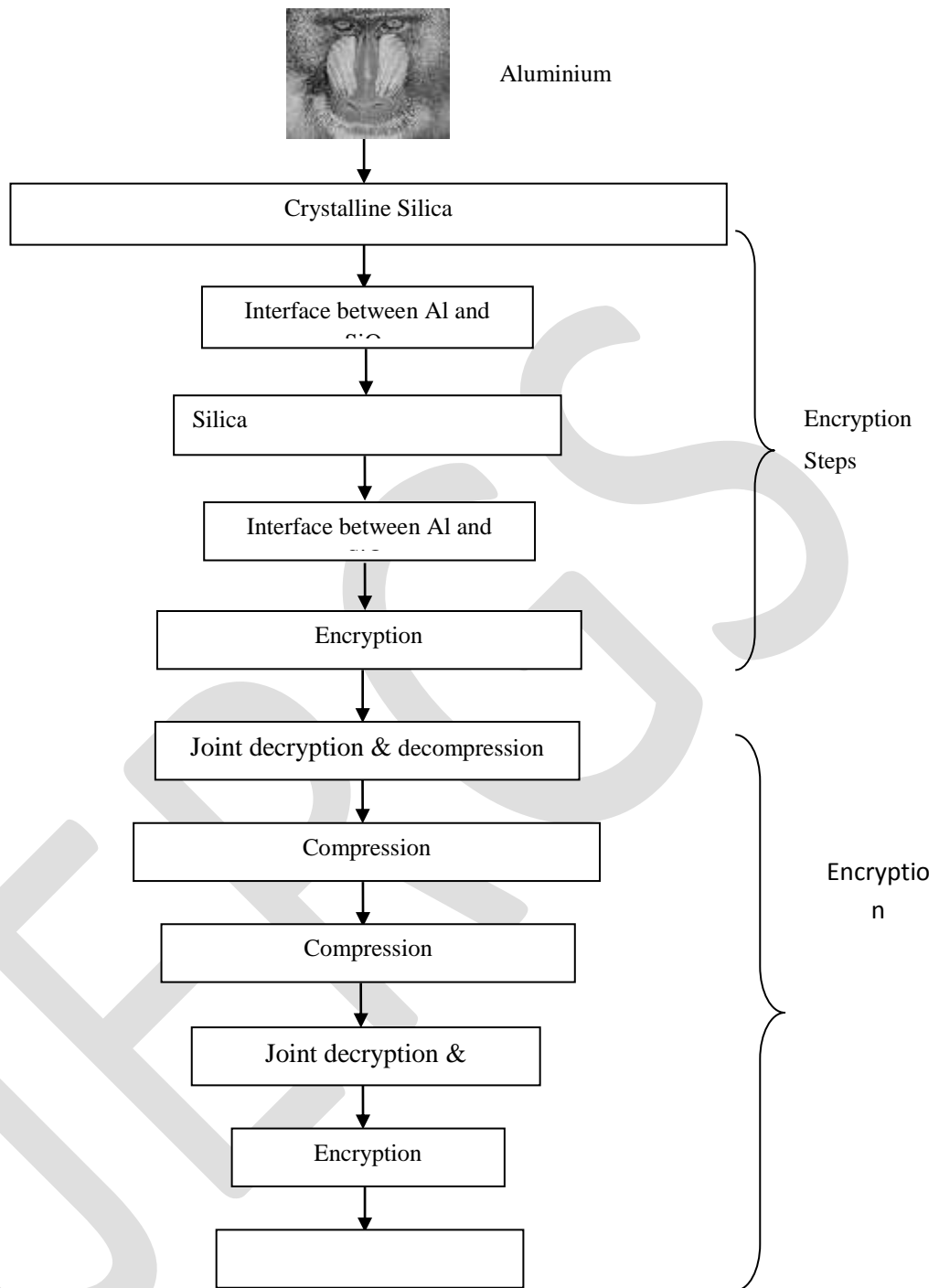


Fig. 4. Flowchart for Image Encryption-Compression Scheme [1]

5. RESULTS EVALUATION

In this section, we will perform experiment to verify the efficiency of our approach. The comparison of the accuracy is done for every method is one with the given values to the proposed work. With our approach result will be evaluated with different parameters as CR (compression ratio), MSE (mean square error) and PSNR (peak signal to noise ratio).

REFERENCES:

- [1] Jiantao Zhou, Xianming Liu, Oscar C. Au and Yuan Yan Tang, "Designing an Efficient Image Encryption-Then-Compression System via Prediction Error Clustering and Random Permutation", IEEE Trans. Inf. Forensics Security, vol. 9, issue 1, January 2014.
- [2] R. Mehala and K. Kuppasamy, "A New Image Compression Algorithm using Haar Wavelet Transformation", International Journal of Computer Applications(0975-8887), International Conference on Computing and Information Technology, 2013.
- [3] X. Zhang, G. Sun, L. Shen, and C. Qin, "Compression of encrypted images with multilayer decomposition", Multimed. Tools Appl., vol. 78, issue 3, Feb. 2013.
- [4] J. Zhou, X. Wu, and L. Zhang, " l_2 restoration of l_∞ -decoded images via soft-decision estimation", IEEE Trans. Imag. Process., vol. 21, issue 12, Dec. 2012.
- [5] D. Klinc, C. Hazay, A. Jagmohan, H. Krawczyk, and T. Rabin, "On compression of data encrypted with block ciphers", IEEE Trans. Inf. Theory, vol. 58, issue 11, Nov. 2012.
- [6] Z. Erkin, T. Veugen, T. Toft, and R. L. Lagendijk, "Generating private recommendations efficiently using homomorphic encryption and data packing", IEEE Trans. Inf. Forensics Security, vol. 7, issue 3, June 2012.
- [7] X. Zhang, G. Feng, Y. Ren, and Z. Qian, "Scalable coding of encrypted images", IEEE Trans. Imag. Process, vol. 21, issue 6, June 2012.
- [8] Nidhi Sethi, Ram Krishna, R. P. Arora, "Image Compression using HAAR Wavelet Transform", IISTE Comp. Engg. & Intelligent Systems, ISSN 2222-1719, 2011
- [9] X. Zhang, Y. L. Ren, G. R. Feng, and Z. X. Qian, "Compressing encrypted image using compressive sensing", in Proc. IEEE 7th IHH-MSP, Oct. 2011.
- [10] M. Barni, P. Failla, R. Lazzeretti, A. R. Sadeghi, and T. Schneider, "Privacy-preserving ECG classification with branching programs and neural networks", IEEE Trans. Inf. Forensics Security, vol. 6, issue 2, June 2011.
- [11] X. Zhang, "Lossy compression and iterative reconstruction for encrypted image", IEEE Trans. Inf. Forensics Security, vol. 6, issue 1, Mar. 2011.
- [12] W. Liu, W. J. Zeng, L. Dong, and Q. M. Yao, "Efficient compression of encrypted grayscale images", IEEE Trans. Imag. Process, vol. 19, issue 4, Apr. 2010.
- [13] T. Bianchi, A. Piva, and M. Barni, "Composite signal representation for fast and storage-efficient processing of encrypted signals", IEEE Trans. Inf. Forensics Security, vol. 5, issue 1, Mar. 2010.

Dynamic Modelling of Biped Robot

Mr. Rahul R Thavai, Mr. Shishirkumar N Kadam

Pillai HOC College of Engineering & Technology- University of Mumbai, rahulthavai1991@gmail.com, 8796273059.

Abstract— Goal of dynamics is to obtain equations of motion of biped. Dynamic model of 11 Degree of freedom biped is formulated. Euler - Lagrange formulation combined with homogeneous transformation matrices are used to derive Equations of motion. Jacobian matrixes are the basic elements in building dynamic model. Jacobian matrixes and Euler- Lagrange equations used to determines its dynamic characteristics such as velocity, acceleration and torque. This is necessary for design as well as for estimation of energy consumption of biped. This paper illustrates the mathematical model of the dynamics equations for the legs into the Sagittal and Frontal planes by applying the principle of Lagrangian dynamics.

Keywords— Degree of freedom (DOF), Denavit–Hartenberg (D-H) parameters, Jacobian, Lagrangian.

1. INTRODUCTION

In the last decade rapid growth in use of Humanoid Robotics results in autonomous research field. Humanoid robots are used in all situations of human's everyday life, cooperating with us. They will work in services, in homes and hospitals, and they are even expected to get involved in sports. Hence, they will have to be capable of doing a diversity of tasks. Humanoid robots resembles human-like in their shape and behavior. They have included in number of applications like replacement of humans in hazardous works such as rescue operations, military operations, disaster scenarios, or restoration movement in people with disabilities.

The first dynamically balanced biped was developed by Kato in 1983. It was named as quasi-dynamic due to static walking. This achievement shifted research to from static to dynamic walking [1]. In 1984, Miura and Shimoyama [2] Modeled BIPER-3 depicting true active balance. It has only three actuators; one to change the angle separating the legs in the direction of motion, and the remaining two which lifted the legs out to the side in the lateral plane. Placement is done using an inverted pendulum. Later this was modified to the seven degree of-freedom BIPER-4 robot. Raibert developed a planar hopping robot [3]. It has a pneumatically driven leg and has three degrees of freedom (pitch motion, and vertical and horizontal translation). A state machine was used to track the current progress.

A dynamic running robot was developed by Hodgins, Koechling and Raibert [4]. This robot was constrained to two dimensional motions. Control system has the three important parameters like body height, foot placement and body attitude; these parameters are controlled through the use of a state machine. The robot was controlled depending upon its current state. Research around this time was focused on developing analytical techniques for designing and controlling robot motion. This leads to complex equations governing the motion of the robot which had no solution and been needed to be approximated or linearized. The zero moment point (ZMP) principle with a control system is used by Takanishiet al [5] to achieve dynamic stability of seven link robot. McGeer [6] showed that a correctly designed biped walker with no actuation and no control could walk down gentle slopes. He considered the pair of pendulum that walk naturally as wheel rolls.

Akihito Sano Junji Furusho [7] used angular momentum of the whole system for feedback-controlled walking. But model fails on sloped surfaces. Zheng et al [8] developed methodology for biped robot control. Estimation of the inclination of supporting foot allows robot to transfer from level walking to climbing the slope. But this methodology fails for walking from a level to a negative slope. Kajita et al [9] restricted the movement of the center of mass (COM) to the horizontal plane to control bipedal dynamic walking. But it was unable to move on uneven surface. Yamaguchi et al. [10] added the feature of a yaw-axis movement to robot WL-12RV. This eliminates the unwanted behavior of the robot to turn at higher velocities that result in 50 percent faster movement than previous robot.

Jong H. Park and Kyoung D. Kim [11] provided solution to move on uneven surface by using gravity compensated inverted pendulum mode (GCIPM). Garcia et al [12] used a double pendulum to show the same. This work concluded that mechanical design is equally, if not more important, than the control method used. This shows that more effort on a correct mechanical system design will simplify the complexity of the control system required. Shadow Robot Group performed research in the United Kingdom and

Developed the Shadow Walker prototype having twelve degrees of freedom. Concept of anthropomorphic design and use of a wooden frame, they have constructed a biped robot using 'air' muscles. Research project done by the University of Waseda in Japan leads to WABIAN Humanoid. They worked on human motion dynamics, human-like mechanism design. Sardain et al [13] generated walking with large velocities.

Zonfrilli et al [14] suggested different biped mechanism to for passive, static, dynamic or purely dynamic walking. Sakagami et al [15] made one of most advanced features biped robot, ASIMO. It process instructions from various types of raw sensory data, able to detect obstacle and identify peoples, Posses map management system for navigation. Its processing is slower due to manipulation of huge database. The compensation for possibility of falling the robot over uneven surfaces is done by Hirukawa et al [16]. Sugahara et al included applications like to take care of elderly people. Zoss et al shows that exoskeletons used for transporting heavy objects. Ekkelen kamp et al design robot for treadmill training so as to reduce physical load on the recovering therapist patient and to offer assistance in leg movements in the forward direction and in keeping lateral balance.

Daan et al implemented pure dynamic approach with open-loop strategy .A predefined time trajectory for the swing leg makes the swing leg move backwards just prior to foot impact. So it moves without requiring local control. Fariz et al [17] had made kinematic formulations by considering position and orientation that results in walking pattern for flat surfaces as well as inclined surfaces.

The research on humanoid biped robot includes various areas such as mechanical design, mathematical modeling, and simulation of biped locomotion. There are many problems that involve kinematics, dynamics, balance and Stability. It makes the study of bipedal robot a complex subject. However, with technological development based on theoretical and experimental research, we have managed to do it. Since the robot have more joints, so the robot has more degrees of freedom. Analysis is related to more variables and the derivation of correlation formulas are also more complex. When we built a humanoid biped robot, we need to make the design of each component by obtaining the mathematical model of each part. The mechanical structure and drive of the biped robot affect their movement speed, power consumption and load directly.

In this paper, we proposed a dynamic model by viewing the kinematic chain of a leg of a biped in forward order. This paper is organized as follows: the forward kinematics for the proposed humanoid robot is obtained using the Denavit-Hartenberg convention.in Section 2. The jacobian matrix which is prerequisite for dynamics is described in Section 3. The discussion about the dynamic model in the Sagittal and Frontal planes using Lagrange equations is in Section 4. Finally, Section 5 presents some important conclusions for biped robot.

2. FORWARD KINEMATICS

Forward kinematics is the task in which the position and orientation of the end-effector is to be determined by giving the configurations for the joints of the robot. The design of biped is based on human body in terms of ratios, body proportions, and range of motion. This paper propose to have sufficient DOF to imitate human motion. The model used consists of 5-links connected through revolute joints, 2-links for each leg and 1-link for torso. The identical legs have hip joint between torso and thigh, knee joints between the thigh and shank, ankle joint between shank and foot, and a rigid body forms the torso. The joint structure of the biped has eleven degrees of freedom, 5 DOF for each leg and 1 DOF for waist or torso. DOF for waist is shared between legs. The Hip joint has 2-DOF, which allows it motion in the sagittal and the lateral plane.

Servos mounted on robot serves as actuators. One servo is mounted on torso, two servos are attached to the hip, one servo is attached to the knee and two servos are attached to the ankle. The mechanical design of the bipedal robot is modular, making it easy to change and replace parts. Forward kinematics is the first step to derive dynamic model of biped. Once the model has been prepared, it is necessary to attach the frames to each joint. The link frame assignment is the basic requirement of Denavit–Hartenberg(D-H)parameter.



Fig 1: Basic model of biped

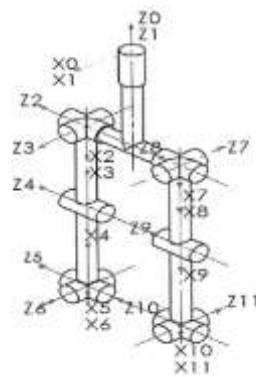


Fig 2: D-H Parameter frame assignment

A 4x4 transformation matrix relating i frame to $i-1$ frame is given by,

$${}^{i-1}H_i = \begin{bmatrix} \cos\theta_i & -\sin\theta_i \cos\alpha_{i-1} & \sin\theta_i \sin\alpha_{i-1} & a_{i-1}\cos\theta_i \\ \sin\theta_i & \cos\theta_i \cos\alpha_{i-1} & -\cos\theta_i \sin\alpha_{i-1} & a_{i-1}\sin\theta_i \\ 0 & \sin\alpha_{i-1} & \cos\alpha_{i-1} & d_i \\ 0 & 0 & 0 & 1 \end{bmatrix}$$

Where,

θ_i = Rotation angle is angle between X_{i-1} and X_i measured about Z_i .

α_{i-1} = Twist angle is angle between lines along joints $i-1$ and i measured about common perpendicular X_{i-1} .

a_{i-1} = link length is the distance between the lines along joints $i-1$ and i along common perpendicular.

d_i = link offset is distance along Z_i from line parallel to X_{i-1} to the line parallel to X_i and are called as Denavit-hartenberg (D-H) parameters.

These are known as D -H parameters and are used to calculate transformation matrix of one link with respect to previous link. Homogeneous transformation from one link to another link is obtained by multiplying continuous chain of matrixes form one to another link.

3. JACOBIAN MATRIX

In this we are interested to derive the velocity relationships that relate the linear and angular velocities of the end-effector to the joint velocities. We will find the angular velocity of the end-effector frame which gives the rate of rotation of the frame and the linear

velocity of the origin. Then we relate these velocities to the joint velocities. Jacobian matrix forms the basic elements in building a dynamic model of biped walking. On the basis of motion i.e rectilinear or rotary, the jacobian matrixes are divided as linear or revolute. In this design, all joints are revolute, so general form of matrix can be written as,

$$J_i = \begin{bmatrix} Jv_i \\ J\omega_i \end{bmatrix} = \begin{bmatrix} Z_{i-1} \times (O_n - O_{i-1}) \\ Z_{i-1} \end{bmatrix} \dots\dots (1)$$

Masses are considered as two concentrated material points such as thigh, shin or leg. We can define the dynamic system as figure 3.

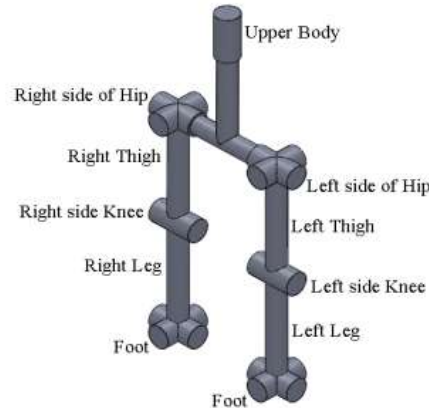


Fig 3: Masses and joints for thigh and shin or legs.

Each mass needs a jacobian matrix J_4 and J_6 means jacobian of thigh and shin. By separating this jacobian matrix into rectilinear and rotary elements, jacobian matrix can be written as shown below. Linear and rotary components of jacobian of thigh are given by,

$$Jv_4 = [Z_0 \times (O_4c - O_0) \quad Z_1 \times (O_4c - O_1) \quad Z_2 \times (O_4c - O_2) \quad Z_3 \times (O_4c - O_3) \quad 0 \quad 0] \dots\dots (2)$$

$$J\omega_4 = [[-l_4 c(\theta_3) (c(\theta_1) s(\theta_2) + c(\theta_2) s(\theta_1)), -l_4 c(\theta_3) (c(\theta_1) s(\theta_2) + c(\theta_2) s(\theta_1)), -l_4 c(\theta_3) (c(\theta_1) s(\theta_2) + c(\theta_2) s(\theta_1)), -l_4 s(\theta_3) (c(\theta_1) c(\theta_2) - s(\theta_1) s(\theta_2)), 0, 0], [l_4 c(\theta_3) (c(\theta_1) c(\theta_2) - s(\theta_1) s(\theta_2)), l_4 c(\theta_3) (c(\theta_1) c(\theta_2) - s(\theta_1) s(\theta_2)), l_4 c(\theta_3) (c(\theta_1) c(\theta_2) - s(\theta_1) s(\theta_2)), -l_4 s(\theta_3) (c(\theta_1) s(\theta_2) + c(\theta_2) s(\theta_1)), 0, 0], [0, 0, 0, -l_4 c(\theta_3) (c(\theta_1) s(\theta_2) + c(\theta_2) s(\theta_1))^2 - l_4 c(\theta_3) (c(\theta_1) c(\theta_2) - s(\theta_1) s(\theta_2))^2, 0, 0]]$$

$$J\omega_4 = [Z_0 \quad Z_1 \quad Z_2 \quad Z_3 \quad 0 \quad 0] \dots\dots (3)$$

$$J\omega_4 = [[0, 0, 0, -c(\theta_1) s(\theta_2) - c(\theta_2) s(\theta_1), 0, 0], [0, 0, 0, c(\theta_1) c(\theta_2) - s(\theta_1) s(\theta_2), 0, 0], [1, 1, 1, 0, 0, 0]]$$

Similarly, Linear and rotary components of jacobian of shin can be calculated as,

$$Jv_6 = [Z \times (O_6c - O_0) \quad Z_1 \times (O_6c - O_1) \quad Z_2 \times (O_6c - O_2) \quad Z_3 \times (O_6c - O_3) \quad Z_4 \times (O_6c - O_4) \quad 0]$$

$$J\omega_6 = [Z_0 \quad Z_1 \quad Z_2 \quad Z_3 \quad Z_4 \quad 0]$$

Where,

$$Z_0 = \begin{bmatrix} 0 \\ 0 \\ 1 \end{bmatrix}$$

$$Z_1 = \begin{bmatrix} {}^0H_1(1,3) \\ {}^0H_1(2,3) \\ {}^0H_1(3,3) \end{bmatrix} = \begin{bmatrix} 0 \\ 0 \\ 1 \end{bmatrix}$$

$$Z_2 = \begin{bmatrix} {}^0H_2(1,3) \\ {}^0H_2(2,3) \\ {}^0H_2(3,3) \end{bmatrix} = \begin{bmatrix} 0 \\ 0 \\ 1 \end{bmatrix}$$

$$Z_3 = \begin{bmatrix} {}^0H_3(1,3) \\ {}^0H_3(2,3) \\ {}^0H_3(3,3) \end{bmatrix} = \begin{bmatrix} -c(\theta_1)s(\theta_2) - c(\theta_2)s(\theta_1) \\ c(\theta_1)c(\theta_2) - s(\theta_1)s(\theta_2) \\ 0 \end{bmatrix}$$

$$Z_4 = \begin{bmatrix} {}^0H_4(1,3) \\ {}^0H_4(2,3) \\ {}^0H_4(3,3) \end{bmatrix} = \begin{bmatrix} -c(\theta_1)s(\theta_2) - c(\theta_2)s(\theta_1) \\ c(\theta_1)c(\theta_2) - s(\theta_1)s(\theta_2) \\ 0 \end{bmatrix}$$

$$O_0 = \begin{bmatrix} 0 \\ 0 \\ 0 \end{bmatrix}$$

$$O_1 = \begin{bmatrix} {}^0H_1(1,4) \\ {}^0H_1(2,4) \\ {}^0H_1(3,4) \end{bmatrix} = \begin{bmatrix} 0 \\ 0 \\ 0 \end{bmatrix}$$

$$O_2 = \begin{bmatrix} {}^0H_2(1,4) \\ {}^0H_2(2,4) \\ {}^0H_2(3,4) \end{bmatrix} = \begin{bmatrix} 0 \\ 0 \\ 0 \end{bmatrix}$$

$$O_3 = \begin{bmatrix} {}^0H_3(1,4) \\ {}^0H_3(2,4) \\ {}^0H_3(3,4) \end{bmatrix} = \begin{bmatrix} 0 \\ 0 \\ 0 \end{bmatrix}$$

$$O_4 = O_4c = \begin{bmatrix} {}^0H_4(1,4) \\ {}^0H_4(2,4) \\ {}^0H_4(3,4) \end{bmatrix} = \begin{bmatrix} l_4 c(\theta_3)(c(\theta_1)c(\theta_2) - s(\theta_1)s(\theta_2)) \\ l_4 c(\theta_3)(c(\theta_1)s(\theta_2) + c(\theta_2)s(\theta_1)) \\ -l_4 s(\theta_3) \end{bmatrix}$$

$$O_6c = \begin{bmatrix} {}^0H_6(1,4) \\ {}^0H_6(2,4) \\ {}^0H_6(3,4) \end{bmatrix}$$

$$= [\{15 (c(\theta_3) c(\theta_4) (c(\theta_1) c(\theta_2)-s(\theta_1) s(\theta_2)) s(\theta_3) s(\theta_4) (c(\theta_1) c(\theta_2)s(\theta_1) s(\theta_2)))+ l_4 c(\theta_3) (c(\theta_1) c(\theta_2) - s(\theta_1) s(\theta_2))\}, \{15 (c(\theta_3) c(\theta_4) (c(\theta_1) s(\theta_2)+c(\theta_2) s(\theta_1))s(\theta_3) s(\theta_4) (c(\theta_1) s(\theta_2) + c(\theta_2) s(\theta_1))) + l_4 c(\theta_3) (c(\theta_1) s(\theta_2) + c(\theta_2) s(\theta_1))\}, \{-15 (c(\theta_3) s(\theta_4) + c(\theta_4) s(\theta_3)) - l_4 s(\theta_3)\}]$$

4. LAGRANGE FORMULATION

The aim to solve dynamics is to obtain equation of motion of system. Because of multiple degree of freedom system, it is difficult to obtain equation of motion. In this paper, principles of Lagrangian dynamics is used for determining the gait locomotion equations for obtaining the torque in each joint of the biped. By representing variables of system as generalized coordinate, we can write equation of motion for an n-DOF system using Euler-Lagrange Equation as,

$$\frac{d}{dt} \frac{\partial L}{\partial \dot{q}_i} - \frac{\partial L}{\partial q_i} = \tau_i \quad \dots\dots (4)$$

$$L = K - P \quad \dots\dots (5)$$

Where L is Lagrangian, K is kinetic energy and P is potential energy.

The kinetic energy of a rigid body is sum of two terms.

$$K = \frac{1}{2} m v^T v + \frac{1}{2} \omega^T I \omega \quad \dots\dots\dots (6)$$

The inertia tensor is required to be transferred into global coordinate, so equation 6 should be multiplied by rotational transfer matrix R.

$$K = \frac{1}{2} m v^T v + \frac{1}{2} \omega^T R I R^T \omega \quad \dots\dots\dots (7)$$

Total kinetic energy is sum of each links.

$$K = \sum_{i=1}^n \left\{ \frac{1}{2} m_i v_i^T v_i + \frac{1}{2} \omega_i^T R_i I_i R_i^T \omega_i \right\} \quad \dots\dots\dots (8)$$

By using the Jacobian matrix, the kinetic energy can be written as the function of the joint variables like Equation 9

$$K = \frac{1}{2} \dot{q}^T \left[\sum_{i=1}^n \{ m_i J_{v_i}(q)^T J_{v_i}(q) + J_{\omega_i}(q)^T R_i(q) I_i R_i(q)^T J_{\omega_i}(q) \} \right] \dot{q} \quad \dots\dots\dots (9)$$

$$K = \frac{1}{2} \dot{q}^T \{ m_4 J_{v_4}(q)^T J_{v_4}(q) + m_6 J_{v_6}(q)^T J_{v_6}(q) + J_{\omega_4}(q)^T R_4(q) I_4 R_4(q)^T J_{\omega_4}(q) + J_{\omega_6}(q)^T R_6(q) I_6 R_6(q)^T J_{\omega_6}(q) \} \dot{q} \quad \dots\dots (10)$$

Inertia matrix D(q) can be given by equation 11

$$D(q) = m_4 J_{v_4}(q)^T J_{v_4}(q) + m_6 J_{v_6}(q)^T J_{v_6}(q) + J_{\omega_4}(q)^T R_4(q) I_4 R_4(q)^T J_{\omega_4}(q) + J_{\omega_6}(q)^T R_6(q) I_6 R_6(q)^T J_{\omega_6}(q) \quad \dots\dots (11)$$

Kinetic energy can be written as,

$$K = \frac{1}{2} \dot{q}^T D(q) \dot{q} = \frac{1}{2} \sum_{j=1}^n d_{ij}(q) \dot{q}_i \dot{q}_j \quad \dots\dots\dots (12)$$

Where D(q) is 6×6 symmetric matrix. Equation 13 shows its elements.

$$D(q) = \begin{bmatrix} d_{11} & d_{12} & d_{13} & d_{14} & d_{15} & d_{16} \\ * & d_{22} & d_{23} & d_{24} & d_{25} & d_{26} \\ * & * & d_{33} & d_{34} & d_{35} & d_{36} \\ * & * & * & d_{44} & d_{45} & d_{46} \\ * & * & * & * & d_{55} & d_{56} \\ * & * & * & * & * & d_{66} \end{bmatrix} \quad \dots\dots\dots (13)$$

Potential Energy of leg is,

$$P = m g h = \sum_{i=1}^n m_i g h_{ci} \quad \dots\dots\dots (14)$$

Lagrangian L is the function of the joint variables given by Equation 15.

$$L = K - P = \frac{1}{2} \dot{q}^T D(q) \dot{q} - P(q) = \frac{1}{2} \sum_{j=1}^n \sum_{i=1}^n d_{ij}(q) \dot{q}_i \dot{q}_j - \sum_{i=1}^n m_i g h_{ci}(q) \quad \dots\dots\dots (15)$$

The partial derivatives of the Lagrangian with respect to the velocity is,

$$\frac{\partial L}{\partial \dot{q}_k} = \frac{\partial}{\partial \dot{q}_k} \left(\frac{1}{2} \sum_{j=1}^n \sum_{i=1}^n d_{ij}(q) \dot{q}_i \dot{q}_j \right) - \frac{\partial}{\partial \dot{q}_k} P(q) =$$

$$\sum_{j=1}^n d_{kj}(q) \dot{q}_j \quad \dots\dots\dots (16)$$

Differential of equation 16 is,

$$\frac{d}{dt} \frac{\partial L}{\partial \dot{q}_k} = \sum_{j=1}^n \dot{d}_{kj} \dot{q}_j + \sum_{j=1}^n \frac{d}{dt} d_{kj} \dot{q}_j = \sum_{j=1}^n \dot{d}_{kj} \dot{q}_j + \sum_{j=1}^n \sum_{i=1}^n \frac{\partial d_{kj}}{\partial q_i} \dot{q}_i \dot{q}_j \quad \dots\dots\dots (17)$$

The partial derivatives of the Lagrangian with respect to the position is

$$\frac{\partial L}{\partial q_k} = \frac{1}{2} \sum_{j=1}^n \sum_{i=1}^n \frac{\partial ij}{\partial q_k} \dot{q}_i \dot{q}_j - \frac{\partial P}{\partial q_k} \dots\dots\dots (18)$$

Euler-Lagrangian equation can be obtained by subtraction of equation 18 from equation 17

$$\sum_{j=1}^n dk_j \ddot{q}_j + \sum_{j=1}^n \sum_{i=1}^n \left\{ \frac{\partial dk_j}{\partial q_i} - \frac{1}{2} \frac{\partial dij}{\partial q_k} \right\} \dot{q}_i \dot{q}_j + \frac{\partial P}{\partial q_k} = \tau_k \dots\dots\dots (19)$$

If we define the Christoffel symbols C_{ijk} and gravity force $g_k(q)$ as in Equation and

$$C_{ijk} = \frac{1}{2} \left(\frac{\partial dk_j}{\partial q_i} + \frac{\partial dk_i}{\partial q_j} - \frac{\partial dij}{\partial q_k} \right) \dots\dots\dots (20)$$

$$g_k(q) = \frac{\partial P(q)}{\partial q_k} \dots\dots\dots (21)$$

Equations of motion are given by equation 22,

$$\sum_{j=1}^6 dk_j(q) \ddot{q}_j + \sum_{j=1}^6 \sum_{i=1}^6 C_{ijk}(q) \dot{q}_i \dot{q}_j + g_k(q) = \tau_k \dots\dots\dots (22)$$

The second term of equation 22, $\sum_{j=1}^6 \sum_{i=1}^6 C_{ijk}(q) \dot{q}_i \dot{q}_j$ has two meanings. When $i = j$, term indicates centrifugal force. When $i \neq j$, term indicates Coriolis Effect. Since the product of inertia is much smaller than moment of inertia, Coriolis effect can be disregarded. So the equations of motion can be written as equation 23.

$$\begin{aligned} \tau_1 &= d_{11}\dot{\theta}_1 + d_{12}\dot{\theta}_2 + d_{13}\dot{\theta}_3 + d_{14}\dot{\theta}_4 + d_{15}\dot{\theta}_5 + d_{16}\dot{\theta}_6 + C_{111}\dot{\theta}_1^2 + C_{221}\dot{\theta}_2^2 + C_{331}\dot{\theta}_3^2 + C_{441}\dot{\theta}_4^2 + C_{551}\dot{\theta}_5^2 + C_{661}\dot{\theta}_6^2 + g_1. \\ \tau_2 &= d_{21}\dot{\theta}_1 + d_{22}\dot{\theta}_2 + d_{23}\dot{\theta}_3 + d_{24}\dot{\theta}_4 + d_{25}\dot{\theta}_5 + d_{26}\dot{\theta}_6 + C_{112}\dot{\theta}_1^2 + C_{222}\dot{\theta}_2^2 + C_{332}\dot{\theta}_3^2 + C_{442}\dot{\theta}_4^2 + C_{552}\dot{\theta}_5^2 + C_{662}\dot{\theta}_6^2 + g_2. \\ \tau_3 &= d_{31}\dot{\theta}_1 + d_{32}\dot{\theta}_2 + d_{33}\dot{\theta}_3 + d_{34}\dot{\theta}_4 + d_{35}\dot{\theta}_5 + d_{36}\dot{\theta}_6 + C_{113}\dot{\theta}_1^2 + C_{223}\dot{\theta}_2^2 + C_{333}\dot{\theta}_3^2 + C_{443}\dot{\theta}_4^2 + C_{553}\dot{\theta}_5^2 + C_{663}\dot{\theta}_6^2 + g_3. \\ \tau_4 &= d_{41}\dot{\theta}_1 + d_{42}\dot{\theta}_2 + d_{43}\dot{\theta}_3 + d_{44}\dot{\theta}_4 + d_{45}\dot{\theta}_5 + d_{46}\dot{\theta}_6 + C_{114}\dot{\theta}_1^2 + C_{224}\dot{\theta}_2^2 + C_{334}\dot{\theta}_3^2 + C_{444}\dot{\theta}_4^2 + C_{554}\dot{\theta}_5^2 + C_{664}\dot{\theta}_6^2 + g_4. \\ \tau_5 &= d_{51}\dot{\theta}_1 + d_{52}\dot{\theta}_2 + d_{53}\dot{\theta}_3 + d_{54}\dot{\theta}_4 + d_{55}\dot{\theta}_5 + d_{56}\dot{\theta}_6 + C_{115}\dot{\theta}_1^2 + C_{225}\dot{\theta}_2^2 + C_{335}\dot{\theta}_3^2 + C_{445}\dot{\theta}_4^2 + C_{555}\dot{\theta}_5^2 + C_{665}\dot{\theta}_6^2 + g_5. \\ \tau_6 &= d_{61}\dot{\theta}_1 + d_{62}\dot{\theta}_2 + d_{63}\dot{\theta}_3 + d_{64}\dot{\theta}_4 + d_{65}\dot{\theta}_5 + d_{66}\dot{\theta}_6 + C_{116}\dot{\theta}_1^2 + C_{226}\dot{\theta}_2^2 + C_{336}\dot{\theta}_3^2 + C_{446}\dot{\theta}_4^2 + C_{556}\dot{\theta}_5^2 + C_{666}\dot{\theta}_6^2 + g_6 \dots\dots\dots (23) \end{aligned}$$

Element of inertia matrix is,

$$d_{11} = (I_{xx4} (c(\theta_3) (1-l_4^2 l_5^2 ((l_5 (c(\theta_3) c(\theta_4) (c(\theta_1) s(\theta_2) + c(\theta_2) s(\theta_1)) - s(\theta_3) s(\theta_4) (c(\theta_1) s(\theta_2) + c(\theta_2) s(\theta_1))) + l_4 c(\theta_3) (c(\theta_1) s(\theta_2) + c(\theta_2) s(\theta_1)))^2/2 + (l_5 (c(\theta_3) c(\theta_4) (c(\theta_1) c(\theta_2) - s(\theta_1) s(\theta_2)) - s(\theta_3) s(\theta_4) (c(\theta_1) c(\theta_2) - s(\theta_1) s(\theta_2))) + l_4 c(\theta_3) (c(\theta_1) c(\theta_2) - s(\theta_1) s(\theta_2)))^2/2 - l_4^2/2 - l_5^2/2 + (l_5 (c(\theta_3) s(\theta_4) + c(\theta_4) s(\theta_3)) + l_4 s(\theta_3))^2/2)^{1/2} + l_4 l_5 s(\theta_3) ((l_5 (c(\theta_3) c(\theta_4) (c(\theta_1) s(\theta_2) + c(\theta_2) s(\theta_1)) - s(\theta_3) s(\theta_4) (c(\theta_1) s(\theta_2) + c(\theta_2) s(\theta_1))) + l_4 c(\theta_3) (c(\theta_1) s(\theta_2) + c(\theta_2) s(\theta_1)))^2/2 + (l_5 (c(\theta_3) c(\theta_4) (c(\theta_1) c(\theta_2) - s(\theta_1) s(\theta_2)) - s(\theta_3) s(\theta_4) (c(\theta_1) c(\theta_2) - s(\theta_1) s(\theta_2))) + l_4 c(\theta_3) (c(\theta_1) c(\theta_2) - s(\theta_1) s(\theta_2)))^2/2 - l_4^2/2 - l_5^2/2 + (l_5 (c(\theta_3) s(\theta_4) + c(\theta_4) s(\theta_3)) + l_4 s(\theta_3))^2/2)) - I_{yx4} (s(\theta_3) (1 - l_4^2 l_5^2 ((l_5 (c(\theta_3) c(\theta_4) (c(\theta_1) s(\theta_2) + c(\theta_2) s(\theta_1)) - s(\theta_3) s(\theta_4) (c(\theta_1) s(\theta_2) + c(\theta_2) s(\theta_1))) + l_4 c(\theta_3) (c(\theta_1) s(\theta_2) + c(\theta_2) s(\theta_1)))^2/2 + (l_5 (c(\theta_3) c(\theta_4) (c(\theta_1) c(\theta_2) - s(\theta_1) s(\theta_2)) - s(\theta_3) s(\theta_4) (c(\theta_1) c(\theta_2) - s(\theta_1) s(\theta_2))) + l_4 c(\theta_3) (c(\theta_1) c(\theta_2) - s(\theta_1) s(\theta_2)))^2/2 - l_4^2/2 - l_5^2/2 + (l_5 (c(\theta_3) s(\theta_4) + c(\theta_4) s(\theta_3)) + l_4 s(\theta_3))^2/2))^{1/2} - l_4 l_5 c(\theta_3) ((l_5 (c(\theta_3) c(\theta_4) (c(\theta_1) s(\theta_2) + c(\theta_2) s(\theta_1)) - s(\theta_3) s(\theta_4) (c(\theta_1) s(\theta_2) + c(\theta_2) s(\theta_1))) + l_4 c(\theta_3) (c(\theta_1) s(\theta_2) + c(\theta_2) s(\theta_1)))^2/2 + (l_5 (c(\theta_3) c(\theta_4) (c(\theta_1) c(\theta_2) - s(\theta_1) s(\theta_2)) - s(\theta_3) s(\theta_4) (c(\theta_1) c(\theta_2) - s(\theta_1) s(\theta_2))) + l_4 c(\theta_3) (c(\theta_1) c(\theta_2) - s(\theta_1) s(\theta_2)))^2/2 - l_4^2/2 - l_5^2/2 + (l_5 (c(\theta_3) s(\theta_4) + c(\theta_4) s(\theta_3)) + l_4 s(\theta_3))^2/2))).$$

Similarly all other $d_{12}, d_{13}, d_{14}, d_{15}, d_{16}, d_{21}, d_{22}, d_{23}, d_{24}, d_{25}, d_{26}, d_{31}, d_{32}, d_{33}, d_{34}, d_{35}, d_{36}, d_{41}, d_{42}, d_{43}, d_{44}, d_{45}, d_{46}, d_{51}, d_{52}, d_{53}, d_{54}, d_{55}, d_{56}, d_{61}, d_{62}, d_{63}, d_{64}, d_{65}, d_{66}$ can be found out.

Each element of the Christoffel symbols is,

$$C_{113} = \frac{1}{2} \left\{ \frac{\partial d_{31}}{\partial q_1} + \frac{\partial d_{31}}{\partial q_1} - \frac{\partial d_{11}}{\partial q_3} \right\} = \frac{\partial d_{13}}{\partial q_1} - \frac{1}{2} \frac{\partial d_{11}}{\partial q_3}$$

REFERENCES:

- [1] T. Kato, A. Takanishi, H. Jishikawa, and I. Kato, The realization of the quasi-dynamic walking by the biped walking machine, *Fourth Symposium on Theory and Practice of Robots and Manipulators* (A. Morecki, G. Bianchi, and K. Kedzior, eds.), (Warsaw), pp. 341–351, Polish Scientific Publishers, 1983.
- [2] H. Miura and I. Shimoyama, Dynamic walk of a biped, *International Journal of Robotics Research*, vol. 3, pp. 60–74, 1984.
- [3] M. H. Raibert, "Legged Robots That Balance". Cambridge, MA: MIT Press, 1986.
- [4] J. Hodgins, J. Koechling, and M. H. Raibert, Running experiments with a planar biped, *Robotics Research: the 3rd Int. Symp. (O. Faugeras and G. Giralt, eds.)*, (Cambridge, MA), pp. 349–355, MIT Press, 1986.
- [5] A. Takanishi, H.-o. Lim, M. Tsuda, and I. Kato, Realisation of dynamic biped walking stabilised by trunk motion on a sagittally uneven surface, *Proceedings of the 1990 IEEE Int. Workshop on Intelligent Robots and Systems (IROS)*, pp. 323–330, 1990
- [6] T. McGeer, Passive dynamic walking, *International Journal of Robotics Research*, vol. 9, pp. 62–82, 1990.
- [7] Sano A., Furusho J., Realization of natural dynamic walking using the angular momentum information, *Proceedings of 1990 IEEE International Conference on Robotics and Automation*, vol. 3, pp. 1476–1481, 1990
- [8] Y. F. Zheng and J. Shen, Gait synthesis for the SD-2 biped robot to climb sloping surface, *IEEE Trans. Robot. Automat.*, vol. 6, pp. 86–96, 1990.
- [9] S. Kajita, T. Yamaura, and A. Kobayashi, Dynamic walking control of a biped robot along a potential energy conserving orbit, *IEEE Transactions on Robotics and Automation*, pp. 431–438, Aug. 1992.
- [10] Yamaguchi, A. Takanishi, and I. Kato, Development of a biped walking robot compensating for three-axis moment by trunk motion, *Proceedings of the 1993 IEEE/RSJ Int. Conference on Intelligent Robots and Systems (IROS)*, pp. 561–566, July 1993.
- [11] J.H.Park and K.I. Kim, Biped robot walking using gravity-compensated inverted pendulum mode and computed torque control, *IEEE Int. Conf. on Robotics and Automation*, pp. 3528–3533, 1998.
- [12] M. Garcia, A. Chatterjee, A. Ruina, and M. Coleman, The simplest walking model: Stability, complexity, and scaling, *ASME Journal of Biomechanical Engineering*, 1998.
- [13] Sardain P., Rostami M., Bessonnet G., An anthro-pomorphic biped robot dynamic concepts and technological design, *IEEE Transactions on Systems Man and Cybernetics*, vol. 28a, pp. 823–838, 1998.
- [14] Zonfrilli F., Oriolo G., Nardi D., A biped locomotion strategy for the quadruped robot Sony ERS-210, *IEEE International Conference on Robotics and Automation (ICRA)*, pp. 2768–2774, 2002.
- [15] Sakgami Y., Watanabe R., Aoyama C., Matsunaga S., Higaki N., Fujimura K., The intelligent ASIMO: system overview and integration, *IEEE/RSJ International Conference on Intelligent Robots and Systems*, pp. 2478–2483, 2002.
- [16] Hirukawa H., Kanehiro F., Kajita S., Fujiwara K., Yokoi K., Kaneko K., Harada K., Experimental evaluation of the dynamics simulation of biped walking of humanoid robots, *Proceedings of IEEE International Conference on Robotics and Automation*, Taipei, China, pp. 14–19, 2003.
- [17] Fariz A., A. C. Amran and A. Kawamura, Bipedal Robot Walking Strategy on Inclined Surfaces using Position and Orientation based Inverse Kinematics Algorithm, *Proceedings of the 2010-11th Int. Conf. Control, Automation, Robotics and Vision Singapore*, pp. 182–186, 2010.

Review on Importance and Advancement in Detecting Sensitive Data Leakage in Public Network

Ms. Revathi Yegappan
PG Scholar, Computer Network Engineering
Dept of Computer Science Engineering
NHCE, Bangalore
Email: revathiyegappan@gmail.com

Dr. S. Mohan Kumar
Associate Professor, Department of Computer Science and Engineering,
New Horizon College of Engineering,
Bangalore.
Email: drsmohankumar@gmail.com

ABSTRACT- Data is one of the most valuable assets in every organization. It is required to detect and prevent the data loss from being stolen or leaked from the organization to the outside world. Data loss may occur intentionally or unintentionally by the internal employees or by the trusted third parties due to mishandling or by mistakes. These data loss causes damage to the organization brands and reputation. Even though there are various techniques to prevent the data loss, but it is essential to detect the leakage of sensitive data as soon as possible before leaving the trusted network. Data loss prevention controls should be effectively implemented in advance in detecting and preventing the sensitive data from being leaked out of an organization.

Keywords: Information Security, Cyber-Crime, Hacks, Attacks, Data Security, Security Risks, Data Leakage, Data Leak Detection, Network Security, Privacy.

INTRODUCTION

Sensitive data could be of different types, it could be related details about a client, employee, Health records of an individual, finance, credit cards details etc. Sensitive data is the information where the disclosure is protected by laws and regulations and mainly by the organization policy. The loss of sensitive data leads to financial damage and the reputation of an organization. This loss of sensitive information affects the organization, customer and the external parties whose information are compromised. Thus the leakage of sensitive information should be prevented from unauthorized transmission of data to the public domain.

Information security controls are employed to protect the sensitive data. An organization need to categorize its data asset and define their sensitivity and identify the level of protection by means of data classification. This classification of data helps to ensure adequate controls are provided to sensitive data .To secure these sensitive data, it is important to know what kind of data is considered to be sensitive, where these sensitive data's are located and who can access those data's.

Data violation is when the sensitive, protected data is viewed, stolen or accessed by unauthorized individual. Data breach involves accessing the personal health information, personally identifiable information, intellectual property. To avoid such data violations Government compliance regulations, industry guidelines provide strict governance on sensitive and personal data.

In any organization data security program is primarily implemented on the devices and media controls. This includes policies, encryption techniques and other necessary safeguards to protect the sensitive information that are stored in storage devices, systems and transportable media. A Data security program should be implemented by considering different factors like Technical safeguards, access controls, monitoring and logging, backup and recovery, data disposal, security training and awareness, auditing and testing, and response program.

While we understand importance of the data security and data loss, it's also necessary understand the impact of the data losses in today scenario. Evolution of science and technology trends impacts business in both positive and negative ways. From our analysis we understand that, most of the current technology trends in Information Technology has created an anxiety on the information security space.

For example the rising market in today's world is the consumer market. E-commerce had made anything and everything possible to buy in today's world. While this is nice to have, it has created high risk areas on information security. Organizations are compelled to provide by accessibility by all means like, mobile, Kiosks, Laptops, I pads, etc. and consumer could be any one. So the information of

organization is available in all the places wherever there is connectivity. This increases susceptibility, sharing of data thru social media and accessible of unintended data owners.

We could also add more to above trends. Cloud revolution has significantly helped the business teams to reduce their Infrastructure cost. The flip side, it has created a risk in terms of Information privacy and challenges in compliances. This one of the reasons why many organizations have not shifted their ERP's to cloud mode.

While we understand the significance of Business Continuity Programs (BCP) in many organizations which is operating 24/7, damages or failures of these systems have created major impact on the financials and loyalty of these companies. While some organization faces the resource crunch situation, human resource do open the gates for third party vendors and contractors to work for their end clients. This will end up in providing complete access and rights to these resources as like an employee. Just in case the right not reset after their contract period or if the monitoring of accessibility is not done properly, it could internally be a high risk situation for the information available in the respective organization.

RELATED RESEARCH WORK

- ❖ Statistics from security firms, research institutions and government organizations show that the numbers of data-leak instances have grown rapidly in recent years. The rising cost of data loss incidents According to a 2010 Ponemon Institute study, the average total cost per data breach has risen to \$7.2 million, or \$214 per record lost. In addition to the costs of incidents increasing, the number of leaks appears to be increasing every year.
- ❖ Papadimitriou.P[et.al],(2009), 'A Model for Data Leakage Detection',[8]-This paper proposes data allocation strategies (across the agents) that improve the probability of identifying leakages. These methods do not rely on alterations of the released data (e.g., watermarks). In some cases "realistic but fake" data records are injected to further improve our chances of detecting leakage and identifying the guilty party.
- ❖ Marecki.J.[et.al],(2010), 'A Decision Theoretic Approach to Data Leakage Prevention',[9]-This paper focus on domains with one information source (sender) and many information sinks (recipients) where: (i) sharing is mutually beneficial for the sender and the recipients, (ii) leaking a shared information is beneficial to the recipients but undesirable to the sender, and (iii) information sharing decisions of the sender are determined using imperfect monitoring of the (un)intended information leakage by the recipients.
- ❖ Jiangjiang Wu[et.al],(2011), 'An Active Data Leakage Prevention Model for Insider Threat',[7]-This paper presents an active data leakage prevention model for insider threat that combines trusted storage with virtual isolation technologies and expresses the protection requirements from the aspect of data object. It shows an implementation framework and give formal description as well as security properties proof.
- ❖ X. Shu and D.Yao[et.al], (2012), 'Data leak detection as a service',[6]- In this paper A network-based data-leak detection (DLD) technique is adopted to detect the accidental leaks due to human errors. The algorithm minimizes the exposure of sensitive data to other network.
- ❖ Alneyadi.S[et.al],(2013), 'Adaptable N-gram classification model for data leakage prevention',[5]- This paper uses N-grams statistical analysis for data classification purposes. The method is based on using N-grams frequency to classify documents under distinct categories. It uses simple taxicab geometry to compute the similarity between documents and existing categories.
- ❖ Yan Wen[et.al],(2014), 'Towards Thwarting Data Leakage with Memory Page Access Interception',[4]-This paper uses Gemini, an instrumentation-free approach, to track data propagation dynamically and then prevent data leakage. Gemini leverages the page fault interrupt mechanism of the operating system, instead of DBI, to track memory page accesses, and then thwart the data leakage. As a result, Gemini is application transparent, i.e., it solves the application compatibility issue.
- ❖ Alneyadi.S[et.al],(2015), 'Detecting Data Semantic: A Data Leakage Prevention Approach',[3]-In this paper, a statistical data leakage prevention (DLP) model is presented to classify data on the basis of semantics. This study contributes to the data leakage prevention field by using data statistical analysis to detect evolved confidential data. The approach was based on using the well-known information retrieval function Term Frequency-Inverse Document Frequency (TF-IDF).
- ❖ Shu, X[et.al],.(2015), 'Fast Detection of Transformed Data Leaks',[1]-In this paper, a detection is coupled with a comparable sampling algorithm it compares the similarity of two separately sampled sequences.
- ❖ Yuri Shapiro[et.al],(2013), 'Content-based data leakage detection using extended fingerprinting',[2]- In this paper an extension to the fingerprinting approach is done based on sorted k-skip-n-grams.

OBSERVATION

- ❖ Exact string matching technique fails to detect data leak in network due to low tolerance for unknown noise.
- ❖ Comparison based on regular expression supports wild card but it is not scalable and practically difficult to deploy.
- ❖ Even though there exists many such solutions to detect and prevent the leakage of confidential data but none of the methods provide absolute protection .Thus the purpose of this research is to provide advancement in detecting the sensitive data leakage in public domain by performing deep content inspection and providing the ability to discover the data leakage as fast as possible .Alert have to be provided about the vulnerability of the data exposure to the user and the administrators.

CONCLUSION

In this paper different data leakage detection models and techniques are premeditated .Thus it is very important to implement DLP controls and information security controls to manage data loss risks. These clear set of controls should be monitored over time and the focus is on defense in depth approach. The data leakage detection and prevention should ensure sensitive data remain safe. The goal of this module is to discover the leakage of confidential data by using a real dataset in public domain and the proposed method try to improve the accuracy and better detection.

REFERENCES:

- [1] Xiaokui Shu, Jing Zhang, Danfeng (Daphne) Yao ,”Fast Detection of Transformed Data Leak”, iee transactions on information forensics and security, vol. 11, no. 3, march 2016
- [2]Shapira, Yuri, Bracha Shapira, and Asaf Shabtai. "Content-based data leakage detection using extended fingerprinting." arXiv preprint arXiv:1302.2028 (2013).
- [3]Alneyadi, Sultan, Elankayer Sithirasenan, and Vallipuram Muthukkumarasamy. "Detecting Data Semantic: A Data Leakage Prevention Approach." Trustcom/BigDataSE/ISPA, 2015 IEEE. Vol. 1. IEEE, 2015.
- [4]Wen, Yan, Jinjing Zhao, and Hua Chen. "Towards Thwarting Data Leakage with Memory Page Access Interception." Dependable, Autonomic and Secure Computing (DASC), 2014 IEEE 12th International Conference on. IEEE, 2014.
- [5]Alneyadi, Sultan, Elankayer Sithirasenan, and Vallipuram Muthukkumarasamy. "Adaptable n-gram classification model for data leakage prevention." Signal Processing and Communication Systems (ICSPCS), 2013 7th International Conference on. IEEE, 2013.
- [6]Shu, Xiaokui, and Danfeng Daphne Yao. "Data leak detection as a service."Security and Privacy in Communication Networks. Springer Berlin Heidelberg, 2012. 222-240.
- [7]Wu, Jiangjiang, et al. "An active data leakage prevention model for insider threat." Intelligence Information Processing and Trusted Computing (IPTC), 2011 2nd International Symposium on. IEEE, 2011.
- [8]Papadimitriou, Panagiotis, and Hector Garcia-Molina. "A model for data leakage detection." Data Engineering, 2009. ICDE'09. IEEE 25th International Conference on. IEEE, 2009.
- [9]Marecki, Janusz, Mudhakar Srivatsa, and Pradeep Varakantham. "A Decision Theoretic Approach to Data Leakage Prevention." Social Computing (SocialCom), 2010 IEEE Second International Conference on. IEEE, 2010.

EXPERIMENTAL STUDY OF PROCESS PARAMETERS AND EFFECT OF TOOL DESIGN ON PROPERTIES OF FRICTION STIR SPOT WELDS

ATMANAND ANIKIVI, VENKATRAO KULKARNI

Assistant Professor, Department of Mechanical Engineering, Sri Venkateshwara College of Engineering, Bangalore – 562157 INDIA

atmanand_623@rediffmail.com, +91-9738331167.

Abstract: Friction stir welding (FSW) has produced a great impact in several industries due to the advantages that this process presents. In particular, the automotive industry has developed a variant of the original process, called Friction Stir Spot Welding (FSSW), which has a strong interest related to the welding of aluminium alloys and dissimilar materials in thin sheets. Aluminium-steel welding is an actual challenge, being FSSW an alternative to produce these joints. However, the information available related to the influence of process parameters on the characteristics of aluminium-steel joints is scarce. In the present investigation Aluminium 8011 was used. Keywords: friction stir spot welding; Aluminium; Microstructure, Macrostructure.

Keywords: friction stir spot welding (FSSW); Aluminium; Tool design; Weld assessment; Microscopic structure; Macroscopic structure; Metallographic studies.

1. Introduction

The application of lightweight metals such as aluminium alloys in transportation industries, especially in automotive industry, is rapidly developed in order to reduce CO₂ exhaust gas and fuel consumption. However, steels are still widely used for structural components because of the lower absolute strength and higher material cost of aluminium alloys. Therefore, assembling both aluminium alloys and steels is necessary to develop hybrid body structures. It is known that fusion welding between aluminium alloy and steel are not reliable because brittle intermetallic compounds are formed along the interface, which results in the lower strength of welds. Recently, joining aluminium alloys to steels are tried by a friction stir welding (FSW) technique, which is a solid state welding process, and successfully achieved high strength welds. A spot welding process using FSW technique has been newly developed, which is called friction stir spot welding (FSSW) or friction spot joining (FSJ). This method is expected to apply to joining for body parts made of aluminium sheet in transportation systems because traditional resistance spot welding of aluminium alloy usually results in poor reliability of joints. FSSW is a solid state joining process as well as FSW, and it is believed that FSSW is suitable for joining dissimilar metals. Consequently, FSSW was applied not only for the joining between dissimilar aluminium alloys but also aluminium alloy and steel.

2. Experimental Details

2.1 Materials

Aluminium 8011:

Metal sheet of aluminium (Al 8011) was used for the experiment. Thickness of the sheets used in the experiment was 3.0 mm.

Table 1: Chemical composition of the material

Chemical composition in % for grade 8011

Fe	Si	Mn	Ti	Al	Cu	Mg	Zn	Impurity
0.6 - 1	0.5 - 0.9	max 0.2	Max 0.08	97.57 - 98.9	max 0.1	Max 0.05	max 0.1	other, each 0.05;

Table 2: Mechanical Properties of the material

Mechanical properties under T=200 C for grade 8011 (8011)

Assortment	Dimension	Direct.	σ_B	σ_T	σ_5	ψ	KCU	Heat treatment
-	Mm	-	MPa	MPa	%	%	kJ / m2	-
soft , GOST 618-73			30-40		2-3			
hard , GOST 618-73			100-120					

2.2 Preparation of Materials

The material aluminium was in the form of a big sheet with uniform thickness of 3 mm. The Aluminium was then shear cut to the dimension of 215x35 mm. Further the workpieces were milled to obtain a perfect flat surface on the edges.



Figure 2. Aluminium work piece.

3. Experimental details of FSSW

3.1 Tool design

The tool design generally involves the selection of tool material and tool dimensions to suit the thickness of base plates. Based on preliminary investigations the tool was selected. The detail of the tool which is used in this investigation is given in the following table. Tungsten carbide tool is used it is not subjected to wear in welding of aluminium sheets.

Table3: chemical composition of tool material

Material	W%	Ni%	Co%
Tungsten carbide	90.0	6.0	4.0

Table4: Details of the tool used for the welding


Tool material	Shoulder dia in mm	Probe dia	Probe height	Shoulder type
WC	25		80	threaded



Figure3.a and b Showing top view and front view of the tool used.

3.2 Experimental set up and welding operation

The entire experiments were carried out on FSW machine. For each trial following procedure is carried out.

- 1) Checking linearity of welding plate.
- 2) The metal sheets to be welded are placed properly in position with the help of jigs and fixtures and bolted tightly for correct alignment throughout the procedure.
- 3) Now the FSW welding head containing the tool is brought in position by hydraulic mechanism. The tool is then made just to touch the surface of the metal. From this position the tool feed is given. Now the welding cycle is started and after the completion of the cycle the tool is drawn back automatically by the hydraulic mechanism.
- 4) Parameters such as tool rotation speed, plunge depth and welding time were given for each work pieces. For each FSSW process the same set up procedure was followed. With the variation in one of the parameters. FSSW analysis parameters. The mechanical performance of a FSSW connection is mainly dependent on the process parameters such as rotational speed (RS), plunge depth (PD) and dwell time (DT).

Table5: summarizes the parameters that were used in the various experiments carried out on FSSW of Aluminium. Showing parameters for the analysis of process parameters.

Welding time sec	Plunge depth mm	Welding condition	Rotational speed RPM	Tensile strength KN
2	5.9	Case 1	1500	3
4	5.9	Case 2	1500	5.3
6	5.9	Case 3	1500	5.3
2	5.9	Case 4	2000	4.3
4	5.9	Case 5	2000	4.3
6	5.9	Case 6	2000	4.6
2	5.9	Case 7	2500	4.2
4	5.9	Case 8	2500	3.6
6	5.9	Case 9	2500	3.1
4	5.8	Case 10	1500	4.5
4	5.7	Case 11	1500	3.5

3.3 Weld assessment

All welds were inspected visually for surface roughness, presence of surface grooves extent of any side flash. The width of the weld should be constant. A reduction of weld width directly after the start of welding is sign that the tool shoulder was not in sufficient contact with workpiece surface and internal voids are assumed to be present. The amount of expelled material should not exceed the amount needed for good welds. The bottom of the welds was examined for checking whether sufficient clamping has been applied.

4. Metallographic studies

Micrography is very essential for the study of structural characteristics of the weld metal. Important phase of metallography is microscopic examination. The weld were prepared for the microscopic and macroscopic examination in a step by step procedure as follows.

1) Grinding

Hand grinding using silicon abrasive was performed. The grit papers of 400, 600, 800, 1000 and 1200 grades were used. This operation was performed as per standards. The emery paper was kept on a clean glass plate kept on a hard and levelled surface of a table. The specimen was generally drawn back and forth across the length of the paper under moderately applied pressure for getting unidirectional and uniform scratches on the surface. During subsequent grinding on successive grades of emery paper, new scratches were formed at right angles, alternately to the scratches formed by the preceding papers by turning the specimen by 90° during each operation. The specimen was cleaned thoroughly with soap in running water and dried before moving on to the next emery sheet. This was done to prevent coarse abrasive particles from the previous papers to be carried on the finer grit papers.

2) Polishing

Disc polishing machine was used for this purpose. Silicon carbide powder of 1000 grit size was uniformly smeared on a clean cloth, fixed to the disk of the polishing machine. The specimen which was hand ground for about 1200 grit size in the preceding operations, was now polished on the rotating cloth at the speeds in the range of 600 -800 rpm and polishing time of about of 10-15 min. depending on the situation, until all the scratches on the surface of the specimen were removed. The specimen was thoroughly cleaned with water and dried. Final polishing was done on a micro cloth. Diamond paste of 3 μm size grit size was smeared on the cloth. The specimen was polished on the rotating cloth for about 5-10 min. until all the scratches were eliminated and a bright mirror surface is obtained. The specimen was again cleaned with soap water, dried and kept ready for the next operation i.e. etching.

3) Etching

The specimen was thoroughly washed in water. Then the etching is done immersing the sample in solution of 5ml HF (48%) in 100ml H₂O for 40-50 sec with intermediate washing in running water. This procedure is repeated for five times before the final etched sample is obtained. After the etching process the specimen were viewed under optical microscope for micrograph and under stereo microscope for macroscopic examination of the weld nugget.

5. Results and Discussions

This chapter deals with the various test results obtained on the experiments conducted. Further the influence of various process parameters is discussed. Results are interpreted and conclusion are derived.

5.1 Results

5.1.1 Tensile test and results

The tensile test were carried on each welded specimen. Tensile-shear tests were carried out in order to evaluate the performance of welds. The Bi-00-201 series of “plug ‘n’ play” test systems are the most cost effective solution to mechanical testing requirements for strength, fatigue and fracture in the 5 to 25 KN force range of static and dynamic loading. The welded specimens are now tested on Nano Servo Hydraulic UTM to evaluate their tensile strength. After fixing the sample in appropriate position, the load is applied gradually by the hydraulic mechanism. For tensile test the graphs of load vs stroke for each sample were obtained from the machine this shows the variation of load bearing capacity with respect to stroke length. For each sample the plot was analyzed and investigated that at how much stroke length the sample has maximum tensile load carrying capacity.

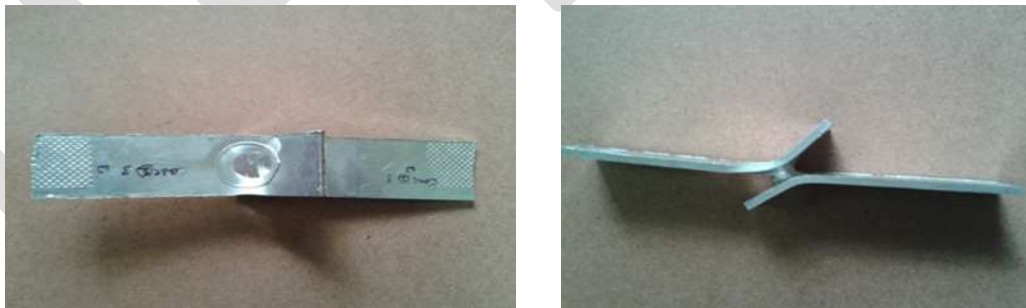
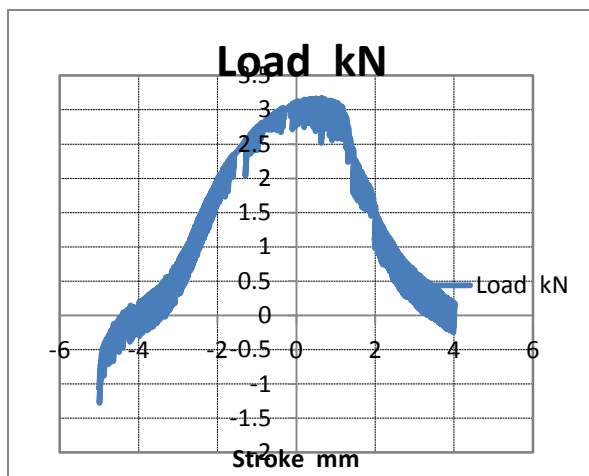


Fig4.A and B specimen after the tensile test (top view) and specimen after the tensile test (side view)

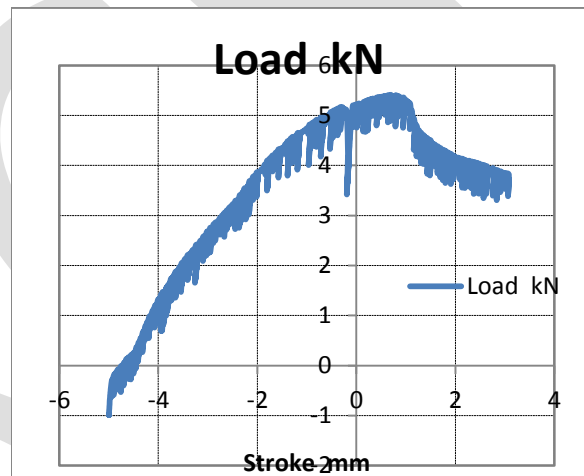


Fig4.C A specimen after the failure

Case 1;



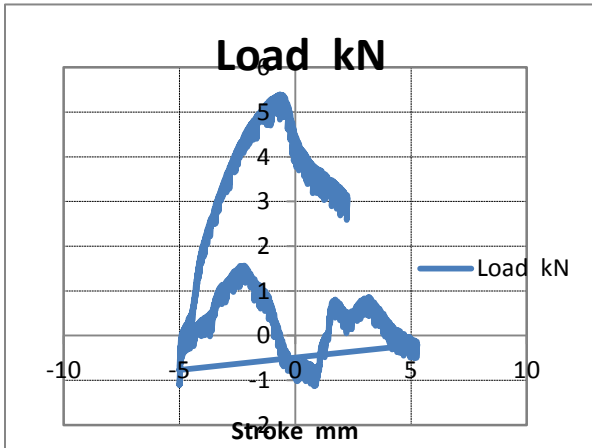
Case2;



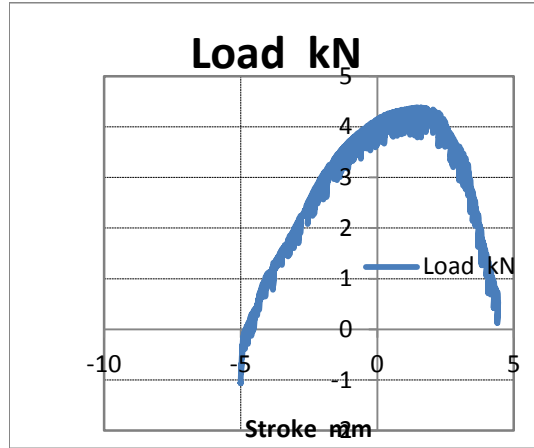
Case1: The graph shows the variation of load with stroke length. The stroke length varies from -4.9952 to 3.8892 mm, a total of 8.8944 mm. The load varies from -1.2771 kN reaches a maximum of 3.1642 kN and then falls back to -0.1278 kN. The maximum load occurs at a stroke length of 0.4887 mm.

Case2: The graph shows the variation of load with stroke length. The stroke length varies from -4.996 to 3.02 mm, a total of 8.016 mm. The load varies from -0.9842 KN reaches a maximum of 5.3899 KN and then falls back to 3.5608kN. The maximum load occurs at a stroke length of 0.5765 mm.

Case 3;



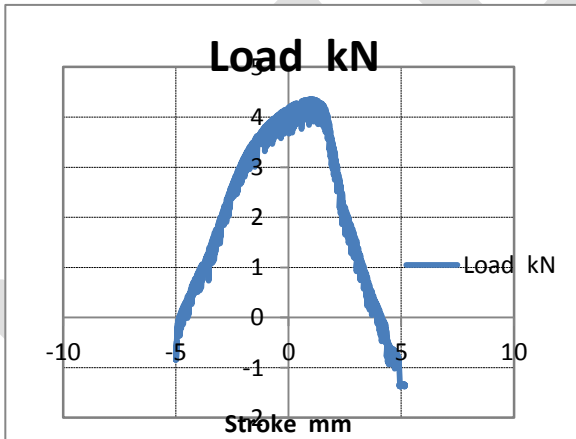
Case 4;



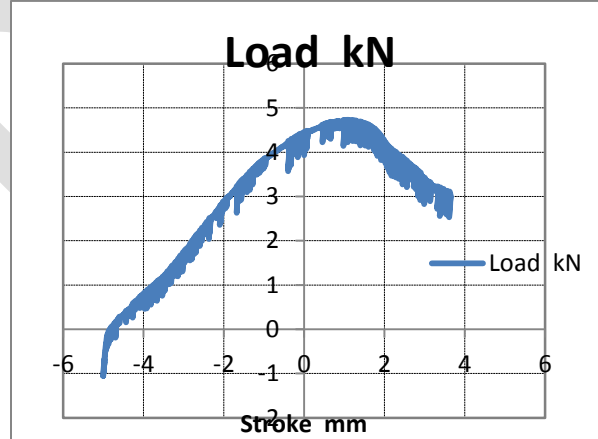
Case3: The graph shows the variation of load with stroke length. The stroke length varies from -5.004 to 2.2243 mm, a total of 7.2283 mm. The load varies from -1.086 kN reaches a maximum of 5.3288kN and then falls back to 2.5864kN. The maximum load occurs at a stroke length of -0.8902 mm.

Case4: The graph shows the variation of load with stroke length. The stroke length varies from --5.001 to 4.388 mm, a total of 9.389 mm. The load varies from -1.0583 kN reaches a maximum of 4.3887kN and then falls back to 0.1326kN. The maximum load occurs at a stroke length of 1.3887 mm.

Case 5;



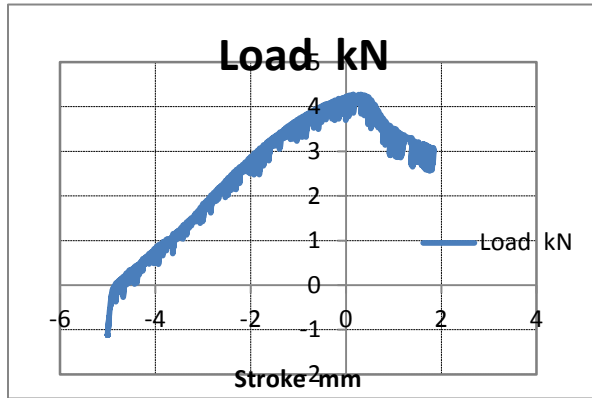
Case6;



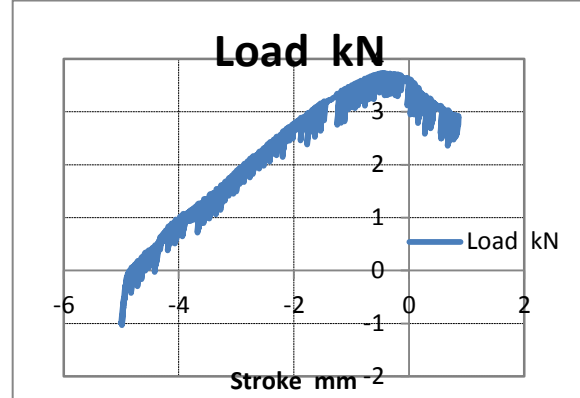
Case5: The graph shows the variation of load with stroke length. The stroke length varies from --5.007 to 4.986 mm, a total of 9.993 mm. The load varies from -0.8391 kN reaches a maximum of 4.35kN and then falls back to -1.3467 kN. The maximum load occurs at a stroke length of 1.0113 mm.

Case6: The graph shows the variation of load with stroke length. The stroke length varies from --5.0018 to 3.4639 mm, a total of 8.4657 mm. The load varies from -1.0464 kN reaches a maximum of 4.716kN and then falls back to 2.6373 kN. The maximum load occurs at a stroke length of 0.9981 mm.

Case7;



Case 8;



Case7: The graph shows the variation of load with stroke length. The stroke length varies from -5.002 to 1.673 mm, a total of 6.675 mm. The load varies from -1.1195 kN reaches a maximum of 4.2504 kN and then falls back to 2.5902 kN. The maximum load occurs at a stroke length of 0.0549 mm.

Case8: The graph shows the variation of load with stroke length. The stroke length varies from -4.991 to 0.7259 mm, a total of 5.7169 mm. The load varies from -0.9941 kN reaches a maximum of 3.7202 kN and then falls back to 2.5615 kN. The maximum load occurs at a stroke length of -0.5126 mm.

6. Microstructure of the Experiments

6.1. Macroscopic and Microscopic structure of welds

Fig. 5 shown below is a macroscopic and microscopic structure of cross section of the welds made at the rotational speed of 2000 rpm and dwell time of 4 seconds. Fig.5a,b,c,d,e, are the cross sections of the FSSW joint which is divided into four main regions, mainly base material (BM), heat affected zone (HAZ),thermo-mechanically affected zone (TMAZ), and stir zone (SZ) respectively. From the fig.5 shown below we may note that the base material exhibits elongated grains and second phase particles parallel to the rolling direction due to work hardening effect. From the thermo-mechanically affected zone we can observe that it possesses highly deformed grains as compared to base material and heat affected zone. The stir zone has a refined and equiaxed grains. And the compact structure is observed in the stir zone and thermo-mechanically affected zone due to dynamic recrystallization occurred in the periphery of the tool pin because of the pin stirring and friction thermal cycle. In the present study, heat input during friction stir spot welding is dependent on tool rotational speed and tool dwell time. The appropriate heat input is obtained by using appropriate rotational speed and dwell time, the grain growth can be negligible even the second-phase particles becomes much finer and smaller with uniform distribution.

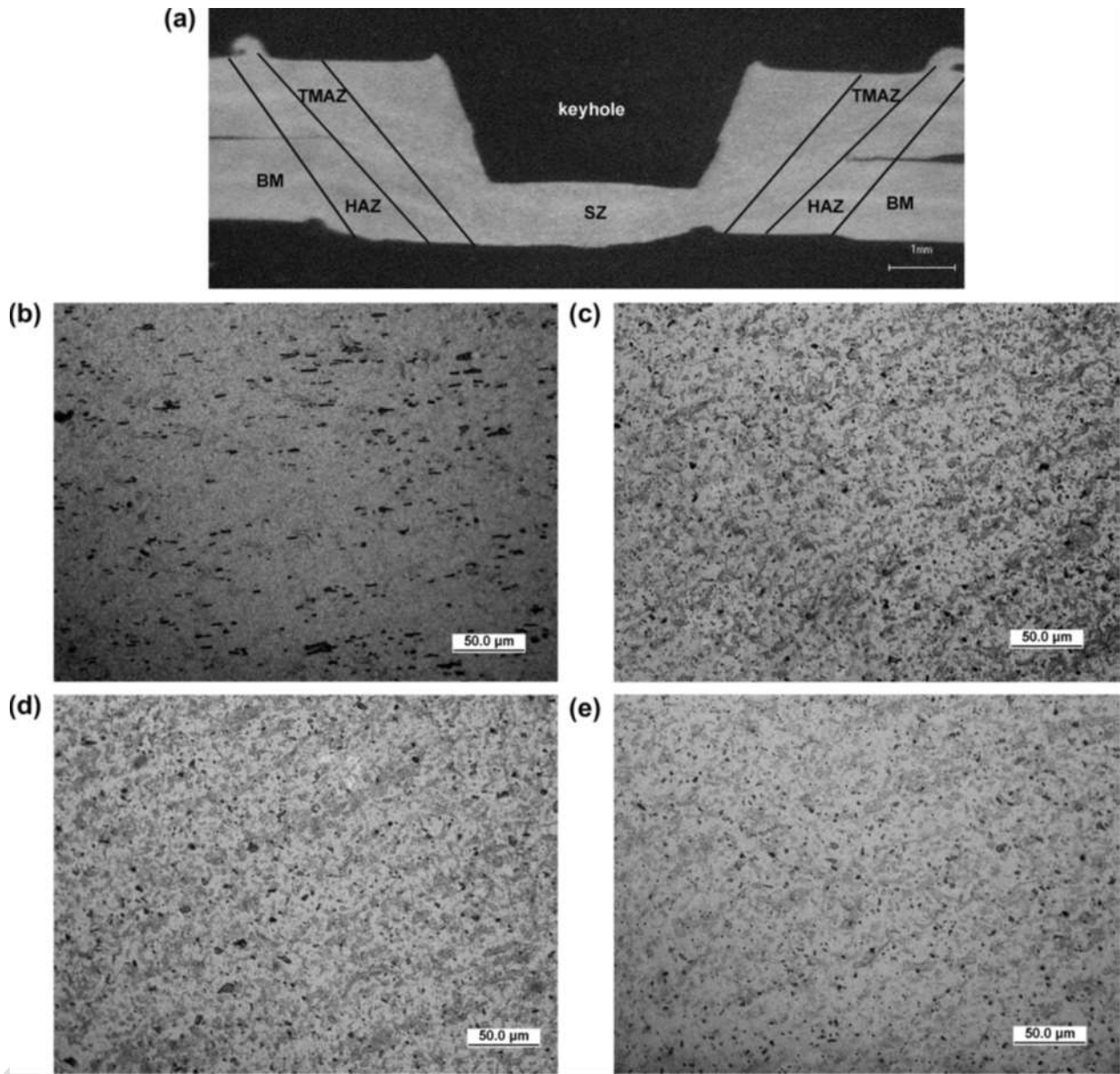
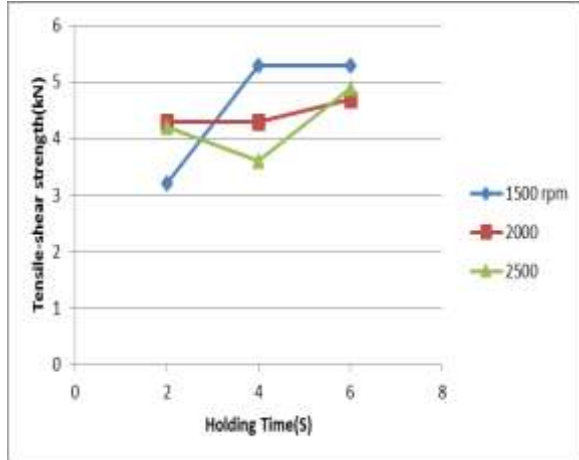


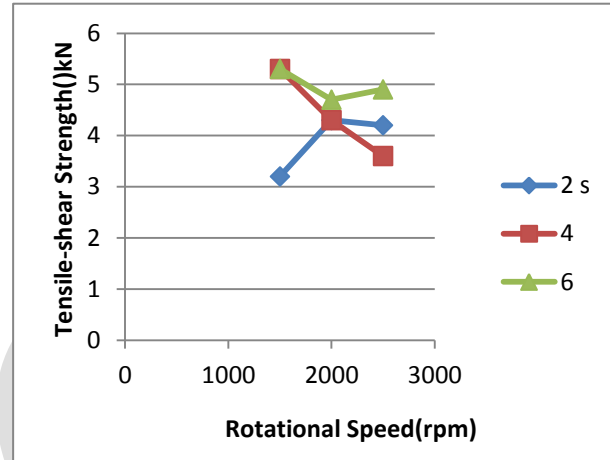
Figure5: Macroscopic and Microscopic structure welds.

7. Discussions:

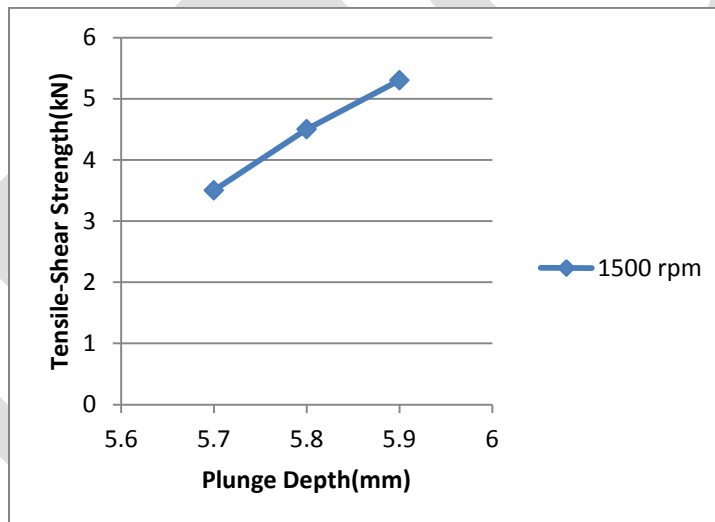
The following are the graphs obtained from the tensile tests of the specimen



Graph tensile – shear strength Vs holding time



Graph Tensile –shear strength Vs rotational speed



Graph Tensile –shear strength Vs plunge depth

8. Conclusions:

- 1) For Lower speed, lower holding time for the given tool failure mode observed is shear fracture.
- 2) Higher speed, higher holding time and higher plunge depth causes good stirring effect, grain refinement and material mixing at the interface of the workpiece. So it was observed that plug fracture occurred in this case.
- 3) At lower value of parameters, the stirring to eliminate the material mixing area is less. i.e. Stirring affected area at lower parameters is less and may be material flow at these parameters is less.
- 4) High speed, high holding time causes good stirring effect, grain refinement and due to high shoulder force material flow is more.
- 5) Increasing the plunge depth causes the expansion of stirring zone and the upward flow of the material in the lower sheet occurs.

REFERENCES:

- [1] C.D. Allen, J.A. Arbegast, Evaluation of friction stir spot welds in aluminium alloys. Paper 2005-01-1252, 2005 SAE World Congress, Society of Automotive Engineers, Detroit, MI, 2005
- [2] H.J. Aval, S. Serajzadeh, A.H. Kokabi, Evolution of microstructures and mechanical properties in similar and dissimilar friction stir welding of AA5086 and AA6061. *Mater. Sci. Eng. A* 528, 8071–8083 (2011)
- [3] Harsha Badarinarayan, 'Fundamentals of friction stir spot welding',] PhD thesis, Missouri University of Science And Technology, United State, 2009.
- [4] Jiahu Ouyang, Eswar Yarrapareddy, Radovan Kovacevic, "Microstructural evolution in the friction stir welded 6061 aluminium alloy (T6-temper condition) to copper" *Journal of Materials Processing Technology*, 2006, 172, pp 110–122.
- [5] J.A. Schneider, in: R.S. Mishra, M.W. Mahoney (Eds.), *Friction Stir Welding and Processing*, ASM International, Ohio, 2007, 37-49.
- [6] M. Shiraly, M. Shamanian, M.R. Toroghinejad, and M. Ahmadi Jazani 'Effect of Tool Rotation Rate on Microstructure and Mechanical Behavior of Friction Stir Spot-Welded Al/Cu Composite' *Journal of Materials Engineering and Performance*, Volume 23(2) February 2014, pp 413-420
- [7] R. S. Mishra, T. A. Freeney, S. Webb, Y. L. Chen, D. R. Herling, G. J. Grant, *Friction Stir Welding and Processing IV*, TMS (2007).
- [8] Tozaki, Y.. "A newly developed tool without probe for friction stir spot welding and its performance", *Journal of Materials Processing Tech.*, 20100401
- [9] Timothy J M., 'Friction Stir Welding of Commercially available Superplastic Aluminium', PhD thesis, Department of Engineering and Design, Brunel University, Brunel, 2008.
- [10] T. Freeney, S. R. Sharma, R. S. Mishra, SAE Technical paper (2006) 2006-2001-0969.
- [11] W. M. Thomas, E. D. Nicholas, J. C. Needham, M. G. Murch, P. Templesmith, C. J. Dawes, G. B. Patent 9125978.8 (1991).
- [12] Zhang, Z.. "Effect of welding parameters on microstructure and mechanical properties of friction stir spot welded 5052 aluminum alloy", *Materials and Design*, 201109.

LIMIT STATE FUNCTION FORMULATION AND TIME VARIANT RELIABILITY ANALYSIS

¹Arup Dey, ²K. M. Mostafizur Rahman Sobuj

¹Graduate Student, Department of Industrial & Production Engineering, Bangladesh University of Engineering and Technology, Bangladesh, arupdey.89@student.sust.edu

²Undergraduate Student, Department of Industrial & Production Engineering, Shahjalal University of Science & Technology, Sylhet-3114, Bangladesh, sobuj@student.sust.edu

Abstract- Most observable phenomena in the world contain certain amount of uncertainty. Probability analysis is used to estimate input and output variables of a system by considering uncertainty. Reliability is the probability that a product performs its intended function over a specified period of time and under specified service conditions. Time-variant stochastic loadings and random deterioration of material properties are inherent in engineering applications [1]. For this type of time dependent uncertainties time variant reliability analysis is used. In time variant analysis limit state function may vary over time. Deterioration of materials properties takes place due to corrosion. In this paper, a time variant limit state function developed to estimate reliability of a fluid flowing pipe over time. Monte Carlo simulation technique is used to compute reliability of pipe at different time with the help of “MATLAB R2008a” software. Due to corrosion reliability is decrease with time. So, the results of analysis can be used to determine time to maintain or change.

Keywords

Time variant reliability, Stress, Limit state function, Random variable, Probability distribution, Monte Carlo simulation

INTRODUCTION

Corrosion defined as the deterioration of material by reaction to its environment. The corrosion occurs because of the natural tendency for most metals to return to their natural state; e.g., iron in the presence of moist air will revert to its natural state, iron oxide. Extreme case of corrosion may lead to failure of the system [2]. Fluid flow is common phenomena for various chemical industries. Normally metallic pipes are used for flow of fluid. Some fluid is dangerous for environment and human being. So, proper and zero failure maintenance needed for hazard fluid flow system. Reliability analysis is used to estimate time to failure. The reliability of a product or system conveys the concept of dependability, successful operation or performance, and the absence of failure. The time-dependent reliability gives the reliability of the system over a specific time interval instead of the reliability at a certain time instant. And results of reliability analysis are used for timely maintenance.

RELIABILITY

Reliability is the ability that a system or component fulfills its intended function under given circumstances over a specified time period. One of the purposes of system reliability analysis is to identify the weakness in a system and to quantify the impact of component failures. It is usually measured by the probability of such ability. A system's reliability is modeled by what is known as its limit state function. The limit state function indicates the state of success or failure.

TIME VARIANT RELIABILITY

The time-dependent reliability gives the reliability of the system over a specific time interval instead of the reliability at a certain time instant. The strength and weakness of the component is not fixed. It changes with aging of system. The probability of failure/success is not just value, but also a function of time. For this, time variant reliability analysis needed for better estimation [3].

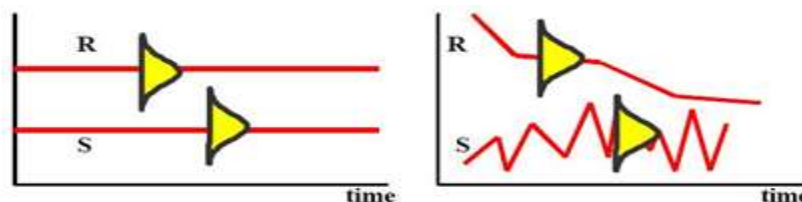


Figure 1: Time invariant and time variant system.

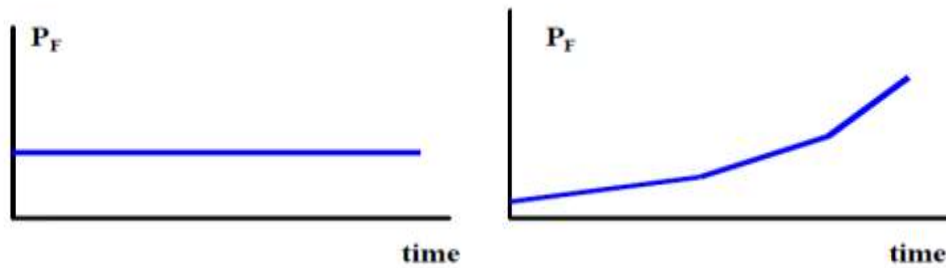


Figure 2: Time invariant and time variant probability of failure.

TIME VARIANT RELIABILITY ANALYSIS MAY BE TWO TYPES:

1. Load may be randomly varying in time: Stochastic processes are introduced in the analyses. It is allow accounting for environmental loading such as wind velocity, temperature or wave height, occupancy, traffic load etc.
2. Material properties may be decaying in time: The degradation mechanisms usually present as initiation phase and propagation phase. Both the initiation duration and propagation kinetics may be considered as random in the analyses. Example of these mechanisms are crack growth and propagation in fracture mechanics, corrosion in steel structures or in reinforce concrete rebar, concrete shrinkage and creep phenomena etc.

These two kinds of dependency may require different methods of analysis. In time-variant reliability analysis for a complicated engineering system may involve the use of many physics-based models and surrogate models, which bring in various types of uncertainty.

A general limit state function for reliability analysis is given by,

$$Z(R, S) = R - S$$

Where, Z = limit state function, R = resistance, S = load

$Z > 0$ FOR SAFE STATE OF SYSTEM.

$Z = 0$, FOR XON LIMIT STATE.

$Z < 0$, FOR FAILURE SET.

There are various types of time dependent problem. So, limit state function also various types for various cases.

1. Load variability
2. Time dependency of the resistance
3. Load and resistance time dependent, no interaction
4. Load and resistance time dependent, interaction

1. Load variability

In the case of only load variability with time, the limit state function can be formulated as:

$$Z(t) = R - S(t)$$

2. Time dependency of the resistance

In this case limit state function is:

$$Z(t) = R(t) - S$$

3. Load and resistance time dependent, no interaction

If both load S and resistance R are time dependent, and then limit state function formulated as:

$$Z(t) = R(t) - S(t)$$

4. Load and resistance time dependent, interaction

Generally, the resistance at time, t may affected by loading at any period of time. This for instance is what happens for mechanisms like fatigue and load of duration rupture.

$$Z(t) = R(S, t) - S(t)$$

Limit state function formulation

Let a thin wall cylindrical pipe which is given in below figure. And internal pressure of the cylinder is P.



Figure 3: Dimensions of cylindrical pipe.

WHERE, r_i = INNER RADIUS, r_o = OUTER RADIUS AND THICKNESS = $T = R_o - R_i$

WHEN THE PRESSURE INSIDE IS LARGER THAN THE PRESSURE OUTSIDE, THE CYLINDER WILL TEND TO SPLIT ALONG A LENGTH AND A CIRCUMFERENCE. THE STRESS PRODUCED IN LONGITUDINAL DIRECTION IS CALLED LONGITUDINAL STRESS AND THE STRESS PRODUCED IN THE CIRCUMFERENTIAL DIRECTION IS CALLED CIRCUMFERENTIAL OR HOOP STRESS.

Longitudinal stress, σ_l

Consider the force trying to split the cylinder about a circumference. The areas acted on by the longitudinal stress, σ_l and the pressure P are calculated in the figure below.



Figure 4: Stress and pressure in longitudinal direction

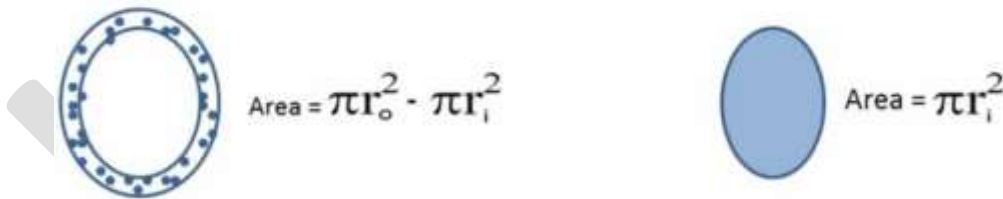


Figure 5: Area of thickness and area of fluid flow (Longitudinal direction)

From force equilibrium equation:

$$\begin{aligned}
 \text{Stress force} &= \text{Pressure force} \\
 (\pi r_o^2 - \pi r_i^2) \times \sigma_l &= \pi r_i^2 \times P \\
 \sigma_l &= \frac{\pi r_i^2}{\pi r_o^2 - \pi r_i^2} \times P \\
 &= \frac{r_i^2}{(r_o + r_i)(r_o - r_i)} \times P \\
 &= \frac{r_i^2}{2r_m t} \times P
 \end{aligned}$$

Circumferential or hoop stress, σ_c

Consider the force trying to split the cylinder about along a length. The areas acted on by the circumferential stress and the pressure are calculated in the figure below.

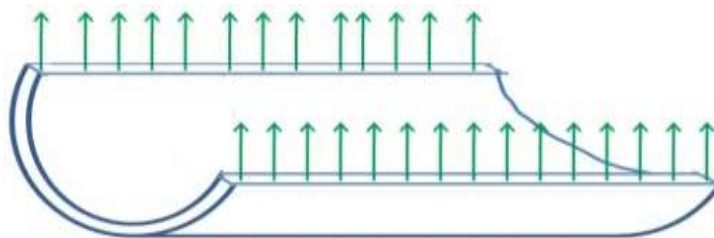


Figure 6: Stress and pressure in circumferential direction

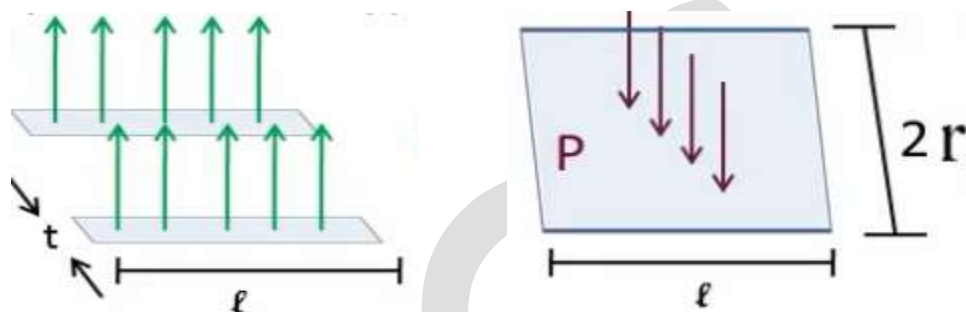


Figure 7: Area of thickness and area of fluid flow (circumferential direction)

From force equilibrium equation:

Stress force = Pressure force

$$2lt \times \sigma_c = 2r_i l \times P$$

$$\sigma_c = \frac{r_i}{t} \times P$$

It is clear that hoop stress is roughly twice the value of longitudinal stress. The wall thickness of the pipe, on almost all occasions is selected based on the thickness required for the internal pressure and allowance. Out of two pressure forces, hoop stress is used for pipe wall thickness calculation and longitudinal force mitigate by using sufficient support [4].

Limit state function

Failure of pipe due to hoop stress occurs when hoop stress force is higher than force [5],

$$F = \frac{4\pi^2 EI}{(\pi(r_o + r_i))^2}$$

$$\text{And } = \frac{lt^3}{12}, \quad = \frac{4E}{(r_o + r_i)^2} \times \frac{lt^3}{12}$$

$$= \frac{Elt^3}{3(2r_o - t)^2}$$

Where, E Modulus of elasticity
 I Moment of inertia

$$\text{So, hoop force} = \sigma_c \times 2lt = \frac{(r_o - t)}{t} \times P \times 2lt = 2l(r_o - t)P$$

If corrosion rate of pipe materials = R mm/y . So, limit state function at time T is given by,

$$Z(P, T, R, E) = F - \sigma_c \times 2lt = \frac{Elt(t - RT)^3}{3(2r_o - t + RT)^2} - 2l(r_o - t + RT)P$$

Where P, R and E are random variable and t, l and r_o are constant.

Monte Carlo simulation

Monte Carlo simulation is a type of simulation that relies on repeated random sampling and statistical analysis to compute the results. This method of simulation is very closely related to random experiments, experiments for which the specific result is not known in advance. In this context, Monte Carlo simulation can be considered as a methodical way of doing so-called what-if analysis. Monte Carlo simulation furnishes the decision maker with a range of possible outcomes and the probabilities they will occur for any choice of action [6].

In Monte Carlo simulation, we identify a statistical distribution which we can use as the source for each of the input parameters. Then, we draw random samples from each distribution, which then represent the values of the input variables. For each set of input parameters, we get a set of output parameters. The value of each output parameter is one particular outcome scenario in the simulation run. We collect such output values from a number of simulation runs.

Variables distribution and parameters

In this problem, for time dependent reliability analysis in limit state function there are seven (07) parameters including time. We considered thickness, outer diameter and length of pipe are constant. And modulus of elasticity, fluid pressure and corrosion rate are random variables. For Monte Carlo simulation, statistical distribution of input parameters is needed to identify from available historical data.

When sufficient data are available, a histogram or frequency diagram can be used to determine the underlying distribution. Also goodness of fit tests is used to assume distribution. Here, due to lack of available data we assume distribution of random variable.

Table 01: Random variables, distribution and Parameters

Variable	E (N/mm^2)	P(N/mm^2)	R(mm/y)
Statistical distribution	Normal	Normal	Normal
Mean	130000	0.5	.08
Standard deviation	8000	.01	.009

Reliability analysis

Reliability analysis can be divided into two broad categories: qualitative and quantitative. The former is intended to verify the various failure modes and causes that contribute to the unreliability of a product or system [7]. The latter uses real failure data (obtained, for example, from a test program or from field operations) in conjunction with suitable mathematical models to produce quantitative estimates of product or system reliability. Here, "MATLAB R2008a" software is used for reliability analysis by Monte Carlo simulation technique. Random number of each input variables repeatedly generated for each time (year) and value of limit state function is recorded. Total no. of positive value is divided by total repeated action to determine reliability of system in every year. Following table show data of reliability for thirty (30) years. Value of constant parameters:

Inner radius of the pipe, $r_i = 500mm$

Thickness of the pipe, $t = 25mm$

Outer radius of the pipe, $r_o = 525mm$

Length of the pipe, $l = 3m = 3000mm$

Table 02: Reliability analysis result

Time (Year)	Reliability	Time (Year)	Reliability
1	1.0000	16	0.8933
2	1.0000	17	0.8783
3	1.0000	18	0.8400
4	0.9967	19	0.8067
5	0.9983	20	0.7667
6	0.9933	21	0.7167
7	1.0000	22	0.6433
8	0.9950	23	0.5717
9	0.9900	24	0.5183
10	0.9850	25	0.4683
11	0.9817	26	0.4133
12	0.9733	27	0.3500
13	0.9633	28	0.2867
14	0.9400	29	0.2700
15	0.9300	30	0.2017

Conclusion

Most of the engineering systems are time dependent. To determine reliability properly, time variant reliability analysis is essential. Probabilistic analysis is plays an important to estimate a system condition by considering uncertainty. Difficulty of reliability is depends of complexity of limit state function, number of random variable, interdependency of variables.

REFERENCES:

- [1] Hu,Zhen (2014), Probabilistic engineering analysis and design under time-dependent uncertainty. Missouri University of Science and Technology.
- [2] Anonymous, http://www.npl.co.uk/upload/pdf/corrosion_control_in_engineering_design.pdf (Accessed 20/08/15)
- [3] A. Vrouwenvelder (TU-Delft/TNO, The Netherlands), Time variant processes in failure probability calculations.
- [4] Anonymous (2014), Lecture: Stress due to internal pressure in pipe & wall thickness calculation.
- [5] Kaminski , Dr. Clemens (2005), Lecture note, CET 1: Stress Analysis & Pressure Vessels. University of Cambridge, UK
- [6] Raychaudhuri, Samik, INTRODUCTION TO MONTE CARLO SIMULATION. Proceedings of the 2008 Winter Simulation Conference; S. J. Mason, R. R. Hill, L. Mönch, O. Rose, T. Jefferson, J. W. Fowler eds.
- [7] Blischke, Wallace R. and Murthy, D. N. Prabhakar (2003), Case Studies in Reliability and Maintenance.
- [8] Ayyub, Bilal M. (1997), Uncertainty Modeling and Analysis in Civil Engineering.

LED ILLUMINATION: A CASE STUDY ON ENERGY CONSERVATION

Mrs. Landge Shubhangi Sudhir

Assistant Professor, shubhangi.landge1@gmail.com, 7774077173

Abstract- This paper deals with the energy saving potential possible by changing the illumination schemes. With increase in energy crisis there is a need of looking for additional energy sources or reduction in energy consumption without losing comfort. Energy audition is the new trend in the present scenario and play a major role in energy saving. One of the energy saving scheme in illumination is, by using natural light and/or use of LEDs. LEDs are having major advantages of longer life & almost negligible power consumption compared to any type of illuminating sources. The case study in a residential township deals with the replacement of existing conventional lighting scheme with LED lighting scheme will have huge energy saving potential, with payback period of even less than 15 months. The LED lighting scheme provides additional advantages as cool light, decreased maintenance cost and longer life.

Keywords – Light emitting diode (LED), compact fluorescent lamp (CFL), Color rendering index (CRI), Correlated color temperature (CCT), Coefficient of variation (CV), surface mounted diode (SMD), efficient lighting technology.

1 INTRODUCTION

Lighting accounts for 7 percent of a typical household's energy bill. One of the easiest ways to save energy is cutting lighting bill. In earlier day's incandescence and fluorescence lamps were mainly used for illumination. But these lamps are extremely inefficient. Only 5 percent of energy they use is converter into visible light. The development in SV, MV and metal halide makes possible to replace this old technology. But none of these technologies could improve the efficacy exceeding 200 lumens per watt and efficiency beyond 60-70%. The recent technology of compact fluorescent lamp (CFL) has improved the efficiency and it has really proved standards. CFLs use about 75 to 80 percent less electricity than an equivalent traditional bulb and can last up to 10 times longer. CFLs are great for replacing standard home light fittings but are more expensive and its illumination decreases with use.

A new kind of lighting became available with the advent of commercial LEDs (Light emitting diode) in the 1960s. LEDs also known as solid state lighting (SSL) are solid light bulbs which are extremely energy-efficient. LEDs will consume less electricity than conventional lighting including CFLs. LED sources are compact, which gives flexibility in designing lighting fixtures and good control over the distribution of light with small reflectors or lenses. These are simple solid state electronic devices that allow electricity to flow through them in one direction to produce a small amount of light. Bulbs for domestic use contain a large number of LEDs so that enough bright light is emitted. Because of the small size of LEDs, control of the spatial distribution of illumination is extremely flexible, and the light output and spatial distribution of an LED array can be controlled with no efficiency loss. Also they can withstand high voltage fluctuations in power supply and have longer operational life. A significant difference from other light sources is that the light is more directional, i.e., emitted as a narrower beam. LED lamps are used for both general and special-purpose lighting. They are still expensive, but they are the most efficient option and their payback period is small

The objective of this paper is to discuss the LED technology along with its benefits and applications over other type of lighting sources. The energy saving potential of LED is verified by replacing the CFL and FTL with LEDs in a residential area.

2 LED TECHNOLOGY-

A. Principle of operation

LED consists of a chip of semiconducting material doped with impurities to create a p-n junction. Like other diodes, current flows easily from the p-side (anode) to the n-side (cathode), but not in the reverse direction. Charge-carriers electrons and holes flow into the junction from electrodes with different voltages. When an electron meets a hole, it falls into a lower energy level and releases energy in the form of a photon.

The wavelength of the light emitted and its color depends on the band gap energy of the materials forming the p-n junction. In silicon or germanium diodes, the electrons and holes usually recombine by a non-radiative transition, which produces no optical emission as these are indirect band gap materials. The materials used for the LED have a direct band gap with energies corresponding to near-infrared, visible, or near-ultraviolet light.

LED development began with infrared and red devices made with gallium arsenide. Advances in materials science have enabled making devices with ever-shorter wavelengths, emitting light in a variety of colors.

LEDs are usually built on an n-type substrate, with an electrode attached to the p-type layer deposited on its surface. P-type substrates, while less common, occur as well. Many commercial LEDs, especially GaN/InGaN, also use sapphire substrate. Most materials used for LED production have very high refractive indices. This means that much light will be reflected back into the material at the material/air surface interface. Thus, light extraction in LEDs is an important aspect of LED production.

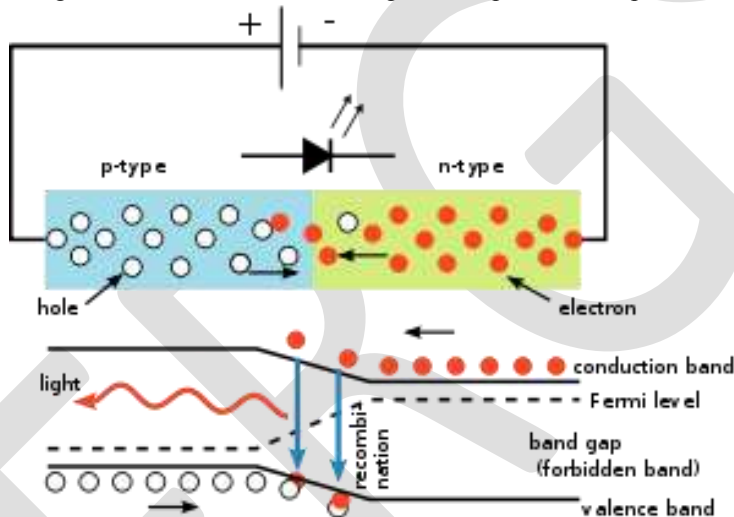


Fig 1. Circuit and Band Diagram of LED.

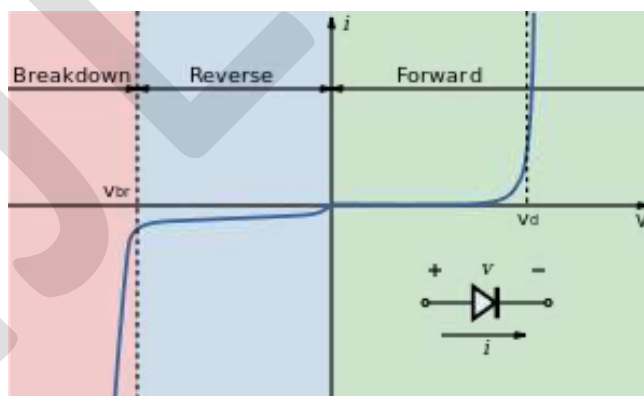


Fig. 2 I-V diagram for a diode.(LED)

B. Development in LED- For over 30 years, LEDs has been used in various areas of application, whether for industrial systems, car lights or advertising. LED technical development continues to step ahead. In the recent years, the white LEDs' luminous efficacy has increased to 130 lumens per watt and more. This is a trend that will continue into the future. The physical effect of electroluminescence was discovered more than 100 years ago.

1951	The development of a transistor marks a scientific step forward in semiconductor physics. It is now possible to explain light emission.
1962	The first red luminescence diode (type GaAsP), developed by American Nick Holonyak, enters the market. This first LED in the visible wavelength area marks the birth of the industrially-produced LED.
1971	As a result of the development of new semiconductor materials, LEDs are produced in new colors: green, orange and yellow. The LED's performance and effectiveness continues to improve.
1993	The first brilliant blue LED was developed and a very efficient LED in the green spectrum range (InGaN diode).
1995	The first LED with white light from luminescence conversion is presented and is launched on the market two years later.
2006	The first light-emitting diodes with 100 lumens per watt are produced. This efficiency can be outmatched only by gas discharge lamps.
2010	LEDs of a certain color with a gigantic luminous efficacy of 250 lumens per watt are already being developed under laboratory conditions. Progress continues to surge ahead. Today, further development towards OLED is seen as the technology of the future.

C. LED Terminology-

- i. **Color rendering index (CRI)** – CRI represents the quality of light and its accuracy to render color correctly. The ideal CRI is 100. Led bulb CRI rating ranges from 70 to 95.
- ii. **Correlated color temperature (CCT)** - it is the measure used to describe the relative color appearance of white light source. CCT indicates whether the light source appears more yellow, orange, gold or more blue in terms of the range of available shades of “white”. White shade can vary from warm white with higher red content to cool white with higher blue content. This is described by color temperature where warm white has lower value of 3000 Kelvin to than cool white of 5000 Kelvin.
- iii. **Coefficient of variation (CV)** - A measurement of illuminance uniformity. The standard deviation of a set of grid values divided by the average.

3 BENEFITS OF LED

LED lighting is very different from other lighting sources such as incandescent bulbs and CFLs. Key differences include:

- i. **Light Source:** LEDs are the size of a fleck of pepper, and a mix of red, green, and blue LEDs is typically used to make white light.
- ii. **Direction:** LEDs emit light in a specific direction, reducing the need for reflectors and diffusers that can trap light. This feature makes LEDs more efficient for many uses such as recessed down lights and task lighting. With other types of lighting, the light must be reflected to the desired direction and more than half of the light may never leave the fixture.
- iii. **Heat:** LEDs emit very little heat. In comparison, incandescent bulbs release 90% of their energy as heat and CFLs release about 80% of their energy as heat. Common incandescent bulbs get hot and contribute to heat build-up in a room. LEDs prevent this heat build-up, thereby helping to reduce air conditioning costs in the home.
- iv. **Long-lasting** - LED bulbs last up to 10 times as long as compact fluorescents, and far longer than typical incandescent.
- v. **Durable** - since LEDs do not have a filament, they are not damaged under circumstances when a regular incandescent bulb would be broken.
- vi. **Mercury-free** - no mercury is used in the manufacturing of LEDs.
- vii. **More efficient** - LED light bulbs use only 2-17 watts of electricity (1/3rd to 1/30th of Incandescent or CFL). LED bulbs used in fixtures inside the home save electricity, remain cool and save money on replacement costs since LED bulbs last so long. Small LED flashlight bulbs will extend battery life 10 to 15 times longer than with incandescent bulbs.
- viii. **Cost-effective** - although LEDs are initially expensive, the cost is recouped over time and in battery savings. LED bulb use was first adopted commercially, where maintenance and replacement costs are expensive. But the cost of new LED bulbs has gone down considerably in the last few years and is continuing to go down. Today, there are many new LED light bulbs for use in the home, and the cost is also less.
- ix. **Light for remote areas and portable generators** - because of the low power requirement for LEDs, using solar panels becomes more practical and less expensive than running an electric line or using a generator for lighting in remote or off-grid areas. LED light bulbs are also ideal for use with small portable generators which is used for backup power in emergencies.

4 LIMITATIONS OF LED

- i. High initial Price- LEDs are currently more expensive (price per lumen) on an initial capital cost basis, than most conventional lighting technologies
- ii. Temperature dependent- LED efficiency and life drop at higher temperature. It limits the use of LED for physical replacement of existing filament and compact fluorescent types. Adequate heat sink is required to increase life.
- iii. Sensitive to Heat- Led lamps are sensitive to excessive heat. LED lamps should be checked for compatibility for use in totally or partially enclosed fixtures as heat buildup could cause lamp failure.
- iv. Voltage sensitive- : LEDs must be supplied with the voltage above the threshold and a current below the rating. Current and lifetime change greatly with a small change in applied voltage. Thus they require a current-regulated supply
- v. Flicker- LED lamps may flicker. The extent of flicker depends on the quality of DC power supply built into the lamp structure.
- vi. Sensitive to Surges Led lamps may be sensitive to electrical surges. It depends on design of lamp. This is generally not an issue with incandescent lamp. Power circuit that supply LED lamp can be protected from electrical surges through the use of electrical protective devices.
- vii. Efficiency- The luminous efficacy of LEDs decreases as the electric current increases. Heating also increases with higher currents which compromise the lifetime of the LED. These effects put limits on the current through LED in high power applications.

5 APPLICATIONS OF LED

LED has an extensive list of applications across a number of industry segments. Some of these are Electric Light Sources, Semiconductor Technology, Audio Electronics, Optics Medical Devices, Computer Peripheral Equipment, Traffic Control Systems, Scanning Equipment, Computer Data Transfer Devices, Heat Transfer & Control Systems, Kitchen Appliances, Dental Equipment, and Automobile Lighting Systems.

While LED can be found across several areas, it's predominantly featured in lighting systems and devices. LED lighting can be used in specific areas as in healthcare centers, cinema halls, hotels, aircraft, automobiles, computer peripherals and other such areas.

- i. Automotive- LED is used in automobiles for interior uses which include indicator lights on dashboard gauges, audio status light, security status light and warning signals. The exterior uses includes third brake lights, left and right rare lamps, turn signals etc.
- ii. Backlight Source-the mobile phone integrate LEDs as surface mounted diode (SMD). One mobile phone takes two LED backlight sources and six SMD LED key lights.
- iii. Display Screen-The LED screen has become the new display medium for advertising and information. It is commonly use in concert, arena and trade show venues. LED display screens have been widely adapted in various fields due its advantages such as high brightness, dynamic visual display, high reliability, low energy consumption, long service life, display content diversity, high durability and low maintenance cost.
- iv. Electronic Equipments- due to attributes such as low power consumption, small size and long life Led have become preferred light source on various electronic equipments. Led is integrated as warning lights and indicators on most electronics.
- v. General Lighting- LEDs are used in advertising billboards, illumination of commercial building exteriors, landmark buildings, bridges, roads, town centers and landscape lighting. Their long life, rich color and easily controlled features with integrated electronics offer a scalable lighting solution. Now a day's LEDs are also used in many airports, subways, hotels, shopping centers and individual homes feature.

6 ENERGY AND COST SAVING OF LEDS

LED is a highly energy efficient lighting technology. Residential LEDs especially ENERGY STAR rated products use at least 75% less energy, and last 25 times longer, than incandescent lighting. The biggest benefit of LED lighting is its lifespan. An LED bulb will last approximately 50,000 hours i.e. five times longer than a CFL bulb. If the bulb is left on for eight hours per day, it will last over 17 years. During that lifespan, an LED bulb will use 300 kilowatt hours of electricity. Widespread use of LED lighting has the greatest potential impact on energy savings. In comparison we need five CFLs to match the 50,000-hour lifespan of an LED. Those five CFLs would use 700 kilowatt hours of electricity. The LED bulb saves 400 kilowatt hours of electricity compared to the CFL and 2,700 kilowatt hours compared to the incandescent bulb.

The table below compares a 60 watt (W) traditional incandescent with energy efficient bulbs that provide similar light levels.

Comparisons between Traditional Incandescent lamp, Halogen Incandescent lamp , CFLs, and LEDs						
	60W Traditional Incandescent	43W Energy-Saving Incandescent	15W CFL		12W LED	
			60W Traditional	43W Halogen	60W Traditional	43W Halogen

Energy \$ Saved (%)	–	~25%	~75%	~65%	~75%-80%	~72%
Annual Energy Cost	\$4.80	\$3.50	\$1.20		\$1.00	
Bulb Life	1000 hours	1000 to 3000 hours	10,000 hours		25,000 hours	

Case study: Replacing conventional lighting system and CFL by LEDs

In residential buildings, lighting accounts for 30 – 40 % of total energy consumption. Lighting is an area which offers many energy efficient opportunities in almost any building, existing as well as new building. A typical residential building has many lighting requirements and each normally has its own set of options for improving lighting efficiency. Lighting control is one of the easiest ways to make substantial energy savings with relatively small investment and is one of the main energy saving measure.

To analyze the performance of LED lighting as energy efficient lighting a case study was conducted in a township. This township has 28 buildings and 1100 flats. Only the lighting provided for lobbies, parking and streetlight is considered for this study. The luminaries used for lobbies and streetlight are CFL and for parking is fluorescent tube light.

In the township there were 782 CFL lamps in lobbies & 148 CFL Lamps for streetlight, which were ON for the purpose of vigilance throughout the night. The tube lights used to ON from 8 PM to 6 PM (Timing use to vary subject to season change). There were 837 fluorescent tube light in parking, which was ON for the purpose of vigilance throughout the night. All the lights (on an average) working for 10 hours a day.

Total power consumption with 40 Watt fluorescent tube light,

$$P_1 = 837 \times 40 = 33480 \text{ Watts.}$$

Total power consumption with 65 Watt CFL,

$$P_2 = 148 \times 65 = 9620 \text{ Watts.}$$

Total power consumption with 11 Watt CFL,

$$P_3 = 782 \times 15 = 11730 \text{ Watts.}$$

Daily energy consumption for 10 hours working of lamps is,

$$E = (33480 + 9620 + 11730) \times 10 = 548.3 \text{ kWhr.}$$

The financial burdon = $548.3 \times \text{Rs. } 8.78 = \text{Rs. } 4,814.074$

Total expenditure in one year = $\text{Rs. } 4,814.074 \times 365 = \text{Rs. } 17,57,137.01$

If these fluorescent lights and CFLs were replaced with LEDs,

a) 11 Watt CFLs in lobbies were replaced by 12 Watt LED lights. Total LED lights required are 782.

Total power consumption = $782 \times 12 = 9384 \text{ Watts}$

b) 40 Watt fluorescent lamps in lobbies were replaced by 12 Watt LED tube lights. Total led tube lights required are 837.

Total power consumption = $837 \times 12 = 10044 \text{ Watts}$

c) 65 Watt CFL in streetlight were replaced by 30 Watt LED lights. Total led lights required are 148.

Total power consumption = $148 \times 30 = 4440 \text{ Watts}$

Daily consumption = $(9384 + 10044 + 4440) \times 10 = 238.68 \text{ kWhr}$

Energy saved per day=548.3 kWhr-238.68 kWhr=309.62kWhr

Financial burden per day=238.68 kWhr×Rs.8.78=Rs. 2095.61

Financial burden per year= Rs. 2095.61×365=Rs. 7,64,897.80

Financial saving per year= Rs.17,57,137.01- Rs. 7,64,897.80

=Rs.9,92,239.21

Cost of LEDs-

- i) LED 12 Watt Rs. 1100.
- ii) LED 30 Watt Rs. 2500.

Total cost involved in replacement of LEDs= 148×Rs. 2500+837×Rs. 1100+782×Rs. 1100

= Rs. 21,50,900

Payback period = total cost of LEDs/ Financial saving per year.

= Rs. 21,50,900/ Rs.9,92,239.21

= 2.16 years

Years=26 months.

It can be seen that energy saving potential is possible by replacing the present system of conventional tube lights and CFL with LEDs. LED last for 75000 to 100000 hours. Taking 75000 hours life, a LED system will last for at least 10 years. These high-quality LEDs with their very long lifetime are getting cheaper, and the market is currently exploding.

7 CONCLUSION

It has been observed that LED illumination is better than any general illumination systems (including CFLs) in terms of energy saving and cost effectiveness. Replacing light bulbs and fluorescent tubes with LEDs will lead to a drastic reduction of electricity requirements for lighting. Since 20-30% of the electricity consumed in industrial economies is used for lighting, considerable efforts are presently being devoted to replacing old lighting technologies with LEDs

REFERENCES:

- [1] Khanna V. K. (2014) Fundamentals of Solid State Lighting: LEDs, OLEDs, and Their Application in Illumination and displays, CRC Press.
- [2] The life and times of the LED – a 100-year history, Nature photonics, vol. 1, April 2007.
- [3] Schubert, E. F. and Kim, J. K. (2005) Solid-State Light Sources Getting Smart, Science, 308, 1274
- [4] Savage, N. (2000) LEDs light the future, Technology Review, vol. 103, no 5, p. 38–44, September–October 2014
- [5] “Model and Predict the Performance of LEDs for Solid State Lighting - Accurately and Quickly“, Technical Note, Lambda Research Corporation 2007
- [6] McKinsey “Lighting the Way”, 2011
- [7] 2011 European Commission green paper “Lighting the future- accelerating the deployment of innovative lighting technologies” R.D. Dupuis and M.R. Krames, J. Light wave Tech. 26, 1154 (2008).
- [8] S. Nakamura and M.R. Krames, Proc. IEEE 101, 2211 (2013).
- [9] Fred Schubert: Light Emitting Diodes, 2nd edition, (2006).

[10] Dr. Norbert Harendt“ Simulation and Optimization of Optical Systems” 2008 Luger Research & LED-Professional.

[11] Ethan Biery, Thomas Shearer, Roland Ledyard, Dan Perkins, Manny Feris “ Controlling LEDs “ Technical white paper May 2014.

[12]Isamu Akasaki, Hiroshi Amano and Shuji Nakamura“ Blue LEDs – Filling the world with new light” The Nobel Prize In Physics 2014, The Royal Swedish Academy of Sciences

IJERGS

Optimization of Drilling Process Parameters on Surface Roughness & Material Removal Rate by Using Taguchi Method

¹S.V. ALAGARSAMY, ²S. AROCKIA VINCENT SAGAYARAJ, ³P. RAVEENDRAN

^{1,3}Department of Mechanical Engineering, Mahath Amma Institute of Engg & Tech, Pudukkottai, Tamil Nadu, India.

²Department of Automobile Engineering, Shanmuganathan Engineering College, Pudukkottai, Tamil Nadu, India.

E-mail: s.alagarsamy88@gmail.com

Abstract— The aim of this work is utilize Taguchi method to investigate the effects of drilling parameters such as cutting speed, feed and depth of cut on surface roughness and material removal rate in drilling of Aluminium alloy 7075 using HSS spiral drill. The Taguchi method, a powerful tool to design optimization for quality, is used to find optimal cutting parameters. Orthogonal arrays, the signal- to- noise ratio, the analysis of variance are employed to analyze the effect of drilling parameters on the quality of drilled holes. A series of experiments based on L16 orthogonal array are conducted using CNC vertical machining centre. The experiment results are collected and analyzed using statistical software Minitab16. Analyses of variances are employed to determine the most significant control factors affecting the surface roughness and material removal rate. ANOVA has shown that the depth of cut has significant role to play in producing higher material removal rate and cutting speed has significant role to play for producing lower surface roughness.

Keywords — AA-7075, Drilling Process, Surface Roughness, Material Removal Rate, Taguchi Method, Signal-to-Noise Ratio, ANOVA.

1. INTRODUCTION

The important goal in the modern industries is to manufacture the products with lower cost and with high quality in short span of time. There are two main practical problems that engineers face in a manufacturing process. The first is to determine the values of process parameters that will yield the desired product quality (meet technical specifications) and the second is to maximize manufacturing system performance using the available resources. Drilling operation is widely used in the aerospace, aircraft and automotive industries, although modern metal cutting methods have improved in the manufacturing industries. The surface quality is an important parameter to evaluate the productivity of machine tools as well as machined components. Hence, achieving the desired surface quality is of great importance for the functional behavior of the mechanical parts. A reasonably good surface finish is desired for improving the tribological properties, fatigue strength, corrosion resistance and aesthetic appeal of the product. Excessively better surface finish may involve more cost of manufacturing. The surface roughness and material removal rate are affected by several factors including cutting tool geometry, cutting speed, feed rate, the microstructure of the work piece and the rigidity of the machine tool. These parameters affecting the surface roughness and drilled hole qualities (roundness, cylindricity and hole diameter) can be optimized in various ways such as Taguchi method. Therefore, a number of researchers have been focused on an appropriate prediction of surface roughness and material removal rate. Aluminium Alloy 7075 are the most widely used non-ferrous materials in engineering applications owing to their attractive properties such as high strength to weight ratio, good ductility, excellent corrosion, availability and low cost. It is used for aircraft fittings, gears and shafts, fuse parts, meter shafts and gears, missile parts, regulating valve parts, worm gears, keys, aircraft, aerospace and defence applications, bike frames, all terrain vehicle (ATV) sprockets. Aluminium Alloys are soft and high strength material. Vinod kumar Vankanti, Venkateswarlu Ganta [1] Investigated the influence of cutting parameters namely cutting speed, feed, point angle, chisel edge width in drilling of glass fiber reinforced polymer composites. The results indicate that feed rate is the most significant factor influencing the thrust force followed by speed, chisel edge width and point angle. Cutting speed is the most significant factor affecting the torque, speed and the circularity of the hole followed by feed, chisel edge width and point angle. Adem cicek Turgay Kivak [2] Studied the effects of deep cryogenic treatment and drilling parameters on surface roughness and roundness error were investigated in drilling of AISI 316 austenitic stainless steel with M35 HSS twist drills. It was found that the cutting speed had a significant effect on the surface roughness and roundness error. Pradeep kumar, P.Packiaraj [3] Presented a Taguchi method to study the influence of process parameters such as speed, feed, drill tool diameter on surface roughness, tool wear, material removal rate and hole diameter error during drilling of OHNS material using HSS spiral drill. It is found that the feed and speed are important process parameters to control surface roughness, tool wear, material removal rate and hole diameter error. Turgay Kivak, Gurcan Samtas, Adem Cicek [4] This paper presented the optimization of drilling parameters using the Taguchi technique to obtain minimum surface roughness (Ra) and thrust force. it was found that the cutting tool was the most significant factor on the surface roughness and that the feed rate was the most significant factor on the thrust force. Chandan Deep

Singh, Rajvir Singh, Swarnjeet Singh [5] In this study the parametric optimization of micro drilling has been studied by considering a number of parameters such as spindle speed, feed rate and drilling tool size on material removal rate (MRR), surface roughness, dimensional accuracy. From the result, the surface roughness are mostly influenced by spindle speed and feed rate. B.Shivapragash, K.Chandrasekaran, C.Parthasarathy [6] The presented work is focusing on multiple response optimization of drilling process for composite Al-TiBr₂. The results shows that the maximum feed rate, low spindle speed are the most significant factors which affect the drilling process and the performance in the drilling process can be effectively improved by using this approach. Many researchers developed many mathematical models to optimize the cutting parameters to get the maximum material removal rate and minimum surface roughness by drilling process.

2. MATERIALS AND METHOD

2.1. Work Piece Material

The work piece material used for present work was Aluminium Alloy 7075. Table 1 and Table 2 shows the chemical composition and mechanical properties of AA7075.

Table 1: Chemical Composition of AA7075

Elements	Composition %
Aluminium	89.58
Silicon	0.4
Copper	0.098
Manganese	1.41
Magnesium	0.055
Chromium	2.33
Zinc	5.95
Ferrous	0.20

Table 2: Properties of AA7075

Property	Value
Tensile Strength	572 Mpa
Yield Strength	503 Mpa
Elongation	11 %
Machinability	70 %
Density	2.81 kg/m ³

2.2. Selection of Process Parameters

In this investigation, machining process parameters like Speed, Feed and Depth of Cut of the drill were considered. According to Taguchi's design of experiments for four parameters and three levels L16 Taguchi orthogonal array was selected. The number of factors and their corresponding levels are shown in Table 3.

Table 3: Machining Parameters and Levels

Process Parameter	Levels			
	1	2	3	4
Speed (rpm)	600	800	1000	1200
Feed (mm/rev)	0.06	0.08	0.10	0.12
Depth of Cut (mm)	1.5	2.5	3.5	4.5

2.3. Methodology

2.3.1. Taguchi Approach

Taguchi method was developed by Dr. Genichi Taguchi. This method involves three stages: system design, parameter design, and tolerance design. The Taguchi method is a statistical method used to improve the product quality. The Taguchi process helps select or determine the optimum cutting conditions for drilling process. Taguchi developed a special design of orthogonal arrays to study the entire parameter space with a small number of experiments only. The experimental results are then transformed into a signal-to-noise (S/N) ratio. It uses the S/N ratio as a measure of quality characteristics deviating from or nearing to the desired values. There are three categories of quality characteristics in the analysis of the S/N ratio, i.e. the lower the better, the higher the better, and the nominal the better. The formula used for calculating S/N ratio is given below.

Smaller the better: It is used where the smaller value is desired.

$$S/N \text{ Ratio} = -10 \log \frac{1}{n} \sum_{i=1}^n y_i^2 \dots\dots\dots(1)$$

Where y = observed response value and n = number of replications.

Nominal the best: It is used where the nominal or target value and variation about that value is minimum.

$$S/N \text{ Ratio} = -10 \log \frac{\mu^2}{\sigma^2} \dots\dots\dots(2)$$

Where σ = mean and μ = variance.

Higher the better: It is used where the larger value is desired.

$$S/N \text{ Ratio} = -10 \log \frac{1}{n} \sum_{i=1}^n \frac{1}{y_i^2} \dots\dots\dots(3)$$

Taguchi suggested a standard procedure for optimizing any process parameters.

2.3.2. ANOVA (Analysis of Variance)

ANOVA is a statistical technique for determining the degree of Difference or similarity between two or more groups of data. It is based on the comparison of the average value of a common component. In this paper, Pareto ANOVA was used which measures the importance of each process parameter of the process. Pareto ANOVA is a simplified ANOVA method, which is based on Pareto principle. The Pareto ANOVA technique is a quick and easy method to analyze results of the parametric design. The Pareto ANOVA technique does not need F -test. This technique identifies the important parameters and calculates the percentage influence of each parameter on different quality characteristics. The use of both Pareto ANOVA technique and S/N ratio approach makes it less cumbersome to analyze the results and hence, make it fast to arrive at the conclusion. From the S/N ratios, the overall S/N ratio is expressed as

$$S/N \text{ Ratio} = \frac{1}{9} \sum_9^1 \left(\frac{S}{N} \right)_i \dots\dots\dots(4)$$

Where, S/N - is the overall mean of S/N ratio and (S/N) is the S/N ratio for i th parameter

The sum of squares due to variation about overall mean is

$$SS = \frac{1}{9} \sum_{i=1}^9 \left(\left(\frac{S}{N} \right)_i - \left(\frac{S}{N} \right) \right)^2 \dots\dots\dots(5)$$

Where, SS - is the sum of squares. For the i th process parameter, the sum of squares due to variation about overall mean is

$$SS_i = \frac{1}{9} \sum_{i=1}^9 \left(\left(\frac{S}{N} \right)_i - \left(\frac{S}{N} \right) \right)^2 \dots\dots\dots(6)$$

Where, SS_i - is the sum of the square for i th parameter and (S/N) is the average S/N ratio of i -th parameter of j -th level

$$\% \text{ contribution} = \frac{SS_i}{SS} \times 100 \dots \dots \dots (7)$$

Table 4: Experimental Results for MRR and Surface Roughness and Corresponding S/N Ratios

S.No	Speed (rpm)	Feed (mm/rev)	Depth of Cut(mm)	MRR (mm ³ /min)	S/N Ratio	Ra (µm)	S/N Ratio
1	600	0.06	1.5	63.617	36.0719	1.17	-1.36372
2	600	0.08	2.5	235.61	47.4439	1.75	-4.86076
3	600	0.10	3.5	577.26	55.2274	1.34	-2.54210
4	600	0.12	4.5	1145.11	61.1769	1.06	-0.50612
5	800	0.06	2.5	235.61	47.4439	0.58	4.73144
6	800	0.08	1.5	113.09	41.0685	1.18	-1.43764
7	800	0.10	4.5	1272.34	62.0921	2.72	-8.69138
8	800	0.12	3.5	923.628	59.3099	1.31	-2.34543
9	1000	0.06	3.5	577.26	55.2274	1.04	-0.34067
10	1000	0.08	4.5	1272.34	62.0921	0.60	4.43697
11	1000	0.10	1.5	176.71	44.9452	0.84	1.51441
12	1000	0.12	2.5	589.04	55.4029	0.73	2.73354
13	1200	0.06	4.5	1145.11	61.1769	0.89	1.01220
14	1200	0.08	3.5	923.62	59.3101	0.97	0.26457
15	1200	0.10	2.5	589.04	55.4029	0.59	4.58296
16	1200	0.12	1.5	254.45	48.1124	1.14	-1.13810

3. RESULTS AND ANALYSIS

Minitab statistical software has been used for the analysis of the experimental work. The Minitab software studies the experimental data and then provides the calculated results of signal-to-noise ratio. The objective of the present work is to minimize surface roughness and maximize the MRR in drilling process optimization. The effect of different process parameters on material removal rate and surface roughness are calculated and plotted as the process parameters changes from one level to another. The average value of S/N ratios has been calculated to find out the effects of different parameters and as well as their levels. The use of both ANOVA technique and S/N ratio approach makes it easy to analyze the results and hence, make it fast to reach on the conclusion. Table 4 shows the experimental results for material removal rate and surface roughness and corresponding S/N ratios.

3.1. Analysis of Signal-to-Noise Ratios

Larger-the-better performance characteristic is selected to obtain material removal rate. Smaller-the better performance characteristic is selected to obtain Surface Roughness.

Table 5: Response Table for MRR

Level	Speed	Feed	DOC
1	49.98	45.49	42.55
2	52.48	52.48	51.42
3	54.42	54.42	57.27
4	51.51	56.01	57.15
Delta	4.44	10.21	14.72
Rank	3	2	1

Table 6: Response Table for Surface Roughness

Level	Speed	Feed	DOC
1	-2.3182	1.0098	-0.6063
2	-1.9358	-0.3992	1.7968
3	2.0861	-1.2840	-1.2409
4	1.1804	-0.3140	-0.9371
Delta	4.4042	2.2938	3.0377
Rank	1	3	2

From the response Table 5 and Fig.2 it is clear that depth of cut is the most influencing factor followed by feed rate and cutting speed for MRR. The optimum for MRR is cutting speed of 1000 rpm, feed rate of 0.12 mm/rev and depth of cut of 3.5 mm. From the response Table 6 and Fig.3 it is clear that cutting speed is the most influencing factor followed by feed rate and depth of cut for surface roughness. The optimum for surface roughness is cutting speed of 1200 rpm, feed rate of 0.06 mm/rev and depth of cut of 2.5 mm.

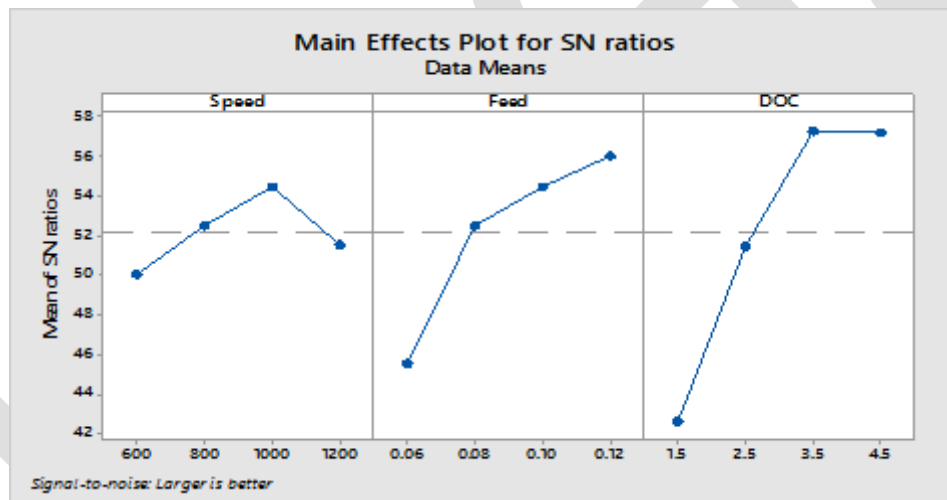


Figure 2: Main Effect Plot for MRR

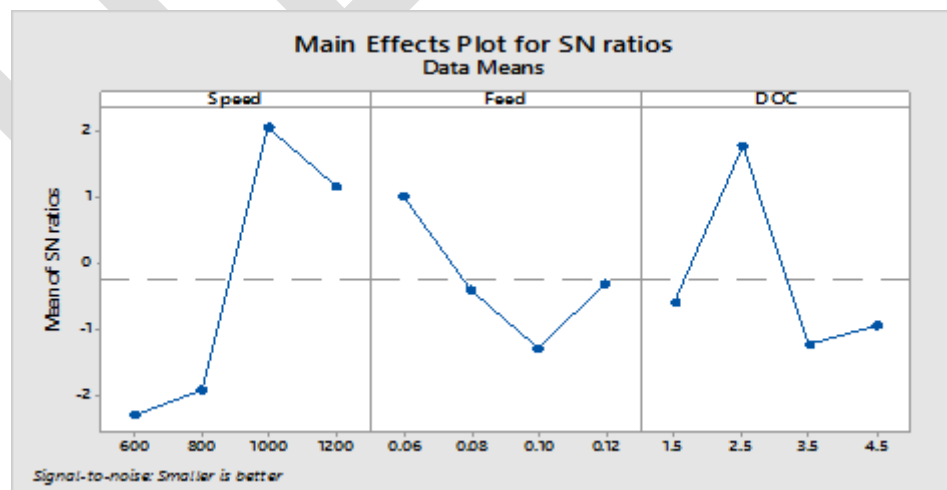


Figure 3: Main Effect Plot for Surface Roughness

3.2. Analysis of Variance (ANOVA)

Taguchi method cannot judge and determine effect of individual parameters on entire process while percentage contribution of individual parameters can be well determined using ANOVA. Using Minitab 17 software ANOVA module can be employed to investigate effect of parameters.

Table 7: ANOVA Results for MRR

Source	DOF	SS	MS	F	% CON
Speed	3	96090	32030	0.37	3.56
Feed	3	541415	180472	2.08	20.11
Doc	3	1533071	511024	5.88	56.96
Error	26	521231	86872	-	0.1936
Total	15	2691807	-	-	100

S = 294.74 R-Sq = 80.64%

Table 8: ANOVA Results for Surface Roughness

Source	DF	SS	MS	F	% CON
Speed	3	1.2067	0.4022	1.08	28.68
Feed	3	0.4295	0.1432	0.39	10.20
Doc	3	0.3420	0.1140	0.31	8.12
Error	6	2.2285	0.3714	-	0.5297
Total	15	4.2067	-	-	100

S = 0.60944 R-Sq = 47.02%

Table 7 & 8 shows the analysis of variance for material removal rate and surface roughness. It is observed that the depth of cut (56.96%) is most significantly influences the material removal rate followed by feed rate (20.11%) and least significant of cutting speed (3.56%). In case of Surface Roughness, speed (28.68%) is the most significant parameter followed by feed rate (10.20%) and least significant of depth of cut (8.12%). In both the cases, error contribution (0.1936%) and (0.5297%) reveals that the inter-action effect of the process parameters is negligible.

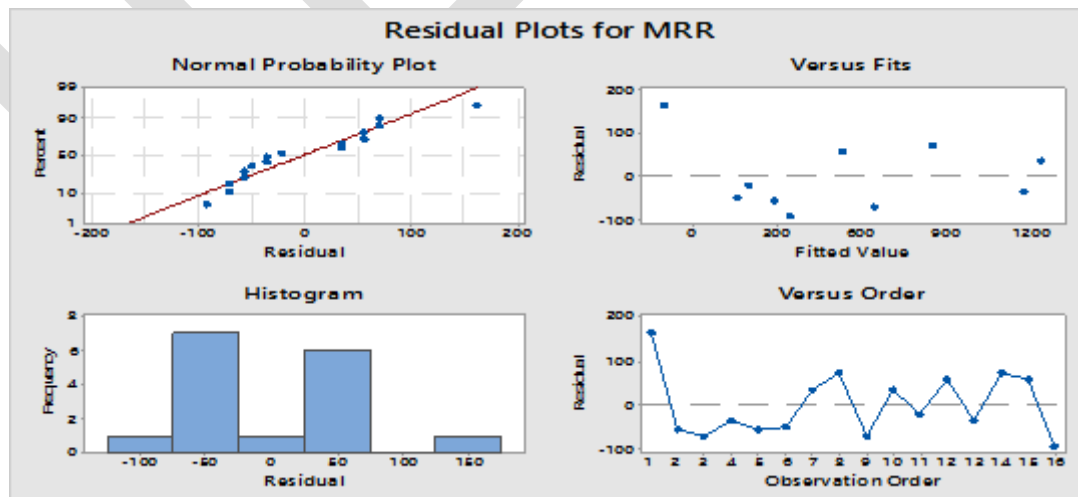


Figure 4: Residual Plot for MRR

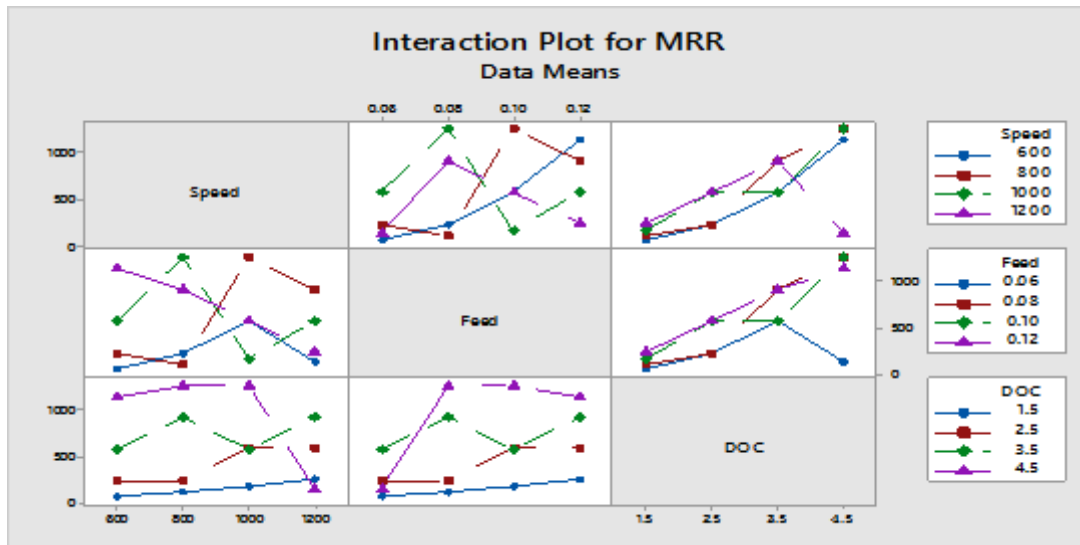


Figure 5: Interaction Plot for MRR

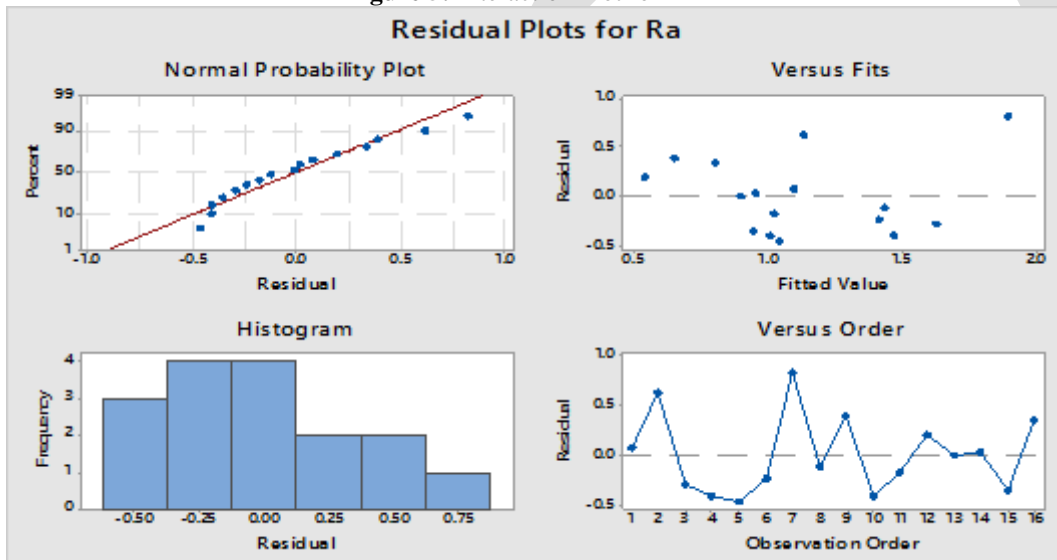


Figure 6: Residual Plot for Surface Roughness

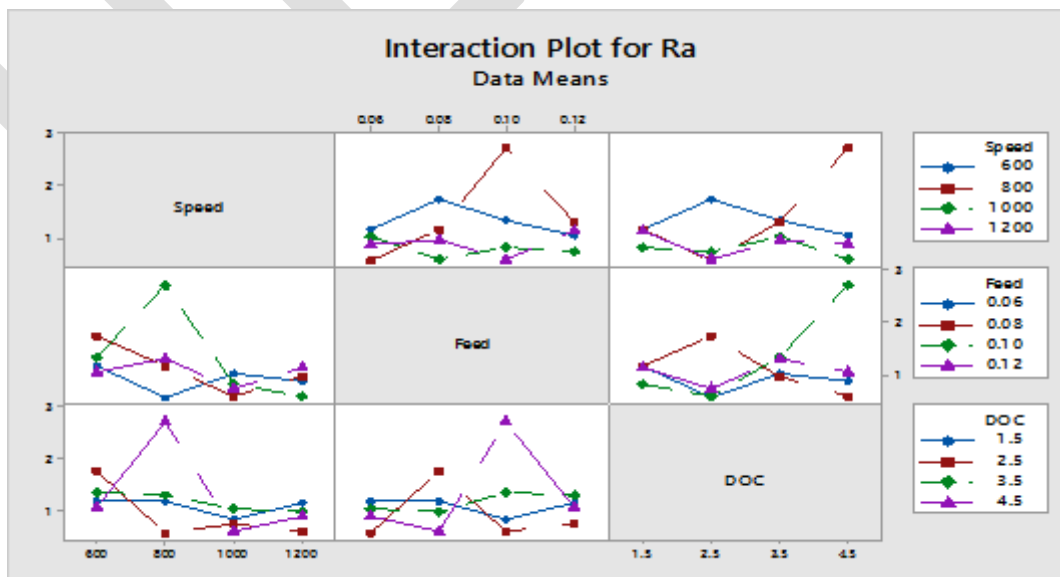


Figure 7: Interaction Plot for Surface Roughness

4. CONCLUSIONS

1. The optimum conditions obtained from Taguchi method for optimizing Material Removal Rate during drilling of Aluminium Alloy 7075 under dry condition are Cutting Speed of 1000 rpm, Feed rate of 0.12 mm/rev and Depth of Cut of 3.5 mm.
2. From response table for S/N ratio of MRR it is clear that Depth of Cut is the most significant factor influencing MRR followed by Feed rate and Cutting Speed is the least significant factor.
3. Analysis of Variances (ANOVA) for S/N ratio for MRR clearly indicates that the Depth of Cut is majorly contributing of about 56.96% in obtaining optimal MRR followed by Feed rate 20.11% and Depth of Cut 3.56%.
4. Optimum conditions for optimizing Surface Roughness are Cutting Speed of 1200 rpm, Feed rate of 0.06 mm/rev and depth of cut of 2.5 mm.
5. From response table for S/N ratio of surface roughness it is clear that Cutting Speed is the most significant factor influencing MRR followed by Feed rate and Depth of Cut is the least significant factor.
6. Analysis of Variances (ANOVA) for S/N ratio for surface roughness clearly indicates that the Cutting Speed is majorly contributing of about 28.65% in obtaining optimal surface roughness followed by Feed rate of 10.20% and Depth of Cut of 8.12 %.

REFERENCES:

- [1]. Turgay Kivak, Gurcan Samtas, Adem Cicek “*Taguchi Method Based Optimisation Of Drilling Parameters In Drilling Of AISI 316 Steel With PVD Monolayer And Multilayer Coated HSS Drills*” Elsevier Measurement 45 (2012) 1547–1557.
- [2]. Adem Cicek, Turgay Kivak, Gurcan Samtas, “*Application Of Taguchi Method For Surface Roughness And Roundness Error In Drilling Of AISI 316 Stainless Steel*” Journal Of Mechanical Engineering 58(2012), 165-174.
- [3]. T. Rajmohan, K. Palanikumar, M. Kathirvel “*Optimization Of Machining Parameters In Drilling Hybrid Aluminium Metal Matrix Composites*” Elsevier Trans. Nonferrous Met. Soc. China 22(2012) 1286-1297.
- [4]. Vinodkumar vankanti, Venkateswarluganta “*Optimization Of Process Parameters In Drilling Of GFRP Composite Using Taguchi Method*” Journal Of Materials Research And Technology.2014; 3(1):35-41.
- [5]. K. Lipin And Dr. P. Govindan “*A Review On Multi Objective Optimization Of Drilling Parameters Using Taguchi Methods*” Akgec International Journal Of Technology. Vol .4, No.2.
- [6]. Reddy Sreenivasulu, And Ch.Srinivasa Rao “*Application Of Grey Based - Taguchi Method To Determine Multiple Performance Characteristics In Drilling Of Aluminium Alloys – Review*” Research Journal Of Engineering Sciences, ISSN 2278 – 9472.Vol. 2(3), 45-51, March (2013)
- [7]. A. Navanth, T. Karthikeya Sharma “*A Study Of Taguchi Method Based Optimization Of Drilling Parameter In Dry Drilling Of Al 2014 Alloy At Low Speeds*” International Journal Of Engineering Sciences & Emerging Technologies, August 2013.ISSN: 2231 – 6604 Volume 6, Issue 1, Pp: 65-75.
- [8]. Yogendra Tyagi, Vedansh Chaturvedi, Jyoti Vimal “*Parametric Optimization Of Drilling Machining Process Using Taguchi Design And ANOVA Approach*” International Journal Of Emerging Technology And Advanced Engineering (ISSN 2250-2459, Volume 2, Issue 7, July 2012).
- [9].B.Shivapragash, K.Chandrasekaran, C.Parthasarathy, “*Multiple Response Optimizations In Drilling Using Taguchi And Grey Relational Analysis*” International Journal Of Modern Engineering Research (IJMER) Vol.3, Issue.2, March-April. 2013 Pp-765-768 ISSN: 2249-6645.
- [10]. Chandan Deep Singh, Rajvir Singh, Swarnjeet Singh “*Effect Of Machining Parameters On Dimensional Accuracy And Surface Roughness During Micro Drilling Of Copper*” International Journal Of Applied Studies (IJAS) Volume: 1, Issue: 1 (Jan 2014), ISSN: 2348 – 1560.

[11]. Shu-Lung Wang, Ting-Yu Chueh “*Analysis Of Material Removal Rate And Surface Roughness On Advanced Ceramics Materials Micro-Hole Drilling*” Public Health Frontier Vol.1 No.1 2012 PP. 11-15.

[12]. Abolfazl Golshan, Danial Ghodsiyeh “*Optimization Of Machining Parameters During Drilling Of 6061 Aluminium Alloy*” Applied Mechanics And Materials Vol. 248 (2013) Pp 20-25.

[13].Yogendra Tyagi, Vedansh Chaturvedi ,Jyoti Vimal “*Parametric Optimization Of CNC Drilling Machine For Mild Steel Using Taguchi Design And Single To Noise Ratio Analysis*” International Journal Of Engineering Science And Technology (IJEST) Vol. 4 No.08 August 2012. ISSN: 0975-5462.

IJERGS

Variable Speed Wind Turbine System Based on PMSG and Improved ZVS FBTL DC-DC Converter

Janani.K, Arun Prasad.B, Raj Kumar.A.

Assistant Professor, Pollachi Institute of Engineering and Technology, urfuturearun@gmail.com, +91-9965877899

Abstract— This paper analyzes a newly developed three level dc/dc converter is presented for wind energy conversion systems. The power generated from the permanent magnet synchronous generator is rectified and fed to the Improved ZVS FBTL converter. A passive filter to reduce the voltage stress and to improve the converter performance. ZVS technique to reduce the conduction losses in the switches. A voltage balancing control strategy is ensured for proper balancing of the input voltage fed to the converter. Whole wind energy conversion system control is to be done with PI controller.

Keywords— Variable speed wind turbine, PMSG, Three level DC-DC converter, ZVS technique, Passive filter, PI controller, Voltage balancing.

INTRODUCTION

Variable speed wind turbine can achieve maximum energy conversion efficiency over wide range of wind speeds. The turbine can continuously adjust its rotational speed according to the wind speed. In doing so the tip speed ratio can be kept at an optimal value to achieve the maximum power conversion efficiency at different wind speed. To make the turbine speed adjustable the wind turbine generator is normally connected to the utility grid through a power converter system. The converter system enables the control of the speed of the generator that is mechanically coupled to the rotor.

Power converters play a vital role in the integration of wind power into the electrical grid. The DC grid, with the advantages such as reactive power and harmonics seems to be promising solution of power collection system for the growing demand in the offshore wind power development. They also make it possible for wind farm to become active element in the power system. The offshore wind turbines may be directly connected into a DC grid to deliver DC power to a medium or high voltage network.

Multilevel converters can obtain high voltage level with low cost, easy available of low voltage devices which reduces the size and cost of the filters and increases the performance of the converter due to the characteristics of the staircase shaped outputs. And also the convenient way of reducing the voltage stress of the converter is by using the multilevel technology which is good one for high voltage and high frequency applications.

When the full bridge two level and half bridge three level converters were considered, the voltage change rate, dv/dt is high which caused large electromagnetic interference in the line connected to the grid. Normally, the voltage level of the dc network would be dozens of kilovolts which is much higher than the input voltage of the dc/dc converter. Hence, a medium frequency transformer (MFT) operated at hundreds of hertz to several kilohertz would be installed in the dc/dc converter. This not only ensures that the input voltage can be boosted to a desired high output voltage, but also achieves the isolation between source and grid.

Full bridge three level converters have a simpler circuit structure and less number of switching devices. Varying from other converter design a passive filter is introduced into the full bridge three level converters which improve the performance of the converter. This filter is used to reduce the stress in the medium frequency transformer. Moreover the voltage balancing control is not possible for two level converters and complicated for sub module based one. In order to reduce the voltage stress and the switching losses in the device, an improved ZVS (Zero Voltage Switching) full bridge three level DC-DC converter is proposed. The converter is capable of

achieving zero voltage switching for all the power switches and the voltage stress is also reduced. Zero Voltage Switching means that the power to the load is switched on or off only when the output voltage is zero volts.

Zero Voltage Switching can extend the life of a controller and of the load being controlled. Varying from other converter design a passive filter is introduced which improves the performance of the converter. The alternating voltage which is obtained from the inverter is fed through the passive filter which reduces the stress and can effectively overcome the problems which occurs due to the non linear characteristics of the semiconductor devices which results in the distorted waveforms. This voltage is fed to the medium frequency transformer (MFT) which in turn steps up the voltage and is been fed to the converter which is essential for a power converter in high power applications. FBTL converter has simple circuit structure and less number of switching devices with improved dynamic response. In this project, an improved ZVS FBTL DC-DC converter is proposed with a voltage balancing control strategy. Wind Energy Conversion Systems (WECS) requires a generator to provide the required power. Many types of generators are available for WECS such as Squirrel Cage Induction Generator (SCIG), Wound Rotor Induction Generators (WRIG), Doubly Fed Induction Generator (DFIG) and Permanent Magnet Synchronous Generator (PMSG).

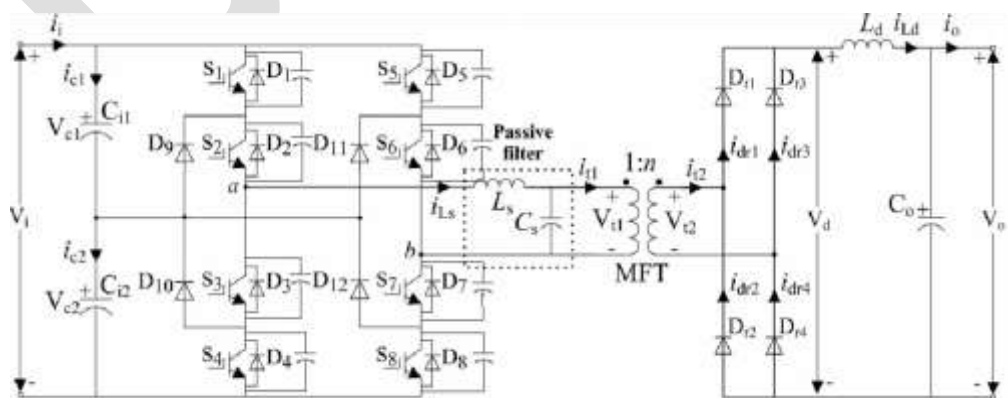
PMSGs are the majority source of commercial electrical energy. A permanent magnet synchronous generator is a generator where the excitation field is provided by a permanent magnet instead of a coil.

IMPROVED ZVS FBTL CONVERTER

Improved ZVS FBTL DC/DC converter, is composed of eight switches (S1–S8), eight freewheeling diodes (D1–D8), four clamping diodes (D9–D12), an MFT, four rectifier diodes (Dr1–Dr4), a passive filter (L_s and C_s), an output filter inductor L_d , an output capacitor C_o , and two voltage divided capacitors (C_{i1} and C_{i2}). These capacitors are used to split the dc voltage V_i into two equal voltages V_{c1} and V_{c2} . Different from the FBTL DC/DC converter, a passive filter is inserted into the Improved ZVS FBTL DC/DC converter as shown to improve the performance of the DC/DC converter which can effectively overcome the problem that the nonlinear characteristics of semiconductor devices results in distorted waveforms associated with harmonics and reduce the voltage stress of the MFT, which is very significant for the power converter in the high power application.

MODULATION STRATEGY

The switches S1–S8 are switched complementarily in pairs with a pulse width modulation (PWM), i.e., pairs S1–S3, S4–S2, S5–S7, and S8–S6, respectively. The duty cycle for S1 is D . The way of phase shifting the PWM for other switch pairs results in the different operation modes. The modulation strategy also includes the voltage balancing control for IFBTL dc/dc converter.



OPERATION MODE I

The PWM waveform for the pairs S8–S6, S5–S7, and S4–S2 lags behind that for pair of S1–S3 by $(D - D_c) T_s / 2$, $T_s / 2$, and $(D - D_c + 1) T_s / 2$ respectively as shown in Fig. 2.7(a). T_s is the switching cycle. The overlap time between S1–S3 and S8–S6 is $D_c T_s / 2$, which is also for S4–S2 and S5–S7. D_c is defined as the overlap duty ratio.

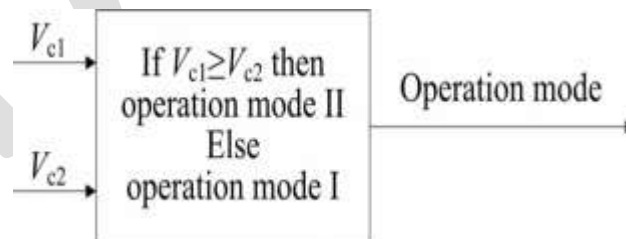
OPERATION MODE II

The PWM waveform for pair S8–S6 leads before that for pair S1–S3 by $(D - D_c) T_s / 2$, and the PWM waveform for pairs S4–S2 and S5–S7 lags behind that for the pair S1–S3 by $(1 - D + D) T_s / 2$ and $T_s / 2$, respectively. The overlap time between S1–S3 and S8–S6, and between S4–S2 and S5–S7 is also both $D_c T_s / 2$. The main difference between the two operation modes is the capacitor charge and discharge situations in each half cycle. In operation mode I, capacitor C_{i2} discharges more energy than capacitor C_{i1} in each half cycle while capacitors C_{i1} and the C_{i2} exchange their situations in operation mode II. In operation mode II, capacitor C_{i1} discharges more energy than capacitor C_{i2} in each half cycle. The two operation modes can be alternatively used for the adaptive voltage balancing control.

The steady-state operations of the converter under the proposed modulation strategy are explained with the assumption that $C_{i1} = C_{i2}$. In one cycle T_s under operation modes I and II, respectively. Voltages V_{ab} , V_{i1} , V_{i2} and currents i_{Ls} , i_{i1} , i_{i2} are all periodic waveforms with period T_s . Currents i_{c1} , i_{c2} and i_{Ld} are with the period $T_s / 2$. Owing to the passive filter in the Improved ZVS FBTL dc/dc converter, the performance of voltages V_{i1} , V_{i2} and currents i_{i1} , i_{i2} associated with the MFT is effectively improved, which is significant for the Improved ZVS FBTL dc/dc converter in the applications of the medium-voltage and high-power system. The charge and discharge situations (i_{c1} and i_{c2}) of capacitors C_{i1} and C_{i2} are the main difference between the operation modes I and II, which would affect the capacitor voltages V_{c1} and V_{c2} . The other performances of the converter are nearly the same.

VOLTAGE BALANCING CONTROL STRATEGY OF IFBTL CONVERTER

The switches S1–S8 are switched complementarily in pairs with a pulse width modulation (PWM), i.e., pairs S1–S3, S4–S2, S5–S7, and S8–S6, respectively. The duty cycle for S1 is D . The way of phase shifting the PWM for other switch pairs results in the different operation modes. The modulation strategy also includes the voltage balancing control for IFBTL dc/dc converter.

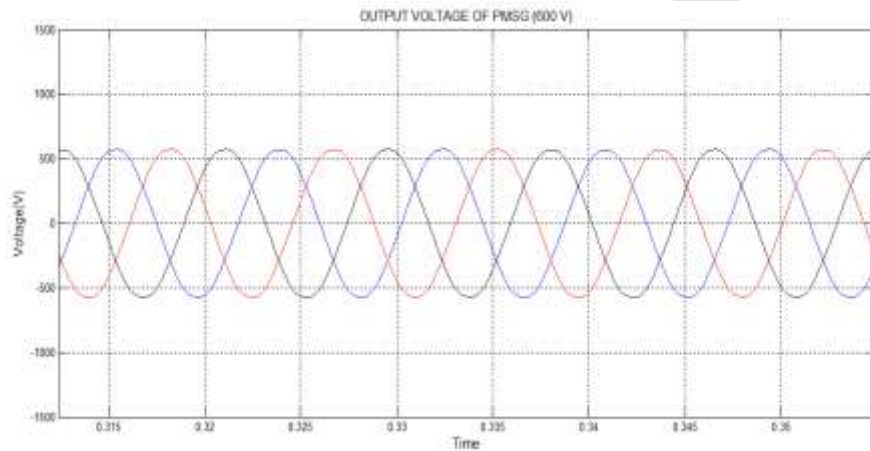


SIMULATION AND TEST RESULTS

Simulation for the permanent magnet synchronous generator fed improved full bridge three level dc/dc converter for wind energy conversion systems is done using MATLAB Simulink. The power generated in the turbine is fed to the grid through an improved full bridge three level dc/dc converter which is used for high and medium power application.

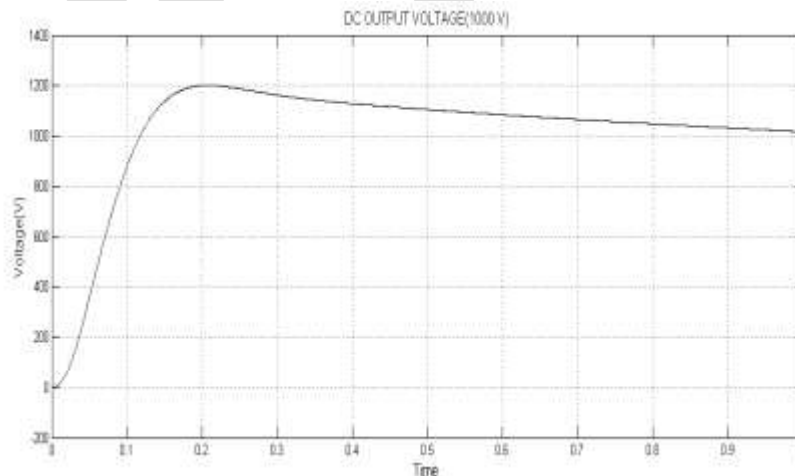
OUTPUT VOLTAGE FROM GENERATOR

Output voltage of 600 V AC is generated from PMSG and is fed to the bridge rectifier.



DC OUTPUT VOLTAGE

DC output voltage of 1000 V obtained from simulation from the Improved ZVS FBTL converter and this stepped up voltage is given to the DC grid.



CONCLUSION

This project has presented the control of the Improved ZVS FBTL dc/dc converter for the wind turbine system to facilitate the integration of wind turbines into a dc grid by transferring power through Improved ZVS FBTL converter efficiently by minimizing

the losses. The converter is designed with variable speed wind turbine and PMSG and also the overall control is done using PI controller and simulated using MATLAB simulink.

REFERENCES:

- [1] C. Meyer, M. Hoing, A. Peterson, and R. W. De Doncker, "Control and design of dc grids for offshore wind farms," *IEEE Trans. Ind. Appl.*, vol. 43, no. 6, pp. 1475–1482, Nov./Dec. 2007.
- [2] N. Y. Dai, M. C. Wong, and Y. D. Han, "Application of a three-level NPC inverter as a three-phase four-wire power quality compensator by generalized 3DSVM," *IEEE Trans. Power Electron.*, vol. 21, no. 2, pp. 440–449, Mar. 2006.
- [3] X. Ruan, B. Li, Q. Chen, S. C. Tan, and C. K. Tse, "Fundamental considerations of three-level dc-dc converters: Topologies, analyses, and control," *IEEE Trans. Circuits Syst. I, Reg. Papers*, vol. 55, no. 11, pp. 3733–3743, Dec. 2008.
- [4] Fujin Deng, and Zhe Chen, "Control of Improved Full-Bridge Three-Level DC/DC Converter for Wind Turbines in a DC Grid", *IEEE Trans. Power Electron*, vol. 28, no. 1, Jan 2013.
- [5] Z. Zhang and X. Ruan, "ZVS PWM full-bridge three-level converter," in *Proc. 4th Int. Power Electron. Motion Control Conf., 2004*, pp. 1085–1090.
- [6] X. Ruan, B. Li, Q. Chen, S. C. Tan, and C. K. Tse, "Fundamental considerations of three-level dc-dc converters: Topologies, analyses, and control," *IEEE Trans. Circuits Syst. I, Reg. Papers*, vol. 55, no. 11, pp. 3733–3743, Dec. 2008.
- [7] Z. Zhang and X. Ruan, "ZVS PWM full-bridge three-level converter," in *Proc. 4th Int. Power Electron. Motion Control Conf., 2004*, pp. 1085–1090.
- [8] P. M. Barbosa, F. Canales, J. M. Burdío, and F. C. Lee, "A three-level converter and its application to power factor correction," *IEEE Trans. Power Electron.*, vol. 20, no. 6, pp. 1319–1327, Nov. 2005.
- [9] J. R. Pinheiro and I. Barbi, "The three-level ZVS-PWM dc-to-dc converter," *IEEE Trans. Power Electron.*, vol. 8, no. 4, pp. 486–492, Oct. 1993.
- [10] S. Kouro, M. Malinowski, K. Gopakumar, J. Pou, L. G. Franquelo, B. Wu, J. Rodriguez, M. A. P'ere, and J. I. Leon, "Recent advances and industrial applications of multilevel converters," *IEEE Trans. Ind. Electron.*, vol. 57, no. 8, pp. 2553–2580, Aug. 2010.
- [11] J. Robinson, D. Jovic, and G. Jo's, "Analysis and design of an offshore wind farm using a MV DC grid," *IEEE Trans. Power Delivery*, vol. 25, no. 4, pp. 2164–2173, Oct. 2010.
- [12] F. Blaabjerg, Z. Chen, and B. S. Kjaer, "Power electronics as efficient interface in dispersed power generation systems," *IEEE Trans. Power Electron.*, vol. 19, no. 5, pp. 1184–1194, Sep. 2004.

Enhanced Fuzzy based Hough Transform for Lane Mark Detection

Manpreet Kaur¹, Ravneet Kaur Sidhu²
Department of Computer Science and Engineering
CT Institute of Technology and Research
Jalandhar, India

E-mail: manpreetb8802@gmail.com¹, ravneet89.sidhu@gmail.com²

ABSTRACT- Lane Detection plays an important role in Intelligent Transportation system and Advanced Driver Assistance Systems. Lane detection is an important aspect of autonomous vehicles. It is also a preventive measure for road accidents. Hough Transform technique uses the edge map obtained from segmentation to detect the lane marks. The threshold value used to segment the image can either be static or dynamic. The overall objective of this paper is to improve the lane detection algorithm using adaptive segmentation and filtering techniques. It has been found that the value used to segment the road image containing lanes has been taken statically. To overcome this, a new lane detection method with an adaptive segmentation value has been proposed. This approach has the ability to boost the lane colorization in efficient manner by utilizing the Additive Hough Transform algorithm with optimized segmentation and filtering techniques. Various parameters like Accuracy, F-measure, Mean Square Error are used for calculating the effectiveness of this technique. The proposed technique yields accurate results as compared to existing techniques.

KEYWORD

ROI; Hough Transform; Otsu; K-means; FCM; Additive Hough Transform; Lane detection, JTF

1. INTRODUCTION

Roads are one of the finest modes of transportation among all modes of transportation. Due to the negligence of drivers, road crashes are continuously increasing day by day. Localizing lane marks painted in the road image is called Lane detection. The major objective of lane recognition is to detect as well as recognize the lane marks painted on the road and then provide these locations to an intelligent system. In intelligent transportation systems, intelligent vehicles cooperate with smart infrastructure to achieve a safer environment and better traffic conditions.

Advanced driver assistance systems (ADAS) are the systems that are designed to assist the driver in its driving process. Lane departure warning system is a part of ADAS whose objective is to detect the lane marks and to warn the driver in the case when the vehicle has tendency to depart from the lane. Many techniques have been made to detect and locate the lane marks. Hough Transform is the most commonly used technique for lane detection but the limitation of Hough Transform is its time complexity to calculate the parameter values. Based on the previous work done in lane detection field, a method is proposed in this paper to detect and localize the lane marks by using Improved Hough Transform based on adaptive segmentation and filtering techniques. This technique yields accurate results in lane detection of straight or curved roads even in the presence of noise present in the image

2. LITERATURE SURVEY

Road safety is the major concern of all the lane detection systems. Most of the road accidents happen when the driver departs from the lane. The Hough Transform (HT) developed by Poly

Hough in 1962 is the most commonly used technique to detect the lane marks. Many varieties and applications to detect the lane lines can be found in the literatures: Yu et al. have proposed a lane detection technique that uses the Hough Transform with a parabolic model under various road and weather conditions. A multi- resolution strategy has been employed to improve the Hough Transform but the method is computationally tractable and less prone when the noise is present in the image [1]. Tseng et al. have proposed a lane detection algorithm that uses Geometry information and Hough transform but the algorithm was time-consuming and also failed when the lane boundaries intersected in a region which is a non-road area [2]. Kim et al. have presented robust lane detection and tracking algorithm based on random sample consensus and particle filtering [3]. An algorithm to detect the painted as well as unpainted roads has been designed by Khalifa that uses Hough Transform for line extraction [4]. Borkar et al. have proposed a lane detection algorithm that is suitable for detecting the lane marks at night. Low resolution Hough Transform has been employed to detect the straight lanes [5]. Wang et al. have used the ideas of region of interest and Random Hough Transform to detect the road edges [6]. Lakshmi et al. have proposed the color segmentation procedure to detect the white and yellow colored lanes on the road [7]. Mariut et al. have

proposed a method that detects the lane marks using Hough Transform and has the tendency to determine travelling direction of the vehicle [8]. Ghazali et al. have proposed an algorithm for detecting unexpected lane changes. The algorithm uses H-maxima approach and improved Hough Transform is applied on the near-field of view to detect the straight lines [9]. Phaneendra et al. have proposed an accident avoiding system that uses Hough Transform to detect the left and right marks and determines the position of the vehicle with respect to these marks and gives a warning message whenever the vehicle departs from the lane [10]. Cho et al. have proposed a lane recognition algorithm that uses multiple region of interest. Hough transform with applied accumulator cells has been applied to detect the lane marks in each region of interest [11]. Yi et al. have discussed the existing lane detection techniques and the benefits and limits of existing lane colorization problems. It has been found that most of the existing researchers have used the Hough Transform algorithm for lane detection and also neglected the overheads of existing techniques. The limitation of Hough Transform is its time complexity to solve trigonometric functions to evaluate parameter values. To reduce the limitations of existing researchers, the author has proposed a modified approach for lane detection called as Additive Hough Transform that accelerates the HT process in computationally efficient manner and making it suitable for real-time lane detection. The algorithm randomly selects two points in the image space and solves them using additive property to obtain a point in the parameter space [13]. After surveying the literature, it has been found that most of the existing researchers have used the Traditional Hough transform that is capable for detecting straight lines only and static threshold is used to segment the image to obtain the edge map. In order to reduce the limitations of existing researchers, a new strategy has been proposed in this paper that consists of enhanced Hough Transform using adaptive segmentation techniques.

3. OVERVIEW OF ALGORITHM

The proposed algorithm works in two steps – pre-processing and post-processing. Pre-processing is low level image processing that deals with images from the camera and generate useful information for detection parts. It includes filtration, ROI selection and gray scale conversion. Initially the road image is captured by the camera and a region of interest is extracted from input image in order to reduce the search area and to save computational time.

Then the gray scale conversion of the image is done to reduce the processing. Post-processing consists of two steps. In first step, image segmentation is done to obtain an edge map which is used as an input by Additive Hough Transform. In second step Additive Hough Transform is applied to detect the lane marks.

3.1 Region of interest

The road image is captured by the camera that is mounted in front of the vehicle. The region of interest is extracted from the original image by cropping the road image. It increases the speed and accuracy of the lane detection algorithm. The maximum region of interest mainly lies in the bottom half of the road image where all the necessary objects such as lane markings, pedestrians and other vehicles are present. On the basis of the dimensions of the image, the region of interest is calculated by reducing each side of the image.

a. Gray-scale Conversion

The RGB image is converted into gray- scale format. Gray-scale conversion transforms a 28 bit, 3 channel RGB color image into 8 bit, one channel and gray-scale image. Generally, road surface can be made up of various obstacles such as shadows, tire skids, oil stains, diverse pavement style which changes the color of the road surface and lane markings to form one image region to another. Due to this, the image is converted into gray scale.

b. Image Segmentation

Image segmentation is an important step in image analysis and object recognition. It divides an image into meaningful structures. Lane detection algorithm uses edge map of the image to detect the lanes. The proposed algorithm consists of clustering based image segmentation technique that is used to segment the road lane image. Fuzzy based segmentation technique divides the road image using an adaptive threshold value which results in better lane detection.

3.3.1 Fuzzy based segmentation

The fuzzy c-means (FCM) algorithm is a clustering algorithm. It was developed by Dunn and Bezdek. The aim of FCM algorithm is to find an optimal fuzzy c-partition by evolving the fuzzy partition matrix iteratively and computing the cluster centers [12]. In order to achieve this, the algorithm tries to minimize the objective function:

$$J_{FCM} = \sum_{i=1}^N \sum_{j=1}^C \mu_{ij}^m (\|x_i - v_j\|)^2 \quad (1)$$

Where m is any real number greater than 1, u_{ij} is the degree of membership of x_i in the cluster j , x_i is the i th data, v_j is the center of the cluster. Membership μ_{ij} is given by:

$$\mu_{ij} = \frac{\|x_i - v_j\|^{\frac{2}{m-1}}}{\sum_{k=1}^c \|x_i - v_k\|^{\frac{2}{m-1}}} \quad (2)$$

c. Hough Transform

Hough Transform (HT) is an efficient tool for detecting straight lines in an image, even in the presence of noise and missing data. The basic principle of the Hough Transform is that every point in the image has infinite number of lines, which pass through it but with a different angle. The goal of the transform is to identify the lines that pass through the most points in the image. These are the lines that most closely match the features in the image. Hough transform algorithm uses an array, called an accumulator, to detect lines. The dimension of the accumulator is equal to the number of an unknown Hough transform parameters. The ρ parameter represents the distance between the line and the origin, and the parameter θ represents the angle of the vector from the origin to the closest point on the line. A count (initialized at zero) in Hough accumulator at point (ρ, θ) is incremented for each line it considers.

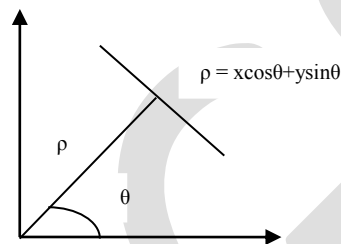


Fig.1 Hough transform for detecting straight lines.

Hough transform is unsuitable for real time applications because high computational time incurred by conventional Hough voting attributed to trigonometric functions and multiplications applied to every edge pixel.

d. Additive Hough Transform

From the various implementation of Hough Transform, it is known that the classic Hough algorithm has heavy calculation burden resulted into ineffectiveness to satisfy real-time request. Therefore, we modify it for detecting both straight and curved roads efficiently as well as for calculating more than one edge point. The idea is to select two points and solve them using the equations (11) and (12).

$$\theta_i = \tan^{-1}((x_i - x_{i+1}) / (y_{i+1} - y_i)) \quad (3)$$

$$\rho = x_i \cos \theta_i + y_i \sin \theta_i \quad (4)$$

The corresponding accumulator units are set to zero in the parameter space. If the points exist in the parameter space the corresponding accumulators count plus 1. If not, the points are inserted into the parameter space.

4. EXPERIMENTS & RESULTS

We have performed the experiments in MATLAB under Hp computer having Intel(R) Core™ i5 processor, 32 bit windows 7 operating system, 4.00 GB RAM and RADEON Graphics. A database of 15 road images has been collected This technique has been implemented on a number of images acquired along the roads with different illumination conditions in different situations such as single/double lane marks, supplementary road marks etc.

4.1 Detection of lane marks using Hough transform and Additive Hough Transform:

Hough Transform and Additive Hough transform techniques have been applied on different test images. The lane detection results of the following four different test images on applying these techniques are shown in Fig. 2. In Fig.2, column (a) represents the original images captured by the camera, column (b) represents the lane detected images obtained on applying the Traditional Hough Transform technique and column (c) represents the lane detected images on applying AHT Hough Transform technique. From subjective evaluation it is evident that more lines are detected by AHT as compared to HT.

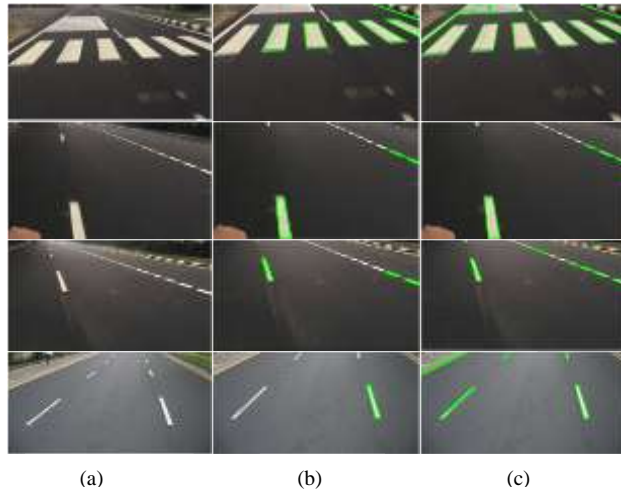


Fig.2 (a) Input Image; (b) Traditional Hough Transform lane detected image; (c) Additive Hough Transform lane detected image.

Performance Evaluation:

Performance Evaluation table shows the analysis of lane detection techniques using different parameters such as Geometric Accuracy, F-measure and MSE. The average values of parameters of conventional and new techniques have been calculated to analyze the performance. Also to evaluate the performance of HT and AHT, the average values of Accuracy, F-measure and MSE are evaluated for 15 images containing lanes. The average values of these parameters are shown in Table1.

a) Accuracy

Accuracy is the major requirement of the lane detection techniques. Geometric accuracy is the accuracy of a resulted image compared to the original image. In Table 1, Accuracy value obtained by HT and AHT techniques for 15 road images containing lane marks is shown. From table values, it is clear that highest value of Accuracy is obtained by AHT as compared to HT.

b) F-measure

F-measure parameter is used to compute the average of information retrieval precision and recall matrices. In Table 1, F-measure value obtained by HT and AHT techniques for 15 road images containing lane marks is shown. From table values, it is clear that highest value of F-measure is obtained by AHT as compared to HT.

c) Mean Square Error

Mean Square Error is a risk function corresponding to expected value of squared error loss or quadrate loss. It is a measure of image quality index. The large value of MSE means the image is a poor quality image. In Table 1, MSE value obtained by HT and AHT techniques for 15 road images containing lane marks is shown. From table values, it is clear that smaller value of MSE is obtained by AHT as compared to HT.

From experimental results and performance measures, it is vivid that results of AHT are more accurate as compared to HT. Therefore AHT yields more accurate lanes as compared to HT technique.

Table 1 Performance evaluation of Accuracy, F-measure and MSE after applying Traditional Hough Transform and Additive Hough Transform techniques on different images.

IMG.	ACCURACY		F-MEASURE		MSE	
	HT	AHT	HT	AHT	HT	AHT
1	0.6802	0.6985	80.3241	83.0168	0.3014	0.2934
2	0.3821	0.4628	62.8943	65.1264	0.5502	0.5328
3	0.8235	0.8468	93.7263	95.8267	0.6215	0.0582

4	0.9017	0.9543	88.1497	90.3047	0.1986	0.1560
5	0.9254	0.9400	96.1005	97.2471	0.0198	0.0192
6	0.9368	0.9487	95.3286	97.0041	0.1024	0.0628
7	0.8553	0.8696	94.9982	97.9587	0.0816	0.0507
8	0.7616	0.7739	91.2109	92.6112	0.1590	0.1365
9	0.8259	0.8926	83.1478	86.2476	0.2517	0.2369
10	0.8016	0.8374	93.2108	94.8521	0.8014	0.6145
11	0.9385	0.9398	87.8435	90.0690	0.1727	0.1465
12	0.9632	0.9759	93.4792	95.2341	0.1285	0.1009
13	0.9112	0.9235	95.2116	97.6785	0.0242	0.0211
14	0.6973	0.7241	90.5387	93.5899	0.0957	0.0729
15	0.8714	0.9234	81.0978	83.8427	0.3014	0.2764
Avg.	0.8183	0.8474	88.4841	90.7073	0.2540	0.1852

4.2 Improved Hough Transform using Fuzzy based segmentation:

Additive Hough Transform (AHT) technique uses an edge map obtained by image gradient processing method as an input for lane detection. The threshold value used to segment the image is taken statically. Therefore adaptive threshold value is required to improve the results further. The Additive Hough Transform technique is applied with Fuzzy Segmentation algorithm. The segmentation results obtained by image gradient processing and Fuzzy segmentation based techniques are shown in Fig.3. From visual perspective, it is clear that the segmentation results of Fuzzy are more accurate than gradient processing method. In Fig. 4, the lane detection results of AHT by using gradient processing and Fuzzy segmentation are shown.

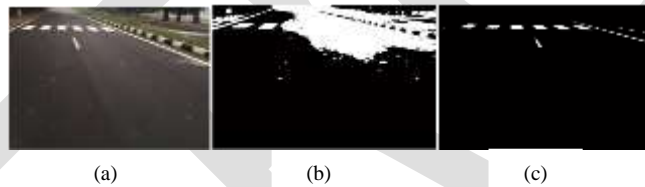


Fig.3 (a) Input Image (b) Gradient processing Segmented Image (c) Fuzzy Segmented Image.

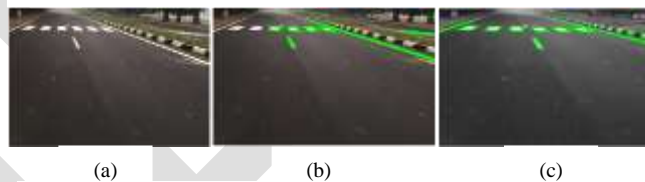


Fig.4 (a) Input Image (b) AHT lane detected Image (c) Fuzzy based HT lane detected Image.

From the experiments, it is clear that Fuzzy based Hough Transform yields better lane detection results as compared to AHT technique.

4.2.1 Fuzzy based Hough Transform:

Fuzzy based Hough Transform technique is implemented on the road images containing lane marks. The improved lane detection results are obtained by Fuzzy based HT as compared to AHT technique. Fig. 5 shows the lane detection results of original image obtained by using AHT and Fuzzy based HT techniques.

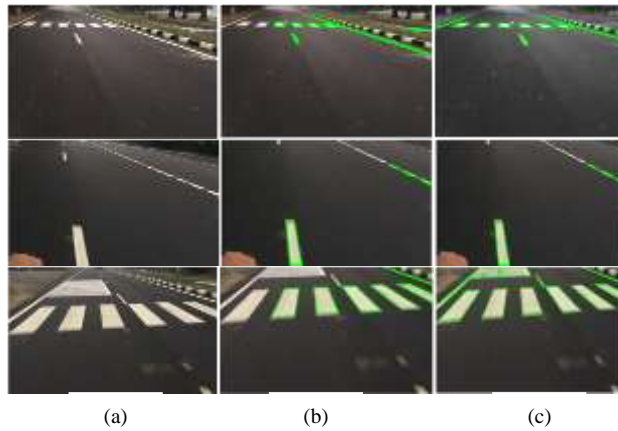


Fig.5 (a) Input Image (b) AHT lane detected Image (c) Fuzzy based HT lane detected Image.

Performance evaluation Table 2 is showing the comparison and complete analysis of AHT and Fuzzy based HT techniques. From the table values, it is clear that the results of Fuzzy based Hough transform technique are more accurate as compared to AHT technique.

Table 2 Performance evaluations of Accuracy, F-measure and MSE on applying AHT and Fuzzy based HT techniques on road images.

IMG.	ACCURACY		F-MEASURE		MSE	
	AHT	Fuzzy based HT	AHT	Fuzzy based HT	AHT	Fuzzy based HT
1	0.6985	0.7537	83.0168	86.5893	0.2934	0.2204
2	0.4628	0.9881	65.1264	99.4013	0.5328	0.0119
3	0.8468	0.9700	95.8267	99.1657	0.0582	0.0157
4	0.9543	0.9998	90.3047	98.4624	0.1560	0.0300
5	0.9400	0.9780	97.2471	99.9972	0.0192	0.0010
6	0.9487	0.9768	97.0041	98.8407	0.0628	0.0220
7	0.8696	0.9633	97.9587	98.8259	0.0507	0.0232
8	0.7739	0.9594	92.6112	98.1054	0.1365	0.0367
9	0.8926	0.9693	86.2476	97.9298	0.2369	0.0406
10	0.8374	0.9500	94.8521	98.4313	0.6145	0.0307
11	0.9398	0.9693	90.0690	97.4172	0.1465	0.0500
12	0.9759	0.9832	95.2341	98.4284	0.1009	0.0307
13	0.9235	0.9535	97.6785	99.1508	0.0211	0.0168
14	0.7241	0.9859	93.5899	97.6178	0.0729	0.0465
15	0.9234	0.9843	83.8427	99.2892	0.2764	0.0141
Avg.	0.8474	0.9590	90.7073	97.8435	0.1852	0.0393

From subjective analysis and performance measures, it is observed that Fuzzy based HT technique gives more accurate lane detection results than AHT technique.

4.3 Enhancement of Fuzzy based Hough Transform using filtering techniques:

Lane detection technique has to locate the lane marks in the presence of noise present in the road image. The noise can be reduced by using different filtering techniques i.e. median filter, mean filter and JTF (Joint Trilateral Filter). Therefore the results of Fuzzy based HT technique are further enhanced by using filters so that it can give more accurate lane detection even in the presence of noise in the road image. In Fig. 6, 7, 8, lane detection results of Fuzzy based HT using mean, median and JTF filters are shown.

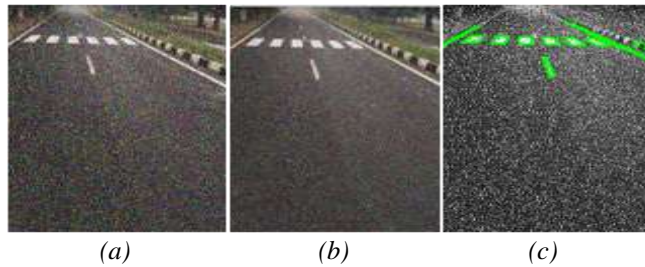


Fig.6 (a) Input Image; (b) Mean Filtered Image; (c) Fuzzy based HT lane detected image with Mean Filter.

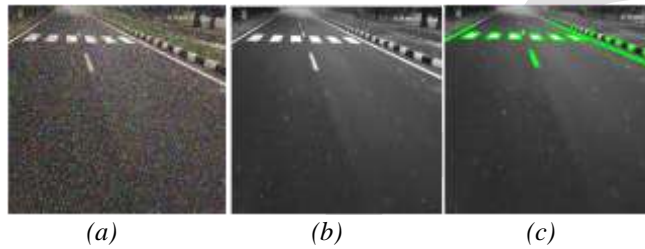


Fig.7 (a) Input Image; (b) Median Filtered Image; (c) Fuzzy based HT lane detected image with Median Filter.

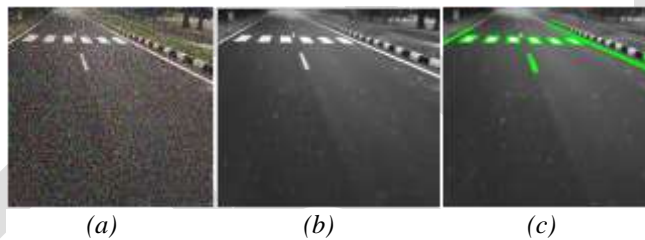


Fig.8 (a) Input Image; (b) JTF Filtered Image; (c) Fuzzy based HT lane detected image with JTF Filter.

From visual analysis, it is clear that the more accurate lanes are detected by Fuzzy based HT with JTF as compared to Mean and Median filter. To analyze the performance of these techniques, the various performance evaluation parameters such as Accuracy, F-measure and MSE are taken. Table 3 is showing the average accuracy value obtained by Fuzzy based HT with mean, median and JTF filters. Table 4 is showing the average F-measure value obtained by Fuzzy based HT with mean, median and JTF filters. Table 5 is showing the average MSE value obtained by Fuzzy based HT with mean, median and JTF filters. From table values it is clear that highest values of accuracy, F-measure and least value of MSE are obtained by Fuzzy based HT with JTF as compared to mean and median filters.

Table 3 Performance evaluations of Accuracy on applying Fuzzy based HT technique with mean, median and JTF on road images.

Image	Accuracy		
	Fuzzy based HT with		
	Mean filter	Median filter	JTF filter
1	0.7582	0.7796	0.7843
2	0.9886	0.9896	0.9902
3	0.9735	0.9798	0.9839
4	0.9985	0.9992	0.9998
5	0.9786	0.9832	0.9948
6	0.9775	0.9789	0.9800
7	0.9645	0.9768	0.9889

8	0.9598	0.9625	0.9720
9	0.9699	0.9708	0.9799
10	0.9529	0.9584	0.9683
11	0.9710	0.9785	0.9875
12	0.9849	0.9893	0.9969
13	0.9580	0.9599	0.9682
14	0.9872	0.9896	0.9979
15	0.9862	0.9886	0.9978
Average	0.9606	0.9656	0.9728

Table 4 Performance evaluations of F-measure on applying Fuzzy based HT technique with mean, median and JTF on road images.

Image	F-measure		
	Fuzzy based HT with		
	Mean filter	Median filter	JTF filter
1	86.9385	86.9650	87.5149
2	99.6385	99.7862	99.9156
3	99.8162	99.9358	99.9713
4	99.2068	99.2367	99.9996
5	99.9980	99.9985	99.9989
6	98.9210	98.9742	99.0852
7	98.9268	98.9776	99.2786
8	98.4638	98.6674	98.9987
9	98.9175	98.9326	98.9886
10	98.4510	98.5572	98.9791
11	98.8138	98.9567	99.2197
12	98.8710	98.9245	98.9518
13	98.9998	99.0016	99.1276
14	99.6275	99.7742	99.8916
15	99.3210	99.4325	99.5874
Average	98.3274	98.4081	98.6339

Table 5 Performance evaluations of MSE on applying Fuzzy based HT technique with mean, median and JTF on road images.

Image	MSE		
	Fuzzy based HT with		
	Mean filter	Median filter	JTF filter
1	0.2196	0.1963	0.1802
2	0.0107	0.0102	0.0095
3	0.0143	0.0134	0.0117
4	0.0291	0.0275	0.0196
5	0.0009	0.0008	0.0005
6	0.0205	0.0197	0.0098
7	0.0225	0.0207	0.0185
8	0.0342	0.0327	0.0291

9	0.0400	0.0389	0.0310
10	0.0301	0.0293	0.0197
11	0.0490	0.0478	0.0372
12	0.0304	0.0287	0.0207
13	0.0149	0.0132	0.0112
14	0.0459	0.0432	0.0399
15	0.0136	0.0124	0.0108
Average	0.0383	0.0356	0.0299

From subjective analysis and performance measures it is vivid that Fuzzy based HT with JTF yields more accurate lane detection results as compared to other filters namely mean and median filters.

4.3.1 Enhanced Fuzzy based Hough Transform using JTF:

In this part of experimental results, Fuzzy based HT technique without filter and Fuzzy based HT with JTF are implemented on the images containing noise such as salt and pepper noise. The enhanced lane detection results are obtained by Fuzzy based HT with JTF as compared to Fuzzy based HT technique. In Fig. 9, the enhanced lane detection results obtained by Fuzzy based HT and Fuzzy based HT with JTF are shown. In Table 6 and 7, the average Accuracy, F-measure and MSE values obtained by Fuzzy based HT without filter and with JTF are shown.

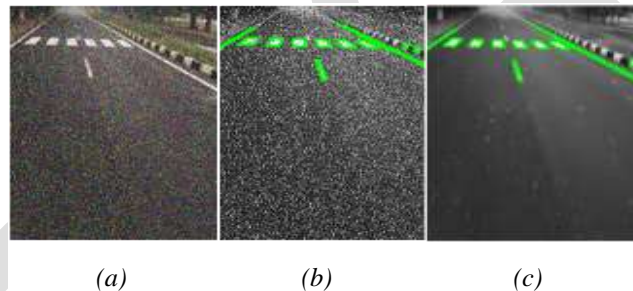


Fig.9 (a) Input Image; (b) Fuzzy based HT lane detected image without filter; (c) Fuzzy based HT lane detected image with JTF.

Table 6 Performance evaluations of Accuracy and F-measure on applying Fuzzy based HT without and with JTF filter on different images.

Image	Accuracy		F-measure	
	Fuzzy based HT (without filter)	Fuzzy based HT with JTF filter (proposed technique)	Fuzzy based HT (without filter)	Fuzzy based HT with JTF filter (proposed technique)
1	0.7537	0.7843	86.5893	0.7843
2	0.9881	0.9902	99.4013	99.9156
3	0.9700	0.9839	99.1657	99.9713
4	0.9998	0.9998	98.4624	99.9996
5	0.9780	0.9948	99.9972	99.9989
6	0.9768	0.9800	98.8407	99.0852

7	0.9633	0.9889	98.8259	99.2786
8	0.9594	0.9720	98.1054	98.9987
9	0.9693	0.9799	97.9298	98.9886
10	0.9500	0.9683	98.4313	98.9791
11	0.9693	0.9875	97.4172	99.2197
12	0.9832	0.9969	98.4284	98.9518
13	0.9535	0.9682	99.1508	99.1276
14	0.9859	0.9979	97.6178	99.8916
15	0.9843	0.9978	99.2892	99.5874
Avg.	0.9590	0.9728	97.8435	98.6339

Table 7 Performance evaluation of MSE on applying Fuzzy based HT without and with JTF filter on different images.

Image	MSE	
	Fuzzy based HT (without filter)	Fuzzy based HT with JTF filter (proposed technique)
1	0.2204	0.1802
2	0.0119	0.0095
3	0.0157	0.0117
4	0.0300	0.0196
5	0.0010	0.0005
6	0.0220	0.0098
7	0.0232	0.0185
8	0.0367	0.0291
9	0.0406	0.0310
10	0.0307	0.0197
11	0.0500	0.0372
12	0.0307	0.0207
13	0.0168	0.0112
14	0.0465	0.0399
15	0.0141	0.0108
Avg.	0.0393	0.0299

From visual analysis and performance measures, it is observed that Fuzzy based HT with JTF results in better lane detection even if the noise is present in the image. Therefore Fuzzy based HT with JTF yields more enhanced lane detection results as compare to existing techniques.

5. CONCLUSION

The lane detection technique is an essence of Intelligent Transportation Systems. It has been found that the value used to segment the image in lane detection algorithm is taken as static. To overcome this limitation, we have introduced a modified Hough approach that uses adaptive segmentation technique such as Fuzzy based segmentation to enhance the segmentation results which in turn results in better lane detection. Also different filtering techniques such as mean, median and JTF have been integrated with the proposed algorithm so that it can efficiently yield more accurate lanes even if the noise is present in the image. From quality measures, it has been analyzed that the value obtained by Fuzzy based HT technique with JTF is more efficient than HT and AHT techniques. Fuzzy based Hough Transform with JTF filter yields more accurate lane results for straight as well as curved images than other techniques. Therefore, the proposed technique is capable to detect straight as well as curved lanes.

REFERENCES:

[1] B. Yu and A. Jain, "Lane Boundary Detection Using a Multi-resolution Hough Transform", in Proceedings IEEE International Conference on Image Processing, vol. 2, pp. 748 – 751, (1997).

- [2] C.C. Tseng, H.Y. Cheng and B.S. Jeng, "A lane detection algorithm using geometry information and modified Hough transform", 18th IPPR conference on Computer Vision, Graphics and Image Processing, (2005).
- [3] Z. Kim, "Robust Lane Detection and Tracking in Challenging Scenarios", in IEEE Transactions on Intelligent Transportation Systems, vol. 9, no. 1, pp. 16 - 26, (2008).
- [4] O.O. Khalifa and A.H.A Hashim, "Vision-Based Lane Detection for Autonomous Artificial Intelligent Vehicles", in IEEE International Conference on Semantic Computing, Berkeley, CA, pp. 636 - 641, (2009).
- [5] A. Borkar, M. Hayes, M. Smith and S. Pankanti, "A layered approach to robust lane detection at night," in IEEE Workshop on Computational Intelligence in vehicles and Vehicular System, pp. 51-57, (2009).
- [6] Z. Teng, J.H. Kin and D.J. Kang, "Real-time Lane detection by using multiple cues", in IEEE International Conference on Control Automation and Systems, pp. 2334 - 2337, (2010).
- [7] J. Wang, Y. Wu, Z. Liang and Y. Xi, "Lane detection based on random Hough transform on region of interesting", IEEE International Conference on Information and Automation, pp. 1735-1740, (2010).
- [8] M. DhanaLakshmi and B.J. Deepika, "A brawny multicolor lane colorization method to the Indian scenarios", International Journal of Emerging Trends and Technology, vol. 2, no. 4, pp. 202-206, (2012).
- [9] F. Mariut, C. Fosala and D. Petrisor, "Lane Mark Detection Using Hough Transform", IEEE International Conference and Exposition on Electrical and Power Engineering, pp. 871- 875, (2012).
- [10] K. Ghazali, R. Xiao and J. Ma, " Road Lane Detection Using H-Maxima and Improved Hough Transform", 4th International Conference on Computational Intelligence, Modeling and Simulation, pp. 2166-8531, (2012).
- [11] N. Phaneendra, G. Goud and V.Padmaja, "Accident Avoiding System Using Lane Detection", International Journal of Research in Electronics and Communication Engineering, vol. 1, no. 1, pp. 1 - 4, (2013).
- [12] S. Lakshmi and V. Sankaranarayanan, "A Robust Background Removal Algorithms Using Fuzzy C-means Clustering", International Journal of Network Security and Applications, vol. 5, no. 2, pp. 93-101, (2013).
- [13] J.H. Cho, Y.M. Jang and S.B. Cho, "Lane recognition algorithm using the Hough Transform with applied accumulator cells in the multi-channel ROI", 18th IEEE International Symposium in Consumer Electronics, pp. 1-3, (2014).
- [14] S.C. Yi, Y.C. Chen and C.H. Chang, "A lane detection approach based on intelligent vision", Computers & Electrical Engineering, vol. 42, pp. 23-29, (2015).

LOCALISED WEATHER MONITORING SYSTEM

Parijit Kedia,

Department of Computer Science, VIT University, Vellore, India, parijitkedia@gmail.com, +919159641802

ABSTRACT – A weather station is a facility equipped with high-tech instruments for predicting future weather phenomenon. This is also used to study the climate of that area. The measurements taken from the station include – temperature, pressure, humidity, wind speed, precipitation. The accuracy predicted by these weather stations is not too high to predict the actual weather condition for a particular area. The error difference may be around 10% which makes a huge difference. Plus, in every city there are 2-3 weather stations only for predicting weather of an area as wide as 426km². The weather stations give the prediction for the whole city and not just a particular area. Each area might have different climate since the weather depends on location. This paper formulates the mechanism to improve the accuracy.

KEYWORDS – Sensors, Accuracy, Algorithms, Analysis, Arduino, Graph, Prediction

INTRODUCTION

Weather prediction is done by extensive analysis of data that is collected over a period of time. The climatic data of a particular location has various attributes like – temperature, pressure, wind, sunlight, rain. All these factors and their intermediaries contribute to the prediction of the climate under consideration. The analysis is done by the based on current data and historical data. Using various algorithms that can model the data.

A small change in weather phenomenon can have a devastating impact on the climate of that area. These may be due to tides, sun rays, and atmospheric pressure. All of these are inter-related. It also becomes difficult to predict future weather more than a few days ahead, since climate is continuously changing. Tomorrow's climate may be further impacted by other meteorological phenomenon.

Human interaction is needed since we need to determine the correct model that needs to be built. Even if we use Artificial Intelligence or Machine Learning Algorithms for the analysis, we need to have the correct model. If model is wrong, then analysis is like a needle in a haystack.

LITERATURE REVIEW

Previous systems that existed are only on collection of climate data or transmission of these data using ZigBee or GSM or Wi-Fi or some remote mechanism. All these system, though they measure the same parameters but they lack one common thing and that is accuracy. People need accurate weather condition of the area they live in. They need to know the weather so that they can thrive and adapt according to it.

Other systems collect data and predict tomorrow's weather data just like that. No patten, no observation are made. This makes the prediction error prone. This method is applicable only to places where there are not so many weather fluctuations occurring in the area i.e. it is stable throughout. Since normal prediction would fail when the outliers are more.

Nowadays, weather station use heavy instruments to determine the weather of the city. These instruments cost high and their accuracy is not too much to rely on.

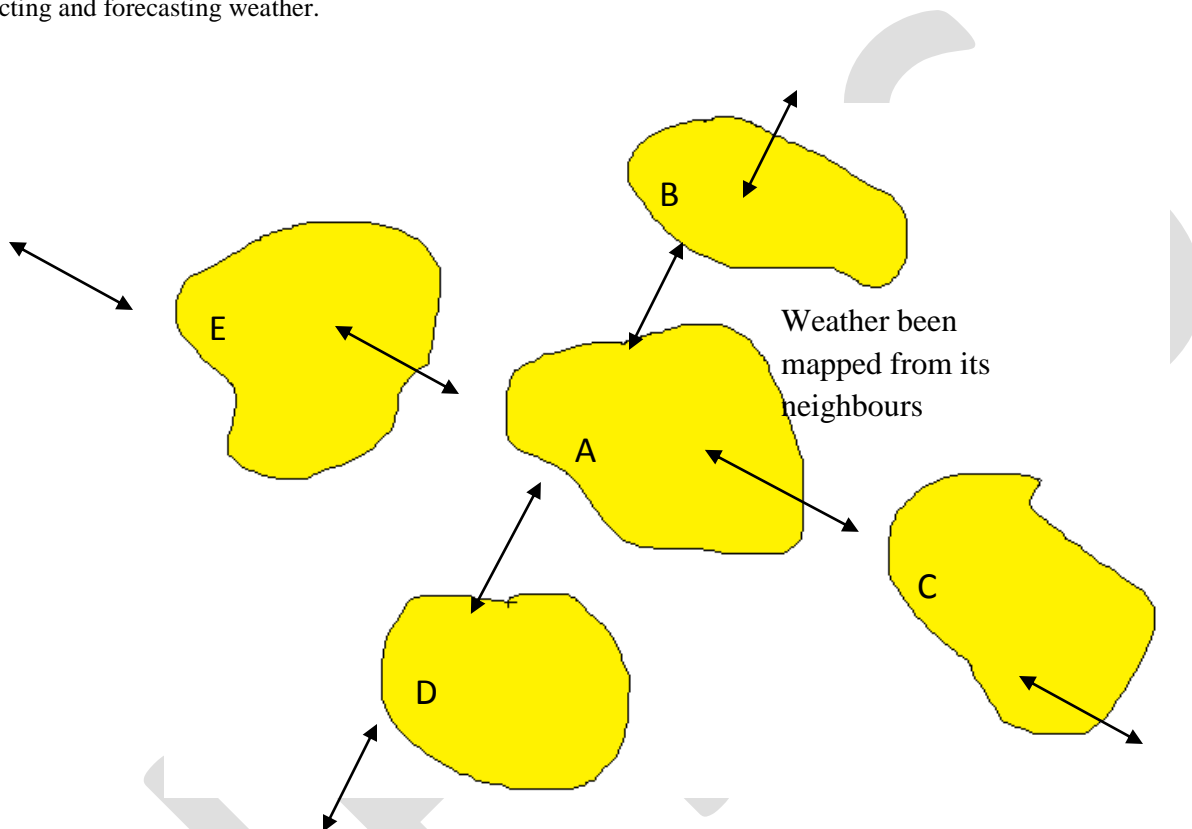
PROPOSED SYSTEM

To improve the accuracy of the above mentioned technique, we would be making the weather stations localized. Now we cannot have the whole unit at each and every area. This would incur a lot of expenses and area. To reduce that we would build a mini weather station on top of every building there is in the city. Suppose, if there are 1 million building, there will be 1 million mini weather stations incorporated on the top just like a Tata Sky antenna is installed. This would help in collecting data from each area of the city, to be specific each building.

Now, consider Location A which is surrounded by location B, C, D and E on 4 sides. Now we can have 5 possibilities of mapping Location A weather i.e. location A weather itself, Location A and B, Location A and C, Location A and D, Location A and E.

All these mapping done together will help in predicting the weather of the Location A to a good accuracy point. Since, weather is dependent and contagious (sort of), learning of the locations dependency will help in resolving/predicting the weather accurately.

An algorithm will be used to learn each locations weather and its neighbouring locations dependencies which will help in currently identifying the climate. Thus people of that area can make plans accordingly depending on the weather predicted by the mini stations. The equipment will be covered in a proper ventilated box, so that it is invulnerable to nature's wrath but in return help in collecting and forecasting weather.



OUTCOME

The expected outcome is to improve the accuracy of the weather being predicted. The error before was around 10%. This proposed mechanism should reduce the error to 2% which is a significant improvement over the previous existing one. The range of the device being installed is limited to 1 building. So the data collected would be over every m^2 . This data would be consistent and similar to the data collected by just 2-3 weather stations. The only difference would be the accuracy of the data to every decimal and forecasting of weather to the actual one.

The result will be displayed on the LCD Screen of each building so that the occupants can check their local area weather. Also, these data can be collected and mapped to be displayed on their states weather report website. They can accurately check the weather of the area they want to visit, travel, etc. Therefore, the people can plan their moves accordingly i.e. at what time should they leave or visit for safe travel.

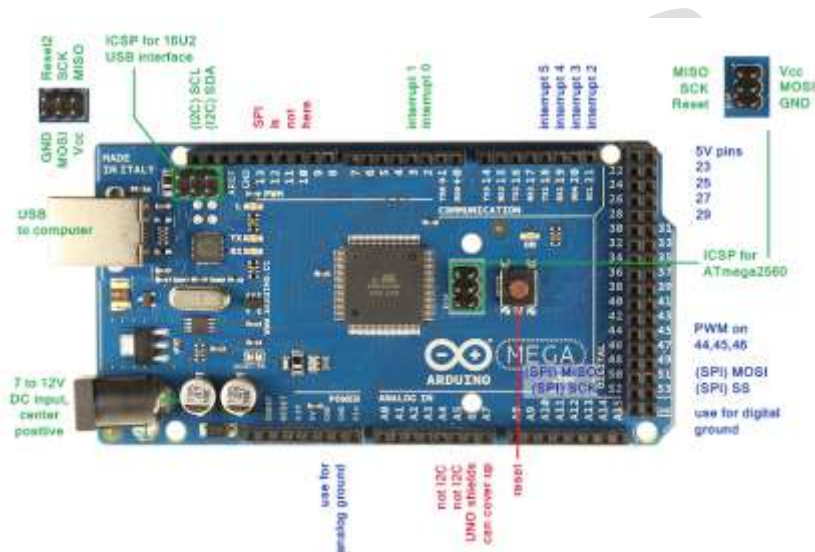
The data being collected will be transmitted to the data center via radio waves since they require no complications required for transmission. The data can be sent via different frequency so that there is very less interference of data. It is a cheaper method of sending data.

The data center collects data from these 1 million houses and maps the data simultaneously to predict weather changes every hour. The data is also collected to report any anomaly that can occur in the near future (just like stock market they vary depending on

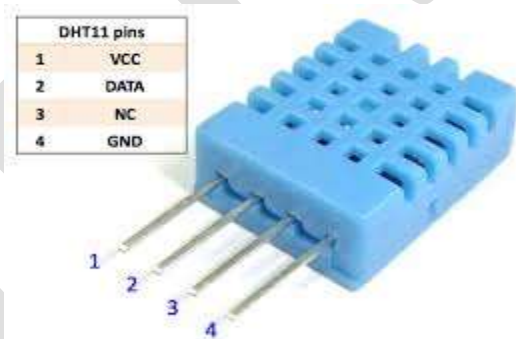
the structures and clues as explained by the Elliotts Wave Theory principle). Also, as said above, the data is mapped for accurate prediction.

COMPONENTS

ARDUINO is an open-source electronics platform based on easy-to-use hardware and software. It is intended for anyone making interactive projects. Arduino senses the environment by receiving inputs from many sensors, and affects its surroundings by controlling lights, motors and other actuators.



DHT11 is a temperature and humidity sensor which has 4 pins. One is voltage, other is ground and third is data pin which is used for transmission of data from sensor to Arduino and last pin is not connected called NC pin.



BMP180 is a pressure sensor module that is connected to Arduino with same concept. One is connected to VCC, other to GND, and to analog pin of Arduino.



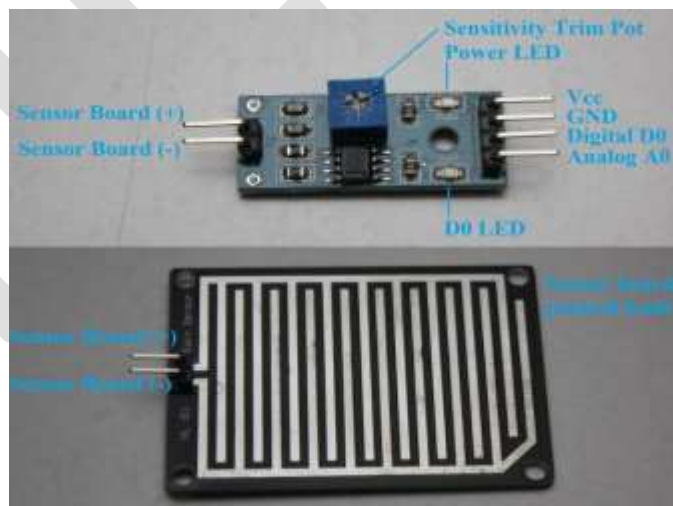
SOUND SENSOR is used for detecting wind modules. The reason behind this is that when wind occurs or when there is a high breeze, air vibrations are created. These air vibrations determine the level of sound which is directly proportional to the wind speed. So, Higher the sound produced, high is the wind speed. This air vibration is similar to the vibration produced in a resonating air column.



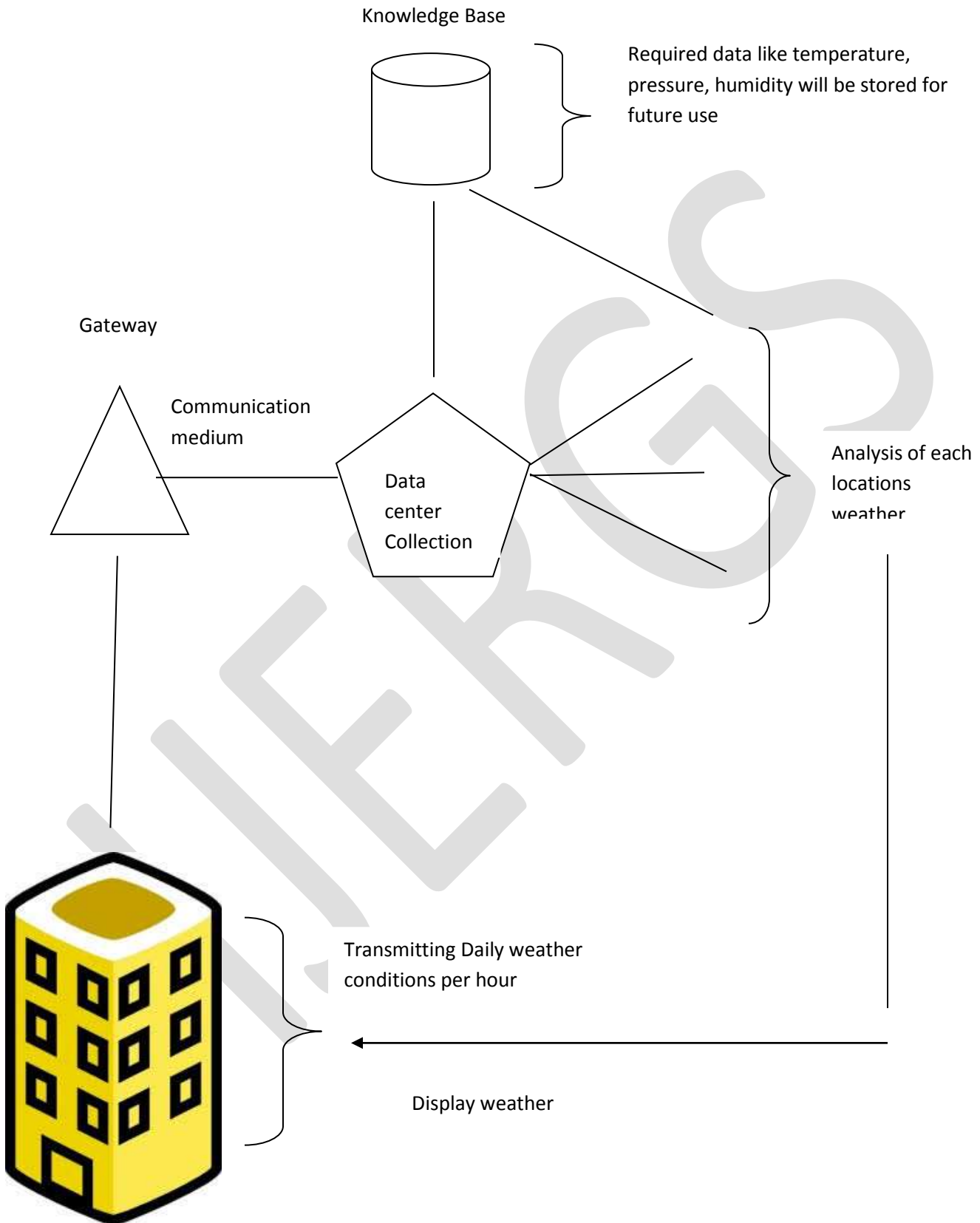
LDR is a light intensity module that maps the sensor value to the intensity of light (inversely proportional) When you increase the external brightness, the sensor values decrease thereby indicating that the light intensity has increased.



Rain Drop Sensor is used for detecting whether rain will be occurring or not. It consist of a board which is connected to an intermediate module. When water is dropped on the board, the resistance inside changes which cause the current to flow thereby indicating that rain is going to happen. The more the water, more rapid changes in the resistance so more current flow. As a result we see fluctuations in values thereby predicting that heavy rain (may be flood) is going to occur.



ARCHITECTURE DESIGN



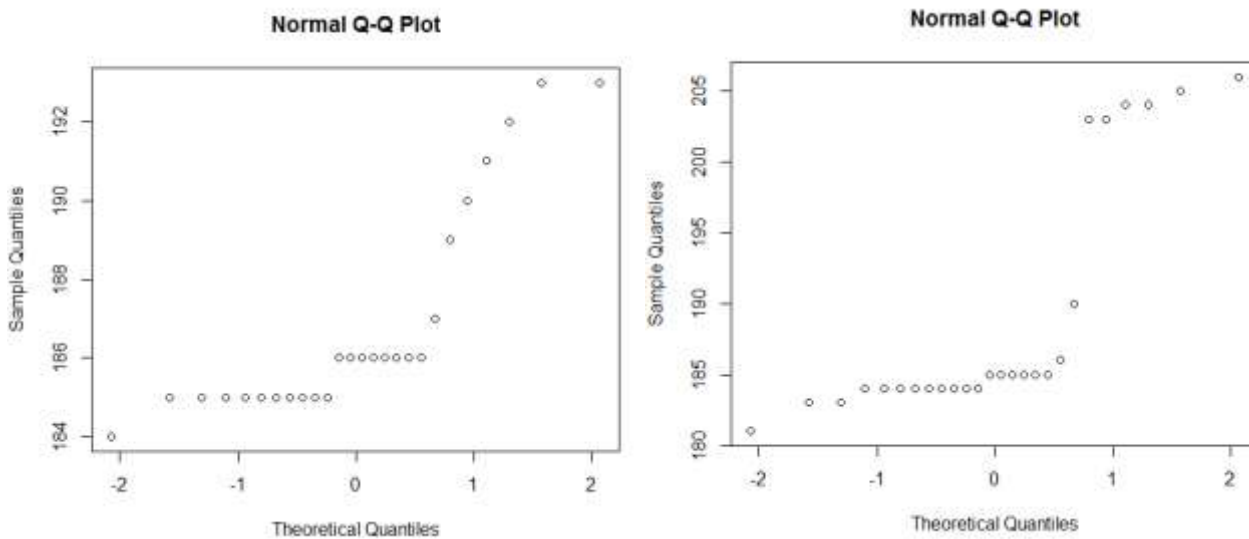
EXPERIMENTAL RESULTS

Suppose a person wants to go to a particular location (say B) from A. Now that person wants to plan his travel accordingly such that he does not have to face the extreme weather conditions of the locations. So he can see the weather of the 2 locations at different time of the day and depending on that he can plan his moves.

For example, Location A will have temperature 35°C at noon and 25°C around 5pm. Location B will have rain occurring in the morning and dry weather by 5pm and the journey time is 1 pm. So, he decides to move at 4 pm where he does not have to face any problems.

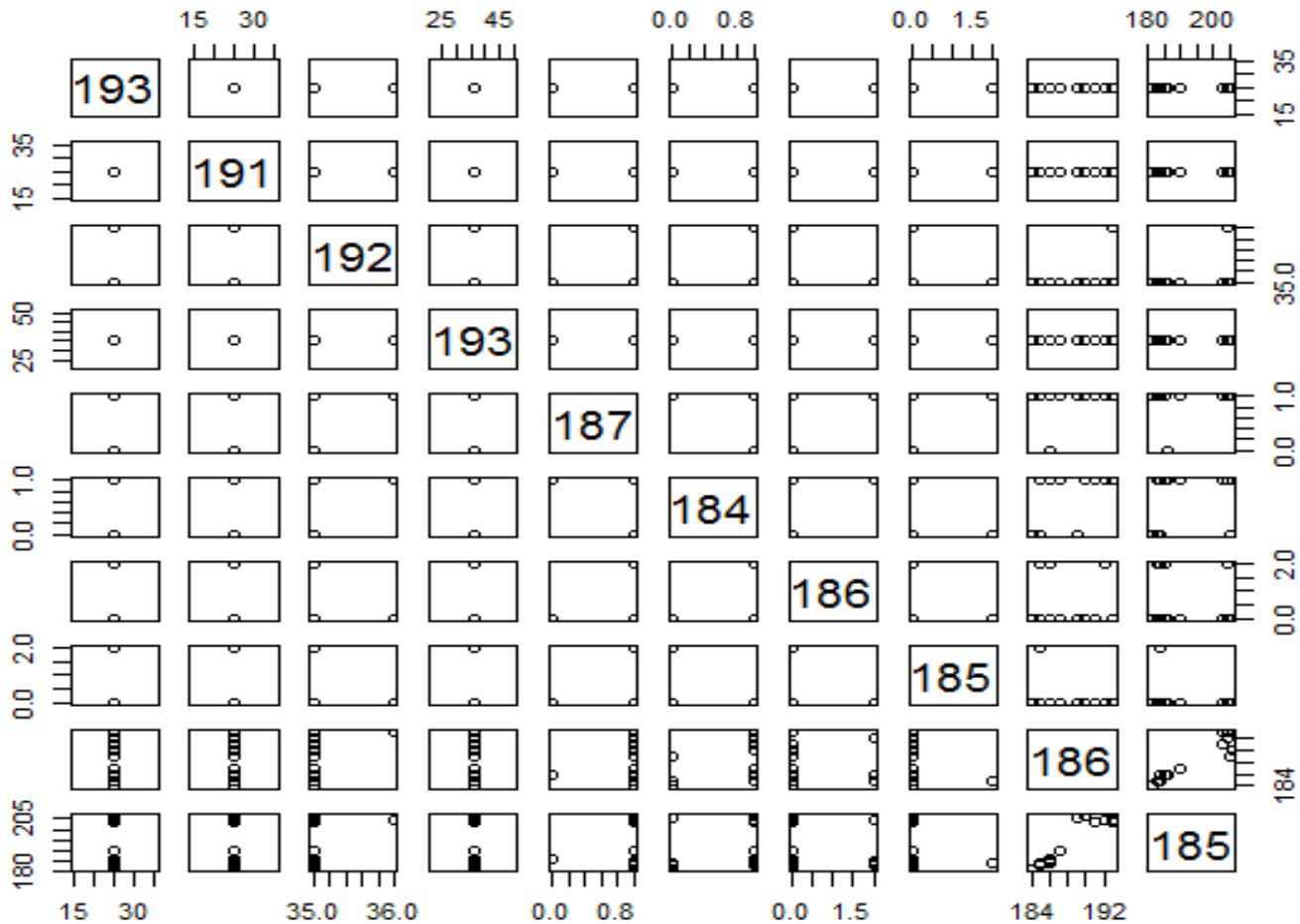
	A	B	C	D	E	F	G	H	I	J
1	Temperat	Temperat	Humidity	Humidity	Rain_A	Rain_B	Light_A	Light_B	Wind_A	Wind_B
2	25.00C	25.00C	36.00%	36.00%	Not Rainir	Not Rainir	193	204	HIGH	HIGH
3	25.00C	25.00C	35.00%	36.00%	Not Rainir	Not Rainir	191	203	HIGH	HIGH
4	25.00C	25.00C	35.00%	36.00%	Raining	Not Rainir	192	204	HIGH	HIGH
5	25.00C	25.00C	35.00%	36.00%	Not Rainir	Not Rainir	193	203	HIGH	HIGH
6	25.00C	25.00C	35.00%	36.00%	Not Rainir	Not Rainir	187	190	HIGH	HIGH
7	25.00C	25.00C	35.00%	36.00%	Not Rainir	Not Rainir	184	181	HIGH	LOW
8	25.00C	25.00C	35.00%	36.00%	Raining	Not Rainir	186	185	HIGH	HIGH
9	25.00C	25.00C	35.00%	36.00%	Not Rainir	Not Rainir	185	184	HIGH	HIGH
10	25.00C	25.00C	35.00%	36.00%	Not Rainir	Not Rainir	186	186	LOW	HIGH

This is the weather data that is collected about the 2 locations A and B in excel format. This data will then be analyzed to determine the weather.



These are qqplots of the light of location A and B simultaneously. With this we can determine the light intensity accurately for a particular location

This graph determines the overall weather of location – A & B. It maps all the factors together and plots into a single graph for prediction. (A pairwise relationship between the location’s attributes.)



Where numbers represent the temperature, humidity, wind, rain, light of A and B respectively.

Various Machine learning algorithms are applied to determine the correlation between the attributes like ART, SOM. Even analysis algorithms are used like RAINFOREST to correctly determine the climate of the location.

CONCLUSION

This work states that the accuracy can be improved even further with well-defined algorithms that can map these data. We can utilize Deep-learning to successfully do that. The data being collected is stored for later use by any other organization which can try and improve the accuracy to upto 100%.

REFERENCES:

- [1] Satoh. F, Itakura. M, "Cloud-based Infrastructure for Managing and Analyzing Environmental Resources", SRII Global Conference, pp.325- 334, 201.
- [2] Kurschl. W, Beer W, "Combining cloud computing and wireless sensor networks", International Conference on Information Integration and Web-based Applications and Services, pp.512-518, 2009.
- [3] Zhengtong. Y, Wenfeng. Z, "The research of environmental pollution examination system based on the Cloud Computing", International Conference on Communication Software and Networks, pp.514-516, 2011.
- [4] Montgomery. K, Chiang. K, "A New Paradigm for Integrated Environmental Monitoring", ACM International Conference Proceeding Series, 2010.
- [5] Wei. Q, Jin. N, Lou X, Ma. R, Xu. J, "Software design for water environment remote monitoring system based on mobile devices", Applied Mechanics and Materials, pp. 2027-2032, 2011
- [6] Kang. J. and Park S. "Integrated comfort sensing system on indoor climate" Sensors and Actuators. 2000. 302- 307.
- [7] Moghavvemi M. and Tan. S. "A reliable and economically feasible remote sensing system for temperature and relative humidity measurement". Sensors and Actuators. 2005. 181-185.
- [8] Campbell Scientific, Data loggers, Sensors and Weather stations, <http://www.campbellsci.co.uk>.
- [9] Visala, Automatic weather stations, <http://www.vaisala.com/en/products>.

[10] Prodata, Affordable automatic weather stations, <http://www.weatherstations.co.uk>.

[11] Sparks L. & Sumner G., "Microcomputer Based Weather Station Monitoring System", Journal of Microcomputer Applications, 7, pp. 233-24, 1984.

[12] Bagiorgas H.S, Margarita N. A, Patentalaki. A, Konofaos. N, Dmetrios P, Matthopoulos & Mihalakakou G., "The Design Installation and Operation of A Fully Computerised, Automatic Weather Station for High Quality Meteorological Measurements", Fresenius Environmental Bulletin, 16-8, pp.948- 962. 2007.

[13] Guo X. & Song Y., "Design of Automatic Weather Station Based on GSM Module", Int. Conf. on Computer, Mechatronics, Control and Electronic Engineering.

[14] Hettiarachchi H.A.P.K. & Fernando I.M.K., "USB Based High Speed Data Acquisition System for an Unmanned Weather Station", 2nd Int. Conf. on e-governance, 2004.

[15] Modicon Inc. Industrial Automation System, "Modicon Modbus Protocol Reference Guide-PI-MBUS-300", Rev. J, June 1996, http://www.modbustools.com/PI_MBUS_300.pdf,

IJERGS

Parametric Investigation for PP Homopolymer (1110MAS) in Plastic Injection Molding Process using Taguchi Method

Amruta Wavare^{1a}, Shahadev Ubale^{2b},

¹ Research Scholar, Department of Mechanical Engineering, MGM's Jawaharlal Nehru Engineering College, Aurangabad, India.

², Department of Mechanical Engineering, MGM's Jawaharlal Nehru Engineering College, Aurangabad, India.

^aamruta.prd15@gmail.com, ^bshahadevubale@jnec.ac.in,

ABSTRACT

This paper deals on an optimization of plastic injection molding process by the effects of processing parameters applying Taguchi methods to improve the quality of manufactured specimen. PP homopolymer 1110MAS is used as the work piece material for carrying out the experimentation to optimize the shrinkage and warpage. The specimen used were of 169*16*3.2 mm dimensions modeled in PRO/Engineer. There are five processing parameters i.e. injection pressure, melt temperature, holding pressure, injection time & cooling time. Taguchi L₁₈ orthogonal array is used to design experimentation with mixed levels of input parameters. The shrinkage and warpage was considered as the quality characteristic with the concept of "the smaller-the-better". The result of minimum shrinkage using the parameter combination of injection pressure 45 bar, Melt Temperature 175 °C, Holding pressure 30 bar, Injection time 4.2 s and cooling time 15 s is 4.133%. Whereas the result of minimum warpage using the parameter combination of injection pressure 45 bar, melt temperature 175 °C, holding pressure 30 bar, injection time 4.5 s and cooling time 20 s is 0.667 mm. It is also predicted that Taguchi method is a good method for optimization of various machining parameters as it reduces the number of experiments.

Keywords: Injection Molding, Taguchi Method, S/N Ratio, Shrinkage and Warpage.

1. INTRODUCTION

Injection molding is the most important process for manufacturing plastic parts. It is suitable for mass producing articles, since raw material can be converted into a molding by a single procedure. In most cases finishing operations are not necessary. An important advantage of injection molding is that with it we can make complex geometries in one production step in an automated process. The injection molding technique has to meet the ever increasing demand for a high quality product (in terms of both consumption properties and geometry) that is still economically priced. Injection Molding is a cyclic process for producing identical articles from a mold, and is the most widely used for polymer processing. The main advantage of this process is the capacity of repetitively fabricating parts having complex geometries at high production rates. Complexity is virtually unlimited and sizes may range from very small to very large. Most polymers may be injection molded, including thermoplastics, fiber reinforced thermo plastics, thermosetting plastics, and elastomers. Critical to the adoption of this high volume, low cost process technology is the ability to consistently produce quality parts.[1]

Taguchi method approach provides a new experimental strategy in which a modified and standardized form of design of experiment (DOE) is used. This technique helps to study effect of many factors (variables) on the desired quality characteristic most economically. By studying the effect of individual factors on the results, the best factor combination can be determined. Taguchi designs experiments using specially constructed tables known as "orthogonal array" (OA). The use of these tables makes the design of experiments very easy and consistent and it requires relatively lesser number of experimental trials to study the entire parameter space.

The experimental results are then transformed into a signal-to-noise (S/N) ratio. Usually, there are three categories of quality

characteristic in the analysis of the S/N ratio, i.e. the-lower-the-better, the-higher-the-better, and the nominal-the-better. The S/N ratio for each level of process parameters is computed based on the S/N analysis. Furthermore, a statistical analysis of variance (ANOVA) is performed to see which process parameters are statistically significant. With the S/N and ANOVA analyses, the optimal combination of the process parameters can be predicted. Finally, a confirmation experiment is conducted to verify the optimal process parameters obtained from the parameter design. Taguchi method stresses the importance of studying the response variation using the signal-to-noise (S/N) ratio, resulting in minimization of quality characteristic variation due to uncontrollable parameter.

Ozcelik et al. [2] has performed research to determine the factors i.e. melt temperature, packing pressure, cooling time and injection pressure that contribute to the mechanical properties such as elasticity module, tensile strength and tensile strain at yield, tensile strain at break, flexural modules and izod impact strength (notched) of Acrylonitrile-Butadiene-Styrene (ABS) moldings was considered. The process is performed by Taguchi's L_9 orthogonal array design was employed for the experimental plan. Signal to noise ratio for mechanical properties of ABS using the Taguchi method was calculated and effect of the parameters on mechanical properties was determined using the analysis of variance.

Ozcelik, et al. [3] has optimized the injection molding process parameters such as melt temperature and packing pressure on the mechanical strength were investigated. Mechanical properties such as tensile strength and izod impact strength (notched) of the specimens were measured by test methods. The effect of molecular orientation on the mechanical properties of the specimens was discussed by Finite Element Analysis.

Mehatand Kamaruddin [4] has optimized the injection molding process parameters such as melt temperature, packing pressure, injection time, and packing time, each at three levels, are tested to determine the optimal combination of factors and levels in the manufacturing process. This study aims to improve the mechanical properties of products made from recycled plastic by utilizing the Taguchi optimization method, instead of coupling the products with additives.

Tsai et al. [5] has performed research to determine the factors that contribute to quality characteristics chosen such as light transmission, surface waviness and surface finish. The factors that been taking into considerations includes Melt temperature, Screw speed, Injection speed, Injection pressure, packing pressure, packing time, mold temperature, cooling rate. Three different regression methods are used, namely, linear, exponential and nonlinear regression. Verification experiments are executed to examine the accuracy of the regression model for predicting quality characteristics of lenses.

Chen, et al. [6] has optimized the injection molding process parameters such as Melt temperature, Mold temperature, Inject speed, Packing pressure with the application computer-aided engineering integrating with statistical technique to reduce warpage variation depended on injection molding process parameters during production of thin-shell plastic components. For this purpose, a number of Mold-Flow analyses are carried out by utilizing the combination of process parameters based on three level of L_{18} orthogonal array table. In this study, regression models that link the controlled parameters and the targeted outputs are developed, and the identified models can be utilized to predict the warpage at various injection molding conditions.

B. Ozcelik and T. Erzurumlu [7] has performed research to determine the factors that contribute to investigate the effects of process parameters for thin shell plastic part were exploited using both design of experiment (DOE), Taguchi orthogonal array and finite element software Mold-flow (FE). The most important process parameters influencing warpage are determined using finite element analysis results based on analysis of variance (ANOVA) method. Artificial neural network (ANN) is interfaced with an

effective GA to find the minimum warpage value. Process parameters such as mold temperature, melt temperature, packing pressure, packing time, cooling time, runner type and gate location are considered as model variables.

Aashiq et al. [8] The purpose of the research is to explore the influence of different mold temperatures on the warpage & shrinkage of the injection molded component's. The simulation software MOLDEX 3D was used for this study, the simulations were done by varying different mold temperatures and their corresponding warpage & shrinkage were collected. So it is required to assure homogeneous mold wall temperature across the entire cavity during the production of injection molded parts.

Babur Ozelik [9] optimized effect of injection parameters and weld line on the mechanical properties of polypropylene (PP) moldings. Melt temperature, packing pressure and injection pressure were investigated to study their effects on the mechanical strength of specimens with/without weld lines. Taguchi's L_9 orthogonal array design was employed for the experimental plan. Signal to noise ratio for mechanical properties of PP using Taguchi method was calculated and effect of the injection parameters and weld line on mechanical properties was determined using the analysis of variance (ANOVA). Linear models were also created by using regression analysis.

Chang,et al. [10] presents a fast and effective methodology for the optimization of the injection molding process parameters of short glass fiber reinforced polycarbonate composites. Various injection molding parameters, such as filling time, melt temperature, mold temperature and ram speed were considered. The methodology combines the use of the GRA (grey relational analysis) method and a CAE Mold-flow simulation software, to simulate the injection molding process and to predict the fiber orientation. At the same time, the fiber orientation was examined by CAE simulation to forecast the shear layer thickness, and simultaneously to check the accuracy of the GRA.

M.-S. Huang and T.-Y. Lin [11] proposes an advanced searching method for setting the robust process parameters for injection molding based on the principal component analysis (PCA) and a regression model-based searching method. This method could effectively reduce the influence of environmental noise on molded parts' multi-quality characteristics in the injection molding process. The design of experiment and ANOVA methods are then used to choose the major parameters, which affect parts quality and are called as adjustment factors. Based on this mathematical model, the steepest decent method is used to search for the optimal process parameters. To verify the performance, computer simulations and experiment of the light-guided plate molding were investigated in this work.

This paper discusses the use of Taguchi method for the injection molding process of PP Homopolymer MAS1110. In this study Taguchi's L_{18} orthogonal table was applied to perform the experimentation. Five controlling factors of injection pressure, melt temperature, holding pressure, injection time & cooling time with three levels for each factor were selected. The volumetric shrinkage and warpage are selected quality objectives as response parameters. By implementing DOE method is utilized to obtain S/N ratio 'smaller is better' approach. The result of minimum shrinkage using the parameter combination of injection pressure 45 bar, melt temperature 175 C, holding pressure 30 bar, injection time 4.2 sec and cooling time 15 sec is 4.133%. Whereas the result of minimum shrinkage using the parameter combination of injection pressure 45 bar, melt temperature 175 C, holding pressure 30 bar, injection time 4.5 sec and cooling time 20 sec is 0.667 mm.

2. METHODOLOGY

The general dimensions of the specimen were 169*16*3.2 mm. The injection molding machine and material used in the experimentation adhered to the following specifications: JIT 80 T(Microprocessor Controlled Injection molding machine) at CIPET, Aurangabad and PP Homopolymer 1110MAS . The process parameters injection pressure, melt temperature, holding pressure, injection time & cooling time, are some of the most significant parameters that affect volumetric shrinkage and warpage, as shown in previous research findings.

Table 1.Physical and mechanical properties of material [CIPET, Aurangabad]

Properties	Test method	Values
Physical properties		
Melt flow index g/10 min	ASTM D 1238	11.0
Density, g/cm ³	ASTM D 1505	0.9
Mechanical Properties		
Tensile strength at yield, MPa	ASTM D 638	42
Elongation at yield, %	ASTM D 638	8
Flexural modulus, MPa	ASTM D 790	1800
Thermal properties		
Heat deflection temperature, °C	ASTM D 648	115
Vicat Softening Point, °C	ASTM D 1525	154

2.1 Range and Levels of Process Parameters

The range of processing parameters is decided by taking number of trial using same material and machine also.

Table 1: Range and levels of process parameters

Name of parameter	Notations used	Unit of parameter	Range of parameter	Levels		
				1	2	3
InjectionPressure	A	bar	45-55	45	50	-
Melt Temperature	B	°C	175-195	175	185	195
Holding pressure	C	bar	30-50	30	40	50
Injection time	D	s	40-45	4	4.2	4.5
Cooling time	E	s	15-25	15	20	25

The selection of an appropriate orthogonal array (OA) depends on the total degrees of freedom of the parameters. Degrees of freedom are defined as the number of comparisons between process parameters that need to be made to determine which level is better and specifically how much better it is. In this study, since each parameter has three levels. Basically, the degrees of freedom for the OA should be greater than or at least equal to those for the process parameters. Therefore, an L₁₈ orthogonal array with five columns and eighteen rows was appropriate and used in this study. The experimental layout for the injection molding parameters using the L₁₈ OA is shown in Table 2. Each row of this table represents an experiment with different combination of parameters and their levels. However, the sequence in which these experiments are carried is randomized.

Table 2: Taguchi L18 orthogonal array

Iteration No.	Input parameters				
	Injection Pressure (bar)	Melt Temperature (°C)	Holding pressure (bar)	Injection time (s)	Cooling time (s)
1	45	175	30	40	15
2	45	175	40	42	20
3	45	175	50	45	25
4	45	185	30	40	20
5	45	185	40	42	25
6	45	185	50	45	15
7	45	195	30	42	15
8	45	195	40	45	20
9	45	195	50	40	25
10	50	175	30	45	25
11	50	175	40	40	15
12	50	175	50	42	20
13	50	185	30	42	25
14	50	185	40	45	15
15	50	185	50	40	25
16	50	195	30	45	20
17	50	195	40	40	25
18	50	195	50	42	15

The test results were evaluated in terms of signal/noise (S/N)ratio. The S/N was calculated by smaller is better for determining effect of injection process parameters on shrinkage and warpage of the specimen. The formula for S/N ratio is as follows

Smaller- the- better -It is used where minimization of the characteristics is intended.

$$S/N = -10 \log_{10} \left[\frac{1}{n} \sum_{r=3}^n \frac{1}{y_i^2} \right] \quad (1)$$

2.3 Response Measurement

A) Shrinkage Measurement

It is the difference between the volume of mould cavity and volume of finished part divided by volume of the mould.

$$S = (V_m - V_p) / V_m \times 100$$

where, V_m is Volume of mould, V_p is Volume of specimen and S is the shrinkage.

V_m is calculated using CAD 2014 & V_p is calculated by Weight/density as density is constant (0.9g/cm^3) and weight of each specimen was taken by using Precision weighing balance AB-204-S FACT after experimentation.

B) Warpage Measurement

Warpage is a distortion where the surfaces of the molded part do not follow the intended shape of the design. The feeler gauge is used to measure the warpage. Feeler gauges usually come with many different metal blades attached. These blades are not sharp and are used to measure gap distance. As such, a feeler gauge is useful when the gap between two surfaces needs to be exact, such as when setting the gap.

3. RESULTS AND DISCUSSION

3.1 Experimental result

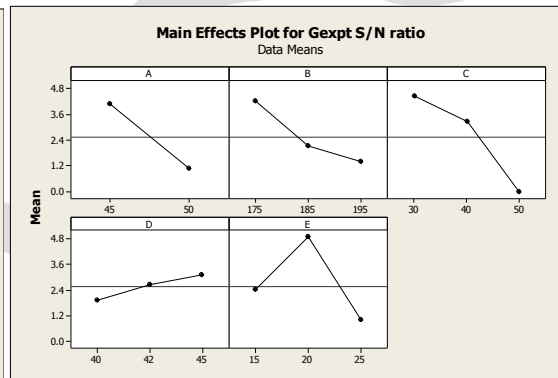
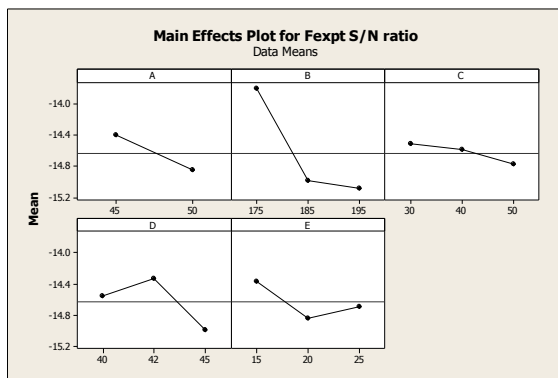


Fig. 3.1 Main Effect plot for volumetric shrinkage S/N ratio

Fig. 3.2 Main Effect plot for warpage S/N ratio

The main effect plots for S/N ratio for shrinkage (experimental) Vs each input parameter are shown in figure 3.1. In the experimental analysis of S/N ratio, factor level will be selected to give maximum S/N ratio as the most suitable factor level. The selection of the most suitable factor level from the graph found that level of factor. It shows that the appropriate set of input parameters is A1 B1 C1 D2 E1 to minimize the volumetric shrinkage from conducting 18 number of experiments parameters namely Injection pressure (A), melt temperature (B), Holding pressure (C), Injection time (D) and cooling time (E). The effect of input parameters on the warpage shown above figure 3.2 for S/N ratio. The main effect plots for S/N ratio for warpage (experimental) Vs each input parameter are shown in figure. It shows that the appropriate set of input parameters is A1 B1 C1 D3 E2 to minimize the volumetric shrinkage from conducting 18 number of experiments parameters namely Injection pressure (A), melt temperature (B), Holding pressure (C), Injection time (D) and cooling time (E).

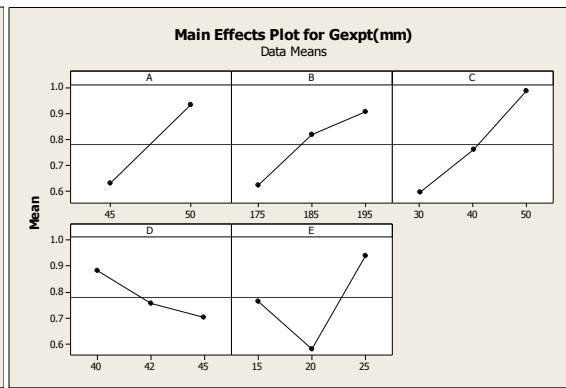
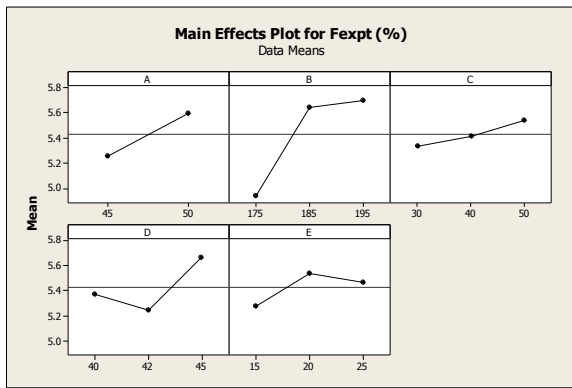


Fig. 3.3 Main Effect plot for Volumetric shrinkage

Fig. 3.4 Main effect plot for warpage

The main effect plots for shrinkage (experimental) Vs each input parameter are shown in figure 3.3. In the experimental analysis of main effect plot, factor level will be selected to give minimum main effect as the most suitable factor level. The selection of the most suitable factor level from the graph found that level of factor which shows that the appropriate set of input parameters is A₁ B₁ C₁ D₂ E₁ to minimize the volumetric shrinkage from conducting 18 number of experiments parameters namely Injection pressure (A), melt temperature (B), Holding pressure (C), Injection time (D) and cooling time(E).

The main effect plots for warpage (experimental) Vs each input parameter are shown in figure 3.4. It shows that the appropriate set of input parameters is A₁ B₁ C₁ D₃ E₂ to minimize the warpage from conducting 18 number of experiments parameters namely Injection pressure (A), melt temperature (B), Holding pressure (C), Injection time (D) and cooling time(E).

4. CONFIRMATION TEST

The purpose of confirmation experiment is to validate the conclusions drawn during the analysis phase. After determining the optimal level of process parameters, a new experiment is designed and conducted with optimum levels of plastic injection molding process parameters.

At the end we get the appropriate set of input parameters from experimentation result was A₁ B₁ C₁ D₂ E₁ to minimize the shrinkage. Whereas we get the appropriate set of input parameters from experimentation result is A₁ B₁ C₁ D₃ E₂ to minimize the warpage.

The confirmation test was conducted for the appropriate set of input parameters i.e for shrinkage it is A₁ B₁ C₁ D₂ E₁ and for warpage it is A₁ B₁ C₁ D₃ E₂.

Table 4.1 Confirmation test for volumetric shrinkage

Iteration No.	A	B	C	D	E	Fexpt
1	45	175	30	4.2	15	4.133

Table 4.2 Confirmation test for warpage

Iteration No.	A	B	C	D	E	Gexpt
1	45	175	30	4.5	20	0.667

The confirmatory experiments were performed using the optimal values and it was found that the experimental values were close enough to the required values. These values gives the reduction in volumetric shrinkage of 3.75 % and for warpage is of 2.54 %. The percentage reduction of response parameters shows that the optimized set of input parameters for plastic injection molding is good enough for minimizing the volumetric shrinkage and warpage also.

5. CONCLUSION

In this work, the experimental investigations has been reported for optimization of parameters influencing the volumetric shrinkage and warpage in plastic injection molding process. The report focuses on the optimization related to parameters of plastic injection molding process using experimentation analysis tool. Taguchi orthogonal array, S/N ratio and ANOVA method are very powerful tools to minimize volumetric shrinkage and warpage and can be successfully employed to improve injection molding of other plastic parts with complex geometry. Based on the results of the experimental analysis carried out, the following general conclusions were drawn

1. The melt temperature was the most influencing parameter followed by injection time, injection pressure, cooling time and holding pressure in sequence for controlling the volumetric shrinkage.
2. The cooling time was the most influencing parameter followed by holding pressure, injection pressure, melt temperature and injection time in sequence for controlling the warpage.
3. The optimal set for minimizing the volumetric shrinkage was of injection pressure 45 bar, Melt Temperature 175 °C, Holding pressure 30 bar, Injection time 4.2 s and cooling time 15 s.
4. The optimal set for minimizing the warpage was injection pressure 45 bar, melt temperature 175 °C, holding pressure 30 bar, injection time 4.5 s and cooling time 20 s.
5. Using the optimal set the volumetric shrinkage reduces to 3.75 % which the least than experimental values.
6. Using the optimal set the warpage reduces to 2.54 %.which the least than experimental values..

REFERENCES:

1. M. V. Kavade and S. D. Kadam "Parameter Optimization of Injection Molding of Polypropylene by using Taguchi Methodology", IOSR Journal of Mechanical and Civil Engineering (IOSR-JMCE) ISSN: 2278-1684 Volume 4, Issue 4PP 49-58, Nov. - Dec. 2012.
2. Babur Ozcelik, Alper Ozbay, Erhan Demirbas "Influence of injection parameters and mould materials on mechanical properties of ABS in plastic injection molding" International Communications in Heat and Mass Transfer, 37 1359–1365, 2010.

3. Babur Ozcelik, Emel Kuram, M. Mustafa Topal “Investigation the effects of obstacle geometries and injection molding parameters on weld line strength using experimental and finite element methods in plastic injection molding” International Communications in Heat and Mass Transfer, 39 275–281, 2012.
4. Nik Mizamzul Mehat, Shahrul Kamaruddin “Optimization of mechanical properties of recycled plastic products via optimal processing parameters using the Taguchi method” Journal of Materials Processing Technology 211 1989– 1994, 2011
5. Kuo-Ming Tsai, Chung-Yu Hsieh, Wei-Chun Lo “A study of the effects of process parameters for injection molding on surface quality of optical lenses” journal of materials processing technology 2 0 9 3469–3477, 2 0 0 9
6. Wen-Chin Chen, Gong-Loung Fu, Pei-Hao Tai, Wei-Jaw Deng “Process parameter optimization for MIMO plastic injection molding via soft computing” Expert Systems with Applications 36 1114–1122, 2009
7. B. Ozcelik, T. Erzurumlu “Comparison of the warpage optimization in the plastic injection molding using ANOVA, neural network model and genetic algorithm” Journal of Materials Processing Technology 171 437–445, 2006.
8. Tolga Bozdana, O mer Eycercoglu “Development of an expert system for the determination of injection molding parameters of thermoplastic materials: EX-PIMM” Journal of Materials Processing Technology 128 113–122, 2002.
9. Mohammad Aashiq, Arun A.P, Parthiban “Investigation of process parameters for an Injection molding component for warpage and Shrinkage” International Journal of Engineering Trends and Technology (IJETT) - Volume4Issue4- ISSN: 2231, April 2013.
10. Babur Ozcelik “Optimization of injection parameters for mechanical properties of specimens with weld line of polypropylene using Taguchi method” International Communications in Heat and Mass Transfer 38 1067–1072, 2011.
11. Shih-Hsing Chang, Jiun-Ren Hwang, Ji-Liang Doong “Optimization of the injection molding process of short glass fiber reinforced polycarbonate composites using grey relational analysis” Journal of Materials Processing Technology 97 186-193, 2000

Phase Change Materials

A. S. Anusha

UG Student, Dept. of Chemical Engineering, Chaitanya Bharathi Institute of Technology, Hyderabad, India,
Contact: +919603435334 e-mail: anusha_addanki@yahoo.co.in

Abstract— Phase Change Materials (PCMs) are the substances that have a high capacity to store and release a large amount of energy in the form of latent heat during change of phase. In fact, PCMs are also known as latent heat storage units. When a substance changes its phase (physical state), energy radiations are absorbed/emitted while its temperature is maintained constant. The latent heat could be put into use. In the current scenario of energy crisis, besides hunting for alternative sources of energy, it is also important to use the available energy resources efficiently. With a broad spectrum of applications in thermal energy storage, minimized fuel consumption, waste heat recovery, cooling machines and computers, space crafts' thermal systems and many more industrial requirements, PCMs pave way to efficient energy management systems. Further research and development would enhance its commercial value. This study elaborates the working principle of PCMs, their classification, parameters that should be verified while selecting a PCM and other techno-economical aspects besides highlighting the merits of their applications in various fields.

Keywords— phase change materials, change of phase, latent heat storage, efficient energy management, thermal energy storage, applications

INTRODUCTION

With the current scenario of increasing energy requirement, shortage of energy resources, there arises a need to use the existing energy resources efficiently besides searching for new sources of energy. This could be accomplished by using phase change materials (PCMs). These are the materials that are mainly used to store thermal energy during the change of phase, usually from solid phase to liquid phase.

OBJECTIVE

The primary concern behind this study is to put into use the latent heat that is absorbed or released during the change of phase of a substance. The substances with high capacity to store and release this latent heat are termed as phase change materials.

PHASE CHANGE MATERIALS

Phase Change Materials (PCMs) are the substances that have a high capacity to store and release a large amount of energy in the form of latent heat during change of phase. They are also known as latent heat storage (LHS) units. ^[6]

Characteristics:

PCMs latent heat storage can be achieved through solid–solid, solid–liquid, solid–gas and liquid–gas phase change. However, the only phase change used for PCMs is the solid–liquid change. Liquid–gas phase changes are not practical for use as thermal storage due to the large volumes or high pressures required to store the materials when in their gas phase. Liquid–gas transitions do have a higher heat of transformation than solid–liquid transitions. Solid–solid phase changes are typically very slow and have a rather low heat of transformation.

Initially, the solid–liquid PCMs behave like sensible heat storage (SHS) materials; their temperature rises as they absorb heat. Unlike conventional SHS, however, when PCMs reach the temperature at which they change phase (their melting temperature) they absorb large amounts of heat at an almost constant temperature. The PCM continues to absorb heat without a significant rise in temperature until all the material is transformed to the liquid phase. ^[7] When the ambient temperature around a liquid material falls, the PCM solidifies, releasing its stored latent heat. A large number of PCMs are available in any required temperature range from –5 up to 190°C. Within the human comfort range of 20°C to 30°C, some PCMs are very effective. They store 5 to 14 times more heat per unit volume than conventional storage materials such as water, masonry or rock.

As one of the goals of latent energy storage is to achieve a high storage density in a relatively small volume, PCMs should have a high melting enthalpy [kJ/kg] and a high density [kg/m³], i.e. a high volumetric melting enthalpy [kJ/m³]. Paraffins have an excellent stability concerning the thermal cycling, i.e. a very high number of phase changes can be performed without a change of the material's characteristics. On the other hand they are flammable and their melting enthalpy and density is relatively low compared to salt hydrates. The problem with salt hydrates is their corrosiveness and the cycling stability, which can often only be guaranteed if certain conditions are met. Another disadvantage of salt hydrates is the so called subcooling. That means that the material does not crystallize at the melting temperature but at a temperature that can be much lower. The subcooling can be reduced by adding so called nucleators into the material.

Figure 1 represents the plot of temperature versus stored heat for an ordinary substance while figure 2 shows the plot of temperature versus heat absorbed when a PCM is used. We can significantly note from these two plots how PCMs can be effective in heat energy storage and temperature control. ^[8]

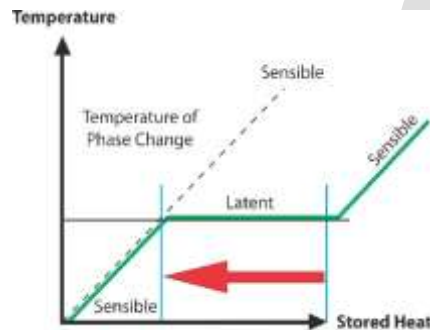


Figure 8

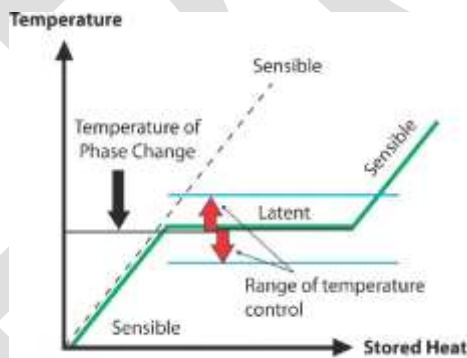


Figure 9

CLASSIFICATION

PCMs are broadly classified as follows ^[9]

Organic PCMs

Organic PCMs are naturally existing petroleum bi-products that have their unique phase-change temperature. These include paraffins and fatty acids. Paraffin (C_nH_{2n+2}) and fatty acids ($CH_3(CH_2)_{2n}COOH$) They are chemically and thermally stable. They have little or no subcooling. They are not corrosive in nature and can be applied comfortably. Yet, they pose certain challenges too. They are flammable in nature. Hence domestically PCMs must be protected with a layer that protects from fire accidents. Organic PCMs have lower melting enthalpy and also have a low density.

Examples of organic PCMs include lauric acid, paraffin wax.

Inorganic PCMs

Inorganic PCMs are engineered hydrated salt solution made from natural salts with water. The chemical composition of salts is varied in the mixture to achieve required phase-change temperature. Special nucleating agents are added to the mixture to minimize phase-change salt separation and to minimize super cooling, that are otherwise characteristic of hydrated salt PCM. They include Salt

hydrates (M_nH_2O). They have high density and have a high melting enthalpy. Hence they have a broad spectrum of applications. Subcooling of inorganic PCMs poses a challenge to their applications. It means that as the substance melts, subsequently another part of the substance solidifies and makes the effect unevenly spread. Besides, they have poor stability. They are corrosive in nature. Hence, corrosion resistant coatings must be given before they are applied.

Examples of inorganic PCMs are calcium-chloride hexahydrate, sodium acetate trihydrate.

Eutectic mixture

A eutectic system is a mixture of chemical compounds or elements that have a single chemical composition that solidifies at a lower temperature than any other composition made up of the same ingredients. This composition is known as the eutectic composition and the temperature at which it solidifies is known as the eutectic temperature. Eutectics may be a combination of Organic-organic, organic-inorganic, inorganic-inorganic compounds.

Example of a eutectic mixture is Water and Ethylene Glycol. Combination of a hydrated salt and water can also form an effective eutectic system.

THERMOPHYSICAL PROPERTIES OF SELECTED PCMS^[1]

Material	Type	Melting point (°C)	Heat of fusion (kJ/kg)	Cost (US\$)
Lauric acid	Organic	44.2	211.6	1.6
Sodium sulfate ($Na_2SO_4 \cdot 10H_2O$)	Inorganic	32.4	252	0.05
Trimethylo-ethane	Organic	29.8	218.0	
Water	Inorganic	0	333.6	0.003

Table 1

Thermal composites

Thermal-composites is a term given to combinations of phase change materials (PCMs) and other (usually solid) structures. A simple example is a copper-mesh immersed in a paraffin-wax. The copper-mesh within paraffin-wax can be considered a composite material, dubbed a thermal-composite. Such hybrid materials are created to achieve specific overall or bulk properties.^[11]

In this case the basic idea is to increase thermal conductivity by adding a highly conducting solid (such as the copper-mesh) into the relatively low conducting PCM thus increasing overall or bulk (thermal) conductivity. If the PCM is required to flow, the solid must be porous, such as a mesh.^[12]

A thermal composite is not so clearly defined, but could similarly refer to a matrix (solid) and the PCM which is of course usually liquid and/or solid depending on conditions.

SELECTION CRITERIA

A material should satisfy the following criteria for being chosen as a PCM:

- *Thermodynamic properties*

The phase change material should possess the Melting temperature in the desired operating temperature range. It should possess High latent heat of fusion per unit volume and high specific heat, high density and high thermal conductivity. [3] It should undergo a congruent melting small volume changes on phase transformation and small vapour pressure at operating temperatures to reduce the containment problem.

■ **Kinetic properties**

A PCM should have High nucleation rate to avoid supercooling of the liquid phase. [5] It should possess High rate of crystal growth, so that the system can meet demands of heat recovery from the storage system.

■ **Chemical properties**

A PCM should possess the following chemical properties [6]:

- Chemical stability
- Complete reversible freeze/melt cycle
- No degradation after a large number of freeze/melt cycle
- Non-corrosiveness, non-toxic, non-flammable and non-explosive materials

■ **Economic properties**

The material being put into use as a PCM must be easily available at a low cost.

WORKING OF A PCM

Let us consider a solid PCM exposed to an environment of varying temperatures. When the temperature rises, the PCM melts and absorbs heat. When the temperature drops, the PCM solidifies, and heat is emitted. During the phase change, the temperature remains constant. Phase change materials (PCMs) therefore take their name from their mechanism of action. Owing to their unique microencapsulation technology, PCMs can be integrated invisibly into the most diverse of construction materials, thus lending them their impressive properties.

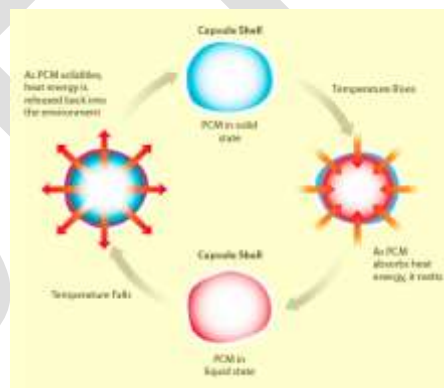


Figure 3

METHODS OF APPLICATION OF PCMs

i. **Macro encapsulation**

The PCM is encapsulated in e.g. cylindrical or spherical modules which are integrated into the storage tank. In order to ensure a good heat exchange between the surrounding heat transfer medium (water or a mixture of water and glycol in most of the cases) and the PCM, the modules should have a high ratio between surface area and volume, i.e. a high heat transfer area per volume unit. This implies that the modules should in principle be as small as possible, which is of course a matter of cost. The

advantages of this kind of integration are the possibility of a relatively simple integration of PCMs into an existing storage tank and the possibility to use PCMs with different melting points in one tank.^[10]

ii. *Microencapsulation*

Paraffins can also be micro-encapsulated with diameters of just a few μm as shown in the figure 3. Due to the small diameter the ratio of surface area to volume is very high and the low thermal conductivity is not a problem. It provides improved heat transfer between the PCM and surroundings because of increased surface area. If these microcapsules are dispersed in a fluid (mostly water), they form a pumpable slurry, that can be used as an energy transport- and storage medium, as a so-called PCM slurry. A microencapsulation of salt hydrates is not possible. Microencapsulation adds cost because it involves several chemical synthesis steps.

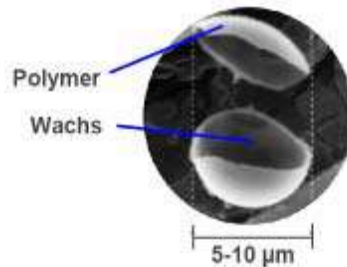


Figure 4

APPLICATIONS OF PCMs

Applications of phase change materials include, but are not limited to^[2]:

- Thermal energy storage
- Conditioning of buildings, such as 'ice-storage
- Cooling of heat and electrical engines
- Cooling: food, beverages, coffee, wine, milk products, green houses
- Medical applications: transportation of blood, operating tables, hot-cold therapies
- Waste heat recovery
- Off-peak power utilization: Heating hot water and Cooling
- Heat pump systems
- Passive storage in bioclimatic building/ architecture (HDPE, paraffin)
- Smoothing exothermic temperature peaks in chemical reactions
- Solar power plants
- Spacecraft thermal systems
- Thermal comfort in vehicles
- Thermal protection of electronic devices
- Thermal protection of food: transport, hotel trade, ice-cream, etc.
- Textiles used in clothing
- Computer cooling
- Turbine Inlet Chilling with thermal energy storage
- Telecom shelters in tropical regions. They protect the high-value equipment in the shelter by keeping the indoor air temperature below the maximum permissible by absorbing heat generated by power-hungry equipment such as a Base Station Subsystem. In case of a power failure to conventional cooling systems, PCMs minimize use of diesel generators, and this can translate into enormous savings across thousands of telecom sites in tropics.

MAJOR CHALLENGES TO PCMs

There are various challenges to PCMs which are illustrated below^[4].

- **Incongruent melting of salt hydrates.**

Many minerals do not melt uniformly. Instead they decompose as they melt. The figure 4 shows the melting pattern of water-NaCl system.

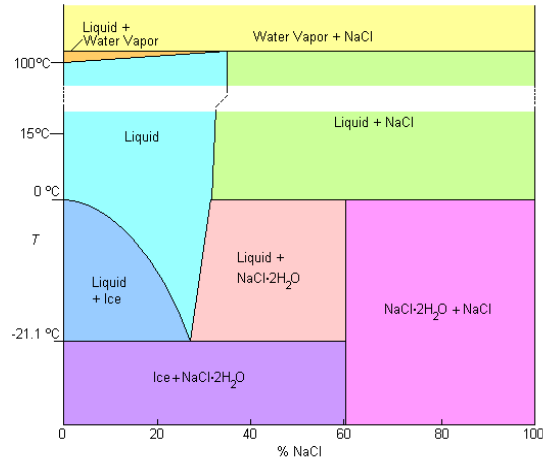


Figure 5

- **Corrosion**

Salt hydrates are corrosive in nature due to the presence of alkaline elements such as sodium, calcium, potassium, etc.



Figure 6

- **Flammability**

Organic PCMs which comprise of paraffins and fatty acids are highly flammable in nature. Application of these substances must be done with utmost care.



Figure 7

- **Expensive microencapsulation**

Microencapsulation provides improved heat transfer between the PCM and its surroundings because of increased surface area but adds cost because it involves several chemical synthesis steps. The final PCM cost varies greatly depending on the approach adopted to encapsulate the PCM.

CONCLUSION

Phase change materials provide an effective and efficient way to save energy and use the available energy efficiently. Easy availability of these materials makes their application comfortable. Depending on the field of application, a suitable PCM must be selected. Further research against unfavorable chemical properties and cost reduction would enhance their commercial value in the global market.

REFERENCES:

- [1] Belén Zalbaa, José Ma Marina, Luisa F. Cabezas, Harald Mehling, "Review on thermal energy storage with phase change materials, heat transfer analysis and applications" Applied Thermal Engineering, Volume 23, Issue 3, February 2003, Pages 251–283
- [2] Sharma, Atul; Tyagi, V.V.; Chen, C.R.; Buddhi, D. (2009). "Review on thermal energy storage with phase change materials and applications". Renewable and Sustainable Energy, Pages: 318–345,
- [3] Hawes DW, Banu D, Feldman D, 'Latent heat storage in concrete II, Solar Energy Materials', 1990, 21, p.61–80.
- [4] Pasupathy, A; Velraj, R; Seeniraj, R (2008). "Phase change material-based building architecture for thermal management in residential and commercial establishments". Pages: 39–64.
- [5] Yinping, Zhang; Yi, Jiang; Yi, Jiang (1999). "A simple method, the -history method, of determining the heat of fusion, specific heat and thermal conductivity of phase-change materials". Measurement Science and Technology 10 (3): 201–205. Bibcode:1999MeScT..10..201Y
- [6] Tammé, Rainer (February 20, 2003). "Phase Change - Storage Systems" (PDF)
- [7] Omer, A (2008). "Renewable building energy systems and passive human comfort solutions". Renewable and Sustainable Energy Reviews 12 (6): 1562–1587.
- [8] Bony, J., Ibanez, M., Puschnig, P., Citherlet, S., Cabeza, L., Heinz, A., (2005), Three different approaches to simulate PCM bulk elements in a solar storage tank, Phase Change Material and Slurry: Scientific Conference and Business Forum, 5.-17. Juni 2005, Yverdon les Bains, Schweiz, S. 99 - 107
- [9] Cabeza, L., (2005), Storage Techniques with Phase Change Materials, Thermal energy storage for solar and low energy buildings, State of the art by the IEA Solar Heating and Cooling Task 32, June 2005, Seite 77-105
- [10] A. Heinz, W. Streicher, "Application Of Phase Change Materials And Pcm-Slurries For Thermal Energy Storage", https://intraweb.stockton.edu/eyos/energy_studies/content/docs/FINAL_PAPERS/8B-4.pdf.
- [11] schoeller®-PCM - Schoeller Textiles
- [12] PCM technology - DuPont™ Energain

Fatigue life evaluation of an Automobile Front axle

Prathapa.A.P⁽¹⁾, N. G.S. Udupa⁽²⁾

¹ M.Tech Student, Mechanical Engineering, Nagarjuna College of Engineering and Technology, Bangalore, India. e-mail: prathap.ap99@gmail.com

²Professor, Mechanical Engineering, Nagarjuna College of Engineering and Technology, Bangalore, India.
e-mail:ngsudupa@gmail.com

Abstract — This paper presents the axle apart from above loads is critically subjected to cyclic and shock loads. In case of four wheelers, Six wheelers and multi axle vehicles role of frontal axle is most important since it drives the rear axle .A robust design of frontal axle involves load calculations and load considerations for four wheeler and six wheeler, Followed by preliminary and detailed design considerations .

In the light, of the above an automobile truck frontal axle is considered for the topic of research to understand its behavior to the loads during service conditions and also at off design conditions for four wheeler and also for six wheeler. The study involves load calculations for various conditions namely four wheeler, six wheeler ,gyroscopic couple ,Fatigue, dead weight and so on .Further , the work is focused on structural evaluation of front axle using FEA approach with preliminary detailed design considerations which, includes Gross weight of the vehicle ,Inertial loads, dynamic loads and Rolling resistance. Commercial FE software (ANSYS) is used to determine the structural integrity of Frontal axle.

Keywords: Front axle, Static analysis, Campbell diagram, modal analysis, FEM

I INTRODUCTION

After years of study, predictable patterns change, the car industry is in its history of product changeover among the most intense. In order to achieve the need to design a medium cars, structural engineers will need to use Rich imaginative concepts. Increase in demand in the automotive designer, Rapid changes, one must first meet the new security requirements, later reduced weight [1]. In order, to meet fuel economy requirements. Experience cannot be extended to new size and performance data of the vehicle, which does not have new standards. Therefore, mathematical modeling is a logical way to explore. Recent, Finite element methods, computer-related digital technologies have opened up the new approaches to the car sets [2].



Figure.1. Dead Front Axle Mechanism of Commercial Truck

Front axle at both ends, an intermediate portion and a circular or elliptical cross-section or I section as shown in Fig 1. Special section (- I, circular, Square) portion of the axle so that it can withstand the bending loads due to weight of the vehicle and the braking torque applied [3]. The dead weight of the vehicle is supporting the front portion of the vehicle, to facilitate the steering. Since, the assembly absorbs the impact transmitted to the irregularities of the road surface and also absorbs torque exerted thereon, due to the braking of the vehicle. Wheel is mounted on the minor axis. Front axle beam quality due to the bending load due to the presence of the vertical force under static conditions of the vehicle, while driving around a corner of the truck a plurality of power leads, e.g., the axial force or torsional force knuckle kingpin, between the pad spring Along the beam and asymmetric length of the interface due to the

centrifugal effect of the vertical load. And turning the truck is braked to stop turning the torque pad and a sporty vehicle deceleration force on the surface of the pad caused the worst situation [5]. The project work on a comprehensive understanding of stress automobile front axle, the strain distribution and the different varieties of conditions to simulate the vibration frequency, and the theoretical basis of scientific designers to improve design quality and shorten the design cycle and reduce design costs [6].

II METHODOLOGY

First and foremost step for the design of the chassis is to find the boundary condition and the placing of the components. The Ergonomics is considered first and according to the ergonomics, the frontal part is constructed. The suspension pick up points are major consideration which can pull off or push off the chassis in the lateral direction during corner entry. A multi axle suspension reduces the sprung mass and hence a distribution of the forces in the unsprung mass. Chassis is to be decided based on the track width and wheelbase dimensions. But the relation between them are profoundly complicated, but few of them can be realized very easily, few of them are listed are below.

A long wheel base should have more stability during braking, and if its polar moment of inertia is not so high, should produce more yaw moment in the corners entry. On the other hand, in slow corners it should have more “under steering tendency” asking for more steering angle and should be less agile.

A wide track will produce less weight transfer and so should give a higher cornering grip potential, but the vehicle will tend to follow wider lines on the track and to have, for example, bigger frontal area.

A wheel base of 3200mm and track width of 1700 is taken with the wheel base to track width ratio of 2. Stability doesn't only depend on these two but also depends on the height of the vehicle. The total height of vehicle is should be designed for the golden ratio of 1.6 has to be achieved without which straight line stability cannot be achieved.

III. CAD AND FEM DESCRIPTION

THE 3D CAD MODEL OF THE FRONTAL DEAD AXLE OF A COMMERCIAL TRUCK IS MODELED USING CATIA V5 R17 SOFTWARE.

The design procedure may vary from Designer to designer. The procedure I followed are listed below.

The idea was to exploit the symmetry of the model, hence only half model is created by creating the base half I section. The end of the I section is modeled with the circular cross section to hold. A spline is created From the cylinder edge which follows the I section. The extended part is now fitted with the Cylinder for the holding; A rectangular pattern of hole is made to accommodate the drill in the model. Now the whole model is created by the symmetry in the y axis.

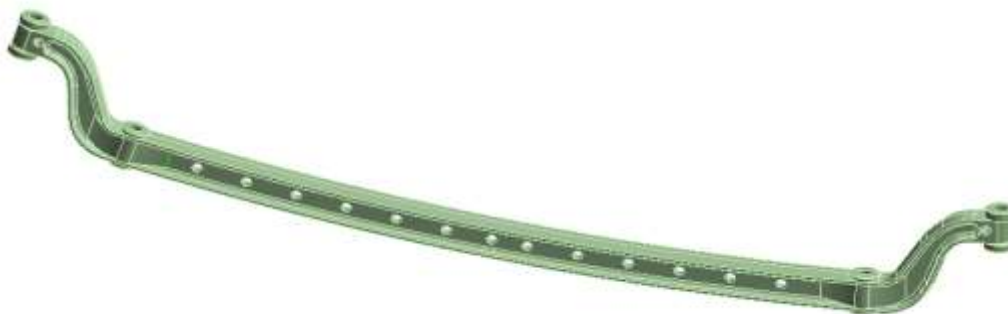


Figure.2. Solid Front Axle Beam

IV.MATERIAL PROPERTIES

The axle material is considered to be ANSI 4340 steel and its mechanical properties are as below:

Table 1: ANSI 4340 Steel mechanical properties for Axle.

Sl.No.	Specification	Value
1.	Density	7.7 - 8.03 gm/cc
2.	Poisson's ratio	0.27-0.30
3.	Elastic Modulus	190-210 Mpa
4.	Tensile Strength	744.6 Mpa
5.	Yield Strength	472.3 Mpa
6.	Elongation	22.0 %
7.	Reduction in Area	49.9 %

V BOUNDARY CONDITIONS

Analysis of Gyroscopic effect on the axle in six wheeler vehicle.

TPYE 1

Boundary conditions applied on the frontal axle when it has Gyroscopic effect, i.e; reaction forces as remote forces acting vertically downwards at king pin and fixed forces where the axle is connected to wheels.

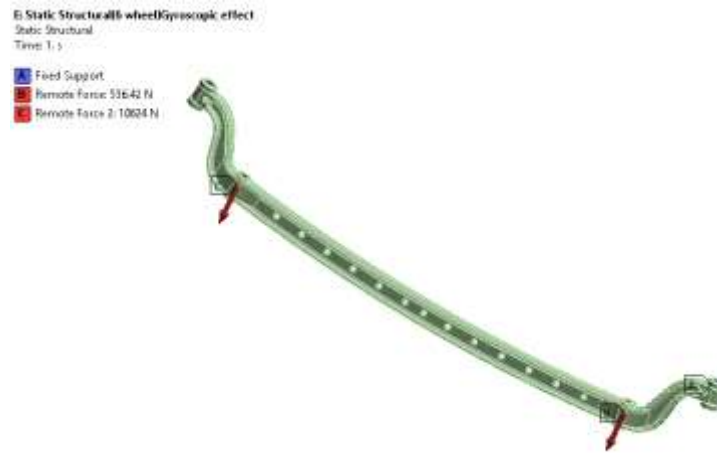


Figure.3. Boundary conditions due to gyroscopic effect

Analysis of Gyroscopic effect on the axle in four wheeler vehicle.

TYPE 2

Boundary conditions applied on the frontal axle when it has gyroscopic effect, i.e.; reaction forces as remote forces acting vertically downwards at king pin and fixed forces where the axle is connected to wheels. Analysis of Gyroscopic effect on the axle in four wheeler vehicle

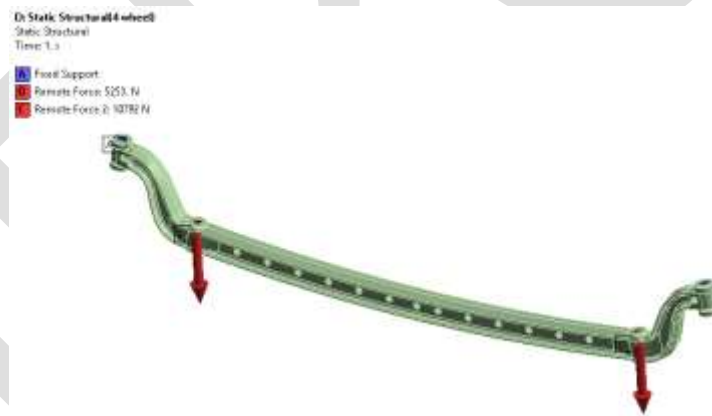


Figure.4. Boundary conditions due to gyroscopic effect

Mesh generation for 3D Model

The Model of the front axle is imported to ANSYS and ideal model is generated using Finite element modelling technique of ANSYS Software. The geometry imported is a 3D model which is meshed considering the SOLID 186 which is dominant, Wherever 186 is not possible SOLID 187 is considered.



Figure.5.Finite element model of Front axle beam

It is very important to consider the type of element using in the analysis. It is seen that the stiffness matrix and interpolating function (Shape function) is different for different elements. The change in the stiffness matrix is due to the degree of freedom of the element, order of the polynomial used for the interpolation function and the type of load that the element can take.

VI. RESULTS AND DISCUSSION

Analysis results of entire axle in four wheeler truck

Von- Mises Stress distribution

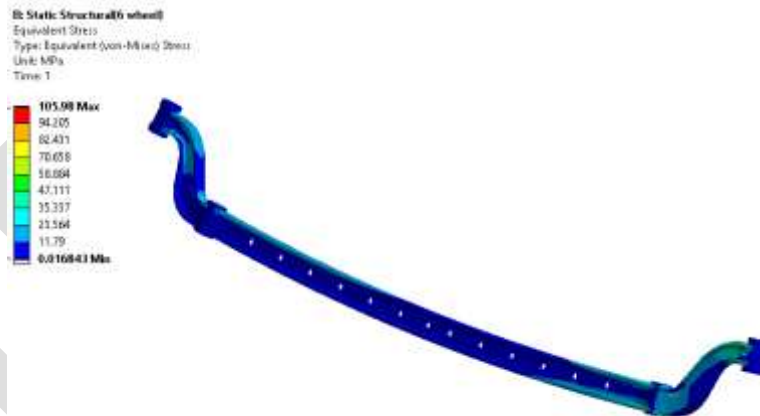


Figure.7. Von mises stress distribution for W_1 and W_2

It is observed that maximum stress is 93.918MPa near the fillet area of the right wheel fixing end and it is less than Yield stress of the material.

Maximum Principal stress determination

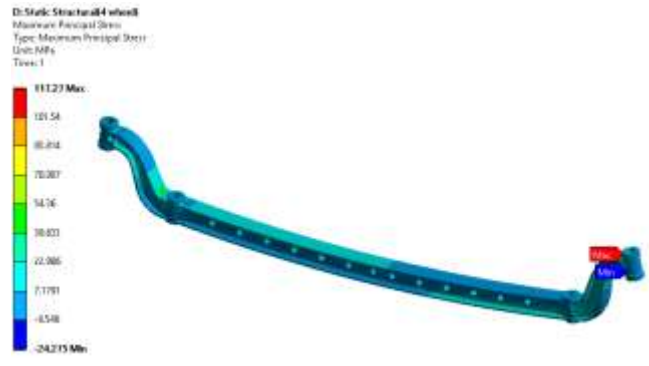


Figure.8. Maximum principal stress distribution for W_1 and W_2

It is observed that maximum stress is 117.27Mpa near the top surface of the right wheel fixing end.

Minimum Principal Stress determination

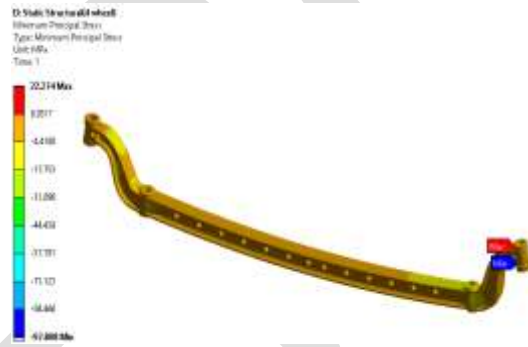


Figure.9. Minimum Principle stress

Maximum Principal Elastic Strain

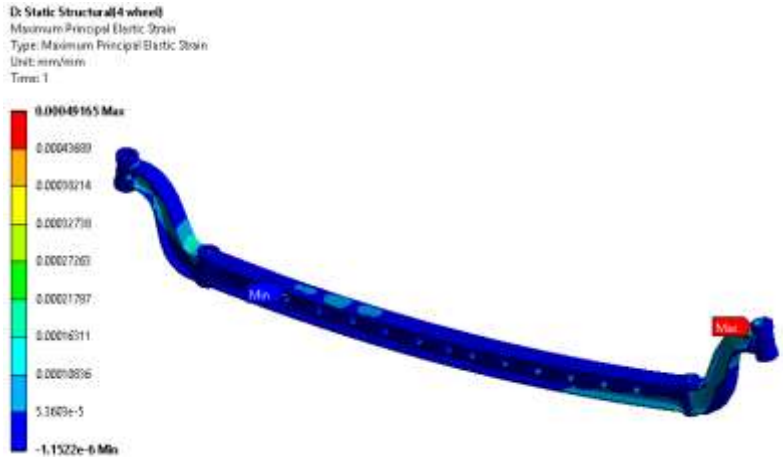


Figure.10.Maximum equivalent strain

Table: 1 Compilation of Results with Gyroscopic effect in 4 wheeler vehicle

Sl.No.	Parameter	Value (Max)
1.	Von Mises Stress	93.918MPa
2.	Maximum Principal stress	117.27MPa
3.	Minimum Principal stress	22.274MPa
4.	Maximum elastic strain	0.0004916

Analysis of Gyroscopic effect on the axle in six wheeler vehicle :

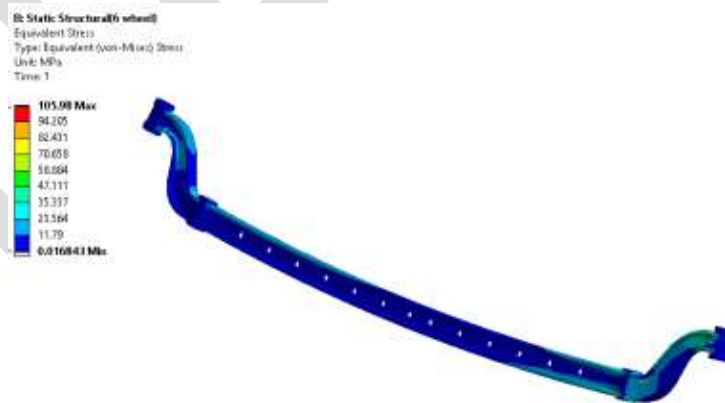


Figure.11. Von mises stress distribution for W_1 and W_2

It is observed that maximum stress is 106.86Mpa near the fillet area of the left wheel fixing end and it is less than Yield stress of the material.

Maximum Principal stress determination

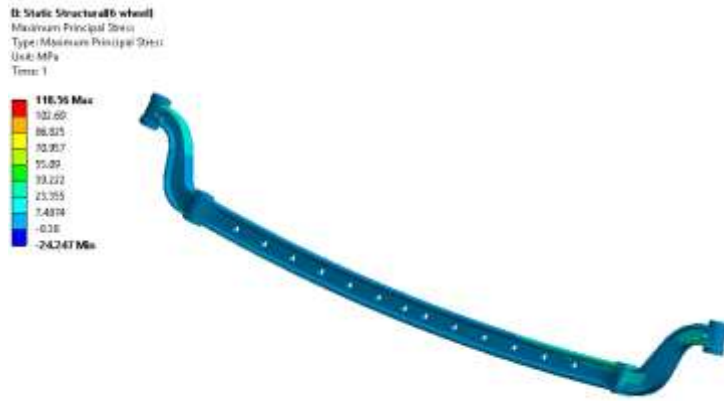


Figure.12. Maximum principal stress distribution for W₁ and W₂

It is observed that maximum stress is 132.81Mpa near the top surface of the left wheel fixing end.

Minimum Principal stress determination.

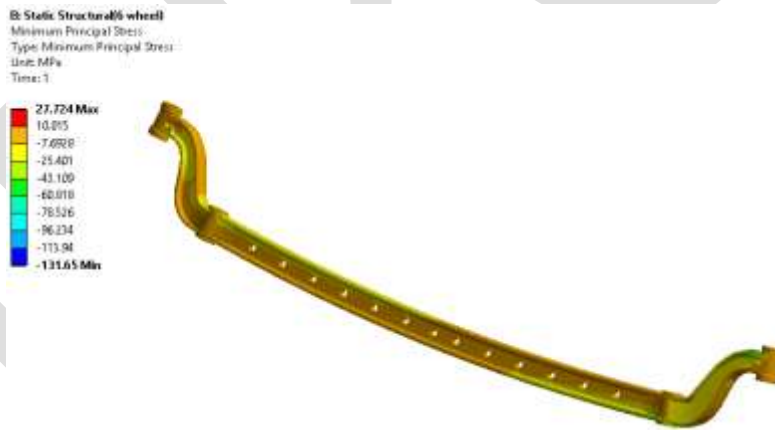


Figure.13. Minimum Principle stress

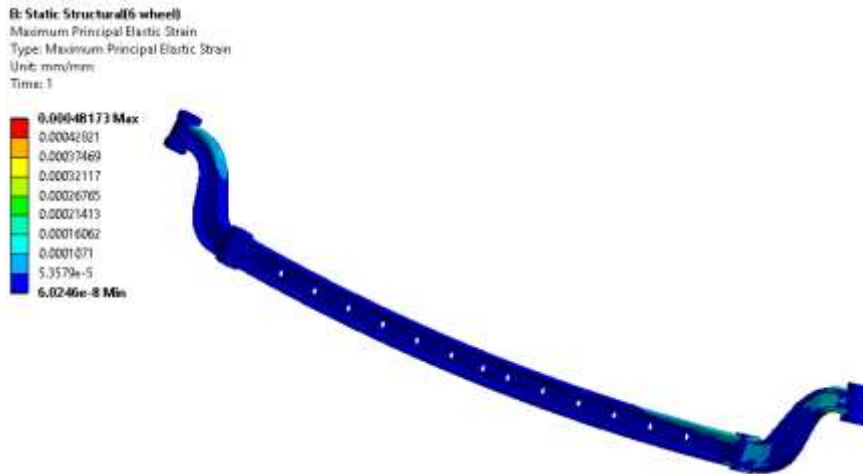


Figure.14. Maximum equivalent strain

Table 2: Compilation of Results with Gyroscopic effect

Sl.No.	Parameter	Value (Max)
1.	Von Mises Stress	105.98MPa
2.	Maximum Principal stress	118.56MPa
3.	Minimum Principal stress	27.724MPa
4.	Maximum elastic strain	0.000481

Fully reversed Cycle:

The cycle consists of the reversal of the load with the scale factor of 1. This fully reversed cycle is used for the analysis purpose.

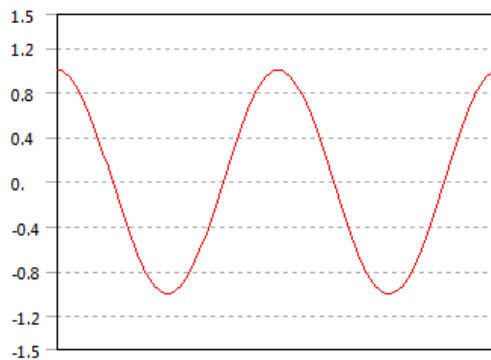


Figure.15. Fully reversed cycle

Life of the component:

Life of the components are always decided by the number of startup and shut down cycles required for the component to initiate crack. The start-up and shown down cycle is shown in the picture.

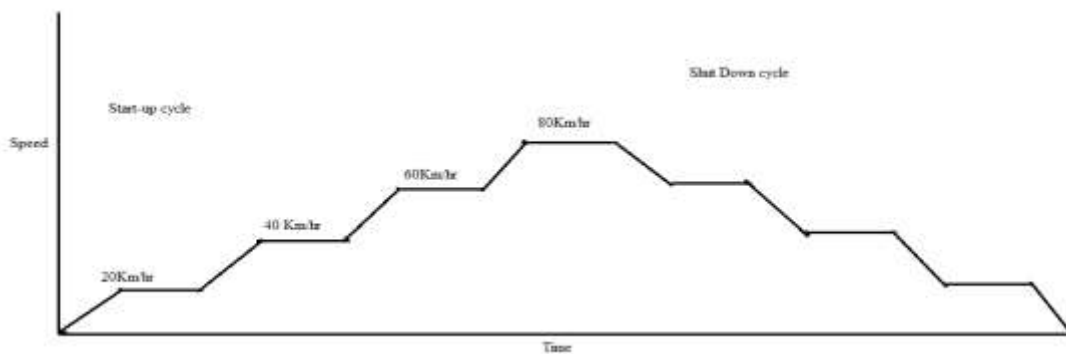


Figure.16. Start up and S`hut down cycle

CONCLUSION:

As the maximum principle stress increases beyond the yield limit, the crack initiation begin to happen as the maximum principle stress acts as tension in the material and shear stresses are completely absent in the material. Minimum principle stress always tends towards zero and doesn't create any serious deformations. Middle principle stress is compressive in nature; it tries to close the crack. If the middle principle is 68% of the yield, then the tensile force cannot open the crack up and the failure is 4 in million as per six sigma standard.

In this case equivalent stress plays a major role and acts as the decision maker. Equivalent stress is the deviatory stress of all the combined effect of stress derived from the strain energy theory is calculated and found to be well within the range.

REFERENCES:

- [1] Kalpan Desai, et al., "Bending stress analysis of rear axle of Maruti-800car", International journal of engineering research and technology ISSN: 2278-0181, volume1, Issue6, August 2012.
- [2] Anupam Singhal, et al., "Failure analysis of automotive FWD flexible driveshaft- A review", International journal of engineering research and applications, ISSN: 2248-9622, volume3, Issue1, Jan - Feb 2013, pp.577-580.
- [3] C Kendall Clarke, et al., "Failure analysis of induction hardened automotive axles", ASM International, 16 May 2008.
- [4] Ji-xin Wang, et al., "Static and dynamic strength analysis on rear axle of small payload off - highway dump trucks", Jilin University, Changchun130025, PR China, volume8, pp.79-86, 2012.
- [5] Lawrence Kashar, "Effect of strain rate on the failure mode of a rear axle", ASM International, volume1, pp. 74-78, 1992.
- [6] Mulani, et al., "FEA analysis of bullock cart axle under static and dynamic condition", International journal of engineering research and technology ISSN: 2321-5747, volume1, Issue2, 2013.
- [7] JavadTarighi, et al., "Static and dynamic analysis of front axle housing of tractor using finite element Methods", Australian journal of agricultural engineering, volume2, pp.45-49, 2011.
- [8] G Rajesh Babu, et al., "Static and modal analysis of rear axle housing of a truck", International journal of mathematical sciences, technology and humanities, volume7, pp.69-76, 2011.

A Real Key Exchange through Set of Rules for Parallel Network File System

¹Dhayalan.D, ²Prabhu.M, ³Rajesh.M, ⁴Prabhakaran.S

¹Assistant Professor, ²PG Scholar, ³PG Scholar, ⁴PG Scholar

Dhayalan@velhightech.com, 9444461494

Department of MCA,

Vel tech high tech Dr.Rangarajan Dr.sakunthala engineering college,

Chennai -62

Abstract: We tend to study the matter of key generation for secure several to several communications. The matter is raised by the proliferation of enormous scale distributed file system supporting parallel access to multiple storage devices. Our work focuses on current web standards for such file systems, i.e. the parallel Network filing system (pNFS) what makes use of Kerberos to determine parallel session keys between consumer and storage devices. Our review of the prevailing Kerberos-based protocol includes a variety of limitations (i) a information server facilitating key exchange between shoppers and storage devices has serious employment which restricts the quantifiability of the protocol (ii) The protocol doesn't give forward secrecy;(iii) information server establish itself all the session keys that area unit used between the shoppers and storage devices and this inherently leads to the key written agreement. During this paper, we tend to propose a spread of genuine key exchange protocols that area unit designed to address on top of problems. We tend to show that our protocols area unit capable of reducing up to more or less fifty four of employment of a information server and at the same time supporting forward secrecy and escrow-freeness.

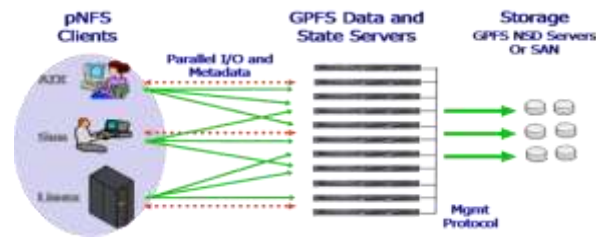
Keywords -- Parallel sessions, Authenticated Exchange, Network file systems, forward secrecy, key escrow.

INTRODUCTION

In a similar classification system, file data is spread across manifold storage devices or nodes to allow coincidental right of entry by manifold tasks of an identical submission. This is often characteristically second-hand in major cluster computing that spotlights on so much on high of the position arrangement and trustworthy admission to nice datasets. That is, superior I/O information measure is accomplished from finish to finish coincidental right of entry to various storage devices within nice calculate clusters, at identical time as data beating is secure through data mirror by suggests that of responsibility broad minded marking algorithms.

A number of instances of so much higher than the bottom presentation equivalent file systems that area unit in manufacture use area unit the IBM General Parallel classification system, Google classification system, Luster, Parallel Virtual classification system, and Panasas classification system; whereas there conjointly continue living investigate comes on spread factor space for storing schemes such as Usra Minor, Ceph, Extremes, and Gfarm. These area unit additional usually than not essential for extremely developed Technicolor information targeted submissions like, seismal processing, digital animation studios, machine fluid dynamics, and semiconductor producing. In these surroundings, a whole lot or thousands of classification system purchasers share information and manufacture extraordinarily elevated collective I/O freight on the classification system at very cheap of peta computer memory unit or T balance storageability.

Our most vital objective during this vocation is to set up well-organized and guarded real key swap over procedures that get along unambiguous requirements of PNFS. Preponderantly, we have a tendency to challenge to induce along the next advantageous possessions, that what is more haven't been adequately accomplished or aren't get able by this Kerberos primarily based solution.



Our goal is to leverage PNFS and GPFS to create the quickest and most ascendible NAS system within the world. The nodes within the GPFS cluster chosen for PNFS access website. Information about final paper submission is available from the conference website.

SECURITY

Previous descriptions of NFS listening fastidiously on straightforwardness and ability, and were supposed to employment well

on intranets and restricted networks. Afterward, the subsequently versions plan to urge higher access and presentation at intervals the Internet surroundings. However, obligation has then become a larger concern. Among several alternative sanctuary problems, user and server authentication at intervals associate open, dispersed, and cross-domain surroundings area unit a tough matter. Key management may be tedious and opulent, however a crucial facet in making certain security of the system.

Moreover, knowledge time alone could also be important in high performance and parallel applications, as an example, persons related to medicine in sequence sharing, monetary knowledge processing and analysis and drug simulation & discovery. Hence, distributed storage devices cause larger risks to varied security threats, like misappropriated modification or stealing of knowledge residing on the storage devices, still as interception of knowledge in transit between completely different nodes at intervals the system. NFS (since version 4), therefore, has been mandating that implementations support end-to-end authentication, wherever a user (through a client) mutually authenticates to associate NFS server. Moreover, thought ought to be to the integrity and privacy (confidentiality) of NFS requests and responses. The RPCSEC GSS framework is presently the core security element of NFS that gives basic security services. RPCSEC GSS permits RPC protocols to access the Generic Security Services Application Programming Interface (GSS-API). The latter is employed to facilitate exchange of credentials between native and remote human activity parties, for example between a consumer and a server, so as to determine a security context.

The GSS-API achieves these through associate interface and a collection of generic functions that area unit freelance of the underlying security mechanisms and communication protocols used by the human activity parties. Hence, with RPCSEC GSS, varied security mechanisms or protocols may be used to produce services like, encrypting NFS traffic and playing integrity check on the entire body of associate NFSv4 decision. Similarly, in pNFS, communication between the consumer and therefore the information server area unit authenticated and guarded through RPCSEC GSS.

The information server grants access permissions (to storage devices) to the client per pre-define access management lists (ACLs). The client's I/O request to a device should embrace the corresponding valid layout. Otherwise, the I/O request is rejected.

In associate surroundings wherever eavesdropping on the communication between the consumer and therefore the device is of sufficient concern, RPCSEC GSS is employed to produce privacy protection.

A.ParallelSessions

Parallel secure sessions between the shoppers and also the storage devices within the parallel Network classification system (PNFS). This Internet standard in associate economical and scalable manner. This can be just like matters that then the antagonist compromises the long-term secret key, it will learn all the subsequence sessions. If associate honest shopper associated an honest device complete matching sessions, they reason anequivalent sessionkey.Second, 2 our protocols offer forward secrecy: one is partly forward securing with relevance multiple sessions inside a period of time.

B. Authenticated Key Exchange

Our primary goal during this work is to style economical and secure genuine key exchange protocols that meet specific requirements of PNFS. The most results of this paper area unit 3 new incontrovertibly secure genuine key exchange protocols. We describe our style goals and provides some intuition of a spread of PNFS genuine key exchange6 (PNFS-AKE) protocols that we take into account during this work.

C. Forward Secrecy

The protocol ought to guarantee the protection of past session keys once the long secret key of a consumer or a memory device is compromised. However, the protocol doesn't offer any forward secrecy. To handle key written agreement whereas achieving forward secrecy at the same time, we tend to incorporate a Diffie- Hellman key agreement technique into Kerberos-like pNFS-AKE-I. However, note that we tend to bring home the bacon solely partial forward secrecy (with relevancy v), by mercantilism potency over security.

SYSTEM FLOW

We have introduced data in our work; data plays a vital role in managing the shopper operation. Metadata performs the fore most task of authentication of user. It generates One-Time-Password (OTP) to authenticate the user access. Once the user/client gets verified the data produce session key that permits user to access resources for specific amount of your time.

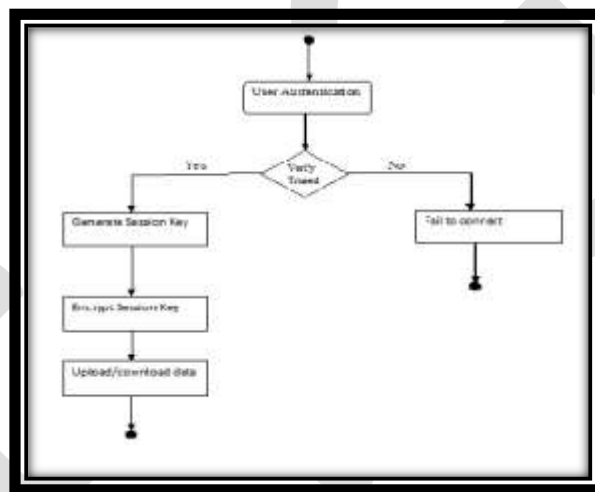


Fig. System flow diagram

3.1 Execution of System

3.1.1.Send()

Send(Ai, start);

if Active Session Index \neq zero then;
 Abort A Active session Index; come M;
Else
 passive attack index = M then;
 sent π_i p;

Return A.

3.1.2.Corrupt()

Corrupt(p);
If session Expire then;

PES SUCS;

Else come corrupt

Message.

3.1.3.Reveal()

```
reveal( $\mu_i$ );  
  proceed as follows:-  
    for instance  $\mu_i$  then;  
      return      sk;
```

3.1.4.Execute()

```
execute( $A_i, B_j$ );  
   $Sk_A \leftarrow H(A, B, k)$ ;  
   $Sk_A \leftarrow Sk_A$ ;  
  Return( $A, B$ );
```

3.1.5 Test()

```
Test( $P^*, i^*$ );  
  Instances outlined  $\pi_i p$ ,
```

wherever $P^* \in SS \cup$ atomic number 55

```
  If instance is outlined  $\pi_i p$  be session key  $Sk_i^* p^*$ ; SIM;  
  If else will  $b=1$  SIM then;  
    Return  $Sk_i^* p^*$ ;  
  Else   A;
```

3.2 Algorithmic Rule

Upon receiving associate I/O request for a file object from C, each S_i performs the following:

- 1) check if the layout σ_i is valid;
- 2) decipher the authentication token and recover key KCS_i ;
- 3) reckon keys $sk_z i = F(KCS_i; IDC, IDS_i, v, sid, z)$ for $z = zero, 1$;
- 4) decipher the encrypted message, check if IDC matches the identity of C and if t is at intervals the present validity period v;
- 5) if all previous checks pass, S_i replies C with key confirmation message victimization key $sk_0 i$.

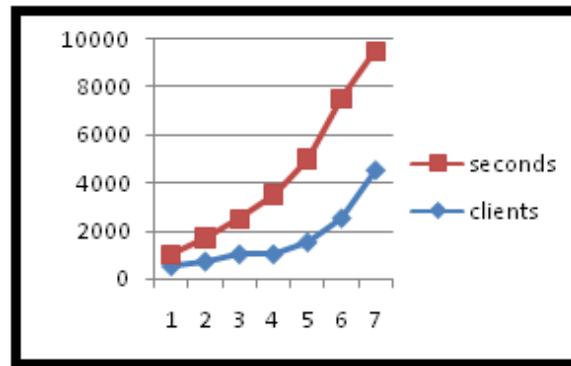


Fig. Computational overhead for sever

3.2.1 Explanation of algorithmic rule

In initiative we tend to are checking if on the market layout is valid or not for more operations and communication. In second step we tend to do the decoding operation on the token that is generated by data server for authentication method. By playacting decryption we are going to recover the key for shopper set. During this third step we are going to reckon the key for storage set for accessing the data information within the storage set. We are going to reckon key by checking the key of shopper set further as id for users. As per the result we are going to come access to user or denied to speak. Fourth step can perform the task of decoding of encrypted message. And it'll additionally check for validation for user access. During this final step if all the on top of method is successfully valid then it'll key confirmation message to User\client.

RELATED WORK

Tele-care Medical data Systems (TMIS) give effective thanks to improve the medical method between doctors, nurses and patients. By up the protection and privacy of TMIS, it's necessary whereas difficult to improve the TMIS so a patient and a doctor will perform synchronous authentication and session key establishment employing a 3-party medical server whereas the secure information of the patient maybe ensured.

In planned system an anonymous many-sided word authenticated key exchange (3PAKE) protocol for TMIS is used. The protocol is predicated on the economical ellipticcurve cryptosystem. For security, we tend to apply the pi calculus based mostly formal verification tool Prove if to indicate that our 3PAKE protocol for TMIS will give obscurity for patient and doctor moreover asachieves synchronous authentication and session key security. The advantage of planned scheme is security and potency that may be utilized in TMIS. For this J-PAKE based mostly protocols area unit used. The disadvantage of planned theme is of it reduced session keys.

Passwords area unit one amongst the foremost common causes of system crashes, as a result of the low entropy of passwords makes systems prone to brute force idea attacks. Due to new technology passwords may be hacked simply.

Automated mathematician Tests still be an efficient, easy to deploy approach to spot automatic malicious login attempts with cheap price of inconvenience to users. Hence during this planned theme the inadequacy of existing and planned login protocols designed to deal with large scale online lexicon attacks e.g. from a bonnets of hundreds of thousands of nodes. during this theme planned a simple theme that strengthens word based mostly authentication protocols and helps forestall on-line dictionary attacks also as many-to-many attacks common to 3-pass SPAKA protocols.

In a public network, once variety of clusters connected to every different is raised becomes a possible threat to security applications running on the clusters. To address this drawback, a Message Passing Interface (MPI) is developed to preserve security services in associate degree unsecured

network. The projected work focuses on MPI instead of other protocols as a result of MPI is one in every of the foremost widespread communication protocols on distributed clusters. Here AES algorithmic rule is employed for encryption/decryption and interpolation polynomial algorithmic rule is employed for key management that is then integrated into Message Passing Interface Chameleon version two (MPICH2) with standard MPI interface that becomes ES-MPICH2. This ESMPICH2 is a new MPI that gives security and authentication for distributed clusters that is unified into crypto graphical and mathematical thought. The major desire of ES-MPICH2 is supporting an outsized sort of computation and communication platforms. The projected system is predicated on each crypto graphical and mathematical concept that ends up in choked with error free message passing interface with increased security.

Password each Key Exchange (PAKE) is one of the vital topics in cryptography. It aims to handle a sensible security problem: the way to establish secure communication between 2 parties only supported a shared countersign while not requiring a Public Key Infrastructure (PKI). Once quite a decade of intensive research during this field, there are many PAKE protocols out there. The EKE and adventurer schemes square measure perhaps the 2_{most} notable examples. Each technique are but proprietary. In this paper, we have a tendency to review these techniques well and summarize varied theoretical and sensible weaknesses. Additionally, we have a tendency to gift a replacement PAKE answer known as J-PAKE. Our strategy is to rely upon well-established primitives like the Zero-Knowledge Proof (ZKP). So far, almost all of the past solutions have avoided victimization ZKP for the concern on potency. We have a tendency to demonstrate the way to effectively integrate the ZKP into the protocol style and meanwhile succeeds } good potency. Our protocol has comparable machine potency to the EKE and SPEKE schemes with clear benefits on security. - Feng Hao1, et al [6] 2.7 we have a tendency to gift a mechanized proof of the password based protocol One-Encryption Key Exchange (OEKE) using the computationally-sound protocol prove Crypto Verif. OEKE could be a non-trivial protocol, and thus mechanizing its proof provides further confidence that it is correct. This case study was conjointly a chance to implement many vital extensions of Crypto Verif, useful for proving several different protocols. we've got so extended Crypto Verif to support the machine Diffie Hellman assumption.

We've got conjointly another support for proofs that believe Shoup's lemma and extra game transformations. Specially, it's currently potential to insert case distinctions manually and to merge cases that no longer have to be compelled to be distinguished. Eventually, some improvements are another on the computation of the probability bounds for attacks, providing higher reductions. specially, we have a tendency to improve over the quality computation of chances once Shoup's lemma is employed, which permits North American country to increase the sure given during a previous manual proof of OEKE, and to indicate that the opponent will test at the most one countersign per session of the protocol. In this paper, we have a tendency to gift these extensions, with their application to the proof of OEKE. All steps of the proof, both automatic and manually radio-controlled, square measure verified by Crypto Verif.

V. SUMMARY OF OUR PROTOCOL

• pNFS-AKE-I:

Our 1st protocol will be thought to be a modified version of Kerberos that enables the shopper to generate its own session keys.

• pNFS-AKE-II:

To deal with key written agreement whereas achieving forward secrecy at the same time, we tend to incorporate a Diffie Hellman key agreement technique into Kerberos-like pNFS-AKE-I. Notably, the shopper C and also the storage device Si every currently chooses a secret worth (that is understood only to itself) and pre-computes a Diffie-Hellman key part. A session secret's then generated from each the Diffie-Hellman parts.

• **pNFS-AKE-III:**

Our third protocol aims to attain full forward secrecy, that is, exposure of a long key affects solely a current session key (with regard to t), but not all the opposite past session keys.

VI. CONCLUSION

We planned 3 real key swaps over protocols for parallel network classification system. Our procedures gift 3 attractive compensations over the gettable Kerberos primarily based pNFS procedure. Primary, the information server implementing our procedures has abundant subordinate work than that of the Kerberos primarily based move toward. Subsequent, 2 our procedures build available forward confidentiality: one is incompletely forward protected [with admiration to manifold assemblies among associate occasion era], at identical time because the extra is totally onward protected [with admiration to associate assembly). Next, we have intended procedure that not solely builds obtainable onward confidentiality, aside from is just too escrowing gratins.

VII. ACKNOWLEDGMENTS

The authors gratefully acknowledge the support for this paper from department of MCA (Vel tech high tech Dr.Rangarajan Dr.sakunthala engineering college), Chennai, India and the anonymous reviewers of this paper.

REFERENCES:

1. Vitality Xie^{1*}, Bin Hu^{1*}, Na Dong¹, Duncan S.Wong²., “Anonymous many-sided Password-Authenticated Key Exchange theme for Telecare Medical data Systems.”
2. Michel Abdalla, David Pointcheval., “Simple PasswordBased Encrypted Key Exchange Protocols.”
3. *A. Sai Kumar **P. Subhadra., “User Authentication to Provide Security against on-line dead reckoning Attacks.”
4. Anupam Datta¹, Ante Derek¹, John C. Mitchell¹, and Bogdan Warinschi²., “Key Exchange Protocols: Security Definition, Proof technique and Applications .
5. R.S.RamPriya, M.A.Maffina., “A Secured and Authenticated Message Passing Interface for Distributed Clusters.
6. Feng Hao¹ and Peter Ryan²., “J-PAKE: genuine Key Exchange while not PKI”
7. Bruno Blanchet., “Automatically Verified Mechanized Proof of One-Encryption Key Exchange”
8. Menezes, P. van Oorschot, and S. Vanstone. Handbook of Applied Cryptography. CRC Press, 1996.
9. Olson and E.L. Miller. Secure capabilities for a petabyte-scale objectbased distributed file system. In Proceedings of the ACM Workshop on Storage Security and Survivability (StorageSS), pages 64–73. ACM Press, Nov 2005.
10. O. O’Malley, K. Zhang, S. Radia, R. Marti, and C. Harrell. Hadoop security design. Yahoo!, Oct2009 attachment/12428537/security-design.pdf.
11. S. Parker. De-risking drug discovery with the use of cloud computing. iSGTW, Jun 18, 2012. <http://www.isgtw.org>.
12. Rosenthal, P. Mork, M.H. Li, J. Stanford, D. Koester, and P. Reynolds. Cloud computing: A new business paradigm for biomedical information sharing. Journal of Biomedical Informatics (JBI), 43(2):342–353. Elsevier, Apr 2010.
13. S. Shepler, B. Callaghan, D. Robinson, R. Thurlow, C. Beame, M. Eisler, and D. Noveck. Network file system (NFS) version 4 protocol. The Internet Engineering Task Force (IETF), RFC 3530, Apr 2003.
14. S. Shepler, M. Eisler, and D. Noveck. Network file system (NFS) version 4 minor version 1 protocol. The Internet Engineering Task Force (IETF), RFC 5661, Jan 2010. [15] R. Sandberg, D. Goldberg, S. Kleiman, D. Walsh, and B. Lyon. Design and implementation of the Sun network filesystem. In Proceedings of the Summer 1985 USENIX Conference, pages 119–130. USENIX Association, Jun 1985.

15. F.B. Schmuck and R.L. Haskin. GPFS: A shared-disk file system for large computing clusters. In Proceedings of the 1st USENIX Conference on File and Storage Technologies (FAST), pages 231–244. USENIX Association, Jan 2002.
16. O. Tatebe, K. Hiraga, and N. Soda. Gfarm grid file system. *New Generation Computing (NGC)*, 28(3):257–275. Springer, Jul 2010.
17. R. Thurlow. RPC: Remote procedure call protocol specification version 2. The Internet Engineering Task Force (IETF), RFC 5531, May 2009.
18. S.A. Weil, S.A. Brandt, E.L. Miller, D.D.E. Long, and C. Maltzahn. Ceph: A scalable, high-performance distributed file system. In Proceedings of the 7th Symposium on Operating Systems Design and Implementation (OSDI), pages 307–320. USENIX Association, Nov 2006.
19. Parallel virtual file systems (PVFS) version <http://www.pvfs.org>

IJERGS

The Innovation of Pervasive Computing

Shweta Ohri

Jagannath International Management School,

Vasant Kunj, New Delhi-70

Emails: shweta.ohri@jagannath.org

Abstract- This paper describes about the recent research topic pervasive computing and its applications. Pervasive Computing interaction systems are rapidly discovering its way into every facet of our lives and change the aspects faster than speed. Large scale of interactive media facades challenges to emergence into existing physical environment and newly built structures, which need to achieve managing capabilities of varied stakeholders, existing work practices and schedules. This technology of Pervasive Computing is inter woven in human lives and due to this it has become the need of time.

1. Introduction

Human social network plays a remarkable role in the information spread in Cyber World. Innovation has changed our lives to an extensive degree and still can possibly transform it in another and emotional way. Due multiplication of innovation into our lives to an expansive degree we spend our lives in an alternate manner when contrasts with our forefathers. Innovation has connected into our everyday life exercises from attempting to recreational exercises. We are presently engaged in interaction with distinctive devices, gadgets and machines.

Pervasive systems refer to construct a universal computing environment where unified and invisible access to computing resources is provided to the user. It aims to make our lives modest through the use of machine interaction by human Pervasive Computing is the latest computing technology which is available in all over the place where the communication taken place. Pervasive computing relies on the convergence of wireless technologies, advanced, electronics and the Internet.

The concept of pervasive computing is based on a simple idea that with advances in technology, computing equipment will grow smaller and gain more power; this would allow small devices to be ubiquitously and invisibly embedded in the everyday human surroundings and therefore provide an easy access to a computing environment. The products are connected to the Internet and the data they generate is easily available. The major technologies such as internet, advanced middleware, operating systems, sensors/actuators, microprocessors, and mobile protocols are used to give support for this technology to function.

Requirements for Pervasive Interaction:

Pervasive applications interfaces ought to be versatile to their surroundings and act as indicated by the situation. They should adapt as per context and don't need explicit interaction from the user. The primary destination of Pervasive Computing is to permit user to emphasize on their task instead on technology. In few previous years we watch numerous applications that accumulate user context through sensors keeping in mind the end goal to do exact things at exact time.

Implicit Human Computer Interaction

Traditional user interfaces were functioned oriented; the user got to whatever the system could do by indicating functions first and afterward their arguments. The central point of IHCI is to emphasize on the user task by preference than stress on technology. IHCI in Pervasive Computing would be hidden and verifiable instead of conventional explicit interaction of user through the system.

Task Oriented Interaction

Pervasive system environment ought to permit the user to focus on the task as opposed to on the technology. Pervasive systems permit the combination of and interaction between task and affective information processing. Pervasive devices with high level of tasks orientation are, consequently, a most significant objective.

Multimodal of Interaction

Multimodal communication furnishes the user with various modes of interfacing with a framework. A multimodal interface gives a few different tools to enter and yield of information. HCI in Pervasive Computing includes versatile to circumstance and backing for multimodal of interaction with the user. This requires an insights work coordinated with an ideal interaction model.

Human Interaction Pattern

Human interaction design in pervasive environment would multimodal of interaction reinforcing with the reliable interface, expressive interface, useful interface, ordered and suitable information.

Natural Human Computer Interaction

Human-computer collaboration has a tendency to rapid change, and advance to something users are used to, which is natural for them, not something they need to learn. Natural Human-Computer Interaction (NHCI) aims to research new intuitive computing system that emerges from human language and behavior into tech applications. NHCI supports interaction with computerized systems without the requirement of external equipment like mice or keyboards. Rather, these will focus on computing systems easy to use and replaced by speech recognitions, context awareness, gestures and body movement. With development in innovation the interaction in Pervasive Computing has an expansion to be carried with natural interactions

Pervasive Computing Challenges

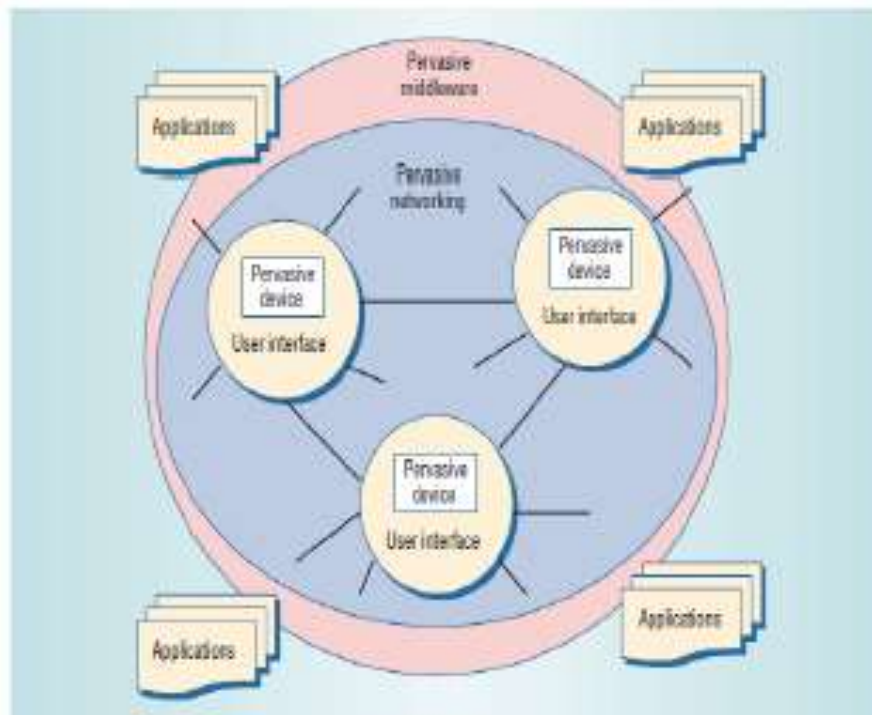
Pervasive Computing has more prominent convince in diverse domains on both local and worldwide situations.. One of the most important and open questions is how to ensure that a computing system is seamlessly and invisibly embedded in the environment and how to minimize the possible impact of its intrusiveness on a user's perception. Generally, there are two mutually complementing approaches to solving the problem of unobtrusiveness of a pervasive system: by miniaturization of devices and embedding of the system's logic into wearable, handheld, and mobile devices, as well as into the environment, and by achieving a level of intelligence of the system that will be able to anticipate the actions of the user in the context of the factors in the environment. As a result, such a pervasive system will "fade into the background" It is critical for analysts to recognize the challenges, objectives, and methods for mounting these technologies in diverse areas to completely aware of its potential. Pervasive Computing would detriment the entire society and absent the limits in computing. In general pervasive technology advancements will be oppressed through an advanced situation that is mindful of their presence. Natural interaction is pervasively available by means of adaptive, sensitive and receptive to their needs, habits and feelings. Progressively, a significant number of the chips around us will sense their surroundings in simple however effective ways. Pervasive Computing, part of procedures and challenges need to be tended to in order to adequately make smart spaces and accomplish miniaturization. Pervasive Computing systems must overcome following challenges. Security outline must consider standards of time and area though Pervasive Computing is expanded in various environments transparently. Protection from Unauthenticated user (security), avoidance of access by an attacker through unverified techniques (integrity), giving availability to user totally (accessibility) and evading an entity from denying previous activities (non-denial) are essential factors the security model. Recognizing kind of exchanging information, conceivable distortion or misuse, shortcomings and features, the security issues in remote system base for network infrastructure can be represented.

- Unauthorized access;
- Viruses attack to destroy security system;
- Undefined security solutions;
- Information hacking by hackers;
- Not have system administrator;
- Weak links;
- Weak infrastructure of application;
- Weak synchronization.

Goals of Pervasive (Ubiquitous) Computing

The principal goal of the Pervasive Computing interaction is to permit user to attention on their everyday task instead of innovation. In last few years we watch numerous applications that accumulate user setting through sensors so as to do right things at correct time. HCI ought to consider usability as well as focus on helping user tasks, demonstrating access to data in most ideal way and focus on all the more influential manifestation of communications. Pervasive Computing systems have utilization sensing, computing and correspondence abilities to watch and react to natural phenomena. Such system will inevitably empower computers too consistently incorporate into ordinary life. They have numerous potential applications in the workplace, home, health awareness, gaming, ecological checking and open transportation.

Architecture for Pervasive Computing



The Pervasive computing architecture has the following four important areas, they are:

- Devices
- Networking
- Middleware
- Applications

Devices

The ubiquitous environment consists of many different types of input and output devices. Some of the system devices such as keyboard, mouse, touchpad, wireless mobile devices, sensors, pagers, mobile phones and smart phones these systems can be used as an input device for a pervasive environment. In that the sensors automatically collect the information about the environment and feed this input directly to the pervasive network.

Networking

All the Pervasive devices are connected with other pervasive or any other communication devices through the distributed network. Why this pervasive device connected through distributed network means, because of the global accessibility of the device. The pervasive devices can be connected through the Local Area Network (LAN) or through Metropolitan Area Network (MAN) or through Wide Area Network (WAN) for the global availability.

Middleware

In order to make a communication between an end-user and a system the pervasive network should need a middleware "kernel". The middle either may be a web application or set of software-bundle. The software-bundle is executing in client-server mode or peer-to-peer mode.

Applications

The Pervasive computing is more environment-centric than web-based or mobile computing. The data which are collected through pervasive environment will be processed by the middleware software and the output will generated based on the present environmental inputs.

I. SMART CLOTHING

- Conductive textiles and inks print electrically active patterns directly onto fabrics.
- Sensors based on fabric monitor pulse, blood pressure, body temperature.
- Invisible collar microphones



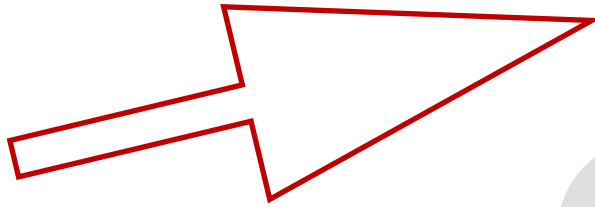
II. INTERACTIVE FLEX POSTERS

- Flexes that communicate with the person automatically in a building and then provide him the information about his office and the venue of his meeting that his held.



III. PILL CAM

- Miniature camera
- Diagnostic device
- It can be swallowed
- Once swallowed it gives the data about the functioning of the vital organs in our body.



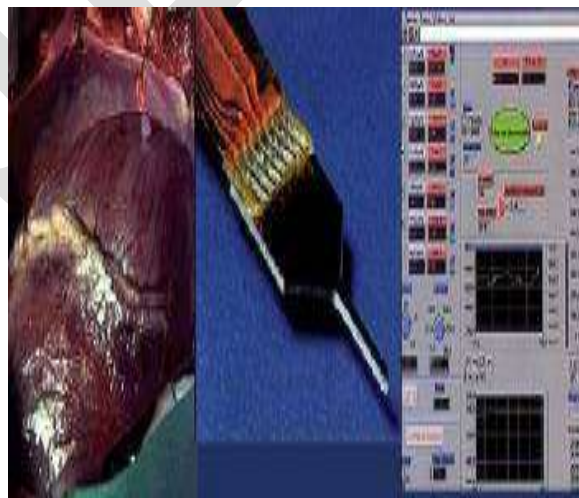
IV. SMART WATCH

- Wrist watches will monitor our sugar



I. DIGITRACKER

- *Digi-tickers* or implanted heart monitors in heart patients will talk wirelessly to computers, which will be trained to keep an eye open for abnormalities.



Conclusions

Technology is rapidly finding its method and changing states faster than speed into every aspect of our lives as a basic need of time. The way of the pervasive environment permits communication between devices whenever and everywhere, so the systems become more pervasive in modern world. Pervasive Computing will be a ripe resource of challenging research issues in computer systems for a long time to come. We will need to address study and explore the challenges in areas outside computer systems. Interaction abilities will need to be emergence with the sorts of computer systems functionalities and answering different applications appearances will oblige us to expand our topic on a few ideas. The role of Pervasive Computing from these areas will need to be integrated into existing physical environment and newly built structures discuss in this paper. Existing innovative abilities give the potential to satisfy Weiser's vision. What has been required is the expression of ideas that will empower designers to deliberately design for physical and cognitive accessibility. Pervasive Computing gives an appealing vision to the future of computing systems. Security, trust and privacy design methods are getting importance in HCI with the advancement of flexibility, nontraditional computing applications that have a solid effect on the personal, natural and instructive privacy of users. To develop security models we recommend to elegant designers by helping they see better work that goes into everyday security, trust and privacy. Hence, research in this field should build familiarity with the impacts of applying specific methods, and should help selecting whatever design methodology is most proper for the configuration of current workload. To accomplish this objective; we propose to develop the security methodologies. A number of the challenges we showing are sensible, applicable and within reach, making them prime challengers for rich future advancements.

REFERENCES:

- [1] Bashir, R.N., Qadri, S., Saleem, R.M., Naeem, M. and Ghafoor, Y. (2014) Human Computer Interaction (HCI) in Ubiquitous Computing. *International Journal of Innovation and Applied Studies*, **9**, 534.
- [2] Weiser, M. (1991) The Computer for the 21st Century. *Scientific American*, **265**, 94-104. <http://dx.doi.org/10.1038/scientificamerican0991-94>
- [3] Fouad, R., Hashem, M., Badr, N. and Talha, H. (2011) Exploring a Hybrid of Geospatial Semantic Information in Ubiquitous Computing Environments. *Global Journal of Computer Science and Technology*, **11(19)**.
- [4] Brodersen, C. and Kristensen, J.F. (2004) Interaction through Negotiation. *Proceedings of the 3rd Nordic Conference on Human-Computer Interaction*, 259-268. <http://dx.doi.org/10.1145/1028014.1028054>
- [5] Sandhu, R. (2013) Shifting Paradigm from Mobile Computing to Ubiquitous/Pervasive Computing. *Indexing Journal Indexing: Our Journal Has Recently Joined International Database for Indexing with DOAJ, Index Copernicus, Open J Gate, CAS, Google Scholar*.
- [6] (2013) Pervasive Computing. *IEEE Computer Society*, **12**, 18-20.[7] Sharifi, A. and Abdulahshah, M.K. (2013). Security Attacks and Solutions on Ubiquitous Computing Network. *International Journal of Engineering and Innovative Technology (IJEIT)*, **3**, 40-45.
- [8] Ye, J. and Dobson, S. Pervasive Computing Needs Better Situation—Awareness. *Awareness Magazine*. <http://dx.doi.org/10.2417/3201201.003943>
- [9] Ismail, A., Hajjar, A.E.S.A. and Ismail, Z. (2011) A New System Architecture for Pervasive Computing. *arXiv Preprint arXiv:1108.2389*.
- [10] Abowd, G.D. and Mynatt, E.D. (2000) Charting Past, Present, and Future Research in Ubiquitous Computing. *ACM Transactions on Computer-Human Interaction (TOCHI)*, **7**, 29-58. <http://dx.doi.org/10.1145/344949.344988>
- [11] Joshi, Y. and Prasad, L. (2012) Pervasive Computing Goals and Its Challenges for Modern Era. *International Journal of Computer Science and Network (IJCSN)*, Volume 1, Issue 3, ISSN 2277-5420. www.ijcsn.org.
- [12] Nielsen, J. (1993) Noncommand User Interfaces. *Communications of the ACM*, **36**, 83-99. <http://dx.doi.org/10.1145/255950.153582>
- [13] Morariu, A., Clipa, B.D., De Lausnay, S., De Strycker, L. and Pentiu, S. (2011) Combining Natural Human-Computer Interaction and Wireless Communication. *Journal of Applied Computer Science & Mathematics*, **5**, 47-52.
- [14] Schmidt, A. (2013) Context-Aware Computing: Context-Awareness, Context-Aware User Interfaces, and Implicit Interaction. In: Soegaard, M. and Dam, R.F., Eds., *The Encyclopedia of Human-Computer Interaction*, 2nd Edition, The Interaction Design

Foundation, Aarhus.

- [15] Chihani, B., Bertin, E. and Crespi, N. (2011) A Comprehensive Framework for Context-Aware Communication Services. Proceedings of the 15th International Conference on Intelligence in Next Generation Networks (ICIN), Berlin, 4-7 October 2011, 52-57. <http://dx.doi.org/10.1109/icin.2011.6081102>
- [16] Chihani, B., Bertin, E., Jeanne, F. and Crespi, N. (2011) Context-Aware Systems: A Case Study. In: Cherifi, H., Zain, J.M. and El-Qawasmeh, E., Eds., Digital Information and Communication Technology and Its Applications, Springer, Berlin, 718-732. http://dx.doi.org/10.1007/978-3-642-22027-2_60
- [17] Karray, F., Alemzadeh, M., Saleh, J.A. and Arab, M.N. (2008) Human-Computer Interaction: Overview on State of the Art. International Journal on Smart Sensing and Intelligent Systems. S. M. Shaheed et al. 50
- [18] Hachman, M. (2002) Canesta Says “Virtual Keyboard” Is Reality. <http://www.extremetech.com/extreme/51958-canesta-says-virtual-keyboard-is-reality>
- [19] Grudin, J. (2011) A Moving Target: The Evolution of HCI. In: Jacko, J., Ed., The Human- Computer Interaction Handbook, 3rd Edition, Taylor & Francis, New York.
- [20] Oviatt, S., Cohen, P., Wu, L., Duncan, L., Suhm, B., Bers, J., et al. (2000) Designing the User Interface for Multimodal Speech and Pen-Based Gesture Applications: State-of-the- Art Systems and Future Research Directions. Human-Computer Interaction, **15**, 263-322. http://dx.doi.org/10.1207/S15327051HCI1504_1
- [21] Gavrilu, D.M. (1999) The Visual Analysis of Human Movement: A Survey. Computer Vision and Image Understanding, **73**, 82-98. <http://dx.doi.org/10.1006/cviu.1998.0716>
- [22] Sibert, L.E. and Jacob, R.J. (2000) Evaluation of Eye Gaze Interaction. Proceedings of the SIGCHI Conference on Human Factors in Computing Systems, The Hague, 1-6 April 2000, 281-288.
- [23] Zacharia, K., Elias, E.P. and Varghese, S.M. (2011) Modeling Gesture Based Ubiquitous Application <http://arxiv.org/abs/1112.2044>
- [24] Poslad, S. (2011) Ubiquitous Computing: Smart Devices, Environments and Interactions. John Wiley & Sons, Chichester.
- [25] Chandini, N., Reddy, N.C.S. and Bashwanth, N. (2014) Pervasive Computing Goals and Its Challenges for New Epoch. International Journal of Advanced Research in Computer and Communication Engineering, **3**, 6437-6439.
- [26] Rao, D.H. (2014) A Scenario Based Approach for Dealing with Challenges in a Pervasive Computing Environment. <http://arxiv.org/ftp/arxiv/papers/1405/1405.6661.pdf>
- [27] Das, S.K., Kant, K. and Zhang, N. (2012) Handbook on Securing Cyber-Physical Critical Infrastructure. Elsevier, Amsterdam.
- [28] Roy, N., Misra, A., Julien, C., Das, S.K. and Biswas, J. (2011) An Energy-Efficient Quality Adaptive Framework for Multi-Modal Sensor Context Recognition. Proceedings of the IEEE International Conference on Pervasive Computing and Communications (PerCom), Seattle, 21-25 March 2011, 63-73. <http://dx.doi.org/10.1109/percom.2011.5767596>
- [29] Rajkumar, R. and Lee, I. (2006) NSF Workshop on Cyber-Physical Systems. 16-17 October 2006, Austin. <http://varma.ece.cmu.edu/CPS/>
- [30] Hayes, G.R., Poole, E.S., Iachello, G., Patel, S.N., Grimes, M., Abowd, G.D. and Truong, K.N. (2007) Physical, Social, and Experiential Knowledge in Pervasive Computing Environments. IEEE Pervasive Computing, **6**, 56-63. <http://dx.doi.org/10.1109/MPRV.2007.82>
- [31] Campbell, A.T., Eisenman, S.B., Lane, N.D., Miluzzo, E., Peterson, R., Lu, H., et al. (2008) The Rise of People-Centric Sensing. IEEE Internet Computing, **12**, 12-21. <http://dx.doi.org/10.1109/MIC.2008.90>
- [32] Leung, A., Sheng, Y. and Cruickshank, H. (2007) The Security Challenges for Mobile Ubiquitous Services. Information Security Technical Report, **12**, 162-171. <http://dx.doi.org/10.1016/j.istr.2007.05.001>
- [33] Pallapa, G., Kumar, M. and Das, S.K. (2007) Privacy Infusion in Ubiquitous Computing. Proceedings of the Fourth Annual International Conference on Mobile and Ubiquitous Systems: Networking & Services, Philadelphia, 6-10 August, 1-8. <http://dx.doi.org/10.1109/mobiq.2007.4451030>

- [34] Ganesh, M. and Krishna, S.M. (2010) Privacy Enhanced Context-Aware Architecture for Ubiquitous Computing. International Journal of Electronics and Computer Science Engineering, **2**, 53-64.
- [35] Khiabani, H., Sidek, Z.M. and Manan, J.L.A. (2010) Towards a Unified Trust Model in Pervasive Systems. Proceedings of the 24th International Conference on Advanced Information Networking and Applications Workshops (WAINA), Perth, 20-23 April 2010, 831-835. <http://dx.doi.org/10.1109/waina.2010.144>
- [36] Campbell, R., Al-Muhtadi, J., Naldurg, P., Sampemane, G. and Mickunas, M.D. (2003) Towards Security and Privacy for Pervasive Computing. In: Okada, M., Pierce, B.C., Scedrov, A., Tokuda, H. and Yonezawa, A., Eds., Software Security—Theories and Systems, Springer, Berlin, 1-15. http://dx.doi.org/10.1007/3-540-36532-X_1
- [37] Forné, J., Hinarejos, F., Marín, A., Almenárez, F., Lopez, J., Montenegro, J.A., et al. (2010) Pervasive Authentication and Authorization Infrastructures for Mobile Users. Computers & Security, **29**, 501-514. <http://dx.doi.org/10.1016/j.cose.2009.09.001>
- [38] Wang, G., Zhou, W. and Yang, L.T. (2013) Trust, Security and Privacy for Pervasive Applications. The Journal of Supercomputing, **64**, 661-663. <http://dx.doi.org/10.1007/s11227-013-0953-4>
- [39] Zhou, B., Shi, Q. and Merabti, M. (2007) Towards Energy-Efficient Intrusion Detection in Pervasive Computing. Proceedings of the IEEE International Conference on communications, Glasgow, 24-28 June 2007, 1417-1422. <http://dx.doi.org/10.1109/icc.2007.238>
- [40] Bharadwaj, S., Vatsa, M. and Singh, R. (2014) Biometric Quality: A Review of Fingerprint, Iris, and Face. EURASIP Journal on Image and Video Processing, **2014**, 34. <http://dx.doi.org/10.1186/1687-5281-2014-34>

Visual cryptography in internet voting for extended security

Archana P.S, Ambily O.

Department of computer Applications, K.V.M college of engineering&IT,INDIA

archanaps92@gmail.com

Abstract— India has an asymmetric federal government, with elected officials at the federal, state and local levels. At the national level, the head of government, Prime Minister, is elected by members of the Lok Sabha, the lower house of the parliament of India. The elections are conducted by the Election Commission of India. All members of the Lok Sabha, except two who can be nominated by the President of India, are directly elected through general elections which take place every five years, in normal circumstances, by universal adult suffrage and a first-past-the-post system.¹ Members of the Rajya Sabha, the upper house of the Indian parliament, are elected by elected members of the legislative assemblies of the states and the Electoral college for the Union Territories of India.

2015 general elections involved an electorate of 863,500,000 people {including all peoples above 18 years } (larger than both EU and US elections combined). Declared expenditure has trebled since 1989 to almost \$300 million, using more than one million electronic voting machines. The size of the huge electorate mandates that elections be conducted in a number of phases (there were nine phases in the 2014 general election). It involves a number of step-by-step processes from announcement of election dates to the announcement of results paving the way for the formation of the new government.

This paper named “Visual cryptography in internet voting for extended security” as the name indicates is a visual cryptography implementation which aims in automating the voting process so that the user can vote from his/her home ,office or anywhere without any geographical restrictions. To ensure secrecy the paper in cooperates the advantages of steganography and visual cryptography together. The secret password is embedded inside an image which is split into two shares. User on entering both the shares correctly can go for voting. Another feature is that the complex tasks going behind the project is hidden from the user so that the system becomes so user friendly.

Keywords----- Biometrics, Internet Voting System (IVS), I-voting, Visual Cryptography (VC), E-voting, 2-2 visual cryptography scheme- n-k visual cryptography

INTRODUCTION

















Elections are conducted in small scale organizations, corporate institutes and on a larger scale, in parliaments too, for appointing board members of that organizational body. These elections restrict the voters to be present at that voting location thus causing inconvenience. This causes an alarming need to bring remote voting systems to effect. Internet voting system using visual cryptography fulfills this need of being able to vote from anywhere without causing security concerns. Almost all fields of life are now automated. But still people have to wait in long queues to do their fundamental right voting. This paper aims in making the voting more secure and effective at the same time making it available for people from any geographical location.

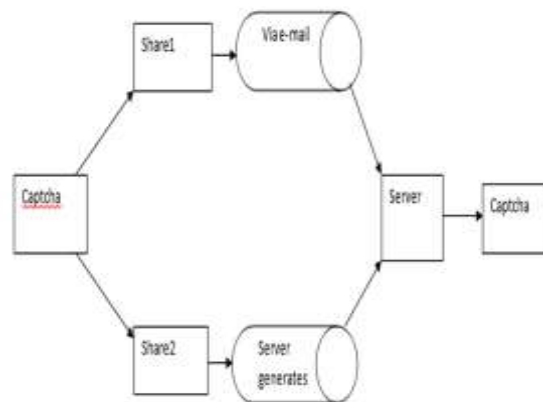
1.1 Internet Voting System

Internet voting system enables a voter to vote over the internet while providing accuracy and security. Internet voting system can be of two types-Poll-site and remote voting. Poll-site voting enables the voter to vote over the internet, at a voting poll. Remote voting enables the voter to vote from anywhere around the globe thus removing geographical restrictions .

1.2 Visual Cryptography

Visual cryptography is an encryption technique that encrypts data using secret key. The encrypted data can be decrypted using human visual system. Thus decryption can be done by someone without the knowledge of cryptography and does not require any decryption algorithm .

Pixel colour	Original pixel	Share 1	Share 2	Share 1 + Share 2
Black				
Black				
White				
White				



MATERIALS AND METHODS

II. INTERNET VOTING SYSTEM USING VISUAL CRYPTOGRAPHY

There are number of visual cryptography schemes as follows.

2.1 Two out of two visual cryptography scheme

In this type of Visual cryptography scheme, the secret image is divided into two shares. This is the simplest kind of visual cryptography. The major application of this scheme is found with IVS that uses 2 out of 2 Visual secret sharing schemes for authentication purpose. To reveal the original image, two shares are required to be stacked together.

2.2 n out of k visual cryptography scheme

This type of visual cryptography scheme divides a secret image into k number of shares. Then the secret image can be revealed from any n number of shares among k. For example, in 3 out of 6 VC scheme, any 3 shares out of 6 shares are sufficient to reveal the secret data. The major problem this scheme is that the user needs to maintain many shares which may result into loss of shares. Also more number of shares means more memory consumption

2.3 k out of k visual cryptography scheme

In This type of visual cryptography scheme secret is divided into k number of shares and for reconstruction of the secret image, all k shares are required. For example, in 6 out of 6 VC scheme, Secret is revealed only after stacking all the 6 shares, where $k=6$. This scheme is not so popular because managing k number of shares is difficult task and it also increases time complexity.

A voting system should be fair enough for both political parties and voters. There are some characteristics of voting system that are as follows-

Authentication: Only authorized voters should be able to vote.

Uniqueness: No voter should be able to vote more than once.

Accuracy: Voting systems should record the votes correctly.

Integrity: Number of casted vote must not be modified.

Verifiability: Possible to verify that votes are correctly counted in the final tally.

Auditability: Reliable and demonstrably authentic election records.

Reliability: Systems should work robustly, even in the face of numerous failures.

This system is developed with due attention to secrecy. User once registered is verified by the admin on validating his ADHAAR CARD. The step by step procedure can be shown as

1. USER REGISTERS
2. ADMIN VIEWS USERS APPLICATIONS
3. HE CROSS CHECKS IT WITH THE IDENTITY PROOF SUBMITTED BY USER.
4. IF FOUND VALID HE/SHE IS APPROVED FOR VOTING
5. USER LOGS IN WITH HIS/HER PASSWORD AND USER ID
6. USER DOWNLOADS SECURITY IMAGE
7. USER DOWNLOADS SECURITY IMAGE SEND TO HIS/HER EMAIL ID
8. UPLOADS BOTH SHARES
9. ADMIN CHECKS WHETHER THE IMAGE SHARES ARE CORRECT (VISUAL CRYPTOGRAPHY)
10. USER MAKES HIS/HER VOTE
12. USER IS NOT ALLOWED TO VOTE AGAIN
13. USER LOGS OUT AND CAN VIEW THE RESULT ONCE IT IS PUBLISHED

AADHAAR

Aadhaar is a 12 digit individual identification number issued by the Unique Identification Authority of India (UIDAI) on behalf of the Government of India. Each individual needs to enroll only once which is free of cost. Each Aadhaar number will be unique to an individual and will remain valid for life. Aadhaar number will help to provide access to services like banking, mobile phone connections and other Government and Non-Government services. Biometric data like fingerprint, iris and palm geometry face is stored in database of Aadhaar. This number will serve as a proof of identity and address, anywhere in India. Any individual, irrespective of age and gender, who is a resident in India and satisfies the verification process laid down by the UIDAI, can enroll for Aadhaar.

ACKNOWLEDGEMENT

The satisfaction that accompanies the successful completion of any task would be incomplete without mentioning the people who make it possible. We are grateful to a number of individuals whose professional guidance along with encouragement have made it very pleasant endeavor to undertake this project. We have a great pleasure in presenting the paper "visual cryptography in internet voting for extended security" under the guidance of Miss: Ambily O.A and for giving us an opportunity to work on this topic. Her encouraging words went a long way in providing the patience and perseverance, which were needed to complete this project successfully. Also her true criticism towards technical issues provided us to concentrate on transparency of our project. We would like to express our gratitude to DR.SV Murugadas, Principal of K.V.M College of Engineering & IT and Prof.S Nagarao, Head of Department of computer applications for their support and guidance. Finally we express our sincere thanks to our parents and all those who helped us directly or indirectly in many ways in completion of this paper.

CONCLUSION

The designed system is used in election processes in clubs, corporate organizations, government elections etc in various forms. The system uses two way authentication as the authentication process is performed on the server side as well as the client side thus providing greater security. The electronic voting system has several advantages like allowing remote voting which removes geographical restrictions to the voter. The encryption technique that is used in our system is visual cryptography which makes use of encrypted shares and decryption is done by human visual system which reduces difficulties in decryption.

REFERENCES:

- [1] Rajendra A B and Sheshadri H S, Visual Cryptography in Internet Voting system, *IEEE*, 2013 ,
Arti Bhise, 2Namrata Borate ,3Aarti Garje,4Yogita Karkal,Secure internet voting,IJES
- [2] Anusha MN Srinivas B K., Remote Voting System for Corporate Companies using Visual Cryptography, *International Journal of Advanced Research in Computer Science and Software Engineering Research*, Volume 2, Issue 6, June 2012
- [3] Puja Devi Rana, Anita Singhrova, Suman Deswal Design and Implementation of K-Split Segmentation Approach for Visual Cryptography, *International Journal of Scientific and Research Publications*, Volume 2, Issue 8, August 2012
- [4] Shivendra Katiyar, Kullai Reddy Meka, Ferdous A. Barbhuiya, Sukumar Nandi, Online Voting System Powered By Biometric Security Using Steganography, *IEEE*, 2011
- [5] J. Alex, Halderman Harri Hursti, Jason Kitcat, Margaret MacAlpine, Travis Finkenauer1 Drew Springall, Security Analysis of the Estonian Internet Voting System, May 2014
- [6] Kohno, Tadayoshi, et al. "Analysis of an electronic voting system." *Security and Privacy, 2004. Proceedings. 2004 IEEE Symposium on*. IEEE, 2004.
- [7]http://newindianexpress.com/states/andhra_pradesh/Maoists-strike-fear-make-off-with-poll-papers-in-agency/2013/07/15/article1684243.ece
- [8] Executive Summary of "Genesis and Spread of Maoist Violence and Appropriate State Strategy to Handle it", Bureau of Police Research and Development, Ministry of Home Affairs, New Delhi
- [9] Dill, David L., Bruce Schneier, and Barbara Simons. "Voting and technology: who gets to count your vote?." *Commun. ACM* 46.8 (2003): 29-31
- [10] Jefferson, David, et al. "Analyzing internet voting security." *Communications of the ACM* 47.10 (2004): 59-64.
- [11] Evans, David, and Nathanael Paul. "Election security: Perception and reality." *IEEE Security & Privacy Magazine* 2.1 (2004): 24-31.
- [12] Agarwal, Himanshu, and G. N. Pandey."Online voting system for India based on AADHAAR ID." *ICT and Knowledge Engineering (ICT&KE), 2013 11th International Conference on*. IEEE, 2013.
- [13] Zissis, Dimitrios, and Dimitrios Lekkas. "Securing e-Government and e-Voting with an open cloud computing architecture." *Government Information Quarterly* 28.2 (2011): 239-251.
- [14] Agarwal, H., & Pandey, G. N. (2013). Impact of E-Learning in Education.*International Journal*.
- [15] SusheelKumar, K., Vijay Bhaskar Semwal, Shitala Prasad, and R. C. Tripathi. "Generating 3D Model Using 2D Images of an Object." *International Journal of Engineering Science and Technology (IJEST)* 3, no. 1 (2011): 406-415.
- [16] Castillo, Jose Miguel, et al. "Prospecting the future with AI." *International Journal of Interactive Multimedia and Artificial Intelligence* 1.2 (2009).
- [17] SusheelKumar, K., Vijay Bhaskar Semwal, Shitala Prasad, and R. C. Tripathi. "Generating 3D Model Using 2D Images of an Object." *International Journal of Engineering Science and Technology (IJEST)* 3, no. 1 (2011): 406-415.
- [18] Vishwanath Bijalwan, Vinay Kumar, Pinki Kumari, Jordan Pascual," KNN based Machine Learning Approach for Text and Document Mining" *International Journal of Database Theory and Application* Vol.7, No.1 (2014), pp.61-70.
- [19] Pinki Kumari and Vikas Pareek, RAKSHITA- A Novel web based Approach for Protecting Digital Copyrights Using Public Key Digital Watermarking and Human Fingerprints" *International conference on methods and models in computer science (ICM2CS-2010)*.
- [20] K. S. Kumar, V. B. Semwal and R. C. Tripathi, "Real time face recognition using adaboost improved fast PCA algorithm", arXiv preprint arXiv:1108.1353, (2011).
- [21] K. S. Kumar, S. Prasad, S. Banwral and V. B. Semwal, "Sports Video Summarization using Priority Curve Algorithm", *International Journal*, vol. 2, (2010).
- [22] K. S. Kumar, V. B. Semwal, S. Prasad and R. C. Tripathi, "Generating 3D Model Using 2D Images of an Object", *International Journal of Engineering Science*, (2011).

Vehicle Tracking Using RFID

1. Jayalakshmi J, 2. Ambily O A

Department of Computer application, Student of MCA, KVM Collage of engineering & IT, Cherthala, INDIA
Email:jayalaksmij1993@gmail.com

Department of Computer application, Faculty of MCA, KVM Collage of engineering & IT, Cherthala, INDIA
Email:ambilybob@gmail.com

Abstract— Smart road checking system is proposed to take off the manual road checking by the police. The system works in such a way that, as the vehicle moves through the RF Detector area, the RF Reader module will read the vehicle ID by scanning the RF chip and the associated computing module will validate the vehicle ID with pre-stored records and automatically checking for all certificates validity. If any invalid details found, the system will make alert to the department via email. So the department can take further actions on the system generated report. Some certificates like pollution, insurance etc. are of short term validity, and those certificates will have to be updated in the specific periods. For this purpose, as per the proposed system users have to link with corresponding department.

Keywords— Radio Frequency Identification, RF reader, RF tag, Transponders, RF chip, Barcode, Road Transport Authority.

INTRODUCTION

Radio-frequency identification (RFID) is an automatic identification method, relying on Storing and remotely retrieving data using devices called RFID tags or transponders. The technology requires the cooperation of an RFID reader and an RFID tag. An RFID tag is an object that can be applied in to an object for the purpose of identification and tracking. This can be done by using radio waves. Some tags can be read from several meters away and beyond the line of sight of the reader. An RFID tag is an object that can be incorporated into a product, here it is vehicles for the purpose of identification and tracking using radio waves.

Smart road checking system is proposed to take off the manual road checking by the police. Now a days there is many road accidents occurs while on road checking. The main reason is the escaping mentality of riders. Sometimes people will have to do unnecessary payments. Tremendous amount of time and power is also wasted due to this type of vehicle checking. Based on the proposed system, the system locks all ways to escape from the checking. As the speed tracking cameras placed near by highways, we implements RF Detectors at each police station limits. Also introducing rule that strictly mentions, each vehicle running on the road should have proper RF chip given while vehicle registration and the vehicles that are registered should get the RF chip from concerned department. The system works in such a way that, as the vehicle moves through the RF Detector area, the RF Reader module will read the vehicle ID by scanning the RF chip and the associated computing module will validate the vehicle ID with pre-stored records and automatically checking for all certificates validity. If any invalid details found, the system will make alert to the department via email. So the department can take further actions on the system generated report. Some certificates like pollution, insurance etc. are of short term validity, and those certificates will have to be updated in the specific periods. For this purpose, as per the proposed system users have to link with corresponding department.

LITERATURE SURVEY

RFID tracking system is also called as Vehicle Tracking application. There is a relative lack of research concerning tracking and monitoring of vehicle movement. This study aims at assessing the feasibility of applying RFID for vehicle tracking purposes. There are different types of tracking devices available in market today.

Radio Frequency Identification (RFID) is an emerging technology that uses wireless radio waves to identify objects from a distance. RFID enables the user to capture real-time information in fast moving and bulky product flows with the aim of achieving a high degree of efficiency and assuring high quality. The components of a typical RFID system include an RFID tag, an RFID reader, an RFID middleware and the backend system. The RFID tag is the identification device attached to the item to be tracked. The RFID reader and antenna are devices that can recognize the presence of RFID tags and read the information stored on them. The aim of

RFID middleware is to process the transmission of information between the reader and other applications after receiving the information. Middleware is software that facilitates communication between the system and the RFID devices. The lower costs and the increasing capabilities of the RFID technique attract attention in keeping track and monitoring the vehicles on the road.

RELATED WORK

Vehicle tracking has increased in use over the past few years and, based on current trends, this rise should continue. Tracking offers benefits to both private and public sector individuals, allowing for real-time visibility of vehicles and the ability to receive advanced information regarding legal existence and security status.

The monitoring system of a vehicle is integration of RFID technology and tracking system. Ben Ammar Hatem and Haman Habib proposed bus management system; integration of RFID and WSN will facilitate the extension of an RFID network eliminating the need of wired installation. The system is suitable for monitor bus traffic inside spacious bus stations and can inform administrators whenever the bus is arriving on time, early or late and information is then displayed on the different wireless displays inside and outside the bus station

COMPONENTS OF RFID

A basic RFID system consist of three components:

- i. An antenna or coil
- ii. A transceiver (with decoder)
- iii. A transponder (RF tag) electronically programmed with unique information

These are described below:

i. ANTENNA

The antenna emits radio signals to activate the tag and read and write data to it. Antennas are the conduits between the tag and the transceiver, which controls the system's data acquisition and communication. Antennas are available in a variety of shapes and sizes; they can be built into a door frame to receive tag data from persons or things passing through the door, or mounted on an interstate tollbooth to monitor traffic passing by on a freeway. The electromagnetic field produced by an antenna can be constantly present when multiple tags are expected continually. If constant interrogation is not required, a sensor device can activate the field. Often the antenna is packaged with the transceiver and decoder to become a reader, which can be configured either as a handheld or a fixed-mount device. The reader emits radio waves in ranges of anywhere from one inch to 100 feet or more, depending upon its power output and the radio frequency used. When an RFID tag passes through the electromagnetic zone, it detects the reader's activation signal. The reader decodes the data encoded in the tag's integrated circuit (silicon chip) and the data is passed to the host computer for processing.

ii. TAGS (Transponders)

An RFID tag is comprised of a microchip containing identifying information and an antenna that transmits this data wirelessly to a reader. At its most basic, the chip will contain a serialized identifier, or license plate number, that uniquely identifies that item, similar to the way many bar codes are used today. A key difference, however is that RFID tags have a higher data capacity than their bar code counterparts. This increases the options for the type of information that can be encoded on the tag. The amount of data storage on a tag can vary, ranging from 16 bits on the low end to as much as several thousand bits on the high end. Of course, the greater the storage capacity, the higher the price per tag. Like all wireless communications, there are a variety of frequencies or spectra through which RFID tags can communicate with readers. Low-frequency tags are cheaper than ultra-high-frequency (UHF) tags, use less power and are better able to penetrate nonmetallic substances.

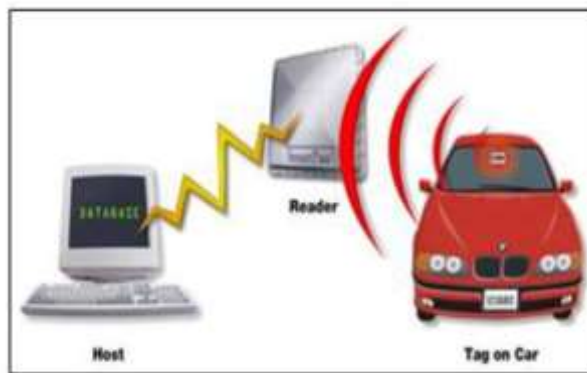
Figure 1: *RFID Tags*



i. RFID Reader

A device used to communicate with RFID Tag. The reader has one or more antennas, which emits radio waves and receive signals back, from the RFID Tag. Also called Interrogator because it interrogates the RFID Tag. Data retrieval - RFID Reader – Device - Emits radio waves - Received by the RFID Tag - Activates the microchip data get transmitted.

Figure 2: A reader is reading RFID tag.



SOLUTION

Current Options

- **Papers (License, Pollution Certificate etc.):**

Traffic police department have been using the traditional techniques of issuing original papers since the start checking.

- **Sticker:**

Police now attaching stickers on Wheelers after checking papers. They paste stickers on every vehicle. Both Road Transport Authority and police officials' informed that the vehicles having no stickers would be considered faulty and illegal and that action would be taken against them.

- **Barcode:**

We may think of Barcode as in some countries departments are using this. But all the above options have modern challenges that may not be overcome easily. Recently huge improvement has been evolved in printing industry and we have found even false money has become impossible to identify. Therefore papers are not enough to overcome the critical situation and very hard to implement in speedy and busy roads. Special stickers may take some time to copy but when it would become older then the fraud owners would take the same chances. About bar code the most important thing is the reader requires to bring very close to the tags (and in line of sight). And paper tags are easily become useless if they are wet and torn.

- **Camera**

Opponents of traffic cameras believe traffic cameras violate privacy and a citizen's right to face his/her accuser. Because this camera photograph people without their knowledge. Another disadvantages of traffic cameras is that they often do not work correctly. The camera and recording system may not be maintained properly. And sometimes the picture is not clear.

New Solution

The main objective of the proposed system is to automate the on road vehicle checking by the police department. For which we are introducing a new concept that every vehicle should have RF Device fitted with the vehicle. By replacing the on road checking and camera placed near by road for checking vehicle, the RF Reading device placed near by the road will read the card details, and automatically validates the owner details and corresponding certificate details. If any mismatch found the system will automatically send alerts to the specific department. Another facility provided by the system is lost vehicle detection and/or vehicle robbery tracking. The owner and police department can see the vehicle position that is the vehicle is under which station limit. So it will be much easier to find out the vehicle. Therefore, the best solution is using Radio Frequency Identification (RFID) Technology.

RFID Advantages

- I. Not requiring line of sight access to be read.
- II. Automatic scanning and data logging is possible without Operator intervention.
- III. Each tag can hold more than just a unique vehicle code.
- IV. Each item can be individually 'labeled'.
- V. With the right technology a plurality of tags can be concurrently read.
- VI. Provides a high degree of security and product authentication – a tag is more difficult to counterfeit than a barcode.
- VII. The supporting data infrastructure can allow data retrieval and vehicle tracking anywhere provided the scanner/reader is close enough to the tag.
- VIII. Since each tag can be unique they can act as a security feature if lost or stolen.

RFID disadvantages

- I. Some common problems with RFID are reader collision. Reader collision occurs when the signals from two or more readers overlap.
- II. Another problem is Tag collision. Tag collision occurs when many tags are present in a small area

ACKNOWLEDGMENT

The satisfaction that accompanies the successful completion of any task would be incomplete without mentioning the people who make it possible. We are grateful to a number of individuals whose professional guidance along with encouragement have made it very pleasant endeavor to undertake this project. We have a great pleasure in presenting the paper "vehicle tracking using RFID" under the guidance of Miss: Ambily O.A and for giving us an opportunity to work on this topic. Her encouraging words went a long way in providing the patience and perseverance, which were needed to complete this project successfully. Also her true criticism towards technical issues provided us to concentrate on transparency of our project. We would like to express our gratitude to DR.SV Murugadas, Principal of K.V.M College of Engineering & IT and Prof.S Nagarao, Head of Department of computer applications for their support and guidance. Finally we express our sincere thanks to our parents and all those who helped us directly or in indirectly in many ways in completion of this paper.

CONCLUSION

Designed as a system is to automate the on road vehicle checking by the police department. For which we are introducing a new concept that every vehicle should have RF Device fitted with the vehicle. By replacing the on road checking the RF Reading device placed near by the road will read the card details, and automatically validates the owner details and corresponding certificate details. If any mismatch found the system will automatically send alerts to the specific department. Another facility provided by the system is

lost vehicle detection and/or vehicle robbery tracking. The owner and police department can see the vehicle position that is the vehicle is under which station limit. So it will be much easier to find out the vehicle.

REFERENCES:

- [1] http://www.ijarcsse.com/docs/papers/Volume_5/4_April2015/V5I3-0561.pdf
- [2] Manish Buhptani, Shahram Moradpour, "RFID Field Guide - Developing Radio Frequency Identification Systems", Prentice Hall, 2005, pp 7-9, 16-225, 160, 231
- [3] Sewon Oh, Joosang Park, Yongioon Lee, "RFID-based Middleware System for Automatic Identification", IEEE International Conference on Service Operations and Logistics, and Information, 2005
- [4] RFID Journal, "<http://www.rfidjournal.com/RFID>"
- [5] Alien Technology Corporation, "Turkish Municipality Gives Green Light to RFID VEHICLE TRACKING", Field Guide, October 2007.
- [6] BEN AMMAR HATEN, HAMAN HABIB, "BUS MANAGEMENT SYSTEM USING RFID IN WSN," EUROPEAN AND MEDITERRANEAN CONFERENCE ON INFORMATION SYSTEM, 2010.
- [7] Kumar Yelamarthi, Daniel Haas, "RFID and GPS integrated navigation system for the visually impaired," 2010.
- [8] Mahammad Abdul Hannan, Aishah Mustapha, Aini Hussain, "RFID and communication technologies for an intelligent bus monitoring and management system," Turkish Journal of Electrical Engineering and Computer Science, pp: 106-120, 2012.
- [9] S. P. Manikandan, P. Balakrishnan, "An Efficient real time query system for public transportation service using Zigbee and RFID," International Journal of Research in Communication Engineering, Vol. 2, No. 2, June 2012.
- [10] Ngai, E.W.T., Li, C.L., Cheng, T.C.E., Lun, Y.H.V., Lai, K.H., Cao, J. et al. (2010). Design and development of an intelligent context-aware decision support system for real-time monitoring of container terminal operations. International Journal of Production Research, 49(12), 3501-3526. <http://dx.doi.org/10.1080/00207541003801291>
- [11] Roy Want "An Introduction to RFID technology", Journal IEEE Pervasive Computing
Volume 5 Issue 1, January 2006, pp-105-113
- [12] Guang-xian Xu, Jian-hui Liu, Zhi-yong Tao, and Xin-chun Li "The Research and Development of the Highway's Electronic Toll Collection System", World Academy of Science, Engineering and Technology 31 2007, pp 383-385.
- [13] A. Chattaraj, S. Chakrabarti, S. Bansal, S. Halder and A. Chandra "An Intelligent Traffic Control System using RFID", IEEE Potentials, vol. 28, no. 3, May-Jun. 2009, pp. 40-43.
- [14] Chong hua Li "Automatic Vehicle Identification System based on RFID", Anti-Counterfeiting Security and Identification in Communication (ASID), 2010, pp 281-284.
- [15] Ben Ammar Hatem, Hamam Habib " Bus Management System Using RFID in WSN",
EMCIS 2010, pp 45-50
- [16] Lejiang Guo, Wei Fang, Guoshi Wang "Intelligent traffic management system based on WSN and RFID" International Conference on Computer and Communication Technologies in Agriculture Engineering 2010, pp 111-114.
- [17] LI Xiangmin, FENG Xu, " Intelligent Toll Collection System Based on RFID
Technology," Industry automation 2007, Vo126, No9, pp. 81-82.
- [18] http://www.transcore.com/markets/Electronic_Vehicle_Registration_Downloads.htm and
http://www.transcore.com/technology/rfid_pdf.htm

[19] Wikipedia "RFID" (2004), Wikipedia, the Free Encyclopedia. 4 Dec. 2004 <http://en.wikipedia.org/wiki/RFID>

[20] <http://RFID.nordic.se>

[21] Vehicle Tracking Systems Overview [Online:]<http://www.roseindia.net/technology/gps/automatic-vehicle-location.shtml>.

[22] Kumar Chaturvedula .U.P , "RFID Based Embedded System for Vehicle Tracking and Prevention of Road Accidents" Vol. 1 Issue 6, August – 2012.

[23] <https://icons8.com/web-app/2354/rfid-tag>

[24] <http://www.trafficparking.com.au/long-range-RFID.php>

IJERGS

A STUDY OF BIOMECHANICAL BEHAVIOUR OF FENESTRATED CAPILLARIES IN THE GLYCOCALYX OF GLOMERULUS

G Lavanya** , Anbarasu S* , Sarathkumar A* , Mohammed Shaheen P P*

** Assistant Professor, Department of Biomedical Engineering Sri Ramakrishna Engineering College

* Dept of Biomedical of Engineering Sri Ramakrishna Engineering College

Abstract- Prognostication of biomechanical behaviour of blood flow in glomerulus is very much necessary to design and construct an artificial kidney under normal conditions. Each kidney contains about 1 million filtering unit (glomeruli). The glomeruli consist of three layers. The glomeruli are made up of many microscopic clusters of tiny blood vessels (capillaries) with small pores. In this work an endeavour is made to find out the characteristics of capillaries when the glomerular filtration is done. The pores (fenestrae) of these capillaries are more responsible for the variation in glomerular filtration rate (GFR). For this analysis, first the artificial model of structure was constructed using Autodesk Inventor software, consisting of 3 parts (Afferent arteriole, Efferent arteriole, Capillaries). The velocity of blood flow in the capillaries and pressure exerted by the blood on the walls, wall shear stress of the capillaries were found out using ANSYS 15.0. This model will help in understanding the characteristics of capillaries while the blood flow occurs for the filtration during glomerular filtration in both normal and diseased conditions..

Keywords— Nephron; Glomerulus; Capillaries; GFR; Afferent arteriole; Efferent arteriole.

1.INTRODUCTION

The nephron is the major part of kidney which plays a major role in urine formation. The human body consists of 2 kidneys each kidney consists of millions of nephrons. Glomerular filtration, Tubular absorption and tubular secretion are the most important 3 process that took place in nephron during urine formation. In this glomerular filtration is most important one were the removal of unwanted particles to the tubule will take place. The glomerular filtration occurs in capillaries of glomerulus which consists of three layers. The endothelial cells of glomerulus, glomerular basement membrane and podocytes. In this the endothelial cells which consists of pores. These pores in the capillaries are responsible for the glomerular filtration which ranging from 30-40nm. A computational analysis of blood through the capillaries were analysed here using the simulation software (ANSYS). A 3d model using Autodesk Inventor software is being constructed and imported in the ANSYS software for the analysis purpose. This analysis will lead to understand the blood rheology in Afferent and Efferent arterioles as well as in the capillaries. The biophysical changes to the blood in capillaries of glomerulus that occur during the urine formation is very much necessary while modelling an artificial kidney.

2.METHODOLOGY

Geometry construction is the most important part of the simulation process. The geometry modelling is carried out by the Autodesk Inventor software which is easy to handle the 3-D model. The model mainly consists of 5 parts afferent arteriole, Efferent arteriole and 3 capillaries which consist of pores. The extended cylindrical tube is adjusted and assembled to develop the geometry. After the geometry construction the model is being imported to the ANSYS software for the further analysis. The analysis process is carried out by the Meshing were inlet and outlet identifications being done. After that for the fluid flow analysis fluent software is used. The laminar flow model is used for this analysis purpose. The model is spitted in to the five cell Zones were three of zones (capillaries) are enabled by the porous zone. The fluid material that used to flow in the model is blood which consists of definite properties.

3.DESIGN AND DEVELOPMENT

For the design criteria the most important is dimensions of the geometry. The recent advancement in the radiological imaging helps to know about the dimensions of the model. The Autodesk Inventor software is more important in this project were the design is being build with certain limitations. Here the afferent arteriole, efferent arteriole and bowman's capsule were separately constructed and

then the assembling is being done. The model is being illustrated in the figure: 1.The Bowman 's capsule which consist of capillaries which is showed in the figure: 2.The dimensions of the geometry is showed in the Table: 1

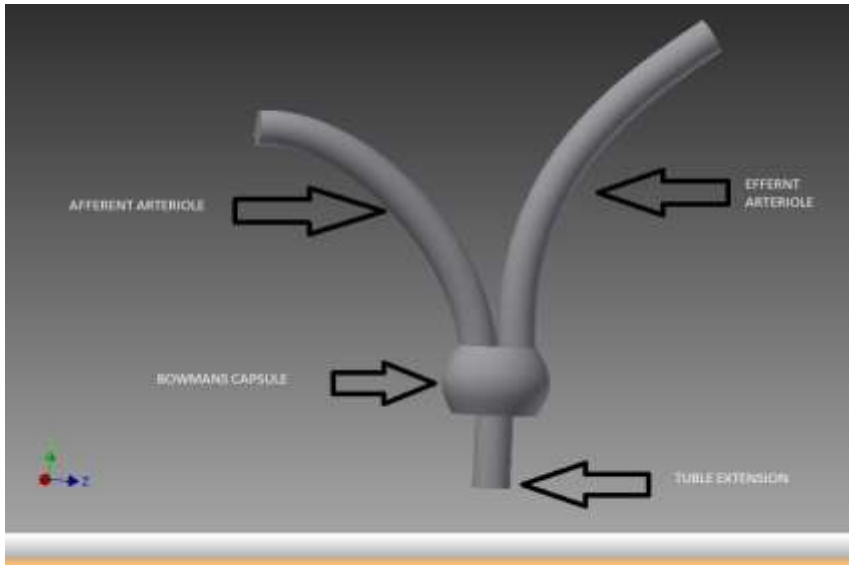


Figure1: The glomerulus model which is constructed using the Autodesk Inventor software.

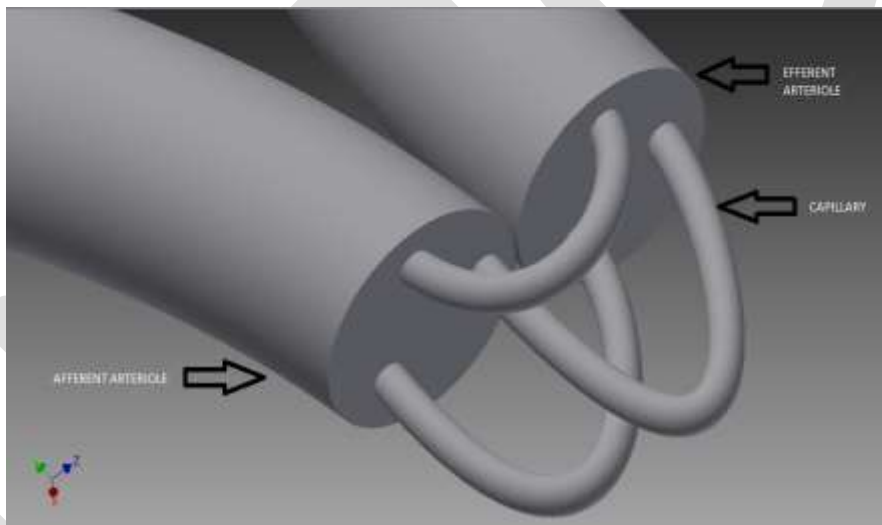


Figure2: The model which is showing capillaries connection between the afferent arteriole and efferent arteriole

3.1 DIMENSIONS OF THE GEOMETRY

PART	LENGTH	RADIUS
AFFERENT ARTERIOLE	45mm	5mm

EFFERENT ARTERIOLE	45mm	5mm
CAPILLARY 1	0.30mm	0.8mm
CAPILLARY 2	0.30mm	0.8mm
CAPILLARY 3	0.35mm	0.8mm

3.2 FLUID FLOW ANALYSIS OF THE GEOMETRY

The step after the geometry construction is the meshing of the model .For that the meshing of the model is being carried out by the meshing software .The inlet and the outlet of the fluid flow is marked for the further reference and it is showed in figure 3.

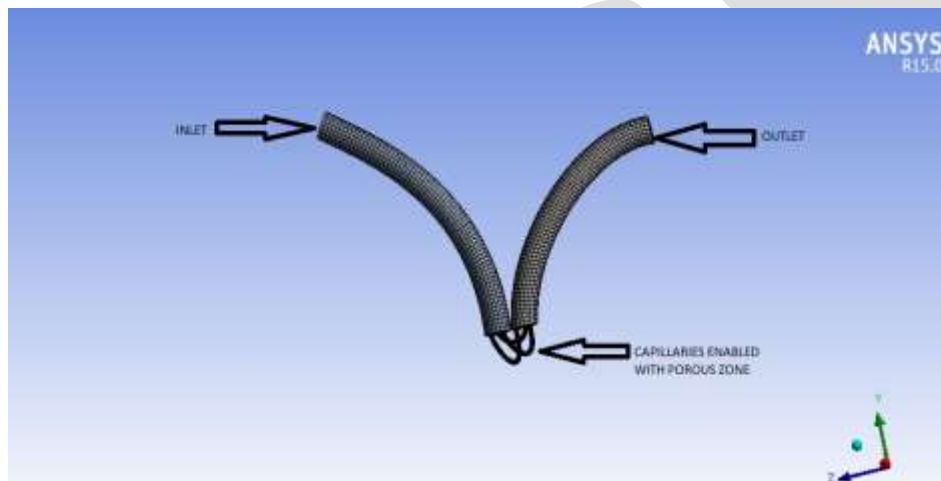


Figure3: Meshing of the geometry for the further reference of fluid flow analysis

4.SETUP CONSIDERATIONS

The setup considerations being started using the fluent software. Here the laminar flow is being selected for the analysis. The fluid here is created for the flow which shows the properties of the blood .Here there are five parts were two are arterioles and three are capillaries which were enabled by the porous zone using cell zone conditions. And the porous zone values were assigned in the boundary conditions

5.RESULT

1.PRESSURE VARIATION ACROSS THE CAPILLARIES

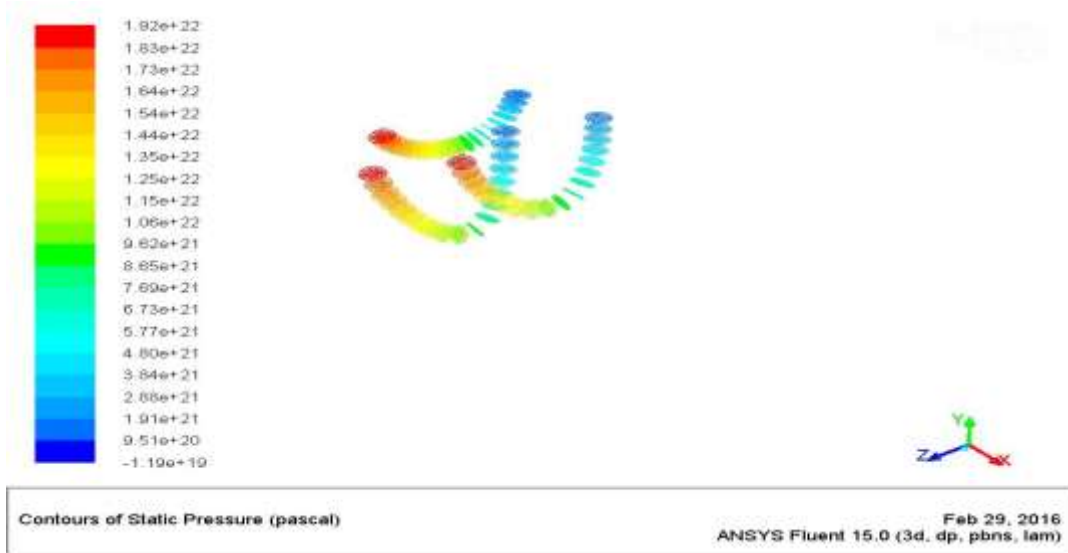


Figure4: Contours of static pressure (Pascal) is illustrated

2. VELOCITY VARIATION ACROSS THE CAPILLARIES

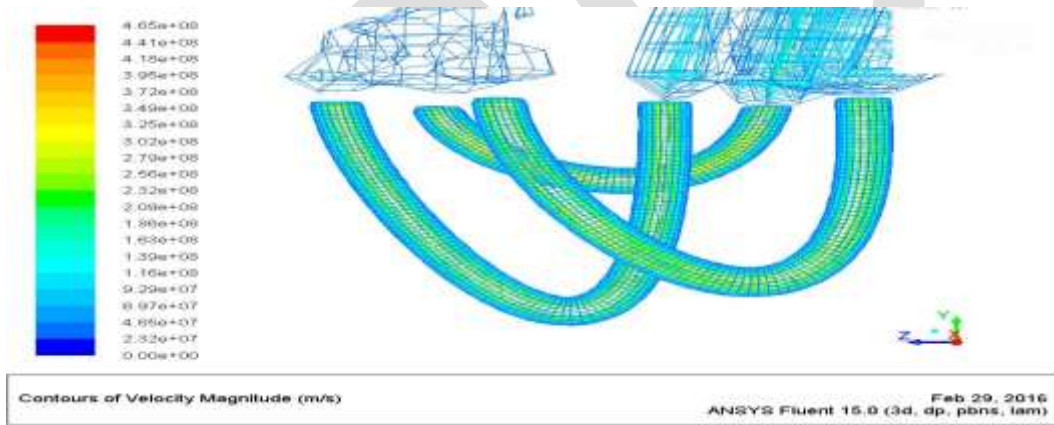
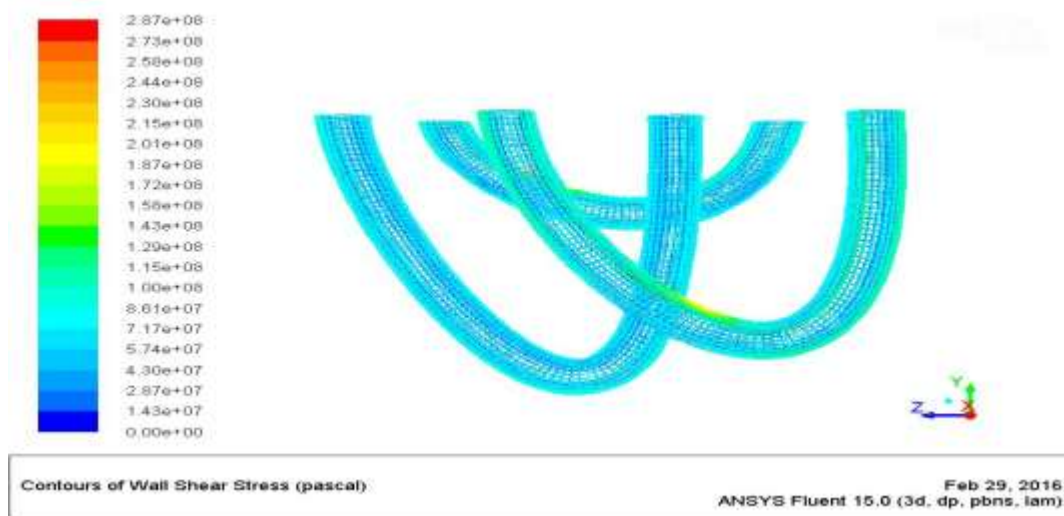


Figure5: Contours of velocity magnitude(m/s) is illustrated

3.WALL SHEAR STRESS ACROSS THE CAPILLARIES



6.CONCLUSION:

This paper describes the physical properties of capillaries that is responsible for glomerular filtration across glomerular layer. Here the velocity, pressure and the wall shear stress across the capillaries is being found. The static pressure is high when the blood enters the capillaries and gradually it decreases when it enter in to the efferent arteriole. The velocity in the arteriole is $0-9029e+07$ and when the fluid reaches the capillaries it get increased to $3.25e+08$. So the velocity is much more higher in capillaries when compared with the arterioles. The wall shear stress in the capillaries will be more in the surface layer so that the filtration made easier for the removal of particles

REFERENCES:

1. Neelam Bajpai, V. upadhyay, P.N pandey, Anil Agarawal, Harish Chandra, "A Newtonian model on the Two phase Renal Blood Flow in Renal Capillaries with special Reference to kidney Infection", IOSR Journal of mathematics (IOSR-JM), Vol.11, 2015, pp.01-11
2. Sapna Ratan Shah, "A mathematical study of blood flow through stenosed artery", International Journal of Universal Science and Engineering, Vol.no 1, 2015, pp.2454-7581
3. Bladimir Saldarrianga, Sergio A. Pinto, Luise. ballesteros "Morphological Expression of the Renal Artery A Direct Anatomical Study in a Colombia Half -Caste Population", International Journal of Morphology, 2008, pp.31-28
4. Sapnas, "Analysis of non -newtonian fluid flow in a stenosed artery", International Journal of Physical Science, Vol.4, 2009, pp.663-671
5. M.D Shihamal Islam, Jerzy Szpunar "Study of Dialyser membrane (polyflux 210H) and Effects of Different Parameters on Dialysis Performance", Open Journal of nephrology, 2013, pp.161-167
6. Omran Bkoush, Diagnostic and Prognostic Value of Proteinuria in Chronic renal disease, clinical studies, Department of Nephrology, Faculty of Medicine, University hospital in Lund, Sweden, 2004
7. Joao Pul o zambon, Renta s magalhaes, Inkap ko, Christina L Ross, Giuseppe orlando, Andrea peloso, Anthony Atala, James I yoo, Research paper, "kidney regeneration, where we are and future perspectives, world Journal of nephrology, 2014, pp.24-30
8. ADALBERT. BOHLE, BERNHARD AEIKENS, ALGUND EEN BOOM, LUDGER FONHOLT WOLF R. UDIGER PLATE, Human Glomerular Structure under normal Conditions and in Isolated glomerular disease, kidney International, Vol.54, suppl.67(1998), pp.186-188
9. Reiner M and Scott Baldiar G.W, "The flow through narrow tube .nature", London, 184:354-359(1959)

Anomalous Absorption of Surface Plasma Wave over a Metal Surface Embedded With Carbon Nano-Tubes

Deepika Goel[#], Prashant Chauhan, Anshu Varshney

Department of Physics and Material Science & Engineering, Jaypee Institute of Information Technology, Noida-201307, UP, India.

Email: deepika7nov@yahoo.co.in

Abstract -The anomalous absorption of surface plasma wave (SPW) by two dimensional arrays of carbon nanotubes, embedded over a metal surface with their length along \hat{x} direction is studied theoretically. As surface wave of frequency ω propagates through the nanotubes, electrons in the nanotubes start oscillating and dissipate their energy via collisions in the nanotubes resulting in resonant absorption of SPW energy at frequency $\omega \approx \omega_{pe} / \sqrt{2}$, where ω_{pe} is plasma frequency of electrons inside the nanotubes. The absorption of SPW by the nanotubes is enhanced and has a sharp peak at resonant frequency. Results revealed that absorption coefficient increases with the density of nanotubes. Effect of lattice permittivity variation on absorption coefficient is also studied

Keywords: Surface plasma waves, carbon nanotubes, Absorption, nanoparticles

INTRODUCTION

The interaction of electromagnetic radiations with carbon nanotubes (CNT) has been a very active area of research due to their outstanding mechanical, thermal, electrical, magnetic, and optical properties that make them an ideal material for optical switches, modulators and saturable absorbers [1-2]. Also, nanoscale dimensions and high carrier mobility makes them potential candidates for high performance electronics and sensing applications [3-5]. Smooth metal surface reradiates the electromagnetic wave energy in the surrounding medium due to high free electron density, resulting in poor absorption. Due to presence of CNT over the metal surface, the electromagnetic waves are absorbed at wave frequency close to the natural frequency of oscillations of the electron cloud [6]. Li et al. [7] have reported the optical absorption spectra of carbon nanotube array having electric field parallel to the tube direction and deduced the relationship between the absorption coefficient and the polarization angle of the array. Ahmed [8] reported the resonant absorption of laser light by two dimensional array of carbon nanotubes occurs at frequency $\omega \approx \omega_{pe} / \sqrt{2}$, where ω_{pe} is plasma frequency of electrons inside the nanotubes. Kumar and Tripathi [9] investigated linear and non linear interaction of laser with an array of carbon nanotubes and observed that surface plasmon resonance occurs at frequency $\omega \approx \omega_{pe} / \sqrt{2}$. The attenuation constant is also resonantly enhanced around these frequencies. The absorption of electromagnetic waves can be greatly enhanced when these waves gets mode converted into surface plasma wave (SPW) [10]. SPW are collective longitudinal oscillations of quasi-free electrons propagating along the interface of a metal and a dielectric medium (or free space). The electric field of these waves decays exponentially away from the interface in both media. The distance to which surface plasma wave lasts is called propagation length. The propagation length of the wave is of the order of 3900 Å in free space and 240 Å in the metal film [11]. The decay is rapid inside the metal as compared to dielectric. Surface plasma wave excites resonant plasma oscillations inside the nanotubes, embedded over the metal surface. At resonant frequency, the absorption constant rises sharply which corresponds to the strong dissipation of the surface wave energy via collisions of the free electrons of the nanotube [8]. Moradi [12] investigated the propagation of the coupled surface plasma waves in the metallic single-walled carbon nanotubes. Bliokh *et al.* [13] depicted both theoretically and experimentally

that resonant excitation of surface plasma waves can achieve total absorption of electromagnetic waves in overdense plasmas. Kumar *et al.* [14] theoretically studied the absorption of SPW energy by metal nanoparticles embedded over the metal surface. Results indicate the increase in absorption coefficient at frequency $\omega_{sp} = \omega_p / \sqrt{3}$, where ω_p is the plasma frequency.

In this paper, we study the absorption of surface plasma waves (SPW) by two dimensional array of carbon nanotubes embedded over the metal surface with their length along \hat{x} direction. The surface plasma wave is propagating over the metal surface in \hat{z} -direction and can be excited by using an attenuated total reflection configuration. It excites resonant plasma oscillations in the nanotubes incurring attenuation of the SPW due to absorption of energy by the nanotubes. Also, we analyse the effect on varying the density of nanotubes and lattice permittivity. This paper has been organised into three sections where introduction is presented as section 1. The propagation of SPW over the metal-vacuum interface and mathematical formalism for absorption of SPW by nanotubes is developed in section 2. Finally, results and conclusions are discussed in section 3.

ABSORPTION OF SURFACE PLASMA WAVES

Consider the metal free-space interface at $x = 0$. The metal occupies the half space for $(x < 0)$ and free space is for $(x > 0)$ as shown in Fig. 1.

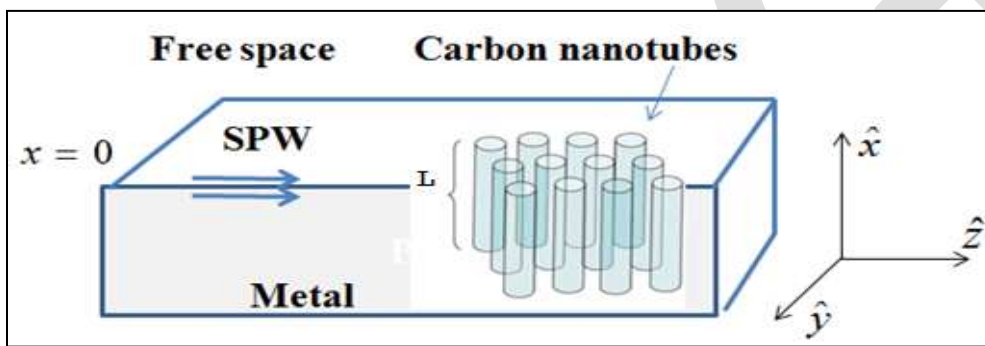


Fig. 10 Schematic of surface plasma wave propagation on metal free space interface embedded with carbon nanotubes.

The metal is characterized by lattice permittivity ϵ_L . The effective permittivity ϵ of metal is given by [8]

$$\epsilon = \epsilon_L - \frac{N\pi r_0^2 \omega_p^2}{(\omega^2 - \omega_{pe}^2 / 2 + i\nu\omega)}$$

ω is the incident surface plasma wave frequency. N is the number of nanotubes per unit area and r_0 is the radius of nanotubes. ν is the electron phonon collision frequency in the metal particle with $\nu^2 \ll \omega^2$ and $\omega_p^2 = 4\pi n e^2 / m$ is the plasma frequency. Here, $-e$ and m are the charge and effective mass of electron. n is the electron density at the metal surface. Suppose the SPW propagates along \hat{z} having electric field components in \hat{x} and \hat{z} directions given by

$$E_1 = \left[\frac{ik_z}{\alpha_1} \hat{x} + \hat{z} \right] A e^{-\alpha_1 x} e^{-i(\omega t - k_z z)} \quad \text{for } x > 0 \quad 2(a)$$

$$E_2 = \left[-\frac{ik_z}{\alpha_2} \hat{x} + \hat{z} \right] A_1 e^{\alpha_2 x} e^{-i(\omega t - k_z z)} \quad \text{for } x < 0 \quad 2(b)$$

where $\alpha_1 = (k_z^2 - \omega^2 / c^2)^{1/2}$ and $\alpha_2 = (k_z^2 - \omega^2 \epsilon / c^2)^{1/2}$. A and A_1 are constants.

Using the boundary conditions i.e. the normal component of \vec{D} and the tangential component of \vec{E} are continuous at the interface $x = 0$, the dispersion relation of surface plasma wave is

$$k_z = \frac{\omega}{c} \left(\frac{\epsilon}{1 + \epsilon} \right)^{1/2} \quad (3)$$

The dispersion relation is derived for low areal density of the nanotubes, so that the SPW field is not modified due to the presence of nanotubes. Consider two dimensional array of carbon nanotubes embedded over the metal surface with their length along \hat{x} direction. The SPW field [Eq. 2(a)] in the free space region ($x > 0$) interacts with the nanotubes. Under the influence of this field, electrons of the nanotube execute oscillations with displacement \vec{s} and their response is governed by the equation of motion, given by [15]

$$m \frac{d^2 \vec{s}}{dt^2} + m\nu \frac{d\vec{s}}{dt} + m \frac{\omega_{pe}^2 \vec{s}}{2} = -e\vec{E}_1 \quad (4)$$

ω_{pe} is the plasma frequency associated with free electrons in nanotube. Taking $\partial/\partial t = -i\omega$, \hat{x} and \hat{z} components of electron velocity are obtained by solving equation (4). These are given by

$$V_x = \frac{Ae\omega}{m(\omega^2 - \omega_{pe}^2/2 + i\nu\omega)} \left(\frac{k_z}{\alpha_1} \right) e^{-i\omega t} \quad (5a)$$

$$V_z = \frac{-ieA\omega}{m(\omega^2 - \omega_{pe}^2/2 + i\nu\omega)} e^{-i\omega t} \quad (5b)$$

The part of \vec{V} in phase with the electric field of SPW gives rise to time average power absorption per electron

$$\epsilon_{abs} = \frac{1}{2} \text{Re}[-e\vec{E}^* \cdot \vec{V}] \quad (6)$$

where \vec{E}^* is the complex conjugate of the SPW electric field in the free space. Substituting the values from equations 2(a), 5(a) and 5(b) in equation (6), we get

$$\epsilon_{abs} = \frac{1}{2} \left(\frac{e^2 A^2 \omega^2 \nu (1 + k_z^2 / \alpha_1^2)}{m((\omega^2 - \omega_{pe}^2/2)^2 + \nu^2 \omega^2)} \right) \quad (7)$$

Suppose the electron density in nanotube is n_e . The effective electron density n_{eff} in the region occupied by the array is

$$n_{eff} = N n_e \pi r_0^2 [8]. \text{ Then, energy absorbed by } n_{eff} \text{ nanotubes in distance } dz \text{ is } dP = -\epsilon_{abs} n_{eff} dz$$

$$dP = - \frac{\omega_{pe}^2 A^2 \nu \omega^2 (1 + k_z^2 / \alpha_1^2) N r_0^2}{8((\omega^2 - \omega_{pe}^2/2)^2 + \nu^2 \omega^2)} dz \quad (8)$$

Using Poynting theorem, the energy flow for surface plasma wave over the metal surface is given by

$$P = - \frac{A^2 c^2 k_z}{16\pi \alpha_1^2 \omega} \left(\frac{k_z^2}{\alpha_1} - \alpha_1 \right) \quad (9)$$

As the SPW propagates, the decay in energy of a beam propagating across a medium is given by $P = P_0 e^{-k_{ip} z}$, k_{ip} is absorption constant. On differentiating this equation w.r.t z and dividing the two equations, we get

$$\int_{P_0}^P \frac{dP}{P} = \int_0^z k_{ip} dz + C \quad (10)$$

where P_0 is the power at $z = 0$, while P is the power of SPW after the absorption length z . Substituting values of dP and P from eqns. (8) and (9) respectively in equation (10), we get the absorption constant k_{ip} , given as

$$k_{ip} = \frac{2N\pi r_0^2 \alpha_1^2 \omega_{pe}^2 \nu \omega^3 (1 + k_z^2 / \alpha_1^2)}{k_z c^2 ((\omega^2 - \omega_{pe}^2 / 2)^2 + \nu^2 \omega^2) (k_z^2 / \alpha_1 - \alpha_1)} \quad (11)$$

Equation (11) is normalized and solved numerically for the parameters, $\omega_{pe} = 4.079 \times 10^{15}$ rad/s and $\nu / \omega_p = 1.5 \times 10^{-2}$.

RESULTS AND DISCUSSION

The resonant absorption of SPW propagating on the metal free space interface embedded with nanotubes is studied. In figure 2, graph is plotted between normalized absorption constant ($k_{ip} c / \omega_p$) versus normalized frequency of SPW (ω / ω_{pe}) for $\epsilon_L = 1$. The absorption constant increases from 0.18 to 0.7 as $N\pi r_0^2$ is increased from 0.005 to 0.015. Resonance is sharply peaked at SPW frequency close to $\omega_{pe} / \sqrt{2}$. Ahmad [8] reported enhanced absorption of laser light by two dimensional arrays of nanotubes and it is sharply peaked around resonance frequency. Nurbek Kakenov *et al.* [16] experimentally studied the reflection spectra from the gold surface with increasing carbon nanotube densities using surface plasmon resonance. The absorption of SPW by nanotubes is facilitated by resonant plasma oscillations inside the nanotubes. The electrons inside the nanotube resonantly absorb SPW energy when the SPW frequency resonates with the surface charge oscillations of the nanotubes i.e. at $\omega = \omega_{pe} / \sqrt{2}$, where ω is the frequency of the SPW. At this frequency, there is sharp increase in absorption constant which corresponds to the strong dissipation of the surface wave energy via collisions of the free electrons of the tube. Absorption constant reduces sharply as one move away from the resonance point. The SPW propagating at the interface is influenced by the properties of the medium. In figures 3, normalized absorption constant ($k_{ip} c / \omega_p$) is plotted on varying lattice permittivity of metals. The plasmon field of the SPW is distorted when the lattice permittivity of the medium is changed [15]. It is observed that for particular value of $N\pi r_0^2 = 0.015$, the absorption constant decreases from 0.7 to 0.36 and resonance peak shifts towards smaller frequencies for variation of ϵ_L from 1 to 9.

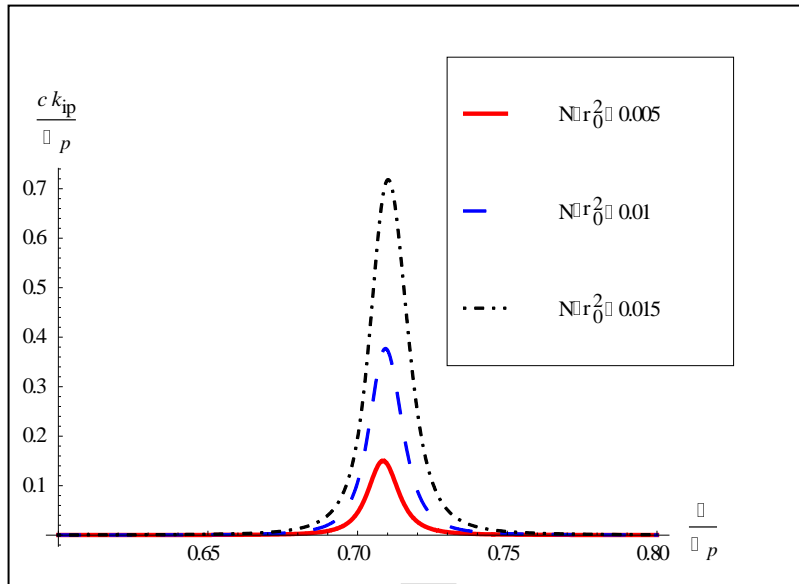


Fig. 2 Variation of normalized absorption constant ($k_{ip}c/\omega_{pe}$) versus normalized frequency (ω/ω_{pe}) for $\epsilon_L = 1$.

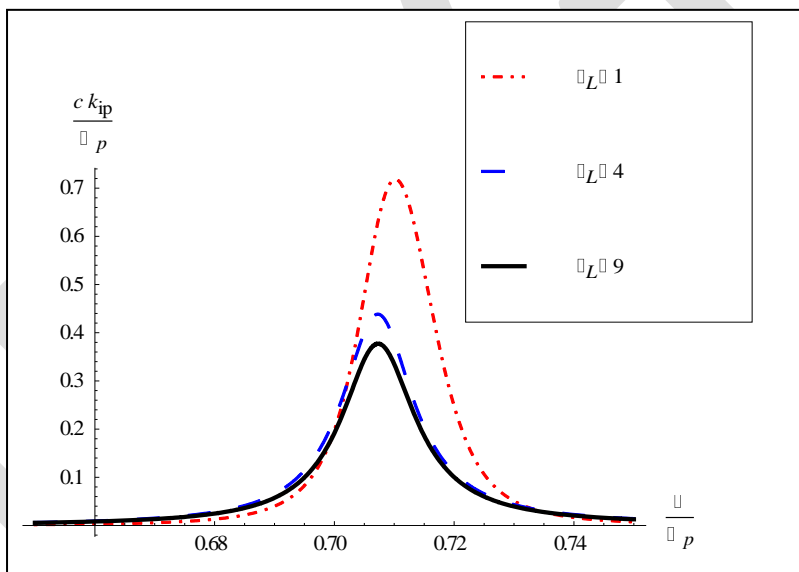


Fig. 3 Plot of normalized absorption constant ($k_{ip}c/\omega_{pe}$) versus normalized frequency (ω/ω_{pe}) on varying ϵ_L .

CONCLUSION

In conclusion, absorption of SPW by carbon nanotubes embedded over the metal surface occurs when SPW frequency becomes $1/\sqrt{2}$ times the plasma frequency associated with free electrons in nanotube. At this frequency, SPW induces a huge localized electric field inside the nanotubes and electrons dissipate their energy via collisions in the nanotubes. The absorption constant rises sharply and increases with the density of the nanotubes. The absorption coefficient is also influenced by the properties of the medium. This could be a good scheme to measure the surface plasma frequency in nanotube.

REFERENCES:

- 1) Dresselhaus M S, Dresselhaus G and Eklund P C 1996 Science of Fullerenes and Carbon Nanotubes, Academic Press, New York.
- 2) Wang C, Badmaev A, Jooyaie A, Bao M Q, Wang K L, Galatsis K and Zhou C W 2011 Radio frequency and linearity performance of transistors using high purity semiconducting carbon nanotubes *ACS Nano* 5, 4169-4176.
- 3) Kakenov N, Balci O, Balci S and Kocabas C 2012 Probing molecular interactions on carbon nanotube surfaces using surface plasmon resonance sensors *Applied Phy. Lett.* 101, 223114.
- 4) Schedin F, Geim A K, Morozov S V, Hill E W, Blake P, Katsnelson M I and Novoselov K S 2007 Detection of individual gas molecules adsorbed on graphene *Nature Mater* 6, 652-655.
- 5) Barone P W, Baik S, Heller D A and Strano M S 2005 Near infrared optical sensors based on single walled carbon nanotubes. *Nature Mater* 4, 86-92.
- 6) Haque M S, Marinelli C, Udrea F and Milne W I 2006 Absorption Characteristics of Single Wall Carbon Nanotubes *NSTI Nanotech, Boston*.
- 7) Li Z M, Tang Z K, Liu H J, Wang N, Chan C T, Saito R, Okada S, Li G D, Chen J S, Nagasawa N and Tsuda S 2001 Polarized Absorption Spectra of Single-Walled 4 Å Carbon Nanotubes Aligned in Channels of an AlPO₄-5 Single Crystal. *Phys. Rev. Lett.*, 87, 127401.
- 8) Ahmad A 2006 Parametric instabilities and plasma effects in nanotubes and nanoparticles. PhD Dissertation, Department of Physics, Indian Institute of technology Delhi, India.
- 9) Kumar M and Tripathi V K 2013 High power laser coupling to carbon nano-tubes and ion Coulomb explosion *Phy. of Plasma* 20, 092103.
- 10) Jonsson G E, Fredriksson H, Sellappan R and Chakarov D 2011 Nanostructures for enhanced light absorption in solar energy devices. *International Journal of Photoenergy* 11, 939807.
- 11) Raether H 1988 Surface plasmons on smooth and rough and on gratings. Springer Tracts in Modern Physics Vol. 111 *Springer, New York*.
- 12) Moradi A 2013 Coupled Surface plasmon-polariton modes of metallic single-walled carbon nanotubes *Plasmonics* 8, 1509-1513 (2013).
- 13) Bliokh Y P, Felsteiner J and Slutsker Y Z 2005 Total absorption of an electromagnetic wave by an overdense plasma *Phys. Rev. Lett* 95, 165003.
- 14) Kumar G and Tripathi V K 2007 Anomalous absorption of surface plasma wave by particles adsorbed on metal surface *Appl. Phys. Lett.* 91,161503.
- 15) Chen F F Introduction to plasma physics and controlled fusion. Vol. 1. *New York: Plenum*.
- 16) Kakenov N, Balci O, Balci S and Kocabas C 2012 Surface Plasmons in metallic nanoparticles: Probing molecular interactions on carbon nanotube surfaces using surface plasmon resonance sensors. *Appl. Phys. Lett.* 101, 223114.

Personalized Shopping App with Customer Feedback Mining and Secure Transaction

Swati H. Kalmegh, Nutan Dhande

Mtech Student, Department of CSE, swatikhalmegh@gmail.com Contact No. 9404725175

Abstract— Reputation-based trust models are important for the success of e-commerce systems. Reputation reporting systems have been implemented in e-commerce systems such as eBay and Amazon (for third-party sellers), where overall reputation scores for sellers are computed by aggregating feedback ratings. Feedback ratings are gathered together for computing sellers' reputation trust scores. A CommTrust system is proposed where the observation made by buyers are mostly used to express opinions about the product in free text feedback review. This paper provides personalized shopping app which suggest customer best seller companies with the help of opinion mining and user preferences and develop a secure transaction system with security techniques (cryptography and steganography).

Keywords— Electronic commerce, commTrust , Encryption, Payment Gateway, Security, Cryptography, Steganography.

INTRODUCTION

Accurate trust evaluation is crucial for the success of e-commerce systems. Reputation-based trust models are important for the success of e-commerce systems. Reputation reporting systems have been implemented in e-commerce systems such as eBay and Amazon (for third-party sellers), where overall reputation scores for sellers are computed by aggregating feedback ratings. For example on eBay, the reputation score for a seller is the *positive percentage score*, as the percentage of positive ratings out of the total number of positive ratings and negative ratings in the past year. But there is one problem called as the "all good reputation" problem, where feedback ratings are over 99% positive on average. Such strong positive bias cannot exactly guide buyers to select sellers to transact with. One possible reason for the lack of negative ratings at e-commerce web sites is that users who leave negative feedback ratings can attract retaliatory negative ratings and thus damage their own reputation.

Although buyers leave positive feedback ratings, they express some disappointment and negativeness in free text feedback comments, often towards specific aspects of transactions. We propose *Comment-based Multi-dimensional trust (CommTrust)*, a fine-grained multi-dimensional trust evaluation model by mining e-commerce feedback comments. With CommTrust, comprehensive trust profiles are computed for sellers, including dimension reputation scores and weights, as well as overall trust scores by aggregating dimension reputation scores. CommTrust is the first piece of work that computes fine-grained multi-dimension trust profiles automatically by mining feedback comments. Reputation-based trust models are widely used in e-commerce applications, and feedback ratings are aggregated to compute sellers' reputation trust scores. The "all good reputation" problem, however, is prevalent in current reputation systems— reputation scores are universally high for sellers and it is difficult for potential buyers to select trustworthy sellers. In this system, based on the observation that buyers often express opinions openly in free text feedback comments, we propose CommTrust for trust evaluation by mining feedback comments. Our main contributions include: 1) we propose a multidimensional trust model for computing reputation scores from user feedback comments; and 2) we propose an algorithm for mining feedback comments for dimension ratings and weights, combining techniques of natural language processing, opinion mining, and topic modeling. This system also provides security at the time of online shopping or transaction. This system provides seller recommendation which is not done in other systems. Also the system provides secure transaction with the security techniques. This system uses two level security model. Two level security model is used to prevent various possible attacks.

OBJECTIVES

- To develop a personalized shopping app which suggest customer best seller companies with the help of opinion mining and users preferences.
- To develop a secure transaction system with security techniques (cryptography and steganography).

LITERATURE REVIEW

Xiuzhen Zhang, Lishan Cui, and Yan Wang, Senior Member, IEEE, "Computing Multi-Dimensional Trust by Mining E-Commerce Feedback Comments"[1]- Reputation-based trust models are widely used in e-commerce applications, and feedback ratings are aggregated to compute sellers' reputation trust scores. The "all good reputation" problem, however, is prevalent in current reputation systems—reputation scores are universally high for sellers and it is difficult for potential buyers to select trustworthy sellers. In this paper, based on the observation that buyers often express opinions openly in free text feedback comments, we propose CommTrust for trust evaluation by mining feedback comments. Extensive experiments on eBay and Amazon data demonstrate that CommTrust can effectively address the "all good reputation" issue and rank sellers effectively. Compute comprehensive multi-dimensional trust profiles for sellers by uncovering dimension ratings embedded in feedback comments [1].

B. Pang and L. Lee, "Opinion mining and sentiment analysis,"[7]- This survey covers techniques and approaches that promise to directly enable opinion-oriented information-seeking systems. An important part of our information-gathering behavior has always been to find out what other people think. This survey covers techniques and approaches that promise to directly enable opinion-oriented information seeking systems. Our focus is on methods that seek to address the new challenges raised by sentiment ware applications, as compared to those that are already present in more traditional fact-based analysis. We include material on summarization of evaluative text and on broader issues regarding privacy, manipulation, and economic impact that the development of opinion-oriented information-access services gives rise to.

J. O'Donovan, B. Smyth, V. Evrim, and D. McLeod, "Extracting and visualizing trust relationships from online auction feedback comments,"[18]- This paper presents a system capable of extracting valuable negative information from the wealth of feedback comments on eBay, computing *personalized* and *feature-based* trust and presenting this information graphically. The algorithm operates on the assumption that online auction transactions can be categorized into a relatively small set of features. Buyers and sellers in online auctions are faced with the task of deciding who to entrust their business to based on a very limited amount of information. Current trust ratings on eBay average over 99% positive and are presented as a single number on a user's profile. This paper presents a system capable of extracting valuable negative information from the wealth of feedback comments on eBay, computing *personalized* and *feature-based* trust and presenting this information graphically.

Y. Zhang and Y. Fang, "A fine grained reputation system for reliable service selection in peer-to-peer networks,"[19]- This paper proposed a manual trust model and an automatic trust model that reduce influence of additional factors on reputation to truly reflect node trust. Distributed peer-to-peer (P2P) applications have been gaining momentum recently. In such applications, all participants are equal peers simultaneously functioning as both clients and servers to each other. A fundamental problem is, therefore, how to select reliable servers from a vast candidate pool.

PROBLEM DEFINATION:

Reputation reporting systems have been implemented in e-commerce systems such as eBay and Amazon (for third-party sellers), where overall reputation scores for sellers are computed by aggregating feedback ratings. But there is one problem called as the "all good reputation" problem, where feedback ratings are over 99% positive on average. Such strong positive bias cannot exactly guide buyers to select sellers to transact with. So to overcome this issue, we propose Personalized shopping app with customer opinion mining and secure payment techniques.

PROPOSED SYSTEM

Online Payment System- 2 Level Security Model

This system proposed personalized shopping app with customer opinion mining and secure payment techniques. 2 level security model is used to prevent 3 possible attacks given

- Shoulder Surfing attack
- Image Disclosure attack
- Email id attack

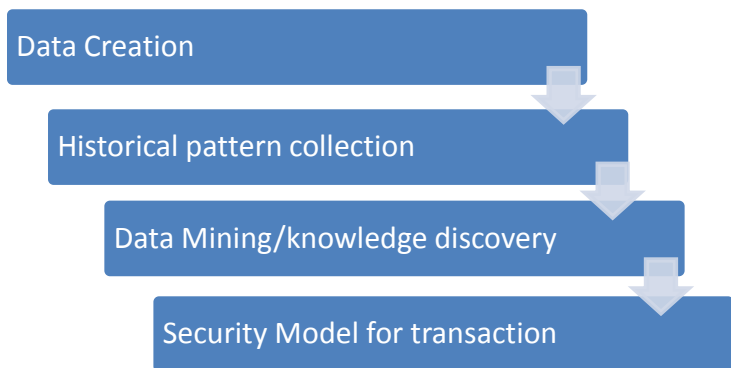


Fig 2: System architecture

- Encoded Image Verification
- One time verification code Authentication

MODULES

1. Admin-

- Create new company login
- View companies reports
- Analysis Reports in textual as well as Graphical format

This below snapshot shows company list.



Admin can manage company that is he can add new company. Admin will also check order details means pending orders, unpaid processed orders and paid orders.



2. Company Admin-

- Analysis Reports in textual as well as Graphical format
- Product Management
- Order Processing
- Ads and Offers management
- Customer feedbacks reports about products

Following snapshot shows the products details i.e. products of all category of particular company.



Field	Value
Customer Name	Sachin Daloke
DOB	12/09/1975
State	Maharashtra
District	Amravati
City	Amravati
Address	855, 88888
Gender	Male
Profession	Business
Annual Income	500000
Mobile	9421473008
Email ID	sachindaloke@gmail.com
UserID	sachin
Password	*****
Repeat Password	*****
Security Question	What is your pet name?

CONCLUSION:

In this way, this system suggest customer best seller companies with the help of opinion mining and user preferences and develop a secure transaction system with security techniques.

REFERENCES:

- [1] Xiuzhen Zhang, Lishan Cui, and Yan Wang "Computing Multi-Dimensional Trust by Mining E-Commerce Feedback Comments" vol. 26, no. 7, July 2014.
- [2] P. Resnick, K. Kuwabara, R. Zeckhauser, and E. Friedman, "Reputation systems: Facilitating trust in internet interactions," *Commun. ACM*, vol. 43, no. 12, pp. 45–48, 2000.
- [3] P. Resnick and R. Zeckhauser, "Trust among strangers in internet transactions: Empirical analysis of eBay's reputation system," *Econ. Internet E-Commerce*, vol.11, no. 11, pp. 127–157, Nov. 2002.
- [4] Jøsang, R. Ismail, and C. Boyd, "A survey of trust and reputation systems for online service provision," *DSS*, vol. 43, no. 2, pp. 618–644, 2007.
- [5] X. Wang, L. Liu, and J. Su, "RLM: A general model for trust representation and aggregation," *IEEE Trans. Serv. Comput.*, vol. 5, no. 1, pp. 131–143, Jan.–Mar. 2012.
- [6] M. De Marneffe and C. Manning, "The Stanford typed dependencies representation," in *Proc. CrossParser*, Stroudsburg, PA, USA, 2008.
- [7] B. Pang and L. Lee, "Opinion mining and sentiment analysis," *Found. Trends Inf. Ret.*, vol. 2, no. 1–2, pp. 1–135, Jan. 2008.
- [8] B. Liu, *Sentiment Analysis and Opinion Mining*. San Rafael, CA, USA: Morgan & Claypool Publishers, 2012.
- [9] D. M. Blei, A. Y. Ng, and M. I. Jordan, "Latent Dirichlet allocation," *J. Mach. Learn. Res.*, vol. 3, pp. 993–1022, Jan. 2003.
- [10] T. Hofmann, "Probabilistic latent semantic indexing," in *Proc. 22nd ACM SIGIR*, New York, NY, USA, 1999, pp.
- [11] Y. Lu, C. Zhai, and N. Sundaresan, "Rated aspect summarization of short comments," in *Proc. 18th Int. Conf. WWW*, New York, NY, USA, 2009.
- [12] Javelin Strategy & Research, "2013 Identify Fraud Report," <https://www.javelinstrategy.com/brochure/276>.
- [13] Anti-Phishing Working Group (APWG), "Phishing Activity Trends Report, 2013," http://docs.apwg.org/reports/apwg_trends_report_q2_2013.pdf.

Design and Manufacturing of Welding Fixture for Fuel tank Mounting Bracket

Prof. A. A. Karad^[1], Brijeshwar Wagh^[2], Ajay Shukla^[3], Niladhari Pyata^[4], Chetan Gujar^[5]

[1] Associate professor, Department of Mechanical Engineering, K.V.N. Naik Institute of Engineering Education and Research, Nashik

[2], [3], [4], [5] Students of B.E. [Mechanical], Department of Mechanical Engineering, K.V.N. Naik Institute of Engineering Education and Research, Nashik

[1] avinash.karad1974@gmail.com, 9860288527

[2] brijeshwarwagh000@gmail.com, 7588844767

Abstract— Fixtures, the component or assembly that holds a part undergoing machining, must be designed to fit the shape of that part and the type of machining being done. The parts to be welded are placed in proper position in fixture and tightened. Welding fixture holds and supports the work piece, prevents distortion in work piece during welding process and withstands high welding stresses. This paper gives detailed information about designing and manufacturing of welding fixture for fuel tank mounting bracket assembly. It contains various tilting and rotating arrangement which makes it versatile during its use. The material used for the fixture is mild steel which is capable of withstanding the load. CO₂ welding is used for the welding the parts of the bracket. It also contains number of locating pins which makes it accurate at the time of working. The coordinate or geometry off these pin position are measured with the help of coordinate measuring machine (CMM).

Keywords— Design, manufacturing, welding fixture, CMM.

1. INTRODUCTION

A fixture is a device for locating, holding and supporting a work piece during a manufacturing operation. Fixtures are essential elements of production processes as they are required in most of the automated manufacturing, inspection, and assembly operations. Fixtures must correctly locate a work piece in a given orientation with respect to a cutting tool or measuring device, or with respect to another component, as for instance in assembly or welding. Such location must be invariant in the sense that the devices must clamp and secure the work piece in that location for the particular processing Operation. Fixtures are normally designed for a definite operation to process a specific work piece and are designed and manufactured individually.

The correct relationship and alignment between the components to be assembled must be maintained in the welding fixture. To do this, a fixture is designed and built to hold, support and locate work piece to ensure that each component is joined within the specified limits. A fixture should be securely and rigidly clamp the component against the rest pads and locator upon which the work is done.

Fixtures vary in design from relatively simple tools to expensive, complicated devices. Fixtures also help to simplify metalworking operations performed on special equipments. Fixtures play an important role on reducing production cycle time and ensuring production quality, by proper locating and balanced clamping methods .Therefore to reduce production cost, fixture design, fabrication and its testing is critical.

Welding is a metal joining process by heating of the materials to a suitable temperature with or without the application of pressure, or by the application of pressure alone, with or without the use of filler metal. Welding is one of the most common processes in the manufacturing industries. The purpose of a welding fixture is to hold the parts to be welded in the proper relationship both before and after welding. Welding fixture will maintain the proper part relationship during welding. The process of fixture designing and manufacturing is considered complex process that requires the knowledge of various areas, such as geometry, tolerances, dimensions, procedures and manufacturing processes. Good fixture design will, of itself, largely determine the product reliability.

Welding fixture is the most common device used to align and retain the various pieces for welding.

1.1 Various element of fixture.

Generally, the entire fixture consists of the following elements.

Locators: A locator is usually a fixed component of a fixture. It is used to establish and maintain the position of a part in the fixture by constraining the movement of the part.

Clamps: A clamp is a force actuating mechanism of a fixture. The forces exerted by the clamps hold a part securely in the fixture against all other external forces.

Fixture Body: Fixture body, or tool body, is the major structural element of a fixture. It maintains the relationship between the fixture elements namely Locator, clamps, supports, and the machine tool on which the part is to be processed.

Supports: A support is a fixed or adjustable element of a fixture. When severe part displacement is expected under the action of imposed clamping and processing. Welding fixtures for work piece comprise the usual locating and clamping elements as used in other fixtures. However, the effect of heat and prevalence of welding spatter must be taken into account while designing hot joining fixtures.

1.2 Design of welding fixture.

Fixture components may be built into various arrangements to accommodate different workpieces. Fixtures must always be designed with economics in mind; the purpose of these devices is to reduce costs, and so they must be designed in such a way that the cost reduction outweighs the cost of implementing the fixture. It is usually better, from an economic standpoint, for a fixture to result in a small cost reduction for a process in constant use, than for a large cost reduction for a process used only occasionally. A common bench vise the left jaw is the immovable surface, and the right jaw is the movable clamp.

Most fixtures have a solid component, affixed to the floor or to the body of the machine and considered immovable relative to the motion of the machining bit, and one or more movable components known as clamps. These clamps (which may be operated by many different mechanical means) allow work pieces to be easily placed in the machine or removed, and yet stay secure during operation. Many are also adjustable, allowing for work pieces of different sizes to be used for different operations. Fixtures must be designed such that the pressure or motion of the machining operation (usually known as the feed) is directed primarily against the solid component of the fixture. This reduces the likelihood that the fixture will fail, interrupting the operation and potentially causing damage to infrastructure, components, or operators.

Fixtures may also be designed for very general or simple uses. These multi-use fixtures tend to be very simple themselves, often relying on the precision and ingenuity of the operator, as well as surfaces and components already present in the workshop, to provide the same benefits of a specially-designed fixture. Examples include workshop vises, adjustable clamps, and improvised devices such as weights and furniture.

The design of welding fixture for any manufacturing process has many objectives. The object are differs from one to another with respect to the type of operation to be done. The design objectives for designing for a welding fixture are

- To hold the part in most suitable position for welding
- To provide proper locating position.
- To provide proper suitable clamping to reduce distortion
- To provide proper heat control of the weld zone
- To provide clearance for filler metal
- To provide ease of operation and maximum accessibility to the point of weld

1.3 Problem statement.

Presently there are no perfect fixtures for the fuel tank mounting bracket, this is otherwise being welded by using hoist hook carriers and rotated to desired positions every time for welding. So it increases manufacturing lead time and increase man and money power also. So, it is necessary to develop a fixture to reduce the cycle time and having mass production.

1.4 Objective.

- **Productivity:** This reduces operation time and increases productivity
- **Skill Reduction:** Any average person can be trained to use fixtures. The replacement of a skilled labor with unskilled labor can effect substantial saving in labor cost.
- **Durable & occupies small space.**

- Retain framework in various position into which it is swung.

1.5 Methodology.

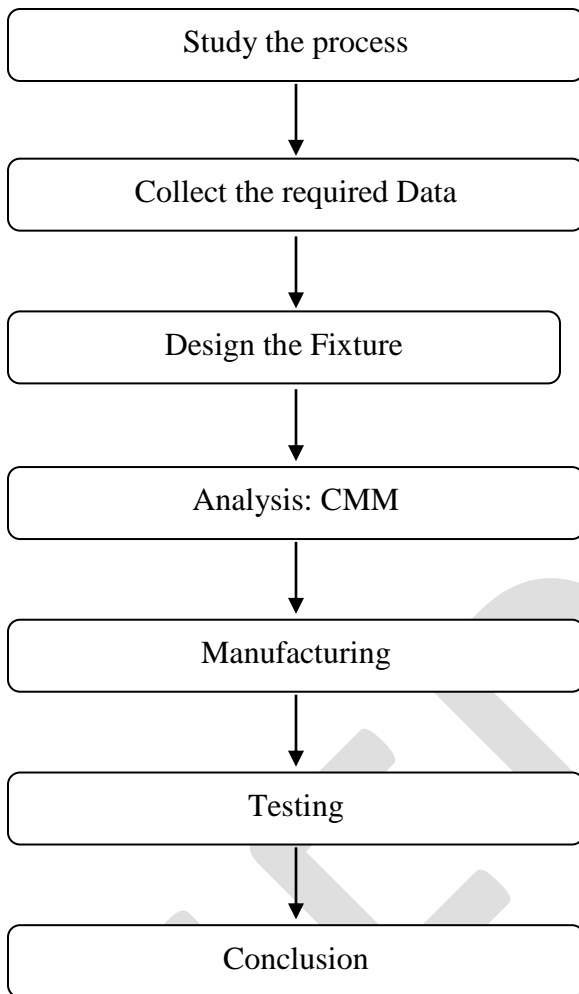


Fig No.1 Methodology flow chart.

The above flowchart shows the methodology of designing and manufacturing the welding fixture. The initial step is start with the material information of the bracket, machine specification, geometric dimensions and tolerances required to achieve on the bracket, and different parts of the bracket and their cad drawing. Then we have collect all the data required for designing the fixture as per the requirement of the bracket and then have to prepare the design the fixture with CAD drawing, after completion of cad model we have to analysis the fixture by CMM that is coordinate measuring machine of the fixture, When it is satisfied then we have to start manufacturing of fixture after that testing should be done either the fixture is made as per the designed and should work proper.

2. INTRODUCTION TO FUEL TANK MOUNTING BRACKET.

We have to design the welding fixture of the fuel tank mounting bracket of the Mahindra's bolero maxi truck. Before this we should have some basic information of the bracket like its parts, of which material it is to be made, etc. It consist of 6 parts as, L channel, L rib, C channel, strip and ribs which are 2 all the parts are made up of cold rolled steel. There 12 welding position from one side.

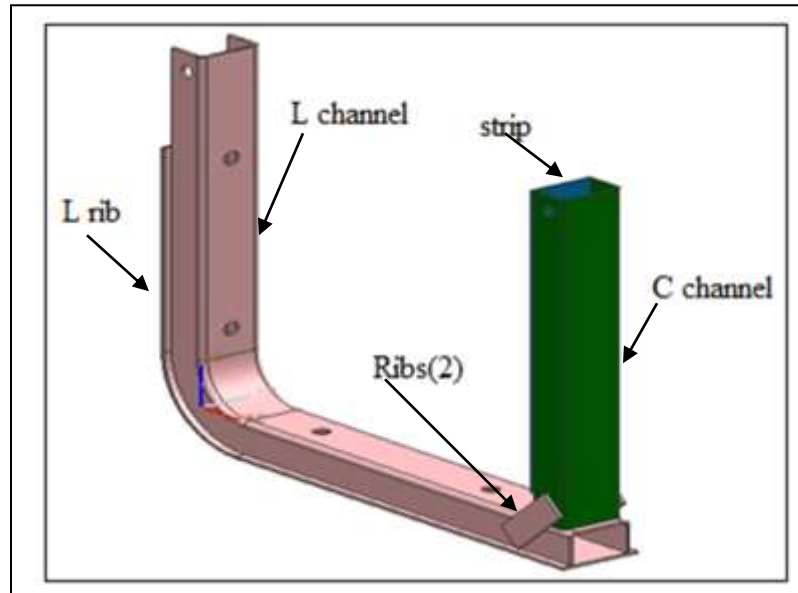


Fig No. 2 Fuel tank mounting Bracket and its parts.

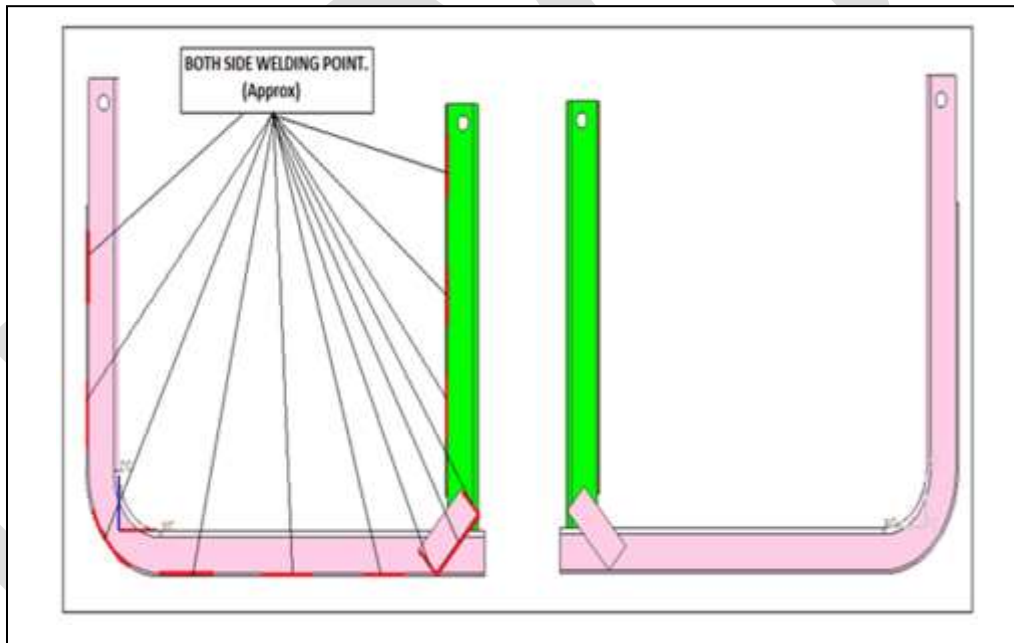


Fig No.3 welding points

3. WELDING FIXTURE FOR FUEL TANK MOUNTING BRACKET

As figure shows the assembly of welding fixture with fuel tank mounting bracket mounted. This welding fixture is specially design for this component to produce mass production and to reduce time consume.

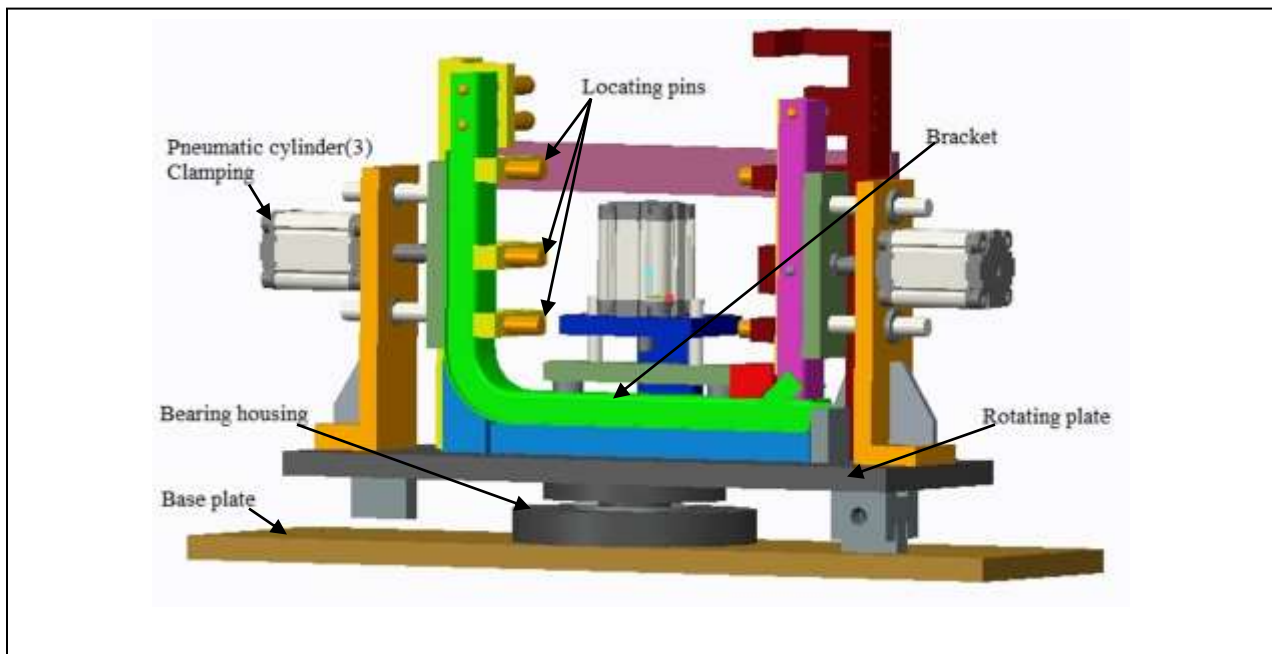


Fig No.4 welding fixture with bracket mounted

Basically this fixture is work as to reduce welder fatigue and to obtain the mass production. As shown in fig the main component is hold and supported in between the locaters and clampers. The rotating plate is mounted in plumber block to till the whole assembly of fixture up to 45° . There is a bearing housing on the rotating plate on which fixture rotating plate is mounted. That fixture rotating plate is rotating about 180° horizontally which reduce the time required to weld as compare to manual welding. Here is the distance is very important thing that should be as the distance is not maintain by the operator or by any technical reason the locaters locate that distance and it should not be accurate and alarm will be generated and the operator got an idea about that there is any misalignment in the component. same way the holes are presented for mounted that fuel tank on it if that holes are not present their or not made by the operator then the alarm will be generated an the operator get an idea that there is anything wrong and had to be solve and any misalignment is present in the fixture the whole system is stop and do not start welding on the component means the welding electrode is not come out from the welding arm.

3.1 Fixture rotating cycle.

- From 0 degree (home Position) to 180 degree, in vertical axis.
- From 0 degree (home Position) to -180 degree, in vertical axis.

3.2 Fixture tilting cycle

- From 0 degree (home position) to 45 degree, in horizontal axis.
- From 0 degree (home position) to -45 degree, in horizontal axis.

3.3 Operation cycle.

- Operator will load all the child parts in fixture. (At this time fixture in Home Position).
- Operator will clamp all the parts with help of pneumatic Cylinder & he will start the welding manually.
- If there is any problem / missing of features while clamping there will be alarm & Co_2 welding machine will not start. When operator willed solved this issue alarm will stop & Co_2 welding machine will ready for welding.

4. COORDINATE MEASURING MACHINEING (CMM) OF WELDING FIXTURE.

A coordinate measuring machine (CMM) is a device for measuring the physical geometrical characteristics of an object. It was carried out to check the positions of the locating points on the bracket are at their proper positions or not. There are total fourteen locating points on the bracket. The co-ordinates of these points were found out with the assistance of CMM and thus a report was generated with the help of software.

The CMM gives the detail idea about the points which are in the tolerance or out of tolerance. We check the co-ordinate of the locating position for the proper fixing of the bracket on the fixture with proper geometry. CMM is used to find the human error developed during the time of manufacturing of the fixture.

This report thus gives information about the different co-ordinates of the holes i.e. locating points.

There are 14 positions in the fixture as per the design and which needs to be located accurate position with respect to each other from reference.

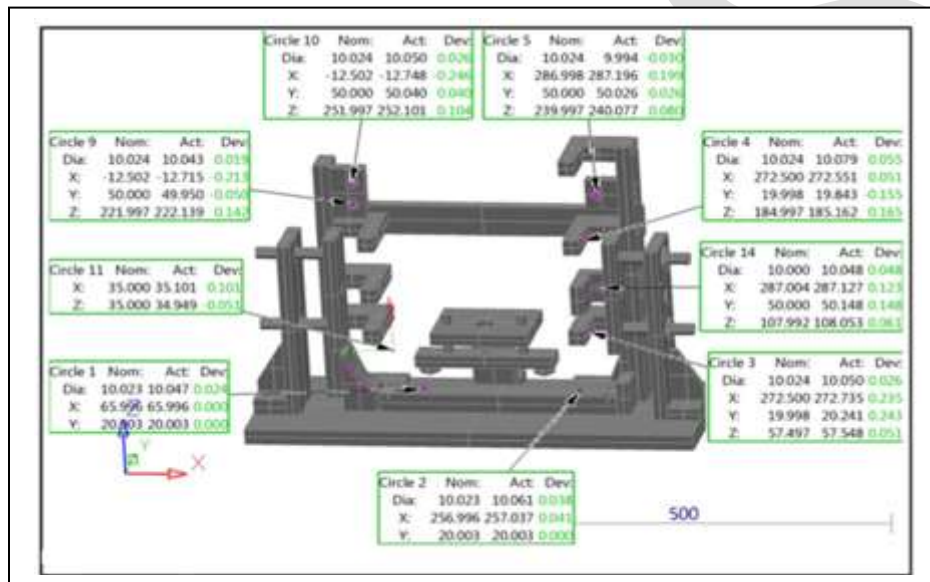


Fig No.5 CMM report 1

The CMM gives the idea about the locating position or locating holes are in tolerance or out of tolerance. The CMM defines the coordinate of the locating position as the manufacturing is done as per the designed. There is no error during manufacturing.

The CMM gives the actual reading of the locating position (circle) as they have high tolerance or low tolerance. It also gives the relation between the nominal and the measured dimensions of the locating position as deviation of the position and it also gives the any error if any.

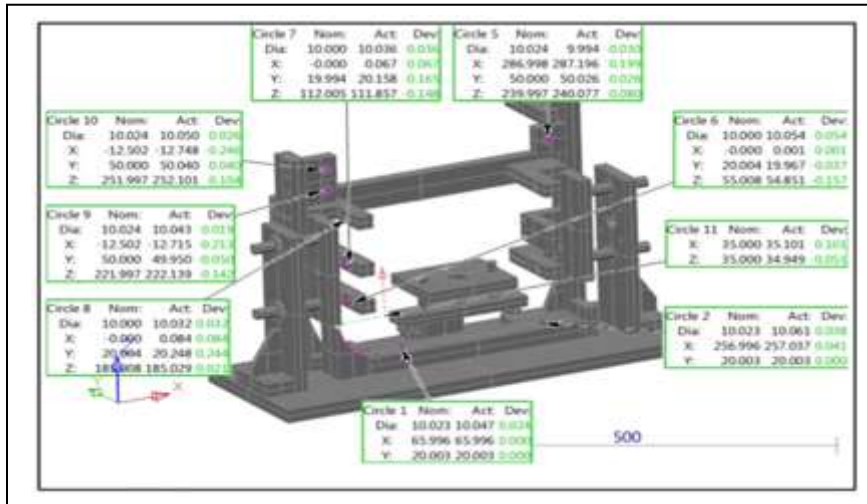


Fig No.6 CMM report 2

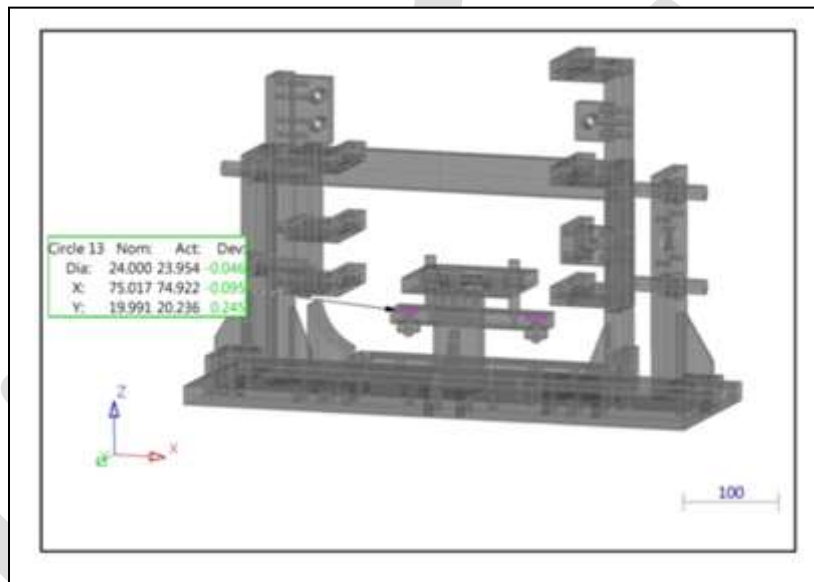


Fig No.7 CMM report 3

5. FUTURE SCOPE.

The welding fixture is designed to reduce the cost of production as well as be elimination being out of work and setting up of tools the fixture will increase the production rate by providing more number of parts in less time. Thus increasing the probability achieved from it. By using number of locating pins for proper location, the accuracy of the fixture increased. Thus allows in improvement of the part to be welded. It also provides an arrangement of interchangeability of the part which makes it flexible and eases the production.

It would also allow controlling quality control expenses of the organization. Thus enabling cost reduction in manufacturing of the parts to be produced. It will also enable to use less skilled labour which shows it reliance and importance and indirectly saving labour charges and number of labors required for the manufacturing process.

The automation part will allow improving the accuracy, reliability on fixture and elimination of wastage of unwanted parts. Last but not least it will improve the safety at work, thereby lowering the rate of accidents.

6. CONCLUSION

The Welding on number of fuel tank mounting bracket without changing the fixture is possible; hence it reduces work in progress, material handling time, work piece setup time and non-productive time. By using this fixture the misalignment occurring during Welding of fuel tank mounting bracket is effectively avoided, hence the accuracy of welding fatigue increases.

The efficiency and reliability of the fixture has enhanced as compared to earlier process. The cycle time required for loading and unloading the parts has reduced, thus improving and enabling interchangeability. It was found that conformability and stability has been achieved with help of fixture. The proposed fixture will hopefully achieve the production target and enhance the efficiency, increasing productivity, reducing elimination of parts, high quality of operation and reduce operation time and also reasonable.

REFERENCES:

- [1] Shailesh S. Pachbhai, Laukik P. Raut, "A Review on Design of Fixtures," International Journal of Engineering Research and General Science, Volume 2, Issue 2, Feb-Mar 2014.
- [2] R. D. Makwana, N. D. Gosvani, "A study on fixture design for complex part," International journal of futuristic trends in engineering and technology, Volume 1 (01), 2014.
- [3] V. R. Basha, J. J. Salunke, "An Advance Exploration on Fixture Design," International journal of engineering research and application, Volume 5, Issue 6 (Part-3), June 2015.
- [4] Siddesh K, Dr. D. Ramegowda, "Design of a welding fixture and analysis for the footrest stand component," International journal of engineering research and technology, Volume 4 Issue 04, April 2015.
- [5] Kalpesh khetani, Jafar Shah, Vishal Patel, Chitan Prajapati, Rohot Bhaskar, "Design and Thermal Stress Analysis of Welding Fixture of a Brake Pedal "International Journal on Recent Technologies in Mechanical and Electrical Engineering (IJRMEE) ,volume 2 issue: 5, May 2015.
- [6] Naveen A M, V A Girish , "Design of welding fixture of head end sub-assembly of motor case" International journal of scientific & technology research volume 3, issue 6, June 2014.
- [7] V. R. Basha, J. J. Salunke, "An Advance Exploration on Fixture Design," International journal of engineering research and application, Volume 5, Issue 6 (Part-3), June 2015.

Dynamic Security Skins

¹Ms.Madhavi Joshi, ²Prof. Y K Patil, ¹Ms.Madhavi Yeole, ¹Ms.Snehalata Bhondave

¹ Student, Department of CSE

¹JSPM College Of Engineering Pune

² Assistant Professor ,Department of CSE

²JSPM College Of Engineering Pune

Abstract- In Dynamic security skin, Passwords are the key to all digital secrets. Passwords stay on the most widely used confirmation method even with their well-known security weakness. Text password is the most accepted form of user authentication on websites due to its relieve and ease. This paper gives a check on different method that were introduce for safe guard of password on a network.

This paper present a scheme, Dynamic protection Skins, that allows a remote web server to prove its self in a way that is easy for a human user to verify & hard for an invader to skit. These schemes include a new password authentication & key-exchange protocol suitable for authenticating users & exchanging keys over an un-trusted network. In small DSS decrease user memory wants. As the final result the DSS provide toughest security.

Keywords —substantiation, domino result, glossary attacks, phishing

INTRODUCTION

In this paper, we studied the case of users authenticate web sites in the context of phishing attacks. Code word authentication protocol come in many flavour, but they all solve the same problem: One party must somehow show to one more party that it knows some password P, typically set in advance. Such protocols range from the trivial to the very complex, [1] and many of them present some form of defence from a diversity of attacks mount by hateful or extremely curious third parties.

In a phishing attack, the attacker spoofs a website (e.g., a financial services website). The enemy draw a casualty to the rascal website, occasionally by embed a linkage in message & heartening the user to snap on the bond.

Security is a division of in a row safety that deals exclusively with sanctuary of websites, web application and web forces. It is the main step to admission to any websites and hence the hackers always try to sneak through the usual security events and gain illegitimate access. Due to the general use of passwords, many security fear are involved in this area. Nowadays, even banking dealings are perform using passwords. Different researchers studied different types of passwords, their profit and drawback.

INFORMATION ANALYSIS

In this project, we inspect the case of users authenticate websites in the situation of phishing attacks. [4] The figure of unique phishing news submitted to APWG in the third section of 2009 reached an all time high of 40,621 in August, a number nearly 5.5 percent higher than the previous record high of 38,514 reported in September 2007.

- Unique Phishing reports submit to APWG, 2009 reached a record 40,621 in August, 5.5 percent more than the previous trace in September, 2007.
- Single Phishing websites reported to APWG reach a record 56,362 in August, displacing the previous record of 55,643 by 1.3 percent in April, 2007.
- The number of hijack brand rise to a proof 341 in August, up more than 10 percent from the earlier record of 310 in March 2009.
- Monetary air force rise back to the top of most under fire business sectors in 2009 after a short disarticulation by expense Services in 2009.
- Entire number of infected computers dropped to 11,001,646 in 2009, representing more than 48.35 percent of the total sample of scanned computers.

The Phishing difficulty show that we as security designers have a distance to travel. Because both attackers and designers use user interface tools, [2] examining this problem yields near into usability design for other time alone and safety areas. We inspect safety properties that make phishing a testing design difficulty.

REFUGE PROPERTIES

- Partial being skills assets :

This aim appears clear, but it implies a diverse come close to towards the design of security systems , humans are not universal principle computer. They are restricted by their natural skills and ability.

- Universal point graphics assets :

Condition , we are structure a scheme with the aim of is calculated to oppose spoofing we must presuppose that standardized realistic designs can be without problems copied.

- Fair arch assets :

We should leave to unusual lengths to check populace beginning mechanically transmission hope based on logos on your own. This model applies to the point out of refuge needle with icons while all right.

- Unenthusiastic customer assets :

Defence is regularly a resulting purpose , Generally users rather to meeting point on their main tasks, with so designers cannot wait for users to be highly enthused to direct their refuge.

➤ Hangar access assets :

This goods encourages us to plan systems that place a high right of way on helping users to keep susceptible data before it trees their run.

DYNAMIC SECUTITY SKINS

Energetic safety Skins is a scheme that allows in the sticks web browser to prove its self in such a way which is easy for being user to know & hard for enemy to satire.

We chose to mechanically recognize real web pages and their contented with aimlessly generated images. In this section we describe some approaches.

1. Browser-Generated Random Images

Assume that the browser generate a random number at the start of every verification deal. This number is known only to the browser, and is used to generate a unique image that will only be used for that transaction. The generated image is used by the browser to create a patterned window border. Once a server is effectively authenticated, the browser presents each webpage that is generated by that server using its own unique window border. The pattern of the window border is at the same time displayed in the user's trusted window. To validate a particular server window, the user only needs to make sure that two patterns match. All non-authenticated windows are displayed by the browser using a radically different, solid, non-patterned border, so that they cannot be mistaken for valid windows.

2. Server-Generated Random Images

We describe an come up to for the server to make images that can be used to mark trusted content. To achieve this, we take gain of some properties of the SRP protocol . In the last step of the protocol, the server presents a hash value to the user, which proves that the server holds the user's verifier. In our scheme, the server uses this value to generate an abstract image, using the visual hash algorithm described above. The user's browser can independently reach the same value as the server and can compute the same image (because it also knows the values of the verifier and the random values supplied by each party). The browser presents the user with the image that it expects to receive from the server in the trusted password window. Neither the user nor the server has to store any images in advance, since images are computed quickly from the seed.

3. Reliable trail towards the key Window

Our addition provides the user with a **trusted password window** that is dedicated to password entry and display of security information. We establish a trusted path to this window by assigning [5] each user a random photographic image that will always appear in that window. We refer to this as the user's *personal image*. The user should easily be able to recognize the personal image and should only enter his password when this image is displayed. As shown in Figure 1, the

personal image serves as the background of the window. The personal image is also transparently overlaid onto the textboxes. This ensures that user focus is on the image at the point of text entry and makes it more difficult to spoof the password entry boxes.



Figure 1 : Trusted Password Window

4. Verifier Based Protocol

We present a simple impression of the protocol to give an insight for how it works. To start, Carol chooses a password, picks a chance salt, and applies a one-way function to the code word to make a verifier. She send this verifier and the salt to the server as a one-time operation. The server will store the verifier as Carol's "password".[3] To login to the server, the only data that she needs to provide is her username, and the server will look up her salt and verifier. Next, Carol's client sends a random value to the server chosen by her client.

The server in turn sends Carol its own random values. Each party, using their knowledge of the verifier and the random values, can reach the same session key, a common value that is never shared. Carol sends a proof to the server that she knows the session key (this proof consists of a hash of the session key and the random values exchanged earlier). In the last step, the server sends its proof to Carol (this proof consists of a hash of the session key with Carol's proof and the random values generated earlier). At the end of this interaction, Carol is able to prove to the server that she knows the password without revealing it.

Secure Remote Password Protocol :

Our goal is to get verification of the user and the server, without significantly altering user password performance or increasing user recall burden. We chose to implement a verifier-based protocol. These protocols differ from square shared-secret confirmation protocol in that they do not entail two parties to share a secret key to authenticate each other. SRP allows a user and server to validate each other over an un-trusted system. We chose SRP because it is lightweight, well analyzed and has many useful properties. Namely, it allow us to preserve the familiar use of passwords, with no require the user to send his password to the server.

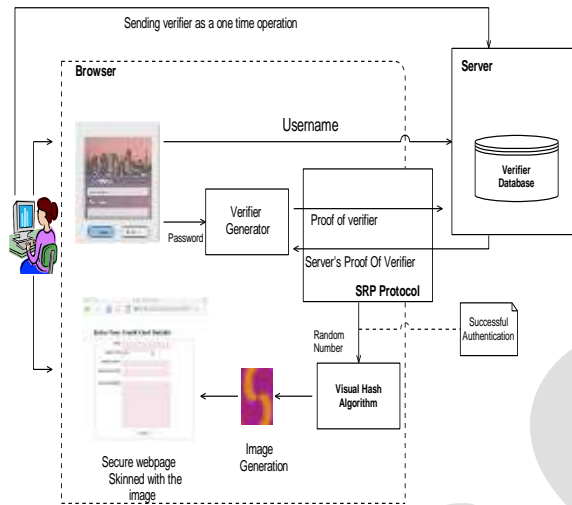


Figure 2: Block Diagram of DSS

CONCLUSION

Our whole project is java based and we know that java is most secured & reliable platform. As we are beginner so we didn't have money to invest in software and java is free to use, we choose database according to that only.

SRP is an improvement[6] on standard login/authentication programs. While adding any type of authentication can be seen as an improvement on current systems, SRP offers the advantages of being both unobtrusive to the day to day lives of users as well as not being too complex (or large) to be implemented in hardware or software, as we have shown.

Finally we are very proud to say that we worked as a team during the whole project work and we tried our best to complete the project according to requirement.

REFERENCES:

- [1] Rachana Dhamija & J.D.Tygar,"The Battle Against Phishing: Dynamic Security Skins"
- [2] Tom Wu,"Secure Remote Password (SRP) Authentication", *Stanford University*.
- [3] RFC 2944 – Telnet Authentication: SRP.
- [4] RFC 2945 – The SRP Authentication and Key Exchange System.
- [5] Patrick Naughton and Herbert Schildt,"Java 2: The Complete Reference", *Osborne/McGraw-Hill*.
- [6] "SRP Design Specifications ,SRP JavaScript Demo", www.srp.stanford.edu

[7] William Stallings, "Cryptography and Network Security: Principles and Practices", Pearson Education, Third Edition
"java information", www.sun.java.com

[8] "phishing information", www.apwg.org

IJERGS

Investigations on Mechanical properties of AL 8011 reinforced with micro B₄C / Red Mud by Stir Casting Method

C. KARTHIKKUMAR¹, R. BARANIRAJAN², I. PREMNAUTH³, P. MANIMARAN⁴

^{1, 2, 3} Students, Department of Mechanical Engineering, Christ College of Engg. And Technology, Puducherry, India

⁴ Assistant Professor, Department of Mechanical Engineering, Christ College of Engg. And Technology, Puducherry, India

Abstract- Aluminium metal matrix composites are emerging as the most versatile materials for unique structural, automotive, aviation, aerospace, defense, marine applications and other structural applications. Because of their excellent interfusion of properties. The potency of Aluminium Matrix Composite can be elevated, when it is reinforced with ceramic particles, which leads the Metal Matrix to elevate their mechanical properties to the reduced weight ratio. In this research a Hybrid Metal Matrix Composite of aluminium alloy is reinforced in conjunction with Boron Carbide of grain size of <10µm and Red Mud of grain size 150µm by using stir casting technique. In which, Red Mud is one of the major dreck material extracted from the bauxite ore of the Alumina during Bayer's Process. Red Mud is contemplated as a dangerous material regarding with NBR 10004/2004, which has been treated under the room condition as a reinforcement with Aluminum Metal Matrix. The samples were casted by varying the proportions in weight percentage by stir casting route. The samples are exposed to tensile, compression, micro hardness test and the dispersion of B₄C and Red Mud in the AMCs was observed in the micrographs. The results prevailed from the mechanical characterization shows the considerable elevation in strength and hardness of the Hybrid Metal Matrix Composite by reducing the weight ratio of the hybrid reinforcements.

Keywords: . Stir casting, hybrid composite, red mud, B₄C

INTRODUCTION

Stir casting is one of the best methods which is widely used worldwide for preparing particle reinforced aluminium matrix composites (PR-ALMC's) in order to produce the complex shapes easily and at a low cost. According to the type morphology and reinforcement, the AMC's are produced by different methods such as stir casting, squeeze casting, spray depositing and powder metallurgy. The above stir casting methods can be categorized under liquid stir casting and solid stir casting. In this investigation we have followed liquid stir casting method to reduce the cost. It involves the incorporation of dispersed phase into a molten metal matrix, followed by its solidification. These aluminium matrix composites are drawing more attention in aviation, aerospace, automobiles and many structural applications due to their good wear resistance with the extraordinary hardness.

Addition of reinforcement to the AMC's can increase the strength of particle reinforced aluminium matrix which imparts good mechanical properties. Addition of reinforcement to the matrix in the stir casting process is a challenging process specially where there is moisture present in the reinforcement materials. Hence the red mud is dried in hot sun for 15 hours [1]. At first B₄C is added to the AMC, where B₄C is a robust material having excellent chemical and thermal stability, High hardness and low density [2]. It is mostly used in nuclear industries due to their good capabilities of absorbing neutrons without creating long living radio nuclides. They are applicable in bullet proof vests, armor tanks, etc. Red mud is the extra ordinary wastage residue produced during the production of Alumina by Bayer's process. It is a insoluble product generated after the digestion from the sodium hydroxide at the higher temperature and the higher pressure which gives the residue of the bauxite which is known as the Red Mud.

EXPERIMENTAL PROCEDURE

The fabrication of aluminium 8011-B₄C-red mud compositions are used in this study and it was carried by stir casting method. In this, firstly the Al 8011 alloy in the form of 25mm diameter rods were placed in a clay graphite crucible. Then it is heated in muffle furnace to the desired temperature of 850 °C. Before the Al is melted, the B₄C of < 10µm is heated in another crucible to the temperature of 250 °C to remove moisture. Red mud is sieved for 150µm for second reinforcement. Then the particulates were mixed into the molten metal. The molten metal was covered with a degassing agent and with the flux to improve the quality of casting and to increase the casting speed of the aluminium 8011. The mixture was stirred by a mechanical stirrer for 5-10 min at a speed of 60 rpm. The temperature of the furnace remains constant at 850 °C during the addition of reinforcement particles.

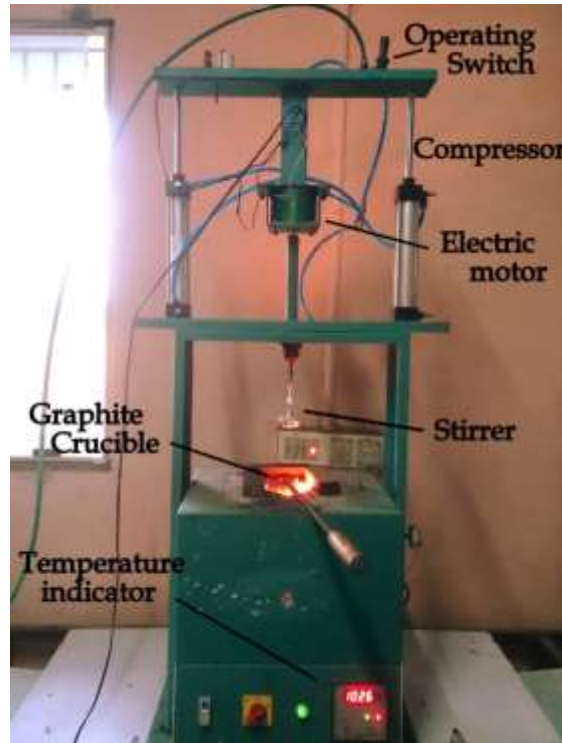


Figure 1. Stir Casting setup for fabrication of (Al8011/ B₄C/ Red Mud)

Then the molten aluminium metal matrix is poured in the preheated die for the preparation of specimen according to the ASTM standard. Same procedure is followed to fabricate AMC's with 1-5% of B₄C and red mud simultaneously. The stir casting set up used for producing composite specimen and the composite castings are shown.

Table 1. Process parameters used for Stir Casting

Parameters	Units	Value
Temperature of Melt	°C	850
Preheated temperature of B ₄ C Particles	°C	250
Preheated temperature of die	°C	400
Spindle Speed	rpm	60
Stirring time	min	10-15
Powder feed rate	g/s	0.8-1.2

EXPERIMENTAL MATERIALS

The following evaluation is associated with the characterization of mechanical properties on Al – Boron Carbide and Red Mud Metal Matrix Composite (MMC) of Aluminium alloy of grade 8011 with the addition of varying weight percentage composition of Boron Carbide and the Red Mud particles by Stir Casting Method. The properties were tested under the laboratory conditions. Variations in the properties are taken into a consideration.

For achievement of the above, a desired experimental setup was prepared to facilitate the preparation samples for the required specification, according to ASTM standards. The experiment was carried out by preparing the samples of varying percentage composition to predict the mechanical properties as well as to measure the Micro Hardness. An analyzed study of a Micro Structure had been conducted by the Optical Microscope to verify the dispersion of hybrid reinforcements.

PREPARATION OF CASTING DIE

Initially the die was made up of a low metal which can be corroded easily within a interval of time. Hence the die was surface finished by using emery papers without damaging the size of ASTM standard. After removing the rusts from the casting die, the die was made to preheated to the temperature of 400 °C for a constant time. Then clamped with two clamps vertically for the regular preparation of the samples without any voids.



Figure 2. Die used for Stir Casting

TESTS PERFORMED

- Tensile Test
- Compression Test
- Micro Hardness Test (BHN)
- Microstructure

Before initializing the testing, the samples were machined to the particular size according to the ASTM standards. Tested samples are being undergone Microstructure testing's by using De- Winton Inverted Trinocular Metallurgical Microscope.

TENSILE TEST

The ultimate tensile strength of various compositions was measured using 5 ton capacity servo hydraulic universal testing machine. Testing of the specimens was in the parallel direction of the applied load. In a stress- strain graph the initial portion of the curve is a straight line and it represents the proportionality of varying stress to strain values according to Hooke's law. When the load is increased continuously, in which the stress of the composite is no more proportional to the strain of the following composite. UTS is the maximum stress that a specimen can bear before its fracture due to the load and its original area. All the tests were conducted according to the ASTM E8-82 standards. The tensile specimens of diameter 16 mm and gauge length 100 mm were prepared by Stir Casting method. Six specimens were tested and the average values of the ultimate tensile strength and Elongation were measured.



Figure 3. Specimens which undergone Tensile Test.

HARDNESS TEST

Hardness test were conducted to find the resistance of plastic deformation of the composites under static or dynamic loads. The micro Vickers Hardness test is used in this present study to examine the hardness of the specimen. In this test the ball indenter of 0.5mm diameter is made to be tested by applying a load of 0.5 Kg for 20 seconds for each specimen. The averages of four varying positions of the specimen were considered as the highest hardness number.



Figure 4. Prepared specimens for Vickers Hardness Test

COMPRESSION TEST

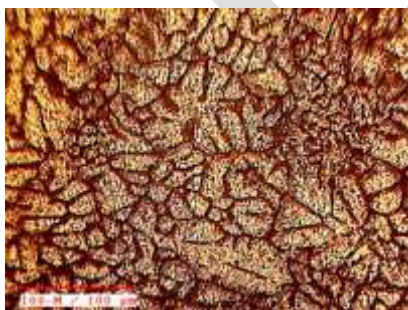
Compression test was carried out using a standard 5 ton capacity universal testing machine. Compression tests were conducted on specimens of 15 mm diameter and 60 mm length machined from the casted composites, by applying the loads gradually; the corresponding strains of the following composite were measured until failure of the specimen. The tests were made according to ASTM E9 at room temperature.



Figure 5. Specimens which were undergone for Compression Test

MICROSTRUCTURE

The microstructures of the varying composites are shown below for the presence of hybrid reinforcements in the Aluminium matrix composites. The Microstructure is studied by using De- Winton Inverted Trinocular Metallurgical Microscope. The samples with the both highest and lowest value for tensile and compression strength were studied for microstructure. The OM revealed the presence of B_4C in the layer of the aluminium matrix and the Red Mud is sedimented in between the matrix which is made the composites to increase its strength.



100X



200X



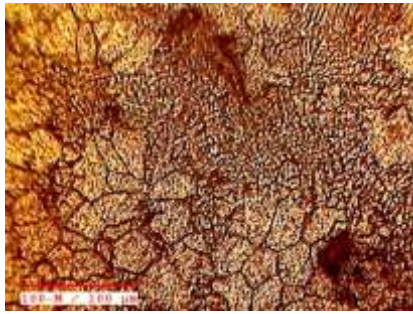
500X

HF

HF

HF

Figure 6. Pure Al without reinforcements



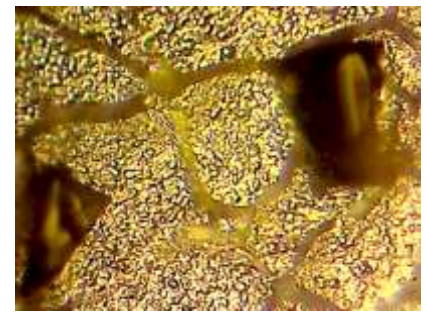
100X

HF



200X

HF



500X

HF

Figure 7. 94% Al + 3% B₄C + 3% Red Mud



100X

HF



200X

HF



500X

HF

Figure 8. 94% Al + 3% B₄C + 3% Red Mud

RESULT AND DISCUSSION

Table 2. Mechanical properties of Al/ Red mud and B₄C composite

Varying Wt% Composition	Tensile Strength Mpa	Hardness BHN	Yield Strength Mpa	Compression strength Mpa	Elongation %
Pure Al	65.315	37.5	57.441	66.426	18
94% Al + 5% B ₄ C + 1% Red Mud	67.543	39.6	55.226	71.141	9.2
94% Al + 4% B ₄ C + 2% Red Mud	71.044	36.6	46.932	61.826	12
94% Al + 3% B ₄ C + 3% Red Mud	77.024	45.4	59.973	76.877	22
94% Al + 2% B ₄ C + 2% Red Mud	72.038	43.7	52.613	65.164	12
94% Al + 1% B ₄ C + 5% Red Mud	70.872	43.4	51.973	70.271	8

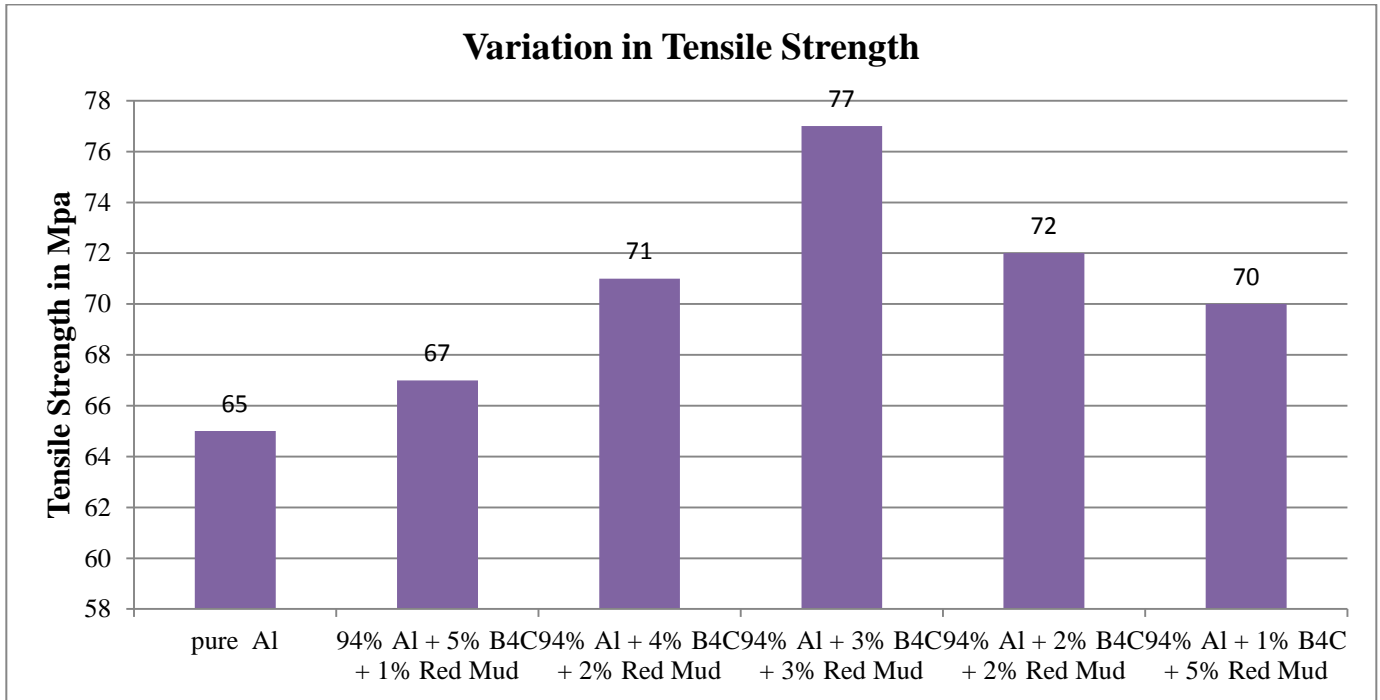


Fig.9 graph shows the variation in tensile strength from 5-1% of B₄C and 1-5% Red mud composite

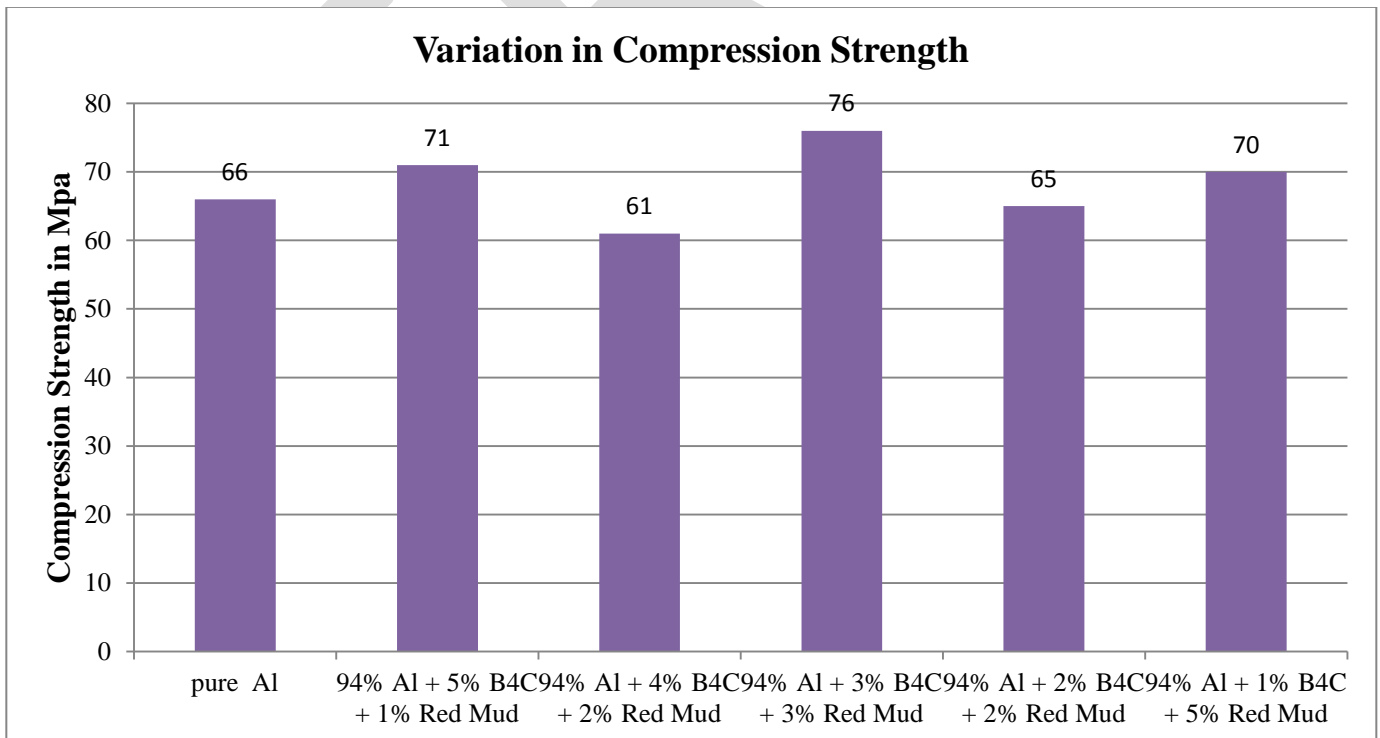


Fig.10 graph shows the variation in Compression strength from 5-1% of B₄C and 1-5% Red mud composite

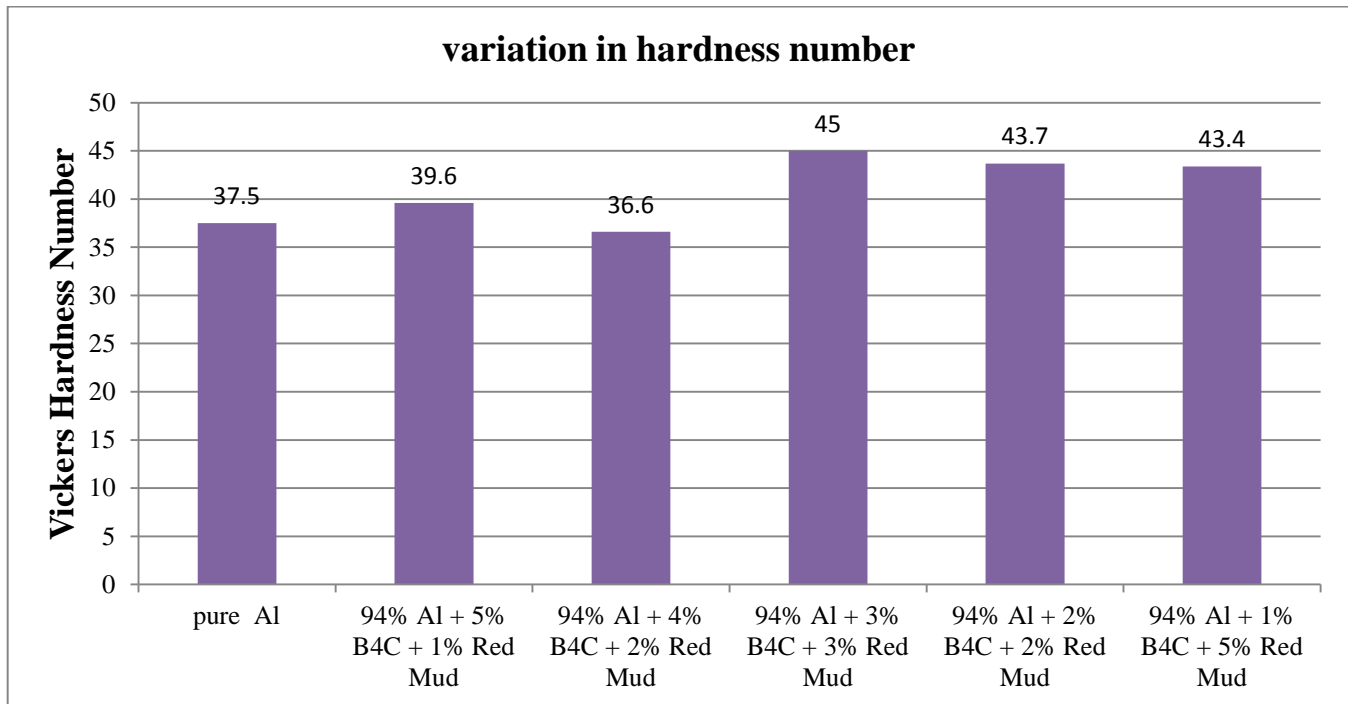


Fig.11 graph shows the variation in Hardness Number from 5-1% of B₄C and 1-5% Red mud composite

It has been observed that at 94% Al + 3% B₄C + 3% Red Mud, there is a considerable increased values in almost all the mechanical properties of the following hybrid composite.

CONCLUSION

Red mud is the waste generated product from alumina plant which can be successfully used as a reinforcing material to produce the particle reinforced aluminium matrix composites (PR-ALMC's) component to be used in the casting environment. It can be successfully used in the place of conventional aluminium intensive materials, and also by saving the usage of about 10 percent of matrix material could be achieved.

There is a good dispersion of red mud in aluminium matrix which improves the hardness of the matrix material of the hybrid composite. The effect is increase in interfacial area between the matrix material and the red mud particles leading to increase in strength appreciably. From this study that the oxide phases like Al₂O₃, Fe₂O₃, TiO₂ etc. have been dispersed uniformly in the interfacial areas of the aluminium matrix thus strengthening the result.

The general conclusion which is revealed from the present work is that by the combination of a matrix material with reinforcement such as B₄C and Red mud particles, it improves mechanical properties like tensile, compression strength, hardness and yield strength. The microstructure studies also indicate the presence of Aluminium dendrite structure with the fine inter metallic particles of B₄C and Red mud reinforced in between interfacial areas of the matrix.

REFERENCES:

- [1] Pradeep.R, "Evaluation of mechanical properties of aluminium alloy 7075 reinforced with silicon carbide and red mud composite", Vol-2, ISSN 2091-2730
- [2] V.C.Uvaraja, N.Natrajan. "Optimization of friction and wear behavior in hybrid metal matrix composites using taguchi technique", 2012, 11, 757-768
- [3] k. Upadhyaya, "composite materials for aerospace applications, developments in ceramics and metal matrix composites", Kamaleshwar Upadhyaya, Ed., warren dale, PA: TMS publications, 1992, pp. 3-24.
- [4] T.W. Clyne, An Introductory Overview of MMC System, Types and Developments, in Comprehensive Composite Materials, Vol-3; Metal Matrix Composites, T. W. Clyne (ed), Elsevier, 2000, pp.1-26.
- [5] V.Vembu, G.Ganesan "Heat treatment optimization for tensile properties of 8011 Al/ 15% Sic metal matrix composite using response surface methodology", Elsevier, Defence Technology 11(2015), 390-39.
- [6] L.M. Manocha, A.R. Bunsell "Advances in composite materials", Pergamon press Oxford, Vol.2, and P1233-1240.
- [7] Mahendra KV, Radhakrisna A Characterization of stir cast Al-Cu-(fly ash +Sic) hybrid metal matrix composites. J Comp Mater 2010;44:989-1005
- [8] S.A. Sajjadi. H.R. Ezatpour, "Microstructure and mechanical properties of Al- Al₂O₃ micro and nano composites fabricated by stir casting", Elsevier, Material science and Engineering A528 (2011) 8765-8771

CAMERA BASED PRODUCT IDENTIFICATION FOR THE VISUALLY IMPAIRED

Prof.Suvarna Bhoir
Information Technology Dept
Xavier Institute of Engineering
Mumbai

Ajeesh Abraham
Information Technology
Xavier Institute Of Engg
Mumbai
Mob No:8097115668

Krupa Wadhaya
Information Technology
Xavier Institute Of Engg
Mumbai

Abstract— This project is developed to make the life of blind people easy. This is a camera based system to scan the barcode behind the image and read the description of the product with the help of Id stored in the barcode. This is very beneficial in case of finding out the description of packaged goods to the blind people and thus helping them in deciding to purchase a product or not especially which are packaged. This is because it becomes very difficult for the blind people to distinguish between the packaged goods. In order to use this system, all the user needs to do is capture the image on the product in the mobile phone which then resolves the barcode which means it scans the image to find out the Id stored. Thus this application really benefits blind and visually impaired people and thus making their work of identifying products easy. This is very easy to use and affordable as it requires a scanner to scan the barcode and a camera phone to take the picture of the image containing the barcode. This is now easy to implement as most of the mobile phones today have the required resolution in order product description. This project can be implemented to scan the barcode to identify the Id stored in it and read out the in any shopping mall, supermarket, Book stores, Medical stores etc.

Keywords— Visually Impaired, Barcode, Smart Phones, Supermarket, Georgie Launcher, Audio Output, TTS (Text to Speech).

INTRODUCTION

The ability to identify products such as groceries and other products is very useful for blind and visually impaired persons, for whom such identification information may be inaccessible. There is thus considerable interest among these persons in barcode readers, which read the product barcodes that uniquely identify almost all commercial products.

The smartphone is a potentially convenient tool for reading product barcodes, since many people carry smartphones and would prefer not to carry a dedicated barcode reader even if the dedicated reader would be more effective. A variety of smartphone apps are available for reading barcodes such as the RedLaser and the ZXing which are for iPhone and Android respectively. A number of portable reading assistants have been designed specifically for the visually impaired. Mobile runs on a cell phone and allows the user to read mail, receipts, fliers, and many other documents. However, the document to be read must be nearly flat, placed on a clear, dark surface (i.e., a non-cluttered background), and contain mostly text. Mobile accurately reads black print on a white background, but has problems recognizing coloured text or text on a coloured background. It cannot read text with complex backgrounds, text printed on cylinders with warped or incomplete images (such as soup cans or medicine bottles).

PROPOSED SYSTEM

The Camera Based Product Identification system (see Fig.1) provides real-time feedback to first help the user find the barcode on a product using a smartphone camera or webcam and then help orient the camera to read the barcode.



Fig 1: Image shows user a barcode recognition system on a smartphone.

Our project takes several video frames per second and analyzes each frame to detect the presence of a barcode in it. The detection algorithm functions even when only part of the barcode is visible in the image, or when the barcode is too far away from the camera to

be read. Moreover, the barcode can appear at any orientation in the image and need not appear with its bars aligned horizontally or vertically. Whenever a barcode has been detected in an image, an audio tone is issued to alert the user.

The audio tone is modulated to help the user center the barcode in the image and bring the camera close enough to the barcode to capture detailed images of it. Specifically, the tone volume reflects the size of the barcode in the image, with higher volume indicating a more appropriate size (not too small or too big) and hence more appropriate viewing distance; the degree of tone continuity (from stuttered to continuous) indicates how well centered the barcode is in the image, with a more continuous tone corresponding to better centering. A visually impaired user first moves the camera slowly so as to find the barcode; further feedback helps the user to move the camera until the barcode is sufficiently well resolved and decoded. If the system reads a barcode and is sufficiently confident of its reading, the system reads aloud the barcode number (or information about the barcode such as the name of the product).

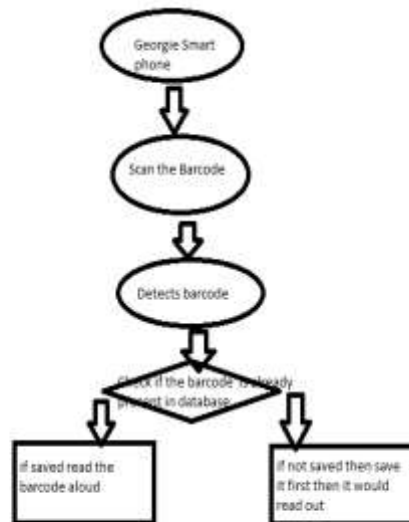


Fig 2: Flowchart of the proposed framework to read text from handheld objects.

Our experience with the system underscores the difficulty that blind users face in using a barcode reader, which requires them to search for barcodes on products in order to read them. This search can take longer on a smartphone-based system due to the much slower rate of processing, smaller detection range and narrower field of view compared with a dedicated system, implying a tradeoff between ease of detection and the burden of having to own and carry a separate device. Empirically we found that the search process tends to be shorter for smaller products (which present less surface area to be searched) and for rectangular packages (curved surfaces are awkward to search, forcing the user to rotate the package relative to the camera). Audio feedback is important for speeding up the search process, and the key to improving our system or other smartphone-based barcode readers in the future lies in improving the feedback.

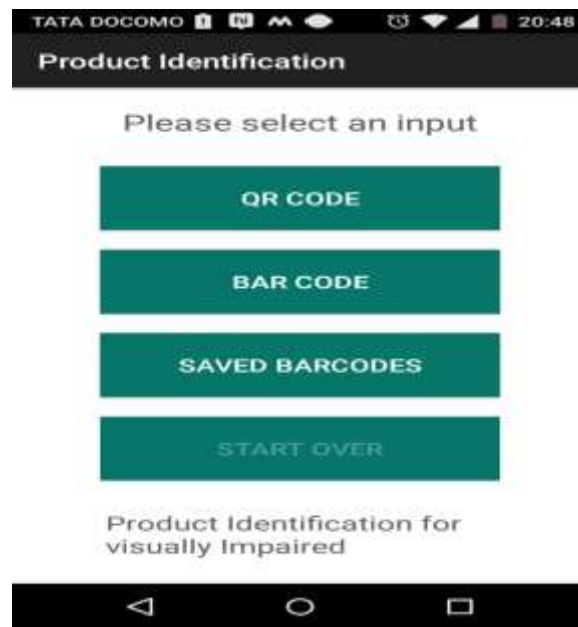


Fig 3: Snapshot of our application

The above image shows us a snapshot of the android application. Our application is developed for Android 4.0(Ice Cream Sandwich) and higher. Our Android application along with the Georgie Launcher could be used well by a visually impaired person as the launcher provides you with the audio output over the clicked button



Fig 4: Snapshot of the saved barcodes in our application.

Once the barcode is detected a description needs to be saved along with it (Fig 4). So the next time the same barcode is read the description saved is read aloud, thus the blind user recognizes the product.

ACKNOWLEDGMENT

We would like to thank Fr.Francis D'mello (Director of XIE) for providing us with such an environment so as to achieve goals of our project and supporting us constantly.

We express our sincere gratitude to our Honorable Principal Mr. Y.D.Venkatesh for encouragement and facilities provided to us.

We would like to place on record our deep sense of gratitude to Prof.Chhaya Narvekar, Head of Dept Of Information Technology, Xavier Institute of Engineering, Mahim, Mumbai, for her generous guidance help and useful suggestions.

With deep sense of gratitude we acknowledge the guidance of our project guide Prof. Suvarna Aranjo. The time-to-time assistance and encouragement by her has played an important role in the development of our project.

We would also like to thank our entire Information Technology staff who have willingly co-operated with us in resolving our queries and providing us all the required facilities on time.

CONCLUSION

This project represents a solution for finding and reading 1D barcodes, intended for use by the visually impaired users. A key feature of the algorithm is the ability to detect barcodes at some distance, allowing the user to rapidly scan packages before homing in on a barcode. Experimental results with a blindfolded subject demonstrate the feasibility of the system. In the future we plan to port our system to a camera phone, and to extend our system to symbologies other than UPC-A, such as the the EAN-13 (which is widespread in Europe).

Experiments with blind/visually impaired volunteer participants demonstrate the feasibility of the system and suggest that its usability is significantly enhanced by real-time feedback to help the user find barcodes before they are read.

We are exploring commercialization options of the application, including collaboration with an organization interested in releasing a consumer-oriented smartphone app that includes detailed information associated with a barcode (e.g., preparation instructions for packaged items).

REFERENCES:

- [1] A. Shahab, F. Shafait, and A. Dengel, "ICDAR 2011 robust reading competition:ICDAR Robust Reading Competition Challenge 2: Reading text in scene images," in Proc. Int. Conf. Document Anal. Recognition, 2011, pp. 1491–1496.
- [2] Advance Data Reports from the National Health Interview Survey (2008). http://www.cdc.gov/nchs/nhis/nhis_ad.htm
- [3] B. Epshtein, E. Ofek, and Y. Wexler, "Detecting text in natural scenes with stroke width transform," in Proc. Comput. Vision Pattern Recognition, 2010, pp. 2963–2970.
- [4] C. Yi and Y. Tian, "Assistive text reading from complex background for blind persons," in Proc. Int. Workshop Camera-Based Document Anal. Recognit., 2011, vol. LNCS-7139, pp. 15–28.
- [5] C. Yi and Y. Tian, "Text string detection from natural scenes by structure based partition and grouping," IEEE Trans. Image Process., vol. 20, no. 9, pp. 2594–2605, Sep. 2011.
- [6] International Workshop on Camera-Based Document Analysis and Recognition (CBDAR 2005, 2007, 2009, 2011). [Online]. Available: <http://www.m.cs.osakafuu.ac.jp/cbdar2011/>
- [7] A. Shahab, F. Shafait, and A. Dengel, "ICDAR 2011 robust reading competition:ICDAR Robust Reading Competition Challenge 2: Reading text in scene images," in Proc. Int. Conf. Document Anal. Recognition, 2011, pp. 1491–1496.
- [8] Advance Data Reports from the National Health Interview Survey (2008).[Online]. http://www.cdc.gov/nchs/nhis/nhis_ad.htm.
- [9] B. Epshtein, E. Ofek, and Y. Wexler, "Detecting text in natural scenes with stroke width transform," in Proc. Comput. Vision Pattern Recognition, 2010, pp. 2963–2970.
- [10] C. Yi and Y. Tian, "Assistive text reading from complex background for blind persons," in Proc. Int. Workshop Camera-Based Document Anal. Recognit., 2011, vol. LNCS-7139, pp. 15–28.
- [11] C. Yi and Y. Tian, "Text string detection from natural scenes by structure based partition and grouping," IEEE Trans. Image Process., vol. 20, no. 9, pp. 2594–2605, Sep. 2011.
- [12] International Workshop on Camera-Based Document Analysis and Recognition(CBDAR 2005, 2007,2009,2011).[Online].Available: <http://www.m.cs.osakafuu.ac.jp/cbdar2011/>
- [13] World Health Organization. (2009). 10 facts about blindness and visual impairment [Online]. Available: www.who.int/features/factfiles/blindness/blindness_facts/en/index.html

- [14] T.Phan,P.Shivakumara and C.L.Tan,“ALaplacianmethodforvideotext detection,” in Proc. Int. Conf. Document Anal. Recognit., 2009,pp. 66–70.
- [15] International Workshop on Camera-Based Document Analysis and Recognition (CBDAR 2005, 2007, 2009, 2011). [Online]. Available: <http://www.m.cs.osakafu-u.ac.jp/cbdar2011/>
- [16] N. Nikolaou and N. Papamarkos, “Color reduction for complex document images,” Int. J. Imaging Syst. Technol., vol. 19, pp. 14–26, 2009.
- [17] KReader Mobile User Guide, knfb Reading Technology Inc.(2008). [On-line]. Available: <http://www.knfbReading.com>
- [18] D. Dakopoulos and N. G. Bourbakis, “Wearable obstacle avoidance electronic travel aids for blind: survey,” IEEE Trans. Syst., Man, Cybern., vol. 40, no. 1, pp. 25–35, Jan. 2010.
- (19) Epshtein, E. Ofek, and Y. Wexler, “Detecting text in natural scenes with stroke width transform,” in Proc. Compute. Vision Pattern Recognit., 2010, pp. 2963–2970.
- [20] A. Shahab, F. Shafait, and A. Dengel, “ICDAR 2011 robust reading competition: ICDAR Robust Reading Competition Challenge 2: Reading text in scene images,” in Proc. Int. Conf. Document Anal. Recognit. 2011, pp. 1491–1496.
- [21] R. Manduchi and J. Coughlan, “(Computer) vision without sight,” Commun. ACM, vol. 55, no. 1, pp. 96–104, 2012.
- [22] The Portset Reader, TVI Technologies for the Visually Impaired Inc., Hauppauge, NY, USA. (2012). [Online]. Available: <http://www.tvi-web.com/products/porsetreader.html>

Repellent activity of essential oil extracted from *Artemisia annua* (Asteracea) grown in Cameroon (Africa) and Luxembourg (Europe)

Nkuitchou-Chougouo K. Rosine D.^{1,4}, Kouamouo Jonas¹, Wannang N. Noel², Yopa K. Nelly¹, Titilayo O. Johnson² Sandjon Bertrand³, Lutgen Pierre⁴, Tane Pierre⁴, Moyou S. Roger⁵.

¹Pharmacy Branch, Faculty of Health Sciences, Université des Montagnes, Bangangté Cameroon P.O.Box 208

²African Centre of Excellence in Phytomedicine Research and Development, University of Jos Nigeria

³Phytorica Laboratory, Pharmacy Bonapriso, Njoh Njoh – street, Douala Cameroon

⁴Iwerliewen Fir Bedreete Volleker (IFBV)-BELHERB, BP 98 Niederaanven, L-6905 Luxembourg

⁵Laboratory of Natural Products, Department of Organic Chemistry, University of Dschang, Cameroon

⁶ Parasitology Laboratory, Institute of Medical Research and the Study of Medicinal Plants (IMPM) Yaoundé Cameroon

Email: nrosinedesiree12@yahoo.com; tel: +237 [677468510](tel:677468510)

Introduction: *Artemisia annua* is an annual plant of China origin well known for its medicinal value due to its diverse chemical composition. The extract of *A. annua* cultivated in Cameroon is rich in essential oil; the larvicidal antibacterial and antifungal properties of *A. annua* had been reported. In the continuation of these works, we investigated the repulsive effect of this plant material.

Materials and methods: The essential oil of *Artemisia annua* of Cameroon and that of Luxemburg were obtained by hydro-distillation of dry leaves of *Artemisia annua* from the two countries. In order to determine their repulsive activities, two methods were used: One of the standard W.H.O (night catch on exposed human legs) and Cage tests (Bigoga models). All methods were validated and the results analyzed using student *t* test.

Results: The turnover of the extraction of the two essential oils gave 0.16%. The repulsive activity was evaluated at the concentration of 0, 50, 100, 200, 300 and 400 part per million (ppm). After the application of the two types of oil by the two methods, we observed that the two plants produced repulsive properties from 50 ppm up to 400 ppm. The time of protection is in an average of 3 hours, but this reduces as the essential oil is diluted.

Conclusion: Essential oil extract from the leaves of *Artemisia annua* cultivated in Cameroon and in Luxemburg have similar repulsive properties on adult *Anopheles gambiae*.

Key words: *Artemisia annua*, *Anopheles gambiae*, essential oil, repulsive, hydro-distillation

INTRODUCTION

Malaria is an infectious disease caused by a parasite of the genus *Plasmodium*, which infects red blood cells. The disease is as old as history and till date, it is a major problem especially in Asia, Africa, Central America, South America and the Caribbean. It remains

the most important parasitic disease affecting mostly children under 5 years and pregnant women [1]. According to WHO, (2015) an estimate of 214 million (with an uncertainty range between 154 million and 289 million) were reported cases of malaria, with about 438,000 (with a margin of uncertainty between 390000 and 636000) deaths [2]. Approximately 3.2 billion people, almost half the world's population, are exposed to malaria risk. This high rate is alarming, thus, scientists around the world have taken from their health priorities the fight against malaria. Recently, Niyondiko and Dembélé introduced soap for protection against the vector [3]. This innovation reinforces the curative control measures (such as ACTs) and preventive (such as bed nets impregnated with long-term consolidation of the domestic environment, sprays, repellants etc) in order to minimize the burden of malaria.

An ethnobotanical study conducted in Kilimanjaro (Tanzania) showed that the most widely used repellent, by the locals are *Ocimum kilimandscharicum* and *Ocimum suave*. The study further showed that the essential oils in these plant material is responsible for activity against bites and perching activity from Anopheles vectors [1].

Much work has been done on *Artemisia annua* in the laboratories of the (Université des Montagnes), and it showed that it is very rich in chemical compounds giving it numerous anti malarial, larvicidal, antibacterial and antifungal properties [4]. So far, positive results have been obtained on the curative plan, but further efforts are still required in terms of prevention.

Optimum protection can be provided by its application as a repellent. It is in this context of continual fight against malaria that we studied the repellent activity of essential oils extracted from *A. annua*.

MATERIALS AND METHODS

Study Sites

The extraction of essential oil from *A. annua* (Cameroon and Luxembourg) was conducted in Phytorica laboratory in Douala (Dr. Bertrand Sandjon) located at the Njoh Njoh - street, with a hydro- distillation device. The study of repellent properties was conducted at night, in the locality of Ebang, so chosen because of the vegetation and climatic condition which favours mosquito growth (10 km from the city of Yaounde on the Yaounde - Obala road in Cameroon) and in the premises of the Parasitology laboratory, in the Institute of Medical Research and the Study of Medicinal Plants (IMPM) in Yaoundé (central region).

Plant Material

A. annua was registered at the Cameroon National Herbarium with voucher number 65647/HNC. Samples used in this study were grown in September 2012 and harvested in February 2013. The

fresh leaves were used.

Extraction of Essential oil

The principle of hydro-distillation was used [5]. 200g of fresh leaves was boiled in 1 L water in a 2L flask for 2 hours. The steam drives essential oils from the product through a column connected to a condenser which condenses the vapor (Figure 1). The hydrosol obtained was then allowed to settle into a separatory funnel in which the previous mixture separates into two immiscible phases. The phase which contains the essential oil floats because it is of lower density than water. The oils extracted were dried using anhydrous sodium sulfate.

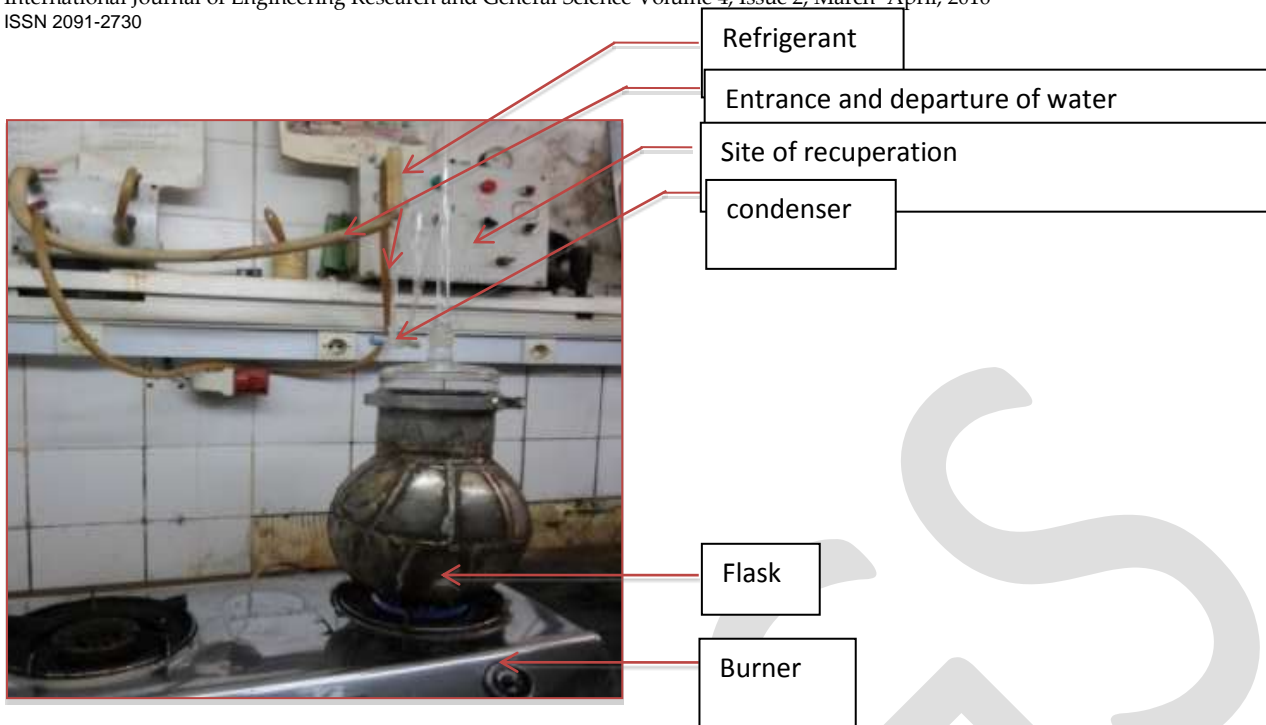


Figure 1: Scheme of Laboratory Phytorica Hydro-distillation

Culturing of *Anopheles gambiae* eggs

The *Anopheles gambiae* eggs were obtained from the insectarium of the Coordinating Organization for the fight Against Endemic Diseases in Central Africa (OCEAC) in Yaounde, Cameroon. This is basically to put in contact with water the *Anopheles* eggs so that they hatch into larvae that later become adult *Anopheles*. The eggs were placed in contact with the source water in plastic plates (3 cm³ of water in plastic plates of 20 cm in diameter). Hatching occurred 48 hours later. Upon hatching, the larvae were fed with a mixture of proteins. The larvae were exposed to the sun during the day (from 8 to 16 hours) and set in the dark at night to observe the circadian cycle they need for their growth.

Breeding process of *Anopheles*

The embryonic development lasted two days and the egg was hatched to release an L1 larva measuring just 1 millimeter. These larvae of *Anopheles* were maintained parallel to the surface of the water. After consecutive molts, the larva reached the stage 4 (L4), measuring 6 to 12 mm. L4 larvae passed to the pupal stage. At the end of this stage, the nymph was immobilized to the surface of the water, the mosquito extended its abdomen and an adult mosquito emerged with a dorsal slit of the exoskeleton (Figure 2).

This emergence lasted only a few minutes though left for 3 days to mature (while feeding them with sugar water) prior to experiment of the test cage method.

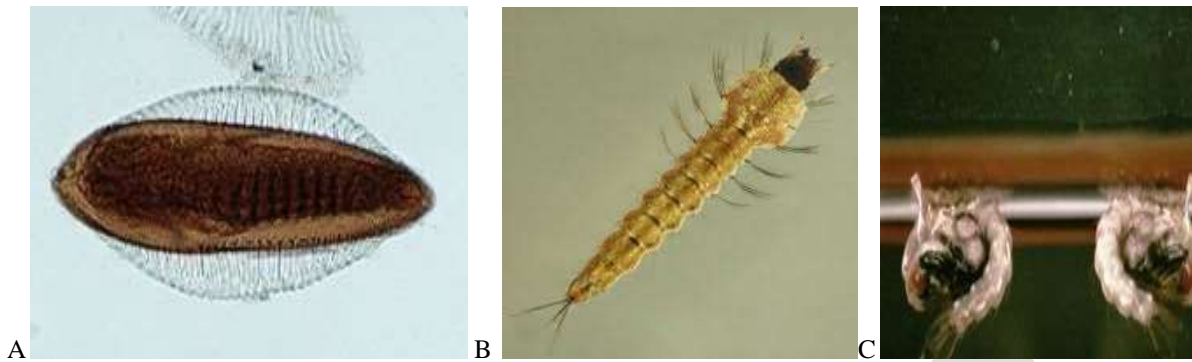


Figure 2: A Eggs, B larvae and C pupae of Anopheles C [16]

We cultured 1500 Anopheles eggs; 1200 eggs (80%) have reached the end of their growth.

Repellant activity

This was achieved in 2 ways: through the night trapping method on human volunteers and by the test method in cages. To afford this, we obtain the inform consent of participants and ethical clearance N^o: 2013/CIE-UdM/Pr was obtained from the ethical institutional comity of “Université des Montagnes”.

The concentrations were made at 0, 50, 100, 200, 300 and 400 ppm by dilution with ethanol. Upon administration of the essential oil by rubbing on the legs of volunteers and observing the perch and bite activities of the vector from 8 pm to 6 am daily (figure3). This experiment was done in a quiet environment, to avoid distraction from noise.



Figure 3: Night trapping method on human volunteers

In the test cages methods, the test was based on observing Anopheles adults movements between an untreated cage and a cage pretreated with increasing concentrations of test material (figure 4).



Figure 4: Test cage of Bigoga model

The test was done under laboratory controlled temperature ($27 \pm 2^\circ\text{C}$) and relative humidity ($80 \pm 2\%$). A 1ml of formulation 50, 100, 200, 300 and 400 ppm of oil fraction was applied on the inner surfaces of which the surface is about 324 cm^2 (treated), and connected to the untreated group [6].

100 female Anopheles were introduced into the cages and mosquito behavior was observed every 30 minutes for three (3) days. The protection time was measured (period between the introduction of the mosquitoes in the treated cage and the time it takes to move to the untreated). If no mosquito returns to the cage treated after 4 hours, the test is stopped and the protection time is rated 4 hours. Each test is repeated 2 times.

RESULTS

Extraction and characteristics of essential oils

Four kilograms of dry leaves of *Artemisia annua* from both sources produced a yield of 0.16% yield (Table I). The characteristics were camphor smell, light green in color and have an oily consistency.

Table I: Extraction yield and characteristics of essential oils

	<i>Artemisia annua</i> from Cameroun	<i>Artemisia annua</i> from Luxembourg
Quantity of dry leaves	4kg	4kg
Weight of E.O	6.5g	6.5g
Yield	0.16%	0.16%
Color	Light green	Light green
Consistency	Oily	Oily
Odor	Aromatic camphor	Aromatic camphor

Repellent activity on volunteers

The harvest consists of 10% of *Mansonia*, *Culex* 60% and 30% *A. gambiae*. Treatment with extract (E.O) of Cameroon reduced *A. gambiae* to 4% and *Mansoni* to 1%. The majority population was *Culex* 95%. Treatment with extract of Luxembourg reduced *A. gambiae* to 25%, the *Culex* was (70%) (Table II)

Table II: Summary of quantities of captured vectors

	Control (witness)	E.O from Cameroun	E.O from Luxembourg
<i>Mansonia</i>	10%	1%	5%
<i>Culex</i>	60%	95%	70%
<i>Anopheles gambiae</i>	30%	4%	25%
Total	100%	100%	100%

Repellent activity in the laboratory

At concentrations of 50 and 100 ppm, the repellent effect of the two essential oils was observed from the 30th minute. This effect was maximal after 1 hour of exposure to 50 ppm. It is from 1:30 min to 100 ppm. This activity later decreased after 150 minutes.

After 4 hours of exposure, residual repellent effect was found to be 10% for *Anopheles* at 100 ppm. There was more repulsive effect at a dose of 50 ppm after 4 hours of exposure.

At 200 ppm, the repellent effect was immediately maximal, resulting in the abandonment of the cage treated with the extracts by all the vectors. This repulsive effect decreased slightly to 150 minutes (2:30 min). At 4 hours, the residual effect was 10%.

At 300 ppm, the protection was 100% at 3 hours. At 4 hours this rate of protection decreased to 30%

A concentration of 400 ppm, the total protection time was 3h 30min. At the fourth time, the repulsion rate was 90% (Figure 5 and 6)

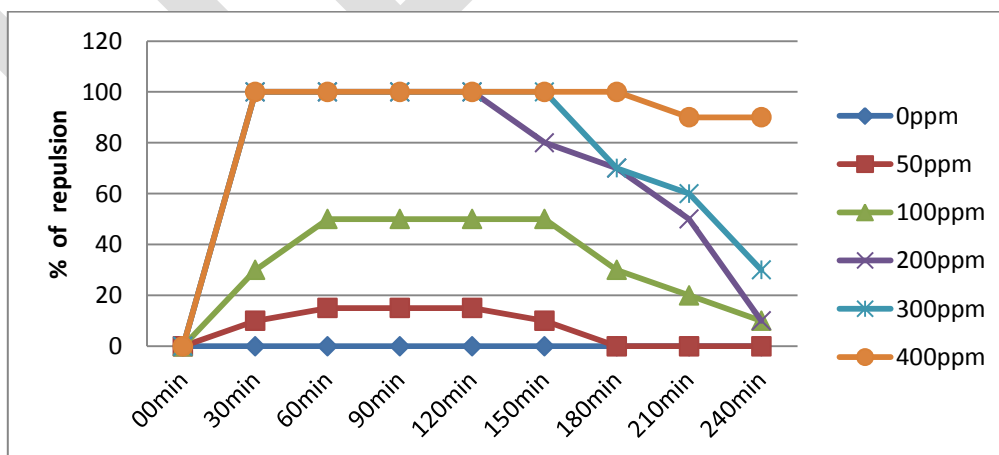


Figure 5: Repulsion of *A. gambiae* in the laboratory (Cameroon)

Luxembourg's essential oil repellent activity is the same as that of Cameroon (Figure 4)

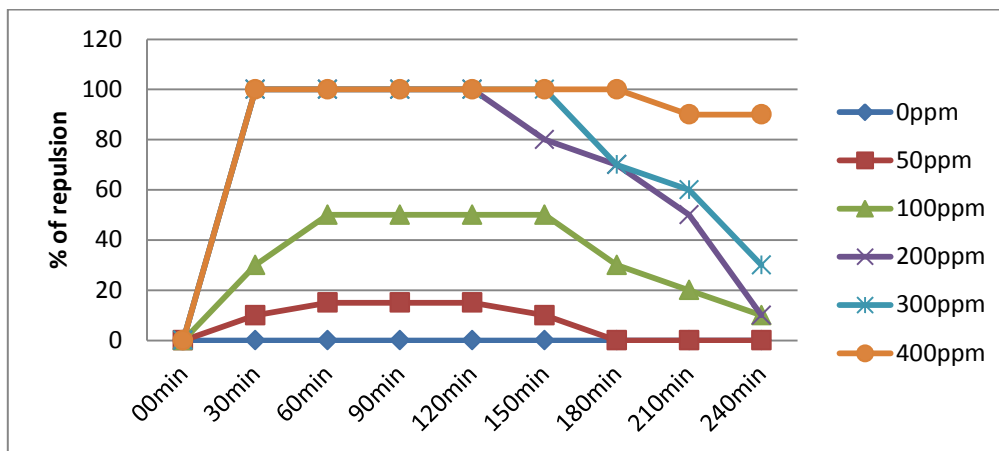


Figure 6: Repulsion of *A. gambiae* in the laboratory (Luxembourg)

DISCUSSION

Hydro- distillation extraction efficiency

The essential oil extracted produced a yield of 0.16 %. In general, the yield of essential oils from aromatic plants is very low. This is the case for example, rose essential oil which has an extraction yield comprised between 0.1 and 0.35% [7]. The yield we obtained in this case is comparable to that found by Valtcho et al in a study on the impact of time on the extraction efficiency of *A. annua* by steam distillation [8]. They obtained yields ranging from 0.05 to 0.35 % for an extraction time ranging from 0 to 240 min, the highest yield corresponding to the longer duration of extraction [8] and comparable performance 0.19% was obtained by Domum of Cameroon in 2012 [4].

Similar results were also cited by Namdeo et al, with yields ranging from 0.14 to 0.66 % of the hydro-distillation of dry leaves of *A. annua* [9]. Zewdinesh et al in turn obtained extraction yields ranging from 0.04 to 1.9%, by solvent extraction, while varying the harvest age and size of plants [10]. Higher yields than ours have been reported with other species of the genus *Artemisia* 1.1% was obtained for *A. absinthium* and 1.2% for *A. arborescens* [11].

Physical characteristics

The aromatic camphor smell of *A. annua* essential oil that we observed may be explained by their high content of camphor (50%) at least demonstrated by studies of Chougouo [12]. Their oily consistency and coloring, have allowed us to say that these two species have consistent characteristics [13]. Indeed, the European Pharmacopoeia specifies that any essential oil should be oily in consistency and sometimes colorful. Similarly, Domum described *A. annua* as oily consistency, with light green color and aromatic camphor smell, with a density of 0.90, an index 19.70 of acid, a saponification value of 25.00, an ester number of 5.30 and positive solubility in alcohol at 75 Å and 95 Å. which is in conformity with our results.

Repellent activity: Activity on volunteers

The chosen site-the town of Ebang (in forest areas) has an adverse weather condition to encourages mosquito growth. Commonly seen were the female Anopheles and other species, namely the Culex (which is the species most represented) and a small number of Mansonia. These three types are responsible for the transmission of various diseases. The *A. gambiae* transmits malaria and lymphatic filariasis, Culex transmits lymphatic filariasis, Japanese encephalitis and other viral diseases, Aedes transmits yellow fever, dengue and lymphatic filariasis and Mansonia transmits lymphatic filariasis [14]. Though this work has some ethical issues, especially when it involved human volunteers, our attention was drawn to a follow-up plan for the treatment of these volunteers.

Repellent activity: Laboratory activity

It is observed that the 2 essential oils possess similar repulsive properties and that the optimum concentration of both is 200 ppm. Protection time varies depending on the concentration used, but it is 2h30min from 200 ppm. Many farmers observed that the cultures of *A. annua* around the house were regress malaria infection, action that would be due to the presence of essential oils in the plant. This hypothesis was verified with our studies because we noticed a growing repulsion depending on the concentration (eg 200 ppm is a time of 2h30min protection, 300 ppm is a time of 3 hours and protection of 400 ppm has a protection time of 3h30min), especially since this repulsion can even explain that secondary metabolites of these plant may have repellent properties on certain insects [15].

This study demonstrated that there was a more marked activity on *A. gambiae*. This action is not noticeable on the Culex at the doses used. The work of Chougouo on the physicochemical characterization of *A. annua* of Cameroon and Luxembourg have identified despite the chemical variability in ecosystem function, 13 volatile compounds that are: camphor, α -pinene, beta- pinene, 3-carene, the α -terpinene, limonene, eucalyptol, artemisia ketone, copaene, the camphene, caryophylène, menthol, and α -terpineol [12]. The differences between the 2 oils related to the amounts of these volatile compounds, scopoletin and artemisinin.

Indeed, analysis of species showed that *A. annua* grown in Cameroon is rich in camphor and menthol but less rich in artemisia ketone, eucalyptol, limonene, copaene than that grown in Luxembourg [16]. Studies have shown that camphor repels flies, mosquitoes, moths and most insects, however, geranium oil (Mainly of camphor) has a very strong repellency against mosquitoes [17, 18]. Which may be by analogy the same case for *A. annua* which is predominantly composed of camphor (50% of all volatile compounds). Also known as repellent a are menthol, camphene, eucalyptol, limonene and α -terpinene [6,18,19,20].

Studies have shown that other compounds, eg α -terpinene which is the major compound found in the leaves of *Chenopodium ambrosioides* Linn have repellent activity on *A. gambiae* [6]. Soybean also repels [21], so also is oil from *Syzygium aromaticum* (cloves) and *Zanthoxylum Limonella* (Makaen)[22]. Citronella oil (solution v/v 1% and 15% v/cream) has a repulsion activity attributed to citral, which is a major oil constituent [19]. The Neem cream provided good protection against *Aedes albopictus*, *Aedes aegypti*, *Culex quinquefasciats*, *Anopheles culcifacies* and *Anopheles subpictus*. The application of cream shows 78% (range 65-95) protection against Aedes, 89% (range 66-100) against Culex and 94.4 % (range 66-100) against Anopheles for 4 hours of protection time [23]. Repulsion rate obtained with DEET, chemical synthesis, is on average of 92 to 100 % for 7h protection time after application [24].

Conclusion

In this study, we conducted by the hydro- distillation, the extraction of essential oil of *Artemisia annua* grown in Cameroon and Luxembourg with an extraction yield of 0.16%. After studies on human volunteers and that conducted in the laboratory, we can conclude that the 2 essential oils could be the alternative to synthetic repellents if properly exploited.

The future scope of this investigation will be to develop an appropriate formulation with suitable synergists, assessment on the product field to determine the effects of toxicology and biological efficiency.

REFERENCES:

- 1- Bernard Germain, Jean vercoutère. Le paludisme. Wikipédia [En ligne]. 2013 avril [consulté le 24.04.2013];1 :[1page]. Consultable à l'URL : <http://fr.wikipedia.org/wiki/paludisme>
- 2- OMS. Paludisme. OMS/paludisme [En ligne]. 2013 mars [consulté le 24.04.2013]; 24: [1page]. Consultable .l'URL: <http://www.who.int/topics/malaria/fr/>
- 3- Lara charmeil. Deux jeunes africains inventent un savon pour lutter contre le paludisme. Camer.be [En ligne]. 2013 avril [consulté le 24.04.2013]; 1:[1page]. Consultable à l'URL: http://www.bbc.co.uk/afrique/region/2013/04/13_04_24_-_paludisme_-_savon.shtml
- 4- Chougouo Kengne Rosine D.; Fotsing Kwetche Pierre R.; Kouamouo Jonas; Domum Tchouanche Bibiane; Somo Moyo Roger and Kaptué Lazare: Antibacterial and Antifungal activity of the Essential Oil Extracted by Hydro-Distillation from *Artemisia annua* Grown in West- Cameroon. British Journal of Pharmacology and Toxicology; 2013; 4(3): 89-94.
- 5- Jacques G. La Commercialisation Des Huiles Essentielles. In:Ganeau, François-Xavier, Collin G, dir. Huiles essentielles: De la plante à la commercialisation-Manuel Pratique. Chicoutimi. Corporation Laseve; 2005; 139-62
- 6- Bigoga J, Saahkem P, Ndindeng S, Ngondi J, Nyegue M, Oben J et al. Larvicidal and Repellent potential of *Chenopodium ambrosioides* Linn Essential oil against *Anopheles gambiae* Giles (Diptera: culcidae). The Open Entomology Journal; 2013. 7(1). 16-22.
- 7- Edward P, Varro E, Lynn RB. Pharmacognosy. LEA et Febiger; 1987; 6
- 8- Valtcho Z, Ferriera J, gonzalez J. Effect of distillation Time of *Artemisia annua* Oil Yield Artemisinin content. San Antonio: Fundamental for life. International annual meetings; 2011;16-19
- 9- Namdeo A, Makhadik K, Kadam S. Antimalarial drug from *Artemisia annua*. Phcog. Mag ISSN; 2: 937 -1296.
- 10- Zewdinesh D, Bizuayehu T, Bisrat D. Leaf, Essential Oil and Artemisinin Yield of *Artemisia annua* L. As influenced by harvesting age and Plant Population Density. World. J Agr. Sci; 2011; 7(4): 404-12.
- 11- Sura B, Sibel K, Serdar G, Nefise U, Sibel K, AhmetU. Antimicrobial and antioxidant properties of *Artemisia* L. Species from Western Anatolia. Tubitak; 2012 ; 36: 75-84.

12- Rosine D. Nkuitchou-Chougouo K., Dalia F. Fomekong, Jonas Kouamouo, Gilbert Hansen, Pierre Lutgen, Marc Flies, Marc Fisher, Simon Swen, Lysette Kouemeni, Denis Wouessidjewe, Titilayo O. Johnson, Jonathan D. Dabak, John Aguiyi, Jean M. Tekam, Lazare Kaptue, Pierre Tane. Physicochemical Characteristics of *Artemisia annua*, an Antimalarial Plant from the Grass- field Regions of Cameroon. Int. J. of Eng. Sci. and Comp.; 2016 ; volume 6, Issue N° 3.

13- Pharmacopée européenne: 4ème édition. 2002

14- OMS. La lutte anti vectorielle-méthodes à usage individuelle et communautaire, [En ligne]. 1999. [consulté le 24.04.2013].1; 1: consultable. l'URL: <http://www.who.int/dsa/catfrançais/lutte antivectorielle.htm>

15- Chang KS, Tak JH, Kim SL, Lee WJ, Ahn YJ. Repellency of *Cinnamomium cassia* bark compounds and cream containing cassia oil to *Aedes aegypti* (Diptera: culicidea) under Laboratory and indoor conditions. Pest Manag Sci; 2006 Novembre; 62(11):1032-8.

16- Rosine D. Nkuitchou-Chougouo K., Jonas Kouamouo, Titilayo O. Johnson, Dalia Fomekong Fotsop, Gilbert Hansen, Pierre Lutgen, Marc flies, Marc Fisher, Simon Sven, Lysette Kouemeni, Mathieu Tene, Denis Wouessidjiwe, Jean M. Tekam, Lazare Kaptue, Pierre Tane. Comparative study of chemical composition of *Artemisia annua* essential oil growing wild in Western Cameroon and Luxembourg by μ -CTE/TD/GC/MS. North Asian International Research Journal of Multidisciplinary ISSN: 2454 – 2326 ; April 2016; Vol. 2, Issue 4.

17- Emie. Zoom sur le camphre. [En ligne]. Avril 2011. [consulté le 02.12.2013] ; 1[1page]. Consultable .l'URL : www.mamzelleemie.com/zoom.sur.le.camphre

18- Flora Medicina Ecole d'herboristerie. Achille mille feuille[En ligne]. Consulté le 02.12.2013.1 [8pages]. Consultable .l'URL : www.antimoustic.com/produits-antimoustiques/repulsifs

19- Girgenti P, Suss L. Repellent activity against *Aedes aegypti* (L.) of formulas based on natural vegetable extracts or synthetic active agents Ann Ig; 2002. juin; 14(3): 205-10.

20- Oyedele AO, Gbolade AA, Susan MB, Adewoyin FB, Soyelu OL, Orofidiya OO. Formulation of an effective mosquito - repellent topical product from lemongrass oil. Phytomedicine; 2002 Avril; 9(3): 259 -62.

21- Mark S, John F. Comparative efficacy of insect repellents against mosquito bites. N Engl J Med 2003 Juin; 33(2); 103-104.

22- Trongtokit Y, Rongsriyam Y, Komalamisra N, Krisa daphong P, Apiwathrason C. Laboratory and field trial of developing medicinal local Thai plant products against four species of mosquito vectors. Southeast Asian J Trop Med Public Health. 2004 Juin; 35(2); 325-33.

23- Dua VK, Nagpal BN, Sharma VP. Repellent action of neem cream against mosquitoes. Indian J Malarial 1995 Juin; 32(2); 47-53.

24- Kweka EJ, Munga S, Mahande AM, Msangi S, Mazigo HD, Adrias AQ et al. Protective efficacy of menthol propylene glycol carbonate compared to N, Ndiethylmethyl benzamide against mosquito bites in northern Tanzania. Parasit vectors 2012 Septembre; 5(5): 189.

A Review on Design Consideration and Need of Fixture in Manufacturing Industries

Prof. A. A. Karad^[1], Brijeshwar Wagh^[2], Ajay Shukla^[3], Chetan Gujar^[4], Niladhari Pyata^[5]

[1] Associate professor, Department of Mechanical Engineering, K.V.N. Naik Institute of Engineering Education and Research, Nashik

[2], [3], [4], [5] Students of B.E. [Mechanical], Department of Mechanical Engineering, K.V.N. Naik Institute of Engineering Education and Research, Nashik

[1] avinash.karad1974@gmail.com, 9860288527

[2] brijeshwarwagh000@gmail.com, 7588844767

Abstract— Fixtures, the component or assembly that holds a part undergoing machining, must be designed to fit the shape of that part and the type of machining being done. A fixture can be designed for the particular job using production tool which make the standard machine tool more versatile to work as specialized machine tool. The fixture designing and manufacturing is considered as the complex process and required knowledge of different areas such as geometry, dimensions, and tolerances, procedure and manufacturing process. This paper gives detailed definition of fixture and also gives the design consideration of fixture associated with the fixture in manufacturing.

Keywords— Fixture, Advantages, Design, Design consideration, manufacturing, welding fixture, CMM

7. INTRODUCTION

A fixture is a device for locating, holding and supporting a work piece during a manufacturing operation. Fixtures are essential elements of production processes as they are required in most of the automated manufacturing, inspection, and assembly operations. Fixtures must correctly locate a work piece in a given orientation with respect to a cutting tool or measuring device, or with respect to another component, as for instance in assembly or welding. Such location must be invariant in the sense that the devices must clamp and secure the work piece in that location for the particular processing Operation. Fixtures are normally designed for a definite operation to process a specific work piece and are designed and manufactured individually.

The correct relationship and alignment between the components to be assembled must be maintained in the welding fixture. To do this, a fixture is designed and built to hold, support and locate work piece to ensure that each component is joined within the specified limits. A fixture should be securely and rigidly clamp the component against the rest pads and locator upon which the work is done.

Fixtures vary in design from relatively simple tools to expensive, complicated devices. Fixtures also help to simplify metalworking operations performed on special equipments. Fixtures play an important role on reducing production cycle time and ensuring production quality, by proper locating and balanced clamping methods. Therefore to reduce production cost, fixture design, fabrication and its testing is critical.

1.1 Purpose

A fixture's primary purpose is to create a secure mounting point for a work piece, allowing for support during operation and increased accuracy, precision, reliability, and interchangeability in the finished parts. It also serves to reduce working time by allowing quick set-up, and by smoothing the transition from part to part it frequently reduces the complexity of a process, allowing for unskilled workers to perform it and effectively transferring the skill of the tool maker to the unskilled worker. Fixtures also allow for a higher degree of operator safety by reducing the concentration and effort required to hold a piece steady.

Economically speaking the most valuable function of a fixture is to reduce labor costs. Without a fixture, operating a machine or process may require two or more operators; using a fixture can eliminate one of the operators by securing the work piece.

The basic purposes of developing and using suitable fixtures for batch production in machine shops are:

- To eliminate marking, punching, positioning, alignments etc.

- Easy, quick and consistently accurate locating, supporting and clamping the blank in alignment of the cutting tool
- Guidance to the cutting tool like drill, reamer etc.
- increase in productivity and maintain product quality consistently
- To reduce operator's labour and skill – requirement
- To reduce measurement and its cost
- Enhancing technological capacity of the machine tools
- Reduction of overall machining cost and also increases in interchangeability.

Hence, provision of fixtures as production tools provides the following:

- Manufacture accurately duplicate and interchangeable parts. Jigs and fixtures are specially designed so that large numbers of components can be machined or assembled identically, and to ensure interchangeability of components.
- Facilitate economical production of engineering components.
- Make operation of parts fairly simple which otherwise would require a lot of skill and time.

1.2 The advantages of using fixture.

- Production increase.
- Low variability in dimension, thereby leading to consistent quality of manufactured product.
- Cost reduction.
- Ensures interchange ability and high accuracy of parts.
- Reduces the need for inspection and quality control expenses.
- Reduces accident, as safety is improved.
- Semi-skilled machine operators can easily use them thereby saving the cost of manpower.
- The machine tool can be automated to an appreciable extent.
- Complex and heavy components can be easily machined.
- Easy assembly operations save labour, and also lead to reduction of defective products.

1.3 Function of Fixture

- Gripping a work piece in the predetermined manner of firmness and location.
- Holding components rigid and prevent movement during working in order to impart greater productivity and part accuracy.
- Supporting and locating every component (part) to ensure that each is drilled or machined within the specified limits.
- Positioning components accurately and maintain relationship and alignment between the tool and the work piece correctly to perform on the work piece a manufacturing operation.

1.4 Element of Fixture

Generally, the entire fixture consists of the following elements

- Locators: A locator is usually a fixed component of a fixture. It is used to establish and maintain the position of a part in the fixture by constraining the movement of the part.
- Clamps: A clamp is a force actuating mechanism of a fixture. The forces exerted by the clamps hold a part securely in the fixture against all other external forces.
- Fixture Body: Fixture body, or tool body, is the major structural element of a fixture. It maintains the relationship between the fixture elements namely Locator, clamps, supports, and the machine tool on which the part is to be processed.
- Supports: A support is a fixed or adjustable element of a fixture. When severe part displacement is expected under the action of imposed clamping and processing. Fixtures for work piece comprise the usual locating and clamping elements as used in other

fixtures. However, the effect of heat and prevalence of welding spatter must be taken into account while designing hot joining fixtures.

8. DESIGN

Fixture components may be built into various arrangements to accommodate different workpieces. Fixtures must always be designed with economics in mind; the purpose of these devices is to reduce costs, and so they must be designed in such a way that the cost reduction outweighs the cost of implementing the fixture. It is usually better, from an economic standpoint, for a fixture to result in a small cost reduction for a process in constant use, than for a large cost reduction for a process used only occasionally. A common bench vise the left jaw is the immovable surface, and the right jaw is the movable clamp.

Most fixtures have a solid component, affixed to the floor or to the body of the machine and considered immovable relative to the motion of the machining bit, and one or more movable components known as clamps. These clamps (which may be operated by many different mechanical means) allow work pieces to be easily placed in the machine or removed, and yet stay secure during operation. Many are also adjustable, allowing for work pieces of different sizes to be used for different operations. Fixtures must be designed such that the pressure or motion of the machining operation (usually known as the feed) is directed primarily against the solid component of the fixture. This reduces the likelihood that the fixture will fail, interrupting the operation and potentially causing damage to infrastructure, components, or operators.

Fixtures may also be designed for very general or simple uses. These multi-use fixtures tend to be very simple themselves, often relying on the precision and ingenuity of the operator, as well as surfaces and components already present in the workshop, to provide the same benefits of a specially-designed fixture. Examples include workshop vises, adjustable clamps, and improvised devices such as weights and furniture.

Designing fixtures depends upon so many factors. These factors are analyzed to get design inputs for fixtures. The list of such factors is mentioned below:

- Study of work piece and finished component size and geometry.
- Type and capacity of the machine, its extent of automation.
- Provision of locating devices in the machine.
- Available clamping arrangements in the machine.
- Available indexing devices, their accuracy.
- Evaluation of variability in the performance results of the machine.
- Rigidity and of the machine tool under consideration.
- Study of ejecting devices, safety devices, etc.
- Required level of the accuracy in the work and quality to be produced.

2.1 Design Consideration in Fixture Design.

- The main frame of fixture must be strong enough so that deflection of the fixture is as minimum as possible. This deflection of fixture is caused because of forces of cutting, clamping of the work piece or clamping to the machine table. The main frame of the fixture should have the mass to prevent vibration and chatter.
- Frames may be built from simple sections so that frames may be fastened with screws or welded whenever necessary. Those parts of the frame that remain permanently with the fixture may be welded. Those parts that need frequent changing may be held with the screws. In the situation, where the body of fixture has complex shape, it may be cast from good grade of cast iron.
- Clamping should be fast enough and require least amount of effort.
- Clamps should be arranged so that they are readily available and may be easily removed.
- Clamps should be supported with springs so that clamps are held against the bolt head wherever possible.
- If the clamp is to swing off the work, it should be permitted to swing as far as it is necessary for removal of the work piece.
- All locator's clamps should be easily visible to the operator and easily accessible for cleaning, positioning or tightening.
- Provision should be made for easy disposal of chip so that storage of chips doesn't interfere with the operation and that their removal during the operation doesn't interfere with the cutting process.

- All clamps and support points that need to be adjusted with a wrench should be of same size. All clamps and adjustable support points should be capable of being operated from the fronts of the fixture.
- Work piece should be stable when it is placed in fixture. If the work piece is rough, three fixed support points should be used. If work piece is smooth, more than three fixed support points may be used. Support point should be placed as farthest as possible from each other.
- The three support points should circumscribe the centre of gravity of the work piece.
- The surface area of contact of support should be as small as possible without causing damage to the work piece. This damage is due to the clamping or work forces.
- Support points and other parts are designed in such a way that they may be easily replaced if they break.

In the design of a fixture, a definite sequence of design stages is involved. They can be grouped into four broad stages of design development.

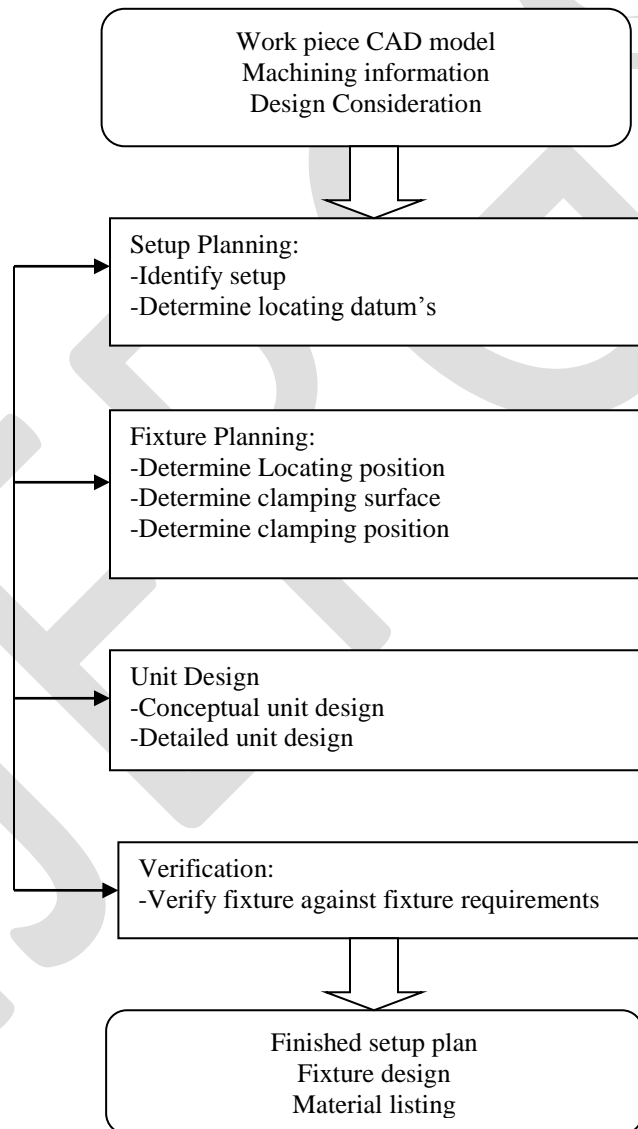


Fig No.1 Steps of fixture Design.

- Stage one deals with information gathering and analysis, which includes study of the component which includes the shape of the component, size of the component, geometrical shape required, locating faces and clamping faces. Determination of setup work piece orientation and position.

- Stage two involves product analysis such as the study of design specifications, process planning, examining the processing equipment's and considering operators safety and ease of use. Determination of clamping and locating position. In this stage all critical dimensions and feasible datum areas are examined in detail and layout of fixture is done.
- Stage three involves design of fixture elements such as structure of the fixture body frame, locators, base plate, clamping and tool guiding arrangement.
- Stage four deals with final design and verification, assembly of the fixture elements, evaluation of the design, incorporating the design changes if any required and completion of design.

9. NEED OF FIXTURE IN MANUFACTURING INDUSTRIES.

Some machining operations are so simple which are done quite easily, such as turning the job is held in position in the chuck and turning operation is done easily. No other device is used to hold the job or to guide the tool on the machine in such an operation.

But some operation are such type in which the tool is required to be guide by means of another device and also some jobs are of such forms which guides the tool is 'jig' and the device which hold the job in position is called 'fixture'.

It serves that to reduce working time by allowing quick set up and smoothing the transition from part to part. It frequently reduces the complexity of a process, allowing for unskilled workers to perform it and effectively transferring the skill of the tool maker to the unskilled worker.

It also allows for higher degree of freedom of operator safety by reducing the concentration and effort required to hold a piece steady. Economically speaking the most valuable function of a fixture is to reduce labour cost by eliminating one of the operators instead of two or three, by securing the work piece.

10. CONCLUSION

Fixture is the manufacturing tool that is employed to reduce interchangeable and identical components. It is unique work holding device designed specifically for machining and assembly.

The paper explained that since the design of fixture is dependent on numerous factors and design consideration of fixture. From the study we can conclude that there are different steps and approaches are available for designing the fixture.

The fixture in manufacturing industries is very useful that reduces the worker fatigue and provides higher degree of freedom of operator safety by reducing the concentration and efforts required to hold the work piece.

REFERENCES:

- [1] Shailesh S. Pachbhai, Laukik P. Raut, "A Review on Design of Fixtures," International Journal of Engineering Research and General Science, Volume 2, Issue 2, Feb-Mar 2014.
- [2] Shrikant V. Peshatwar, L.P Raut, "Design and development of Fixture for eccentric shaft: A Review," International Journal of Engineering Research and Applications, Vol. 3, Issue 1, February 2013.
- [3] V. R. Basha, J. J. Salunke, "An Advance Exploration on Fixture Design," International journal of engineering research and application, Volume 5, Issue 6 (Part-3), June 2015.
- [4] R. D. Makwana, N. D. Gosvani, "A study on fixture design for complex part," International journal of futuristic trends in engineering and technology, Volume 1 (01), 2014.
- [5] Kiran Valandi, M. Vijaykumar, Kishor Kumar S., "Development, fortification and analysis of fixture," International journal of innovative research in science, Volume 3, Issue 4, April 2014.

Critical Analysis of Job satisfaction in Service industry: A Review

Akshyakumar S.Puttewar¹, Dr.R.D.Askhedkar², Dr.C.C.Handa³

¹ Assistant Professor, Department of Mechanical Engineering, DBACER, Nagpur.

email id: asputtewar@gmail.com Mobile: 9860107880

^{2,3} Professor, Department of Mechanical Engineering, KDK college of Engineering, Nagpur

Abstract — Job satisfaction represents one of the most complex areas facing today's managers when it comes to managing their employees. Many studies have demonstrated an unusually large impact on the job satisfaction on the motivation of workers, while the level of motivation has an impact on productivity, and hence also on performance of business organizations. Unfortunately, job satisfaction has not still received the proper attention from neither scholars nor managers of various business organizations.

Keywords— Job satisfaction, Indicators, factors of job satisfaction, Approach of job satisfaction

INTRODUCTION

A successful organization is one which is capable to create an environment where the potential of each employee is realized and actively applied in achieving the objectives of an organization. In the modern world, the level of employee's engagement and the quality of work are directly proportional to the success of an organization and contributes towards its growth. So managers are always concerned with identifying ways to boost morale, increase productivity and gain competitive advantage. So a major focus is on factors influencing productivity rather than enhancing the quality of product.

Factors influencing productivity can be classified into two categories: Controllable or internal factors & Non-controllable or external factors. Controllable (internal factors) includes Product, Technology, Plant & equipment, materials, Human factors(job satisfaction), Work methods, Management style, Financial Factors, Sociological factors. Non-controllable (external factors) includes Natural Resources, Government policy, and infrastructure. From the above mentioned factors, job satisfaction is major factor which influence productivity.

An employee will incline towards the growth and success of the organization only if he is satisfied with his work as well as with the organization. So, in order to access the level of satisfaction of employees, it is important to know exactly what matters most to them. Job satisfaction is one's attitude towards his job (positive or negative). The basic element of employee job satisfaction is satisfaction in work and the work environment. One of the most widely used definitions in organizational research is that of Locke (1976), who defines job satisfaction as "a pleasurable or positive emotional state resulting from the appraisal of one's job or job experiences". Job satisfaction is defined as all the feelings that an individual has about his/her job[1].Wadhwa and Wadhwa[2]defines job satisfaction as the orientation that employee has towards his work. He believes that jobs are important as they help in achieving organizational objectives. Employee job satisfaction is determined by the presence of job pleasure and absence of job discontent. Job discontent and job pleasure are important ingredients of job satisfaction [3]. The behavior of an employee is influenced by his attitude and values. An employee, who is happy, is always satisfied with his work and this improves the quality.

INDICATORS OF JOB SATISFACTION

Job satisfaction benefits the organization in many ways. It is also a good indicator of longevity. The various measures of job satisfaction are as follows [3]:

1. Helps In Employee Retention
2. Increase Productivity
3. Reduce Turnover, Recruitment, Training Cost
4. Improved Teamwork
5. Increased Quality of Service
6. Enhances Employee Loyalty
7. Reduce Absenteeism

8. Deliver Superior Value To Customers
9. Increased Performance
10. Happiness/Joy/Pleasure of Employee

FACTORS AFFECTING JOB SATISFACTION

There are variety of factors that makes people feel positive or negative about their job. Job satisfaction can be influenced by variety of factors. One of the biggest prelude to the study of job satisfaction was the Hawthorne studies. These studies primarily credited to Elton Mayo [4] of the Harvard Business School, sought to find the effects of various conditions (most notably illumination) on workers' productivity. These studies ultimately showed that novel changes in work conditions temporarily increase productivity (called the Hawthorne Effect). It was later found that this increase resulted, not from the new conditions, but from the knowledge of being observed. This finding provided strong evidence that people work for purposes other than pay, which paved the way for researchers to investigate other factors in job satisfaction.

A research conducted by Mosammod Mahamuda Parvin and M M Nurul Kabir [5], shows that salary, efficiency in work, fringe supervision, and co-worker relation are the most important factors contributing to job satisfaction. Daljeet Singh Wadhwa et.al. [6] in their research identified that environmental, organizational and behavioral factors are the probable causes behind employee job satisfaction have a positive impact on job satisfaction. Another study by Nawaraj Chaulagain and Deepak Kumar Khadka [7] conducted among Healthcare Professionals reported that responsibility, opportunity to develop, staff relations and patient care were significantly influencing factors for job satisfaction. According to Ethica Tanjeen [8] some factors that are point of high concern to employees regarding their satisfaction are job security, promotion, relationship with superiors. The factors that lead to lowest satisfaction are freedom, relationship with immediate supervisor and promotion. As success of an organization depends mostly on the performance of employees so they need to be satisfied. Jaime X. Castillo and Jamie Cano [9] found that Hygienic and motivation factors are responsible for job satisfaction. The findings imply that employee were most satisfied with the content of their job and least satisfied with the context in which their job was performed.

Factors that lead to hold positive or negative job perceptions can be summarized as follows.

Recognition

It is an act of notice, praise, or blame supplied by one or more superior, peer, colleague, management person, client, and/or the general public. Recognition is also a factor of motivation in Hertzberg's two factor theory.

Promotion

Promotion refers to designate an actual change in upward direction in job status. The promotion to the next level will result in positive changes such as pay, autonomy and supervision.

Pay

These are the sequences of events in which compensation plays a major role. There is no doubt that monetary rewards may play a very influential role in determining job satisfaction. Salaries not market related, can lead to dissatisfaction.

Interpersonal Relations

It involves relationships with superiors, subordinates, and peers or colleague. If the employee experiences the healthy relationship with others within the organization so it will boost the morale and satisfaction toward the job and lead to the higher productivity.

Supervision

The supervisor's willingness to delegate responsibility and/or to teach subordinates is known as supervision. If workers view their superiors as fair, competent and sincere, the level of job satisfaction will be high. Vice-versa workers that perceive employers as unfair, incompetent and selfish will therefore experience a lower level of job satisfaction.

Policy and Administration

These are events in which some or all aspects of the organization were related to job satisfaction. Organizational policy plays an important part in the satisfaction of employee toward the job. These should be framed keeping in view of employee's needs and desire.

Working Condition

Physical working conditions and facilities are equally significant for job satisfaction of employees, viz:- Canteen, Proper lighting, Drinking water, crèches, clean washrooms.

Work Itself

The 'work itself' plays a critical role in determining how satisfied a worker is with the job:- the actual job performance related to job satisfaction.

METHODS /APPROACH OF JOB SATISFACTION

The content theory of job satisfaction rests on identifying the needs and motives that inspire people. The theory focuses on the inner needs driving people to act in that work environment. Suggesting management by observing employees behavior, can determine and predict their needs.

Abraham H. Maslow developed a need hierarchy theory. According to this theory, the urge to fulfill need is a prime factor in motivation of people at work. Human being strives to fulfill a wide range of needs. Human needs are multiple, complex and interrelated. Human needs form a particular structure or hierarchy. Physiological needs are at the base of the hierarchy while self-actualization needs are at the apex. Safety (security) needs, social needs and esteem (ego) needs are positioned in between. Lower-level needs must at least partially be satisfied before higher level needs emerge. As soon as one need is satisfied, another need emerges. This process of need satisfaction continuous from birth to death.

According to Herzberg, maintenance or hygiene factors are necessary to maintain a reasonable level of satisfaction among employees. These factors do not provide satisfaction to the employees but their absence will dissatisfy them. Therefore these factors are called dissatisfies. These are not intrinsic parts of a job but they are related to conditions under which a job is performed. On the other hand motivational factor are intrinsic parts of the job. Any increase in these factors will satisfy the employees and help to improve performance. But a decrease in these factors will not cause dissatisfaction.

In 1964, Vroom defined motivation as a process, controlled by the individual, which governed choices among alternative forms of voluntary activities. Motivation is a product of an individual's expectancy that a certain effort will lead to the intended performance, the instrumentality of this performance to achieving a certain result, and the desirability of the result (known as valence) for the individual. Expectancy theory explains the behavioral process of why individuals choose one behavioral option over another. It also explains how they make decisions to achieve the result they desire. Vroom introduces three variables within his expectancy theory: valence (V), expectancy (E), and instrumentality (I).

In 1963, John Stacey Adams introduced the idea that fairness and equity are key components of a motivated individual. Equity theory is based in the idea that individuals are motivated by fairness, and if they identify inequities in the input/output ratios of themselves and their referent group, they will seek to adjust their input to reach their perceived equity. Adams' suggested that the higher an individual's perception of equity, the more motivated they will be, and vice versa - if someone perceives an unfair environment, they will be demotivated [10].

CONCLUSION

Job satisfaction represents one of the most complex areas facing today's managers when it comes to managing their employees. Unfortunately, job satisfaction has not still received the proper attention from neither scholars nor managers of various business organizations. Many studies have demonstrated an unusually large impact on the job satisfaction on the motivation of workers, while the level of motivation has an impact on productivity, and hence also on performance of business organizations. Researchers have used qualitative approach for identifying the factors of job satisfaction and to find their correlations. Thus, quantitative approach is still not used for studying job satisfaction phenomenon. So, there is a need to study and model job satisfaction using quantitative approach.

REFERENCES:

- [1] Spector, P.E., 1997. Job Satisfaction: Application, Assessment, Causes, and Consequences. SAGE Publications, London.
- [2] Wadhwa, D., and Wadhwa, D. (2011). A Study on factors influencing employee job satisfaction - A study in cement industry of Chhattisgarh. International Journal of Management and Business Studies, Vol. 1 (3), pg. 10-15.

- [3] Rajesh K. Yadav , Nishant Dabhade , ‘A Case Study - with Overview of Job Satisfaction’, Indian journal of economics and development, vol1(8), 136-146, aug2013.
- [4] Elton Mayo, The Human Problems of an Industrial Civilization (New York, The Macmillan Company. 1933; reprinted by Division of Research, Harvard Business School, 1946), p. 114.
- [5] Mosammod Mahamuda Parvin, M M Nurul Kabir, “Factors Affecting Employee Job Satisfaction of Pharmaceutical Sector”, Australian Journal of Business and Management Research, Vol.1 No.9 ,December-2011, pp.113-123.
- [6] Daljeet Singh Wadhwa et.al, “A Study on Factors Influencing Employee Job Satisfaction -A Study in Cement Industry of Chhattisgarh”, IJMBS Vol. 1, Issue 3, September 2011, pp.109-111
- [7] Nawaraj Chaulagain and Deepak Kumar Khadka, “Factors Influencing Job Satisfaction among Healthcare Professionals at Tilganga Eye Centre, Kathmandu, Nepal”, International Journal of Scientific & Technology Research Volume 1, Issue 11, December 2012, pp.32-36
- [8] Ethica Tanjeen, “A study on factors affecting job satisfaction of Telecommunication industries in Bangladesh”, IOSR Journal of Business and Management (IOSR-JBM), Volume 8, Issue 6 (Mar. - Apr. 2013), pp. 80-86
- [9] Jaime X. Castillo and Jamie Cano, “Factors Explaining Job Satisfaction Among Faculty”, Journal of Agricultural Education Volume 45, Number 3, 2004, pp.65-74.
- [10] Rao V S P (2009). Human resource management – Text and cases, Excel books – New Delhi, 299–306.
- [11] Brikend Aziri, “Job Satisfaction: A Literature Review”, Management Research and Practice Vol. 3 Issue 4 (2011) pp: 77-86
- [12] Hong Lu, Alison E. While, K. Louise Barriball, “Job satisfaction and its related factors: A questionnaire survey of hospital nurses in Mainland China”, Elsevier International Journal of Nursing Studies 44 (2007) 574–588

THE ROLE OF SOFT SKILLS IN THE DEVELOPMENT OF EMPLOYEE IN AN ORGANISATION

¹Prof Anil Chand, ¹Dr. Jaimini Tipnis

¹Associate Professor, Sinhgad Institute of Business Administration

Research, Pune.

S.No. 40/4, Near Octroi Post, Kondhwa-Saswad Road,

Tel: Cell: 8600141456

Email: sail.jaimini271@gmail.com, anilchand_sibar@sinhgad.edu

Abstract:-“Soft Skill is an organized activity for increasing the knowledge and skills of people for a definite purpose. It involves systematic procedures for transferring technical know-how to the employees so as to increase their knowledge and skills for doing specific jobs with proficiency. “

Politeness and Soft Skills are the act of increasing the knowledge & skills of an employee for doing a particular job. Soft Skill improvement means growth of the individual in all respects. While giving training involves the development of skills that are usually necessary to perform a specific job. The purpose of soft skill is to bring about improvement in the performance of work.

“The use of soft skills the terms training & development in today's employment setting is far more appropriate than 'training' alone since human resources can exert their full potential only when the learning process goes far beyond simple routine. Therefore the soft skills improvement is an important part of every organization”.

Soft Skills improvement is a continuous process and not a one-shot affair, and since it consumes time and entails much expenditure, it is necessary that a training program or policy should be prepared with great thought and care, for it should serve the purposes of the establishment as well as the needs of employees. A successful training program presumes that sufficient care has been taken to discover areas in which it is needed most and to create the necessary environment for its conduct.

Key words:- Soft skill, Self-Management skill, Feedback system, Development, skill training program Assessment, type of soft skill

Introduction

Presenting to adults is very different than presenting to children. Time is a precious commodity for working adults. They generally want to do things efficiently and quickly the path of least resistance. This includes learning about software where the learning presentation must be clear, concise, organized and to the point in order to make the maximum use of time. Adults also want to know how something will benefit them personally, especially in relation to their job. The soft skill guidelines within this job aid have been developed from business literature and are specifically designed for adults.

The section on creating effective presentations is designed to be generic with tips and suggestions that can be applied to a variety of presentation situations. This portion of the job aid includes developing presentations and visual aid design. For the section on communication process this job aid will touch on issues such as interpersonal skills, barriers to communication, giving and receiving feedback and, most importantly, rehearsal and practice. The final portion of this job aid includes a presentation.

A person's soft skill is an important part of their individual contribution to the success of an organization. Particularly those organizations dealing with customers face-to-face are generally more successful, if they train their staff to use these skills. Screening or training for personal habits or traits such as dependability and conscientiousness can yield significant return on investment for an organization. For this reason, soft skills are increasingly sought out by employers in addition to standard qualifications.

What are soft skills?

Before going any further in debating the importance of soft skills we have to clarify the question "What exactly are soft skills?" This basic question is not easy to answer, because the perception of what is a soft skill differs from context to context. A subject may be considered a soft skill in one particular area, and may be considered a hard skill in another. On top of it the understanding of what should be recognized as a soft skill varies widely. Knowledge in project management for instance is "nice to have" for an electrical engineer, but it is a "must to have" for a civil engineer. Training in cultural awareness might be useful for a chemist, but it is an absolute necessity for public or human resources management in societies of diverse cultures.

Interesting enough the internationally renowned encyclopedias has little to say about soft skills. The online encyclopedia "Wikipedia" gives a very broad definition of soft skills, which leaves much room for discussion:

"Soft skills refer to the cluster of personality traits, social graces, facility with language, personal habits, friendliness, and optimism that mark people to varying degrees. Soft skills complement hard skills, which are the technical requirements of a job."

Examples of soft skills

- Communication skills

- Critical and structured thinking
- Problem solving skills
- Creativity
- Teamwork capability
- Negotiating skills
- Self-management
- Time management
- Conflict management
- Cultural awareness
- Common knowledge
- Responsibility
- Etiquette and good manners
- Courtesy
- Self-esteem
- Sociability
- Integrity / Honesty
- Empathy

Why are soft skills important?

After having elaborated so much on soft skills, the answer to why they are considered as being so important is still open. There are numerous reasons for having a critical look at a person's soft skills. One straightforward reason is today's job-market, which in many fields is becoming ever increasingly competitive. To be successful in this tough environment, candidates for jobs have to bring along a "competitive edge" that distinguishes them from other candidates with similar qualifications and comparable evaluation results. And where do they find this competitive advantage? In bringing along additional knowledge and skills, added up by convincing personal traits and habits. This sounds familiar.

Understandably, employers prefer to take in job candidates who will be productive from a very early stage on. If a graduate from university first has to be trained on putting more than three sentences together, how to do a proper presentation, or how to chat in a pleasant and winning manner with colleagues and customers,

1. **Conflict Management:** Conflict is natural and inevitable. Project Manager should know techniques to manage conflicts & use them appropriate to the situation. I dealt about this topic in [this post](#).
2. **Coaching:** This is similar to competency skill I pointed out in the blog theme. Project Manager need to have necessary competency so that they can develop competency in team members which help them to perform their project activities in the expected level.
3. **Negotiation & Team Building:** These skills need more personal involvement from a Project Manager than just focus on output. This one identified under “Relationship & Recognition” in Leadership Rubik Cube. Better relationship with the team & other stakeholders creates a positive environment towards successful execution of the project. All other skills like Communication, Trust Building, Conflict Management, Influencing helps in doing better negotiation & team building activities.
4. **Decision Making:** A decision by organization’s management gives birth to a new project :-) Facing challenges, finding options, deciding to go with one particular option – are part and parcel of a Project Manager’s day-to-day life. Decisions of a Project Manager at each level affects the project outcome. Therefore it is essential skill for a PM.
5. **Political & Cultural Awareness:** Politics in organization is as long as it creates healthy competition among different groups that leads to organization’s growth. PM need to create awareness about the organizational politics & use it appropriately for project success. With increase in global projects, it is inevitable for PMs to understand the cultural differences in the team around the world and work with them accordingly.

Soft Skills List – Self Management Skills

Self-Management Skills address how you perceive yourself and others, manage your emotions, and react to adverse situations. Only when you build an inner excellence can you have a strong mental and emotional foundation to succeed in your career.

1. **Growth mindset** – Looking at any situation, especially difficult situations, as an opportunity for you to learn, grow, and change for the better. Focusing your attention on improving yourself instead of changing others or blaming anyone.
2. **Self-awareness** – Knowing and understanding what drives, angers, motivates, embarrasses, frustrates, and inspires you. Being able to observe yourself objectively in a difficult situation and understand how your perceptions of yourself, others, and the situation are driving your actions.
3. **Emotion regulation** – Being able to manage your emotions, especially negative ones, at work (e.g. anger, frustration, embarrassment) so you can think clearly and objectively, and act accordingly.

4. **Self-confidence** - Believing in yourself and your ability to accomplish anything. Knowing that all you need is within you now. “Those who believe in themselves have access to unlimited power” – wisdom from Kung Fu Panda
5. **Stress management**- Being able to stay healthy, calm, and balanced in any challenging situations. Knowing how to reduce your stress level will increase your productivity, prepare you for new challenges and supports your physical and emotional health, all of which you need for a fulfilling, successful career.
6. **Resilience** – Being able to bounce back after a disappointment or set back, big or small, and continue to move onward and upward.
7. Skills to **forgive and forget**- Being able to forgive yourself for making a mistake, forgive others that wronged you, and move on without “mental or emotional baggage.” Freeing your mind from the past so you can focus 100% of your mental energy on your near and long-term career goals.
8. **Persistence and perseverance** – Being able to maintain the same energy and dedication in your effort to learn, do, and achieve in your career despite difficulties, failures, and oppositions.
9. **Patience** – Being able to step back in a seemingly rushed or crisis situation, so you can think clearly and take action that fulfills your long term goals.
10. **Perceptiveness** – Giving attention and understanding to the unspoken cues and underlying nuance of other people’s communication and actions. Often times, we are too busy thinking about ourselves and what we are saying, we leave little room to watch and understand others’ action and intentions. If you misinterpret other’s intention, you can easily encounter difficulties dealing with people and not even know why.

IMPORTANCE OF SOFT SKILLS:-

Soft Skills plays an important role in human resource development. It is necessary, useful and productive for all categories of employees and supervisory staff. Soft Skill is important as it gives various benefits to employers and employees. It is very important in the present age as developments in science and technology are introducing radical changes in the industrial field. Soft Skill is actively and intimately connected with all personnel or managerial activities. It is an integral part of the whole management program, with all its many activities functionally inter-related. Soft Skill is a practical and vital necessity because it enables employees to develop and rise within the organization, and increase their “market value”, .Soft Skill , moreover, heightens the morale of the employees, for it helps in reducing dissatisfaction, complaints, grievances and absenteeism, reduces the rate of turnover. It moulds the employees’ attitudes and helps them to achieve a better co-operation with the company and a greater loyalty to it. The importance of Soft Skill has been expressed in these words.

HOW SORT SKILL BENEFIT TO THE ORGANIZATION

Be kept to the minimum by the skillful employees. These will lead to lower cost of production per unit. The major benefits of Soft Skills to the organization are:

- + Behave Politely
- + Good Communication.
- + Standardization of procedures + Less quarrel.
- + Economical operations + Higher morale
- + Preparation of future managers + Better management

OBJECTIVES OF THE STUDY

- 1) To understand the need of soft skills in the development of HR.
- 2) To study the useful soft skills method which are useful to improve the politeness of employees?
- 3) To understand the performance of the employee after attending soft skill training program.
- 4) To know the best soft skill training given to the employee.

SCOPE OF WORK

- 1) The study will help to understand the need of soft skills in the development of HR.
- 2) This study will try to know awareness and involvement of the organization in the respect of training and development functions.
- 3) To study the HRD functions undertaken by organization.
- 4) It aim to cover the effective training& development activities under taken at. For the sake of improvement development of efficiency and activity
- 5) Lead to improved probability and more positive attitudes towards profit orientation.

RESEARCH METHODOLOGY

Research is a search for facts. It answers the questions and gives solution to the problems. Research is an organized enquiry. it seeks to find explanations to unexplained phenomenon to classify doubtful facts and to current the misconceived facts.

METHOD OF DATA COLLECTION:

1) Primary data:

The primary data was collected through:

- 1) Observation
- 2) Interview schedules
- 3) Personnel visit to obtain the necessary information.

2) Secondary data:

Secondary data was obtained from

- 1) Company records
- 2) Magazines
- 3) Annual reports etc.

DATA ANALYSIS:

Sampling unit:-

Employees of 'SONAI INDAPUR DAIRY & MILK PRODUCTS LTD'

Sampling technique:-

Simple random technique.

Sample size:-

A sample of 60 employees was selected for this survey.

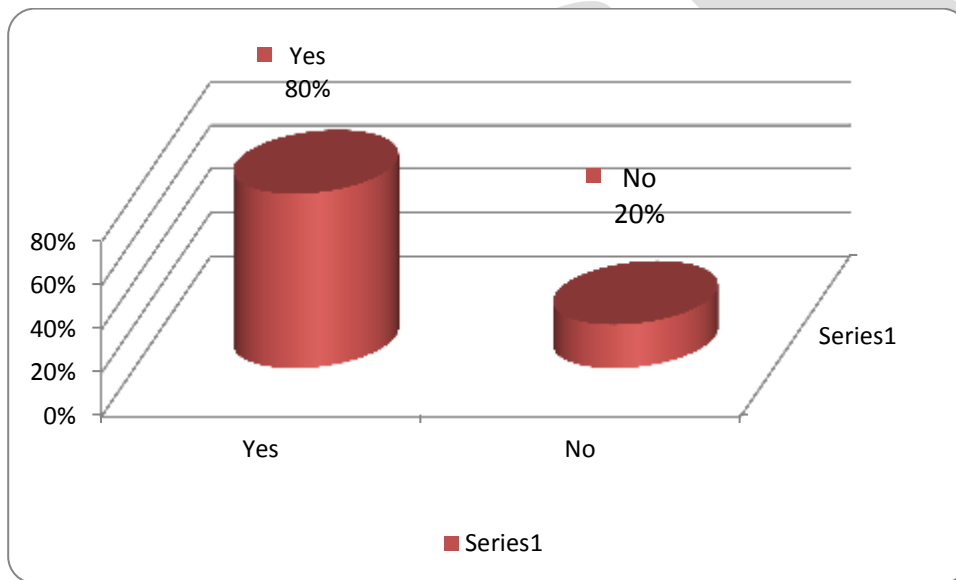
Tool for analysis:-

- 1) Percentage method.

DATA ANALYSIS AND INTERPRETATION

1. Have you attended any soft skill training programs?

Sr. No.	Options	Frequency	Percentage
1	Yes	48	80%
2	No	12	20%
	Total	60	100%



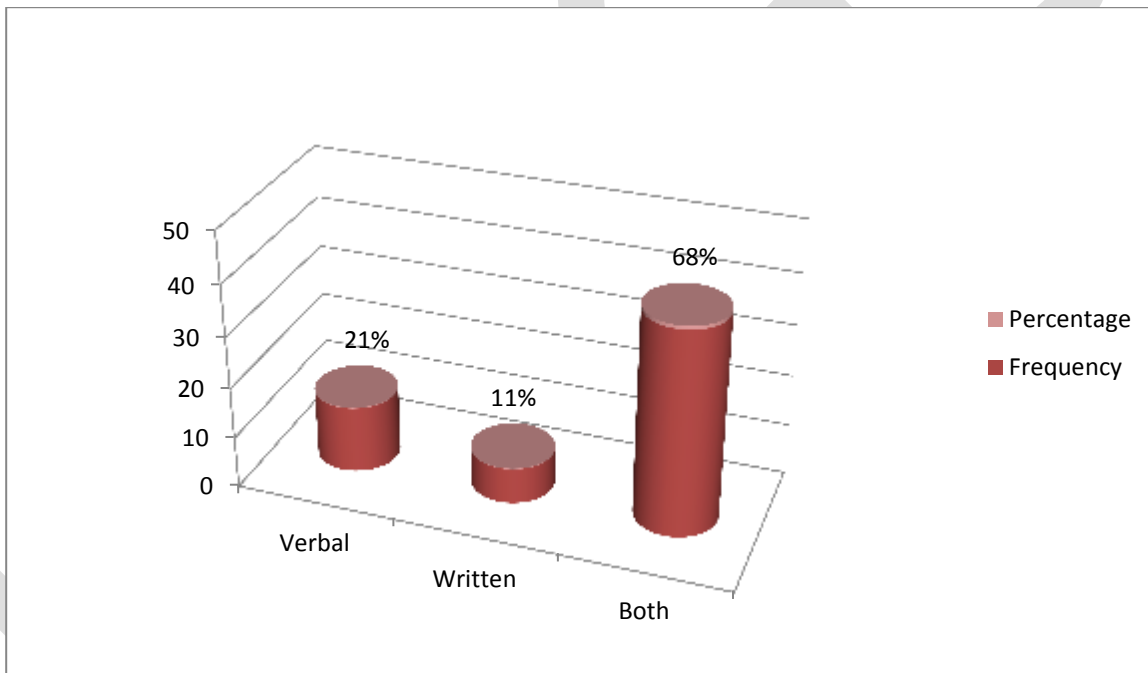
From the above table it is found that 80% employees attended soft skill training programs arranged by the organization while 20% of them have not attended such programs.

Hence maximum employees have attended soft skill training and development program organized by the company.

2) Which are the channels of communication used in the program's are :-

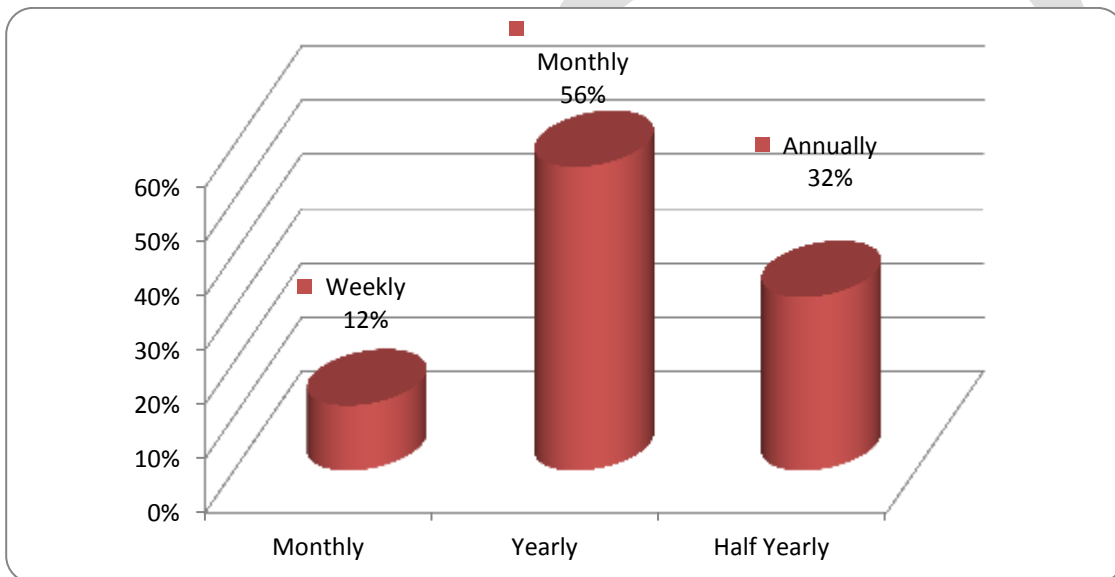
Sr. No.	Options	Frequency	Percentage
1	Verbal	13	21%
2	Written	07	11%
3	Both	40	68%
	Total	60	100%

From the above table it is found that 21% of employees said that verbal communication is used in program, 11% said that written communication is used while 68% selected both the options i.e. both verbal and written communications are used in soft skill training and development programs of the organization.



3) How many times soft skill training program in arranged in your organization?

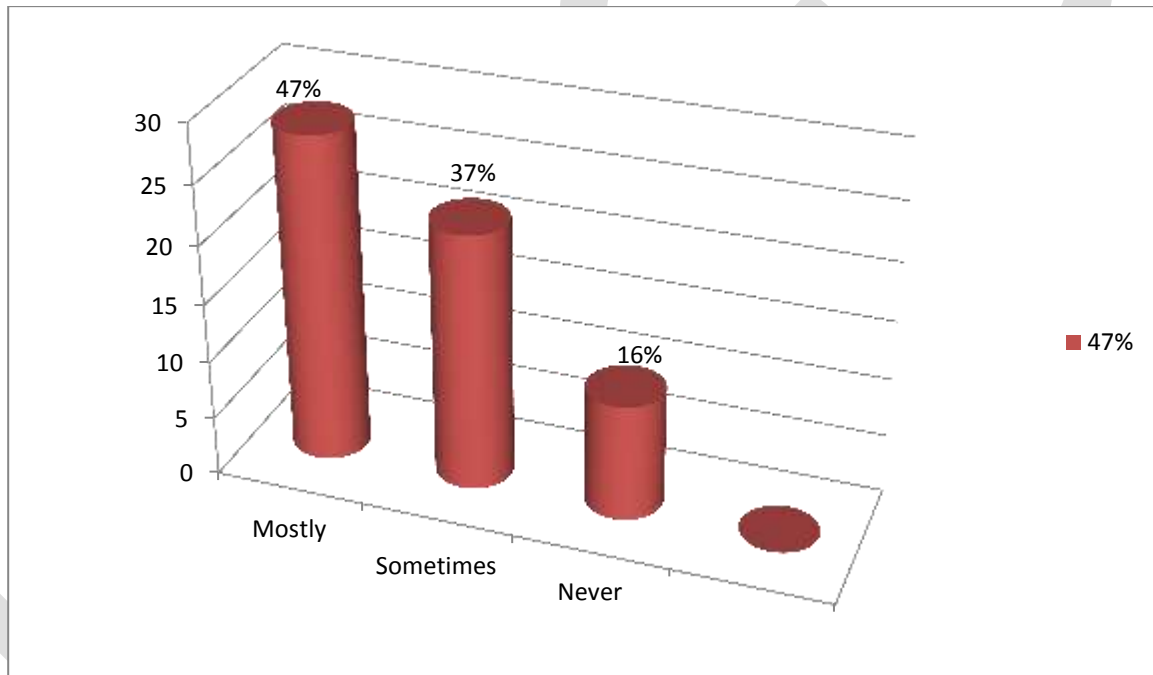
Sr. No.	Options	Frequency	Percentage
1	Weekly	07	12%
2	Monthly	34	56%
3.	Annually	19	32%
	Total	60	100%



From the above table it is found that 56% employees said that Soft Skill Training program are arranged Monthly in their organization, 32% said that these programs are arranged half yearly while 12% employees said that soft skill training program is arranged in their organization Weekly.

4) You were able to pass on knowledge and skills provided from the soft skill training programmes to your subordinates.

Sr. No.	Options	Frequency	Percentage
1	Mostly	28	47%
2	Sometimes	22	37%
3	Never	10	16%
	Total	60	100%

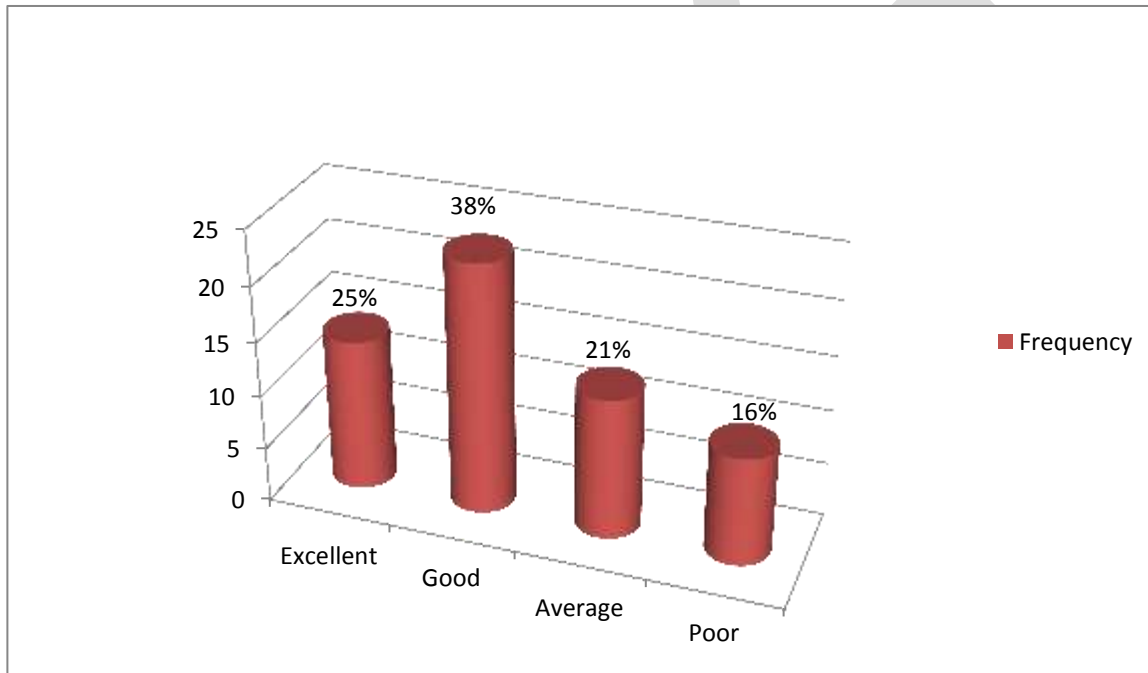


From the above table it is found that 47% employees mostly pass on knowledge and skills to their subordinates, 37% do this some times and 16% do not do this any time.

Hence maximum employees pass on knowledge and skills provided from the soft skill training to their subordinates.

5) How would you rate the soft skill training programme?

Sr. No.	Options	Frequency	Percentage
1	Excellent	14	25%
2	Good	23	38%
3	Average	13	21%
4	Poor	10	16%
	Total	60	100%

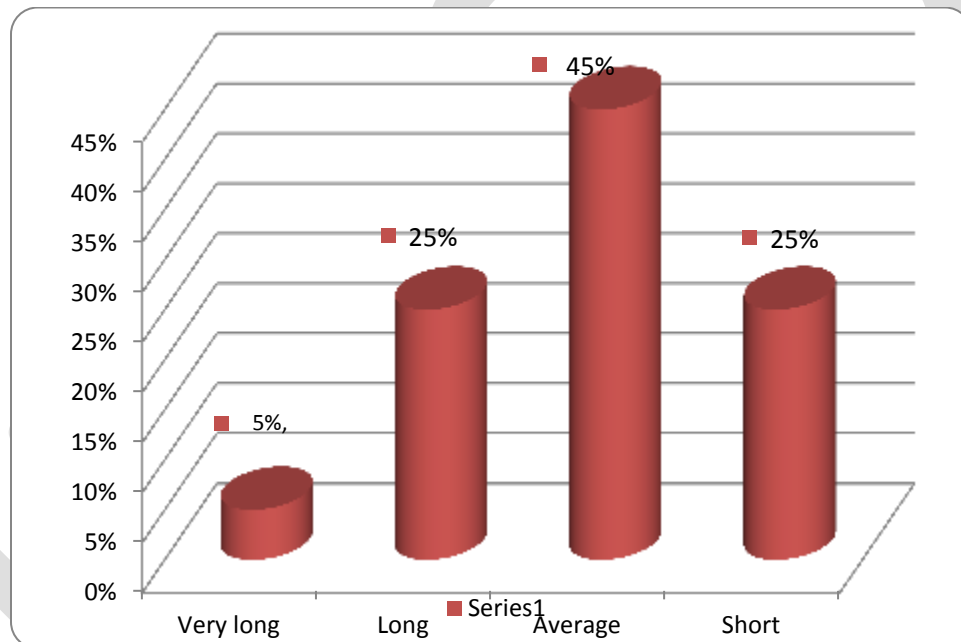


From the above table it is found that 25% employees rate soft skill training as excellent, according to 38% it is good, 21% says that it is average and 16% rate soft skill training as poor.

Hence maximum employees say that soft skill training in their organization is excellent.

6) Time period of soft skill training ?

Sr. No.	Options	Frequency	Percentage
1	Very long	03	05%
2	Long	15	25%
3	Average	27	45%
4	Short	15	25%
	Total	60	100%

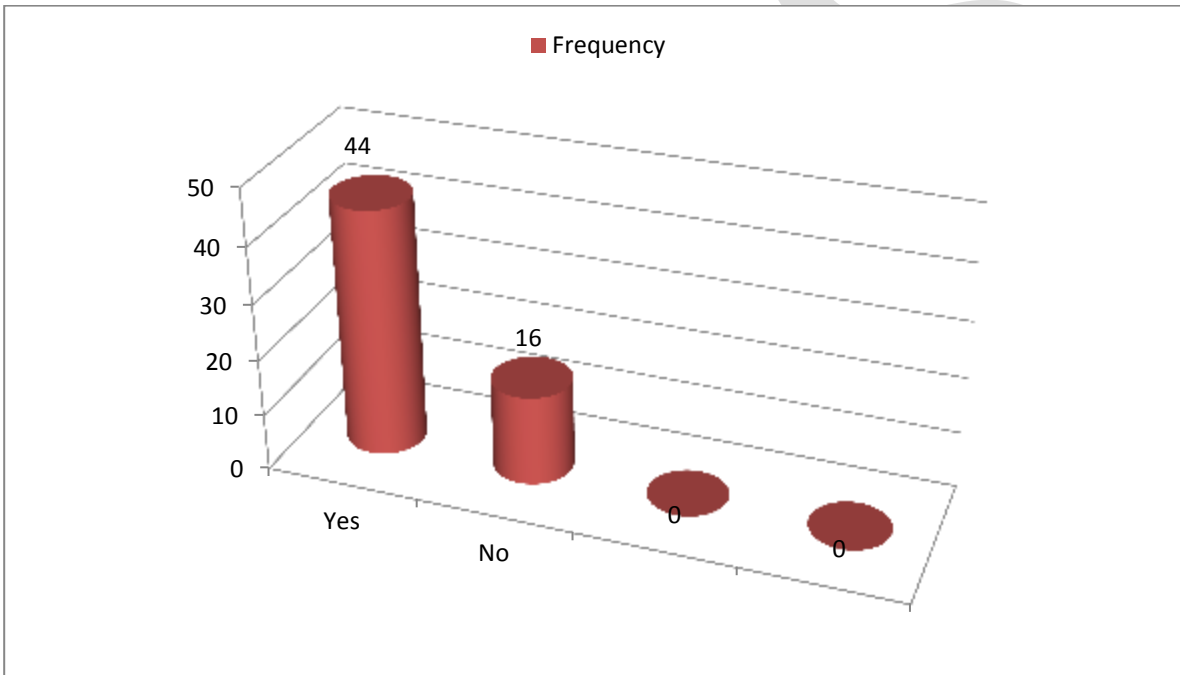


From the above table it is found that 5% employees said that soft skill training period of organization is very long, 25% thinks it is long, 45% said that soft skill training period is average while 25% said that soft skill training period of organization is short.

Hence maximum employees said that the soft skill training period in their organization is short.

7) Is there a system of feedback?

Sr. No.	Options	Frequency	Percentage
1	Yes	44	73%
2	No	16	27%
	Total	60	100%



From the above table it is found that 73% said that there is feedback system available while 27% are not agree with that.

Hence maximum employees said that there is a feedback system in their organization.

CONCLUSION

- 1) Conclude the results of the study have been quite a satisfactory one.
- 2) The employees seem to be quite satisfied with the soft skill training process at Dairy and are keen to attend more soft skill training in the future.
- 3) However, there have been found certain loopholes in areas like the Soft Skill Training Needs Identification and the Feedback System adopted in company.
- 4) Also, the post evaluation of the Soft Skill training is almost missing in the Dairy.
Recommendations have been provided in the study, which if implemented, could help the Dairy to quite an extent in improving the system.
- 5) To assess the need of training and according to the need training should be given.

REFERENCES:

1. Audibert, G. and James, M The softer side: Advisor today 2002,97(2),72
- [2] Hewitt Sean(2008) "9 soft skills for success", www.askmen.com
- [3] Martin carole (2008) "how to stand out from a crowd of candidates", www.career_intelligence.com
- [4] Thacker A Rebecca and Yost A Christine(2002), "Training Students to become effective workplace team leaders" Team Performance Management, Vol.8, No3/4, pp.89
- [5] Tobin P(2006), Managing Ourselves - Leading Others". ICEL2006, Inspiring Leadership :Experiential learning and leadership development. Vol.2, pp36

WEBSITES

- 1) https://en.wikipedia.org/wiki/Soft_Skills_and_development
- 2) <http://softskillanddevelopment.naukrihub.com/>
- 3) <http://www.managementstudyguide.com/softskilltraining-and-development.htm>
- 4) <http://www.businessdictionary.com/definition/softskilltraining-and-development.html>

Experimental Analysis of Vortex Tube with Modified Nozzle: Provided with Internal Taper

M. Surendra Reddy¹, K. Jayasimha Reddy¹, Din Bandhu¹

¹Assistant Professor, G. Pulla Reddy Engineering College (Autonomous), Kurnool, A. P., India

Email: dinosingh@hotmail.co.uk; Contact No.: +91-9525874626

Abstract: Vortex tube is a simple, non-conventional cooling device having no moving parts, which is compact and simple to produce both cold and hot air from the source of compressed air without affecting the surroundings. When high pressure air is tangentially injected, a strong vortex flow will be created which will split into two air streams: heat escapes through the outer periphery at one end, cold escapes through core at the other end. The primary ingredient that involves the performance of vortex tubes is a nozzle and orifice. In this work the performance of vortex tube is investigated with different diameters of orifice and a modified nozzle: providing with different levels of internal taper towards the hot end at various pressure and mass flow. The modified nozzle provided with taper boost up the desired flow pattern, makes the air to travel towards the hot end without disturbing the next coming air at the inlet. The experimental investigations were carried out based upon the maximum temperature drop. It is discovered that the effect of nozzle design is more important than orifice in getting higher temperature drops. The experimental results showed that these modifications could remarkably improve the functioning of the vortex tube. In this work the best combination of modified nozzle and orifice with suitable conditions is suggested for better performance of the vortex tube.

Keywords: Nozzle taper, vortex flow, orifice, temperature drop, diaphragm, internal taper, pressure, temperature.

INTRODUCTION

Fig. 1 illustrates a simple vortex tube. It is a simple device which separates the high energy molecules from low energy molecules. When high pressure air is injected through tangential nozzle a strong vortex flow will be created which will be spiral down through the tube and blocked by a conical valve. The air at high temperature near boundary of the tube will escape through the periphery. Whereas the air at a lower temperature at the center is reversed by conical valve and pass through the orifice which is located near the nozzle.

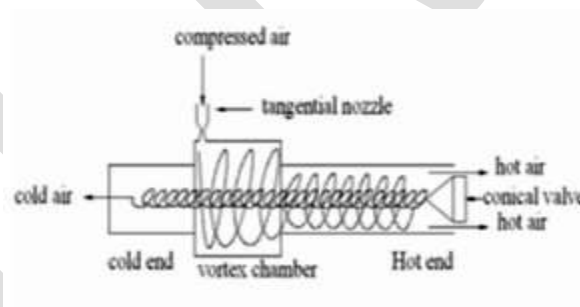


Fig. 1: Flow pattern in Vortex Tube

LITERATURE REVIEW

The vortex tube was invented quite by accident in 1928. George Ranque, a French physics student, was experimenting with a vortex-type pump he had developed when he noticed the warm air exhausting from one end, and cold air from the other. Ranque soon forgot about his pump and started a small firm to exploit the commercial potential for this strange device that produced hot and cold air with no moving parts [1]. However, it soon failed and the vortex tube slipped into obscurity until 1945 when Rudolph Hilsch, a German physicist, published a widely read scientific paper on the device [2]. Ahlborn et al. studied the temperature separation in a low pressure vortex tube and they state that separation is due to the secondary circulation [3]. Behera et al. carried out a simulation of vortex tube using CFD [4]. Aljuwayh et al. studied the mechanism of flow and energy separation inside the vortex tube using renormalization group(RNG) k-e and standard-e models. He used a two-dimensional axisymmetric model along with the effects of the rotational velocity and reported that RNG k-e model predicts better the function of the vortex tube [5]. Eiamsa had experimentally studied the effect of the nozzle numbers on the performance of a vortex tube [6]. Pinar et al. investigated the effects of inlet pressure, nozzle number and fluid type factors on the tube vortex performance by means of Taguchi method [7]. Promvonge and Eiamsaard reported the effects of the number of inlet tangential nozzles, the cold orifice diameter and the tube insulations on the temperature reduction and isentropic efficiency of the vortex tube [8]. Skye et al. (2006) obtained the inlet and outlet temperatures in experimental and

numerical form and compared them with each other [9]. He used a standard two dimensional turbulence k- ϵ model for simulating. He studied numerically the effect of length to diameter ratio (L/D) and stagnation point occurrence, importance in flow patterns [10-12].

CONSTRUCTION DETAILS

The vortex tube consists of the following components:

The design details of Vortex tube: diameter D= 10mm; Vortex tube length L= 1702mm; L/D =17; Diameter of cold orifice D_c=3, 4, 5 mm; Nozzle taper = 0.16, 0.24, 0.3; Material= MS steel.



Fig. 2: Parts of Vortex Tube used for experiments

EXPERIMENTAL PROCEDURE

Before starting the experiment the compressor is run for 15 minutes to get stable compressor pressure. Throughout the experiment the input conditions are maintained constant. Then the compressed air is fed to the inlet of the vortex tube, from there a small portion of the air is directly coming out through cold orifice. The remaining air swirls inside the vortex chamber and travel towards hot end. At the hot end the flow is partially restricted by a control valve. When the pressure of the air near the valve is made more than outside by partially closing the valve, a reversal axial flow through the core of the hot side starts from the high pressure region to low pressure region. During this process, heat transfer takes place between reversed stream and forward stream. Therefore, air stream through the core gets cooled below the inlet temperature of the air in the vortex tube, while air stream in forward direction gets heated up. The experiment is started with conical valve in fully closed position and corresponding readings were noted. By controlling the opening of the valve the temperature of the cold air and its temperature can be varied. The aim of this experiment is to study the variation of temperature at hot end and cold end with respect pressure variation and valve position variation. The cold gas leaves the central diaphragm near the entrance nozzle, while the hot gas discharges through the periphery at the far end of the tube. The control valve is also used to control the flow rate of the hot stream. This would help to regulate cold mass fraction. Thermometers are used to measure inlet, hot and cold stream temperatures. The mass flow rates of the cold air and hot air discharges are measured by standard pipe orifice flow meters and their ratio called a cold mass fraction is changed by regulating the cone shaped valve opening.

RESULTS AND DISCUSSION

The performance of vortex tube was marked by cooling effect (ΔT_c) and heating effect (ΔT_h). They are defined as follows:

$$\Delta T_c = T_i - T_c,$$

$$\Delta T_h = T_h - T_i,$$

Where, T_i is the inlet temperature, T_c is the outlet temperature of cold end, T_h is the outlet temperature of hot end.

Fig. 3 shows the variation of temperature drop with inlet pressure for considered combinations of nozzle and diaphragm at 25% opening of the valve towards hot end. The graph shows that the temperature drop increases with increase in inlet pressure. The maximum temperature drop of 280°C is obtained for the combination of nozzle3-diaphragm1 at 25% opening towards hot end for 12 bar pressure. It is observed that the temperature drop increases with increase in nozzle taper for small diameter diaphragm at all 25% opening towards hot end. Whereas, as using higher diaphragm the temperature drop decreases with increase of nozzle taper for 25% opening towards hot end. This is because at low diaphragm diameter, With increase of nozzle taper the air at the nozzle exit tends to move towards hot end which improves the desired flow pattern and there by the temperature drop increases. The lowest temperature obtained is nearly 4°C for a diaphragm having 3mm diameter and it is around 5°C and 10°C for 4 mm and 5 mm diaphragms respectively.

Fig. 4 shows the variation of temperature drop with inlet pressure for considered combinations of nozzle and diaphragm at 50% opening of the valve towards hot end. The graph shows that the temperature drop increases with increase in inlet pressure. The maximum temperature drop of 26°C is obtained for the combination of nozzle2-diaphragm2 at 50% opening towards hot end at 12 bar pressure. The graph indicates that the effect of diaphragm area is more predominant in getting higher temperature drops. The lowest temperature obtained is nearly 7°C for diaphragm having 3mm diameter and it is around 6°C and 12°C for 4 mm and 5 mm diameter diaphragms respectively. This is because as the supply air pressure is increased it might help to speed up the flow and increase the mass flow rate which leads to strong swirl flow into the vortex tube. This gives rise to high friction dissipation between the boundaries of the flow and a higher momentum transfer from the core region to the wall region. Due to which we get maximum temperature separation at higher pressure.

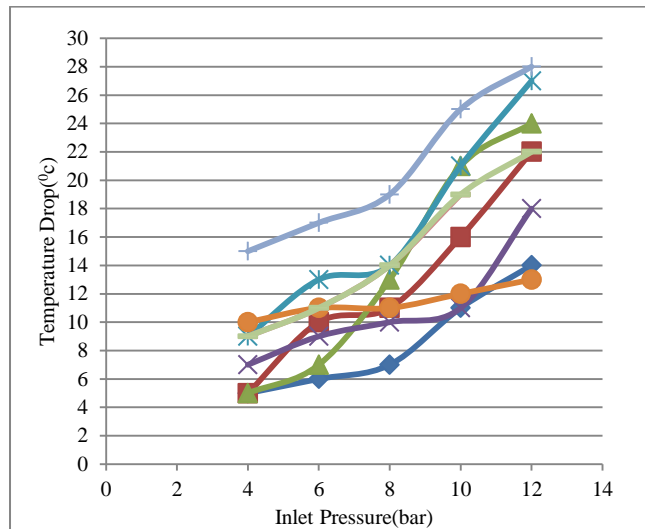


Fig. 3: Pressure v/s temperature drop at 25% opening towards hot end

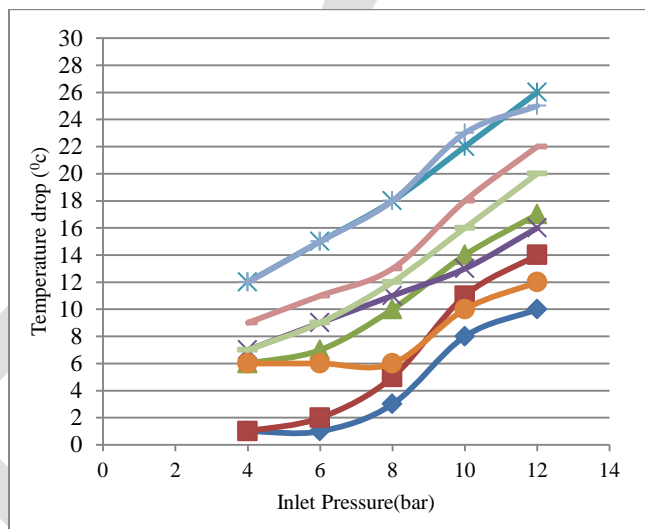


Fig. 4: Pressure v/s temperature drop at 50% opening towards hot end

Fig. 5 shows the variation of temperature drop with inlet pressure for considered combinations of nozzle and diaphragm at 50% opening of the valve towards hot end. The graph shows that the temperature drop increases with increase in inlet pressure. The maximum temperature drop of 23°C is obtained for the combination of nozzle3-diaphragm1 at 75% opening towards hot end at 12 bar pressure. This is because as the opening of the valve increases more air escapes from the pipe easily through cold end which in turn decreases maximum temperature drop. The lowest temperature obtained is nearly 9°C for diaphragm having 3mm diameter and it is around 10°C and 15°C for 4 mm and 5 mm diameter diaphragms respectively.

Fig. 6, 7, and 8 shows the effect of pressure on temperature rise for considered combination of nozzles and diaphragm with different opening percentage towards the hot end. The trend of temperature rise is similar to that of temperature drop that increases with increase of pressure. The temperature rise is higher at smaller opening towards the hot end. The maximum temperature rise obtained is decreasing with increase of diaphragm diameter whereas; it is effective at moderate nozzle taper. This is because at higher diaphragm diameter the air from the inlet escapes through diaphragm without moving towards the hot end. Either low taper or higher taper of nozzle does not give effective rise in temperature because at lower taper the air after tangential entry takes the swirl flow and hits the inlet air which disturbs the flow pattern and at higher taper the air particles can't be closely packed and the advantage of sliding friction between adjacent layers loses. Using nozzle3 with diaphragm1 at 25% opening towards hot end gives a maximum temperature rise of 20°C.

The effect of inlet pressure on temperature drop and temperature rise is shown in Fig. 8. It can be observed that maximum temperature drop is obtained at 12bar for nozzle3-diaphragm1 at 25% opening towards hot end. As the pressure increases the temperature drop also increases this is because as the inlet pressure increases the intensity of swirl increases and at high swirl intensities the heat exchange between two layers becomes predominant. That causes the central stream of air to get cooled giving of heat to the layer at the periphery. The rate of temperature drop increase is slow at low pressure and is high at high inlet pressure.

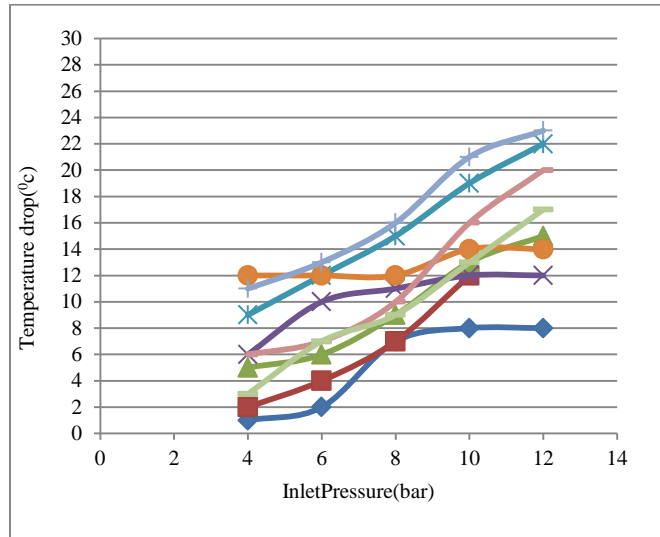


Fig. 5: Pressure v/s temperature drop at 75% opening towards hot end

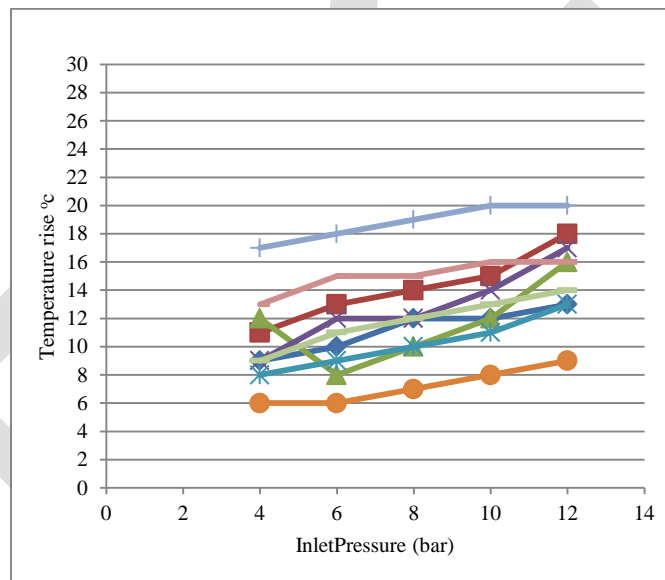


Fig. 6: Pressure v/s temperature rise at 25% opening towards hot end

Fig. 6 shows the variation of temperature rise with inlet pressure for considered combinations of nozzle and diaphragm at 25% opening of the valve towards hot end. The graph shows that the temperature rise increases with increase in inlet pressure. The maximum temperature rise of 20°C is obtained for the combination of nozzle3-diaphragm1 at 75% opening towards hot end at 12 bar pressure. This is because at higher diaphragm diameter the air from the inlet escapes through diaphragm without moving towards the hot end. Either low taper or higher taper of nozzle does not gives effective rise in temperature because at lower taper the air after tangential entry takes the swirl flow and hits the inlet air which disturbs the flow pattern and at higher taper the air particles can't be closely packed and the advantage of sliding friction between adjacent layers loses.

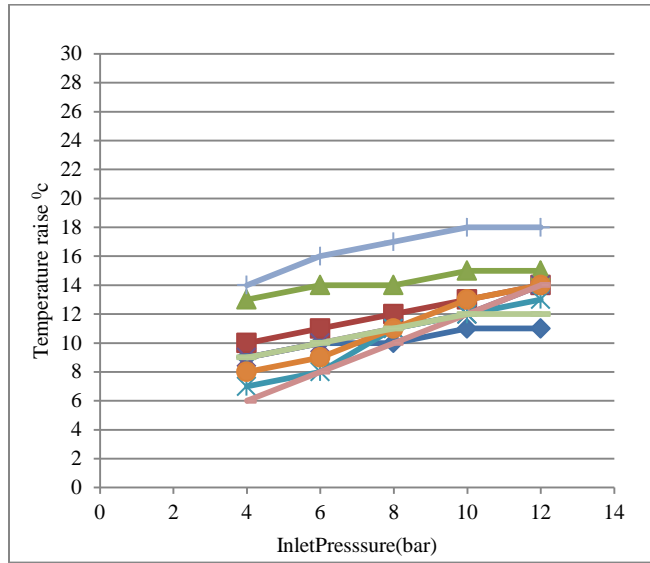


Fig. 7: Pressure v/s temperature rise at 50% opening towards hot end

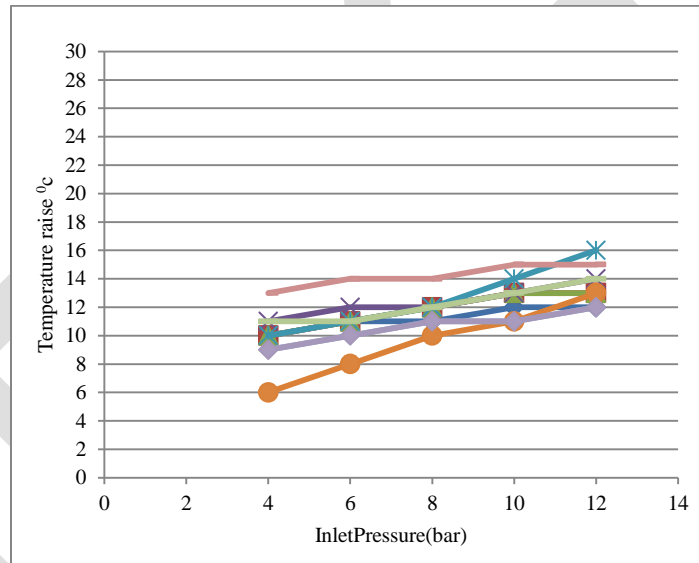


Fig. 8: Pressure v/s temperature rise at 75% opening towards hot end

The effect of inlet pressure on temperature drop and temperature rise is shown in Fig. 8. It can be observed that maximum temperature drop is obtained at 12 bar for nozzle3-diaphragm1 at 25% opening towards hot end. As the pressure increases the temperature drop also increases this is because as the inlet pressure increases the intensity of swirl increases and at high swirl intensities the heat exchange between two layers becomes predominant. That causes the central stream of air to get cooled giving of heat to the layer at the periphery. The rate of temperature drop increase is slow at low pressure and is high at high inlet pressure.

- The maximum temperature difference of 28°C is obtained towards cold end side while 20°C is obtained towards hot end side.
- With increase in inlet pressure cooling effect, heating effect increases. Minimum cold end temperature of air obtained is 4°C while maximum hot end temperature of air obtained is 52°C.
- The maximum temperature drop of 28°C is obtained for nozzle3-diaphragm1 (3 mm) at 25% opening towards hot end whereas the maximum temperature rise of 20°C is obtained for nozzle3-diaphragm1 (3 mm) at 25% opening towards hot end.
- The diameter of the orifice influences the expansion that takes place in the vortex chamber. When the diameter of the orifice is 3 mm, it produces best cooling effect. When the diameter of the orifice is 5 mm, it produces best heating effect, because both the hot air and cold air as flowing out were mixed together which further affected the cold air to have higher temperature. When the diaphragm diameter is 3 mm and 4 mm, it has higher back pressure and makes the temperature

reduction at the cold tube lower, it shows that the diameter of the diaphragm is an important factor for the energy separation. The optimum diaphragm diameter obtained in present study is 3 mm.

CONCLUSION

From the series of tests conducted on the performance of vortex tube with modified nozzle, the following conclusions are drawn:

1. The temperature drop at cold end and temperature rise at hot end increases with increase of inlet pressure.
2. The temperature drop increases with increase in nozzle taper for small diameter diaphragm at all % opening towards hot end. Whereas, by using higher diaphragm the temperature drop decreases with increase of nozzle taper for all % opening towards hot end.
3. The lowest temperature obtained is nearly 4°C for a diaphragm having 3mm diameter and it is around 5°C and 10°C for 4 mm and 5 mm diameter diaphragms respectively.
4. The maximum temperature obtained is nearly 52°C for a diaphragm having 3 mm diameter and it is around 50°C and 48°C for 4 mm and 5 mm diameter diaphragms respectively.
5. The lowest temperature obtained is nearly 4°C for 25% opening towards hot end and it is around 6°C and 9°C for 50% and 75% opening towards hot end.
6. The maximum temperature obtained is nearly 52°C for 25% opening towards hot end and it is around 50°C and 48°C for 50% and 75% opening towards hot end.
7. The temperature rise at hot end decreases with increase of diaphragm diameter.
8. The temperature rise is lower at either low or too higher nozzle taper.
9. The temperature drop at cold end and temperature rise at hot end decreases with increase of percentage opening of control valve towards hot end.
10. The diaphragm of 3mm diameter with nozzle3 Taper at 25% opening through hot end is the optimum combination which gives a maximum temperature drop of 28°C and maximum temperature rise of 20°C. After comparing the performance parameters of vortex tube for different combinations of nozzle and diaphragm and for different throttle valve openings it is concluded that for nozzle3-diaphragm1 at 25% opening towards hot end provides maximum performance of vortex tube with modified nozzle.

REFERENCES:

- [1]. Ranque, "Experiments on expansion in vortex with simultaneous exhaust of hot air and cold air". Le journal de Physique et le Raiuum(Paris)pp 112-114(1965)
- [2]. R. Hilsch, The use of the expansion of gases in a centrifugal field as cooling process,
- [3]. Ahlborn Rev. Sci. Instrum. 18 (2) (1947) 108–113.
- [4]. Behera U and Paul PJ (2005) CFD analysis and experimental investigation towards the optimizing the parameter of Ranque-Hilsch vortex tube. Int. J. Heat Mass Transfer. 48, 1961-1973.
- [5]. Aljuwayhel, N. F., Nellis, G. F., Parametric and Internal Study of the Vortex Tube Using CFD Model, Int.J. Refrigeration, 28 (2005), 3, pp. 442-450
- [6]. Eiamsa-ard, S., Promvonge, P., Investigation on the Vortex Thermal Separation in a Vortex Tube Refrigerator, Science Asia, 31 (2005), 3, pp. 215-223
- [7]. Pinar, A. M., Uluer, O., and Kirmaci, V., 2009, Optimization of Counter Flow Ranque-Hilsch Vortex Tube Performance Using Taguchi Method, International Journal of Refrigeration, Vol. 32 (6), pp. 1487-1494.
- [8]. Promvonge, P., and Eiamsa-ard, S., 2005, Investigation on the Vortex Thermal Separation in a Vortex Tube Refrigerator, Science Asia, Vol. 31 (3), pp. 215-223.
- [9]. Bramo, A. R., Pourmahmoud, N., A Numerical Study on the Effect of Length to Diameter Ratio and Stagnation Point on the Performance of Counter Flow Vortex Tube, Aust. J. Basic & Appl. Sci., 4 (2010), 10, pp. 4943-4957.
- [10]. Bramo, A. R., Pourmahmoud, N., Computational Fluid Dynamics Simulation of Length to Diameter Ratio Effect on the Energy Separation in a Vortex Tube, Thermal Science, 15 (2011), 3, pp. 833-848
- [11]. Skye, H.M., G.F. Nellis and S.A. Klein, "Comparison of CFD analysis to empirical data in a commercial vortex tube," Int. J. Refrigeration., 29 (2006) 71-80.
- [12]. Pourmahmoud, N., Bramo, A. R., the Effect of L/D Ratio on the Temperature Separation in the Counter Flow Vortex Tube, IJRRAS, 6 (2011), 1, pp. 60-68

DESIGN AND DEVELOPMENT OF AUTOMATIC MAINS FAILURE PANEL FOR DIESEL GENERATOR

Dashpute Ajit, Pathan Mohsin, More Prashant. , Kamble Vijaykumar

Savitribai Phule Pune University, India,

Department of Electrical Engineering, AISSMS's Institute Of Information Technology, Pune, India.

ajit.dashpute21@gmail.com, mohsinpathan58@gmail.com, prashantmore.more64@gmail.com

Abstract --Electricity is an essential commodity in our day to day life, electricity forms the basics of any developing country or a developed country. Electricity is required in Domestic, industrial and commercial purposes. Thus, electricity is very important. Failure in electricity supply or interruption in the supply has many adverse effect on Electrical equipments and Control systems. The purpose of this project is to design and build a system that is called Automatic Main Failure (AMF) System which can automatically allow switching from Mains power supply to a battery as backup power supply. Depending upon the Control unit ,[1] there are three main types of AMF units 1) by using Microcontroller in AFM unit itself, 2) by using PLC (Programmable Logic Control) programming for control action & 3) with the help of Relay Mechanism .In this paper a Relay based system is discribed for control action. Elements which are used they are voltage sensor(PFD), Overload Relay and Air Circuit Breaker. The system is continously monitoring the voltage level from the mains. If the voltage is dropped below the allowed level, this system will switch the Load to Generator(Auxillaury supply) and switch back to the Mains when the voltage is back to nominal required normal level.An interlocking of both the ACB is done to avoid any mal operation of switching of ACB. Some delay is also introdused in the system to avoid the transient condition fault in witch the source will not have to shift .Continouty of supply to load is achieved with the help of AMF unit.

Keywords: Phase Failure Detector; Overload Relay; Air Circuit Breaker; Battery Charger; Delay Timer; MCB, Bus bar .

I. INTRODUCTION

Automatic Main Failure (AMF) System is a system which can automatically transfer the switch from Mains power supply to Auxiliary when anomaly such voltage drop, over-voltage and outage or blackout is occurred at the main power & any Power Quality problem regarding the supply will also cause the system to operate. [2]AMF continuously monitor the level of voltage and the output is given to the Control Circuit. Feedback from the Overload relay, Low voltage monitoring relay will generate the signal for both the ACB to be operates corresponding and switch the supply accordingly.

A. Objectives.

The objectives of this project is to:

- i) Design a system that allows switching from mains power to backup power when anomaly is detected.
- ii) Design an automatic system using Relay Operating Control system.

TABLE 1. Main Components and their Specification used in the system.

Component List	Ratings
Phase Failure Detector	415-440 VAC
Overload Relay	440V ,6 Amp
Air Circuit Breaker	415V,800 Amp
Battery charger	24 V DC 10 Amp
Delay Timer(ON delay)	240VAC
Single Pole MCB	230/400V , 16 Amp

B. Problem Statement

- i. A device will not operate efficiently due to the voltage drop
- ii. A device may damage due to overvoltage
- iii. Time Consuming, to switch the source manually.

II. FUNCTIONAL DETAIL

A. Phase Failure Detector.

It is an electro mechanical device used in power system engineering to protect a load from damage due to failure in any of the phases supplying power to the load. It automatically cuts off the load from supply if one of the individual phase becomes faulty. A phase failure detector is particularly important component in many assembly plants using the mains power supply. A significant reduction in value due to uneven load conditions will cause serious problems.

Phase Failure Detector will operate in following conditions;

- i) Unbalanced Voltage
- ii) Single Phase or Phase loss
- iii) Overload Condition
- iv) Power Outage
- v) Phase Reversal

It monitor both Generator as well as Mains side parameter. Any above mentioned condition will cause PFD to operate & give signal to ACB as well as control signal is generated

B. Overload Relay

A thermal Overload relay is used for monitoring the over load in the system. Which causes the over current flow from supply side to the load side.

This overcurrent will responsible for many damage that will occur in the system. Equipment fail to operate, life time of electrical machine will get reduced, and mal operation of other connected unit etc. are the main impact of this overload or current to the system.

Thermal Overload relay is a bimetallic strip having different thermal properties like the melting or binding temperature of one strip will be less than that of other. In case overload, this high inrush current flowing through the relay will cause the one strip to be milt & relay contacts will get closed this gives the signal to control unit

As per given feedback signal from thermal overload relay ACB & other control signal generated.

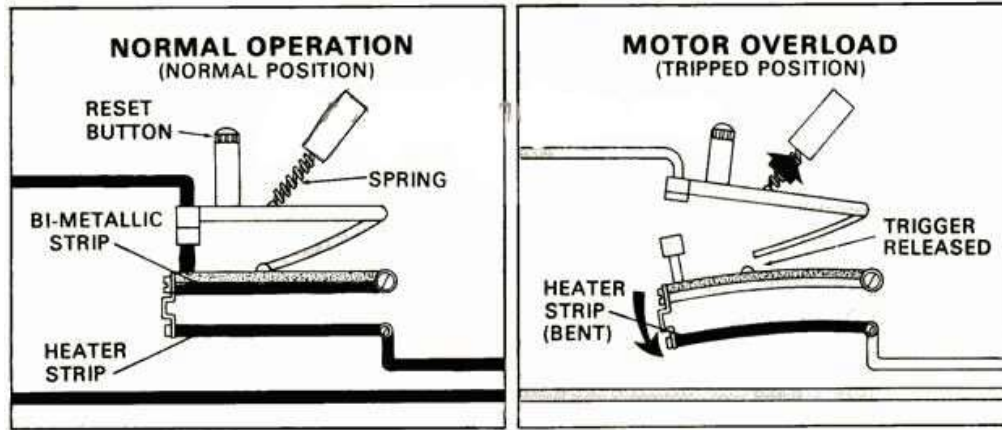


Fig. 1 : Overload Relay

C. Air Circuit Breaker

Air circuit breaker is a device used to provide Overcurrent and short circuit protection for circuits ranging from 800Amps to 10000 Amps. Air circuit breakers are usually used in low voltage applications below 450 volts. ACB prevents the re-establishment of arcing after current zero by creating a situation where in the contact gap will withstand the system recovery voltage .For interrupting arc it creates an arc voltage in excess of the supply voltage.

[3]There are three main methods by which this arc voltage get reduced.

- i) *By cooling the Arc plasma*
Medium between the contactors of ACB has high temperature during the Arc reformation due to which free electrons are radially developed by collision, to avoid this a cooling system is provided in-between.
- ii) *By lengthening the Arc path*
As the length of Arc is increased, it require more voltage to restrike Arc between the contactors. Metallic strip tangential to contactor are used to increase the length of Arc.
- iii) *By Splitting of Arc into 'n' no. series*
A series of non-conducting fringes are present above the Arc area .This causes the Arc to split in no. of small Arc directed upward resulting to avoid the reformation of Arc

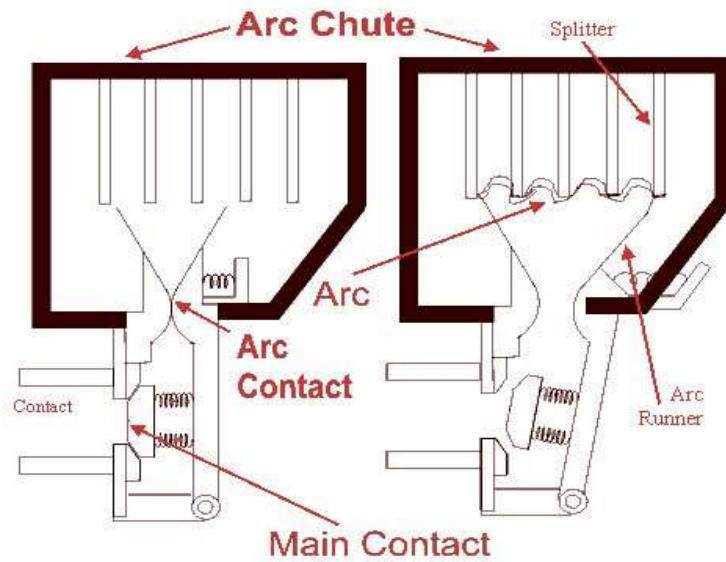


Fig. 2 : Air Circuit Breaker

An interlocking of both ACB is done to avoid the unconditional or fault occurs in the control signal generated .Both the ACB will operate one after another. If any fault occurs in the one ACB then other ACB will not operate

D. Delay Timer

It is a device which is used to add a delay in operation. There are two types of timer, ON delay timer & OFF delay timer. In ON delay timer, when time has expired the contacts close until voltage removed. In OFF delay timer, control input for opening of contacts cause timer to start & contacts will not be operates until the time out .On delay timer used to avoid transient fault operation.

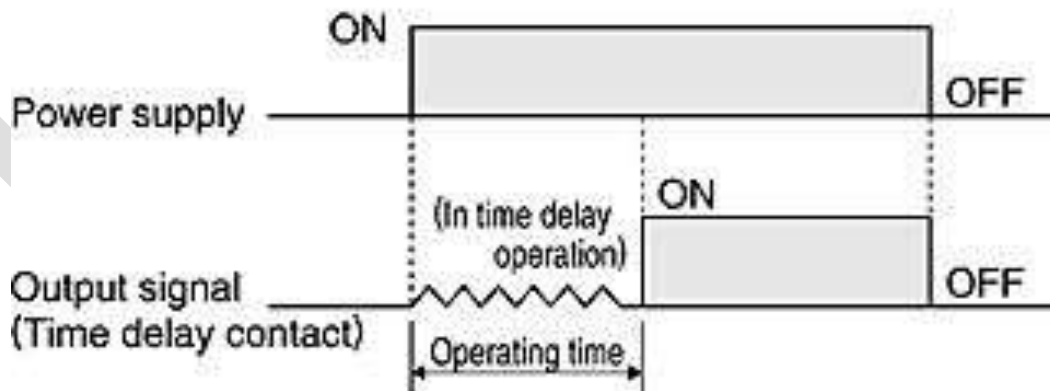


Fig. 3 : Delay time

III. OVERALL SYSTEM DESIGN

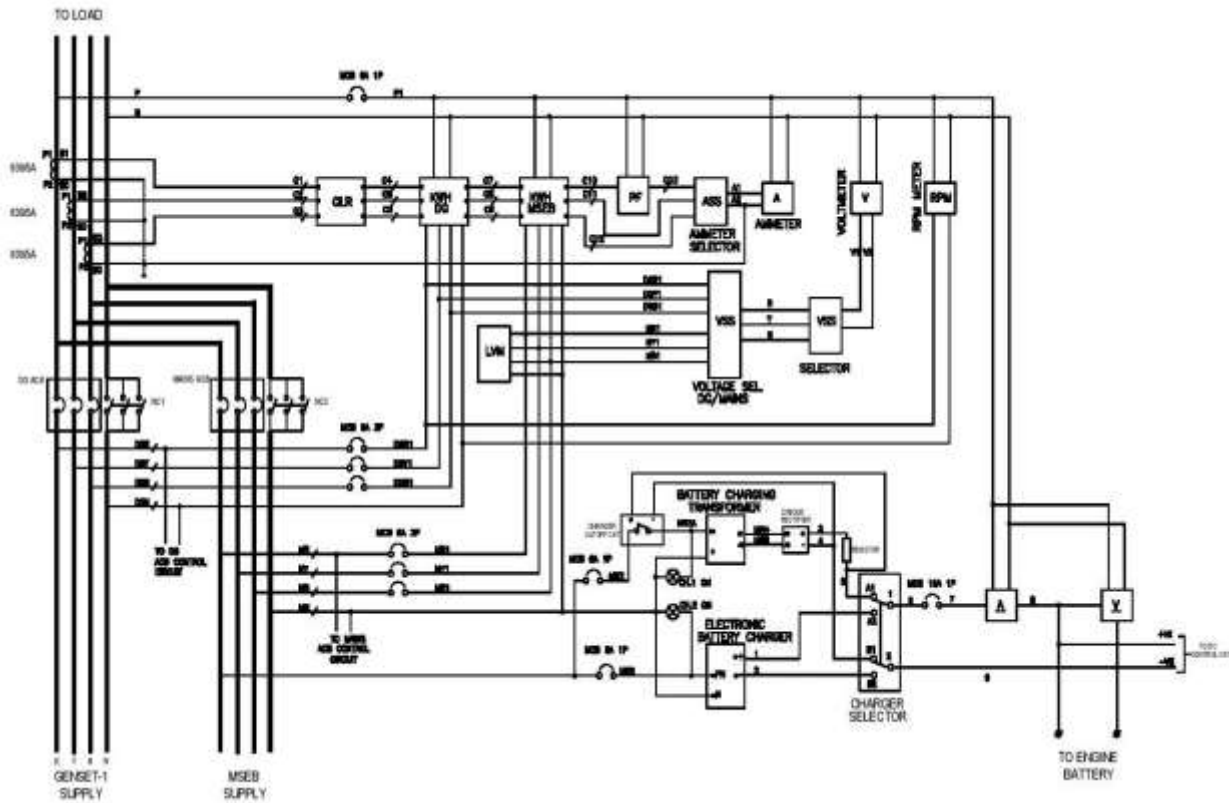


Fig. 4 : Line diagram

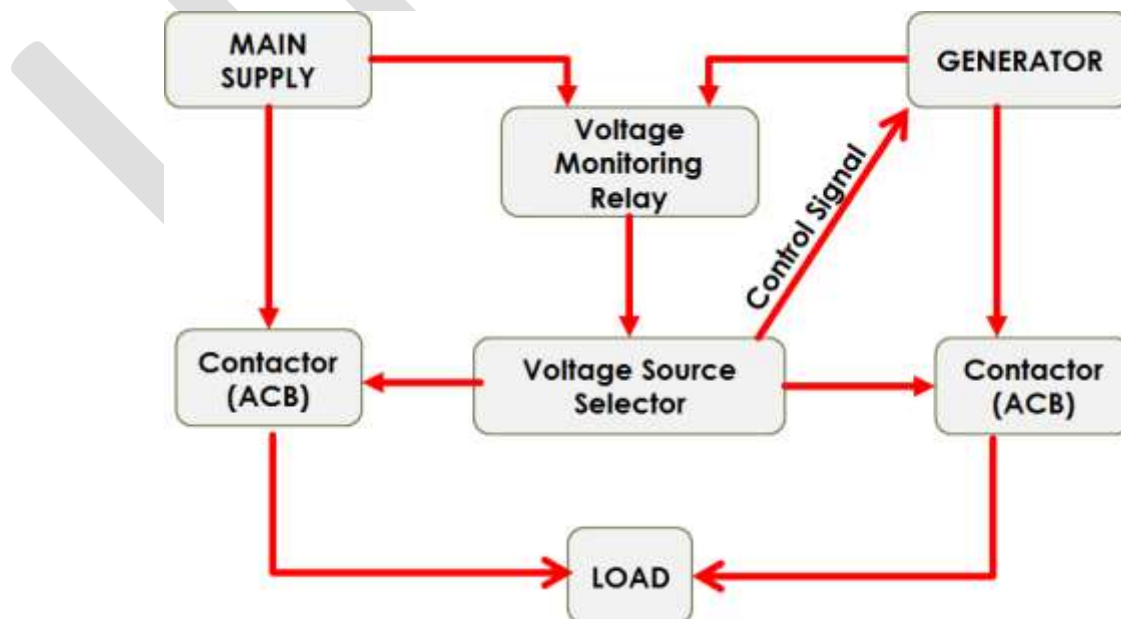


Fig. 5 : Block diagram

Above fig. 5 of block diagram represents the function of AMF panel. Each block represent the main part of panel. Power from mains supply is continuously monitored by PFD with the help of relay unit. It gives signal to the ACB for its operation / protection. When fault occurs in the mains supply PFD detects the fault and disconnect the mains supply form the load side by tripping the ACB. Generator will start automatically. When generator runs at rated RPM & frequency then the ACB (DG) will operate & supply is given to the load form the generator. A delay is introduced in the system to avoid the transient fault condition.

panel.

Power from mains supply is continuously monitored by PFD with the help of relay unit. It gives signal to the ACB for its operation / protection .when fault occurs in the mains supply PFD detects the fault and disconnect the mains supply form the load side by tripping the ACB. Generator will start automatically. when generator runs at rated RPM & frequency then the ACB(DG) will operate & supply is given to the load form the generator. A delay is introduced in the system to avoid the transient fault conditio

IV. DESIGN CONSIDERATIONS

In the designing of AMF panel for 250 KVA load, Active power & Maximum Rated current are calculated to determine rating of contactor to be used as well as cable size.(Assume PF=0.8 & Balanced Load)[1]

$$\text{Active power } P = \text{Apparent Power} \times \text{Power Factor}$$

$$\text{Active power } P = 250 \times 10^3 \times 0.8$$

$$\text{Active power } P = 200\text{kW}$$

$$\text{Power} = 3 I_p V_p \cos \phi$$

$$I_p = \frac{\text{Power}}{3 V_p \cos \phi}$$

$$I_p = \frac{200 \times 10^3}{3 \times 240 \times 0.8} = 347.22 \text{ Amp}$$

(Tolerance of 25%)

$$\text{Maximum Fault Current} = I_p + (0.25 \times I_p)$$

$$\text{Maximum Fault Current} = 347.2 + (0.25 \times 347.22) = 434.025 \text{ Amp}$$

$$\text{Required Cable should carry a current of at least} == 434.025 \times 1.5 = 651.03 \text{ Amp}$$

$$\text{Bus bar size for 800 Amp} = 7 \times 75 \text{ mm}$$

(IEC 60439 – 2: 2000)

Each control equipment are selected as per the above current rating of system. Connection Diagram of panel is made & final wiring of equipment are carried out after mounting of each

V. CONCLUSION

Auto mains failure panel with generator starting/shut down facility has been designed to help man reduce the stress and loss of time associated with the starting and shutting down of the alternative sources of supply (generator)

It will automatically switch the source when the voltage is lower than required value. And supply of electricity is obtained.

REFERENCES:

- [1] L.S. Ezema "Design of Automatic Change over Switch With Generator Control Mechanism" ISSN-L:22223-9553 Vol. 3, No.3,nov 2012
- [2] Jonathan Gana Kolo" Design and Construction of an Automatic Power Changeover Switch" AU J.T. 11(2):(Oct. 2007)
- [3] S.M. Chaudhari "Switchgear and Protection" .Techmax publication.
- [4] Google.com
- [5] wikipedia
- [6] online search engines

Security in Cloud Computing using Hybrid of Algorithms

Jasleen Kaur¹, Sushil Garg²

[1]Student,M.tech(CSE),RIMT,Mandi Gobindgarh,Punjab

E-mail: jasudhingra@gmail.com

Contact No.: 9914341118

[2]Principal, ,RIMT,Mandi Gobindgarh,Punjab

Abstract-Cloud Computing is a fast evolving technology in the field of IT industry. It is well known for its on demand service to the users remotely over Internet. It provides the users with the resources as per their demand and also enables the users to pay as per their usage of resources. Also, it helps the users to access the cloud from anywhere over Internet. This is a big advantage of cloud computing since one need not carry all the documents always since cloud access is global. Although the cloud storage is centralized but cloud access can be done remotely. This means that it is possible that there can be security breaches or any intruder attack while fetching or storing the data onto cloud. So, security of cloud is really important. So, this paper introduces a new security approach using hybrid of two algorithms: RSA as Digital Signature and Blowfish Algorithm.

Keywords- cloud computing, security, deployment models, service models, security, RSA as digital signature, Blowfish algorithm

1 Introduction

Cloud Computing is being viewed as an emerging field in the world of IT industry as it provides scalable “on demand service” to the users over Internet. Cloud Computing aims at providing resources to the users as per their demand only. Cloud allows users to pay as per their requirement and need not pay for the not required resources hence saving money. It is a smart way to use or share resources as it provides business to many people remotely and at the same it lets customers get the resources of their choice all at one place over Internet. Thus, buyer and vendor need not come face to face in order to make the deal and both can be served for their purposes remotely over Internet through Cloud Computing. There are a lot of companies that have come up with their own clouds such as Google, Amazon, Microsoft,IBM,Oracle and so on, to help people get the benefits of cloud services. The cloud provides services on three different layers: Software as a Service(SaaS), Platform as a Service(PaaS) and Infrastructure as a Service(IaaS). These layers have been explained below. Also, cloud is of various types such as Private Cloud, Public Cloud, Hybrid Cloud and Community Cloud. These types are discussed further.

1.1 Deployment Models

There are different deployment models in cloud computing. These are:

- a.) Private Cloud: Private Cloud is the one in which cloud infrastructure is established within the organization and provides limited access to the users. Since, only privileged users can access the resources on the cloud, it is considered as most secure of all other deployment models. It is deployed where the number of users accessing the information is small.
- b.) Public Cloud: Public Cloud is the one in which cloud infrastructure is shared among different organizations. The public cloud is managed by some third party who lease out the resources to the organizations as per their demand. Hence, the public cloud supports the feature pay-as-you-go pricing. Public clouds are vulnerable to data tampering as there are multiple organizations accessing the applications on sharing basis and hence, it may give easy access to some intruder.
- c.) Hybrid Cloud: Hybrid Cloud is the combination of different clouds. As it is the combination of models, it offers the advantages of multiple deployment models. It provides ability to maintain the cloud as recovery of data is easy in this cloud. It provides more flexibility.
- d.) Community Cloud: Community Cloud is the one in which the cloud infrastructure is shared between different organizations with same interests or concerns. The organizations having same requirements (like security, policy, etc.) agree to share the resources from the same party or cloud vendor. Hence, community cloud is basically a public cloud with enhanced security and privacy just like that in private cloud. The infrastructure may be maintained within the organization or outside the organization.

1.2 Cloud Computing Service Models

- a.) Infrastructure as a Service (IaaS):

IaaS is the last layer of the cloud computing stack and this layer provides the consumers with various facilities like that of storage, processors, servers, networking and other hardware facilities and as well as some software facilities like virtualization and file system. This layer controls and manages various operations required by the consumer. It allows the consumers to equip resources as per their demand. It allows the users to deploy their applications or software services effectively and they may access resources with all their rights. In IaaS, an organization leases out its resources to the consumer and the consumer pays back on per-use basis.

b.) Platform as a Service (PaaS):

PaaS is the layer that lies above the IaaS in the stack. It deals with providing development as well as deployment options to the consumers. It basically provides an environment for developing the application with some built-in tools which have some pre-defined functions which help the user to build the application as per requirement. Also, once the application is developed, it may be deployed within the same environment. But, the application so developed becomes environment specific and cannot be run on any other vendor's environment. It also supports the feature of renting of resources and the consumers have to pay on per-use basis.

c.) Software as a Service (SaaS) :

SaaS is the topmost layer in the stack and lies above the PaaS layer. It provides deployment of the end product or software or some web application on the IaaS and PaaS services and provides access to different consumers through some network, probably Internet nowadays. The services of this layer are perceived and manipulated by the consumers. The consumers access these services through Internet once the software has been deployed. The license to these services may be subscription based or usage based. The consumer may extend the services (subscription as well as scalability) based on the demand.

2 Literature Survey

A.) Sanjoli and Jasmeet [7], "Cloud data security using authentication and encryption technique", propose blend of two cryptographic algorithms, EAP-CHAP(Extensible Authentication Protocol- Challenge Handshake Authentication Protocol) and Rijndael Encryption Algorithm. EAP is used to provide authenticated access to the cloud environment. CHAP, a method of EAP, is implemented for authentication purpose. This is then followed by encryption using Rijndael Encryption Algorithm. The complete methodology involves few steps. In the first step, Cloud Service Provider (CSP) receives an authentication request from the user. In the second step, CSP sends acknowledgement after verifying the user identity using EAP-CHAP. In the third step, once the user is authenticated, the user encrypts the data using Rijndael Encryption Algorithm and uploads the encrypted data on to the server of CSP. The data is saved in encrypted form on to the server. Hence, when the user receives any encrypted data from CSP, it can be decrypted using same key same as that used for encryption. In this paper, client side security has been focused and encryption is in the hands of user for providing better security.

B.) Shirole and Sanjay[6], "Data Confidentiality in Cloud Computing with Blowfish Algorithm", propose a system that uses encryption technique to provide reliable and easy way to secure data for resolving security challenges. Scheduler performs encryption on plain data into cipher data followed by uploading of ciphered data on the cloud. When the data is to be retrieved from the cloud, it is obtained in plain data format and is stored on the system. This preserves data internally. And hence, this builds a relationship of cooperation between operator and service provider. This model uses OTP(One-Time Password) for authentication purpose and Blowfish algorithm for encryption purpose.

C.) Garima and Naveen [5], "Triple Security of Data in Cloud Computing", state that cloud computing is a networking model which is connected to a number of servers and is based on client server architecture providing various facilities due to its flexible infrastructure. According to this paper, since cloud computing is internet based technology, so, security stands as a major concern and introduce a mechanism to protect the data in the cloud using combination of two cryptographic algorithms and steganography. This paper proposes blend of two cryptographic algorithms viz.a.viz., DSA(Digital Signature Algorithm) and AES(Advanced Encryption Standard) and Steganography. DSA is used for authentication purpose, AES is used for encrypting the data and Steganography is used for further encryption. The working involves signing of the data in the first step. The signature is generated by first applying a hash function on the data and this gives compact form of data which is called message digest. The message digest is then signed using sender's private key. Once the message is signed, the data is encrypted along with the signature using AES. Once encryption is completed using AES algorithm, the data is further encrypted using steganography. Steganography hides message along with another media which does attract the attention of the intruder and hence the data is protected. This complete mechanism is implemented on ASP.NET Platform and ensures to achieve authenticity, data integrity and security of data in the cloud. This paper concludes that time complexity of the complete mechanism is high since it is one by one process.

D.) Parsi and Sudha[4], "Data Security in Cloud Computing using RSA Algorithm", state that cloud computing is an emerging technology and is fast becoming the hottest area of research. To provide data security in cloud environment, RSA algorithm has been implemented to provide the same. RSA stands for Ron Rivest, Adi Shamir and Len Adleman. RSA is public key cryptography. In the proposed system, RSA is used for both encryption and decryption of data. The process involves encryption of data and then uploading it onto the cloud. For decryption of data, required data is downloaded from the cloud, cloud provider authenticates the user and then the data is decrypted. RSA is used to provide authenticated access to intended user only and hence makes the system secure. The working of RSA consists of two keys: public key and private key. Public key is distributed and shared with others while the private key is only available with the original data owner. Thus, Cloud Service Provider(CSP) perform the encryption and decryption is performed by the consumer or cloud user. Hence, once the data is encrypted using public key, private key must be known in order to decrypt the data. RSA algorithm has three steps: Key Generation, Encryption and Decryption. Key generation is done between CSP and user and then encryption and decryption are performed further. The proposed system provides authenticated access and prevents any intruder access. Hence, the system is made secure.

3 Proposed Work

The hybrid algorithm that has been implemented is a combination of two popular and most widely used cryptographic symmetric and asymmetric algorithms viz.a.viz., RSA as Digital Signature and Blowfish Algorithm. RSA as Digital Signature is used for authentication and verification purpose and Blowfish is used for encryption and security purpose.

RSA was introduced by Ron Rivert,Adi Shamir and Leonard Adleman in 1977. Initials of their names has been used to name the popular algorithm, RSA.

RSA falls under public key cryptography. RSA as Digital Signature aims at providing authentication and non-repudiation of the message. It means that the message that the receiver receives is received from the intended sender and also the message is not duplicated.

Two keys are used for signing the document: public key and private key. The private key, as the name suggests, is kept secret with the sender and is not shared globally and hence is used for signing the document. The public key is shared globally and is used for authentication of the sender by receiver. The working of RSA as Digital Signature has following steps:

- a.) Firstly a message digest of the document is prepared using the hash function.
- b.) Signing of the document is performed using the private key generated using RSA algorithm.
- c.) Verification of the document is performed using the public key generated using RSA algorithm.

Once the document is signed, further encryption is performed by Blowfish algorithm in order to make a secure system.

Blowfish algorithm, was introduced by Bruce Schneier in 1993, is a very famous fast secret key cryptography. The working of this algorithm is complex and is hard to be broken by any intruder. This will make the system secure and will prevent any breach of security. Blowfish has a block size of 64-bit and a variable key length which varies from 32 bits up to 448 bit. The process has 16-round Feistel cipher and large key-dependent S-boxes are used for encryption/decryption purpose. The working includes of following steps:

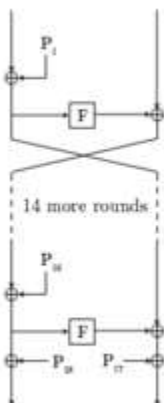


Fig. 1 The Feistel structure of Blowfish

- a.) The diagram above is pictorial representation of Blowfish. Each row represents 32 bits.

b.) The algorithm uses two subkey arrays: the 18-entry P-array and four 256-entry S-boxes.

c.) The S-boxes take 8-bit input and give 32-bit output.

d.) In every round, an entry from P-array is taken, and after the final round, each half of the data block is XORed with one of the two remaining unused P-entries.

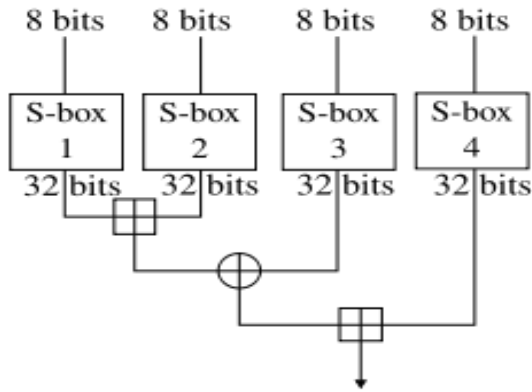


Fig. 2

e.) The diagram above shows Blowfish's F-function.

- Firstly, the input is divided into four eight-bit quarters.
- These quarters are then given as input to the S-boxes.
- The outputs are added modulo 2^{32} and XORed and a final output of 32-bit are obtained.

f.) Decryption is performed using these steps, except that P1, P2, ..., P18 are used in reverse order.

4 Working Of Hybrid Algorithm

The Proposed Algorithm consists of blending of two algorithms: RSA as Digital Signature and Blowfish Algorithm. RSA as Digital Signature provides non-repudiation and authentication of the document while Blowfish is used for encryption and decryption purpose. Once the document is signed and encrypted using the hybrid algorithm, two copies of digital signature are created out of which one is stored locally and another is uploaded onto the cloud along with encrypted message. For decryption, document will be decrypted using Blowfish and then digital signatures are matched with the copy of digital signature stored onto cloud.

Step1. Key Generation Algorithm using RSA

Public key and private key will be generated using RSA algorithm.

The steps for RSA algorithm are:

- a.) Choose two distinct large random prime numbers p and q .
- b.) Find $n = pq$, where n is the modulus for public and private keys.
- c.) Find the totient: $\phi(n) = (p-1)(q-1)$.
- d.) Choose an integer e such that $1 < e < \phi(n)$, and e and $\phi(n)$ have no factors other than 1, where e is declared as the public key exponent.
- e.) Find d to satisfy the congruence relation $d \times e = 1$ modulus $\phi(n)$; d is the private key exponent.
- f.) The public key is (n, e) and the private key is (n, d) . All the values d, p, q and ϕ must be kept secret.

Step2. Generation of Digital Signature

- a.) Before signing the document, the sender creates a message digest using a hash function.

- b.) Message digest is basically a crushed form of entire message and so any hash function may be used for creating the message digest.
- c.) Once the message digest M , is created it may be used for signing the document using private key.
- d.) The private key (n,d) is used to sign the document using $S=M^d \text{ mod } n$.
- e.) After the document is signed, the document is further encrypted.

Step3. Encryption of the document

- a.) Once the document is signed, it is ready to be encrypted.
- b.) For encryption, Blowfish algorithm is used.
- c.) It has 16 round Fiestel structure and key dependent S-boxes.
- d.) Basic operation performed in this algorithm is XOR logic function.
- e.) XOR operation is performed on the output of each row.
- f.) After 16 rounds of XOR operation, the encryption process is complete.

Step4. Decryption of the document

- a.) The decryption process is achieved using reverse of Blowfish algorithm.
- b.) This process gives the message digest generated during digital signing of the document.

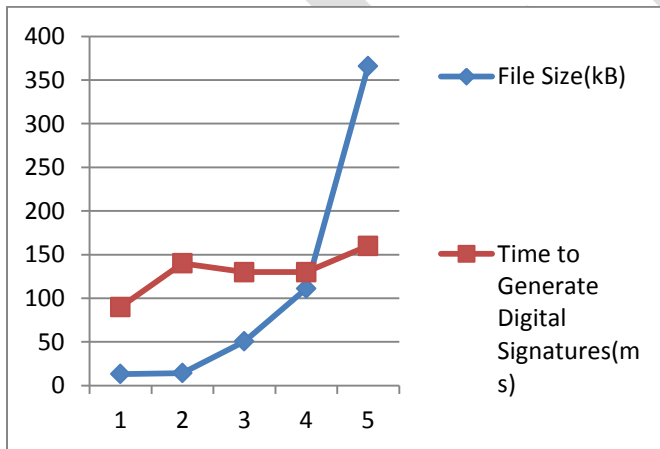
Step5. Verifying the Digital Signature

- a.) The receiver verifies the sender by matching the digital signatures obtained after decryption with that saved onto the cloud.
- b.) If the signatures match, the sender is verified.

5 Results

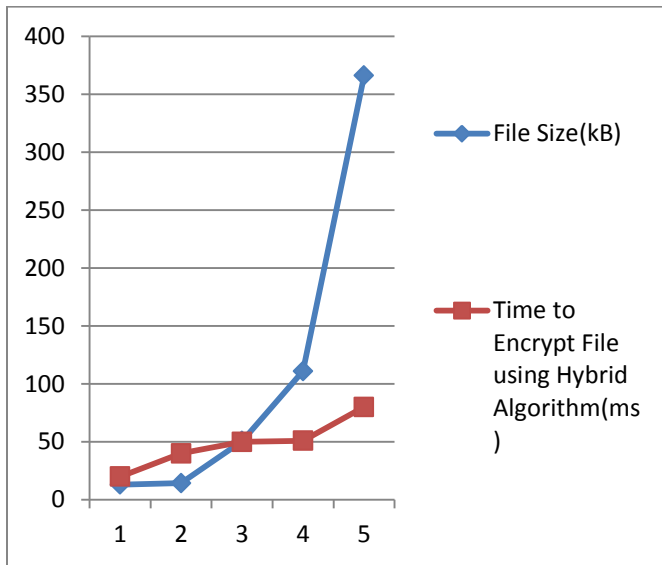
The algorithm is implemented using Java NetBeans and results have been simulated using CloudSim. Following results have been obtained for different file sizes.

a.) Time to Generate Digital Signatures



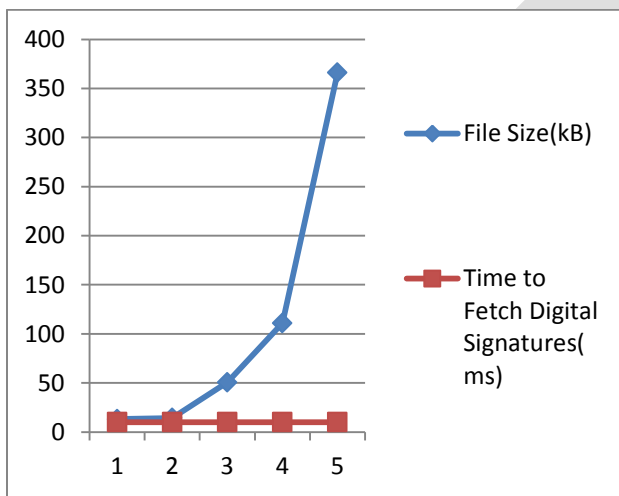
Time to generate digital signatures varies proportionally with file size. As the file size increases so does the generation time increases.

b.) Time to Encrypt Message using Hybrid Algorithm



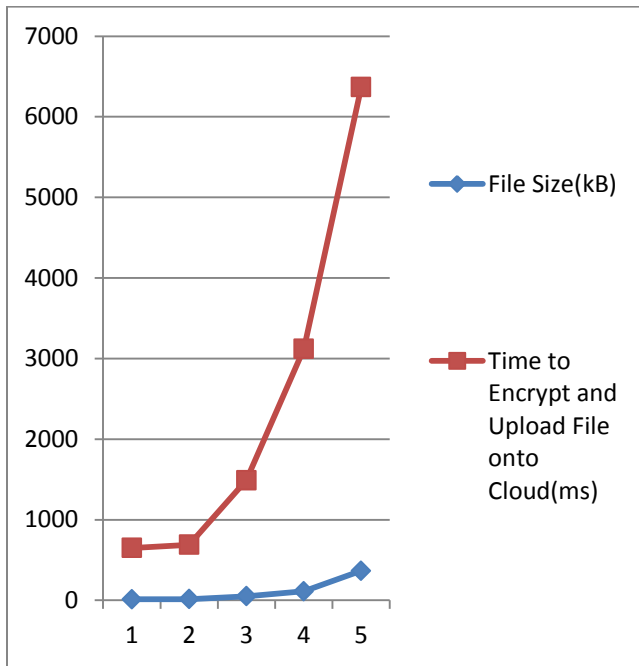
Time to encrypt file using hybrid algorithm varies proportionally with file size. As the file size increases so does the encryption time increases.

c.) Time to Fetch Digital Signatures from Cloud



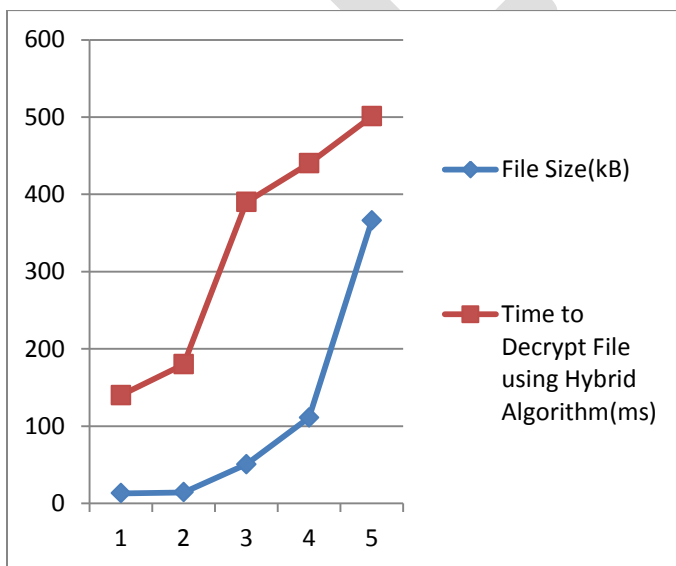
Time to fetch digital signatures is independent of file size. It remains constant for all file sizes.

d.) Time to Encrypt and Upload File onto Cloud



Time to encrypt and upload file onto cloud varies proportionally with file size. As the file size increases, encryption and upload time increase.

e.) Time to Decrypt File



Time to decrypt file is directly related to file size. As file size increases, decryption time increases.

6 Conclusions

The implemented algorithm is a hybrid of two algorithms. From above results, it can be concluded that new Hybrid Algorithm is fast since it takes few milliseconds to encrypt and decrypt the message. Also, it is secure since the encrypted code cannot be understood easily. This is advantageous as it makes the new algorithm secure and fast too. Blending of these two algorithms has fetched the better of two worlds of public key cryptography and secret key cryptography.

REFERENCES:

- [1] http://en.wikipedia.org/wiki/Category:Cloud_computing_providers
- [2] <http://www.cloudcomputingchina.cn/Article/luilan/200909/306.html>
- [3] http://searchcloudcomputing.techtarget.com/sDefinition/0, sid201_gci1287881,00.html
- [4] Kalpana, Parsi, and Sudha Singaraju. "Data security in cloud computing using RSA algorithm." *IJRCCT* 1.4 (2012): 143-146.
- [5] Saini, Garima, and Naveen Sharma. "Triple Security of Data in Cloud Computing." *International Journal of Computer Science & Information Technologies* 5.4 (2014).
- [6] Subhash, Shirole Bajirao. "Data Confidentiality in Cloud Computing with Blowfish Algorithm." *International Journal of Emerging Trends in Science and Technology* 1.01 (2014).
- [7] Singla, Jasmeet Singh. "Cloud data security using authentication and encryption technique." *Global Journal of Computer Science and Technology* 13.3 (2013).
- [8] Naik, Uma, and V. C. Kotak. "Security Issues with Implementation of RSA and Proposed Dual Security Algorithm for Cloud Computing."
- [9] Somani, Uma, Kanika Lakhani, and Manish Mundra. "Implementing digital signature with RSA encryption algorithm to enhance the Data Security of cloud in Cloud Computing." *Parallel Distributed and Grid Computing (PDGC), 2010 1st International Conference on.* IEEE, 2010.
- [10] Hashizume, Keiko, et al. "An analysis of security issues for cloud computing." *Journal of Internet Services and Applications* 4.1 (2013): 1-13.
- [11] Rani, Sunita, and Ambrish Gangal. "Cloud security with encryption using hybrid algorithm and secured endpoints." *International journal of computer science and information technologies* 3.3 (2012): 4302- 4304.
- [12] Saravanan, N., et al. "An implementation of RSA algorithm in google cloud using cloud SQL." *Research Journal of Applied Sciences, Engineering and Technology* 4.19 (2012): 3574-3579.
- [13] <http://cloudcomputingcafe.com/>
- [14] Devi, G., and M. Pramod Kumar. "Cloud Computing: A CRM Service Based on a Separate Encryption and Decryption using Blowfish algorithm." *International Journal Of Computer Trends And Technology* 3.4 (2012): 592-596.
- [15] Kaur, Randeep, and Supriya Kinger. "Analysis of Security Algorithms in Cloud Computing."
- [16] Thakur, Jawahar, and Nagesh Kumar. "DES, AES and Blowfish: Symmetric key cryptography algorithms simulation based performance analysis." *International journal of emerging technology and advanced engineering* 1.2 (2011): 6-12.
- [17] Kumar, K. Vijay, Dr N. Chandra Sekhar Reddy, and B. Srinivas Reddy. "Preserving Data Privacy, Security Models and Cryptographic Algorithms in Cloud Computing." *International Journal of Computer Engineering and Applications* 7.1 (2015).
- [18] Kaur, Jasleen, et al. "SURVEY PAPER ON SECURITY IN CLOUD COMPUTING." (2015).
- [19] Kaur, Jasleen, and Sushil Garg. "Security in Cloud Computing using Hybrid of Algorithms."

A NEW SIMPLIFIED ASYMMETRICAL MULTILEVEL INVERTER TOPOLOGY WITH FUNDAMENTAL SWITCHING CONTROL

D.Dhanunjaya Naidu¹,D.Vijaya Kumar²

¹*P.G.Student, Dept. of EEE, AITAM Engineering college, AP, India, naidudhanu0303@gmail.com*

²*professor, HOD, Dept. of EEE, AITAM Engineering college, AP, India, vijayakumar@gmail.com* ²*Professor*

Abstract— Multilevel inverters have been a widely accepted solution for high voltage and high power applications. Their performance is highly superior to that of conventional two-level inverters due to reduced harmonic distortion, lower electromagnetic interference, and higher dc link voltages. Their main disadvantage is their complexity, requiring a great number of power devices and passive components, and a rather complex control circuitry. In this paper a new inverter topology for generation of fifteen levels of output voltage with reduced number of switches is presented. This topology requires fewer components compared to existing inverters (particularly in higher levels) and requires fewer carrier signals and gate drives. The inverter is controlled by fundamental switching scheme to have a minimum power loss as compared to PWM scheme. The performance of the proposed topology is demonstrated through the simulation in MATLAB/SIMULINK platform and the results demonstrating the operation of the proposed topology as multilevel inverter is presented.

keywords— Multilevel inverter, power electronics, fundamental switching.

INTRODUCTION

Multilevel power conversion was first introduced more than two decades ago. The general concept involves utilizing a higher number of active semiconductor switches to perform the power conversion in small voltage steps. There are several advantages to this approach when compared with the conventional power conversion approach [1]. Another important feature of multilevel converters is that the semiconductors are wired in a series-type connection, which allows operation at higher voltages. However, the series connection is typically made with clamping diodes, which eliminates overvoltage concerns. Furthermore, since the switches are not truly series connected, their switching can be staggered, which reduces the switching frequency and thus the switching losses. One clear disadvantage of multilevel power conversion is the higher number of semiconductor switches required. It should be pointed out that lower voltage rated switches can be used in the multilevel converter and, therefore, the active semiconductor cost is not appreciably increased when compared with the two level cases. However, each active semiconductor added requires associated gate drive circuits and adds further complexity to the converter mechanical layout. Another disadvantage of multilevel power converters is that the small voltage steps are typically produced by isolated voltage sources or a bank of series capacitors. Isolated voltage sources may not always be readily available, and series capacitors require voltage balancing [2]. Some applications for these new converters include industrial drives, flexible ac transmission systems (FACTS), and vehicle propulsion. One area where multilevel converters are particularly suitable is that of renewable photovoltaic energy that efficiency and power quality are of great concerns for the researchers. There are several classical topologies of inverters that are reported by the researchers [3]. Multilevel inverters with reduced number of switches has also become a popular area. Inverter topologies where not all the semiconductor switches involved in output generation are also presented by the researchers [4].

This paper presents an overview of a asymmetrical fifteen level inverter topology with reduced number of switches. The dc sources are assigned with magnitude arranged in a binary fashion. The inverter is divided into two parts namely level and polarity generator whose function is to generate the necessary levels and reversing of the polarity respectively. The inverter is switched with fundamental switching strategy and the generation of control pulses is analyzed. The proposed topology is simulated using Sim power system toolbox of matlab and the results are presented.

POWER STAGE

Fig. 1 shows the power circuit of the proposed 15-level inverter topology. In conventional multilevel inverters, the power switches are operated to produce a high- frequency waveform in both positive and negative polarities. However there is no need to use all the switches for production of bipolar levels. This is the basic idea that has been put into practice by the proposed topology. The output voltage is synthesized by two stages namely level generator which is responsible for the generation of levels requires in positive polarity and secondly the polarity generator stage which is responsible for generating the polarity of the output voltage. The power semiconductor switches employed in the level generator should have high switching frequency capability for generating the required

levels. Whereas the power switches employed for polarity generation operates at the line frequency. The positive levels generated by the level generator is fed to a full-bridge inverter (polarity generator) which will generate the required polarity of the output voltage. In the proposed topology fundamental switching scheme is employed in which no high frequency PWM is required [5]. The operating modes of the inverter is as shown in Fig. 4. For the simulation V_{pu} is considered to be 25V. The required output positive voltage levels produced by the level generator are generated as follows:

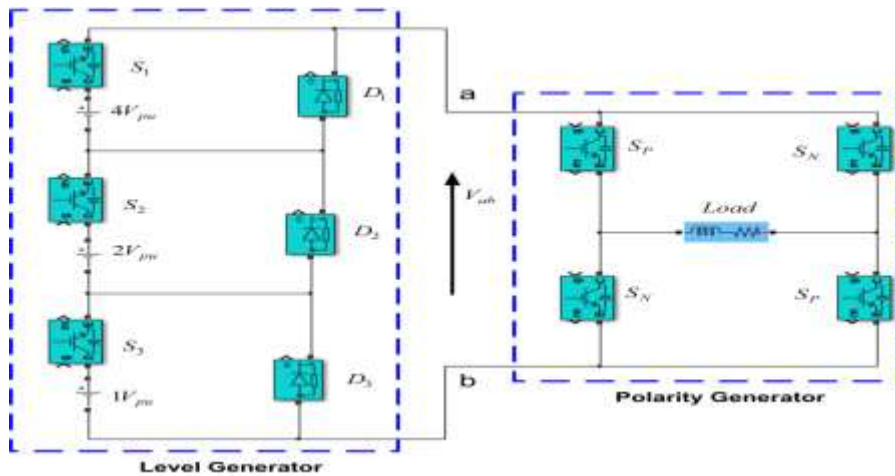


Fig. 1:Proposed asymmetrical 15-level inverter topology.

State 1: $V_{ab} = 0V$ -To obtain this state of level 0 all the switches are turned OFF.

State 2: $V_{ab} = 25V$ -To obtain this state of level 1 switches S_3, S_P are ON and remaining switches are OFF.

State 3: $V_{ab} = 50V$ -To obtain this state of level 2 switches S_2, S_P are ON and remaining switches are OFF.

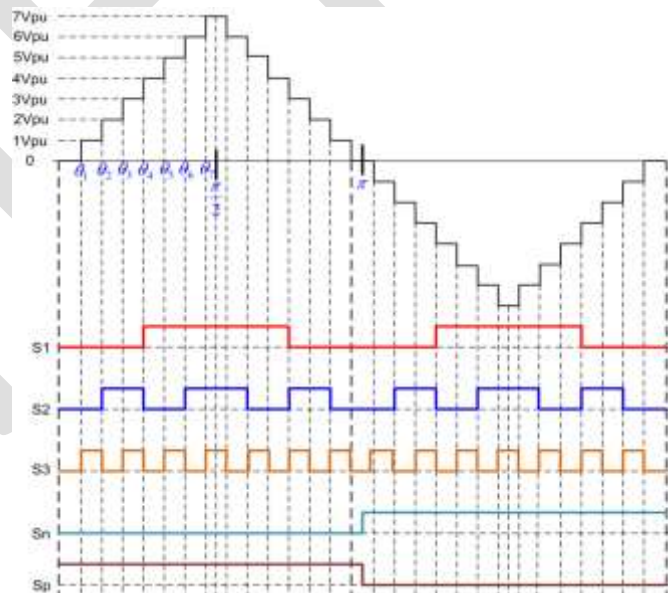


Fig.2: Stepped-voltage waveform consists of the output of proposed inverter topology.

State 4: $V_{ab} = 75V$ -To obtain this state of level 3 switches S3, S2, SP are ON and remaining switches are OFF.

State 5: $V_{ab} = 100V$ -To obtain this state of level 4 switches S1, SP are ON and remaining switches are OFF.

State 6: $V_{ab} = 125V$ -To obtain this state of level 5 switches S1, S3, SP are ON and remaining switches are OFF.

State 7: $V_{ab} = 150V$ -To obtain this state of level 6 switches S1, S2, SP are ON and remaining switches are OFF.

State 8: $V_{ab} = 175V$ -To obtain this state of level 7 switches S1, S2, S3, SP are ON and remaining switches are OFF.

Fig. 2 shows the Stepped-voltage waveform consists of the output of proposed inverter with switching angles for 10 IGBTs. According to the operating states and the output voltage level to be generated the gate pulses for all the switches are derived. The switching angles are used to obtain the switching pulses using a sine wave reference as shown in Fig. 3.

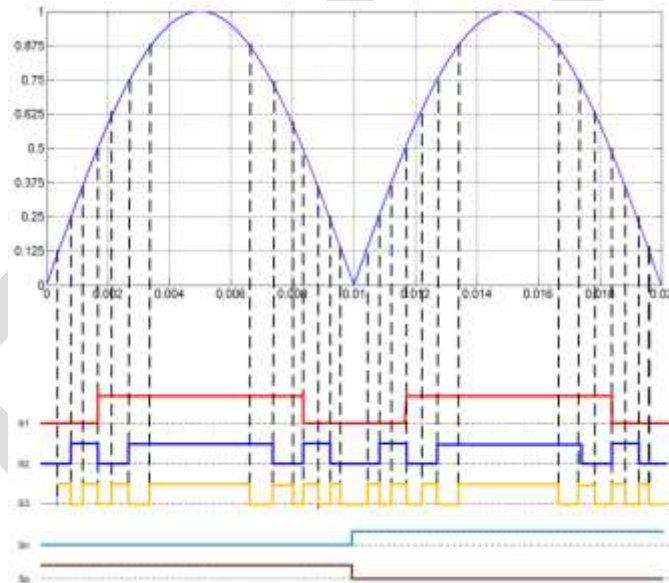


Fig. 3:Reference sine wave and gating signals.

The logic function for the switches is derived from the above waveform as follows. Where V_{ref} is the reference sinusoidal wave.

$$S_1 = \{1 \rightarrow (V_{ref} > 0.5)\}$$

$$S_2 = \{1 \rightarrow ((0.125 < V_{ref}) * (V_{ref} < 0.5)) + (0.75 < V_{ref})\}$$

$$S_3 = \{1 \rightarrow ((0.125 < V_{ref}) * (V_{ref} < 0.25)) + ((0.375 < V_{ref}) * (V_{ref} < 0.5))\}$$

$$+ ((0.625 < V_{ref}) * (V_{ref} < 0.75)) + (0.875 < V_{ref})\}$$

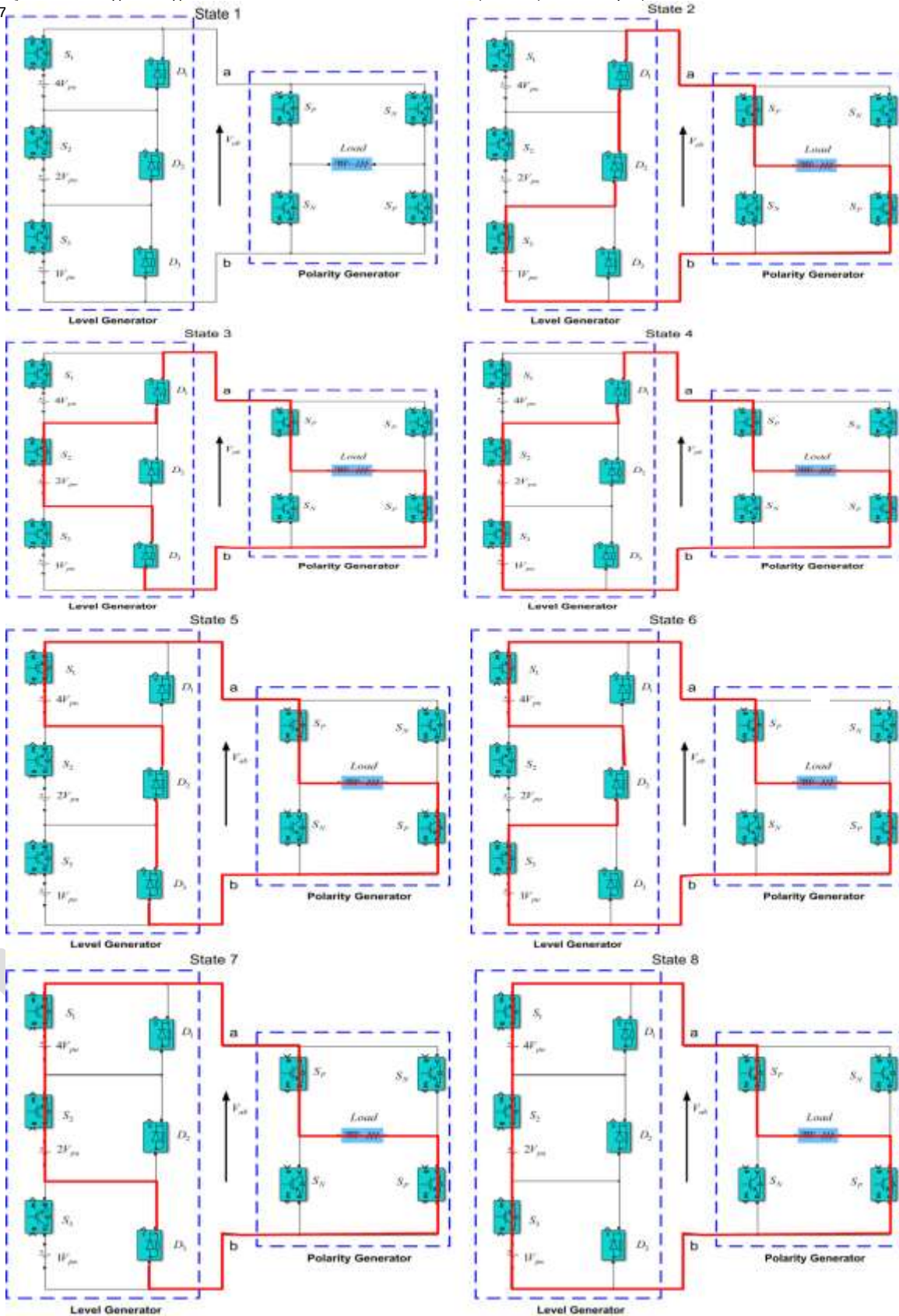


Fig.4: Operating states of the proposed inverter.

SIMULATION RESULTS

In order to verify the proposed inverter topology simulations are carried out on MATLAB/SIMULINK platform. Fig. 5 shows the implementation of the power circuit and the control scheme in Matlab/Simulink.

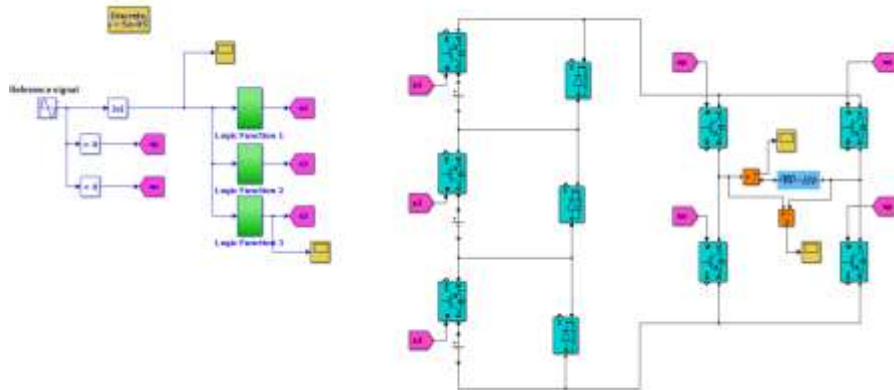


Fig.5: Simulink diagram of the proposed inverter topology implemented in Matlab.

The output waveforms of the inverter feeding a resistive load of 150Ω is shown in Fig. 6. The %THD of the current is 6.63 without any filtering.

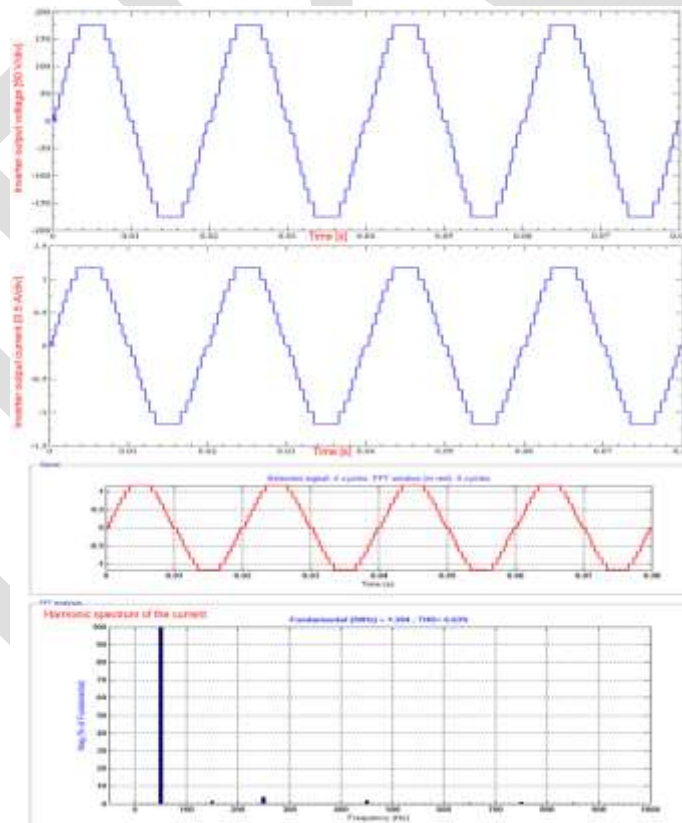


Fig. 6: Output waveform of the inverter feeding resistive load.

The output waveforms of the inverter feeding a resistive-inductive load of 150Ω and 50mH is shown in Fig. 7. The %THD of the current is 4.3 which is in comply with the IEEE 519-1992 standard.

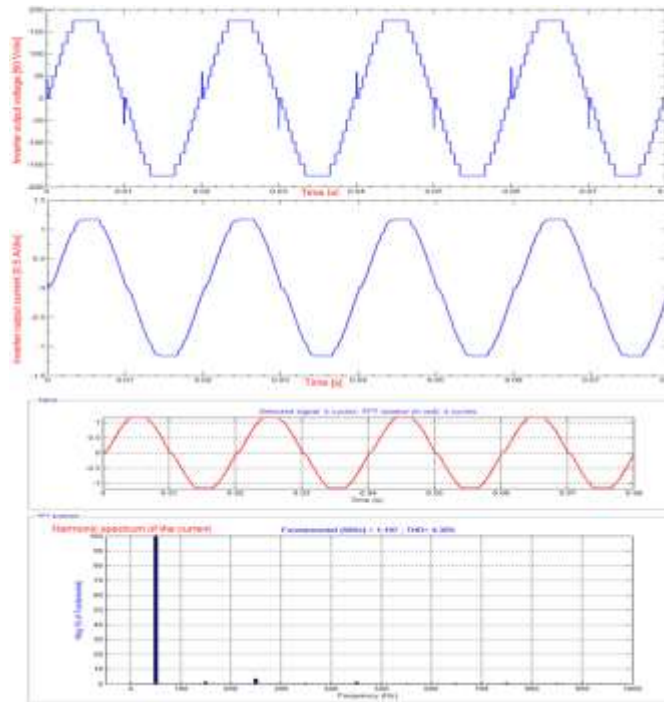


Fig.7: Output waveform of the inverter feeding resistive-inductive load.

TABLE I
 COMPARISON OF COMPONENTS REQUIRED FOR PROPOSED TOPOLOGY WITH OTHER POPULAR INVERTERS

	<i>Neutral point clamped</i>	<i>Cascaded</i>	<i>Flying capacitor</i>	<i>Proposed</i>
<i>Main switches</i>	12	12	12	10
<i>Main diodes</i>	12	12	12	10
<i>DC bus capacitors</i>	6	3	6	3
<i>Total number</i>	30	27	30	23

Table I shows the comparison of number of components required for the proposed topology with other popular inverters. It can be seen that the proposed inverter requires less number of components for same level generation and hence has a better efficiency and performance.

CONCLUSION

In this paper a new inverter topology which has superior performance, offering improved output waveforms and lower THD over conventional topology in terms of number of switches required, cost, control system and reliability. The proposed topology and fundamental switching scheme result in a near-sinusoidal waveform. As a result, a significant reduction of output voltage THD is obtained, and the modulation scheme has been discussed in detail. The complexity of PWM for this topology is low since it only needs to generate PWM gating pulses for generation of positive level only. The results obtained clearly shows the effectiveness of the proposed topology as a multilevel inverter with reduced number of switches as a promising topology for multilevel power conversion.

REFERENCES:

- [1] Wu, B., *High-Power Converters and AC Drives*, Hoboken, NJ John Wiley and Sons, Inc., 2006.
- [2] S. R. Stala, "Application of balancing circuit for dc-link voltages balance in a single-phase diode-clamped inverter with two three level legs," *IEEE Trans. Ind. Electron.*, vol. 58, no. 9, pp. 4185-4195, Sep. 2011.
- [3] J. Rodriguez, J. S. Lai, and F. Z. Peng "Multilevel inverters: A survey of topologies, controls, and applications," *IEEE Trans. Ind. Electron.*, vol. 49, no. 4, pp. 724-738, Aug. 2002.
- [4] N. Sandeep, P. Salodkar, and P. S. Kulkarni, A new simplified multilevel inverter topology for grid-connected application," in *Proc. IEEE Students' Conference on Electrical, Electronics and Computer Science (SCEECS)*, Bhopal, India, pp. 1-6, Mar. 2014.
- [5] Z. Sang, C. Mao, and D. Wang, "Staircase control of hybrid cascaded multi-level Inverter," *Electric Power Components and Systems*, 42(1), pp. 23-34, 2014.
- [6] T.L.Skvarenina, the power electronics hand book. Boca Raton, FL: CRC Press, 2002.
- [7] K.A.Corzine, J.R.Baker, and Jayden, "reduced parts-count-multilevel rectifiers." In conf.Rec.IEEE-IAS Ammu.meeting, Chicago, IL, Sept.2001, cad-Rom.
- [8] T.A.Meynard and H.Foch, "multilevel converters and derived topology for high power conversion." In proc.1995 IEEE 21st int.conf. Industrial electronics, control, and instrumentation, nov.1995, PP.21-26
- [9] N.S.Choi, J.G.Cho, and G.H.Cho "a general circuit topology of multilevel inverter." In proc. IEEE PESC 91, June 1991, PP.96-103.
- [10] D.W.Kang et al. "improved carriers wave-based SVPWM method using phase voltage redundancies for generalized cascaded multilevel inverter topology." In proc.IEEE APEC, New Orleans, LA, Feb.20000, PP.542-548

A survey on wormhole attacks on Wireless Mesh Networks and its detection

Shalki Naresh
(Pursuing M. Tech, CSE)
Maharishi Ved Vyas Engineering College, Kurukshetra University

Er. Navjot Singh
(Assistant Professor, CSE)

shalkinaresh@gmail.com, +91-9419966981

Abstract— Wireless Mesh Networks (WMNs) have come out as an economical and extensible technology that can offer low-cost, high bandwidth, better coverage, etc to meet the needs of lot of people with different properties. But because of its open nature and wireless transmission; it is prone to many attacks of which the wormhole is the severe one. In this attack, the attackers form a tunnel between them; overhear the packets, forward them to each other and packets are replayed at the other end of network. The main objective of this paper is to study the wormhole attack related to WMNs and to study the various detection mechanisms of wormhole. The various wormhole detection schemes like: shared information among communicating access points, cluster-based detection, detection using hop-count, etc are also studied. The effect of these given schemes on wormhole and network is also evaluated. Thus the research study is based on WMNs, wormholes, wormhole detection and its effect.

Keywords— Wireless Mesh Networks, Denial of services, Wormhole attack, Authentication Server, Mesh Points, time division duplex, time division multiple access, Pair wise Master Key Security association, Mobile Ad Hoc Network, Wormhole detection based on Neighbor's Neighbor scheme, Random Walk Route Scheme.

INTRODUCTION

WIRELESS MESH NETWORKS: A mesh network consists of radio nodes which is used for communication purposes is called Wireless Mesh Network (WMN). A WMN is a dynamic network which is self-organizing and self-configuring. The nodes of WMN's automatically establish an ad hoc network and also maintain their mesh connectivity [7].

With increase in interest in multi-hop wireless communications, wireless mesh networks (WMNs) have come out as an affordable and scalable solution to obtain broadband packet data communications across wide areas. WMNs can offer increased network coverage and enhanced load balancing across the network in comparison with typical single-hop wireless networks. The more advantages of WMN's are node failures robustness, deployment and maintenance ease, and its initial deployment cost is low [1].

Wireless mesh networks (WMNs) came out as an encouraging technology which yields low-cost, high-bandwidth wireless access services in various fields. A common WMN is introduced in Figure 1 which comprises of group of stationary mesh routers (MRs) which made backbone of mesh and a group of mesh clients which communicate along mesh routers. Security is used to evaluate performance of WMN's. The most challenges which we are facing in the security of WMN's are due to open nature and multi-hop cooperative communication environment in WMN's. These network services aspects are more unprotected specifically for attacks that come within the network [8].

Security is critical problem in WMN's because of wireless open nature and multi-hops due to which it caught variety of attacks such as wormhole, physical disruption, node compromise, etc.

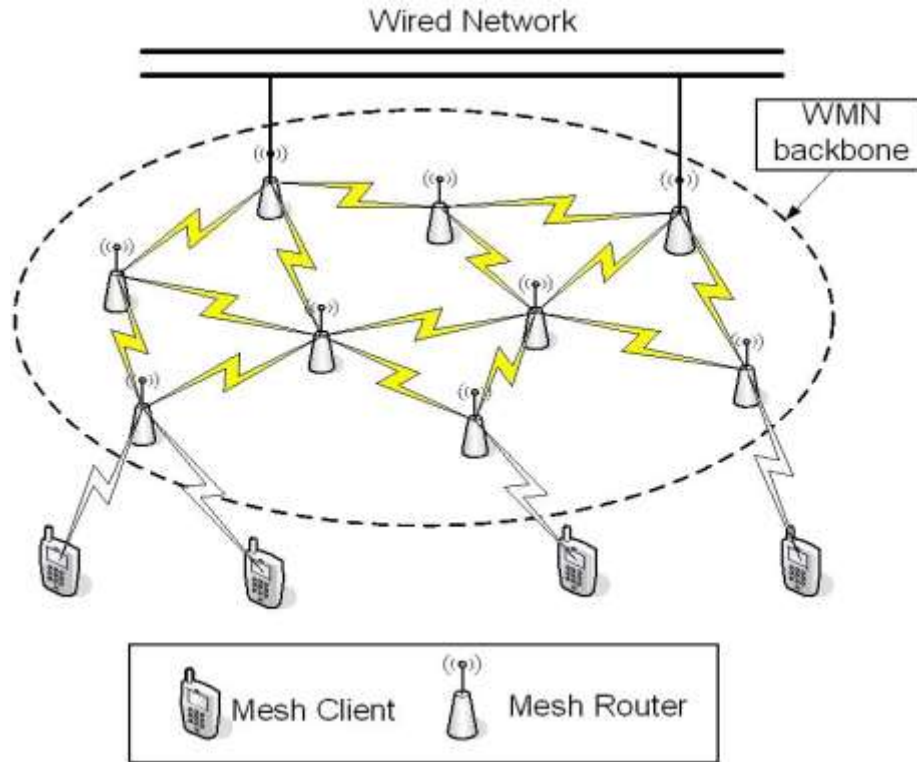


Figure 1: A typical WMN

SECURITY ISSUES

The security is important feature of observing application in WMNs. WMN's catches Denials of Service (DoS) attacks because of the use of multi-hop routing in WMN's. A DoS attack is one in which the network remains unavailable for its users and unable to respond to user in particular waiting time. It floods the server with huge number of requests so that the server is unable to service the authorized user. The DoS attack is done to exhaust the network resources by overloading it with packets form its exposed nodes which includes mesh routers and mesh clients. However because of limited bandwidth, routing functionalities, mobility, etc, associated with each node of WMN's, it introduce many probabilities to cast a DoS attack. Various DoS attacks on WMN's are being shown below in Table 1 [7].

Layer	Attack	Defense Mechanisms
Physical layer	Jamming , Scrambling	Spread-spectrum, priority messages, lower duty cycle, region mapping, mode
MAC Layer	Unfairness, Mac Misbehavior, Selfish MAC	Small frames, Error-correction code Rate limitation
Routing Layer	Black hole , Greyhole , Wormhole , Jellyfish ,Byzantine ,Sybil , Cache Poisoning, Message Bombing	Authentication, packet leases by using temporal and geographic information, monitoring, probing, redundancy checking

MODELS OF AUTHENTICATION FOR WMN's

In WMN's, the AAA-server can be employed for authentication, authorization and accounting of devices and users inside the WMN (deployed in the mesh point) or outside of WMN yet reachable over an IP network through mesh portal. The authentication of mesh point, mesh access point and a simple station involves different procedures. The process of authentication is consistently related to the server, but there is always a direct communication between mesh points. The existing authentication models are:-

A. Centralized Authentication Model

In centralized authentication model of WMN, the IEEE 802.11i security association method is used. The 802.11s of WMN contains the attributes of both IBSS and ESS configurations of IEEE 802.11i. The execution of 802.11s is based on the 802.11i security architecture; thus the Authenticator and Supplicant part are placed in each MP (modulation parameter) [4].

In link establishment, the 802.1i authentication and key management performs separate IEEE 802.1X authentication processes which are executed on a server in two steps. Then in each of two steps the security association is provided by server through Pair wise Master Key (PMKSA). The first step includes the IEEE/802.1X authentication between client device which is initiator mesh point (as supplicant) and the AS (Authentication server) through peer mesh point which is network device (as authenticator) whereas second step includes IEEE/802.1X authentication between network device as peer mesh point (as supplicant) and the authentication server (AS) through initiator mesh point (as authenticator). A PMKSA (Pair wise Master Key Security Association) is established by IEEE 802.1X/EAP authentication [4].

Since WMN's are distributed in nature so it should be self-organized and requires supporting distributed authentication. Node mobility and speedy link establishment with neighbor nodes need freedom from central entities. Thus the need to opt distributed authentication is:

- Because of centralized Authentication Server (AS), there must be transfer of authentication information between AS and mesh points when two mesh points establishes link between them or mutually authenticate one.
- In centralized authentication model, Authentication server (AS) is single point of failure. If AS fails the authentication of new MP's (mesh points) is impossible.

B. Distributed Authentication Model

In Distributed authentication model there is no centralized AS and is related to IBSS under 802.11i. The functions of authentication server are supported by every mesh point (MP) in the WMN. During the process of authentication every mesh point is able to act as Supplicant, Authenticator and an Authentication Server. The security association specifications for Distributed model are the same RSNA as applied in the central model except for the central AS. In distributed model the role of AS is performed by the mesh points. IEEE802.1i key management and authentication is used in link establishment phase to get security association. For security association, this step gives Pair Wise Master Key and also pair wise and group wise transient keys. The link must be established by each mesh node, so a table is used to handle multiple security associations that must implemented in each mesh point [4].

In IEEE 802.1X authentication, every mesh point demands from its local IEEE 802.1X entity to forms a Supplicant port for the peer mesh point (MP). Then the authentication will be initiated by Supplicant port to the peer MP by sending an EAPOL-Start message. The local IEEE 802.1X is also requested by the mesh point to form an Authenticator port for the peer MP when receives an EAPOL-Start message. When two mesh points are initially authenticated, data frames (except IEEE 802.1X messages) are not allowed to flow between them until both of each MP's have well finished Authentication and Key Management and have supplied the encryption keys. This model has its own drawbacks as this model is based on transitivity of trust i.e. any node of WMN can provide certificate to other node if it trust it. Thus there is series of trust (transitivity) which may lead to network congestion and to security breaches [4].

Drawbacks of existing models are follows:

- a. Fully central:
 - i. Traffic congestion.
 - ii. Single point of failure of Authentication server.
 - iii. Saving information of all Mesh Points at server side is unpractical.
- b. Fully distributed
Transitive trust or chain of trust leads to security breaches.

WORMHOLE ATTACK

An attack in which two attackers are attached by high-speed off-channel link and placed strategically at different ends of a network is called wormhole attack. The wormhole link can be formed by many ways e.g., by Ethernet cable, by optical link, long range wireless communications, etc. The attacker records the overheard data and forward it to one another and the packets are replayed at other end of the network. They make distant nodes believe that they are their nearby neighbors by replaying valid network messages and thus all communications between damaged nodes is enforced to go through attacker nodes [3]. This attack prevents nodes from determining valid paths that are more than two hops away and affects network functionality. A strong attack results in a separation or breakdown of a network. Figure-2 shows a wormhole attack in which the packets received by node X are replayed at Y by the attacker, and vice versa. The packets which are broadcasted near X and moves via wormhole will arrive earlier at Y as compared to those which usually cover several hops to move from a location near X to Y. Thus by forwarding routing messages they makes A and B to believe that they are neighbors, and then by excluding particular messages they distort communications between A and B [2].

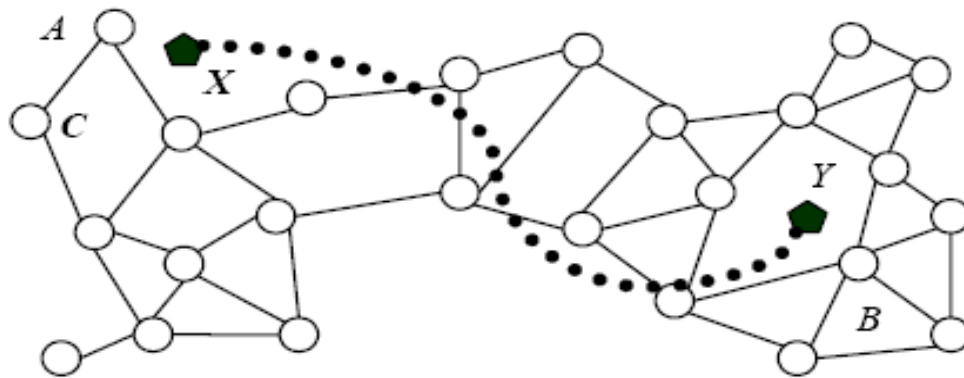


Figure 1. Wormhole attack.

A) Types of Wormhole Attacks:

Wormhole attacks can be:

- 1) *Packet encapsulation wormhole*: In this form of wormhole attacks, the data packets are encapsulated and there are some nodes between malicious nodes. The hop count does not increase as encapsulated data packets are sent between malicious nodes. Due to this the routing protocols using hop count are adaptable to this attack.
- 2) *Packet Relay wormhole*: This wormhole attack is initiated by more than one malicious nodes and data packets of two far away sensor nodes are relayed by malicious nodes so that they appear as neighbors to them. This attack is also known as “Replay-Based attack”.
- 3) *Protocol Distortion wormhole*: In this attack the routing protocol is distorted by malicious node and traffic is attracted by it. The ‘shortest delay’ or ‘smallest hop count’ routing protocols are affected by this wormhole attack.
- 4) *High-quality/Out-of-band Channel wormhole*: In this wormhole attack, a single-hop, high-quality, out-of-band-link called tunnel is formed between malicious nodes. A tunnel can be formed by direct wired or directional wireless link. This attack is difficult to launch as it needs special hardware [9].

B) Detection mechanisms of Wormhole attack:

The techniques to detect wormhole attacks are:

- 1) *Centralized approach*: In this approach, data from neighborhood of each node is sent to a central entity. The received data is used to build a model of whole network and is checked for inconsistencies. The inconsistencies that may appear because of wormholes, depends on information provided by local nodes. The approaches under it are:-

- Statistical Detection of wormhole
- Wormhole Detection using multi-dimensional Scaling approaches

- 2) *Decentralized approach*: In this approach, each node builds model of its own neighborhood by the use of data collected locally, so there is no need of central entity. Since it doesn't need central entity thus can be used in many applications [10]. The various approaches under it are:

- Wormhole Detection based on distance estimation

- Anchors positional information method of wormhole detection
- Method based on directional range information for wormhole detection.

LITERATURE SURVEY

Hyunok Lee et.al (2008) an assignment protocol based on control time slot is made for large wireless mesh networks (WMNs) which are established upon time division duplex (TDD) and time division multiple access (TDMA). In this protocol, every wireless mesh router has a broadcast time slot which maintains a minimum average signal-to-interference-plus-noise ratio (SINR) with all its adjoining routers. This protocol is implemented in fully distributed way and is topology-dependent which uses contention-based reservation mechanisms. It also uses the mechanisms of negative acknowledgement, busy tones and selection strategy based on greedy time slot. This protocol includes the whim of co-channel interference and radio propagation. A computer simulator which applies radio propagations on large scale and regards all co-channel interferences within network is generated. By simulations, the performance of protocol is calculated for many factors of wireless system which includes shadowing. Thus, a power control scheme for better utilization of time slots is given. Also, an algorithm based on power control has been given and its uses have been determined. Results shows that in all simulated scenarios this protocol assures minimum average SINR for pair of neighbor links and is robust, adaptable and scalable [1].

V.S. Shankar Sriram et.al (May 2009) in wormhole attack, an attacker which has limited resources and without any cryptographic break can cause destruction on wireless networks. At first, the research says that it is possible only on Ad hoc networks, but now it is deduced that it can be done on any infrastructure based wireless LANs. With a successful wormhole attack, an attacker can disrupt routing and can deny services of the network. Architecture for determining the likelihood of wormhole attack as well as corrective measures for avoiding such attacks is proposed. The mechanism involves use of Neighbor discovery with link verification so that in and out traffic of neighboring AP's can be monitored and also it uses hop neighbors data structures so that false neighbors can be detected. The threat of this attack is reduced by this mechanism and no location information and clock synchronization is required [2].

Debdutta Barman Roy et.al (April 2009) in case of wireless system with multi-hops, there is need of cooperation between different nodes to relay packets between them due to which it encounters a variety of security risks such as wormhole attack. In wormhole attack, a malicious node at one location records the traffic and tunnels it to other attacker which is far away and which replays it. In Ad-Hoc networks, a feasible and strong authentication method for nodes along with lightweight cryptography is used for routing security. Sadly, wormhole attack cannot be trapped by cryptographical measures because it does not create separate packets. The packets already present in the network are replayed in this attack. Earlier methods of wormhole detection needs specialized hardware, such as extremely accurate clocks, directional antennas, etc. But in this paper a counter-measure based on clusters is used for detecting wormhole attacks, which lessens those drawbacks and systematically reduces the wormhole attack in MANET. A simulation is done on 30 nodes and on many guard nodes which shows the productivity of this proposed algorithm [3].

Divya Bansal et.al (2010) a wireless mesh network and issues related to the deployment of WMN's is discussed of which security is serious one. The main point of security is authentication of users and devices in the network. In IEEE 802.11s based mesh networks, there is no particular security architecture which serves large number of applications. A centralized and distributed authentication schemes for WMN's are discussed. Due to multi-hop characteristic of WMN's, 802.11i cannot be used as security standard because it is based on central security mechanism. And distributed mechanism because of its trust issue can't be implemented. So an approach based on threshold and Clustered Certificate Authority is given which serves best of both centralized and distributed authentication architecture and use of which can restricts the entry of malicious nodes [4].

Nadher M. A. Al_Safwani et.al (8-9 June, 2011) security is the important matter for providing the shielded communication among mobile nodes in hostile environment. The wireless ad-hoc network is unsafe against attacks by malicious nodes. By using QualNet 4.5 simulator, the influence of various attacks on mobile Ad Hoc Network (MANET) system has been figure out in this paper. The active and passive attack on MANET is studied and the performance of MANET with and without these attacks is measured. The data link and network layer of nodes in MANET is simulated. The results are used to evaluate the formation of MANET nodes for security. The study is used for performance analysis of MANET and what-if' analysis is performed for optimization of nodes [5].

Pushpendra Niranjana et.al (April 2012) because of wireless transmissions in MANET, it is subjected to more security issues than wired one. The paper focus on tunneling attacks in which there is no need of exploiting the nodes of network and can easily interfere route establishment. A new method which does not requires modification of protocol and detection of suspicious routes is presented. The method detects the attacker nodes directly by using hop-count and time delay analysis from user's viewpoint without particular environment assumptions. The work is simulated by the use of OPNET. The method detects 75% of attacks in 5 minutes. Since searched routes parts are selected for multipath transmissions so probability of occupying routes by attack is also reduced [6].

Huaiyu Wen et.al (September 20, 2013) security is a cause of concern for Wireless Mesh Networks (WMNs) cause of its vast use. It is easy for an attacker to launch a wormhole attack on WMN's because of its open nature and can't be prevented by using cryptographic protocols. To increase the capability and possibility of detection of wormhole attack, a highly capable detection algorithm which is based on 2-hop neighbor known as Wormhole Detection based on Neighbor's Neighbor scheme (WDNN) is proposed. Also to prevent wormhole routes that attract routing traffic based on least count a Random Walk Route scheme (RWR) is given. In WDNN, by extending the range of transmission of 2-hop neighbor, the network topology fabricated by wormholes can be identified without the use of clock synchronization or additional hardware. In RWR, the route other than the low latency link created by wormholes is chosen. The security analysis by using these techniques proves that it can detect and prevent wormhole attacks. The simulation result of protocols reveals that it can get 100% wormhole detection rate and routes can be prevented from being attacked against traditional routing protocols [7].

Rakesh Matam et.al (2013) wormhole attack is an acute attack on WMN's and when is critically placed it can disturb the bulk of routing communications. Almost all of the earlier wormhole defense mechanisms are not fully secured from wormhole attacks launched in participation mode. This paper presents wormhole-resistant secure routing (WRSR) algorithm that reveals the existence of wormhole during route discovery and seclude it. In contrast to other schemes that start the detection of wormhole on observing packet loss, WRSR analyses route requests that traverse a wormhole and avoids the formation of such routes. In WRSR, a unit disk graph model is used to decide the mandatory and enough condition for analyzing a wormhole-free path. The most interesting aspect of WRSR is its capability to prevent from all types of wormhole attacks (hidden and Byzantine) without using extra hardware like synchronized clocks or timing information, global positioning system, etc [8].

Priti Gupta et.al (2014) Wireless Mesh Network is a rising technology that can be implemented to construct a network which can increase the coverage of internet access for satisfying the different needs of many people. WMN's are more prone to wormhole attacks as compared to other attacks. In a common wormhole attack, two or more forms a tunnel between them by the use of adequate communication medium. This paper provides algorithm for identifying wormhole in WMN's which is based on calculation of directional neighbor list and neighbor list of source node. This algorithm gives the rough location of nodes and calculates the effect of wormhole on each node so that corrective measures can be implemented. The performance of algorithm can be evaluated by the variation of wormholes in the network [9].

Himani Gupta et.al (May 2015) wireless mesh networks are widely used and are liable to the many attacks because of lack of security; one of such attack is wormhole. In such attack, attacker nodes by planning established a tunnel between them by using systematic wireless medium. In this paper, a wormhole detection algorithm is described for wireless mesh networks in which wormholes is detected by the calculations of neighbor and directional neighbor list of nodes. It gives the probable location of the nodes and tells us about the consequence of wormhole attack on all nodes that helps us in implementation of the network. The evaluation of the performance is done by changing the number of wormholes in the network and then the throughput and packet delivery ratio in these situations are explored. GloMoSim is used as simulator [10].

CONCLUSION OF SURVEY

The literature above reviewed can be concluded as:

Author & Year	Work	Technique Used	Findings
Hyunok Lee 2008	Fully distributed control time slot assignment protocol for WMN's	Contention based reservation mechanisms, busy tones and negative acknowledgments.	Minimum average SINR in all simulated scenarios; protocol is adaptable, scalable and robust
V.S Shankar Sriram 2009	Methodology for securing wireless LANs against wormhole attack	Shared information among communicating access points, neighbor discovery and link verification	Prevent rouge access point from behaving as false neighbors, reduce wormhole threat, no need of location information and Clock synchronization
Divya Bansal 2010	Threshold based authorization model for authentication of node in WMNs	Threshold Cryptography and principle of threshold numbers	Combines both central and distributed authentication models and restricts the entry of malicious bots
Pushendra Niranjan 2012	Wormhole attack detection using hop count and time delay	Hop count, Time delay, OPNET simulator	Detects wormhole effectively: 75% in 5 mins, further occupying of routes by attack is reduced
Huaiyu Wen 2013	2-hop neighbor detection and prevention of wormhole attacks	WDNN: Wormhole detection based on Neighbor's Neighbor scheme RWR: Random Walk Route Scheme	Faked topology detected, Least cost route by wormhole is detected, fraction of compromised nodes fall quickly.
Rakesh Matam 2013	Wormhole-resistant secure routing for WMNs	Unit disk graph model, shorter alternate path to detect wormhole	Defend against all wormholes (hidden and byzantine) without any extra hardware
Priti Gupta 2014	Scheme to detect wormhole in WMNs	Neighbor list, directional neighbor list	Gives approximate location of nodes and effect of wormhole on each node
Himani Gupta 2015	Partially distributed authentication solution for securing WMN from wormhole attacks	Neighbor list, directional neighbor list, GloMoSim, Directional ranges	Constant throughput while PDR increases proportionally with increase in number of nodes and detects high percentage of attack

CONCLUSION

In this paper the WMNs are studied and the various security concerns related to WMNs are also studied. The wormhole attacks on WMNs and its detection methods are studied. The methods of detection are studied and are compared. The alternative solutions are: shared information among communicating access points which averts the rouge points from acting as neighbors and there is no need of location information and clock synchronization, hop count detection which detects 75% attack in 5 mins, 2-hop neighbor detection in which WDNN and RWR are used by which Faked topology detected, least cost route by wormhole is detected, fraction of compromised nodes fall quickly, etc. So there is no particular solution to this problem as different methods for different architecture are available.

REFERENCES:

[1] Hyunok Lee, Donald C. Cox, "A fully- distributed control time slot assignment protocol for large wireless mesh networks", 978-1-4244-2677-5/08/\$25.00 c 2008 IEEE.

- [2] V.S.Shankar Sriram, Ashish Pratap Singh, G.Sahoo, "Methodology for Securing Wireless LANs Against Wormhole Attack", International Journal of Recent Trends in Engineering, Issue. 1, Vol. 1, May 2009.
- [3] Debdutta Barman Roy, Rituparna Chaki, Nabendu Chaki, "A new cluster-based wormhole intrusion detection algorithm for mobile ad-hoc networks", International Journal of Network Security & Its Applications (IJNSA), Vol 1, No 1, April 2009.
- [4] Divya Bansal, Sanjeev Sofat, "Threshold based Authorization model for Authentication of a node in Wireless Mesh Networks", Int. J. of Advanced Networking and Applications Volume: 01, Issue: 06, Pages: 387-392 (2010).
- [5] Nadher M. A. Al_Safwani, Suhaidi Hassan, Mohammed M. Kadhun, "Mobile Ad-hoc networks under wormhole attack: A simulation study", Proceedings of the 3rd International Conference on Computing and Informatics, ICOCI 2011,8-9 June, 2011 Bandung, Indonesia.
- [6] Pushpendra Niranjana, Prashant Srivastava, Raj kumar Soni, Ram Pratap, "Detection of WormholeAttack using Hop-count and Time delay Analysis", International Journal of Scientific and Research Publications, Volume 2, Issue 4, April 2012 ISSN 2250-3153.
- [7] Huaiyu Wen, Guangchun Luo, "Wormhole Attacks Detection and Prevention Based on 2-Hop Neighbor in Wireless Mesh Networks", Journal of Information & Computational Science 10:14 (2013) 4461-4476 (September 20, 2013).
- [8] Rakesh Matam, Somanath Tripathy, "WRSR: wormhole-resistant secure routing for Wireless mesh networks", EURASIP Journal on Wireless Communications and Networking 2013.
- [9] Priti Gupta, Suveg Moudgil, "A Novel Scheme to Detect Wormhole Attacks in Wireless Mesh Network", International Journal of Computer Science and Information Technologies (IJCSIT), Vol. 5 (3), 2014, 4798-4801.
- [10] Er. Pinki Tanwar, Himani Gupta, "Partially Distributed Authentication Solution for Securing WMN against Wormhole Attacks", International Journal of Advanced Research in Computer Science and Software Engineering Volume 5, Issue 5, May 2015.

Smart Concrete – A New Technology

Patil Gaurao S., Patil Nikhil M., Dhange Ankush B.,
Jadhav Swati B., Jaybhaye Archana L.

(Student, Department of Civil Engineering, Imperial college of Engineering, Pune, India)

gaurav.ptl@gmail.com
patilnikpatil24@gmail.com
arbdhange07@gmail.com

Abstract – Due to temperature gradients, surface cracks can occur at very early ages in concrete structures. Because the hydration has just started it is possible that these cracks can heal with continuing hydration. The aim of this research was to investigate if cracks that arise at early ages can heal and under what conditions. Primarily the strength of healed cracks was considered. When water flows through cracks smaller than 0.2 mm, the flow will decrease and can stop completely. This is called self healing. Precipitation of calcium carbonate and clogging by loose particles are the most mentioned causes.

Keywords—Bacillus Sphaericus, Filling of cracks, Peptone, Self healing, Calcium carbonate, Corrosion resistance, Compressive strength

INTRODUCTION:

Concrete is the most widely used construction material because of its high compressive strength, relatively low cost etc. One adverse property of concrete is its sensitivity to crack formation as a consequence of its limited tensile strength. For that reason, concrete is mostly combined with steel reinforcement to carry the tensile loads. Although these rebars restrict the crack width, they are mostly not designed to completely prevent crack formation. Cracks endanger the durability of concrete structures as aggressive liquids and gasses may penetrate into the matrix along these cracks and cause damage. Consequently, cracks may grow wider and the reinforcement may be exposed to the environment. Once the reinforcement starts to corrode, total collapse of the structure may occur. Therefore, it seems obvious that inspection, maintenance and repair of concrete cracks are all indispensable. However, crack repair becomes difficult when cracks are not visible or accessible. Moreover, in Europe, costs related to repair works amount to half of the annual construction budget. In addition to the direct costs, also the indirect costs due to loss in productivity and occurrence of traffic jams carry a severe economic penalty. Accordingly, self-healing of cracked concrete would be highly beneficial. Self-healing is actually an old and well known phenomenon for concrete as it possesses some natural autogenous healing properties.

However, autogenous healing is limited to small cracks, is only effective when water is available and is difficult to control. In 1969, self-healing properties were for the first time built-in inside polymeric materials.

PRINCIPLE:

Concrete is a construction material that is used world-wide because of its first-rate properties. However, the drawback of this material is that it easily cracks due to its low tensile strength. It is a well-known fact that concrete structures are very susceptible to cracking which allows chemicals and water to enter and degrade the concrete, reducing the performance of the structure and also requires expensive maintenance in the form of repairs. In this paper, the following notable points regarding classification of bacteria, self-healing of cracks in concrete, chemical process for crack remediation, self-healing mechanism of bacteria, application of bacteria in construction field, Advantages and disadvantages of bacterial concrete etc., are observed and identified from the other research works. Cracking in the surface layer of concrete mainly reduces its durability, since cracks are responsible for the transport of liquids and gases that could potentially contain deleterious substances. On the other hand the concrete structures show some self- healing capacity, i.e. the ability to heal or seal freshly formed micro-cracks.

LITERATURE REVIEW:

Bacterial Concrete: New Era for Construction Industry

International Journal of Engineering Trends and Technology (IJETT) – Volume 4 Issue 9- Sep 2013

Concrete which forms major component in the construction Industry as it is cheap, easily available and convenient to cast. But drawback of these materials is it is weak in tension so, it cracks under sustained loading and due to aggressive environmental agents which ultimately reduce the life of the structure which are built using these materials. This process of damage occurs in the early life of the building structure and also during its life time. Synthetic materials like epoxies are used for remediation. But, they are not compatible, costly, reduce aesthetic appearance and need constant maintenance. Therefore bacterial induced Calcium Carbonate (Calcite) precipitation has been proposed as an alternative and environment friendly crack remediation and hence improvement of strength of building materials. The concept was first introduced by Ramakrishna, Journal publication on self-healing concrete over the last decade. A novel technique is adopted in re-mediating cracks and fissures in concrete by utilizing Microbiologically Induced Calcite or Calcium Carbonate (CaCO_3) Precipitation (MICP) is a technique that comes under a broader category of science called bio-mineralization. MICP is highly desirable because the Calcite precipitation induced as a result of microbial activities is pollution free and natural. The technique can be used to improve the compressive strength and stiffness of cracked concrete specimens. Research leading to microbial Calcium Carbonate precipitation and its ability to heal cracks of construction materials has led to many applications like crack remediation of concrete, sand consolidation, restoration of historical monuments.

MATERIALS:

1. Cement –

Ordinary Portland cement of grade 53 available in local market is used in the investigation. The cement used has been tested for various properties as per IS: 4031-1988 and found to be confirming to various specifications of IS: 12269-1987 having specific gravity of 3.0.

2. Coarse Aggregate –

Crushed granite angular aggregate of size 20 mm nominal size from local source having specific gravity of 2.71 is used as coarse aggregate.

3. Fine Aggregate –

Natural river sand having specific gravity of 2.60 and confirming to IS-383 zone II is used.

4. Water –

Locally available portable water confirming to standards specified in IS 456-2000 is used.

5. Microorganisms –

Any of the following bacteria may be used for the process:

- Bacillus sphaericus
- Bacillus cohnii
- Bacillus halodurans
- Bacillus pseudofirmus
- Bacillus subtilis

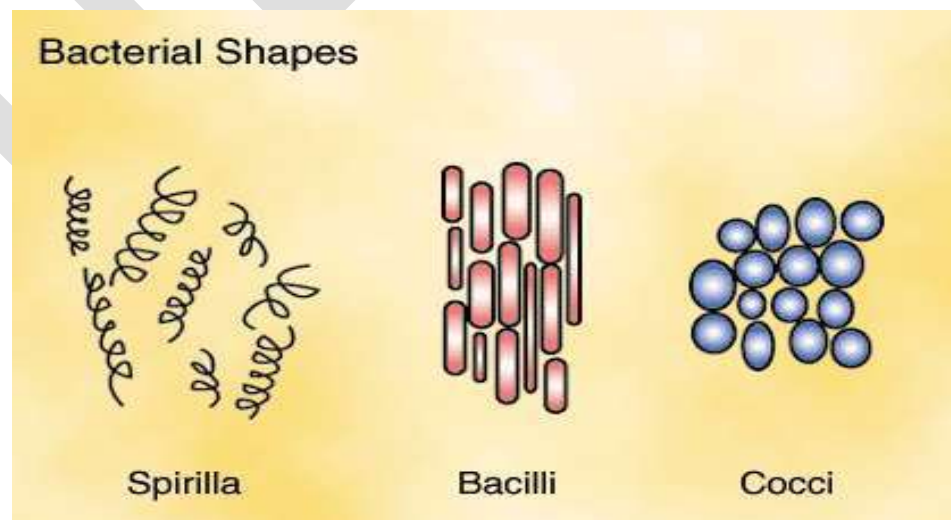


Fig.1 Shapes of Bacteria

METHODOLOGY –

The following steps are involved in the implementation of the project and are not limited to

- Literature Survey
- Collection of Required RAW materials
- Designing of concrete M20 Grade mix as per IS 10262-2009
- Culturing of Calcite Depositing Bacteria
- Casting and curing of controlled concrete cubes, beams and cylinders
- Creating a fault plane for bacterial concrete application
- Application of cultured bacteria for cracked Surface
- Strength and durability tests on healed concrete
- Comparison of strength and durability characteristics of controlled M20 grade concrete and bacteria healed concrete
- Discussions and conclusions to be done on the results obtained.



Fig. 2 Bacteria



Fig. 3 Nutrient Agar



Fig.4 UV rays machine

ADVANTAGES:

- Helpful in filling of cracks in concrete.
- Helpful to reduce leakage of residential building.
- Helps to reduce permeability in concrete.
- Helpful to reduce corrosion of reinforced concrete.
- It increases durability of concrete.

DISADVANTAGES:

- It is quite costly than normal concrete so becomes uneconomical.
- It is not suitable for Indian atmospheric condition.
- It gives better results only if comes in contact with water.
- Process of activation of bacteria is tedious.
- It takes more time for working of bacteria in concrete.

CONCLUSION:

The microbial induced calcite precipitation reaction may cause lower amount of capillary pores and clogging of the pores, which reduces chloride ion transport in concrete. The use of bacterial cells has thus become a viable solution not only to some durability problems but also as an environmentally responsible course of action. The new method of self healing design to repair cracks in cracked concrete was suggested, and self healing properties of cracked concrete using various mineral admixture were investigated. This microbe proved to be efficient in enhancing the properties of concrete by achieving a very high initial strength increased and thus we can conclude that the produced calcium carbonate has filled some percentage of void volume thereby making the texture more compact and resistive to seepage.

REFERENCES:

- [1] M.V. Seshagiri Rao, V. Srinivasa Reddy, M. Hafsa, P. Veena And P. Anusha "Bioengineered Concrete - A Sustainable Self-Healing Construction Material", Department Of Civil Engineering, Jntuh College Of Engineering Hyderabad, India
- [2] "Studies on Strength Characters of Self Healing Bacterial Concrete" Project Reference No. 37s0747 College: Acharya Institute Of Technology, Bangalore

[3] Jagadeesha Kumar B G1, R Prabhakara2, Pushpa H31associate Prof., Civil Engineering, “Bio Mineralization Of Calcium Carbonate By Different Bacterial Strains And Their Application In Concrete Crack Remediation” , M S Ramaiah Institute Of Technology, Bangalore, India.

[4] Srinivasa Reddy V1, Achyutha Satya K2, Seshagiri Rao M V3, Azmatunnisa M41&2, “A Biological Approach To Enhance Strength AndDurability In Concrete Structures”, Department Of Civil Engineering, JntuhCeh, Hyderabad -500085, India

[5] Ravindranatha Rao, Udaya Kumar, SuhasVokunnaya, Priyodip Paul, Ioannou Orestis assistant Professor-Selection Grade “Effect Of Bacillus Flexus In Healing Concrete Structures”, Department Of Civil Engineering, Manipal Institute Of Technology, Manipal, India

[6] Pradeepkumar.A, Assistant Professor, “An Experimental Work on Concrete by Adding Bacillus Subtilis”, Dept. Of Civil Engineering, Veltech Engg College, International Journal of Emerging Technologies and Engineering (IJETE).Volume 2 Issue 4, April 2015, ISSN 2348 – 8050

[7] S. Sunil Pratap Reddy, M. V. Seshagiri Rao, P. Aparna and Ch. Sasikala, “Performance of Ordinary Grade Bacterial (Bacillus Subtilis) Concrete”, Department Of Civil Engineering, Cjits, Jangaon, Warangal, India

[8] Rajesh K. Verma, LeenaChaurasia, Vishakha Bisht, Manisha Thakur, “Bio-Mineralization and Bacterial Carbonate Precipitation In Mortar And Concrete”, Bio Concrete Laboratory, Environmental Science And Technology Group, Central Building Research Institute, Roorkee, India bioscience And Bioengineering Vol. 1, No. 1, 2015, Pp. 5-11

[9] Ravindranatha, N. Kannan, Likhith M. L. Assistant Professor “Self-Healing Material Bacterial Concrete”, Department Of Civil Engineering, M. I. T - Manipal, Karnataka, India

Probabilistic Network Model (PNM) Based Data Aggregation Method for Load Balancing In WSN

Ms. Jayashree A. Vanmali¹, Prof. Rahul Patil²

¹PG Scholar, Computer Engineering Department, Bharati Vidyapeeth College Of Engineering, Navi Mumbai, India

²Assistant Professor, Computer Engineering Department, Bharati Vidyapeeth College Of Engineering, Navi Mumbai, India

Email: jagruti.vanmali@yahoo.com

Abstract— Data aggregation is the process of collecting and aggregating the useful data. Data aggregation is considered as one of the fundamental processing procedures for saving the energy. Advancement in computing technology has led to the production of wireless sensors capable of observing and reporting various real world phenomena in a time sensitive manner. However such systems suffer from bandwidth, energy and throughput constraints which limit the amount of information transferred from end-to-end. Data aggregation is a known technique addressed to alleviate these problems but is limited due to their lack of adaptation to dynamic network topologies and unpredictable traffic patterns. In WSN, data aggregation is an effective way to save the limited resources. The main goal of data aggregation algorithm is to gather and aggregate data in an energy efficient manner so that network lifetime is enhanced. Wireless sensor nodes are very small in size and have limited processing capability and very low battery power. This restriction of low battery power makes the sensor network prone to failure. Data aggregation is a very crucial technique in WSNs. Data aggregation helps in reducing the energy consumption by eliminating redundancy. Most of the existing DAT construction works are based on the ideal Deterministic Network Model (DNM), where any pair of nodes in a WSN is either connected or disconnected. Under this model, any specific pair of nodes is neighbors if their physical distance is less than the transmission range, while the rest of the pairs are always disconnected. However, in most real applications, the DNM cannot fully characterize the behaviors of wireless links due to the existence of the transitional region phenomenon. The load-balance factor is also neglected when constructing DATs in current systems. And most of the current literatures investigate the DAT construction problem under the DNM.

In this project we are concentrating on load balancing factor and also on construction of DAT using Probabilistic Network Model (PNM). Therefore, it is focused on constructing a Load-Balanced Data Aggregation Tree (LBDAT) under the PNM. More specifically, three problems are investigated, namely, the Load-Balanced Maximal Independent Set (LBMIS) problem, the Connected Maximal Independent Set (CMIS) problem, and the LBDAT construction problem. LBMIS and CMIS are well-known NP-hard problems and LBDAT is an NP-complete problem. LBDAT will be NP-Complete and will be constructed in three steps: Load-Balanced Maximal Independent Set (MDMIS), Connected Maximal Independent Set (CMIS) and Load-Balanced Parent Node Allocation (LBPNA). Approximation algorithms and performance ratio analysis will also be covered. The simulation is done using NS2 tool.

Keywords— Sensor node, Data collection, Data aggregation, WSN, Network load balancing, Data Aggregation Trees (DATs), Load-Balanced Data Aggregation Tree (LBDAT), Deterministic Network Model (DNM), Probabilistic Network Model (PNM)

INTRODUCTION

Wireless sensor networks have limited computational power, limited memory and battery power, hence increased complexity for application developers which results in applications that are closely coupled with network protocols. In Wireless Sensor Networks (WSNs), sensor nodes periodically sense the monitored environment and send the information to the sink (or base station), at which the gathered/collected information can be further processed for end-user queries. In this data gathering process, data aggregation [1,2,4] can be used to fuse data from different sensors to eliminate redundant transmissions, since the data sensed by different sensors have spatial and temporal correlations. Hence, through this in-network data aggregation technique, the amount of data that needs to be transmitted by a sensor is reduced, which in turn decreases each sensor's energy consumption so that the whole network lifetime is extended.

Data coming from multiple sensor nodes is aggregated as if they are about the same attribute of the phenomenon when they reach the same routing node on the way back to the sink. Data aggregation is a widely used technique in wireless sensor networks. The security issues, data confidentiality and integrity, in data aggregation become vital when the sensor network is deployed in a hostile environment. Data aggregation is a process of aggregating the sensor data using aggregation approaches. Sensor nodes are deployed in remote environments to a multi-hop WSN over a wide range of area. Very rarely do the users have global information on the sensor nodes' distribution. That is why when users request state-based sensor readings of the attributes like temperature and humidity in an arbitrary area, networks may suffer the unpredictable heavy traffic. This problem needs data aggregation to comply with user requirements and manage overlapped aggregation trees of multiple users efficiently.

Data Gathering is a fundamental task in Wireless Sensor Networks (WSNs). Data gathering trees capable of performing aggregation operations are also referred to as Data Aggregation Trees (DATs). Existing works spend lots of efforts on aggregation scheduling and not on the DAT construction problem. Existing DAT construction works are based on the ideal Deterministic Network Model (DNM), where any pair of nodes in a WSN is either connected or disconnected. They did not consider the load-balance factor when they construct a DAT. Without considering balancing the traffic load among the nodes in a DAT, some heavy-loaded nodes may quickly exhaust their energy, which might cause network partitions or malfunctions.

Key Points in data aggregation are as follows:

- i. Nodes sense attributes over the entire network and route to nearby nodes.
- ii. Node can receive different versions of same message from several neighboring nodes.
- iii. Communication is usually performed in the aggregate.
- iv. Neighboring nodes report similar data.
- v. Combine data coming from different sources and routes to remove redundancy.

Most of the existing DAT[5] construction works are based on the ideal Deterministic Network Model (DNM), where any pair of nodes in a WSN is either connected or disconnected. Under this model, any specific pair of nodes is neighbors if their physical distance is less than the transmission range, while the rest of the pairs are always disconnected. However, in most real applications, the DNM cannot fully characterize the behaviors of wireless links due to the existence of the transitional region phenomenon. The load-balance factor is also neglected when constructing DATs in current systems. And most of the current literatures investigate the DAT construction problem under the DNM.

In this paper we are discussing on load balancing factor and also on construction of DAT using Probabilistic Network Model (PNM). Therefore, it is focused on constructing a Load-Balanced Data Aggregation Tree (LBDAT) under the PNM. More specifically, three problems are investigated, namely, the Load-Balanced Maximal Independent Set (LBMIS) problem, the Connected Maximal Independent Set (CMIS) problem, and the LBDAT construction problem. LBMIS and CMIS are well-known NP-hard problems and LBDAT is an NP-complete problem.

The main contributions of this paper are summarized as follows:

- i. Analysis of Data aggregation technique
- ii. Constructing a Load-Balanced Data Aggregation Tree (LBDAT) under the PNM
- iii. Investigation of three problems namely, the Load-Balanced Maximal Independent Set (LBMIS) problem, the Connected Maximal Independent Set (CMIS) problem, and the LBDAT construction problem
- iv. Simulation using NS-2.34 under Fedora Linux environment.

METHODOLOGY

WSNs are one of the most important technologies which are used in a variety of applications. To impact these applications in a real-world environment, we need more efficient strategies to guarantee secure communication on the sensor readings as well as to maximize the whole network lifetime. Since the sensor nodes are equipped with limited energy batteries, the energy conservation is the primary challenge for WSNs. We solved the LBDAT construction problem in three phases in this paper. First, we constructed a Load-Balanced Maximal Independent Set (LBMIS), and then we selected additional nodes to connect the nodes in LBMIS, denoted by the Connected MIS (CMIS) problem. Finally, we acquired a Load-Balanced Parent Node Assignment (LBPNA). After LBPNA is determined, by assigning a direction of each link in the constructed tree structure, we obtain an LBDAT.

A. Data Aggregation overview[13]

Data aggregation is the process of collecting and aggregating the useful data. Data aggregation is considered as one of the fundamental processing procedures for saving the energy. A data aggregation scheme is energy efficient if it maximizes the functionality of the network. If we assume that all sensors are equally important, we should minimize the energy consumption of each sensor. As soon as a query is sent by the BS to a sensor, the first step followed is to handle the query. This is followed by data collection from sources and aggregation of that data.

Network Data aggregation is of two types:

- a. Address-centric (AC) and
- b. Data-centric (DC)

a) Address-centric (AC)

In AC routing protocol [2], query is routed to a specific address or a given sensor based on the address specified in the query. Each source independently Address Centric Routing sends data along the shortest path to sink (“end to-end routing”). Data is then sent from this specific location to the BS(Base Station). The source with the address specified in the query, sends its data directly to the BS.

b) Data-centric (DC)

However, in DC routing [2], based on the condition specified in the query, all sensors satisfying that condition, need to respond and therefore, the query is broadcast to all the nodes (within range) in the network.

B. Probabilistic Network Model (PNM) based data aggregation method

We solve the LBDAT construction problem in three phases in this paper. First, we construct a Load-Balanced Maximal Independent Set (LBMIS), and then we select additional nodes to connect the nodes in LBMIS, denoted by the Connected MIS (CMIS) problem. Finally, we acquire a Load-Balanced Parent Node Assignment (LBPNA). After LBPNA is determined, by assigning a direction of each link in the constructed tree structure, we obtain an LBDAT. In this subsection, we formally define the LBMIS, CMIS, LBPNA, and LBDAT construction problems sequentially. The proposed method can be implemented using following flow(Fig.1)[13].The simulation parameters[13] are shown in table 1.And data aggregation for different network based schemes[1] are shown on Fig.2.

TABLE1
Simulation Parameters

Parameter/Specification	Details
No. of Nodes	50
Topology (Area)	500x500
NS2 version	NS2.34
Simulation Time	100 sec
Maximum Packet sent per second	1000
Energy threshold	0.3dbm

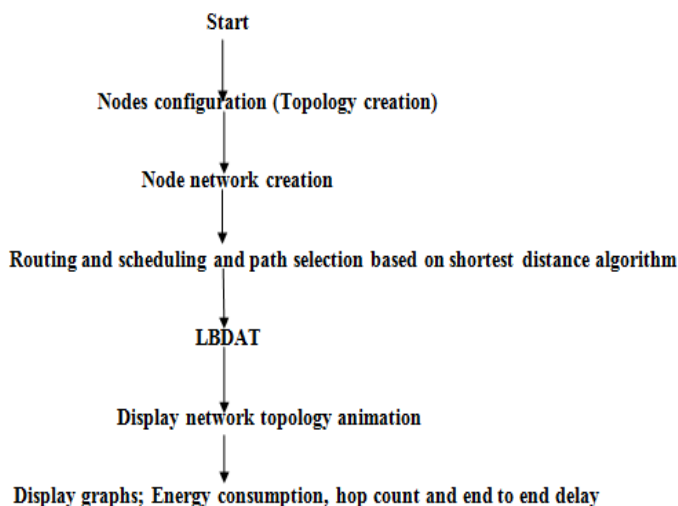


Fig.1.Method Flow

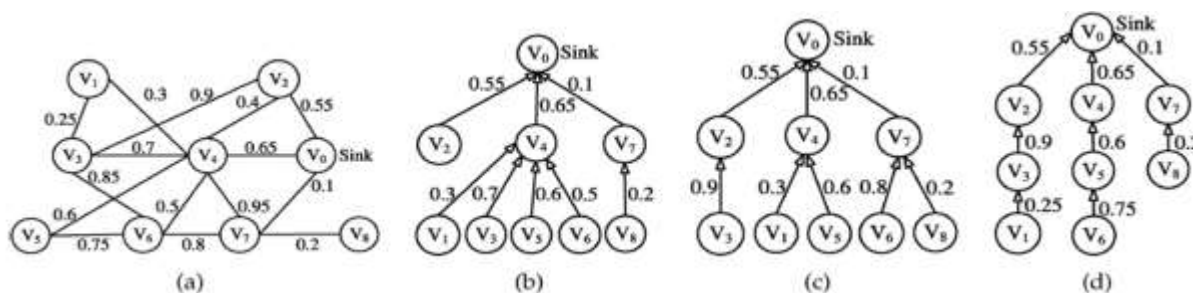


Fig.2.Data aggregation: Probabilistic WSN(a), DATs(b and c), and an LBDAT(d)

In this paper, we addressed the fundamental problems of constructing a load-balanced DAT in probabilistic WSNs. We first solved the CMIS problem, which is NP-hard, in two phases. In the first phase, we found the optimal MIS such that the minimum potential load of

all the independent nodes is maximized. To this end, a near optimal approximation algorithm is provided. In the second phase, the minimum-sized set of LBMIS connectors are found to make the LBMIS connected. The theoretical lower and upper bounds of the number of non-leaf nodes are analyzed as well. Subsequently, we studied the LBDAT construction problem and provided an approximation algorithm by using the linear relaxing and random rounding techniques. After an LBPNA is decided, by assigning a direction to each link, we obtain an LBDAT.

SIMULATION RESULTS

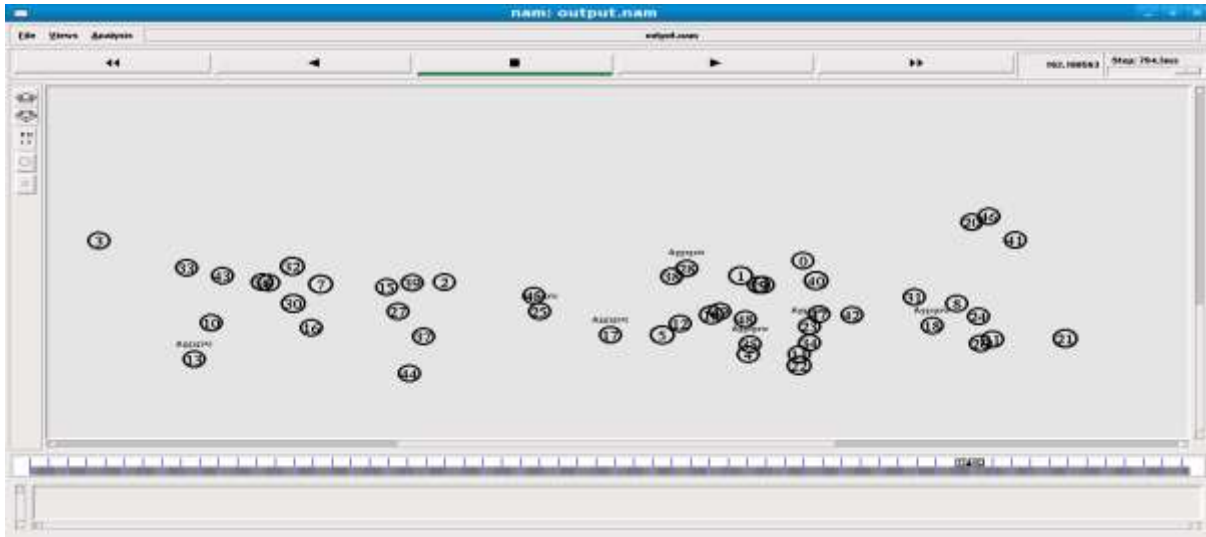


Fig.3.Animation View in NS2

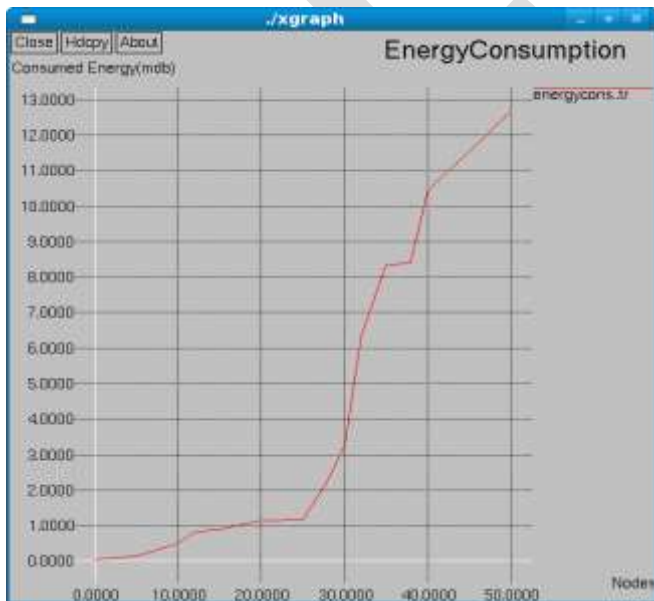


Fig.4.Energy Consumption graph

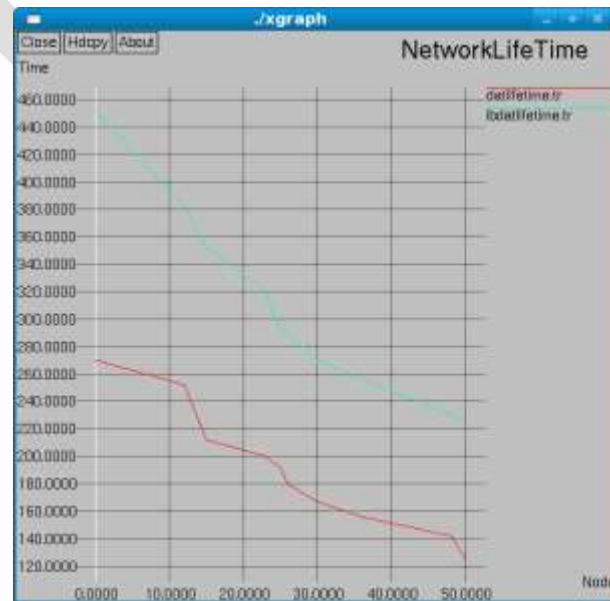


Fig.5.Network Life time graph

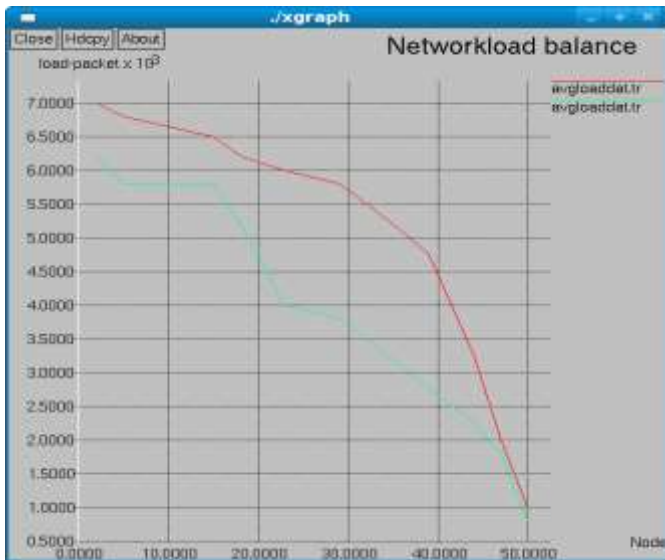


Fig.6.Network Load Balance graph

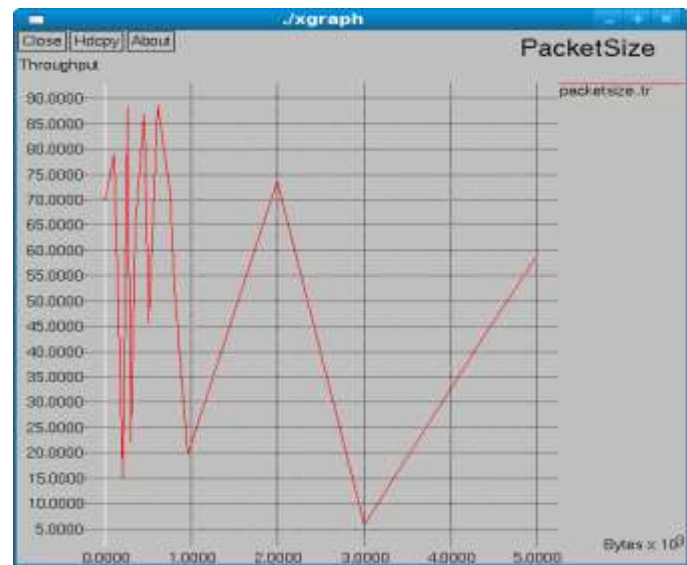


Fig.7.Packet size graph

CONCLUSION

From the simulations, we can study the parameters for the mentioned method. The network life time, energy consumptions and load balancing signifies the significance and effectiveness of the method. We studied the WSN and data aggregation in WSN. In this paper we concentrated on load balancing factor and also on construction of DAT using Probabilistic Network Model (PNM). Therefore, it is focused on constructing a Load-Balanced Data Aggregation Tree (LBDAT) under the PNM as shown in figure 6. More specifically, three problems are investigated, namely, the Load-Balanced Maximal Independent Set (LBMIS) problem, the Connected Maximal Independent Set (CMIS) problem, and the LBDAT construction problem. LBMIS and CMIS are well-known NP-hard problems and LBDAT is an NP-complete problem. LBDAT will be NP-Complete and will be constructed in three steps: Load-Balanced Maximal Independent Set (MDMIS), Connected Maximal Independent Set (CMIS) and Load-Balanced Parent Node Allocation (LBPNA). The results show importance of the method.

REFERENCES:

- [1] Jing (Selena) He, Shouling Ji, Yi Pan, Yingshu Li, "Constructing Load-Balanced Data Aggregation Trees in Probabilistic Wireless Sensor Networks", IEEE Transactions on Parallel and Distributed Systems, Volume:25, Issue:7, Issue Date :July 2014.
- [2] S. Madden, R. Szewczyk, M.J. Franklin, and D. Culler, Supporting Aggregate Queries Over Ad-Hoc Wireless Sensor Networks, WMCSA'02.
- [3] H.O. Tan, and I. Korpeoglu, Power Efficient Data Gathering and Aggregation in Wireless Sensor Networks, SIGMOD Record 32(3):66-71, 2003.
- [4] H.O. Tan, I. Korpeoglu, and I. Stojmenovic, Computing Localized Power-Efficient Data Aggregation Trees for Sensor Networks, TPDS'11.
- [5] S. Ji and Z. Cai, Distributed Data Collection in Large-Scale Asynchronous Wireless Sensor Networks under the Generalized Physical Interference Model, ToN, 2012.
- [6] X. Chen, X. Hu, and J. Zhu, Minimum Data Aggregation Time Problem in Wireless Sensor Networks, LNCS, 3794:133-142, 2005.
- [7] P.J. Wan, S. C.-H. Huang, L. Wang, Z. Wan, and X. Jia, Minimum latency aggregation scheduling in multi-hop wireless networks, MobiHoc, 2009.
- [8] S. Ji, J. He, A. S. Uluogac, R. Beyah, and Y. Li, Cell-based Snapshot and Continuous Data Collection in Wireless Sensor Networks, TOSN, 2012.
- [9] Y. Xue, Y. Cui, and K. Nahrstedt, Maximizing Lifetime for Data Aggregation in Wireless Sensor Networks, MONET, 2005.
- [10] H. Lin, F. Li, and K. Wang Constructing Maximum-Lifetime Data Gathering Trees in Sensor Networks with Data Aggregation, ICC, 2010.

[11] Ankit Tripathi, Sanjeev Gupta, Bharti Chourasiya, "Survey on Data Aggregation Techniques for Wireless Sensor Networks", International Journal of Advanced Research in Computer and Communication Engineering Vol. 3, Issue 7, July 2014.

[12] Imanishimwe Jean de Dieu, Nyirabahizi Assouma, ManiraguhaMuhamad, Wang Jin, and Sungyoung Lee, "Energy-Efficient Secure Path Algorithm for Wireless Sensor Networks", Hindwi Publishing, International Journal of Distributed Sensor Networks ,Volume 2012.

[13] Jayashree A.Vanmali, Prof. Rahul Patil,"A Data Aggregation Method for Balancing Load under Probabilistic Network Model (PNM) ",International Journal of Application or Innovation in Engineering & Management,2015.

IJERGS

Specialized Automated Tool Grinding Machine

Tushar Doshi, Parin Dave, Rahul Deorukhkar, Amit Dubey, Prof.Sanjay Lohar

Mechanical Engineering Department,tusharsdoshi@gmail.com,9172898644

Abstract— This paper is focused on the design of an Automated fixture for Grinding of Single Point cutting Tool (SPCT). This aims to reduce tool grinding time, improve tool geometry, tool life, surface finish of job. The automation is achieved by use of Arduino Micro-controller. Precise angle of orientation and feed is given by the use of stepper motors to actuate a fixture holding the tool .This paper focus on design of a low cost and specialized automatic grinding machine capable of grinding complex geometry of tools for use in small industries , small workshops .

Keywords— Automated, Grinding, Single Point Cutting Tool, Gear Box, Lead Screw, Angles,CNC.

INTRODUCTION

Single Point Cutting Tools (SPCT) are widely used for lathe operations such as turning, facing and tapering of metal. Their cutting action depends upon Shear force exerted by proper cutting tool tip geometry. Optimum cutting tip geometry is essential for resisting cutting forces as well as dissipating frictional heat generated at the work piece tool interface. These tools undergo wear as a result of constant friction and heating at the work piece-tool tip interface. . Currently SPCT (Single Point Cutting Tool) machine tools are available pre-fabricated , with no room for customisation and at a higher cost or are ground by hand Grinding. Manual Grinding has the following draw backs :It is not possible for an operator to consistently reproduce the tool geometry with accuracy leading to variation in surface finish of jobs produced on individual machines i.e. reduced uniformity.The tool grinding performance will vary between operators depending on their experience leading to variation in performance from machine to machine which again reduces uniformity and quality conformance.It requires the operator to stop operations leading to increased downtime and inefficient utilization of time.In order to manage the above mentioned problems a low cost, specialized CNC TGM is the proposed solution. Using a fixture improves the economy of production by allowing smooth operation and quick transition from part to part, reducing the requirement for skilled labor by simplifying how workpieces are mounted, and increasing conformity across a production run. A fixture differs from a jig in that when a fixture is used, the tool must move relative to the workpiece; a jig moves the piece while the tool remains stationary. Automation of Grinding fixtures is possible through the use of actuation mechanism and drives such as stepper motors controlled through programmable micro-controllers. Micro-controllers afford high precision and holding torque which is used to orient the tool to be ground in the correct position and maintain this position against grinding force. This ability of Automated grinding fixtures is invaluable for achieving optimum tool geometry with maximum precision. The program used for actuating the fixture can be specialized for each individual tool so that the same fixture can be used for re-grinding a wide range of tools and complex geometries .

EXPERIMENTAL SETUP

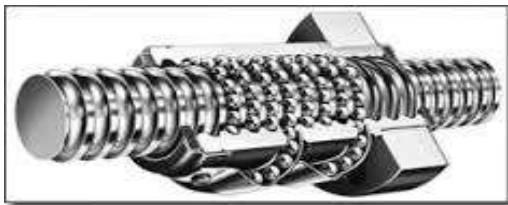
Machine structure is the “backbone” of the machine tool. It integrates all machine components into a complete system. The machine structure is crucial to the performance of the machine tools since it is directly affecting the static and dynamic stiffness, as well as the damping response of the machine tool. A carefully designed structure can provide high stiffness, result in higher operation bandwidth and more precise operation. A small-scale machine tool generally requires even higher stiffness than the ordinary large-scale machine tool since it is usually operated at higher speeds. Lower frame is made up of standard angles of 65*5mm dimensions. Other Upper

frame are made up of mild steel as its cost is low and it gives high strength. All frames are made with high precision and with high accuracy. Other components are mounted on this rigid frame of mild steel.

DESCRIPTION OF COMPONENTS

WORM AND WORM GEAR BOX- A **worm drive** is a gear arrangement in which a **worm** (which is a gear in the form of a screw) meshes with a **worm gear** (which is similar in appearance to a spur gear). The two elements are also called the **worm screw** and **worm wheel**. This type of gear box are use for low rpm and high torque.

BALL/ LEAD SCREWS- A ball screw is a mechanical linear actuator that translates rotational motion to linear motion with little friction. A threaded shaft provides a helical raceway for ball bearings which act as a precision screw. As well as being able to apply or withstand high thrust loads, they can do so with minimum internal friction.



In a ball screw actuator, ball bearings reduce friction and distribute the load. (Courtesy of Danaher Motion)

Fig.1., BALL/LEAD SCREW

BALL BEARINGS-A ball bearing is a type of rolling-element bearing that uses balls to maintain the separation between the bearing races. The purpose of a ball bearing is to reduce rotational friction and support radial and axial loads



Fig.2., BALL BEARING

LINEAR RODS- Linear rods are rigid strong Mild Steel shafts which are used to carry the load without affecting the motion and supports linear movement. Linear rods with linear bearing assembly are used to carry the loads and supports the structures in linear motions the total load of the structure is taken away by the linear rod bearing assembly and therefore the load on ball screw is reduced and causes precise smooth linear motion.



Fig.3 LINEAR ROD

LINEAR BALL BEARINGS- A linear bearing is to provide free motion in linear direction. The load is carried away by the linear bearing and reduces friction slides over linear rods. A linear-motion bearing or linear slide is at features smooth motion, low friction, high rigidity and long life. They are economical, and easy to maintain and replace.

SHAFT END SUPPORTS- Shaft supports are used to support linear rods /shafts rigidly without slip. Shaft support blocks are used for end or intermittent support where loads are light and slight shaft deflection is not a concern

SHAFT COUPLINGS- A Shaft Coupling is a device used to connect two shafts together at their ends for the purpose of transmitting power.. The primary purpose of couplings is to join two pieces of rotating equipment N



Fig.4., SHAFT V. COUPLER.

POWER SUPPLY- 24V 10.4AMPS SMPS(Switch Mode Power Supply) adapters are used for stepper motors and for powering micro-controller.

MICROCONTROLLER BOARD –Micro stepper motor driver (RMCS_1102) 18 to 50V,5 Amps board is used as the motion control board. RMCS-1102 is micro-stepping drive designed for smooth and quiet operation is chosen to drive the NEMA 23 stepper motor RMCS-1102 achieves micro-stepping using a synchronous PWM output drive. RMCS-1102 receives PULSE/STEP, DIRECTION inputs from the microcontroller and generates high rated PWM output signals to stepper motor



FIG.5 MICRO CONTROLLER

STEPPER MOTOR- A stepper motor is a brushless, synchronous electric motor that converts digital pulses into mechanical shaft rotation in a number of equal steps .The motor's position can then be commanded to move and hold at one of these steps without any feedback sensor (an open-loop controller).A NEMA 23 stepper motor is a stepper motor with a 2.3 x 2.3 inch size is chosen to drive the motion of the axes. NEMA 23 stepper motors are high torque about 19KG-Cm holding torque .NEMA 23 stepper motors have 1.8 degree step angle with 2.5A rated current.

BENCH GRINDER-A bench grinder is a type of [benchtop grinding machine](#) used to drive [abrasive wheels](#). These types of grinders are commonly used to hand [grind cutting tools](#) and perform other rough grinding. Depending on the grade of the grinding wheel it may be used for sharpening cutting tools such as [lathe](#) tools or [drill bits](#).



FIG.6 BENCH GRINDER

CALCULATIONS

Worm and Worm Drive-In proposed design, we required to move the shaft at 3 rpm. But Motor Speed is 150 rpm. Therefore for achieving the reduction ratio of 50:1 we are employing a worm drive. Where the input data are as follows,

$$P = 8 \text{ Watt.}$$

$$N_1 = 150 \text{ rpm.}$$

$$N_2 = 3 \text{ rpm.}$$

No. of Teeth on Worm and Gear

As the operation is light duty, from design data book we have, service factor = 1.2

$$[P] = 9.6 \text{ Watt.}$$

$$i = 50$$

$$\text{No. of starts } Z_1 \geq \frac{40}{i+1}$$

$$\text{Hence, } Z_1 = 1 \text{ and } Z_g = 50$$

Helix Angle

$$\text{Let, } q = 11$$

$$\text{Hence, } \lambda = \tan^{-1}\left(\frac{1}{11}\right) = 5.19^\circ$$

$$\beta_w = 90 - 5.19 = 84.81^\circ$$

$$\beta_g = 5.19^\circ$$

Virtual Teeth

$$Z_{wv} = \frac{Z_w}{(\cos \beta_w)^3} = 1350.98$$

$$Z_{gv} = \frac{Z_g}{(\cos \beta_g)^3} = 50.62$$

Weaker Material

From design data book we have,

For worm : Case hardened steel (C-45)

$$\sigma_b = 135 \text{ N/mm}^2 \quad \sigma_u = 630 \text{ N/mm}^2 \quad \sigma_c = 149 \text{ N/mm}^2$$

For wheel : Bronze steel (Chilled)

$$\sigma_b = 110 \text{ N/mm}^2 \quad \sigma_u = 390 \text{ N/mm}^2 \quad \sigma_c = 149 \text{ N/mm}^2$$

Worm gear are always 20° Full Depth Involute.

$$y_{wv} = 0.154 - \frac{0.912}{1350.98} = 0.1533$$

$$y_{gv} = 0.154 - \frac{0.912}{50.62} = 0.13598$$

$$\text{Hence, } \sigma_{bw} * y_{wv} = 20.695$$

$$\sigma_{bg} * y_{gv} = 18.36$$

Therefore, Gear is weaker.

Module Determination

From design data book we have,

$$a = \left(\frac{50}{11} + 1 \right) * \left(\left(\frac{540 * 11}{50 * 1490} \right)^2 * 305.6 \right)^{\frac{1}{3}}$$

$$a = 6.92 \text{ cm} = 69.2 \text{ mm}$$

$$\text{But, } a = 0.5 * m_x * (q + Z_g)$$

$$\text{Hence, } m_x = 0.227 \text{ cm} = 2.27 \text{ mm}$$

Selecting standard module from PSG, hence $m_x = 3 \text{ mm}$.

CACULATION OF LEAD SCREW TORQUE

Nominal Diameter-20 mm

Mean Diameter- 19 mm

Core Diameter- 18 mm

Pitch- 5 mm

Assuming coefficient of friction between nut and screw-

$$\mu=0.15$$

$$\alpha=\tan^{-1} 0.15$$

$$\alpha=8.58$$

Helix Angle- β

$$\tan \beta = p/\pi * \text{Mean Dia.}$$

$$B=\tan^{-1} 5/ \pi * 19$$

$$B=4.788$$

$\alpha > \beta$,hence it is SELF-LOCKING.

Weight Of Fixture- 60Kg~589N

Reaction Force- $F= \mu R$

Assuming coefficient of friction between Ball bearing and linear rod-

$$\mu=0.15$$

$$F=0.15*589$$

$$=88.35N$$

Total weight to be push by lead screw-

=Weight of fixture + back pressure

Assuming back pressure=100N

$$\text{Total weight}=100+88.35$$

$$=188.35N$$

Torque required

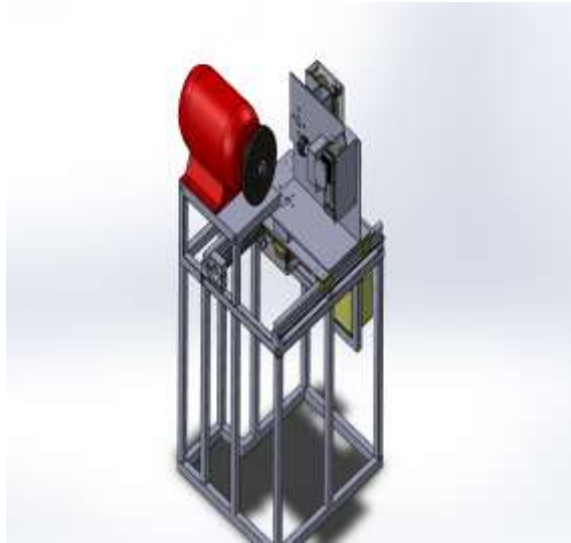
$$W * \frac{Dm}{2} * \tan(\beta + \alpha)$$

$$T = 188.35 * \frac{0.019}{2} * \tan(4.78 + 8.58)$$

$$T = 0.42Nm \sim 0.5Nm$$

Selecting Stepper Motor of 1Nm torque

ACTUALDESIGN



OBSERVATION TABLE

DESCRIPTION (ANGLES)	IDEAL ANGLES	AUTOMATED ANGLES
Side Rake	15°	14.8°
End Cutting Edge	5°	5.1°
End Relief	5°	4.8°
Back Rake	0°	0.1°
Side Relief	5-6°	5°
Nose Radius	0.5-3mm	1.5mm

CONCLUSION:

With the increasing demand for small scale high precision parts in various industries, the market for small scale machine tools has grown substantially. Using small machine tools to fabricate small scale parts can provide both flexibility and efficiency in manufacturing approaches and reduce capital cost, which is beneficial for small business owners. In this thesis, a small scale three axis CNC milling machine is designed and analyzed under very limited budget. X

REFERENCES:

- [1] Zelinski, Peter (2013-11-08), "Hybrid machine combines milling and additive manufacturing", Modern Machine Shop.
- [2] Roe, Joseph Wickham (1916), English and American Tool Builders, New Haven, Connecticut: Yale University Press
- [3] Zelinski, Peter (2014-02-21), "The capacity to build 3D metal forms is a retrofittable option for subtractive CNC machine tools", Modern Machine Shop Additive Manufacturing supplement.
- [4] [Hartness, James](#) (1910), [Hartness Flat Turret Lathe Manual](#), Springfield, Vermont, USA: Jones and Lamson Machine Company, p. 89
- [5] Malakooti, B; Deviprasad, J (1989). "An Interactive Multiple Criteria Approach for Parameter Selection in Metal Cutting". Operations Research 37 (5): 805-818.
- [6] K. Kadirgama et al. 2011, "Tool Life and Wear Mechanism" "<http://umpir.ump.edu.my/2230/>
- [7] R.S.Khurmi(1979),J.K Gupta,"Machine Design".S Chnad publication.
- [8] V.B Bhandari(1994)"Design of Machine Element"Third edition.
- [9] Altintas, Yusuf. Manufacturing Automation: Metal Cutting Mechanics, Machine Tool Vibrations, and CNC Design. Cambridge University Press, 2000
- [10] S. Lopez , Mechanical Engineering Department (VCET)," Production Process Notes" Vol-1,2.
- [11] www.google.com
- [12] Websites-www.mirandatools.in

Secure Message Transmission

Babar Khalid, Shoaib Farooqui, Rajesh Nair, Priyanka Kedar

bkhalid797@gmail.com Contact no.: +919767871805

Department of computer engineering
Dhole Patil College of Engineering,
Pune Maharashtra.

Abstract: we are living on a fully digital horizon where security must be a serious threat. If you are willing to transmit confidential information over internet then you have to ensure security first. At first glances, our civilization may appear to be somewhat progressive. With the passing of everyday we are going towards the more digitized. We are enjoying fully paperless society but somewhere we are afraid of being hacked. Because it is important for person to protect own's identity from them those who are prowling in the distance. Security and privacy are the key factors if you are willing to transmitting the data over internet. we have to rethink about security of data over internet. In this paper we offered a safe zone for the customers which providing the security and privacy to the users confidential data. So, enjoy the privacy. In this paper we proposed two mechanism as 1) GRID authentication system; 2) compression and subtraction based encryption decryption mechanism.

INTRODUCTION

We are living in 21st century, a digital world. The main problem in digital world is how to protect confidential information. The first thing you want for security is authentication. So you have to protect your identity from intruders. But what if your data is stolen while data is transmitting over internet. So then you have to secure the data while data is transmitting over internet. What really occurs with data present into a computer system? However, it is also possible that something or someone within adjacent proximity to the computer read the information as well. That something or someone else might most probable be a Shoulder surfer. Dr. Fred Cohen, an esteemed frontrunner in information security and information defense organizes shoulder surfing as an occurrence that encompasses 'observing over people's shoulder as they use data or information system'.

The most mutual technique used for verification is textual password. The dimness of this technique like eaves dipping, social engineering and shoulder surfing are well known. Illogical and lengthy passwords can ensure the system security. However the key challenge is it's problematic to remember. Studies have exposed that users have an affinity to pick short passwords that are easy to recap. Inappropriately, these passwords be able to guess easily. [1] The another procedure is biometrics. But these two systems have their own disadvantages. Biometrics, such as finger prints, iris scan or facial recognition have been introduced but not yet broadly agreed. [2] Such configurations are expensive, and the identification procedure can be slow are two major disadvantages of these systems. There are numerous graphical password systems that are proposed in the last period. But they also suffering from shoulder surfing. [3] There are graphical password mechanisms offered which are unaffected to shoulder surfing but they have their own drawbacks like winning more period for user to login or having patience levels.

But according to our study the key problem is the attackers try to get access to the password which the user types. But what if the user does not know the password which will allow him to access? And what if user do not enter the actual password? And every time the password entered is different. Sounds a bit strange but this is what our system does. Are you afraid of being? Don't be! It's not that easy.

In this paper we proposed two techniques to protect user's confidential information. One is GRID based authentication scheme with OTP (one time password) which provide secure authentication to users.

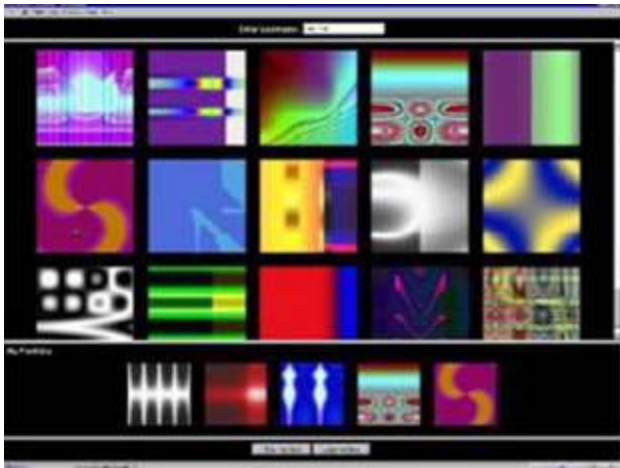
And second is for security of data over internet key exchange is the mechanism for certifying network security. For key exchange over the internet, both security and confidentiality are desired [1]. It enhances the security of the web based system and makes it difficult for the attackers to decipher the keyword of the user. This technique we can call it as cryptography. In this technique we used compression based encryption and decryption mechanism to enhance information security. And here we use DHKE as transmission security [1].

Thus, now just forget to believe that you have been lacerated and enjoy the privacy. We providing you the safe zone where your identity and confidential data are safe. So, enjoy privacy...

EXISTEING SYSTEMS

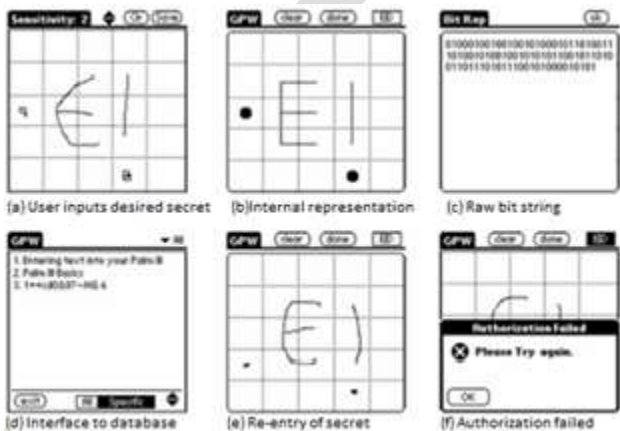
R. Dhamija, and A. Perrig. "Déjà Vu: A User Study Using Images for Authentication". In 9th USENIX Security Symposium, 2000[10].

Dhamija and Perrig suggested a graphical verification mechanism where user will choose images as a password to identify user's genuineness [10]. In this sytem user have to recognize the preselected images for verification at login time from a set of images as illustrated in below figure. But this mechanism has disadvantage as it is vulnerable to shoulder surfing.



Jermyn, I., Mayer A., Monroe, F., Reiter, M., and Rubin. "The design and analysis of graphical passwords" in Proceedings of USENIX Security Symposium, August 1999[12].

Jermyn Projected a new system called "Draw- a-Secret" (DAS) as described in figure where the user is necessary to draw the picture on a 2D grid. If the drawing traces the same grids in the same order as drawn during registration time, then the user is verified [12]. This system also not ensuring security from shoulder surfing.



A. F. Syukri, E. Okamoto, and M. Mambo, "A User Identification System Using Signature Written with Mouse," in *Third Australasian Conference on Information Security and Privacy (ACISP)*: Springer-Verlag Lecture Notes in Computer Science (1438), 1998, pp. 403-441[11].

Syukri established a technique where user will draw a signature using a mouse as shown below for authorization at login time[11]. This method included two phases 1.registration and 2.verification. user draws a signature using mouse at registration time and then system extracts the signature area. at the verification time it takes the user signature as input and does the standardization and then extracts the factors of the signature. The drawback of this system is the falsification of signatures as it is not possible for users to draw a signature always as it is. It is challenging to draw the signature in the same edges at the time of registration. In this

technique the user must click on the approximate areas. So, this system is ineffective for authentication process. This system ensuring security to keystroke login but somewhere exposed by shoulder surfer.



Haich Haichang Gao, Zhongjie Ren, Xiuling Chang, Xiyang Liu UweAickelin, "A New Graphical Password Scheme Resistant to Shoulder-Surfing[14].

Haichang offered a shoulder-surfing resilient system as shown below where the user is essential to draw a arc transverse to their password images prepared fairly than clicking on them straight. This graphical scheme chains DAS and Story arrangements to deliver genuineness to the user [14]. But this system is also vulnerable to shoulder surfing.



Suwarna jungari, Vrushali Bhujbal, Shital Sonawane, prof. Shital Salve: "authentication session password scheme using texts and colors", 2014[8].

S. Jungari offered a pair based authentication system in which User has to enter the password dependent on secret pass. The session password holds of letters and digits. Here intersection of pair is selected to submit as a password. Row of first letter and column of second letter where interacting is selected to submit the password. The intersection letter is part of the session password. This is repetitive for all pairs of secret pass [8]. This system is resistant to keystroke login but it is vulnerable to shoulder surfing.

W	H	1	7	P	N
M	Z	F	E	6	X
I	J	0	O	K	R
S	D	2	A	G	L
B	8	C	5	9	T
3	4	Q	Y	U	V

Proposed system:

Here we proposed pair based authentication system with OTP (one time password). Proposed authentication system is similar to pair based authentication system but in proposed system we eliminated disadvantages of pair based system. Pair based system has disadvantages like password must contain even number of digits while in proposed authentication system can include even as well as odd number of digits as a password. And we included OTP which is resistant to shoulder surfing and also enhance the security of the system. OTP must be included with user defined password. In proposed authentication system user have to enter predefined password as well as OTP at the time of login.

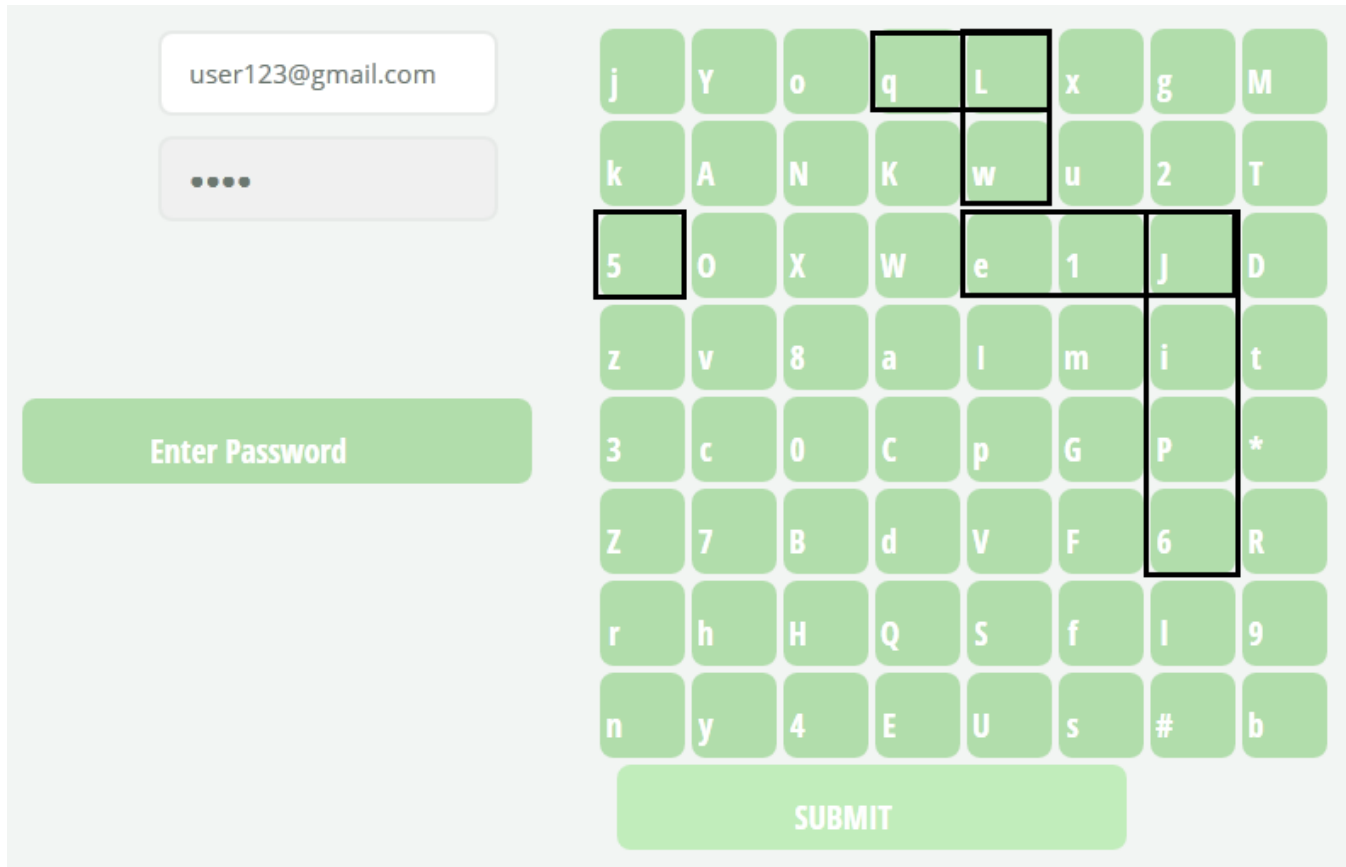
It means that for example user defined password is “asd73” and OTP received is “69” then user have to submit “asd7369” as a password in GRID. Advantage of this system is it ensures security since at every login time GRID changes. GRID contains 26 small characters, 26 capital characters and 10 digits.

26 small characters + 26 capitals + 10 digits;
 26+26+10=64;
 So, 64 values will be visible on GRID.

j	Y	o	q	L	x	g	M
k	A	N	K	w	u	2	T
5	O	X	W	e	1	J	D
z	v	8	a	l	m	i	t
3	c	0	C	p	G	P	*
Z	7	B	d	V	F	6	R
r	h	H	Q	S	f	l	9
n	y	4	E	U	s	#	b

How to use

The intersection of a passwords two digits will be considered as a selection point on the GRID. It means that user have to select passwords two digits pairs intersection at login time. For example “qwe” is a user defined password and OTP received is “65” then user have to submit “LJ5” as a password as L is a intersection of row(q) and column(w) ; J is a intersection of row(e) and column(6) and 5 is selected as it is because 5 itself an intersection for 5. Which is described clearly in below figure.



Security analysis:

As discussed above GRID changes every time so that it is ensuring security. This mechanism is resistant to shoulder surfing, keystroke login and hidden camera attack due to dynamic password. Every time user get OTP and every time user submit password is always differ. So, this nature of authentication ensuring more security according to previous authentication systems.

Shoulder surfing: in proposed authentication system Grid is used where user do not submit actual password and user also enter OTP at login time. So, that system is resistant to shoulder surfing attack or hidden camera attack. Every time GRID changes and it will resistant to guessing as well.

Keystroke login: this system is resistant to keystroke login as here user submit password using GRID and keyboard interface is not needed in this authentication system.

Existing authentication system vs proposed system:

Objectives	Textual	Graphical	Biometric	Draw a secret	Proposed system
Implementation	Easy	Quit complex	Complex	Complex	complex
Accuracy	High	High	Low	Low	high
Security	Low	Low	High	Moderate	high
Hardware required	Not required	Not required	Required	Not required	Not required
Memory required	Less	Moderate	more	Less	Less
Cost	Low	Moderate	High	Low	Low
Time required to authenticate user	Less	More	less	More	less

Key exchange mechanism:

The key exchange is between the core cryptographic mechanisms for certifying network security. For key exchange over the internet we have to ensure security and privacy [1]. The internet key exchange protocol to ensure internet security, which state key exchange mechanism used to produce common keys for use in internet protocol security standard [3]. If you are willing to transmit the confidential information over internet then you have to worry about security and privacy of your information. Security is first element for information over internet. Information security over internet is serious threat now a days. Today we are living in a fully paperless world and that’s why we have to rethink about security of data over internet.

Deniable internet key-exchange

[1]Andrew chi-chih Yao and Yunlei Zhao proposed family of privacy-preserving authenticated DHK[1] Protocols titled deniable Internet key-exchange (DIKE), both in the traditional PKI situation and in the identity-based setting. The newly established DIKE protocols are of intellectual simplicity and real-world adeptness. They deliver useful privacy security to both protocol applicants, and growth innovation and new assessment to the IKE conventional [3] [4] and the SIGMA protocol [5].

Internet Key-exchange (IKE)

One of the simple safe communication mechanism is key formation protocol that is known as Internet Key Exchange (IKE). It is the characteristic of Internet protocol Security (IPSec) offered by the IETF in 1998 [3, 4]. But, people have many blames for this protocol, generally for its complication [6]. The IKE and IPSec used to deliver safekeeping services and confidentiality for communication protocols. The standard of IKE has gone over two generations. 1) IKEv1 [3] uses public-key encryption as the verification mechanism. 2) IKEv2 [1] uses signatures as the authorization mechanism, with the SIGMA protocol [5] as the basis.

Internet Protocol Security (IPSec)

IPSec is the Internet Engineering Task Force (IETF) suggested standard for “layer 3 real-time Communication securities [6].” In a real-time security classification, an initiator, called Alice, establish communication session with a responder system, called Bob. They substantiate to both by verifying awareness of some secret, and then launch a secret key for the safety of the rest of the session. We use the word “real-time” to separate it from a procedure such as protected e-mail, in which Alice be able to generate an encrypted, signed message for Bob without interrelating with Bob [4].

By functioning under layer 4, IPSec preserve the problem of an active attacker critically breach at a distance a session by injecting a single volatile package. Solutions like SSL, which function above TCP, are exposed to this risk. While IPSec can be well-ordered without modifications to applications, the power of IPSec cannot be cracked till the API is altered to notify requests of the endpoint identifier, and applications are reformed to use the data in the altered API.

Proposed system

The main goal of proposed system is to enhance the security over transmission of data and authentication process in web applications. It makes difficult for the attackers to decipher the keyword and ensures the security of information navigating over internet.

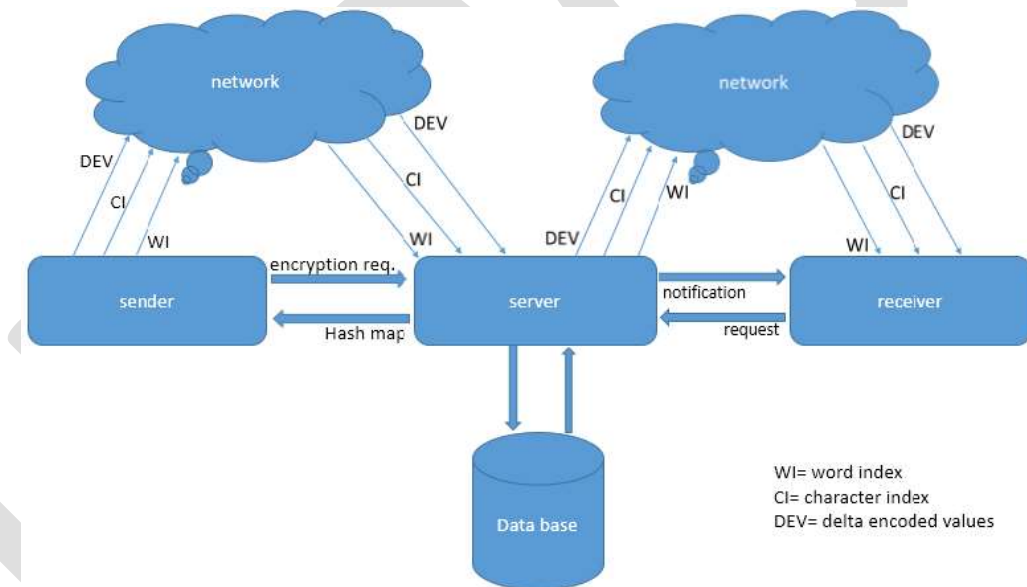
Proposed system provide a safe zone to users who willing to transmit their confidential information over internet. Here we are using grid based authentication with OTP as a front end security. Here user register his/her user name and password at registration

time. And at the login time user have to submit user name and password. Here user submit password using GRID. Password contains user defined password + OTP (received by message).

For example, user selected password is “qwe45” and OTP received is “65”, then user have submit password “qwe4565” in GRID.

At the back-end we provide a security to user’s confidential data transmitting over internet. Here we developed a new encryption and decryption technique for ensuring security to data from attacker to decipher. In this system original message is divided into three portions as word index, character index and delta encoded value as described below:

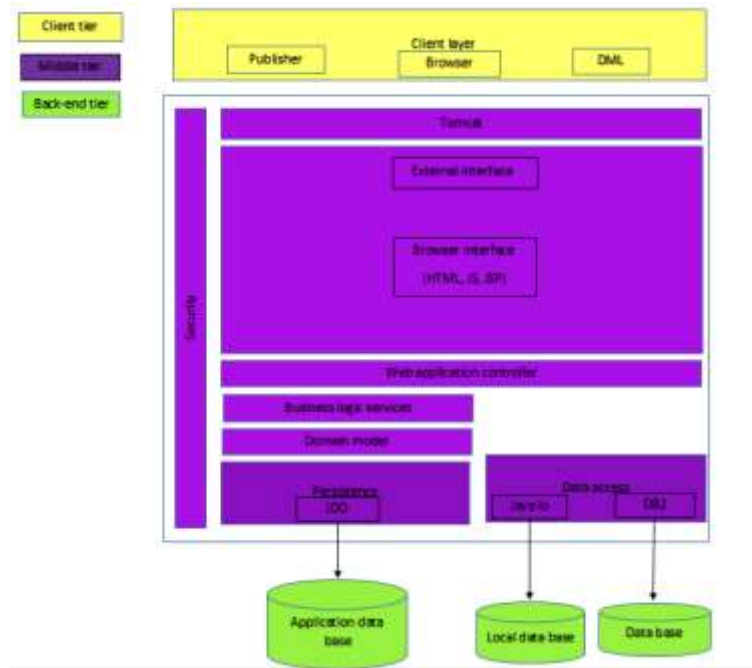
- Here we get word index as each new word typed will get assigned a word index number (wi).
- But if word types is already in the list then it will stored in to compressed list.
- If all the words got appropriate values then we proceed to character index.
- Now we assign a new character index (CI) value to each character in the word which is differ otherwise equivalent CI as assigned to same words.
- Now we will proceed to delta encoded value and fetch the hash map value (generated and received from server) of each character and then we assign first character value as same as in the hash map. And then second characters hash map value will be minimized from first character hash map value. And then this new value will be used to minimization of next characters hash map value.
- This process will be followed for all the characters in the message and then what we will get is the delta encoded value.
- Now all values (word index, character index, and delta encoded value) are to be append one value to a one individual message. At the last all the values are to be sent as an individual message for security enhancement.
- Now whenever server get message from the sender it will notify the appropriate receiver about message.
- Now whenever receiver login to the system and request for the message, server will send ciphered text (WI, CI, and delta encoded value) to the receiver system And delete that message from the server to enhance the information security.
- Then decryption takes place at the receiver system and original message will be sent to the receiver by e-mail. This process is clearly described in below figure.



Message entered by user is encrypted at client side and then ciphered text is sent to server and stored on to the server. Server store encrypted message in message data base and then notify appropriate receiver about message. Whenever receiver login into the system and request for the message, server sent ciphered values to the receiver and decryption take place at the receiver end. Then original message will be sent to receivers email address.

System architecture:

A system architecture is the theoretical model that explains the structure, activities, and more understandings of a system. Architecture view is describe all technologies and interfaces used for implementation of this system. The fundamental body of a structure, their associations with each other and to the atmosphere, and the ethics leading its intention and evolution. A detailed system architecture is illustrated in below figure.



MATHEMATICAL MODEL

$U = \{U_1, U_2, U_3 \dots U_n\}$ (User)
 $S = \{Server\}$ (Server)
 $M = \{M_1, M_2, M_3 \dots M_n\}$ (Message)
 $K = \{K_1, K_2, K_3 \dots K_n\}$ (Key)
 $HT = \{HT_1, HT_2, HT_3 \dots HT_n\}$ (Hash Table)
 $RN = \{RN_1, RN_2, RN_3 \dots RN_n\}$ (Random no.)
 $DEV = \{DE_1, DE_2, DE_3 \dots DE_n\}$ (Delta encoded values)
 $WI = \{WI_1, WI_2, WI_3 \dots WI_n\}$ (word index)
 $CI = \{CH_1, CH_2, CH_3 \dots CH_n\}$ (character index)
 $DB = \{Udb, Mdb\}$ (data base, user data base, message data base)
 $L = \{success, failure\}$
 $MTG = \{U, S, M, K, HT, RN, DEV, WI, CI, DB, L\}$

Compression based message encryption

Here we will see how message encryption mechanism work when user enter original text message.

Whenever user select to send the message at the same time server generate grid and send GRID value to the client machine. Now as user submit their original text message client machine start encryption process. How mechanism work is as follows:

Let word token $WT=n$; current character $k=0$; stored array $j=0$; word index $WI= i$; character index $CI= empty$; and then three events will be followed by mechanism to encrypt the message.

Event 1:

Now read the text message and if space arrived in the text we will consider it as a word-end. So, word token is increased by 1. So, now $WT_n=WT_{n+1}$.

And then if word previously read is in not registered in the list then $WI=i+1$; otherwise store word into compressed list and increase token WT_{n+1} .

This process is followed by all the words in the text message and what will produced is word index of all words from the text message.

Event 2:

Now here access the word array created in event 1. And split words into characters and let current character as k; current character index $CI=y$; $CI(k)=x$;

Now read characters one by one and increase $CI(k)=y+1$ if k is not there in the CI array. Else $CI(k)=CI(x)$. Follow this steps for all characters present in the text and we will get character index of all characters.

Event 3:

Now assume q = current character; hash-map value= $HM(q)=q_{ij}$ (i^{th} and j^{th} location of q in the hash-map); delta encoded value (q)= $DEV(q)$ =empty; and p =previous characters DEV;

Now $DEV(q)=HM(q)$ if and only if $DEV(q)$ =empty;

Otherwise $DEV(q)=(DEV(p)-HM(q))$.

This step is followed by all the characters in the text and we will get delta encoded value.

Hence, at the end of the three events we got WI, CI, and DEV. And message is encrypted successfully.

Results

Authentication:

Below chart illustrate the result of user login time as how much time system takes to authenticate the user at login time. It describe the time taken by system to authenticate the different users. This time also depend on network speed.

users	Time(ms)
1	10
2	9
3	10
4	11
5	9
6	10
7	9

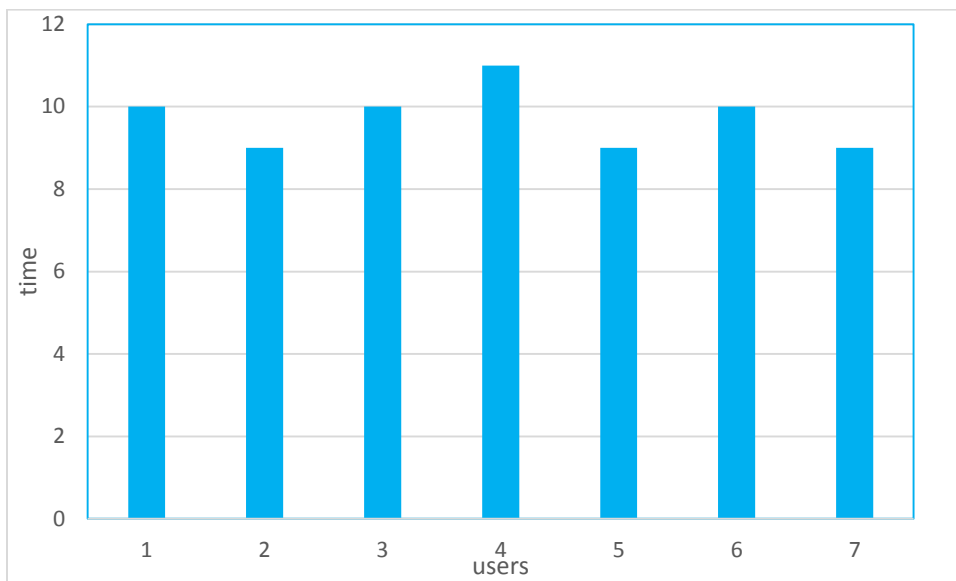


Chart shown above is describing the result in terms of login time. It shows how much time taken by system to authenticate which user. It shows time taken by system to authenticate 7 users.

ACKNOWLEDGMENT

We are grateful to prof. Priyanka Kedar for very supportive clarification and suggestions, as well as very helpful suggestions about this project.

Conclusion

In this paper, we proposed a safe zone for the user willing to transmit confidential information over internet. Here we proposed message encryption technique for ensuring data security over internet which is followed by GRID based authentication system using OTP which is resistant to shoulder surfing as well as keystroke login.

REFERENCES:

- [1] A. C. Yao and Y. Zhao, "privacy-preserving Authenticated Key-Exchange over Internet" January 2014.
- [2] S. Al-Riyami and K. Paterson, "Certificate less public-key cryptography," in *Proc. Asiacrypt 2003*, pp. 452–473.
- [3] D. Harkins and D. Carreal, "The Internet key-exchange (IKE)," *IETF (The Internet Engineering Task Force), New York, NY, USA, Tech. Rep. 2409, Nov. 1998.*
- [4] C. Kaufman, "Internet key exchange (IKEv2) protocol," *The Internet Engineering Task Force, London, U.K., Tech. Rep. 4306, Dec. 2005.*
- [5] H. Krawczyk, "SIGMA: The 'SIGn-and-MAC' approach to authenticated Diffie-Hellman and its use in the IKE-protocols," in *Proc. CRYPTO 2003*, pp. 400–425.
- [6] D. Boneh and M. Franklin, "Identity-based encryption from the weil pairing," in *Proc. CRYPTO 2001*, pp. 213–229.
- [7] A. C. Yao and Y. Zhao, "Deniable Internet key-exchange," *IACR (The International Association for Cryptologic Research), San Diego, CA, USA, Tech. Rep. 2011/035, Jan. 2011.*
- [8] Suwarna jungari, Vrushali Bhujbal, Shital Sonawane, prof. Shital Salve: "authentication session password scheme using texts and colors", 2014.
- [9] VAISHNAVI PANCHAL, CHANDAN P. PATIL a user study using "Authentication schemes for session password" March 2013.

[10] R. Dhamija, and A. Perrig. "Déjà Vu: A User Study Using Images for Authentication". In *9th USENIX Security Symposium*, 2000.

[11] A. F. Syukri, E. Okamoto, and M. Mambo, "A User Identification System Using Signature Written with Mouse," in *Third Australasian Conference on Information Security and Privacy (ACISP): Springer-Verlag Lecture Notes in Computer Science (1438)*, 1998, pp. 403-441.

[12] Jermyn, I., Mayer A., Monroe, F., Reiter, M., and Rubin. "The design and analysis of graphical passwords" in *Proceedings of USENIX Security Symposium*, August 1999.

[13] *Real User Corporation: Pass faces*, www.passfaces.com.

[14] Haichang Gao, Zhongjie Ren, Xiuling Chang, Xiyang Liu UweAickelin, "A New Graphical Password Scheme Resistant to Shoulder-Surfing

[15] M SREELATHA , M SHASHI , M ANIRUDH "Authentication Schemes for Session Passwords using Colour and Images" May 2011.

[16] M. Bellare and P. Rogaway, "Entity authentication and key distribution," in *Proc. CRYPTO 1993*, pp. 273–289.

[17] Babar Khalid, shoaib Farooqui, Rajesh nair, Priyanka Kedar, "privacy for key exchange and authentication process using grid", *IJSRD/vol. 3,issue 09,2015/ISSN:2321-0613*

Low Contrast Image Enhancement Technique By Using Fuzzy Method

Ajay Kumar Gupta

Research Scholar

Ajay3914@gmail.com

Cont. 8109967110

Siddharth Singh Chauhan

Asst. Prof., IT Dept

Siddharth.Inct@gmail.com

Manish Shrivastava

HOD, IT Dept

Contact.manishshrivastava@gmail.com

Abstract—: One of the most interesting and challenging area in image processing research is to enhance low Contrast images. Many images may suffer from poor contrast and noise due to the inadequate lighting during image acquiring. So it is required to enhance the contrast of image as well as remove the noise that increase image quality. This paper presents a fuzzy based enhancement technique for low contrast grayscale image. Proposed works transforms the gray scale image from spatial domain to fuzzy domain, then modify the fuzzy domain by using the pal king membership function which modify image from low contrast to high contrast, And finally, transforms the gray scale image from modified fuzzy domain back to spatial domain by using defuzzification method. The performances of the proposed method are compared with the other existing methods. The proposed method gives better quality enhanced image and needs minimum processing time rather than the other methods.

Keywords— Defuzzification, Image Enhancement, Fuzzy domain, Grayscale, Membership Function, Spatial Domain, Histogram Equalization.

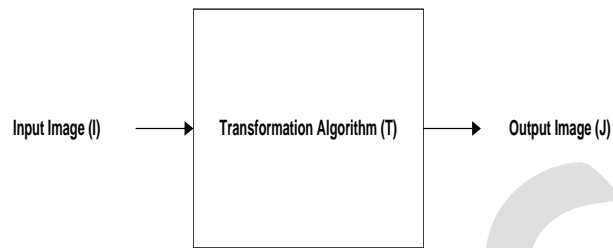
INTRODUCTION

Many important areas like machine vision, remote sensing, dynamic and traffic scene analysis, biomedical image analysis and autonomous navigation required good contrast images with preserving details [1]. But most of the images suffer from poor/low contrast because of inadequate lighting during image acquiring, it may be by wrong setting of aperture size or due to speed of shutter or it may be by nonlinear image intensities mapping. Thus, image enhancement is required whenever one wants to increase the quality of the image. So Image enhancement is one of the fundamental task applied in image processing that improve interpretability and appearance of the image. It provides better input image for further image processing task [2].

Image enhancement can be used in many fields where images are to be analyzed such as satellites images analysis, medical image analysis etc. We can define the Image enhancement technique as transforming an image X into image Y using transformation function T. The values of pixels in images X and Y are denoted by x and y, respectively. As said, the pixel values x and y are related by the expression,

$$y = T(x) \quad (1)$$

Where T is a transformation algorithm that converts a pixel value x into a pixel value y . The results of this transformation are converted into the grey scale range or color image. If grey scale digital images are used then, the results are mapped back into the range $[0, L-1]$, where $L=2^k$, k is the number of bits in the image being considered. So, for example, suppose if we are using an 8-bit image then the range of pixel values lie between 0 and 255. This theory can be extended for the color images also [3].



1. Image Enhancement technique

In next section, we are presenting the research work of some prominent authors in the same field and explaining a short description of various techniques used for image enhancement.

LITERATURE REVIEW

Image enhancement can be classified into two groups namely frequency domain and spatial domain methods. In the frequency domain method, the enhancement is conducted by modifying the frequency transform of the image. Meanwhile in the latter method, image pixels are directly modified to enhance the image. However, computing the enhancement in frequency domain is time consuming process even with fast transformation technique thus made it unsuitable for real time application [4].

There are many image enhancement methods have been proposed. A very popular technique for image enhancement is histogram equalization (HE). This technique is commonly employed for image enhancement because of its simplicity and comparatively better performance on almost all types of images. The operation of HE is performed by remapping the gray levels of the image based on the probability distribution of the input gray levels. It stretches the dynamic range of the image's histogram and resulting in overall contrast enhancement [5]. Various researches have been performed on Histogram Equalization, and many methods have already been proposed. But Most of the HE techniques could cause a washed-out effect on the appearance of the enhanced image and/or amplify existing noises [2]. In addition, due to the poor and low contrast nature of the acquired image, vagueness and ambiguity are introduced and have led to the increment of uncertainty in the image information. This vagueness in the image appears in the form of imprecise boundaries and intensities during image digitization.

Therefore, fuzzy sets theory [6] has been proposed as a problem solving tool between the precision of classical mathematics and the inherent imprecision of the real world. The imprecision possessed by the acquired image can be perceived qualitatively by human reasoning. However, there is no specific quantification to describe the imprecision and thus machine may not understand them. Realizing this limitation to a great extent, fuzzy logic tools empower a machine to mimic human reasoning.

In the image enhancement field, the fuzzy set theory has been widely utilized by other researchers [1,4,7-14]. Pixel property such as gray tone intensity is modeled into a fuzzy set using a membership function. The image is considered as an array of fuzzy singletons having a membership value that denotes the degree of belonging to specific property.

In 2000 H.D. Cheng et.al [7], proposed a novel adaptive direct fuzzy contrast enhancement method, sigmoidal membership function is used to map an image from spatial to fuzzy domain. The resultant image obtained is properly enhanced. When transforming the image from one color space (RGB) to another color space (HSV, HIS, YIQ) hue is unaltered only the intensity and saturation components are changed, as a result gamut problem will occur. So in [8], S.K.Naik tried to keep the transformed values within the range of the RGB space so as to avoid the gamut problem. Although the image is enhanced, the clarity of the enhanced image is not good.

In 2006 Madasu Hanmandlu, and Devendra Jha [4] proposed that Gaussian membership function to fuzzify the image information in spatial domain. They introduce a global contrast intensification operator (GINT), which contains three parameters, viz., intensification parameter, fuzzifier, and the crossover point, for enhancement of color images. They define fuzzy contrast-based quality factor and entropy-based quality factor and the corresponding visual factors for the desired appearance of images. By using the proposed technique, they observed a visible improvement in the image quality for under exposed images, and the entropy of the output image is decreased.

In 2009 Madasu Hanmandlu. et.al [9] presented a new approach for the enhancement of color images using the fuzzy logic technique. To provide an estimate of the underexposed and overexposed regions in the image, an objective measure called exposure has been defined. This measure serves as the dividing line between the underexposed and overexposed regions of the image. For the process of enhancement, The hue, saturation, and intensity (HSV) color space is employed. The hue component is preserved to keep the original color composition intact. For the enhancement of the luminance component of the underexposed image a parametric sigmoid function is used. A power-law operator is used to improve the overexposed region of the image, and the saturation component of HSV is changed through another power-law operator to recover the lost information in the overexposed region.

In 2011 Gang Li et.al [10] proposed image enhancement operation that used the value of grey entropy in the neighborhood window as parameters to measure the level of current pixel being edge point. This paper described a fuzzy mapping based on translation transformation, which can increase the stability of the algorithm; making use the grey entropy of pixels in neighborhood to judge the level of edge for pixels, the dynamic adaptive selection of central point of neighborhood in fuzzy contrast enhancement was achieved, and can increase the local gray contrast of the image, rich the texture layer of the image, improve the quality of the image, make it more adaptive for further treatment and analysis.

In 2012 Khairunnisa Hasikin and Nor Ashidi Mat Isa [11] presented a fuzzy grayscale enhancement technique for low contrast image. Most of the developed contrast enhancement techniques improved image quality without considering the non uniform lighting in the image. Here, the fuzzy grayscale image enhancement technique is proposed by maximizing fuzzy measures contained in the image. Then, to enhance the image, membership function is modified by using power-law transformation and saturation operator..

Image enhancement algorithms offer a wide variety of approaches for modifying images to achieve visually acceptable images. The choice of such techniques is a function of the specific task, image content, observer characteristics, and viewing conditions. In this section, there is a survey on various techniques for image enhancement. Our paper presents a enhancement technique for low contrast grayscale image. The paper first, transforms the gray scale image from spatial domain to fuzzy domain, then maximizes the fuzzy measures contained in the image by using the membership function that is modified to enhance the image by using power-law transformation. And finally, defuzzification is applied that transforms the gray scale image from modified fuzzy domain back to spatial domain.

The paper is organized as follows: Section III describes the proposed work implementation and algorithm which describes the method that we have defined for image enhancement. Section IV Shows experimental results of proposed method and comparison with other image enhancement Methods. Section V Describes the conclusion and future work of proposed method.

PROPOSED METHOD

Image representation in fuzzy set notation

An image X of size M*N having gray levels ranging from L_{\min} to L_{\max} can be modeled as an array of fuzzy singletons. Each element in the array is the membership value representing the degree of brightness of the gray level l ($l = L_{\min}, L_{\min} + 1, \dots, L_{\max}$). In the fuzzy set notation, we can write

$$\mu_{ij} = (X_{ij} - X_{\min}) / (X_{\max} - X_{\min}) \quad (2)$$

Where $\mu_{i,j}$ denotes the degree of brightness possessed by the gray level intensity $x_{i,j}$ of the (i,j)th pixel.

Modification of Membership Function

The goal of our proposed method is to take care of the fuzzy nature of an image and the fuzziness in the definition of the contrast to make the contrast enhancement more adaptive and more effective, and to avoid over-enhancement/under-enhancement. So for adaptive fuzzy contrast enhancement fuzzification is applied by Modification of memberships function $\mu_{i,j} \rightarrow \mu'_{i,j}$ by using following PAL and KING transformation or the intensification operator (INT),

$$\mu_{ij} = T(\mu_{ij})$$

$$\mu'_{ij} = \begin{cases} 2 * [\mu_{ij}]^2 & 0 \leq \mu_{ij} \leq \mu_c \\ 1 - 2 * [1 - \mu_{ij}]^2 & \mu_c < \mu_{ij} \leq 1 \end{cases}$$

It transforms the membership values that are above 0.5(default value) to much higher values and membership values that lower than 0.5 to much lower values in a nonlinear manner to obtain good enhancement image otherwise show the not enhancement image.

Adaptive fuzzy contrast enhancement using defuzzification

Defuzzification for the generation of new gray levels X'_{ij} by the inverse transformation G^{-1} .

$$X'_{ij} = G^{-1}(\mu'_{ij})$$

$$X'_{ij} = X_{\min} + \mu'_{ij} * (X_{\max} - X_{\min})$$

:

Thus, the final image obtained by the defuzzification process, is the required enhanced image for the input image, X'.

PERFORMANCE ANALYSIS

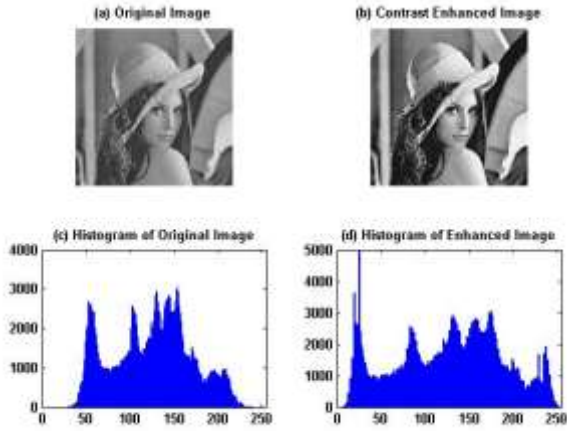
The proposed method has been implemented on Intel Core 2 CPU 2GHz using Matlab R2009b. 20 standard images (size: 400x264) obtained from California Institute of Technology database which consist of underexposed and overexposed regions are considered as test images.

The enhanced image is analyzed in terms of its output quality and quantitative analysis such as index of fuzziness (IOF), contrast, peak signal to noise ratio (PSNR) and processing time.

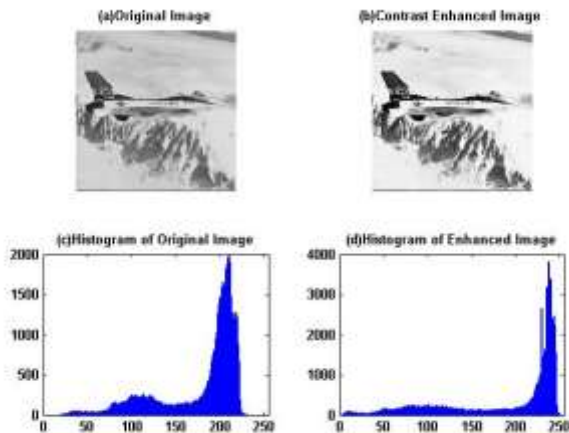
In order to demonstrate the performance of the proposed method, we compared the experimental results of the proposed approach with other state of the art methods namely fuzzy set theory [1], conventional approach of NINT [6], application of fuzzy IF-THEN rules

(fuzzy rule-based) [12], Pal-King method [15] fuzzy quantitative measure [13] and fuzzy local enhancement [14], are widely used in image enhancement.

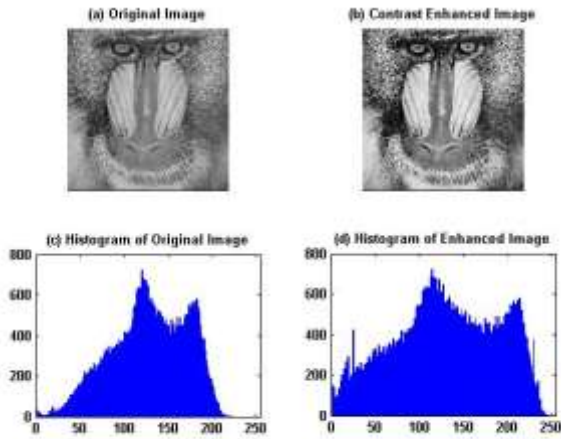
The enhanced images produced by the proposed methods are presented in Fig.1 to 4. For the subjective qualitative analysis of processed image appearance, the test images namely 'Lena', 'plane', 'Baboon' and 'Paper' are shown in these figures. The original images have poor brightness in the underexposed regions and brightness is higher in the overexposed regions.



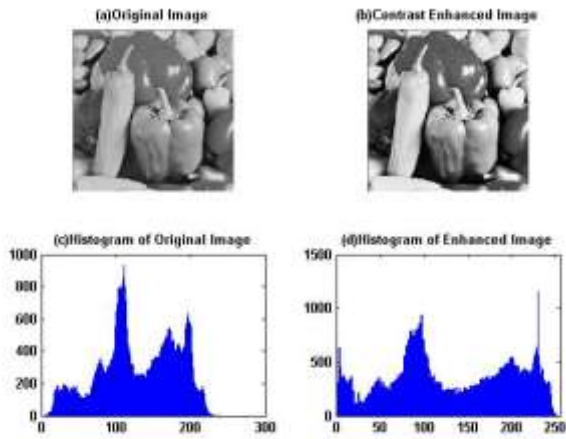
2. (a) original image (Lena) ,(b) enhanced image c) Histogram of Original Image (d) histogram of Enhance image



3. (a) original image (Plane) ,(b) enhanced image c) Histogram of Original Image (d) histogram of Enhance image



4. (a) original image (Baboon) ,(b) enhanced image c) Histogram of Original Image (d) histogram of Enhance image



5. (a) original image (Paper) ,(b) enhanced image c) Histogram of Original Image (d) histogram of Enhance image

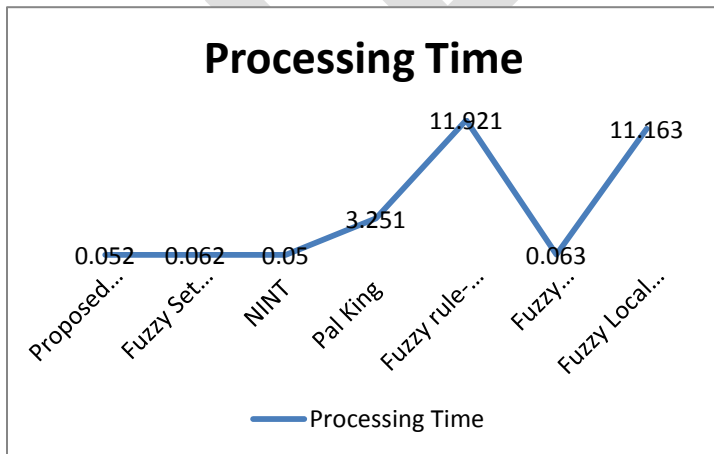
The qualitative analysis presented in the Figures 2 to 5 can be supported by quantitative analysis presented in TABLE I. The average analysis for 20 standard images of proposed method, NINT, fuzzy rule-based, fuzzy quantitative analysis ,Pal King method and fuzzy local enhancement presented in TABLE I are discussed. For each analysis, the best results obtained are made bold.

TABLE I indicates that the proposed method has the best performances in terms of smallest IOF, highest PSNR and obtained good contrast. However, in terms of the average execution time, NINT has the fastest processing time because NINT is less complex and treated the whole image as mixed region without considering overexposed and underexposed regions.

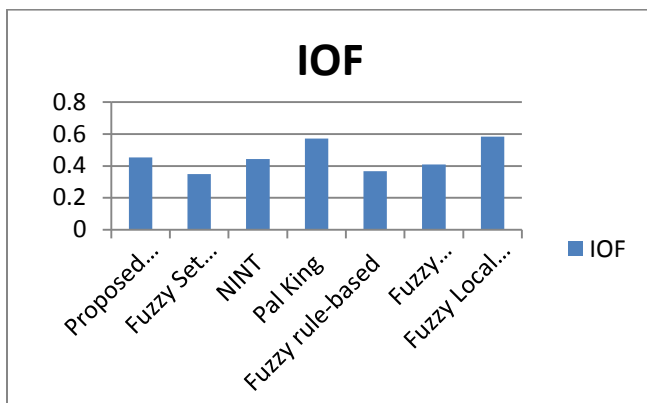
TABLE I. QUANTITATIVE ENHANCEMENT ANALYSES FOR 20 STANDARD IMAGES (AVERAGE VALUES)

Method\Analysis	Processing Time T(s)	IOF	PSNR (dB)	Contrast
Proposed Method	0.052	0.454	34.23	70.7151
Fuzzy Set Enhancement	0.062	0.349	22.039	71.969
NINT	0.050	0.443	13.947	88.391
Pal- King	3.251	0.572	18.92	89.1
Fuzzy rule-based	11.921	0.367	19.096	78.793
Fuzzy Quantitative Measure	0.063	0.410	15.417	82.654
Fuzzy Local Enhancement	11.163	0.584	19.063	81.929

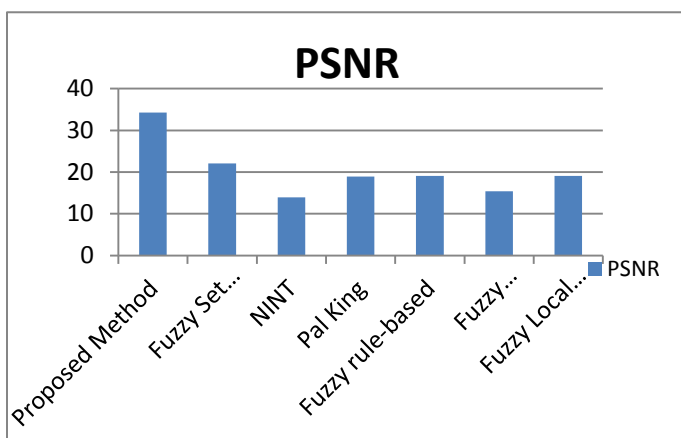
Fig.6 shows the computational time of the proposed method with other enhancement methods . Fig.7 shows comparison graph of the IOF among proposed method and other enhancement methods. Fig.8 shows comparison graph of the proposed method and other enhancement methods with respect to PSNR Calculation .



6. The Execution Time(sec) comparison of Our proposed Method with other existing method



7. The IOF comparison of Our proposed Method with other existing method



8. The PSNR comparison of Our proposed Method with other existing method

CONCLUSION

In this paper Pal King Membership function is defined to enhance the image and algorithm is proposed. The proposed algorithm is implemented in MATLAB 7.8. This proposed algorithm is able to overcome the drawbacks of spatial domain methods like thresholding, histogram equalization and frequency domain methods. This algorithm is able to get good contrasted image which increases the brightness of the low contrasted images. This algorithm is tested on different type of images. The experimental result shows that the brightness is increased as compared to previous one. Future work can be extended for other images then grayscale images to obtain better result with accuracy.

REFERENCES:

- [1] Khairunnisa Hasikin and Nor Ashidi Mat Isa, "Enhancement of the low contrast image using fuzzy set theory"14th International Conference on Modelling and Simulation, IEEE,2012.
- [2] S.S. Bedi1, Rati Khandelwal2,"Various Image Enhancement Techniques- A Critical Review" International Journal of Advanced Research in Computer and Communication Engineering Vol. 2, Issue 3, March 2013
- [3] Raman Maini and Himanshu Aggarwal , " A Comprehensive Review of Image Enhancement Techniques" JOURNAL OF COMPUTING, VOLUME 2, ISSUE 3, MARCH 2010, ISSN 2151-9617.
- [4] M. Hanmandlu and D. Jha, "An Optimal Fuzzy System for Color Image Enhancement," Image Processing, IEEE Transactions on, vol. 15, pp. 2956-2966, 2006.
- [5] Manpreet Kaur, Jasdeep Kaur, Jappreet Kaur," Survey of Contrast Enhancement Techniques based on Histogram Equalization" (IJACSA) International Journal of Advanced Computer Science and Applications, Vol. 2, No. 7, 2011.

- [6] L. A. Zadeh, "Outline of a New Approach to the Analysis of Complex Systems and Decision Processes," Systems, Man and Cybernetics, IEEE Transactions on, vol. SMC-3, pp. 28-44, 1973.
- [7] H.D. Cheng, Huijuan Xu, "A novel fuzzy logic approach to contrast enhancement", Pattern Recognition , 33 , 2000, 809-819.
- [8] S.K. Naik, C.A. Murthy, "Hue-preserving color image enhancement without gamut problem", IEEE Trans. Image Process.,12, 2003, 1591–1598.
- [9] Madasu Hanmandlu, Senior Member, IEEE, Om Prakash Verma, Nukala Krishna Kumar, and Muralidhar Kulkarni, "A Novel Optimal Fuzzy System for Color Image Enhancement Using Bacterial Foraging", IEEE transactions on instrumentation and measurement, vol. 58, no. 8, august 2009.
- [10]Gang Li, Yala Tong,Xinping Xiao, "Adaptive Fuzzy Enhancement Algorithm of Surface Image based on Local Discrimination via Grey Entropy", Elsevier Procedia Engineering 15 (2011) 1590 – 1594, 2011.
- [11]Khairunnisa Hasikin and Nor Ashidi Mat Isa, "Enhancement of the low contrast image using fuzzy set theory"14th International Conference on Modelling and Simulation, IEEE,2012.
- [12]X.-Y. Wang, T. Wang, and J. Bu, "Color image segmentation using pixel wise support vector machine classification," Pattern Recognition, vol. 44, pp. 777-787, 2011.
- [13]D.-l. Peng and A.-k. Xue, "Degraded image enhancement with applications in robot vision," in Systems, Man and Cybernetics, 2005 IEEE International Conference on, 2005, pp. 1837-1842 Vol. 2.
- [14]E. E. Kerre and M. Nachtegael,"Fuzzy techniques in image processing," Physica-Verlag, 2000.
- Pal S K, King R A."Image enhancement using smoothing with fuzzy sets," IEEE Trans. Systems, Man & Cybernetics, 1981, 11(7): 494-501

Health Effect of Prolonged Standing at Work & Its Control Measures: A Review

Shaikh Abdus Samad (ME Manufacturing Scholar); Prof R D Shelke (HOD)

Department of Mechanical Engineering, Everest's Educational Society's Group of Institutions College of Engineering & Technology, Aurangabad

as.shaikh@gmail.com | +91 7276 571737

Abstract – Many nations significantly depend upon manufacturing industries. Manufacturing Industries depends upon their employees. Ergonomics at work is now became essential part of day-to-day work which directly / indirectly depend upon quality & quantity of work done by any person. Pain is a very common and disabling condition among industrial workers. Most of the industrial workers lost productive time due to pain which reduced performance of the worker. The use of ergonomic is considered a critical means to alleviate the pain associated with standing work and, as a result increase in quality & quantity of productivity. This paper is a review of person working in manufacturing industries. This type of study is important that concern the shop floor worker working in a prolonged standing position on a regular basis. Prolonged standing can cause sore feet, swelling of the legs, varicose veins, general muscular fatigue, and low back pain, stiffness in the neck and shoulders, and other health problems.

Keywords – Ergonomics, Prolonged Standing, Kinesiology, Health effect of Prolonged Standing, Control Measure to reduce health hazard of Prolonged Standing, Engineering Control to reduce health hazard of Prolonged Standing, Administrative Control to reduce health hazard of Prolonged Standing.

1 INTRODUCTION

Ergonomics (or human factors) is the scientific discipline concerned with the understanding of interactions among humans and other elements of a system, and the profession that applies theory, principles, data and methods to design in order to optimize human well-being and overall system performance. [09]

Standing position is most suitable position among industrial workers at work. Most kind of job in manufacturing industry does not permit the worker to perform the job in sitting position. While performing or working, workers need adequate degree of freedom especially operating large machine and huge workpieces, reaching of materials and tools, and pushing and pulling of excessive loads.

Working in standing can be considered as most suitable & natural position because the mobility of legs having large degree of freedom. However, when workers spent prolonged time in standing position throughout their working hours (more than 50% of total working hours), they might feel discomfort and experienced muscle fatigue at the end of workday, it will vital contributor to decrease workers performance in industry. Prolonged standing posture can cause many temporary as well as permanent health effect which include but not limited to sore feet, swelling of the legs, varicose veins, general muscular fatigue, and low back pain, stiffness in the neck and shoulders, and other health problems.

2 HEALTH EFFECT

Millions of workers in the India have suffered from injuries due to prolonged standing, and resulted billion days sick leave a year. Worker who performs processes jobs in prolonged standing posture can cause many temporary as well as permanent health effect which include but not limited to discomfort in the legs, sore feet, swelling of the legs, varicose veins, general muscular fatigue, and low back pain, stiffness in the neck and shoulders, and other health problems.

2.1 WORK-RELATED MUSCULOSKELETAL DISORDERS (WMSD)

Work related musculoskeletal disorder (WMSD) is a common health problem throughout the industrialized world and a major cause of

disability. WMSD are conditions of the nerves, tendons, muscles, and supporting structures of the musculoskeletal system that can result in fatigue, discomfort, pain, local swelling, numbness, tingling, joint compression, etc... WMSD usually develop from accumulative impairment resulting from prolonged exposure to excessive levels of physical as well as psychosocial strain at work. The major risk factors for WMSD in the workplace include but not limited to: Heavy manual handling; Repetitive and forceful actions; Vibration; Awkward static postures that arise from badly designed workstations, tools, equipment, working methods; Poor work organization. [04] [05] [10] [11] [12] [13]

2.2 POSTURAL KYPHOSIS

Proper posture is often referred to as a "neutral spine", Postural kyphosis is improper posture or a "non-neutral spine". Postural kyphosis is the most common type, normally attributed to slouching, can occur in both the old and the young. In the young, it can be called 'slouching' and is reversible by correcting muscular imbalances. Often prolonged working with improper posture with non-neutral spine regularly can cause Slouching in workers. [10]

2.3 VARICOSE VEINS

Veins that have become enlarged and twisted, especially within the legs, ankles and feet of an effected individual called Varicose Veins. Varicose veins have also been associated with chronic heart and circulatory disorders and hypertension as well as complications related to pregnancy. Among the working age population one out of five hospitalizations from varicose veins are as a result of prolonged standing. Prolonged standing leads to impeded blood flow and stasis in the veins in the lower limbs, which can cause varicose veins. [06] [10]

2.4 CAROTID ATHEROSCLEROSIS

Standing for prolonged periods can lead to certain cardiovascular disorders. Prolonged standing at work significantly associated with the progression of carotid atherosclerosis in men. Prolonged standing can change the distribution of blood in the extremities. This in turn causes the blood to pool and reduces the circulating blood plasma volume leading to hemodynamic changes that impact the body and it can influence the progressions of carotid atherosclerosis. Atherosclerosis can lead to coronary artery disease, carotid artery disease, peripheral artery disease, and aneurysms. [03] [06] [07] [08] [10] [15]

2.5 JOINT COMPRESSION

Prolonged Standing places significant pressure on the joint of the hips, knees, ankle and feet but without any significant movement of it. This reduces the normal lubrication and cushioning of synovial joints, causing them to wear and tear. [10]

2.6 MUSCLE FATIGUE

Muscle Fatigue is the most disabling condition (around 1/3rd of all worker injury and illness as per OSHA) among workers. Muscles kept in a constant stress position quickly become exhausted and can result in pain and swelling in the lower back, legs, ankles and feet. Prolonged standing experiences muscle fatigue which persists short period of time at end, this might differ person to person. [02] [10]

2.7 PREGNANCY

Prolonged standing increase risk for high blood pressure, spontaneous abortion, preterm birth, low birth weight among working pregnancy women. [01] [12] [10]

3 CONTROL MEASURES

Researcher use many control measure to reduce health hazard due to prolonged standing. These control measures can broadly classified in Engineering Control & Administrative Control. These ergonomic practices not fully but somehow found to be effective to reduce health hazard due to prolonged standing. Prevention is better than cure. Control the Hazard of prolonged standing need to be treated as a priority so that related injuries can be eliminated or minimized further prevent permanent injury. [07][08][13][14][15]

3.1 ENGINEERING CONTROLS

Control of Hazard of Prolonged standing using engineering technique is called Engineering Control. Engineering Control includes, but not limited to, providing Ergonomic Flooring, Ergonomic Footwear & Ergonomic Workstation. Research shows these techniques are effective but unable to fully eliminate Hazard of Prolonged Standing. [07][08][13][14][15]

3.2 ADMINISTRATIVE CONTROLS

Where Engineering Control difficult to be implementing, Administrative Controls are used to minimize the Hazard of Prolonged Standing. Administrative Control includes, but not limited to, work-rest scheduling, arrange work such as worker could not adopt one posture long time, providing rest intervals, Training & Education about Good body posture & Ergonomic way to acquiescent fatigue etc... Experts suggest to move around and change positions throughout the day. It is best not to sit in one position for more than 20 minutes, or to stand in one position for more than 8 minutes. Research shows that Administrative Control is more effective than Engineering Control, to control the hazard of prolonged standing. [07][08][13][14][15]

CONCLUSION

Based on review of the literature, it can be concluded that performing jobs in prolonged standing has contributed numerous health effects such as Work-related Musculoskeletal Disorders (WMSD), chronic venous insufficiency, Postural Kyphosis, Varicose Veins, Joint-Compression, Muscle Fatigue, Problem in Pregnancy, Preterm Birth, Spontaneous Abortion, and Carotid Atherosclerosis. However, those injuries can be minimized through application of engineering and administrative controls. Developed Nations more concern on Ergonomic at work than developing nations. Ergonomically design work spaces are more prevalent in Europe & America Region. Developed Nations have work spaces design anthropomorphically for their region but not such case in developing nation. Developing nation's industrial workers lack ergonomic knowledge & good body posture during working

REFERENCES:

- [1] Bonde JP, et. al., "Miscarriage and occupational activity: a systematic review and meta-analysis regarding shift work, working hours, lifting, standing, and physical workload", *Scandinavian Journal of Work, Environment & Health*, 2013;39(4):325-334
- [2] Jeremy Brownie, et. al., "Muscle fatigue and discomfort associated with standing and walking: Comparison of work surfaces", *The Proceedings of the 19th Triennial Congress of the International Ergonomics Association*. Melbourne, August 2015.
- [3] Krause N, et. al., "Standing at work and progression of carotid atherosclerosis", *Scandinavian Journal of Work, Environment & Health*, 2000;26(3):227-236
- [4] Roseni Abdul Aziz, et. al., "Musculoskeletal disorders in body regions and its associated risk factors among electronics workers in Malaysia", *The Proceedings of the 19th Triennial Congress of the International Ergonomics Association*. Melbourne, August 2015.
- [5] S. C. Mali, et. al., "An Ergonomic Evaluation of an Industrial Workstation: A Review", *International Journal of Current Engineering and Technology*, Volume: 5, Issue: 3, June 2015.
- [6] Finn Tuchsén, et. al., "Standing at work and varicose veins", *Scandinavian Journal of Work, Environment & Health*, 2000;26(5):414-420
- [7] Prof. R. D. Vaidya, et. al., "Ergonomics Evaluation of Body Posture of Worker In SSI", *Journal of Emerging Technologies and Innovative Research (JETIR)*, Volume: 1 Issue: 6, November 2014.
- [8] N. A. Ansari, et. al., "Evaluation of work Posture by RULA and REBA: A Case Study", *IOSR Journal of Mechanical and Civil Engineering (IOSR-JMCE)*, Volume: 11, Issue: 4, Aug 2014.
- [9] "www.iea.cc", 12th March 2016 @ 05:19 PM
- [10] "www.en.wikipedia.org", 12th March 2016 @ 05:19 PM
- [11] Sandip B. Wanave, et. al., "Study and Assessment of Body Posture of the Operator Working in Transformer Manufacturing Industry through RULA", *International Journal of Research in Advent Technology*, Volume: 2, Issue: 2, February 2014.
- [12] Siti Noor Azizzati Mohd Noor, et. al., "A Review of Studies Concerning Prolonged Standing Working Posture", *Advanced Engineering Forum*, Volume: 10, December 2013.
- [13] Mohd Hafiz Zani, et. al., "An overview of ergonomics problems related to CNC machining operations", *Advanced Engineering Forum*, Volume: 10, December 2013.
- [14] Isa, H., et. al., "Electromyography analysis associated with prolonged standing in metal stamping industry", *Journal of Advanced Manufacturing Technology*, Volume: 7, Issue: 1, June 2013.
- [15] N. A. Ansari, et. al., "Study and Justification of Body Postures of Workers Working In SSI by Using Reba", *International Journal of Engineering and Advanced Technology (IJEAT)*, Volume: 2, Issue: 3, February 2013.

Smart Ticketing Using Wi-Fi Technology

Farhana Siddiqui¹, Sayyed Mohammed Askari²
Dept. of Computer Engineering
M.H.Saboo Siddik College of Engineering Mumbai India
1 khanfarhana_ali@hotmail.com
2 sayyed.askari@gmail.com

Abstract: To Travel in public rail transport system is more efficient than other means, like travelling by road where the issue of traffic is always a major problem of public as well as the administration. But, to travel in the railways getting a ticket is a tedious task which uses lots of time and efforts of the commuters. To overcome these problems of ticketing the administration has implemented lots of new ways by which a person can book a ticket. But somehow those methods have not delivered up to the expectation, and there is still a long queues at the traditional ticketing counters to get the ticket. With the help of technology our project propose to help in reducing the problem. In todays time almost every traveller has a smartphone device which is embedded with wi-fi. With the help of that device the passenger can book a ticket on its own device without standing in a queue and get a copy of the ticket on its own device. The application does not requires an internet connection but it connects to railways server via wi-fi router on the station to book ticket. Also the ticket is stored in the database of railways so the travellers can get it when they are required to.

Keywords- Wi-Fi Router, Android, Internet.

INTRODUCTION

Train travel is the most cost effective and time efficient travelling system in major cities for public transport. These System provide trains which arrive on scheduled time and comparatively at lower cost. With these benefits this system is most preferred mode of travelling by the people which has made it also the most crowded system. With more and more people travelling the time and queue at ticket counter has increased exponentially. To make the system more efficient we have proposed a system in which the passenger does not require to stand in long and time consuming queues and also does not require to carry a physical ticket. With the help of our system a commuter can get the required ticket for its destined journey with its own smart device. The device is embedded with wi fi which will help the commuter to connect to the railway server with the help of an application and wi fi router installed at station and book a ticket very quickly. In this system commuter does not require to stand in a long queue like at traditional booking windows and also at recent smart ticketing machines during the peak hours of morning and evening. Also it get you a e-ticket which is loss proof and environment friendly. Allowing the commuter to book the ticket from the station without using any cost increasing service like Internet, SMS, GPS,EDGE/GPRS, 3G/4G etc. which other system fails to provide.

LITERATURE SURVEY

Indian railways has become technologically a lot more advanced in past few years. Railways have in cooperated several new and better functionalities in the system to supply higher degree of service to the users. For booking of a ticket there has been immeasurable problems caused to the commuters in order to make the booking of ticket easy the railways have introduced several technological options like on-line ticket booking, Coupons, Smartcards etc. For long journeys it introduced an e-ticketing facility whereby the user can book a ticket through a website and get an e-ticket, which is needed to be shown to the ticket checker whenever required. However in cities suburban railways still had crowds at each counters which provides ticket. To get out of this problem M-ticketing(mobile ticketing) was introduced within which user will be able to get the tickets in their mobile devices.[1]

Recently there has been a service in which sms protocol is used was implemented for booking of a ticket, in this the user who has a mobile device along with a working sms function can avail the benefits of this service. For getting a ticket booked the user needs to send a sms for every request in order to get a response which is also a response sms. This system reduced the efforts to stand in ticket queues.[2]

Another service to get a ticket booked in that the application after booking the ticket generates a ticket in the form of a QR code(Quick Response Code) which the ticket inspector can use to verify the ticket form its database system for its authenticity and validation. In addition to this it shows the details of schedule ,routes details along with the cost for the user. The mode of payment can be cards credit/debit or through prepaid cards. The database is also maintained for user information.[3]

EXISTING SYSTEM

In Indian railway the Mumbai local railways provides multiple ways for ticket booking for its commuters

WINDOW TICKET

It is oldest and most widely used mode for ticket booking. In this method a person issues a ticket to the commuters one at a time, so during peak hour there are long queues at window to get a ticket . This causes waste of time and efforts of everyone standing in queue making it most time ineffective.

COUPONS

To overcome the problem of long and never ending queues the railways introduced coupon system which requires the commuter to buy a coupon book which has coupons of different denominations. For every journey commuter needs to get coupons validated by using a validating machine installed at every station. But, not every time there is right amount of coupon denomination left with the person to get it validated. Some times a person has to get coupon validated which is of more value than the actual fare for the journey. Also the coupons can be reused by removing the validation marks causing loss to the railways.

SMART CARDS

This is an expensive system which is implemented by the railways which provide its commuters an ease of ticket booking. For using this the commuter needs to buy a smart card and recharge it with certain amount. The machine at station are often crowded during peak hours. Also the machines are often not working properly . The maintenance of these machines are also very high.

M-TICKETING

Taking the help of technology the railways have introduced m-ticketing mobile application which allows the user to book a ticket on the mobile device itself. But to book the user needs to have an internet service like EDGE/GPRS, 3G/4G connection to start the booking. Also the account is to be recharged using online transaction. But, the user cannot book a ticket when they are near to the station making them to book the ticket before reaching the station[4].

PROPOSED SYSTEM

In this system which we are presenting the user shall go to the station from where he/she wants to start the journey and use the android application to get a ticket. The user for the first time needs to get registered at ticketing counter from any stations. After registration the user will get a unique id which will be used every time user connects to the system. The system requires the user to add money in to their account from which the fares will be deducted. The money can be added to the account of the user through various methods such as from ticket counters or from online transaction of credit or debit cards. For railways the database is maintained which stores the user information such as ticket information amount present in the account of any particular User ID.

For this system to work a wifi router is installed at every station. The user needs to connect to the railway server using a the wifi router with the help of our android application. After the connection is successfully made the user will be able to book a ticket.

To book a ticket the user will have to select the destination where he/she wants to go and also select the route preferred. After that the class in which the intention of travel is for then the number of tickets required if some one else are also accompanying. Then if the ticket to be used for return journey then that condition should be checked and submit the information. After the submit it done the application will check every field and the amount of ticket should be less than the amount in the user account to get a confirmed booking. After a successfully booking a ticket the user will get a message which will act as a ticket.

In the span of usage user will require to the account to be added with more money for that user can use the ticket counter or online transaction to refill his/her account.

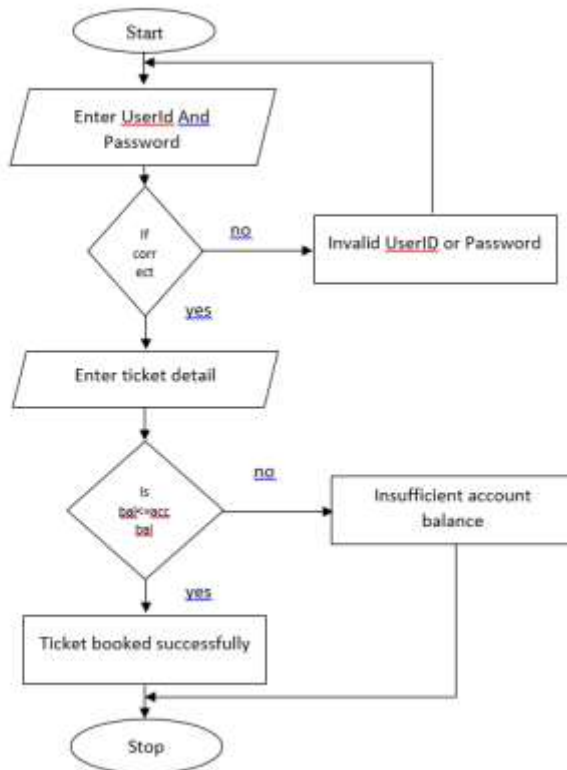


Fig: Flowchart

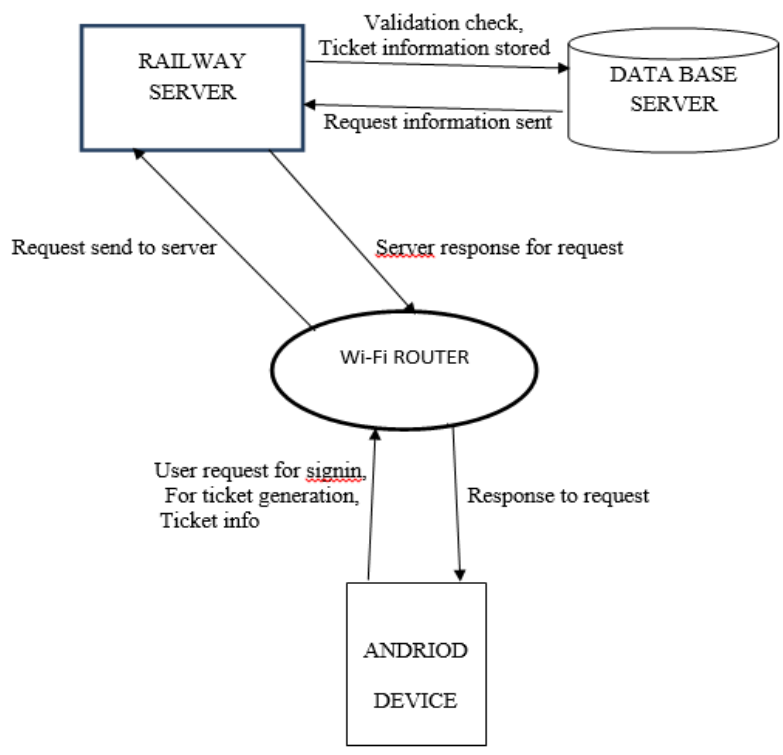


Fig: Block diagram

IMPLEMENTATION

This system to book a ticket on mobile without standing in a queue and also without internet or any other cost increasing service. This will reduce the efforts of the user and also providing a better facilities to them. The Implementation of this system requires to maintain a database for keeping records with a wifi access point or a router. To implement the system we require following,

MICROSOFT SQL SERVER

It is a relational database management system by Microsoft, this software helps us to maintain the database and also provide it for different functions. We are using the software for storing the information of the user and also to retrieve the information of the data whenever required by us. The database will store the information such as UserID, Password, Name, Account Balance, Ticket information, etc.[5]

ANDROID APPLICATION

Android is a mobile OS by google on which most of the devices run today. It is the most used OS by the people. Its application is developed for android because of its wider reach and more number of users. The application is used to book the ticket it will connect to the database with the help of wifi router. [6]

WIFI ROUTER

It is a device which performs the function of router also providing a wireless access point. For our system the router is connected to the database and provide the access point of the mobile application to connect to the database acting as a middleware in the system.[7]



Fig: Server home page

The screenshot shows a window titled "UInfo" with a header "USER INFORMATION". Below the header are seven input fields: "First Name", "Middle Name", "Last Name", "Address", "DOB" (with a date picker showing "30 March 2016"), "Email id", and "User Password". At the bottom center is a button labeled "NEXT".

Fig: User Registration Form

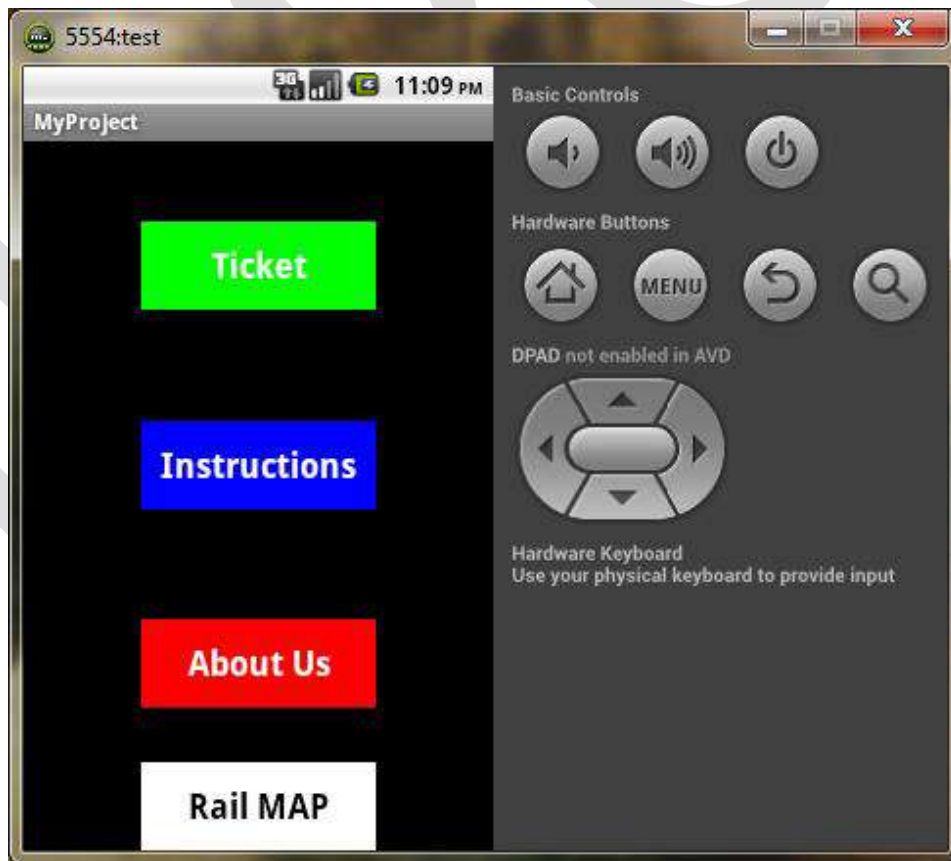


Fig: Main Page of Mobile Application



Fig: Ticket Form

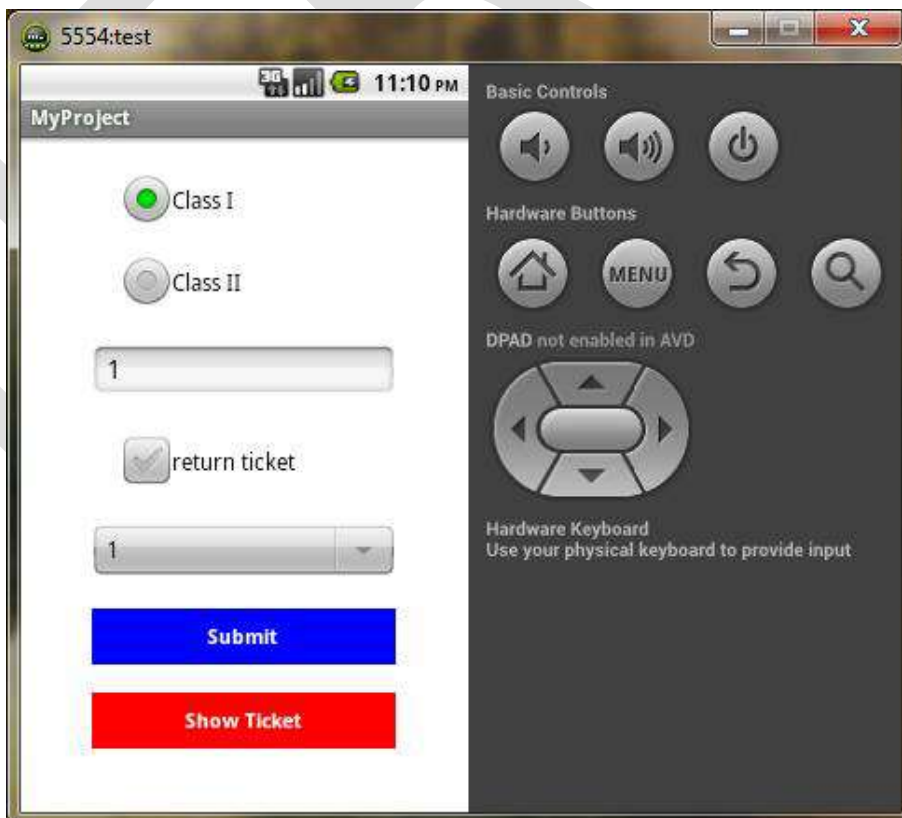


Fig: Ticket form



Fig: Error message for invalid id password



Fig: Ticket after successful booking

ACKNOWLEDGMENT

We would like to express our gratitude and thanks to our college M.H. Saboo Siddik College Of Engineering for providing us with the opportunity the this wonderful project.

CONCLUSION

The Proposed model of our application will reduce the user effort to complete the booking of a ticket by allowing mobile devices to book and store ticket information. This will also help in the efforts of green environment. The application is user friendly for all and also has higher efficiency.

FUTURE ENHANCEMENTS

In future we would like to introduce the system of online transaction and online registration which will make the system further more efficient. Since the application is only for the android we would like to make it available it for other platforms as well like IOS, Windows etc.

REFERENCES:

- [1]. Karthick.SI, Velmurugan, 'Android Suburban Railway Ticketing with GPS as Ticket Checker', IEEE International Conference on Advanced Communication Control and Computing Technologies (ICACCCT), pp. 63-66, 2012.
- [2]. Sadaf Shaikh, Gayatri Shinde, Mayuri Potghan, Tazeen Shaikh, Ranjeetsingh Suryawanshi, 'Urban Railway Ticketing Application', International Journal of Advanced Research in Computer Science and Software Engineering, pg130-132,2014.
- [3]. Savita Dubey, 'Queue-less Ticketing System for Local Trains', International Journal of Infinite Innovations in Technology, Vol.2, 2014
- [4]. Indian Railway https://www.utsnmobile.indianrail.gov.in/RDS/images/HELP_ANDROID_Paperless.pdf
- [5]. Microsoft SQL Server (04 April 2016). Retrieved from https://en.wikipedia.org/wiki/Microsoft_SQL_Server
- [6]. Android Operating System (04 April 2016). Retrieved from https://en.wikipedia.org/wiki/Android_%28operating_system%29
- [7]. Wireless Router (04 April 2016). Retrieved from https://en.wikipedia.org/wiki/Wireless_router

Heat Transfer Analysis of Gas Turbine Rotor Blade Through Staggered Holes Using CFD

Priyanka Singh*, O P Shukla**

* M. Tech Student Department of mechanical engineering Millennium Institute of technology Bhopal(M.P)

(pink_i_singh08@yahoo.com)

** Assistant professor of mechanical engineering Millennium Institute of Technology Bhopal (M.P)

(opshukla0132@gmail.com)

ABSTRACT- In a gas turbine engine, the turbine blade operated higher temperature than the melting point of the blade material. Cooling of gas turbine blades is a major consideration for continuous safe operation of gas turbines with high performance. Several methods have been suggested for the cooling of blades and one such technique is to have radial holes to pass high velocity cooling air along the blade span. In the present work CFD analysis is used to examine the heat transfer analysis of gas turbine with six different model consisting of 5,9&13 inline one row of holes and compared with 9&13 model in staggered holes arranged in the three rows and developed a new model with 14 holes in the staggered arrangement. The prediction is commonly used CFD software FLUENT (a turbulence realizable k-e model with enhanced wall treatment). On evaluating the contour plot of the pressure, velocity & velocity vector we found that the temperature distribution on the 13 staggered holes, uniformly distributed along the blade area, as compared to 13 inline holes. And the heat transfer is also increases in the 13 & 14 staggered holes arrangements.

KEY WORDS- Computational fluid dynamics (CFD), Inline holes, Staggered holes, Heat transfer rate, CAD, Turbulent-Intensity model.

I INTRODUCTION

The gas turbine used in power plant, where a great amount of energy produces for its weight and size. Gas turbine engine is a single turbine section which is made from Disk or Hub, and this disk or hub holds number of turbine blades. Turbine section is connected to compressor section through shaft, and this shaft is also called as Spool. There are two types of compressor section can be used Axial or Centrifugal. In compressor the temperature and pressure of air increases and air will be compressed. Most of the gas turbine engines having twin spool design means high pressure spool and low pressure spool but some gas turbines using three spools, Intermediate pressure spool between the high and low pressure spool.

METHODES OF COOLING

Components of gas turbine can be cooled by **air** or **liquid cooling**. Liquid cooling is more attractive because of high specific heat capacity and evaporative cooling but liquid cooling having problem of corrosion, choking, and leakage. Air cooling allows the discharged air into main flow without any problem. For air cooling less quantity of air required such as 1.5-3% of main flow and blade temperature can be reduced by 250-300C. There are many types of cooling used in gas turbine blades.

1. Internal Cooling

- Convection cooling.
- Impingement cooling.

2. External Cooling

- Film cooling.
- Cooling effusion.
- Pin fin cooling.

II LITERATURE REVIEW

K hari brahmaiah et.al.[1]- Examine the heat transfer analysis of gas turbine with four different models consisting of blade with and without holes and blades with varying number of holes(5,9&13) were analyzed. Transfer rate and temperature distribution, the blade with 13 holes is considered as optimum. Steady state thermal and structural analysis is carried out using ANSYS software with different blade materials of Chromium steel and Inconel-718. While comparing these materials Inconel-718 is better thermal properties and induced stresses are lesser than the Chromium steel.

R d v Prasad et.al.[2]- Examine steady state thermal& structural performance for N155& Inconel 718 nickel-chromium alloys. Using finite element analysis Four different models consisting of solid blade and blades with varying number of holes (5, 9&13 holes) were analyzed of cooling holes. The analysis is carried out using ANSYS software package. While comparing materials, it is found that Inconel 718 is better suited for high temperature .the graphs drawn for temperature distribution, von-misses stresses and deflection, the blade with 13 holes is considered as optimum. the induced stresses are minimum and the temperature of the blade is close to the required value of 800C.

B deepanraj et.al.[3]- using finite element analysis thermal and structural performance due to loading condition, with material properties of Titanium- Aluminum alloy. Six different models with different number of holes (7, 8, 9, 10, 11&12) were analyzed. Using ANSYS, bending stress, deflection, temperature distribution, for number of holes are analyzed. It is found that when the numbers of holes are increased in the blade the temperature distribution falls down. For the blade configuration with 8 holes, the temperature near to the required value i.e., 800C is obtained.

G. Narendranath et.al.[4]- examine the first stage rotor blade off the gas turbine analyzed using ANSYS 9.0. The material of the blade was specified as N155. Thermal and structural analysis is done using ANSYS 9.0 Finite element analysis software. The temperature variations from leading edge the trailing edge on the blade profile is varying from 839.5310C to 735.1620C at the tip of the blade. It is observed that the maximum thermal stress is 1217 and the minimum thermal stress is the less than the yield strength value i.e., 1450.

V.Vijaya Kumar et.al.[5] - examine the “preliminary design of a power turbine for maximization of an existing turbojet engine”. For a clear understanding of the combined mechanical and the thermal stresses for the mechanical axial and centrifugal forces. The peripheral speed of rotor and flows velocities is kept in the reasonable range so to minimize losses. In which the base profiles is analyzed later for flow condition through any of the theoretical flow analysis method such as “potential flow approach”.

III METHODOLOGY

CFD (computational fluid dynamics) analyzes thermal analysis by computer based simulation these analysis are based on the fluid flow, heat transfer, and related phenomenon such as chemical reactions. This project uses CFD analysis of flow and heat transfer. The application areas of gas turbine are aerodynamics lift and drag (i.e. airplane or windmill wings), power plant combustion, chemical processes, heating/ventilation and even biomedical engineering (simulating blood flow through arteries and veins). CFD analysis is carried out in the various industries are used in R&D and manufacture of aircraft, combustion engines, as well as many other industrial products.

Basic steps to perform CFD analysis-

1) Preprocessing-

- **CAD Modeling-** The generation of model is done on the CAD modeling. In the working plane the key points created and these points are joined by spline curves through spline command in CAD to obtain a smooth contour. By extrude command the contour (2D model) is then converted into area and then volume (3D model) was generated. The hub is generated through rectangle command a rectangle is created in 2D model and then this 2D model is converted into 3D model and then extrude command is used. And finally these two volumes are combined into single volume.

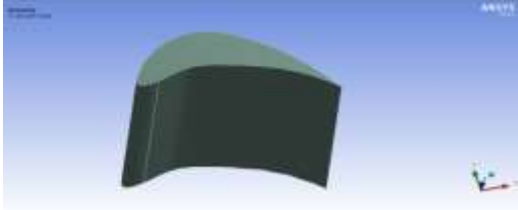


Fig .1 Turbine Blade Profile

- **Meshing-** In this operation, the CAD geometry is discretized into large numbers of small elements and nodes. The arrangement of nodes and elements in space in a proper manner is called mesh. Various models of blade profile with holes and their meshing are shown in figure.

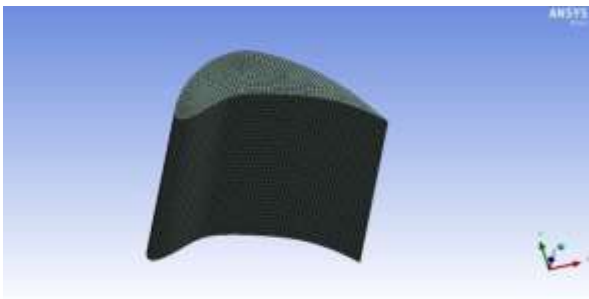


Fig.2 Meshing of the blade profile



Fig 3 Meshing of Five inline holes.

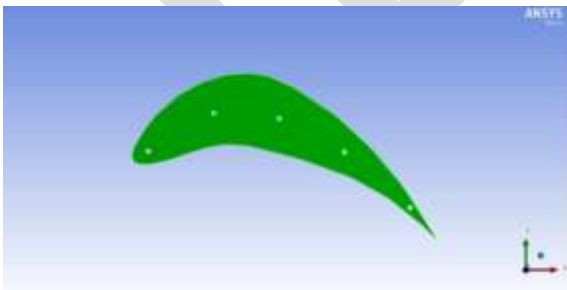


Fig.4 Blade profile with holes.

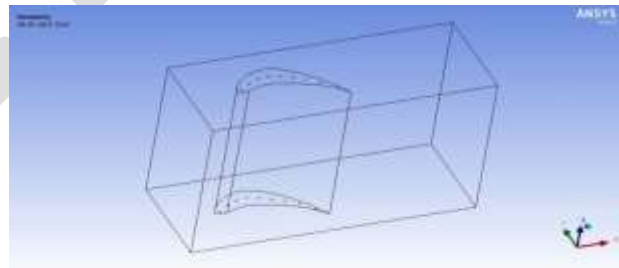


Fig 5 CAD Model of 9 inline holes

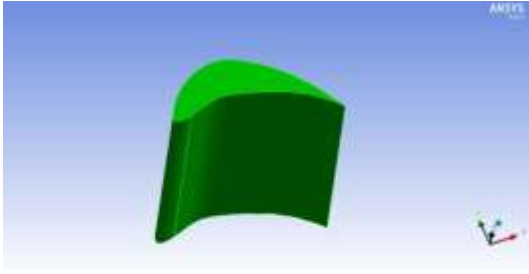


Fig 6 Blade profile of 9 inline holes



Fig 7 Blade profile 9 staggered holes

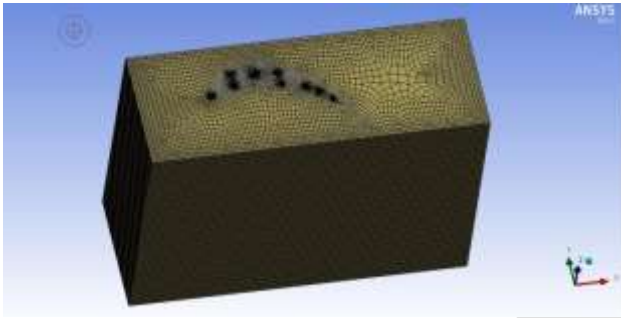


Fig 8 meshing of 9 staggered holes.

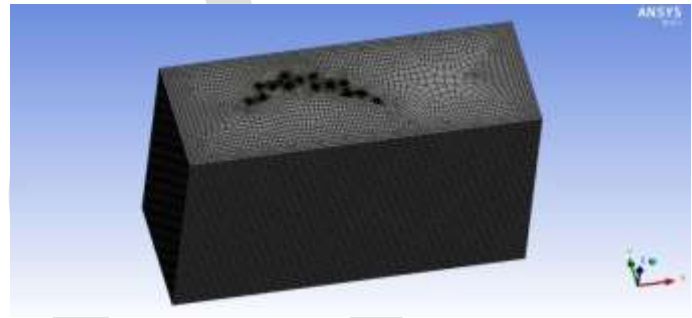


Fig 11 Meshing of 14 staggered holes.

2) Solution -

- **Type of solver-** Pressure based.
- **Physical model-** Turbulent (k-e), energy equation.
- **Material property-** Property of fluid such as air.
- **Boundary condition-** Pressure, velocity inlet, velocity outlet wall etc.
- **Solution method-** Choosing the solution method such as momentum equation, turbulent energy equation etc.
- **Solution initialization-** Initialize the solution to get the initial solution of the problem.
- **Run solution-** Run the solution by giving no of iteration for solution to converge.

3) **Post processing-** Post processing is used for viewing and interpretation of result. The results can be viewed in various animations, graph etc.

IV NOMENCLATURE

α Coefficient of thermal expansion

E Young's modulus

μ Poisson's ratio

L Length

D Diameter of shaft

N Speed of turbine in RPM

K Thermal conductivity

d Diameter of cooling air passage

Details of turbine blade-

D = 1308.5 mm, N = 3426 RPM, L = 117mm, d = 2mm

Table 1- Mechanical properties of Chromium steel and Inconel 718

Properties	Units	Chromium steel	Inconel 718
E	Mpa	80705	205005
P	Kg/cu m	7754	8192
K	W/m-k	24.5	25.8
μ	- - -	0.291	0.293
Cp	j/kg-k	435.801	586.253
Melting point	•C	1415	1346
Yield stress	Mpa	656	1068

V RESULT ANALYSIS

The temperature distribution and total heat transfer rate of the blade depends on the heat transfer coefficient for gases and the thermal conductivity of the material. The calculation of heat transfer coefficient is doing by some iterative methods such as turbulence realizable(k-e) models. It is observed that the maximum temperatures are prevailing at the leading edge of the blade. There is a temperature fall from the leading edge to the trailing edge. In first observation of the blade with 9 inline holes drilled readily to pass the cooling air through cooling holes , it can be observed from the fig 12 the temperature at the cooling holes is lower.

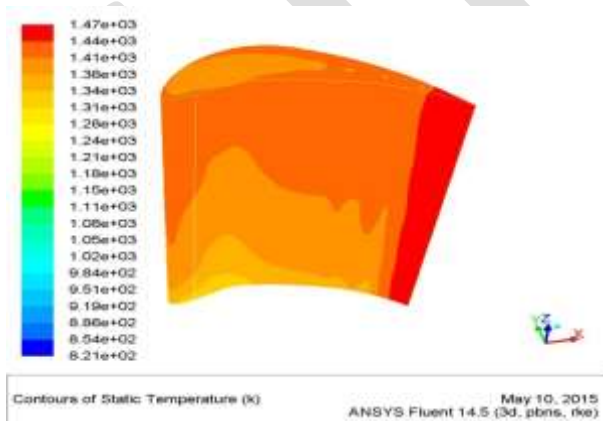


Fig 12 Contour of static temperature 9 inline holes.

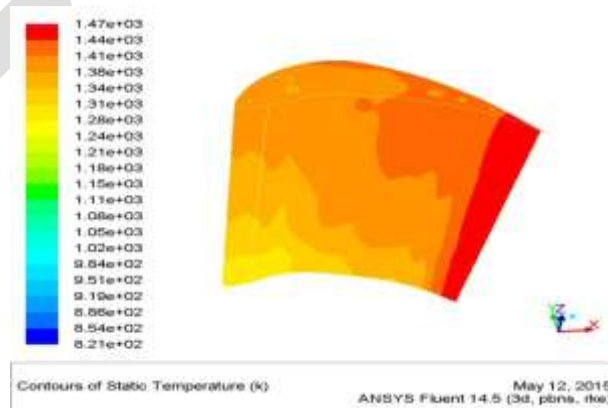


Fig 13 Contour of static temperature 9 staggered holes.

But if I drilled the 9 holes in staggered form then the temperature variation are shown in figure. The temperature of the blade is lower more then inline drilled holes. The blade temperature decreases 1397.663K to 1343.653K in the same number of the holes only

changing on the arrangement. In the fig 13 holes are drilled in the one line then the blade temperature were obtained as 1301.362K. and on the staggered 13 holes two row the temperature were obtained as 1303.689K. but the uniformity of the temperature distribution is better in the fig 13 as compared to 12

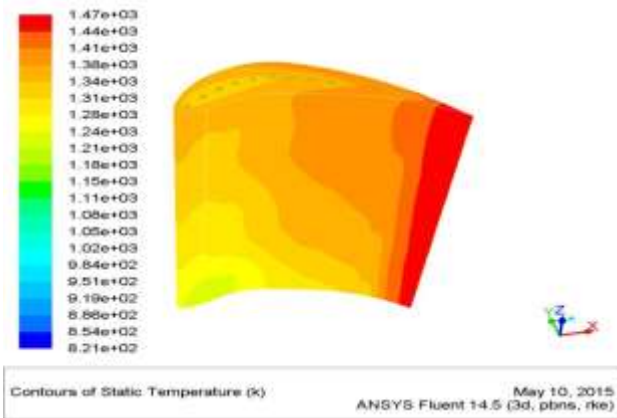


Fig 14 Countour of static temperature of 13 Inline holes.

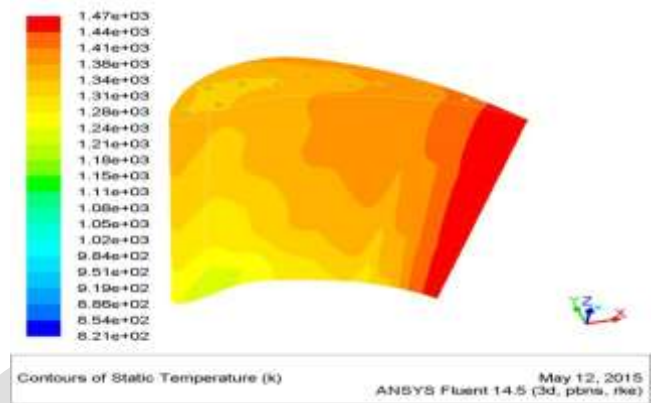


Fig 15 Countour of static temperature of 13 Staggered holes.

Up to the 13 inline holes studies are concerned that the number of holes are restricted because RDVPrasad obtained the minimum temperature as 1099.96K at the 13 holes and K Hari Brahmaiah also obtain 1112K but I obtained the 1303.689K at the 13 holes in staggered form. As both are explained that the decreasing temperature will lead to lower the thermal efficiency, because larger portion of air is utilized for cooling purpose and reduced quantities of air flows into the combustion chamber of gas turbine plant. The reduced mass flow rate of the gas and the decreased temperature of the blade will reduce the power output and efficiency of the plant. But at the 13 holes I obtained the temperature 1303.689K at the same material. So that I have studied on the 14 holes drilled in the staggered form and the temperature is obtained as 1291.784K.

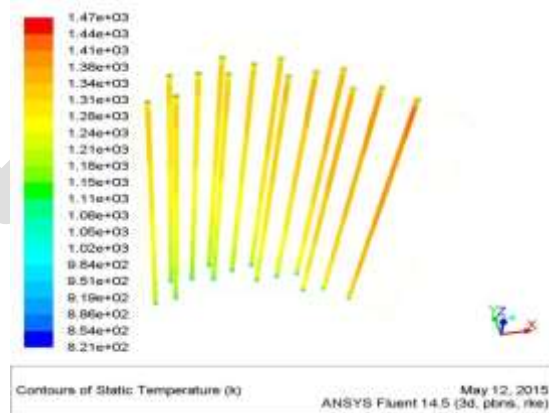
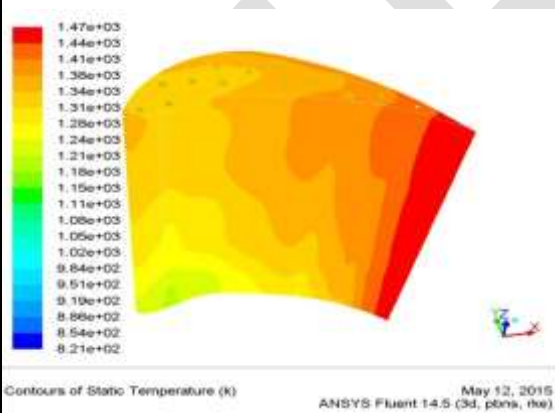


Fig 16 Contour of static temperature of 14 staggered holes. Fig 17 contour of static temperature 14 holes on the whole blade.

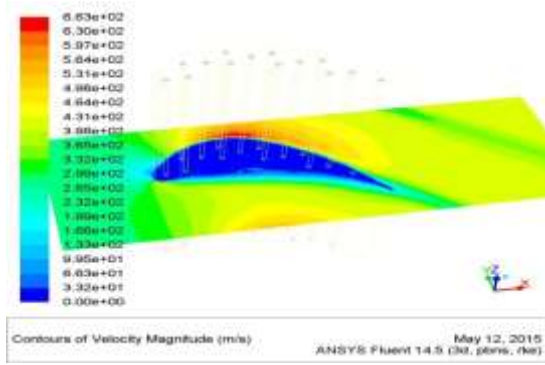


Fig 17 Contour of velocity magnitude of 14 staggered holes.

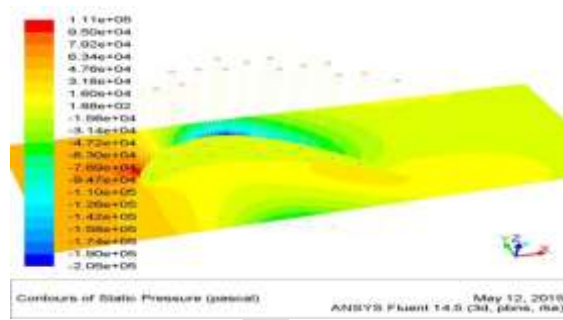


Fig 18 Contour of static pressure 14

Staggered holes.

By observing the fig 18,19&20 the static pressure of the blade is decreases with the increasing number of holes. But due to the reason of the thermal efficiency we can not increase the number of holes from optimum value. As K Hari Brahmaiah discussed that Inconel 718 material is best suited for the blade cooling because it gives maximum heat transfer rate and lesser amount of stresses and strain then Chromium steel. So that I taking that references and supposing the Inconel 718 is a best material.

Table 2 Total heat transfer rate Vs No of holes (inline) [Inconel 718]

No of holes	0	5	9	13
Total heat transfer rate (watts)	72.5	2190	3862	5032

Table 3 Total heat transfer rate Vs No of holes (staggered)[Inconel 718]

No of holes	9	13	14
Total heat transfer rate (watts)	3752	5081	5336.5

Table 4 Blade leading edge temperature Vs No. of holes(inline)

No of holes	0	5	9	13
Blade leading edge temperature(K)	1473.15	1374.138	1397.663	1301.362

Table 5 Blade leading edge temperature Vs No. of holes(staggered)

No of holes	9	13	14
Blade leading edge temperature (K)	1343.653	1303.689	1291.984

VI CONCLUSION & FUTURE SCOPE

CFD analysis of gas turbine blade is carried out with different models consisting of staggered varying number of cooling holes.

- In the overall stresses the temperature show the significant effect in the turbine blade.
- The blade leading edge is minimum for the blade consisting of 14 staggered holes and the total heat transfer rate is maximum.
- In the maximum curvature of the blade profile the temperature distribution is almost uniform.
- In the blade section the temperature is linearly decreasing from the tip to the root .

Further scope will be that we can increasing the number of holes up to the 16 in staggered form because staggered holes consumes less area as compared to inline holes. And it will give more heat transfer rate as well as minimum leading edge temperature. And also the strength of the blade is main consideration.

REFERENCES:

- [1] K Hari Brahmaiah, M. Lava Kumar, "Heat transfer analysis of gas turbine blade through cooling holes". International journal of computational engineering research (IJCER) Vol 04, Issue 7, July-2014.
- [2] R D V Prasad, G. Narasa Raju, M S S Srinivasa Rao, N Vasudeva Rao "Steady state thermal & structural analysis of gas turbine blade cooling system". International journal of engineering research & technology (IJERT) vol 2, issue 1, January-2013.
- [3] B. Deepanraj, P. Lawrence and G. Sankaranarayanan "Theoretical analysis of gas turbine blade by finite element method" scientific world. Vol 9 no 9, July 2011.
- [4] G Narendranath, S. Suresh "Thermal analysis of a gas turbine rotor blade by using ansys" International journal of engineering research and applications (IJERA) Vol 2, issue 5, Sep-Oct 2012.
- [5] V.Vijaya kumar, R. Lalitha Narayana, CH.Srinivas "Design and analysis of gas turbine blade by potential flow approach" V. Vijaya kumar et al Int. Journal of Engineering Research and Application, Vol. 4, Issue 1 (Version 1), January 2014
- [6] Sushil Sunil Gaikwad, C. R. Sonawane, "**Numerical Simulation Of Gas Turbine Blade Cooling For Enhanced Of Heat Transfer Of The Blades Tip**" IJRET: International Journals of Researches in Engineering and Technology eISSN: 2319-116 .Dec 2013.
- [7] Sridhar Paregouda, Prof. Dr. T. Nageswar Rao "**CFD Simulations on Gas turbine blades and Effect of Hole Shapes on leading edges Film Cooling Effectiveness**" International Journals of Modern Engineering Research (IJMER) Vol. 3, Issue. 4, Oct-. 2013
- [8] Honami, S., Shizawa, T., and Uchiyama, "**Behaviors Of The Laterally Inject Jets In Film Coolings: Measurements Of Surface Temperature And Velocity or Temperature Field Within The Jets,**" Vol. 116, ASME Journal of Turbo machineries, Vol 09 September 2013.
- [9] Harish. Sankar, J. P. Vikas, W.Nrisimhendrar Varun, "**Experimental & Numerical Investigation Of Effects Of Blowing Ratios in Film Cooling Effectiveness And Heat Transfer Coefficients Over Gas Turbine Blade Leading Edges Film Cooling's Configuration**" International Journal of Engineering Researches & Technology (IJERT) Vol. 2 Issue 8, August – 2013
- [10] T.Madhusudhan, Dr.K.Ramchandra, , Dr.H.Maheshappa"**Needs For Analysis Of Stresses Concentration Factor In Inclined Cutouts Of Gas Turbine Blade,**"Jawaharlal Nehru National College of Engineerings Shimoga, Karnataka, India. March-2012
- [11] Sanford Fleeter, Chem Zhou, Elias N. Houstis "**Fatigue Life Prediction of Turbomachine Blading**" Purdue University, enh@cs.purdue.edu Jan-2012
- [12] Cun-liang, L., Hui-ren, Z., Jiang-tao, B. and Du-chun, "**Film Cooling Performances Of Converging Slots-Hole Row On A Gas Turbine Blades**" International Journal of Heat and Mass Transfer. Dec 2011

Solar-Wind Hybrid Energy Generation System

Pritesh P. Shirsath¹, Anant Pise², Ajit Shinde³,

B.E., Department of Electronics, NMIET, Savitribai Phule Pune University, Pune, India - 410507

pssh23@gmail.com¹, anantpise1992@gmail.com², ajitshinde50@gmail.com³

Abstract— As the race for global industrialization begin late in 18th century, the developing technology made humans to depend on energy, so as the energy crisis begins, in this modern era, electricity become a most essential need of human beings, from household to industrial work. So, the purpose of the project is to generate electricity without using non-renewable resources and pollution. Since, renewable standalone energy generation system have disadvantages, which need to be overcome by hybrid systems. Wind and solar energy have being popular ones owing to abundant, ease of availability and convertibility to the electric energy. This work covers realization of hybrid energy system for multiple applications, which runs under a designed circuitry to utilize the solar and wind power. And a designed circuitry for more efficient results, and inverters to convert the electrical energy as per demand.

Keywords—Hybride Energy; Solar System; Wind Energy; Renewable Energy; Clean Energy; Electrical Energy Generation

INTRODUCTION

Hybrid Renewable Energy Systems (HRES) are becoming popular as stand-alone power systems for providing electricity in remote areas due to advances in renewable energy technologies and subsequent rise in prices of petroleum products. A hybrid energy system, or hybrid power, usually consists of two or more renewable energy sources used together to provide increased system efficiency as well as greater balance in energy supply.

Most of us already know how a solar/wind power generating system works, all these generating systems have some or the other drawbacks (considering standalone system), like Solar panels are too costly and the production cost of power by using them is generally higher than the conventional process, it is not available in the night or cloudy days. Similarly Wind turbines can't operate in high or low wind speeds.

Solar hybrid power systems are hybrid power systems that combine solar power from a photovoltaic system with another power generating energy source. This would create more output from the wind turbine during the winter, whereas during the summer, the solar panels would produce their peak output. Hybrid energy systems often yield greater economic and environmental returns than wind, solar, geothermal or trigeneration stand-alone systems by themselves.

PROPOSED SYSTEM

Block/System Diagram

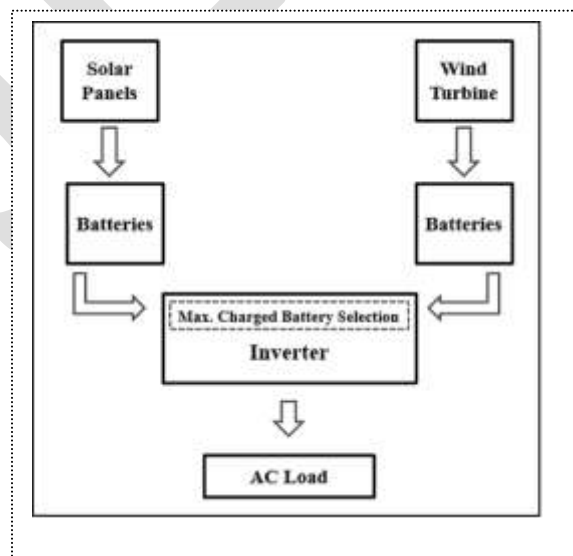


Fig.1. Block diagram of proposed system.

Block/System Description

The proposed system is the hybrid/combination of two individual system as, solar system and wind system. The block wise description is as follows,

Solar Panel:

Solar panel / PV panel are used to convert the renewable power coming from the sun into electrical energy. The principle of working solar panel is with semiconductors. Since, the whole eco-system on planet earth is dependent on sun energy and it's a huge source of never ending energy. Due to ace of availability, easily interpretation, amount of source and popularity it is preferred for project.

Solar panels are photovoltaic which, generates electrical energy using sun light radiations. Depending on the position and intensity of the sun radiation the amount of electrical DC energy will produced. For the proposed project specifications and design, a 12V, 150 watt off grid solar panel is required. The standard size of the panel, available in the market, 48inch x 22inch x 2inches is most suitable however, other sizes can be considered.

Wind Turbine:

The wind is available 24 hours in earth's eco system. Wind turbine having large blades which are joined to rotor of generator leading to produce electrical energy as moves by flow of wind. Wind power is also renewable, never energy source and easily available within atmosphere. Wind turbine power plants are much more popular providing much more efficiency considering the space of implementation.

Wind Turbine is mechanical system/machine which generates electrical energy from renewable wind energy source. Depending on the speed of the wind the amount of electrical AC energy will produced. For the project, a 500 watt, having 3 blades of 1 meter radius, wind turbine generator will be needed. The height of the wind turbine should be 18 meters. For foundation of it a 2 x 2 x 4 m space required.

Batteries:

The electrical energy produced by the system is need to be either utilized completely or stored. Complete utilization of all the energy produced by the system for all the time is not possible. So, it should be store rather than useless wasting it. Electrical batteries is the most relevant, low cost, maximum efficient storage of electrical energy in the form of chemical reaction. Hence, batteries are preferred.

The energy generated from the proposed project is need to be store. So, two batteries is needed. One is attached to wind turbine for which a 120AmpH battery will be required, which will be fair enough full fill the storage capacity for targeted value. The second battery is 80AmpH is preferred for storing solar energy. But, as per application/ storage and demand battery capacity can be variable.

Inverter:

Inverter is a electronic system, converters direct current into alternating current, i.e. DC into AC. The stored electrical energy in the batteries is DC in nature. And it cannot utilized for various kinds of load. So, for delivering AC supply to the load inverter system is required. Inverter is either analog or digital kind. Digital inverter is microcontroller based which increase the buildup cost of the system also, is uses MOSFET technology providing more efficiency. But, considering the financial aspect and resolution the proposed project designs and build the inverter analog in nature.

The input energy is in DC (12V) form stored in the batteries. It will convert it into AC with ~230V, 500W (the maximum value of load to be attach), ~50Hz specification matching with the house hold mains supply. At output, AC loads can be attach.

Maximum Charged Battery Selection:

Maximum charged battery selection, a specially designed circuit used to detect the maximum amount of stored electrical energy in each batteries. It is attached within the inverter circuit. So, the inverter box/block will enclosed this. The circuit is made up of transistor family device like BJT's, MOSFET's along with diodes, resistors and capacitors.

LITERATURE SURVEY AND METHODOLOGY USED

Name of IEEE/Journal Paper	Method/Algorithm Used	Results
Hybrid system of PV solar/wind & fuel cel [3]	Use of wind power, solar cell, fuel cell	Concept is two or more renewable power source connected to grid
Control of Hybrid Solar-Wind system with acid battery [5]	Use of Solar power, Wind power, Acid battery, Micro-Controller	Electric lead acid batteries are device provide electrical energy from Chemical
Design & Implementation of Domestic Solar-wind	Use of Solar Energy, Wind Energy, Solar	Portion of energy requirement for home has been

Hybrid Energy System battery and MPPT. supplied.
 Fig.2. Comparative study of surveyed paper.
 [6]

Referring, Ugur FESLI, Raif BAYIR, Mahmut OZER has proposed project on, "Design & Implementation of Domestic Solar-Wind Hybrid Energy System".

It state that, the demand for more energy is full filled by using renewable source like wind power, solar power. This can be archived by using hybrid energy system connected to grid i.e. wind power energy generation and solar energy generation produces energy without fluctuations.

The system proposed uses a designed circuit consist of transistor and relay. This circuits added in the inverter, while input is taken from batteries. As, any one battery get fully charged, the circuit gets activated, due to fully charge battery triggers the transistor. The activated circuit is make the poles of relay for contact and the charge battery gets selected to provide the DC supply to inverter.

EXISTING SYSTEM

Completely Renewable Hybrid Power Plant (solar, wind, biomass, hydrogen) a hybrid power plant consisting of these four renewable energy sources can be made into operation by proper utilization of these resources in a completely controlled manner. Hybrid Energy Europe - USA. Caffese in Europe introduce hybridizing HVDC transmission with Marine hydro pumped Energy Storage via elpipes.The project of Caffese is 3 marine big lakes producing 1800 GW and transmission with elpipes. A part 1200 GW produce waterfuels-windfuels-solar fuels 210 billion liter year. (IEEE Power and Engineering Society-General Meeting Feb.9.2011, Arpa-E, Doe USA, MSE Italy, European Commission-Energy-Caffese plan and Consortium)

The Hassi R'Mel power station in Algeria, is an example of combining concentrating solar power (CSP) with a gas turbine, where a 25-megawatt (MW) CSP parabolic trough array supplements a much larger 130 MW combined cycle gas turbine plant. Another such integrated solar combined cycle power station is the Yazd power station in Iran (*also see ISCC*).

ADVANTAGES

The advantages covered by the propose system are listed as,

- Overcoming disadvantages of standalone renewable electrical energy generation system.
- Producing much more efficiency as two or more renewable energy generation system working together in the terms of electrical energy generation.
- Since, the system doesn't have microcontroller or microprocessor the complexity of system testing and understanding became easy in terms of difficulties.
- System maintains is remarkably reduced and becomes easy.
- Renewable energy sources like, sun, wind,. Are utilized so, no waste production.
- Producing clean, friendly to environment, renewable energy.
- Once the system is designed and developed or manufactured, the installation of system is easy.
- Within certain time period the installation cost gets covered.
- If the system gets damaged in case, no need of changing entire system or subsystem. Just, changing a damage component will work out.

DISADVANTAGES

There's no system without having a disadvantage. So as, the system have disadvantages as follow:

- The first time installation cost is huge in terms of finance.
- The circuit designing complexity is more as there in no micro-computer for controlling action.

APPLICAATION

Some of the applications for the purpose system are listed follow,

- The system is used for domestic purpose.
- Street lighting, Traffic signals.
- Various monitoring systems.
- Powering up for communication system.
- Pump irrigation Systems.
- Small Boats like yatch.
- As per requirement of electrical energy the system can be either designed or updated for higher energy requirement.
- When ac mains supply is not available, the proposed system can be used as emergency system with only few changes.
- So, it can be used for almost every electronic, mechanic, viz. system needing/ require electric energy to work on.

FUTURE SCOPE

As the awareness of non-renewable sources and pollution causes by them, the clean energy production with renewable sources is widely preferred and day by day implementation of such sources going on, so, research and resources are also increasing for such plants and projects.

As the first time installation cost is higher due to design and manufacturing perspective. The system can be monitories using graphical user interference on computer. So, the whole information will be available to user and/or stored regarding further applications and development.

ACKNOWLEDGMENT

The proposed project have been sponsored by “Prof. N. J. Jadhav,” for the wind turbine. The project is constructed under the guidance of “Prof. Priya Choughule”. And, being most motivator and helpful in all aspects regarding to the project “Prof. Nabin Das.” Thank you for the efforts and engorgement taken to make it successful.

REFERENCES:

- [1] T.S. Balaji Damodhar and A. Sethil Kumar, “Design of high step up modified for hybrid solar/wind energy system,” Middle-East Journal of Scientific Research 23 (6) pp. 1041-1046, ISSN 1990-9233, 2015.
- [2] Wala Elshafee Malik Elamin, “Hybrid wind solar electric power system,” report, University of Khartoum, Index-084085, July 2013.
- [3] Sandeep Kumar and Vijay Garg, “Hybrid system of PV solar/wind & fuel cell,” IJAREEIE, Vol. 2, Issue 8, ISSN 2320-3765, August 2013.
- [4] Rakeshkumar B. Shah, “Wind solar hybrid energy conversion system- literature review,” International Journal of Scientific Research, Vol. 4, Issue 6, ISSN 2277-8179, June 2015.
- [5] Ugur FESLI, Raif BAYIR, Mahmut OZER, “Design & Implementation of Domestic Solar-Wind Hybrid Energy System”, Zonguldak Karaelmas University, Department of Electrical and Electronics Engineering, Zonguldak, Turkey.
- [6] Nazih Moubayed, Ali El-Ali, Rachid Outbib, “Control of an Hybrid Solar-Wind System with Acid Battery for Storage”, Wseas Transactions on Power System, Labortory of Science in Information and System (LSI), Axi-Marseille University, France

Night Time Vehicle Detection Using Tail Lights: A Survey

Swathy S Pillai, Radhakrishnan B

PG Scholar, Dept. of Computer Science and Engineering, Baselios Mathews II College of Engineering
Sasthamcotta, Kerala, India Ph: 9895759462
swathysp@gmail.com

Asst. Professor, Dept. of Computer Science and Engineering, Baselios Mathews II College of Engineering
Sasthamcotta, Kerala, India
radhak77@rediffmail.com

Abstract- The main challenge during night-time driving is the visibility of the road ahead. The major challenge rests in controlling accidents during night as the night conditions differ from the day in environment conditions, vehicle lighting etc. The reduced cost of cameras and optical devices helped in installing front-mounted intelligent systems for identifying forward collision avoidance and mitigation. During night, vehicles in front are generally seen by their tail lights. The turn signals are mostly important because they signal lane change and potential collision. This survey presents a car recognition system by identifying and segmenting tail lights in the night-time road environment.

Keywords

Segmentation, Edge detection, Taillight, Blob detection, Connected component analysis, Symmetry score, Nakagami-m distribution .

INTRODUCTION

This paper gives a literature review on various techniques used in identifying vehicles during night. The usage of Computer Vision ideas has helped lot with road safety and security. The appearance of vehicles during night time is different when compared to its daylight conditions such as environment lighting, reflection of light on the body of vehicles, color of vehicles etc. Thus a different image processing approach is essential for night time road environment. This method seeks on segmenting the tail lights of vehicles and classifying them. When vehicles are viewed from behind at night, they are primarily visible by the red color of tail lights. All car models have their own peculiar physical and structural features which make them distinctive from each other and the appearance of brake lights is one of those features. For the technique to be most efficient, ideally a tweaked camera is used which filters only the red lights, thereby eliminating image bleeding.



(a)

Fig 1 Tail light of vehicle

(b)

Brake light of Vehicle

TECHNIQUES

Segmentation

Segmentation is the process by which an image is fenced off into smaller parts so that processing of an entire image can be more meaningful and easier i.e. process of partitioning a digital image into set of pixels. The process of segmentation makes an image meaningful and easy for analysis and it assigns label for every pixel so that same characteristics are shared by pixels with same label.

BhavinkumarM.Rohit et.al. [1] used the segmentation approach and introduced low light video frames which have low exposure value images. The idea behind using the low exposure image frames is that factors such as street lights, unwanted reflections from vehicles

body, sign boards reflections can be removed and only the bright red color and head lights of oncoming vehicles are visible in the image frame. Segmenting the red color from other noises is the major issue in identifying the tail lights.

Binamrata Baral et.al. [2] explains Special Theory Based Segmentation techniques such as Genetic Algorithm, Neural Network, Clustering and Wavelets based segmentation techniques. Genetic algorithm depends upon the process of natural selection and uses techniques such as selection, cross over and mutation. In neural based, the principle of ANN is used. For clustering Fuzzy C-means and K-means clustering is implemented and in wavelet based wavelet transforms of image is used for feature extraction.

JunbinGuo et.al. [3] explained OTSU algorithm for tail light segmentation for identification of vehicles at night. In this after analyzing the histogram of image the lower boundary for thresholding is determined by counting the average number of higher gray scales. Next, between the lower boundary and the highest gray scale of the image, the optimal threshold is calculated by Otsu method and the image is divided into pixels based on this threshold. The resultant object I_{result} can be computed by,

$$I_{result}(x, y) = \begin{cases} 1 & \varphi_{\theta RC}(x, y) > T \\ 0 & \varphi_{\theta RC}(x, y) < T \end{cases} \quad (1)$$

where $\varphi_{\theta RC}$ is the image and T the threshold value.

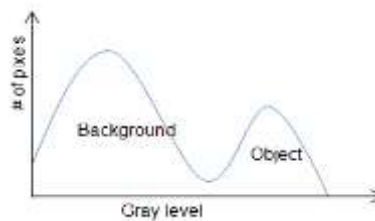


Fig 2 Histogram showing apparent classes using thresholds T_1 and T_2

Edge detection

The edges of an image indicates higher frequency region within that image. Edge detection refers to the process of identifying and locating abrupt changes in pixel intensity which characterize boundaries of an image. Detection of edges is applicable in image segmentation, data compression image reconstruction and so on. There are two types of edge detection; first order and second order edge detection. The techniques of edge detection are Sobel, Prewitt and Canny edge detection.

P.Srinivaset.al.[4] implemented Canny edge detection in order to detect the vehicle tail light. The algorithm smoothens the image and finds the gradient to highlight regions with high spatial derivatives. The non-maxima regions are then suppressed and two threshold values are set. The value is set to zero if the magnitude is below the first threshold, it is considered as edge if the magnitude is above second threshold and a path is obtained if magnitude lies between the two.

M.Kalpana et.al.[5] explained edge detection operators such as differential operator like Robert, Prewitt and Sobel operators, Log operator and Canny operator. Among these operators the most commonly used is the Canny operator. Even after edge detection various noises exists in the detected image and then wavelet transformation has been used to remove that.

Manoj K Vairalkaret.al.[6] proposed Sobel edge detection for image detection. The Sobel detector is selected after verifying the edge orientation, noise environment and edge structure. Depending upon the output of these variables the techniques implemented for edge detection are gradient and laplacian detection. The Sobel operator is associated with a pair of 3x3 convolution kernel, one obtained by rotating the other one at 90° . The gradient magnitude G is given by,

$$|G| = \sqrt{(G_x^2 + G_y^2)} \quad (2)$$

where G_x and G_y are magnitude in x and y direction respectively.

Filtering and Enhancement

Filtering is the process of modifying or enhancing an image by removing the noises from it and is a neighborhood operation in which the output image pixel value is obtained by applying some algorithms to the neighborhood pixel values of the input pixel. Image enhancement is the process by which the specific features of an image is brought out by histogram equalization, median filtering *etc.* Enhancement makes it easier to identify the key features of an image.

Bharti Sharma et.al. [7] proposed an algorithm for vehicle detection in which the filtering of the output image is done after applying the threshold value to the vehicle . Shape index is computed to extract the target object as it extracts the bright target object more precisely. Shape Index (SI) is calculated as,

$$SI = \frac{Perimeter}{\sqrt[4]{Area}} \quad (3)$$

By these operations vehicle is detected.

PushpalataPatilet.al. [8]explained a method for vehicle detection by image processing in which image enhancement is done with the help of a computer. The main objective is to create an image that is more suitable for specific applications. The technique implemented enhances the image by image's joints and lineaments. To emphasize brightness differences associated with linear features contrast enhancement is used.

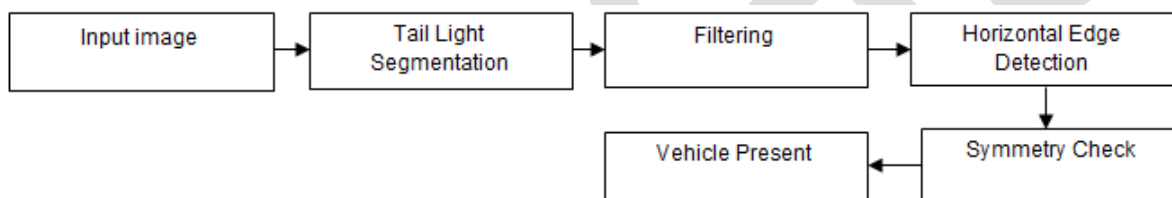


Fig 3 Vehicle Detection Steps

LITERATURE SURVEY

BhavinkumarM.Rohit et.al [1] describes a system for detecting vehicles based on their rear lights. They used the segmentation approach and introduced low light video frames which have low exposure value images. The idea behind using the low exposure image frames is that factors such as street lights, unwanted reflections from vehicles body, sign boards reflections can be removed and only the bright red color and head lights of oncoming vehicles are visible in the image frame. Segmenting the red color from other noises is the major issue in identifying the tail lights. The red layer is firstly extracted from the rear light and is then converted to the gray image. The gray frame is then subtracted from the red frame and all the unwanted noises are removed by median filter. A threshold value is set to convert the obtained image to its corresponding binary image. Then the blob analysis techniques are used to calculate the area and the corresponding bounding boxes. Blob detection methods are aimed at detecting regions in an image that has similar as well as difference in their properties. Depending upon the symmetry, tail lights for same vehicle is identified and the nuisance are rejected.

Chen et al.[11] uses segmentation for identifying the bright object and verifies the segmented regions by spatial clustering based on the symmetric properties such as shape, texture and relative position. The Nakagami-m distribution approach is used to detect turn signals by scatter modeling of tail lights. The turn signals are detected using contrast enhancement in which intensity for the image is obtained. In order to avoid the noise generated from the non-tail lights a step function is applied and preprocessed. Thus obtained tail light is modeled using the Nakagami-m distribution. After this the color space regulation on the CIE xy chromaticity has been introduced to verify detected turn signals. For recognizing the direction of the detected turn signal as the reflectance strength of the area near turn signals is larger than that of other areas, vehicle reflectance is first decomposed. The bounding area is analyzed and in order to overcome the variation of an event pattern, a training algorithm is adopted like AdaBoost. Using this algorithm the classifiers of left and right turn signal directions are trained.

Noppakun Boonsim et.al. [12] present a new algorithm to detect a vehicle ahead by using taillight pair. Tail light detection is implemented by two steps tail light candidate extraction and tail light verification. The tail light candidate extraction phase includes extraction of color pixels from the input image and candidate extraction process segments red pixel regions containing white. By applying symmetry score of size, shape and position candidates the tail light verification is done. The symmetry of position is considered by estimating y-direction distance of each pair by,

$$DS (P_k) = (1 - \frac{|H_i + H_j|}{H_i + H_j}) \times 100 \quad (4)$$

Where DS is y-distance symmetry score of pair P_k . H_i and H_j are the y axis-distance between border and center of C_i and C_j , respectively. Next, size symmetry is then checked to justify area characteristic equality using.

$$AS (P_k) = (1 - \frac{|A_i - A_j|}{A_i + A_j}) \times 100 \quad (5)$$

Where AS is defined as size (area) symmetry score of pair P_k . A_i and A_j are the area of candidate C_i and C_j consecutively. Then the symmetry of shape is checked by analyzing aspect ratio of candidate width and height.

$$ARS (P_k) = (1 - \frac{|ARS_i - ARS_j|}{ARS_i + ARS_j}) \times 100 \quad (6)$$

Where ARS is the aspect ratio symmetry score of pair P_k . ARS_i and ARS_j represent the aspect ratio of candidate C_i and C_j respectively. position symmetry score is experimentally defined as the most significant value following by size and shape symmetry Score

$$\text{Symmetry Score (SS)}_k = 0.8 * DS_k + 0.1 * AS_k + 0.1 * ARS_k \quad (7)$$

Finally, the maximum symmetry score will be considered to confirm the position of TLs. The symmetry score of TL should be more than 80. If the score is less than the threshold value, test images will be discarded. This is the equation to verify TL positions.

$$\text{TL pair} = \text{Max (Symmetry Score (} P_k)) > 80 \quad (8)$$

Yen Lin Chen et.al.[13] explained an effective system for detecting and tracking moving vehicles during night has been explained. Using image segmentation and pattern analysis techniques the vehicles tail light are detected and identified. The main process done in this paper is the classification of car and motorbike tail lights.

A moving car is modeled as a rectangular patch, a tracked component group TG_k^t has been implemented and given by,

$$\tau_{r1} \leq W \frac{(TG_k^t)}{H(TG_k^t)} \leq \tau_{r2} \quad (9)$$

where τ_{r1} and τ_{r2} are threshold values 2.0, 8.0 and W, H represents the width and height of the bright objects. TG_k^t should be symmetrical and well aligned such that

$$\tau_{\alpha1} \left(\frac{W(TG_k^t)}{H(TG_k^t)} \right) \leq |TG_k^t| \leq \tau_{\alpha2} \left(\frac{W(TG_k^t)}{H(TG_k^t)} \right) \quad (10)$$

where $\tau_{\alpha1}, \tau_{\alpha2}$ are threshold values 0.4 and 2.0. The width of TG_k^t of a potential car should be in a reasonable ratio with respect to the lane width,

$$\tau_{\omega1} \cdot LW(TG_k^t) \leq W(TG_k^t) \leq \tau_{\omega2} \cdot LW(TG_k^t) \quad (11)$$

where $LW(TG_k^t)$ is the approximate lane width associated with TG_k^t . The threshold $\tau_{\omega1}$ and $\tau_{\omega2}$ are 0.5 and 0.9, respectively.

To identify motorbike a single tracked component TP_i^t can be identified as,

$$\tau_{m1} \leq \frac{W(TP_i^t)}{H(TP_i^t)} \leq \tau_{m2} \quad (12)$$

where the threshold values τ_{m1} and τ_{m2} are 0.6 and 1.2.

Ronan O' Malley et.al.[14] explains segmenting red lamps and pairing to combine it with target vehicle. RGB color space is converted to HSV and cross relation method is used to pair the red light.

Table 1 Color thresholds

	Hue	Saturation	Value
Red	340° - 30°	0 - 30	80 - 100
White	All	0 - 20	99-100

Along the line adjoining the center region of light the cross relation is calculated. The cross relation matrix γ between two lamp image segments is calculated by,

$$\gamma = \sum_{x,y} \frac{(T(x,y) - \bar{T})(I(x,y) - \bar{I})}{\sigma_T \sigma_I} \quad (13)$$

CHALLENGES

Although many techniques have been implemented for vehicle detection during night, accidents caused by heavy vehicles can't be controlled yet. The methods implemented for detection are not used for heavy vehicles as their taillight orientation is different from that of cars and motorbikes. It is difficult to identify the vehicle if the lights are under repairing condition. The techniques available for detection uses computer vision techniques and so it requires high cost for its implementation.

CONCLUSION

This survey paper reviews different techniques used for the detection and identification of taillights of vehicles during night. Various vehicle detection methods are explained using the image segmentation techniques. In this paper many image processing techniques such as Segmentation, Edge detection, Filtering and image enhancement are discussed. By combining these methods the tail light are detected and the accidents during night are controlled up to some extent. More studies and researches are required in this field for further detection of all vehicles.

REFERENCES:

- [1] Bhavinkumar M. Rohit, Mitul M. Patel, "Nighttime vehicle Tail light detection in low light video frame using Matlab", International Journal for Research in Applied Science & Engineering Technology, Volume 3 Issue V, May 2015.
- [2] BinamrataBaral, SandeepGonnade, ToranVerma, "Image segmentation and Various Segmentation Techniques- A Review", International Journal of Soft Computing and Engineering, Volume-4, Issue-1, March 2014.
- [3] JunbinGuo, JianqiangWang, XiaosongGuo, Chuanqiang Yu and Xiaoyan Sun, "Preceding Vehicle Detection and Tracking Adaptive to Illumination Variation in Night Traffic Scenes Based on Relevance Analysis" Sensors 2014, 19 August 2014.

- [4] P.Srinivas, Y.L. Malathilatha, Dr. M.V.N.K Prasad, “Image Processing Edge Detection Technique used for Traffic Control Problem”, International Journal of Computer Science and Information Technologies, Vol. 4 (1), 2013, 17 – 20.
- [5] M. Kalpana, G. Kishorebabu, K.Sujatha, “Extraction of Edge Detection Using Digital Image Processing Techniques”, International Journal Of Computational Engineering Research, Vol. 2 Issue.5.
- [6] Mr. Manoj K. Vairalkar, Prof.S.U.Nimbhorkar, “Edge Detection of Images Using Sobel Operator”, International Journal of Emerging Technology and Advanced Engineering, volume 2, Issue 1, January 2012.
- [7] Bharati Sharma, Vinod Kumar Katiyar, Arvind Kumar Gupta and Akansha Singh, “the Automated Vehicle Detection of Highway Traffic Images by Differential Morphological Profile”, Journal of Transportational Technologies, Scientific Research, April 2014.
- [8] PushpalataPatil and Prof. SuvaranaNandyal, “Vehicle Detection and Traffic Assessment Using Images”, Advance in Electronic and Electric Engineering, Volume 3, Number 8 (2013).
- [9] Basavaprasad B, Ravi M, “A Comparative Study On Classification Of Image Segmentation Methods With A Focus On graph Based Techniques”, International Journal of Research in Engineering and Technology, Volume 3, May 2014.
- [10] XiaohuaShu, Liming Liu, Xiaowei Long, Pei Shu, “Vehicle Monitoring Based On Taillight Detection”, International Conference on Intelligent Systems Research and Mechatronics Engineering.
- [11] Duan-Yu Chen, Member, IEEE, Yang-JiePeng, Li-Chih Chen, and Jun-Wei Hsieh, Member, IEEE, “Nighttime Turn Signal Detection by Scatter Modeling and Reflectance-Based Direction Recognition”, IEEE SENSORS JOURNAL, VOL. 14, NO. 7, JULY 2014.
- [12] Noppakun Boonsim, SimantPrakoonwit, “An Algorithm for Accurate Taillight Detection at Night”, International Journal of Computer Applications, Volume 100– No.12, August 2014.
- [13] Yen-Lin Chen, Member, IEEE, Bing-Fei Wu, Senior Member, IEEE, Hao-Yu Huang, and Chung-Jui Fan, “A Real-Time Vision System for Nighttime Vehicle Detection and Traffic Surveillance”, IEEE TRANSACTIONS ON INDUSTRIAL ELECTRONICS, VOL. 58, NO. 5, MAY 2011.
- [14] Gonzalez, R. C., Woods, R. E., And Eddins, Digital image processing using MATLAB, 2nd Ed. Gatesmark Publishing, Knoxville, TN,2009.
- [15] Mahdi Rezaei, ReinhardKlette, Mutsuhiro Terauchi, “Robust Vehicle Detection and Distance Estimation Under Challenging Lighting Conditions”, ARTICLE in IEEE TRANSACTIONS ON INTELLIGENT TRANSPORTATION SYSTEMS · MARCH 2015.
- [16] <http://www.wikipedia.org/>

An Overview Of Mammogram Noise And Denoising Techniques

Athira P¹, Fasma K.K¹, Anjaly Krishnan²

¹P.G Scholar, ²Assistant Professor, Thejus Engineering College

¹E-mail: athiraponnoth@gmail.com

Abstract— Mammogram is a mammography exam used to aid in the diagnosis of breast diseases in women. This paper mainly focuses on the biomedical image processing area. Noise is an inevitable parameter that must be considered in the medical images. The main problem of mammogram is that like other medical data it is also affected with noise during the acquisition of the mammogram images. So it is a challengeable task for researchers to denoise the mammogram images while preserving the important features of the image. The main noises affecting the mammogram images are salt and pepper, gaussian, speckle and poisson noise. In previous days, noises in the mammogram images are denoised by the linear methods like mean and weiner filters. But the main problem of linear filtering is that it produces blurring effect and incomplete noise filtration. To overcome this limitation nonlinear filtering techniques like wavelet based denoising were proposed. In this paper, light is thrown on some important type of mammogram noises and its denoising techniques.

Keywords— Mammogram, Denoising, Salt and pepper, Gaussian noise, Speckle noise, Poisson Noise, Mean, Median, Wavelets, Wiener filter, Adaptive transforms.

INTRODUCTION

In the recent times among the various types of cancer breast cancer is one of the leading global health concerns. Mammogram is an easy and affordable method for diagnosing the microcalcification and clinically hidden lump tissues in the breast at the early stage of cancer. Breast cancer can be defined as a malignant tumor that starts in the cells of the breast. A malignant tumor is a group of cancer cells that can grow into (invade) surrounding tissues or spread (metastasize) to distant areas of the body. The female breast is made up mainly of lobules (milk-producing glands), ducts (tiny tubes that carry the milk from the lobules to the nipple), and stroma (fatty tissue and connective tissue surrounding the ducts and lobules, blood vessels, and lymphatic vessels). Most breast cancers begin in the cells that line the ducts (ductal cancers) [3]. Sometimes the malignant tumor may begin in the cells of lobules, while a small number start in other tissues. Lobular cancers are begins in the milk carrying ducts and spreads beyond it. It is the second most common type of breast cancer. Detecting the breast cancer in the earlier stages is the most effective way to be surviving the breast cancer. Mammography is used for the early detection of masses in the breast and thereby reducing the death rate. Mammogram unit uses low energy X-rays to see inside the breast. There are different types of mammography like digital mammography, computer aided detection and breast tomosynthesis. Even though there are so many methods to diagnosing the breast cancer, it remains difficult to interpret some cases. Since the mammogram images are noisy and low contrast the radiologists may confused to diagnoses the cancer. In the present, the miss diagnosis rates of the radiologists about 10-30%.

The main aim of mammogram denoising is to preserve the important features of the image while filtering out the noise. In previous days, noises in the mammogram images are denoised by the linear methods like mean and weiner filters. But the main problem of linear filtering is that it produces blurring effect and incomplete noise filtration. To overcome this limitation nonlinear filtering techniques like wavelet based denoising were proposed. This paper presents the noise and denoising techniques on mammogram images.

The paper is structured as follows: the noise model section gives a brief description about the noise and also describes about different types of mammogram noises. It mainly consists of salt and pepper, speckle, poisson and gaussian noise. Next section presents an overview of denosing techniques. Both linear and nonlinear filters are described in that section.

NOISE MODEL

Noise is a random fluctuation of image intensity and appears as grains in the image. The ambient conditions affect the imaging sensors in the camera. The noise may arise in the image as effects of basic physics-like photon nature of light or thermal energy of heat inside the image sensors [4]. When a noise is affected in an image the pixels in the image show different intensity values instead of true pixel values. Noise can be added to an image during accusation and transmission of image. The noisy image can be modeled as

$$g(x,y)=f(x,y)+n(x,y) \quad (1)$$

Where $f(x, y)$ is the original image pixel, $n(x,y)$ is the noise and $g(x, y)$ is the resulting noisy pixel.[1]

TYPES OF NOISES

a) Salt and Pepper Noise: Salt and pepper noise is also called impulse valued noise. Other terms are spike noise, random noise or independent noise. Due to this noise black and white dots appear in the image. The main reason behind the appearance of salt and pepper noise are sharp and sudden changes of image signal and dust particles in the image acquisition source or over heated faulty components[4]. Due to this noise image is corrupted to a small extent. When image is affected by this noise image pixel values are replaced by noisy pixel values either maximum or minimum pixel value i.e., 255 'or' 0 respectively, if number of bits are 8 for transmission. Salt and pepper noise is present in the mammogram images because of the dust particle in the mammogram unit .This noise introduce dark and white dots in the images as shown in fig 2.

254	207	210		254	207	210
97	212	32	→	97	0	32
62	106	20		62	106	20

Fig 1: The central pixel value is corrupted by salt and Pepper noise [6]

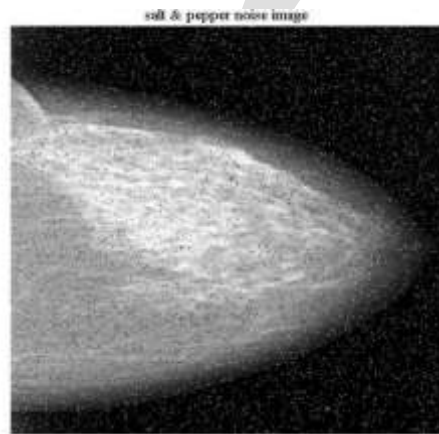


Fig 2: Salt and pepper image

b) Speckle Noise: Speckle noise can be considered as a multiplicative noise. This noise can exist in an image similar to Gaussian noise [2]. This noise can be modeled as shown below

$$J = I + n * I \quad (3)$$

Where, J is the speckle noise image, I is the input image and n is the noise image with mean 0 and variance V [4]. This noise is due to the dust particle in the image accusation source .Fig 3 shows the image with speckle noise.

c) Poisson Noise: Poisson noise is also called photon noise. This noise is due to the statistical behavior of electromagnetic waves such as x-rays, visible lights and gamma rays. In a mammogram image poisson noise is due to the change in the number of photons in the mammogram unit.The root mean square value of this noise is proportional to the square root intensity of the image.Due to this noise different pixel of the image suffered by independent noise value. As the name indicates this type of noise has a Poisson distribution and the probability distribution function given by [9]

$$f(k, \lambda) = \frac{\lambda^k e^{-\lambda}}{k!} \quad (4)$$

k –number of occurrences of an event

λ –Positive real number



Fig 3: Speckle noise image

d) Gaussian noise: This noise model follow Gaussian distribution. That means each pixel in the noisy image is the sum of the random Gaussian distributed noise value and the true pixel value. The noise is mainly due to electronic circuit noise and sensor noise[10]. Figure 4 shows the image with Gaussian noise.

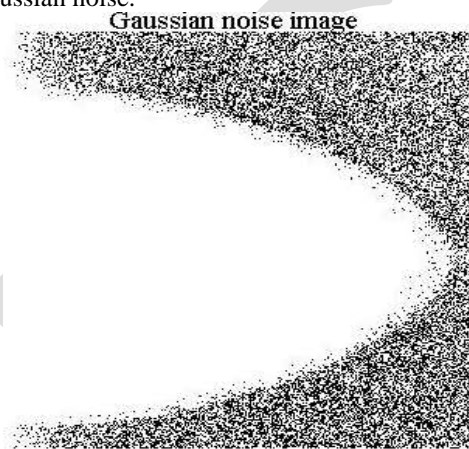


Fig 4:Gaussian noise image

This type of noise has a Gaussian distribution, which has a bell shaped probability distribution function given by

$$P(x)=\frac{1}{\sigma\sqrt{2\pi}} e^{-\frac{(x-\mu)^2}{2\sigma^2}} \quad (2)$$

Where $P(x)$ is the Gaussian distribution noise in image, μ is the mean and σ is the standard deviation respectively [4]. The Graphical representation of the probability distribution function is shown in Figure 5

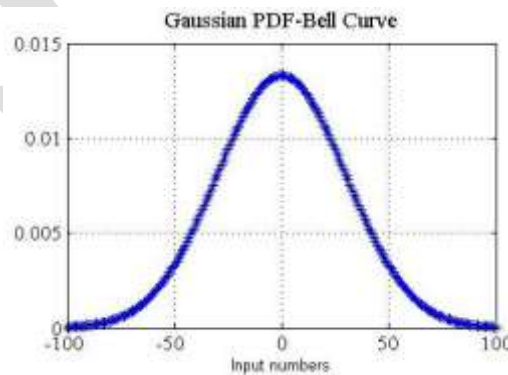


Fig 5: PDF of Gaussian noise

DENOISING METHODS

Image denoising plays an important role in image processing for the analysis of images. Image denoising can be defined as the recovery of the original image which is impure by the noise. Among the large number of denoising algorithm the best one should remove the noise completely from the image, while preserving the important features. The image $s(x,y)$ is the original image. It is blurred by a linear operation and noise $n(x,y)$ is added to the original image form the degraded image $w(x,y)$. This noisy image is given to denoising technique which give the denoised image $z(x,y)$.

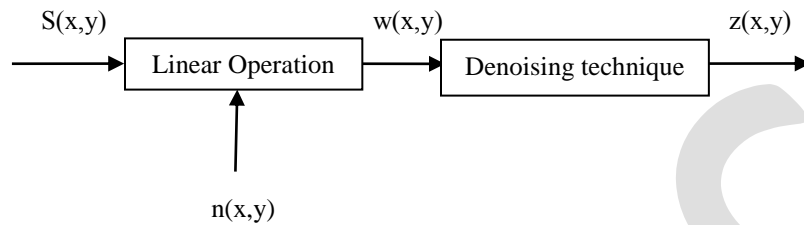


Fig 6: Denoising concept[2]

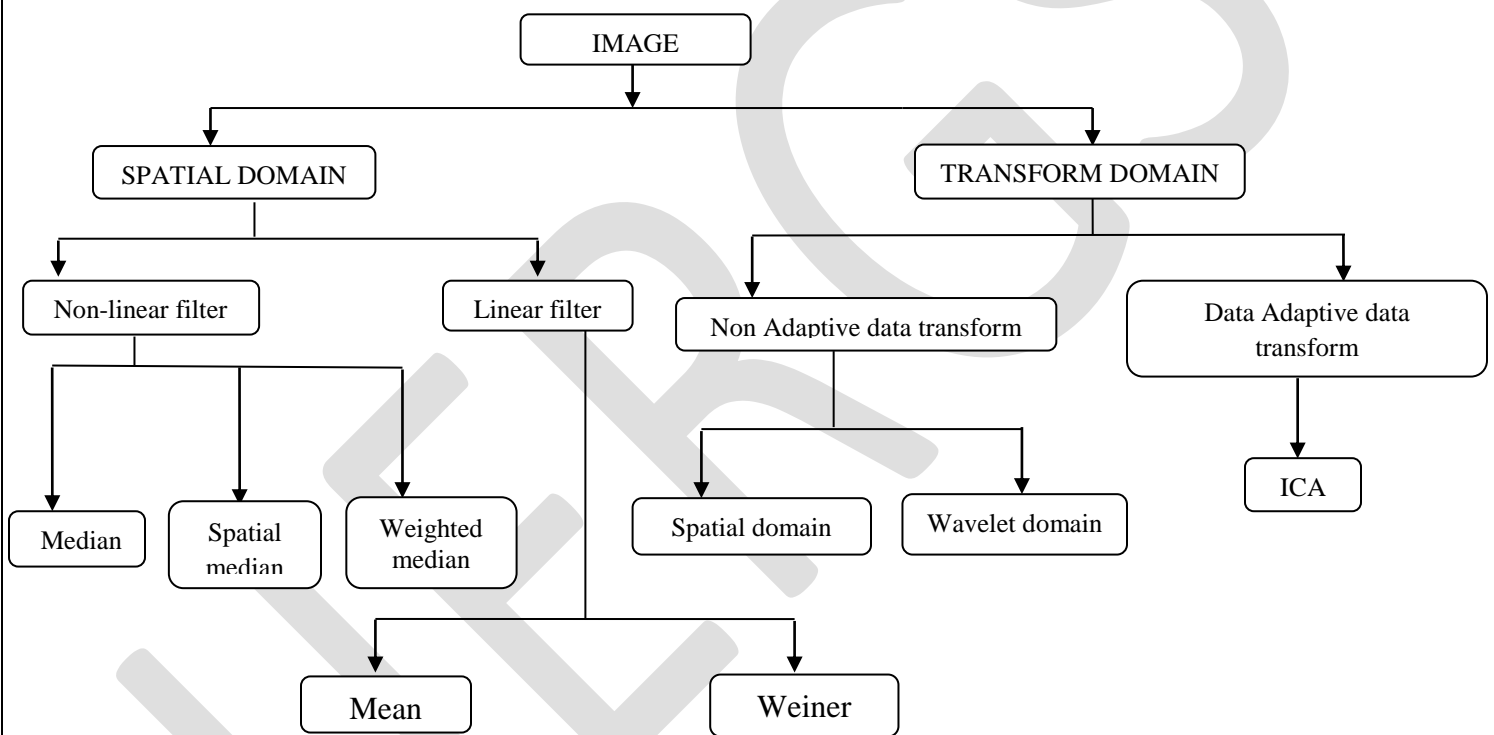


Fig 7: Classification of Image Denoising Techniques [7]

The Linear operation means the addition or multiplication of the noise $n(x,y)$ to the signal $s(x,y)$. Fig 7 shows the various types of denoising techniques that are used in the mammogram images. Spatial filtering methods and transform domain filtering methods are the two basic approaches in image denoising.

A) Spatial Filtering

Spatial Filtering is a traditional way to remove noise from image data .Non-linear and linear filters are the two types of spatial filters.

1) Linear Filters

Linear filters are based on the constraint of linearity which produces time varying input signals to produce output signals. Linear filter improve the images in many ways: sharpening the edges of objects, reducing random noise, correcting for unequal illumination, deconvolution to correct for blur and motion, etc. But the main problem of linear filter is that it may produce blurring effect.

1.1 Mean: Mean filter is a simple averaging linear filter. In mean filter the center value in the window is replaced by a sliding window filter. Each pixel value in the image is replaced with the average value of its neighbors, including itself [6]. Mean filter is mainly used when an image is corrupted with salt and pepper noise. Mean filter changes the noise affected white and dark values closer to the pixel values of the surrounding ones. If the noise in certain region is needed to be removed mean filter is used. That is when only a part of the image needs to be processed mean filter is used. In fig 5 8, 4,7,2,1,9,5,3 and 6 are the pixel values. The mean of the pixel value is obtained by taking the average of these values. Here the mean is 5.so the central value is replaced by 5.

Unfiltered Values

8	4	7
2	1	9
5	3	6

*	*	*
*	5	*
*	*	*

$$8+4+7+2+1+9+5+3+6=45; 45/9=5$$

Fig 8: In this Center value which is previously 1 in the unfiltered value is replaced by the mean of all nine values that is 5,[6]

1.2 Wiener filter: Wiener filter is used to filter out noise that has corrupted a signal. It is based on statistical approach. For denoising wiener filter requires the spectral information of the noise and the original signal. The filters are designed according to the desired frequency response. This filter is mainly used to remove the additive noise. The main aim of wiener filter is to reduce the mean square error [6]. The two parts of wiener filter are inverse filtering part and noise smoothing part. The deconvolution and removing the noise with a compression operation are performed in the inverse filtering part

2. Non Linear Filters

Non linear filters are mainly used for removing the non additive noise. The main drawback of linear filter is that it produces blurring effect and incomplete noise filtration during the denoising of an image. To overcome this disadvantage nonlinear filters are used.

2.1 Median filter: The median filters have a moving window principle similar to the mean filter. It is a simple method which is based on the order statistics. It is used for smoothing the images. The amount of intensity variation between one pixel and the other pixel is reduced by using median filter. In this filtering method it replaces the original pixel value by the median value of some neighboring pixel. For calculating the median value first sorting all pixel values into ascending order and then replace the pixel being calculated with the middle pixel value. If the number of pixel values is even, then the average of the two middle pixel values is used to replace [6]. In the case of signal dependent noise the performance of median filtering is not satisfactory

10	5	20
14	80	11
8	3	22

3,5,8,10,11,14,20,22,80



Median (central value 80 is replaced by 11)

Fig 9: Method of Median Filter [6]

B) Transform domain

1. Non-adaptive transforms

1.1 Spatial-Frequency Filtering: Spatial frequency filtering uses low pass filters with fast fourier transform. In this method the filter is designed based on the desired frequency response. The method is time consuming and may produce artificial frequencies in the processed image.

1.1.1 Wavelet transform: Wavelet transform is one of the powerful tool for signal and image processing. This arithmetic function will split the data into different frequency component[12].Since it is a multiresolution transform it give both time and frequency information. It is another form of representing an image and it does not change information content in the image. The non redundant

image representation is provided by discrete wavelet transform (DWT) which also provide better spatial and spectral information. Because of this reason DWT is attracted more in image denoising. In DWT the signal is passed through two complementary filters which give approximation and detail component of the signal. This step is known as the decomposition or analysis. The inverse of this step is known as the reconstruction or synthesis. The analysis and synthesis step is done by the mathematical operation discrete wavelet transform and inverse discrete wavelet transform respectively. The original image is transformed into four pieces when DWT is applied. The four pieces are normally labeled as A1, H1, V1 and D1 as the schematic depicted in Fig.6. The A1 is called the approximation, can be further decomposed into four sub-bands. The remaining bands are called detailed components. To obtain the next level of decomposition, sub-band A1 is further decomposed [8]. The main advantage of DWT is that it is a multiresolution transform. In image denoising first image is divided into different sub bands and then thresholding algorithms are applied to the wavelet coefficients. Finally inverse wavelet transform is applied which give denoised image. Wavelet transform also have some disadvantages. Lack of shift invariance and lack of directional selectivity are the two main drawback of DWT.

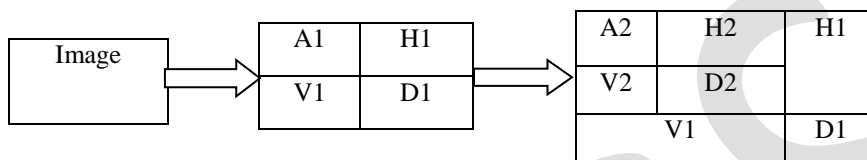


Fig.10:DWT based Wavelet decomposition to various levels[8]

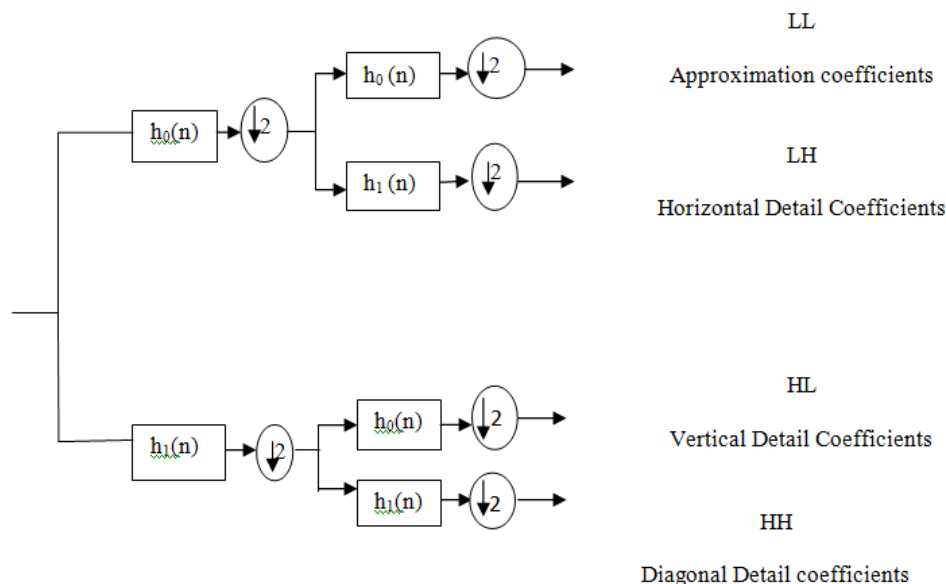


Fig 11: 2D DWT with single stage decomposition [8]

2.2 Adaptive transforms

According to the characteristics of the image inside the filter the behavior of the adaptive filter changes. Independent Component Analysis (ICA) is one of the adaptive transform which gained wide spread attention. The ICA method is used to represent a set of multidimensional data vectors in a basis in which the component are independent as possible[11] For denoising of non gaussian data ICA is used. The advantage of using ICA is that it's assumption of signal to be Non-Gaussian which helps to denoise images with Non-Gaussian as well as Gaussian distribution. One of the disadvantage of ICA when compared to wavelet transform is that it's computational cost [1].

CONCLUSION

Denoising of mammogram images is indeed a challenging task for the domain experts. The accuracy of tumor prediction mainly relies upon the efficiency of the denoising techniques. In this paper different types of mammogram noises and its denoising techniques have been discussed. It is evident from this study that gaussian, speckle, salt and pepper and poisson noises play a major role in distorting the mammogram image. As the linear filters produce blurring effect nonlinear filters are used. As per the research wavelet based denoising outperformed the linear denoising techniques.

REFERENCES:

- [1] Toran Lal Sahu Mrs. Deepty Dubey” A Survey on Image Noises and Denoise Techniques” International Journal of Advanced Research in Computer Engineering & Technology (IJARCET) Volume 1, Issue 9, November 2012
- [2] Chandrika Saxena, Prof. Deepak Kourav” Noises and Image Denoising Techniques: A Brief Survey” Versha Rani et al, Journal of Global Research in Computer Science, 4 (4), April 2013, 166-171
- [3] Samir Kumar Bandyopadhyay” Breast Cancer Prevention and Early Detection”
- [4] Mr. Rohit Verma Dr. Jahid Ali” A Comparative Study of Various Types of Image Noise and Efficient Noise Removal Techniques” International Journal of Advanced Research in Computer Science and Software Engineering 3(10), October - 2013, pp. 617-622
- [5] Ajay kumar boyat and brijendra kumar joshi” A review paper: noise models in digital image processing”signal & image processing : an international journal (SIPIJ) vol.6, no.2, april 2015
- [6] Priyanka kamboj and versha rani “A Brief study of various noise model and filtering techniques “versha rani et al, journal of global research in computer science, 4 (4), april 2013, 166-171
- [7] Barjinder Kaur, Manshi Shukla” Image Denoising and its Methods: A Survey” Barjinder Kaur et al, International Journal of Computer Science and Mobile Computing, Vol.3 Issue.6, June- 2014, pg. 234-238
- [8] Er. Manpreet Kaur , Er. Gagandeep Kaur A P” A Survey on Implementation of Discrete Wavelet Transform for Image Denoising” International Journal of Communications Networking System
- [9] Nawazish naveeda, ayyaz hussainb, m. Arfan jaffara,tae-sun choic” quantum and impulse noise filtering from breast mammogram images” computer methods and prog ram sin biomedicine 108(2012) 1062–1069
- [10]Prabjot Kaur and Sheo Kumar” Survey of Image Noise Technique” SSRG International Journal of Computer Science and Engineering (SSRG-IJCSE) – EFES April 2015
- [11]P.Mayo,F.Rodenas,and G.Verdu”Comparing Methods to Denoise Mammographic Images”
- [12]Harish Kumar.N,Amutha.S and Dr.Ramesh Babu D.R”Enhancement of Mammographic Images using Morphology and Wavelet Transform”ISSN:2229-6093

Review of Structural Considerations Due To Load Development In Silo Design

Dr. Amit Bijon Dutta Ph.D.

Mecgale Pneumatics Pvt. Ltd., dutta.ab@gmail.com,+91-9637000048

Abstract— The loads which bulk materials exert on silo structures are generally divided into two categories: one due to initial fill and second which resulting due to the flow. Initial fill loads develop, as the name implies, when an empty silo is filled without any withdrawal taking place. The term flow-induced loads are on the other hand, to some extent of a misnomer since it implies that the material must be in motion for these loads to build up. The loads which bulk materials exert on silo structures are generally divided into two categories: one due to initial fill and second which resulting due to the flow. Initial fill loads develop, as the name implies, when an empty silo is filled without any withdrawal taking place. The various types of flow are Initial Fill, Mass Flow – Single Outlet, Funnel Flow – Single Outlet, and Multiple Outlets Material Flow Properties. Force resultants factors like tension, vertical force & upper section, bending in flat walls, horizontal bending on a circular wall vertical bending of upper wall, vertical force on a flat bottom and tension and forces on ring beam are also considered in the review.

Keywords— Silo, Design, Loads, Janssen Theory, Ring Beam, Stress.

INTRODUCTION

Studies of the design and construction of silo started in 1882 when Roberts made his first test on silo of rectangular shape 15m high for calculating pressure. The first lateral and vertical pressure were defined in 1895 by Janssen. After that, his formulas have been continuously applied, although to date problem have not been ceased[1]. Around the nineteen sixties a strong drive was undertaken to define calculate the pressure produced by the stored material on the wall hopper.

The economic cost of repairs to this essential –though frequently neglected – component of a bulk material handling system is generally on a very high. The owner faces direct financial losses due to production and repairs, personnel in the environs are exposed to danger. In this paper I shall elaborate on some of the problems that can occur causing the reason of failure

SILO LOADS FOR DESIGN CONSIDERATIONS:

The loads which bulk materials exert on silo structures are generally divided into two categories: one due to initial fill and second which resulting due to the flow. Initial fill loads develop, as the name implies, when an empty silo is filled without any withdrawal taking place. The term flow-induced loads are on the other hand, to some extent of a misnomer since it implies that the material must be in motion for these loads to build up. In fact, the lone requirement is that there be some extraction of material which allows the flow induced loads to build up. As this occurs, flow can be stopped and then restarted without having any appreciable consequence on the silo loads. In addition, the velocity of discharge is usually not an important variable in affecting the magnitude of the silo loads. The primary reason for it is that most bulk materials are not viscous or visco-elastic, so their velocity of movement has little effect on their frictional properties[2].

INITIAL FILL

As with all of the loading conditions explained herein, it is suitable to consider first the vertical-sided portion of the silo (also called as the cylinder section), and after that the hopper (i.e., sloped/inclined section of the silo where the cross-sectional area is changing with height). If a silo is filled at a point that is coinciding narrowly with the silo's center line, the loads which develop on the cylinder walls are normally of smaller amount than those which are flow induced and are therefore of little interest as far as structural design is apprehensive about. If there is some reason to consider these loads, Janssen equation is recommend with a 'Kj' value (ratio of pressures, horizontal to vertical) of 0.4 and with wall friction angle 'φ' equal to a value determined from. For a circular cylinder of diameter D, the Janssen equation is:

$$p = \frac{\gamma D}{4\mu} [1 - e^{-4\mu K_j Z/D}] \quad (1)$$

$$\tau = \mu p \quad (2)$$

$$\mu = \tan\phi' \quad (3)$$

Refer TAXONOMY section at end of paper for a description of terms in equations[8].

Other types of fill conditions can result in loads on the cylinder walls which are bigger than those which are flow-induced. In particular, consider the conditions which occur when filling is off-centered in a silo, or if it is filled along a ridge (such as would occur if a continuous belt tripper fill system are used). Pressures around the silo perimeter at any elevation caused by these conditions can be calculated using the following method[9]:

- a) At any point on the cylinder's perimeter, measure vertically up the wall to the elevation where the material surface contacts the wall, z_1 .
- b) Cut the surface profile with a horizontal slice at the elevation just determined (i.e., where the contact of material to the surface the wall). Calculate the volume of the surcharge above that slice, and then divide that volume by the area of the slice, to give an effective additional head above the slice, z_2 .
- c) Apply Janssen's equation, using $z = z_1 + z_2$.
- d) Repeat the same for sufficient points around the perimeter of the silo to define the distribution.

Even as this condition is usually rather localized to a region immediately below the material surface, it can take place at any height as the silo is being filled. As far as the hopper section is concerned, we believe that the following equation satisfactorily predicts the preliminary fill pressures which act normal (i.e., perpendicular) towards the walls of a converging conical hopper, independent of what type of flow pattern occurs during discharge.

$$p = \gamma \left(\left(\frac{h-z}{ni} \right) + \left(\frac{q}{\gamma} - \frac{h}{ni} \right) \left(1 - \frac{h}{ni} \right)^{ni+1} \right) \quad (4)$$

$$ni = 2 \left(1 + \frac{\tan \phi}{\tan \theta c} \right) - 3 \quad (5)$$

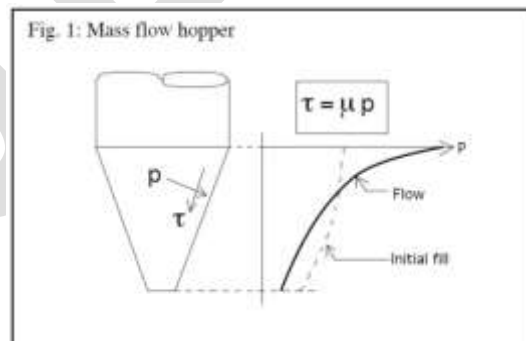
Note that "z" in equation (4) begins with a zero value at the top of the hopper, not at the top of the cylinder as in equation (1). The value of q can be calculated by taking the Janssen horizontal pressure p at the bottom of the cylinder and dividing by Kj (0.4 is the recommended value)[3]

For hopper geometries other than conical, numerical integration of the equations of equilibrium is essential. As will be shown below, in the case of a mass flow hopper the initial fill loads preside over the structural design of the hopper in more or less, its bottom two-thirds, whereas flow-induced loads govern in the upper third as shown in Fig.1. In the majority funnel flow hoppers, their structural design can be based upon initial fill loads.

MASS FLOW – SINGLE OUTLET

Mass flow is a condition in which *the entire* material is in motion even if a single part is withdrawn. As indicated in the SILO DESIGN segment above, particles are able to be flow at different velocities and still satisfy the necessities for mass flow as long as they are moving.

A mass flow bin or silo can still exhibit a no flow condition of arching if the outlet is too small relative to the particle size (arching due to interlocking) or if the outlet passage is too small relative to the cohesive strength of the materials. Mass flow silos can also develop self-induced vibrations as material discharges[7].



If we assume that the outlet size is large enough to put off the formation of a stable arch, and in addition that self-induced vibrations do not occur on discharge, the loads that develop on the silo walls are moderately well defined. In the cylinder section, a good quality starting point is to use the Janssen equation but with a range of Kj and wall friction values as follows:

$$0.25 \leq Kj \leq 0.6 \quad (6)$$

$$\phi' \text{ calc.} = \phi' \text{ meas.} \pm 5^\circ \quad (7)$$

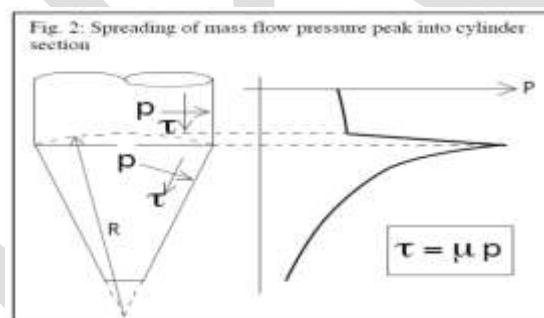
The “plus” sign must only be used in this equation when calculating upper limit of shear stresses for cylinder buckling calculations, or else the “minus” sign should be used. If an applicable silo code predicts higher pressures, it must be used in the hopper sector; it is also recommend that the use of the following equation [8] to calculate flow induced loads in conical hoppers:

$$p = \gamma K f \left(\left(\frac{h-z}{ni} \right) + \left(\frac{q}{\gamma} - \frac{h}{ni} \right) \left(1 - \frac{h}{ni} \right)^{ni+1} \right) \quad (8)$$

$$K f = \frac{1}{\left(\frac{3}{2} \left(1 + \frac{\tan \phi}{\tan \theta c} \right) - \frac{1}{6(\sigma'/\gamma B) \tan \theta c} \right)} \quad (9)$$

$$n f = 2 K f \left(1 + \frac{\tan \phi}{\tan \theta c} \right) - 3 \quad (10)$$

The value of “z” starts at zero in equation (8) at the top of the hopper, as in equation (4). The value of q can be computed by taking the Janssen horizontal pressure ‘p’ at the cylinder bottom and dividing by ‘Kj’. To be conservative, a minimum value of ‘Kj’ be supposed to be used for the calculation of ‘p’. These equations result in high pressures in roughly the upper third of the mass flow hopper than occur during preliminary fill, but lower pressures at the bottom two-thirds of the hopper segment. Refer Fig. 1. Since the rapid switch in the state of stress which occurs at the top of a mass flow hopper section, a little increase in wall pressure is time and again experienced in the section of the cylinder just above the hopper top. To account for this condition, it is recommended that the crest pressure be spread all along the vertical wall as depicted in Fig. 2. First, draw a circular arc centered on the theoretical apex of the conical hopper, and passing through the top of the cone. The elevation of the highest point on the arc is approximately the utmost elevation on which the peak pressure increase is experienced. The wall pressure allocation below this elevation (down to the top of the cone) may be assumed linear. A silo in which the filling and the withdrawal points are positioned along the vertical centerline, and which also behaves in mass flow, will probably experience a little non-uniformity of pressures in the region of its circumference.



This could be caused by the wall being out-of-round or out-of-plumb, the intrusion of manufacture joints, or segregation of the contained bulk material. It is common practice, although by no means always correct, to balance for these effects by multiplying the calculated wall pressure ‘p’ by some “over pressure factor” for purpose of design. Recommendation is that this should be a *minimum* requirement, and that a designer be supposed to make a rational attempt to calculate approximately pressure non-uniformities and their effects.

FUNNEL FLOW – SINGLE OUTLET

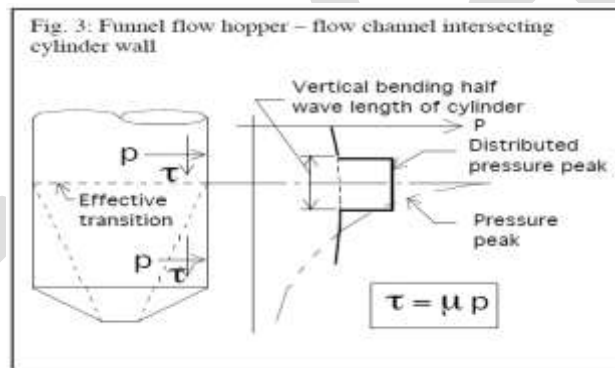
It have been noted above, there is no flow all along the hopper walls in a funnel flow pattern (except when the hopper is being emptied at the closing stages of the ejection sequence), it is rational in most cases to consider with the intention of the design pressures acting normal to the hopper walls are similar to those which occur during initial fill. Therefore no additional calculations are desirable for the hopper section. This presumes that the outlet size in addition to feeder arrangements are such that no arching or rat holing can occur as material is discharged. It is also important so as to, there be no self-induced silo vibrations acting to magnify pressures.

As far as the cylinder section is concerned, there are two main circumstances to consider. First, if the flow channels do not overlap the cylinder wall, it will be safe and reasonable to presume so as to the pressures acting alongside the walls will be the same as throughout initial fill. If, on the other hand, the flow channel do interconnect the cylinder wall, one must consider whether or not the flow channel is centered (*i.e.*, cylinder wall intersects at the same elevation approximately its circumference). If the flow channel is centered, one can presume a Janssen stress field above *the effective transition* (*i.e.*, the height at which the flow channel intersects the cylinder walls).

With mass flow cylinder pressures, it is recommended using a range of 'Kj' and wall friction values as described above. At the efficient transition wherever the flow channel strikes the wall, there is a rapid enhancing in wall pressure owing to the convergence which the material is undergoing. Within the flow channel itself, it is rational to assume that the pressures would vary as if this was a mass flow hopper other than with the hopper angle replaced by the flow channel angle, as well as the wall friction value replaced by the internal friction of sliding particles on each other. It have not been well defined as how this pressure distribution is transmitted to the vertical walls. It is safe, but probably somewhat conventional, to assume so as to, the pressure which acts normal to the cylinder walls is the same pressure which acts normal to the flow channel.

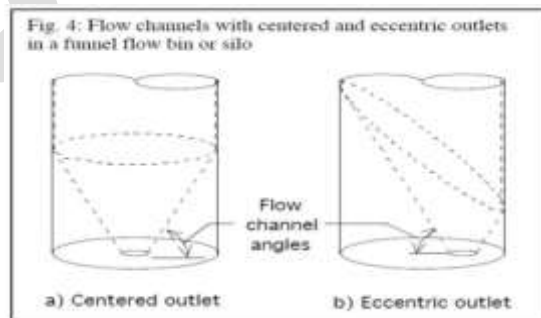
As by means of the conditions which occur at the bottom of a cylinder just above a mass flow hopper, there is a few sequence of this pressure peak, which occurs just above the effective transition in a funnel flow silo. It is recommend that the total radial external force given by the peak pressure, multiplied by the effective area in excess of which it acts and converted in to smaller uniform pressure spread over a wall height equal to one vertical bending half wave length. This ought to be centered at the elevation of the effective transition. Refer Fig. 3.

Several studies have been conducted in an attempt to predict the shape of flow channels in funnel flow bins. One of the older and better known studies was performed by Giunta[11]. He postulated that for a silo having a circular outlet by means of a diameter large and sufficient enough to prevent arching and rat holing, the flow channel shape would consist of a cone emanating from the outlet and flaring out to some diameter. In the upper portion of the bin or silo, he postulated that the flow channel shape should be cylindrical with a diameter set by the maximum size of the conical flow channel. Giunta tested his theory on eighteen inches diameter flat-bottom bin having a single, central outlet. Test materials included pulverized coal, industrial starch, and iron ore concentrate. He found reasonably good agreement between the actual flow channel shape and his theory. There are a number of restrictions in applying Giunta's work as pointed out by Carson *et al.*



In both of the above cases, the wall pressure will be fundamentally constant at any elevation unless the outlet is near the wall. Only after that will the steep flow channel intersect the wall. However, if this occurs, the resulting horizontal bending moments can be exceptionally large because of the extremely non-uniform wall pressures. Furthermore, the authors found that by means of eccentric outlets, the resultant flow channel expanded at roughly the same angle as in a bin with a centered outlet, as well as the eccentric flow channel's axis of symmetry if approximately vertical. Refer Fig. 4.[8][11]

Unfortunately, the studies failed to recognize any correlation between steady state flow channel angle and material flow properties such as useful angle of internal friction or angle of repose.



Clearly, much more work needs to be done with larger models, additional bulk solids, and full scale silos previous to any definitive conclusions can be reached[4][5].

MULTIPLE OUTLETS

If more than one outlet is there in a silo, it is necessary to design the silo structurally to withstand the worst possible loading condition. This usually occurs when one or more of the outlets are active while the others are inactive. Even if all of the outlets be active but are discharging at different rates, preferential flow channels can develop even though functionally it is designed for mass flow silo. To account for these various design conditions, the silo need to be designed as funnel flow loading conditions with an off-centered flow channel occurring above one or more of the active outlets. The nearly all severe combination of flow channels must be considered when calculating the eccentric loads.

MATERIAL FLOW PROPERTIES

Most silo design codes include, either in the code itself or in the commentary section, a tabulation of “distinctive” properties of a numeral of bulk materials. One should approach the data in such tables very vigilantly. Interpolating properties or guessing properties on the basis of superficial similarities in the description of materials must be strongly avoided. It is important to remember that it is not possible to know, or to look up, the requisite flow properties of a granular material from its generic name alone. This is true not only of the bulk material by means of itself, but also of the surface on which it is sliding. For example, providing values or a range of values, intended for wall friction of “coal on steel” sounds simple but can be very misleading. Before using such data, one be supposed to consider the following questions[3]:

- What type of coal (*e.g.*, bituminous, lignite, anthracite) that was considered for developing the data in this table?
- The particle size, moisture content, ash content, etc. of the coal that is to be described?
- Type of steel and what surfaces finish were used for the tests? If carbon steel be used, was the variation as of smooth, polished surface to a rough surface (*e.g.*, due to corrosion) considered? In case of stainless steel is used, was the surface rough (mill finish plate) or smooth (2B finish sheet or polished plate)? If the steel have been mechanically polished, was the direction of polish lines taken into account? Such tabulations make available a disservice to designers in that they tempt the engineer to use them in spite of the warnings provided either within the table or in accompanying text. An engineer can be lulled into a sense that they have some quantitative data that is functional for design, whereas in fact, no assumption is valid.

Material flow tests ought to be run whenever possible to precisely quantify the flow properties (and range of flow properties) of the bulk material to be handled. This is predominantly important when the bulk material being handled is not free flowing, or as soon as its flow properties are unknown, uncertain, or variable. Defining whether or not a material is “free flowing” is to some extent subjective and a matter of debate. In our opinion, the best way to define this is to base it on the flow property of the bulk material and how do the flow properties dictate the type of flow which will occur in a given bin or silo. For example, if it is recognized (either through experience or through flow properties tests) that a given bulk material will not form a steady arch or rathole in a given silo or bin, one might rationally conclude that the material in this silo should be “free flowing.” This same material in another silo having a different flow pattern or silo dimensions may no longer be considered “free flowing.” [11] If tests are to be done, we recommend the following:

- ✓ *Effective angle of internal friction and Flow function:* Material’s cohesive strength and internal friction angles measurement generally, run on the fine fraction of the bulk material, since it is the fines which exhibit most strength. Furthermore, concentrations of fines are generally inescapable because of particle segregation. Once these parameters have been measured, it is possible to follow design process to calculate minimum outlet dimensions to prevent arching as well as decisive rat hole diameters. *Bulk density* usually this is measured by consolidating the bulk material to various pressures and after that measuring the resultant bulk density at those pressures. Such tests should be run both on the fine fractions well as on the full particle size range. The bigger value must be used while calculating bin loads.
- ✓ *Wall friction.* Generally it is easier to execute this test on the fine fraction of the material, and the resulting values typically don’t differ significantly by means of particle size. It is significant to run this test on both the material of construction of the cylinder section as well as with the purpose of the hopper. Consideration is supposed to be given to variations in the preliminary condition of the silo walls as well as situation that can occur subsequent to usage owing to abrasive wear, corrosion, etc. In general, the smoother the wall surface, the higher the wall pressure acting against it.
- ✓ *Abrasive wear.* A tester is accessible which can quantitatively predict the actual life of a bin or silo wall material due to a bulk material sliding along it. This tester may also be used to determine the change in wall friction due to wear. Each of the parameters can vary by means of the same bulk solid if any one or more of the following conditions change:
 - ❖ Moisture content
 - ❖ Time of storage at rest
 - ❖ Particle size distribution
 - ❖ Temperature
 - ❖ Chemical changes

Note that we have not incorporated in the above listing the measurement of the value of K_j . In our opinion, this parameter is more silo dependent than material-dependent. Therefore, attempts to measure its value for a given bulk solid are inappropriate.

FORCE RESULTANTS TENSION

In a circular bin or hopper wall with uniform pressure lying on the circumference, the lone horizontal force resultant is the ring tension. It is easy to calculate and accommodate during the design phase. If the hopper bottom is supported at the top edge (*i.e.*, the junction with the vertical wall), it will be loaded in tension the length of the line of slope, along with the ring tension. This becomes easy to calculate and design but it is important to check for meridional bending[11].

VERTICAL FORCE & UPPER SECTION

There are vertical compressive forces in the walls of the upper silo section due to the buildup of wall friction effects from the top surfaces downward to the level of the support. This is the sum of the horizontal outward pressures at every addition of depth, multiplied by the depth increment and the wall friction coefficient. Include to it any loads from the roof closure as well as self weight. The decisive buckling stress in the wall is the decisive factor governing the thickness requisite to carry this vertical compression. This condition seldom dictates the depth of reinforced concrete walls:[4] however is a major consideration in designing thin-walled steel or aluminum silos.

BENDING IN FLAT WALLS

Flat walls come into view in rectangular bins or hoppers, or in a chisel-shaped hopper between circular upper sections along with a slotted outlet. This type of bending is always in combination with tension in the plane of the wall. Within the upper section of a bin, vertical compression might also be present. A flat reinforced concrete wall in bending must have two layers of reinforcement, sufficiently anchored at the ends by lap splices running into the adjoining walls. In a steel design it is regularly assumed that the tension and or compression are carried by the wall plate, and the bending is carried by the external stiffeners[8]. The horizontal walls of a rectangular or conical/ chisel-shaped hopper, operating in mass flow, have to remain as practically flat as possible, or the pattern of mass flow may be lost.

HORIZONTAL BENDING ON A CIRCULAR WALL

This occurs majorly due to resultant of a funnel flow, single eccentric flow channel reaching the upper bin wall. The horizontal radial external pressure of the material on the wall is not uniform on the circumference, so out-of-round bending is induced. Non-uniform pressures inside symmetrically filled and emptied silos can also result in bending which needs to be evaluated. Combined bending along with tension effects can best be calculated using a finite element model of the bin wall which is loaded by the internal pressures is calculated over the whole circumference and height. Alternatively, a hand calculation for bending plus tension on the ring can be performed. The most important effect on a steel plate shell is the reduction in vertical buckling strength resultant from an increase in the radius of curvature when the shell deflects out-of-round. In case of construction of reinforced concrete, the reinforcing steel must be provided in two layers, with sufficient capacity for the bending and ring tension at any point. [7]

VERTICAL BENDING OF UPPER WALL

In mass flow, and also in case of funnel flow at the point so as to the flow channel strikes the wall and a peak pressure develops at the effective transition. This might be on the full perimeter or an isolated patch, and is also transient. In funnel flow this crest pressure possibly will be several times greater than the pressures above and below, and occurs on a very shallow band. The resultant force is bending in the vertical direction. In a concrete wall the result may be the development of horizontal cracks.

VERTICAL FORCE ON A FLAT BOTTOM

It is calculated using a value of ' K_j ' which will maximize the vertical pressure. One must retain information that a huge portion of the gross weight of contained material is carried by the bottom when the diameter to height ratio is small[9]. This portion decreases quickly as the height-to-diameter ratio increases.

FORCES AT RING BEAM

Perhaps the most common and typical, design of a steel silo is circular, with a vertical upper section and conical bottom hopper, supported at discrete points all around the circumference of a ring beam at the junction amid the two parts. A R.C.C. silo will usually have a steel bottom hopper supported from a ring beam which may be separate from the vertical wall, or constructed into the wall.

This ring beam accumulates the meridional tension as of the hopper shell, in addition to, possibly the gross weight of the bin by vertical friction load from the upper wall.[2] A horizontal and vertical component of tension is contributed from the hopper.

The horizontal factor from the hopper creates compression within the ring beam. The summation of the vertical forces creates bending, shear, and torsion in the ring beam. The bending moments are negative (tension at top) above the support points, and positive at mid-span. Shear occurs at the supports. The curvature of the beam allows the torsion to develop, and is at a maximum at the points of contra flexure of the spans[11].

An extra force results is the rolling moment. The line of action of the vector sum of the forces applied to the ring beam is unlikely to pass all the way through the shear center of the beam cross section. The beam therefore tends to be rolled inside out. The net result of rolling is an extra vertical moment, applied at all points on the circumference. The ring beam has to be designed to provide accommodation all these forces in combination.

OTHER CONSIDERATIONS: FEEDER DESIGN

In addition to the geometry and construction materials (MOC's) of the silo, equally important is the type of feeder which is used, as well as details of the interface between the hopper and the feeder. This is particularly important if a mass flow design is to be considered in which, the feeder must ensure that the outlet area is fully "live". Feeder design is equivalently important with funnel flow or expanded flow silos since, depending upon the details of the interface, the flow channel[12] may either be centred or eccentric. Also important is the operation of a gate at the outlet. If a gate is used in whatever thing should be a full open or full closed position, it may upset the development of mass flow or the type of flow channel that may develop in funnel flow or expanded flow. A partially closed gate – even if only just projecting into flowing material – can avert flow along significant portions of the hopper wall.

CONCLUSIONS

The best approach to the design any silo, hopper or bin, for bulk materials is one which is reasoned, thorough, conservative, and based on parameters measured. Design engineers are not legally protected by only following a code of practice. Compliance with the local codes is, of course, essential, but it should never, by itself, be regarded as a sufficient condition to the performance of an acceptable satisfactory design. It is the accountability of the design engineer to ensure that the design is based on complete and sound knowledge of the materials being handled, that the design is competent, and that it covers all anticipated loading combinations.

The construction of any silo, hopper or bin, should be always executed by a qualified and experienced team that understands the stipulation and specifications as per the design and the consequences of not following them. It is the joint responsibility of the designer, builder, and owner that structure constructed/fabricated is of an acceptable standard and satisfactorily fulfills the intent of the design.

It is then the accountability of the owner to properly maintain the structural and other components. It is also the owner's responsibility to ensure that any intended alteration in usage, liner material, discharge geometry or hardware, or any other specified or pre defined parameter, is preceded by a design review for strengthening applied as required.

The design, construction, and utilization of a silo, at all phases, it is supposed to be bear in mind that if a silo is designed, built/fabricated and erected, and operated properly it will have a long and safe life. It must also be noted and understood, that in the event of a failure, the cost of repairs or re-fabrication or reconstruction, litigation, and insurance approximately always add up to several times the cost of doing the job properly in the first place.

TAXONOMY

- D = cylinder diameter
- h = hopper height
- Kf = defined by equation
- Kj = Janssen ratio of horizontal to vertical Pressure
- nf = defined by equation
- p = pressure acting normal to a silo or hopper wall
- q = vertical pressure acting at top of hopper
- z = vertical coordinate

- Z_1 = vertical distance along cylinder wall starting at point of intersection of top pile
- Z_2 = additional vertical height added to z_1 to account for pile height
- γ = bulk density
- θ_c = conical hopper angle (measured from vertical)
- μ = coefficient of sliding friction between bulk solid and wall surface
- τ = shear stress acting along wall surface in direction of flow
- ϕ' = wall friction angle between bulk solid and wall surface

REFERENCES

- [1] R. T. Jenkyn and D. J. Goodwill, Silo Failures: Lessons to be Learned, *Engineering Digest*, Sept. 1987.
- [2] A. W. Jenike, Effect of Solids Flow Properties and Hopper Configuration on Silo Loads, In *Unit and Bulk Materials Handling* (Loeffler, F.J., and C.R. Proctor, eds.), ASME, 1980, pp 97-106.
- [3] T. Johnston, Analysis of Silo Failures from Asymmetric Flow, *Presented at the 1991 Spring Convention, American Concrete Institute*, Boston, MA, March 17-21, 1991.
- [4] Blight G E 1985 Int. J. Bulk Solids Storage in Silos
- [5] Carson J W and Goodwill D J, The Design of Large Coal Silo for Safety, Reliability and economy. *Bulk Solid Handling Vol. 4 No.1*,pp 173-177,1984.
- [6] J. W. Carson and R. T Jenkyn, How to Prevent Silo Failure with Routine Inspections and Proper Repair, *Powder and Bulk Engineering 4 No. 1*, January 1990
- [7] J. W. Carson and R. T Jenkyn, Load Development and Structural Consideration in Silo Design
- [8] A challenge for designers of steel silos - Jim Durack & Professor Charlie Tranberg – USQ
- [9] Silo Problems – Juan Ravenet, *Bulk Solid Handling Vol.1 Number 4*, December 1981.
- [10] Giunta J.S. Flow Pattern of Granular Materials in Flat Bottom Bins, *Translations of the ASME Journal of Engineering Industry*, 91,Ser. B, No.2, Pg. No. 406-413.
- [11] J. W. Carson and R. T Jenkyn Load Development and Structural Consideration in Silo Design, Jenike & Johanson Inc.
- [12] Jenike A.W.: Effect of Solid Flow Properties and Hopper Configuration in Silo Loads *Unit of Bulk Material Handling* (Loeffler. F.J. and C.R. Proctor,eds), 1980 ASME, PP. 97-106

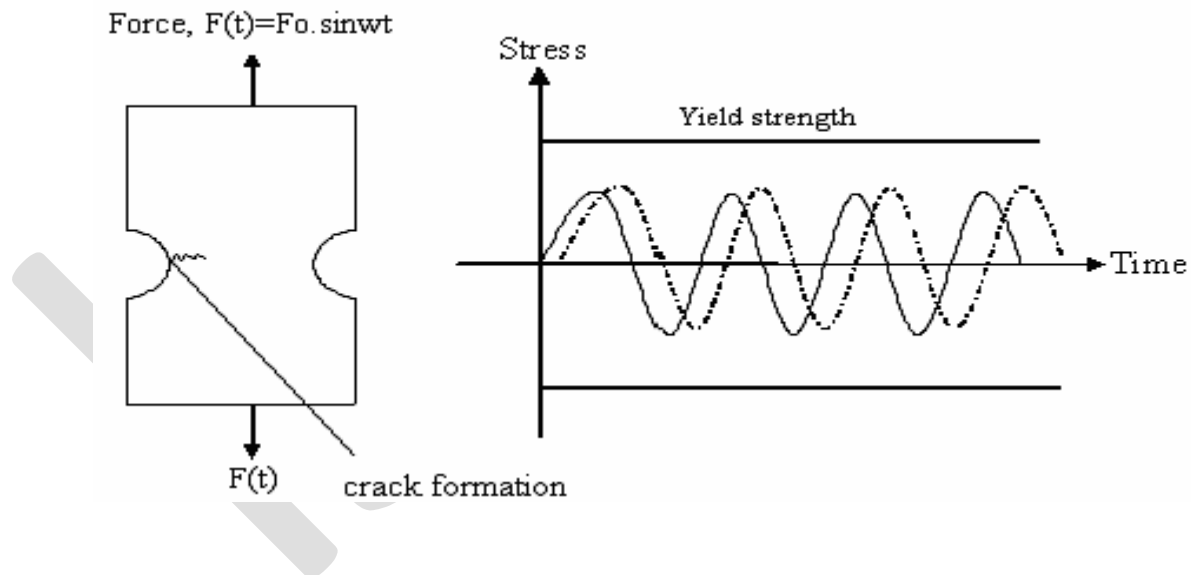
Design and Development of Fatigue Testing Machine

Chirag Surati, Patel Hiral

- 1) UG Student, Mechanical Department, suratic60@gmail.com , +91-9586158177
- 2) UG Student, Mechanical Department, patelhiral.ph43@gmail.com , +91-8866165805

Abstract: Fatigue testing facilities are first classified in accordance with a number of features which include purpose, type of loading, and method of load application and transmit as well as control system. It is built on the understanding obtained from a vibration analysis of the force transfer function from the load cell of the machine to a fabricated calibration bar. Performing the dynamic characterization in practice consists of making a frequency sweep with the strain gage equipped calibration bar. All the proceeding steps of analysis required to predict an upper bound of the linear measurement error is conveniently handled by software. The machine we made is concept machine and we are not taking into account any of the features like efficiency & output of the machine, servicing cost of the machine etc. The machine made by us is based on the machines used in the different industries. We obtain the s-n curves on the basis of the testing of different types of material which are being tested. The result that we get after the testing should match the standard s-n curve of that material

INTRODUCTION: Fatigue occurs when a material is subjected to repeated loading and unloading. If the loads are above a certain threshold, microscopic cracks will begin to form at the surface. Eventually a crack will reach a critical size, and the structure will suddenly fracture (break). The shape of the structure will significantly affect the fatigue life; square holes or sharp corners will lead to elevated local stresses where fatigue cracks can initiate. A careful study of the broken parts in almost any scrap yard will reveal that the majority of failures occur at stress below the yield strength. This is a result of the phenomenon called fatigue which has been estimated to be responsible for up to 90% of the in-service part failures which occur in industry. If a bar of steel is repeatedly loaded and unloaded at say 85% of its' yield strength, it will ultimately fail in fatigue if it is loaded through enough cycles.



FATIGUE FAILURE

Fatigue: It is the process of progressive permanent structural change occurring in a material which is subjected to conditions that produce fluctuating stresses and strains at some point and that may turn in cracks or complete fracture after a sufficient number of fluctuations. If the maximum stress in the specimen does not exceed the elastic limit of the respective material, the specimen returns to its initial condition when the load is removed. A given loading may be repeated many times, provided that the stresses remain in the elastic range. These conclusion is correct for loadings repeated even a few more times. However, it is not correct when loadings are repeated thousands or millions of times. In such cases, rupture will occur at a stress much lower than static breaking strength and this phenomenon is known as fatigue.

Material properties: A fundamental requirement for any durability assessment is knowledge of the relationship between stress and strain and fatigue life for a material under consideration. Fatigue is a highly localized phenomenon and it's depends very much on the stresses and strains experienced in critical regions of a component or structure. The relationship between uniaxial stress and strain for a given material is unique, consistent and moreover independent of location. However, the most critical locations are at notches even when loading is uniaxial.

Cumulative Damage Analysis: The cumulative damage analysis for a critical region in a component consists of several closely interrelated steps as can be seen combination of the load history (Service Loads), stress concentration factors (Stress Analysis) and cyclic stress-strain properties of the materials (Material Properties) can be used to simulate the local uniaxial stress-strain response in critical areas. Through this process it is possible to develop good estimates of local stress amplitudes, mean stresses and elastic and plastic strain components for each excursion in the load history. The damage contribution of these events is calculated by comparison with material fatigue data generated in laboratory tests on small specimens. The damage fractions are summed linearly to give an estimate of the total damage.

Fatigue Failure Mechanism: A fatigue failure begins with a small crack; the initial crack may be so small and cannot be detected. The crack generally develops at a point of localized stress concentration like discontinuity in the material, such as a change in cross section, a keyway or a hole. Once a crack is initiated, the stress concentration effect become greater and the crack propagates. Consequently the stressed area decreases in size, the stress increase in magnitude and the crack propagates more rapidly. Until finally, the remaining area is unable to sustain the load and the component fails suddenly. Thus fatigue loading results in sudden, unwarned failure.

Factors that affect the fatigue life:

- 1) The size of the member
- 2) Environmental operating conditions
- 3) Type of load (uni-axial, bending moment...etc.)
- 4) Load history (constant, variable random load etc.)
- 5) Frequency of cyclic load

Stages of fatigue failure:

Fatigue failures often occur quite suddenly with catastrophic (disastrous) results and although most insidious for metals and polymers are also susceptible to sudden fatigue failures. The process occurs by the initiation and propagation of cracks and, the fracture surface is close to perpendicular to the direction of maximum tensile stress. Applied stresses may be axial (tension-compression), flexural (bending) or torsion (twisting) in nature. There are three possible fluctuating stress-time modes possible. The simplest is completely reversed constant amplitude where the alternating stress varies from a maximum tensile stress to a minimum compressive stress of equal magnitude. The second type, termed repeated constant amplitude, occurs when the maxima and minima are asymmetrical relative to the zero stress level. Lastly, the stress level may vary randomly in amplitude and frequency which is merely termed random cycling small compared with the size of cross section. At the same time, the sizes of these cracks whose depth is small compared with the size of the cross section. This process forms the third stage of fatigue damage. Fatigue is gradual process of damage accumulation that proceeds on various levels beginning from the scale of the crystal lattice, dislocations and other objects of solid state physics up to the scales of the structural components.

1. Fatigue failures generally involve three stages

Crack initiation:

- Areas of localized stress concentrations such as fillets, notches, key ways, bolt holes and even scratches or tool marks are potential zones for crack initiation

- Crack also generally originate from a geometrical discontinuity or Metallurgical stress raiser like sites of inclusions.

- As a result of the local stress concentrations at these locations, the induced stress goes above the yield strength (in normal ductile materials) and cyclic plastic straining results due to cyclic variations in the stresses. On a macro scale the average value of the induced stress might still be below the yield strength of the material.

- During plastic straining slip occurs and (dislocation movements) results in gliding of planes one over the other. During the cyclic stressing, slip a saturation result which makes further plastic deformation difficult.

- As a consequence, intrusion and extrusion occurs creating a notch like discontinuity in the material.

Crack Propagation:

- This further increases the stress levels and the process continues, propagating the cracks across the grains or along the grain boundaries, Slowly increasing the crack size.

- As the size of the crack increases the cross sectional area resisting the

Applied stress decreases and reaches a thresh hold level at which it is Insufficient to resist the applied stress.

Final fracture:

- As the area becomes too insufficient to resist the induced stresses any further a sudden fracture results in the component basic features of failure appearance.

- A fatigue failure, therefore, is characterized by two distinct regions. The first of these is due to progressive development of the crack, while the second is due to the sudden fracture. The zone of sudden fracture is very similar in appearance to the fracture of a brittle material, such as cast iron, that has failed in tension. The crack propagation zone could be distinguished from a polished appearance.

How to Analyze Fatigue:

Two principal factors govern the amount of time it takes for a crack to start and grow sufficiently to cause component failure:

The component material and the stress field. The main ways to calculate fatigue life: Stress Life (SN)

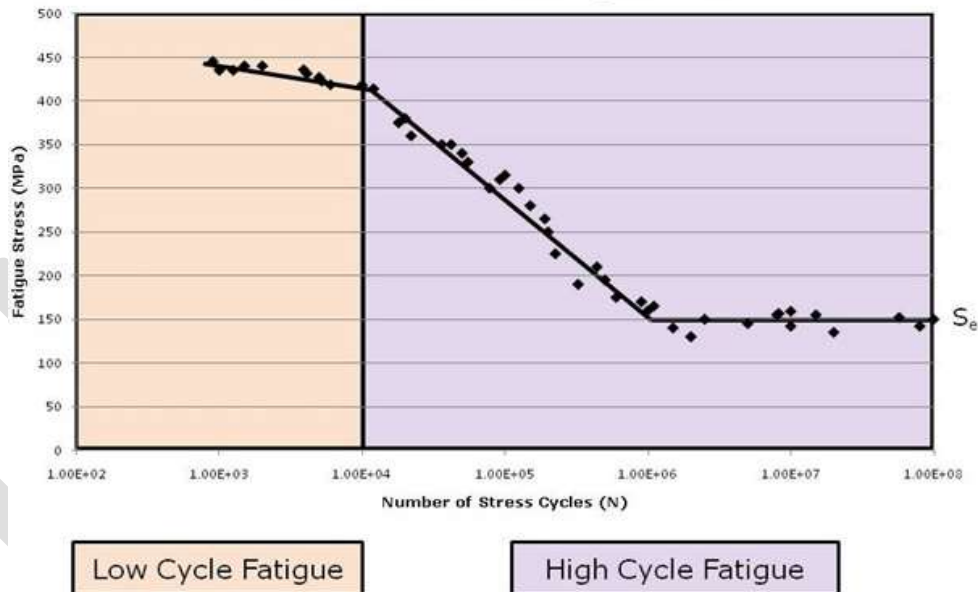
STRESS-LIFE BASED APPROACH (S-N METHOD)

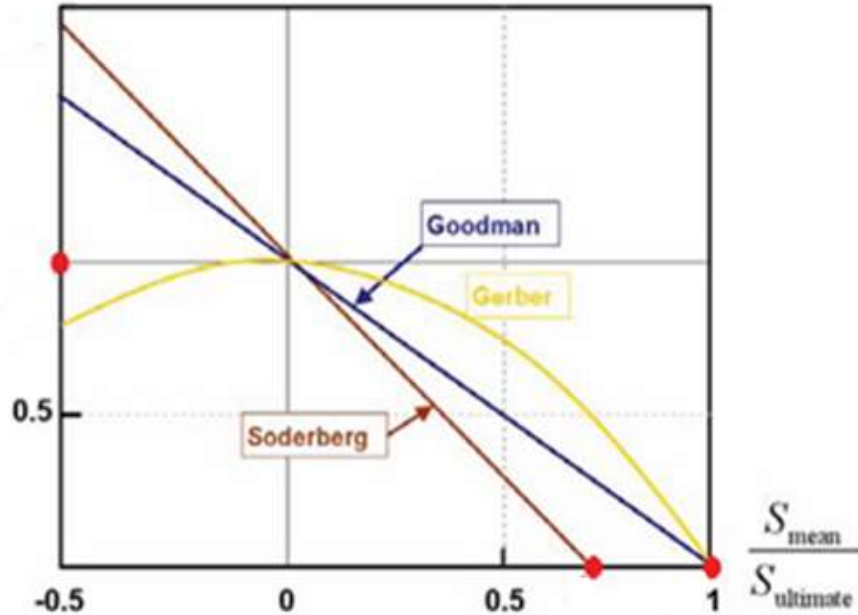
The Stress Life approach predicts the component's fatigue life based upon a standard material test for failure. It gives results based upon the whole fatigue life and as such does not break down the process into the three stages. The Stress Life Approach is based upon the calculation of varying elastic stresses, which means it cannot be applied to low cycle fatigue (failures with 10,000 load cycles). However, this approach is very accurate for high cycle fatigue, which is the realm of most industrial applications. Considerable material data has been published for materials tested using this method.

The basis of the stress-life method is the Wohler S-N curve, that is a plot of alternating stress, S , versus cycles to failure, N . The data which results from these tests can be plotted on a curve of stress versus number of cycles to failure. This curve shows the scatter of the data taken for this simplest of fatigue tests. The approach known as stress-based approach continues to serve as a widespread used tool for the design of the aluminum structures. Comparing the stress-time history at the chosen critical point with the S-N curve allows a life estimate for the component to be made. Stress-life approach assumes that all

stresses in the component, even local ones, stay below the elastic limit at all times. It is suitable when the applied stress is nominally within the elastic range of the material and the number of cycles to failure is large. The nominal stress approach is therefore best suited to problems that fall into the category known as high-cycle fatigue. High cycle fatigue is one of the two regimes of fatigue phenomenon that is generally considered for metals and alloys. It involves nominally linear elastic behavior and causes failure after more than about 10^4 to 10^5 cycles. This regime associated with lower loads and long lives, or high number of cycles to produce fatigue failure. As the loading amplitude is decreased, the cycles-to-failure increase.

Mock Carbon Steel Fatigue Data





The Gerber, Goodman and Soderberg methods denote the predicted failure behavior according to the mean correction lines shown with the same names. The Gerber method uses a quadratic, non-conservative approach related to the endurance limit and ultimate tensile strength, which is generally applicable to ductile materials. The Goodman approach relies on a conservative, linear relationship between the same parameters. The Soderberg line is the most conservative of all relationships as it links S_e to the tensile yield strength. The intersection of the alternating and mean stresses can provide some sense of the likelihood of failure according to the different standard lines.

All three methods apply only when all associated S-N curves are based on fully reversed loading. Moreover, these corrections only become significant if the applied fatigue load cycles have large mean stresses compared to the stress range. Testing has shown that fatigue failure generally occurs somewhere in the region between the Goodman line and the Gerber line. Thus, to give some leeway in a design, it is most practical to use the more conservative of the two as the upper boundary.

Design:

Materials used to made equipment:

Motor

Specimen

Bearing

Shaft

Nut

Collet

Design calculation for shaft diameter:

$$P = 2 * \pi * N * T / 60, \quad P = \text{Power Transfer}, \quad T = \text{Torque Transfer}$$

$$N = \text{R.P.M. of Shaft}, \quad \text{Power of Motor} = 1\text{Hp}$$

* $T = \pi \cdot 16 \cdot \text{Shear Stress} \cdot D^3$, $T = \text{Torque}$

$D = \text{Diameter of Shaft}$

Design calculation for bearing:

* $P = W/A$, $P = \text{Pressure Exerted on Bearing}$

$A = \text{Area of Bearing}$, $A = 3.14 \cdot r^2$

$r = \text{Radius of Shaft}$

* Total Frictional Torque, $T = .667 \cdot 1 \cdot W \cdot r/m$

$W = \text{Load Applied}$

$r = \text{Radius of Shaft}$

$1/m = \text{Poissons Ratio}$

* Power Lost in Friction, $P = 2 \cdot 3.14 \cdot N \cdot T/60$

$P = \text{Power Lost}$,

$N = \text{R.P.M. of Shaft}$,

$T = \text{Total Friction Torque}$

* Heat generated at bearing, $H = P \cdot 60 \text{ (KJ/min)}$

$P = \text{Power Lost}$

Acknowledgment:

I feel privileged in expressing most important and essential acknowledgement to PROF. CHINTAN.K.PATEL for his invaluable esteemed guidance and encouragement for perusing the project. I am also thankful to other professors for their correct guidance.

Conclusion:

After successfully performing, "the conclusion is given that in the starting in initial condition at normal motor speed there is no breakdown in the component, But after some time if we apply some load to the down side of the component then crack is initiated and at certain point and time there is sudden breakage in component".



REFERENCES:

1) Scientist: ABASS ADEYINKA AZEEZ

Reference: Ives De Baere, Department of Mechanical Construction and Production, Ghent University, Gent, Belgium

2) Scientist: J.R. Davis, ASM Specialty Handbook: Aluminum and Aluminum Alloys, ASM International, 1993

3) Scientist: G. Di Franco, G. Marannano, A. Pasta and G. Virzì Mariotti Crack propagation Reference: Beck, T., Lohe, D., Baumgartner, F., 2002, The Fatigue Behaviour of an Aluminium Foam Sandwich Beam Under Alternating Bending – Advanced Engineering Materials, vol. 4, n. 10, pp 787-790

4) Reference: J. Schijve fatigue of structures and materials. Dordrecht, Boston: Kluwer Academic press, 2001.

5) Scientist: Gbasouzor Austine Ikechukwu REFERENCE: Proceedings of the World Congress on Engineering and Computer Science 2013 Vol I WCECS 2013, 23-25 October, 2013, San Francisco, USA

6) References: [1] Dieter, G.E., Mechanical metallurgy, 1988, SI metric edition, McGraw-Hill, ISBN 0-07-100406-8. [2] Hashemi, S. Foundations of materials science and engineering, 2006, 4th edition, McGrawHill, ISBN 007-125690-3.

7)References: Ali M 2005 Int. J. Fatigue 2733 Broek D and Bowles C O 1971 J. Inst. Metals 99255 Chawla N, Andres C, Jones J W and Allison J E 1998 Met. Trans. A292843 Di Russo E, Conserva M, Gatto F and Maricus F 1973 Met. Trans. A4 1133

8)References: SS-ISO 3800 Stephens, R. I., Bradley, N. J., Horn, N. J., Gradman, J. J., Arkema, J.M. & Borgwardt, C. S. (2005).

9) References: Belingardi G, Cavatorta MP, Paolino DS. "Repeated impact response of hand lay-up and vacuum infusion thick glass reinforced laminates". International Journal of Impact Engineering, Vol. 35, No. 7, pp 609-619, 2008.

10)References Arnet, H. and Vollertsen, F.,1995. Extending Laser Bending for the Generation of Convex Shapes. ImechE Part B, Journal of Engineering Manufacture. Vol. 209; pp: 433–442.

11) www.Fatiguetesting.com

12) www.Scribd.com

13) En.wikipedia.org/wiki/gantt.chart

14) www.asminternational.org

IJERGS

ECG DENOISING TECHNIQUES: A SURVEY

¹Shamya C, ¹Shilpa Unnikrishnan M K, ²Smitha P B
¹PG Scholar, ² Assistant Professor ,Dept. of ECE, Thejus College of Engineering
Email: Shamya27@gmail.com

Abstract— This paper describes about different techniques for ECG denoising. This paper focuses on biomedical signal processing area. ECG The ECG signal is a graphical representation of electrical activity generated by rhythmic contractions of the heart. ECG signal is corrupted by presence of different noises like power line interference, channel noise, baseline wander, electromyogram (EMG) Noise, electrode contact noise, and motion artifacts that may lead to wrong interpretation in diagnosis. Efficient denoising techniques are required for the accurate diagnosis of cardiac problems.

Keywords— Electrocardiogram, Denoising, Emperical mode decomposition, Discrete wavelet transform, Adaptive filtering, Bayseian filtering, Kalman filter.

INTRODUCTION

Signal processing plays a significant role in biomedical engineering and diagnostics. For efficient diagnosis of various diseases. Signal processing has a dominant contribution in pattern analysis and feature extraction. Every year, around 25% of deaths in the world are caused by cardiac disorders like arrhythmia.

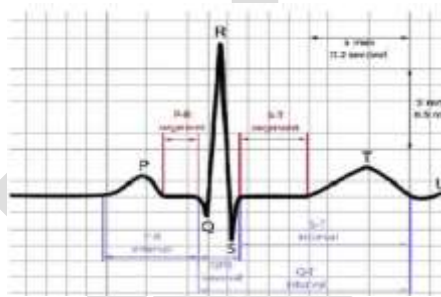


Fig 1: Normal ECG waveform [1]

The electrocardiogram is a diagnostic tool that is used to assess the electrical and muscular functions of the heart. An ECG signal represents the cardiac activity of the human heart recorded by placing electrodes on the skin and is used by the physicians for clinical diagnosis of cardiac abnormalities. The ECG signal is a representation of electrical activity generated by rhythmic contractions of the heart and it can be measured by placing electrodes on the body's surface. An electrode lead, or patch, is placed on both arm and leg and

Six leads are placed across the chest wall. The signals generated at the electrodes are recorded [1].

Fig.1 depicts a normal ECG signal. Each ECG signal of normal heart. It consists of six continuous electromagnetic peaks, ie, PQRST and U. The P wave reflects the activation of the right and left atria. The QRS complex shows depolarization of the right and left ventricles. The T wave, which is generated after QRS complex shows ventricular activation [3]. On the reading of ECG, the atrial repolarization is not recorded. The electrocardiogram can also be used to measure the rate and rhythm of the heartbeat, as well as provides the evidence of blood flow to the heart muscle. The ECG signal will be corrupted due to the presence of different types of artifacts and interferences such as Power line interference, Electrode contact noise, Muscle contraction, Base line drift, Instrumentation noise generated by electronic and mechanical devices, Electrosurgical noise.

The rest of the paper is organized as follows: Noises in ECG signal describes about the different types of noise interfering with the ECG signal. The Section ECG denoising techniques explains about different denoising techniques.

NOISES IN ECG SIGNAL

Power line interference, Electrode contact noise, Motion artifacts, Muscle contraction, Base line wander, Instrumentation noise generated by electronic devices and Electrosurgical noise [2] are the different type of noises which contaminate the ECG signal.

1. POWER LINE INTERFERENCE

Amplitude of the power line Interference is half of peak-to-peak ECG amplitude. Common causes for the 50 Hz interferences are the following

1. stray effect created due to the loops in the cables
2. improper grounding of ECG machine or disconnected electrode on the patient's body
3. Electromagnetic interference produced from the power lines
4. 50 Hz signals is induced in the input circuits of the ECG machine due to the presence of electrical equipments such as air conditioner, elevators and X-ray units draw heavy power line current.

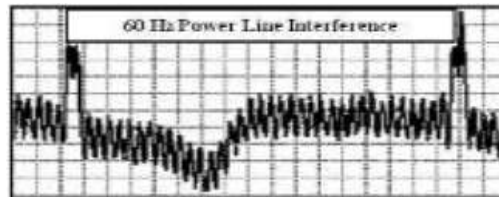


Fig 2: 60 Hz Power Line Interference

2. ELECTRODE CONTACT POTENTIAL

The improper contact of the electrodes between patient and measuring system creates electrode contact noise. It has a duration of 1 sec and amplitude of which is maximum recorded output of ECG signal with frequency of 60Hz [2].

3. MOTION ARTIFACTS

When the ECG is recorded, movement of the patient will cause changes in electrode skin impedance. Duration of this noise is 100-500ms and its amplitude is 500% peak to peak ECG amplitude [2].

4. ELECTROMYOGRAPHY NOISE

Muscle contractions also known as EMG (electromyography) noise which is produced by the patient's movement and is responsible for artefactual millivolt level potentials change in the ECG signal. The standard deviation of this type of noise is 10% of peak to peak ECG amplitude with duration of 50ms and the frequency content being dc to 10 KHz [2].

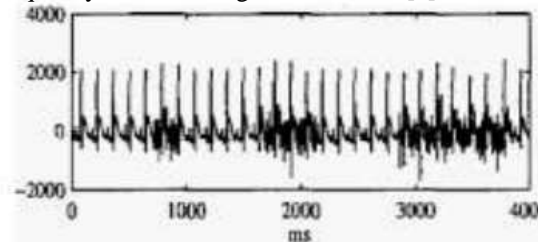


Fig 3: EMG noise in ECG signal

5. BASELINE WANDER

Baseline wander is caused by respiration or due to patient movement which may produce problems in the peak detection. Due to the presence of wander, T peak would be higher than R peak which might lead to misinterpretation of detected T peak as R peak. Amplitude variation is 15% of peak to peak ECG amplitude [2].

ECG DENOISING TECHNIQUES:

ECG signal is recorded from patient's body by placing electrodes on patient body. ECG signal when acquired from patient body is interfered by presence of different noises like power line interference, channel noise, baseline wander, electromyogram (EMG) Noise, electrode contact noise, and motion artifacts that may lead to wrong interpretation in diagnosis. Efficient denoising techniques are required for the accurate diagnosis of cardiac problems. Different ECG denoising techniques are explained below.

1. WAVELET BASED TECHNIQUE

Based on Wavelet theory for ECG signal denoising, Mashud Khan proposed Signal-Noise residue algorithm [5]. The algorithm is based on assumption that a raw ECG signal is linear combination of noise and ECG signal. Accurate estimation of noise is enabled by

the use of symmlet 8 mother wavelet with highest number of vanishing moments and multiscale decomposition of the signal. This helps to remove the noise with minimal computation.

L Chmelka et. al. in [4] used a wavelet based Wiener filter to suppress the EMG noise from ECG signal. The filtering is done by modifying the coefficients of wavelet transform depending on estimated noise level. For pilot estimation, hybrid thresholding based wavelet filtering is used. The results obtained show that these filters are good for filter banks with short impulse response while worst for filter banks with long impulse response.

Wei Zhang et. al. in [9] proposed a sub-band adaptation filtered algorithm based on wavelet transform that extracts a weak ECG signal in a strong noisy environment. It is a hybrid approach which uses a fixed sub-band decomposition and the decorrelation property of wavelet transform and property of adaptation filter. The algorithm successfully improves the extracting precision and speed and provides strong stability.

P. Mithun et. al. in [10] proposed a denoising technique for suppressing EMG noise and motion artifact in ECG signal based on wavelet. Advantages of this approach is that it does not require a reference as required in adaptive filtering techniques and also it does not require multi-channel signals as required by ICA-based techniques. Also identification of R-peaks as required in the cubic spline and EMD based techniques are not needed. Selected wavelet basis function is discrete Meyer wavelet. Combining the features of hard and soft thresholding, EMG noise was reduced while by limiting the wavelet coefficients Motion artifact was reduced.

Donghui Zhang in [11] proposed an approach based on discrete wavelet transform for baseline wander correction and denoising. In order to reduce the high-frequency noise, wavelet shrinkage method using Empirical Bayes posterior median is used. The Symmlet wavelet with order 8 and decomposition level up to 6 is used as the mother wavelet.

Gordan Cornelia et. al. in [12] used wavelet transform to filter and analyze noisy ECG signal. All relevant noise are removed by using wavelet thresholding. A three level wavelet decomposition was used to decompose the signal. The Daubechies db1 and db3 wavelets, the symlet sym2 and the first order coiflet coif-1 wavelets were used for analysis and it was found that the best results are obtained with the db3 wavelet, and the worst ones with the sym wavelet.

Omid Sayadi proposed an bionic wavelet transform (BWT) [15] for ECG denoising. The most distinguishing characteristics of BWT is that its resolution in the time-frequency domain can be adaptively adjusted not only by the signal frequency but also by the signal instantaneous amplitude and its first-order differential [15]. In denoising first the BWT is optimized and then the BWT coefficients are calculated after that hard thresholding and soft thresholding is done. This algorithm has many advantages like the signal denoised by BWT is a smoothed version, Single artifacts do no longer exist, Interference removal is achieved by properly adjusting the center frequency of mother function and the number of decomposition levels [16], For higher input SNR more improvement is obtained.

2. FIR AND IIR FILTER

Seema rani et. al. in [6] made a comparative study on the use of FIR and IIR filters for removing baseline noises present in ECG signal. Two parameters considered to evaluate the suppression of baseline noises are Spectral density and average power of signal. Based on the obtained implementation results, though FIR and IIR filters both have removed the baseline noises, IIR filters are efficient as there is a phase delay in FIR filtered waveforms. Produced due to large order of FIR filter. Also the computational complexity, memory requirement and power dissipation of IIR filter is less than FIR filters which makes IIR filters the better choice for removal of baseline noises.

Ying -Wen Bai et. al. in [7] made a comparative study of general notch filter, comb notch filter and equiripple notch filter. The performance is measured with respect to mean square error. It is observed that the equiripple notch filter retains the detail of practical signal effectively at the expense of higher filter order while the comb and general notch filters weaken the features of the ECG signal.

Mahesh Chavan et. al. in [3] designed a digital FIR equiripple notch filter which remove power line interference from ECG signal. Even though higher order filter is required, this filter reduces powerline interference successfully. The higher order implementation increases the computational complexity and makes it difficult to realize the higher order filter. Also the delay in response is increased. Reduction in signal power is more in the Equiripple method when compared with the windowing technique. Window method need less number of elements while Equiripple method need more computational elements, Thus computational time is the major limiting parameter of the Equiripple type digital filter.

A technique is proposed in [7] for the improvement of raw and noisy ECG signals by using window based FIR filters. The performance of denoising is measured by calculating the SNR of the processed ECG signal and then correlation coefficient was determined to find the degree of mismatch between raw ECG and filtered noisy ECG. The designed FIR filter with Kaiser window works excellent as compared to the Gaussian, Blackman and Blackman-Harris filter in removing baseline wandering and power line interference under different noisy conditions.

Mohandas Choudhary et. al. in [14] made comparative study between Butterworth, Chebyshev Type-I and Chebyshev Type-II based on parameters signal to noise ratio and average power for their use in suppression of noise in ECG signal. It is concluded that Butterworth low pass filter shows better performance when compared to other filters.

3. EMPIRICAL MODE DECOMPOSITION:

Empirical Mode Decomposition is proposed in [6] method to remove high frequency noise and baseline wander. The signal is decomposed as sum of several intrinsic mode functions which represent simple oscillatory mode. The first several Intrinsic Mode Functions (IMF) contains the noise components. In order to achieve the denoising and baseline wander removal, different IMF are processed. partial signal reconstruction causes high frequency denoising. The method is suitable for real noise cases too.

Md. Ashfanoor Kabir et. al. in [8] proposed a new windowing method in the Empirical Mode Decomposition domain. This method preserves the QRS complex information in the first three high frequency intrinsic mode functions. Characteristic time scales in the signal. The intrinsic oscillatory modes are identified by used to identify the intrinsic oscillatory modes and then the signal is decomposed into intrinsic mode functions. The noisy signal is enhanced in the Empirical Mode Decomposition domain and then transformed into the wavelet domain in which an adaptive thresholding scheme is applied to the wavelet coefficients to preserve the QRS information. In order to reduce the noise that remains after even after the Empirical Mode Decomposition, an adaptive soft thresholding is performed in the Discrete Wavelet Transform domain.

The paper proposed in [18] uses the empirical mode decomposition method Decomposition (EMD) of signal into sum of intrinsic mode functions (IMF) with a final residue is the important feature of EMD. Shifting process is used to estimate the IMFs. In this paper both FIR filter and EMD are used for removing PLI by passing the first IMF through FIR low pass filter and proposes a new technique for removing base line wander. In this technique first determine the number of IMFs that are affected by base line wander noise and then subtract those IMF and final residue from noise ECG signal. The ECG signal is taken from the MIT- BIH database. Parameter used in this paper is RMSE which is calculated for both EMD based method and filter based method and concluded that EMD based method is better and appropriate than filter based method and also have reduced computational complexity [18].

4. BAYESIAN FILTERING:

A nonlinear Bayesian filtering frame-work is proposed by Kazi M D in [16] for the filtering of single channel noisy ECG recordings. The necessary dynamic models of the ECG are based on a modified nonlinear dynamic model, previously suggested for the generation of a highly realistic synthetic ECG. An automatic parameter selection method is also used to facilitate the adaptation of the model parameters to a vast variety of ECGs. This approach is evaluated on several normal ECGs, by artificially adding white and colored Gaussian noises to visually inspected clean ECG recordings, and studying the SNR and morphology of the filter outputs. The results of the study demonstrate superior results compared with conventional ECG denoising approaches such as band-pass filtering, adaptive filtering, and wavelet denoising over a wide range of ECG SNRs. The method is also successfully evaluated on real non-stationary muscle artifact. This method may therefore serve as an effective framework for the model-based filtering of noisy ECG recordings.

5. ADAPTIVE FILTERING:

A least-mean-square algorithm based adaptive filters for removing power line interference from ECG signal is proposed in [16] combines different adaptive filter algorithms: least-mean-square (LMS), Block LMS (BLMS), delay LMS (DLMS), adjoint LMS, filtered -X (XLMS), normalized LMS (NLMS) and fast Fourier transform BLMS (FFT BLMS) for the removal of power line interference from the ECG signal. The real ECG signal and the 50Hz power line interference is generated by using MATLAB. Different performance parameters such as power, SNR, %PRD, ESD are compared. This paper concluded that LMS and NLMS are appropriate than other adaptive filters. As the SNR of LMS filter is lower than NLMS filter. Therefore performance of NLMS is better than LMS for removing 50Hz PLI [16].

The paper proposed in [17] presents the removal of power line interference from the ECG signal by comparing the performance of two adaptive filters: normalized least-mean-square (NLMS) adaptive filter and recursive-least- square adaptive filter with a traditional notch filter in both time and frequency domain. Real ECG signal is taken from the MIT-BIH database and the 50 Hz Power line interference is generated by using MATLAB. For performance measurement different parameters are used such as power spectral density (PSD), spectrogram, signal to noise ratio (SNR), percent root mean square difference (%PRD) and mean square error (MSE). comparison is made between the adaptive filters and notch filter. The high SNR, low %PRD and low MSE and better PSD of adaptive NLMS shows the effectiveness of this filter as compared to others. This paper concluded that adaptive NLMS filter performs better than adaptive RLS and notch filter for removing 50Hz noise properly.

MA Mneimneh et. al. in [13] proposed an adaptive Kalman filter for the real time removal of baseline wandering. Both the ECG signal and the baseline wandering can be removed using the Kalman filter. The comparison of the proposed approach is made with moving averaging and cubic spline baseline removal techniques which distortion is minimum in case of the proposed approach. Due to adaptability and convergence factor of Kalman filter the approach fails to remove baseline wander under high frequency changes. Table 5 shows comparison between baseline removal techniques [13].

CONCLUSION

This survey includes the work by different researchers on signal denoising techniques. ECG signal is corrupted by different type of noises like power line interference, channel noise, baseline wander, Electromyogram (EMG) Noise, electrode contact noise, and motion artifacts. Adaptive filtering is the best filtering technique for ECG signal with low frequency SNR. Wavelet technique can be used if signal beat to beat variation is high. EMD can be used to remove high frequency noise.

REFERENCES:

- [1] Mohandas Choudhary, Ravindra Pratap Narwaria "Suppression of Noise in ECG Signal Using Low pass IIR Filters" "International Journal of Electronics and Computer Science Engineering, page No:2238-2243.
- [2] Sarang L. Joshi, Rambabu A. Vatti, Rupali V.Tornekar, "A Survey on ECG Signal Denoising Techniques" International Conference on Communication Systems and Network Technologies,2013
- [3] Mahesh S Chavan, R A Agrawala, M.D. Uplane. "Design and implementation of Digital FIR Equiripple Notch Filter on ECG Signal for removal of Power line Interference" 4th Wseas International Conference on Electronics, Control & Signal Processing , 2005.
- [4] L Chmelka, J Kozumplik "Wavelet-Based Wiener Filter for Electrocardiogram Signal Denoising" .0276-6547/05.Computers in cardiology 2005;32: 771-774.IEEE-2005.
- [5] Mashud Khan, Faizen Aslam, Tahir Zaidi, Shoab A. Khan." Wavelet Based ECG Denoising Using Signal-Noise Residue Method" .978-1-4244-5089-3/11 , IEEE,2011
- [6] Seema Rani , Amarpreet kaur , J S Ubhi. "Comparative study of FIR and IIR filters for the removal of Baseline noises from ECG signal" International Journal of Computer Science and Information Technologies Vol 2 (3), 2011
- [7] Ying -Wen Bai, Wen-Yang Chu, Chien-Yu, Yi -Ting , Yi- Ching Tsai and Cheng-Hung Tsai "Adjustable 60 HZ Noise Reduction by a Notch Filter for ECG signal" International and Measurement Technology conference Itlay 18-20 May 2004
- [8] Md. Ashfanor Kabir , Celia Shahnaz." ECG Signal Denoising Method Based on Enhancement Algorithms in EMD and Wavelet Domains." 978-1-4577-0255-6/11.IEEE-2011.
- [9] Wei Zhang, Xu Wang, Linlin Ge , Zhuo Zhang." Noise Reduction in ECG Signal Based on Adaptive Wavelet Transform". Proceedings of the 2005 IEEE Engineering in Medicine and Biology 27th Annual Conference Shanghai, China, September 1-4, 2005.
- [10] Wei Zhang,Xu Wang , Linlin Ge , Zhuo Zhang." Noise Reduction in ECG Signal Based on Adaptive Wavelet Transform". Proceedings of the 2005 IEEE Engineering in Medicine and Biology 27th Annual Conference Shanghai, China, September 1-4, 2005.
- [11]P. Mithun, Prem C. Pandey, Toney Sebastian, Prashant Mishra, and Vinod K. Pandey." A Wavelet Based Technique for Suppression of EMG Noise and Motion Artifact in Ambulatory ECG". 33rd Annual International Conference of the IEEE EMBS Boston, Massachusetts USA, August 30 - September 3,2011.
- [12] Donghui Zhang. " Wavelet Approach for ECG Baseline Wander Correction and Noise Reduction" Proceedings of the 2005 IEEE Engineering in Medicine and Biology 27th Annual Conference Shanghai, China, September 1-4, 2005.
- [13]Gordan Cornelia, Reiz Romulus. "Ecg Signals Processing Using Wavelets". University of Oradea: Electronics Department, Oradea, Romania.
- [14]MA Mneimneh, EE Yaz, MT Johnson, RJ Povinelli." An Adaptive Kalman Filter for Removing Baseline Wandering in ECG Signals".Computers in Cardiology 2006;.
- [15]Omid Sayadi , Mohammad Bagher Shamsollahi, "ECG Denoising with Adaptive Bionic Wavelet Transform" , in Proceedings of the 28th IEEE EMBS Annual International Conference New York City, USA, Aug 30- Sept 3, 2006.
- [16]Md. Maniruzzaman, Kazi Md. Shimul Billah, Uzzal Biswas, and Bablu Gain, 2012, "least-mean-square algorithm based adaptive filters for removing power line interference from ECG signal", ICIEV 2012.
- [17]Uzzal Biswas, and Md. Maniruzzaman,2014, "Removing power line interference from ECG signal using adaptive filter and notch filter", International conference on electrical engineering and information &communication technology (ICEEICT) 2014.
- [18]S. A. Anapagamini and R. Rajavel , 2013, "Removal of Artifacts in ECG using Empirical Mode Decomposition", international conference on communication and signal processing, 2013.

AN OVERVIEW OF CAD SYSTEMS FOR LUNG CANCER DETECTION

¹Shilpa Unnikrishnan M.K., ¹Shamya C, ²Neenu P.A.

¹PG Scholar, ²Assistant Professor, Dept. of ECE, Thejus Engineering College, Thrissur

shilpaunnimk@gmail.com

Abstract— Lung cancer is one of the acute types of cancers with the least survival rate. Manual evaluation of the lung CT scan is an exhaustive task. Thus the use of computerized systems can provide the assistance to the expert practitioners in the comprehensive assessment of the medical information. Lung CAD system focuses on the detection of the potential abnormalities namely nodules which can either be malignant or benign. This paper reviews the techniques involved in CAD systems in biomedical image processing domain that offer the detection of the abnormal growth of cells in the lungs.

Keywords— CAD, Classification, False positives, Lung nodules, Region growing, Segmentation, Thresholding

INTRODUCTION

Lung cancer is regarded as one of the most dangerous diseases which pose threat to the existence of mankind. In spite of moderate improvements in the treatments of the lung cancer, the prognosis is however inferior as the survival rate after the diagnosis is depreciating even with the development of several equipments [19]. The survival of lung cancer is closely related to the stage at the time of diagnosis. The root cause of this deadly disease is the tobacco smoking. It is highly difficult to detect the presence of malignancy as it does not exhibit noticeable symptoms. Various Computer Aided Detection (CAD) systems have been developed as a second opinion to the diagnostic interpretation of the physician. The establishment of the Computed Tomography (CT) imaging modality paved the way for the detection of tumours inside the pulmonary structures. The lung CT images depict the abnormalities in lungs with better clarity, low distortion and a minimum amount of noise.

CAD system is regarded as an inevitable tool in medical radiology which aims at improving the performance of radiologists providing high sensitivity in the efficient diagnosis of the various diseases. Pulmonary CAD system[1] has been a phenomenal and revolutionary step, in the early and premature detection of lung abnormalities. The systems make use of the CT scan images to determine the pathologic condition of the patient by extracting the features of the potential abnormalities. Computerized detection helps to reevaluate the diagnostic decision if necessary. The CAD systems include systems for automatic detection of nodules and 3D reconstruction of lung systems, which assist the radiologists in their final decisions. Various image processing techniques are applied on the medical images to enhance the image and to use for the further clarification of diagnosis.

The paper is arranged in the following way: The section Overview of Computer Aided Detection Systems presents a brief description of CAD systems and the following section depicts the CAD Systems for lung cancer detection in detail which includes the architecture review of CAD systems for lung cancer detection and the various techniques involved in each stage.

OVERVIEW OF COMPUTER AIDED DETECTION SYSTEMS

Computer Aided Detection (CAD) is a proven clinical tool that assists the physicians for the detection of deadly diseases. These systems provide a second opinion in the interpretation of the diagnostic results. CAD refers to pattern recognition software that identifies suspicious features on the image and attracts the attention of the radiologist, in order to reduce false negative readings. The Radiologist reviews the examination and then activates the CAD system and performs the reevaluation of the results before issuing the final diagnostic results. CAD has its enormous impact in the medical industry as it provides the clinical interpretation in the detection of the deadly diseases. CAD techniques attract the attention from the in different fields. The main research task in the development of CAD systems is to improve the performance for widely applying the system in medical field.

The performance of a computer-aided cancer detection and diagnosis system needs integration of many independent and self-contained systems to achieve the best performance. The in-depth knowledge of the subsystems including the feature extraction and classification systems are required to attain the improved performance of the whole system. Even though CAD systems are proven to

improve the efficiency of radiologists in the detection of nodules, they are not widely used in clinical practice. As a result, CAD systems have become one of the most prominent areas of research in medical image processing.

The practice of radiology comprises of the visual perspective of an image and the interpretation or cognition. Manual strategies such as double reading can be adopted but as it is an exhaustive task, computerized systems have been developed. To provide workflow efficiency, the potential of CAD system with associated tools is highly accepted. CAD algorithms are developed to find out the same features that a Radiologist looks for during case review. But a further investigation is demanded as it may lead to some perception error and from there to wrong diagnostic interpretation. The CAD algorithms require a digital data set of the image for analysis. The medical images are usually in Digital Imaging and Communications in Medicine (DICOM) format compatible with the open source software.

CAD SYSTEMS FOR LUNG CANCER DETECTION

A well-developed computerized system for the detection and extraction of abnormalities provides the assistance to experts regarding the classification of image features into normal and abnormal categories. The use of digital computers in the detection of lung nodules in pulmonary CT images was first reported by in the early 60s [4]. The lung nodule detection system was established only after twenty years. Due to the lack of computational resources and advanced image processing techniques the first results were not so interesting. Current researches, however, have been showing that the accuracy of diagnosis with the advancing techniques in the biomedical image processing. The parameters including the speed, sensitivity and reduction of false positives were improved in the late 90s. Thresholding was used for nodule selection and Artificial Neural Networks for elimination of false positives. The main problem encountered was the low level of automation of systems because scanners were used for X-ray films, which is usually a manual process.

I. Lung Cancer and Lung Nodules

Lung cancer is treated as a worldwide predicament and is a major reason behind the cancer-related deaths in humans around the globe. It is one of the most deadly cancers with the least survival rate after diagnosis. Survival from lung cancer is directly related to its growth at its detection time. The earlier the detection is, the higher the chances of successful treatment are. Lung cancer is caused by uncontrollable irregular growth of cells in lung tissue which proliferate in an uncontrolled way [18]. It occurs after repeated inserts to the genetic material of the cell. Early detection of lung tissue abnormalities can help lung patients getting early treatment for their illness. Lung cancer often has no symptoms until it has metastasized due to the limited number of pain receptors in the lungs. The most frequently used imaging technique in the lung cancer diagnosis is Computed Tomography. Early detection of lung cancer, which is typically viewed in the form of pulmonary nodules, is an efficient way of improving the survival rate.

Lung nodules are the potential abnormalities that are roughly spherical with round opacity and a having a diameter of upto approximately 30mm. Based on their relative positions, the nodules are classified into well-circumscribed, vascularized, juxta-pleural and pleural-tail[3]. This classification is very significant since the intra-parenchymal nodules are having high probability of malignancy. Well-circumscribed nodule is located centrally in the lung without any connections to vasculature. Vascularized nodules are connected to the vessels even though it is located centrally in the lung. The name of pleural-tail nodule is due to a portion of the nodule being connected to the pleural surface by a thin tail. Juxta-pleural nodule has a large portion connected to the pleural surface. This is a straightforward classification technique to label a nodule by analysing its position and connections which can be supportive in the detection of the lung cancer. CT scan images depict the pulmonary abnormalities in a more accurate way. A nodule is defined as a rounded and irregular opaque figure on a CT scan. Fig 1 shows transaxial CT images of the four types of lung nodules namely well-circumscribed, vascularized, juxta-pleural and pleural tail nodules shown from left to right.

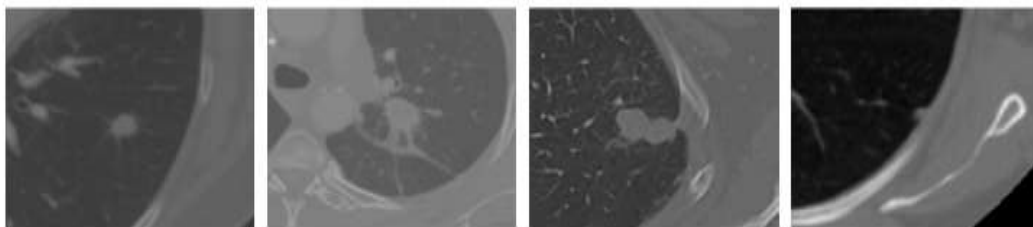


Fig 1: Transaxial CT images[1]

II. Architecture Review of Lung Cancer CAD systems

CAD systems for detecting pulmonary nodules are usually composed of five subsystems namely acquisition, preprocessing, segmentation, nodule detection and elimination of false positives [3].

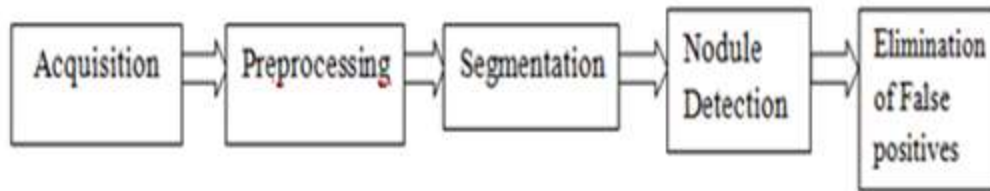


Fig 2. CAD system Architecture [4]

The CAD system architecture is shown in Fig 2. Acquisition of images involves obtaining the CT scan image from either public or private database. Preprocessing stage includes the resizing of the images, image enhancement, noise removal, extraction of ROI and segmentation of the nodule. The main objective of nodule segmentation is to accurately define the region of measurement from where the best information using an adequate set of features can be obtained. The thresholding approach in segmentation involves application of a threshold of intensity to perform the separation as the darker shades in CT scans represent the lung tissues when compared to other organs. Nodule detection aims at the determining the pulmonary nodules in the image.

The main issue that persists in the CAD systems is to discriminate true nodules from other pulmonary structures. The main relevance of pulmonary nodules is that they often represent the initial radiographic findings of lung cancer. The best method to segment the tumour regions is the Region growing method because the borders are thin and connected each other. Initially, the possible nodules detected are segmented and their features are extracted. The main extracted features are intensity values of pixels, morphology and texture. After the identification and characterization of nodules, the CAD system tries to eliminate false positives. In order to eliminate FP, classifiers are used. A classification system generally consists of training and testing phases. The classifier is trained to learn the parameters of the system in the first phase and the testing phase is to evaluate the success of the classifier. The commonly used classifiers are Support Vector Machines, Artificial Neural Networks etc.

1. Image Acquisition

CT scan images for the Lung CAD systems are obtained from the public databases[5] namely, Early Lung Cancer Action Program (ELCAP), Lung Image Database Consortium (LIDC) in national imaging archive and Medical Image Database. Beyond the public lung image database private database obtained from the hospitals are also used. Image quality in CT scanning is affected by various parameters namely radiation dose, slice thickness, detector efficiency etc. The low dose CT scan is used for reducing the exposure to the radiation by trading off the image quality.

2. Preprocessing

Preprocessing in the Lung CAD system refers to the steps necessary to enhance the image quality by eliminating the artifacts due to noise which can improve the visibility of the extracted pulmonary nodule. This stage removes defects caused by the image acquisition process. Types of filters used in preprocessing[13] stage are Laplacian of Gaussian filter, Ring Average filters, Median filters, Morphological filters, Selective Enhancement Filter etc. The LoG filter enhances the blob like structures with respect to the variation in intensity. Takahiro et al. [17] proposed a selective enhancement filters for the enhancement of blob like structures and for suppressing the vessel like structures.

For the extraction of lungs two techniques are suggested namely rule-based reasoning and pixel classification [6]. Pixel classification includes sequence of steps, tests, and rules. These include techniques like Local Thresholding, Region Growing, Edge Detection, and Morphological operations. In pixel classification, each pixel from the image is classified into an anatomical class. A rule-based thresholding technique is implemented by Naveed Ejaz et.al [6]. A threshold based on the density histogram was selected and the lung mask is obtained so as to separate the lung parenchyma from the other anatomic structures on the CT scan images. Disha et.al [7] proposed image slicing algorithm for the extraction of lung region. To enhance the quality of image various morphological operations like opening, closing followed by erosion, dilation were applied to remove any irrelevant information in the image.

3. Segmentation

The lung CT image needs the segmentation of the anatomical structures including lungs, lung lobes, airways, vessels etc. Due to the similar densities of the pulmonary structures and the behaviour of the scanners used, segmentation is considered to be a complex task. Several techniques have discussed the segmentation activity. Based on the accuracy, processing time and level of automation, the

segmentation procedures are evaluated. The main techniques in segmentation of lung regions are thresholding approach, segmentation by deformable models, shape and edge based approaches[3],[13].

In the segmentation approach based on thresholding, a threshold of intensity to perform the separation is utilized. This approach can be performed iteratively or used in combination with Otsu's thresholding, morphological operations, edge detection algorithms [7] etc. Gao et.al [14] proposed an accurate segmentation method with four steps namely the extraction of the airway from lung region, removal of pulmonary arterial and venous vessel trees by finding a suitable threshold, application of a large threshold to separate right and left lung and morphological smoothing of lung boundary. The accuracy of the thresholding approach lies mainly upon image acquisition protocol and acquisition type. The main issue behind this type of technique is that its accuracy is deteriorated by the type of equipment that makes the acquisition and the location of nodules.

Deformable models are curves or surfaces, for image segmentation, which deform themselves according to the influence of internal and external forces. The main types of deformable models used for segmentation of lung images are active contours and level set based deformable models[8]. The deformable model started from an initial segmentation obtained by a threshold estimated from CT data. The major drawbacks of this segmentation are its initialization process, speed issue and the inability of external forces to capture the lack of homogeneity in regions of the lung.

The extensive use of edge detector filters and wavelet transforms comprises of the edge based segmentation algorithms. The first derivative Gaussian filters are used to point out an outline of lung borders in [15]. Laplacian of Gaussian (LoG) operator was used to find a continuous lung contour which was combined together to extract the final lung region. Edge point detection method using spatial edge detection filters with closed contour for lung boundaries was proposed.

4. Nodule Detection

Lung nodules detection aims at determining location of lung nodules. Accuracy of lung nodule segmentation and the method for false positive reduction are the main parameters which affects the detection performance [5]. Isolated solid nodules are easy to detect as the contrast between tissue and air is clearly visible. But if the nodules are pleural-attached or vascularized, the detection becomes difficult. Nodule segmentation is crucial for the diagnostic and treatment procedures for monitoring the tumour growth in the lung. The main techniques used for the candidate nodule detection are thresholding, morphological processing, template matching, adaptive thresholding, region growing method etc.

Armato et al. [9] applied multiple gray-level thresholds to the volumetric lung regions to identify nodule candidates. It analyses the complete lung with a grayscale threshold method and searches for voxel in the lung. If the grayscale of a voxel is between the threshold, the voxel is marked by the algorithm and a 3D region growing with an eight neighbour relation is started. The first relation is done with a low threshold followed by the one with the high threshold. These regions are marked for further processing and analysis. Template matching methods [13] are used to segment the solitary pulmonary nodules. With this approach, circular or semicircular nodules can be identified. To identify the nodules situating inside and on the boundaries of lung area, Assefa et.al [16] developed both circular and semicircular templates. The structure of the lesion is irregular as they are connected to the vasculature or pleural region. In the Region growing method [11] regions are constructed and the region grows from this seed by comparing the neighbouring voxel values based on some user criterion such as pixel intensity. The disadvantage of this approach is that nodule detection is semi-automated. Contextual clustering has been combined with region growing for reducing the segmentation steps in [13]. It outperformed the conventional algorithms by providing high accuracy.

5. Elimination of False Positives

False Positives (FP) are the non-nodule structures detected as nodules. The known CT artifacts which are caused by breathing or the heart beat, or partial volume effect also increase the FPs. False positives are to be eliminated for the better accuracy of the CAD system. The increase in the number of false positives is contributed by the attached vessels and airways[5]. Thus the reduction of false positives must be performed correctly to identify the pulmonary nodule. Each and every region is individually analysed for finding the true positive nodule candidate.

Classifiers are used for evaluation of the nodules. Feature extraction is an important step in the system which involves the extraction of information about size, shape, texture and intensity values. Classification is mainly composed of training phase and testing phase. Training phase includes the supervised training and validation process. In testing phase, the lung CT scan images are compared with the extracted features in the reference model. Khin Mya Mya Tun [12] proposes a CAD system with Artificial Neural Network as the classifier. In classification, feed-forward neural network is used to classify the lung cancer stages. This system can know the condition of lung cancer at early stages, so it can play a very important and essential role to avoid serious stages. Rule Based Classification [13] can be used to separate nodules and non-nodule structure. Suzuki et.al [14] proposes a multiple massive-training Artificial Neural Network to reduce the number of false-positive results. An MTANN is a highly nonlinear filter which uses input images and

corresponding teaching images for training. To reduce background level effects in chest radiographs, a background-trend-correction technique, followed by contrast normalization, is applied to the input images for the MTANN. Multi MTANN provided acceptable level of sensitivity with reduction of false positives.

CONCLUSION

In this paper, an overview of CAD systems for lung cancer detection has been discussed. With the least survival rate, lung cancer is proved to be one of the most dangerous catastrophic threats among the cancer related fatalities. Automation introduced in the detection of the cancer laid the foundation for the improved medical assistance. The generic CAD system architecture is designed in such a way so as to obtain a considerable amount of accuracy and sensitivity with minimum number of false positives. Various methods for the computerized detection techniques have been examined. Collaborative efforts are required for the wide establishment of computer aided detection systems in medical sector for the prognosis of the lung cancer and its related ailments.

REFERENCES:

- [1] Gonçalves., "Automatic Lung Nodule Classification in Chest Computerized Tomography Images"., International Conference on Machine Vision Applications, 2015.
- [2] S.Shaik Parveen, Dr.C.Kavitha., "A Review on Computer Aided Detection and Diagnosis of Lung Cancer Nodules"., International Journal of Computers & Technology Volume 3 No. 3, Nov-Dec, 2012.
- [3] Macedo Firmino et.al., "Computer-aided detection system for lung cancer in computed tomography scans: Review and future prospects"., BioMedical Engineering OnLine 2014.
- [4] Rakesh Kumar Khare, G. R. Sinha, Sushil Kumar., "CAD for Lung Cancer Detection: A Review"., IJMTER 2015
- [5] Ashish kumar dhara et.al., "Computer-aided Detection and Analysis of Pulmonary Nodule from CT Images: A Survey., IETE Technical Review, 29:4, 265-275
- [6] Naveed Ejaz et.al., "Implementation of Computer Aided Diagnosis System for Lung Cancer Detection"., Lecture Notes on Software Engineering, Vol. 1, No. 4, November 2013.
- [7] Disha Sharma, Gagandeep Jindal., "Identifying Lung Cancer Using Image Processing Techniques"., ICCTAI 2011.
- [8] Bin Chen., "Automated Segmentation of Lung Nodules and Pulmonary Blood Vessels and Follow-up Analysis of Lung Nodules from 3D CT Images"
- [9] Armato SG et.al., "Computerized detection of pulmonary nodules on CT scans"., Radiographics 1999, 19(5):1303-11.
- [10] A.Prabin, DR. J.Veerappan., "Automatic Segmentation Of Lung Ct Images By Cc Based Region Growing"., Journal of Theoretical and Applied Information Technology October 2014. Vol. 68 No.1.
- [11] Khin Mya Mya Tun., "Feature Extraction and Classification of Lung Cancer Nodule using Image Processing Techniques"., International Journal of Engineering Research & Technology (IJERT) ISSN: 2278-0181
- [12] Cambron N. Carter., "CAD system for lung nodule analysis"., Thesis and dissertations, University of Louiseville.
- [13] Bhavanishankar .K and Dr. M.V.Sudhamani., "Techniques for Detection of Solitary Pulmonary Nodules in Human Lung and their classifications -A Survey"., International Journal on Cybernetics & Informatics (IJCI) Vol. 4, No. 1, February 2015.
- [14] Q. Gao, S.Wang, D. Zhao, and J. Liu, "Accurate lung segmentation for X-ray CT images", in Proceedings of the 3rd International Conference on Natural Computation (ICNC '07), vol. 2, pp. 275-279, 2007.
- [15] P. Campadelli, E. Casiraghi, and D. Artioli, "A fully automated method for lung nodule detection from postero-anterior chest radiographs", IEEE Transactions on Medical Imaging, vol. 25, no. 12, pp. 1588-1603, 2006.
- [16] Mickias Assefa et al., "Lung nodule Detection Using Multi Resolution Analysis", proc. IEEE, International Conference on Complex Medical Engineering, ICME, pp.457-461, 2013.
- [17] Takahiro Miyajima et al., "Classification of Lung Nodules Temporal Subtraction Image Based on Statistical Features and Improvement of Segmentation Accuracy", proc. 12th IEEE International Conference on Control, Automation and Systems, Jeju Island, Korea, pp.1814-1817, 2012.
- [18] M.V. Sprindzuk et al. "Lung cancer differential diagnosis based on the computer assisted radiology: The state of the art", Polish journal of Radiology, Pol J Radiol, 75(1): 67-80, 2010.
- [19] World health organization Cancer: www.who.int/gho/ncd/mortality_morbidity/cancer/en

AN OVERVIEW OF TURBOCODES

Jeena Thomas¹, Ranjitha C R¹, Indrasena N V²

¹PG Scholar, ²Assistant professor,

Dept.of Electronics & Communication, Thejus College of Engineering

¹Email: ttjeena@gmail.com

Abstract— This paper focus on the various encoding and the decoding schemes of turbo codes and representing various design parameters of the turbo coding scheme. Turbo code is one of the high performance forward error correction codes used in communication systems, it offers the performance nearer to the Shannon limit. The commonly using Turbo encoder is parallel concatenated recursive systematic convolutional encoders separated by an input output mapping device is known as an interleaver. Similarly the Turbo decoding can be done using different algorithms. BCJR algorithm is the commonly used decoding algorithm for Turbo codes. This paper proposes a brief study about the different decoding algorithms such as Viterbi algorithm, BCJR algorithm, SOVA algorithm, Log-map decoding algorithm.

Keywords— Turbo encoder, Turbo decoder, Interleaver, RSC code, BCJR algorithm, Viterbi algorithm, SOVA algorithm.

INTRODUCTION

Error-control codes, also called error-correcting codes or channel codes, are the key component of digital transmission system. Channel coding is obtained by providing controlled redundancy into the transmitted digital sequence. Turbo codes is the new class of high-performance forward error correction (FEC) codes, and which is the first practical codes closely approach to the channel capacity. The Turbo code has the capacity nearer to the Shannon limit. Shannon limit is the theoretical maximum information transfer rate of the channel. A basic 1/3 rate turbo code is obtained by the parallel concatenation of two 1/2 rate recursive systematic convolutional encoder separated by an interleaver. There are two kinds of convolutional codes ; non-systematic convolutional (NSC) and recursive systematic convolutional (RSC) codes. By combining the turbo code with a multi-level modulation the spectral efficiency of turbo coded systems can be increased [12]. The turbo coded systems, which are spectral efficient can be classified into two. They are the non-binary turbo code combined with a multi-level modulation and the other one is the coded modulation (CM) with the binary turbo code. The recursive systematic convolutional codes are the main component of Turbo Codes. Those are based on Linear Feedback Shift-Registers (LFRS) and act as pseudorandom scramblers. There are several parameters affect the performance of turbo codes such as component decoding algorithms, number of decoding iterations, generator polynomials, constraint lengths of the component encoders and interleaver type. For a concatenated scheme, the Turbo decoding algorithm should not limit itself to passing hard decisions among the decoders then the turbo code work properly. The initially proposed turbo codes were parallel concatenated convolutional codes (PCCC).Then, the serial concatenated convolutional codes (SCCC) and the hybrid concatenated convolutional codes (HCCC) were proposed.

TURBO CODE ENCODER

Turbo code is one of the high performance forward error correction codes used in communication systems, it offers the performance nearer to the Shannon limit. It is the first practical codes, which closely approach the channel capacity. The general form of Turbo encoder involves two recursive systematic convolutional (RSC) encoders separated by an interleaver. These two encoders used are normally identical and it is said to be symmetrical. If the modulo sum of two valid code words resulting a valid codeword which is known as linear codes. The Turbo code is a linear code. A linear code is said to be 'good' if that has high-weight codewords.

A. Parallel Concatenated ConvolutionalCodes (PCCC)

Turbo-codes is also known as parallel-concatenated recursive systematic convolutional code [1]. The Turbo code has the parallel structure, in which recursive systematic convolutional (RSC) codes working in parallel is used to create the "random" versions of the message.

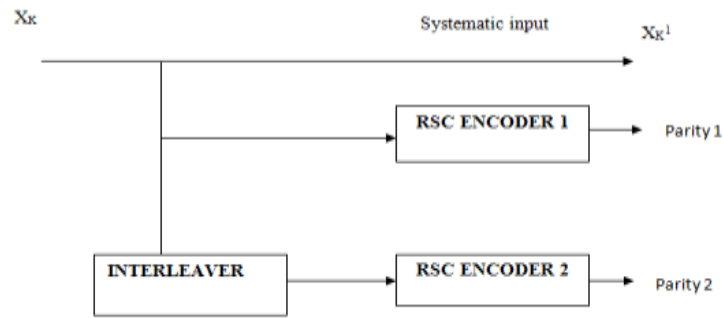


Fig 1: Turbo encoder [1]

Usually two parameters are used to describe convolutional codes that are code rate 'r' and constraint length 'k'. So that code rate can be expressed as 'k/n'. The state information of the convolutional encoder is stored by using the shift registers. In order to avoid the excessive decoding complexity RSC encoder with short constraint length is considered. The RSC encoder can be created from the conventional non-recursive non-systematic convolutional encoder by feeding back one of its encoded output to its input.

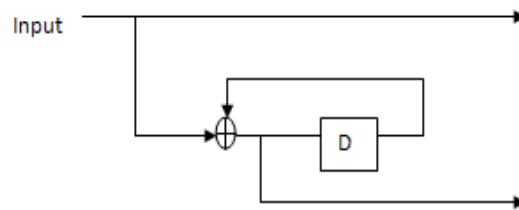


Fig 2: Recursive Systematic Convolutional Encoder[2]

The recursive systematic convolutional encoder tends to produce higher weight code words. So that it is well suitable for turbo codes as compared to non-recursive systematic convolutional encoders.

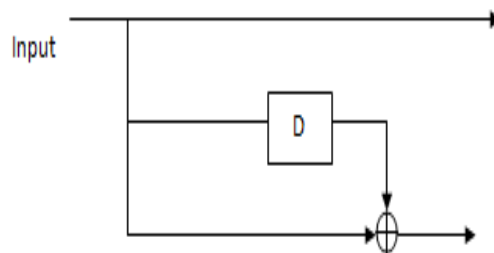


Fig 3: Non-recursive Systematic Convolutional Encoder[2]

Two or more RSC codes, each with a different interleaver is involved in the parallel structure. Interleaver is a device, which permutes the data sequence in some predetermined order. The codeword is formed by considering only one of the systematic outputs from the two component encoders. The systematic output from the other component encoder is the permuted version of the systematic output, which is already selected. A bit-error probability of 10^{-5} is obtained using a rate 1/2 code over an additive white Gaussian noise (AWGN) channel. Recursive systematic convolutional code [2], which has a feedback path that adds the content of the shift register to the input bit. At low signal to noise ratio it offers better performance. Interleaver is an input output mapping device, which change the positions of the bits in each block of data before it enters the second encoder. So the encoder input is not correlated. The interesting property of the RSC code is only a small fraction of finite weight information sequence gets low redundancy coded sequences at the encoder's output. [6].

For high data rates longer interleavers are used. Long interleavers [2] introduce long delays for lower data rates. The BER performance improved with the interleaver size increases is known as interleaver gain. In order to maximise interleaver gain parallel concatenated convolutional codes are use recursive convolutional encoders. For every input information bit, the PCCC outputs a three-

bit code word that consists of the systematic bit, and the parity bits, which are generated using the two recursive systematic convolutional encoders. The selection of choice of component codes and interleaver type are the key parameters considering in the performance of a turbo code. RSC code has an infinite impulse response but in the NRC code the impulse response is finite. Because of this RSC code and NRC code has different minimum weight input. The main factor in the designing of convolutional codes is the constraint length. The constraint length is measured as the number of memory elements plus one.

B. Serial Concatenated Convolutional Codes (SCCC)

In SCCC have the outer code and the inner code which is separated by using the interleaver. As a result decoupling takes place at the output of encoder from the input of the inner encoder [2]. A rate 1/3 SCCC that is formed by the rate 1/2 outer code, which is the non-recursive convolutional (NRC) code, and the rate 2/3 inner code, which is recursive convolutional (RC) code.

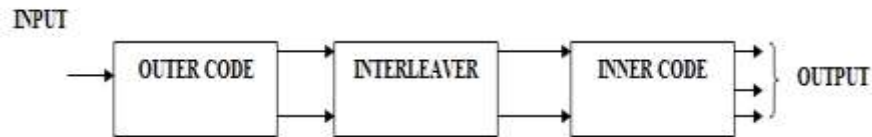


Fig 4: Serial Concatenated Convolutional Codes (sccc) [2]

Parallel concatenated convolutional codes perform better for high BER values. While or low BER values SCCC's perform very well. This performance varies depending on the interleaver size. The performance of an SCCC improves with increasing the interleaver size. For an SCCC to attaining an interleaver gain, a recursive inner encoder must be used. To maximize this interleaver gain the NRC outer code is necessary.

C. Hybrid Concatenated Convolutional Codes (HCCC)

It is the combination of PCCCS and SCCC's. HCCC's become SCCC's without upper branch [3] and it becomes PCCCS without outer code. The disadvantage of HCCC is that they introduce significant amount of delay. For low coding rates HCCC's are known for better performance. Because of using two encoders and one interleaver, the decoding delay is significant. So that HCCC's provide good performance for extremely high data rates, in which the resulting delay is tolerable. The Turbo code depends on several factors such as memory size, generating polynomials, number of decoding iterations, interleaver type and interleaver size [13].

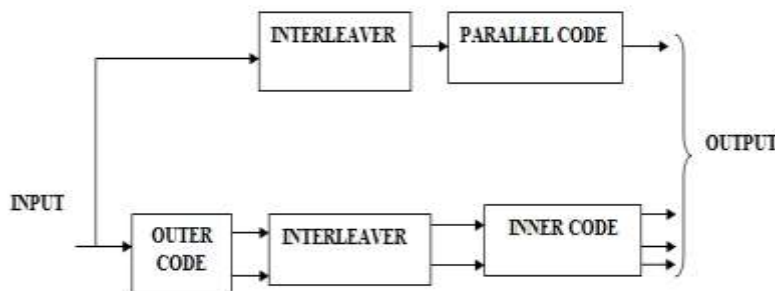


Fig 5: Hybrid Concatenated Convolutional Codes (hccc) [2]

TURBO DECODERS

Decoding of convolutional code in the turbo code can be done by passing soft information from one decoder to the next. The Turbo decoder [7] comprises of two serially interconnected soft-in soft-out (SISO) decoders. The decoding takes place on the noisy versions of systematic bits and two sets of parity bits to produce an estimate of original message bits. There are two kinds of decoding algorithms, soft output viterbi algorithm (SOVA), which is proposed by Hagenauer and Hoher based on the Viterbi algorithm and the BCJR algorithm proposed by Bahl, Cocke, Jelinek and Raviv.

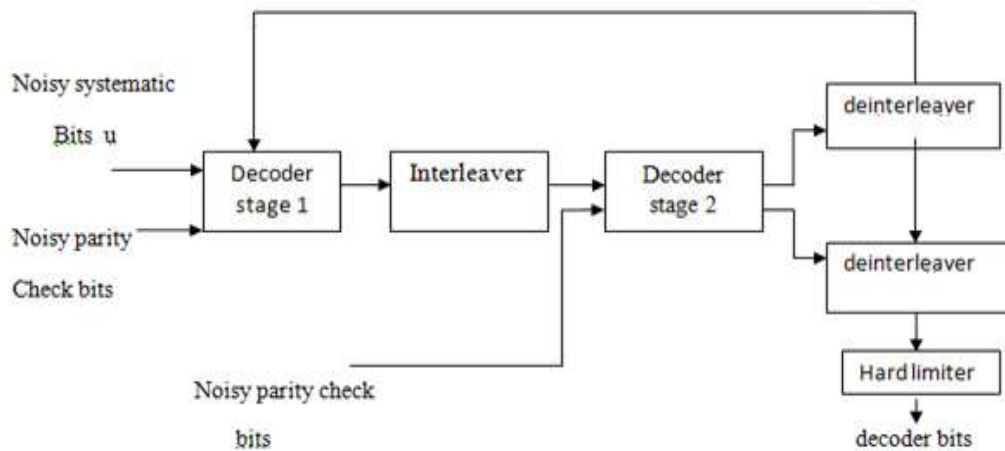


Fig 6: Turbo decoder [7]

For decoding of turbo codes different types of algorithms are available [3]. The trellis-based estimation is the base of each of the algorithm and is classified into two types. They are sequence estimation algorithms and symbol-by-symbol estimation algorithms. Sequence estimation algorithms can be classified as Viterbi algorithm, SOVA (soft output Viterbi algorithm) and improved SOVA.

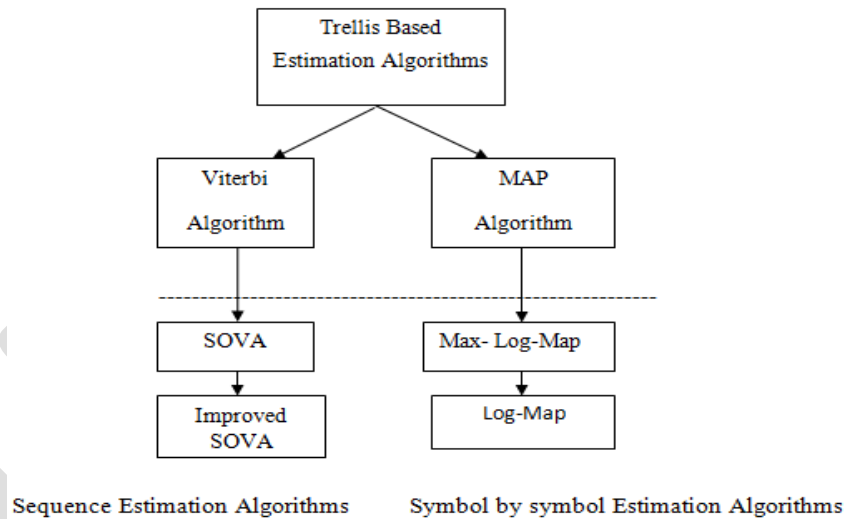


Fig 7: Decoding algorithms for Turbo codes [4]

Symbol-by-symbol estimation algorithms are classified as the MAP algorithm, Max-Log-Map and the Log-Map algorithm. Sequence estimation algorithms are less complex than symbol-by-symbol estimation algorithms. The BER performance of the symbol by symbol algorithm is much better than the sequence estimation algorithms. The algorithms namely The MAP, SOVA, LOG-MAP, MAX-LOG-MAP, improved SOVA produces soft outputs [4]. Viterbi algorithm is a hard-decision output decoding algorithm and the SOVA is soft-output producing Viterbi algorithm. Maximum a-posteriori algorithm, is named as BCJR algorithm, which is an optimal decoding technique for linear codes that minimizes the probability of symbol error. This is in contrast to the commonly used Viterbi algorithm. The maximum length sequence estimation (MLSE) is the principle of the viterbi algorithm. The Viterbi algorithm reduces the sequence (or word) error probability.

A. BCJR ALGORITHM

The BCJR algorithm is implemented to solve the maximum a posteriori probability detection problem, which is a soft input soft output decoding algorithm with two recursions that is forward and backward both involve soft decisions invented by Bahl, Cocke, Jelnek and Raviv. The viterbi algorithm is an algorithm, which operates on the principle of the maximum likelihood decoding. The maximum likelihood decoder, which examine received sequence and detect a valid path which has the smallest hamming distance from the received sequence. The viterbi algorithm is a soft input hard output algorithm, in which only the forward recursion involving soft decisions is possible. The BCJR algorithm is more complex than the viterbi algorithm because of backward recursions.

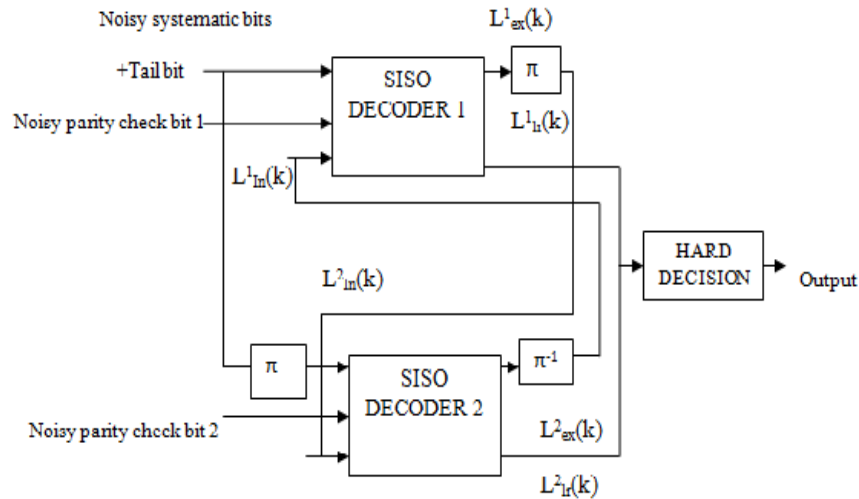


Fig 8: Structure of a Turbo Decoder based on either SOVA or the BCJR Algorithm [8]

In decoding section the received sequence is partitioned into three, that are systematic bits, and parity check bits 1 and 2 [8]. Here the systematic bits, parity check bits 1 and a priori information, which is taken from SISO Decoder 2 is taken as the input to SISO Decoder 1 and the decoder 1 outputs extrinsic information and the log likelihood ratio as a result of estimation of a bit sequence by use of SOVA. SISO Decoder, which produces a-posteriori information by decoding a-priori information. Systematic information, parity information and a priori information are the inputs to the SISO Decoder.

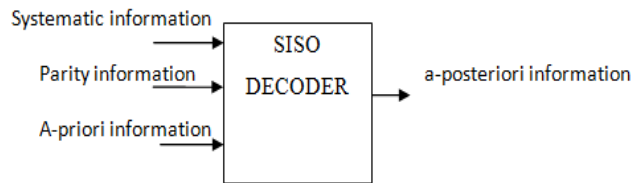


Fig 9: Structure of the SISO Decoder [8]

Consider $u = (u_1, u_2 \dots u_N)$ be the information bits represented by the binary random variables. In the case of systematic encoders, one of the outputs $x_s = (x_{s1}, x_{s2} \dots x_{sN})$ is similar to the information sequence u and the next is the parity information sequence output $x_p = (x_{p1}, x_{p2} \dots x_{pN})$. In the MAP decoding scheme [4], the decoder decides whether $u_k = +1$ or $u_k = -1$, which depends on the sign of the log-likelihood ratio (LLR). In the case of radix-2 trellises the log domain computations of the BCJR algorithm can be separated into three main categories that are branch metric computation, forward / backward metric computation and combination of forward and backward state metrics.

The interleaved version of the extrinsic information is provided as an input to decoder 2, where it is used as a priori information and the decoding is performed together with an interleaved version of the systematic bits and the parity check bits. SISO decoder 2 – also based on SOVA like SISO decoder 1, which outputs extrinsic information and a log likelihood ratio. For a second iteration the SISO decoder takes the deinterleaved version of extrinsic information and the log likelihood ratio and is used as a-priori information in SISO decoder 1. Two LLR outputs after the number of iterations are used to make a hard decision. In the case of BCJR decoding of a convolutional turbo encoder 8 to 10 iterations are conducted.

B. VITERBI DECODING ALGORITHM

The viterbi algorithm was introduced in 1967. The maximum likelihood decoding of convolutional codes can be executed by using this algorithm [8]. This algorithm works by rejecting the less likely paths and keeping the most likely path through the trellis in each node. A hard decision on the transmitted sequence means that the path selection leaves with a single path in the Trellis. By using this algorithm the maximum likelihood sequence can be found. At the early point of the decoding process, loss of valuable information takes place due to the hard decision making. a- priori information the viterbi algorithm accepts the soft-inputs in the form of but it

does not produce soft-outputs. By using the encoders Trellis diagram viterbi algorithm works as maximum likelihood sequence estimator. So that it selects a path with the highest likelihood by looking all possible sequences Trellis diagram.

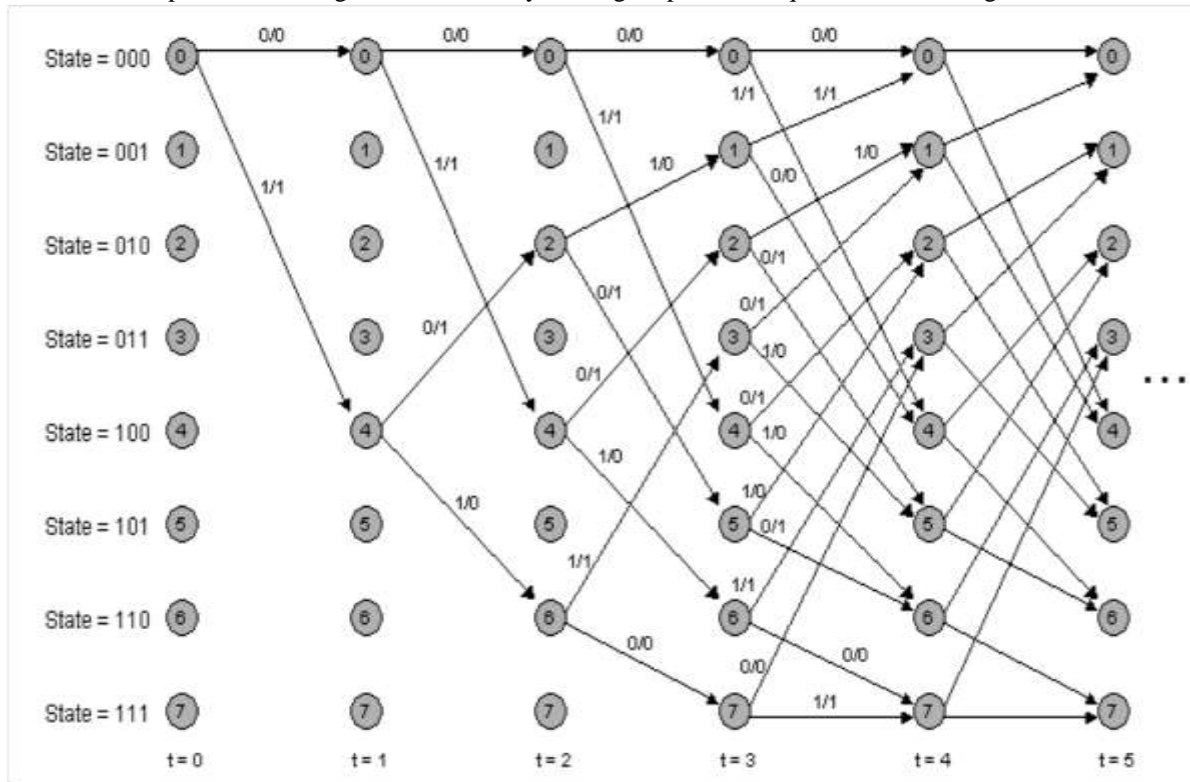


Fig 10: Trellis Diagram for one 8 State Constituent Encoder [8]

It finds which path has the highest likelihood by considering the Hamming distance between incoming bits and possible transitions in the encoder (or Trellis) as a metric. The BCJR algorithm, which produces a soft estimate for each bit by considering the incoming bits as a maximum a- posteriori probability (MAP) detection problem. But the viterbi algorithm finds the most likely sequence and instead of maximizing the likelihood function for each bit it estimates several bits at once. So BCJR algorithm has the best performance than the Viterbi algorithm. Consider a constituent encoder with its trellis diagram, at which several possible paths are available. The amount of memory required to calculate the all possible paths is very large. So to reduce the amount of memory viterbi introduces paths through the Trellis diagram with smallest Hamming distance are known as survivor paths. Consider K is the constraint length of the encoder that is the encoders memory plus one ($K = M+1$), the Viterbi only takes 2^{K-1} survivor paths. The Viterbi algorithm works well on the small frames on the Trellis diagram. So for each iteration, decision of the best path is calculated. The decoding window moving forward through the branch and depends on the code in the Frame new decisions are made.

C. SOVA ALGORITHM

SOVA algorithm is proposed by Hangenauer and Hoehner 1989. It is a modified form of Viterbi algorithm [3]. The reliability of bit sequences or the a- posteriori probabilities of the state transitions are produced by this algorithm. There are two major modifications used from the Viterbi algorithm to SOVA, those are the maximum likelihood path selected by path metrics is modified and the algorithm is modified to provide soft output to every decoded bit. At low Signal to noise ratio SOVA's estimation of probability is good. This algorithm has higher similarities to the viterbi algorithm except some modifications like computing the transition and bit reliabilities. If there is a difference between two path metrics then the reliability of bits is updated. In addition to the most likely path sequence, a reliability value of each estimated bit is calculated using this sub-optimum algorithm. In the SOVA algorithm the soft output is updated by considering two path sequences, which is named as survivor and concurrent path sequences. Several modifications are done to improve the SOVA algorithm. That is the normalisation of the extrinsic information is takes place by multiplying using a correcting factor, which depends on the variance of the decoder output and by inserting two or more correcting coefficients the correlation in the decoder input is achieved.

D. ITERATIVE TURBO DECODING

In the first iteration consider the first component decoder. The decoder receives the transmitted systematic bits, and the parity bits, from the first encoder [4]. Half of the parity bits must be punctured at the transmitter to obtain the half rate code. For the punctured bits the turbo decoder must insert zeros in the soft channel output. Then the soft channel inputs are processed by the first component decoder to produce its estimate of the conditional LLRs of the data bits. Consider u_k be the input information bit, The a-posteriori log likelihood ratio in the first iteration from the first component decoder is represented by using $L_{11}(U_k / Y)$. The first component decoder will have no a-priori information about the bits in the case of first iteration [12]. The channel sequence containing the interleaved version of the received systematic bits, and the parity bits from the second encoder received by the second component decoder. In the case of Turbo decoder, if the parity bits generated by the encoder are punctured before transmission it will need to insert zeroes in to this sequence. Decoder can use the conditional LLR provided by the first component decoder to generate a-priori LLRs. extrinsic information from the component decoder is used as the a-priori LLRs in iterative turbo decoder. Then arrange the decoded data bits after being interleaved by the same order as they were encoded by the second encoder. At the end of the first iteration the second component decoder uses the received channel sequence and the a-priori LLRs to produce its a-posteriori LLRs. Then the first component encoder again processes its received channel sequence at the second iteration. When iterative process is continues average the BER of the decoded bits will fall.

D. LOG MAP DECODING ALGORITHM

The MAP decoding algorithm and the LOG MAP Decoding algorithm [9] is based on the same idea. But the benefit of this algorithm is it simplifies the computation by discarding the multiplicative operations. The multiplicative operations, which is computationally more expensive by comparing it in to the addition operations in terms of the processing speed of the microprocessor. The implementation of this algorithm is very difficult that is to store the probabilities in the computation of the log-likelihood ratio it needs large amount of memory. The decoder structure used in this algorithm is shown in below, where Λ_2 , Λ_1 represents the a-priori information and Λ_{1e} , Λ_{2e} represents the a-posteriori information.

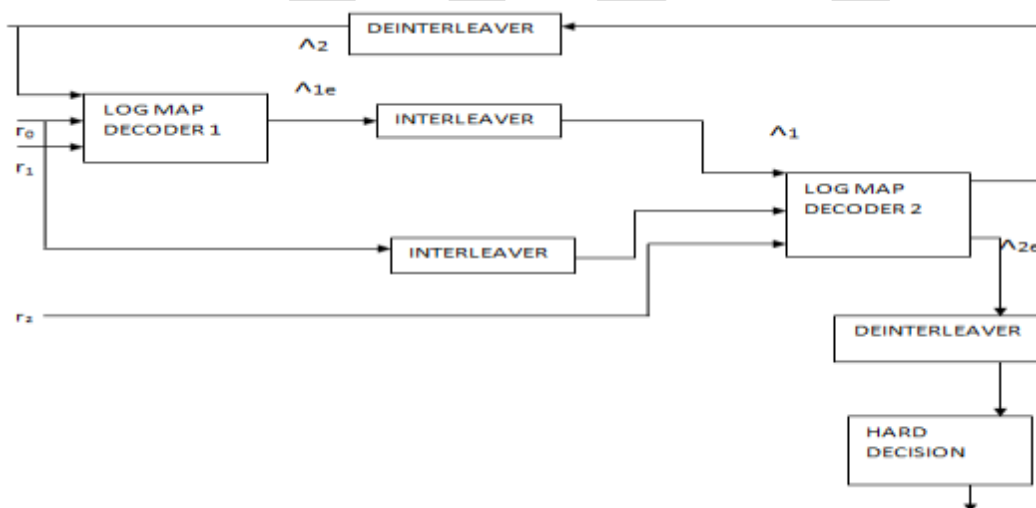


Fig 9: Log-MAP algorithm [9]

CONCLUSION

The Turbo code is a high performance forward error correcting code. The forward error correction is capable of locating the positions, where the errors occurred and which is corrected. The Turbo code has the parallel structure, in which Recursive systematic convolutional (RSC) codes working in parallel is used to create the “random” versions of the message. Two or more RSC codes, each with a different interleaver is involved in the parallel structure. Then the details about the serial concatenated convolutional code and the hybrid concatenated convolutional code are also described. Turbo decoding is takes place on the noisy versions of systematic bits and two sets of parity bits to produce an estimate of original message bits. The Log-MAP algorithm has high performance as compared with soft output viterbi algorithm decoding scheme ie, MAP decoding scheme takes an approximation from this SOVA decoder. So that MAP algorithm gets superior performance than the soft output viterbi algorithm.

REFERENCES:

- [1] Raffi achiba mehrnaz mortazavi booz,allen & hamilton, inc mclean, virginia william fizell “Turbo code Performance and Design Trade-offs” miltatcom jteo falls church, virginia. 0-7803-6521-6/\$10.(0c0) 2 000 ieee.
- [2] Sarpreet Singh, Rupinder kaur “Techniques for Turbo Decoding Using Parallel Processing, Comparative Analysis” International Journal of Advanced Research in Computer Science and Software Engineering.
- [3] Poonam, Mr. Bhavneesh Malik, Mr. Gaurav Kochar. “ A Review on Turbo Codes using Different Algorithms” International Research Journal of Engineering and Technology (IRJET).
- [4] Jason P. Woodard and Lajos Hanzo. “Comparative Study of Turbo Decoding Techniques: An Overview” ieee transactions on vehicular technology, vol. 49, no. 6, november 2000.
- [5] Claude Berrou, Ramesh Pyndiah, Patrick Adde, Catherine Douillard and Raphaël Le Bidan. “An Overview of Turbo Codes and Their Applications” GET/ENST Bretagne, Laboratoire TAMCIC (UMR CNRS 2872), PRACom Technopôle Brest Iroise.
- [6] Simon haykin. “Communication Systems” fourth edition, john wiley&sons inc.
- [7] Jesper Kjeldsen. “Turbo Coding” Aalborg University Institute for Electronic Systems.
- [8] Prathyusha Allala. “Genetic Optimization of Turbo Decoder” the School of Electrical Engineering and Computer Science and the Russ College of Engineering and Technology.
- [9] Rupinder kaur, Sarpreet Singh. “Parallel Processing Based Turbo Decoder Design using Viertibi Algorithm” International Journal of Application or Innovation in Engineering & Management (IJAIEM).
- [10] A. Burr. “Turbo-codes: The Ultimate Error Control Codes” electronics & communication engineering journal august 2001.
- [11] Guido montorsi. “Unveiling Turbo codes: Some Results On Parallel Concatenated Codes” conference paper · october 1995.
- [12] Sorin adrian barbulescu. “Iterative Decoding of Turbo codes and other Concatenated Codes” The school of electronic engineering faculty of engineering university of south Australia.

A survey on secure and energy efficient LEACH protocol

Rashim Rana Er. Anoop Arya
(Pursuing M. Tech, CSE) (Assistant Professor, CSE)
Maharishi Ved Vyas Engineering College, Kurukshetra University

rashimrana02@gmail.com, +91-8572088409

Abstract— WSN is a network in which sensor nodes are placed in an area so that physical information like military surveillances, transport monitoring, habitat monitoring, etc can be gathered. These sensor nodes sense the data and send it to the B for evaluation for which the data aggregation is done. The data aggregation is achieved by using LEACH routing protocol. LEACH protocol is clustering algorithm which is self organizing in nature and form clusters on the basis of the signal strength of the sensors. In this paper, the WSN and security requirements for secure data aggregation are studied. Also the LEACH protocol with its phases and various attacks on LEACH are studied. In this paper techniques for energy efficiency is also apply. Thus, the research in this paper is based on WSN, its security requirements, its energy efficiency, LEACH, LEACH attacks and its effect on WSN.

Keywords— Wireless sensor network, base station, Low-Energy Adaptive Clustering Hierarchy, Time division multiple access, Cluster head, carrier sensing multiple access, medium access control.

INTRODUCTION

The Wireless sensor networks is an infrastructureless and highly distributed network in which small lightweight wireless nodes are present. In this sensor nodes are independent and power limited sensing devices which are deployed in the region to sense different types of physical information from the environment[9].

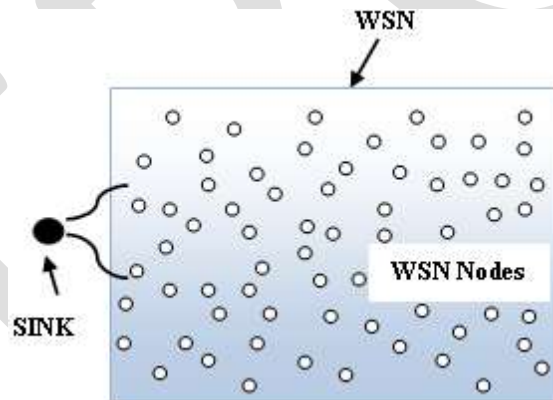


Figure 1: Illustration of WSN Network [8]

Sensors are having the ability to communicate through wireless channels and the energy computational power and memory are constrained in the sensors. The environmental data is monitor by the WSN this is the major application of the WSN. WSN transmit this data to the central node which is called as the sink node. The sink node initiate some specific action on the basis of analyzed data. The sink node analyse the data and compute the minimum or maximum or computation of average. Either sink node or network analyse the data. Every sensed data is transmitted to the sink node if analysis is carried out at that node. The required aggregate is computed by sink node when it received the data from all the node. This method is used for aggregating the data and it is called All-Node data aggregation scheme. In this approach if the amount of transmitted data increases then the consumption of energy also increases. The over all lifetime of WSN increases the aggregated data amount in the network.

In data aggregation scheme the neighboring node send the information to the aggregator node which compute the aggregate and send the aggregated data to the sink node. The number of transmission reduces and the bandwidth and energy utilization is improving by the the data aggregation. There are some security issue are present. The security in data aggregation is achieve by the secure data aggregation[2]

Sensor node energy consumption is affected by the routing protocol. Three routing protocols of wireless sensor network are :

a). Flat Based Routing Protocol:

The same role and functionality in transmitting and receiving data is play by all the nodes. In this the selection of specific set of sensor nodes to be queried is very typical due to lack of global identification with random deployment of sensor nodes. The query is send to different part of the field by base station and wait for result data from only selected parts of field. This method is called data centric routing.

b). Hierarchical Routing Protocol:

Different roles are assign to the node in this network like members of cluster, cluster head etc.This routing is mainly consider as two layer architecture in this one layer responsible for cluster head selection and other for the routing.

c). Location Based Routing Protocol:

The location tell the address of the sensor node. The signal strength give the estimate about the distance between the nodes. In this some location based scheme demand that the nodes go to the sleep mode if they are not doing any activity for saving the energy.

Hierarchical-based routing protocols are avoid redundancy and they are the best. In this network energy is used efficiently and lifetime and scalability is enhanced. In this protocol, nodes are making the clusters in which higher energy nodes are used to process and forward the data, while other nodes can be used to sense the data. Data aggregation and fusion for reducing the size of transmitted message for the base station is done by cluster head[8]

Security Requirements

In this section of secure data aggregation two types of confidentiality requirements are considered.

1. Generic Confidentiality : The content of data is not access by the sensor node and they are not participate in the data aggregation.
2. End-to-End confidentiality : Sensors actively participating to the aggregation mechanism do not access the data that is already aggregated.

Network Model

In this we consider a network which consist of small devices and a sink node.The two type of nodes are present in this sensor nodes (SN-nodes) they senses the actual data and Aggregator nodes (AG-nodes) they are responsible for sending queries and combining answers which are send by the children and a message is forward to the parent which contains the intermediate aggregation result of the queries and their answers.The organization of nodes in the form of m-ary tree. The tree structure is as shown in fig. 1 In Fig.1. S_0, S_1, \dots, S_{2m} are sensing nodes and SG_1, \dots, SG_m are aggregating nodes, where l is the level of the node in the tree. The root of the tree is calles sink node[2].

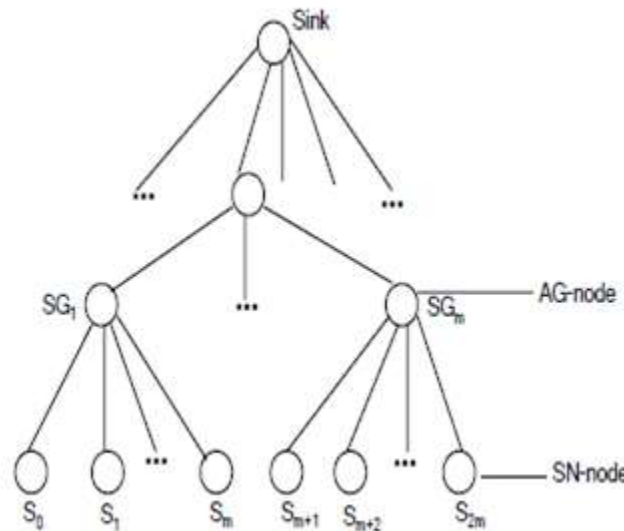


Figure 2: Tree structure of nodes in the network. In each level K nodes are present. Nodes of leaf level are sensing nodes(SN-N odes) and others are aggregated nodes(AG-Nodes).

LEACH (Low-Energy Adaptive Clustering Hierarchy)

A dynamic hierarchical clustering algorithm for sensor networks is called Low Energy Adaptive Clustering Hierarchy (LEACH) is introduced by Heinzelman, *et al.* This is a protocol, which is cluster based and in which distributed cluster formation is done. LEACH selects some sensor nodes as cluster-heads randomly and this role is rotated for equal distribution of the energy load among the sensors in the network. In LEACH the data is compressed by the cluster head which is upcoming from nodes of the same cluster and an aggregated packet is send to the BS by the cluster head for reducing the amount of information that is send to the BS. TDMA/Code division multiple access MAC is used for reducing inter-cluster and intra-cluster collisions. Randomized rotation of cluster head is conducted after a given interval of time for obtaining uniform energy dissipation in the sensor network.[10]

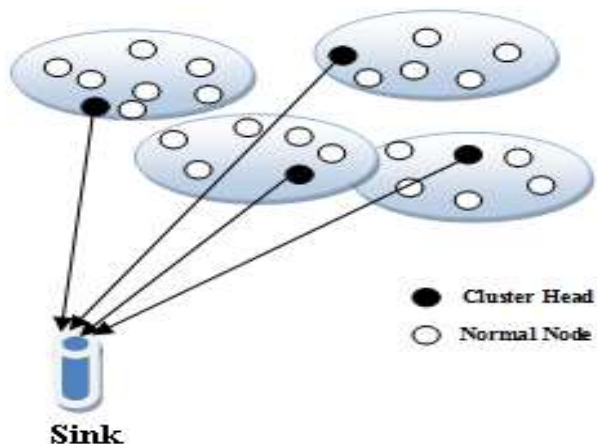


Figure 3: LEACH Routing Topology[8]

LEACH protocol operation is split into two phases:

- □ Setup phase
- □ Steady phase

Setup phase

The set-up phase organize the cluster and select the cluster-heads. At the starting each node is independent of the other nodes . A number is generated by each sensor node which is called random number such that $0 < \text{random} < 1$ and this number is compares with a pre-defined threshold $T(n)$. The sensor node becomes cluster-head for that round if the $\text{random} < T(n)$, else it becomes cluster. The threshold is given $T(n)$ below:

$$T(n) = \begin{cases} P & \text{if } n \in G \\ \frac{1}{1 - P(r \bmod (1/P))} & \text{else} \end{cases}$$

Where,

P is the probability of the node being selected as a CH.

r is the number of rounds.

G is the set of nodes that haven't been CH in the last $1/p$ rounds \bmod denotes modulo operator.

The next $1/p$ rounds are not select those nodes which are selected as a cluster head in the previous r rounds. When CH is selected the CH use a CSMA MAC protocol for broadcasting an advertisement message to its neighbours which are placed in the new cluster head. The join-request message which contain the IDs of the nodes is send by using CSMA for joining with the cluster which snd the strongest strength signal to the nodes. The TDMA schedule is set up by the CH for data transmission coordination in the cluster and propogate it to its cluster members.The collision is prevented between data messages by TDMA scheme and TDMA also conserves energy between non cluster head nodes. At that point all nodes know their TDMA slots and steady state phase is started.

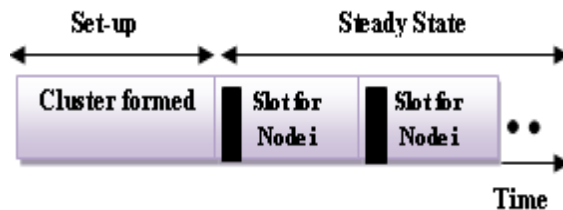


Figure 3: Period of LEACH [8]

Steady State Phase

In this phase the surrounding sense by the cluster members and sensed data is transmit to their CH on the basis of the TDMA schedule which is received in the setup phase. For saving the energy for other slots the sensor node go to the sleep mode. When all the data is received by the CH which is send by its cluster members. The CH compute the aggregated data and send this aggregated data to the BS. After some time the network is go back to the setup phase for entering to the next round. In the next round the CH selection is occure.

ATTACKS ON LEACH

Some of the Attacks on LEACH are as follows.

a). Selective forwarding attack

The message is faithfully forward to the destination by the node. Certain messages are not forward by the malicious node . The malicious node drop the message and ensure that the message is not reach to the intended destination. This attack is called selective forwarding attack.

b). Sybil attack

In a Sybil Attack, the multiple identities of a node to other nodes in the sensor networks is shown by the malicious node. By creating new false identities of the nodes or stealing identities of other nodes in the network this attack is done. In this a single node may be used many times. This attack causes many affects like consuming energy,increasing traffic,packet dropping, reducing network life time etc

c). Hello flood attack

The HELLO packets are send by the sensor nodes to the neighbours for alerting them about the attack. These packets are send only with in the transmission range. But an attacker some times sends the flood of false HELLO packets. After receiving the packets from an attacker the nodes consider that the attacker is suited inside the transmission range but in actual it is far away from the nodes. In this the nodes transmit the messages unnecessarily and reduces their energy.

LITERATURE SURVEY

Wendi B.Heinzelman.et.al(2002) When we set hundreds or thousands of cheap microsensor nodes in a network they allows users for combining the data from the individual nodes by accurately monitoring a remote environment. In this network robust wireless communication protocols are required which are energy efficient and provide low latency. In this paper, the author develop a protocol architecture called LEACH for microsensor networks that combines the idea of both media access and energy-efficient cluster-based routing with application-specific data assembling for the achievement of good performance in terms of latency, system lifetime and application-perceived quality. A new distributed cluster formation technique in LEACH is used that enables self-organization of numbers of nodes, rotating cluster head positions for even distribution of the energy load among all the nodes and algorithm for adapting cluster. Author's results show that the system lifetime improve by LEACH by an order of magnitude compared with general-purpose multihop approaches[1].

A.S.Poornima. et. al (2010) In WSN large number of nodes are consist of with limited communication capabilities, sensing and computation. In such network resource constrained nodes are present and transmission of data in this is a energy-consuming operation. By reducing the number of bits transmitted on a network the lifetime of a network is increased. The data aggregation method is used for reducing the data transmission. The issues of security such as confidentiality , data integrity and freshness in data aggregation become essential When the WSN is deployed in a remote or hostile environment where sensors are prone to node failures. For achievement of security in data aggregation we use secure data aggregation schemes. In this paper the author propose a Secure Data Aggregation scheme which provides end-to-end data privacy. In this 30%-50%. of the average number of bits transmitted are reduced [2].

Abderrahim Beni Hssane.et.al(2010) In WSN for increasing the lifetime and scalability of a network we can use a clustering algorithm. In this paper, the author propose a Position-Based Clustering (PBC). algorithm in this algorithm he evaluate a distributed energy-efficient clustering algorithm for heterogeneous WSNs. PBC is an improvement of LEACH-E. The ratio between the remaining energy of network and residual energy of each node give the probabilities on the basis of that probabilities the PBC elected the cluster heads. In this 2 level hierarchy is used by selecting a intermediate node for the data transmission. Moreover, in this a new technique is used for cluster formation which not only based on the received signal strength of the cluster head's advertisement but also on its position. The lifetime of the whole network is increased by this algorithm and in performs it is better than LEACH, LEACH-E and SEP [3].

Mortaza Fahimi Khaton Abad.et.al(2011) Research on WSN has received much attentive as they offer an advantage of monitoring different kinds of environment by sensing physical phenomenon. The important application of the sensor network applications are scalability, Prolonged network lifetime and load balancing. For achieving these goals cluster sensor nodes technique is used. In this paper the author introduce an LEACH based energy efficient clustering algorithm for sensor networks. WSN uses LEACH which is the most popular cluster-based structures. TDMA and MAC both are used by LEACH for balancing the energy consumption. The proposed protocol integrated some feature to LEACH for reducing the consumption of energy in each round. The result of proposed work shows a significant reduction in network energy consumption compared to LEACH[4].

Tripti Sharma.et.al(2012) WSN is the network in which power-limited sensing devices are present these are called sensors. These sensors spread in a region for sensing different types of information which is present in the environment. The considerable amount of energy is dissipated when these sensors sense and transmit data to other sensors nodes which are present in the network. In this paper, F-MCHL is propose which is a homogeneous energy protocol. In LEACH protocol on the basis of threshold values clusters are formed; whereas, in the proposed protocol we use fuzzy logic approach for electing the cluster-head based on two form - energy and proximity distance. The master cluster head is elected out of the previously elected cluster heads. Master cluster head is having the maximum residual energy if the energy is low so it is not called as a master cluster head. In conventional LEACH all cluster heads are send the aggregated information to the BS but in the proposed protocol only master cluster head is used for sending the information to the BS. Simulation results on MATLAB shows that this proposed protocol provides better stability period, higher energy efficiency and lower instability period as compared to LEACH protocol. Results obtained shows that an suitable Master cluster-head election can enhance the lifetime of the network and reduce the energy consumption[5].

Mona El_Saadawy.et.al(2012) Security solutions for WSN are not developed easily due to the dangerous nature of wireless medium and limited availability of resources in WSN. The encryption/decryption algorithms are the most essential part of the secure communication and their implementation is very intricate in WSNs. since they integrated routines that having very complex and intense computing procedures. In WSN the designing of a secure clustering protocol that achieves the desired security goals while keeping an acceptable level of energy consumption is a very challenging task. LEACH protocol is a basic clustering-based routing protocol for WSNs. S-LEACH is the modified version of LEACH which protect against the outside attack by using cryptographic technique. This paper proposes MS-LEACH for enhancing the security of S-LEACH by offering data confidentiality and node to CH authentication by using pairwise keys which is shared between their cluster members and the CHs. MS-LEACH has efficient security properties and achieves all goals of the WSN security. The result shows that the protocol accomplish the in demand security goals and perform better than other protocols in terms of energy consumption, network[6].

Baiping Li.et.al(2012) A WSN is a group of sensor nodes which are able for monitoring different types of environments for applications that include biological detection, home security, diagnosis and machine failure. For long period of time the gathering of sensed information in an energy efficient manner is not easy in the sensor network. In WSN the amount of data transmitted between sensor nodes and the base station is reduced by the help of data fusion. The LEACH protocol is best solution for data collection problem, where formation of small number of clusters are done in a self-organized manner. On the basis of LEACH protocol, a low energy-consumption chain-based routing protocol LEACH-CC is proposed. In the new protocol each node will send information about its energy level and current location to the BS for its characterization. The simulated annealing algorithm is run for determining the clusters for that round. Then a chain routing is set between clusters for decreasing the amount of nodes which communicate with the BS. Finally, the results show that LEACH-CC performs better and it not only extends the lifetime of the network, but also improves the energy efficiency[7].

Alisha Gupta.et.al(2013) Encryption schemes which are operated over ciphertext are of extreme importance for WSN & specially in LEACH protocol. Energy is the salient limit of LEACH. Due to this limitation, the designing of a confidentiality scheme for WSN is important by doing this the sensing data can be transmitted to the receiver efficiently and securely and at the same time energy consumed must be minimum. Hence the author proposed LEACH-HE in which homomorphic encryption is added to LEACH protocol. The homomorphic encryption is the confidentiality scheme in LEACH-HE. In this encryption technique algebraically aggregation of data is occur. The decryption of data is not occur hence energy consumption is less. In this proposed work results are obtained in terms of three forms - amount of data transmitted, total energy consumed and number of nodes alive. The performance of LEACH_HE is somewhat similar to LEACH[8].

Muneer Alshowkan.et.al(2013) Working with WSN is a challenging task because in this many challenges are present such as the limited resource in processing power, energy and storage. The security maintenance in WSN is a challenging task due to presence of

limited energy. The aim of the paper is reducing the power consumption and improving the current security mechanisms in WSN. The energy routing protocol is provided by LEACH and it do not cover the security requirements. Alternatively, this paper aims to design LS-LEACH (Lightweight Secure LEACH) which is more secure and energy efficient routing protocol. Authentication algorithm is added to this for assuring authenticity, data integrity and availability. Furthermore, this paper shows the improvement over LEACH protocol which make it more secure and tell how the energy efficiency is increased [9].

Mayur S.et.al(2015) Hierarchical routing protocol is used by many application in WSN for routing of the sensed data to the sink, LEACH is one of those application and it is the first and most widely used hierarchical distributed clustering protocol in WSN. Security is the most important factor in WSN because they are prone to intrusion and different types of network attack. The joining of nodes in a cluster head on the bases of Received Signal Strength (RSS) of HELLO packets which are received from CHs making it susceptible to HELLO Flood attack. HELLO Flood attack is detected by either cryptographic approach this approach is less suitable in terms of battery power and memory or non cryptography approach the packet are sending for detection which increases communication overhead as the energy needed for transmission of packet is more than the energy needed for processing. In this author proposed a detection scheme for HELLO Flood attack on the basis of cryptography and non cryptography solutions. The no. of transmission of test packets is reduced in this paper and in this location dependent key(LDK) management scheme is used which provides the security[10].

CONCLUSION OF SURVEY

The literature above reviewed can be concluded as:

Author and year	Work	Technique	Conclusion
Wendi B. Heinzelman 2002	Design Application Specific Protocol for WSN	WSN	The high performance which is needed under the tight constraints of the wireless channels are provided by LEACH
A.S.Poornima 2010	Securing the End-to-End Data Aggregation in WSN	Aggregation scheme and homomorphic encryption	In the SEEDA protocol the no. of bits which are transmitted are reduced from 30%-50%.
Abderrahim Beni Hssane 2010	Design Position-Based Clustering protocol for An Energy-Efficient Clustering Hierarchy for Heterogeneous WSN	Heterogeneous WSN model, Radio energy dissipation model, LEACH	PBC provides better use and optimization of energy dissipation in the network.
Mortaza Fahimi Khaton Abad 2011	LEACH Algorithm is modify for WSN	Clustering	The network energy of modified LEACH is high and the Dead nodes in modified LEACH is less.
Tripti Sharma 2012	Design Fuzzy Based Master Cluster Head Election Leach Protocol in Wireless Sensor Network	LEACH ,LEACH-C,CHEF	In this stability period is extended and energy is well distributed. In this the cluster are well separated from each other.
Mona El_Saadawy 2012	Security of S-LEACH is enhanced for WSN	Use cryptography with S-LEACH	MS-LEACH is better in terms of average power consumption, average work lifetime,average network throughput and average normalized routing load.
Baiping Li 2012	Study LEACH Protocol and apply add some new techniques for its improvement	LEACH, Radio Energy Model for LEACH-CC, LEACH-Centralized with Chain	In LEACH-CC the distribution of energy load among the nodes increase quality and the lifetime of the network. If the size of network increases the further improvement by LEACH-CC are shown.
Alisha Gupta 2013	Implement the LEACH protocol by using homomorphic	Homomorphic encryption	In LEACH protocol if we add homomorphic encryption the protocol become more secure. The no. of bits

	encryption		transmitted are same in both LEACH_HE and LEACH. Hence by these performance parameters we conclude that adding homomorphic encryption to LEACH donot degrades the performance.
Muneer Alshowkan 2013	Design a new secure and Energy Efficient Routing Protocol for WSN	LEACH, clustering and data aggregation	The, network life time, system throughput and the total energy consumption of the network become better after improving the LEACH protocol.
Mayur S 2015	Security of LEACH Protocol is enhanced from HELLO Flood Attack in WSN Using LDK Scheme	Location Dependent key	The performance of the network is improved by the proposed work. In this detection time and energy for detection are less used. In this work LEACH function smoothly in the HELLO Flood Attack.

CONCLUSION

In this paper the WSNs are studied and the various security concerns related to WSNs are also studied. The LEACH protocol and attacks on this are studied. The methods of security on LEACH are studied. The alternative solutions for security and energy efficiency are : In LEACH protocol if we add homomorphic encryption the protocol become more secure and this technique donot degrades the performance. The position based clustering protocol provides better use and optimization of energy dissipation in the network. The network energy of modified LEACH is high and the Dead nodes in this is less. For making the networking more secure and energy efficient we can use any of the given techniques as given in the paper and some other techniques are also available we use these as per the requirement.

REFERENCES:

- [1] Wendi B. Heinzelman, "An Application- specific Protocol Architecture for Wireless Microsensor Networks" IEEE TRANSACTIONS ON WIRELESS COMMUNICATIONS, VOL. 1, NO. 4, OCTOBER 2002.
- [2] A.S.Poornima, B.B.Amberker, "SEEDA : Secure End-to-End Data Aggregation in Wireless Sensor Networks" IEEE 2010.
- [3] Abderrahim Beni Hssane, Moulay Lahcen HASNAOUI, Mostafa SAADI, "Position-Based Clustering: An Energy-Efficient Clustering Hierarchy for Heterogeneous Wireless Sensor Networks" International Journal on Computer Science and Engineering Vol. 02, No. 09, 2010.
- [4] Mortaza Fahimi Khaton Abad , Mohammad Ali Jabraeil Jamali, "Modify LEACH Algorithm for Wireless Sensor Network" International Journal of Computer Science Issues, Vol. 8, Issue 5, No 1, September 2011 ISSN (Online): 1694-0814
- [5] Tripti Sharma , Brijesh Kumar, " F-MCHEL: Fuzzy Based Master Cluster Head Election Leach Protocol in Wireless Sensor Network" International Journal of Computer Science and Telecommunications Vol. 3, Issue 10, October 2012.
- [6] Mona El_Saadawy, Eman Shaaban, " Enhancing S-LEACH Security for Wireless Sensor Networks" IEEE 2012
- [7] Baiping Li, Xiaoqin Zhang, "Research and Improvement of LEACH Protocol for Wireless Sensor Network" International Conference on Information Engineering Lecture Notes in Information Technology, Vol.25, 2012
- [8] Alisha Gupta , Vivek Sharma, " Implementation of LEACH Protocol using Homomorphic Encryption" International Academy of science, Engineering and technology
- [9] Muneer Alshowkan, Khaled Elleithy, Hussain AlHassan, "LS-LEACH: A New Secure and Energy Efficient Routing Protocol for Wireless Sensor Networks" 17th IEEE/ACM International Symposium on Distributed Simulation and Real Time Applications.

[10] Mayur S, Ranjith H.D, “Security Enhancement on LEACH Protocol From HELLO Flood Attack in WSN Using LDK Scheme”
International Journal of Innovative Research in Science, Engineering and Technology (An ISO 3297: 2007 Certified Organization)
Vol. 4, Issue 3, March 2015

[11] Vikas Nandal and Deepak Nandal, “Maximizing Lifetime of Cluster-based WSN through Energy-Efficient Clustering Method”:
IJCSMS Vol. 12, Issue 03, September 2012

[12] Meenakshi Diwakar and Sushil Kumar., “Energy Efficient Level Based Clustering Routing Protocol For Wireless Sensor Networks” IJASSN, Vol 2, No.2, April 2012

IJERGS

Harnessing Piezoelectricity from Various Mechanical Stresses at Different Surroundings

Pranjali Uday Rakhe¹

Parul Singh²

¹Department of Electrical Engineering, Sardar Patel College of Engineering, Mumbai, Maharashtra, India
prakhe.95@gmail.com, +91 9021011477

²Department of Electrical Engineering, Sardar Patel College of Engineering, Mumbai, Maharashtra, India
parulsingh2102@gmail.com, +91 7738288501

Abstract— In our age, depleting natural resources have created a thirst to look for alternate sources of energy. Piezoelectricity is one such pragmatic solution to our energy crisis. In our paper, we will be discussing the applications of piezoelectricity in various surroundings. The exhibition of mechanical stress on a piezoelectric crystal produces some voltage which is capable of driving low power electric equipment. A responsive sub-flooring system made up of blocks that depress under the force of foot traffic if installed at public places, can power display boards and lights at public places such as railway and bus stations, cinema halls and so on. Piezoelectricity can also be incorporated to drive devices in offices, homes and gyms. This human powered electricity generation when coupled with efficient storage systems will give rise to a reliable source of energy which can be utilized whenever required. By harnessing energy from piezoelectric crystals, humans will be made aware of their contributions to the environment by helping produce a steady supply of energy from piezoelectric elements.

Keywords— Piezoelectricity, mechanical stress, vibration, crystal, pressure, renewable energy, electricity.

1. INTRODUCTION

The world's supply of fossil fuels is large, but finite. With each passing day, exhaustible energy sources are depleting resulting in the urge to look for alternative sources such as wind energy, hydro-power, solar energy, piezoelectricity, etc. Piezoelectricity is one such form of energy which is easy to harvest and can be installed easily at public places to harness electricity. Piezoelectricity is the development of electric charge produced by the application of mechanical stress on a piezoelectric crystal. It is the linear electromechanical interaction between the electrical and mechanical state in crystalline materials that do not exhibit symmetry. Electricity harvested from piezoelectric crystals may not be enough to power high voltage appliances, but such form of electricity can act as supplementary power sources such as batteries, lamps, display systems, radio, etc. In this paper, we will be describing the application of piezoelectricity at public places to power appliances at these places.

2. WORKING PRINCIPLE

Many materials exhibit piezoelectricity. Some are naturally occurring whereas some are chemically synthesized. Quartz, Berlinite (AlPO_4), Sucrose, Rochelle Salt, Topaz, mineral macedonite (PbTiO_3), bone, silk, wood, enamel, DNA are some naturally occurring piezoelectric materials. Barium titanate (BaTiO_3), lithium niobate (LiNbO_3), potassium niobate (KNbO_3) are some synthetic ceramics exhibiting piezoelectricity. Piezoelectric crystals do not exhibit symmetry. Such crystals are electrically neutral. When a mechanical force is applied on a piezoelectric crystal, the structure is deformed, pushing some atoms closer or farther, thereby upsetting the balance of positive and negative charge. Hence net electrical charges appear on opposite, outer faces of the crystal. In the following section, we have described the different sources from where piezoelectricity is harnessed. Further on, we have proposed a new idea which can be used in this field.

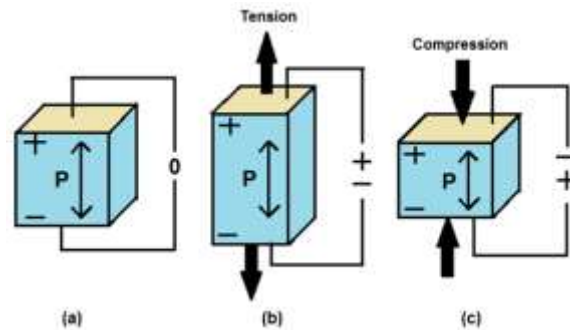


Fig.1. Piezoelectricity generated when the piezoelectric crystal is deformed

3. APPLICATIONS OF PIEZOELECTRICITY (PRE-EXISTING WORK)

3.1. RAILWAY STATIONS

The floorings at railway stations in Tokyo and Shibuya in Japan have piezoelectric ceramics embedded within. The electricity developed is used to power the energy-hungry parts of the station such as the electrical lighting system and the ticket gates.

3.2. HIGHWAYS

Vehicular traffic produces vibrations which can easily generate ample amount of electricity via piezoelectric materials laid underneath the road. This electricity produced can power the automatic gates and display systems at the toll booths.

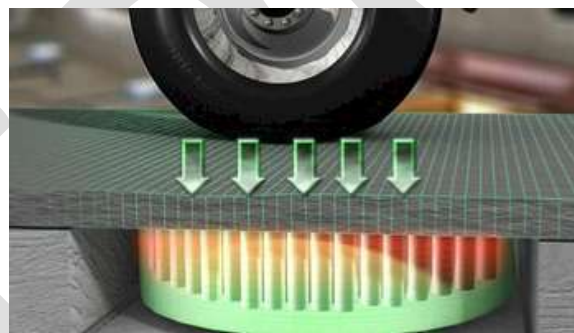


Fig.2. Pressure exerted by vehicular traffic activating piezoelectric crystals

3.3. FLOORINGS

Door mats, tiles and floors of sidewalks can have piezoelectric crystals underneath. The pressure exerted by people walking on them can be stored in capacitors acting as supplementary storage during power shortage. The energy generated via pedestrian traffic weight on sidewalks is used to power the lights along the roads.

3.4. GYMS

The treadmills at gyms can have piezoelectric crystals under the belt. When a person works on the treadmill, his weight along with vibrations can produce sufficient mechanical stress on the piezoelectric crystals so as to produce enough energy to power iPads or any other form of display systems in front of the treadmill.

3.5. DANCE CLUBS

In London, a dance club has incorporated piezoelectric crystals in its floorings. The impact of the foot movements by those using the dance floor is powerful enough to generate sufficient electricity so as to power the lights at the club.

4. PROPOSED WORK

4.1. PIEZOELECTRICITY POWERED STUDY LAMPS

A person sitting on the chair of study tables will produce sufficient mechanical stress so as to produce electricity that will power the lamp on the table. Once the person gets up, the stress acts no more, thereby turning off the lamp when not in use.

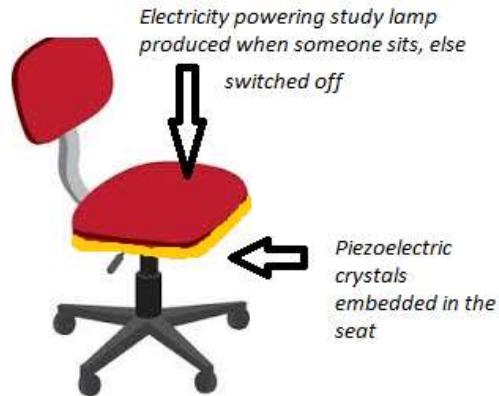


Fig.4. Piezoelectricity powered study lamp

4.2. VEHICLE METERS POWERED BY PIEZOELECTRICITY

Auto-rickshaw and taxi meters can also be powered using piezoelectricity. Piezoelectric ceramics when embedded underneath the driver's seat can act as a responsive system. When the driver is seated, his weight will turn on the meter. The electricity produced can be stored in capacitors which can be used when the driver is not in his seat and the meter is still running.

4.3. PIEZOELECTRIC LIFTS

The weight exerted by lift users can produce enough stress to compress the embedded piezoelectric material and power digital displays. Assuming that, on an average, 2 people are always in the lift the time delay is also drastically reduced. Furthermore, during peak office hours, more people will use lifts leading to more power output, which can then be stored for later usage.

The following table describes the weight requirements and its corresponding wattage for the production of piezoelectricity from the application of human weight. The power outputs described in the table can be used to drive the vehicle meters, lamps and display systems. From this table, it can be estimated that if an average person weighing around 55 kgs, sits on the piezoelectric chair, he will produce 0.065 watts/sec and time taken to light up a 9 Watt CFL will approximately be 2 minutes 30 seconds. Also, the minimum requirement for small voltage digital displays is 1-2 watts. Hence time required to power the digital display system will be from 15.38 second to 30.7 seconds.

Calculation:

0.065 watts/sec for 55 kgs.
To light up a 9-13 watt CFL, time required will be $9/0.065 = 2.307$ minutes;
 $13/0.065 = 3.33$ minutes

Weight (in kgs)	Power (in watts)
40	0.05
45	0.055
50	0.06
55	0.065
60	0.07
70	0.08
75	0.09

Table.1.Power output for corresponding weight

To light up a low power digital display, time required will be $2W/0.065=30.7$ secs and $1W/0.065=15.38$ secs. Assuming that there are two people in a lift, approximate weight inside the lift is now 100 kgs. Power produced will be 0.12 watts. Therefore time delay is:

Max=16.66secs (2/0.12) Min=8.33 secs (1/0.12)

To avoid this time delay in the lighting up of bulb, it can be noted that a person can use the chair when not using the bulb or the vehicle. The electricity generated from the piezoelectric chair during this period can be stored in lithium metal hydride batteries. This stored electricity can be in turn used during the initial time, before the system lights up on its own via real time piezoelectricity production.

5. OUTPUT OBTAINED FROM PIEZOELECTRIC MATERIALS

It has been observed from pre-existing experiments that power output from a single piezo-film was in the range of $0.2\mu W$. The direct application of a piezo-film as a power source is not practical. The outputs from a single piezo-film can produce a root-mean-squared voltage of 1.18V which is high enough to be stored in a nickel metal hydride battery. After the rechargeable battery charged up completely, it was discharged through a load of 10 kΩ for 1 hour. During this discharging period, the current measured maintained at 760 mA and the potential difference across the resistor was 1.2V which is nearly equal to a power of 0.9 watts. The output obtained from a piezoelectric crystal is an alternating signal. In order to make this signal usable for low power devices it has to be first converted into digital signal. This is done by using AC to DC converter. It consists of a simple diode rectifier. This is followed by a capacitor, which gets charged by the rectifier to a predefined voltage. At this point, the switch closes and the capacitor discharges through the device.

6. INCREASING THE PRODUCTIVITY

Power obtained from a single piezoelectric material is very low. To increase the productivity of the piezoelectric materials, they can be placed in series or parallel. However, series connection of piezoelectric materials is preferred over the parallel, as the series connection increases the voltage output of the system.

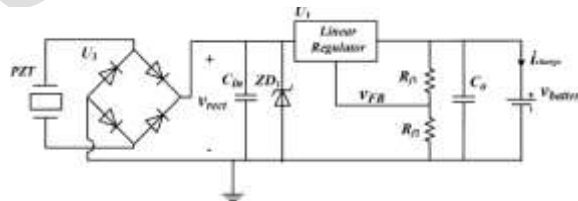


Fig.5. AC to DC converter used to harvest energy from a piezoelectric material

7. LIMITATIONS

Although piezoelectricity has its own advantages, there are some limitations that can be incurred during installation. The piezoelectric sheets have stress-strain limits. A sheet can be stretched to a strain of approximately 500 microstrain (micrometers per meter) in regular use. Higher surface strains can be achieved, but the statistics of survival get worse. Also, the initial costs of installation of the entire piezoelectric circuit are high owing to the high costs of AC to DC converters used. These converters are manufactured primarily by countries like USA and Germany and their costs range from 30-35\$. In the foreseeable future it is expected that India will start producing its own AC to DC converters which will reduce the installation costs drastically.

8. FUTURE PROSPECTS

The field of piezoelectricity is still in its infancy. Studies are going on to use the properties of piezoelectric materials in various fields. Some of the proposed concepts that can be used are:

8.1. BRIGHT WALK

A design for a pair of shoes has been proposed that is equipped with piezoelectric devices. It utilizes kinetic energy generated while walking and converts it into usable electrical energy.

8.2. P-ECO ELECTRIC VEHICLE

P-Eco is a car design proposed by some designers. It describes a car which runs on piezoelectric batteries. The vibrations produced by the car will act as mechanical stress for the piezo-elements thereby feeding power to the car. Besides these proposed applications, several other models have been developed such as hearing aids for the deaf, self-powering tablets, self-heating piezoelectric shower that works without consuming electricity, etc. Piezoelectricity is a promising field as it provides sufficient energy for low power sources in an eco-friendly way.

8.3. USE AT CRYOGENIC TEMPERATURES

Researchers are studying the use of piezoelectric crystals at cryogenic temperatures (near zero Kelvin). Since piezoelectricity functions on the basis of electric dipoles, these dipoles remain unaffected by changes in temperature. Hence this quality of piezoelectric materials can be used in the extremely cold parts of the world.

9. CONCLUSION

This paper presents the usability of piezoelectricity in various surroundings such as public places. The advantages of piezoelectric materials are more than its limitations, hence it is expected that this field will witness in-depth research to exploit its advantages. Although most of the applications of piezoelectric effect have been proposed, two new applications have been mentioned that can be tested and put to use. By using piezoelectric materials at public places, people can be made aware of their contributions to the society and can hence, be encouraged to use this eco-friendly, cost effective and efficient method of electricity generation.

REFERENCES:

- [1] Jedol Dayou, Man-Sang, C. Dalimin, M.N. and Wang S., "Generating electricity using Piezoelectric material" Borneo Science, 24 March 2009, Pg 47-51.
- [2] Kim Diamond, "Breakthroughs in Piezoelectric Power: Raising Public Awareness is a Step in the Right Direction for U.S. Sustainable Development", April 17 2009, Energy Pulse, Energy Central.
- [3] Tanvi Dikshit, Dhawal Srivastava, Abhijeet Gorey, Ashish Gupta, Parag Parandkar and Sumant Katiyal, "Energy harvesting via Piezoelectricity", BIJIT-BVICAM's International Journal of Information Technology (July-December 2010), Pg 265-270.
- [4] J. Ryall, "Japan harnesses energy from footsteps", The Telegraph, 12 December 2008.
- [5] Kiran Boby, Aleena Paul K, Anumol.C.V, Josnie Ann Thomas, Nimisha K.K, "Footstep Power Generation using Piezoelectric transducers", Dept of EEE, MACE, Kothamangalam.
- [6] Roundy S., Wright P. K. and Rabaye J., "A. study of low level vibrations as a power source for wireless sensor nodes", Computer Communications 26 (2003) 1131– 1144.
- [7] Y. C. Shu and I. C. Lien, "Analysis of power output for piezoelectric energy harvesting systems", Smart Materials and Structures 15 (2006), pp. 1499-1512.

[8] Steven R. Anton and Henry A. Sodano, "*A review of power harvesting using piezoelectric materials*", (2003- 2006), *Smart Materials and Structures* 16 (2007).

[9] Zhong Lin Wang, Xudong Wang, Jinhui Song, Jin Liu, and Yifan Gao, "*Piezoelectric Nanogenerators for Self-Powered Nanodevices*", Vol. 7, No. 1 January–March 2008, *IEEE Pervasive Computing*, Computer Society.

IJERGS

A brief study on LDPC codes

¹Ranjitha CR,¹ Jeena Thomas,² Chithra KR

¹PG scholar,² Assistant professor, Department of ECE, Thejus engineering college
Email:cr.ranjitha17@gmail.com

Abstract: Low-density parity-check (LDPC) codes are a class of linear block LDPC codes. The name comes from the characteristic of their parity-check matrix which contains only a few 1's in comparison to the amount of 0's. This paper represents LDPC code characteristics, encoding and iterative decoding approaches to achieve channel capacity. Low-density-parity-check codes have been studied a lot in the last years and large progresses have been made in the understanding and ability to design iterative coding systems. The transmission quality is basically concerned with the probability of bit error at the receiver with respect to communication. This is an attempt to obtain highest capacity with minimum error rate by implementing modern codes named as LDPC (Low Density Parity Check codes). At the present time, LDPC codes has received a superior interest because of the error correction performance and world wide applications.

Keywords: LDPC, Encoding, Decoding, Construction, Tanner graph, Hard decision decoding, Soft decision decoding

INTRODUCTION

Error correction codes are one of the widely using tools available for achieving reliable data transmission in communication systems. For a wide variety of channels, the Noisy Channel Coding Theorem of Information Theory proves that the probability of decoding error can be made to approach zero exponentially with the code length if properly coded information is transmitted at a rate below channel capacity. It has been over 70 years since Claude Shannon published his famous "A Mathematical Theory of Communication", the foundation of the vast fields of channel coding, source coding and information theory, in which Shannon proved the existence of channel codes that are able to provide reliable communication as long as the code rate does not exceed the channel capacity. During the 1990s, the situation changed dramatically with the invention of Turbo Codes and the rediscovery of low-density parity-check (LDPC) codes, both of which have near-capacity performance. Coding schemes play an essential role in ensuring successful transmission of information, which is represented by a sequence of bits, from one point to another. In order to combat channel noise, coding strategy is devised that can construct codewords by adding redundancy to the transmitted bits, such that the original information can be perfectly decoded even with a certain number of errors. One of the most advanced classes of channel codes is the class of LDPC codes, which were first proposed by R.G Gallager in the early 1960s and rediscovered and generalized by MacKay et al. in the 1990s. As strong competitors to Turbo Codes, LDPC codes are well known not only for their near-capacity performance but also for their manageable decoding complexity[1]. More importantly, LDPC codes have some of the advantages of linear block codes, such as their simplicity and sparse (low-density) parity-check matrices which can be depicted as a graphical model called a Tanner graph (TG).

The name of LDPC code arrives from parity-check matrix concept which has only few one's when compared with zeros. Nowadays parallel architecture is also in use which will again increase the performance. Thus these codes are suited for implementation of current systems. The forward error correction codes are used more frequently on those days due to highly structured algebraic block and convolution codes. Nowadays LDPC codes are commonly used in Wi-max for microwave communications, CMMB i.e. china multimedia mobile broadcasting, Digital video broadcasting and for Wi-Fi standard. Low Density Parity Check (LDPC) codes gained significant research attention in current years due to their powerful decoding performance than turbo codes. All LDPC decoding algorithms are usually iterative in nature, so the performance and cost of using LDPC codes are partly determined by the choice of decoding algorithm. The decoding algorithm operate by exchanging messages between basic processing nodes. Design of power efficient LDPC encoders and decoders with low biterror rate (BER) in low signal-to-noise ratio (SNR) channels is critical for these environments.

REPRESENTATION OF LDPC CODES

The paper [2] explained, Low-density parity-check codes are error correction codes specified by a matrix containing mostly 0's and only a small number of 1's. Such a structure give both: a lower decoding complexity and good distance properties. Generally there are two methods to represent LDPC codes. Like all linear block codes they can be described via matrices and second method is a graphical representation. The parity check matrix is a $m \times n$ matrix with m number of rows and n number of columns. An example of parity check matrix is given in the figure 1.

$$H = \begin{pmatrix} 0 & 1 & 0 & 1 & 1 & 0 & 0 & 1 \\ 1 & 1 & 1 & 0 & 0 & 1 & 0 & 0 \\ 0 & 0 & 1 & 0 & 0 & 1 & 1 & 1 \\ 1 & 0 & 0 & 1 & 1 & 0 & 1 & 0 \end{pmatrix}$$

Figure 1: Example of parity-check matrix[2]

We can now define two numbers describing these matrix. A w_r for the number of 1's in each row and w_c for each columns. For a matrix to be called low-density the two conditions $w_c \ll n$ and $w_r \ll m$ must be satisfied. In order to do this, the parity check matrix should usually be very large, so the example matrix given above can't be really called low-density. The graphical representation of the above parity check matrix is given in the figure 2.

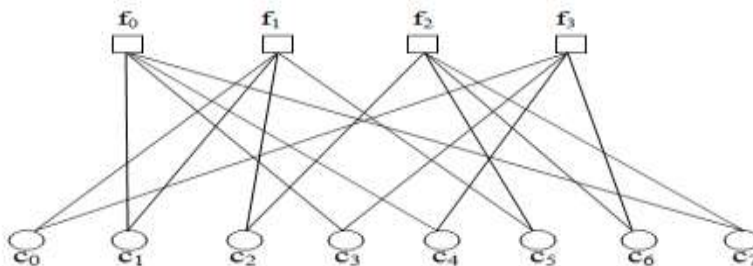


Figure 2. Tanner graph corresponding to the parity check matrix[2]

Tanner introduced an effective graphical representation for the LDPC codes. Tanner graphs are bipartite graphs. That means that the nodes of the graph are separated into two distinctive sets and edges are connecting nodes of two different sets[8]. The two types of nodes in a Tanner graph are called variable nodes (v-nodes) and check nodes (c-nodes). Considering the graph, there is no connectivity between C_0 and F_0 hence the first place is having 0,1 in the second place means that connectivity lies between F_0 and C_1 . Check nodes are specified as m nodes that are number of parity bits and variable nodes are n which are known as number of bits in code word.

If w_c is constant for every column and $w_r = w_c \cdot (n/m)$ is also constant for every row then the LDPC code is called a regular LDPC code. If H is low density but the numbers of 1's in each row or column are not constant the code is called an irregular LDPC code.

DIFFERENT ENCODING SCHEMES OF LDPC CODE

Encoding of codes, specially for higher block length codes can be quite difficult to implement in hardware but there are several methods for generating H such that encoding can be done via shift registers[7]. If the generator matrix G of a linear block code is known then encoding can be done using Parity check matrix H . The cost of the method depends on the Hamming weights i.e. the no of 1's in G . If the vectors are dense, then cost of encoding using this method is proportional to n^2 . If G is sparse then this cost becomes linear with n . Here note that by performing Gauss-Jordan elimination on H to obtain it in the form a generator matrix G for a code with parity-check matrix H which can be found as per following[3].

$$H = [A \quad I_{n-k}] \tag{1}$$

Where A is $(n-k) \times k$ binary matrix and I is the size $(n-k \times n-k)$ identity matrix. The generator matrix is then

$$G = [I_k \quad A^T] \tag{2}$$

The message can encode into code words for LDPC Codes which requires the generation of parity check matrix H . The encoding method is through the use of a generator matrix, denoted by G . A code word C is formed by multiplying source input u by the generator matrix which is represented as

$$C = u * G \tag{3}$$

The above explained method is the basic concept about the LDPC encoding. Many other methods are proposed by different authors to reduce the complexity of the LDPC encoding. Compared to turbo codes which is widely used in communication systems the main disadvantage of LDPC code is the complexity of encoding technique, in paper 'Efficient Encoding of Low-Density Parity-Check Codes'[11] by Thomas J. Richardson and Rüdiger L considered the encoding problem for LDPC codes specified by sparse parity-check matrices. The efficiency of the encoder arises from the sparseness of the parity-check matrix H and the algorithm can be applied to any (sparse) H . Although the example is binary, the algorithm applies generally to matrices H whose entries belong to a field F also assume that the rows of H are linearly independent. Assume given an $m \times n$ parity-check matrix H over F . By definition, the associated code consists of the set of n -tuples x over F such that

$$Hx^T = 0^T \tag{4}$$

Probably the most straightforward way of constructing an encoder for such a code is the following. By using Gaussian elimination H is converted to an equivalent lower triangular form as shown in Fig. 3.

n-m m

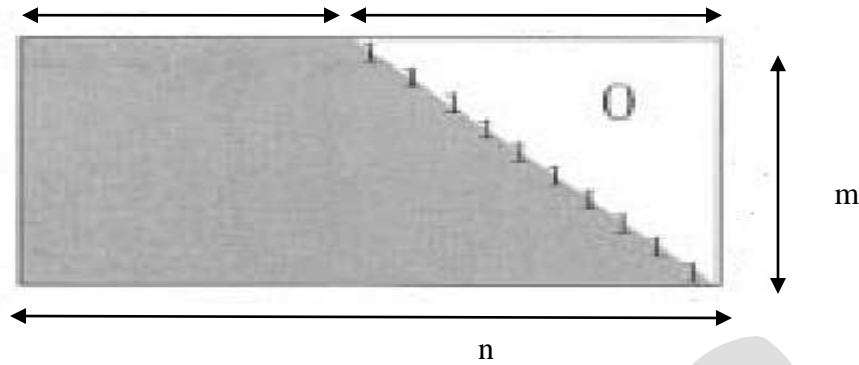


Figure .3. An equivalent parity-check matrix in lower triangular form.

Split the vector x into a systematic part s , $s \in F^{n-m}$ and a parity part p , $p \in F^m$ such that $x=(s,p)$. Construct a systematic encoder as follows:

- i) Fill s with the $(n-m)$ desired information symbols.
- ii) Determine the m parity-check symbols using back-substitution.

More precisely, for $l \in [m]$ calculate

$$P_l = \sum_{j=1}^{n-m} H_{l,j} s_j + \sum_{j=1}^{l-1} H_{l,j+n-m} p_j \quad (5)$$

The complexity of this scheme is Bringing the matrix H into the desired form requires $O(n^3)$ operations of preprocessing. The actual encoding then requires $O(n^2)$ operations since, in general, after the preprocessing the matrix will no longer be sparse.

The proposed encoder in this paper is motivated by the above example. Assume that by performing row and column permutations only we can bring the parity-check matrix into the form indicated in Fig. 4. We say that H is in approximate lower triangular form. Note that since this transformation was accomplished solely by permutations, the matrix is still sparse. More precisely, assume that we bring the matrix in the form

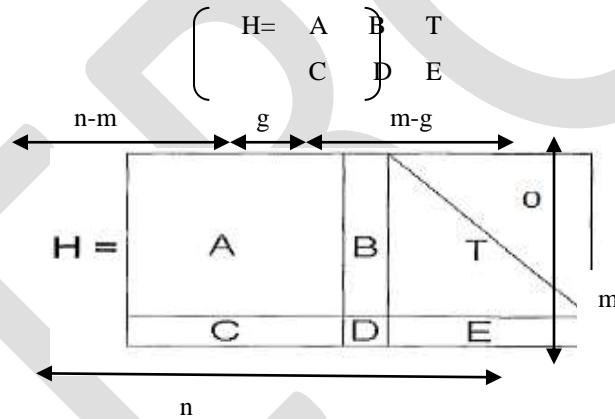


Figure 4. The parity-check matrix in approximate lower triangular form.

Where A is $(m-g) \times (n-m)$, B is $(m-g) \times g$, T is $(m-g) \times (m-g)$, C is $g \times (n-m)$, D is $g \times g$ and E is $g \times (m-g)$ matrices. Further, all these matrices are sparse matrices and T is lower triangular with ones along the diagonal. Multiplying this matrix from the left by

$$\begin{pmatrix} I & 0 \\ -ET^{-1} & I \end{pmatrix} \quad (6)$$

We get

$$\begin{pmatrix} A & B & T \\ -ET^{-1}A+C & -ET^{-1}B+D & 0 \end{pmatrix} \quad (7)$$

Let $x=(s,p_1, p_2)$ where s denotes the systematic part, p_1 and p_2 combined denote the parity part, p_1 has length g , and p_2 has length $(m-g)$. The defining equation $Hx^T=0^T$ splits naturally into two equations, namely

$$As^T + Bp_1^T + Tp_2^T = 0 \quad (8)$$

and

$$(-ET^{-1}A+C)s^T + (-ET^{-1}B+D)p_1^T = 0 \quad (9)$$

define $\Phi = -ET^{-1}B+D$ and assume for the moment that Φ is non singular. then

$$p_1^T = -\Phi^{-1}(-ET^{-1}A+C)s^T \quad (10)$$

Hence, once the $g \times (n-m)$ matrix $-\Phi^{-1}(-ET^{-1}A+C)s^T$ has been precomputed, the determination of can be accomplished in complexity $O(g \times (n-m))$ simply by performing a multiplication with this (generally dense) matrix. In the similar manner p_2 can also precomputed with less complexity. So the proposed system consist only two steps mainly, preprocessing and actual encoding. In the preprocessing step, we first perform row and column permutations to bring the parity-check matrix into approximate lower triangular form with as small a gap g as possible.

DIFFERENT DECODING SCHEMES OF LDPC CODES

There are different type of iterative decoding algorithms are used for decoding the LDPC codes. They are mainly classified as hard decision decoding and soft decision decoding respectively. The decision made by the decoder based on the received information is called a hard-decision if the value of bit can either be 0 or 1. If the decoder is able to distinguish between a set of values between 0 and 1, then it is called a soft-decision decoder[5]. The decoding of LDPC code is performed through iterative processing using the Tanner graph, to satisfy the parity check conditions. The condition $CH^T=0$ is the parity check condition, where C is the codeword and H is the parity check matrix. If $CH^T=0$ then the received codeword is said to be valid, that is the received code word is error free.

A. HARD DECISION DECODING

Bit flipping algorithm is the best example for hard decision decoding. In bit flipping decoding the message would be binary, different from belief propagation decoding. In belief propagation decoding the probabilities of incidence of the code word bits constitute the message. The message and the edges in the tanner graph are passed together in bit flipping algorithm. The message send by the message node contain the information that the bits available at the message node is zero or one to the check node. The check node returns a response message to the message node. This response is initiated by using the parity check equation which is based on the modular sum of bits available at the check node is equal to zero. Let the code word be $C = [11001000]^T$ and the received cord word $Y = [10001000]^T$. This implies error occurred in C . The fig.2 illustrate the tanner graph, used for the decoding algorithm. The steps involved in the bit flipping algorithm is given below. Explained in[2]

- Step1: All message nodes send a message to their corresponding check nodes connected to it. In this case, the message is the bit they believe to be correct for them. Here C_2 receives 0 (as per the codeword received Y) and it will send to f_1 and f_2 . Similarly all message nodes will send messages to their corresponding check nodes as illustrated in the table 1.
- Step 2: Every check nodes calculate a response to their connected message nodes using the messages they receive from step 1. The response from check node is calculated by using parity check equations which force all message nodes to connect to a particular check node to sum to 0 (mod 2). If sum of bits received is zero then the same bit which they received from the message node will send back. If it is not zero the the check node will flip the bit that received from message node and send back. Move to step 3.
- Step 3: The message nodes use the messages they get from the check nodes and they received from transmitter to decide if the bit at their position is a 0 or a 1 by majority rule. The message nodes then send this hard-decision to their connected check nodes. Table2 illustrate this step.
- Step 4: Repeat step 2 until either exit at step 2 or a assigned number of iterations has been passed.

Table 1: Overview of messages received and sent by the check nodes[2]

c-node	Activities
f_0	Received: $C_2=0$ $C_4=0$ $C_5=1$ $C_8=0$ Sent: $1-C_2$ $1-C_4$ $0-C_5$ $1-C_8$
f_1	Received: $C_1=1$ $C_2=0$ $C_3=0$ $C_6=0$ Sent: $0-C_1$ $1-C_2$ $1-C_3$ $1-C_6$
f_2	Received: $C_3=0$ $C_6=0$ $C_7=0$ $C_8=0$ Sent: $0-C_3$ $0-C_6$ $0-C_7$ $0-C_8$
f_3	Received: $C_1=1$ $C_4=0$ $C_5=1$ $C_7=0$ Sent: $1-C_1$ $0-C_4$ $1-C_5$ $0-C_7$

Table 2:Message nodes decisions for hard decision decoder.[2]

Message nodes	Y_1	Message from check node		Decision
C_1	1	$f_2=0$	$f_4=1$	1
C_2	0	$f_2=1$	$f_1=1$	1
C_3	0	$f_2=1$	$f_3=0$	0
C_4	0	$f_1=1$	$f_4=0$	0
C_5	1	$f_1=0$	$f_4=1$	1
C_6	0	$f_2=1$	$f_3=0$	0
C_7	0	$f_3=0$	$f_4=0$	0
C_8	0	$f_1=1$	$f_3=0$	0

The bit flipping algorithm can be classified and explained in the paper [12], ‘Hard decision and soft decision algorithms of LDPC and comparison of LDPC with Turbo codes, RS codes and BCH codes’.

Weighted Bit-Flipping Algorithm(WBF):

The WBF algorithm finds the most unreliable message node of each individual check. The magnitude the received value y_i determines the reliability of the hard decision z_i , the least reliable message node's magnitude for each individual check during the algorithm's first step is given by:

$$Y_m^{\min} = \min_{n \in N(m)} |y_n| \quad (11)$$

where $|y_n|$ denotes the absolute value, i.e., the magnitude of the n^{th} message node's soft value while Y_m^{\min} is the lowest magnitude of all message nodes participating in the m^{th} check. In the iterative WBF process, the bit sequence z obtained by hard decision is multiplied with the transpose of H matrix, and the resultant syndrome vector s is derived. For each message node at the position n , the WBF algorithm computes:

$$E_n = \sum_{m \in M(n)} (2s_m - 1) y_m^{\min} \quad (12)$$

where E_n is the error term, it is used to evaluate the probability that the bit position n would be flipped. Thus in the next step of WBF algorithm, the bit having highest error term E_n will be regarded the least reliable bit and hence flipped, i.e., flip the particular bit in z which has the highest error term E_n . The forgoing steps are repeated until an all zero syndrome vector is obtained.

Improved Weighted Bit-Flipping Algorithm (IWBF):

The WBF algorithm considers the check node based information during the assessment of the error term E_n . By contrasting, the IWBF algorithm proposed by Zhang and Fossorier increased the performance of the WBF algorithm by considering both the check node and message node based information during the evaluation of E_n . As seen in the WBF, when the error term E_n is high, the corresponding bit is likely to be an erroneous bit and hence it to be flipped. However when the soft value $|y_n|$ of a certain bit is high, the message node itself is expressing some confidence that the corresponding bit should not be flipped. Hence the above equation can be modified as:

$$E_n = \sum_{m \in M(n)} (2s_m - 1) y_m^{\min} - \alpha |y_n| \quad (13)$$

this equation considers the extra information provided by the message node itself, thus a message node having higher soft value has a lower chance of being flipped, regardless having a high error term E_n .

Gradient Descent Bit-Flipping Algorithm(GDBF):

The numerical problem for a differentiable function, the GDBF method is a natural choice. The partial derivative of $f(x)$ with respect to the variable $x(k) \in [1, n]$ can be derived from the definition of $f(x)$:

$$\partial / \partial x_k f(x) = y_k + \sum_{i \in M(k)} \prod_{j \in N(i) \setminus k} x_j \quad (14)$$

Consider the product x_k and partial derivative of x_k in x given as:

$$x_k \partial / \partial x_k f(x) = x_k y_k + \sum_{i \in M(k)} \prod_{j \in N(i)} x_j \quad (15)$$

one better way to finding the position of flipping is to choose the position at which the absolute value of partial derivative is large.

Reliability-Ratio Based Weighted Bit-Flipping Algorithm(RRWBF):

The optimum value has to be found specifically for each particular column weight and its value should be optimized for each individual SNR are the main drawbacks of I-WBF. In RRWBF introduce a new quantity termed as the reliability ratio (RR) defined as:

$$R_{mn} = \beta \cdot |y_n| / |y_m^{\max}| \quad (16)$$

Where $|y_m|$ is used to denote the highest soft value of all the message nodes participating in the m^{th} check. The variable β is a normalization factor for ensuring that we have $\sum_{n: n \in N(m)} R_{mn} = 1$.

Hence, instead of calculating the error term E_n using y_m^{\min} , propose the employment of the following formula:

$$E_n = \sum_{m \in M(n)} (2s_m - 1) / R_{mn} \quad (17)$$

the rest of the RR-WBF algorithm is same as the standard WBF algorithm and the iteration will be terminated when a all zero syndrome vector obtain.

Self Reliability Based Weighted Bit Flipping Algorithm(SRWBF):

According to the previous methods there are two kind of information need to be considered in evaluating the error term for each bit: the information from check node and the intrinsic information. It is noticed that the $2s_m - 1$ term may bring enough information from check nodes. Hence, the self reliability $|y_n|$ should be considered more in contrast to the reliability of the neighbor variable nodes participating in same check nodes. In consideration of this, a new self reliability ratio based weighted bit flipping decoding algorithm is introduced. The new error term used is:

$$E_n = \sum_{m \in M(n)} (2s_m - 1) / |y_n| \quad (18)$$

The ignorance of the reliability of neighbor variable nodes can largely reduce the decoding complexity.

Check Reliability Based Bit-Flipping (CRBF) Algorithms:

Two CRBF algorithms are proposed: the soft check reliability based bit flipping (soft-CRBF) algorithm, which proposes the received channel values when decoding, and its hard decision counterpart which sends the hard decision counter which sends the hard decision demodulated bit streams to the decoder. The soft CRBF outperforms the WBF decoding algorithm and its variants and is comparable to SPA for some LDPC codes.

Two novel check reliability based soft decision bit flipping decoding algorithms are used to improve the performance of the WBF algorithm and its variants for decoding LDPC codes. At each iterations, the cost/ reliability for each bit is computed. The bit with reliable is flipped. The check reliability is also defined for each check node and is used to update the related bit node reliabilities. The sum of bit cost/reliability is to be a relaxed version of the ML decoding metric.

B. SOFT DECISION DECODING

Soft-decision decoding gives better performance in decoding procedure of LDPC codes which is based on the idea of belief propagation. In soft scheme, the messages are the conditional probability that in the given received bit is a 1 or a 0. The sum-product algorithm is a soft decision message-passing algorithm. Prior probabilities for the received bits is the input probabilities as here they were known in advance before running the LDPC decoder. The bit probabilities returned by the decoder are called the a posterior probabilities[4].

In the paper [3], the sum-product algorithm is a soft decision message-passing algorithm which is similar to the bit-flipping algorithm described in the previous section, but the major difference is that the messages representing each decision with probabilities in SPA. Whereas bit-flipping decoding on the received bits as input, accepts an initial hard decision and the sum-product algorithm is a soft decision algorithm which accepts the probability of each received bit as input. For example here initially take a guess that suppose a binary variable x , then it is easy to find $P(x = 1)$ given $P(x = 0)$, since $P(x = 1) = 1 - P(x = 0)$ and so here it is needed to store one probability value for x . Log likelihood ratios are introduced here to do so. They are used to represent the metrics for a binary variable by a single value as per following:

$$L(x) = \text{Log} (P(x=0)/P(x=1)) \quad (19)$$

The aim of sum-product decoding algorithm here is first to compute the maximum a posteriori probability (MAP) for each codeword bit. Now here it is the probability that the i -th codeword bit is a 1 conditional on the event N and that all parity-check constraints are satisfied[10]. The sum-product algorithm iteratively computes an approximation of the MAP value for each code bit. The a posteriori probabilities returned by the sum-product decoder are only exact MAP probabilities if the Tanner graph is cycle free[9]. The extra information about bit i received from the parity-checks is called as extrinsic information for bit i . Until the original a priori probability is returned back to bit i via a cycle in the Tanner graph, the extrinsic information obtained from a parity check constraint in the first iteration is independent of the a priori probability information for that bit and information provided to bit i in subsequent iterations which remains independent of the original a priori probability for bit i . In sum-product decoding the extrinsic message from check node j to variable node i , $E_{j,i}$, is the LLR of the probability that bit i causes paritycheck j to be satisfied.

The probability that the parity-check equation is satisfied if bit i is a 1 is,

$$P_{j,i}^{\text{ext}} = 1/2 - 1/2 \pi_{r \in B_{j,i}^{\neq i}} (1 - 2P_r^{\text{int}}) \quad (20)$$

Where $P_{j,i}^{\text{ext}}$ is the current estimate, available to check j , of the probability that bit i is a one. If bit i is a zero, The probability that the parity-check equation is satisfied is thus $(1 - 2P_{j,i}^{\text{ext}})$. Here it is expressed as a log-likelihood ratio,

$$E_{j,i} = \text{LLR } P_{j,i}^{\text{ext}} = \text{Log} [(1 - 2P_{j,i}^{\text{ext}}) / P_{j,i}^{\text{ext}}] \quad (21)$$

We get,

$$E_{j,i} = \text{Log} [1 + \pi_{r \in B_{j,i}^{\neq i}} \tan h (M_{j,i}' / 2)] / [1 - \pi_{r \in B_{j,i}^{\neq i}} \tan h (M_{j,i}' / 2)] \quad (22)$$

Where,

$$M_{j,i}' = \text{LLR} (P_{j,i}^{\text{int}}) = \text{log} [(1 - P_{j,i}^{\text{int}}) / P_{j,i}^{\text{int}}] \quad (23)$$

Here Each bit has access to the input a priori LLR, r_i , and the LLRs from every connected check node. The total LLR of the i -th bit is the sum of these LLRs:

$$L_i = \text{LLR} (P_i^{\text{int}}) = r_i + \sum_{j \in A_i} E_{j,i} \quad (24)$$

The messages sent from the bit nodes to the check nodes, $M_{j,i}$, are not the full LLR value for each bit here. The equation $Hx[\text{mod } 2] = 0$ is satisfied (where $x[\text{mod } 2]$ is received codeword) or maximum number of iterations set.

The paper [13] 'Channel Coding using Low Density Parity Check Codes in AWGN' compared performance between a hard decision decoding algorithm (bit flipping) and a soft decision decoding algorithm (belief propagation). The analysis is based on the Bit Error Rate of decoding outputs. The result shows that the Soft decision decoding gives better performance than the hard decision decoding. LDPC code with soft decision decoding enhances the system performance and makes the long distance communication fast and error free.

APPLICATION OF LDPC CODES

It is error correcting codes in DVB-s2 standard for satellite communication for digital television. It is also used in Ethernet 10 base T. It is also a part of Wi-Fi 802.11 standard. The optional parts of it are 802.11 ac and 802.11n. It is also used in OFDM networks where data transmission to be without error. It is even with low bit rate also.

CONCLUSION & FUTURE SCOPE

Low-density parity-check (LDPC) code, a very promising near-optimal error correction code (ECC), is being widely well thought-out in next generation industry standards. LDPC code implementations are widely used in DVB-S2, T2 or Wi-MAX standards. Unlike many other classes of codes, LDPC codes are already equipped with very fast (probabilistic) encoding and decoding algorithms. These algorithms can recover the original codeword in the face of large amounts of noise. The iterative decoding approach is already used in turbo codes but the structure of LDPC codes give even better results. In many cases they allow a higher code rate and also a lower error floor rate. Furthermore they make it possible to implement parallelizable decoders..

REFERENCES:

- [1] R. G. Gallager, 'Low-Density Parity-Check Codes'. Cambridge, MA: M.I.T. Press, 1963.
- [2], Bernhard M.J. Leiner, LDPC Codes – a brief Tutorial Stud.ID.: 53418L bleiner@gmail.com, April 8, 2005.
- [3] Namrata P. Bhavsar, Brijesh Vala, ' Design of Hard and Soft Decision Decoding Algorithms of LDPC'. International Journal of Computer Applications (0975 – 8887)
- [4] Ashish Patil, Sushil Sonavane, Prof. D. P. Rathod, "Iterative Decoding schemes of LDPC codes", International Journal of Engineering Research and Applications (IJERA), March -April 2013.
- [5] Sarah J. Johnson, 'Introducing Low-Density Parity-Check Codes', School of Electrical Engineering and Computer Science, The University of Newcastle, Australia.
- [6] William E Ryan, ' An introduction to LDPC codes', department of electrical and computer engineering. The University of Arizona, Australia, 2003.
- [7] M. Jadhav, ankit pancholi, dr. A. M. Sapkal, 'Analysis and implementation of soft decision decoding algorithm of ldpc', pune university phase-i, d,-402, g.v 7, ambegaon, pune (india), [IJETT], 2013.
- [8] B. Vasic , Ivan B. Djordjevic, Low density parity check code and iterative decoding for long haul optical communication system, Journal of light wave technology , vol.21.no.2. February 2003
- [9] Lakshmi.R, Tilty Tony, Abin Johns Raju, An Analytical Approach to The Performance of Low Density Parity Check Codes, International Conference on Advanced Computing and Communication Systems (ICACCS -2013), Dec. 19 21, 2013
- [10] Vikram Arkalgud Chandrasetty, Syed Mahfuzul Aziz, FPGA Implementation of a LDPC Decoder using a Reduced Complexity Message Passing Algorithm , Journal of Networks, Vol. 6, no. 1, January 2011
- [11] Thomas J. Richardson and Rüdiger L. Urbanke 'Efficient Encoding of Low-Density Parity-Check Codes' IEEE TRANSACTIONS ON INFORMATION THEORY, VOL. 47, NO. 2, FEBRUARY 2001.
- [12] CHINNA BABU.J, V.USHA SREEE, and S.PRATHYUSHA, 'Hard decision and soft decision algorithms of LDPC and comparison of LDPC with Turbo codes, RS codes and BCH codes'. Proceedings of 09th IRF International Conference, 27th July-2014, Bengaluru, India, ISBN: 978-93-84209-40-7.
- [13] Rinu Jose and Ameenudeen P.E, 'Channel Coding using Low Density Parity Check Codes in AWGN'. International Conference on Emerging Trends in Technology and Applied Sciences (ICETTAS 2015)

Impact of Atmospheric Temperature on (UHF) Radio Signal

Joseph Amajama

Department of Physics, University of Calabar – Nigeria, joeamajama2014@yahoo.com, +2347036357493

Abstract— Radio signal strengths from Cross River State Broadcasting Co-operation Television (CRBC-TV), (4⁰57'54.7"N, 8⁰19'43.7"E) transmitted at 35mdB and 519.25 MHz (UHF) were measured using a Cable TV analyzer in a residence along Etta-abgor, Calabar (4⁰57'31.7"N, 8⁰20'49.7"E) simultaneously with the meteorological components (weather parameters): atmospheric temperature, atmospheric pressure, relative humidity and wind speed and direction to ascertain the impact of atmospheric temperature on radio signals. The meteorological components with signal strength were measured half hourly from the residence for over 24 hrs to draw a justifiable inference on the impact of the atmospheric temperature on the radio signal. Results indicated that radio signal strength is inversely proportional to atmospheric temperature; provided that, other measured meteorological components were observed constant, including the wind speed and direction. The correlation of the signal strength and atmospheric temperature was $r = -0.93$ and the equation $S = K/T$ at constant atmospheric pressure, relative humidity and wind speed and direction was postulated, where S, T and K are Signal strength, Atmospheric temperature and Constant respectively.

Keywords— Meteorological components, Atmospheric temperature, Radio Signal, Signal strength, Ultra High Frequency (UHF).

INTRODUCTION

Generally, with increasing altitude there is a regular decline in temperature within the troposphere. Consequently, there is a readily distinguishing impact on some “radio propagation modes” and radio-communications that take place in this sphere [11]. Until the “tropopause” is attained there is a continuous decline in temperature in the troposphere. Here (at the tropopause) the temperature starts to rise and levels out the temperature gradient. The mercury is about -50°C at this point [11].

The air refractivity of the troposphere performs a beneficial purpose in the radio communications applications that use “tropospheric radio wave propagation”. The air refractivity depends on the temperature, pressure and humidity of the atmosphere [3]. The atmospheric temperature has an effect on the air refractivity. The air refractivity is directly proportional to the atmospheric temperature and simultaneously other meteorological parameters (exclusive of wind) [15].

The atmospheric condition (weather) has a significant effect on signal [13] [7]. The condition of the atmosphere or meteorological state can cause signal losses. Signal path losses are an essential factor in the plan of any radio communications system [12]. Basically, signal path loss is the degradation in strength of a signal as it travels through a particular region or medium [4] [12].

The following are some of the factors that may cause path losses during propagation. They are: free space path losses, absorption losses, diffraction losses, multipath, terrain, buildings and vegetations and the atmosphere [4]. The major elements of the atmosphere that constitute the weather are the atmospheric temperature, pressure, humidity and wind speed and direction. The atmospheric temperature is a measure of the average kinetic energy of air molecules at 2 m (6 feet) above the surface [8]. Atmospheric temperature has a slight negative effect on signal from earlier studies [5].

This research work focuses its search light on the impact of the atmospheric temperature from a residence at Etta-abgor in the Calabar metropolis on radio signal of about 519.25 MHz and 35mdB which is the frequency and signal strength of transmission respectively of the Cross River Broadcasting Corporation Television (CRBC-TV), Calabar, Cross River State, Nigeria.

To score the goal of this work, signal strength evaluations in the Etta-abgor residence were made simultaneously with the meteorological components (atmospheric temperature and pressure, relative humidity and wind speed and direction) to investigate the atmospheric temperature bearing on radio signal.

METHODOLOGY

The Radio Wave Experiments

The campaign was carried out in a residential area (Etta-abgor) within the Calabar metropolis in Cross River State, Nigeria. The main object of the experiments was to obtain statistical data of signal strengths and meteorological components in the aforementioned residential area to determine the impact of the atmospheric temperature on radio wave signal. Signal strengths were obtained every 30 mins at the residential area for over 24 hrs and simultaneously, the meteorological components: atmospheric temperature and pressure and relative humidity and wind direction and speed were recorded to probe the impact of the atmospheric temperature on the signal. The measurement of the signal strength was made using the Digital Community – Access (Cable) Television (CATV) analyzer with 24 channels, spectrum 46 - 870 MHz, connected to a domestic receiver antenna of height 4.23 m.

To be able to reach a justifiable conclusion on the impact of the atmospheric temperature on the signal, the dependence of the signal strength on relevant parameters was analyzed. These relevant parameters were the: atmospheric temperature and pressure,

relative humidity and the wind speed and direction. The received signal was measured only on the downlink and the receiver antenna was adjusted until the best obtainable result of signal strength was captured on the cable analyzer before recording.

Relevant Properties of the Digital CATV Analyzer

Digital Community – Access (Cable) Television (CATV) analyzer with 24 channel spectrum, model “DLM3-T”, operates over a frequency range of 5 - 65 MHz for lower band (mobile transmit, base receive) and 46 - 870 MHz for upper band (base transmit, mobile receive). The channel spacing is 8 MHz. It is specially designed to provide a band of the free “off-air channels” and provides a relative reading of signal strength that is aided by a unidirectional antenna in alignment. It can measure signal levels of 0 - 100 mdB and has an inbuilt rechargeable batteries that can provide power to an “antenna pre-amp” to accurately give a set-up location. Its maximum sensitivity is approximately -100 mdB. TV images and test data are displayed simultaneously, efficiently and conveniently [2].

Sites Descriptions

The site (4°57'31.7"N, 8°20'49.7"E) where the weather was under study to ascertain the impact of the atmospheric temperature on the signal strength was a residential area in the Calabar metropolis – Nigeria. It is at Atta-agbor. There are scanty trees with predominantly low height buildings of about 2 m to 3 m.

Measurement Method

To determine the impact of the atmospheric temperature on radio signal, the CATV analyzer was stationed in an apartment and the 4.23 m high antenna was connected to it and mounted outside. The atmospheric temperature and pressure, relative humidity and the wind speed and direction and corresponding signal strength were taken every 30 mins for over 24 hrs.

Sampling with the CATV analyzer

Measurements with the digital CATV analyzer being time dependent were made approximately every sixty seconds (60 s). The average signal strength value (mean of minimum and maximum reading) was recorded when the images were sharpest.

RESULT AND ANALYSIS

The result of the experiments is analyzed below. To determine the impact of the atmospheric temperature on radio signals, some data or measurements extracted/excepted from the whole were used to determine the impact of mentioned parameter above on the signal strength, through the curve that was produced.

Analysis of the impact of atmospheric temperature on radio signal strength

The four meteorological components that govern our weather are the atmospheric temperature, atmospheric pressure, relative humidity and wind speed and direction.

Fig. 1 below shows the graphical relationship between signal strength and atmospheric temperature.

TABLE 1

Measurement of Signal strength (mdB) at different atmospheric temperature, at uniform relative humidity of 94%, near uniform atmospheric pressure of 29.92(±0.02) inHg and uniform wind speed and direction of 0mph NA

Atmospheric temperature (°F)	Signal strength (mdB)	Relative humidity (%)	Atmospheric pressure (inHg)	Wind (mph)	Time (hour)
77.0	9.4	94	29.91	0 NA	22:30
78.5	9.0	94	29.94	0 NA	8:00
78.0	9.3	94	29.94	0 NA	8:30
79.5	7.8	94	29.94	0 NA	11:30
79.0	8.0	94	29.94	0 NA	12:00

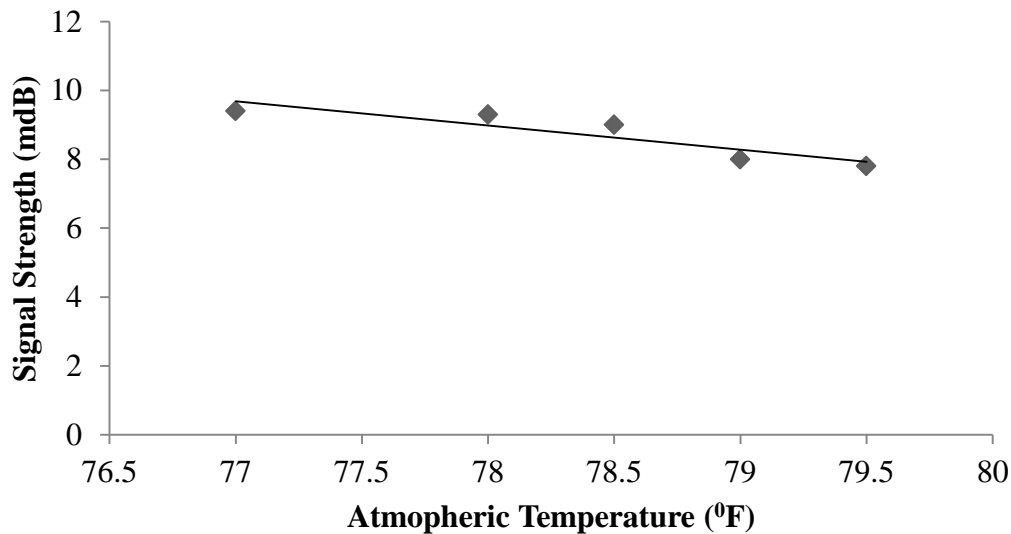


Fig. 1. Relationship between signal strength (mdB) and atmospheric temperature (°F), at uniform atmospheric pressure of 29.92 (± 0.02) inHg, uniform relative humidity of 94 % and uniform wind speed and direction of 0 mph NA.

Fig. 1 shows the relationship between signal strength and atmospheric temperature, at a uniform humidity of 94 %, uniform atmospheric pressure of 29.92 (± 0.02) inHg and uniform wind speed and direction of 0 mph NA. The signal strength decreased with a slight rise in temperature. Mathematically, the correlation between the two parameters is -0.94 in value. Hence, the higher the temperature: the lower the signal strength. In other words, the signal strength is inversely proportional to temperature, provided that other meteorological components, atmospheric pressure, relative humidity and wind speed and direction are observed constant.

If S (dB) and T (°F) symbolize Signal strength and Atmospheric temperature respectively, it can be postulated that $S \propto \frac{1}{T}$ or $ST=K$ (i.e. $S_1T_1=S_2T_2$ where S_1T_1 and S_2T_2 represent initial and final state conditions) at the same atmospheric temperature and pressure, relative humidity and wind direction and speed, where K is a constant.

SUMMARY, CONCLUSION AND RECOMMENDATION

Summary

In this work, experiments have been carried out to characterize the propagation of radio signals through the atmosphere to determine the impact of the atmospheric temperature on propagating radio signal.

Results from the meteorological components at the residence in Etta-agbor: atmospheric temperature and pressure, relative humidity, wind speed and direction revealed that; increase in temperature results in the degradation of signal strength, observing other meteorological components constant. The correlation between the signal strength and temperature was found to be $r = -0.94$. The phenomenon that explains this is that there is a collision between increasing raining particles of light from the sun as temperature increases with the radio signals, this attenuates the signal strength. This is true since electromagnetic waves which radio signal (radio wave) is a member share the same properties and are reflected or diffracted or refracted when they encounter an obstacle [1] [6] [9] [10] [14].

Conclusion

In conclusion, it was observed from the residential area in Etta-agbor, Calabar-Nigeria, that the atmospheric temperature was inversely proportional to the signal strength, provided that the meteorological components: atmospheric temperature and pressure and relative humidity were observed constant including wind speed and direction. Hence $ST = K$ at same atmospheric pressure, relative humidity and wind speed and direction; where S = Signal strength, T = Atmospheric temperature and K = Constant.

Recommendation

Since the investigation the impact of the atmospheric temperature with this new methodology, on radio signal is a pioneering or ground breaking research, other students or researchers should be encouraged to further investigate this postulations with sufficient data in different climates to verify the claim and ascertain the impact of other meteorological components on radio signal.

ACKNOWLEDGMENT

A million and one thanks go to the Cross River Broadcasting Cooperation (CRBC) for granting a ready access to their Community Access Television (CATV) analyzer throughout the course of this research.

REFERENCES:

- [1] Dell, W. R., Groman, J. & Timms, H. (1994). *The world book encyclopedia*. Chicago: World Book Incorporated.
- [2] Editors of BM/E Magazine. Broadcast Antenna System Handbook (2nd ed.) (1973). New York: Tab Books, 117 – 124.
- [3] Amajama, J. (2015). Association between Atmospheric radio wave refractivity and UHF Radio signal. *American International Journal of Research in Formal, Applied and Natural Sciences*, 13(1), 61 – 65.
- [4] Ian, P. (Ed.) (2015). Radio signal path loss. In radio electronics. Retrieved April 3, 2015, from www.radio-electronics.com.
- [5] Jari, L. & Isma, H. (2015). Effect of temperature and humidity on radio signal strength in outdoor wireless sensor. *Proceedings of the federated conference on computer science and information systems*. 5, 1247 – 1255.
- [6] Liew, S. C. (2015). Principles of remote sensing. Retrieved January 14, 2015 from <http://www.crisp.nus.edu.sg/-research/tutorial/em.htm>.
- [7] Meng, Y. S., Lee, Y. H. & Ng, B. C. (2013). The effects of tropical weather on radio wave propagation over foliage channel. *IEEE transaction on vehicular technology*, 58(8), 4023 - 4030.
- [8] Weather parameters (2015). Retrieved November 10, 2015, from cees.tamtu.edu/cees/weather/parameters.html.
- [9] Parker, S. P. (1982). *McGraw-Hill concise encyclopedia of science and technology* (4th ed.). New York: McGraw-Hill, 213 – 265.
- [10] Rappaport, T. S. (1996). *Wireless communications*. New Jersey: Pearson Prentice Hall, 495 -502.
- [11] Tropospheric propagation (2015). In Wikipedia. Retrieved April 5, 2015, from http://en.wikipedia.org/wiki/tropospheric_propagation.
- [12] Wayne T. (2001). *Electronic communications systems: fundamentals through Advanced*. New Jersey: Prentice-Hall, 39.
- [13] Yeeken, O. O. & Michael, O. K. (2011). Signal strength dependence on atmospheric particulates. *International Journal of electronics and communication engineering*, 4(3), 283 – 286.
- [14] Young, H. D. & Freedman, R. A. (1998). *University physics* (9th ed.). California: Addison-Wesley Longman, 958 -960.
- [15] Amajama, J. (2015). Mathematical relationship between Radio refractivity and its meteorological components with a near linear mathematical equation to determine radio refractivity. *International Journal of Inovative science, Engineering and Technology*, 2(12), 953 – 957.

ANALYSIS OF A CONCEPT FOR PRUDENTIAL UTILISATION OF EXCESS POWER GENERATED IN IC ENGINES DURING CLUTCH ENGAGEMENT PROCESS

¹Aravind Mohan K S, ²Dr. Aboobacker Kadengal

¹Department of Mechanical Engineering,

Lal Bahadur Shastri College of Engineering, Kasaragod
Kerala, India - 671542

Ph No. : +91 8891367362

aravindmohan010@gmail.com

²Associate Professor & Dean (PG),

Department of Mechanical Engineering,

Lal Bahadur Shastri College of Engineering, Kasaragod
Kerala, India

Abstract— With increasing number of vehicles taking the roads, traffic congestion has become a routine problem in all major cities and towns. For a vehicle moving throughout these long queues, the engine may either be in an idling situation or the power may be drawn along with partial engagement of the clutch plates. In such cases, the engine power is not efficiently used during vehicles traction, as the engine will be operating with maximum efficiency at rated load and it will decrease with deviations from rated load condition on either direction. For a typical internal combustion engine, the fuel consumption would increase with increased brake power productions. The rate of increment in specific fuel consumption of the engine is much lesser for low brake power than for higher brake power. So when the clutch plates are fully engaged at low partial loads or partially engaged, additional rate of consumption of fuel for producing additional power will be very low compared to for producing the same amount additional power at higher loads, where it is highly needed. Hence additional (surplus) power can be produced at low load conditions such as idling or partially engaged clutch conditions, and harnessed and utilized later on when the vehicle demands high power at higher values of specific fuel consumption. The concept is validated on a typical test engine in the laboratory, and the results are normalized so that it can be applied for any engine.

Keywords-- idling, clutch, traction, internal combustion engine, brake power, specific fuel consumption, energy conservation

1. INTRODUCTION

Traffic congestion is one of the major problems faced by all metropolitan cities around the globe. Most of the major roads and intersections in and around city premises may contain long standing queues of commuter and public transportation vehicles during peak hours and this trend is most probable to increase moving on to the future.

Once the vehicle is moving through these long queues, it is obvious that using the clutch mechanism, the drivers can put the vehicle's engine at partial loads or no load depending on the power requirement. When in a partially clutched or fully disengaged engine stages, there is slippage or otherwise no literal contact between the driving and driven shafts on either sides of the clutch setup, as described in the Machine Design reference books like Shigly[1]. In both these cases it is evident that the complete power that can be produced by the engine remains underutilized for vehicular traction, instead only a fraction of the power that can be produced is drawn from the engine. Venu, [2] gives a comprehensive analysis of the transmission procedure during engagement and disengagement of the clutch plates and a relative velocity created between the pressure plate and friction plate\clutch disk, in a clutch setup, during its operation. This slippage owing to the power that can be produced not being efficiently utilized, can incur additional fuel consumption. Even though this may seem to be a small quantity, over the number of cycles and duration of time that the vehicles spend on traffic blocks, it can build up into a much bigger loss as evidenced by S. Gangopadhyay and P. Parida [3]. In such cases the no load runs of the can be analogous to idling of engine because in the long queues at the intersections and traffic blocks the idling can be due to the clutch plates being partially engaged or fully disengaged from the engine crank shaft. Gangopadhyay S. and Parida P.[3] puts forth a more general analysis in idling losses, rather than being limited to a specific data on power losses due to partial clutching or fully disengaged engine runs. Till date the scope of conserving this underutilized power is not thought about and the fuel losses during partial clutching was seen as an unavoidable one and a compulsory wastage incurred by the vehicle in its run through the busy roads and intersections. This kind of engine run can be termed as a fuel surplus condition while more fuel than what is required is burned in the engine cylinders.

On the other hand it is just the contrary, once the vehicle demands high power like in the cases of a steep slope or an overload. If the power demanded is so high, the engine fails to meet up with this demand, simply because the demanded power may just be or even over that threshold of power or torque which that engine could provide. This condition can be termed as fuel starvation since even though at full throttles the engine fails to meet up with the demanded high powers.

Even though the two problems mentioned above are the extreme conditions of an engine's run, if a balance could be struck between the two, the power deficit during the fuel starvation can be met up with the underutilized power, available in surplus during the clutch engagement/disengagement processes when the engine is left and no loads or partial loads. Surprisingly this has not been done before to satisfactory extends and thus this paper aims to throw light to the following two areas:

- The feasibility of harnessing that underutilized power present during engagement or disengagements of clutch plates, at the lower rungs of an engine's run (5-15% of rated load) when it consumes lesser fuel for unit rise in BP and then providing it to the upper rungs of its run (maximum power productions accounting roughly to 175-200% of the rated load) when unit rise in brake power consumes high quantities of fuel (section 2 and section 3).
- To substantiate this claim to a larger extend and to see if this nascent idea could stand, a case study was done on a test engine and was thereby projected to a higher powered engine of the same characteristics (section 4).

2. THE PROBLEM STATEMENT

The stages of the engine, during clutch engagement and disengagement processes, first at partial loads and then at no loads, when it is fully disengaged from transmission, are the areas of interest. Hence the situation is explained as follows:

- Engine partially loaded: By partial engagement of the clutch plates, a slippage is allowed between the driving shaft and driven shaft on either side of the clutch assembly. By doing so the complete power, which can be produced by the engine, is not passed on to the driven shaft and to the subsequent mechanical components to follow. Thereby the power drawn is only a fraction of what is produced by the engine,
- Engine fully disengaged from transmission: the aim of fully disengaging the engine is to cut off power from the driving shaft to the driven shaft. The clutch plates disengage to isolate the engine and the power flow is terminated at the clutch setup. As no power is drawn from the engine for transmission purposes, the brake power produced at the rated speed is a small fraction of the engine capacity and the engine remains underutilized.

It is interesting to note that both the above conditions tend to occur at the first 10-25% of the brake power values that can be produced by the engine because once the clutch disks are disengaged, the primary intension is to temporarily cut off the power drawn from engine and when this is done, the engine tends to attain its rated speed, provided it is at zero fuel throttling.

For a typical internal combustion engine, the mechanical efficiency curve, as shown in Fig.1 takes the peak value at rated conditions. Once the engine is partially loaded, during the engagement/disengagement process of clutch plate, the efficiency values of the engine shift to the off design conditions at either sides of the peak in fig 1. To expect a continuous and reliable performance, the engine must be operated at its rated conditions. Partial loading of the engine is most likely to fall towards the left of the peak value efficiency. Hence it is safe for any secondary power harnessing device to engage onto the engine till the rated power conditions are reached, provided the fuel consumption is in check and economical.

Let at the so called partial or full disengagement of clutch plates during the lower Brake Power regions in an engine's run, 'x' kW is the Brake power produced at a fuel consumption of y cc/sec. Since there is no full contact between the driving and driven shafts on either sides of the clutch plate, as stated by Venu [2], the whole of the 'x'kW value is not utilized for traction. Instead only a fraction of it is consumed while the other fraction is left unused. The following sections articulates the feasibility of harnessing that unused fraction of power and utilizing it later on when high power is being demanded of the engine.

2.1 THEORETICS OF THE CLAIM

When engine is disengaged by the separation of the clutch plates, the load is taken off from the engine and the engine runs at its rated speed. The power produced at this speed comes well under the earlier said low Brake Power regions of 10-25% of the rated BP.

From the principles of mechanics,

$$P \propto T \cdot \omega_{\text{rated}}$$

According to the above expression, when more power is needed for traction, the speed being constant, torque must be increased. This in turn increases the fuel consumption. Thus it can be claimed from this equation that the torque, (thereby the fuel consumption) for 10-25% of maximum BP must be much lesser than the torque (and hence fuel consumption), at a power which is 80-95% of maximum BP.

i.e. Fuel Consumption at (0.1 to 0.25) of $BP_{\text{max}} \ll$ Fuel Consumption at (0.8 to 0.9) of BP_{max}

The above concept is illustrated graphically in figure 2. For a typical IC engine, the fuel consumption would increase with increase in power outputs. Hence in an ideal case, the TFC vs. BP graph for an IC engine should have an increasing trend of slope as shown in Fig. 2. The left and right sides of the graph can be characterized by fuel consumptions at low BP or no loads and high BP productions respectively. On further closer analysis of the graph, it's more evident that even though throughout its range the slope is increasing, the rate of increase is gentle at the beginning stages, against the high rate of slope increase towards the end.

Consider the initial stages of the curve in fig 2. Here the curve progresses with minute increments in its slope. This trend of a gentle slope increase is evident to more than half of the curve's progress. This is the region where the engine produces low BP's and the gentle slope increments can be due to the comparatively low fuel consumption of the engine when operating in this region. The referred region is shown in fig 2 as region P. In this region, large fluctuations or variations in the BP would account to only a corresponding small variation in the fuel consumed as marked in the graph.

Once the engine is in low BP production conditions, namely when it's in Idling or partially loaded conditions, the operation of the engine would possibly be in region P. Hence it can be summed up that when complete power is not drawn from the engine, as in the above working stages, the generated surplus BP is most likely to be in this region.

The Specific fuel consumption, SFC, can indicate how efficiently the engine is using the fuel supplied to produce work at that particular instant or in other words, the total fuel consumed (TFC) for a unit rise in BP produced gives the SFC as in Heywood [4].

As the slope is gentle in this region P, it can be inferred from the graph that in region P, for a unit increment of load on the engine or for a unit thrust force increase produced by the engine, it accounts for only a very small increment of fuel consumed. In other words, the SFC values would be comparatively lower in this region owing to the gentle slope.

Towards the later end stages of the curve, the vehicle demands high BP from the engine, region Q in Fig.2. The region Q is to be noted for its highly steep rise in slope of the curve, which is due to the high fuel consumption incurred by the engine for producing these high BP values. In this region, the increments in load exerted on the engine would need larger changes in fuel consumed. Each small increment in the BP produced would get the engine to consume comparatively higher amount of fuel, i.e. the SFC is higher for the region Q.

The reason for this huge fuel consumption is very obvious because an engine's operation can only fall under region Q once high torque is demanded for the traction, like in the cases of an upward slope, sudden cruising demands etc. In all these mentioned cases the high power can be produced by increased throttling and burning more fuel and the increase in each unit of BP produced is at an expense of higher fuel consumed.

In an ideal case, the specific fuel consumption would remain unchanged throughout the engine's operations irrespective of the power outputs. But it is very evident from fig 2 and fig 5, the change in the amount of fuel consumed once the operation of the engine is shifted from region P to region Q. An economic comparison can be made between the two regions characterized by the higher SFC values in region Q to the lower values in region P, to substantiate the claim. In region P the initial values are of the order of 0.03 c.c./ kW sec (section 4, table a) and the final values in region Q are in the order of 5.4 c.c./ kW sec, implying a 180 fold increase in fuel that is being consumed in the final stages of the graph. Subsequently the cost incurred for fuel in the production of a unit BP increase in region Q is 180 times that of in region P.

Hence the claim made is that, the power which remains underused in the engine due to partial or no load conditions during clutch engagement\disengagement, can be harnessed and later on supplied when the condition demands more power from engine i.e. when each unit of Brake power is produced at a higher expense of fuel consumption.

3. METHODOLOGY

The above sections illustrated the possibility of application of a power harnessing procedure to an engine's operation. In this section the methodology of the same is explained.

Along with the vehicular traction power, other auxiliary devices also feed from the engine. Let the total power accounted for traction and the auxiliary devices be termed the primary power and the load exerted on the engine, the primary load. This primary load may vary according to the vehicles demand during its run. In a TFC vs. BP curve the primary load can range to anywhere in the graph from origin to region P or region Q, indicating an unrestricted domain for the primary load. When the vehicle is in normal run, characterized by normal throttling of the fuel pump, the complete BP generated by the engine is used up as primary power since the BP being produced is just sufficient for the primary loads.

Consider the vehicle in a wait and move mode within a queue during heavy traffic congestions. The engine will, in majority of its run, be in partial and occasional no loads, owing to continuous clutch engagements and disengagements. This may normally come under low BP production stage, the region P. Since the vehicle is made to run at a partially clutched stage, complete power that can be produced by the engine is not required as primary power and higher Brake powers could be produced than what is required for the primary loads, indicating a scope for defining a secondary power. Secondary power is that power that can be used to run a power harnessing device. Be it hydraulic, pneumatic, electric or a hybrid of any of these. The secondary load is the load that can be exerted by these devices on the engine crank shaft. The secondary loads can only be exerted on the engine

when it is operating in low BP production conditions i.e. in region P in Fig 2 and below the maximum efficiency point in Fig 1. Hence the secondary power that can be harnessed from the engine strongly depends on the primary power, since only that underutilized amount of BP above the primary power, can be utilized for satisfying the secondary loads. Mathematically speaking, during partially loaded/no load stages,

$$\text{Primary loads} + \text{Secondary loads} + \text{losses} = \text{BP produced}$$

Hence the secondary loads can be applied strictly under the following two constrains:

- The engine should be operating in region P,
- Sum of primary and secondary loads must be equal to than the BP being produced

3.1 POWER EXTRACTION AND APPLICATION

When during the normal run of a vehicle there is a sudden load drop on the crank shaft due to partial loading or no loading due to clutch engagements, the primary power demanded of the engine is reduced. As said earlier an additional secondary load can be exerted on the crank shaft, provided collectively the primary and secondary loads do not exceed the BP that can be produced with the same fuel consumed. Say here, 50-55 kW as in the case of engine B, beyond which there is higher rate of fuel consumed. Or else the secondary loads will be loaded onto the engine when it is operating under high BP production conditions, i.e. in region Q. This may occur at an expense of high fuel consumption which is not economical and not desired. So the secondary loads can be engaged on the crank shaft as much as the primary load is disengaged from the engine owing to clutch disk disengagements. Further when the vehicle demands very high power from the engine. Like for the situation of a very steep slope, sudden cruising demands etc. Even if the engine produces its maximum possible value of BP, it may not be sufficient to meet these requirements in some cases. This maximum power produced would be at a very high quantity of fuel consumed and each unit rise in the BP would be at the cost of high quantities of fuel consumed. i.e. the SFC would come to very high values. So at these conditions there is a chance that the maximum power produced will be lesser than what the primary loads demand. Or in other words the primary power required is greater than BP produced.

Graphically speaking this may occur at the extreme right end of region Q in a TFC vs. BP graph. So any external boosting power available for the vehicle above the BP value, produced by engine, can be useful here. It is in this situation that the energy stored using the secondary power, that was harnessed earlier, can be put to use. If this energy can fill up the dearth in power between the primary load demand and BP produced, it can meet up with the vehicles demand of high power for that situation. Even if not fully but to a partial extend, the BP along with this energy discharge which was harnessed and stored earlier can be fed to meet up to the demand of primary loads.

Hence when each unit of BP increase consumes enormous amount of fuel, the excess power produced when unit BP rise consumed lesser fuel, can be used to give a boost up to the vehicular traction.

4. SUPPORTIVE EXPERIMENT

In order for a more practical insight to the above theoretical proposal, the engine's behavior during clutch engagement/disengagement needs to be studied. The condition can be an analogy to the state of an engine under 10-25% of its full load. The feasibility of fuel surplus and power starving conditions can be best explained if a plot between the fuel consumption and Brake Power is made. Hence a load test on an engine was conducted with a sole aim of knowing its fuel consumption at the different brake power ranges that it can produce.

4.1 NON DIMENSIONALISATION AND SCALING

The decision of selecting any engine and not a specific engine was taken up with the concept of non dimensionalisation and further scaling in mind. Hence any engine operating parameters selected can be non-dimensionalised with suitable scaling relations. These operating parameters can be correlated from the test engine and to any similar engine. Another advantage of plotting such a graph is that once a plot between the Total Fuel Consumption (TFC) and Brake Power (BP) is made, the first differential of the equation of the graph will give the specific fuel consumption, SFC. SFC is the fuel consumption for a unit brake power increase made. Hence in the expected case, the SFC at 80% full load must be much greater than the SFC at 10-20% of the full load.

4.2 EXPERIMENT

Engine A: Test Engine

Engine Type : 4-stroke, Air Cooled Diesel Engine

Power : 4.4kW

TFC	: 0.3749cc/sec
-----	----------------

Engine B: Scaled Engine

Engine Type	: 4-stroke, 2.5 L Diesel Engine
-------------	---------------------------------

Power	: 88 kW
-------	---------

TFC	: 5.79cc/sec
-----	--------------

Load testing was done on Engine A. Engine B is characteristically similar to engine A but possesses higher credentials of power outputs. This engine was considered so as to analyze this claim of power harnessing in a more real time situation. This can be achieved with the concept of non-dimensionalisation using rated values and then projecting it to the higher engine. It is explained in the following paragraphs.

The values of Mean BP and Mean TFC of engine A, obtained from testing, were non dimensionalised using the rated BP and rated TFC of engine A to obtain a set of non-dimensional ratios (the values were simply divided with the corresponding rated quantities). Since engine B is of similar characteristics of that of A, these ratios when multiplied with the rated quantities of engine B, a satisfactory set of performance values of engine B can be obtained. These values are shown in Table (b).

Once a plot for TFC vs. BP was made for the engines, the first differential of the curve equation, at the particular values of BP, would give the SFC values at that point.

Fig 3 and Fig 4 shows the plots between TFC and BP for engine A and engine B respectively, with the values from Tables (a) and (b) respectively. A 6th degree polynomial curve was the best fit for both the plots with the regression coefficient $R^2=0.9986$ for both plots. The equation of the curve is shown besides the respective graphs.

Consider the equation of the TFC vs. BP curve for engine B (fig 4).

$$y_2 = 5E-09x_2^6 - 9E-07x_2^5 + 6E-05x_2^4 - 0.0019x_2^3 + 0.0267x_2^2 - 0.126x + 2.3318$$

Differentiating the equation with respect to x_2 ,

$$(dy_2/dx_2) = 3E-8x_2^5 - 4.5E-6x_2^4 + 24E-4x_2^3 - 5.7E-3x_2^2 + 0.0534x_2 - 0.126$$

Since $y_2 = \text{TFC}$ and $x_2 = \text{BP}$,

$(dy_2/dx_2) = \text{Slope}$, which is the TFC for that unit increase in BP. This fuel consumed for unit rise in BP is known as Specific Fuel Consumption(SFC). The values of SFC also is shown in the table s (a) and (b).

Fig 5 shows the SFC vs BP graph for engine B.

4.3 OBSERVATIONS AND FURTHER ANALYSIS.

Consider Fig 4, the TFC vs. BP plot for engine B. The curve proceeds with an increasing pattern in slope when fitted with a 6th degree polynomial curve. When analysed closely it can be seen that for a range of BP from 0 kW to around 50-55 kW, the mode of increase for slope is very gradual and gentle. In this region, the TFC is ranging from 0 to around 5cc/sec. So it can be said that for variations of load in this region, the consumed fuel quantity is very small. For example, in region P, for an increase of 10 kW load on the crank shaft, say from 10kW to 20kW, the additional fuel consumed is less than 0.1cc/sec.

The same can be spoken in the SFC vs. BP graph (Fig 5). For this region corresponding in the SFC vs. BP graph (fig 5), a unit thrust force increase occurs at a very small amount of fuel consumed. i.e. the SFC is comparatively smaller in this region. Hence this will be the region of operation for the engine under low power production conditions like idling or no loads and for partial loads.

Now consider the region beyond the BP values of 50-55kW. Let this region be termed as region Q for easy reference. In this region, from the TFC vs. BP graph (fig 4) it can be seen that the slope is increasing at a much chaotic rate. It implies the fuel consumption takes the upward trend of increase in this region. Once extrapolated, it can be made much obvious that the fuel consumption would further soar to very high values in a second, for higher BP production by the engine. For example, in this region Q, for an increase of 10 kW load on the crank shaft, say from 62 kW to 72 kW, the

additional fuel consumed is more than 18cc/sec. Comparing the two examples, it is to be specially noted for an equal amount of BP rise of 10 kW, the difference in fuel consumption, once the region of operation of the engine changes from P to Q.

The situation of region Q is much more evident once the SFC values are analyzed (table b). For this region corresponding in the SFC vs. BP graph (fig 5), a unit brake power increase occurs at a bigger quantity of fuel consumed. i.e. the SFC is comparatively higher in this region.

5. RELATED WORK

Methodologies to improve upon the efficiency and additional systems that harness power have been a heavily researched area ever since the IC engines came into the forefront. With vehicles becoming so prominent in today's world of limited fossil fuel supplies and escalating carbon emissions into the atmosphere, this has further become a more stressed upon topic these days. Under normal driving conditions, the efficiency of an IC engine is approximately 20% as stated by Fyffe J.[5]. This value is an alarmingly low one considering the otherwise limited options onto which we can migrate from an IC engine. All these have given the term 'power harnessing' from an IC engine more weight. Hence any sort of efficient energy retrieval method is most welcome in today's world.

Hybrid engines have come to the forefront in the last decade or so owing to the need of energy savings to increase the overall efficiency and decrease emission hazards. So has efficiency and power improving methods come into prominence, like Heat Recovery from exhaust gas proposed by Jadhao J.S. and Thombare D.G. [6], mechanical supercharging, turbocharging, pressure wave supercharging of the engine as in Heywood [4], modifying specific thermodynamic processes in the basic operating power cycle of the engine as in the Thermodynamics reference book Cengel [7], an alternative thermodynamic operating cycles for the engine, like the eco cycle proposed by Postrzednik S., Zmudka Z. [8] etc. to name a few.

A hybrid electric vehicle with an electric motor aiding the IC engine, helps to keep the efficiency of the same at its peak point as proposed by Fyffe J. [5], while providing additional power as and when required by the vehicle and storing that power which is lost due to idling of the engine, when the vehicle moves through congested roads. Modern Hybrid Electric Vehicles (HEV) even reduces the energy lost due to idling of engine by shutting it off and restarting it when needed called start-stop system as proposed by Reddy S.S., Tharun K.S [9]. Electric regenerative braking in HEV's considers recovering the maximum braking energy and harnessing it. Jin L., Chen P. et al. [10] and Reddy S.S., Tharun K.S[9] puts forth regenerative braking, and [10] the same in an electric vehicle driven by in-wheel motors. This broad area of electric hybrids too does not touch upon harnessing the underutilized power during clutch engagements and disengagements in a vehicle.

A hydraulic hybrid as proposed by Rohanhatti [11] also aims to improve upon the overall efficiency of the system. It uses hydraulic accumulators and motors for the hydraulic cycle along with the IC engine. The additional power is stored as hydraulic energy to be used later on when required. A hydraulic Regenerative system by Kumar [12] converts the kinetic energy to pressure energy when a vehicle is decelerating. The energy generated due to the momentum rate change is stored in hydraulic accumulators and is later on used to aid traction. A similar concept is implemented in the Hydraulic Launch Assist (HLA) produced by Eaton Corporation to improve vehicle efficiency in its stop and go process.

In a very inspiring paper by Huang Y., Yang F. et al.[13], it is specified how engine braking can be avoided by disengaging the clutch when the vehicle is braked and slowed down, letting the engine to run on no loads. An automatic clutch then engages onto the engine, connecting it to an Integrated Starter and Generator system and the power then produced by the engine generates electricity aiding regeneration.

6. FUTURE SCOPE AND EXPANSIONS

This paper claimed a nascent idea of harnessing underutilized power during partial or no load engine runs and an engine test substantiated this claim. It is found that there is scope for considerable amount of power that can be harnessed at various operating stages of an engine during clutch engagements and disengagements. A hydraulic and an electric power tapping system may be developed to harness power from an engine during clutch engagements and disengagements without overly loading the engine so that the load exerted by the power tapping systems can be within the engine's low BP producing stage.

The hydraulic power tapping system harnesses the energy at low BP production when the engine is clutched and stores it as pressure energy of a fluid in a hydraulic accumulator setup as proposed by Gangwar G.K., Tiwari M. et al. [14]. When the vehicle demands high power, this compressed fluid at high pressure may be allowed to expand through a turbine producing work which can aid traction.

The electric power tapping is done by using the power that is harnessed from engine during clutching, to run an alternator to generate electricity which charges the main battery or feeds the auxiliary devices of the engine.

A comparative study between hydraulic power tapping and electric power tapping system will be done so as to determine which system is more efficient in using the harnessed power.

7. CONCLUSIONS

Once a vehicle is in partial or no loads due to clutch engagements and disengagements, complete power that can be produced by the engine is not utilized for vehicle traction. Only a fraction of it is used up, the rest remains underutilized. The paper provided a case study on whether this underused power could be harnessed during clutch engagements and disengagements under low BP production conditions and then used later on when the vehicle demands high power. An engine test validated the scope for this power harnessing methodology and an economic analysis gave a 180 fold increase in the cost incurred in the fuel that is consumed for higher values of brake power produced when compared to the lower brake power production conditions.

REFERENCES:

- [1] Richard G. Budynas and J. Keith Nisbett, "Shigley's Mechanical Engineering Design", McGraw Hill Education private limited, Edition 8, ISBN: 0-390-76487-6.
- [2] Venu M.K.K., "Design Optimization of Clutches in an Automatic Transmission", Chalmers University of Technology Sweden, Master's Thesis 2013: 28.
- [3] Gangopadhyay S. and Parida P., "Estimation of Fuel Loss during Idling at signalized intersections in Delhi", Indian Roads Congress (IRC), Vol. 12, pp.61-69, 2009.
- [4] John B. Heywood, "Internal Combustion Engine Fundamentals", McGraw Hill Education (India) private limited, ISBN: 9781259002076, 1259002071.
- [5] Fyffe J., "The Reports of My Death Have Been Greatly Exaggerated- An Internal Combustion Engine's Story", Stanford Energy Journal, Issue 4: Sustainable Transportation, April 2014.
- [6] Jadhao J.S., Thombare D.G., "Review on exhaust gas heat recovery for IC engine", International Journal of Engineering and Innovative Technology(IJEIT), Vol. 2, Issue 12, June 2013.
- [7] Yunus A Cengel, Michael A Boles, "Thermodynamics: An Engineering Approach" McGraw Hill Education (India) private limited, Edition 7, ISBN: 9780071072540, 0071072543.
- [8] Postrzednik S., Zmudka Z., "Improving of IC Engine Efficiency through Dropping of the charge exchange work", Journal of KONES Internal Combustion Engines, Vol 11, No. 3-4, 2004.
- [9] Reddy S.S., Tharun K.S., "Eco Friendly Vehicle (Hybrid Electric Vehicle)", International Journal of Engineering Trends and Technology (IJETT), Vol. 4, Issue4, April 2013.
- [10] Jin L., Chen P., Liu Y., "An Analysis of Regenerative Braking and Energy Saving for Electric Vehicle with In-Wheel Motors", International Journal of Control and Automation, Vol. 7, No.12, pp. 219-230, 2014.
- [11] RohanHatti, "Hydraulic Hybrid Vehicle", International Journal of Engineering Research and General Sciences (IJERGS), Vol. 3, Issue 1, January-February, 2015.
- [12] ER. Amitesh Kumar, "Hydraulic Regenerative Braking System", International Journal of Scientific & Engineering Research, Vol. 3, Issue 4, April-2012
- [13] Huang Y., Yang F., Ouyang M., Chen L., Gao G., He Y., "An Efficient Energy Regeneration System for Diesel Engines", World Electric Vehicle Journal, Vol. 4, pp. 000525-000531, 2010.
- [14] Gangwar G.K., Tiwari M., Sing R.B., Dasguptha K., "Study of different Type of Hydraulic Accumulators their characteristics and applications", International Journal of Research in Aeronautical and Mechanical Engineering(IJRAME), Vol. 2, Issue 2, pp. 56-63, February 2014

Table A

Mean BP in kW (x)	Mean TFC in cc/sec (y)	(dy/dx) = SFC in cc/kW sec
0.1229	0.1307	-

Table B

BP in kW (x)	TFC in cc/sec (y)	(dy/dx) = SFC in cc/kW sec
2.4583	2.0186	-

0.2458	0.1522	0.03697373	4.9167	2.3507	0.02728528
0.3688	0.1539	0.06477715	7.3750	2.3774	0.05406984
0.4917	0.1548	0.06768961	9.8333	2.3908	0.07614056
0.6146	0.1581	0.05820138	12.2917	2.4412	0.11489106
0.7250	0.1634	0.04662353	14.5000	2.5236	0.18154500
0.8458	0.1698	0.03615627	16.9167	2.6221	0.30802528
0.9500	0.1736	0.03166718	19.0000	2.6814	0.47706000
1.0688	0.1794	0.03315907	21.3750	2.7711	0.75499734
1.1771	0.1868	0.04082914	23.5417	2.8852	1.10341450
1.2833	0.1909	0.05355252	25.6667	2.9477	1.54763778
1.3875	0.1960	0.06991859	27.7500	3.0263	2.09511000
1.5031	0.2048	0.09094820	30.0625	3.1627	2.84852467
1.6042	0.2135	0.11033054	32.0833	3.2977	3.64593056
1.6875	0.2203	0.12615147	33.7500	3.4020	4.41000000
1.8000	0.2297	0.14635680	36.0000	3.5479	5.60664000
1.9125	0.2358	0.16474538	38.2500	3.6417	7.00800750
2.0250	0.2532	0.18170950	40.5000	3.9103	8.63050500
2.1375	0.2672	0.19891365	42.7500	4.1264	10.49053500
2.2500	0.2791	0.21958652	45.0000	4.3105	12.60450000
2.3625	0.2900	0.24881288	47.2500	4.4785	14.98880250
2.4521	0.3100	0.28294425	49.0417	4.7871	17.09169137
2.5635	0.3312	0.34658029	51.2708	5.1158	19.97441511
2.6750	0.3646	0.44454551	53.5000	5.6312	23.16736500
2.7865	0.3922	0.59117907	55.7292	6.0566	26.68649213
2.9250	0.4505	0.86792344	58.5000	6.9568	31.53946500
2.9531	0.5263	0.94013093	59.0625	8.1285	32.59194873
3.1719	0.6494	1.74843245	63.4375	10.0286	41.59317627
3.2813	0.8621	2.36147514	65.6250	13.3139	46.66011328
3.3906	1.1494	3.15624921	67.8125	17.7519	52.12469678
3.6094	1.9231	5.44426142	72.1875	29.7002	64.30709619

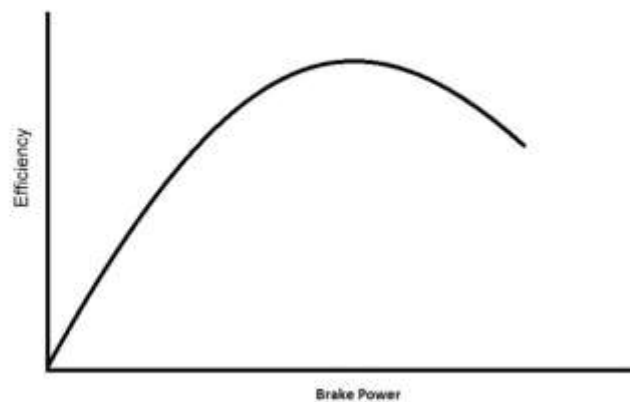


Fig. 1

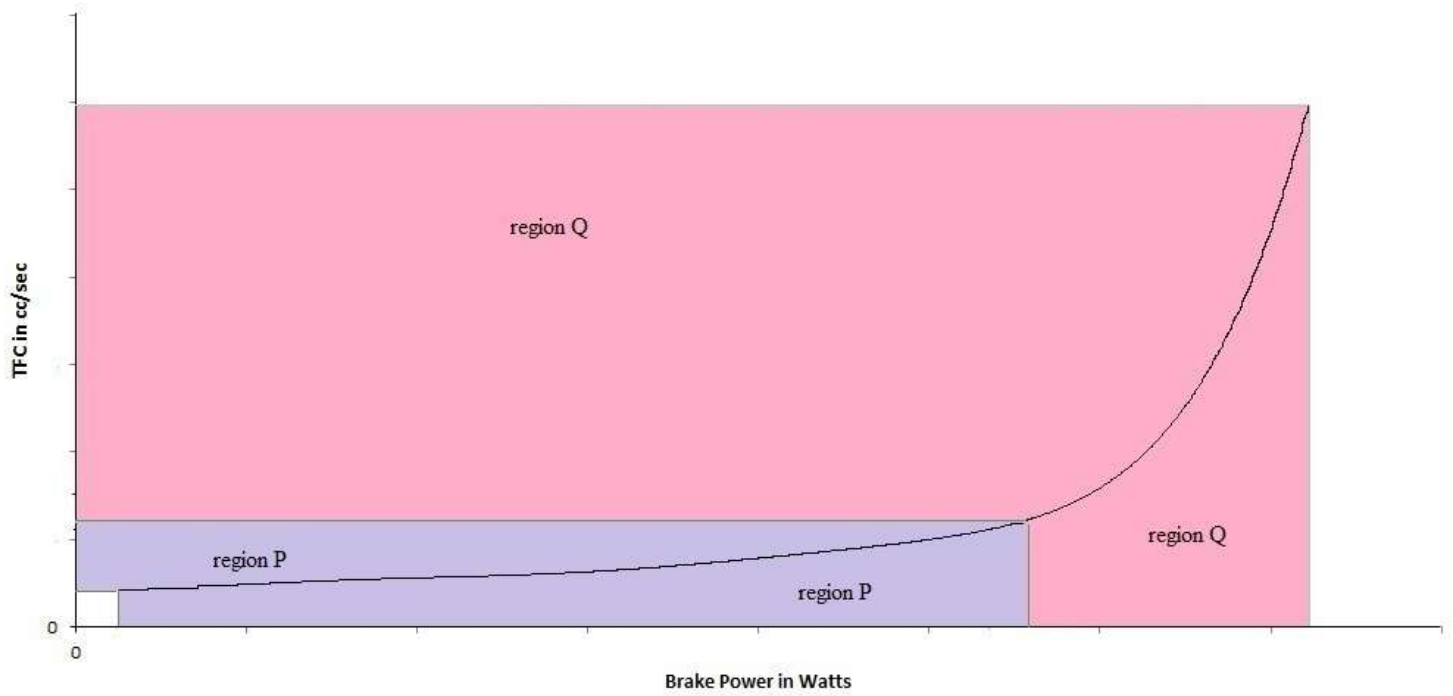


Fig 2.TFC vs. BP

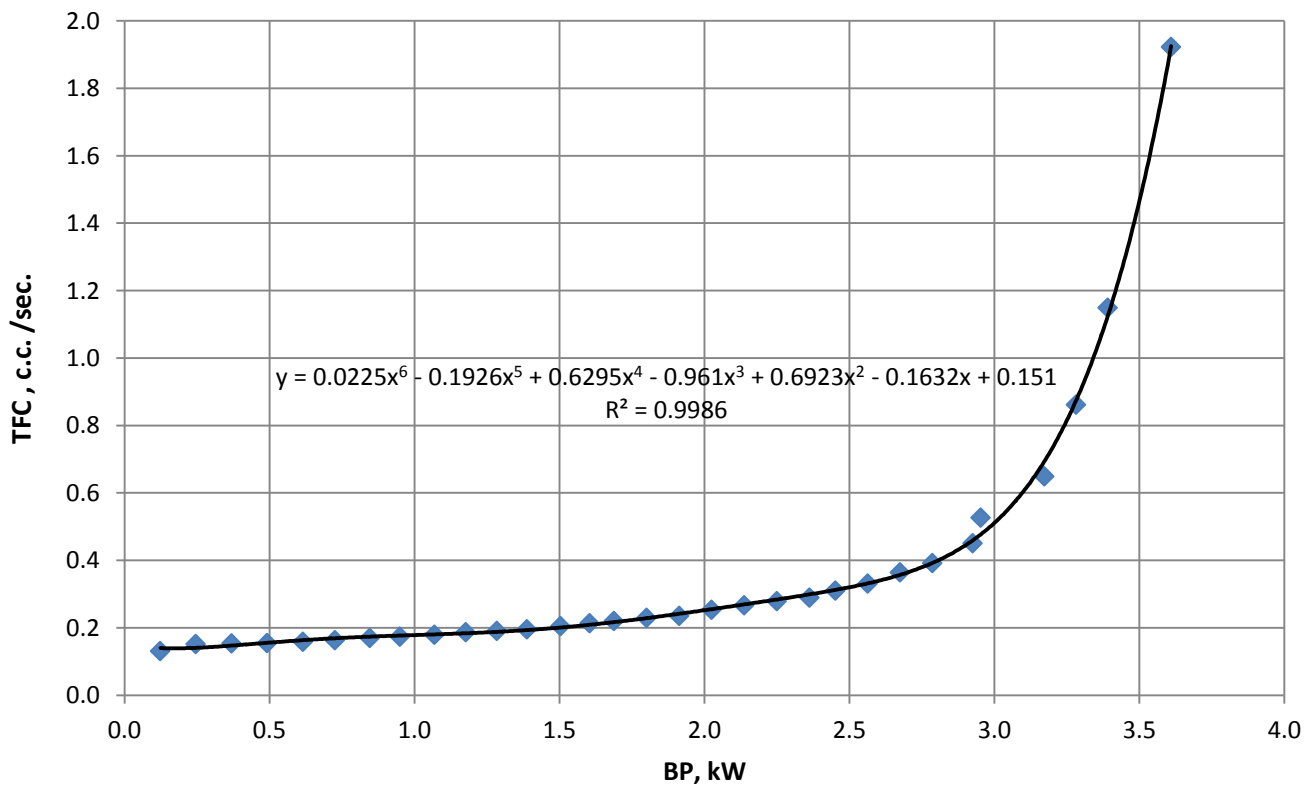


Fig.3, TFC vs BP (Engine A)

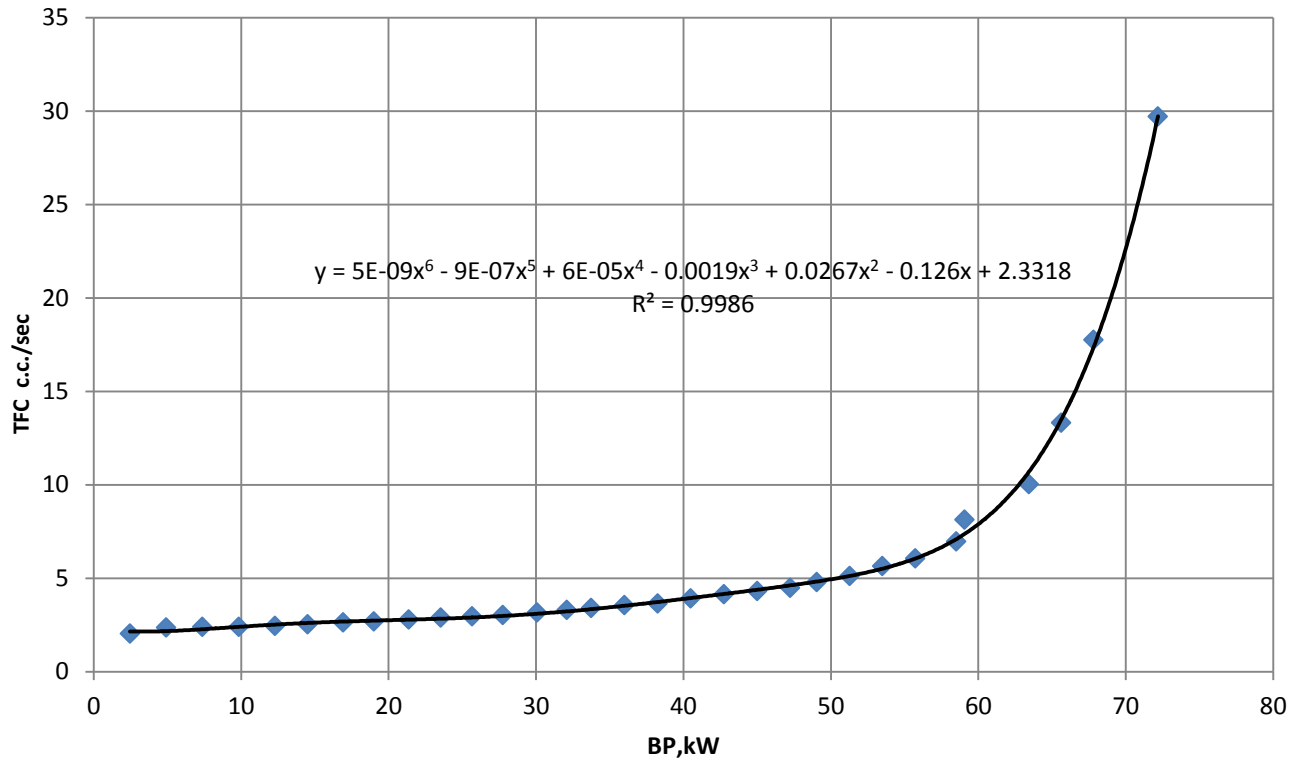


Fig. 4, TFC vs BP (Engine B)

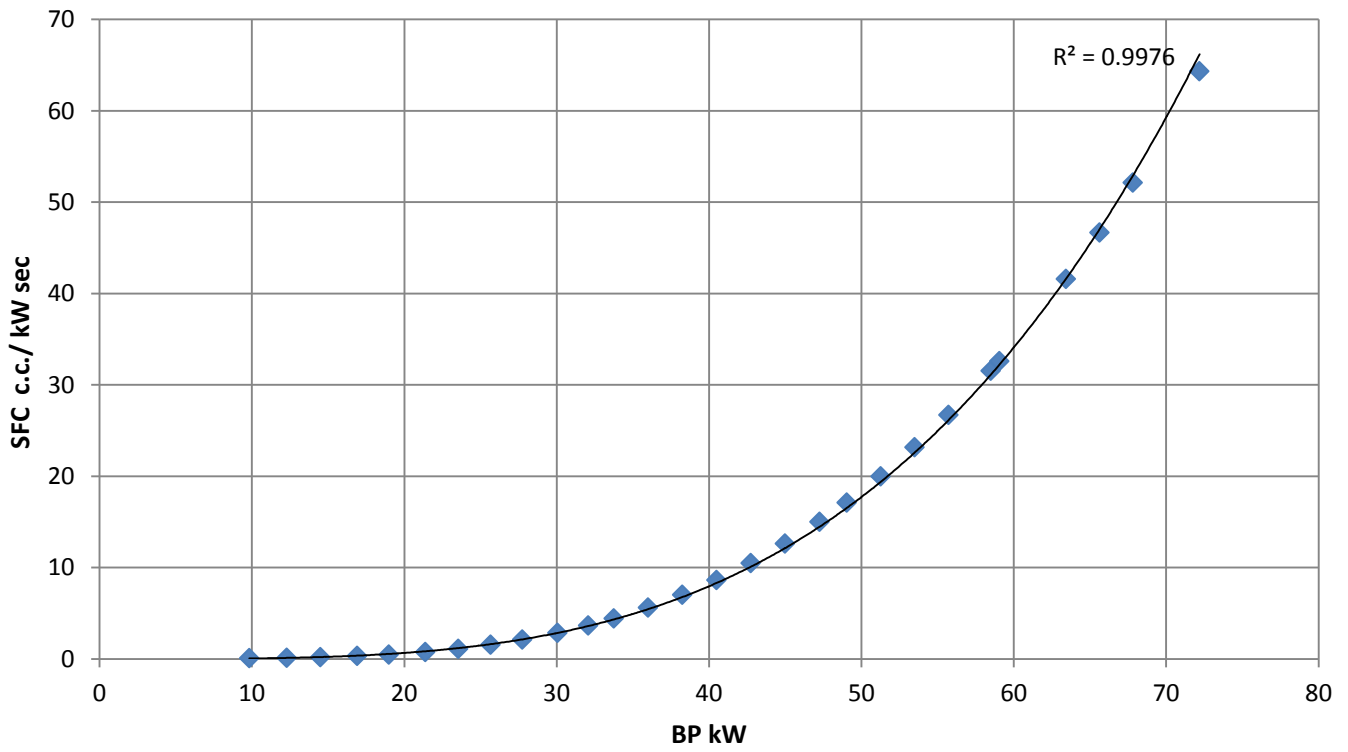


Fig. 5, SFC vs BP (Engine B)

To Establish Relation Between Destructive and Non-Destructive Tests on concrete

Nilam Bhosale¹, P.A. Salunkhe²

Assistant Professor¹, Dept. of Civil Engg., P.D.V.V.P. College of Engg, Ahmednagar, M.H., India, nilam17.bhosale@gmail.com
Assistant Professor², Dept. of Civil Engg., P.D.V.V.P. College of Engg, Ahmednagar, M.H., India, salunkhepriyanka21@gmail.com
Contact -9764544363

Abstract— Non destructive test methods are used to examine the properties and compressive strength of hardened concrete. In existing concrete structures there was no direct relation between the results of non destructive tests. This paper describes the correlation between Rebound hammer, Ultrasonic pulse velocity, core compressive strength and cylinder compressive strength of hardened concrete. It also describes the relation between bond strength and cube compressive strength and comparison of modulus of elasticity by different standards. An experimental program was carried out, involving both destructive and non destructive methods applied to different concrete mixtures, such as M20, M25 and M30. The slab of 2000 x 1000 x 200 mm were casted for each grade of concrete and cores were extracted from the slab. Also the Cylinders of size 100 x 200 mm were casted to compare the results. Cubes of size 150 x 150 x 150 mm and cubes of size 150 x 150 x 150 mm with inserted bar of size 16mm were casted and tested for compressive strength and pull out test respectively. Relationships were derived for rebound hammer, pulse velocity, compressive strength of cores and cylinders, compressive strength of cube and bond strength. The results show good behavior for these methods.

Keywords— Non destructive test (NDT), Rebound hammer, Ultrasonic pulse velocity, Compressive strength, Pullout test, core test, Cores, Cylinders.

INTRODUCTION

The Non Destructive Techniques have been grown during recent years. One of the prime objectives of Non- Destructive Testing (NDT) is to certify that the component being examined is fit for the intended service. These techniques are used for assessment of quality of construction.

Concrete has significantly influenced the nature of engineering projects. Concrete, as a composite material, is generally composed of cement, sand, aggregate, water, mineral admixtures and chemical admixtures. Considerable work has been conducted to develop rapid, non destructive tests (NDTs) that provide a reproducible measure of concrete quality in a structure. Unfortunately, as is usually the case in concrete testing, all these NDT generate results that are affected by various parameters such as aggregate type and size, age, moisture content, and mix proportion. Therefore, the correlation between measured properties and strength differs for various concretes and must be limited to the concrete in question. However, the NDTs are also convenient and have been used for many years in quality management of engineering materials. These tests are useful in determining the differences in concrete quality from one part of a structure to another. [1]

For fresh concrete it involves casting specimens of concrete and testing them for various properties. The concrete cube test and cylinder tests are the most popular tests and are used as the standard method of measuring compressive strength for quality control purpose.

Properties of hardened concrete have been examined by applying many non destructive techniques. Some of the non destructive evaluation techniques are Ultrasonic waves, Core testing, rebound hammer test, Pull out test. A known relationship between the result of in situ testing and the strength of concrete requires for the estimation of in place concrete strength. For existing construction the relationship has to be assessed on site correlation of non destructive test results to strength of core. [2]

The main objective of this paper is to develop a relationship between core compressive strength, casted cylinder compressive strength, Ultrasonic Pulse Velocity, Rebound strength. Also it develop relation between cube compressive strength & bond strength and found modulus of elasticity by different standard codes.

EXPERIMENTAL PROGRAM

A. Test specimen and testing programme

In this proposed work NDT methods are used to find compressive strength of concrete & to find relation between NDT methods and compressive strength. For that purpose slabs, cylinders, cubes, cubes with inserted bar were casted. For casting of a specimens 43 grade JK cement is used. Locally available river sand is used as fine aggregate. Locally available coarse aggregate

of size 20 mm and 10 mm were used. The coarse aggregate were crushed ballast type aggregate which are found in Deccan trap region. The properties of material used are as follows:

MATERIAL USED:

- 1) Maximum size of aggregate = 20 mm.
- 2) Cement type = 43 grade JK cement.
- 3) Specific gravity of cement = 3.15
- 4) Specific gravity of fine aggregate = 2.77
- 5) Specific gravity of coarse aggregate = 2.8
- 6) Water absorption of coarse aggregate = 0.5%
- 7) Water absorption of fine aggregate = 1.1%
- 8) Free moisture content:
 - i) Coarse aggregate = Nil.
 - ii) Fine aggregate = 1%

Concrete mix design of grades M20, M25 and M30 were prepared using IS10262-1982. The mix proportions listed in table no. 1 were adopted for this experimental work:

TABLE I
MIX PROPORTION OF CONCRETE PER CUBIC METER

Concrete grade	M20	M25	M30
Cement (Kg/m ³)	394.38	439.290	460
Water (Kg/m ³)	199.16	193.68	194.12
20mm crushed aggregate (Kg/m ³)	682.67	676.37	659.55
10mm crushed aggregate (Kg/m ³)	557.28	553.39	562.58
Natural sand (Kg/m ³)	593.14	573.35	461.21

Using above mix proportions cased test specimens are as follows:

1. For compressive strength of concrete, three Cube of size 150mm X 150mm X 150mm for each grade of concrete were casted.
2. For Bond strength of concrete, three Cube of size 150mm X 150mm X 150mm with inserted bar of dia. 16mm for each grade of concrete were casted.
3. For extracting cores, slab of size 2000 mm X 1000 mm X 200mm for each grade of concrete was casted.
4. For comparing results of cores, five moulds of cylinder of size 100 X 200 mm for each grade of concrete were casted.

Casted cube after 28 days were tested to obtain compressive strength using standard compression testing machine. Pull out test were done on cube of inserted bar of dia. 16mm.

From pull out test bond strength is to be calculated. The bond strength between concrete and steel is calculated by formula, Load divided by surface area of inserted bar (i.e. πdl).

After 28 days from casting date of slab 10 cores of 100mm diameter were extracted from each slab. The cores were drilled perpendicular to the direction of casting, so that drilled sample becomes undisturbed sample. The cores were extracted by using core cutter machine. Core test is direct method of assessing in-situ strength of concrete in a structural element. Drilled cylindrical core is removed from structure; tests may be performed on core to determine compressive strength and static modulus of elasticity of concrete is calculated from compressive strength.

In Rebound hammer test twelve hammer impacts were equally distributed on two opposite sides of each core and cylinder specimen that is sides which have been lying sideward during concreting. The rebound strength was calculated as the average of the twelve readings.

Ultrasonic Pulse Velocity Test operates on principle that stress wave propagation velocity is affected by quality of concrete. Pulse waves are induced in materials and the time of arrival measured at the receiving surface with a receiver. Electromagnetic timing circuits enable the transit time T of the pulse to be measured.

Longitudinal pulse velocity (in km/s or m/s) is given by:

$$V = L / T$$

Where V = Pulse velocity, L = Path length, T = time taken by the pulse to traverse that length.

Ultrasonic pulse velocity is influenced by elastic modulus, strength of concrete, density and moisture content.

After rebound hammer and ultrasonic pulse velocity test, the same cores and cylinders were destructively tested to obtain crushing strengths using standard compression machine.

TEST RESULTS

The following results were tabulated after testing specimen of cores and cylinders for rebound hammer, pulse velocity test and compressive strength. Also cubes and cubes with inserted bars were tested for compressive strength and bond strength respectively.

A. For M20 grade of concrete

**TABLE II
CORE TEST RESULT**

Sample No.	Rebound strength inclination angle = 0 ⁰	UP V km/s	Comp. strength N/mm ²	Equivalent cube strength IS 516-1959	Density kN/m ³
1	20.6	3.88	21.7	25.75	23.82
2	21.39	3.94	22.4	26.74	24.97
3	20.34	3.88	21.5	25.43	23.87
4	21.2	3.9	21.8	26.50	22.74
5	20.9	3.9	21.7	26.13	23.65
6	19.77	3.84	21.1	24.71	23.74
7	21.98	3.95	22.8	27.48	24.65
8	23.02	4.02	23.7	28.78	24.89
9	21.49	3.92	21.9	26.86	23.87
10	21.18	3.92	22.1	26.48	23.96
Avg.	21.19	3.91	22.07	26.49	23.04

**TABLE III
CYLINDER TEST RESULT**

Sample No.	Rebound strength inclination angle = 0 ⁰	UPV km/s	Comp. strength N/mm ²	Equivalent cube strength IS 516 -1959	Density kN/m ³
1	21.9	4.07	22.5	27.38	24.94
2	23.74	4.25	24.6	29.68	23.02
3	21.55	4.06	21.9	26.94	23.77
4	23.74	4.18	24.4	29.68	24.42
5	22.28	4.16	23.2	27.85	25.81
Avg.	22.64	4.14	23.32	28.30	23.39

**TABLE IV
CUBE TEST RESULTS**

Sample No.	Load (kN)	Compressive strength (N/mm ²)	Average Compressive strength (N/mm ²)
1	550.3	24.46	27.1
2	615.4	27.35	
3	663.6	29.49	

**TABLE V
PULL OUT TEST RESULTS**

Sample No.	Load (kN)	Bond strength (N/mm ²)	Average Bond strength (N/mm ²)	Average Bond strength (N/mm ²) AS per IS 456-2000
1	43.69	6.45	7.45	1.92
2	59.88	8.84		
3	47.82	7.06		

B. For M25 grade of concrete

**TABLE VI
CORE TEST RESULTS**

Sample No.	Rebound strength inclination angle = 0°	UPV km/s	Comp. strength N/mm ²	Equivalent cube strength IS 516-1959	Density kN/m ³
1	25.39	4.07	25.8	31.74	25.66
2	25.13	4.06	25.7	31.41	24.89
3	25.63	4.09	25.9	32.04	23.74
4	25.58	4.08	25.9	31.98	24.16
5	24.76	4.02	25.5	30.95	23.43
6	25.82	4.1	26	32.28	24.67
7	24.36	4.02	25.5	30.45	23.22
8	25.73	4.1	26	32.16	24.18
9	25.79	4.11	26.1	32.24	24.23
10	26.05	4.09	26.2	32.56	25.11
Avg.	25.42	4.07	25.86	31.78	24.33

**TABLE VII
CYLINDER TEST RESULTS**

Sample No.	Rebound strength inclination angle = 0°	UPV km/s	Comp. strength N/mm ²	Equivalent cube strength IS 516-1959	Density kN/m ³
1	25.92	4.25	27	32.40	24.4
2	25.26	4.2	26.1	31.58	23.48
3	26.59	4.3	27.7	33.24	24.72
4	26.76	4.3	28.4	33.45	24.48
5	24.91	4.15	25.8	31.14	23.59
Avg.	25.88	4.24	27	32.36	24.13

**TABLE VIII
CUBE TEST RESULTS**

Sample No.	Load (kN)	Compressive strength (N/mm ²)	Average Compressive strength (N/mm ²)
1	803.5	35.71	32.36
2	762.3	33.88	
3	618.8	27.50	

**TABLE IX
PULL OUT TEST RESULTS**

Sample No.	Load (kN)	Bond strength (N/mm ²)	Average Bond strength (N/mm ²)	Average Bond strength (N/mm ²) AS per IS 456-2000
1	65.23	9.63	8.55	2.24
2	56.15	8.29		
3	52.36	7.73		

C. For M30 grade of concrete

TABLE X
CORE TEST RESULTS

Sample No.	Rebound strength inclination angle = 0°	UPV km/s	Comp. strength N/mm ²	Equivalent cube strength IS 516-1959	Density N/m ³
1	26.33	4.05	27.8	32.91	23.29
2	26.62	4	28.2	33.28	23.48
3	27.73	4.07	29.4	34.66	23.12
4	27.74	4.06	29.6	34.68	24.19
5	27.18	4.02	28.5	33.98	24.11
6	27.73	4.04	28.9	34.66	24.58
7	27.07	4.05	29.1	33.84	24.78
8	28.69	4.16	31.4	35.86	25.34
9	28.46	4.12	30.8	35.58	25.26
10	28.85	4.13	30.8	36.06	26.17
Avg.	27.64	4.07	29.45	34.55	24.4

TABLE XI
CYLINDER TEST RESULTS

Sample No.	Rebound strength inclination angle = 0°	UPV km/s	Comp. strength N/mm ²	Equivalent cube strength IS 516-1959	Density kN/m ³
1	27.02	4.3	29.8	33.78	23.67
2	27.39	4.28	30.9	34.24	24.36
3	28.75	4.43	36.2	35.94	24.75
4	28.85	4.4	34.9	36.06	24.44
5	28.13	4.35	33.9	35.16	24.94
Avg	28.03	4.35	33.14	35.036	24.43

TABLE XII
CUBE TEST RESULTS

Sample No.	Load (kN)	Compressive strength (N/mm ²)	Average Compressive strength (N/mm ²)
1	806.4	35.84	35.09
2	784.6	33.27	
3	813.16	36.16	

TABLE XIII
PULL OUT TEST RESULTS

Sample No.	Load (kN)	Bond strength (N/mm ²)	Average Bond strength (N/mm ²)	Average Bond strength (N/mm ²) AS per IS 456-2000
1	64.21	9.48	9.56	2.4
2	58.52	8.64		

3	71.53	10.56		
---	-------	-------	--	--

TABLE XIV
 MODULUS OF ELASTICITY OF CONCRETE

	IS 456-2000	ACI 318-1995	BS 8110-1985 (PART2)	IS 13311-1992 (PART1)
FORMULA	Ec =	Ec =	Ec,28 = Ko +	<i>Dynamic modulus of elasticity</i>
Grade of Concrete	$5000 \cdot \sqrt{f_{ck}}$ (N/ mm ²) X10 ⁻³ (kN/mm ²)	$57000(f_{ck})^{1/2}$ (Psi) X 145.0377 X10 ⁻³ (kN/mm ²)	0.2 f_{cu,28} (kN/mm ²)	$= E = \frac{\rho(1+\mu)(1-2\mu)E^2}{1-\mu}$ (N/ mm ²) X10 ⁻³ (kN/mm ²)
M20	26.69	24.36	25.70	29.99
M25	29.27	26.68	26.86	33.67
M30	30.64	27.82	27.51	33.81

Where,

Ec=Static modulus of elasticity

Ed= Dynamic modulus of elasticity

D. COMPARISON OF RESULTS

From observation table comparison of average rebound strength, average UPV and average compressive strength of cylinders and cores for M20, M25 and M30 grades of concrete is done. It observed that, 1. Average rebound strength of cylinders is greater than average rebound strength of cores. 2. Average UPV of cylinders is greater than average UPV of cores. 3. Average compressive strength of cylinders is greater than average compressive strength of cores.

The relation between average compressive strength of cubes (f_{cube}) and average compressive strength cylinders (f_{cyl}) are developed from above results is given below:

TABLE XV
 RELATION BETWEEN CUBE AND CYLINDRICAL COMPRESSIVE STRENGTH.

Grade	Relation between f _{cube} and f _{cyl}	Relation between f _{cube} and f _{cyl} as per IS 516-1959
For M20	f _{cube} = 1.16 f _{cyl}	f _{cube} = 1.25 f _{cyl}
For M25	f _{cube} = 1.20 f _{cyl}	f _{cube} = 1.25 f _{cyl}
For M30	f _{cube} = 1.06 f _{cyl}	f _{cube} = 1.25 f _{cyl}

Calibration curves for rebound method and Ultrasonic pulse method are drawn using regression analysis. The relations were drawn by plotting the rebound number and Pulse velocity against the compressive strength.

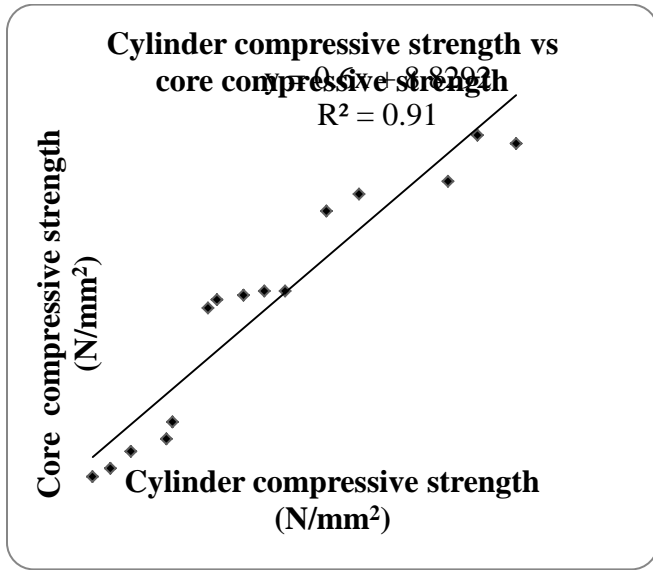


Fig.1: Cylinder compressive strength vs core compressive strength.

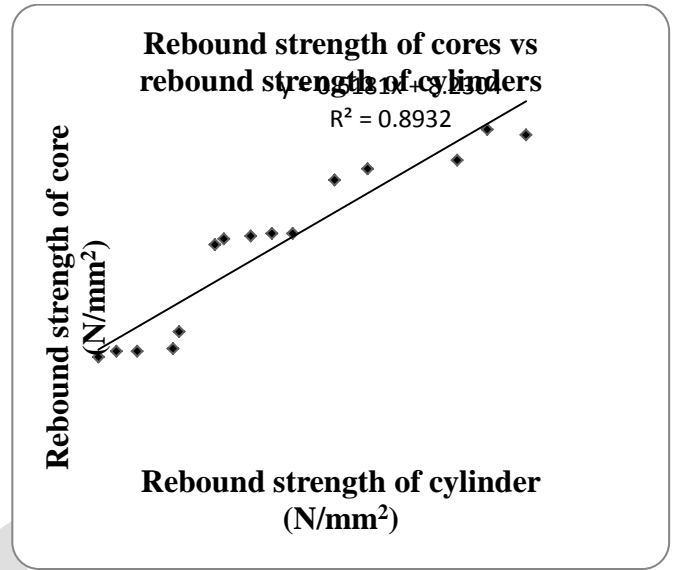


Fig.2: Rebound no. of cylinders vs rebound no. of cores.

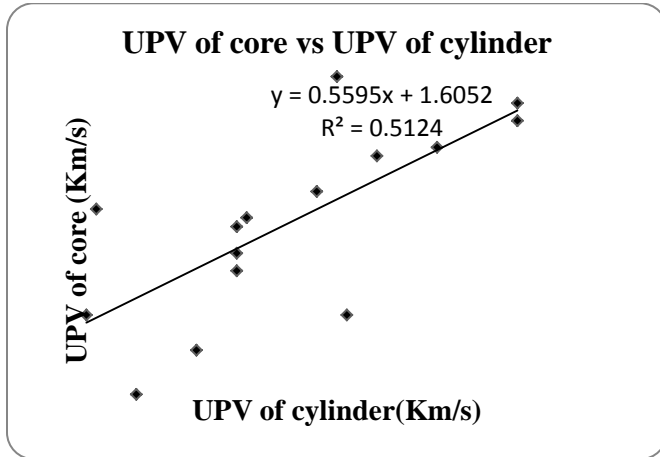


Fig.3: UPV of cylinders vs UPV of cores

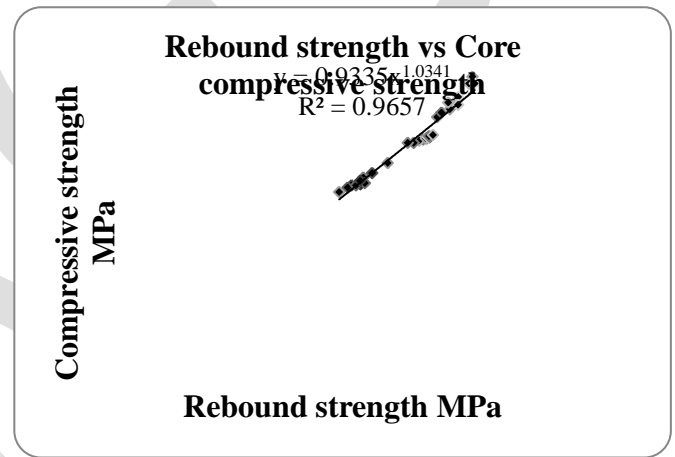


Fig.4: Core compressive strength vs rebound strength.

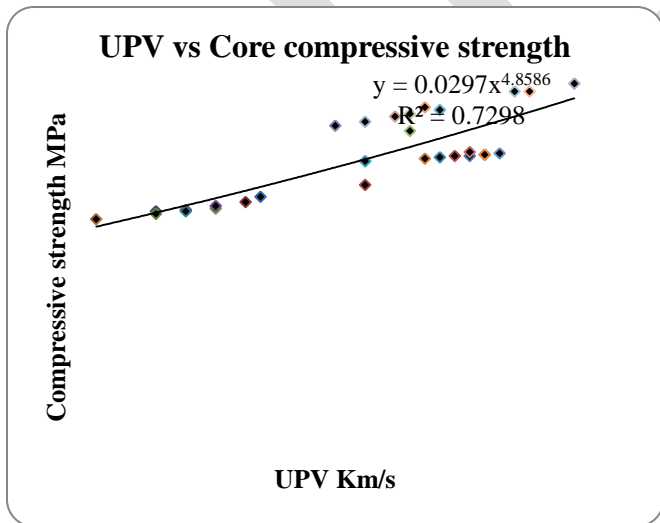


Fig.5: Core compressive strength vs UPV.

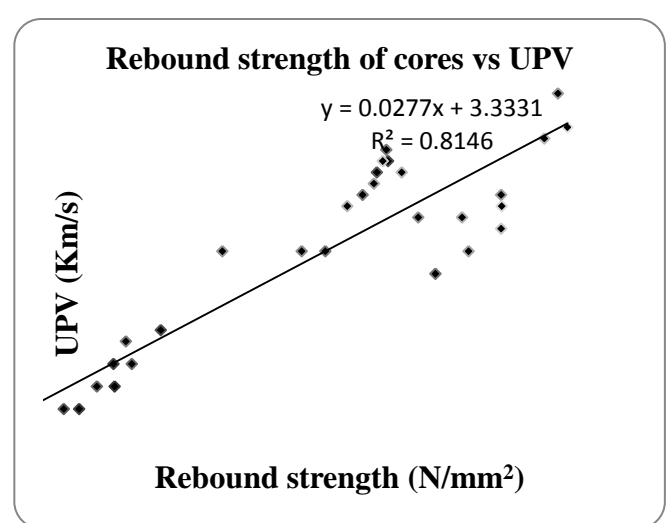


Fig 6: Rebound strength of cores vs UPV

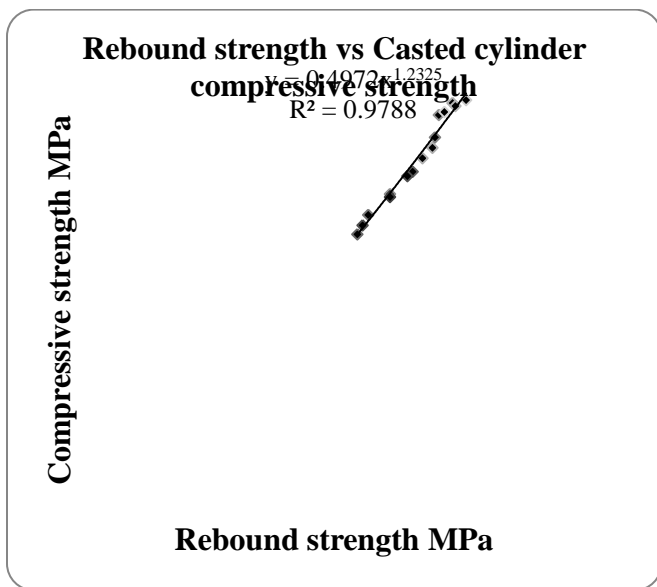


Fig.7: Cylinder compressive strength vs rebound strength

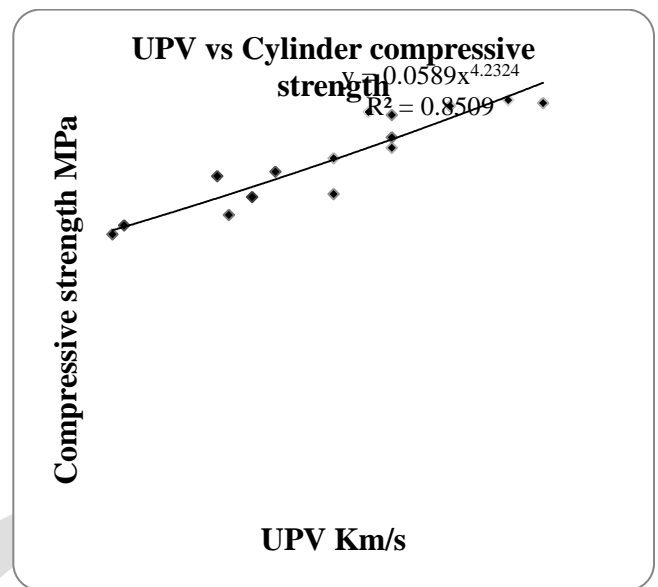


Fig.8: Cylinder compressive strength vs UPV.

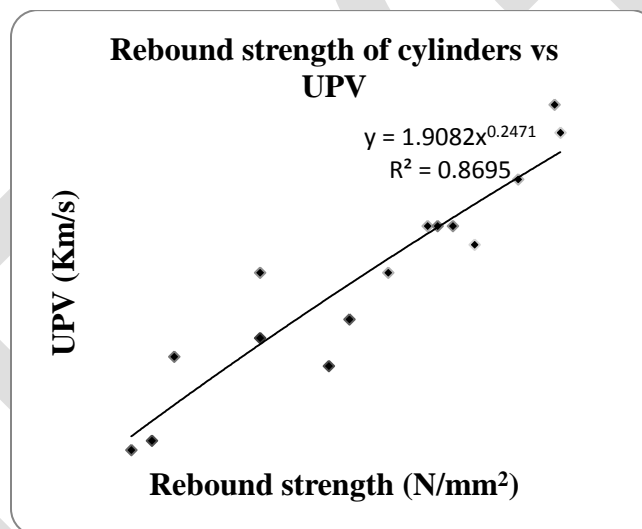


Fig 9: Rebound strength of cylinders vs UPV.

REGRESSION ANALYSIS

In the proposed work statistical methods are used for explanation of the tests results and the prediction of concrete strength. Statistical concepts indispensable in the analysis of any test result related to the mechanical strength of the concrete which obtained in lab from the compressive strength test carried out to a sample of core even in a standard cylinder form.

This work included to predict the analytical relationships between

1. Crushing strength of core with casted cylinder
2. Crushing strength of core with rebound strength.
3. Crushing strength of core with UPV.
4. Crushing strength of casted cylinder with rebound strength.
5. Crushing strength of casted cylinder with UPV.
6. Crushing strength of cubes with bond strength.

For analysis process of the results regression analysis method was used. The goal of regression method is to fit a line through points (results) so that the squared deviations of the observed points from that line are minimized. In regression analysis we obtain a set of coefficients for an equation.

EQUATIONS OF RELATIONSHIP AFTER REGRESSION ANALYSIS

Different regress model of curve between rebound number, Pulse velocity and the compressive strength of concrete core according to the experimental data is given below:

TABLE XVI

REGRESS MODEL BETWEEN REBOUND STRENGTH, PULSE VELOCITY AND THE COMPRESSIVE STRENGTH OF CONCRETE CORE FOR COMBINATION OF M20, M25 AND M30 GRADE OF CONCRETE

Type of Equations	Core compressive strength vs Rebound strength Relations	Core compressive strength vs UPV relations	Rebound strength of core vs UPV relations
Linear	$f_{cor} = 1.099 R_{cor} - 1.428$ $R^2 = 0.962$	$f_{cor} = 30.53 U_{cor} - 96.93$ $R^2 = 0.700$	$U_{cor} = 0.027 R_{cor} + 3.333$ $R^2 = 0.814$
Exponential	$f_{cor} = 8.786e^{0.043} R_{cor}$ $R^2 = 0.976$	$f_{cor} = 0.193e^{1.214} U_{cor}$ $R^2 = 0.729$	$U_{cor} = 3.384e^{0.006} R_{cor}$ $R^2 = 0.815$
Logarithmic	$f_{cor} = 26.25\ln(R_{cor}) - 58.28$ $R^2 = 0.946$	$f_{cor} = 122.0\ln(U_{cor}) - 143.9$ $R^2 = 0.700$	$U_{cor} = 0.674\ln(R_{cor}) + 1.860$ $R^2 = 0.830$
Polynomial	$f_{cor} = 0.075 R_{cor}^2 - 2.566 R_{cor} + 42.46$ $R^2 = 0.985$	$f_{cor} = -5.686 U_{cor}^2 + 76.00 U_{cor} - 187.8$ $R^2 = 0.700$	$U_{cor} = -0.002 R_{cor}^2 + 0.166 R_{cor} + 1.671$ $R^2 = 0.858$
Power	$f_{cor} = 0.933 R_{cor}^{1.034}$ $R^2 = 0.965$	$f_{cor} = 0.029 U_{cor}^{4.858}$ $R^2 = 0.729$	$U_{cor} = 2.340 R_{cor}^{0.168}$ $R^2 = 0.832$

TABLE XVII

REGRESS MODEL BETWEEN REBOUND STRENGTH, PULSE VELOCITY AND THE COMPRESSIVE STRENGTH OF CASTED CYLINDER FOR COMBINATION OF M20, M25 AND M30 GRADE OF CONCRETE.

Type of Equations	Cylinder compressive strength vs Rebound strength Relations	Cylinder compressive strength vs UPV relations	Rebound strength of Cylinder vs UPV relations
Linear	$f_{cyl} = 1.304 R_{cyl} - 6.314$ $R^2 = 0.975$	$f_{cyl} = 26.38 U_{cyl} - 85.10$ $R^2 = 0.848$	$U_{cyl} = 0.042 R_{cyl} + 3.174$ $R^2 = 0.875$
Exponential	$f_{cyl} = 7.583e^{0.049} R_{cyl}$ $R^2 = 0.981$	$f_{cyl} = 0.386e^{0.997} U_{cyl}$ $R^2 = 0.849$	$U_{cyl} = 3.296e^{0.009} R_{cyl}$ $R^2 = 0.876$
Logarithmic	$f_{cyl} = 32.44\ln(R_{cyl}) - 77.97$ $R^2 = 0.969$	$f_{cyl} = 111.8\ln(U_{cyl}) - 134.7$ $R^2 = 0.849$	$U_{cyl} = 1.046\ln(R_{cyl}) + 0.861$ $R^2 = 0.868$
Polynomial	$f_{cyl} = 0.035 R_{cyl}^2 - 0.459 R_{cyl} + 15.61$ $R^2 = 0.977$	$f_{cyl} = -10.04 U_{cyl}^2 + 111.5 U_{cyl} - 265.5$ $R^2 = 0.850$	$U_{cyl} = 0.001 R_{cyl}^2 - 0.052 R_{cyl} + 4.355$ $R^2 = 0.882$
Power	$f_{cyl} = 0.497 R_{cyl}^{1.232}$ $R^2 = 0.978$	$f_{cyl} = 0.058 R_{cyl}^{14.232}$ $R^2 = 0.850$	$U_{cyl} = 1.908 R_{cyl}^{0.247}$ $R^2 = 0.869$

TABLE XVIII

RELATION BETWEEN CASTED CYLINDER AND CORE TEST RESULTS.

Types of equation	Cylindrical compressive strength vs core compressive strength	Rebound strength of casted cylinder vs Rebound strength of core.	UPV of casted cylinder vs UPV of core.
Linear	$f_{cor} = 0.6f_{cyl} + 8.829$ $R^2 = 0.91$	$R_{cor} = 1.098 R_{cyl} - 3.589$ $R^2 = 0.948$	$U_{cor} = 0.539U_{cyl} + 1.710$ $R^2 = 0.557$
Exponential	$f_{cor} = 13.17e^{0.023} f_{cyl}$ $R^2 = 0.890$	$R_{cor} = 7.484e^{0.046} R_{cyl}$ $R^2 = 0.941$	$U_{cor} = 2.248e^{0.135} U_{cyl}$ $R^2 = 0.559$
Logarithmic	$f_{cor} = 17.32\ln(f_{cyl}) - 31.87$ $R^2 = 0.935$	$R_{cor} = 27.51\ln(R_{cyl}) - 64.57$ $R^2 = 0.949$	$U_{cor} = 2.295\ln(U_{cyl}) + 0.683$ $R^2 = 0.562$
Polynomial	$f_{cor} = -0.034 f_{cyl}^2 + 2.586 f_{cyl} - 19.25$ $R^2 = 0.958$	$R_{cor} = -0.020 R_{cyl}^2 + 2.152 R_{cyl} - 16.75$ $R^2 = 0.949$	$U_{cor} = -1.373 U_{cyl}^2 + 12.18 U_{cyl} - 22.95$ $R^2 = 0.607$
Power	$f_{cor} = 2.648 f_{cyl}^{0.681}$	$R_{cor} = 0.574 R_{cyl}^{1.157}$	$U_{cor} = 1.736 U_{cyl}^{0.577}$

	$R^2 = 0.921$	$R^2 = 0.945$	$R^2 = 0.563$
--	---------------	---------------	---------------

TABLE XIX
RELATION BETWEEN CUBE COMPRESSIVE STRENGTH AND BONDS STRENGTH.

Sr. No	Relations	Function	R ²
1	Linear	$f_{bd} = 0.256f_{ck} + 0.43$	0.975
2	Exponential	$f_{bd} = 3.237e^{0.030} f_{ck}$	0.985
3	Logarithmic	$f_{bd} = 7.845\ln(f_{ck}) - 18.50$	0.965
4	Polynomial	$f_{bd} = 0.020 f_{ck}^2 - 0.987 f_{ck} + 19.43$	1
5	Power	$f_{bd} = 0.339 f_{ck}^{0.934}$	0.977

CONCLUSIONS

The following conclusions are drawn from the results obtained from the experimental work

1. The following relations are drawn by considering different parameters such as compressive strength, Rebound number and ultrasonic pulse velocity of casted cylinders & cores which are extracted from casted slab:

- Relation between the compressive strength of cylinders and compressive strength of cores is $f_{cor} = -0.034f_{cyl}^2 + 2.586f_{cyl} - 19.25$.
- The relation between rebound strength of cylinders and rebound strength of cores are $R_{cor} = -0.020R_{cyl}^2 + 2.152R_{cyl} - 16.75$ and $R_{cor} = 27.51\ln(R_{cyl}) - 64.57$.
- The relation between rebound ultrasonic pulse velocity of cylinders and ultrasonic pulse velocity of cores is $U_{cor} = 1.373U_{cyl}^2 + 12.18U_{cyl} - 22.95$.

2. The following relations are drawn by considering different parameters such as compressive strength, Rebound strength and ultrasonic pulse velocity of cores which are extracted from casted slab:

- The relation between rebound strength and compressive strength of cores is $R_{cor} = -0.050f_{cor}^2 + 3.487f_{cor} - 31.16$.
- The relation between ultrasonic pulse velocity and compressive strength of cores is $U_{cor} = -0.003f_{cor}^2 + 0.181f_{cor} + 1.410$.
- The relation between rebound strength and ultrasonic pulse velocity of is $U_{cor} = -0.002 R_{cor}^2 + 0.166 R_{cor} + 1.671$.

3. The following relations are drawn by considering different parameters such as compressive strength, Rebound number and ultrasonic pulse velocity of casted cylinders:

- The relation between rebound strength and compressive strength of cylinders is $R_{cyl} = -0.037f_{cyl}^2 + 2.712f_{cyl} - 19.85$.
- The relation between ultrasonic pulse velocity and compressive strength of cylinders is $U_{cyl} = 0.022f_{cyl} + 3.64$.
- The relation between rebound strength and ultrasonic pulse velocity of cylinders $U_{cyl} = 0.001R_{cyl}^2 - 0.052R_{cyl} + 4.355$.

4. There is well-built relationship between the cube compressive strength and bond strength. $f_{bd} = 0.020f_{ck}^2 - 0.987f_{ck} + 19.43$, $R^2 = 1$. As R-square value is close to 1.0 it indicates that almost all of the variability with the variables specified in the model.

5. Modulus of elasticity is calculated by IS 456, BS 8110-1985 and ACI 318-1995 code. After comparing the results it is found that modulus of elasticity calculated by IS 13311-1992 i.e. dynamic modulus of elasticity (Ed) is greater than the static modulus of elasticity (Ec) calculated by other methods.

The relation between static modulus of elasticity (Ec) and dynamic modulus of elasticity (Ed) is given below.

- For M20 $E_d = 1.12 E_c$
- For M25 $E_d = 1.15 E_c$
- For M30 $E_d = 1.10 E_c$

REFERENCES:

- Jen-Chei Liu, Mou-Lin Sue and Chang-Huan Kou "Estimating the Strength of Concrete Using Surface Rebound Value and Design Parameters of Concrete Material" Tamkang Journal of Science and Engineering, Vol. 12, No. 1, pp. 17 (2009).
- Tony Zheng, "Role of Advanced Non-Destructive Tests in Construction and Repair of Concrete Structures" Building & Construction, Research and Consultancy (BCRC), Perth, WA, Australia.
- M. Yaqub, M. Anjum Javed "Comparison of Core and Cube Compressive Strength of Hardened Concrete" 31st Conference on our world in concrete & structures at Singapore, 16 - 17 August 2006.
- Mohammadreza Hamidian, Ali Shariati, M. M. Arabnejad Khanouki, Hamid Sinaei, Ali Toghrolfi and Karim Nouri "Application of Schmidt Rebound Hammer and Ultrasonic Pulse Velocity Techniques for Structural Health Monitoring" 22 Nov 2011.
- Dr. Isam H. Nash't, Saeed Hameed A'bour, Anwar Abdullah Sadoon, "Finding an Unified Relationship Between Crushing Strength of Concrete and Non-destructive Tests" 3rd MENDT - Middle East Nondestructive Testing Conference & Exhibition Bahrain, Manama 27-30 Nov 2005.

- [6] Hassan R. Hajjeh, "Correlation between Destructive and Non-Destructive Strengths of Concrete Cubes Using Regression Analysis" Contemporary Engineering Sciences, Vol. 5, no. 10, 493 – 509, 2012.
- [7] Sanjeev Kumar Verma, Sudhir Singh Bhadauria, and Saleem Akhtar, "Review of Nondestructive Testing Methods for Condition Monitoring of Concrete Structures," Journal of Construction Engineering, vol. 2013, Article ID 834572, 11 pages, 2013. doi:10.1155/2013/834572
- [8] Ferhat Aydin and Mehmet Saribiyik "Correlation between Schmidt Hammer and destructive compressions testing for concretes in existing buildings" Scientific Research and Essays Vol. 5(13), pp. 1644-1648, 4 July, 2010.
- [9] IS: 516 – 1959, Methods of Tests For Strength of Concrete, Bureau of Indian Standards, New Delhi, 1959.
- [10] IS: 10262 – 1982, Recommended Guidelines For Concrete Mix Design, Bureau of Indian Standards, New Delhi, 1982.
- [11] IS: 13311 (Part 1 & Part 2): 1992, Non-Destructive Testing of Concrete -Methods of Test, Bureau of Indian Standards, New Delhi, 1992.
- [12] "Guidebook on non-destructive testing of concrete structures" IAEA, VIENNA, 2002 IAEA–TCS–17 ISSN 1018–5518.

FPGA implementation of Integer DCT for HEVC

M. Murali ¹, V. Sandhya ², P. Harika ³

¹PG scholar in ECE, ²Asst. Prof, ³Asst. Prof

Department of ECE, BVC Engineering College, Odalarevu, ¹+91-9010449605

murali.marlapudi@gmail.com, vsandhya445@gmail.com, harika.pangam@gmail.com.

Abstract--In this paper, area-efficient architectures for the implementation of integer discrete cosine transform (DCT) of different lengths to be used in High Efficiency Video Coding (HEVC) are proposed. An efficient constant matrix multiplication scheme can be used to derive parallel architectures for 1-D integer DCT of different lengths such as 4, 8, 16, and 32. Also power-efficient structures for folded and full-parallel implementations of 2-D DCT is implemented with proposed architecture. The proposed architecture with 32-point length is 29.2% and 9.2% area efficient, also results in 13.1% and 2.8% less Area-Delay product respectively when compared to basic and existing models.

Also pruning is applied to proposed architecture to improve the performance which results in 50.78% decrease in area Delay product for 32-point integer DCT.

Key Words-High Efficiency Video Coding (HEVC), integer discrete cosine transform (DCT), video coding.

I. INTRODUCTION

In digital image processing, data compression is necessary to improve efficiency in storage and transmission. Transformation is one popular technique for data compression. By first transforming correlated pixels into weakly correlated ones, and after a ranking in their energy contents, for example, and retaining only the most significant components, high compression ratio is possible [1]. Since inverse transformation is needed to reproduce the original image from the compressed data, it is important that the transform process be simple and fast. The family of orthogonal transforms [2] is well suited for this application because the inverse of an orthogonal matrix is its transpose. In real-time applications, a transform is most likely implemented using a dedicated chip. Thus the shorter bit length (integer cosine transform) ICT will lead to a simpler IC structure and shorter computation time.

II. HEVC (High Efficiency Video Coding)

The discrete cosine transform has found a wide range of applications in signal and image processing [3], [4], especially in image compression. It has become the heart of international standards in image compression such as JPEG and MPEG [5]. In some applications, the input data consists of integer vectors or integer matrices. But the output of DCT does not consist of integers. For lossless coding it would be of great interest to be able to characterize the output completely again with integers. In the JPEG-2000 proposal [6], the use of the integer DCT-II for lossless image coding is recommended. However, up to now, lossless coding schemes are hardly based on integer DCTs which have been studied in recent years [7], [8], [9], [10], [11].

HEVC is said to double the data compression ratio compared to H.264/MPEG-4 AVC at the same level of video quality. It can alternatively be used to provide substantially improved video quality at the same bit rate. The design of most video coding standards is primarily aimed at having the highest coding efficiency. Coding efficiency is the ability to encode video at the lowest possible bit rate while maintaining a certain level of video quality. There are two standard ways to measure the coding efficiency of a video coding standard, which are to use an objective metric, such as peak signal-to-noise ratio (PSNR), or to use subjective assessment of video quality. Subjective assessment of video quality is considered to be the most important way to measure a video coding standard since humans perceive video quality subjectively. The Discrete Cosine Transform (DCT) plays a vital role in video compression due to its near-optimal de-correlation efficiency and high energy compaction. HEVC supports DCT of different sizes such as 4,8,16 and 32 and it is a loss compression technique. Integer DCT integrates both loss and lossless coding scheme perfectly.

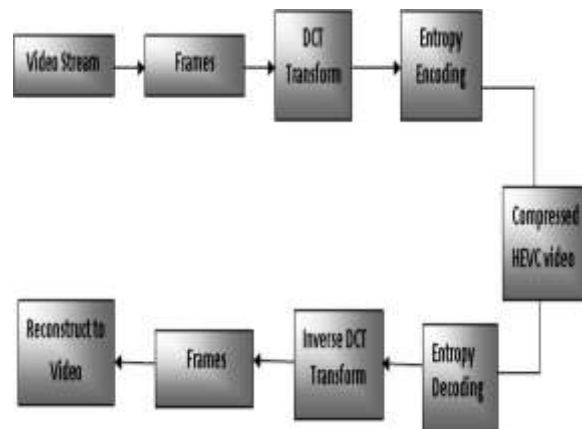


Figure1: Flow of HEVC Mechanism

III.ALGORITHM

Integer DCT can be generated by make use of Matrix. The 4-point Integer DCT generation depends on 2x2 matrices that are obtained from a 4x4 matrix as given below. The shown matrix is observable to be orthogonal symmetric. The need of symmetry in the matrix is already been stated. The 8x8 and 16x16 matrices for implementation of higher order Integer DCT operations are as shown below.

$$\begin{bmatrix} 64 & 64 & 64 & 64 \\ 83 & 36 & -36 & -83 \\ 64 & -64 & -64 & 64 \\ 36 & -83 & 83 & -36 \end{bmatrix}$$

$$\begin{bmatrix} 64 & 64 & 64 & 64 & 64 & 64 & 64 & 64 \\ 89 & 75 & 50 & 18 & -18 & -50 & -75 & -89 \\ 83 & 36 & -36 & -83 & -83 & -36 & 36 & 83 \\ 75 & -18 & -89 & -50 & 50 & 89 & 18 & -75 \\ 64 & -64 & -64 & 64 & 64 & -64 & -64 & 64 \\ 50 & -89 & 18 & 75 & -75 & -18 & 89 & -50 \\ 36 & -83 & 83 & -36 & -36 & 83 & -83 & 36 \\ 18 & -50 & 75 & -89 & 89 & -75 & 50 & -18 \end{bmatrix}$$

$$\begin{bmatrix} 64 & 64 & 64 & 64 & 64 & 64 & 64 & 64 & 64 & 64 & 64 & 64 & 64 & 64 & 64 \\ 90 & 87 & 80 & 70 & 57 & 43 & 25 & 9 & -9 & -25 & -43 & -57 & -70 & -80 & -87 & -90 \\ 89 & 75 & 50 & 18 & -18 & -50 & -75 & -89 & -89 & -75 & -50 & -18 & 18 & 50 & 75 & 89 \\ 87 & 57 & 9 & -43 & -80 & -90 & -70 & -25 & 25 & 70 & 90 & 80 & 43 & -9 & -57 & -87 \\ 83 & 36 & -36 & -83 & -83 & -36 & 36 & 83 & 83 & 36 & -36 & -83 & -83 & -36 & 36 & 83 \\ 80 & 9 & -70 & -87 & -25 & 57 & 90 & 43 & -43 & -90 & -57 & 25 & 87 & 70 & -9 & -80 \\ 75 & -18 & -89 & -50 & 50 & 89 & 18 & -75 & -75 & 18 & 89 & 50 & -50 & -89 & -18 & 75 \\ 70 & -43 & -87 & 9 & 90 & 25 & -80 & -57 & 57 & 80 & -25 & -90 & -9 & 87 & 43 & -70 \\ 64 & -64 & -64 & 64 & 64 & -64 & -64 & 64 & 64 & -64 & -64 & 64 & 64 & -64 & -64 & 64 \\ 57 & -80 & -25 & 90 & -9 & -87 & 43 & 70 & -70 & -43 & 87 & 9 & -90 & 25 & 80 & -57 \\ 50 & -89 & 18 & 75 & -75 & -18 & 89 & -50 & -50 & 89 & -18 & -75 & 75 & 18 & -89 & 50 \\ 43 & -90 & 57 & 25 & -87 & 70 & 9 & -80 & 80 & -9 & -70 & 87 & -25 & -57 & 90 & -43 \\ 36 & -83 & 83 & -36 & -36 & 83 & -83 & 36 & 36 & -83 & 83 & -36 & -36 & 83 & -83 & 36 \\ 25 & -70 & 90 & -80 & 43 & 9 & -57 & 87 & -87 & 57 & -9 & -43 & 80 & -90 & 70 & -25 \\ 18 & -50 & 75 & -89 & 89 & -75 & 50 & -18 & -18 & 50 & -75 & 89 & -89 & 75 & -50 & 18 \\ 9 & -25 & 43 & -57 & 70 & -80 & 87 & -90 & 90 & -87 & 80 & -70 & 57 & -43 & 25 & -9 \end{bmatrix}$$

The even positions and odd positions of output vector of 4-point integer DCT can be obtained by matrix multiplication with vectors [a(0) a(1)] and [b(0) b(1)] as stated below.

$$\begin{aligned} y(0) &= \begin{bmatrix} 64 & 64 \end{bmatrix} a(0) \\ y(2) &= \begin{bmatrix} 64 & -64 \end{bmatrix} a(1) \\ y(1) &= \begin{bmatrix} 83 & 36 \end{bmatrix} b(0) \\ y(3) &= \begin{bmatrix} 36 & -83 \end{bmatrix} b(1) \end{aligned}$$

Here the intermediate vectors [a(0) a(1)] and [b(0) b(1)] are obtained from input vector [x(0) x(1) x(2) x(3)] as stated below

$$\begin{aligned} a0 &\leq x0 + x3; a1 \leq x1 + x2; \\ b0 &\leq x0 - x3; b1 \leq x1 - x2; \end{aligned}$$

Finally the multiplication of the above stated matrices with intermediate vectors will result in following equations.

$$Y(0)=64xa(0)+64xa(1)$$

$$Y(2)=64xa(0)-64xa(1)$$

$$Y(1)=83xb(0)+36xb(1)$$

$$Y(3)=36xb(0)-83xb(1)$$

To solve these equations an eight 8x8 multipliers and four 16 bit adder / subtractions are needed. As already known the implementation of digital multiplier in hardware requires number of adders and consumes considerable area and consumes considerable power, eventually result in more delay causes performance degradation of overall circuit.

In-order to optimise the design metrics the implementation of multiplier must be replaced, the obvious solution is shifters. As already known a simple left shift is equivalent to multiply by two, the output vector generation equations of 4-point integer DCT stated can be obtained using shifters replaced by multipliers is given below.

$$Y(0)=(<<6)a(0)+(<<6)a(1)$$

$$Y(2)=(<<6)a(0)-(<<6)a(1)$$

$$Y(1)={{<<6}+{<<1}}[{{<<3}+1}+1]b(0)+{{<<2}}[{{<<3}+1}]b(1)$$

$$Y(3)={{<<2}}[{{<<3}+1}]b(0)-{{<<6}+{<<1}}[{{<<3}+1}+1]b(1)$$

The implementation shown may not require any multiplications but requires six, four, two and two shifters respectively of 6-bit, 4-bit, 2-bit, 1-bit wide and four 16-bit adder/subtractor. The generalised algorithm for input vector of N-bit wide for implementation of integer DCT is as given below:

$$\begin{bmatrix} y(0) \\ y(2) \\ \cdot \\ \cdot \\ y(N-4) \\ y(N-2) \end{bmatrix} = \mathbf{C}_{N/2} \begin{bmatrix} a(0) \\ a(1) \\ \cdot \\ \cdot \\ a(N/2-2) \\ a(N/2-1) \end{bmatrix}$$

$$\begin{bmatrix} y(1) \\ y(3) \\ \cdot \\ \cdot \\ y(N-3) \\ y(N-1) \end{bmatrix} = \mathbf{M}_{N/2} \begin{bmatrix} b(0) \\ b(1) \\ \cdot \\ \cdot \\ b(N/2-2) \\ b(N/2-1) \end{bmatrix}$$

$$a(i) = x(i) + x(N - i - 1)$$

$$b(i) = x(i) - x(N - i - 1)$$

$$m_{N/2}^{i,j} = c_N^{2i+1,j} \text{ for } 0 \leq i, j \leq N/2 - 1$$

IV. PROPOSED ARCHITECTURE

The proposed architecture implementation is based on shift and add/subtract design of existing model but implemented with an architecture where hardware resources are reused to miniature the hardware requirement so as to reduce design metrics of VLSI such as area, delay, power and cost. The following flow shows the implemented design of proposed algorithm for implementation of four point integer DCT.

$$Y(0)=(<<6)a(0)+(<<6)a(1)$$

$$Y(2)=(<<6)a(0)-(<<6)a(1)$$

$$Y(1)={{<<6}+{<<1}}[{{<<3}+1}+1]b(0)+{{<<1}}[{{<<1}}[{{<<3}+1}]]b(1)$$

$$Y(3)={{<<1}}[{{<<1}}[{{<<3}+1}]]b(0)-{{<<6}+{<<1}}[{{<<3}+1}+1]b(1)$$

Here the digital block (<<1)[<<3+1] is reutilized while performing operations. Because of the reuse, algorithm requires shifter 6-bit, 3-bit and 1-bit wide respectively six, two and four. Also four 16-bit wide adders or subtractors are required.

TABLE1-Comparison of Hardware Resources Requirement

4-Point	Six-shifters	Three-shifters	Two-shifters	One-shifter
Existing	6	4	2	2
Proposed	6	2	0	4

TABLE1 above shows the Comparison between Existing and Proposed algorithms in terms of hardware resource requirement considering number of shifters required for each algorithm. The proposed architecture requires half the number of 3-bit shifters and hence area may be saved to lot extent. Implementation of hardware architecture for above algorithm will be appear as shown in the following Figure2. Architecture in Figure2 can be viewed as input addition/ subtraction unit, shifting unit and output addition/subtraction unit. Multiplication with constant 64 can be obtained as input vector left shifted by six bits and multiplication by 36 and 83 can be obtained as stated in the algorithm and hardware implementation is as shown in figure(b) below where 3-bit shifter and 1-bit shifter are reused for the calculation of both 83 and 36 multiplications. The implementation of 8, 16 and 32 point integer DCT architectures can also be done in the same way as shown in Figure2 for 4 point. Figure3 shows the implementation of hardware for constant multiplication for 8 point integer DCT implementation.

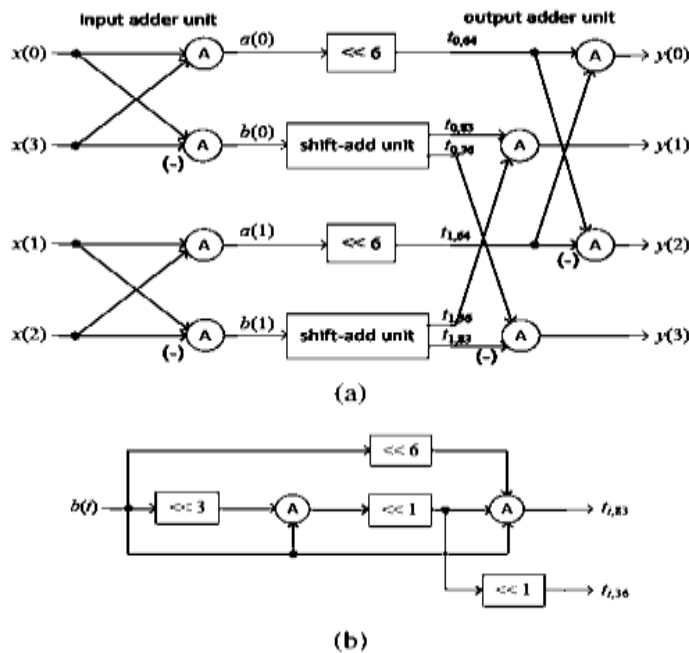


Figure2: Proposed Architecture for 4-point Integer DCT

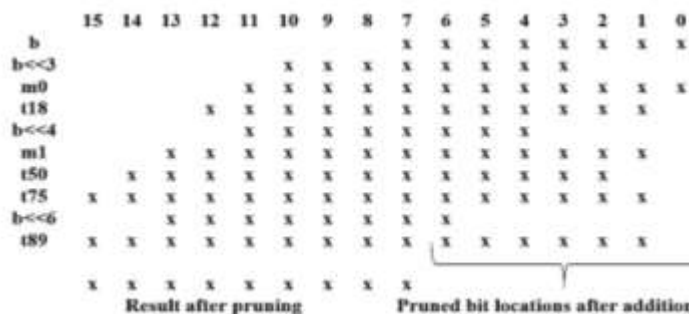


Figure3: Proposed Pruning scheme for 8-point DCT

Here one 3-bit shifter and two 1-bit shifters are reused to decrease the hardware requirement.

Image processing applications are less concern to accuracy, because of the eye persistence. Hence pruning is applied to the proposed architecture to further improve the design metrics. Figure3 shows the pruning concept applied in shift and add unit for 8-point Integer DCT, where after shift-add operation the resultant values are pruned to 9 instead of 16 to reduce the complexity of output addition unit and to reduce the transmission band width.

V.RESULTS

Integer DCT for High Efficient Video Coding implemented with varied input vectors from 4-point to 32-point and synthesized for Vertex-E FPGA. Obtained readings are tabulated in TABLE2. The implemented shift and add units with data flow from input vector to the output pad through internal hardware for calculating product of the input applied vector with Integer DCT matrix coefficients for 8-point and 16-point implementations are shown in Figure4 and Figure5 respectively. Also the implemented 2 dimensional integer DCT with dataflow is shown in figure6. The readings furnished here shows number of LUTs required, amount of Delay produced and Area-Delay Product having considerable importance in VLSI design of 4,8,16 and 32 point Integer DCT implementations using Basic algorithm, Existing algorithm and proposed algorithm.

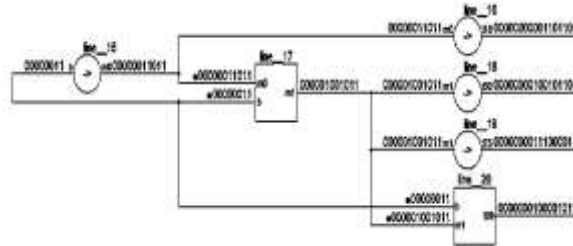


Figure4: Implemented shift and add unit for proposed 8-point architecture

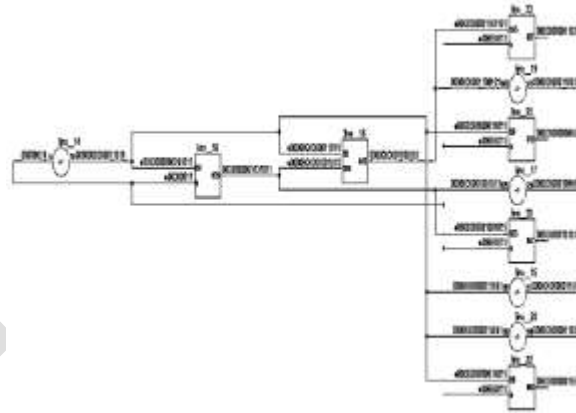


Figure5: Implemented shift and add unit for proposed 16-point architecture

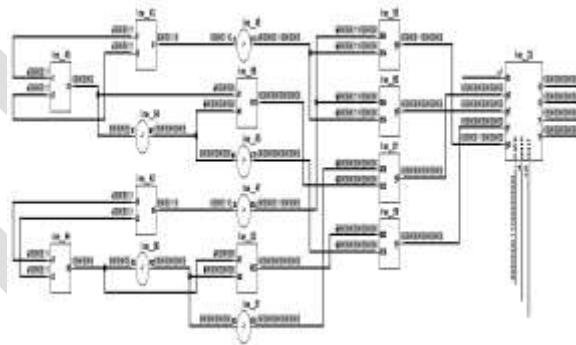


Figure6: Implemented 2D integer DCT for 4X4 input

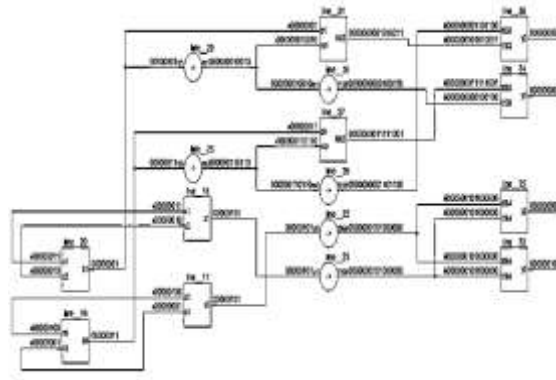


Figure7: Implemented 4-point Integer DCT with pruning.

From the readings the proposed algorithm is the best in performance in terms of area occupancy and delay produced. The proposed architecture with 32-bit length is 29.2% and 9.2% area efficient, also results in 13.1% and 2.8% less Area-Delay product respectively when compared to basic and existing models. Also implemented pruned architecture results in 50.78% decrease in area Delay product for 32-point integer DCT compared to proposed architecture. Figure8 shows the comparison of Area consumed and Delay produced among the Basic, Existing, proposed and proposed-pruned algorithms.

TABLE2 - Comparison among Basic, Existing and Proposed Architectures.

Design	N	LUT's	Delay(ns)	ADP
Basic	4	158	22.097	3.491
	8	863	24.503	21.146
	16	2927	33.937	99.333
	32	10007	47.435	474.68
Existing	4	135	20.159	2.721
	8	553	23.137	12.794
	16	2356	37.628	88.651
	32	8453	51.026	431.32
Pro-posed	4	129	20.05	2.586
	8	510	24.523	12.506
	16	1924	37.367	71.894
	32	7740	54.169	419.26
Proposed after pruning	4	114	20.05	2.285
	8	413	24.983	10.317
	16	1466	33.836	49.603
	32	5593	49.714	278.05

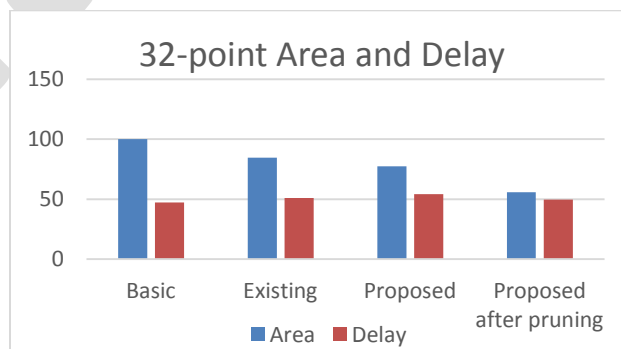


Figure8: Comparison of Area and Delay

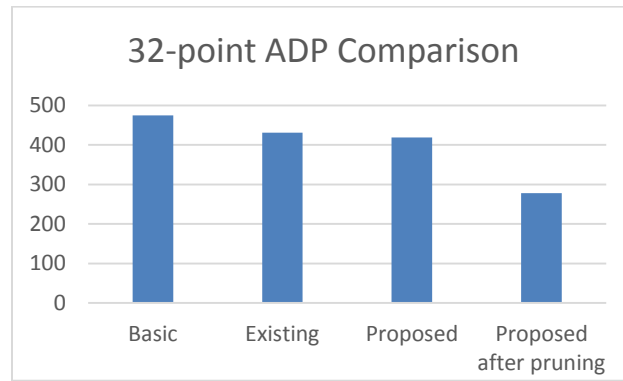


Figure9: Comparison of Area-Delay Product

Here the observed readings show that proposed algorithm occupies very less area and provides less amount of delay. Also the proposed design results in less area delay product as shown in figure9. Hence the proposed architecture optimised in terms of Design metrics. Also the proposed pruned architecture shows considerable improvement in Area-Delay-Product.

CONCLUSION

A new architecture for implementation of 4,8,16 and 32 point 1D integer DCT for HEVC is implemented and synthesized for Vertex-E FPGA. Also found that the implemented design consumes less number of LUTs and produces less amount of delay hence result in less Area Delay Product and Power Delay Product when compared to Existing and Basic methods. Also 2D integer DCT implemented in 4,8,16 and 32 point input vector. The proposed architecture with 32-bit length is 29.2% and 9.2% area efficient, also results in 13.1% and 2.8% less Area-Delay product respectively when compared to basic and existing models. Also pruning is applied to proposed architecture to improve the performance which results in 50.78% decrease in area Delay product for 32-point integer DCT. The pruned architecture for 4,8,16 and 32 point Integer DCT architectures were synthesized.

REFERENCES:

- [1] A. Rosenfeld and A. Kak, Digital Picture Processing. New York: Academic. New York, 1982.
- [2] A. K. Jain. "A sinusoidal family of unitary transforms." IEEE Trans. Pattern Analysis Much. Inrel., vol. 4, pp. 356-365, Oct. 1979.and Consent), JCT-VC L1003, Geneva, Switzerland, Jan. 2013.
- [3] K.R. Rao, P. Yip, Discrete Cosine Transform: Algorithms, Advantages, Applications, Academic Press, Boston, 1990.
- [4] G. Strang, The discrete cosine transform, SIAM Rev. 41 (1999) 135–147.
- [5] V. Bhaskaran, K. Konstantinides, Images and Video Compression Standards: Algorithms and Architectures, Kluwer, Boston, 1997.
- [6] M.W. Marcellin, M.J. Gormish, A. Bilgin, M.P. Boliek, An overview of JPEG-2000, in: Proc. Data Compression Conf., 2000, pp. 523–541.
- [7] W.K. Cham, P.C. Yip, Integer sinusoidal transforms for image processing, Internat. J. Electron. 70 (1991) 1015–1030.
- [8] L.Z. Cheng, H. Xu, Y. Luo, Integer discrete cosine transform and its fast algorithm, Electron. Lett. 37 (2001) 64–65.
- [9] K. Komatsu, K. Sezaki, Reversible discrete cosine transform, in: Proc. IEEE Internat. Conf. Acoust. Speech Signal Process. 1998, pp. 1769–1772.
- [10] J. Liang, T.D. Tran, Fast multiplier less approximations of the DCT: The lifting scheme, IEEE Trans. Signal Process. 49 (2001) 3032–3044.
- [11] W. Philips, Lossless DCT for combined lossy/lossless image coding, in: Proc. IEEE Internat. Conf. Image Process. Vol. 3, 1998, pp. 871–875

Melanoma: A Review On Various Segmentation Techniques

Rinchu Baburaj¹, Varnya C¹, Nikhil C.R²

¹P.G Scholar, ²H.O.D

Department of Electronics and Communication Engineering, Thejus Engineering College, Thrissur

E-mail- rinjoos92@gmail.com

Abstract— This paper highlights the various segmentation algorithms used in the automated melanoma detection. The application of biomedical image processing for diagnostic purpose is a non invasive technique. In order to identify skin cancer at an early stage without performing unnecessary biopsies, digital images of melanoma skin lesion have been investigated. Different segmentation techniques which aids in the efficient detection of malignant melanoma has reviewed in this paper. Among the implemented algorithms, wavelet network shows better segmentation results for skin cancer images. Automatic border detection is a challenging task in dermoscopic images.

Keywords— Melanoma, Segmentation, Dermoscopy, Thresholding, Clustering, Region Merging, Contour, Wavelet Networks

INTRODUCTION

Digital image processing plays a vital role in the area of research and has opened a wide range of new research prospects. Image processing is a profound key that can modify the outlook of many designs and proposals. Digital image processing refers to the automatic processing of digital image by means of digital computer. The basic steps involved in image processing are image acquisition, pre-processing, segmentation, enhancement of image, image compression, and restoration. In this, image segmentation has become a very significant task in today's scenario. Segmentation is usually the primary step in any computer aided analysis of images. The segmentation process converts an image into more easy and meaningful way to analyze. It is typically used to extract boundaries and curves in the images. Application areas of segmentation includes content based image retrieval, locating objects in satellite images, biometric recognition, detection of tumors, tissues in medical field.

Image segmentation is the process of dividing a digital image into multiple regions or set of pixels with homogenous properties.[2] This partitioning should be done until the region of interest in specified application has been separated. The objective behind segmentation is to simplify the representation of image for further processing. The result of segmentation is a set of segments that collectively forms the entire image. Accurate segmentation of medical images is very important for the analysis and diagnosis of abnormalities in different parts of the body. Segmentation becomes important since it further aids in the classification of extracted lesion as benign or malignant. Malignancy insists the need for analysis and thereafter medical examination. In order to avoid unnecessary biopsies, accurate classification which proceeds after accurate segmentation is needed. Performance of segmentation algorithm is greatly influenced by the properties of image selected. Thus it is not necessary that a segmentation algorithm suited for a particular medical image provides excellent results for other medical images also.

Skin cancer is considered as the most common type of cancer which accounts for considerable amount of death in human world wide. In U.S by current status, a skin cancer will develop in one in five people during their life time. Skin cancer can be broadly grouped as melanoma and benign skin cancers. Benign Melanoma is simply the appearance of moles on skin. These type of skin disease usually starts in the basal cells or squamous cells. Such cells are found at the base portion of the outer layer of the skin. [14]The continuous exposure of skin to sunlight is considered as the major reason behind skin cancers. Basal cell or squamous cell cancers can be cured if found and treated early. Malignant Melanoma is the appearance of sores that cause bleeding. It is the most deadly and dangerous form of skin cancer. It arises from the cancerous growth in pigmented skin lesion. Malignant Melanoma is named after the cell melanocyte, from which it presumably arises,. If diagnosed at the primary stage, the disease is curable. The World Health Organization approximates that more than 70230 people a year in the world die from too much sun, mostly from malignant type skin cancer. Early detection of this cancer can help its curability.

Dermoscopy, also known as Dermatoscopy or Epiluminescence Light Microscopy is non-invasive diagnosis technique for the in vivo observation of pigmented skin lesion[2]. It is a new kind of imaging technique used to examine skin lesion with an equipment called dermatoscope. Analysis of dermoscopic images plays an important role in the early diagnosis of malignant melanoma. But this conventional method is time consuming and subjective even for trained dermatologists. Due to these limitations, there is currently a great interest in the development of computer aided diagnosis systems that can assist the clinical evaluation of dermatologists. The

standard approach in automatic dermoscopic image analysis has three stages like image segmentation ,feature extraction and feature selection and lesion classification. The segmentation becomes the most important stage since it affects the accuracy and precision of subsequent steps. Existence of great varieties of lesion shapes, sizes and colors along with different skin type and textures makes the task difficult. In addition, some lesions have irregular boundaries and shows a smooth transition between lesion and skin. Other difficulties include the presence of dark thick hairs covering the lesion, existence of specular reflections and spurious edge points.[12]. Basic steps involved in the computer aided diagnosis of melanoma detection are shown below

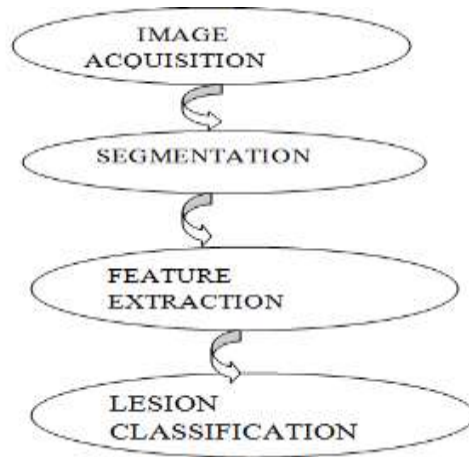


Fig: Steps for melanoma detection using CAD

In all image processing systems , the first step is to acquire an digital image from a random source defined as image acquisition. The collected image is then preprocessed for noise removal and segmented for obtaining the region of interest .Important features are extracted and are used for classifying the lesion as benign and malignant melanoma .These forms the elementary steps in all computer aided detection systems.

SEGMENTATION

Segmentation is the one of challenging tasks in digital image processing. The segmentation technique is employed to separate the lesion pigment from the healthy skin. Dermoscopic images are a great challenge for segmentation algorithms due to the different diversities in skin and lesion. In some images there is a low contrast or smooth transition between lesion and the surrounding skin. More over ,these images usually contains some intrinsic skin features like hairs ,black frames ,skin lines, blood vessels and air bubbles. Large number of segmentation algorithms have been suggested to overcome these difficulties .These algorithms can be broadly divided into 4 types[16]

A.Thresholding based Segmentation: Thresholding is one of the easiest method of segmentation where a gray scale image is transformed into binary image. Thresholding techniques have the advantage of being computationally simple and fast, and produce good results on images where there is good contrast between the lesion and the surrounding skin/ however, in the dermoscopic images these methods generally produce inconsistent results, since there is low contrast and a smooth transition between the lesion and the skin, which leads the algorithm to fail.[2]

B. Region-Based Segmentation: In this method the image is separated or clustered into small regions based on common properties of an images. Generally, region-based methods have difficulties when the pigmented skin lesions resent a great variety of colors or textures along with different skin types which leads to over segmentation.[16]

C. Edge Based Segmentation: This technique selects weather the pixels of an image belong to the edge or not. It is one of the simple segmentation method in image processes. The existence of weak edges in the images resulting from a smooth transition between lesion and skin is the main problem behind the edge based approach. Another drawback of this is the presence of noise points in the image which can be derived from some image artifacts like hairs, air bubbles and skin lines. The result can be convergence of contour to noise points and incorrectly segmented skin lesion.[8]

D.Clustering based segmentation: This is based on grouping of samples known as clusters, directly applied or extended to the high dimensional data. This technique is mostly used for gray scale images. Clustering mainly involves the partitioning of a feature space

into homogeneous regions. [12]

EXISTING ALGORITHMS

Thresholding Algorithm

H Gangster presents a thresholding based segmentation technique for melanoma recognition in [17]. Thresholding is one of the simplest segmentation technique used for melanoma detection. It comes under similarity based approach. It can be sub divided into two types global thresholding and adaptive (local) thresholding. Global thresholding uses a single threshold value throughout the entire image. It is a iterative process which considers the mean of all pixels as the initial threshold after grouping based on this initial threshold a new threshold value which is the average of mean of pixel intensities of each group is calculated. Then the pixels are regrouped based on the new threshold. This iterative process continuous till the difference between the new threshold and the previous one becomes negligibly small. The local thresholding works by dividing the image into small regions and using separate threshold value for each sub regions. The output is a binary image showing the segmented portions. Thresholding method performs fairly well for images with good contrast between foreground and the background but not for images with sharp peaks. Another advantage is that they does not require any prior knowledge about the image. This method usually fails due to the over lapping of two regions of the images. [1][19]

K Means Clustering

In K means method developed by MacQueen [18], the image pixels are divided among the clusters based on some distance metrics between cluster centroids and all pixels. The objective of K means clustering is to partition and image into mutually exclusive clusters. This is done by minimizing the selected distance metrics. The number of clusters is fixed with a prior knowledge of the image. Initially the distance between each pixels and all cluster centroids including the one pixel is located is calculated. Based on this distance metric, the pixels are reassigned to the nearest centroid, thus a new centroid is obtained based on this pixel relocation. This iterative process continuous till all the pixels have been grouped into their nearest centroid and the centroid value changes no further. K means algorithm is easily programmable and computationally economical. The output is sensitive to initial choice of clusters. [2]

Fuzzy C Means clustering

Fuzzy C means proposed by Besdek [20] is a soft computing technique and a variant of K means. Fuzzy C means is an unsupervised technique that finds application in feature analysis, clustering, and classifier designs. FCM is robust and retains more information from the original image than K means algorithm. The main objective of Fuzzy method is to minimize an objective function iteratively by introducing certain fuzziness for the belongingness of each image pixels into each cluster [21]. The degree to which each pixel belongs to a cluster is given by the membership value. The crucial problem associated with this clustering is the assignment of clusters approximately by the user that is the user may not assign the correct number of clusters for the specific application. Although this is an effective method the resulting membership value does not correspond well to the degree of belonging of the data. Also becomes inaccurate in noisy environment [2].

Statistical Region Merging

In statistical region merging proposed by Nock and Neilson [10] regions are considered as set of pixels with homogenous properties. These are iteratively grown by combining smaller regions. It is a merging segmentation where the merging of two or more regions is based on a statistical test. This statistical test works with a predicate which specify the deviation in the intensities of test regions. Thus the basic components of the algorithm can be defined as the merging predicate and the order of the merging. It is very important that any two regions in an image can be merged if and only if they satisfy the statistical test conditions. So the test conditions need to be applied for all regions before merging which will be time consuming. The algorithm has an advantage of ease to implement and it can handle images with multiple channels and noises [5].

Active Contour Models

Active contour models are parametric snake models presented by Kass [22]. This contour models locks on to the nearby edges under the influence of a user imposed constrained energy and the energy of the image. Snake is a spline which is controlled by an energy minimizing function. And it relies on the image gradient for edge detection. Active contours are often attracted by spurious edges due to artifacts and reflections which does not belong to the lesion boundaries. Therefore robust methods which are able to discard the influence of edges introduced, defined as adaptive snakes that employs estimation based on expectations maximizations algorithms for detecting contour segments. But disadvantage is that the capture range of the snake is limited and requires experts initialization also the snake do not detect curvatures in the images [8].

Gradient Vector Flow

Automatic lesion boundary detection in dermoscopic images using gradient vector flow segmentation is introduced by B Erkol in [3]. The gradient vector flow is an well known algorithm successfully used in medical imaging applications. The object boundaries are

approximated by an elastic contour which is initialized by the user. The contour is then modified based on differential equations. The gradient vector flow field allows long range attraction of the contour towards the object boundaries. The initialization of this algorithm is automatic. The method works by placing a circle with a given radius on the images. Here the circle center is given by the center of the segment region which is obtained by adaptive thresholding [23].

Fuzzy-Based Split and Merge Algorithm (FBSM)

J Maeda introduces a Fuzzy based split and merge segmentation technique in [25]. The algorithm originally aims at unsupervised perceptual segmentation of natural color images. First, the algorithm extracts color and texture features from an original image. Chrominance is used as color features and statistical geometrical features are used as texture features. Then a split and merge technique is executed in four steps: simple splitting, local merging, global merging and boundary refinement. A fuzzy based homogeneity measure is used to estimate the similarity of any adjacent regions. This combines the resemblance of color and texture features with different degrees of importance. This measure simplifies the complex mechanism of integrating different features by symbolic representation[12]

Iterative Thresholding

A novel approach for analyzing melanoma images using thresholding segmentation is proposed by Abbas Hussien Miry in [26]. In iterative segmentation the RGB image space is transformed into two intensity images. For that initially image is transformed into HVC color space, since the human color perception is closely related to HVC color space. Subsequently this is converted into intensity images. After rescaling the image with gray level histogram the higher and lower values in the lesion are compared. Two membership values are obtained which specifies the degree of certainty of pixels. Threshold values for two intensity images are then calculated, finally resulting to a binary image. Morphological operations are also performed to obtain the final lesion.[11]

Otsu's Algorithm

Otsu's algorithm is one of the oldest segmentation techniques presented by Scholar Otsu in 1979. It is a kind of global thresholding which depends on gray value of image. It is a widely used simple and effective thresholding method[27]. It is one of the leading ways for automatic thresholding which transforms the gray scale image to binary image. Otsu supports pixel density of an image and iterates the set of all values by measuring the pixel range of each side of an image. Otsu method was one of the efficient thresholding segmentation methods for general real world images considering uniformity and shape dimension measures but takes too much time to be practical for multilevel threshold selection

Wavelet Network Method.

Komal Lawand introduces a new concept of wavelet Networks for segmentation of dermoscopic images in [9]. Wavelet network is a novel approach that combines the wavelet decomposition and neural network capacity of self learning. That is neurons in the conventional neural network are replaced by wavelets in wavelet networks. For the wavelet network formation, the Mexican hat wavelet is first selected as the mother wavelet and the lattice structure is formed by choosing different shift and scale parameters. The set of effective wavelet is obtained by using two stages of screening. Finally the network weights are calculated using the orthogonal least square algorithm. Red, Green and Blue matrix value of the dermoscopic images are given as the input to the wavelet network. Then the image is segmented and the exact boundary of the skin lesion is obtained as the output. Wavelet networks take the full advantage of characteristics of wavelet transform and neural network ability of universal approximation which makes them an excellent segmentation technique for melanoma images.

CONCLUSION

The research in dermoscopic images has been increased considerably for the early detection of severe skin cancer. This paper evaluates different segmentation techniques used for tracking the boundary of skin cancer lesions. The result of each algorithm is greatly influenced by type of images used for analysis. Among the implemented algorithms, wavelet Network gives accurate segmentation results for dermoscopic images. Due to the time-frequency localization of wavelet transform and self learning characteristics of Neural Networks, Wavelet Network is more effective and robust.

REFERENCES:

- [1] Rahil Garnav i, Mohammad Aldeen, M. Emre Celebi, George, Sue Finch (2010), "Border detection in dermoscopy images using hybrid thresholding on optimized color channels", Elsevier
- [2] A.A. Haseena Thasneem, R. Mehaboobathunnisa, M. Mohammed Sathikand S. Arumugam "comparison of different segmentation algorithms for dermoscopic images" May 2015
- [3] B. Erkol, R. H. Moss, R. J. Stanley, W. V. Stoecker, and E. H. V. tum, "Automatic lesion boundary detection in dermoscopy images using gradient vector flow," *Skin Res. Technol.*, vol. 11, no. 1, pp. 17–26, Feb. 2005.
- [4] H. Zhou, M. Chen, L. Zou, R. Gass, L. Ferris, L. Drogowski, and J. Rehg, "Spatially constrained segmentation of dermoscopy images," in *Proc. 5th IEEE Int. Symp. Biomed. Imag.: Nano Macro*, May 2008, pp. 800–803.

- [5] M. E. Celebi, H. A. Kingravi, H. Iyatomi, Y. A. Aslandogan, W. V. Stoecker, R H. Moss, "Border detection in dermoscopy images using statistical region merging" *SkinRes.Technol.*, vol.14,no.3, pp. 347–353, Aug. 2008.
- [6] NidhaKhdhair El Abbadi and Abbas HussienMiry(2013), "Automatic Segmentation of Skin" Lesions Using Histogram Thresholding", *Journal of Computer Science*, Vol.10, Issue.4, pp.632-639.
- [7] M. Zortea, S. O. Skrvseth, T. R. Schopf, H. M. Kirchesch, and F. Godtlielsen, "Automatic segmentation of dermoscopic images by iterative classification," *Int. J. Biomed. Imag.*, vol. 2011, p. 19, 2011.
- [8] Teresa Mendonc,a, Andr'e R. S. Marc,al, Angela Vieira "Comparison of Segmentation Methods for Automatic Diagnosis of Dermoscopy Images" *IEEE EMBS Cité Internationale*, Lyon, France August 23-26, 2007.
- [9] Komal Lawand "Segmentation of Dermoscopic images" *IOSR Journal of Engineering* Vol. 04, Issue 04 ,April.2014 Pages 16-20.
- [10] F. Nielsen and R. Nock, "On region merging: The statistical soundness of fast sorting, with applications", *IEEE International Conference on Computer Vision and Pattern Recognition*, Vol. 2, pp. 19-26, 2003.
- [11] D. Saranya, M. Malini "A Review of Segmentation Techniques on Melanoma Detection" 2015, *IJARCSSE*
- [12] M. Silveria, J. C. Nascimento, J. S. Marques, A. R. S. Marcal, T. Mendonca, S. Yamauchi, J. Maeda, and J. Rozeira, "Comparison of segmentation methods for melanoma diagnosis in dermoscopy images," *IEEE Trans. Signal Process.*, vol. 3, no. 1, Mar. 2009
- [13] RudyMelli, CostantinoGrana, Rita Cucchiara(2006), "Comparison of color clustering algorithms for segmentation of dermatological images"
- [14] Gurkirat Kaur, Kirti Joshi " Automatic Detection and Segmentation of Skin Melanoma Images"-An Introduction Sep 2015
- [15] R. C. Gonzalez and R. E. Woods, *Digital Image Processing*. Englewood Cliffs, NJ: Prentice–Hall, 2002, pp. 123–135
- [16] H.Castillejos,V.Ponomaryov,andL.N.-de-Rivera,V.Golikov,"Wavelet transform fuzzy algorithms for dermoscopic image segmentation," *J. Comput. Math. Meth. Med.*, vol. 2012, pp. 41–52, 2012
- [17] H. Ganster, P. Pinz, R. Rohrer, E. Wildling, M. Binder, and H. Kittle, "Automated melanoma recognition," *IEEE Trans. Med. Imag.*, vol. 20,no. 3, pp. 233–239, Mar. 2001
- [18] J. B. MacQueen, "Some Methods for classification and analysis of multivariate observations", *Proceedings of the Fifth Berkeley Symposium on Mathematical Statistics, and Probability*, Vol. 1, pp. 281-297, 1997
- [19] Nikil Pal and Sankar Pal, "A review on image segmentation techniques", *IEEE Transactions on Pattern Recognition*, Vol. 26, No. 9, pp. 1277-1294, 1993.
- [20] James C Bezdeck, Robert Ehrlich and William Full, "FCM - The Fuzzy c-means Clustering Algorithm", *Computers and Geoscience*, Vol. 10, No. 2-3, pp. 191-203, 1984.
- [21] G. C. Karmakar, L. Dooley and S. M. Rahman, "A survey of fuzzy rule based image segmentation techniques", *First IEEE Pacific-Rim Conference on Multimedia*, pp. 350-353, 2000.
- [22] M. Kass, A. Witkin and D. Terzopoulos, "Snakes: Active contour models", *International Journal on Computer Vision*, Vol. 1, pp. 321-331, 1987
- [23] C. Xu and J. Prince, "Snakes, shapes, and gradient vector flow," *IEEETrans. Image Process.*, vol. 7, no. 3, pp. 359–369, Mar. 1998
- [24] J. Maeda, A. Kawano, S. Saga, and Y. Suzuki, "Number-driven perceptual segmentation of natural color images for easy decision of optimal result," in *Proc. Int. Conf. Image Processing*, 2007, vol. 2, pp. 265–268.
- [25] J. Maeda, A. Kawano, S. Saga, and Y. Suzuki, "Unsupervised perceptual segmentation of natural color images using fuzzy-based hierarchical algorithm," in *Proc. SCIA*. New York: Springer, 2007, vol.4522, *Lecture Notes in Computer Science*, pp. 462–471
- [26] Abbas Hussien Miry " Iterative Thresholding and Morphology Operation based Melanoma Image Segmentation".
- [27] Vala J, Baxi. A review on Otsu image segmentation algorithm. *IJARCET*. 2013; 2(2):387–9

Productivity Improvement By Maynard Operation Sequence Technique

Prof. A. A. Karad¹, Mr. Nikhil K. Waychale², Mr. Nitesh G. Tidke³,

¹ Professor, Department of ME, K. V. N. Naik Institute of Engineering, Education & Research, Nashik.

² B.E. Student, K. V. N. Naik Institute of Engineering, Education & Research, Nashik.

³ B.E. Student, K. V. N. Naik Institute of Engineering, Education & Research, Nashik.

¹ avinash.karad1974@gmail.com, ² waychalenikhil@gmail.com, ³ niteshtidke5@gmail.com,

Abstract— To sustain in business under the current global situation of fierce competition a company needs to reduce or eliminate the idle and/or down time of operations in addition to improvement of the current working methods. The problems and challenges of an auto company engaged in assembling car rear floor assembly are attributable to non-optimal operations with inefficient capacity planning. This study is conducted through application of Maynard Operation Sequence Technique (MOST) in the rear floor assembly section to capture the workflow activities using systematic and descriptive workflow data block for the value adding, value engineering and methods engineering analysis. Thus through the process redesign and process flow analysis, material handling and workflow are improved. Consequently, it has been possible to reduce the production cycle time to cater the higher level of demand with shorter Takt time reducing the current level of manpower.

Keywords— Maynard Operation Sequence Technique (MOST), Bottlenecks, Takt Time, Existing Time, Proposed Time, Increment of Production Rate, Amount of Investment.

1 INTRODUCTION

MOST is a work measurement technique that concentrates on the movement of objects. It is used to analyze work and to determine the normal time that it would take to perform a particular process/operation. MOST is a powerful analytical tool to measure every minute spent on a task. It makes the analysis of work a practical, manageable and cost effective task. It was originally developed by H. B. Maynard & Company Inc. and has three versions- Basic MOST (for the activities between 20 s to 2 min.), Mini MOST (for the activities shorter than 20 s) and Maxi MOST (for the activities above 2 min.). MOST is used primarily in industrial setting to set the standard time in which a worker should perform a task. MOST analysis is a complete study of an operation or sub-operation typically consisting of several method steps and corresponding sequence model. MOST is comprised of Work study, method study, and work measurement. In the organization under study, the excess time in operator's activity and fatigue of worker. Therefore, the real work was to identify the NVA activities and finding the reasons of fatigue in workers and reduce or minimize them. The highly practical, efficient and cost effective time estimation technique - MOST is used for this purpose. The Basic MOST System satisfies the most work measurement situations in the manufacturing arena. Every company very likely has some operations for which Basic MOST is the logical and most practical work measurement tool. Consequently, only three activity sequences are needed for describing manual work.

2 METHODOLOGY

The Basic MOST work measurement technique therefore comprises the following sequence models:

General Move Sequence- For the spatial movement of an object freely through the air.

A B G A B P A
Get Put Return

Where A = Action Distance
B = Body Motion
G = Gain Control

P = Placement

These sub-activities are arranged in a sequence model, consisting of a series of parameters organized in a logical sequence. The sequence model defines the event or actions that always take place in a prescribed order when an object is being moved from one location to another. The common scale of index numbers for all MOST sequence models is 0, 1, 3, 6, 10, 16, 24, 32, 42 and 54. The time value for a sequence model in basic MOST is obtained by simply adding the index numbers for individual sub-activity and multiplying the sum by 10.

Controlled Move Sequence- For the movement of an object when it remains in contact with a surface or is attached to another object during the movement. The controlled move sequence model is A B G M X I A, in which A B G – Get, M X I – Move or Actuate, A – Return

Where M – Move Controlled
 X – Process Time
 I – Alignment

Tool Use Sequence- For the use of common hand tools. However, the Tool Use sequence model does not define a third basic activity normally it is a combination of General Move and Controlled Move activities. The tool use sequence model is ABG ABP *ABP A, in which ABG – Get Tool, ABP – Put Tool, * - Use Tool, ABP –Aside Tool, A – Return

MOST is a predetermined motion time system that is used primarily in industrial settings to set the standard time in which a worker should perform a task. The time units used in MOST are based on hours & parts of hours called TMU (Time Measurement Unit). The following conversion is provided for calculating standard times:

- 1 TMU = 0.00001 hour
- 1 TMU = 0.0006 minute
- 1 TMU = 0.036 second
- 1 hour = 100, 000 TMU
- 1 minute = 1, 667 TMU
- 1 second = 27.8 TMU

3 EXPERIMENTATION

The existing assembly line consists of six workstations. The assembly is done by spot welding process with the help of movable spot welding guns. Time measurement for existing production line carried out by applying MOST technique. Time measured individually for each workstation. Existing time required for each workstation determined as below.

Table 3.1- Existing Time For Work Stations

W/s No.	Name Of The Work Station	Gun No.	Men	Time In Sec.	Time In Min.
1	Fixture 1	IG14	2	80.2	1.34
2	Fixture 2	IG29	2	91.8	1.53
3	Fixture 3	SG36	2	100.08	1.67
4	Welding Table	CO ₂ -01	2	95.39	1.59
5	Fixture 4	SG23& SG34	3	214.80	3.58
Total			11	582.27	9.70

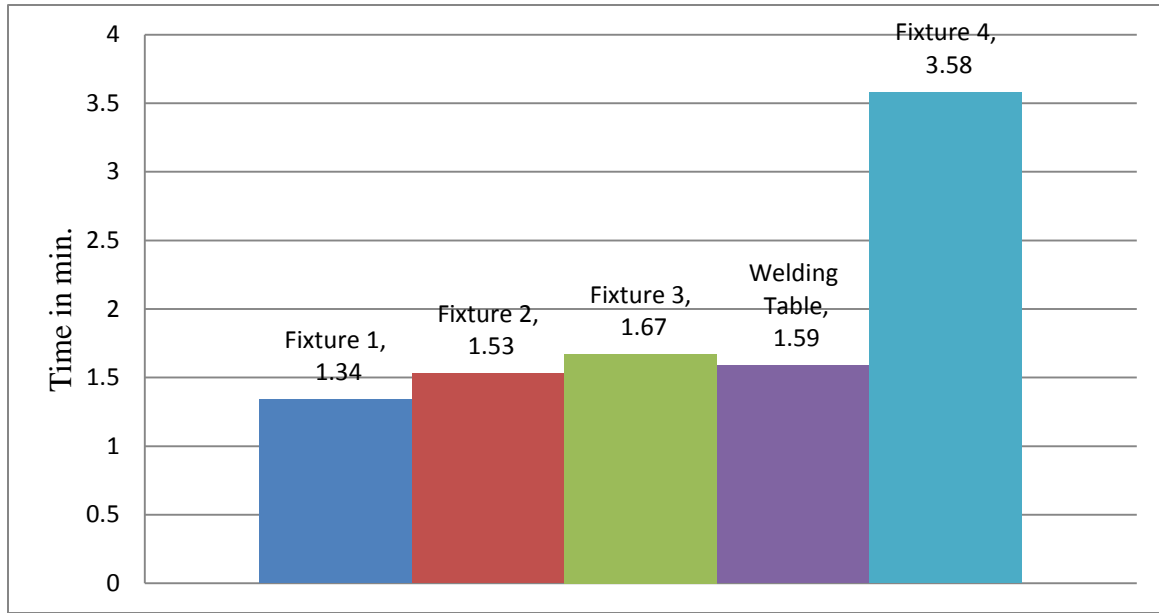


Figure 3.1- Existing Time For Work Stations

As shown in the above chart, fixture 4 required maximum time to complete work. Therefore work station 5 is identified as a bottleneck operation. For bringing the competitive advantages, attempt is to be made first to reduce the cycle time through incorporation of positive changes within the bottleneck work station. By applying the MOST technique, process flow, working procedure (also called standard operation procedure (SOP)) and layout of the plant, it can be easily identified that the work station cycle time can possibly be reduced by modifying the working method. To reduce bottleneck work station time, one more work station added next to the bottleneck work station in the assembly line. The operations performed by bottleneck work station partly divided with newly added work station. Thus production flow maintain smooth. There is no fatigue and saturation of work.

Table 3.2- Proposed Time For Work Stations

W/s No.	Name Of The Work Station	Gun No.	Men	Time In Sec.	Time In Min.
1	Fixture 1	IG14	2	80.2	1.34
2	Fixture 2	IG29	2	91.8	1.53
3	Fixture 3	SG36	2	100.08	1.67
4	Welding Table	CO ₂ -01	2	95.39	1.59
5	Fixture 4	SG34	2	88.32	1.47
6	Fixture 5	SG43	1	100.32	1.67
Total			11	556.11	9.27

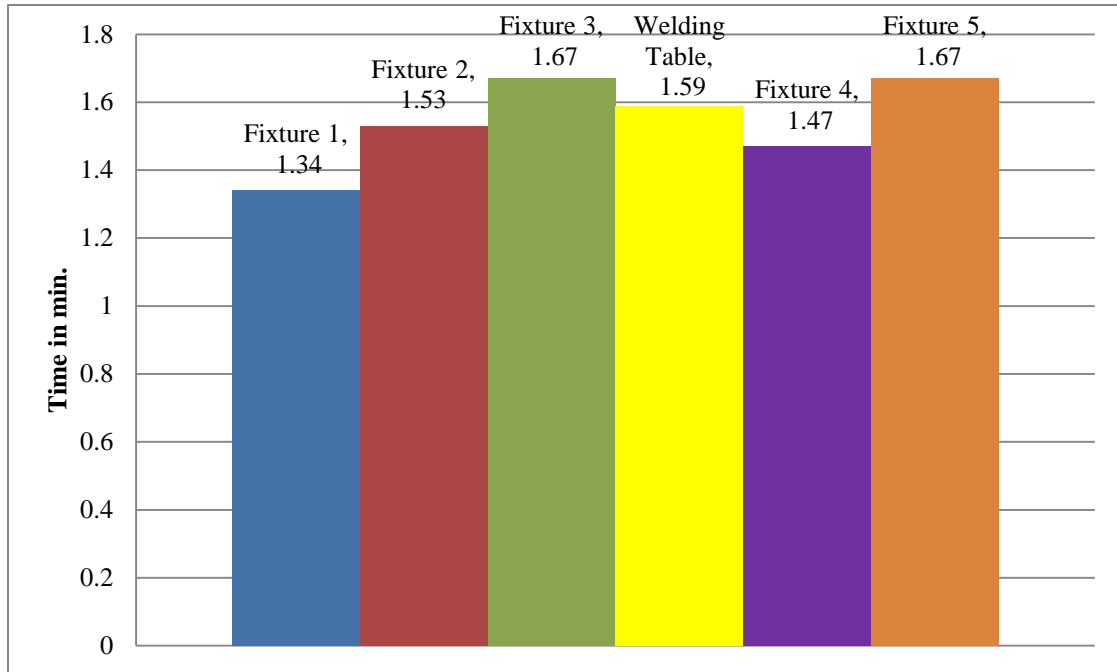


Figure 3.2- Proposed Time For Work Stations

As shown in the above chart, by adding one more work station time required by bottleneck work station is minimized. Also manpower required by work station 4 is reduced to 2 men. Manpower required by new workstation is 1 man. Minimization of time required for bottleneck work station results in to balancing of assembly line by avoiding fatigue and saturation of work.

4 RESULTS AND DISCUSSION

To assess the improvement in production rate, the Takt time of the considered assembly line is determined by dividing the total available time with the customer demand.

Table 4.1- Information Available To Work Out The Takt Time

Available Working Time (Min.)	Total Activity Time (Min.)	Highest Work Station Time (Min.)	Daily Required Quantity
480	10.694	1.67	280

$$\begin{aligned}
 \text{Takt Time} &= (\text{Available working time})/(\text{Daily required quantity}) \\
 &= 480/280 \\
 &= 1.71 \text{ min.}
 \end{aligned}$$

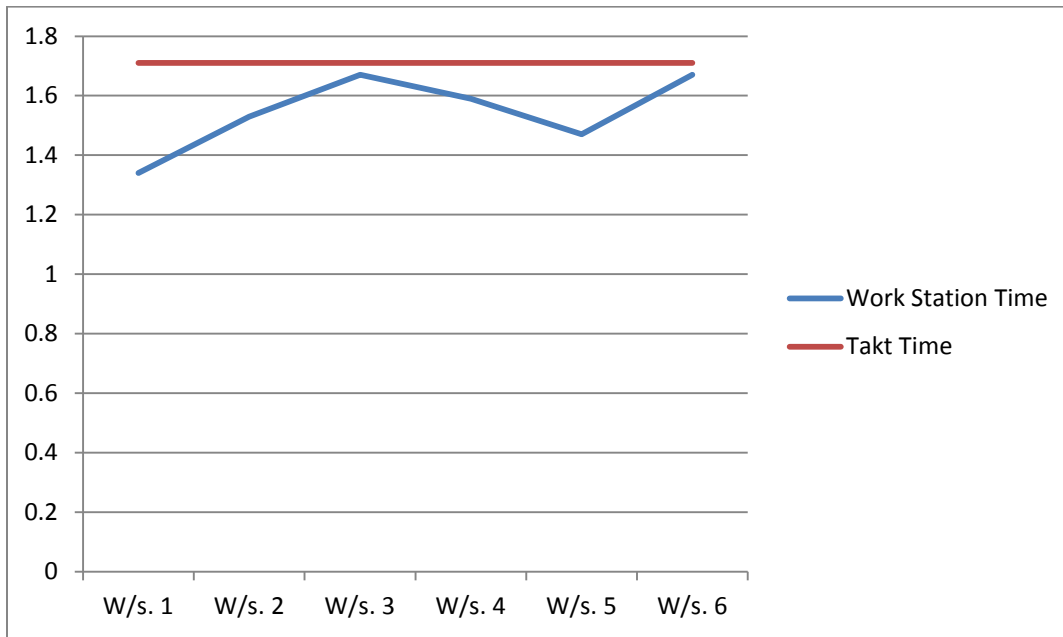


Figure 4.1- Takt Time

As the calculated Takt time for the assembly line is as 1.71 minutes per piece, the customer demand of 280 pieces per day cannot be entertained by the current practice. However, by bringing the proposed changes in assembly lines it is possible to satisfy the demand on time as well as increase the productivity.

Table 4.2- Manpower requirement

Type Of Assembly Line	Shift Time		Total Manpower	Largest W/s. Time In Min.
	Day	Night		
Current Assembly Line	11	6	17	3.58
Proposed Assembly line	11	0	11	1.67

As shown in the above table, proposed changes in the assembly line reduce manpower up to 11 men. As the daily required quantity is achieved in only day shift, manpower of 6 men work in night shift saved in proposed assembly line. The amount of investment save is given below.

$$\begin{aligned}
 \text{Investment saved/Year} &= \text{Manpower} * \text{Average salary per year} \\
 &= 6 \text{ (men)} * 3 \text{ (lakh)} \\
 &= 18 \text{ lakh}
 \end{aligned}$$

Hence we can save amount of investment up to 18 lakh per year by implementing the proposed changes in the current assembly line. The time saved to complete task in largest workstation is given below.

$$\begin{aligned}
 \text{Time Saved/Unit Quantity} &= \text{Largest W/s. Time In Current Assembly Line} - \text{Largest W/s. Time In Proposed Assembly Line} \\
 &= 3.58 - 1.67 = 1.91 \text{ Min.}
 \end{aligned}$$

5 CONCLUSION

It is evident that to sustain in this competitive industrial environment, a company needs to reduce or eliminate the idle and/or down time, improve the working methods, standardize the time as well as enhance the overall capacity planning and in this respect the MOST can play a vital role. In this research, a possible way of improving the productivity of undertaken by an auto company is presented. The result shows that by modifying the methods, it is possible to bring the competitive advantages in terms of satisfying the customer demand, well balancing the process flow as well as ensuring the economic benefits. Thus the incorporation of the MOST to estimate the standard times for various elemental tasks involved in different operations, inclusion of simple tools and jigs to perform a task in shorter time with minimum effort from operators and manoeuvring the distribution of activities in different workstations to balance production lines can substantially improve the productivity of an industry from the current level. In future, a research study with the application of the MOST can be explored from a wider perspective through implementation in a single or mixed model assembly lines having large number of work stations.

REFERENCES:

2. N. M. Karim, H. M. Emrul Kays, A. K. M. N. Amin and M. H. Hasan, "Improvement Of Workflow And Productivity Through Application Of Maynard Operation Sequence Technique (MOST)", Proceedings of the 2014 International Conference On Industrial Engineering And Operation Management, Bali, Indonesia, January 7-9, 2014.
3. Ingale Mahesh. Vishwanath, Sunil J Kadam, Pandit Shamuvel Vinod, Mulla M.L., "Improvement Of Productivity By New Approach-Lean Enterprise By MOST Way", International Journal Of Innovative Research In Science Engineering And Technology, Vol.3, Issue 6, June 2014.
4. Mr. Ankit Mishra, Mr. Vivek Agnihotri & Prof. D. V. Mahindru, "Application Of Maynard Operation Sequence Technique (M.O.S.T) At Tata Motors And Adithya Automotive Application Pvt Ltd., Lucknow For Enhancement Of Productivity-A Case Study", Global Journal Of Researches In Engineering :- B (Automotive Engineering), Vol.14, Issue 2, Version 1.0, Year 2014.
5. Tarun Kumar Yadav, "Measurement Time Method For Engine Assembly Line With Help Of Maynard Operating Sequencing Technique (MOST)", International Journal Of Innovation In Engineering And Technology (IJJET), Vol.2, Issue 2, April 2013.
6. Rajesh Kanda, Shalom Akhai, Ripunjaya Bansal, "Analysis Of MOST Technique For Elimination Of Idle Time By Synchronization Of Different Lines", International Journal Of Research In Advent Technology, Vol.1, Issue 4, November 2013.
7. R. M. Belokar, Yashveer Dhull, Surender Nain, Sudhir Nain, "Optimization Of Time By Elimination Of Unproductive Activities Through MOST", International Journal Of Innovation Technology And Exploring Engineering (IJITEE), Vol.-1, Issue -1, June 2012.
8. Mr. Pramanbra Kumar Gupta, Mr. Saurabh Singh Chandravat, "To Improve Work Force Productivity In A Medium Size Manufacturing Enterprise By MOST Technique", IOSR Journal Of Engineering (IOSRJEN), Vol.2, Issue 10, Page No.8-15, October 2012.
9. Jan Zurek, Robert Cieslak, Marcin Suszynsky, "Practical Evaluation Of Methods Of Research In Assembly Time Consumption", Committee Of Mechanical Engineering Pas-Poznan Division, Vol. 32, No. 4, 2012.
10. Vikram K. V., Dr. D. N. Shivappa, Jaganur Sangamesha, "Establishing Time Standards For Fixing Body Side Panel To The Chassis In Assembly Line Using MOST", Proceedings Of The National Conference On Trends And Advances In Mechanical Engineering, Oct. 19-20, 2012.
11. Liang Ma, Weizhang, HuanzhaFu, Yang Guo, Damien Chablat, Froud BENNIS, "A Framework For Interactive Work Design Based On Motion Tracking, Simulation And Analysis", Ma L., Zhang W, Fu. H,Guo Y, Chablat D, Bennis F., "A Framework For Interactive Work Design Based On Digital Work Analysis And Simulation", Human Factors And Ergonomics In Manufacturing Vol.20(4), Page No.339-352 April 2010.
12. Feri Afrinaldi, Muhmad Zarneri Mat Saman, Awaluddin Mohamad Shaharoun, "The Evaluation Methods Of Disassemblability For Automotive Components – A Review And Agenda For Future Research", Journal Mekanikal, No. 26, 49-62, December 2008.
13. Janxin Jiao, Mitchell M. Tseng, "A Pragmatic Approach To Product Costing Based On Standard Time Estimation", International Journal Of Operations & Production Management, Vol. 19, No. 7, PP.738-755, 1999.

A Review on Iris Feature Extraction Methods

Fasna K K¹, Athira P¹, Remya Krishna J S²

¹PG Scholar, ²Assistant Professor,

Dept. of Electronics & Communication, Thejus College of Engineering

Email: fasimoideen@gmail.com

Abstract— Iris biometry has been gaining its attention during the recent years in the various cooperative and non-cooperative environments. The stability and unique features of iris lead to its increased usage for personal recognition in various fields like airport, border security, harbors, etc. All the researches are going on in the area of iris recognition to increase its accuracy and speed of recognition. The reduced time for personal recognition improves the performance of the recognition system and reduces the amount of false recognition. The difficulty of forging and using an imposter lead to the wide acceptance of iris biometry. The various methods used in iris recognition proposed by various researches are reviewed in this paper. All these methods give importance to increase the speed of recognition.

Keywords— Iris recognition, feature extraction, Gabor, DCT, DWT, Contourlet Transform, ICA, PCA, GLCM

INTRODUCTION

Biometry is gaining more attention during the recent years. Biometrical identification refers to the physiological and behavioral characteristics of a person to recognize an individual. There are several types of biometry including voice, signature, fingerprint, face, iris, hand, keystroke dynamics, etc. The physiological characteristics include iris, face, hand, fingerprint, etc. Behavioral characteristics are voice, signature, keystroke dynamics, etc. Among all the existing biometrics, iris is the most efficient one in terms of accuracy. Iris provides unique set of features to represent an individual. These features are stable throughout the life time of an individual. Iris has distinct phase information. Iris biometry is also very reliable since it is an externally visible part of the eye and hence does not need the contact of an individual to acquire it unlike hand, fingerprint, etc.

The basic steps included in an iris recognition system are image acquisition, preprocessing, iris localization and segmentation followed by the extraction of features, and finally the formation of feature vector and identification between a genuine and an imposter image. Image acquisition implies the capturing of iris images under sufficient illumination conditions. Improper acquisition may lead to addition of noises in the acquired images. Preprocessing step includes the noise removal and pupil extraction. The pupil in an eye image does not carry any useful information, and thus can be removed which will help in the localization of iris. Then the iris area will be identified and segmented out. This segmented iris is used to form the feature vector of an iris. After this feature extraction the feature vectors are compared using any classifiers to identify the authorized persons.

A biometric system mainly consists of two phases namely the enrollment phase and verification phase. In the enrollment phase, the images are collected and feature extracted to form the feature vector and is then stored in a database. In the verification phase, the query image which is to be tested is preprocessed and then feature extracted. Thus formed feature vector will be compared against those stored in the database to identify the authorized persons.

FEATURE EXTRACTION

Iris has a unique texture and thus can uniquely represent each of the individual. Feature extraction methods extract the distinctive features present in an iris image. Features give both the local and global information about the iris. It quantifies some significant characteristics in an iris. There exist several algorithms for efficient feature extraction. Normally feature extraction methods can be grouped as signal processing methods and statistical processing methods. The first method includes both the spatial domain and frequency domain methods. The latter one exploits the spatial dependencies between the pixels. Features can be general features or domain specific features. General features normally refer to the features like color, texture, shape, etc. they can be referred as pixel level features, local features and global features. The features that are computed pixel- wise whereas the local features are those which are computed on subdivisions of an image and global features refers to those which are computed for the entire image. Domain specific features normally refer to the features in an application specific domain such as face, fingerprint, etc. Some of the methods that are used to extract the iris features are briefly reviewed below.

a) Gabor filter

J.Daugman [17] introduced gabor filters for iris recognition and he got patent for this paper. Gabor filters can provide finest conjoint representation of signal in both space and spatial frequency. A Gabor filter is created by modulating either a sine wave or a cosine wave with a gaussian. Since the sine wave is perfectly confined in frequency, but not in space, this modulation provides the optimum conjoint localization in both space and frequency. Modulation of the sine wave with a Gaussian wave results in space localization, along with the loss of localization in frequency.

Quadrature pair of Gabor filters is used for the decomposition of a signal, with an imaginary part defined by a sine modulated by a Gaussian and a real part defined by a cosine modulated by a Gaussian. The real filters are known as the even symmetric components while the imaginary filters are known as odd symmetric components. The frequency of a sine wave specifies the center frequency of the filter, meanwhile the bandwidth is defined by the gaussian bandwidth. The iris features are extracted by the application of 2D gabor filters. By varying the wavelengths and the orientation of filters, several banks of gabor filters comprising 15, 20, 25, 30, 35 filters are applied on images. 2D gabor filter can be defined as:

$$G(x, y; \theta, f) = \exp\{-(1/2)[(x'^2/\delta x'^2) + (y'^2/\delta y'^2)]\} \cos(2\pi f x') \quad (1)$$

$$x' = x \cos\theta + y \sin\theta \quad (2)$$

$$y' = y \cos\theta - x \sin\theta \quad (3)$$

where δx and δy symbolize the spatial size of the filter, θ denotes the orientation angle, f gives the frequency of the filter. Since a gabor filter possess both the real and imaginary parts, it will yield 20 real and 20 imaginary outputs when an input image is convolved with a bank of 20 filters. By combining both of these real and imaginary parts, an output feature vector of about 2048 bit length can be generated.

Gabor filters can be applied on multichannel basis in some methods. In this method, the filters will be applied locally on several parts of the image instead of applying to the entire image at once. The entire iris image is represented by the global information which is formed by combining the local information calculated from each part of the iris. This technique is done by dividing the entire original image into a number of equal parts needed to compute the local information. A number of banks of gabor filters will be applied on these divided sub images. Then the feature vector is formed by collecting information extracted from these sub-images. Thus formed feature vector will be the result of combination of local feature vectors of both the real and imaginary outputs. This resultant feature vector is then used for comparison.

b) Log-Gabor Filter

D.field [19] and P.Yao, X.Ye [20] introduced log-gabor filters which are gaussian on the logarithmic scale. The normal gabor filters are the traditional choice of filters in feature extraction. Usually, they are suffered with two main restrictions; the maximum bandwidth is confined to roughly one octave and also in the case of seeking broad spectral content with maximum spatial localization, these filters are not optimal. Thus a logarithmic gabor filter called log-gabor filter is introduced as an alternative to the normal gabor filter. This log-gabor filter is based on the fact that when viewed on a logarithmic frequency scale, the natural images can be better coded using filters having Gaussian transfer function. Gabor functions are having gaussian transfer functions when observed on a linear frequency scale. The frequency response of a log-gabor filter can be given as:

$$G(f) = \exp\{-0.5 \times \log(f/f_0)^2 / \log(\sigma/f_0)^2\} \quad (4)$$

Here f_0 denotes the center frequency and σ represents the bandwidth of the filter. There are two important characteristics to be noted. Firstly, the log-gabor functions do not have a dc component, and secondly, at higher frequencies the transfer function of a log-gabor filter has an extended tail [2].

c) Discrete Cosine Transform

D. M. Monro introduced DCT for the feature extraction in [4]. Discrete cosine transform can be used for expressing a signal as a sum of sinusoids. Similar to the DFT, DCT is also meant to work on the data points which are discrete. The noticeable difference between these two is that the DCT make use of cosine functions only whereas the DFT uses both the sine and cosine functions. For very highly correlated images the DCT always shows exceptional energy compaction. DCT represents any signal or function as the sum of sinusoids for various amplitudes and frequencies.

DCT can be expressed mathematically as;

$$F(u, v) = a(u) a(v) \sum_{x=0}^{M-1} \sum_{y=0}^{N-1} f(x, y) \cos(\pi(2x+1)u/2M) \cos(\pi(2y+1)v/2N) \quad (5)$$

$$\text{where } \alpha(u) = \left\{ \begin{array}{l} (1/\sqrt{M}), u = 0, \\ \sqrt{2/M}, u = 1, 2, \dots, M - 1 \end{array} \right. \quad \& \quad \alpha(v) = \left\{ \begin{array}{l} (1/\sqrt{N}) \text{ for } v = 0, \\ \sqrt{2/N}, v = 1, 2, \dots, N - 1 \end{array} \right.$$

When DCT is applied to an image, all the low frequency coefficients will get concentrated on the top left most corners of the DCT spectrum. Thus it can be said that DCT compresses all the information present in the image and considers only those coefficients which are present at the left hand top most corners. The main unique distinguishable features of the subject are represented by these low frequency components whereas the finer details are represented by the high frequency components. For recognition based applications, usually the low frequency components which are residing on the top left most corners are extracted. It is because for such applications, these low frequency components are more than enough. The high frequency components are discarded in these cases.

The Discrete Cosine Transform requires fastest algorithms for its computation. It is real, orthogonal and separable. DCT is similar to DFT in the case of real numbers since the fourier transform of real and even function is real and even. The DCT helps in achieving a clear frequency distribution when it is applied on an image. The low frequency components possess more information than the high frequency components. The low frequency components get accumulated on the left top most corner. In order to compute 2D DCT, the 1D DCT is applied initially on the rows and then to the columns. The coefficients obtained after DCT is used to form the feature vector needed for comparison. For the case of basis vectors with real valued components DCT is a competent method.

d) Discrete Wavelet Transform

W. Boles and B. Boashah [21] introduced a human identification technique using the wavelet transform. Unlike DCT, Wavelet transform provides the real time representation of a signal in both time and frequency. The most significant difference is that the wavelet transform offers a flexible time frequency window. This window gets narrowed while witnessing the high frequency activities. Similarly, it gets widened while observing the low frequency activities. Thus the wavelet transform provides multiresolution analysis with the help of this window. It is said to be multiresolution since it offers good spatial resolution for higher frequencies and good frequency resolution for lower frequencies. This type of approach is more appropriate for those signals having lesser higher frequency components and more low frequency components

The DWT decomposes the image into four parts namely approximation, horizontal details, vertical details and diagonal details. The approximation part represents more information compared to the detail parts. The approximation part corresponds to the low frequency components. For further decomposition DWT is again applied on the approximation part to achieve the multiresolution. In iris recognition applications, the iris region gets decomposed to components at different resolutions. Thus the frequency data gets localized so that the features occurring at the same position and resolution become matched. Different types of wavelets are being used for this application.

e) Contourlet Transform

Amir and Hamid [23] developed an iris extraction algorithm based on contourlet transform. The main concept behind the Contourlet transform is that a sparse image expansion can be obtained by the application of multiscale transform tailed by a local directional transform. The nearby basis functions at the same scale are grouped into linear structures. The CT is obtained by the application of directional decomposition after the multiscale decomposition. Thus it offers multiple numbers of different directions at a single scale. Contourlet transform makes sense in the feature extraction applications because of its properties like directionality and anisotropy. The directional energies of the curvelet coefficients in each of the sub image create the anisotropic feature vector.

The Curvelet Transform is constructed by the multiscale decomposition with the Laplacian pyramid followed by the directional decomposition of sub bands using the directional filter bank. Thus the texture details from a set of directional sub bands are collected at various scales in different orientations. Thus intrinsic geometrical structures are obtained for the iris image. The contour segments detection is made possible by the local directional transform using the directional filter bank whereas the edges or point detection is made possible with the help of wavelet-like transform (Laplacian Pyramid). This combination of laplacian pyramid and double filter bank is called as pyramidal directional filter bank.

f) Principal Component Analysis

Jin-Xin Sh, and Xiao-Feng Gu [12] identified the use of principal component analysis for feature extraction. PCA is invented by Karl Pearson in 1901. This classic technique is mainly used for the suppression of higher dimensional data sets to the lower dimensions for the purpose of data analysis and visualization, compression of data and for the extraction of features. This analysis mainly involved the computation of eigen value decomposition and singular value decomposition for data covariance matrix and data matrix respectively after mean entering the data of each attribute. The features obtained after PCA are usually spatial global features. PCA thus performs the data reduction by transforming the original data into a much smaller dimensional feature space.

PCA is normally used to find patterns in the higher dimensional data. This technique involves the suppression of a larger number of correlated variables to a lesser number of uncorrelated variables. These lesser number of uncorrelated variables is called the principal components. These components usually represent the maximum variance possible and thus revealing the internal structure of the data. PCA can be considered as one of the simplest eigen vector based multivariate analyses.

The first principal component identified represents the maximum variance with the following component accounts for the remaining maximum variance possible. In such a way, the strength of variations in different directions for an image is computed. Both the eigen vectors and eigen values are computed by PCA. The principal components are those eigen vectors which are having the largest eigen value. It is also called as the discrete Karhunen-Loeve transform, the Hotelling transform or proper orthogonal decomposition (POD) depending on the application it is used. PCA find the principal components which represent the maximum variance possible by a set of linear transformed components. Thus PCA can be considered as an unsupervised linear feature extraction algorithm involving a linear mapping using the eigen vectors having the highest eigen values. The study of the eigen value decomposition of a covariance matrix is called as the Principal Component Analysis

g) Independent Component Analysis

Jin-Xin Sh and Xiao-Feng Gu [12] employed feature extraction method based on Independent Component Analysis. ICA is one of the analysis techniques for the source separation which aims at recovering the original signal from a set of known observations where each of the observations corresponds to an unknown mixture of the original signal, which is possible in case of statistically independent original signal and are under mild conditions on mixture. The ICA computes the inverse of the mixing matrix if the mixing performed is linear. Instead of the eigen vectors in PCA, ICA computes the independent source vectors. These higher dimensional vectors are a linear combination of a set of unknown independent source vectors. Using the estimates of the computed independent source vectors, ICA can reconstruct the original signal. The coefficients of expansion of ICA are taken as feature vectors for irises. Being independent the ICA source vectors are much closer to natural features present in an image and thus can easily identify the differences between irises. ICA characterizes a multidimensional random vector as a linear grouping of independent components which are random variables that are not gaussian. ICA mainly depends on the correlation information between the patterns.

h) Grey Level Co-occurrence Matrix

Amir and Hamid [23] and V. V. S. Tallapragada [16] developed an iris extraction algorithm based on GLCM. A grey level co-occurrence matrix defines the distribution of co-occurring values at a specified offset level. This matrix is created by considering the direction and distance between each pixel. Texture representation is done by those features which are derived from this matrix. This non-filter based technique mainly relies on the second order statistics of the pixel intensities and computes the joint probability distribution function of the grey levels present in an image. The mathematical definition of the co-occurrence matrix is the probability $P_d(i, j)$ of two pixels, with grey level values i and j respectively and are parted by a distance vector d , of an image I of size $N \times M$ is given as;

$$P_d(i, j) = (|\{(r, s)(t, v) : I, I(t, s) = i, I(t, v) = j\}|) / NM \quad (6)$$

GLCM is a statistical measure which defines the texture by computing the frequency of occurrence of pairs of pixel in a given spatial relationship and with defined values. since the GLCM is based on the spatial relationship between the pixel of interest and the pixel to its immediate right, it is also called as grey level spatial dependence matrix. The size of the GLCM matrix represents the number of grey levels present in the corresponding image. The joint pdf of the pairs of pixels define the spatial relationship between them, which is usually described in terms of the lineal distance between pixels and the angle between them. Normally 14 features representing the visually recognizable properties of image are extracted from the GLCM matrix. These texture representing features are energy, entropy, contrast, variance, correlation, homogeneity, sum average, sum entropy, sum variance, difference variance, maximum correlation coefficient, and finally the information measures of correlation.

CONCLUSION

Iris recognition has been increasing its popularity during the recent years. The various methodologies used for the feature extraction in an iris recognition system proposed by several researches are reviewed in this paper. Iris biometry has been gaining its popularity due to its stability and uniqueness in the life time. All the methodologies reviewed in this paper have its own importance depending on the area of application of these methods. Researches are still going on to increase the accuracy and to reduce the time required for recognition.

REFERENCES:

- [1] Saadia Minhas, Muhammad Younus Javed, "Iris Feature Extraction Using Gabor Filter", 2009 International Conference on Emerging Technologies, IEEE.
- [2] A.T. Kahlil, F.E.M. Abou-Chadi, "Generation of Iris Codes Using 1D Log-Gabor Filter", 2010 International Conference on Computer Engineering and Systems (ICCES), IEEE.
- [3] D. M. Monro, S. Rakshit, and D. Zhang, "DCT-Based Iris Recognition", IEEE Transactions On Pattern Analysis And Machine Intelligence, Vol. 29, No. 4, April 2007.
- [4] Abhiram M.H., Chetan Sadhu, "Novel DCT Based Feature Extraction for Enhanced Iris Recognition", 2012 ICCICT, Oct. 19-20, Mumbai, India.
- [5] Mrinalini I R, Pratusha B P, "Enhanced Iris Recognition Using Discrete Cosine Transform And Radon Transform", IEEE Sponsored 2nd ICECS 2015.
- [6] A Deshpande, S Dubey, H Shaligram, A Potnis, Satishkumar Chavan, "Iris Recognition System using Block Based Approach with DWT and DCT", 2014 IEEE (INDICON).
- [7] P.P.Chitte, J.G.Rana, R.R.Bhambare, V.A.More, R.A.Kadu, M.R.Bendre, "IRIS Recognition System Using ICA, PCA, Daugman's Rubber Sheet Model Together", IJCTEE, volume 2.
- [8] H.B.Kekre, S D.Thepade, J Jain , N Agrawal, "IRIS Recognition using Texture Features Extracted from Haarlet Pyramid", International Journal of Computer Applications, 2010.
- [9] S D. Thepade, P Bidwai, "Iris Recognition using Fractional Coefficients of Transforms, Wavelet Transforms and Hybrid Wavelet Transforms", 2013 ICCCCM.
- [10] Minakshi R.Rajput, "Iris feature extraction and recognition based on different transforms", International Journal of Engineering Research and Development, Nov 2013.
- [11] Aparna Gale, S.S.Salankar, "Performance Analysis on Iris Feature Extraction Using PCA, Haar Transform and Block Sum Algorithm", IJEAT, April 2015.
- [12] J. Xin Sh, X.Feng Gu, "The Comparison of Iris Recognition Using Principal Component Analysis, Independent Component Analysis and Gabor Wavelets", ICCSIT, 2010, IEEE.
- [13] T C Meetei, Shahin Ara Begum, "Performance Evaluation of Feature Selection Methods for ANN Based Iris Recognition", ICETACS 2013, IEEE.
- [14] S N.Talbar, R M.Bodade, "Feature Extraction Of Iris Images Using Ica For Person Authentication", 2007 IEEE ICSPC 2007.
- [15] P. S Vanthana, A. Muthukumar, "Iris Authentication Using Gray Level Co-occurrence Matrix And Hausdorff Dimension", IEEE, 2015 ICCCI.
- [16] V.V.S Tallapragada, E.G.Rajan, "Iris Recognition Based on Combined Feature of GLCM and Wavelet Transform", 2010, IEEE.
- [17] J. Daugman (1993). "High Confidence Visual Recognition of Persons by a Test of Statistical Independence", IEEE Tans. Pattern Analysis and Machine Intelligence.
- [18] J. Daugman (2004). "How iris recognition works", IEEE Trans. CSVT, vol. 14, no. 1.
- [19] D. Field (1987). "Relations between the statistics of natural images and the response properties of cortical cells", Journal of the Optical Society of America.
- [20] P. Yao, J. Li, X. Ye, Z. Zhuang, and B. Li. "Iris Recognition Algorithm Using Modified Log-Gabor Filters", Proc. 18th International Conference on Pattern Recognition 2006.
- [21] W. Boles and B. Boashash (1998). "A human identification technique using images of the iris and wavelet transform", IEEE Transactions on Signal Processing, vol. 46, no. 4.
- [22] Li Ma, T. T., Yunhong W., and Dexin Z., (2004). Efficient iris recognition by Charactering Key Local Variation. IEEE Transactions on Image Processing.
- [23] Amir A. and Hamid, R.P, "A novel method for iris feature extraction based on contourlet transform and co-occurrence matrix", IADIS, 2009.

Construction of low complexity Array based Quasi Cyclic Low density parity check (QC-LDPC) codes with low error floor

Pravin Salunkhe, Prof D.P Rathod

Department of Electrical Engineering, Veermata Jijabai Technological Institute (VJTI), Mumbai, India.

pravinms22@gmail.com

Abstract— Low Density Parity Check (LDPC) codes are class of linear block error correcting codes and are very popular due to their Shannon capacity approaching performance. Due to their low decoding complexity they outperform the existing convolutional and turbo codes and find use in many wire and wireless applications. This paper gives an overview about construction of Quasi Cyclic regular LDPC based on shifting identity matrix. The algorithm produces Parity check matrix which is free of cycle 4 and hence giving girth of at least 6. Simulation shows that with sum product decoder we can achieve good Bit Error rate (BER) and also gain the advantage of memory efficient circuit due to quasi cyclic structure of parity check matrix.

Keywords— Quasi Cyclic-LDPC codes, message passing, regular LDPC, irregular LDPC, circulant permutation matrix, Tanner Graph, girth.

INTRODUCTION

Low-Density Parity-Check (LDPC) codes were first invented by Gallager in 1962 [1]. Initially these codes were ignored but recently they were rediscovered and shown to perform near Shannon's limit [2],[3],[4],[5],[6].

A regular LDPC code is described by parity check matrix H having following properties: (1) each row has α 1's ; (2) each column has β 1's ; (3) number of 1's common between any two rows denoted by λ is no greater than 1; (4) α and β are small compared to code length n . Fourth property ensures that number of 1's. α and β are also called as row weight and column weight respectively. Third property ensures that there is no cycle of length 4 in Tanner graph [7]. From fourth property it is clear that number of 1's are small or low compared to total entries in H matrix and hence the name low density parity check code.

LDPC codes can be represented in two ways. One by using parity check matrix and second by using Tanner graph or *bipartite graph*. A *bipartite graph* is one in which the nodes can be partitioned into two classes, and there is no edge connection between two nodes of the same class. A *Tanner graph* for an LDPC code is a bipartite graph such that: (1) In the first class of nodes, there is one node for each of the n bits in the codeword and are also referred as bit nodes. (2) In the second class of nodes, there is one node for each of the m parity checks which is equal to number of rows of matrix H and are also called as check nodes. (3) Connection of edge is made from bit node to a check node if the bit is included in the parity check matrix [8]. Loop in the Tanner graph is called as cycle and the number of edges in cycle is called as girth. Girth 4 can affect the performance of decoding LDPC code and hence removal of girth 4 is necessary. If the column or rows weights of H matrix are not constant then it is called as irregular LDPC.

Consider the following regular LDPC H matrix having constant row and column weight. Tanner graph for given matrix is shown in figure 1.

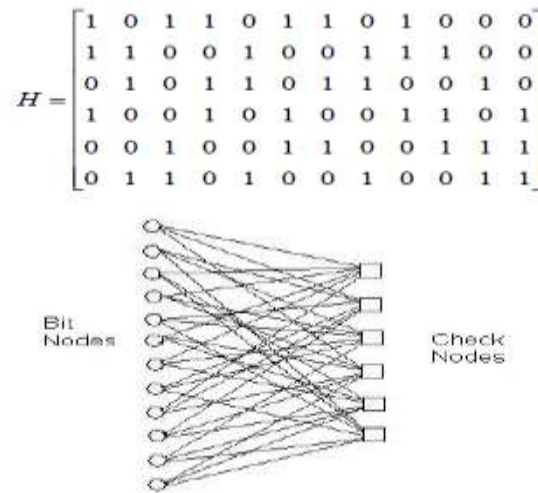


Fig. 1. A parity check matrix H and its corresponding Tanner graph

ARRAY BASED QUASI CYCLIC LDPC CODES

The major disadvantage of LDPC code is that more amount of memory is needed to store parity check matrix. This problem can be solved by Quasi Cyclic LDPC (QC-LDPC) codes [11]-[13] since their parity check matrices include circulant matrices and hence can be encoded with the shift registers. The codes are quasi cyclic because we can obtain another codeword by simply cyclically shifting a codeword within each block of circulant.

A (r,t) regular quasi cyclic matrix H can be represented based on cyclic shifting $\rho \times \rho$ identity matrix as :

$$H = \begin{bmatrix} I_{\alpha_{11}} & I_{\alpha_{12}} & \cdot & \cdot & \cdot & I_{\alpha_{1t}} \\ I_{\alpha_{21}} & I_{\alpha_{22}} & \cdot & \cdot & \cdot & I_{\alpha_{2t}} \\ \cdot & \cdot & \cdot & \cdot & \cdot & \cdot \\ \cdot & \cdot & \cdot & \cdot & \cdot & \cdot \\ \cdot & \cdot & \cdot & \cdot & \cdot & \cdot \\ I_{\alpha_{r1}} & I_{\alpha_{r2}} & \cdot & \cdot & \cdot & I_{\alpha_{rt}} \end{bmatrix} \quad (1)$$

where $\alpha_{ij} \in \{0,1,\dots,\rho-1\}$ and $I_{\alpha_{ij}}$ ($1 \leq i \leq r, 1 \leq j \leq t$) represents $\rho \times \rho$ matrix obtained by cyclically shifting identity matrix to the left by α_{ij} times. From above structure it is clear that H matrix has t ones in each row and r ones in each column.

Array codes [9] proposed by J. L. Fan are regular quasi cyclic in nature and they are free of cycle 4. For prime number ρ and for positive integer $r \leq t$, they are given by following form:

$$H = \begin{bmatrix} I & I & I & \dots & I \\ I & \alpha & \alpha^2 & \dots & \alpha^{t-1} \\ I & \alpha^2 & \alpha^{2 \times 2} & \dots & \alpha^{2 \times (t-1)} \\ \dots & \dots & \dots & \dots & \dots \\ \dots & \dots & \dots & \dots & \dots \\ I & \alpha^{r-1} & \alpha^{2 \times (r-1)} & \dots & \alpha^{(r-1) \times (t-1)} \end{bmatrix} \quad (2)$$

where I is $\rho \times \rho$ identity matrix and α is $\rho \times \rho$ left or right cyclic shift of identity matrix and $\alpha^0 = I$. For example, when ρ is 5,

$$\alpha = \begin{bmatrix} 0 & 1 & 0 & 0 & 0 \\ 0 & 0 & 1 & 0 & 0 \\ 0 & 0 & 0 & 1 & 0 \\ 0 & 0 & 0 & 0 & 1 \\ 1 & 0 & 0 & 0 & 0 \end{bmatrix} \quad \text{or} \quad \alpha = \begin{bmatrix} 0 & 0 & 0 & 0 & 1 \\ 1 & 0 & 0 & 0 & 0 \\ 0 & 1 & 0 & 0 & 0 \\ 0 & 0 & 1 & 0 & 0 \\ 0 & 0 & 0 & 1 & 0 \end{bmatrix} \quad (3)$$

H matrix defined by above form has t ones in each row and r ones in each column. This has rank $\rho r - r + 1$.

E. Eleftheriou proposed modified array LDPC [10] having following form:

$$H = \begin{bmatrix} I & I & I & \dots & I & I & \dots & I \\ O & I & \alpha & \dots & \alpha^{j-2} & \alpha^{j-1} & \dots & \alpha^{k-2} \\ O & O & I & \dots & \alpha^{2(j-3)} & \alpha^{2(j-2)} & \dots & \alpha^{2(k-3)} \\ \dots & \dots & \dots & \dots & \dots & \dots & \dots & \dots \\ \dots & \dots & \dots & \dots & \dots & \dots & \dots & \dots \\ O & O & \dots & O & I & \alpha^{j-1} & \dots & \alpha^{(j-1)(k-1)} \end{bmatrix} \quad (4)$$

where I and O are $\rho \times \rho$ identity matrix and null matrix respectively. k and j are positive integers such $k, j \leq \rho$ and α is $\rho \times \rho$ left or right cyclic shift of identity matrix. Here H is full rank matrix and upper triangular nature of matrix helps in encoding in linear time. Clearly above matrix gives irregular QC-LDPC code.

Error performance of regular and irregular QC-LDPC codes

The decoding procedure can be described in terms of message passing or sum-product algorithm (SPA) algorithm [8] in which all variable nodes and all check nodes iteratively pass messages along their edges. The values of the code bits are updated accordingly with each iteration. The algorithm continues until a valid codeword is generated or until the completion of a specified number of iterations.

Simulations are done for both regular and irregular QC-LDPC codes. Figure 2 shows the BER for regular QC-LDPC and Figure 3 shows the BER of irregular LDPC codes. For regular QC-LDPC BER of $0.0028 (10^{-2})$ for BPSK modulated code length of 184 bits over additive white Gaussian noise at 4 dB Signal-to-Noise ratio (SNR) is obtained. Similar BER of 10^{-2} at 4dB SNR is obtained for irregular QC-LDPC codes.

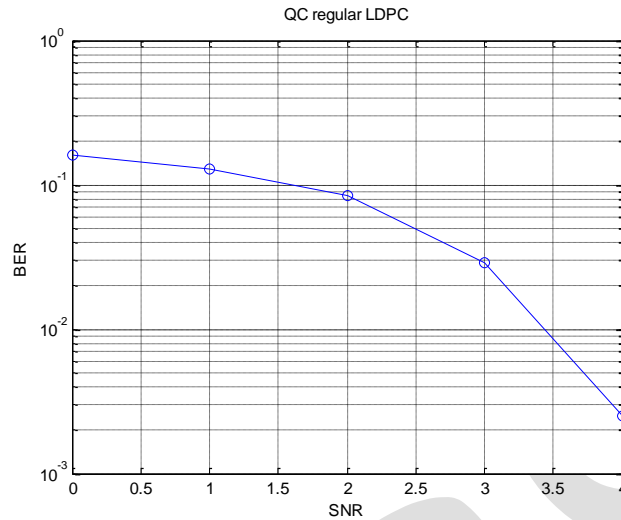


Fig. 2. BER for Regular QC-LDPC code

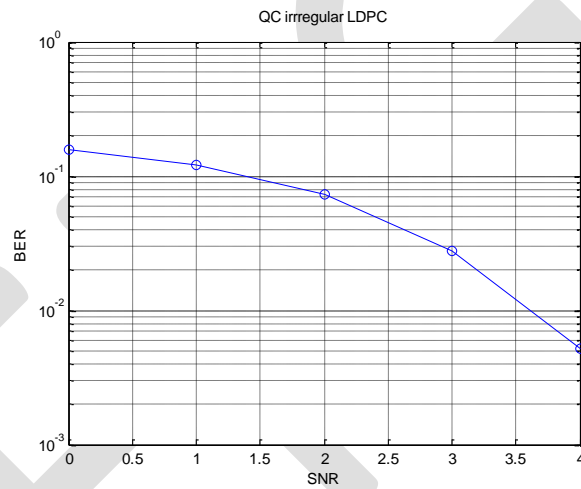


Fig. 3. BER for Irregular QC-LDPC code

CONCLUSION

Array based QC-LDPC codes, obtained by shifting identity matrices have been simulated. Rank and BER property of LDPC codes resulting from this are studied. Simulation shows that given different parameters r, t, ρ, k etc. parity-check matrix H can be easily constructed for regular and irregular QC-LDPC codes with low complexity as compared to random and algebraic construction of LDPC codes. The advantage of this construction method is that parity-check matrix H is free of cycle 4. Due to their low encoding complexity and low error floor they are good competitors to other LDPC codes constructed from finite geometry and other methods. Another advantage is because of quasi cyclic structure decoding can be performed by using shift registers giving memory efficient circuit.

REFERENCES:

- [1] R. G. Gallager, "Low density parity check codes," IRE Trans. Inform. Theory, vol. IT-18, pp. 21–28, Jan. 1962. Rice Straw" Wageningen UR Food & Biobased Research ,Number Food & Biobased Research number 1176 ,ISBN-number 978-90-8585-755-6, December 31st, 2009
- [2] D. J. C. MacKay and R. M. Neal, "Near shannon limit performance of low density parity check codes," Electronics Letters, vol. 32, no. 18, pp. 1645–1646, 1996.
- [3] D. J. C. MacKay, "Good error-correcting codes based on very sparse matrices," IEEE Trans. Inform. Theory, vol. 45, pp. 399–432, Mar. 1999.
- [4] T. J. Richardson, M. A. Shokrollahi, and R. Urbanke, "Design of capacity-approaching irregular low-density parity-check codes," IEEE Trans. Inform. Theory, vol. 47, pp. 619–637, Feb. 2001.
- [5] S. Y. Chung, J. G. D. Forney, T. J. Richardson, and R. Urbanke, "On the design of low-density parity-check codes within 0.0045 db of the shannon limit," IEEE Commun. Lett., vol. 5, pp. 58–60, Feb. 2001.
- [6] Y. Kou, S. Lin, and M. Fossorier, "Low density parity check codes: A rediscovery and new results," *IEEE Trans. Inform. Theory*, vol. 47, pp. 2711–2736, Nov. 2001.
- [7] R. M. Tanner, "A recursive approach to low complexity codes," IEEE Trans. Inform. Theory, vol. IT-27, pp. 533–547, Sept. 1981.
- [8] S. Lin and J. D. J. Costello, *Error Control Coding: Fundamentals and Applications*. Englewood Cliffs, NJ: Prentice Hall, 1983.
- [9] J. L. Fan, "Array codes as low-density parity-check codes," in *Proc. 2nd Int'l Symposium on Turbo Codes and Related Topics*, Brest, France, pp. 543-546, Sept. 2000.
- [10] E. Eleftheriou and S. Olcer, "Low-density parity-check codes for multilevel modulation," in *Proc. IEEE Int. Symp. Information Theory (ISIT2002)*, Lausanne, Switzerland, Jun./Jul. 2002, p. 442
- [11] Q. Huang, Q. Diao and S. Lin, "Circulant decomposition: Cyclic, quasi-cyclic and LDPC codes," *Information Theory and its Applications (ISITA)*, 2010 International Symposium on, Taichung, 2010, pp. 383-388.
- [12] Z. Li, L. Chen, L. Zeng, S. Lin and W. Fong, "Efficient Encoding of Quasi-Cyclic Low-Density Parity-Check Codes," in *IEEE Transactions on Communications*, vol. 53, no. 11, pp. 1973-1973, Nov. 2005. doi: 10.1109/TCOMM.2005.858628.
- [13] Q. Huang, Q. Diao, S. Lin and K. Abdel-Ghaffar, "Cyclic and quasi-cyclic LDPC codes: New developments," *Information Theory and Applications Workshop (ITA)*, 2011, La Jolla, CA, 2011, pp. 1-10. doi: 10.1109/ITA.2011.5743581.

REVIEW ON STEGANOGRAPHY USING TEXTURE SYNTHESIS

Varnya C¹, Rinchu Baburaj¹, Harikrishnan N²
¹PG Scholar, ²Assistant Professor
Dept of ECE, Thejus Engineering College
Email:¹1992ammuv5@gmail.com

Abstract— Steganography is the art of hiding data in a media such as image, video or audio files. This paper describes different texture synthesis mechanisms as well as steganographic techniques for the secure transmission of information with more capacity. Mainly, steganography is a type of an invisible communication which is recently being used in different applications. The data embedding capacity and the increased PSNR values are the major issues facing in steganography. To solve these issues, many algorithms have been put forward in these years. Texture synthesis is one of the efficient methods which can be used to improve the data embedding capacity. In this method, the data is hidden in the cover image which is generated by the method of texture synthesis which adds more data embedding capacity. It is a challenging task to generate high quality synthesis results. So different texture synthesis methods and data hiding schemes are analysed here.

Keywords— Cover Image, Data Embedding, Patch based synthesis, Pixel, Steganography, Stego Image, Texture synthesis, Tiling

1. INTRODUCTION

Steganography is a useful tool which allows covert transmission of information through the communication channel. Comparing to cryptography, in steganography the data hidden will not be much visible to attackers. Various formats of media such as audio, image and video can be used as cover for hiding the data[1]. But due to the ease of use and memory requirements, digital images are more popularly used as cover images for steganographic techniques.

Normally all digital file formats can be used for steganography as cover objects but an important property of redundancy is needed for hiding data. Redundancy can be explained as the amount of bits of an object that provide accuracy far greater than needed for the object's use and display. Redundant bits are those bit patterns in an image that do not disturb the visible features even if the bits are altered. Digital images[2] and audio files will obey this property but studies have found that other file formats can also support this redundancy. All digital file formats contain sequence of binary digits 0 and 1. So, the steganographic technique can be simply applied to the binary sequence by altering the one or two bits in the original sequence. The pixels of an image constitute the light intensities at specific points on the image. In an 8 bit image, each pixel will be an 8 bit sequence of 0's and 1's. So even if the least significant bit of the sequence is changed, it will not affect the entire image.

Texture is something which is composed of repeated patterns and it exactly looks like a uniform image. Texture synthesis is the process of creating repeated patterns of textures from a smaller texture image known as the source texture by taking the advantage of its structural content. Texture synthesis finds its application in a wide variety of areas like graphics, image enhancement techniques, animation etc[3]. Nowadays steganographic data hiding schemes are also being used together with texture synthesis methods. By the addition of coding techniques and cryptographic techniques along with the above mentioned methods, the data hiding capacity and security[4] can be improved.

The entire paper is organized as follows: In section 2, different texture synthesis techniques are reviewed and finally out of which the most efficient technique is identified. Section 3 analyses various steganographic techniques in digital images and at last, the most useful data hiding technique is found. Section 4 describes methods that combine both steganography and texture synthesis and finally the better method is identified.

2. TEXTURE SYNTHESIS

Textures are images that contain some repeating patterns and also they will possess the possibility of certain random variations. The two important properties of a texture are:

- The generated texture output should look like input
- The algorithm that is used to generate the output must be easy to use

The generated texture synthesized image possesses two properties such as local and stationary because each pixel in the texture image is visually related to a small set of its neighborhood pixels. Out of various algorithms proposed and presented, some of the texture synthesis methods are analyzed below.

2.1. Tiling Methods

This is one of the most simple and easy method of synthesizing a large texture from a smaller input texture. In this technique, multiple copies of the input sample are simply copied and pasted side by side to generate the output texture. The method presented by Cohen *et al.* [5] is a simple and stochastic tiling system for non-periodically tiling a plane using a number of Wang Tiles. The tiles then filled with textures, uniform images or uniform patterns will obtain a continuous representation. Wang Tiles are basically squares in which each edge is assigned a particular color which can be Red, Blue, Green and Yellow as shown in figure 2.1. Matching colored edges are aligned to tile the plane as shown in figure 2.2. Tiling requires all neighboring edges between tiles to have matching colors. This

method of tiling is named after Hao Wang in 1961 that any set of tiles that can produce a valid tiling of the plane must also be able to produce a periodic tiling of the plane.

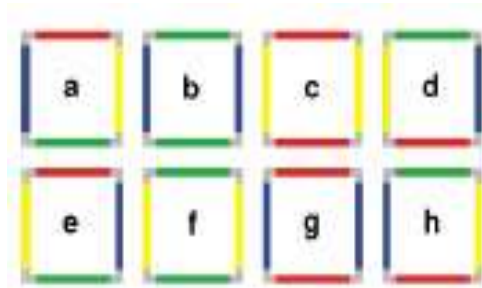


Fig 2.1: Eight Wang Tiles that can stochastically tile the plane [5]

New methods to fill the tiles with 2D texture, 2D Poisson distributions, or 3D geometry to efficiently create non-periodic texture as needed was presented. They also demonstrated how to fill individual tiles when combined with Poisson distributions that maintain their statistical properties.

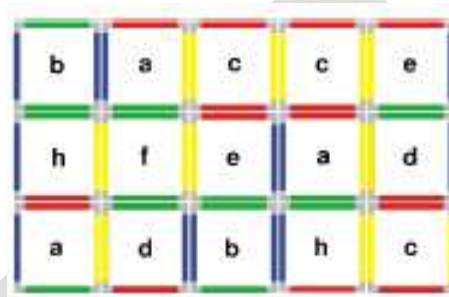


Fig 2.2: Align tiles to match edge color to create non-periodic tilings[5]

Edge coloring and the synthesis of textures ensures that the tiles always fit together. But a problem arises if an object or a visible artifact of the texture is placed across the tile corners. In this case, the vertical edge color constraint imposes all tiles with same colored opposite vertical edges to include the remainder of this object to ensure the fitting condition. Since the same object is also on the horizontal edge, all tiles that contain the corresponding horizontal edges needed to be placed similarly. This results in visible repetitive patterns which creates visual artifacts. To avoid this problem, a solution is found by coding the corners of a tile as an additional bit of information, by essentially coloring the corners as well as the edges. For example, in a single tile, $2^4 = 16$ possibilities of corner codings can occur. From their studies, they understood that the larger set of tiles provides increased degrees of freedom.

The method introduced by Weiming Dong *et al.*[6] is an optimized approach that can stably synthesize an ω -tile set of large pattern diversity and high quality. For that, an extendable rule is introduced to increase the number of sample patches to vary the patterns in a ω -tile set. In contrast to the other concurrent techniques that randomly choose sample patches for tile construction, the current technique uses Genetic Algorithm to select the feasible patches from the input example. This operation ensures the quality of the whole tile set. This is an approach for tile-based texture synthesis that is based on the optimization of tile set quality within a Genetic Algorithm (GA)-based framework.

2.2 Pixel – Based Methods

Due to the disadvantage aroused from tiling method because of the overlapping error and visible seams in the pasting edges, another method is introduced which is known as the pixel based texture synthesis. The method synthesizes a texture in scan line order by finding and copying pixels with the most similar local neighborhood.

A simple and efficient pixel based method is presented by Efros and Leung[7] in 1999. Their algorithm uses an input source image and a uniform white noise image which is having the size and dimension of the output texture. In this, a single pixel is generated at a time from an initial seed. A fixed size window with user specified size is taken which is centered on the currently synthesizing pixel. The more matching pixel is searched and copied in the output target. This process is repeated until all pixels in the target image are generated. This is illustrated in figure 2.3.

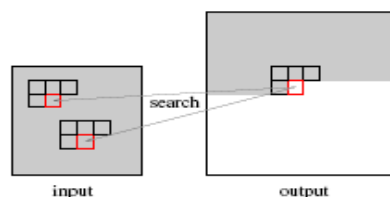


Fig 2.3: Pixel based synthesis

The paper presented by Wei and Levoy[8] uses a deterministic algorithm and the output texture is generated in a scan line order. This method improves the speed of the synthesis procedure by using tree structured vector quantization (TSVQ)[9] to match the target pixel with the neighborhood pixels. This fastest algorithm has a largest memory requirement. But it failed to synthesize the texture images of flowers, leaves, pebbles etc.

A slightly modified technique is introduced by Heeger and Bergen[10] which uses a multi resolution approach. The method uses an input texture and a modified noise image whose histogram is modified which matches with the input texture. The algorithm iterates by matching the noise histogram with the input texture image by using an image pyramid representation. It can be an image pyramid[11] or Laplacian pyramid. After some threshold iterations, the process can be stopped.

2.3 Patch based methods

In patch based methods, a single patch is generated at a time as shown in figure 2.4. In the previous method, only a single pixel is getting generated. So comparing to the existing methods, patch based method is much faster and is being widely used for texture synthesis applications[12].

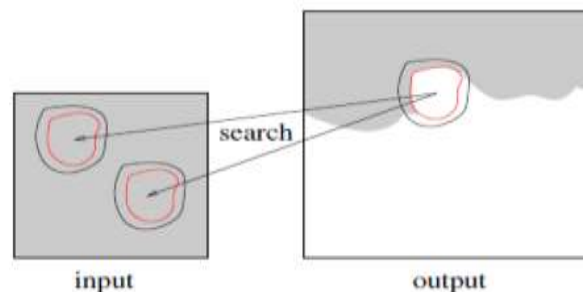


Fig 2.4: Patch based synthesis

Here the patches are copied block by block in a raster order. Upper left corner is initialized first. Then a square block is selected, which is taken as the candidate neighbour. Then next best matching patch is selected and is placed in the target image which overlaps with the other. Image quilting algorithm put forward by Efros and Freeman[13] minimizes the overlapping error introduced during the patch based texture synthesis. This implement a minimum error boundary cut in between the tiles copied as shown in figure 2. 5. The image quilting algorithm is as follows:

- Select a random patch from the input texture and initialize it as the seed to perform the texture synthesis and place it in the upper left corner.
- The process is done from left to right and top to bottom as:
 - Select the best fit patch to be pasted next using an exhaustive search.
 - Calculate the overlapping area between the current patch and the already processed patches using the L2 norm. The minimum error boundary path is identified and add that new patch to the output texture

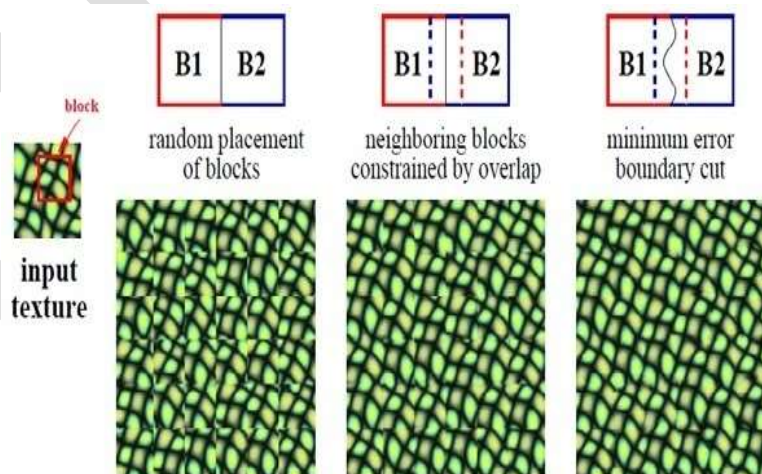


Fig 2.5: Quilting texture[13]

Liang, Liu and *et al.*[14] introduced a fast and new algorithm to generate texture using the method of texture synthesis. The texture generation was based on a non-parametric estimation of Markov Random Field [15] density function. This method assumes the texture as Markov Random model and the stochastic process is assumed to be stationary and local. Markov Random Field model is chosen

because of its accuracy in modeling a variety of textures[16]. The method is both applicable to texture synthesis which depends on some constraints as well as which is independent of constraints. Constraint based texture synthesis is found in applications like texture synthesis for hole-filling and tileable texture synthesis. Here the constraint is a randomness parameter. The parameter is used to control the randomness of the synthetic texture. In this paper, an input sample texture 'Iin' is used to generate an output synthetic texture 'Iout' by making use of this patch based algorithm. A patch 'Bk' is selected from the input texture 'Iin' and is copied in the target image in each step to generate the output texture. For the ease of work, the patch size taken for pasting is taken a fixed size of 'Wb x Wb'.

By analyzing various steganographic techniques, patch based texture synthesis is found to be the most useful algorithm for synthesizing textures. This method generates a single patch at a time and thus it is a faster method. Also in order to avoid the visual artifacts and overlapping error, an image quilting algorithm is also used with the patch based texture synthesis method. Comparing to all other methods this technique is widely used.

3. STEGANOGRAPHY

Steganography is the technique of hiding secret data and can be called as a type of invisible communication. Steganography differs from cryptography in the fact that in the case of steganography, the source and stego image can't be easily distinguished. The technique which is used to hide the data must be selected such that even after hiding the data the media should not affect any kind of distortions. In order to hide data in images, the noisy or redundant areas[17] are to be found first. Because in that areas, while the bits of pixels are changed, it will not get noticed.

In the paper proposed by Johnson and Jajodia[18], steganographic techniques are explained in detail. Number of ways exist to hide the data in images. The most popular approaches are:

- LSB replacement
- Masking and filtering
- Algorithms and transformations

For a 24 bit image, 3 bits of data can be hidden in each byte of the pixels. If the data before hiding is compressed using coding and compression schemes, more amounts of data can be hidden in the cover image. The data is hidden by replacing the least significant bits by the bits in the secret data. The change in the least significant bit will not affect the cover image since LSB bits are redundant bits. So the resulting stego image will exactly look like the input cover image. Masking and filtering methods are restricted to 24 bit and gray scale images. In lossy compression, watermarking techniques can be applied without destructing the image. Masking technique is much better than LSB insertion if factors such as cropping, compressing and image processing are taken into consideration. In algorithms and transformations, the data in its frequency domain is hidden into transformed coefficients of the pixel values of the cover image. This provides high embedding capacity and resists malicious attacks. Some of the transform domain techniques are Discrete Wavelet transform (DWT), Discrete Fourier Transform (DFT), Discrete Cosine Transform (DCT).

From the study and analysis of different steganographic techniques, it is found that LSB replacement is the most simple and efficient technique for data hiding. In LSB replacement, in order to hide the data, only the least significant bits of pixel information are changing. Since they are the redundant bits, it does not affect the pixel information much if altered. This will avoid visual artifacts and distortions in the cover media where data is hidden.

4. STEGANOGRAPHY IN SYNTHESIZED TEXTURE

Otori and Kuriyamma[19] introduced the data hiding technique in texture synthesis. For that, they used pixel based texture synthesis and data hidden in the synthesized texture. In this method they conceal data in dotted patterns and then they are directly painted on the blank image as shown in figure 4.1. The final output texture is generated by performing the pixel based texture synthesis in the above image. Thus every pixels are generated until complete texture is obtained. Finally the dotted patterns get masked in the synthesized texture. For extracting the data, the print out of the stego image is taken before the data detection mechanism. The capacity of this method depends on the number of dotted patterns used for data hiding. However, this method has a small rate of error in data retrieval.

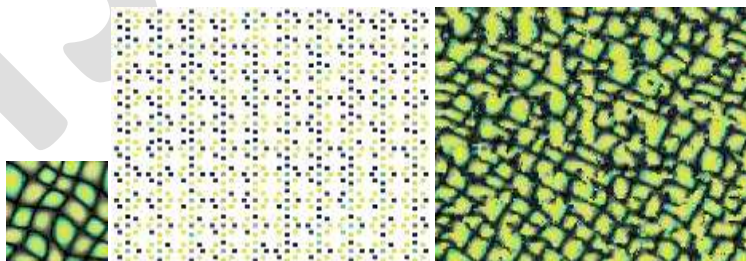


Fig 4.1: Input image, dotted pattern and the synthesized texture[19]

In the paper titled Robust data hiding on texture images by Otori and Kuriyamma[20], a regularly arranged dotted patterns painted with the color features that of the input image is hidden with the data. These dotted patterns are finally masked and this is having high quality compared to the existing texture synthesis methods. The hidden data can be recovered from the image printed like 2D bar

codes. They also used the pixel based texture synthesis. The colors in the input image are grouped with a specific color component which is known as a coded component. The component value depends on the brightness of a particular position. A threshold level is also set in order to improve the robustness.

A new reversible data hiding scheme is put forward by Kuo-Chen Wu and Chung-Ming Wang[21] which used a patch based texture synthesis algorithm and yielded a better output. Initially an index table is generated from the secret key which records the location to paste the source patches. By pasting the source patches, in the preferred locations, a composition image is generated. Then, patch based texture synthesis method is performed in the composition image. The data is hidden in the image which is synthesized by using LSB replacement technique and is transmitted. At the receiver side, proper recovery steps are carried out. The important advantages of this method are that the data embedding capacity is increased and a normal steganalytic algorithm cannot defeat this approach. Also the source texture i.e, the input image can be perfectly retrieved without any distortion and the source texture can be again used for another round of steganography.

5. CONCLUSION

Steganography uses different approaches for the secure communication of information. Many different algorithms are combined in order to improve the efficiency and capacity of the data hiding methods. The most simple and one of the efficient methods is the LSB insertion technique. Steganography together with the texture synthesis methods is explained here. Texture synthesis process resamples an input texture and produces an output texture which is having a user specified size and having more data embedding capacity. From the review of different texture synthesis methods, it is found that patch based texture synthesis is the most fastest and efficient method for synthesizing a texture. So it is widely used in applications such as 3D Graphics, computer vision and animation industry. Due to the simplicity and effectiveness, LSB replacement is considered to be the better steganographic technique.

REFERENCES:

- [1] F. A. P. Petitcolas, R. J. Anderson, and M. G. Kuhn, "Information hiding a survey," *Proc. IEEE*, vol. 87, no. 7, pp. 1062–1078, Jul. 1999.
- [2] T. Morkel, J.H.P. Eloff, M.S. Olivier, "An Overview Of Image Steganography", Information and Computer Security Architecture (ICSA) Research Group Department of Computer Science.
- [3] Amruta G. Chakkarwar, "The Novel Approach To Enhance Image Using Texture Synthesis", *International Journal of Engineering Research & Technology (IJERT)* Vol. 2 Issue 4, April – 2013 ,ISSN: 2278-0181.
- [4] Venkata Keerthy S, Rhishi Kishore T K, Karthikeyan B, Vaithianathan V, Anishin Raj M M, "A Hybrid Technique for Quadrant Based Data Hiding Using Huffman Coding", *IEEE Sponsored 2nd International Conference on Innovations in Information Embedded and Communication Systems ICIIECS'15*, 2015.
- [5] M. F. Cohen, J. Shade, S. Hiller, and O. Deussen, "Wang tiles for image and texture generation," *ACM Trans. Graph.*, vol. 22, no.3, pp. 287–294, 2003.
- [6] Weiming Dong, Ning Zhou, Jean-Claude Paul, "Optimized Tile-Based Texture Synthesis".
- [7] Alexei A. Efros and Thomas K. Leung, "Texture synthesis by non-parametric sampling", *IEEE International Conference on Computer Vision*, pages 1033–1038, Corfu, Greece, September 1999.
- [8] L.-Y. Wei and M. Levoy, "Fast texture synthesis using tree-structured vector quantization," in *Proc. 27th Annu. Conf. Comput. Graph. Interact. Techn.*, 2000, pp. 479–488.
- [9] [Cosman, P.C.](#), [Oehler, K.L.](#), [Riskin, E.A.](#), [Gray, R.M.](#), "Using Vector Quantization For Image Processing", [Proceedings of the IEEE](#), Sep 1993.
- [10] David J. Heeger and James R. Bergen, "Pyramid-based texture analysis/synthesis" *SIGGRAPH'95: Proceedings of the 22nd annual conference on Computer graphics and interactive techniques*, pages 229–238, New York, NY, USA, 1995. ACM.
- [11] Peter J. Burt, Edward H. Adelson, "The Laplacian Pyramid as a Compact Image Code", *IEEE Transactions On Communications*, Vol. Com-31, No. 4, April 1983.
- [12] Liu-yuan Lai, Wen-Liang Hwang, and Paruvelli Sreedevi, "Texture Synthesis Technique Using Different Sized Patches", *Institute of Information Science, Academia Sinica, Taiwan*.
- [13] A. A. Efros and W. T. Freeman, "Image quilting for texture synthesis and transfer," in *Proc. 28th Annu. Conf. Comput. Graph. Interact. Techn.*, 2001, pp. 341–346.
- [14] L. Liang, C. Liu, Y.-Q. Xu, B. Guo, and H.-Y. Shum, "Real-time texture synthesis by patch-based sampling," *ACM Trans. Graph.*, vol. 20, no. 3, pp. 127–150, 2001.
- [15] Zhu, S. C., Wu, Y, And Mumford, D. 1998. "Filters, random-fields and maximum-entropy (Frame)", *Int. J. Comput. Vis.* 27, 2 (March), 107–126.

- [16] Renjie Chen, Ligang Liu, Guangchang Dong, “ Local resampling for patch-based texture synthesis in vector fields”, Int. J. of Computer Applications in Technology ,2004.
- [17] N. Provos and P. Honeyman, “Hide and seek: An introduction to steganography,” IEEE Security Privacy, vol. 1, no. 3, pp. 32–44, May/Jun. 2003.
- [18] N. F. Johnson and S. Jajodia, “Exploring steganography: Seeing the unseen,” Computer, vol. 31, no. 2, pp. 26–34, 1998.
- [19] H. Otori and S. Kuriyama, “Data-embeddable texture synthesis,” in Proc. 8th Int. Symp. Smart Graph., Kyoto, Japan, 2007, pp. 146–157.
- [20] Hirofumi Otori and Shigeru Kuriyama, “Robust Data Hiding on Texture Images”, 2009 Fifth International Conference on Intelligent Information Hiding and Multimedia Signal Processing, Toyohashi University of Technology.
- [21] Kuo-Chen Wu and Chung-Ming Wang, “Steganography Using Reversible Texture Synthesis”, IEEE Transactions On Image Processing, Vol. 24, No. 1, January 2015

Optimization of Resistance Spot Welding Process Parameter by Taguchi Method

Prof. A. A. Karad¹, Mr. V. S. Shete², Mr. N. V. Boraste³

¹ Professor, Department of ME, K. V. N. Naik Institute of Engineering, Education & Research, Nashik.

² B.E. Student, K. V. N. Naik Institute of Engineering, Education & Research, Nashik.

³ B.E. Student, K. V. N. Naik Institute of Engineering, Education & Research, Nashik.

¹ avinash.karad1974@gmail.com, ² vaibhavshete14@gmail.com, ³ borastenikhil@gmail.com

Abstract— Experimental investigation on resistance spot welding has been carried out using L9 Taguchi orthogonal array. Mild steel material has been considered for experimental work. The spot welding input parameters, which are considered for this work are electrode force on plate, welding time and welding current, however tensile strength of nugget has been taken as output parameter. L-9 orthogonal array Results show that Welding current has significant impact on the tensile strength of nugget. The best suitable value of input parameters were found as follows Electrode Force(KGF)536, Welding time(cycle)24, Welding current(KA)10. The output value maximum tensile strength is found to be 330.00(MPA).

Keywords— Spot Welding, Tensile Strength, Taguchi Method, S/N Ratio, ANOVA Optimization.

INTRODUCTION

Resistance welding is a popular welding process due to its high speed and low cost combination. It also provides excellent reproducibility. Resistance spot welding (RSW) is one of the key metal joining techniques for high volume production in the automotive, biomedical and electronics industry. Large-Scale Resistance Spot Welding has become the predominant means of auto body assembly, with an average of two to six thousands spot welds. Increasing application of very thin metal sheets in manufacturing electronic components and devices, Small-Scale Resistance Spot Welding is attracting more and more researchers' attention. This work presents an approach to determine the effect of the process parameters (electrode force, weld time and welding current) on tensile strength of resistance weld joint for mild steel with the help of Taguchi method. The Taguchi method, which is effective to deal with responses, was influenced by multi-variables. This method drastically reduces the number of experiments that are required to model the response function compared with the full factorial design of experiments. The major advantage of this technique is to find out the possible interaction between the parameters. It is more resistant to general corrosion and pitting than conventional nickel chromium stainless steels such as 302-304. It has the following characteristics: Higher creep resistance, excellent formability, Rupture and tensile strength at high temperatures, Corrosion and pitting resistance.

Identifying The Important Process Control Variables:

Some of the important process control variable which influences the tensile strength and other characteristics of the spot welding are current, welding time, holding time, squeezing time, pressure, electrode diameter. But in our study we consider only welding time, welding current and electrode force. So by general spot welding heat equation

$$H= I^2Rt$$

Where, H= heat generated, I= Current, R=resistance, t=time

In this study Cycle time, Current and the electrode force were considered as the parameters to study their effect on the tensile strength of mild steel.

Experimentation

Preparation of the samples: - prepared the sample of dimension 100 x 25 mm for tensile strength and then join the two pieces by spot welding and set the range of parameter and calculate the tensile strength. This technique was used to prepare Mild steel. This method is most economical use in Mild steel. In this process the three different range electrode force, welding time, welding current.

The chemical composition of these steels was analyzed as listed in Table 1

Table1: Chemical Composition of Mild Steel

C %	Mn %	P%	S %	Si%	Cu%	Ni%	Cr
0.01	0.84	0.02	0.00	0.42	0.06	10.0	17.2
6	43	817	586	98	61	7	2



Fig 1: Test specimens after tensile testing on UTM m/c

Steps In Performing A Taguchi Experiment:

The process of performing a Taguchi experiment follows a number of distinct steps they are

Step1: Formulation of the problem—the success of any experiment is dependent on a full understanding of the nature of the problem.

Step2: Identification of the output performance characteristics most relevant to the problem.

Step3: Identification of control factors, noise factors and signal factors (if any). Control factors are those which can be controlled under normal production conditions. Noise factors are those which are either too difficult or too expensive to control under normal production conditions. Signal factors are those which affect the mean performance of the process.

Step4: Selection of factor levels, possible interactions and the degrees of freedom associated with each factor and the interaction effects.

Step5: Design of an appropriate Orthogonal Array (OA).

Step6: Preparation of the experiment.

Step7: Running of the experiment with appropriate data collection.

Step8: Statistical analysis and interpretation of experimental results.

Step9: Undertaking a confirmatory run of the experiment Copper alloy electrodes and the welding parameters according to the Taguchi L9 method as listed in Table 3 were used in the experiment.

Table 2: L9 Table Formulation

Expt.	Electrode force	Welding current	Welding time
1	1	1	1
2	1	2	2
3	1	3	3
4	2	1	2
5	2	2	3
6	2	3	1
7	3	1	3
8	3	2	1
9	3	3	2

Table 3 Process Parameters With Their Values At Three Levels

LEVEL	1	2	3
ELECTRODE FORCE	460	498	536
WELDING CURRENT	10	13	16
WELDING TIME	18	21	24

Result and Discussion:

The signal-to-noise concept is closely related to the robustness of a product or process design. Robustness has to do with a product's ability to cope with variation and is based on the idea

Table no. 4 Tensile Strength Response According To L9 Array

EXPT	ELECTRODE FORCE (KGF)	WELDING CURRENT (KA)	WELDING TIME (CYCLE)	TENSILE STRENGTH (MPA)
1	460	10	18	298.18
2	460	13	21	269.96
3	460	16	24	269.00
4	498	10	21	281.57
5	498	13	24	307.00
6	498	16	18	278.29
7	536	10	24	330.00

8	536	13	18	279.93
9	536	16	21	269.78

Electrode force(KGF)	Welding Current(KA)	Welding Time(cycle)	TS (MPA)	SNRA
----------------------	---------------------	---------------------	----------	------

that quality is a function of good design. A robust design or product delivers strong "signal". It performs its expected function and can cope up with variations ("noise"), both internal and external. Since a good manufacturing process will be faithful to a product design, robustness must be designed into a product before manufacturing commences. According to Taguchi, if a product is designed to avoid failure in the field, then factory defects will be simultaneously reduced. There is no attempt to reduce variation, which is assumed to be inevitable, but there is a definite focus on reducing the effects of variation. "Noise" in processes will exist, but designing a strong "signals" into a product can minimize their effect. The dimensionless signal-to-noise ratio is used to measure controllable factors that can have such a negative effect on the performance of a design. It allows for the convenient adjustment of these factors. Provided that a process is consistent, adjustments can be conveniently made using the signal-to-noise ratio to achieve the desired target.

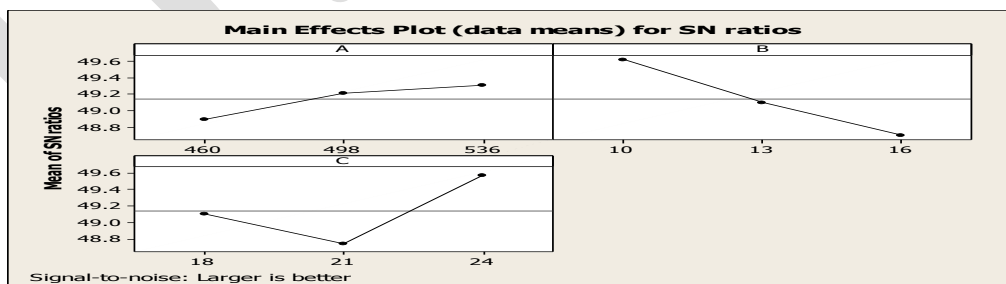
The signal to noise ratio (S/N ratio) was used to measure the sensitivity of the quality characteristic being investigated in a controlled manner. In Taguchi method, the term 'signal' represents the desirable effect (mean) for the output characteristic and the term 'noise' represents the undesirable effect (signal disturbance, S.D) for the output characteristic which influence the outcome due to external factors namely noise factors. The S/N ratio can be defined as:

$$S/N \text{ ratio, } \eta = -10 \log (\text{MSD})$$

where, MSD :mean-square deviation for the output characteristic.

Sample of dimension 100 x 25 mm were cut from a complete Mild steel sheet of 1.2 mm thickness. Then the pieces were joined by spot welding.

Graph 1: Effect of various parameters



460	10	18	298.18	49.4896
460	13	21	269.96	48.6067
460	16	24	269.00	48.5950
498	10	21	281.57	48.9917
498	13	24	307.00	49.7428
498	16	18	278.29	48.890
536	10	24	330.00	50.3703
536	13	18	279.93	48.9410
536	16	21	269.78	48.620

Table 6: Response Table

Level	Electrode force (kgf)	Welding Current(ka)	Welding Time(cycle)
1	48.90	49.62	49.11
2	49.21	49.10	48.74
3	49.31	48.70	49.57
Delta	0.41	0.92	0.83
Rank	3	1	2

Analysis Of Variance:

The main aim of ANOVA is to investigate the design parameters and to indicate which parameters are significantly affecting the output parameters. In the analysis, the sum of squares and variance are calculated. F-test value at 95% confidence level is used to decide the significant factors affecting the process and percentage contribution is calculated. Larger F – value indicates that the variation of the process parameter makes a big change on the performance. The analysis of variance (ANOVA) is applied in order to test the equality of several means, resulting in what process parameters (factors) are statistically significant.

Table 6: Results Of ANNOVA For T-S Strength

Source	DF	Seq SS	Adj SS	Adj MS	F Ratio	P Value	% C
A	2	327.6	327.6	163.8	0.70	0.588	9.46
B	2	1442.9	1442.9	721.4	3.09	0.245	41.69
C	2	1223.1	1223.1	611.6	2.62	0.277	35.33
Error	2	467.5	467.5	233.7			13.50
Total	8	3461.0					100

$$S = 15.2881 \quad R\text{-Sq} = 86.49\% \quad R\text{-Sq(adj)} = 45.98\%$$

Conclusion:

Experiments have been carried out using L-9 Taguchi orthogonal array. Nine standard combinations of input parameters have been tried to get the betterment of response. It is revealed by experiments the input variable Electrode force (KGF)) 536, Welding current (KA) 10, Welding time (CYCLE) 24 however the best output value observed to be 330.00(MPA). This gives an edge to weld maker to get the optimal/near optimal input process parameters.

REFERENCES:

- [1] Aravinthan Arumugam, MohdAmizi Nor, "Sopt Welding Parameter Optimization To Improve Weld Characteristic For Dissimilar Metals", International Journal Of Scientific & Technology Research Volume 4, 01, January 2015.
- [2] Manoj Raut And Vishal Achwal, "Optimization of Spot Welding Process Parameters For Maximum Tensile strength." International Journal of Mechanical Engineering and Robotics Research Vol. 3, No. 4, October 2014.
- [3] Makwana Brijesh V, Mr. Ruchir Desai, Mr. Pradhyuman Parmar, "Optimization Of Process Parameter For RSW Process Of Austenitic SS304 using Response Surface Method" International Journal For Technological Research In Engineering Volume 1, 9, April-2014.
- [4] Shaikshafee, Dr. B. BaluNaik, Dr. K. Sammaiah, Dr. Mohd. Mohinoddin, "RSW Process Parameters Optimization by Taguchi Method", IOSR Journal Of Mechanical and Civil Engineering (IOSR-JMCE) e-ISSN: 2278-1648, p-ISSN: 2320-334X, Volume 11, 5 Ver.II (Sept.-Oct. 2014), PP 46-54.
- [5] Saurabh Kumar Gupta, K.N. Pandey, "Application Of Taguchi Method For Optimization Of Friction Stir Welding Process Parameter to Joining of Al Alloy", Advanced Material Manufacturing & Characterization Volume 3, 1(2013).
- [6] Dr. D. R. Prajapati, Daman Vir Singh Cheema, "Optimization Of Weld Crack Expansion Defect Of Wheel Rim By Using Taguchi Approach: A Case Study". International Journal Of Innovative Research In Science, Engineering Technology, Vol. 2, Issue 8, August 13.
- [7] Norasiah Muhammad, Yupiter HP Manurung, Mohammad Hafidzi, Sunhaji Kiyai Abas, Ghalib Tham, M. Ridzwan Abd. Rahim "A Quality Improvement Approach for Resistance Spot Welding using Multi-objective Taguchi Method and Response Surface Methodology, International Journal on Science and Engineering, Vol.02, 2012, No.3 P17-22.
- [8] Hamid Eisazadeh, Mohsen Hamedi, Ayob Halvae "New Parametric study of nugget size in resistance spot welding process using FEM". Advanced Welding & Joining Department, Korea Institute of Industry technology, 2011, P 925 – 930.
- [9] A.G Thakur, T.E Rao, M.S Mukhedkar and V.M. Nandedkar, 2010 "Application Of Taguchi Method for RSW of Galvanized Steel", ARPN Journal Of Engineering and Applied Sciences Vol.5, No. 11, November 2010.
- [10] K. Kishore, P.V. Gopal Krishna, K. Veladri and Ali Syed Qasim "Analysis of Defects in Gas Shielded Arc Welding of AISI 1040 Steel Using Taguchi Method". ARPN Journal of Engineering and Applied Sciences, vol. 5, no. 1, 2010, p1p. 37 - 41.
- [11] A.G.Thakur, V.M.Nandedkar, Application of Taguchi Method to Determine Resistance spot welding conditions of Austenitic Stainless Steel AISI 304, Journal of Scientific & Industrial Research, vol 69, Sept 2010, P 680-683.
- [12] Ugur Esme, "Application of Taguchi method for Optimization of resistance spot Welding process" The Arabian journal of science and Engineering, Volume 34, Number 2B, 2009, P521-52.

Fingerprint Recognition Improvement Using Histogram Equalization and Compression Methods

Nawaf Hazim Barnouti

Baghdad, Iraq

E-mail-nawafhazim1987@gmail.com, nawafhazim1987@yahoo.com

Abstract— Biometrics refers to metrics related to human characteristic. Biometric systems work on physiological and behavioral biometric data to recognize people. Fingerprints are common biometric that have been used to identifying people for many years. Fingerprint identification also known as hand print is the process of comparing two instances of friction ridge skin impressions from human fingers or toes to determine whether these impressions have come from the same person. FVC2000 fingerprint database is used in this work. Pre-processing methods are applied on the images database to increase the recognition rate. Histogram equalization is used and shows improvement in result. Compression methods are used to decrease the redundancy of the image and also to store or transfer data in an efficient structure. PCA is used for feature extraction and dimension reduction. PCA is popular and will generate training set of images database. City block distance classifier is the final step of fingerprint recognition.

Keywords— Fingerprints, FVC2000, TIFF, HE, LZW, PCA, City block, Euclidean distance, Recognition rate

INTRODUCTION

Fingerprints is an impression in its narrow sense left by the friction ridges and actually widely examined from several points of view. Scientific studies on their embryogenesis can be found. Several papers have been written on the inheritance of specific fingerprint features and they include statistically linked to all kinds of common human features (gender) and some more obscure ones (sexual orientation, high blood pressure) [1]. Finger scan technology is deployed biometric with a number of different vendors offering a wide range of solutions. Fingerprints are deposited on a good suitable surface such as metal or glass. Biometric systems work on physiological and behavioral biometric data to recognize a person. The behavioral biometric parameters (signature, speech, gait and keystroke) change with environment and age. Although physiological features such as fingerprint, palm print, face and iris will still unchanged during the life time of a person. The biometric system work as identification mode or verification mode based on the need of an application. The verification mode validates a person identity by comparing taken biometric data with pre made template databases. The identification mode also known as hand print identification recognize a person identity by performing matches against several fingerprints biometric templates.

Fingerprints are commonly applied in daily life for more than 100 years because of its feasibility, reliability, distinctiveness, permanence, accuracy, and acceptability. Fingerprint is a pattern of ridges, furrows and minutiae that are taken using inked impression on a paper or sensor. Fingerprint sensor is an electronic device used to capture a digital image of a fingerprint pattern. High quality fingerprint included 25 to 80 minutiae based on sensor resolution and finger position on the sensor. The false minutiae are the false ridges breaks because of insufficient amount of ink and cross connections as a result of over inking. It is not easy to extract reliably minutia from poor quality fingerprint impressions arising from very dry fingers and fingers mutilated by scars, scratches due to accidents, injuries. Minutia based fingerprint recognition includes Thinning, Minutiae matching, Minutiae extraction and Computing matching score [2].

Fingerprint image obtaining is without question the most important and critical step in an automated fingerprint authentication system, because it determines the final fingerprint image quality which has a drastic effect on overall system performance. Captures the digital image of a fingerprint pattern known as live scan and it can be done by placing the finger on the surface of a fingerprint reader as shown in figure 1. This live scan is digitally done to generate a biometric template (a collection of extracted features) that is collected and used for matching process. The commonly used fingerprint sensor technologies are optical, ultrasonic and capacitive. Siemens ID Mouse comes under the capacitive type of fingerprint sensors. Capacitance sensors use the principles related to capacitance in order to form fingerprint images [3].



Figure 1: Fingerprint Readers.

FVC2000 FINGERPRINT DATABASE

The Fingerprint Verification Competition (FVC) is an international competition involved in fingerprint verification software examination. A subset of fingerprint impressions obtained with different sensors was presented by registered people to help them adjust the parameters of their methods. People were requested to provide registration and match executable files of their methods. The analysis was executed at the organizers facilities applying the submitted executable files on database, obtained with the same sensors as the training set. Table 1 shows the database most important information.

Table 1: FVC2000 Information.

Call for participation	November, 1999
Submission Deadline	June 1st, 2000
Registration Deadline	March 1st, 2000
Evaluation Period	July–August, 2000
Notes	Anonymous part. not allowed
Registered Participants	25 (15 withdrew)
Results Presentation	Barcelona, September 2000
Website	http://bias.csr.unibo.it/fvc2000
HW/SW Implementation	Pentium III (450 MHz) FVC Test suite v1.0 Windows NT

FVC2000 competition attempted to set up the first common benchmark, helping academic institutions and companies to unambiguously evaluate overall performance and monitoring improvements in their fingerprint recognition algorithms. In FVC2000, the “universal” sensor is in fact a collection of four various sensors to more beneficially handle the latest advances in fingerprint sensing techniques. Databases 1 and 2 were collected by applying two small size and low cost sensors. Database 3 was collected by applying a high quality optical sensor. While, images in Database 4 were synthetically generated. Each database was divided into a sequestered “test” set of 800 images (set A) and an open “training” set of 80 images provided to people for method tuning (set B). The four different databases (DB1, DB2, DB3 and DB4) were collected using different sensors technology [4]. Table 2 shows the features of these databases.

Table 2: FVC2000 (DB1, DB2, DB3 and DB4) Features.

#	Image	Set A	Set B	Resolution
---	-------	-------	-------	------------

	Size	(w*h)	(w*h)	
DB1	300x300	100*8	10*8	500 dpi
DB2	256x364	100*8	10*8	500 dpi
DB3	448x478	100*8	10*8	500 dpi
DB4	240x320	100x8	10x8	About 500 dpi

IMAGE FORMAT

TIFF (Tagged Image File Format) is a file format for mainly strong images, as well as photographs and line art. It is probably the most common and flexible of the present public domain raster file formats. Originally created by the company Aldus, jointly with Microsoft, for use with PostScript printing. TIFF is a common format for high color level images, along with JPEG and PNG. TIFF format is generally supported by image manipulation applications, and by faxing, scanning, optical character recognition, and many other applications. TIFF is a complex format that includes a very wide range of choices. Even if this makes it useful as a general format for interchange between professional image editing applications, it makes helping it in additional application include web browsers difficult [10]. Figure 2 shows samples taken from DB1 and DB3.

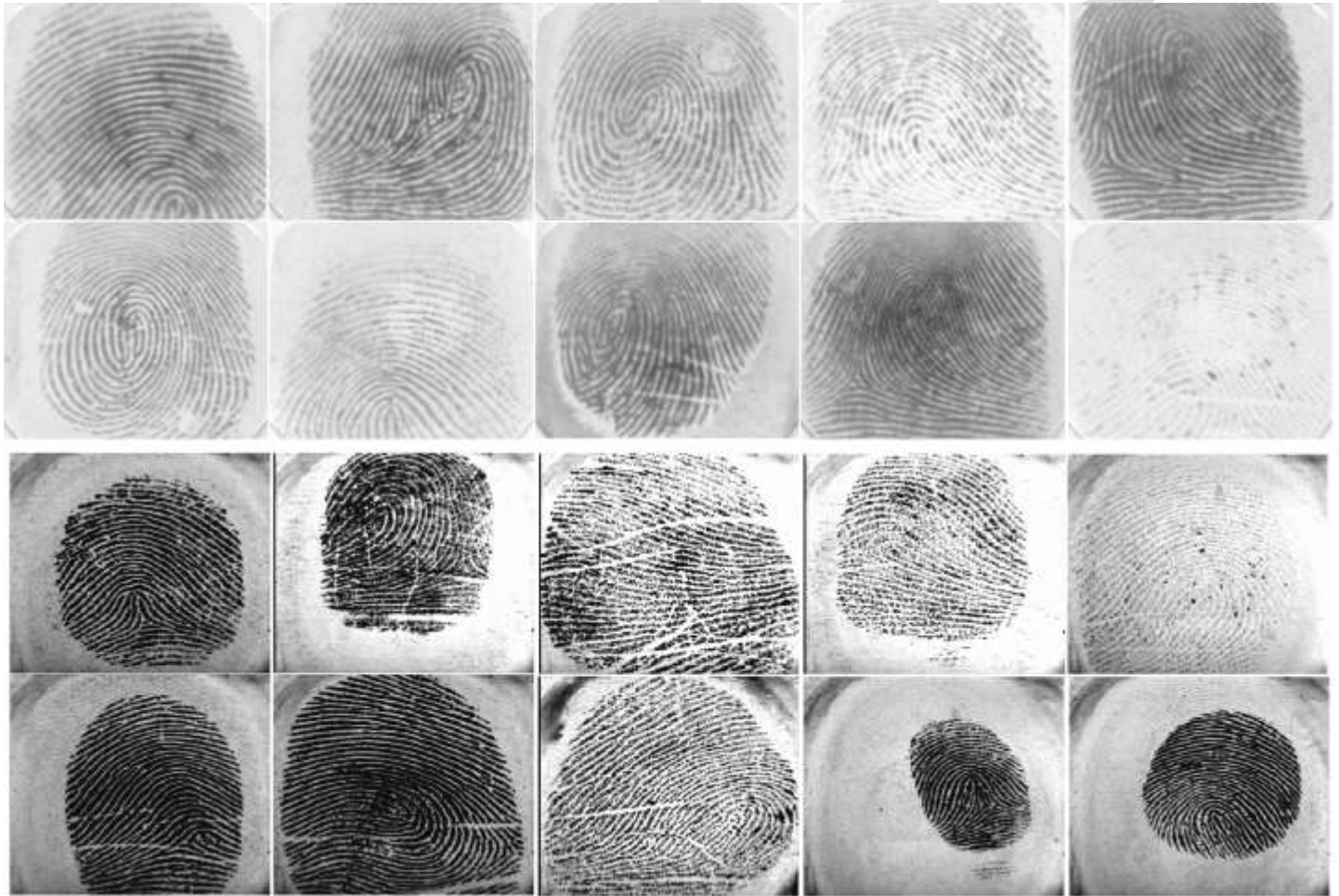


Figure 2: Sample Images Taken from DB1 and DB3.

IMAGE PRE-PROCESSING

Image enhancement improvement is a basic problem in computer vision and image processing. It's the process of modifying the pixel's intensity of the input image by using mathematical operations to generate better output images. Many methods have been developed in image processing during the last decades. It's nearly become a pre-processing part of many areas like medical image processing and as a preprocessing part of texture synthesis, speech recognition, and a lot of additional image and video processing applications [6]. Contrast is created by the difference in luminance reflectance from two adjacent areas. Enhancement methods mainly fall under two basic categories spatial and frequency domain methods. Spatial domain methods are usually more popular than the frequency based methods, as they are developed on direct manipulation of pixels in image. Spatial domain methods have been developed for visualizing the impact effect. Some of these methods makes use of simple linear or nonlinear intensity level transformation functions, while others use complex analysis of different image features that include edge and connected component information [7].

1. HISTOGRAM EQUALIZATION

Contrast enhancement improvement issue in digital images was resolved by using different methods, but Histogram Equalization (HE) method is the most popular. Histogram Equalization method flattens the histogram and extends the dynamic selection of intensity values by applying the cumulative density operation. Even so, you will discover major draw backs in Histogram Equalization especially when executed to process digital images. First of all, HE transforms the histogram of the input image into a uniform histogram by importing the whole selection of gray levels uniformly over the histogram of an image, with a mean value that could be in the center of gray levels range. Consequently, the mean brightness of the output image is usually at the center or close to it when it comes to discrete implementation. In terms of images with high and low mean brightness value, you can find an important change in the view of the enhanced image. Secondly, histogram equalization performs the enhancement depending on the global content of the image [7]. Basically, histogram equalization highlights the edges and borders between different objects, but may decrease the local details of these objects and not adequate for local enhancement. Another result to do this merge is the production of over saturation artifacts and enhancement [8]. For image $I(x, y)$ with K discrete level, the gray values histogram is determined using the occurrence probability of the gray level i , as shown in the equation below:

$$Prob(i) = \frac{n_i}{N} \quad \text{Where } 0 \leq i \leq K - 1 \quad (1)$$

Where N is the total number of pixels in the image, n is the total number of pixels with the same intensity level, and K is the total number of gray level in the image. Figure 3 shows fingerprint image before and after applying the histogram equalization.



Figure 3: Fingerprint Image Before and After Applying HE.

2. IMAGE COMPRESSION

Images become very important and used in many application areas. Because of the large amount of data images need to be compressed. Image compression is an application of data compression that encodes the original image with number of bits. Data compression has an important part in the different areas of storage. The purpose of image compression would be to decrease the redundancy of the image and also to store or transfer data in an efficient structure [11]. The primary objective of such system is to decrease the storage amount as much as possible, and the decoded image shown in the monitor can be similar to the original image as much as can be [9]. Image Compression can be either lossy or lossless. Lossless compression methods is suitable for archival purposes and for medical imaging. Lossy compression methods are suitable for natural images such as photographs in applications. The high quality at a given compression rate is the main purpose of images compression. Now consider an encoder and a decoder. When the encoder will receive the original image file, the image file is going to be converted into a series of binary data, frequently known as

the bit stream. The decoder after that receives the encoded bit stream and decodes it to form the decoded image. If the total data amount of the bit stream is lower than the total data amount of the original image, then this is called image compression [13] [14]. Figure 4 shows the full compression process. TIFF (Tagged Image File Format) is the image format used in FVC2000 database.

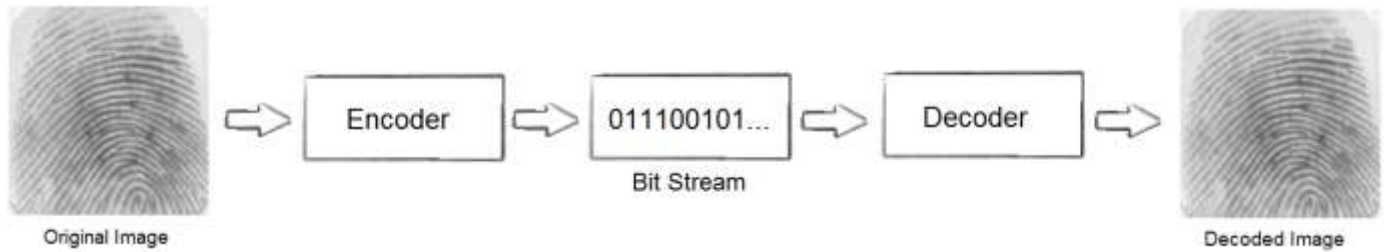


Figure 4: Image Compression Process.

PRINCIPAL COMPONENT ANALYSIS (PCA)

Building the image space by using the PCA method. The PCA is feature extraction and dimension reduction method. PCA is a popular linear projection technique, and also known as eigenspace projection, Karhunen and Loeve (KL) transformation, or Hotelling. It reduces dimensionality by extracting the principal components of multidimensional data. PCA can extract the important features, capture the nearly variable data components of samples, and then select numerous significant individual from all the feature components [5]. Through PCA, an efficient and simple recognition process can be obtained compared with other methods. Recognitions that use PCA features also perform better in singular variation cases for each individual. Raw intensity data are used for recognition and learning without mid-level or low-level processing [12].

PCA method Steps are as follows:

1. Collect images from fingerprint database.
2. Represent images as a single vector.
3. Compute average mean.

$$AverageMean = \frac{1}{M} \sum_{n=1}^M TrainImage(n) \quad (2)$$

Where M is the total number of the training images.

4. Subtract original image from average mean.

$$S = TrainImage - AverageMean \quad (3)$$

5. Compute covariance matrix.

$$Covariance = \frac{1}{M} \sum_{n=1}^M S(n) S^T(n) \quad (4)$$

6. Calculate eigenvalues and eigenvectors.
7. Sort and eliminate eigenvalues.
8. Build training matrix.

DISTANCE MEASUREMENT

The distance between two images is a major concern in image recognition and computer vision. The final step of fingerprint recognition is measuring the distance between two images. Image similarity is the distance between the vectors of two images. The distances among feature space representations are used as the basis for recognition decisions. Many existing image distance methods suffer from complicated measure computations, leading to a difficulty in combining the metric with some fingerprint recognition methods.

1. CITY BLOCK DISTANCE

City block distance, which also known as L1 distance or Manhattan distance classifier, is the summation of the absolute difference between two vectors. It is especially used for discrete types of descriptors. City block distance is a true distance function because it responds to triangle inequality. It also assumes a triangular distribution [15]. Suppose X is the training images and Y is the test image. City block distance then can be calculated from the equation below:

$$d(X, Y) = |X - Y| = \sum_{i=0}^{\text{No.Of Images}} |X_i - Y_i| \tag{5}$$

2. EUCLIDEAN DISTANCE

Euclidean distance is widely used to classify and compute the similarity between images because it is faster than other classifiers and is simple. Euclidean distance examines the root of square differences between the coordinated of a pair of objects. A minimum Euclidean distance classifier is the most suitable condition for normally distributed classes [15]. Euclidean distance can be calculated from the equation below:

$$d(X, Y) = \sqrt{\sum_{i=1}^{\text{No.Of Images}} (X_i - Y_i)^2} \tag{6}$$

RESULT AND DISCUSSION

In this analysis, FVC2000 fingerprint database that contain four databases (DB1, DB2, DB3, and DB4) is used with different number of training and testing images to evaluate the performance and recognition rate. TIFF (Tagged Image File Format) is a file format for FVC2000 fingerprint database. Table 3 shows the recognition rate of DB1 and DB3 without applying any pre-processing on images. The recognition rate will increase when the number of training images is increased. The recognition rate was weak and not acceptable. Therefore, images pre-processing methods are applied. Image pre-processing methods are important and applied to perform better results. Histogram equalization and Image compression are applied.

Table 3: Recognition Rates (DB1 and DB3).

No. of Testing Images	No. of Training Images	DB1 Recognition Rate	DB3 Recognition Rate
7	1	22.86 %	18.57 %
6	2	22.67 %	20 %
5	3	24 %	22 %
4	4	27.5 %	24.5 %
3	5	33.33 %	50 %
2	6	45 %	50 %
1	7	45 %	50 %

1. HISTOGRAM EQUALIZATION

The widely accepted histogram equalization cannot correctly enhance all the part of an image. When the original image is irregularly illuminated, certain information will be either too dark or too bright. These methods are generally the most applied histogram adjustment methods. HE is used to create a uniformly distributed image over the whole brightness scale, and HE helps the input image histogram to have a predefined shape. HE improve and increase the recognition rate. Table 4 shows the recognition rate of DB1 and DB3 using HE. Histogram of the image is equalized as shown in figure 5.

Table 4: Recognition Rate (DB1 and DB3) Using HE.

No. of Testing Images	No. of Training Images	DB1 Recognition Rate	DB3 Recognition Rate
7	1	40 %	31.43 %
6	2	43.33 %	32.33 %
5	3	48 %	40 %
4	4	57.5 %	47.50 %
3	5	66.67 %	63.33 %
2	6	75 %	65 %
1	7	75 %	70 %

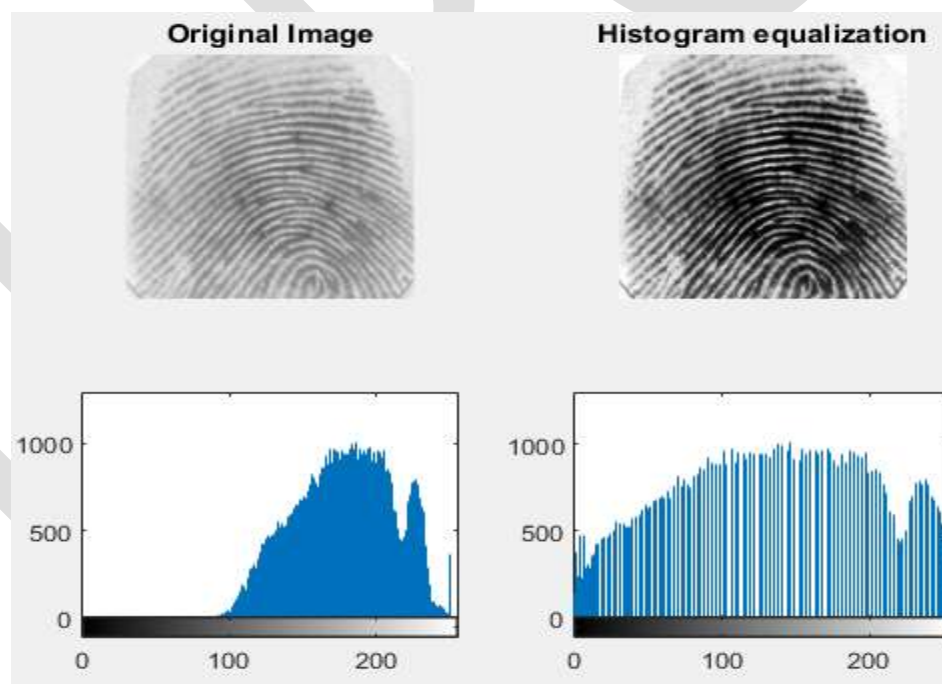


Figure 5: Image After Applying Histogram Equalization.

2. IMAGE COMPRESSION

In this analysis TIFF format is used in the FVC2000 database. Many compression methods can be applied. The compression reduces the size of files to save storage space and to save time when transmitting it. Compression play a center role in communication technology and is part of modern life. Lossless compression methods are useful in image archiving. Lossless means there is no quality loss due to compression. LZW data compression is a universal lossless method created by Abraham Lempel, Jacob Ziv, and Terry

Welch. LZW is one of the adaptive dictionary methods. LZW is simple to implement and has the potential for very high throughput in hardware implementation. LZW compression works better with images that have solid colors. LZW is also suitable for compressing text files. Many other lossless methods can be used. Pack Bits is simple and fast method for run length encoding.

CONCLUSION

Fingerprints are important area of biometrics and used in many applications. In this work Databases 1 and 3 of FVC2000 (Fingerprint Verification Competition) are used. PCA used for feature extraction and dimension reduction. City block distance is used for matching process. Different number of training and testing images are used. Increasing the training images will increase the recognition rate. The results without use any Pre-processing methods was weak and not acceptable. Histogram equalization and Image compression methods are used. The recognition rate increased when applying the histogram equalization in each database 1 and 3. Image compression also important and used to reduce the time and the size of files to save storage space.

REFERENCES:

- [1] Kücken, Michael, and Alan C. Newell. "Fingerprint formation." *Journal of theoretical biology* 235, no. 1 (2005): 71-83.
- [2] Raja, K. B. "Fingerprint recognition using minutia score matching." *arXiv preprint arXiv:1001.4186* (2010).
- [3] Mazumdar, Subhra, and Venkata Dhulipala. "Biometric Security Using Finger Print Recognition." *University of California, San Diego* (2008): 3.
- [4] Maio, Dario, Davide Maltoni, Raffaele Cappelli, James L. Wayman, and Anil K. Jain. "FVC2000: Fingerprint verification competition." *Pattern Analysis and Machine Intelligence, IEEE Transactions on* 24, no. 3 (2002): 402-412.
- [5] Kale, Piyush G., and C. S. Khandelwal. "IRIS & Finger Print Recognition Using PCA for Multi Modal Biometric System." (2016).
- [6] Rao, Raghuveer M., and Manoj K. Arora. "Overview of image processing." In *Advanced Image Processing Techniques for Remotely Sensed Hyperspectral Data*, pp. 51-85. Springer Berlin Heidelberg, (2004).
- [7] Krishna, A. Sri, G. Srinivasa Rao, and M. Sravya. "CONTRAST ENHANCEMENT TECHNIQUES USING HISTOGRAM EQUALIZATION METHODS ON COLOR IMAGES WITH POOR LIGHTNING." *International journal of computer science, engineering and applications* 3, no. 4 (2013): 15.
- [8] Raju, A. "A comparative analysis of histogram equalization based techniques for contrast enhancement and brightness preserving." (2013).
- [9] Wei, Wei-Yi. "An introduction to image compression." *National Taiwan University, Taipei, Taiwan, ROC* (2008).
- [10] Aguilera, Paula. "Comparison of different image compression formats." *Wisconsin College of Engineering, ECE 533* (2006).
- [11] Kaur, Simrandeep, Verma, Sulochana. "Design and Implementation of LZW Data Compression Algorithm." *International Journal of Information Sciences and Techniques (IJIST)*, 3, no. 4 (2012).
- [12] Melo, Ernande F., and Hélio M. de Oliveira. "A Fingerprint-based Access Control using Principal Component Analysis and Edge Detection." *arXiv preprint arXiv:1502.01880* (2015).
- [13] Vijayvargiya, Gaurav, Sanjay Silakari, and Rajeev Pandey. "A Survey: Various techniques of image compression." *arXiv preprint arXiv:1311.6877*(2013).
- [14] Dheemanth, H. N. "LZW Data Compression." Volume 3 Issue, (2014): 22.
- [15] Gawande, Mohit P., and Dhiraj G. Agrawal. "Face recognition using PCA and different distance classifiers."

DATA COMPRESSION AND EXPANSION USING DISCRETE WAVELET TRANSFORM IN ENCRYPTED DOMAIN

VITTHAL SHELKE¹, PROF. R.A.PATIL²

1 Student, (M Tech) Department of Electrical Engineering, VJTI, Mumbai. Shelkey247@gmail.com, 9011502844.

2 Associate Professor, Department of Electrical Engineering, VJTI, Mumbai

ABSTRACT

The signal processing after encryption that is in cryptosystem is relatively somewhat new topic. The data size to store available information require large memory, so here we are proposing a method called multilevel discrete wavelet transform (DWT) in encrypted domain. We are suggesting a frame work for carry out DWT and its inverse DWT in the encrypted domain. With this proposed framework we carry out multilevel DWT and inverse DWT in Homomorphic encrypted domain. Encryption is the process of encoding data. The purpose of encryption is to ensure data security. Homomorphic encryption is useful of encrypted information for data computation.

Keywords-Dataprocessing, Discrete wavelet transform (DWT), Inverse Discrete wavelet transform (IDWT), Encryption, Decomposition, DFT, FFT

INTRODUCTION

Data processing [1] in encrypted domain is somewhat new topic. This new technique gives two kinds of application uses in the future. The first kind of application is in the scenario of network media distribution. The customer may be asked to embed a water mark in the media to find out illegal copies. Since the plain media can be easily attacked during the process of watermarking, a solution for this is to embed the watermark in the encrypted media, whose content is protected by the cryptosystem. Signal processing the encrypted domain provide powerful and accurate tools to carry out implementation quiet possible. The second Application is to protect privacy. Consider a case of a remote access system based on biometric data, the users sensitive information related to authentication will be stored in server. If server is unsecure or misused then, user will face some serious problems. Processing in the encrypted domain along with Cryptographic protocols in the encrypted domain. Cryptographic protocols [2], [3], can give an effective solution to the server store the user information in encrypted form in Data base. The signal processing in encrypted domain plays important role. But not all cryptosystem [4],[5],[6],[7] like advanced encryption standard (AES) and data encryption standard (DES) Does not retain the symmetrical relation with the plain text. The Homomorphic Cryptosystem [8] keep the algebraic structure of plain text Homomorphic cryptosystem are of two type. one is partially Homomorphic cryptosystem and fully Homomorphic cryptosystem which give permission to carry out addition and multiplication.

The Homomorphic Cryptosystem [8] was first introduced by Rivest. There are two operations regarding to each other one in the cipher text domain and other in plain text domain. consider two plain text m_1 and m_2 .

Then

$$D\{E[m_1] \circ E[m_2]\} = m_1 \diamond m_2 \quad (1)$$

where $D\{\}$ is decryption and $E\{\}$ is encryption

RELATED WORK

There have been works on signal processing in encrypted domain. Bianchi [9][10] investigated on implementation of discrete Fourier transform (DFT) and fast Fourier transform (FFT) in encrypted domain but due to limitation in encrypted domain discrete wavelet transform is used. DWT is general scheme for signal processing. This paper contains the performing of DWT actually. DWT can extract different type of information from given data or called media. DWT can be used as for application like water marking [11], reducing memory space, feature extraction.

PROCEDURE

The important feature to choose wavelet transform is that it allows Multiresolution decomposition and here we are taking image into consideration so an image that is decomposed by using wavelet transform can be reconstructed completely.

LL	HL
LH	HH

1st level.

LL	HL	HL
LH	HH	
LH		HH

2nd level .

LL	HL	HL	HL
LH	HH		
LH		HH	HH
LH			

3rd level.

Figure 1: wavelet decomposition

The resulting decomposition contain two-dimensional array Coefficients containing four sub levels. As LL (low low), HL (high low), LH (low high) and HH (high high). The LL level again can be decomposed in the same manner as in 1st level decomposition .like that we can produce any levels of decomposition.In this manner image is decomposed. Now here we are using discrete wavelet transform (DWT)

DISCRET WAVELET TRANSFORM

In Signal Processing the discrete wavelet transform based result better than DCT.The discrete wavelet transform (DWT) is a linear transformation that operates on adata vector whose length is an integer power of two, transforming it into a numerically different vector of the same length. It is a tool that separates data into different frequency components, DWT give temporal resolution that is it give frequency and location information.

According to Mallet algorithm [12] Discrete wavelet transform is defined as

DWT

$$a_j(k) = \frac{1}{\sqrt{2}} \sum_{l \in \mathbb{Z}} h_a(2k - l)a_{j-1}(l) \tag{2}$$

$$d_j(k) = \frac{1}{\sqrt{2}} \sum_{l \in \mathbb{Z}} g_a(2k - l)a_{j-1}(l) \tag{3}$$

where

$J=1,2,3,\dots$

$a_j(k)$ is the approximation coefficient.

$d_j(k)$ is detail coefficients.

and

$h_d(k)$ = low pass decomposition filter coefficient.

$g_d(k)$ = high pass decomposition filter coefficient.

Both the plain text and cipher text are always represented by integers in encryption. So for this all the data and parameters are represented with the help of integers.

Generally the filter coefficients are $h_d(k)$ and $g_d(k)$ are Real numbers. So in order to implement DWT in encrypted domain we have to consider integers instead of real numbers. The obtained integers instead of real numbers are obtained by quantization process as,

$$H(k) = \lfloor Qh_d(k) \rfloor \tag{4}$$

$$G_d(k) = \lfloor Qg_d(k) \rfloor \tag{5}$$

Where $\lfloor \cdot \rfloor$ is round of function.

According to discussion as we talked above we give the recursive definition of DWT

$$A_j(k) = \sum_{l \in \mathbb{Z}} H_d(2k - 1)A_{j-1}(l) \tag{6}$$

$$D_j(k) = \sum_{l \in \mathbb{Z}} G_d(2k - 1)A_{j-1}(l) \tag{7}$$

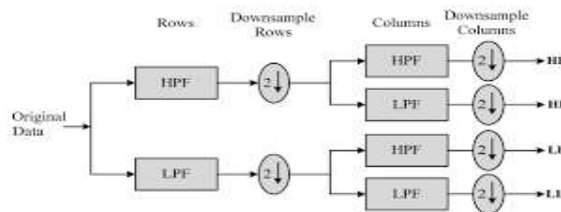


Figure 2: The block diagram of DWT:

In order to implement discrete wavelet transform DWT in encrypted domain we have to consider some issues, one of them is whether we are able to recover original Data from decryption. Other is to obtain plain wavelet coefficient.

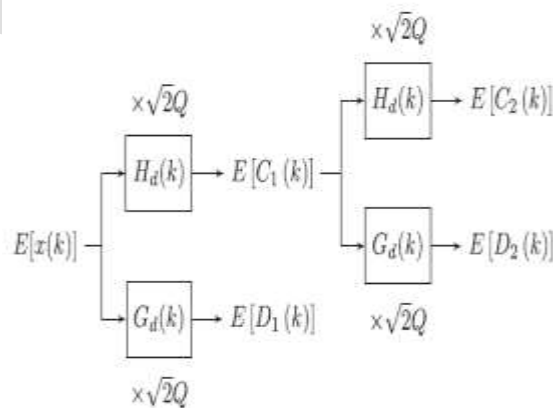


Figure 3: Block diagram of two levels DWT in encrypted domain

INVERSE DISCRETE WAVELET TRANSFORM

The mallat algorithm for[12] Inverse discrete wavelet transform(IDWT) is given as

$$a_j(k) = \frac{1}{\sqrt{2}} \sum_{l \in \mathbb{Z}} h_r(k - 2l)a_{j+1}(l) + g_r(k - 2l)d_{j+1}(l) \tag{8}$$

where

h_r ,lowpass filter coefficients.

g_r ,high pass filter coefficients.

In encrypted domain to Implement Inverse discrete wavelet transform(IDWT) the filter coefficients 1st converted suitable form that is in integer form.

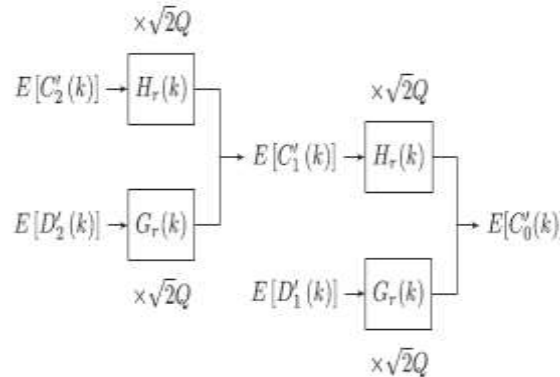


Figure 4: Block diagram two-level IDWT in the encrypted domain

METHODS FOR REDUCE DATA EXPANSION

While performing discrete wavelet transform and inverse discrete wavelet transform data is expanded due to expanding factor

A) Data expansion came into account due to absence of Normalization factor $\frac{1}{\sqrt{2}}$ in (6) and (7) and other is quantization process. So for that considers scale factor Q determine the precision of approximation of discrete wavelet transform and inverse discrete wavelet transform integers.

B) Rational filter coefficient:

Consider rational filter coefficients such as Haar wavelet. This can be expressed as two prime numbers which are relative as quotient.

$$Q \text{ mod } L=0$$

This can be achieved by using Haar wavelet.

Multiplicative inverse method does not require not additional information about input. It is applicable to both cases, that is for discrete wavelet transform and inverse discrete wavelet transform. In Multiplicative inverse method the scaling factor Q is selected relatively prime. Multiplicative inverse method used to increase performance in application as data hiding, data compression and also feature extraction.

CONCLUSION

This paper shows the implementation of discrete wavelet transform DWT in the encrypted domain and problem of data expansion due to quantization process is tackled. And also proposed frame work to implement discrete wavelet transform and inverse discrete wavelet transform in Homomorphic cryptosystem. DWT and IDWT is implemented using rational filter coefficients. Also multiplicative inverse method is discussed to improve capacity of signal processing.

REFERENCES:

- [1] Z. Erkin, A. Piva, S. Katzenbeisser, R. Lagendijk, J. Shokrollahi, G. Neven, and M. Barni, "Protection and retrieval of encrypted multimedia content: Whencryptography meets signal processing," EURASIPJ. Inf. Security, vol. 2007, pp. 1–20, Jan. 2007.
- [2] A. Yao, "Protocols for secure computations," in Proc. 23rd Annu. Symp. Foundations Computer Science, 1982, pp. 160–164.
- [3] O. Goldreich, S. Micali, and A. Wigderson, "How to play ANY mental game," in Proc. 19th Annu. ACM Conf. Theory Comput., 1987, pp. 218–229.
- [4] T. Elgamal, "A public key cryptosystem and a signature scheme based on discrete logarithms," IEEE Trans. Inf. Theory, vol. 31, no. 4, pp. 469–472, Jul. 1985.
- [5] P. Paillier, "Public-key cryptosystems based on composite degree residuosity classes," in Proc. Adv. Cryptology, 1999, pp. 223–238.
- [6] I. Damgård and M. Jurik, "A generalisation, a simplification and some applications of Paillier's probabilistic public-key system," in Proc. Public-Key Cryptography, 2001, pp. 119–136.
- [7] C. Gentry, "Fully homomorphic encryption using ideal lattices," in Proc. 41st Annu. ACM Symp. Theory Comput., 2009, pp. 169–178.
- [8] R. Rivest, L. Adleman, and M. Dertouzos, "On data banks and privacy homomorphisms," in Foundations of Secure Computation. Cambridge, MA, USA: MIT Press, 1978, pp. 169–178
- [9] T. Bianchi, A. Piva, and M. Barni, "On the implementation of the discrete Fourier transform in the encrypted domain," IEEE Trans. Inf. Forensics Security, vol. 4, no. 1, pp. 86–97, Mar. 2009.
- [10] M. Barni, P. Failla, R. Lazzeretti, A. Sadeghi, and T. Schneider, "Privacy-preserving ECG classification with branching programs and neural networks," IEEE Trans. Inf. Forensics Security, vol. 6, no. 2, pp. 452–468, Jun. 2011
- [11] P. Zheng and J. Huang, "Walsh-Hadamard transform in the Homomorphic encrypted domain and its application in image watermarking," in Proc. 14th Inf. Hiding Conf., 2012, pp. 240–254.
- [12] S. Mallat, "A theory for multiresolution signal decomposition: The wavelet representation," IEEE Trans. Pattern Anal. Mach. Intell., vol. 11, no. 7, pp. 674–693, Jul. 1989

Microstrip Line Digital Balanced Phase Shifter

Arati Arun Bhonkar, Dr. Udaysingh Sutar

ME (Pursuing) AISSMSCOE Pune, bhonkararati91@gmail.com and +91-9657210969

Abstract— Phase shifters finds application in areas like phase modulators, frequency up converters, phased array antenna systems, mobile communication system, WLAN and in PLL systems. For better detection of target in defence systems or surveillance systems phase shifters are needed to be installed on antenna systems to provide beam steering electronically without use of mechanical scanning for positioning. This proposed phase shifters are designed for 2.3 - 2.7 GHz (ISM band). 90° and 45° balanced structure provides better immunity against electromagnetic interference. Proposed design provides phase error around -2° to 5.67° for 45° phase shifter and 0.48° to 1.6° for 90° phase shifter. It also provides desired insertion loss.

Keywords— Microstrip lines, beam-steering, phased array antennas, MMIC, HEMT technology, ABCD matrix, phase error.

INTRODUCTION

Phase shifters are used in electronic warfare and active phased array radar systems. To achieve proper detection of ships in rough sea and heavy rain condition beam - steering antennas are required. Their significant applications like traffic control, regulation and collision avoidance radars in S band make them suitable to be installed on ships, aircrafts, and missiles in detection system. Beam-steering antennas are also used in smart base station antennas for WLAN and cellular communication. This is achieved through use of phased arrays. Here phase shifters are used to control main beam of antenna array. To achieve direction of beam's main lobe to be changed with time (scanning), rotation of antenna is required. However, mechanical rotation of single antenna is costly and time consuming. Hence electronic scanning should be done, which is possible using phased array antennas. This is done by varying electronically phase of radiating element. Electronically steerable phased array antenna is achieved by placing phase shifter on each radiating element [2].

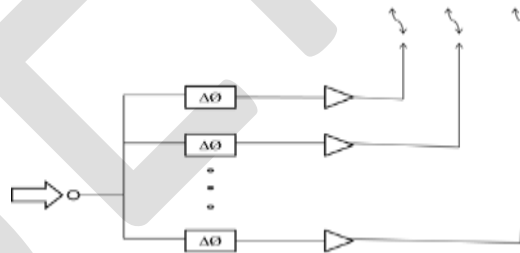


Fig. 1 A standard phased array antenna system

A phase shifter is a two port device whose fundamental function is to provide a change in phase of RF signal with negligible attenuation. Depending on the nature of the insertion phase (i.e., whether switchable continuously or in discrete steps), phase shifters are further classified into analog and digital. Analog phase shifter generates continuous phase difference corresponding to continuous variation of control signal, whereas digital phase shifter separates phase into predetermined states that are changed by digitally controlling each bit. Also they are categorized as balanced and unbalanced type or single ended. Balanced structures have symmetrical configuration and they provide better immunity to electromagnetic interference. Fig. 2(a) shows one element of balanced phased array system. For balanced antenna and balanced RFIC, single ended phase shifter needs two baluns to transform signal from balanced to single ended and vice versa. However in fig. 2(b) balanced phase shifter connects balanced antenna and balanced RFIC directly and reduce circuit size and complexity [1].

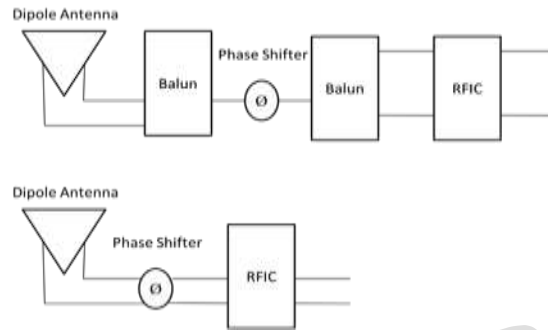


Fig. 2 (a) Single ended phase shifter, (b) Balanced phase shifter

LITERATURE SURVEY

In electronic warfare and active phased array radar systems they are used in transmit/receive module to adjust phase and hence they should be fabricated in MMIC (Monolithic Microwave Integrated Circuit) technology that achieves small size, light weight, low cost and low power consumption. To use phase shifters in electronic warfare they must operate in ultra wide bandwidth. Insertion loss, operating bandwidth and constant phase shift within the bandwidth are major concern in design of phase shifters [4].

Phase shifters are key elements in beam steering systems such as phase array antennas. Here multiple antennas are used and delay is added to signal of each antenna. It also utilizes beam forming technique which transmits the signal in specific direction that reduce power dissipated from transmitter [5].

Traditionally phase shifters are fabricated using III-V technologies like GaAs. Design of phase shifters with low cost light weight and low power consumption is of prime importance hence, HEMT technology is used. The high mobility of electrons and high quality factor of passives in these technologies achieves low insertion loss. Silicon substrates reduce their implementation costs significantly. In the 4-bit balanced active phase shifter is implemented by the vector sum method. However, the active components are unilateral, which makes it difficult to use as a reciprocal circuit in transmit /receive (T/R) module [3].

DESIGN

45° Balanced Digital Phase shifter:

45° loaded line phase shifter is as shown in fig 3. By controlling the input signal to be differential or common mode, $\lambda/8$ transmission lines can be either short circuited stub as shown in fig. 3(a) or open circuited stubs in fig. 3(b). A loaded transmission line and its equivalent circuit are shown in fig. 7. Transmission line of electrical length θ_i and impedance Z_i with two switchable susceptances B_1 and B_2 in fig. 4 represents ABCD matrix as

$$\begin{bmatrix} A & B \\ C & D \end{bmatrix} = \begin{bmatrix} 1 & 0 \\ jB_i & 1 \end{bmatrix} \begin{bmatrix} \cos\theta_i & jZ_i \sin\theta_i \\ jY_i \sin\theta_i & \cos\theta_i \end{bmatrix} \begin{bmatrix} 1 & 0 \\ jB_i & 1 \end{bmatrix} \quad (1)$$

$$= \begin{bmatrix} (\cos\theta_i - B_i Z_i) \cos\theta_i & j(Z_i \sin\theta_i) \\ j(2B_i \cos\theta_i + Y_i \sin\theta_i - B_i^2 Z_i \sin\theta_i) & (\cos\theta_i - B_i Z_i) \end{bmatrix} \quad (2)$$

where $i=1$ or 2 (switching states 0 or 1).

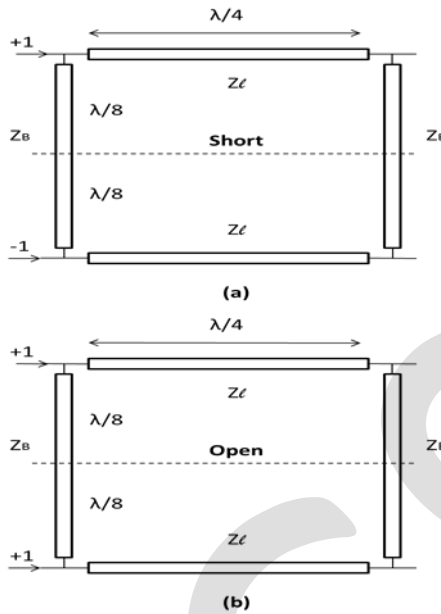


Fig. 3 45° balanced digital loaded-line phase shifter
(a) Odd mode (b) Even mode

ABCD matrix of transmission line of electrical length θ_{ei} and impedance Z_{ei} ,

$$\sqrt{Y_{ei}} = Y_{\ell} [1 - (B_i Z_{\ell})^2 + 2B_i Z_{\ell} \cot \theta_{\ell}] \quad (3)$$

$$\cos \theta_{ei} = \cos \theta_{\ell} - B_i Z_{\ell} \sin \theta_{\ell} \quad (4)$$

In our case $B_1 = Z_B$ (S.C.), $B_2 = -Z_B$ (O.C.), $\theta_{\ell} = 90^\circ$,

Phase difference $\Delta\theta$ of two states is obtained as

$$\theta_{e1} = \cos^{-1}(-Z_B \cdot Z_{\ell}) \quad (5)$$

$$\theta_{e2} = \cos^{-1}(Z_B \cdot Z_{\ell}) \quad (6)$$

$$\Delta\theta = \theta_{e2} - \theta_{e1} \quad (7)$$

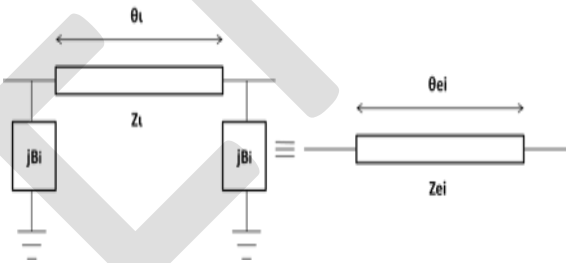


Fig. 4 Loaded transmission line connected with two Susceptance and its equivalent transmission line

Calculated values of 45° balanced digital phase shifter is given in table I.

TABLE I
CALCULATED VALUES OF 45° BALANCED DIGITAL PHASE SHIFTER

θ_{ℓ}	Z_{ℓ}	$ B_i $	θ_{stub}	Z_{stub}
90°	45.9Ω	8.5×10^{-3}	45°	117.6Ω

90° Balanced Digital Phase Shifter :

To realize 90° phase shifter with broader bandwidth, loaded line phase shifter with three shunt susceptance can be used. 90 phase shifter is shown in fig. 6. Following same procedure of 45 phase shifter design equations will be

$$B^2 = \frac{2B^1}{(B^1 Z_{\ell})^2 + 1} \quad (8)$$

$$\theta e_i = 180^\circ + \tan^{-1} \left(\frac{2B^1 Z_o}{1-(B^1 Z_o)^2} \right) \quad (9)$$

where $i=1$ or 2 , is insertion phase of one of two states. Since $B1$ in equation (9) only changes sign while changing state, phase difference of even and odd mode should be,

$$\Delta\theta = (\theta e_2 - \theta e_1) = 2 \tan^{-1} \left(\frac{2|B_1 Z_o|}{1-(B_1 Z_o)^2} \right) \quad (10)$$

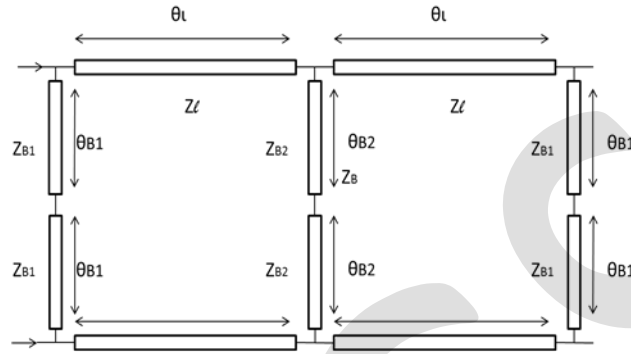


Fig. 5 90° balanced digital phase shifter

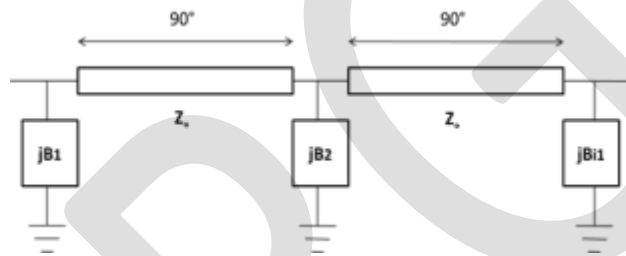


Fig. 6 3 Element loaded- line phase shifter

Calculated values of 90° balanced digital phase shifter is shown in table II.

TABLE II
 CALCULATED VALUES OF 90° BALANCED DIGITAL PHASE SHIFTER

θ_l	Z_o	θ_{stub1}	Z_{stub1}	θ_{stub2}	Z_{stub2}
90°	50Ω	45°	120.7Ω	45°	71Ω

IMPLEMENTATION

45° and 90° phase shifters are implemented using Agilent's ADS (Advanced Design System) EM simulation software. Circuit is first implemented in schematic and after fine tuning in circuit simulator it is simulated in EM simulator. These balanced digital phase shifters are implemented using microstrip lines with Rogers RO4003 substrate of thickness 0.508mm and dielectric constant of 3.58.

Design and results of 45° phase shifter:

Fig. 7 shows schematic of 45° phase shifter with physical dimension to be used in design using microstrip. Layout design from schematic is shown in fig. 8.

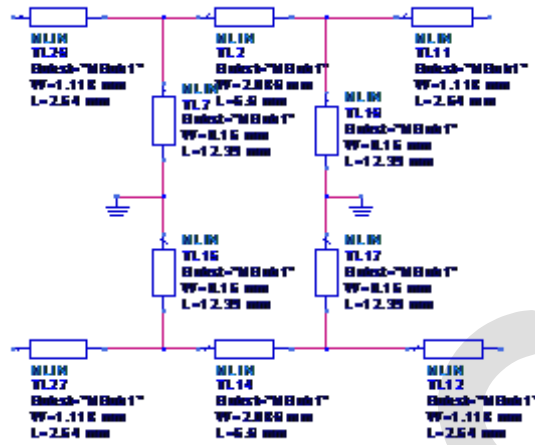


Fig. 7 Schematic of 45° phase shifter

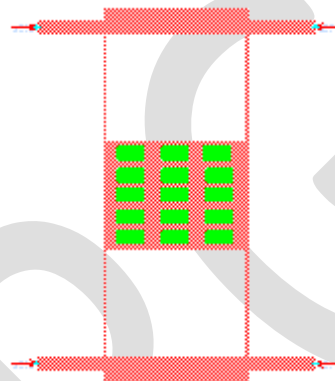
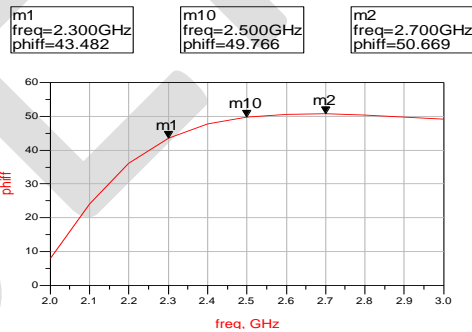
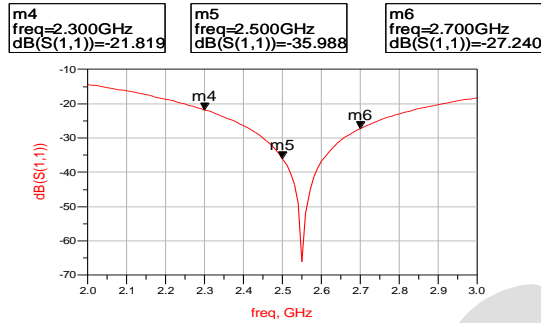


Fig. 8 Layout and results of 45° phase shifter

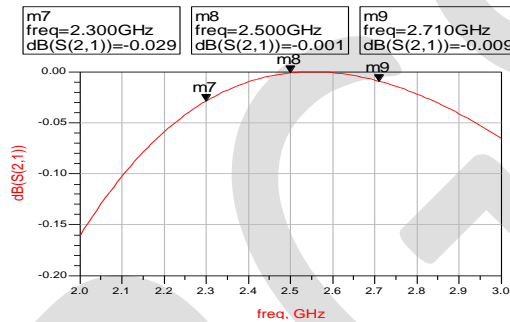
Simulated results of designed circuit for the range from 2.3- 2.7GHz from fig. 9 shows desired phase shift, insertion loss and return loss. Insertion loss is approximately 0.01 to 0.03dB.



(a)



(b)



(c)

Fig. 9 Results of 45° Phase shifter (a) Phase-shift (b) Return loss (c) Insertion loss

Design and results of 45° phase shifter:

Schematic and dimensions for 90 ° phase shifter are depicted in fig.10 while layout is shown in fig. 11. Simulated results including phase shift insertion loss and return loss are shown in fig.12. Insertion loss is around 1.8dB.



Fig. 10 Schematic of 90° phase shifter

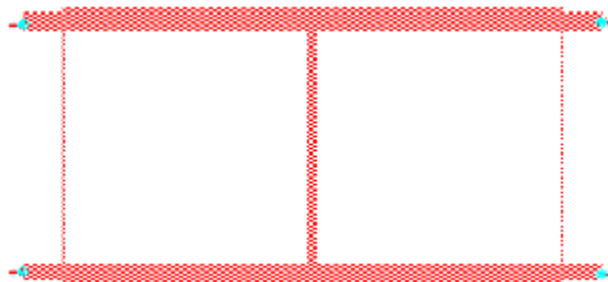
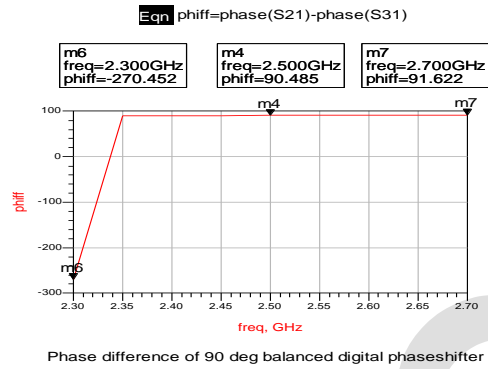
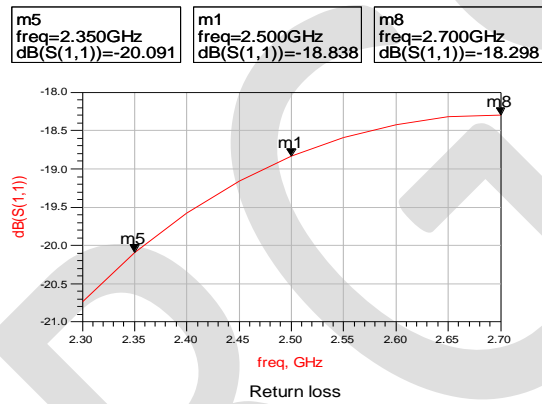


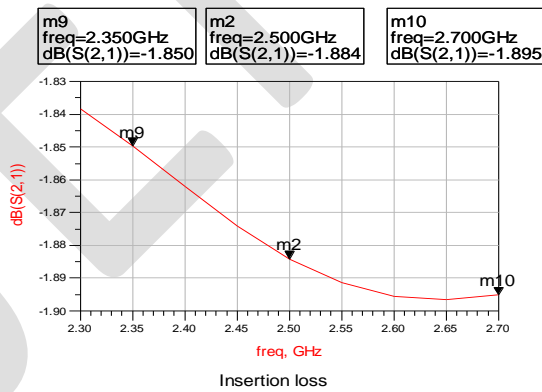
Fig. 11 Layout and results of 45° phase shifter



(a)



(b)



(c)

Fig. 12 Results of 90° Phase shifter (a) Phase-shift
 (b) Return loss (c) Insertion loss

From results we got -2 to 5.67 phase error for 45 phase shifter and 0.48 to 1.6 phase error for 90 phase shifter.

APPLICATIONS

- Phase Modulators
- Frequency Up-converters
- Phase Array Antenna Systems
- Mobile Communication systems

- Direct receiving in Digital Satellite Systems(DSS)
- Satellite modems and modems in WLAN network
- Digital Phased Locked Loop

ACKNOWLEDGMENT

I acknowledge S M Wireless Solution, Pune (sister concern of RFIC solutions USA) for providing Agilent's ADS (Advanced Design System) simulation platform. Even I am thankful to Prof. Dr. Udaysingh Sutar (Head of Department AISSMSCOE, Pune) for providing resources for the project work.

CONCLUSION

45° and 90° balanced digital phase shifters have been proposed in the paper. Both these balanced phase shifters are loaded by $\lambda/8$ open and short circuited stubs. Using both circuits and some control and switching circuitry different phase shifts can be achieved. Circuit has less phase error around -2° to 5.67° for 45° phase shifter and 0.48° to 1.6° for 90° phase shifter.

REFERENCES

- [1] Yun-Wei Lin, Yi- Chieh Chou, and Chi- Yang Chang, "A Balanced Digital Phase Shifter by Novel Switching-mode Topology," IEEE Transactions on Microwave Theory and Techniques, vol.61, no. 6, June 2013.
- [2] Puneet Anand, Sonia Sharma, Deepak Sood, C. C. Tripathi, "Design of Compact Reconfigurable Switched Line Microstrip Phase Shifters for Phased Array Antenna," 1st International Conference on Emerging Technology Trends in Electronics, Communication and Networking, 2012.
- [3] Seyedreza Hadian Ameri, Amir Pourhossien, "A 6-bit Digital Phase Shifter by using HEMT Technology," IEEE 8th International Colloquium on Signal Processing and its Applications, 2012.
- [4] Yong-Sheng Dai, "A novel miniature 122 GHz 90° MMIC Phase Shifter with Microstrip Radial Stubs," IEEE Microwave and Wireless Components, vol. 18, no.2, February 2011.
- [5] Y.Wang, M. E. Bialkowski, and A. M. Abbosh, "Double Microstrip-Slot Transitions for Broadband $\pm 90^\circ$ Microstrip Phase Shifters," IEEE Microwave and Wireless Components Letters, vol. 22, no. 2, February 2012.
- [6] Jun Zhang, S.W. Cheung and Qi Zhu, "Design of 180° Switched-line Phase Shifter with Constant Phase Shift Using CRLH TL," IEEE Antennas and Propagation Society International Symposium (APSURSI), 2014.
- [7] Jun Zhang, "Design of High Power Capacity Phase Shifter with Composite Right/Left-Handed Transmission Line," IEEE Transactions on microwave theory and techniques microwave and optical technology letter, Vol.54, No. 1, Jan 2012.
- [8] S. H. Yeung, Q.Xue, and K. F. Man, "Broadband 90° Differential Phase Shifter constructed using a pair of Multisection Radial line Stubs," IEEE Trans. Microwave Theory Techniques, vol. 60, no. 9, pp. 2760–2767, Sep. 2012.
- [9] X. Tang and K. Mouthaan, "Phase-shifter Design using Phase-slope Alignment with Grounded Shunt Stubs," IEEE Trans. Microwave Theory Techniques., vol. 58, no. 6, pp. 1573–1583, Jun. 2010.
- [10] J. C. Lu, C. C. Lin, and C. Y. Chang, "Exact Synthesis and Implementation of New High-order Wideband Marchand baluns," IEEE Transactions Microwave Theory Techniques, vol. 59, no. 1, pp. 80–86, Jan. 2011.
- [11] Shib Shankar Singh, "Design and Realization of S-band GaAs MMIC Two Bit Phase Shifter for Phase Array Radar Antenna Applications," IEEE Proceedings of International Conference on Microwave, 2008.
- [12] S. H. Yeung, Q.Xue, and K. F. Man, "Broadband 90° Differential Phase Shifter constructed using a pair of Multi-section Radial Line Stubs," IEEE Transactions Microwave Techniques, vol. 60, no. 9, pp. 2760-2767, Sept. 2012.

De-noising Techniques for Biomedical Images

Siddhartha Avhad, Prof.R.A.Patil

VJTI, Mumbai, avhadsiddhartha@gmail.com

Abstract—In Medical imaging system, biomedical images reveal internal structures hidden inside human body. It is also used for diagnosis of diseases. Database of such images used for research work. These images may get corrupted by noise during acquisition and transmission due to patient movement, inaccurate instrumental setup, surrounding noise, etc. These noisy effects decrease the performance of visual and computerized analysis. As biomedical images contain many important details, such noises are unwanted and hence to be removed while processing. Many approaches have been proposed to remove such noises. Mainly two approaches are used for de-noising of biomedical images: filter based and second is Wavelet based. This paper surveys these techniques and provides comparative analysis depending on different parameters. Filter based techniques are conventional like averaging filter, median filter, Wiener filter, adaptive filter, etc. while Wavelet-based technique is an advanced technique used in de-noising of biomedical images.

Keywords—Image de-noising, Median filter, Wiener filter, Wavelet Thresholding, PSNR, Discrete Wavelet Transform, Hard Thresholding, Soft thresholding

I. INTRODUCTION

An image plays an important role in the area of research and technology like Bio-medical images in Medical imaging system. But during Acquisition, Processing and Transmission, an image will inevitably be mixed with a certain amount of noise which deteriorates the quality [7]. In the diverse fields, scientists are faced with the problem of recovering original images from such noisy images. So, it is necessary to deal with image noise in order to deal with a high level processing which required in bio-medical applications like PET scan, CT scan, MRI scan, etc. The removing of noise from any affected image is called as de-noising which remove the noise and retain the important image features as much as possible [12]. According to actual image characteristic, noise statistical property and frequency spectrum distribution rule, Researchers have developed many methods of eliminating noises. Traditionally, we can find many noise reduction methods, many of them are in spatial or frequency domain by filtering. Spatial Low-pass filters smooth away noise but also blur edges in images while the high-pass filters can make edges even sharper and improve the spatial resolution but also amplify the noisy background [2]. In the recent years there has been a fair amount of research on wavelet thresholding and threshold selection for image de-noising. Wavelet analysis is a time-frequency analysis method used on the concept of wavelet transform with good time-frequency localization, so it has been widely applied in the field of image de-noising [8]. There are different wavelet thresholding approaches out of which hard and soft thresholding are well-known. This paper makes comparative study between such thresholding techniques and different several standard filters that are largely used for noise suppression.

II. TYPES OF NOISE

Noise produces undesirable effects such as unseen lines, corners, blurred objects and disturbs background scenes etc. There are the four types of noise categories in an image: 1. Gaussian noise; 2. Salt and pepper noise; 3. Poisson noise; 4. Speckle noise [1].

1. Gaussian noise : Gaussian noise is also called as electronic noise as it arises in amplifiers or detectors. This noise is additive in nature which is caused by thermal noise. Gaussian noise is independent at each pixel and signal intensity. Gaussian noise equally affects each and every pixel of an image [5].

2. Salt and pepper noise: It is also called as impulsive noise generated during data transmission. Image pixel values are replaced by corrupted pixel values either maximum 'or' minimum pixel value. The maximum or minimum values are dependent upon the number of bits used. Here, corresponding value for black pixels is 0 while for white pixels it is 1. The salt and pepper noise is generally caused by faulty of pixel elements in the camera sensors, faulty memory locations, or timing errors in the digitization process[5].

3. Poisson Noise: It is also called as quantum (photon) noise or shot noise. The poisson noise is appeared due to the statistical nature of electromagnetic waves such as x-rays, visible lights and gamma rays.

4. Speckle noise: Speckle is a granular 'noise' that inherently exists in and degrades the quality of the medical ultrasound and optical coherence tomography images. Speckle noise results from the patterns of constructive and destructive interference shown as bright and dark dots in the image

III. DE-NOISING TECHNIQUES

Different types of Filtering techniques and Wavelet thresholding techniques are used for image de-noising. Wavelet transform has been used as a good image representation and analysis tool mainly due to multi-resolution analysis, data separability, compaction and sparsity features in addition to statistical properties. Image de-noising based on the wavelet transform is mainly completed by wavelet thresholding in wavelet domain. There are two types of wavelet thresholding: 1. Soft thresholding 2. Hard thresholding.

A. FILTER BASED IMAGE DE-NOISING

- **Median Filter:** The median filter is a nonlinear digital filtering technique, used to remove noise in image. Median filtering is very widely used in digital image processing because; it preserves edges while removing noise able to remove noise. Hence, there is no reduction in the sharpness of the image. But when noise density exceeds 50% in an image, the edge details of the original image cannot be preserved by standard median filter. Comparatively, its performance is not that much better than Gaussian blur for high levels of noise, whereas, for speckle noise and salt and pepper noise (impulsive noise), it is particularly effective.

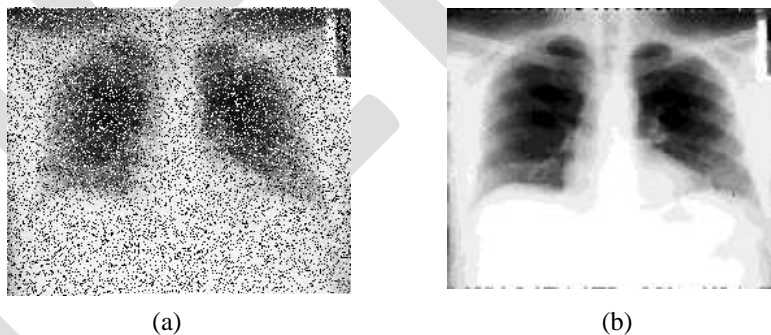


Figure 1: a) Biomedical Image with Salt and pepper noise b) Median filtered image

- **Wiener Filter:** Wiener filter is a linear filter. It is used to deblur an image. It preserves the edges and other frequency parts of an image. It uses pixel wise adaption; hence this technique is also called as adaptive filtering technique [5]. It minimizes the mean square error (MSE) between the estimated random process and the desired process. Wiener deconvolution can be useful when the point-spread function (PSF) and noise level are known or can be estimated.
- **Gaussian Filter:** It is a low pass filter whose impulse response is a Gaussian function. Gaussian filters have the properties of having no overshoot to a step function input while minimizing the rise and fall time. It filters the input signal using a Gaussian FIR filter. It smoothes the image in order to remove the noise in prior to apply canny edge detection algorithm.

B. WAVELET BASED IMAGE DE-NOISING

The simpler way to remove noise or to reconstruct the original image using the wavelet coefficients used the result of decomposition in wavelet transform, is to eliminate the small coefficient associated to the noise[1].

Wavelet threshold de-noising has three steps as follows:

- 1) An image is decomposed into multi-scale wavelet transform.
- 2) Setting a certain threshold, thus the wavelet coefficients are processed to remove noise as much as possible, eliminate the smaller wavelet coefficient, and larger wavelet coefficients retained.
- 3) Taking inverse wavelet transform.

There are two methods of processing of wavelet coefficients has hard threshold and soft threshold.

i. Soft Threshold: Soft threshold is the absolute value of the signal compared with the threshold value, if the absolute value is greater than the threshold becomes the product, the sign function of the absolute value multiplied with the difference of the threshold and the absolute value i.e. Soft threshold shrinks coefficients above the threshold in absolute value. The false structures in hard thresholding can overcome by soft thresholding[1].

$$\hat{W}_{j,k} = \begin{cases} \text{sgn}(W_{j,k}) (|W_{j,k}| - \lambda) & \text{if } |W_{j,k}| \geq \lambda \\ 0 & \text{otherwise} \end{cases} \dots\dots\dots(1)$$

ii. Hard Threshold: Hard threshold is a “keep or kill” procedure. Hard threshold is the absolute value of the signal compared with the threshold. It is less than or equal to the threshold point becomes zero, and the point is greater than the threshold unchanged [8].

$$\dots\dots\dots(2) \quad \hat{W}_{j,k} = \begin{cases} W_{j,k} & \text{if } |W_{j,k}| \geq \lambda \\ 0 & \text{otherwise} \end{cases}$$

The Bayes Shrink method is one of the wavelet based approach to remove noise from biomedical image. It has been attracting attention recently as an algorithm for setting different thresholds for every sub band. Bayes Shrink uses soft thresholding. The purpose of this method is to estimate a threshold value that minimizes the Bayesian risk assuming Generalized Gaussian Distribution (GGD) prior [13].

$$t_B = \sigma^2 / \sigma_S \dots\dots\dots(3)$$

Where σ^2 is the noise variance and σ_S is signal variance without noise.

From the definition of additive noise we have,

$$w(x, y) = s(x, y) + n(x, y) \dots\dots\dots(4)$$

Since the noise and the signal are independent of each other, it can be stated that,

$$\sigma_w^2 = \sigma_S^2 + \sigma^2 \dots\dots\dots(5)$$

σ_w^2 can be computed as shown below:

$$\sigma_w^2 = \frac{1}{n^2} \sum_{x,y=1}^n w^2(x, y) \dots\dots\dots(6)$$

The variance of the signal, σ_S^2 is computed as,

$$\sigma_S = \sqrt{\max(\sigma_w^2 - \sigma^2, 0)} \dots\dots\dots(7)$$

$$PSNR = 10 \log_{10} \left(\frac{255^2}{MSE} \right) \text{ db} \quad \dots\dots\dots(8)$$

$$MSE = \frac{1}{MN} \sum_{i=1}^M (x, y) \sum_{j=1}^N (X(i, j) - P(i, j))^2 \quad \dots\dots\dots(9)$$

V. COMPARISON OF WAVELET THRESHOLDING & FILTER BASED DENOISING TECHNIQUES:

PSNR (PEAK SIGNAL TO NOISE RATIO)				
NOISE	NOISE VARIANCE	MEAN FILTER	MEDIAN FILTER	BAYES SHRINK
GAUSSIAN NOISE	0.001	24.0598	25.4934	33.7031
	0.002	23.2251	24.3480	29.9001
	0.003	22.5261	23.4147	27.7650
	0.004	21.9796	22.6049	26.0865
	0.005	21.4536	22.0205	25.1235
	0.01	19.5569	19.7703	22.0446
SPECKLE NOISE	0.001	24.8274	26.6157	44.0220
	0.002	24.5114	26.1260	40.0535
	0.003	24.2207	25.6708	38.3935
	0.004	23.9316	25.2771	35.6827
	0.005	23.7015	24.8599	34.3460
	0.01	22.6357	23.4053	30.9207

Table 1: Comparison of Filtering and Wavelet based approaches based on PSNR values [13]

VI. CONCLUSION

This paper surveys different techniques of image denoising based on filter based and Wavelet based approach. Each method has its merits and demerits based on different parameters like PSNR, MSE, etc. After comparing these methods as shown in table 1, it is observed that Bayes shrink method is more suitable for biomedical image denoising as it has better PSNR values for particular noise variance than other filter based methods. But it is more complex than filter based approach. Hence, to achieve good performance, it is necessary to combine Bayes shrink approach and Filter based techniques.

VII. REFERENCES

- [1] Ayushi Jaiswal, Jayprakash Upadhyay, Ajay Somkuwar, 'Image de-noising and quality measurements by using Filtering and wavelet based techniques', International Journal of Electronics and Communications (Elsevier), pp.699-705, 2014.
- [2] Fei Xiao, Yungang Zhang, 'A Comparative study on Thresholding Methods in Wavelet-based Image de-noising', Advanced in Control Engineering and Information science (Elsevier), pp.3998-4003, 2011.
- [3] G. Andria, F. Attrivissimo, G. Cavone, N. Giaquinto, 'Linear filtering of 2-D wavelet coefficients for denoising Ultrasound medical images', Measurement (Elsevier), pp.1792-1800, 2012.
- [4] Sachin D Ruikar, Dharmal D Doye, 'Wavelet-based Image de-noising Technique', International Journal of Advanced Computer Science and Applications (IJACSA), Vol. 2, No.3, pp.49-53, March 2011.
- [5] Kalpana, Harjinder Singh, 'Review paper: to study the Image De-noising techniques', International Research Journal of Engineering and Technology (IRJET), Vol. 2, No.8, pp.127-129, Nov. 2015.
- [6] Dipalee Gupta, Siddhartha Choubey, 'Discrete Wavelet Transform for Image Processing', International Journal of Emerging Technology and Advanced Engineering (IJETA), Vol. 4, No.3, pp.598-602, March 2015.
- [7] Hong-qiao Li, Sheng-qian Wang, Cheng-zhi Deng, 'New Image De-noising Method Based Wavelet and Curvelet Transform', IEEE International Conference on Information Engineering, pp.136-139, 2009.
- [8] Shunyong Zhou, Xingzhong Xiong, Wenling Xie, 'A Modified Image De-noising Algorithm by Labeling and 3D Wavelet Transform', IEEE International Conference on Computer Application and System Modeling (ICCASM), pp.44-47, 2010.
- [9] M. Nikpour, H. Hassanpour, 'Using diffusion equations for improving performance of wavelet-based image denoising techniques', IET Image Processing, Vol. 4, Issue 6, pp. 452-462, 2010.
- [10] Jing Tiano and Li Chen, 'Adaptive Image de-noising using a Non-Parametric Statistical Model Of Wavelet Coefficients', IEEE International Symposium on Intelligent Signal Processing and Communication Systems (ISPACS), Dec. 2010.
- [11] B. Dhiyanesh, K. S. Sathiyapriya, 'Image Inpainting and Image Denoising in Wavelet Domain Using Fast Curve Evolution Algorithm', IEEE International conference on Advanced Communication Control and Computing Technologies (ICACCCT), Dec. 2010.
- [12] Hedao P, Swati S. Godbole: 'Wavelet thresholding approach for image denoising', IJNSA Vol.3, issue 4, pp.16-21, 2011.
- [13] Anutam and Rajni, 'Comparative analysis of filters and wavelet based Thresholding methods for image denoising', CSCP, pp.137-148, 2014.

Smart Utilization of Urban and Rural Land

Ghuge Pravin V., Shirsat kedar, Patil Gaurao S., Dahe Akshay N.,
(Student, Department of Civil Engineering, Imperial college of Engineering, Pune, India)

pravinghuge2@gmail.com

onlykts@gmail.com

gaurav.ptl@gmail.com

daheakshay@gmail.com

Abstract – Land is the most important component of the life support system. It is the most important natural resource which embodies soil and water, and associated flora and fauna involving the ecosystem on which all man's activities are based. Land is a finite resource. Land availability is only about 20% of the earth's surface. Land is crucial for all developmental activities, for natural resources, ecosystem services and for agriculture. Growing population, growing needs and demands for economic development, clean water, food and other products from natural resources, as well as degradation of land and negative environmental impacts are posing increasing pressures to the land resources in many countries of the world. For India, though the seventh largest country in the world, land resource management is becoming very important. India has over 17% of world's population living on 2.4% of the world's geographical area. After independence the population of our country increase's day by day. Due to that the problems like shortage of basic amenities, shortage of lands, and increase in the population rate are occurred. Due to increase in the population rate the price of lands are increases day by day. To overcome such problem the proper smart utilization of land is necessary.

In this report the smart utilization of land is done with respect to proper land zoning, create and maintain the basic infrastructure, transportation, rural community development, plantation, landscaping & wasteland reclamation, smart waste management and smart services.

Keywords — Smart utilization of urban & rural land, proper land zoning, create & maintain basic infrastructure, non-agriculture permission, rural community development, transportation, plantation, landscaping & wasteland reclamation, smart waste management, smart services.

INTRODUCTION:

In India large amount of land is used for dumping the waste. If proper techniques like source reduction, recycling, proper disposal of waste are used, we can reduce the wastage of land for such purpose. For smart utilization of land proper land zoning is the major consideration is to be considered. The land zoning is classified as Residential zone, Commercial zone, Industrial zone, Institutional /Public/Semipublic zone, Transportation & Recreation zone.

Non-agriculture used of land is plays an important role in smart land utilization. During post independence period & especially during last ten years industrialization is taking place in India particularly in Maharashtra on very wider scale. New cities & towns are coming into existence so also the then small existing towns & cities have now developed into Great metropolitan cities. Million & millions of people are migrating from other distance states in Maharashtra in search of jobs and means of livelihood & getting themselves permanently settled. Consequently the non-agricultural use of agricultural lands is increase beyond limitations. There is constant continuous increase in the constructions of the residential houses, industries & commercial complexes. Multi story projected buildings in large numbers in almost all cities, towns, metropolitan cities & various industrial estates including various Maharashtra Industrial Development Industries (M.I.D.Cs).

Smart utilization of land plays an important role in rural community development, agriculture & food production. Traffic issue is the major problem in our country now days. If the proper transportation system is provided by using smart land utilization we can defiantly overcome from this problem.

Plantation & landscaping is also plays an important role in smart utilization of land. Loss of vegetation cover leads to loss of soil erosion, which ultimately creates wasteland. This is one of the pressing problems of our country as loss of soil has already ruined large amounts of cultivable lands. If it remains unchecked, it will affect the remaining lands. That's why the wasteland reclamation is important.

By considering all above parameters we can do the smart utilization of urban & rural land which is beneficial to the overall development of our country.

LITERATURE REVIEW:

- I. R.K. Lallianthanga, Robert Lachhanhima Sailo (2013)
 1. It is imperative to develop land use plans which can counteract the detrimental effects on environment, and at the same time improve productivity of land.
 2. Indian Remote Sensing satellite data (LISS-III and Cartosat-I) had been used for generating various thematic layers like land use, slope, soil, drainage, etc.
 3. The analysis in a GIS system helped in bringing out maps and statistics with constructive options for alternate land use plans which are expected to be both productive and sustainable.
 4. The study incorporates standard techniques of remote sensing and geographic information system. Visual interpretation and on-screen digitization techniques were used for classifying and delineating the various land use / land cover classes from the satellite data.
- II. William A. Fischel
 1. Zoning allows municipalities to shape their residential environments and their property-tax base.
 2. Voters in most communities will accept developments that raise the value of their major personal asset, their homes.
 3. The efficiency of zoning thus depends on the transaction costs of making mutually advantageous trades between existing voters and development-minded landowners.
 4. High transactions costs of selling zoning plus the endowment effect that zoning confers probably create land-use patterns with excessively low densities in American metropolitan.

PROBLEM STATEMENTS AND OBJECTIVE:

Day by day the value of land is increasing. There will be need of proper land utilization. We are trying to do smart utilization of land with respect to the proper zoning, proper establishment of infrastructure with proper land use, smart waste management, plantation & landscaping etc. is necessary. We take a problem statement on a small village named as Malegaon (Najik Kinhi) Tal. Malegaon Dist. Washim. We try to doing the smart utilization of land with considering above all parameters So that in future there will be no shortage of all the requirements for the people and it will helpful to become India Smart country in the world.

OBJECTIVES:

1. Reduce the wastage of land by providing smart waste management.
2. Create a proper utilization of land with help of proper zoning.
3. To create & maintain basic infrastructure.
4. Oxygen control with the help of plantation & landscaping.
5. Increase the efficiency of land by using smart techniques like ground water recharge, rain water harvesting, biogas & vermiculture.
6. Smart utilization of land by forming echo-chain

METHODOLOGY:

1. The methodology adopting is a mix of literature survey.
2. By taking studies of MRTP ACT, Development Plan, Non-Agriculture permission procedure, Land Acquisition Act regarding land utilization policy
3. Conducting the survey of the villages & find out the present issue.
4. Design an eco chain STP, WTP, & Biogas plant for improve efficiency of land.

DATA COLLECTION AND ANALYSIS:

The area of village 1519.1 Ha. The village is located at Malegaon Taluka in Washim District. The village is under development. Following data is collected from village for the analysis:

1. Zoning of the land is not done properly.
2. There is no proper transportation system available in village.
3. The roads are not properly constructed.
4. There is lot of illegal construction is done in the village.
5. The ground water table is very low.
6. There is one big lake but the proper utilization of this lake is not done.

7. There is no proper drainage system, lack of basic amenities etc.

The following table shows the basic information regarding this village:

Sr. No.	Location	Malegaon(N.K.),Tal.Malegaon Dist.-Washim, Maharashtra
1	Area In Hector	1519.1Ha
2	Number of Household	264
3	Population	1109
4	Male	559
5	Female	550
6	Number of Catalas	1590
7	Population Under Age 0.6	136
8	Population Under Age Male 0.6 Male	65
9	Population Under Age 0-6 Female	71

Firstly we carried out the survey of the village. Then we found out above issues regarding land utilization. After that we create a proper land zoning with the help of MRTP Act.1966. Providing residential zone, industrial zone, commercial zone, recreational zone, farming zone etc. We also provide educational facilities, temples, proper transportation facilities, parking, gardens etc. We have design the W.T.P. & S.T.P. for 1500 people of that village. After treating of waste water, the remaining water is used for plantation which is plays an important role in oxygen control. By using biogas plant, it becomes helpful for cooking purpose and solar panels are provided for street lights.

Following Figure shows Eco chain of village for dumping of waste to reduce wastage of land:

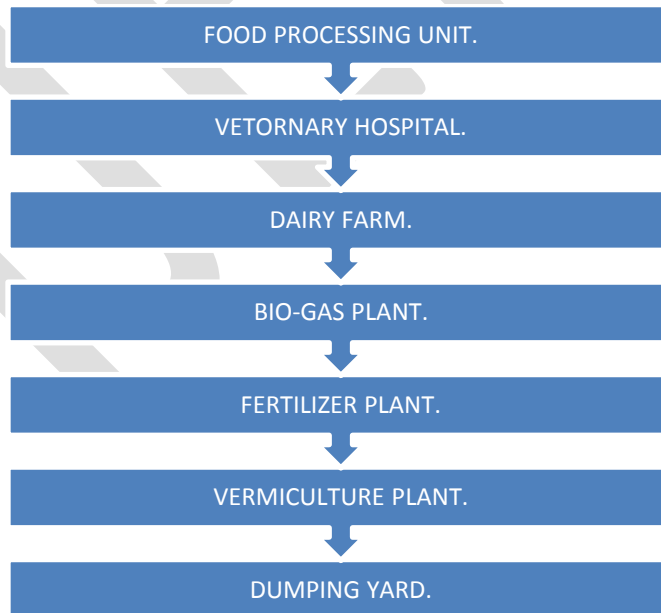


Fig. 1.Eco chain

Following are the advantages of Eco chain:

- By Formation of the chain, the land wastage for dumping of the waste is reduces & the proper land utilization is done.
- By Providing Smart services like Bio gas plant, solar energy, Rain water harvesting the rural community development is achieved.

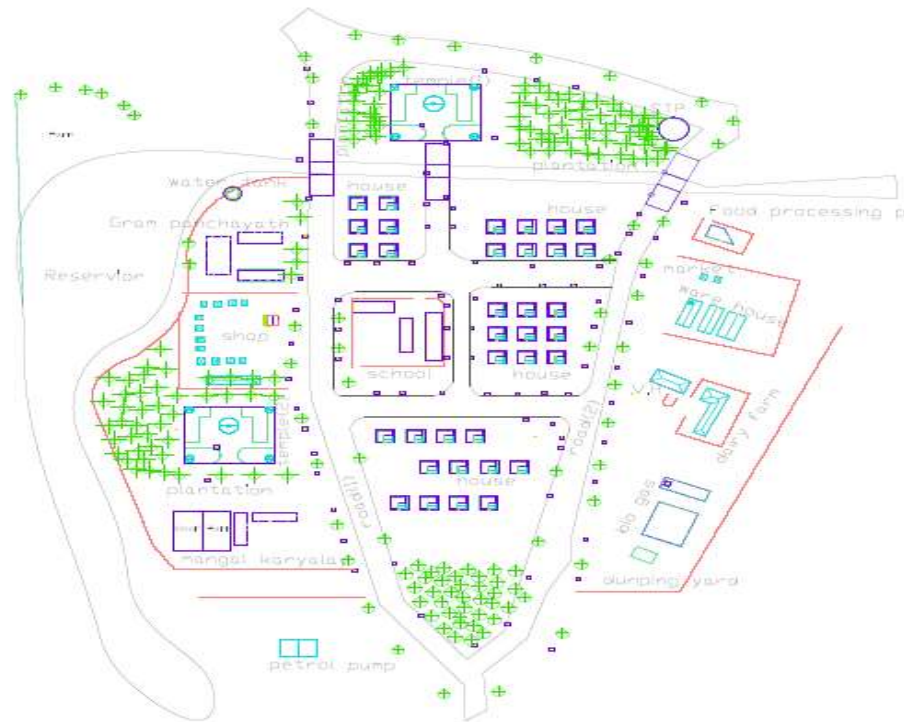


Fig. 2 Smart utilization of land at Malegaon (N.K.) village.

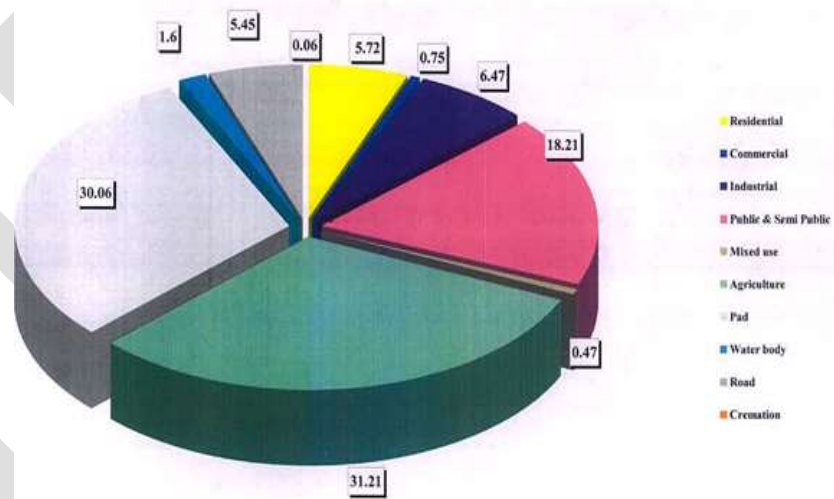


Fig.3 Land use zoning of Malegaon (N.K.) Village

CONCLUSION:

After the study of Malegaon (N. K.) Village, we can conclude that the smart utilization of land can be done with the help of proper zoning, establishing the basic infrastructure, proper land use, smart waste management, plantation & landscaping .The wastage of land can be reduced by providing proper eco-chain maintained at its proper level. With the help of smart services like Rain water harvesting, Biogas, Vermiculture, we can improve the efficiency of the land. It also useful for the rural community development. The land is a finite source so the proper utilization of the land is necessary for future development.

REFERENCES:

- [1] A. Apte, V. Cheernam, M. Kamat, S. Kamat, P. Kashikar, and H. Jeswani “Potential of Using Kitchen Waste in a Biogas Plant” , August 2013.
- [2] Momah O.L. Yusuf, Nwaogazie, L. “Effect of Waste Paper on Biogas Production from Co-digestion of Cow Dung and Water Hyacinthine Batch Reactors”, December 2008.
- [3] G. Raghuram Simi Sunny “Right to Fair Compensation and Transparency in Land Acquisition, Rehabilitation and Resettlement Ordinance”, July 2015.
- [4] Attila Meggyes and Valéria Nagy “Biogas and Energy Production by Utilization of Different Agricultural Wastes”, 2012
- [5] R.K. Lallianthanga, Robert Lalchhanhima Sailo “Land use planning for sustained utilization of resources using Remote Sensing & GIS techniques: A case study in Mamit District, Mizoram, India”, 2013.

STUDY ON SPLITTING TENSILE STRENGTH OF HYBRID LENGTH STEEL FIBER REINFORCED CONCRETE UNDER ELEVATED TEMPERATURE

Deepthy.S.Nair, Asst.Professor,civil Engg.Dept

M.G university,91deepthy@gmail.com,9496321124

Abstract— Concrete is a composite material likely exposed to high range of temperatures during its service life. The relative properties of concrete after such an exposure are of great importance in terms of the durability of buildings. The constituents of concrete have different properties and also depends on moisture and porosity. A complete understanding of the behavior of concrete under elevated temperature after a thermal excursion is essential for reliable design evaluations and assessments. The properties of concrete changes with respect to time and the environment to which it is exposed, an assessment of the effects of concrete is also important in performing safety evaluations.

Keywords— Concrete, Temperature, Split tensile strength

INTRODUCTION

Exposure of concrete to elevated temperature affects its mechanical and physical properties. Temperature affects produce dimensional changes, loss of structural integrity, release of moisture and gases resulting from the migration of free water could adversely affect plant operations and safety. Steel fibres are relatively short and closely spaced as compared with continuous reinforcing bars or wires. The study focuses on the effect of temperature on fiber reinforced concrete by incorporating two different length hooked steel fibers.

LITERATURE REVIEW

Balazs and Lubloy [1] investigated the properties of concrete may be considerably influenced by high temperatures. These properties are depends on the maximum temperature and the composition of the concrete. Water-cement ratio (W/C), type of cement, type of aggregate and porosity are also influenced by the temperature. The deterioration of concrete at high temperatures is manifested as deterioration of the material itself and the deterioration of the structural performance. *Bangi and Horiguchi* [2] investigated on effect of fibre type and geometry on maximum pore pressures in fibre-reinforced high strength concrete at elevated temperatures. Fibre type and geometry, significantly contributes towards pore pressure.

The objectives of the study are;

- Study the effect of steel fibers on compressive strength of concrete
- To predict the performance characteristics of steel fibers with different percentages (0%,0.5%,1%) on concrete with temperatures(Ambient temperature,200°C,400°C)
- To minimize the experimental procedure according to Box-Behnken Design for optimization.

MATERIALS AND METHODOLOGY

The materials selected for this experimental study includes normal natural coarse aggregate, Manufactured sand as fine aggregate, cement, superplasticizer, both end hooked steel fiber and potable drinking water. Potable clean drinking water available in the water supply system was used for casting as well as for curing of the test specimens. Hooked end Steel fibers of two different diameters 0.55mm with 35mm length and 0.75mm diameter with 60mm and aspect ratio of 63.63 and 80 were used. The manufacturer is Stewols private limited,Nagpur. The super plasticizer used was MASTER RHEOBUILD 918 a product of BASF India Pvt. Ltd, Ernakulam.

MIX-DESIGN

The mix design is carried out as per relevant Indian standard Code Specification [7]. Mix designing is carried out to arrive at the quantities required for 1 m³ of concrete and mix designation as shown in Table I.

TABLE I. QUANTITY REQUIRED FOR 1M³ MIX

W/C	Proportion of Steel Fiber	Water (Kg)	Cement (Kg)	F_a (Kg)	C_a (Kg)	Steel Fiber (Kg)
0.35	0	160	460	660	1240	0
	0.5	159	457	656	1233	39
	1	158	455	653	1237	78
0.4	0	160	400	700	1260	0
	0.5	159	398	696	1253	39
	1	158	396	693	124	78
0.45	0	160	360	730	1260	0
	0.5	159	358.2	726	1253	39
	1	158	356.4	722	1247	78

MATERIALS AND METHODOLOGY

- *Box -Behnken Design*

Box– Behnken designs are experimental designs for response Surface Methodology, devised by George E.P.Box and Donald Behnken in 1960 [8]. Response Surface Methodology (RSM) is an empirical optimization technique for evaluating the relationship between experimental outputs (or responses) and factors called x₁, x₂, and x₃. Box–Behnken is a spherical, revolving design. In this study Box-Behnken design with three variable and three-level factor to reduce the numbers of experiment adopted. Three control factors, namely, water-cement ratio, steel fiber percentage, and temperature are used in this experimental work. In the present investigation 3 set of factors are involved and hence we require a 3³ set that is requiring 27 replications and a 3³ full factorial design. But according to Box–Behnken designs it can be reduced to 13 sets and the design points reside in the middle of the sides and at the corner points of a cube. Figure I. Shows the model for Box–Behnken design. The model is designed using the equation:(1)

$$y = \beta_0 + \beta_1x_1 + \beta_2x_2 + \beta_3x_3 + \beta_{11}x_1^2 + \beta_{22}x_2^2 + \beta_{33}x_3^2 + \beta_{12}x_1x_2 + \beta_{13}x_1x_3 + \beta_{23}x_2x_3 \tag{1}$$

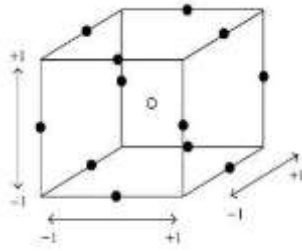


Figure I.
 Box Behnken Design For Three Factors

TEST ON FRESH PROPERTIES OF CONCRETE – SLUMP TEST

It is used to study the workability of prepared concrete during the progress of work and to check the uniformity of concrete. The details of mixes corresponds to slump are shown in Table II.

TABLE II.
 DETAILS OF MIXES CORRESPONDS TO SLUMP

Mix Designation	W/C ratio	Superplastizer (% of cement)	Slump Obtained (mm)
R0.35	0.35	0.5	66
R0.4	0.4	0.5	80
R0.45	0.45	0.5	95

HEATING OF THE SPECIMENS

The study includes the effect of temperature on the concrete. The specimens were heated in the electric oven. After attaining desired temperature, one hour is provided to the specimen to maintained in that level for reaching steady state condition. After that the oven was switched off and allow the specimen to cool off. It is observed that the mass of the specimen decreases after subjected to temperature and the loss in concrete mass is considerably less in steel fiber reinforced specimen compared to the control mix specimen.

RESULT ANALYSIS BY BOX-BEHNKEN DESIGN USING REGRESSION TECHNIQUE

Experiments were performed using the Box–Behnken experimental design. Box–Behnken experimental design is a type of response surface methodology. Response surface methodology is an empirical optimization technique for evaluating the relationship between the experimental outputs and factors called x_1 , x_2 , and x_3 . For obtaining the results for Box-Behnken design, analysis of variance has been calculated to analyze the accessibility of the model and was carried in Microsoft Office Excel 2007.

Box–Behnken Regression was done and the values were compared with the obtained value. The coefficient of determination (R^2) is defined as the ratio of the explained. variation to the total variation, and is a measure of the degree of fit. A good model fit should yield an R^2 of at least 0.8. The coefficient of determination (R^2) is defined as the ratio of the explained variation to the total variation. The test result of the experimental specimen and by using Box–Behnken design as shown in the Table. III

Table.III

BOX-BEHNKEN DESIGN
RESULTS

Designation	Temperature (°C)	Steel fiber (%)	Predicted Compressive Strength (N/mm ²)	Predicted Split Tensile Strength (N/mm ²)
R _{0.35} S ₀ T ₂₀₀	200	0	45.05	3.09
R _{0.35} S _{0.5} T ₀	27	0.5	53.01	4.87
R _{0.35} S _{0.5} T ₄₀₀	400	0.5	49.92	3.53
R _{0.35} S _{1.0} T ₂₀₀	200	1	54.60	5.29
R _{0.4} S ₀ T ₀	27	0	38.60	3.12
R _{0.4} S ₀ T ₄₀₀	400	0	34.44	2.07
R _{0.4} S _{0.5} T ₂₀₀	200	0.5	41.20	3.40
R _{0.4} S _{1.0} T ₄₀₀	400	1	44.40	4.14
R _{0.4} S _{1.0} T ₀	27	1	45.64	5.05
R _{0.45} S _{1.0} T ₂₀₀	200	1	43.74	4.30
R _{0.45} S _{0.5} T ₀	27	0.5	42.93	3.74
R _{0.45} S _{0.5} T ₄₀₀	400	0.5	40.62	3.13
R _{0.45} S ₀ T ₂₀₀	200	0	36.49	2.50

Box-Behnken design was successfully adopted and the experiments were designed choosing the input parameters for the levels selected. Response surface methodology using Box-Behnken design proved very effective and time saving model for studying the influence of process parameters on response factor by significantly reducing the number of experiments and hence facilitating the optimum conditions. The predicted values and experimental values are approximately same and hence the model is fit. The conclusions obtained from the test results are:

- The split tensile strength increases with the increase in the % of steel fibers.
- As temperature increases the strength decreases in the case of 0% steel fiber mixes.
- As in the case of 1% steel fiber the tensile strength is very much higher compared to the control mix specimen

ACKNOWLEDGMENT

I thank God, the almighty for his blessings without which nothing would have been possible. I also wish to extend my heartfelt thanks to Dr. JobThomas, Asst. Professor, Department of Civil Engineering, School of Engineering, CUSAT for his cooperation, guidance and most generous help. I extend my thanks to all the faculty members of Civil Engineering Department and to all my friends for their guidance.

REFERENCES:

- [1] Gyorgy L.Balazs, Eva Lubloy (2012) “*Post-heating strength of fiber-reinforced concretes*” fire safty journal, Vol. 49, pp 100-106.
- [2] Mugume Rodgers Bangi , Takashi Horiguchi (2012)“*Effect of fibre type and geometry on maximum pore pressures in fibre-reinforced high strength concrete at elevated temperatures,*” cement and concrete research,Vol.42, pp 157-161.
- [3] R.H. Haddad, R.J. Al-Saleh, N.M. Al-Akhras(2008) “*Effect of elevated temperature on bond between steel reinforcement and fiber reinforced concrete*”fire safty journal, Vol.36, pp 459-466.
- [4] A.Lau, M. Anson (2006) “*Effect of high temperatures on high performance steel fibre reinforced concrete*”cement and concrete research”, Vol.36, pp 1698-1707.
- [5] Gai-Fei Peng , Song-Hua Bian , Zhan-Qi Guo , Jie Zhao , Xin-Lai Peng, Yu-Chuang Jiang (2008), “*Effect of thermal shock due to rapid cooling on residual mechanical properties of fiber concrete exposed to high temperatures*” Construction and Building Materials, Vol. 22, pp 948-955.
- [6] IS 2386: 1963, *Methods of test for Aggregates for Concrete, Part I & III*, Bureau of Indian Standards, New Delhi.
- [7] IS 10262: 2009, *Guidelines for Concrete Mix Design Proportioning*, Bureau of Indian Standards, New Delhi.
- [8] Qiu et al.(2014), *Application of Box–Behnken design with response surface methodology for modelling and optimizing ultrasonic oxidation of arsenite with H₂O₂* , Central European Journal of Chemistry, vol pp164-172 Central European Journal of Chemistry, Vol 12,PP 164-172

Detecting Power Grid Synchronization Failure on Sensing Bad Voltage or Frequency Documentation

Assistant Prof. Karan Gupta, Shreyas Gupta, KummadVerma, Anil Singh, Abhimanou Sharma

Department of Electrical Engineering, GCET, Jammu, karan74_gupta@yahoo.com, 9796623311

Abstract—In modern power system, electrical energy from the generating station is delivered to the ultimate consumers through a huge network of transmission and distribution. There are several power generation units connected to the grid such as hydro, thermal, solar, wind etc to supply power to the load. Thus, for satisfactory operation of loads, it is desirable that consumers are supplied with substantially constant voltage and frequency.

In this paper we present the development of a system to detect the synchronization failure of any external supply source to the power grid on sensing the abnormalities in frequency and voltage. For feasible transmission, the frequency and voltage of the AC supply should be within the limits as decided by the grid, depending upon the demand of the power supply. As per CENTRAL ELECTRICITY AUTHORITY OF INDIA Regulations 2010, variation of the system voltage should be of $\pm 5\%$ and that for frequency close to 50 Hz and shall not allow it to go beyond the range 49.2 to 50.3 Hz or a narrower frequency band specified in the Grid Code, except during the transient period following tripping. In case these limits are exceeded and the demand for power is more than the demand for supply, it results in grid failure. In such situations, the feeder unit is completely disconnected from the grid, causing islanding situation. Thus synchronization is needed between the grid and the feeder unit, so as to prevent the large scale brown out or black out of the grid power. In this paper, we are presenting a system which can warn the grid in advance so that alternate arrangements are kept on standby to avoid complete grid failure. Methods of detecting islanding are clearly grouped into three categories as a function of their operating mode. These three categories are:

- Active methods resident in the grid tied inverter
- Passive methods resident in the grid tied inverter
- Methods not resident in the DG but communicating the DG and the utility

This paper is based on passive method to detect the synchronization failure of any external supply source to the power grid on sensing the abnormalities in frequency and voltage.

Keywords—Islanding, Grid, Voltage Variation, Frequency Variation, Active methods, Passive methods

INTRODUCTION

Energy provides the power to progress. Availability of sufficient energy and its proper use in the country can result in its people rising from subsistence level to highest standard of living. Energy exists in different forms in nature but the most important form is the electrical energy. The modern society is so much dependent upon the use of electrical energy that it has become a part and parcel of our life. Several new trends have already employed in the electricity infrastructure. It includes the expansion of the existing grid with micro grids and mega grids, extensive sensors, data processing, visualization tools, etc. Increasing electrical energy demand, modern lifestyles and energy usage patterns have made the world fully dependant on power systems thus the need of a reliable and stable power system grid. However, the power system is a highly nonlinear system, which changes its operations continuously. Therefore, it is very challenging and uneconomical to make the system be stable for all disturbances. At present, the interest toward the distributed generation systems, such as photovoltaic arrays and wind turbines, increases year after year. But wind turbines and generally DGs will have affects in the power system network that one of these influences is an islanding phenomenon. Islanding refers to the condition in which a distributed generator (DG) continues to power a location even though electrical grid power from the electric utility is no longer present. Islanding situations can damage the grid itself or equipments connected to the grid and can even compromise the security of the maintenance personnel that service the grid. According to IEEE1547 standard, islanding state should be identified and disconnected in 2 seconds. This leads to idea of Automatic detection of Grid synchronization failure concept. Thus, the main consideration in our paper is to detect islanding in a grid.

ISLANDING

Islanding is a critical and unsafe condition in which a distributed generator, such as a solar system, continues to supply power to the grid while the electric utility is down. This condition is caused due to an excessive use of distributed generators in the electrical grid. Solar power generators, wind generators, gas turbines and micro generators such as fuel cells, micro turbines, etc. are all examples of distributed generators. The fact that anyone could supply electricity back to the grid causes the problem of islanding. It is a condition in which a distributed generator like solar panel or wind turbine continues to generate power and feed the grid, even though the electricity power from the electrical utility is no longer present. Also it exposes utility workers to life critical dangers of shocks and burns, who may think that there is no power once the utility power is shut down, but the grid may still be powered due to the distributed generators.

To avoid this problem, it is recommended that all distributed generators shall be equipped with devices to prevent islanding. The act of preventing islanding from happening is also called anti-islanding. Islanding causes many problems, some of which are listed below:

- **Safety Concern:** Safety is the main concern, as the grid may still be powered in the event of a power outage due to electricity supplied by distributed generators, as explained earlier. This may confuse the utility workers and expose them to hazards such as shocks.
- **Damage to customer's appliances:** Due to islanding and distributed generation, there may be a bi-directional flow of electricity. This may cause severe damage to electrical equipment, appliances and devices. Some devices are more sensitive to voltage fluctuations than others and should always be equipped with surge protectors.
- **Inverter damage:** In the case of large solar systems, several inverters are installed with the distributed generators. Islanding could cause problems in proper functioning of the inverters.

WAYS TO DETECT AND RESOLVE ISLANDING

There are many ways to detect islanding. These are categorized as under:

- **Active islanding detection:** Active detection methods involve the technique of constantly sending a signal back and forth between the distributed generator and the grid to ensure the status of electrical supply. In active methods, small disturbances are injected into the power system and its responses due to the injected disturbances are monitored. These methods change the balancing power between loads and generations, reduce the power quality of the power systems and are not suitable for wind farms with numerous wind turbines. Reactive power export error detection method, impedance measurement method, slip mode frequency shift algorithm (SMS), active frequency drift (AFD), active frequency drift with positive feedback (AFDPF), automatic phase-shift (APS) and adaptive logic phase shift (ALPS) are a few examples of active islanding detection methods.
- **Passive islanding detection:** Passive detection methods, on the other hand, make use of transients in the electricity (such as voltage, current, frequency, etc.) for detection. Passive methods continuously monitor the system parameters such as voltage, frequency, harmonic distortion, etc. Based on the system characteristics, one or more of these parameters may vary greatly when the system is islanded. The passive methods do not affect the waveform of the high voltage. This is beneficial since it does not give rise to power quality issues such as voltage dips. Setting a proper threshold can help to differentiate between an islanding and a grid connected condition. Rate of change of output power of DG, rate of change of frequency, voltage unbalance and harmonic distortion are a few examples of passive islanding detection methods.
- **Methods not resident in the DG but communicating the DG and the utility:** Methods not resident in the DG side but implemented on the EPS side are much complicated and expensive. The most important ones can be summarized as:
 - **Introduction of impedance** – Small impedance, normally capacitive, is placed after the PCC on the EPS side. It only gets connected when the breaker DG-EPS is opened, unbalancing the local load.
 - **PLC Communication** – Uses the “Power Line Communications Carrier” technology to test if the DG is working isolated. SCADA Systems – With the help of a Supervisory Control and Data Acquisition System the EPS is checked and the potential islands detected.

The quickest and easy way to prevent any problems is to shut off the distributed generator when requested by the utility.

ARRANGEMENT FOR DETECTING POWER GRID SYNCHRONIZATION FAILURE ON SENSING BAD VOLTAGE OR FREQUENCY

The block diagram shown in fig.1. This system is based on a microcontroller of 8051 family. The microcontroller monitors the under/over voltage being derived from a set of comparators. As the frequency of the mains supply cannot be changed, the project uses a variable frequency generator (555-timer) for changing the frequency, while a standard variac is used to vary the input voltage to test the functioning of the project. A lamp load (indicating a predictable blackout, brownout) is being driven from the microcontroller in

case of voltage/frequency going out of acceptable range. Further the project can be enhanced by using power electronic devices to isolate the grid from the erring supply source by sensing cycle by cycle deviation for more sophisticated means of detection.

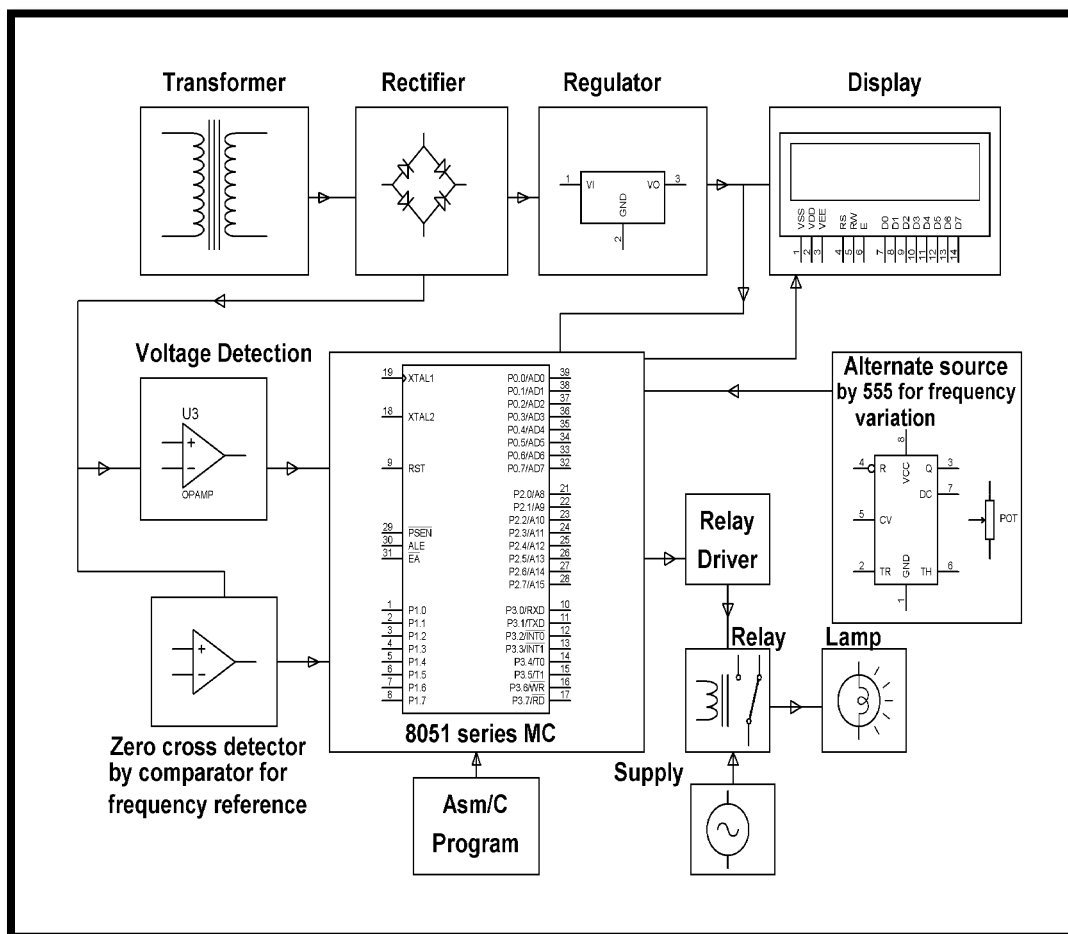


Fig.1- Block diagram

The components required are as follows: Microcontroller (At89s52/At89c51), Power Supply, 555 Timer, Lm358, Lm339, Relays, Bc547, Liquid Crystal Display, Led, In4007, Resistors, Capacitors.

VOLTAGE SENSING PART

The microcontroller is connected to the zero voltage sensing circuit to ensure the frequency of the supply is at normal frequency of 50Hz. A Voltage Regulator is used to get variable voltage. Initially both the presets are adjusted such that both the output pins of the OPAMP IC are at normal low and normal high level. At this point the lamp is glowing as the voltage is in the range. The Voltage Regulator is adjusted so as to get the input AC voltage more than the normal value. Now the normally high pin of the OPAMP IC will go low, giving an interruption pulse to the pin of the microcontroller. The microcontroller accordingly sends a high logic pulse to switch off the relay driver, which in turn de-energizes the relay driver making the lamp to turn off. Similarly when the Variable Regulator is adjusted so as to get input AC voltage less than the normal value, at some point, the normally low pin of the OPAMP IC goes high and the microcontroller on receiving this interruption, sends a high logic signal to the relay driver to switch off the relay and hence the lamp which stops glowing

FREQUENCY SENSING PART

The Voltage Regulator is adjusted such that the AC input voltage is at its normal value. The microcontroller pin is connected to the output of the 555 timer through a PNP transistor. The timer works in a stable mode to produce signals at frequencies which can be adjusted using the variable frequency. This output is connected to the internal timer of the microcontroller which accordingly calculates the frequency of the frequency, the relay driver is triggered, which in turn energizes the relay and the AC supply is given to the lamp which turns off once the frequency of the pulses goes beyond the normal frequency or less than the normal.

ACTUAL VIEW OF PROJECT

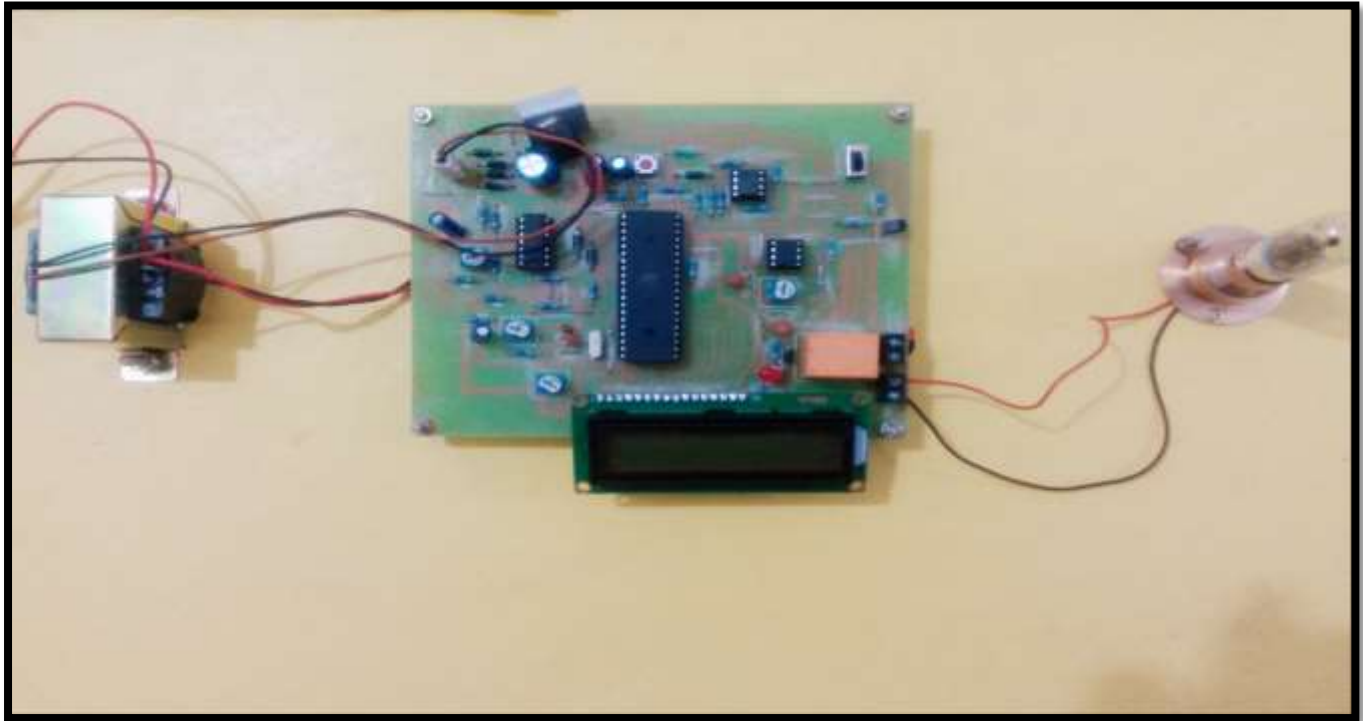


Fig.2 Actual View of Project

CONCLUSION

This paper gives brief idea about indicator which senses the abnormalities in voltage as well as in frequency so as to detect the synchronization failure of any external supply source to the power grid. This type of indicators are much needed in most crowded EHV substations where number of voltage levels, number of sources, number of power transformers and number of load lines are existing. In short it will be beneficial in case of complicated substation because at present the facility available is FTR i.e. Frequency Trip Relay and UFR i.e. Under Frequency Relay which performance function of directly disconnection of particular feeder which may cause sudden rise of voltage on system bus. Also there is a chance for the power system to get imbalance in the absence of such indications and automatic disconnection i.e. islanding.

REFERENCES:

- [1] Hèctor Beltran, Francisco Gimeno, Salvador Seguí-Chilet and Jose M. Torrelo Instituto de Tecnología Eléctrica Av. Juan de la Cierva, 24 - Parc Tecnològic 46980 Paterna, València (Spain) paper on “Review of the Islanding Phenomenon Problem for Connection of Renewable Energy Systems.
- [2] Amin Safari paper on —A Novel Islanding Detection Technique for Distributed Generation (DG) Units in Power Systeml. February, 2013 International Journal of Advanced Science and Technology Vol. 51
- [3] J. McCalley, W. Jewell, T. Mount, D. Osborn, and J. Fleeman, BA wider horizon: Technologies, tools, and procedures for energy systems planning at the national level, [IEEE Power Energy Mag., vol. 9, no. 3, pp. 42–54, May/Jun. 2011].
- [4] J. Duncan Glover, Mulukutla S. Sarma, and Thomas J. Over byes Power System Analysis and design, fourth edition chapter 1,2.
- [5] J. B Gupta's 10th edition power system part 2 transmission and distribution of electrical power pg 367.
- [6] <http://en.m.wikipedia.org/wiki/Islanding>.
- [7] CANMET (2004). “An assessment of distributed generation islanding detection methods and issues for Canada.” CANMET Energy Centre.
- [8] Bas Verhoeven, “ Probability of islanding in utility network due to grid connected photovoltaic power systems.”
- [9] H.Karimi, A.Yazdani, and R.Iravani, negative-sequence current injection for fast islanding detection of a distributed resource in it, IEEE trans. On power electronics, VOL. 23, NO.1, JANUARY 2008.
- [10] S.N. Singh ,S.C. Srivastva, Electric power industry reconstructing in India, Present Scenario and future prospects, Senior Members, IEEE.

- [11]Text Book-"The 8051 Microcontroller and Embedded systems" by Muhammad Ali Mazidi and Janice GillispieMazidi, Pearson Education
- [12]Mr. NitinDhama, "Developing Islanding Arrangement Automatically For Grid on Sensing Voltage or Frequency Beyond Range," IJERMT Mag., vol.2, no.2, pp.184-187, March 2015.
- [13]Eider Robles, Salvador Ceballos, JosepPou, Member, IEEE, Jos'e Luis Mart'in, Member,IEEE, Jordi Zaragoza, Student Member, IEEE, and Pedro Ibañez,Member, IEEE paper on "Variable- Frequency Grid-Sequence Detector Based on A Quasi-Ideal Low-Pass Filter Stage and a Phase-Locked Loop".OCTOBER 10VOL.25, NO. 10, IEEE TRANSACTIONS ON POWER ELECTRONICS.
- [14]B.Roberts, "Capturing Grid Power," IEEE Power Energy Mag., vol.7, no.4, pp.32-41, Jul./Aug.2009.

IJERGS

Mechanical Properties of Al6061 Based Metal Matrix Composites Reinforced with Ceramic Particulates and Effect of Age Hardening on its Tensile Characteristics

G.Shaikshavali¹, Dr. E.Venugopal goud², M.Murali mohan¹

¹Assistant Professor, G. Pulla Reddy Engineering College (Autonomous), Kurnool, A. P., India

²Associate Professor, G. Pulla Reddy Engineering College (Autonomous), Kurnool, A. P., India

Email: shaikshavali.vali@gmail.com; Contact No.: +91-9014161577

Abstract: Aluminium materials has a huge requirement in the fields of automotive, aerospace and different engineering applications in order to meet requirements of various fields a material with good mechanical and thermal properties is developed which is metal matrix composites in which aluminium alloys is used as common matrix phases and reinforced used are different material particulates and fibers. Experimental MMC components are being developed for use in aircraft, satellites, jet engines, missiles, and space shuttle. In present study ceramic materials is used as reinforcements for MMCs such as Sic, Al₂O₃, B₄C and TiB₂. Al6061 is used as base matrix material. Metal matrix composites are fabricated using different ceramic reinforcements and Al6061 material using liquid metallurgy technique in this study stir casting method is used. Four different MMCs are produced with 10% Sic, 10%, Al₂O₃, 10% B₄C and 10% TiB₂. Mechanical properties are studied for the obtained cast composites of Al6061-10% Sic, 10%, Al₂O₃, 10% B₄C and 10% TiB₂ by conducting hardness test, tensile test and impact test. The obtained results were compared and graphically charted to characterize the different composite material.

Keywords: Metal Matrix Composites, Al6061, Ceramic materials, stir casting method.

INTRODUCTION

Aluminium material has less density than steel, with good corrosion resistance and mechanical properties, aluminium and its alloys have been widely used in various sectors such as automotive and aerospace. Aluminium metal matrix composites reinforced with ceramic particles has improved strength, high elastic modulus, impact strength and increased wear resistance, MMCs are becoming very popular as they exhibit superior strength-to-weight ratio. Al alloy based metal matrix composites are presently used in several applications such as pistons, pushrods, cylinder liners and brake discs. The manufacturing techniques of the aluminium metal matrix composites are classified into three types namely. Liquid state methods, Semisolid methods and Powder metallurgy methods

In liquid state methods, the metal matrix composites are produced by incorporating the ceramic particulates into a molten metallic matrix and casting the material in moulds. In this present study stir casting technique is used. Stir Casting is a liquid state method of producing composite materials in which preheated reinforcement materials are mixed with a molten metal by means of a stirrer, after proper mixing the liquid composite material is then casted in moulds as per required shapes.

Aluminium 6061 is a metal alloy with low density and high thermal conductivity, but it has poor wear resistance. To overcome this drawback, Al 6061 alloy is reinforced with ceramic materials so that its hardness, young's modulus and wear resistances are increased. Ceramic materials generally used to reinforce Al alloys are Si_c, Ti_c, TiB₂, ZrB₂, AlN, Si₃N₄, Al₂O₃, TiB₂ and SiO₂.

LITERATURE REVIEW

The literature survey regarding the above alloy systems and their composites are as follows.

Ravi et al. [1] conventional stir casting is an attractive processing method for produced AMCs as it is relatively inexpensive and conducive for a wide selection of materials and processing conditions. Pradeep R et.al [2] observed the study of mechanical properties of Al- Silicon Carbide Metal Matrix Composite (MMC) of Aluminium alloy of grade 7075 with addition of varying weight percentage composition such as Si_c8%+Al7075, Si_c6%+ Al7075, Si_c4%+Al7075, Si_c2%+ Al7075 by stir casting technique. The experimental result reveals that the combination of a matrix material with reinforcement SiC particles, improves mechanical properties like tensile strength, compressive strength, hardness and yield strength.

Ramesh et al. [3] investigated the mechanical properties of Al 6061-TiB₂ in-situ composites fabricated by liquid metallurgy route using Al 6061 as the matrix material and Al-10% Ti and Al-3% B as reinforcements. The developed in-situ composites exhibited considerable improvement in the mechanical properties as compared to the base metal S.Dhinakaran [4] investigated the

Characteristic of Boron Carbide Particulate Reinforced Aluminum Metal Matrix Composites produced by stir casting technique in his studies Al 6061 was used as base material and reinforced with the varied percentages of B₄C. 3%, 6% and 9% with particle size of 220µm. Cocen and Onel [5] investigated evaluated the porosity content of a Si_C/Al-5%Si-0.2% Mg composite sample from the difference between the calculated density and experimentally observed density. It was reported that the composite in the as-cast condition contained some porosity, which was reduced in the extruded condition.

Demir and Altinkok [6] investigated and evaluated the density and porosity of a dual-ceramic (Al₂O₃ and Si_C)-reinforced Al composite by the Archimedes principle and reported that the relative density increases with both infiltration temperature and pressure. The density of aluminium matrix composites increased with reinforcement fraction, and the density of Al 7075-Al₂O₃ composites was observed to be more as compared to that of Al 6063-SiC composites for the same reinforcement content. G. Straffelini et.al. [7] Reported that the matrix hardness has a strong influence on the dry sliding wear behavior of Al6061-Al₂O₃ composites. A. Martin et. al. [8] in the studies of tribological behavior on Al6061-Al₂O₃ composites concluded that a characteristic physical mechanism involves during the wear process.

From the above discussion it can be concluded that the not enough data is available on the mechanical properties of ceramic particulates reinforced Al6061 composites. Hence, the present studies are aimed to fabrication Al6061 ceramic reinforced composites with all the ceramic materials containing 10% age of weight of ceramic particles in each casting and to study their density, hardness and mechanical properties the castings are to be obtained with the following compositions Al6061-10% Si_C, 10%, Al₂O₃, 10% B₄C and 10% TiB₂.

MATERIAL & METHODS

Base Materials used

Aluminum alloy 6061 is light weight material with density of 2.7 gm/cm³ it is a heat-treatable alloy with strength higher than 6005A. It has very good corrosion resistance and very good weld ability Aluminum 6061 has an excellent heat and electricity conductor and in relation to its weight is almost twice as good a conductor as copper.

Table 1 Chemical Composition of Al6061

Element	Si	Fe	Cu	Mn	Mg	Cr	Zn	Ti	Al
Weight %	0.62	0.23	0.22	0.03	0.84	0.22	0.10	0.1	Bal

Reinforcements used

Silicon carbide (Si_C) is a chemical compound of carbon and silicon it is produced by high temperature electro chemical reaction of sand and carbon. Silicon carbide has low density high strength and high hardness and good elastic modulus.

Aluminium oxide (Al₂O₃) is a refractory ceramic oxide also called as alumina which is synthetically produced white in colour crystalline substance. Alumina is made from bauxite, a naturally occurring ore containing variable amounts of hydrous (water-containing) aluminum oxides. Alumina has high temperature resistant good mechanical properties.

Boron carbide (B₄C) s an extremely hard material it is used in refractory applications because to its high melting point and thermal stability, it is also used as abrasive powders and coatings due to its extreme abrasion resistance it has high hardness and low density and it is commonly used in nuclear applications as neutron radiation absorbent.

Titanium diboride (TiB₂) Titanium diboride (TiB₂) is a known ceramic material with high strength and durability it has high melting point, hardness, strength to density ratio, and high wear resistance properties. Titanium diboride has high electrical conductivity they can be easily machined in electrical discharge machining (EDM)

Table 2 Properties of ceramic reinforcements

Properties	Silicon carbide (SiC)	Aluminium oxide (Al ₂ O ₃)	Boron carbide (B ₄ C)	Titanium diboride (TiB ₂)
Density gm/cm ³	3.2	3.89	2.52	4.52
Melting point °C	2750	2072	2763	2970
Elastic Modulus (Gpa)	410	300	450	461.4
Hardness (HB500)	2800	1175	3100	3250

EXPERIMENTAL PROCEDURE

The aluminium 6061 based ceramics reinforced metal matrix composites are prepared using stir casting machine. Four different metal matrix composite materials were produced using different ceramic particulates. The weight percentages of Al6061 and ceramics for producing MMCs are

1. 90% of Al6061 is added with 10% SiC
2. 90% of Al6061 is added with 10% Al₂O₃
3. 90% of Al6061 is added with 10% B₄C
4. 90% of Al6061 is added with 10% TiB₂

The required quantities of Aluminium 6061 alloy is melted in the Inconel crucible of stir casting machine as shown in figure 1 the alloy melted completely at 800 °C. Slag was removed from the molten metal by adding hexachloro ethane (degassing) tablet, once the alloy is melted the preheated ceramic particulate SiC is poured in the Inconel crucible in required quantities which contains molten Al6061 alloy, silicon carbide is preheated till 250 °C using muffle furnace as shown in figure 2. the stirring processes is started using mechanical stirrer, stirring is done at a speed of 250 rpm for 10 mins. The molten metal was poured in the preheated cast iron mould (preheat temperature 400 °C) as shown in figure 3 and MMCs are produced in round bars as shown in figure 4. The same process is repeated for producing other three metal matrix composites.



Fig. 1 shows stir casting machine



Fig. 2 shows Muffle furnace



Fig. 3 Cast iron mould



Fig. 4 Casted metal matrix composite materials

RESULTS AND DISCUSSION

Hardness test

To evaluate the hardness properties of produced metal matrix composites Rockwell hardness testing machine is used, the results of the Rockwell hardness tests are obtained for both the base alloy and the composites.

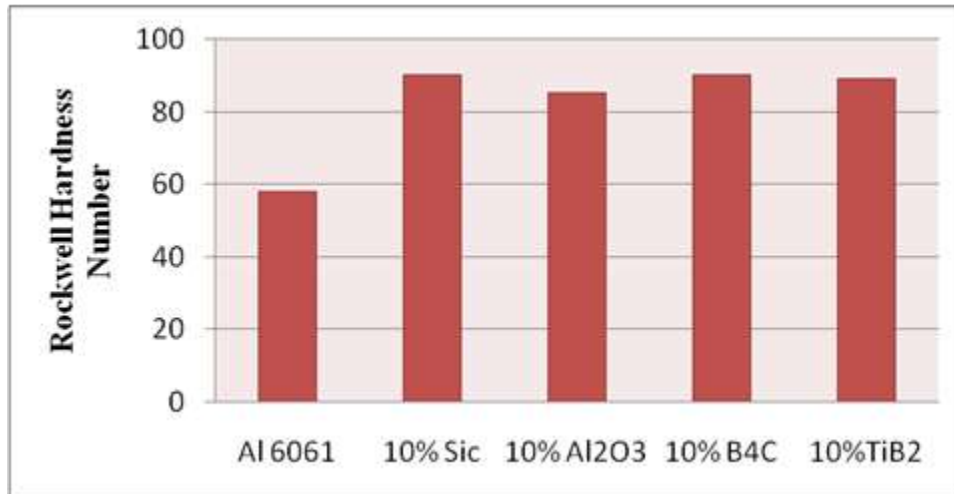


Fig. 5: Hardness tests of composite materials

From figure. 5 it is seen that the hardness of metal matrix composites is more when compared to base Al6061 alloy and it is observed that the composites reinforced with silicon carbide (SiC), and boron carbide (B₄C) and Titanium diboride (TiB₂) has more hardness compared to aluminium oxide (Al₂O₃).

Tensile test

The tensile test determines the ability of a material to withstand loads before elongation the testing is conducted using Tensometer testing machine the metal matrix composites were machines as the required dimensions for the test. Ultimate tensile strength is calculated as it is the maximum stress that a material can with stand under tensile loading.

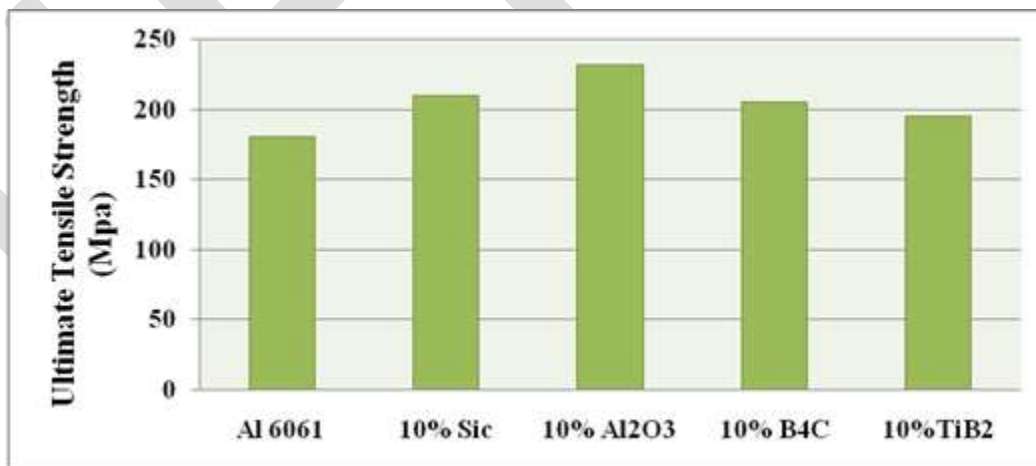


Fig. 6: Ultimate tensile strength of composite materials

From figure 6, it is clear that the tensile strength increased from 180 MPa of Al6061 to 212 Mpa in Al6061+10% Si_C MMC, the ultimate tensile strength of MMCs reinforced with 10%, Al₂O₃, 10% B₄C and 10% TiB₂ is more than the base Al6061 alloy and it is observed that the ultimate tensile strength of composite reinforced with aluminium oxide (Al₂O₃) is more than the other ceramics reinforced MMCs.

Impact test

The impact test is conducted using Charpy impact test, it is a standardized high strain-rate test which determines the amount of energy absorbed by a material during fracture. The test specimens were machines as per the required dimensions.

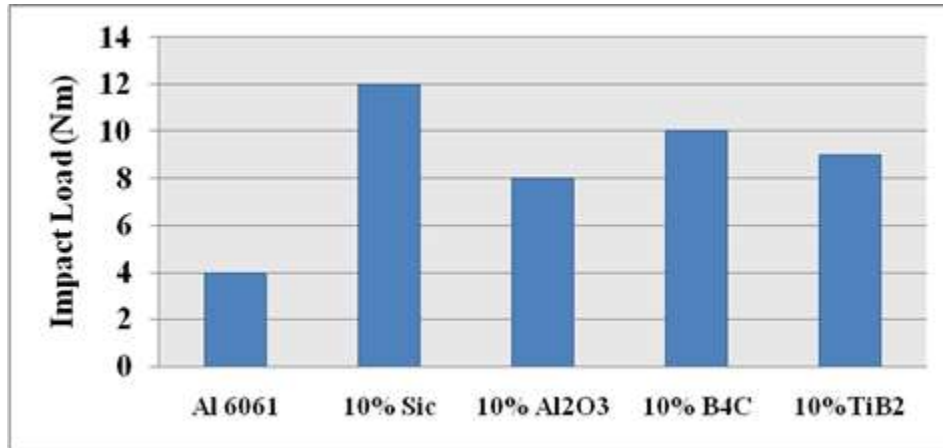


Fig. 7: Impact tests of composite materials

Figure 7 shows that the metal matrix composites reinforced with ceramic particulates has more impact resistance strength than the base Al6061 alloy, composite which is reinforced with ceramic aluminium oxide (Al₂O₃) has more impact strength than the other composites which are reinforced with silicon carbide (Sic), and boron carbide (B₄C) and Titanium diboride (TiB₂).

Age Hardening

Age hardening is done by solutionizing the samples at 525 0C for 10 hours and then cooled in water after cooling the specimens were artificially aged at 1650C for 8 hours and Effect of age hardening on the tensile strength of Al 6061 Metal matrix composites reinforced with ceramics is studied.

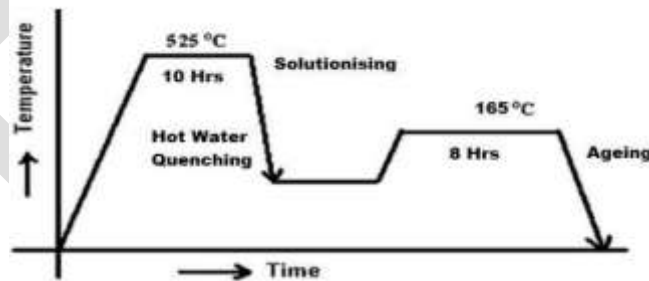


Fig. 8: Diagram representing age hardening process

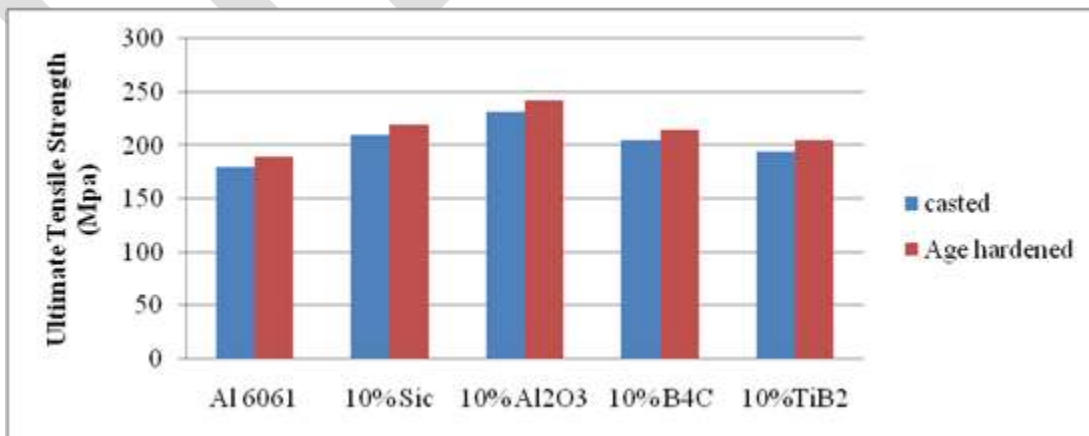


Fig. 9: Comparison of ultimate tensile strength of casted MMCs and MMCs after age hardening

From figure 9 it is observed that the age hardening of metal matrix composites has increased the ultimate tensile strength of MMCs. The strain to fracture was less affected by the volume fraction of ceramic reinforcements and ageing treatment.

CONCLUSION

Al6061 based ceramics reinforced metal matrix composites have been successfully fabricated using stir casting machine with different types of ceramic particulates. The mechanical properties such as hardness, tensile and impact strength of composites are studied. Following conclusions can be drawn from this study

1. Liquid metallurgy techniques were successfully adopted in the preparation of Al6061-10% Sic, Al6061-10%, Al₂O₃, Al6061- 10% B₄C and Al6061-10% TiB₂. Metal matrix composites.
2. Hardness test study revealed that the hardness of ceramic reinforced metal matrix composites is more than the base Al6061 alloy. Al6061-10% Sic, and Al6061- 10% B₄C composite materials exhibit more hardness than other reinforced composites.
3. Tensile test results show that the Al6061-10%, Al₂O₃ MMC material has good ultimate tensile strength property when compared to other ceramic reinforced MMCs.
4. This present study reveals that the impact strength of ceramic reinforced metal matrix composites is more than the base Al6061 alloy. Highest impact strength is seen in composite reinforced with silicon carbide (Sic).
5. The age hardening process has increased the tensile strength of the metal matrix composites.

Future studies can be carried out on processing and evaluation mechanical properties of different aluminium alloy combinations with reinforcements like AlN, BN, MgAl₂O₄ and Graphite. Tribological studies and other mechanical properties evaluation of the above produced MMCs can also be investigated.

REFERENCES:

- [1] KR. Ravi, VM .Sreekumar, RM. Pillai, Chandan Mahato, KR. Amaranathan, R. Arulkumar. Optimization of mixing parameter through a water model for metal matrix composites synthesis. *Mater des.* 28 (2007) 871-881.
- [2] Pradeep, R., Praveen Kumar, B.S and Prashanth: Evaluation of mechanical properties of aluminium alloy 7075 reinforced with silicon carbide and red mud composite, *International Journal of Engineering Research and General Science*, Vol. 2, Issue 6, (1081-88), 2014.
- [3] Ramesh CS, Pramod S, Keshavamurthy R. A study on microstructure and mechanical properties of Al 6061-TiB₂ in-situ composites. *Materials Science and Engineering A.* 2011; 528:4125–32.
- [4] S.Dhinakaran^{1,a} T.V.Moorthy Fabrication and characteristic of boron carbide particulate reinforced aluminum metal matrix composites *International Journal of Engineering Research Science*, Vol. 3, Issue 7, (1051-78), 2014.
- [5] Cocen, U, & Onel, K. (2002). Ductility and strength of extruded SiCp/aluminium alloy composites. *Composites Science and Technology*, 62, 275–282. Elsevier, United Kingdom
- [6] Demir, A, & Altinkok, N. (2004). Effect of gas pressure infiltration on microstructure and bending strength of porous Al₂O₃/SiC-reinforced aluminium matrix composites. *Composites Science and Technology*, 64, 2067–2074. Elsevier, United Kingdom.
- [7] G.Straffelini, F.Bonollo, A.Tiziani, “Influence of matrix hardness on the sliding behavior of 20 vol% Al₂O₃-particulate reinforced 6061 Al metal matrix composite”, *Wear* 211 (1997) 192-197.
- [8] Martin, J. Rodriguez, J. Llorca, “Temperature effects on the wear behavior of particulate reinforced Al-based composites”, *Wear* 225–229 (1999) 615–620.
- [9] Arun. L.R, Saddam Hussain. Dr. Suneel Kumar N.Kulkarni, “Dynamic behaviour of hybrid aluminium6061 metal matrix reinforced with sic and fly ash particulates” *International Journal of Innovative Research in Science, Engineering and Technology* Vol. 2, Issue 6, June 2013.
- [10] F.Toptan, A.Kilicarslan, M. Cigdem, I.Kerti. Processing and microstructural characterization of AA1070 and AA6063 matrix B₄Cp reinforced composites. *Mater Des* 31 (2010) s87-s91.

COLOUR REMOVAL OF TEXTILE DYEING EFFLUENT USING LOW COST ADSORBENTS

Ms.A.Kavitha¹, Ms.G.Sai Pooja², Ms.M.Kaaviyarshini³

¹ASSISTANT PROFESSOR, DEPARTMENT OF CIVIL ENGINEERING, SRIGURU INSTITUTE OF TECHNOLOGY, COIMBATORE.

^{2,3}STUDENT, DEPARTMENT OF CIVIL ENGINEERING, SRIGURU INSTITUTE OF TECHNOLOGY, COIMBATORE.

¹corresponding author E-mail id:kavitha.civil@sriguru.ac.in

Abstract - Many industries like dye industries, textile, paper and plastics use dyes in order to colour their products and also consume substantial volumes of water. As a result they generate a considerable amount of coloured wastewater. The presence of small amount of dyes (less than 1 ppm) is highly visible and undesirable. For the present study the sample effluent is collected from yarn dyeing industry, Coimbatore. The physico-chemical characteristics of the dyeing effluent is carried out according to the standard methods. The characteristics of adsorbents were studied and the selection of natural adsorbents for the colour removal in dyeing effluent is carried out. Experiments were performed to investigate the adsorption capacities of locally available low cost bio-adsorbents like cotton seeds, coconut coir pith, groundnut shell, cotton shell powders to remove colour in a textile industry wastewater. Experimental investigation was carried out to identify the effect of adsorbent dosage, contact time, agitator speed, pH, temperature by using Batch adsorption method. From the experimental investigations, the maximum colour from the textile industry wastewater was obtained at an optimum adsorbent dosage of 300 mg, an optimum contact time of 75 min., an optimum temperature of 330 K and an optimum agitator speed of 600 rpm and optimum pH of 7. Further, from the validation experiments, it was found that the maximum colour removal percentage in textile industry wastewater is about 75.25, 79.9, 86.75 and 81.7 % respectively for Cotton seeds, Coconut coir pith, Groundnut shell, Cotton shell. This result was higher than the results obtained by different process parameters for various bio adsorbents. Finally, from the results of adsorption study, it was concluded that bioadsorbents used as a coagulant for removing the colour from textile industry wastewater especially peanut hulls powder because of its higher adsorptive capacity than other bio-adsorbents used in this study. The experimental data for the adsorption process were well fitted by the Langmuir adsorption isotherm model relative to the fit of the Freundlich adsorption model.

Keywords—Decolourisation, Natural Adsorbents, Cotton Seeds, Coconut coir pith, Groundnut shell, Bioadsorbents, Peanut hulls, Efficiency of adsorbents

1. INTRODUCTION

Adsorption is a process that occurs when a gas or liquid solute accumulates on the surface of a solid or a liquid (adsorbent), forming a molecular or atomic film (the adsorbate). It is different from *absorption*, in which a substance diffuses into a liquid or solid to form a solution. The term sorption encompasses both processes, while desorption is the reverse process. Adsorption is operative in most natural physical, biological, and chemical systems, and is widely used in industrial applications such as activated charcoal, synthetic resins and water purification. Similar to surface tension, adsorption is a consequence of surface energy. This chapter explains the methods and materials involved for the colour removal. Activated carbon (AC) as many known as a solid, porous, black carbonaceous material and tasteless. Marsh (1989) defined AC as a porous carbon material, usually chars, which have been subjected to reaction with gases during or after carbonization in order to increase porosity. AC is distinguished from elemental carbon by the removal of all non-carbon impurities and the oxidation of the carbon surface.

2. EXPERIMENTAL SECTION

AC manufactured by the pyrolysis of carbonaceous materials of vegetable origin, such as wood, coal, peat, fruit stones, and shell or synthetic polymer followed by activation of the chars obtained from them (Manocha,2003). The pyrolysis of any carbonaceous material in absence of air involves decomposition of organic molecules, evolution of tarry and gaseous products, and finally in a solid porous carbon mass. An adsorbent with highly developed porosity and correspondingly large surface area is obtained only by activating the carbonized material either by physical or chemical activation. The processing of AC basically involves selection of parameters that effecting the activated carbon production, carbonization process and types of activation. The low cost bio-adsorbents like cotton shells, cotton seeds, ground nut shell and coconut coir pith were collected from the local areas and washed repeatedly with distilled water to remove dust and soluble impurities. Initially all bio-adsorbents were kept for drying at room temperature in a shade for 10 h and then heating in an air oven at 473 K for 24 h. Then they crushed and passed through 15-20 mesh. Then, the prepared cotton shells, cotton seeds, ground nut shell and coconut coir pith powders were kept in a refrigerator at a temperature of 278 K. This method used to avoid the decomposition, because cotton shells, cotton seeds, ground nut shell and coconut coir pith are agro-based products.

2.1 PHYSIO-CHEMICAL ANALYSIS OF DYEING EFFLUENT SAMPLE

The physio-chemical analysis of the effluent is essential for the treatment technique. For the present study, collected a textile industry wastewater samples from yarn dyeing industry, Coimbatore city, Tamil Nadu, with the help of airtight sterilized bottles. Then, took the wastewater samples to the Environmental Laboratory and then they were stored in refrigerator at 278 K for analyzing colour intensity.

TABLE 2.1 Physico-Chemical Characteristics of Effluent

S.NO	CHARACTERISTICS	VALUE
1	Chlorides	513.31 mg/l
2	PH	10.5
3	Temperature	30 ⁰ C
4	Colour	Dark green
5	Odour	Pungent
6	Turbidity	250 NTU
7	Sulphates	660 mg/l
8	Total hardness as CaCO ₃	459 mg/l
9	BOD	220 mg/l
10	COD	500 mg/l

TABLE 2.2 Proximate analysis of selected adsorbents

CHARACTERISTICS	COTTON SEEDS	COCONUT COIR PITH	GROUND NUT SHELL	COTTON SHELL
Ph	5.5	5.8	6.2	6
Bulk density	2.11	2.16	2.22	2.18
Attrition	13	15	22	19
Moisture content	8.5%	9.2%	9.7%	9.5%
Ash content	8.2%	7.56%	7%	7.23%
Surface area	1188m ² /g	1127.6 m ² /g	1263.6 m ² /g	1242 m ² /g
Iodine removal	660mg/g	682mg/g	702mg/g	690mg/g
Methylene blue number	18g/100g	20.5g/100g	24.6g/100g	22.30g/100g

3. RESULTS AND DISCUSSION

The parameter such as pH, time, temperature, agitation speed, adsorbent dosage for various are discussed. The colour removal in a textile industry wastewater is to be achieved by using bio-adsorbents like Cotton seeds, Coconut coir pith, Groundnut shell, Cotton shell.

3.1 ADSORPTION EXPERIMENTS

Conducted batch adsorption experiments by shaking a series of five glass bottles containing 250 ml textile industry wastewater with different adsorbent dosage (100, 200, 300, 400 and 500 mg), different pH value (4, 5, 6, 7, 8, 9, 10) different contact time (25, 50, 75, 100 and 125 min.), different temperature (300, 310, 320, 330 and 340 K) and different agitator speed (200, 400, 600, 800 and 1000 rpm) . The bottles were tightly fixed in the shaker. The shaking proceeded for 3 hrs to establish equilibrium, after which the mixture was left to settle for 1 h. The filtrate’s absorbance was determined by means of the UV-VIS spectrophotometer. By referring to the calibration curve of the absorbance, the percentage reduction of colour from a textile industry wastewater could be obtained. From Fig.2.1, it may be observed that upto some wavelength absorbance increased with wavelength increased, beyond which, the absorbance decreased. The point at which the absorbance decreased is called point of deflection and the wavelength corresponding to the point of deflection is called maximum wave length. The observed maximum wavelength from Fig is 495 nm.

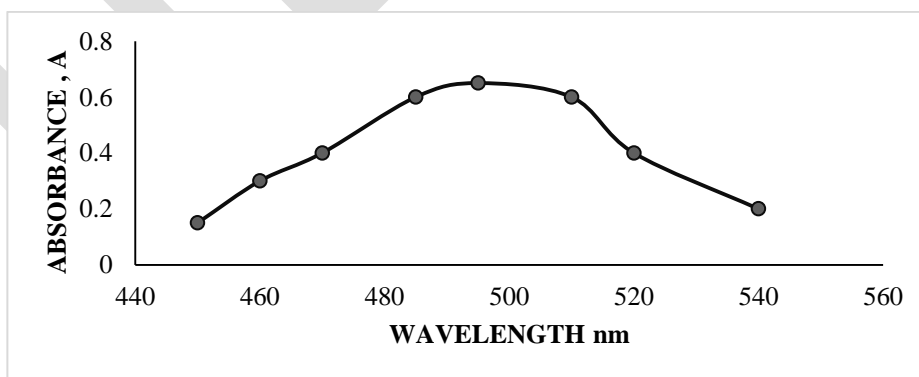


Fig-3.1 Absorbance curve for the textile effluent sample

3.2 EFFECT OF ADSORBENT DOSAGE

The percentage reduction of colour in a textile industry wastewater with pH of 7 against adsorbent dosage from 100 to 500 mg with an increment of 100 mg by different bio-adsorbents at contact time of 60 min., temperature 300 K and agitator speed of 400 rpm. The results revealed that colour removal percentage was low at the beginning and then increased with adsorbent dosage increased. This is because, the active sites in the bio-adsorbents could not be effectively utilized when the dosage was low and thereafter bio-adsorbents could be effectively utilized. When the bio-adsorbent dosages are higher, it is more likely that a significant portion of the available active sites remain uncovered, leading to lower specific uptake. From the fig no.2.2 it may be found that an optimum adsorbent dosage at which maximum colour removal is 300 mg and the colour reduction percentage is 75, 78.0, 83.5 and 79.5 % respectively for Cotton seeds, Coconut coir pith, Groundnut shell, Cotton shell.

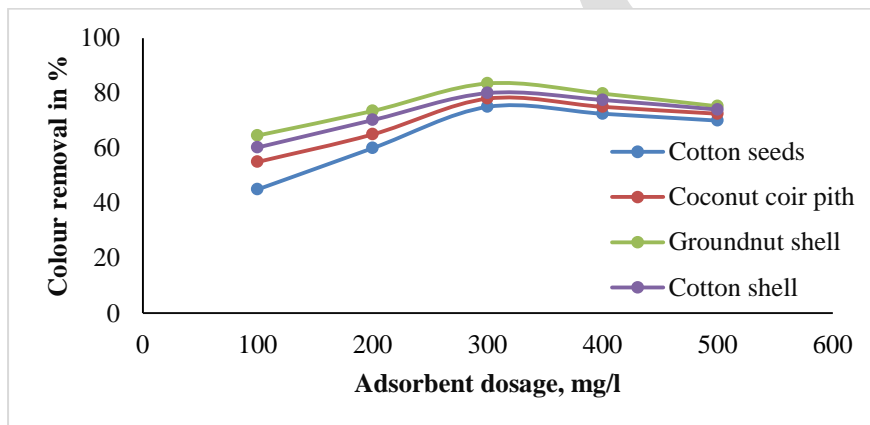


Fig-3.2 Effect of adsorbent dosage on colour removal

3.3 EFFECT OF CONTACT TIME

The percentage reduction of colour in a textile industry wastewater with pH of 7 against contact time from 25 to 125 min. with an increment of 25 min. by different bio-adsorbents at an optimum adsorbent dosage of 300 mg, temperature of 300 K and agitator speed of 400 rpm. The results revealed that the rates of percent colour removal are lower at the beginning of the experiment is probably due to the larger surface area of bioadsorbents was not contacted properly with the textile industry wastewater. Further, as contact time increased, the colour removal percentage also increased, is due to larger surface area of bio-adsorbents was contacted properly with a textile industry wastewater. As surface adsorption sites become exhausted, uptake rate is controlled and transported the adsorbate from the exterior to interior sites of bio-adsorbents. From Fig.2.3, it may be found that an optimum contact time at which maximum colour removal is 75 min. and colour reduction percentage is 72.5, 75, 80.67 and 76.67 % for Cotton seeds, Coconut coir pith, Groundnut shell, Cotton shell respectively.

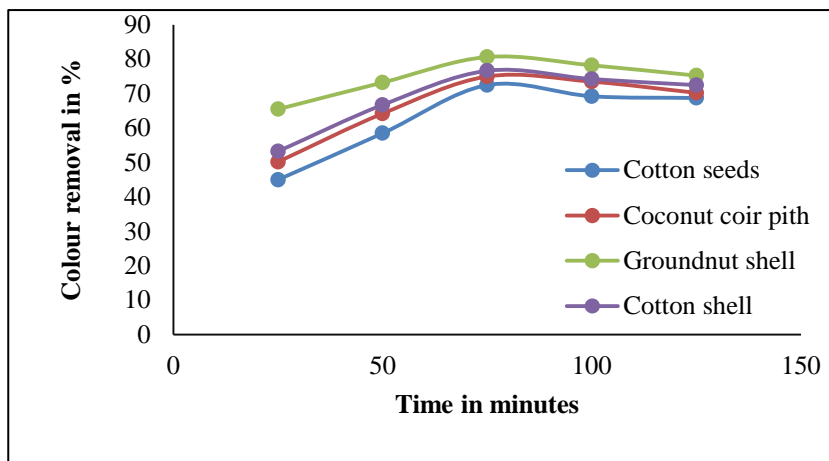


Fig-3.3 Effect of time on colour removal

3.4 EFFECT OF TEMPERATURE

The effect of temperature onto colour removal in a textile industry wastewater with pH of 7 by different bio-adsorbents was investigated at a temperature from 300 to 340 K, with an increment of 10 K and at an optimum adsorbent dosage of 300 mg, an optimum contact time of 75 min and agitator speed of 400 rpm. The percentage of colour removal continuously increased as temperature increased. However, maximum colour removal was obtained at a temperature of 330 K and thereafter equilibrium was attained. Increasing the temperature is known to increase the rate of diffusion of the adsorbate molecules across the external boundary layer and in the internal pores of the adsorbents particle, owing to the decrease in the viscosity of the solution. Thus, a change in temperature will change the equilibrium capacity of the adsorbents for a particular adsorbate. From Fig.2.4, it may be found that an optimum temperature at which maximum colour removal is 330 K and colour reduction percentage is 72.8, 76.2, 81.5 and 77.25% for Cotton seeds, Coconut coir pith, Groundnut shell, Cotton shell respectively.

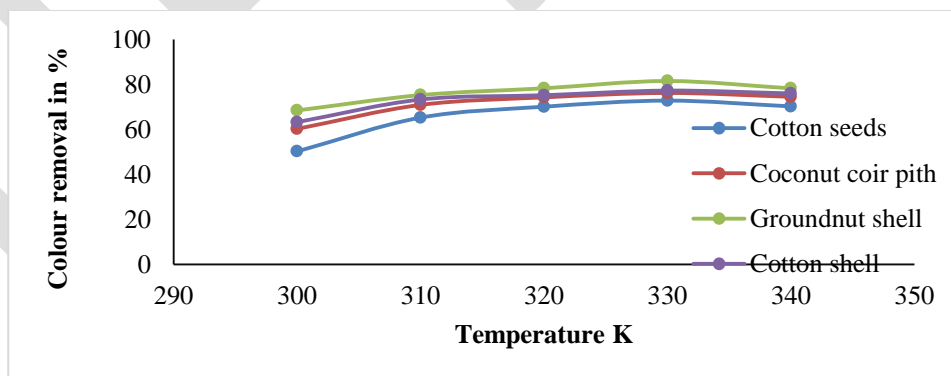


Fig-3.4 Effect of temperature on colour removal

3.5 EFFECT OF AGITATOR SPEED

The influence of agitator speed onto colour removal in a textile industry wastewater with pH of 7 by different bio-adsorbents is to be examined at agitator speed from 200 to 1000 rpm with an increment of 200 rpm and at an optimum adsorbent dosage of 300 mg, contact time of 75 min, and temperature of 330 K. It can be seen that continuous Increment in percentage removal with increasing agitator speed upto 600 rpm, beyond which colour removal attained the equilibrium. From Fig.2.5, it may be found that an optimum

agitator speed at which maximum colour removal is 600 rpm and colour reduction percentage is 73.8, 76.9, 82.3 and 78.4 % for Cotton seeds, Coconut coir pith, Groundnut shell, Cotton shell respectively.

3.6 EFFECT OF PH

The influence of effect of pH in colour removal in a textile industry wastewater with different bio-adsorbents is to be examined at pH varies from 4 to 10 at an optimum adsorbent dosage of 300 mg, contact time of 75 min, and temperature of 330 K, agitator speed of 400 rpm. It can be seen that continuous increment in percentage removal with increasing pH value upto 7, beyond which colour removal attained the equilibrium. From Fig.2.6, it may be found that an optimum pH value at which maximum colour removal is 7 and colour reduction percentage is 72.75, 75.75, 81.25 and 78.25 % for Cotton seeds, Coconut coir pith, Groundnut shell, Cotton shell respectively.

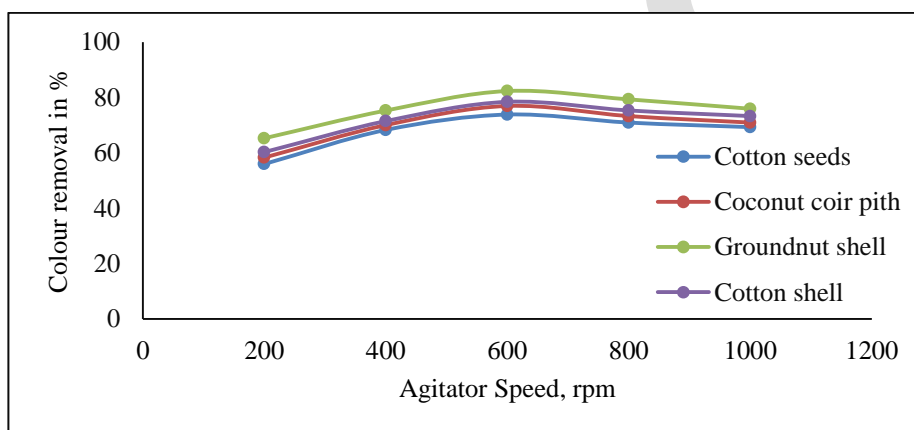


Fig-2.5 Effect of Agitator Speed on Colour Removal

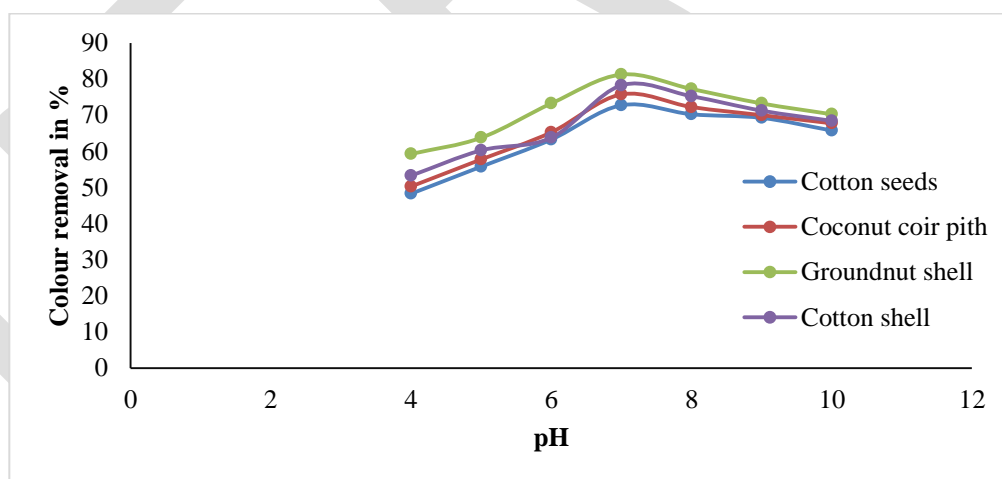


Fig – 3.6 Effect of pH on colour removal

3.7 VERIFICATION EXPERIMENT

In order to validate the above experiments in reducing the colour from textile industry wastewater, a separate experiment has been performed with an optimum adsorbent dosage of 300 mg, an optimum contact time of 75 min, an optimum temperature of 330 K and an optimum agitator speed of 600 rpm and optimum pH value of 7. The maximum colour removal percentage by different bio adsorbents in a textile industry wastewater is shown in Figure 2.7. The results showed that maximum colour removal percentage in a textile industry wastewater is about 75.25, 79.9, 86.75 and 81.7 % respectively for Cotton seeds, Coconut coir pith, Groundnut shell,

Cotton shell. Furthermore, it may also be found from that the maximum colour removal percentage in a textile industry wastewater was higher than each selected process parameters of different bio-adsorbents. Based on the results, it was concluded that bio-adsorbents may be used for removing the colour in a textile industry wastewater. Furthermore, over all experimental results at different process parameters have shown that maximum adsorption capacity of bio-adsorbents in the order of colour removing from textile industry wastewater is Groundnut shell followed by cotton shell, coconut coir pith and cotton seeds.

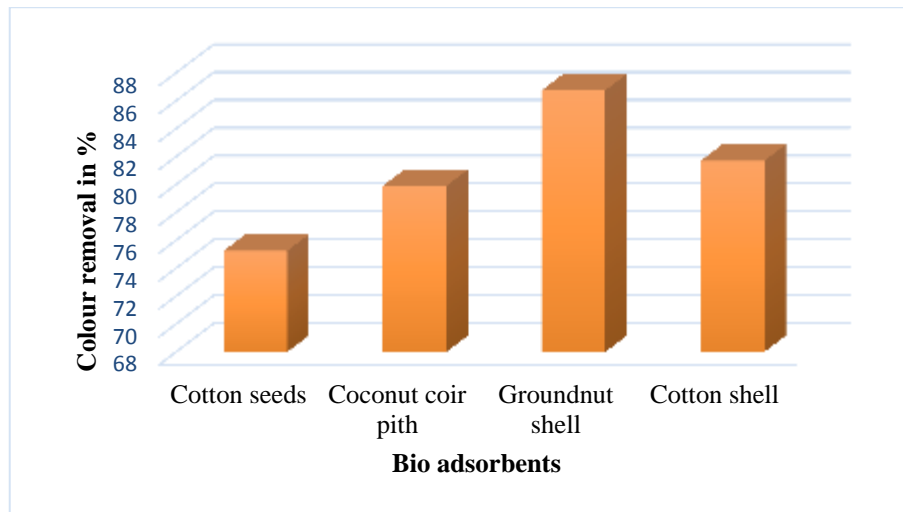


Fig -3.7 Maximum Colour Removal Percentage by Different Bio-Adsorbents

3.8 Adsorption isotherm

Adsorption isotherms, which are the presentations of the amount of solute adsorbed per unit of adsorbent, as a function of equilibrium concentration in bulk solution at constant temperature were studied. If a quantity, q of adsorbate is adsorbed by a porous solid adsorbent at constant temperature and the steady state equilibrium concentration, then the function q describes the adsorption isotherm. It shows the adsorption isotherm for the dye adsorption on groundnut shell, cotton shell, coconut coir pith and cotton seeds. The isotherm rises in the initial stages with higher slope at low C_e and q_e values. This indicates that, initially there are numerous readily accessible sites and confirms the monolayer coverage of dye. A variety of isotherm equations have been in use, some of which have a theoretical foundation and some being of mere empirical nature. In the present work, Langmuir and Freundlich isotherm has been tested.

Table 3.8.1 Adsorption isotherm for dye adsorption on Cotton seeds

S.NO	C_e (mg/l)	q (mg/g)
1	24	7.6
2	30.6	8.94
3	37.6	10.24
4	46	11.4
5	56.3	12.37
6	67	13.3

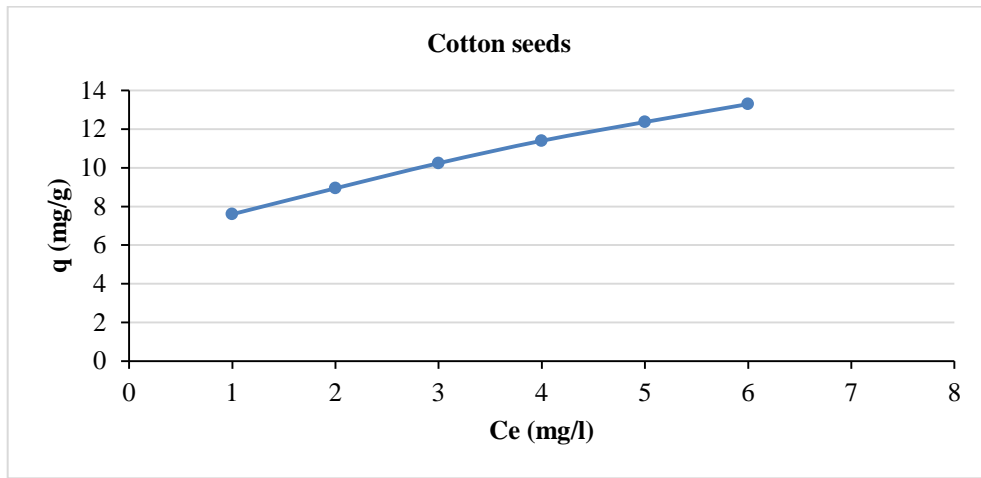


Fig -3.8.1 Adsorption isotherm for dye adsorption on Cotton seeds

Table 3.8.2 Adsorption isotherm for dye adsorption on Coconut coir pith

S.NO	Ce (mg/l)	q (mg/g)
1	20.3	7.97
2	27.3	9.27
3	35	10.5
4	42	11.8
5	54	12.6
6	61.5	13.85

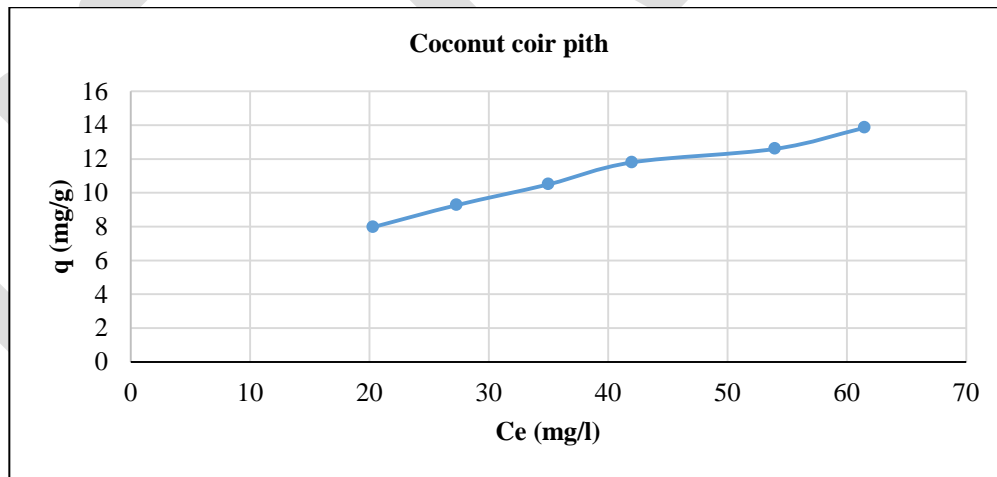


Fig-3.8.2 Adsorption isotherm for dye adsorption on Coconut coir pith

Table 3.8.3 Adsorption isotherm for dye adsorption on Groundnut shell

S.NO	Ce (mg/l)	q (mg/g)
1	13.7	8.63
2	18	10.2
3	23.4	11.66

4	29.3	13.07
5	37.3	14.27
6	43.8	15.62

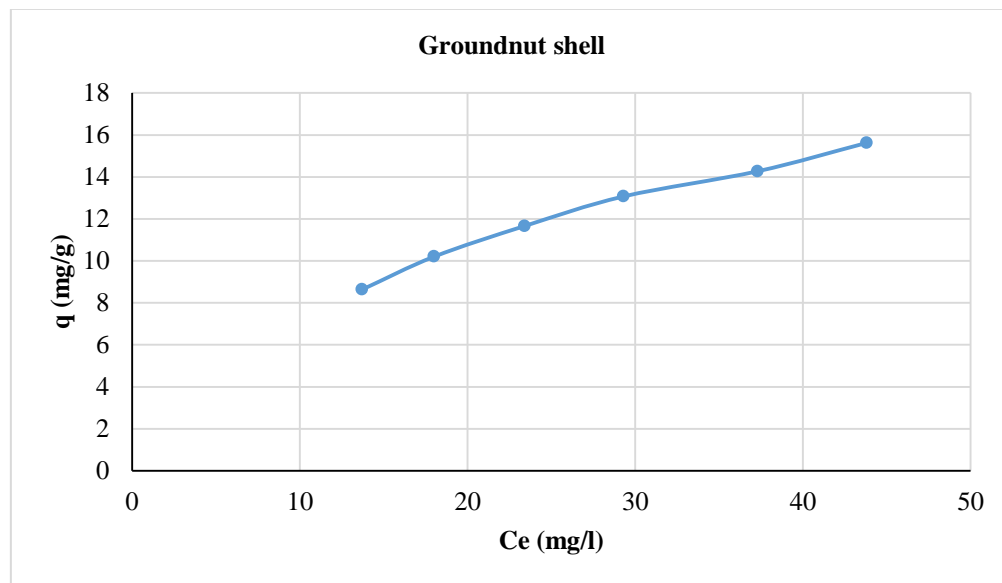


Fig- 3.8.3 Adsorption isotherm for dye adsorption on Groundnut shell

Table 3.8.4 Adsorption isotherm for dye adsorption on Cotton shell

S.NO	Ce (mg/l)	q (mg/g)
1	19.8	8.02
2	25.1	9.49
3	31	10.90
4	39	12.10
5	47.2	13.28
6	57.5	14.25

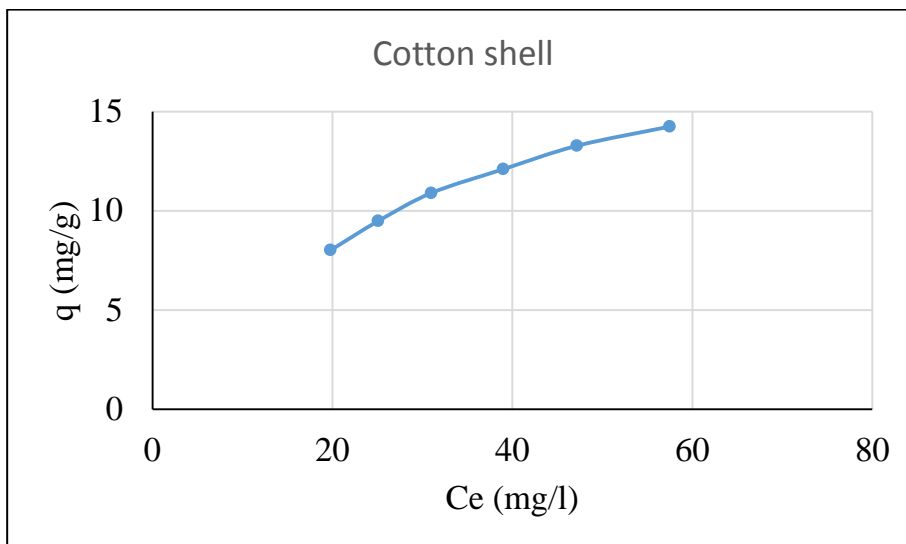


Fig- 3.8.4 Adsorption isotherm for dye adsorption on Cotton shell

3.9 Langmuir isotherm

According to Langmuir model, adsorption occurs uniformly on the active sites of the adsorbent, and once an adsorbate occupies a site, no further adsorption can take place at the site. The Langmuir model is given by following Eq (1),

$$C_e / q_e = 1/q_m KL + C_e / q_m \text{ ----- (1)}$$

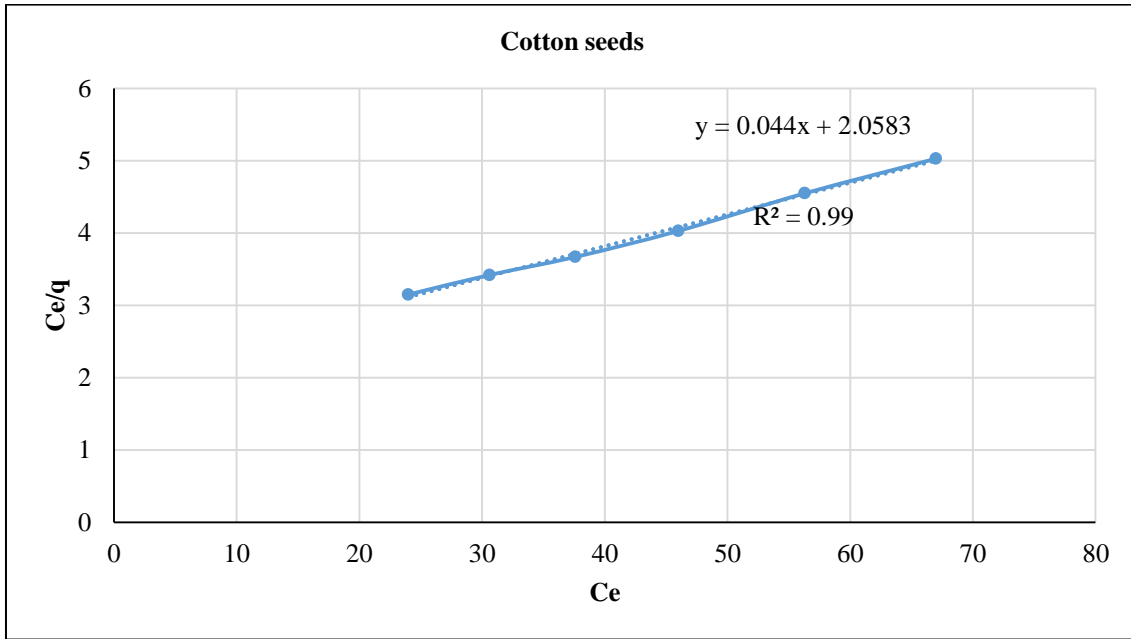
Where, C_e is the equilibrium concentration mg/L, q_e is the amount of dye adsorbed at equilibrium (mg/g) and q_m is q_e for a complete monolayer (mg/g); KL is sorption equilibrium constant (L/mg). A plot of C_e/q_e versus C_e (Fig. 6, Table 6) should indicate a straight line of slope $1/q_m$ and an intercept of $1/KLq_m$ [40-41]. The Langmuir parameters can be used to predict the affinity between the adsorbate and adsorbent using the dimensionless separation factor, RL , defined by Eq. (2)

$$RL = 1 / (1 + KL C_e) \text{ ----- (2)}$$

The value of RL lies between 0 and 1 for favorable adsorption, while $RL > 1$ represents unfavourable adsorption, and $RL = 1$ represents linear adsorption while the adsorption process is irreversible if $RL = 0$. The adsorption of dye on ABC follows the Langmuir isotherm model for metal adsorption. The dimensionless parameter RL values lies between 0.09623 to 0.4128 is consistent with the requirement for favorable adsorption. The high value of correlation coefficient R^2 indicates a good agreement between the parameters and confirms the monolayer adsorption of dye onto the adsorbent surface.

Table 3.9.1 Langmuir adsorption isotherm for dye adsorption on Cotton seeds

S.NO	Ce	Ce/q
1	24	3.15
2	30.6	3.42
3	37.6	3.67
4	46	4.03
5	56.3	4.55
6	67	5.03



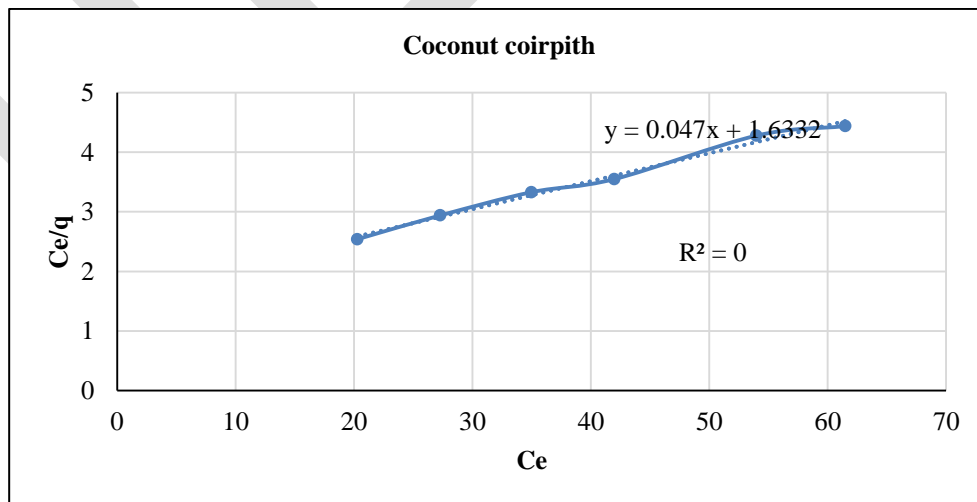
Slope of the curve = $1/qm =$

0.044 , Intercept of the curve = $1/KL qm = 2.0583$
 $qm = 22.72 \text{ mg/g}$, $KL = 0.021$ and $R^2 = 0.9973$

Fig 3.9.1 Langmuir adsorption isotherm for dye adsorption on Cotton seeds

Table 3.9.2 Langmuir Adsorption isotherm for dye adsorption on Coconut coir pith

S.NO	Ce	Ce/q
1	20.3	2.54
2	27.3	2.94
3	35	3.33
4	42	3.55
5	54	4.28
6	61.5	4.44

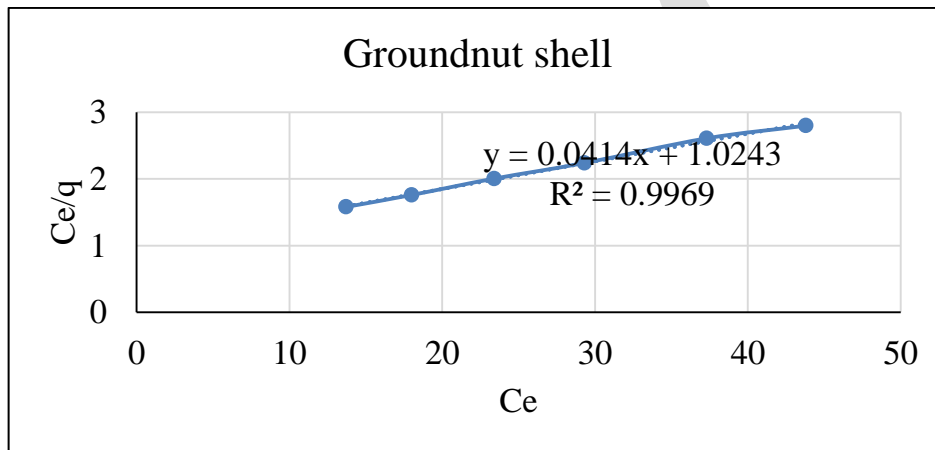


Slope of the curve = $1/qm = 0.047$, Intercept of the curve = $1/KL qm = 1.6332$
 $qm = 21.27 \text{ mg/g}$, $KL = 0.028$ and $R^2 = 0.99$

Fig 3.9.2 Langmuir Adsorption isotherm for dye adsorption on Coconut coir pith

Table 3.9.3 Langmuir Adsorption isotherm for dye adsorption on Groundnut shell

S.NO	Ce	Ce/q
1	13.7	1.58
2	18	1.76
3	23.4	2.006
4	29.3	2.24
5	37.3	2.61
6	43.8	2.80

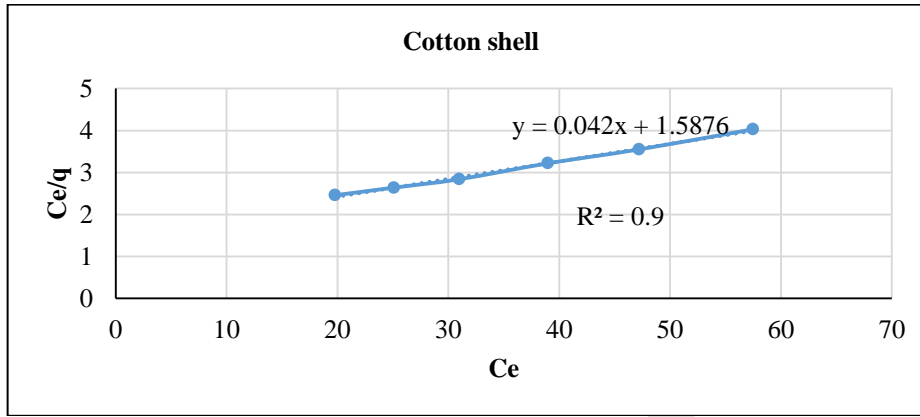


Slope of the curve = $1/q_m = 0.0414$, Intercept of the curve = $1/K_L q_m = 1.0243$
 $q_m = 24.15 \text{ mg/g}$, $K_L = 0.04$ and $R^2 = 0.9969$

Fig – 3.9.3 Langmuir Adsorption isotherm for dye adsorption on Groundnut shell

Table 3.9.4 Adsorption isotherm for dye adsorption on Cotton shell

S.NO	Ce	Ce/q
1	19.8	2.46
2	25.1	2.64
3	31	2.84
4	39	3.22
5	47.2	3.55
6	57.5	4.03



Slope of the curve = $1/q_m = 0.042$, Intercept of the curve = $1/K_L q_m = 1.5876$

$q_m = 23.80 \text{ mg/g}$, $K_L = 0.026$ and $R^2 = 0.997$

Fig – 3.9.4 Adsorption isotherm for dye adsorption on Cotton shell

3.10 Freundlich isotherm

Freundlich isotherm model was also used to explain the observed phenomenon (Freundlich, 1906)[43]. The Freundlich isotherm is represented by $\log q_e = \log K_f + 1/n \log C_e$

Where, C_e is the equilibrium concentration (mg/L), K_f and n are constant incorporating all factors affecting the adsorption process such as adsorption capacity and intensity, respectively. A plot of $\log q_e$ vs $\log C_e$ from values in Table gives a linear trace with a slope of $1/n$ and intercept of $\log K_f$. K_f and n calculated from the intercept and slope of the plots were found to be 5.899 and 4.038 respectively. The K_f value is related to the adsorption capacity; while the $1/n$ value is related to the adsorption intensity. $1/n$ values indicate the type of isotherm to be irreversible ($1/n = 0$), favourable ($0 < 1/n < 1$) and unfavourable ($1/n > 1$). Therefore ABC which has n value of 0.2476 implies effective adsorption. The value of the correlation coefficient, R^2 , obtained in this case indicates that the Freundlich model gave a poorer fit to the experimental data than the Langmuir isotherm model.

Table 3.10.1 Freundlich adsorption isotherm for dye adsorption on Cotton seeds

S.NO	$\log C_e$	$\log q_e$
1	1.38	0.88
2	1.48	0.95
3	1.57	1.01
4	1.66	1.05
5	1.75	1.09
6	1.82	1.12

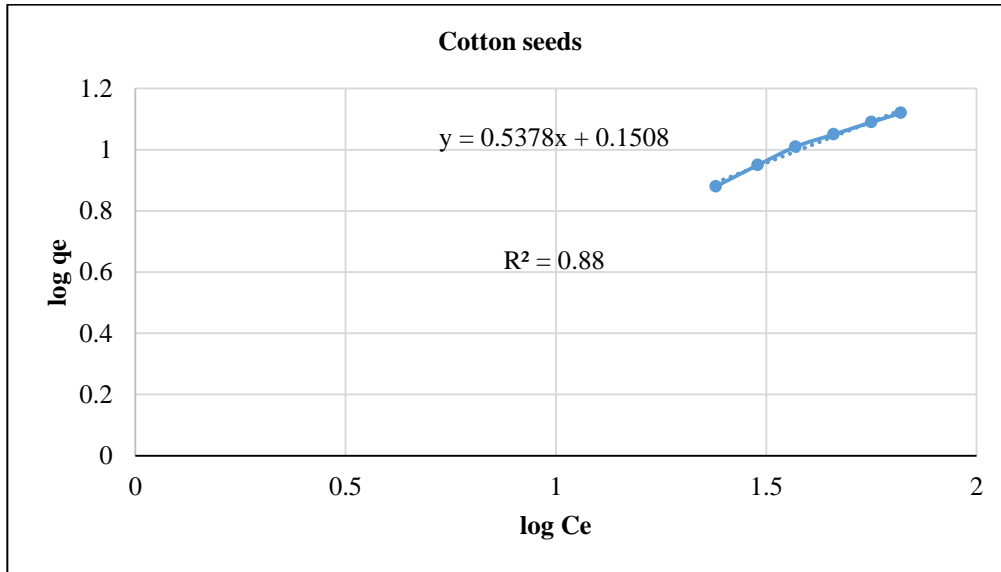


Fig 3.10.1 - Freundlich adsorption isotherm for dye adsorption on Cotton seeds

Slope = $1/n = 0.5378$, Intercept = $\log K_f = 0.1508$, $R^2 = 0.8876$

Table 3.10.2 Freundlich Adsorption isotherm for dye adsorption on Coconut coir pith

S.NO	log Ce	log qe
1	1.30	0.90
2	1.43	0.96
3	1.54	1.02
4	1.62	1.07
5	1.73	1.10
6	1.78	1.14

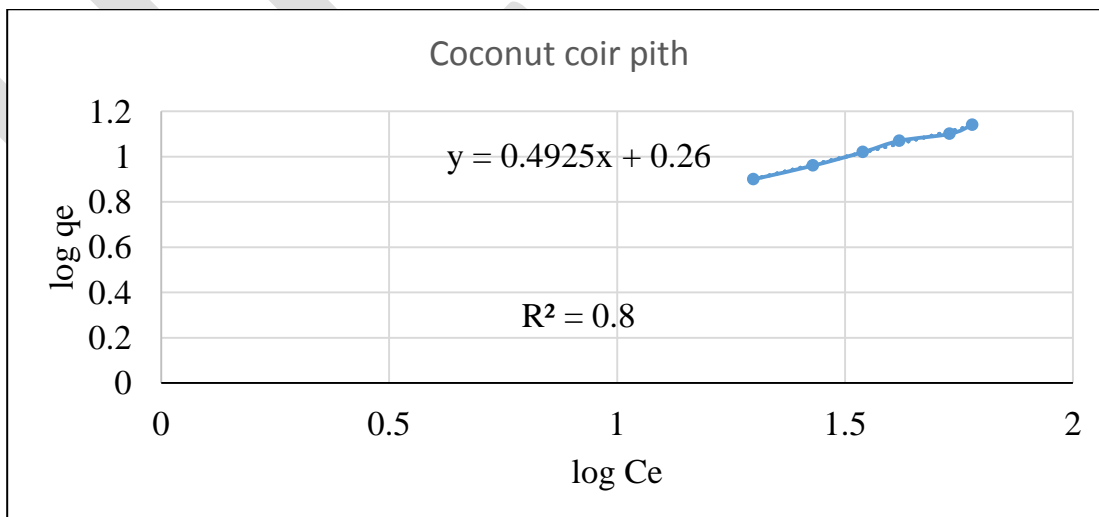


Fig 3.10.2 - Freundlich Adsorption isotherm for dye adsorption on Coconut coir pith

Slope = $1/n = 0.4925$, Intercept = $\log K_f = 0.26$, $R^2 = 0.882$

Table 3.10.3 Freundlich Adsorption isotherm for dye adsorption on Groundnut shell

S.NO	log Ce	log qe
1	1.136	0.93
2	1.25	1.008
3	1.36	1.06
4	1.46	1.11
5	1.57	1.15
6	1.64	1.19

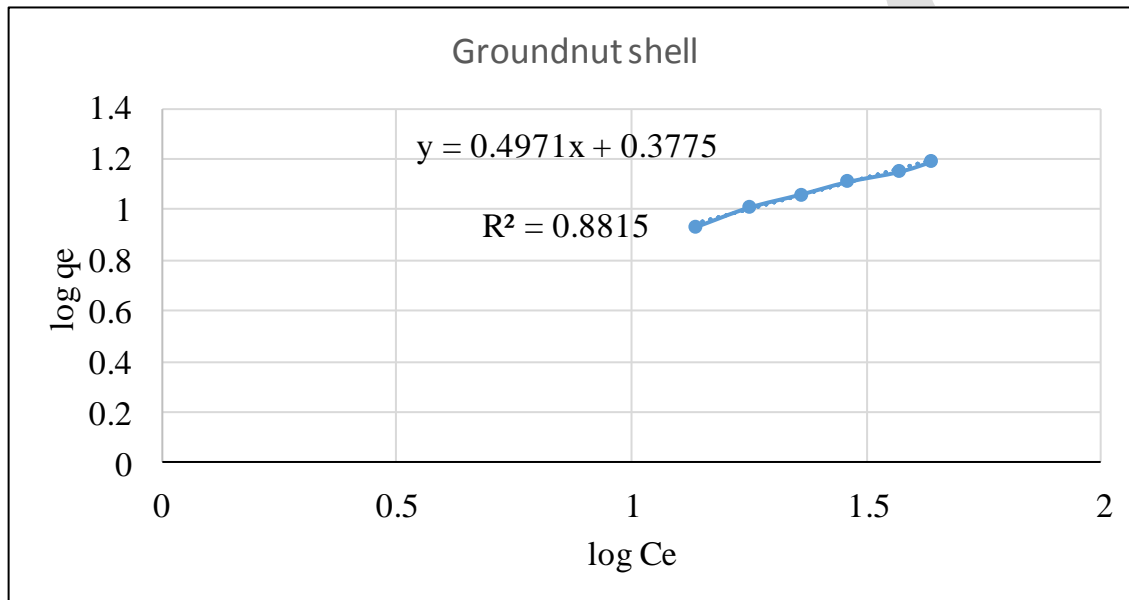


Fig 3.10.3 - Freundlich

Adsorption isotherm for dye adsorption on Groundnut shell

Slope = $1/n = 0.4971$, Intercept = $\log K_f = 0.3775$, $R^2 = 0.8815$

Table 3.10.4 Adsorption isotherm for dye adsorption on Cotton shell

S.NO	log Ce	log qe
1	1.29	0.39
2	1.39	0.42
3	1.49	0.45
4	1.59	0.50
5	1.67	0.55
6	1.75	0.60

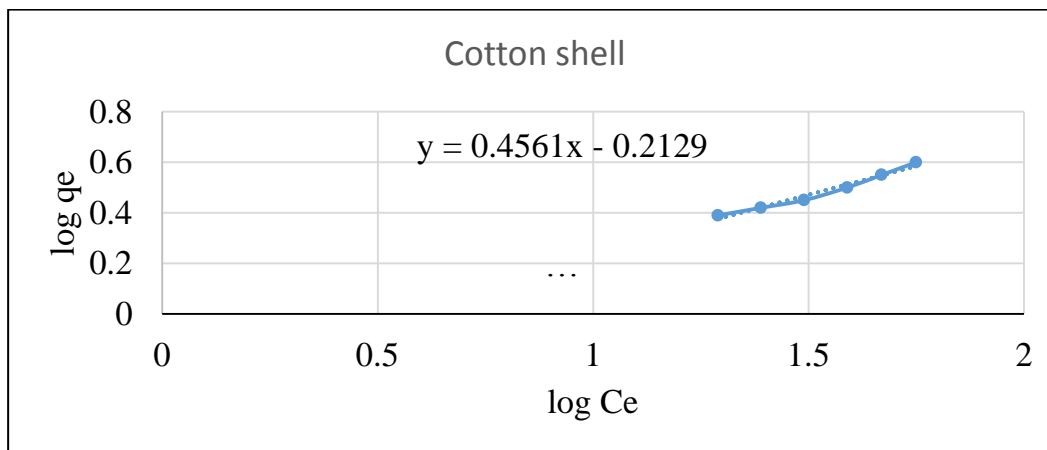


Fig 3.10.4 - Adsorption isotherm for dye adsorption on Cotton shell

Slope = $1/n = 0.4561$, Intercept = $\log K_f = 0.2129$, $R^2 = 0.8732$

3.11 SUMMARY

The effect of using various parameters have been analysed through this study. The experimental investigation of varying such parameters and their optimum values will be analysed in next phase of the project. The colour removal efficiency of using such adsorbents is expected to be 70-80%. In the present study, the batch adsorption study was conducted to find out suitability of bio-adsorbents for removing colour in a textile industry wastewater. The ability of bio-adsorbents for removing colour in a textile industry wastewater with different dosage, different contact time, different temperature and different agitator speed were monitored for this present study. The maximum percentage reduction of colour in a textile industry wastewater by different bio-adsorbent were obtained at an optimum adsorbent dosage of 300 mg, an optimum contact time of 75 min., an optimum temperature of 330 K and an optimum agitator speed of 600 rpm. From the validation experiments, it found that maximum colour removal percentage in a textile industry wastewater is about 74.2, 79.3, 85.6 and 80.7 % respectively for neem leaves, orange peels, peanut hulls and coconut coir pith powders. These results of validation experiment were higher than the results obtained by different process parameters. Furthermore, over all experimental results have shown that maximum adsorption capacity of bio-adsorbents in the order of colour removing from a textile industry wastewater is peanut hulls powder followed by coconut coil pith powder, orange peels powder and neem leaves powder. Finally, from the results of adsorption study, it was concluded that bioadsorbents may be used as a coagulant for removing colour from a textile industry wastewater especially peanut hulls powder because of its higher adsorptive capacity than other bio adsorbents used in this study.

4. ACKNOWLEDGEMENT

We take this opportunity to express our thanks to department of Civil Engineering, Sriguru Institute of technology to undertake this work and allow us to present our findings as our contribution to the development of knowledge in the field of Environmental Engineering and also wish to express my sincere thanks to my parents and all my friends for their support

5. CONCLUSION

In the present study, the batch adsorption study was conducted to find out suitability of bio-adsorbents for removing colour in a textile industry wastewater. The maximum percentage reduction of colour in a textile industry wastewater by different bio-adsorbent were obtained at an optimum adsorbent dosage of 300 mg, an optimum contact time of 75 min., an optimum temperature of 330 K and an optimum agitator speed of 600 rpm and pH 7. From the validation experiments, it found that maximum colour removal percentage in a textile industry wastewater is about 75.25, 79.9, 86.75 and 81.7 % respectively for Cotton seeds, Coconut coir pith, Groundnut shell, Cotton shell. These results of validation experiment were higher than the results obtained by different process parameters.

Furthermore, over all experimental results have shown that maximum adsorption capacity of bio-adsorbents in the order of colour removing from a textile industry wastewater is groundnut shell followed by cotton shell, Coconut coir pith and cotton seeds. Finally, from the results of adsorption study, it was concluded that bio adsorbents may be used as a coagulant for removing colour from a textile industry wastewater especially groundnut shell powder because of its higher adsorptive capacity than other bio-adsorbents used in this study. The experimental data for the adsorption process were well fitted by the Langmuir adsorption isotherm model relative to the fit of the Freundlich adsorption model. The Langmuir adsorption capacity was determined as 22.72 mg/g, 21.27 mg/g, 24.15 mg/g, 23.80 mg/g, for adsorption on Cotton seeds, Coconut coir pith, Groundnut shell, Cotton shell.

REFERENCES:

- [1] - Salman J.M. and Alsaad K.—Adsorption of 2,4-dichlorophenoxyacetic acid onto date seeds activated carbon: Equilibrium, Kinetic and thermodynamic studies|| *Int.J.Chem.Sci.*, vol.10, no.2 , pp. 677-690, 2012.
- [2]- Abbas A.F and Ahmed M.J. —Optimization of Activated Carbon Preparation from Date Stones by Microwave Assisted K₂CO₃ Activation || *Iraqi Journal of Chemical and Petroleum Engineering IJCPE* .vol.15, no.1 , pp.33- 42, 2014.
- [3]- Viswanathan B., Indra Neel P. and Varadarajan T. K. — *Methods of Activation and Specific Applications of Carbon Materials*|| National Centre for Catalysis Research Department of Chemisry, Indian Institute of Technology, Madras Chennai, India, 2009.
- [4]- C. Namasivayam, N. Muniasamy, K. Gayatri,M. Rani & K. Ranganathan (1996), Removal of dyes from aqueous solutions by cellulosic waste orange peel, *Bio-resource Technology*, Vol. 57, pp. 37-43.
- [5]- Mohammed M.A., Shitu A. and Ibrahim A. —Removal of Methylene Blue Using Low Cost Adsorbent: A Review|| *Research Journal of Chemical Sciences*, vol. 4, no 1, pp.91-102, 2014.
- [6]- Oladipo M.A., Bello I.A., Adeoye D.O., Abdulsalam, K.A.and Giwa, A.A.— Sorptive Removal of Dyes from Aqueous Solution: A Review || *Advances in Environmental Biology*, vol. 7, no.11, pp. 3311-3327, 2013.
- [7]- Gottipati R. and Mishra S. —Process optimization of adsorption of Cr(VI) on activated carbons prepared from plant precursors by a two-level full factorial design|| *Chemical. Engineering Journal*, vol. 160 , no. 1, pp. 99–107, 2010.
- [8]- Mutah M., Akira K., Zaiton A. M., Jafariah J., Mohd Razman S. and Nor Eman I. —Production of sugarcane bagasse based activated carbon for Cd²⁺ removal using factorial design || *International Journal of Innovative Technology and Exploring Engineering*, vol. 2, no. 4, pp. 2278-3075, 2013.
- [9]- Fung P.P.M., Cheung W.H. and McKay G. —Systematic Analysis of Carbon Dioxide Activation of Waste Tire by Factorial Design|| *Chinese Journal of Chemical Engineering*, vol. 20, no. 3, pp.497—504, 2012.

Partial Product Compression Methods: A Study and Performance Comparison Using a Tree Structured Multipliers

Parameshwara M. C* and Srinivasaiah H. C⁺

*Assistant Professor, Department of E & CE, Vemana Institute of Technology, VTU, Bangalore-34, Karnataka, India.

*Email:pmcvit@gmail.com, Phone: +919620902171

⁺Professor, Department of TCE, Dayananda Sagar College of Engineering, VTU, Bangalore-78, Karnataka, India.

⁺Email:hcsrinivas@gmail.com

Abstract— This paper presents the study and performance comparison of two traditional ‘partial product compression methods’ (PPCMs) viz. Wallace and Dadda in terms of the design metrics (DMs) such as power, delay, power-delay-product (PDP), and Area. For performance comparison an $N \times N$ -bit unsigned ‘tree structured multipliers’ (TSMs) have been considered as a case study with ‘ N ’ being varied from 5 to 16 bits. To design TSMs a low PDP 3:2 counter (1-bit Full adder) along with half adder (HA) cells have been considered. Further all the TSMs are designed in the Cadence’s virtuoso tool environment using 90 nm based ‘generic process design kits’ (GPDK) and simulated using Spectre simulator with BSIMv3v (Level 49) based transistor models. The power, delay, and PDP DMs of TSMs under consideration are extracted at nominal room temperature with supply voltage of $V_{DD}=1.2$ V and input signal frequency $F_{in} = 200$ MHz. This study and comparison of TSMs provides an insight to tradeoff among the Wallace and the Dadda PPCMs in terms of DMs.

Keywords— Tree structured multipliers, 1-bit adder, Arithmetic circuits, Low power adder, 3:2 counter, 28-T hybrid adder, Partial product compression, Wallace multipliers, Dadda Multipliers.

INTRODUCTION

The rapid advancements that are taking place in modern ‘wireless communication technologies’ (WCT) mirrored by the advancements in ‘semiconductor technologies’ (ST), demands the design of energy efficient wireless communication systems [1, 2, 3] to establish a seamless communication between the two end users. The transceiver being an important block of wireless communication system plays an important role in meeting the stringent requirements that are imposed by both WCT and ST. Further the transceivers are classified into two types viz. analog and digital. The digital transceivers are the natural choice for energy efficient wireless communication systems because of their important features like low phase noise, easily programmable, higher integration, very precise and controllable performance etc. [4, 5]. The digital transceiver is augmented with many sub-systems, among these the frequency synthesizer is one important sub-system that needs a greater attention in view of meeting the stringent requirements imposed by the modern WCT. The traditional frequency synthesizers are classified into viz. analog, digital, and analog and mixed mode. Among these the digital frequency synthesizers such as ‘direct digital frequency synthesizer’ (DDFS) is more popular because of its unique characteristics such as low power, low phase noise, high resolution, and good spectral purity. Traditionally the DDFS can be designed using the conventional architectures such as ROM or ROM less or sine computation techniques [6, 7, 8, 9, 10]. Among these DDFS architectures, most of the architectures employs the multiplier as a computational element to perform various ‘digital signal processing’ (DSP) operations. Thus the performance of multiplier is very important in meeting the performance of frequency synthesizer and there by the overall performance of the transceiver of a wireless communication system.

The block diagram of an $N \times N$ -bit unsigned multiplier is as shown in Figure 1, where ‘ N ’ is the number of bits in the multiplier (X) (or multiplicand (Y)). In this paper the word sizes of both X and Y are chosen to be equal. Further the block diagram shown in the Figure 1 has three important sub-blocks viz. the ‘partial product generation’ (PPG), the ‘partial product compression’ (PPC), and the final ‘carry propagation’ (CP) sub-blocks. The inputs for the PPG block are an ‘ N ’ bit multiplier ‘ X ’ and multiplicand ‘ Y ’, these inputs are either in binary or recoding formats such as Booth radix-4, ‘canonical signed digit’ (CSD), ‘minimal signed digit’ (MSD) or any other recoding formats and using these inputs the PPG block generates the partial products. In this paper both ‘ X ’ and ‘ Y ’ have been considered as natural binary numbers thus a two input ‘AND’ gate array is used to generate the partial products. The total number of partial products that are generated corresponding to an ‘ N ’ bit X and Y are N^2 partial products. The output of PPG that is N^2 partial products are applied as an input to the PPC block. The PPC block sums up the entire partial products efficiently using either the Wallace tree or the Dadda tree [11, 12] approach and reduces to two rows. The most critical element of the PPC techniques is a 3:2 counter, which is a 1-bit full adder (FA). A counter compresses $(k-1)$ rows of partial products into $\log_2(k)$ partial products [13]. The final two rows of compressed partial products that have been derived from the output of the PPC blocks are the input for the CP block. The CP block adds final two rows of the partial products generated at the output of PPC and produces an ‘ W ’ bit product term ‘ Z ’ (Figure-1), where the size of $W=2 \times N$ bits.

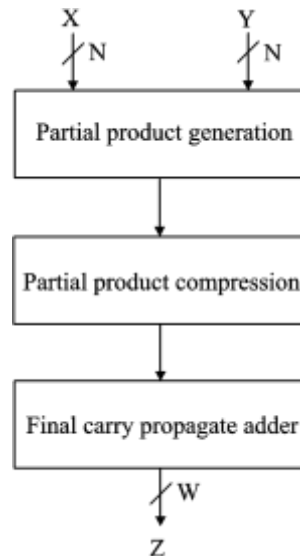


Figure 1: Block diagram of unsigned $N \times N$ -bit multiplier

PARTIAL PRODUCT COMPRESSION METHODS (PPCMs)

The most critical blocks in a conventional high speed multipliers are PPC and CPA blocks, these two blocks are very important in determining the overall speed of a multiplier. In general, the method of achieving the PPC using a 2:2 counter and a 3:2 counter is as shown in the Figure-2. Traditionally there are two partial product compression techniques viz. Wallace tree [11] and Dadda [12] tree based approaches and these are more frequently used to compress the partial products. The method of adding the partial products using Wallace and Dadda methods are illustrated using the 'dot' diagrams and is shown in Figure 3 for a $N=12$ -bits. In this figure, each 'dot' in a particular 'Column-Row' represents an individual partial product, generated from the logical 'AND' operation of the respective bits of 'X' and 'Y'. To explain the PPCM an unsigned 12×12 multiplier is taken as a case study.

PPCM based on Wallace approach:

The Figure-3a is a PPCM based on Wallace tree approach, here the method of achieving the PPC between the PPG and final CPA is shown in five different stages viz. Stage-1 (S1), Stage-2 (S2), Stage-3 (S3), Stage-4 (S4), and Stage-5 (S5). The very first step in a Wallace tree based TSM is the generation and reorganization (shifting) of PPs. The main functionality of individual stages is explained as follows: In the S1 all the individual PPs that are generated out of PPG block in the form of a '12-rows' \times '12-columns' matrix (herein referred as 'PP matrix (PPM)') is reorganized into the form of '12-rows' \times '23-columns' (herein referred as RPPM). To reorganize the 12×12 PPM into the 12×23 RPPM, the PPs in each row starting from the row-1 (R1) to the final row-12 (R12) are arranged such that each row under consideration is shifted towards left by 1-bit in position from its respective previous row. For $N=12$ -bit, a total of 144 PPs are generated in PPG block and are reorganized into 12-rows and 23-columns. Each row of PPM contains about 12 individual PPs, after reorganization the PPs in each row starting from R1 to R12 are spread over 23-columns that is from column-1 (C1) to column-23 (C23). The 12 PP rows that are spread in 23-columns are grouped as group-1 (G1), group-2 (G2), group-3 (G-3), group-4 (G4) (Figure: 2a), where each group contains 3-rows. The 3-PP rows of each group are simultaneously compressed into 2-PP rows by using a 3:2 counter and 2:2 counters. The method of PP rows compression is explained as below:

Let ' R_i ' be the i^{th} row of the group under consideration, where ' i ' varies from 1, 2, 3, N,

Let ' C_j ' be the j^{th} column of the group under consideration, where ' j ' varies from 1, 2, 3, 2N, and

Let ' PP_{ij} ' be the individual partial product of i^{th} row and j^{th} column in the group under consideration

Considering the R1-R3 of G1 in S1, the $PP_{1:1}$ and $PP_{3:14}$ are the PPs that are not subjecting to compression (represented by dark solid circle '●') and are carried forward to the next stage (S1). The " $PP_{1:2}$ and $PP_{2:1}$ " and " $PP_{2:13}$ and $PP_{3:13}$ " are compressed by using a 2:2 counters. For example the PPs in the C2: $PP_{1:2}$ and $PP_{2:1}$ that are subjecting to compression are shown in the Figure- 2a. The PPs in the remaining respective rows and respective columns are compressed by using a 3:2 counters. For example the PPs in the C3 that are $PP_{1:3}$, $PP_{2:2}$, and $PP_{3:1}$, subjecting to compression are shown the Figure: 2b below. The Sum and Cout outputs of a 3:2 counter (1-bit FA) are represented by solid circles with cyan and red colors respectively. Whereas, the Sum and Cout outputs of a 2:2 (1-bit HA) counter are represented by solid diamonds with cyan and red colors respectively. Thus the total 12-rows of PPs are reduced to 8-rows of PPs using a set of 3:2 counters and 2:2 counters in each group.

The second stage of compression that is S2 has total 8 rows of PPs, out of these 8-rows the first 6-rows of PPs are organized into two groups with each group being 3-rows of PPs. The last 2-rows of PPs remain ungrouped and are carried forward to the

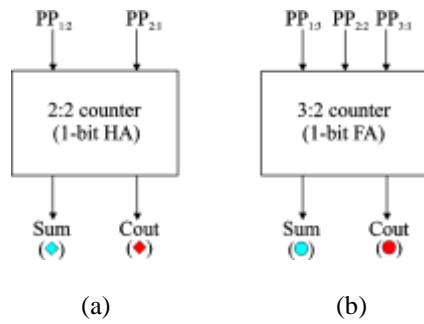


Figure 2: An example of PPC using a) 2:2 counter b) 3:2 counter

next stage for further PPs compression. The grouped PPs are subjected to compressions using a set of counters, this result into the reduction of 6-rows of PPs into 4-rows of PPs. The next level of PPs compression will be carried in the third stage (S3). The stage three (S3) has a total

6-rows of PPs, which are organized into 2-groups and these groups are subjected to PPs compression using appropriate number of counters (3:2 and 2:2 counters). After PPs compression the 6-rows of PPs in S3 will reduce to 4-rows. These 4-rows are further subjected to compression till the number of rows will reduce to 2-rows. The 4-rows of PPs that are the result of PPs compression of S3 will be further grouped and compressed in the next stage (S4). The S4 has total 4-rows of PPs, the first 3-rows of PPs are organized into one group and the remaining 1-row of PPs ungrouped and is carried forward to the next level for PPs compression. After compression of PPs the 3-rows of PPs will reduce to 2-rows of PPs, these 2-rows of PPs along with the 1-row of PPs (uncompressed in S4) are subjected to compression in the next stage S5. The stage S5 has total 3-rows of PPs; these 3-rows of PPs are organized into single group and compressed using a set of counters. After compression the 3-rows of PPs will reduce to 2-rows, thus the PPs compression will be stopped at this level. Finally the 2-rows of the compressed PPs will be added by using CPA adder to get the final product.

PPCM based on Dadda approach:

The PPCM using Dadda based approach is shown in Figure 3b, here also the generated PPs in the form of PPM is converted into the form of RPPM. The RPPM has total 12-rows of PPs and these rows are divided into 4-groups with each group being 3-rows. The divided groups are compressed and reduced to two rows and these two rows of PPs are further added by a CP adder to generate the final product of a multiplier. The compression of PPs into two rows is achieved through different stages viz. S1-S5 using 3:2 and 2:2 counters as shown in the Figure 3b. The number of stages required to compress the PPs can be determined by using Dadda algorithm. The important steps of Dadda algorithm for determining the number of stages required to compress the PPs in 12×12 multiplier are explained as follows:

Let $S_F = 2$ be the height (number of PPs rows) of the final stage or height of the CP stage, then the height of its preceding stages is calculated as given below.

$$S_5 = \lceil 1.5 \times S_F \rceil = 3$$

$$S_4 = \lceil 1.5 \times S_5 \rceil = 4$$

$$S_3 = \lceil 1.5 \times S_4 \rceil = 6$$

$$S_2 = \lceil 1.5 \times S_3 \rceil = 9$$

$$S_1 = \lceil 1.5 \times S_2 \rceil = 13$$

Since the multiplier under consideration is 12×12 , therefore the maximum height of 13 is unnecessary and hence the Dadda algorithm converges. The Figure 3b is the dot diagram of 12×12 bit multiplier using Dadda based PPCM and has total 5-stages viz. S1, S2, S3, S4, and S5. The S1 is the RPPM and has a total of 12 PPs rows, the 12 rows are further divided into 4-groups viz. G1, G2, G3, and G4 with each group being 3-rows. Since the height of the S1 is 12, to achieve the S2 height = 9, the G1, G2, and G3 of S1 are subjected to PP compression using appropriate number of 3:2 and 2:2 counters. This results in stage S2 with the height = 9. Thus the stage S2 has a total 9 rows of PPs in the form of RPPM and these rows are further divided into 3 groups G1, G2, and G3 with each group being of 3-rows of PPs. Further the G1, G2, and G3 of S2 are subjected to compression to achieve the height of S3 = 6. The S3 has total 6 rows of PPs and grouped into G1 and G2. These groups that is G1 and G2 of S3 are subjected to PPs compression to achieve a height of S4 = 4. Further in the 4 rows of S4, the first 3-rows are grouped as G1 and last row is remain ungrouped and is carried forward to the next stage. The G1 of S4 is subjected to the PPs compression to achieve a height of S5 = 3. Thus S5 has a total 3 PPs rows and these 3 PPs rows are grouped as G1, the G1 is subjected to PPs compression to achieve a height of final CP stage = 2.

MICRO ARCHITECTURES OF TSM

The critical units of PPCM and final CP adder of the TSM is the 2:2 and 3:2 counters as shown in Figure-2. The 2:2 counter is a half adder that takes two input signals viz. A and B and produces the two output signals viz. the Sum and the Cout. The 3:2 counter is a pseudo 1-bit adder that takes 3-input signals viz. A, B, and Cin and produces two output signals viz. the Sum and the Cout. The micro-architectures of these counters are as shown in Figure 4. The Figure 4a is the micro-architecture of 2:2 counter (1-bit HA), this architecture has been designed by using static CMOS logic and it conceives a total 16-transistors (16Ts). The Figure 4b is the micro-architecture of 3:2 counter (1-bit FA), this architecture has been derived using a 'mixed logic style' (MLS) and conceives a total 28Ts [14]. The MLS based 3:2 counter (herein referred as 'MLSFA') combines the best advantages of the static CMOS logic and CMOS transmission gate logic. The MLSFA has the low power and low PDP advantages as compared to any other 1-bit FAs as reported in the literature [15].

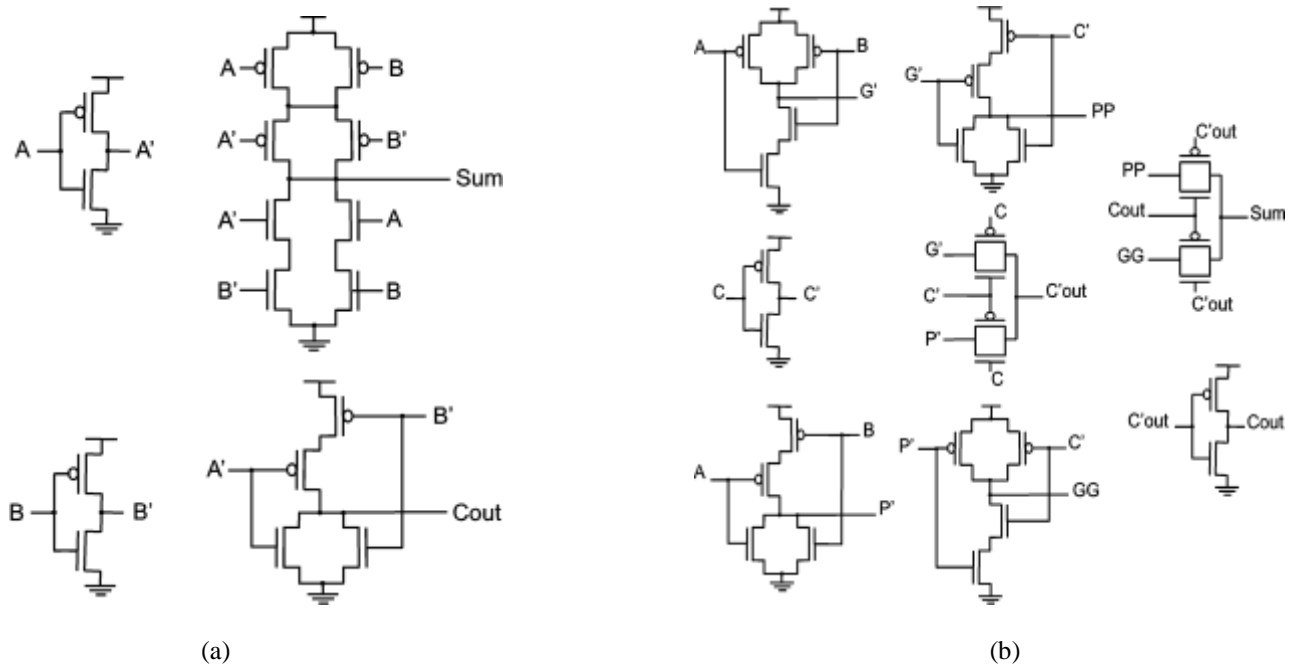


Figure 4: Schematic of a) 2:2 counter (1-bit HA) b) 3:2 counter (1-bit FA)

SIMULATION ENVIRONMENT TO EXTRACT DESIGN METRICS

The test bench that is used to extract DMs such as power, delay, and PDP of a TSM under consideration is as shown in the Figure 5. The 'circuit under test' (CUT) is the Wallace based or the Dadda based $N \times N$ bit TSM. All the TSMs under consideration are designed by using 1-bit FA and 1-bit HA as shown in Figure 4. To extract the DMs of a CUT under consideration we have used standard input test patterns as suggested in [16] and these patterns are listed in the Table-1. In the Table-1, the N in the first column represents the multiplier size, the 'PL' in the second column represents the 'propagation length' of the final CP adder, the 'X' and 'Y' represents the critical vectors that are used to derive the DMs of the respective N bit multiplier.

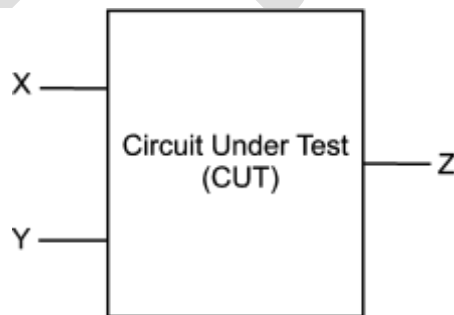


Figure 5: Test bench used to extract the power, propagation delay, and PDP of TSMs under consideration

All the TSM simulations have been carried out under common process-voltage-temperature (PVT) conditions with input signal clock frequency $F_{in} = 200\text{MHz}$. From the Table-1, it is observed that the set of test vectors (X and Y) for each N value are different. Also the propagation length (PL) varies corresponding to each set of test vectors and is linearly increasing with respect to N.

TABLE I
 INPUT TEST VECTORS USED TO EXTRACT WORST CASE POWER AND DELAY OF TSMS

N	PL	Multiplier (X)	Multiplicand (Y)	Product (Z)
5	8	11011	10011	1000000001
6	8	011011	010011	1000000001
7	9	1101011	1000011	1110000000001
8	13	1111011	11000111	1100000000000001
9	14	1110101	111100111	111000000000000001
10	14	0111010	0111100111	111000000000000001
11	18	1111110	1110000111	111000000000000000001
12	18	0111111	0111000011	111000000000000000001
13	21	1011011	1111011100	1011000000000000000000001
14	24	1000000	0011111101	1000000000000000000000001
15	25	0100110	1001111100	110000000000000000000000001
16	28	1011010	1110000110	101000000000000000000000000001

PERFORMANCE COMPARISON OF TREE STRUCTURED MULTIPLIERS

The performance comparison of TSMS under consideration is discussed in terms of the DMs such as power, delay, and PDP. The DMs of the $N \times N$ TSMS that are extracted using the test bench of Figure-5 are listed in the Table- 2. From the Table-2, the important points that are observed for both ‘Wallace tree based TSM’ (WTSM) and ‘Dadda based TSM’ (DTSM) are discussed as below.

- Considering the first row of Table-2, with $N=5$ and $PL=8$; the power dissipation of the WTSM ($14.27\mu W$) is low as compared to DTSM ($14.82\mu W$), whereas the delay of WTSM (0.311 ns) and DTSM (0.312 ns) are comparable. Further the PDP of WTSM (4.45 fJ) is less than that of DTSM (4.62 fJ). The hardware requirement is same for both the TSMS. Thus for $N=5$ the WTSM is power and energy efficient than that of DTSM.
- From the second row of the Table-2, with $N=6$ and $PL=8$, again the WTSM is power and energy efficient as compared to DTSM. Whereas the hardware requirement in terms of adders is less for DTSM as compared to WTSM.
- Observing the third row of the Table-2, with $N=7$ and $PL=9$, the power and delay of WTSM and DTSM are comparable. Whereas the DTSM is more area efficient as compared to WTSM.
- For $N=8$ to $N=16$, it is observed that the DTSM outperforms the WTSM in terms of DMs viz., power, delay, PDP, and area.
- Considering the last row of Table-2, with $N=16$ and $PL=28$; the power dissipation of the WTSM ($181.5 \mu W$) is higher than that of a DTSM ($174.5 \mu W$), whereas the delay of WTSM (1.1 ns) is low as compared to DTSM (0.95 ns). Further the PDP of WTSM (199.6 fJ) is also higher than that of DTSM (166 fJ). Also the hardware requirement in terms of adders is more for WTSM as compared to DTSM.
- Thus from the comparison table, it is observed that the Wallace tree based PPCM is a good a choice for $N=5$ to $N=7$, whereas for $N > 7$, the choice is the Dadda based PPCM.

CONCLUSION

In this paper, the two traditional PPCMs have been compared in terms of power, delay, PDP, and area (in terms of adders) by using two conventional TSMs. To compare the performance of PPCMs, the WTSM and DTSM (in which the PPCMs were embedded) are designed for the sizes of $N=5$ to $N=16$ and simulated using Cadence's EDA tools based on 90nm GPDK. The TSMs have implemented using a 2:2 counter and a 3:2 counters in Cadence's Virtuoso and simulations were carried out using Cadence's Spectre simulator based on 90nm BSIMv3v (level 49) transistor models. All the simulations of the circuits under considerations were carried out at common PVT conditions with $f_{in} = 200$ MHz. From the simulation results it is observed that, for $N=5$ to 7, the WTSM (based on Wallace tree PPCM) has better power and energy efficiency as compared to DTSM (based on Dadda PPCM). For $N > 7$ the DTSM has better performance in terms of power, delay, PDP, and area than the WTSM. Thus depending on the size of 'N' and an application, one can have an option to choose the required PPCM to trade-off between the DMs.

REFERENCES:

- [1] Cheng-Xiang Wang et al.: "Cellular architectures and key technologies for 5G wireless communication networks" IEEE Communications Magazine, pp. 122-130, Feb. 2014.
- [2] F. Akyildiz, David M. Gutierrez-Estevez, and Elias Chavarria Reyes: "The evolution to 4G cellular systems: LTE-Advanced". Elsevier Journal of Physical Communication, 2010, pp. 217-244.
- [3] '2013PIDS_Summary.pdf', <http://www.itrs.net/ITRS>.
- [4] Bennet C. Wong, and Henry Samueli, "A 200MHz All-Digital QAM Modulator and Demodulator in 1.2 μ m CMOS for Digital

- Radio Applications,” IEEE Journal of Solid State Circuits, vol. 26, no 12, pp. 1970-1979, Dec. 1991.
- [5] F. P. Chan, M. P. Quirk, and R. F. Jurgens, “High-Speed Digital Baseband Mixer,” TDA Progress Report 42-81, Communication System Research Section, January-March, pp. 63-80, 1985.
- [6] Byung-Do Yang, Jang-Hong Choi, Seon-Ho Han, Lee-Sup Kim, and Hyun-Kyu Yu, “An 800 MHz Low-Power Direct Digital Frequency Synthesizer With an On-Chip D/A Converter,” IEEE Journal of solid-state circuits, Vol. 39, no. 5, pp. 761-774, May 2005.
- [7] Loke Kun Tan, and Henry Samuelli, “A 200MHz Quadrature Digital Synthesizer/Mixer in 0.8 μ m CMOS,” IEEE Journal of Solid State Circuits, Vol. 30, No. 3, pp. 193-200, March 1995.
- [8] A. Yamagishi, M. Ishikawa, T. Tsukahara, and S. Date, “A 2-V, 2-GHz low-power direct digital frequency synthesizer chip-set for wireless communication,” IEEE J. Solid-State Circuits, vol. 33, pp. 210-217, Feb. 1998
- [9] A. M. Sodagar and G. R. Lahiji, “Mapping from phase to sine-amplitude in direct digital frequency synthesizers using parabolic approximation,” IEEE Trans. Circuits Syst. II, vol. 47, pp. 1452-1457, Dec. 2000.
- [10] J. M. P. Langlois and D. Al-Khalili, “ROM size reduction with low processing cost for direct digital frequency synthesis,” in Proc. IEEE Pacific Rim Conf. Communications, Computers and Signal Processing, pp. 287-290, Aug. 2001.
- [11] C. S. Wallace, “A suggestion for parallel multipliers,” IEEE Trans. Electron Comput., vol. EC-13, no. 1, pp. 14-17, Feb. 1964.
- [12] L. Dadda, “Some schemes for parallel multipliers”, Alta Frequenza, vol. 34, March 1965.
- [13] Wen-Chang Yeh, and Chein-Wei Jen, “High-speed booth encoded parallel multiplier design,” IEEE Trans. Computers, Vol. 49, No. 7, pp. 692-701, July 2000.
- [14] Parameshwara M. C. and Srinivasaiah H. C. “Study of Power-Delay Characteristics of a Mixed-Logic-Style Novel Adder Circuit at 90nm Gate Length”, IJCA, vol. 119, no 4, pp 27-33, June 2015.
- [15] Parameshwara M. C. and Srinivasaiah H. C. “Choice of Adders for Multimedia Processing Applications: Comparison of Various Existing and a Novel 1-Bit Full Adder”, IOSR, vol. 10, no 3, pp 69-73, May 2015.
- [16] Henrik Eriksson, Per Larsson-Edefors, and Daniel Eckerbert, “ Toward Architecture-Based Test-Vector Generation for Timing Verification of Fast Parallel Multipliers,” , IEEE Trans. VLSI systems, vol. 14, no. 4, April 2006.

Performance analysis of fiber reinforced composite spring Embedded with steel wire

Bhaskar U¹, Guruchethan A M², Devendra Reddy M³

^{1,2,3}Assistant Professor, MED, SVCE, Bengaluru, ²guruchethanam@gmail.com, +919591275426

Abstract— Helical spring is the most common element that has been used in many automobile suspension systems. In this work, hybrid spring are fabricated using the composite material and steel wire as a core material, helical spring related to light vehicle suspension system under the effect of a uniform loading has been studied and finite element model has been developed to compare with analytical solution. In the present work three different types of hybrid helical springs using cross-woven glass fiber, cross-woven carbon fiber and combined glass and carbon fiber along with a steel wire as a core material have been fabricated. Tests were conducted on these specimens to study their mechanical behavior. The spring rate and deflection with respect to various loading condition have been evaluated. The results of these parameters with respect to the above three specimen have been compared with one another. The present study is an attempt to observe the feasibility of replacing composite coil spring in place of conventional steel spring. It is concluded that through a modification in the cross-section design of coil spring and with a proper material combination, it is possible to improve the properties of composite coil springs.

Keywords— Composite material, helical spring, glass fibre, steel wire, spring constant, spring deflection, filament winding.

INTRODUCTION

Springs are crucial suspension elements on automobiles which are necessary to minimize the vertical vibrations impacts and bumps due to road irregularities and create a comfortable ride. Coil springs are commonly used for automobile suspension and industrial applications. Presently the automobile production companies are showing an interest for replacement of conventional steel helical spring with composite helical spring due to their high strength to weight ratio property. The replacement of steel parts by composite materials yields, significant weight savings. But as with many new materials, design and manufacturing problems arise. The composite materials made it possible to reduce the weight of the springs without any reduction of load carrying capacity and stiffness. Studies were conducted on the application of the composite spring for automobiles and then compared to steel spring efficiency. Hybrid springs are also adopted for replacing the conventional spring to increase the efficiency of hybrid springs they are manufactured by combining the different material in different composition. The effect of hybridization on hybrid springs with standard cross-section was investigated and optimum hybrid spring was determined according to cost and maximum loading capacity, it is determined that carbon/epoxy plies are used for outer layers and are more advantageous. But the outer ply subjected to force was damaged thus this layer should be particularly reinforced.

The main factor to be considered in the design of the spring is the strain energy of the material. The type of stresses acting in the compression loading of the spring is the direct shear and torsion. The stiffness of the spring is also very important property which is obtained by load divided by deflection. For the purpose of saving energy and improving the performance of the shock absorbers, with light weight and high quality, composite materials have to be used for to present vehicles. With more number of electric vehicles and hybrid vehicles are entering into the market in the present-days.

In this study spring for two wheelers is taken for replacement, Glass fiber and carbon fiber is used to manufacture the composite hybrid helical spring. But as with many new materials, design and fabrication problems arise. The main reason is that fiber reinforced plastic composites are anisotropic materials, which are quite different from traditional materials. Hence the applications of composites in the manufacture of springs are not yet popular. Fiber reinforced polymers have been developed for many applications, mainly because of the potential weight savings, the possibility of reducing noise, vibrations and ride harshness due to their high damping factors, the absence of corrosion problems, which lowers maintenance costs, which has favorable impact on the manufacturing costs. However, due to the availability and cost limitation, the present work was restricted to the study of helical spring made from glass fiber and carbon fiber cross woven. It presents advantages over graphite/ epoxy such as lower sensitivity to cracks, impact and wear damage.

Several papers were devoted to the application of composite materials for automobiles. I Rajendran studied the applications of composite structures for automobiles and design optimization of a composite leaf spring. Chang-Hsuan et al. (2007) have investigated the mechanical behaviors of helical composite springs. They have developed four different types of springs made of unidirectional laminates, rubber core unidirectional laminates, unidirectional laminates with a braided outer layer and rubber core

unidirectional laminates with a braided outer layer. Faruk (2009) investigated the dynamic behavior of composite coil springs of arbitrary shape. Abdul et al. (2010) have investigated the influence of ellipticity ratio on the performances of woven roving wrapped composite elliptical springs both experimentally and numerically. Many more researchers have been investigated on elliptical springs, leaf springs and C springs. Research on fiber reinforced composite helical spring is not popular due to manufacturing difficulties. This paper discusses the feasibility of using fiber reinforced composite helical spring for automobile suspension. It is well documented in the literature that the energy storage capacity of rectangular spring is more: also found that less amount of work is carried out on this variety of springs. Hence for the experimentation rectangular cross section is chosen

MATERIALS AND METHODS

Materials

The fibers chosen for the spring design are cross-woven glass fiber and cross-woven carbon fiber with steel wire as a core material for fabrication, In order to facilitate the wetting of fibers; epoxy resin is selected. L-12/K-6 Lapox epoxy system for laminating applications is used. The properties of the material are given in Table1.

Table 1: Properties of E-glass/ Epoxy Resin

Properties	E-Glass/Epoxy
Young’s modulus in fiber direction, E ₁ (GPa)	53.8
Young’s modulus in transverse direction, E ₂ (GPa)	17.9
Shear modulus, G ₁₂ (GPa)	8.96
Major Poisson’s ratio, v ₁₂	0.25
Minor Poisson’s ratio, v ₂₁	0.08
Strength in fiber direction, X ₁ (MPa)	1.03*10 ³
Strength in transverse direction, X ₂ (MPa)	27.58
Shear strength, S (MPa)	41.37

Design of Composite hybrid helical spring	Design of conventional spring
• Outer diameter : 60mm	1. Outer Diameter : 55mm
• Mean diameter : 48mm	2. Mean Diameter : 50mm
• Width of wire : 12mm	3. Diameter of wire : 10mm
• Thickness of wire : 10mm	

Calculation of the width and thickness of the rectangular spring

The stress in the rectangular section spring. The axial deflection in the rectangular section spring.

$$\tau_{max} = KFD \frac{1.5h+0.96b}{b^2} h^2$$

Where $K = \frac{4c-1}{4c-4} + \frac{0.615}{c} = \frac{b}{h}$

b= width of the spring and h= Thickness of the spring in mm.

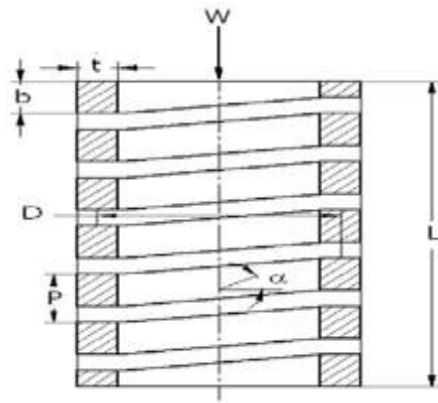


Fig 1: Spring with rectangular cross-section



Fig 2: Helical groove cutting process.

Fabrication

The manufacturing process followed in this work is a variation of filament winding process. In this method a mandrel as shown in Figure 2 is prepared with Mild steel or any other material.

In this, the mandrel having a shape of the spring profile is fixed between the centers of the lathe. A mould release agent silicone-gel/grease is applied on the mandrel. Since the load acting on the compression is shear, the fiber is cut in 90 degree orientation as shown in Fig 4. In order to form the hybrid helical spring the stainless steel strip is used in between the fibers at the center of the spring thickness.

The measured quantity of Epoxy resin matrix material is taken. The fiber tape with steel strip after dipping in the epoxy resin is wound on the mandrel. This process of winding the tape on the mandrel is continued till the thickness of the spring is obtained on the mandrel. After the completion of winding, the shrink tape is wound on the mandrel as shown in Fig 3. The mandrel with the fibers kept for curing in atmospheric temperature for 48 hours. After curing the spring is removed from the mandrel by turning operation in a lathe as shown in the Fig 3(a). The cured spring has the dimension of $L=180\text{mm}$, $D_0=60\text{mm}$, $D=48\text{mm}$, $b=12\text{mm}$, $t=10\text{mm}$ and $n=9$. The same procedure is followed for glass and carbon fiber springs. And for glass/carbon fiber springs, one layer of carbon fiber and one layer of glass fibers are to be bonded with resin for winding on the mandrel. Fabricated springs are shown in the Fig 5.



Fig 3: Tube strip wound on mandrel



Fig 3(a): Tube strip is removed from mandrel



Fig 4: Fiber and steel strip with 90° orientations

Fig 5: Models of the helical spring

Experimental Methods

The main parameters to be considered in the application of spring stiffness, failure load, maximum compression and physical dimensions. There is no deviation obtained in the physical dimension of the fabricated spring. Experiments were conducted as per ASTM standards and the results are shown in table 2.

Table 2: Details of composite and conventional steel spring

Properties	Composite spring	Conventional spring
Spring constant (N/mm)	4	5
Maximum Compression (mm)	80	85
Load at Max compression (N)	175	6461.52
Failure Load (N)	1000	7000
Shear stress (N/mm ²)	15.185	82.270
Weight of spring (g)	260	560
Pitch (mm)	22	24

RESULTS AND DISCUSSION

The main objective of this study is to find the feasibility of replacing metal coil spring with the composite hybrid spring for automotive suspension and to study their mechanical properties. In order to improve reliability of the Experimental results for three sets of springs were fabricated and tests were conducted on these springs. Experimental results are compared with theoretical results by graphical representation Fig 6.

Load-Displacement curve for Hybrid Spring Models

The load-deflection or stiffness test results for three different springs are obtained automatically from the Universal testing machine manually operating which generates the load-deflection.

The load-deflection curves for the three types of springs are shown in Fig 6. A linear cure is obtained for all the three types of springs. A small variation is observed in the curves of the specimens are observed in the three spring. This variation is due to the

dimensional variations in the fabrication process. The values of the load and the deflection of all the three springs are given in Table 3 and the corresponding curves are shown in Figure 6.

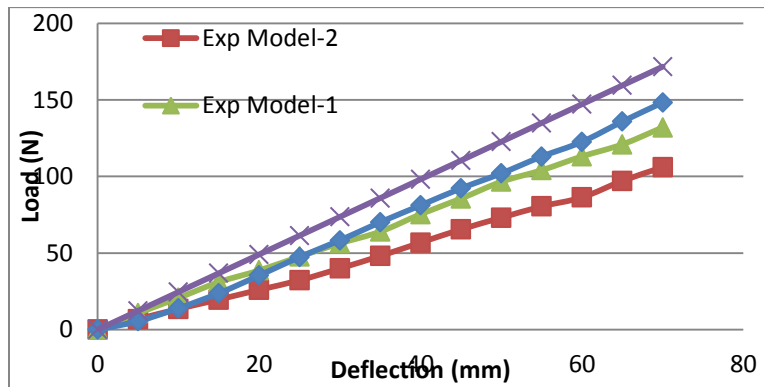


Fig 6: Load- deflection plots for Theoretical and Experimental spring models

Table 3: The values of Load and Deflection of Three spring models

Displacement (mm)	Composite Hybrid Spring			Theoretical
	Model-1	Model-2	Model-3	Spring
	Load (N)	Load (N)	Load (N)	Load(N)
0	0	0	0	0
5	10.693	6.867	5.494	12.265
10	20.699	13.534	13.931	24.531
15	30.999	19.62	23.741	36.797
20	38.652	25.996	35.316	49.063
25	47.676	32.176	47.383	61.329
30	56.309	39.926	58.272	73.595
35	63.961	48.069	70.142	85.861
40	75.341	56.80	81.128	98.127
45	85.543	65.433	92.214	110.394
50	96.531	73.085	102.024	122.659
55	104.084	80.442	113.012	134.925
60	113.109	86.328	122.625	147.191
65	120.957	97.119	135.869	159.457
70	132.043	106.046	148.323	171.723

Load-Stiffness plot for composite Hybrid spring Models

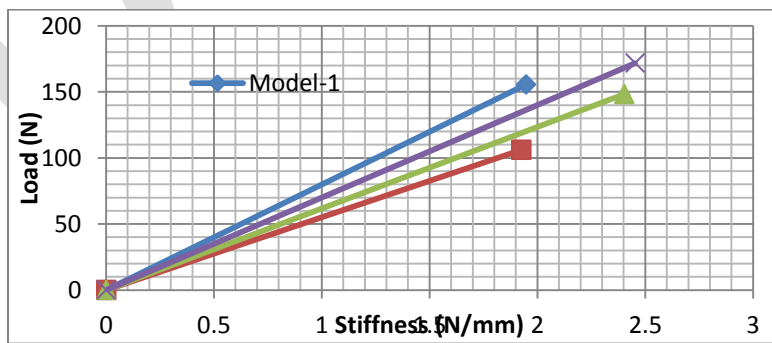


Fig 7: Load-Stiffness plot for Composite hybrid spring

The load- stiffness for composite hybrid spring is as shown in the above fig 7. It is clearly observed from the above graph that the stiffness of the spring model-3 is very close to the theoretical spring model than the remaining models 2 & 3.

Load-Deflection Curve for conventional steel spring over composite hybrid spring

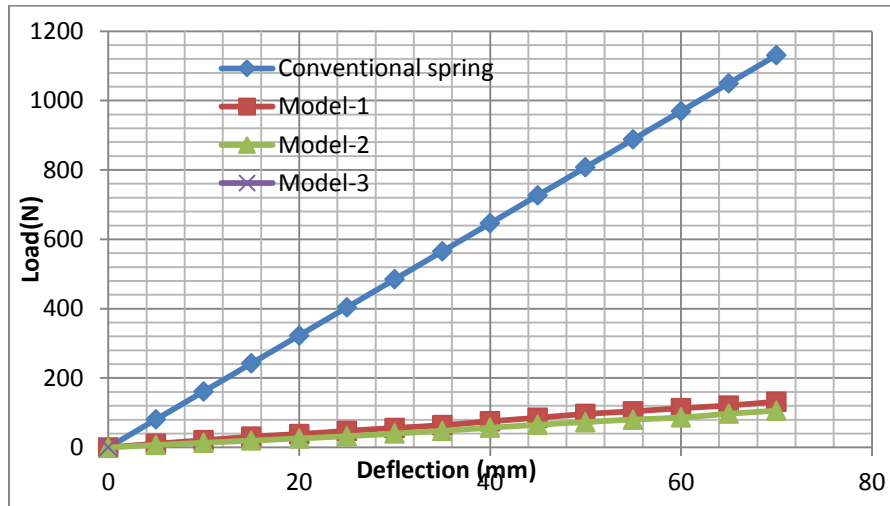


Fig 8: Load-Deflection plot for conventional spring over composite spring

The above graph shows the comparison of the conventional steel spring with composite hybrid helical spring. It is observed that the conventional steel spring having more load carrying capacity over the composite hybrid spring, among the composite hybrid spring the model-3 has more load carrying capacity than the model 1 & 2.

Weight of composite hybrid helical spring

The weight of the composite helical compression spring is obtained theoretically by considering the area and length of the rectangular wire and density of the composite material. The fiber volume fraction and mass matrix volume fraction is calculated by using the rule of mixture method

Table 4: Weight of the spring obtained

Spring number	Fiber volume fraction	Theoretical Weight (grams)	Fiber mass fraction	Experimental Weight (grams)	Difference in weight (grams)
Model-1	0.55	283	0.726	246	37
Model-2	0.60	293.72	0.765	256	37.72
Model-3	0.70	313.92	0.835	260	53.92

The theoretical weight of the conventional steel helical spring is 548 grams. The average experimental weight of the composite material hybrid spring is 254grams, in which the spring contains of steel strip of weight 40grams. As compared to the weight of the metal spring and experimental weight of the composite hybrid spring 53.65% of weight reduction is achieved.

CONCLUSION

Composite hybrid springs with different combination were subjected to different test under different loading condition. The test results have drawn the following conclusions.

- Load deflection results for hybrid helical spring shows large variations in deformations up to 171.723N. Subsequently the variations in deformations reduced as there is lesser gap between the coils
- On comparing the deflection values of hybrid composite helical springs with that of conventional steel spring, it is observed that 60% of the load that is required for steel spring is sufficient for the full compression of hybrid composite spring.

- For a set of specific design parameters of the helical compression spring on comparing with the conventional steel helical spring for the similar set of parameters the weight of the hybrid composite spring is 54% less than the conventional steel spring.
- The axial stress computed on the steel spring is about 945.9MPa, whereas the stress on composite helical spring is 19.523MPa.

In order to achieve better stiffness results on hybrid composite helical springs it is required to incorporate certain modification in the design parameters and material combination.

REFERENCES:

- 1] Chang-Hsuan Chiu, Chung-Li Hwan, Han-Shuin Tsai, Wei-Ping Lee. "An experimental investigation into the mechanical behaviors of helical composite springs", vol-77(2007), 331-340.
- 2] Bruno KAISER and Christina BERGER. "Recent findings to the fatigue properties of helical springs"
- 3] James M. Meagher and Peter Altman. "Stresses from flexure in composite helical implantable lead spring" S1350-4533(96) 00022-7.
- 4] D. Abdul Budan, T.S. Manjunatha. "Investigation on the Feasibility of Composite Coil Spring for Automotive Applications", vol 46(2010).
- 5] B S Azzam. "An optimum design for composite helical springs", AL -Jouf 2014, Egypt.
- 6] V Yildirim. "Free vibration of uniaxial composite cylindrical helical springs with circular section". Journal of Sound and Vibration, vol-239(2), 2001, 321-333.
- 7] W.H. Wong, P.C. Tse, K.J. Lau, Y.F. Ng. "Spring constant of fibre-reinforced plastics circular springs embedded with nickel-titanium alloy wire" vol 65(2004), 319-328.
- 8] Gulur Siddaramanna Shiva Shankar*, Sambagam Vijayarangan, "Mono Composite Leaf Spring for Light Weight Vehicle – Design, End Joint Analysis and Testing" vol. 12, No.3.2006
- 9] B. Ravi Kumar, Swapan K. Das, D.K. Bhattacharya. "Fatigue failure of helical compression spring in coke oven batteries". Engineering Failure Analysis 10 (2003) 291–296.
- 10] H.A. Al-Qureshi. "Automobile leaf springs from composite materials" vol 118(2001), 58-61.
- 11] Faruk Firat Calim. "Dynamic analysis of composite coil springs of arbitrary shape" Vol 40(2009), 741-757.
- 12] Mehdi Bakhshesh and Majid Bakhshesh. "Optimization of Steel Helical Spring by Composite Spring". International journal of multidisciplinary science and engineering, vol.3, No.6, June 2012.

A SENSORLESS SLIDING MODE CONTROL BASED INDUCTION MOTOR DRIVE FOR INDUSTRIAL APPLICATION

¹ LAVANYA.S ² MOHAMED APPAS.J ³ SURESH KUMAR.P ⁴ VIJAYALAKSHMI.V ⁵JENIFER ROSNEY.J

DEPARTMENT OF ELECTRICAL AND ELECTRONICS ENGINEERING
MAHARAJA INSTITUTE OF TECHNOLOGY, COIMBATORE
EMAIL: jeniferrosney.john@gmail.com/ Ph.No. 9566650283

Abstract— Parameter identification plays an important role in speed estimation schemes. This paper presents a speed estimation scheme based on second-order sliding-mode super twisting algorithm (STA) and model reference adaptive system (MRAS) estimation theory, in which both variations of stator resistance and rotor resistance are deliberately treated. A stator current observer is designed based on the STA, which is utilized to take the place of the reference voltage model of the standard MRAS algorithm. The observer is insensitive to the variation of rotor resistance and perturbation when the states arrive at the sliding mode. Derivatives of rotor flux are obtained and designed as the state of MRAS, thus eliminating the integration. Furthermore, in order to improve the near-zero speed operation, a parallel adaptive identification of stator resistance is designed relying on derivatives of rotor flux and stator current. Compared with the first-order sliding-mode speed estimator, the proposed scheme makes full use of the auxiliary sliding-mode surface, thus alleviating the chattering behavior without increasing the complexity. The robustness and effectiveness of the proposed scheme have been validated experimentally.

Keywords— DC link, Induction Motor, Inverter, Inverse Park transformation, Model reference adaptive system, PI controller, Park Transformation, PWM, Rectifier, Sliding Mode Technique.

1. INTRODUCTION

With the invention of vector control technique the induction motor (IM) became popular for variable-speed drives and motion control. In indirect vector control of IM, flux and torque are decoupled under estimation of the slip speed with appropriate information of the rotor time constant. The accuracy of motor parameters, particularly, the rotor time constant plays an important role for the accuracy of the indirect vector method. To cope with that, recently, variable- structure controls (VSC), and in particular, sliding-mode control (SMC) system, have been applied for electric motor drive. The SMC-based drive system has many attractive features such as: 1) it is robust to parameter variations and model uncertainties and insensitive to external load disturbance; 2) it offers a fast dynamic response, and stable control system; 3) it can handle some nonlinear systems that are not stable by using linear controller; and, 4) it requires an easy hardware/software implementation. However, due to discontinuous nature, it has some limitations in electrical drives and shows high-frequency oscillations as chattering characteristics.

The chattering makes various undesirable effects such as current harmonics and torque pulsation. In recent years, the chattering issue has become the research focus of many scholars. Generally, introducing a thin boundary layer around the sliding surface can solve the chattering problem by interpolating a continuous function inside the boundary layer of switching surface. However, the slope of the continuous function is a compromise between control performance and chattering elimination. Also, asymptotic stability is not guaranteed and may cause a steady-state error.

2. OBJECTIVES OF THE THESIS

The objectives of the thesis are listed below:

- To reduce the overshoot of the DC link in existing system.
- To measure the speed without sensors.
- To use sliding mode technique to estimate speed.
- To acknowledge the efficient working of the existing system using this proposed system in the company.
- To design a model sufficient to prove the result.

3. BLOCK DIAGRAM OF EXISTING SYSTEM

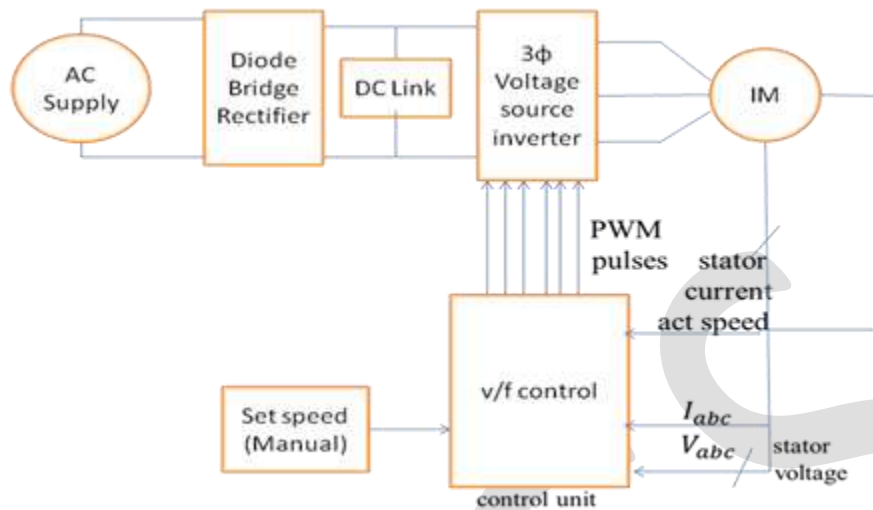


Fig 3.1: Block diagram of existing system.

The above block diagram shows the existing system, in this AC Supply given to diode bridge rectifier circuit. The input supply is converted to DC. The DC link circuit act as a mediator reducing the harmonics and over shoots. The DC link circuit output is input to three Phase voltage source inverter. The voltage source inverter drives the induction motor by converting by DC input to AC output. By using sensor we calculate actual speed, current, voltage. It is given to conventional PI controller and V/F controller and its compare the actual speed and set speed. The feedback is given to the PWM generator. The PWM generator is triggers the voltage source and thus the induction motor is controlled using direct input method.

3.1 DRAWBACKS

- Using more sensors.
- Cost is high.

4. BLOCK DIAGRAM OF PROPOSED SYSTEM

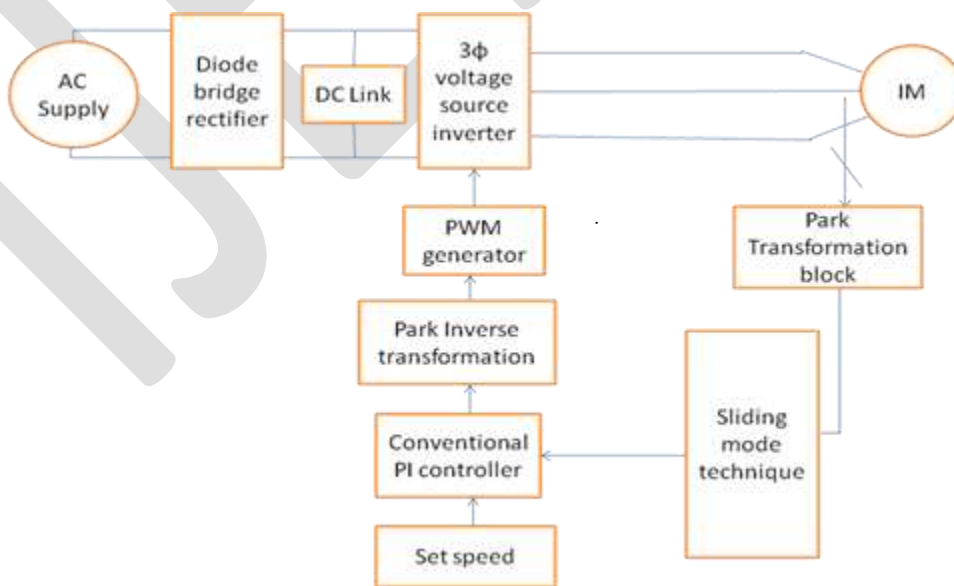


Fig 4.1 Block diagram of proposed system.

The above block diagram shows the proposed system, in this AC Supply given to diode bridge rectifier circuit. The input supply is converted to DC. The DC link circuit act as a mediator reducing the hormones and over shoots. The DC link circuit output is input to three Phase voltage source inverter. The output current of voltage source inverter is given to park transformation. The park transformation converts the three phase current (I_a, I_b, I_c) to two phase current (I_d, I_q). From this current is taken as a reference and its used in sliding mode technique. In sliding mode technique we calculate the actual speed, magnetic flux, torque, rotor position. The output is given to control unit then it compare the actual speed and set speed. The feedback is given to inverse park transformation. The inverse park transformation is convert two phase current (I_d, I_q) to three phase current (I_a, I_b, I_c). The output current is given to the PWM generator and it triggers the voltage source and thus the induction motor is controlled using direct input method.

4.1 DRAWBACKS

The conventional H- Bridge inverter produces only two levels of output, it contains higher order of harmonics say third level . Say 50% of THD. The system consists of power electronics filters like inductive and capacitive for filtering purpose. This increases the cost and weight of the system. To overcome these drawback a new modified system is proposed .

5. UNIVERSAL BRIDGE

The power bridges example illustrates the use of two Universal Bridge blocks in an ac/dc/ac converter consisting of a rectifier feeding an IGBT inverter through a DC link. The inverter is pulse-width modulated (PWM) to produce a three-phase 50 Hz sinusoidal voltage to the load. In this example the inverter chopping frequency is 4000 Hz.

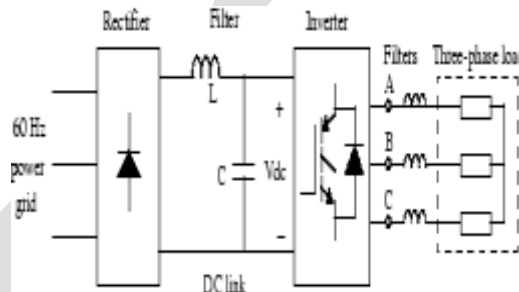


Fig 5.1 Example of universal bridge.

The IGBT inverter is controlled with a PI regulator in order to maintain a 1 pu voltage (380 Vrms, 50 Hz) at the load terminals. A Multimeter block is used to observe commutation of currents between diodes 1 and 3 in the diode bridge and between IGBT/Diodes switches 1 and 2 in the IGBT Bridge. Start simulation. After a transient period of approximately 40 ms, the system reaches a steady state. Observe voltage waveforms at DC bus, inverter output, and load on Scope1. The harmonics generated by the inverter around multiples of 2 kHz are filtered by the LC filter. As expected the peak value of the load voltage is 537 V (380 V RMS).

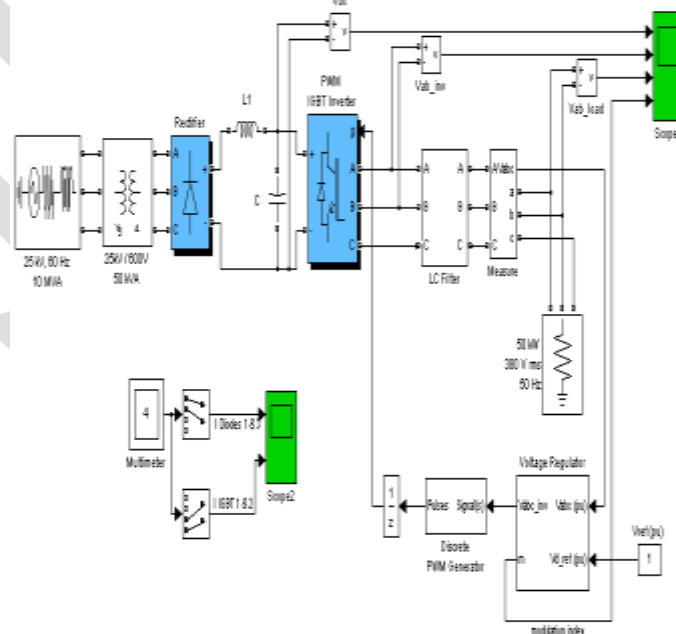


Fig 5.1 Simulation diagram of universal bridge.

In steady state the mean value of the modulation index is $m = 0.8$, and the mean value of the DC voltage is 778 V. The fundamental component of 50 Hz voltage buried in the chopped inverter voltage is therefore

$$V_{ab} = 778 \text{ V} * 0.612 * 0.80 = 381 \text{ V RMS}$$

Observe diode currents on trace 1 of Scope2, showing commutation from diode 1 to diode 3. Also observe on trace 2 currents in switches 1 and 2 of the IGBT/Diode bridge (upper and lower switches connected to phase A). These two currents are complementary. A positive current indicates a current flowing in the IGBT, whereas a negative current indicates a current flowing in the antiparallel diode.

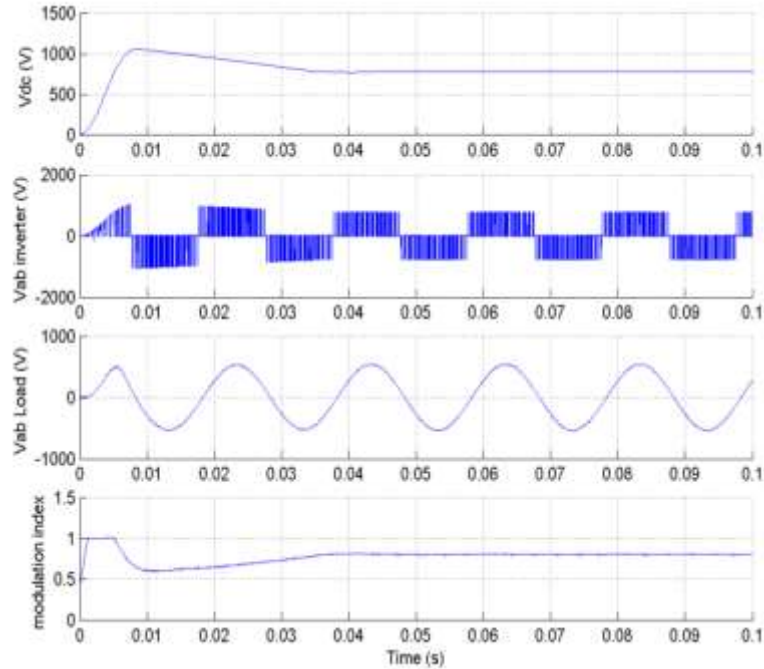


Fig 5.2 Time(s) vs Modulation index, Vab load(v), Vab inverter(v), Vdc(v)

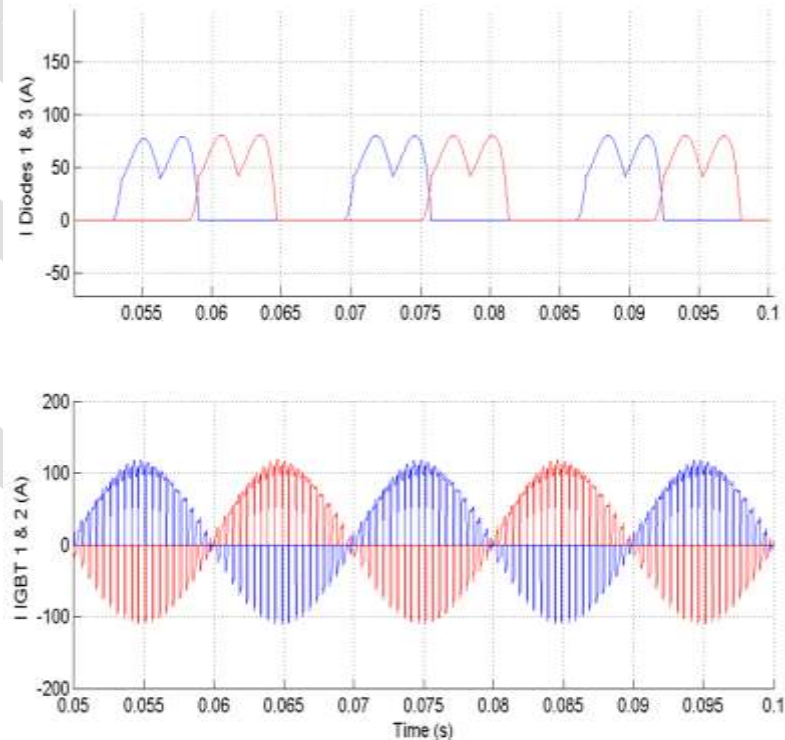


Fig 5.3 Time(s) vs IGBT & Diode

6. INTRODUCTION TO PARK TRANSFORMATION

Perform Park transformation from three-phase (abc) reference frame to dq0 reference frame. The ransformations section of the Control and Measurements library contains the abc to dq0 block. This is an improved version of the abc_to_dq0 Transformation block. The new block features a mechanism that eliminates duplicate continuous and discrete versions of the same block by basing the block configuration on the simulation mode. If your legacy models contain the abc_to_dq0 Transformation block, they continue to work. However, for best performance, use the abc to dq0 block in your new models.

6.1 DESCRIPTION

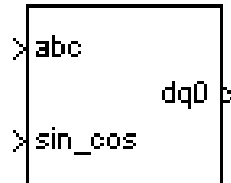


Fig 6.1: Park transformation.

The abc_to_dq0 Transformation block computes the direct axis, quadratic axis, and zero sequence quantities in a two-axis rotating reference frame for a three-phase sinusoidal signal. The following transformation is used:

$$V_d V_q V_0 = 23(V_a \sin(\omega t) + V_b \sin(\omega t - 2\pi/3) + V_c \sin(\omega t + 2\pi/3)) = 23(V_a \cos(\omega t) + V_b \cos(\omega t - 2\pi/3) + V_c \cos(\omega t + 2\pi/3)) = 13(V_a + V_b + V_c),$$
 where ω = rotation speed (rad/s) of the rotating frame.

The transformation is the same for the case of a three-phase current; you simply replace the $V_a, V_b, V_c, V_d, V_q,$ and V_0 variables with the $I_a, I_b, I_c, I_d, I_q,$ and I_0 variables.

This transformation is commonly used in three-phase electric machine models, where it is known as a Park transformation. It allows you to eliminate time-varying inductances by referring the stator and rotor quantities to a fixed or rotating reference frame. In the case of a synchronous machine, the stator quantities are referred to the rotor. I_d and I_q represent the two DC currents flowing in the two equivalent rotor windings (d winding directly on the same axis as the field winding, and q winding on the quadratic axis), producing the same flux as the stator $I_a, I_b,$ and I_c currents.

You can use this block in a control system to measure the positive-sequence component V_1 of a set of three-phase voltages or currents. The V_d and V_q (or I_d and I_q) then represent the rectangular coordinates of the positive-sequence component.

You can use the Math Function block and the Trigonometric Function block to obtain the modulus and angle of V_1 :

$$\downarrow V_1 \downarrow \angle V_1 = G V_{2q} + V_{2d} = \text{atan2}(V_q/V_d).$$

This measurement system does not introduce any delay, but, unlike the Fourier analysis done in the Sequence Analyzer block, it is sensitive to harmonics and imbalances.

6.2 DIALOG BOX AND PARAMETERS

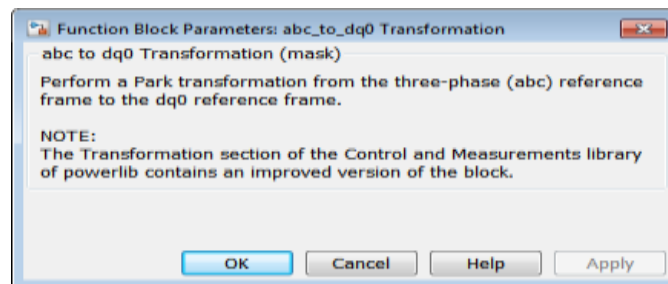


Fig 6.2: Dialog box and parameters.

6.3 INPUTS AND OUTPUTS

abc

Connect to the first input the vectorized sinusoidal phase signal to be converted [phase A phase B phase C].

sin_cos

Connect to the second input a vectorized signal containing the $[\sin(\omega t) \cos(\omega t)]$ values, where ω is the rotation speed of the reference frame.

dq0

The output is a vectorized signal containing the three sequence components [d q o], in the same units as the abc input signal.

7. INTRODUCTION TO INVERSE PARK TRANSFORMATION

The Four Axis instance of this VI requires fixed size four elements arrays (one per axis) for all inputs, and returns fixed size four element array outputs. Calculates the Inverse Park Transform portion of the field-oriented control (FOC) commutation algorithm. The Inverse Park Transform modifies the flux,torque (d,q) rotating reference frame into a two phase orthogonal system (alpha,beta). The output is called the voltage vector. The data type you wire to any input determines the polymorphic instance to use.

7.1 Inverse Park Transformation (Single Axis)

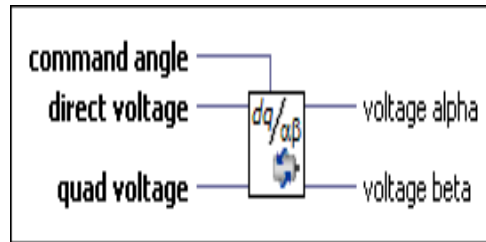


Fig 7.1 Single axis of inverse park transformation.

command angle—Specifies the calculated flux angle for the Park and Inverse Park transforms, in pi radian

direct voltage—Specifies the direct voltage value calculated by the flux/torque loop for use with the Inverse Park Transform.

quad voltage—Specifies the quad voltage value calculated by the flux/torque loop for use with the Inverse Park Transform.

voltage alpha—Specifies the alpha voltage calculated by the Inverse Park Transform for the Space Vector Modulation function.

voltage beta—Specifies the beta voltage calculated by the Inverse Park Transform for the Space Vector Modulation function.

7.2 Inverse Park Transformation (Four Axis)

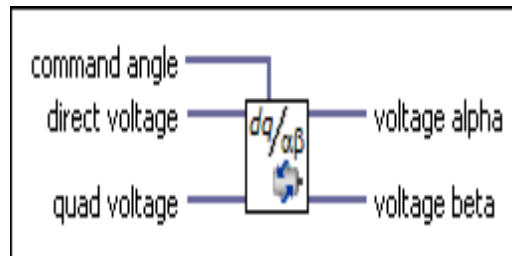


Fig 7.2 Four axis of inverse park transformation.

command angle—Specifies the calculated flux angle for the Park and Inverse Park transforms, in pi radians.

direct voltage—Specifies the direct voltage value calculated by the flux/torque loop for use with the Inverse Park Transform.

quad voltage—Specifies the quad voltage value calculated by the flux/torque loop for use with the Inverse Park Transform.

voltage alpha—Specifies the alpha voltage calculated by the Inverse Park Transform for the Space Vector Modulation function.

voltage beta—Specifies the beta voltage calculated by the Inverse Park Transform for the Space Vector Modulation function.

7.3 DETAILS

Use the Inverse Park Transform function to calculate the Inverse Park Transform portion of the field-oriented control (FOC) commutation algorithm, which modifies the flux, torque (d,q) rotating reference frame in a two phase orthogonal system (alpha, beta).

The Inverse Park Transform uses the following equations:

$$v_{\alpha} = v_d \cos \theta - v_q \sin \theta$$

$$v_{\beta} = v_d \sin \theta + v_q \cos \theta$$

Where

v_{α} is the alpha voltage,

v_d is the direct voltage,

v_q is the quad voltage,

v_{β} is the beta voltage, and

θ is the angle of rotation for the transformed reference frame.

The following figure shows the NI Soft Motion FOC commutation algorithm block diagram, and the location of the Inverse Park Transform within it.

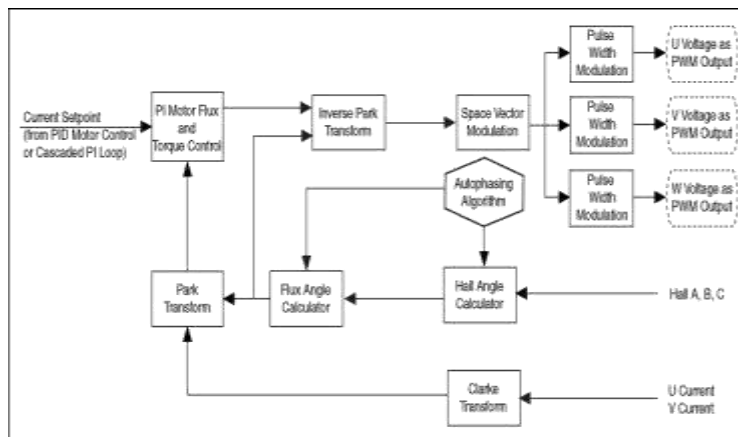


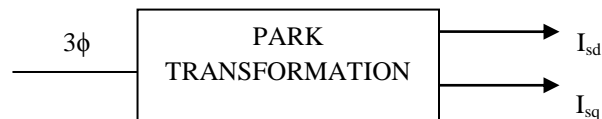
Fig 7.3 Block diagram NI Soft Motion FOC commutation algorithm.

7.4 FIXED-POINT DETAILS

The Motor Control VIs use fixed-point values when possible. When you wire fixed-point values to Motor Control VIs, the VIs usually return values that do not lose any bits of word length. However, if the operation creates a value that exceeds the maximum word length that LabVIEW accepts, overflow or rounding conditions can occur. LabVIEW accepts a maximum word length of 64 bits. Refer to Using the Fixed-Point Data Type in the FPGA Module help for information about how fixed-point numbers might impact timing.

8. SLIDING MODE TECHNIQUE

8.1 STATOR CURRENT:



The park transformation converts the three phase current to two phase (Isd, Isq)

I_{abc} = Stator current

I_{sd} = Stator direct current

I_{sq} = Stator quadrature current

8.2 STATOR VOLTAGE:



The park transformation converts the three phase current to two phase (V_{sd}, V_{sq})

V_{abc} = Stator voltage

V_{sd} = Stator direct voltage

V_{sq} = Stator quadrature voltage

STATOR FLUX :

$$\varphi_{sd} = \int V_d - R_s \cdot I_{sd} \quad (1)$$

$$\varphi_{sq} = \int V_q - R_s \cdot I_{sq} \quad (2)$$

Where,

$$I_{sd} = \frac{2}{3} \left(I_a - \frac{1}{2} I_b - \frac{1}{2} I_c \right) \quad (3)$$

$$I_{sq} = -\frac{2}{3} \left(-(\sqrt{3}/2) I_b + (\sqrt{3}/2) I_c \right) \quad (4)$$

φ_{sd} = Direct stator flux

φ_{sq} = Quadrature stator flux

V_d = Direct voltage

V_q = Quadrature voltage

R_s = Stator Resistance

MAGNITUDE OF STATOR FLUX :

$$\text{Magnitude of stator flux} = \sqrt{(\varphi_{sd}^2 + \varphi_{sq}^2)} \quad (5)$$

ROTOR POSITION:

$$\theta = \tan^{-1} \left(\frac{\varphi_{sq}}{\varphi_{sd}} \right) \quad (6)$$

Where,

θ = Rotor position.

TORQUE ESTIMATOR:

$$T_e = (3/2) p (\varphi_{sd} * I_{sq} - \varphi_{sq} * I_{sd}) \quad (7)$$

Where,

P – no of poles

$$\text{Slip} = T_e * (R_r / 2) \quad (8)$$

Where,

T_e = Estimated torque

R_r = Rotor resistance

ELECTRICAL SPEED:

$$\text{Electrical speed} = (\text{speed of field-slip}) / \text{square of rotor flux} \quad (9)$$

$$\text{Speed of rotor field} = \varphi_{rd} * \varphi_{r\beta} - \varphi_{rq} * \varphi_{r\alpha} \quad (10)$$

ROTOR FLUX :

$$\varphi_{rd} = (L_M / L_R) \varphi_{sd} \quad (11)$$

$$\varphi_{rq} = (L_M / L_R) \varphi_{sq} \quad (12)$$

MECHANICAL SPEED:

$$\omega_m = (1/2) * \text{Electrical speed.} \quad (13)$$

Where,

ω_m = Mechanical speed

In sliding mode technique we calculate the actual speed, magnetic flux, torque, rotor position. The output is given to control unit then it compare the actual speed and set speed

9. SIMULATIONS AND RESULTS

The detailed description about the result of the proposed system with the help of MATLAB and the results of the simulated system is drawn here.

9.1 SIMULATION DIAGRAM

The simulation diagram of proposed system is shown below.

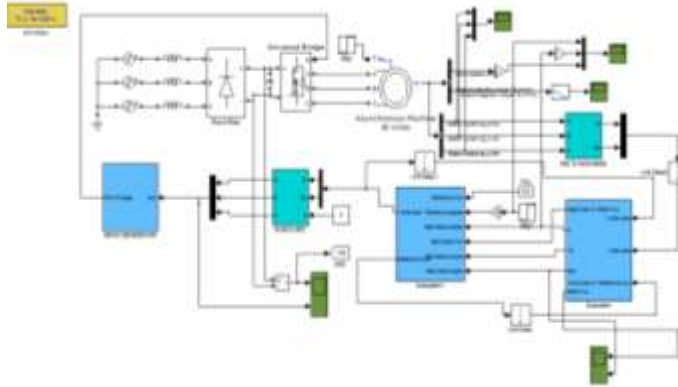


Fig 9.1: Simulation diagram of the proposed system.

9.2 TRIGGER CIRCUIT SPWM GENERATOR

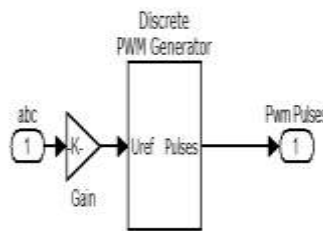


Fig 9.2: Circuit diagram of SPWM generator.

The output from the inverse park transformation is fed into selector bus and the gain is added with it. The output from the gain is fed into SPWM generator the PWM pulses are produced.

9.3 TRIGGER CIRCUIT PARK TRANSFORMATION

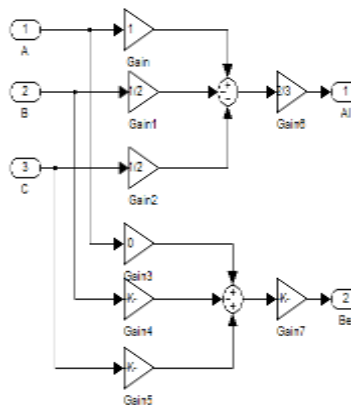


Fig 9.3: Circuit Diagram of A1-Be to ABC.

The stator current is fed into the gain and is summed up in the summing point and three phases converted into two phase stator current.

9.4 TRIGGER CIRCUIT INVERSEPARK TRANSFORMATION

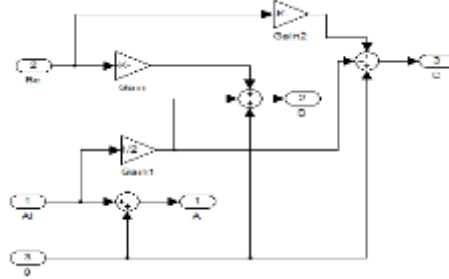


Fig 9.4: Circuit diagram of inverse park transformation.

In this circuit by adding gains and summing point with references the two phase again converted into three phase.

9.5 TRIGGER CIRCUIT PI CONTRLLER

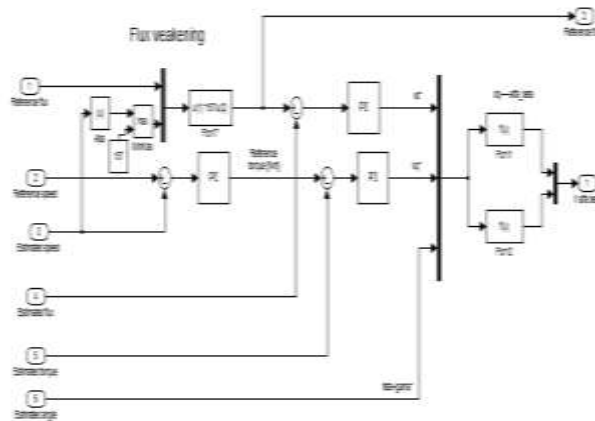


Fig 9.5 : Circuit diagram of PI controller.

The reference speed, estimated speed ,reference flux, estimated flux, estimated angle ,estimated torque are given to control unit.It compares the actual speed and set speed and its given to the inverse park transformation.

9.6 TRIGGER CIRCUIT SLIDING MODE

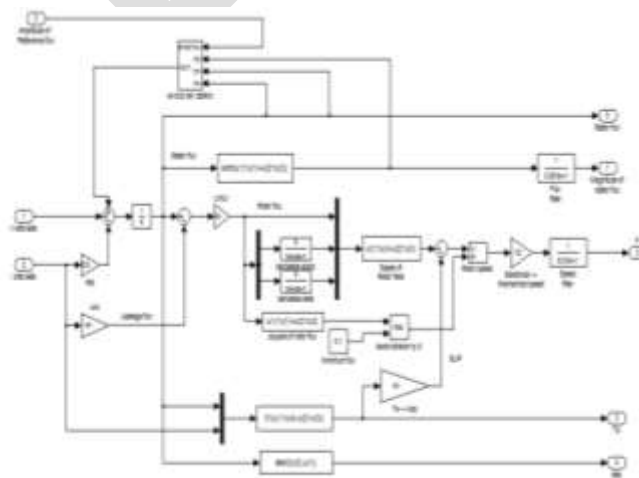


Fig 9.6: circuit diagram of sliding mode control.

The flux and voltage are taken as reference and the feedback current is fed into gain then it is given to derivative alpha and beta. Then the output is given to the speed of rotor flux and it is converted as electrical to mechanical speed .The final estimated speed is obtained.

9.7 OUTPUT OF SIMULATION MODEL

9.7.1 SPEED CHARACTERISTICS

X axis: Time in seconds
Y axis: speed in rpm

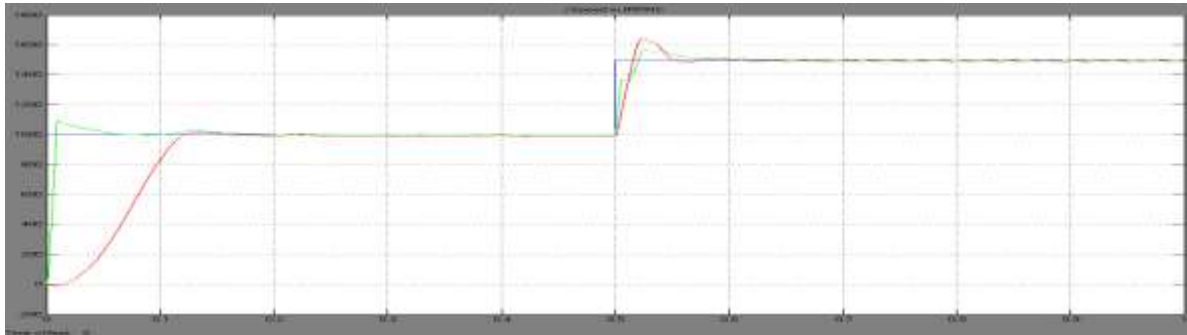


Fig 9.7: Time Vs Speed characteristics.

In the above graph shows the characteristics of Speed.

- The blue colour line shows the estimated speed.
- The pink colour line shows the reference speed.
- The green colour line shows the actual speed.

9.7.2 VOLTAGE CHARACTERISTICS

X axis : Time in seconds
Y axis : Direct current voltage (V_{dc})

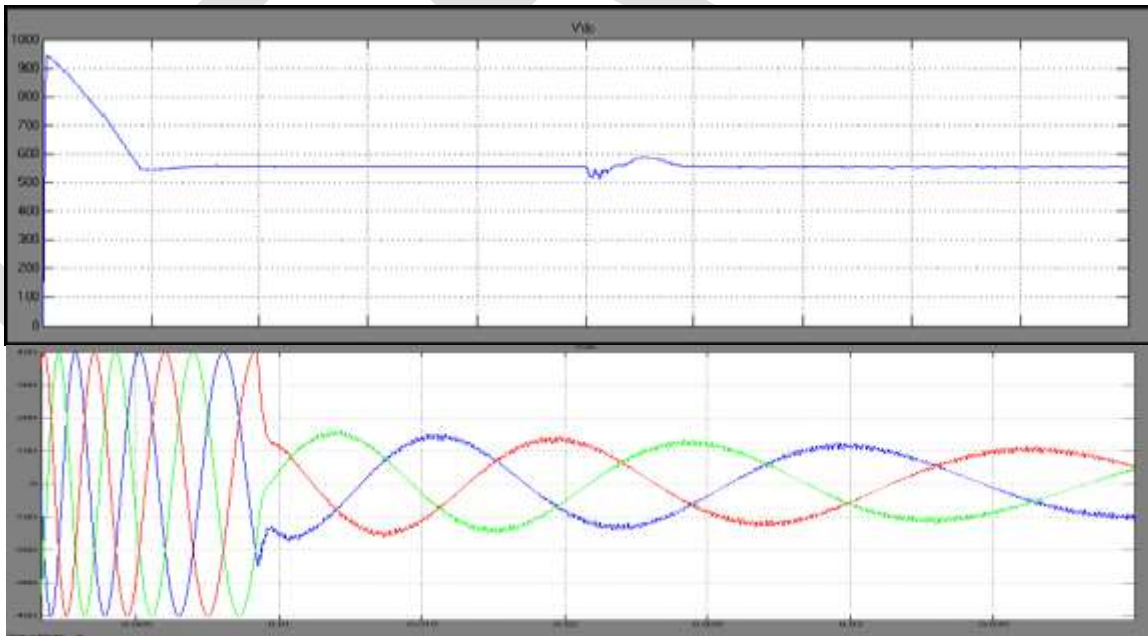


Fig 9.8(a) and (b) : Time Vs voltage (V_{dc}).

In the above graph shows the characteristics of voltage.

- The blue colour line shows the estimated speed.
- The pink colour line shows the reference speed.
- The green colour line shows the actual speed.

9.7.3 TORQUE CHARACTERISTICS

X axis : Time in seconds
Y axis : Direct current voltage (V_{dc})

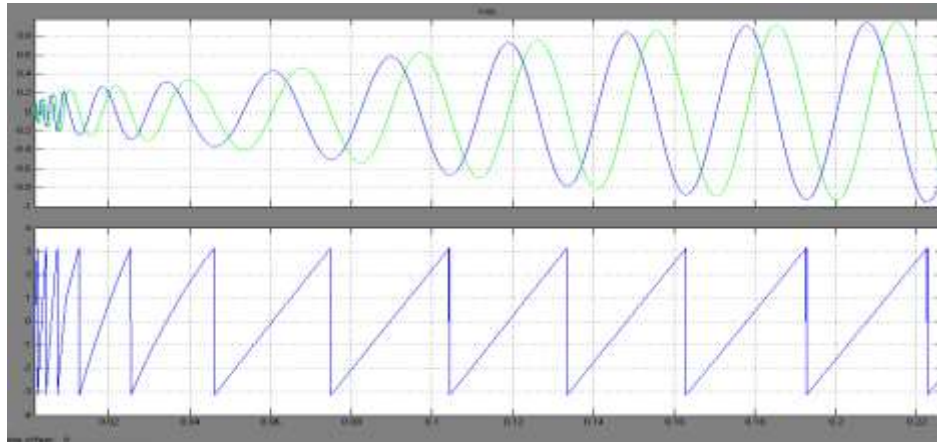


Fig 9.9 (a) and (b) : Time Vs voltage (V_{dc}).

In the above graph shows the characteristics of torque.

- The blue colour line shows the estimated speed.
- The pink colour line shows the reference speed.
- The green colour line shows the actual speed.

9.7.4 STATOR FLUX CHARACTERISTICS

X axis : Time in seconds
Y axis : Speed in rpm

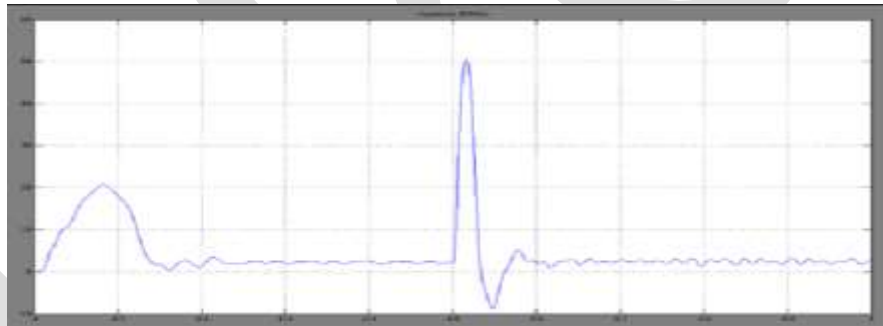


Fig 9.10 : Time Vs Speed

In the above graph shows the characteristics of stator flux.

- The blue colour line shows the estimated speed.
- The pink colour line shows the reference speed.
- The green colour line shows the actual speed.

9.7.5 STATOR CURRENT CHARACTERISTICS

X axis : Time in seconds
Y axis : Speed in rpm

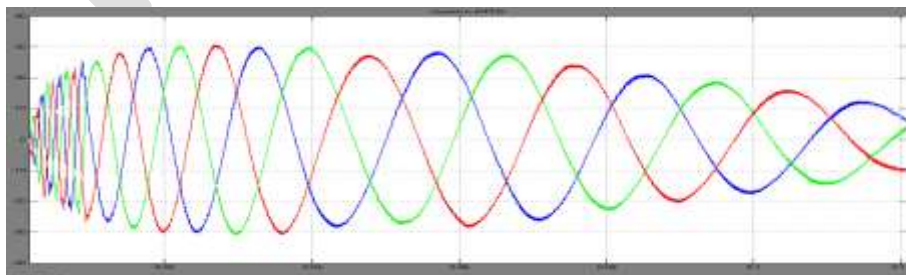


Fig 9.11 : Time Vs Speed.

In the above graph shows the characteristics of stator current.

- The blue colour line shows the estimated speed.
- The pink colour line shows the reference speed.
- The green colour line shows the actual speed.

10. CONCLUSION

This paper presents a modified speed-sensorless control scheme based on second-order sliding-mode STA and MRAS estimation theory. The estimation scheme has been obtained by combining a second-order sliding-mode current observer with a parallel speed and stator resistance estimator based on rotor flux-based MRAS. Both the error in instantaneous phase position and the error in amplitudes are used respectively for speed estimation and R_s identification, thus overcoming the problems of R_s variation, particularly for low-speed operation.

The STA-based observer is utilized to take the place of the reference voltage model of the standard MRAS. Derivatives of rotor flux are obtained and designed as the state of MRAS, thus eliminating the integration. Moreover, by making full use of auxiliary surfaces, the observations are insensitive to rotor parameter perturbation with the alleviation of chattering behavior at the same time. The proposed scheme is insignificantly more complex than its counterpart with speed estimation only, so it is easy to implement in the already existing MRAS-based speed estimator. However, since the scheme is designed based on the mathematical model of IM, its observability is generally lost at zero magnetic field frequency. Machine state observability can be improved by additional stator voltage change injection, which is considered to be the further work.

REFERENCES:

1. Akin. B and Bhardwaj. M, "Sensored field oriented control of 3-phase induction motors", Texas Instrument Guide, Dallas, TX, USA. [Online]. Available: www.ti.com/litv/pdf/sprabp8.
2. Araki. M and Taguchi. H, "Two-degree-of-freedom PID controllers," *Int. J. Control, Autom., Syst.*, vol. 1, no. 4, pp. 401–411, Dec. 2003.
3. Barrero. F, Gonzalez. A, Torralba. A, Galvan. E, and Franquelo.L.G, "Speed control of induction motors using a novel fuzzy sliding-mode structure," *IEEE Trans. Fuzzy Syst.*, vol. 10, no. 3, pp. 375–383, Jun. 2002.
4. Cupertino. F, Naso. D, Mininno. E, and Turchiano. B, "Sliding-mode control with double boundary layer for robust compensation of payload mass and friction in linear motors," *IEEE Trans. Ind. Appl.*, vol. 45, no. 5, pp. 1688–1696, Sep./Oct. 2009.
5. Chien. C. J, "A combined adaptive law for fuzzy iterative learning control of nonlinear systems with varying control tasks," *IEEE Trans. Fuzzy Syst.*, vol. 16, no. 1, pp. 40–51, Feb. 2008.
6. Faa-Jeng. L, Po-Huan. C, Chin-Sheng. C, and Yu-Sheng. L, "DSP-based cross-coupled synchronous control for dual linear motors via intelligent complementary sliding mode control," *IEEE Trans. Ind. Electron.*, vol. 59, no. 2, pp. 1061–1073, Feb. 2012.
7. Franklin. P and Powell. J. D, *Emami-Naeini Feedback Control of Dynamic Systems*, vol. 4. Englewood Cliffs, NJ, USA: Prentice-Hall, 2006, p. 2.
8. Gadoue. S. M, Giaouris. D, and Finch. J. W, "MRAS sensorless vector control of an induction motor using new sliding-mode and fuzzy-logic adaptation mechanisms," *IEEE Trans. Energy Convers.*, vol. 25, no. 2, pp. 394–402, Jun. 2010.
9. Garrido. A. J, Garrido. I, Amundarain. M, Alberdi. M, and De la Sen. M, "Sliding-mode control of wave power generation plants," *IEEE Trans Ind. Appl.*, vol. 48, no. 6, pp. 2372–2381, Nov./Dec. 2012.
10. Hongyi. L, Jinyong. Y, Hilton. C, and Honghai. L, "Adaptive sliding-mode control for nonlinear active suspension vehicle systems using T-S fuzzy approach," *IEEE Trans. Ind. Electron.*, vol. 60, no. 8, pp. 3328–3338, Aug. 2013.
11. Jinhui. Z, Peng. S, and Yuanqing. X, "Robust adaptive sliding-mode control for fuzzy systems with mismatched uncertainties," *IEEE Trans. Fuzzy Syst.*, vol. 18, no. 4, pp. 700–711, Aug. 2010.
12. Kim. Y. K and Jeon. G. J, "Error reduction of sliding mode control using sigmoid-type nonlinear interpolation in the boundary layer," *Int. J. Control Syst.*, vol. 2, no. 4, pp. 523–529, 2004.
13. Kung. C. C and Su. K. H, "Adaptive fuzzy position control for electrical servo drive via total-sliding-mode technique," *Proc. Inst. Elect. Eng.—Elect. Power Appl.*, vol. 152, no. 6, pp. 1489–1502, Nov. 2005.
14. C. Lin, T. Liu, M. Wei, L. Fu, and C. Hsiao, "Design and implementation of a chattering-free non-linear sliding-mode controller for interior permanent magnet synchronous drive systems," *IET Elect. Power Appl.*, vol. 6, no. 6, pp. 332–344, Jul. 2012.
15. Lorenz. R, "A simplified approach to continuous on-line tuning of fieldoriented induction machine drives," *IEEE Trans. Ind. Appl.*, vol. 26, no. 3, pp. 420–424, May/June. 2002.
16. Orowska-Kowalska. T, Kaminski. M, and Szabat. K, "Implementation of a sliding-mode controller with an integral function and fuzzy gain value for the electrical drive with an elastic joint," *IEEE Trans. Ind. Electron.*, vol. 57, no. 4, pp. 1309–1317, Apr. 2010.

17. Pupadubsinet al. P., "Adaptive integral sliding-mode position control of a coupled-phase linear variable reluctance motor for high-precision applications," IEEE Trans. Ind. Appl., vol. 48, no. 4, pp. 1353–1363, Jul./Aug. 2012.
18. Rong-Jong. W, "Fuzzy sliding-mode control using adaptive tuning technique," IEEE Trans. Ind. Electron., vol. 54, no. 1, pp. 586–594, Feb. 2007.
19. Rong-Jong. W and Kuo-Ho. S, "Adaptive enhanced fuzzy sliding-mode control for electrical servo drive," IEEE Trans. Ind. Electron., vol. 53, no. 2, pp. 569–580, Apr. 2006.
20. Roopaei. M, Zolghadri. M, and Meshksar. S, "Enhanced adaptive fuzzy sliding mode control for uncertain nonlinear systems," Commun. NonlinearSci. Numer. Simul., vol. 14, no. 9/10, pp. 3670–3681, Sep./Oct. 2009.

IJERGS

Lean, Green and DMADV Tool Based Approach for an Effective Execution of Residential Building Construction Improvement

Gourav Tiwari¹, S.Kesavan²

¹Department of Civil Engineering, S.R.M University, Chennai, Tamilnadu, India

²Department of Civil Engineering, S.R.M University, Chennai, Tamilnadu, India

(Email- gouravedifice@gmail.com, Kesavan.s@ktr.srmuniv.ac.in)

Abstract— in this paper introduce how to use the principal of LEAN and SIX SIGMA in Residential Foundation Project and how to make Eco- Friendly and Green Foundation. Construction industry is major source of pollution and wastage. By the help of Lean and Six Sigma Principle, wastage problem and Harmful impact of construction material on environment and human health can be reduce.

Keywords— Lean, Six Sigma Tool, Eco-Friendly Materials, Green Buildings, Pollution, Foundation, Voice of customer.

I. INTRODUCTION

This Research Paper Based on Application of Lean and Six Sigma Principal on Construction of Spread Footing Foundation. Construction industry is a major source of Pollution. By the help of Lean and Six sigma tool water supply system can be Redesign and impact of harmful construction material on environment can be reduce.

II. TOOL

a. Lean-Lean is Principal introduce by Toyota. Lean shows the wastage of material and how to reduce the amount of wastage during the production.

b. Green-In this research paper Green word refers to reduce unhealthy Construction Impact on human body, because due to construction is major source of pollution emission.

c. DMADV-DMADV (Define, Measure, Analysis, Design, Verify) it is tool of six sigma. It is use for development of New product, New process.

Design: Define is the First Step of the Lean and Six Sigma Process. It consists of defining the problem, the process and the Customer.
Tools- Project Charter, Voice of Customer, SIPOC (Supply, Input, Process, Output, Customer)

Measure: This phase consist of data analysis and find out the reasons of waste in the Process.
Tool- Cause & Effect Diagram or Fishbone Diagram.

Analysis: It is consist of statistical analysis of the problem.
Tools- Process Analysis, Data Analysis.

Design- It is consist of improvement of alternatives.

Verify: The Performance of design should be according to customer needs.

III. CASE STUDY

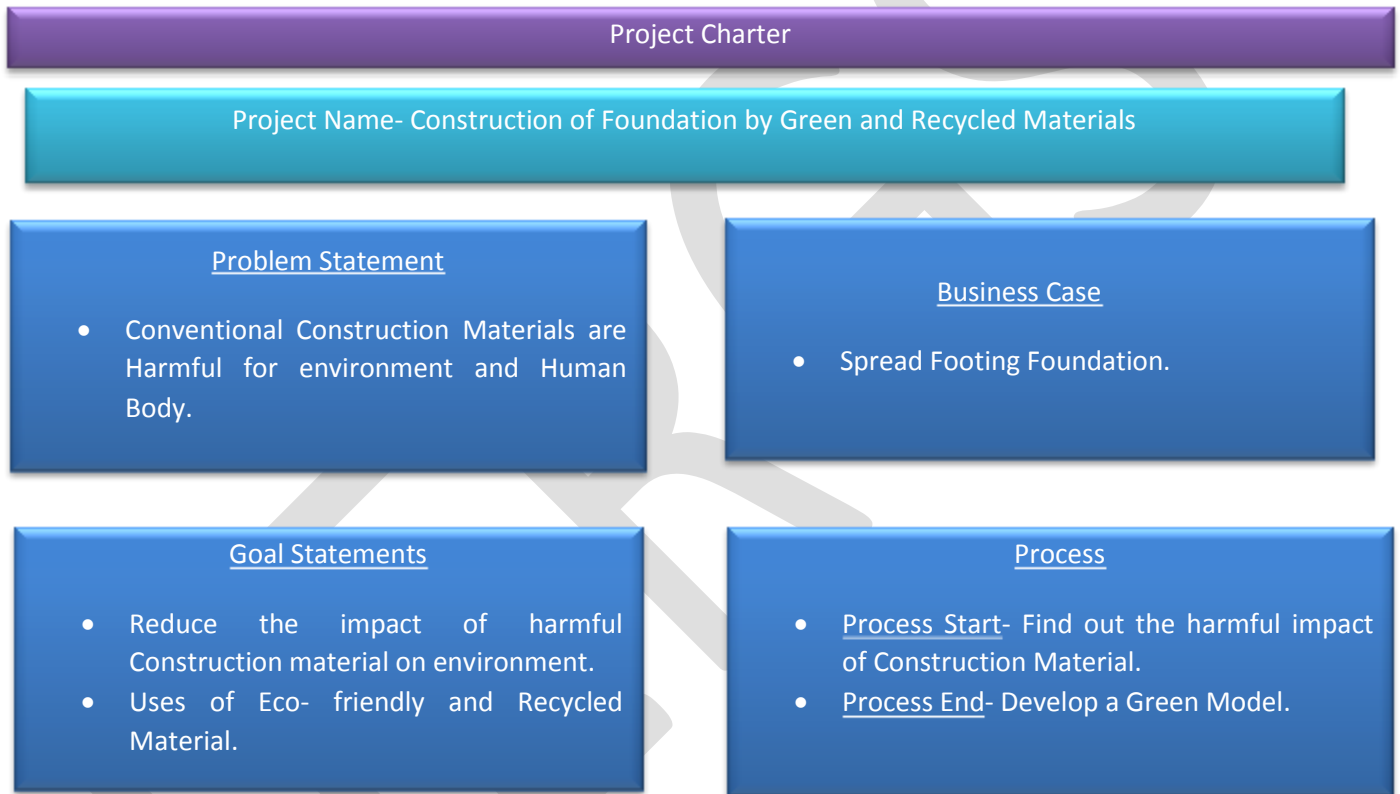
For application of lean and six sigma tool (DMADV). We are taking a construction of spread footing foundation. General Specifications:

Table 1
 General Specifications of Spread Footing Foundation

Width of Concrete Base	80 cm
Width of 1 st footing	60 cm
Width of 2 nd footing	50 cm
Height of plinth	60 cm
Height of Wall	3.50 m
Thickness of wall	30 cm

Define Phase

Step 1- Define aim of Project.
 Tool- Project Charter.



Step 2- Define Customer Requirement.
 Tool- Voice of Customer Translation matrix.

Table 2
 Voice of Customer Translation matrix

Customer Comment	Customer Requirement
Red List Building Materials are harmful to living creatures including Human or Environment	Uses of Non- Toxic and Non Chemical Materials

P.V.C responsible for Cancer Causing Vinyl Chloride monomer and ethylene dichloride	Find Out the Alternative of P.V.C
Silica can cause chronic obstructive pulmonary disease	Uses of Green Materials
Lead Found in Paints. It causes Kidney, nervous system and other Organ Damage	Uses of Eco Friendly Paints
Asbestos is found in insulation, pipe covering, Roof materials, acoustical materials, Fire proofing Insulation it can cause COPD	Find Out the Alternative Solution of Asbestos
The Cement industry is one of the primary Product of CO2.	Find out the Eco- Friendly Cement and Concrete.

Step 3- Define Process.
Tool- SIPOC.



Measure Phase

Tool- Fishbone Diagram.

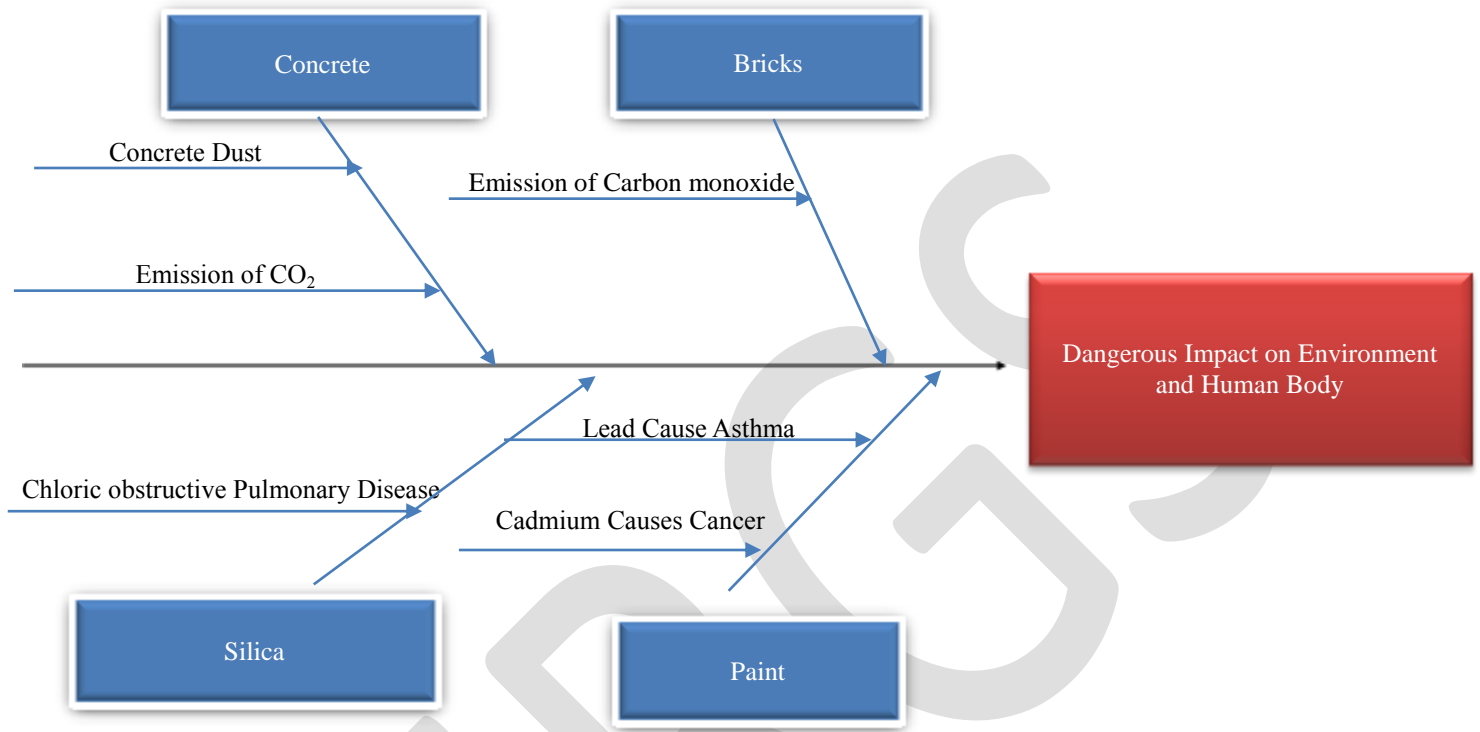


Fig. 1
Fishbone Diagram

Analysis Phase

Tool- Process Analysis, Data Analysis.

Fly ash- sand-lime-Gypsum Brick

Use- for Walls in housing and all type of Building Construction

Table 3
Properties of Fly ash- sand –lime –Gypsum Brick

Compressive Strength	80-150 kg/cm ²
Unit Weight	3-3.5 kg/brick
Water absorption	8-10 %
Density	1800-1950 kg/m ³

Clay Fly ash Burnt Brick

Use- For Walling

Table 4
Properties of clay fly ash Burnt Brick

Compressive strength	75-150 kg/cm ²
Water absorption	12-16%
Unit Weight	2.5-3 kgs

Bulk Density	1600-1825 kg/cm ²
Colour	Red

Marble Slurry Bricks
Use- For walling

Table 5
Properties of Marble Slurry Bricks

Compressive strength	93 kg/cm ²
Water absorption	14%
Volume of Brick	1687.5 cm ²
Colour	White/grey

Cellular Light Weight Concrete
Use- Reduction of Dead Weight of Foundation

Table 6
Properties of Cellular Light Weight Concrete

Range of densities	400-1800 m ³
Compressive strength	10-250 kg/ sq.cm
Water absorption	5% by Weight
Thermal Conductivity	0.082-0.555 w/mk

Eco- Friendly Paints

Major Manufactures of Natural Paints.

Table 7
List of Natural Paints Manufactures

Aglaia	Livos	Auro
EcoDesign's Bioshield	SoyGuard	Silacte
Anna Sova	Green Planet Paints	Master Blend

Major Manufactures of Zero Volatile Organic Compound Paints.

Table 8
List of Zero VOC Paints Manufactures

Earth paint	ECOS Paints	AFM Safecoat
ICI Life master	Best Paint Company	American Pride
Sherwin Williams	Mythic Paints	Homestead Paints

Major Manufactures of Low Volatile Organic Compound Paints.

Table 9
List of Low VOC Paints Manufactures

Benjamin Moore Aura	Benjamin Moore Saman	Cloverdale Horizon
Cloverdale EcoLogic	Miller Paints	Timber Ox Green

Design Phase

Table 10
Design of Foundation

Item No.	Description of Item	No.	Length	Breadth	Ht. or Depth	Quantities	Total Quantities
1	Earthwork in Excavation in Foundation	1	6.00m	.80m	.90m	4.32	4.32 cu.m
2	Lime Concrete in Foundation	1	6.00m	.80m	.30m	1.44	1.44 cu.m
3	1 st Class Eco Friendly brick work in lime Mortar in foundation and Plinth						
	1 st Footing	1	6.00m	.60m	.20m	.72	
	2 nd Footing	1	6.00m	.50m	.20m	.60	
	Plinth Wall up to G.L	1	6.00m	.40m	.20m	.48	
	Plinth Wall up to G.L	1	6.00m	.40m	.60m	1.44	
							Total= 3.24 m ³
4	1 st Class Eco Friendly Brickwork in lime Mortar for Superstructure	1	6.00m	.30m	3.50m	6.3	6.3 m ³
5	Non- Toxic White Washing	1	6.00m	-	3.50m	21.0	21.0 m ²
6	Non –Toxic Colour Washing	1	6.00m	-	4.10 m	24.6	24.6 m ²

IV. CONCLUSION

Overall, by the help of Design tool of Six Sigma Spread Footing Foundation can be Redesign and Eco-friendly construction will be possible. By the help of lean and six sigma tool Pollution can be reduce and also reduce the toxic impact of materials on human health. Any existing system can be redesign and it will be economical in compare to current price model and also reduce the wastage of materials by new system.

REFERENCES:

- [1] Arpad Horvath “Construction Materials and the Environment”
- [2] Center for Health Environment & Justic “Toxic chemicals in products and building materials purchased by New York Schools and Government Agencies”.
- [3] Jane Anderson “The embodied Impact of Construction Materials”.
- [4] Raid al Amor “Analysis of lean construction practices at Abu Dhabi construction industry”.
- [5] Sunil V. Desale, Sharad V. Dwadhar “An application of lean and six sigma principle for constructional process improvement in Indian organization”.
- [6] Sneha.p.sawant, Smita V. Pataskar “Applying six sigma principles in construction industry for quality improvement”
- [7] Abdul-Aziz Ali Bhawani “Improving construction processes by integrating lean, green, and six-sigma”.
- [8] Sunil v. Desale, Sharad V. Dwadhar “Eliminating waste in construction by using lean and six sigma Principal” by.
- [9] Mehmet Tolga “Critical Success factor for six sigma” by.
- [10] Atul Porwal “Construction waste management at source: A building information modelling based system dynamics approach”.
- [11] Seung Heon Han, M.ASCE, Myung Jin Chae, Ph.D, P.E, Keon Soon Im, P.E; and Ho Dong Ryu. “Six sigma Based Approach to improve performance in construction operations”.
- [12] Sophia Lisbeth Hsu “Life Cycle Assessment of Materials and Construction in Commercial Structure: Variability and Limitations”.

Arduino Based: Smart Light Control System

Deepak Kumar Rath

Undergraduate Student, Instrumentation & Electronics Engineering

College of Engineering and Technology, Bhubaneswar

Email:deepak.cetb@gmail.com Mob: +91-8895900066

Abstract— This world is full of different kind of light sources some are natural ones while others are man-made light sources. The man-made light sources have only two modes of operation that is switch on and switch off there is no intermediate level that can be set according to the surrounding lighting condition and at the end everything needs to be controlled manually. These lead to wastage of electricity and at the same time a manual control is not effective in the modern era. In this paper, we purpose an advanced light control system which is capable of replacing the old generation light control system. The system is implemented on an embedded platform & is equipped with a photo sensitive detector (LDR) which gives the required input for operation .The working of our light control system is based on the amount of luminous energy in the environment at that moment of time. Depending upon the light intensity at that instant the lighting of the lighting system is adjusted. The embedded main board including the Microcontroller chip, memory (flash), and communication port are used as a processing module for the input that we get from peripheral devices (LDR).Application of such a system can be implemented in workstations, park lights, street lighting system, head lights of automobiles and much more.

Keywords—Arduino Uno, LDR, Relay, Lighting Units Arduino Programming, Automatic Control, Energy Efficient

INTRODUCTION

We are living in the world where everything goes to be automatic from your washing machine to your ceiling fan. The world revolves around the word automation and the ones that are automated are said to be of next generation because they limit the involvement of humans. They are self-sufficient to operate on their own and thereby, saving time and cost by being more efficient than the manual ones. But lighting systems have yet to make its move in these automated crusade. We have just started the crusade in our attempt here.

The main objective of this project is to implement an auto-intensity control of LED-based on LDR which is interfaced to an Arduino board. As the surrounding light decreases slowly from evening to night, the light intensity gradually increases and then gets gradually decreased from night to early dawn hence saves energy .Thus, the lights switch on at the dusk and light intensity increases till midnight and regressively decrease till dawn and then finally switch off automatically. The process repeats every day. As stated earlier, application includes: park lights, street lights, head light in automobile and many unexplored options. Relay is used to provide isolation between Arduino and 220 volt AC supply.

The goal is to reduce the amount of energy consumed and thereby reducing the cost incurred due to energy loss thus proving to be a cost-effective strategy.

LITERATURE REVIEW

Controlling lighting system by means of LDR and Arduino together is relatively a new concept. After going through many research papers which were related to field of lighting system, I found that there are papers only about street light system and that too most of them are Passive Infrared receiver based and few are LDR based but they are controlled by means of timers and analog circuits. Some were controlled by wireless GSM/GUI networks .That being said they are no papers which coin all the lighting system under one umbrella and use LDR and Arduino system as their fundamental architecture to control it.

Ancient Lighting system have been confined to two options on and off, due to it had their own share of disadvantage. This kind of operation meant energy loss due to continuous operation at maximum voltage though actual requirement might be less depending upon the outside lighting condition. The simplest solution to it is by calibrating the lights according to the outside lighting condition. This is what we are aiming for in our smart lighting system.

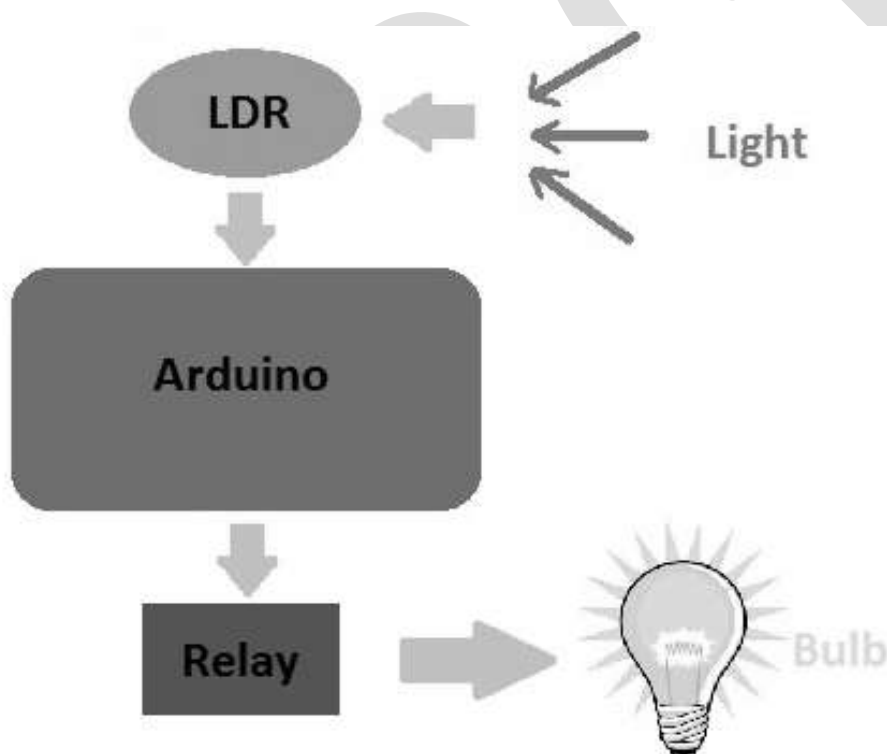
PROPOSED SYSTEM

As stated earlier our main objective is to provide an efficient & energy saving lighting system by evaluating the outside lighting condition and then adjusting the lights accordingly. The circuit mainly consists of a sensing element known as LDR, which is followed by processing unit Arduino which takes input for sensing element and gives its output to the LEDs (lighting units). Though other units like relays, transistors are also be used for higher voltage supply.

The LDR senses the light and sends the data to Arduino. The Arduino analyse the data and gives its response to the LEDs through the relay mechanism. The Arduino is programmed in such a way it automatically adjusts the lights to give most accurate result possible.

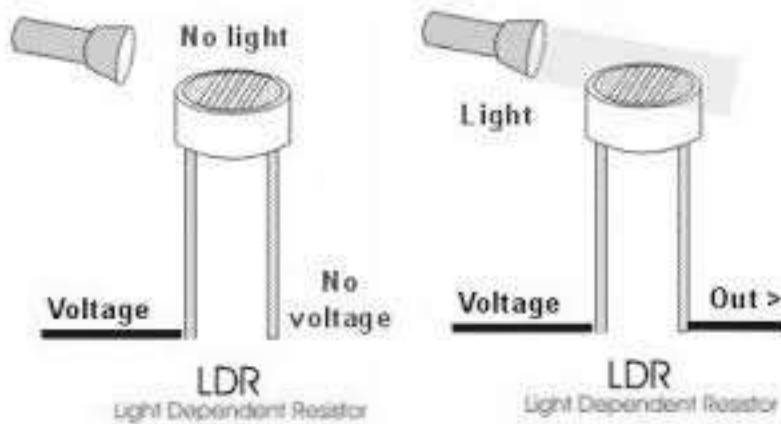
ARCHITECHTURE DESIGN

The pictorial representation of our model is given below:



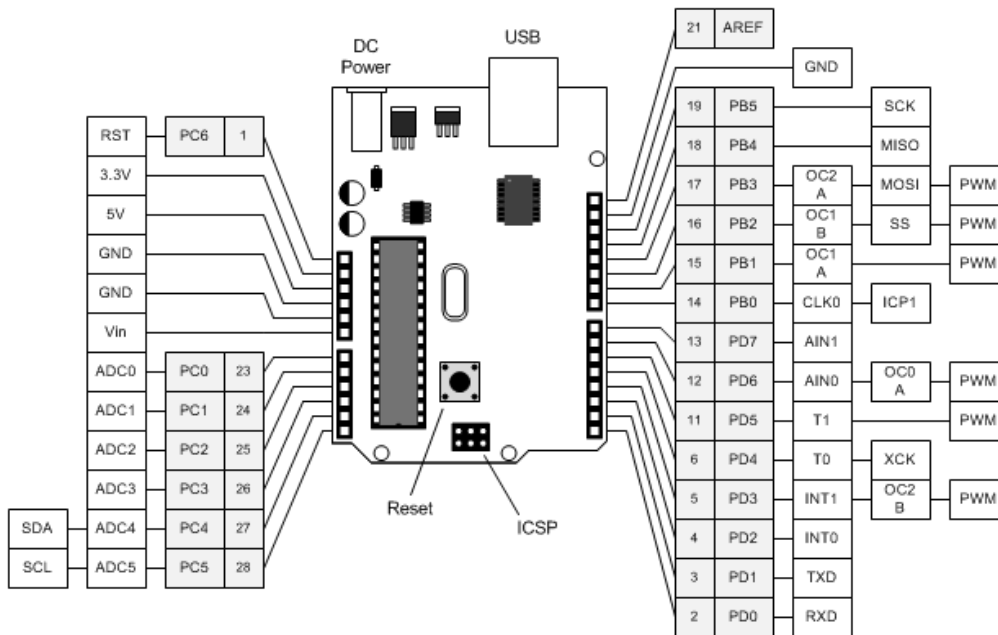
CIRCUIT COMPONENTS:

- 1) LIGHT DEPENDENT RESISTOR (LDR) SENSOR



Light Dependent Resistor as the name suggest the resistance is dependent upon the light incident on it. The light dependent resistor resistance changes with intensity of light, with increase in light intensity the resistance offered by the sensor decreases and with decrease in light intensity the resistance offered by the sensor increases. Hence it acts as variable resistor with change in light intensity. These helps in finding the amount of light intensity at that instant of time and thus helping in regulating the lighting of our lighting system accordingly.

2) ARDUINO UNO



Arduino is an open-source physical platform based on microcontroller board having the ATmega32 series controllers and Integrated Development Environment for writing and uploading codes to the microcontroller. It has input and output pins for interaction with the outside world such as with sensors, switches, motors and so on. To be precise it has 14 digital input/output pins (of which 6 can be used as PWM outputs), 6 analog inputs, a 16 MHz quartz crystal, a USB connection, a power jack, an ICSP header and a reset button. It contains everything needed to support the microcontroller .It can take supply through USB or we can power it with an AC-to-DC adapter or a battery Arduino acts as the processing module of the

system. It takes input from the LDR, process the data and gives the output to LEDS directly or through a relay and a transistor mechanism

3) LEDS

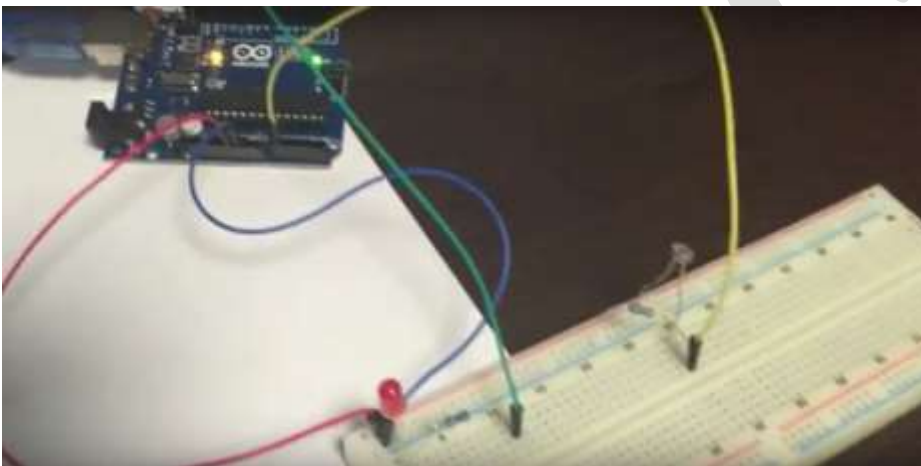
A light-emitting diode (LED) is a pn junction diode, which emits light when activated. When we apply voltage across its leads, electrons are able to recombine with holes within the LED, releasing energy in the form of photons which gives the light. Hence, it is a two-lead semiconductor light source

Light emitting diodes represents our lighting system and the amount of light emitted by it is directly related to the amount of light in the environment that is when outside light is less than the light given by LEDS is more and visa-versa.

RELAY

In this project whenever high voltage supply has to be used then relay is used to provide isolation between low voltage circuitry and high voltage circuitry. Arduino is also used to provide control signal to relay whenever intensity of light falls below a certain level. Control signal generated from pin 13 of Arduino which is used as an output pin was given to relay which is finally given to the lights.

WORKING PRINCIPLE

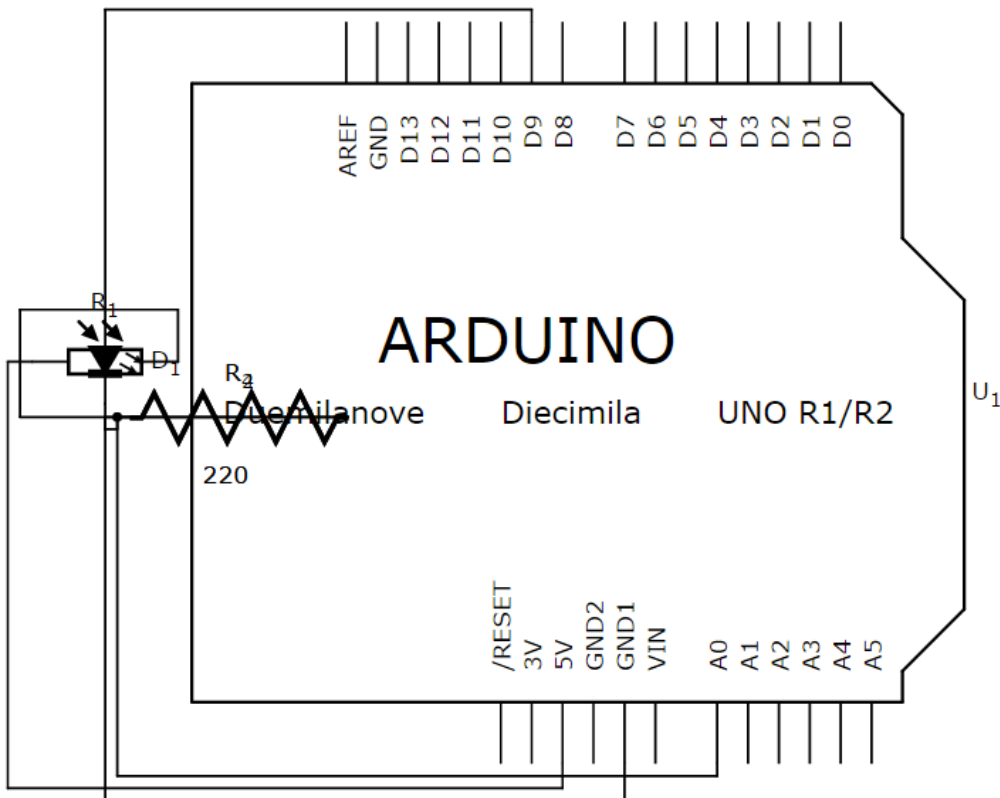


The working of our model is very simple. The supply is given through the power jack. From the Arduino we take 5v supply and connect it to one of the terminal of photo resistor and other end is connected to a resistor of 10k which acts as a voltage divider and then final connected to ground. The output is given by output pin 13 of the Arduino which is connected to the led through a 220ohm resistor. The other end of LED is perfectly grounded. As this is a working porotype here, we haven't shown the usage of relays but if required they can be connected just before the lights (LEDS) for isolation purposes.

The LDR senses the amount of light in the atmosphere at that moment of time and accordingly sends the data is to Arduino .The Arduino converts the data received into various discrete levels .For example from 0 to 1023 discrete levels for a given data then 0 represents maximum darkness and 1023 represents maximum brightest so light is received is converted into one of the discrete value from 0 to 1023.Now depending upon the discrete value that we get (0 to 1023) we adjust the output voltage accordingly from 0 to 5v.So,when complete darkness (night time)that is discrete level 0 than the output is 5v as a result LED is brightest or when partially dark(dawn/evening) that is discrete level of 512 then the output is 2.5 v as a result LED is half of the maximum brightest or when completely bright that is discrete level 1023 then the output voltage is 0v as a result LED switched off. Thus, the LED not only just automatically switches on and off but also adjust the amount of light emitted according to the outside condition. The usage of such kind of application in the headlights of cars, park lights, street lights is very useful.

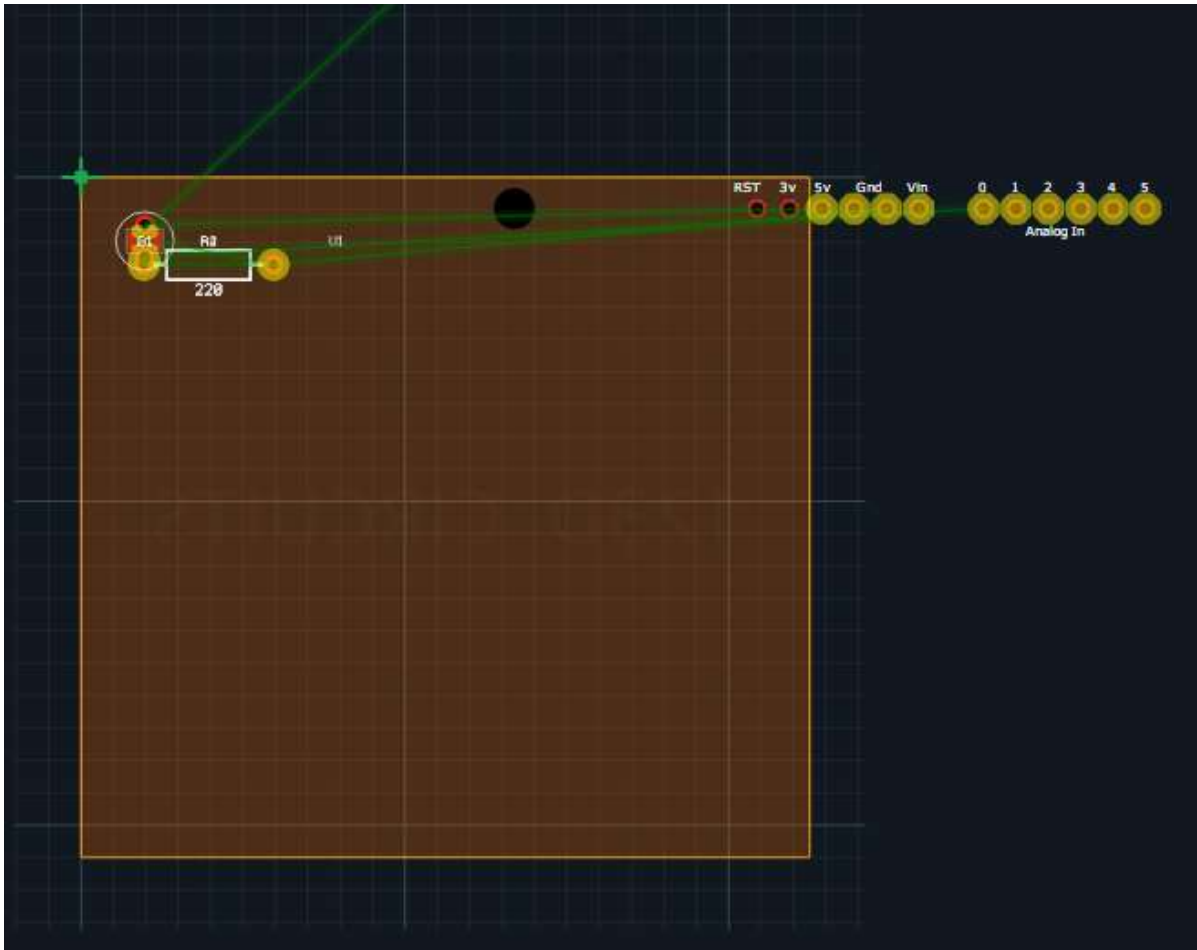
SCHEMATICS VIEW:

The schematic diagram of the smart lighting system is given below:



PCB VIEW:

The PCB diagram of the smart lighting system is given below:



The relays and transistors are externally connected and are not give in the above views as it is only required when with a higher AC voltage supply is used as a supply. These can be used in the case of street lighting and park lighting system where isolation is important for safety.

CONCLUSION

This Arduino based project will provide a competent method for lighting systems and make the whole process of energy saving easier and efficient. With a capability to change the amount of light emitted depending upon the outside condition is no doubt an innovation with many future application apart from the fact that it can also be used in many present day tech such as head lights, street light, park lights, industrial lights and many more. The usage of the smart lighting system will undoubtedly change the world that we see today.

REFERENCES:

- [1] Wang Xiao-Yuan, Andrew L. Fitch, Herbert H. C. Iu, Victor Sreeramand Qi Wei-Gui “Implementation of an analogue model of a memristor based on a light-dependent resistor”2012 Chinese Physical Society and IOP Publishing Ltd Chinese Physics B, Volume 21, Number 10

- [2] A.A.Nippun Kumaar, Kiran.G, Sudarshan TSB, " Intelligent Lighting System Using Wireless Sensor Networks", International Journal of Ad hoc, Sensor & Ubiquitous Computing (IJASUC) Vol.1, No.4, December 2010, pp 17-27
- [3] Y. K. Tan; T. P. Huynh; Z. Wang, " Smart Personal Sensor Network Control for Energy Saving in DC Grid Powered LED Lighting System", IEEE Trans. Smart Grid
- [4] O'Reilly, Fergus, and Joe Buckley. "Use of wireless sensor networks for fluorescent lighting control with daylight substitution." Proceedings of the Workshop on Real-World Wireless Sensor Networks (REANWSN). 2005.
- [5] Divya, Guddeti, et al. "Design and Implement of Wireless Sensor Street Light Control and Monitoring Strategy along with GUI." IJITR (2016): 78-81.
- [6] Prasetyo, William Tandy, Petrus Santoso, and Resmana Lim. "Adaptive Cars Headlamps System with Image Processing and Lighting Angle Control." Proceedings of Second International Conference on Electrical Systems, Technology and Information 2015 (ICESTI 2015). Springer Singapore, 2016.
- [7] Qi, Liang, MengChu Zhou, and WenJing Luan. "Emergency Traffic-Light Control System Design for Intersections Subject to Accidents." (2016).
- [8] Huynh, T. P., Y. K. Tan, and K. J. Tseng. "Energy-aware wireless sensor network with ambient intelligence for smart LED lighting system control." IECON 2011-37th Annual Conference on IEEE Industrial Electronics Society. IEEE, 2011.
- [9] Subramanyam, B. K., K. Bhaskar Reddy, and P. Ajay Kumar Reddy. "Design and development of intelligent Wireless Street light control and monitoring system along with GUI." International Journal of Engineering Research and Applications (IJERA) Vol 3 (2013): 2115-2119.
- [10] Fitch, Andrew Lewis, et al. "Realization of an analog model of memristor based on light dependent resistor." Circuits and Systems (ISCAS), 2012 IEEE International Symposium on. IEEE, 2012.
- [11] Tran, Duong, and Yen Kheng Tan. "Sensorless illumination control of a networked LED-lighting system using feedforward neural network." Industrial Electronics, IEEE Transactions on 61.4 (2014): 2113-2121.
- [12] Kim, Sangil, et al. "Design of lighting Fluorescent lamp and AC LED control board using MCU." Journal of the The Korean Institute of Power Electronics (2010): 252-253.
- [13] Song, Sang-bin, Woo-young Cheon, and Young-^ㄹ. Yu. "Design of a LED lighting bar replacement neon sign." Journal of the Korean Institute of Electrical Engineers (2006): 1671-1672.
- [14] Tran, Duong, and Yen Kheng Tan. "Sensorless illumination control of a networked LED-lighting system using feedforward neural network." Industrial Electronics, IEEE Transactions on 61.4 (2014): 2113-2121.

Performance Evaluation of Adaptive Filters for Noise Cancellation

J.L.Jini Mary¹, B.Sree Devi², G.Monica Bell Aseer³

¹ Assistant Professor, Department of ECE, VV college of Engineering, Tisaiyanvilai.

² Assistant Professor, Department of ECE, VV college of Engineering, Tisaiyanvilai.

³ Assistant Professor, Department of ECE, VV college of Engineering, Tisaiyanvilai.

¹ jini@vvcoc.org, ² sree@vvcoc.org, ³ monica@vvcoc.org

Abstract—VLSI implementation of adaptive noise canceller based on least mean square algorithm is implemented. First, the adaptive parameters are obtained by simulating noise canceller on MATLAB. Simulink model of adaptive noise canceller was developed and the noise is suppressed to an extreme extent in recovering the original signal. The objective of adaptive interference cancellation is to obtain an estimation of the interfering signal and to subtract it from the corrupted signal and hence obtain a noise free signal. For this purpose, the filter uses an adaptive algorithm to change the value of the filter coefficients, so that it acquires a better approximation of the signal after each iteration. The LMS, and its variant NLMS, RLS are the adaptive algorithms widely in use. This paper presents a comparative analysis of the LMS(Least Mean Square), NLMS(Normalized LMS) and RLS(Recursive Least Square) Filters in case of noise cancellation and the effects of parameters- filter length and step size have been analyzed and the relation between the filters has been established. Finally, the performances of the algorithms in different cases have been compared.

Keywords—Noise cancellation, Adaptive filters, Adaptive Algorithms, LMS Filter, NLMS Filter, RLS Filter, Noise Cancellation

1 Introduction

Adaptive filters, as a segment of digital signal systems have been widely used in communication industry as well as in applications such as adaptive noise cancellation, adaptive beam forming, and channel equalization. In general FIR structure has been used more magnificently than IIR structure in adaptive filters. The output of FIR filters is the convolution of its input with its coefficients which have constant values. However, when the adaptive FIR filter was contrived, this required appropriate algorithm to update the filter's coefficients. The algorithm used to update the filter coefficient is the Least Mean Square (LMS) algorithm which is known for its simplification, low computational complexity, and better performance in different running environments. Recursive Least Squares algorithm is abstention in convergence than the LMS but its very complex to implement. Hence detaining system performance in terms of speed and FPGA area used.

1.1 Adaptive Filters

A filter is a device that maps its input signal to another output signal facilitating the extraction of the desired information contained in the input signal. Time-invariant filters have fixed internal parameters and structure.

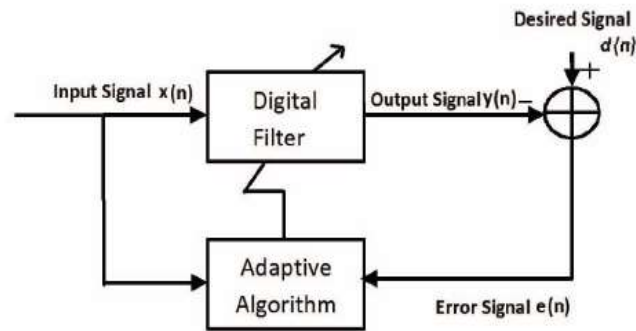


Figure 1.1. Block Diagram of Adaptive Filter

An adaptive filter is time-varying since their parameters are continually changing in order to meet certain performance requirements. The general setup of an adaptive filtering environment is shown in Figure 1.1. where n is the iteration index, $x(n)$ denotes the input signal, $y(n)$ is the adaptive filter's output signal, and $d(n)$ defines the reference or desired signal. The error signal $e(n)$ is the difference between the desired $d(n)$ and filter output $y(n)$. The error signal is used as a feedback to the adaptation algorithm in order to determine the appropriate updating of the filter's coefficients.

1.2 Adaptive Noise Cancellation

Methods of adaptive noise cancellation were proposed by Widrow and Glover in 1975. The primary aim of an adaptive noise cancellation algorithm is to allow the noisy signal through a filter which suppresses the noise without disturbing the desired signal.

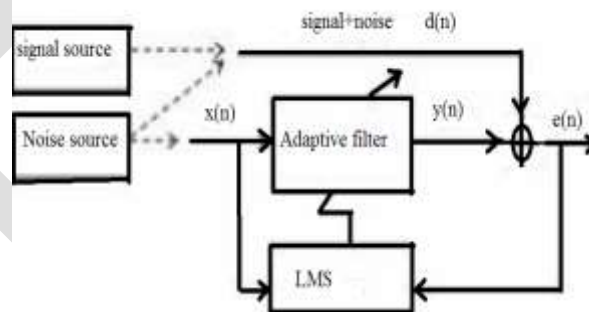


Figure 1.2. Block Diagram of adaptive noise canceller

The basic block diagram is given in Fig. 1.2. An adaptive filter automatically adjusts its own impulse response through an LMS algorithm. Adaptive Noise Canceller (ANC) has two inputs – primary and reference. The primary input receives a signal from the signal source that is corrupted by the presence of noise, uncorrelated with the signal. The concept of adaptive noise cancelling, an alternative method of estimating a signal corrupted by additive noise or interference is to pass it through a filter. The mode uses a “primary” input which is epithetical an corrupted signal (source + noise) and a “reference” input containing noise correlated in some anonymous way with the primary noise.

1.3 Flow chart for adaptive noise canceller

The Flowchart for Adaptive noise canceller is shown in figure 1.3. Adaptive noise canceller works on principle of correlation cancellation. One is desired input D_{in} and another reference correlated noisy input X_{in} . The desired input signal which is corrupted by noise can be obtained by appealing main input signal $X(k)$ and noisy input signal $N(k)$ to adder. This adder adds input signal and

noisy signal and endow corrupted signal. It further supplied to FIR filter as an input signal. The FIR filter has its endemic impulse response.

FIR filter convolutes input signal with its intrinsic impulse response. Then FIR filter consign a desired output signal. This is the first iteration which cannot solve the problem completely. And then forward to adaptive LMS algorithm as a input signal.

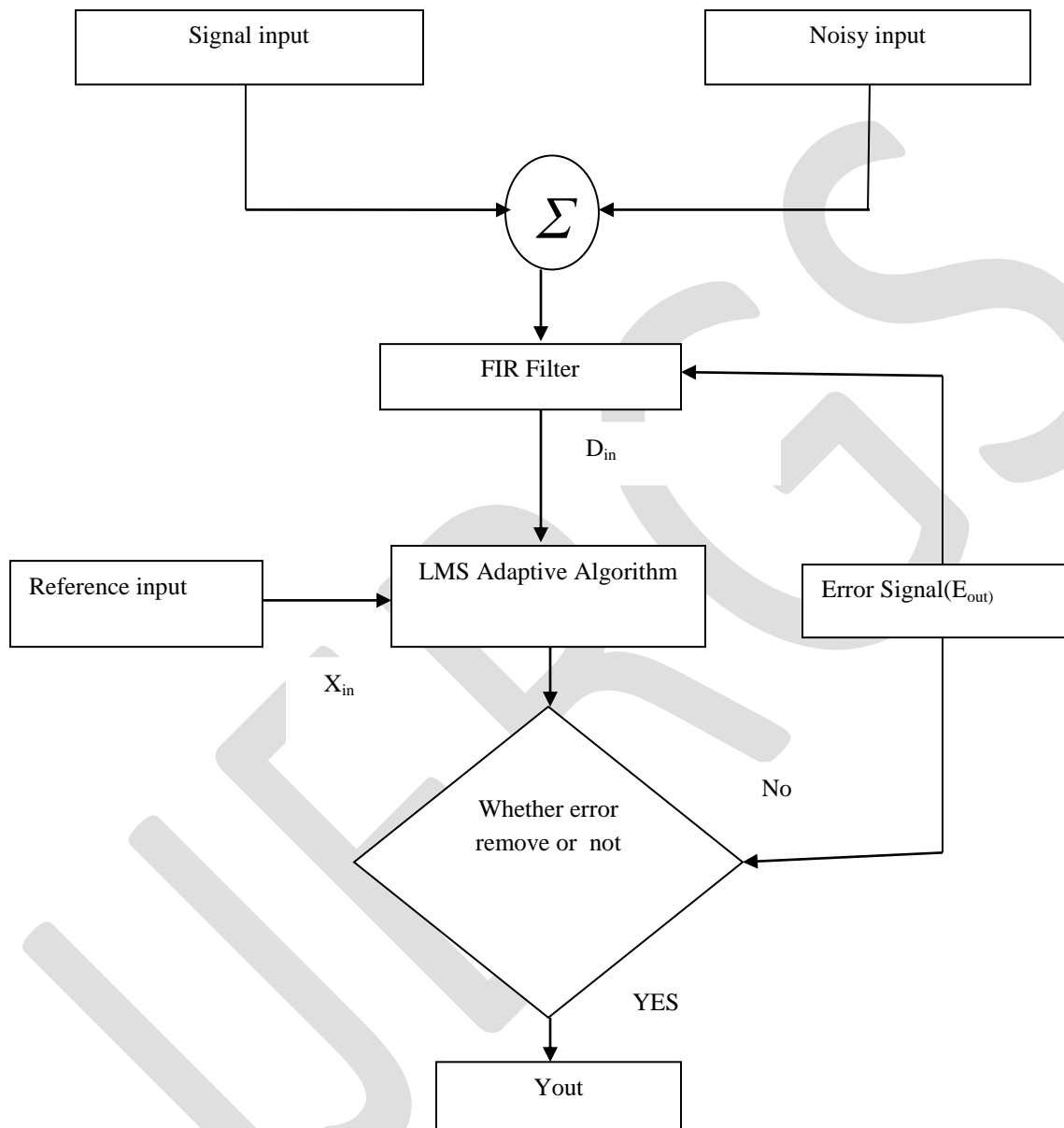


Figure 1.3. Flow chart for Adaptive noise canceller

Another reference noisy correlated input is also given to adaptive LMS algorithm. LMS algorithm continuously contemplate input signal with reference signal for adjusting the filter coefficients. After every iteration, the filter coefficients get upgraded. Its output is further applied to FIR filter again which will again perform filtering to give error output signal. After the certain number of iterations, we will get the required noise free output. The adaptive filter digress from a fixed filter in that it automatically amend its own impulse response. Reconcile is accomplished through an algorithm that responds to an error signal.

2 LMS Algorithm

The Least Mean Square or LMS algorithm is a stochastic gradient algorithm that iterates each tap weight in the filter in the direction of the gradient of squared amplitude of an error signal with respect to that tap weight.

The LMS is an approximation of the steepest descent algorithm, which uses an Instantaneous estimate of the gradient vector. The assess of the gradient is based on sample values of the tap input vector and an error signal. The algorithm iterates over each tap weight in the filter, moving it in the direction of the approximated gradient. The idea behind LMS filter is to use the method of steepest descent to find a coefficient vector which minimizes a cost function.

Least mean square (LMS) algorithm is stochastic gradient algorithm developed by Widrow and Hoff in 1959 and widely used in adaptive signal processing applications.

From Fig. 1.2, the output of the filter $y(n)$ is given by

$$Y(n)=w^T(n)x(n) \quad (2.1)$$

Where $w(n)$ is weight vector and the error signal is given by

$$e(n)=d(n)-y(n) \quad (2.2)$$

Substituting (2.1) in (2.2) yields

$$e(n)=d(n)-w^T(n)x(n) \quad (2.3)$$

According to the mean square error criterion Optimum filter parameters w_{opt} should make $\xi=E\{e^2(n)\}$ as minimum.

The mean square error can be expressed as $\xi=E\{d^2(n)\}-2w^T r_{xd}+w^T R_{xx} w$ (2.4)

Where $r_{xd}=E\{x(n) d(n)\}$, is cross-correlation vector and $R_{xx}=E\{x(n) x^T(n)\}$, is autocorrelation matrix. It can be seen that the mean square error ξ is a quadratic function of W , and the matrix R_{xx} is positive definite or positive semi definite, so it must have a minimum value. Due to this gradient of W is zero, the minimum when w_{opt} meet $\nabla \xi=0$ and when R_{xx} get a unique solution $w_{opt}=R_{xx}^{-1} r_{xd}$ is considered.

In LMS algorithm the gradient of the instantaneous squared error can be used instead of the gradient of the mean square error. To update the weights for each iteration of the adaptive filter a step size parameter μ is introduced to control speed of convergence of the algorithm.

$$w(n+1)=w(n)+2\mu e(n)x(n) \quad (2.5)$$

The step size parameter affects the stability, convergence speed and steady state error so to reduce steady state error small step size is used but it decreases the speed of the convergence of the algorithm. For better speed of convergence the step size value is increased but this affects the filter stability.

2.1 Simulink model for LMS filter

Environmental noise polluted sinusoidal signal is extracted. Noise signal is modeled as Gaussian noise. The two signals were added and subsequently fed into the simulation of LMS adaptive filter. The test block diagram of the noise canceller in Simulink is shown in Fig. 2.1. System inputs are Sinusoidal signal and Gaussian noise signal. The system outputs are the sinusoidal signal after filtering. By using manual switch LMS Adaptive filter Step size parameter is changed between high and low constant values. Gaussian noise generator is used for generating the noise signals. The step size value to the LMS filter was 0.001.

Select the Adapt port check box to create an Adapt port on the block. When the input to this port is nonzero, the block continuously updates the filter weights. When the input to this port is zero, the filter weights remain constant.

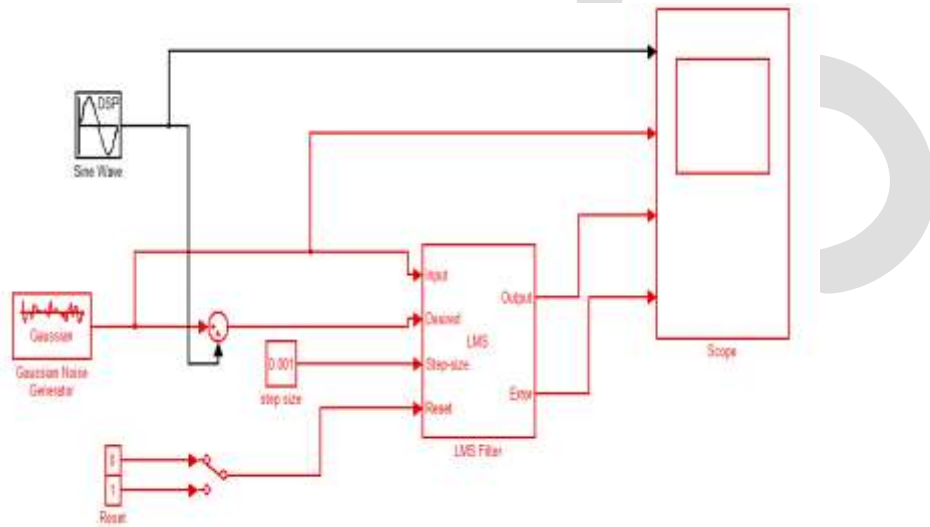


Figure 2.1. Simulink model for LMS

If the Reset port is enabled and a reset event occurs, the block resets the filter weights to their initial values. The LMS filter length used here is 32. If the step size parameter is at higher constant value the response is fast but showing less accurate and if step size factor is at lower constant value the response may be slow but it is showing more exact performance.

2.2 Experimental Results

Figure 2.2 shows the scope output of the LMS Filter. If the step size parameter is at higher constant value, the response is fast but showing less accurate results and if step size factor is at lower constant value the response may be slow but it is showing more exact performance.

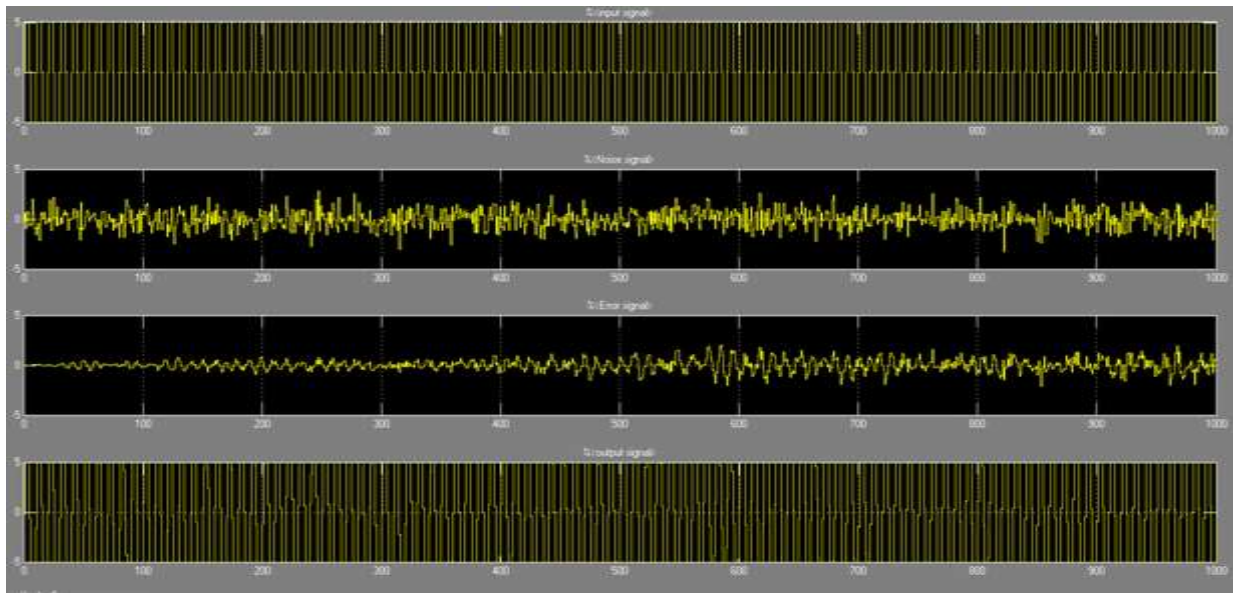


Figure 2.2 Scope output of LMS filter

3 NLMS Algorithm

In many adaptive filter algorithms Normalized least mean square algorithm (NLMS) is also derived from conventional LMS algorithm. The normalized LMS (NLMS), algorithm utilizes a variable convergence factor that minimizes the instantaneous error. Such a convergence factor usually reduces the convergence time but increases the misadjustment. In order to improve the convergence rate the updating equation of the conventional LMS algorithm can be employed variable convergence factor μ . The value of $\mu\sigma^2 x$ directly affects the convergence rate and stability of the LMS adaptive filter. The NLMS algorithm is an effective approach to overcome this dependence, particularly when the variation of input signal power is large, by normalizing the update step-size with an estimate of the input signal variance, $\sigma^2 x(n)$. In practice, the correction term applied to the estimated tap-weight vector $w(n)$ at the n -th iteration is 'normalized' with respect to the squared Euclidean norm of the tap input $x(n)$ at the $(n-1)$ -th iteration,

$$w(n + 1) = w(n) + \frac{\mu}{\|x(n)\|_2} e(n)x(n) \quad (3.1)$$

Apparently, the convergence rate of the NLMS algorithm is directly proportional to the NLMS adaptation constant μ , i.e. the NLMS algorithm is independent of the input signal power. Theoretically, by choosing μ so as to optimize the convergence rates of the algorithms, the NLMS algorithm converges more quickly than the LMS algorithm.

The variation of signal level at the filter input and selecting a normalized correction term, we get a stable as well as a potentially faster converging adaptation algorithm for both uncorrelated and correlated input signal. It has also been stated that the NLMS is convergent in the mean square if the adaptation constant μ (note that it is no longer called the step size) satisfies the following condition:

$$0 < \mu < 2$$

Despite this particular edge that NLMS exhibits, it has slight problem of its own. Consider the case when the input vector $x(n)$ is small. However, this can be easily overcome pending a positive constant to the denominator such that

$$w(n + 1) = w(n) + \frac{\mu}{c + \|x(n)\|_2} e(n)x(n) \quad (3.2)$$

Where the denominator is the normalization factor. With this, we obtain a more robust and reliable implementation of the NLMS algorithm.

4 Recursive Least Square (RLS) Algorithm

The Recursive Least Squares (RLS) filter is a better filter than the LMS filter, but it is not used as often as it could be because it requires more computational resources. The LMS filter requires $2N+1$ operation per filter update, whereas the RLS filter requires $2.5N^2 + 4N$. It has been successfully used in system identification problems and in time series analysis where its real-time performance is not an issue.

The Recursive least squares (RLS) adaptive filter is an algorithm which recursively finds the filter coefficients that minimize a weighted linear least squares cost function relating to the input signals. This is in contrast to other algorithms such as the least mean squares (LMS) that aim to reduce the mean square error. In the derivation of the RLS, the input signals are considered deterministic, while for the LMS and similar algorithm they are considered stochastic. Compared to most of its competitors, the RLS exhibits extremely fast convergence. However, this benefit comes at the cost of high computational complexity, and potentially poor tracking performance when the filter to be estimated changes.

In general, the RLS can be used to solve any problem that can be solved by adaptive filters. For example, suppose that a signal $d(n)$ is transmitted over an echoic, noisy channel that causes it to be received as

$$x(n) = \sum_{k=0}^q b_n(k)d(n-k) + v(n+1) \tag{4.1}$$

Where $v(n)$ represents additive noise. To recover the desired signal $d(n)$ by use of a p -tap FIR filter,

$$d(n) = \sum_{k=0}^{p-1} W_n(k) x(n-k) = W_n^T x(n) \tag{4.2}$$

Where

$$X_n = [x(n) \quad x(n-1) \quad \dots \quad x(n-p+1)]^T \tag{4.3}$$

is the vector containing the p most recent samples of $x(n)$.

To estimate the parameters of the filter W , and at each time n we refer to the new least squares estimate by W_n . As time evolves, to avoid completely redoing the least squares algorithm to find the new estimate from w_{n+1} , in terms of W_n .

5 Performance Evaluation of LMS ,NLMS and RLS

Table 5.1. Comparison of LMS and RLS with mean variance

Parameter	LMS	RLS
Mean	0.0057	0.0125

Variance	0.86	0.55
Multiplications	$2N+3$	$3(N+1)^2+3(N+1)$
Additions	$2N+2$	$3(N+1)^2+3(N+1)$
Time Elapsed	5.5ms	9.8ms

Table 5.2. Comparison of LMS NLMS RLS Table

Algorithm	MSE	%noise reduction	Complexity	Stability
LMS	2.5×10^{-2}	98.62%	$2N+1$	Highly stable
NLMS	2.1×10^{-2}	93.85ss	$5N+1$	Stable
RLS	1.7×10^{-2}	91.78%	$4N^2$	Less stable

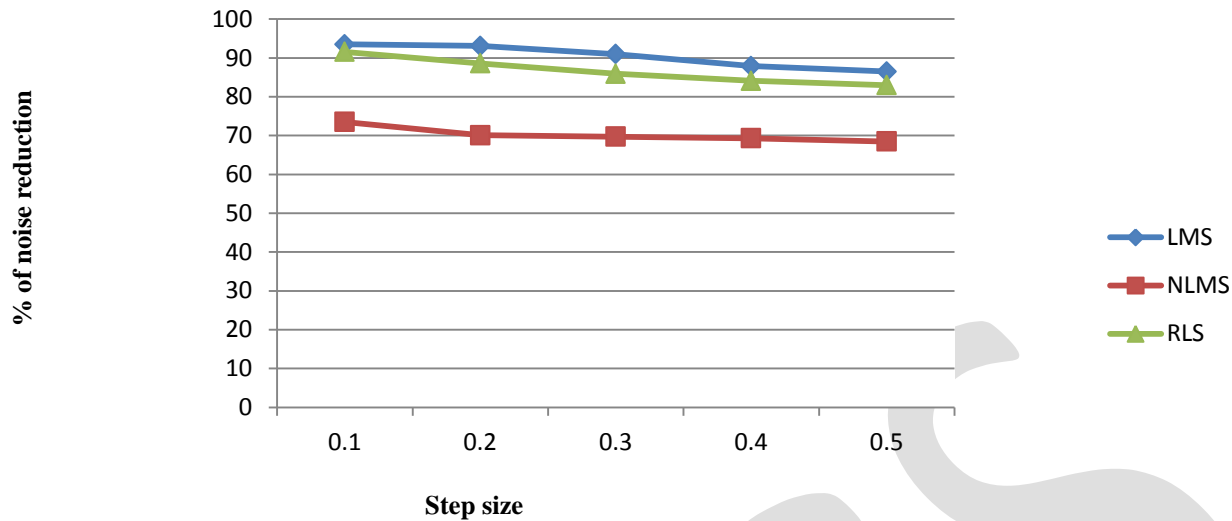


Figure 7.1 Comparison of adaptive filters with step size and % of noise reduction

From the table 5.1 and 5.2, the LMS Filter have higher stability. The percentage of noise reduction is greater in LMS algorithm. The complexity is reduced in the LMS algorithm. NLMS and RLS have low complexity but the tracking performance is poor compared with LMS filter. Fixed filter length 10 is taken for evaluation. It can be observed that for both the LMS and the NLMS, a particular optimum step size produces best approximation of the original signal. The value of the optimum step size is larger for the LMS than the NLMS. However, as the filter length is increased, the gap closes down since the value decreases for the LMS and increases for the NLMS. Another notable difference is that the curve for the LMS ascends sharply before reaching optimum level, and descends slowly afterwards. For the NLMS, it is the reverse.

6 CONCLUSION

Efficient Adaptive Noise canceller has been designed and simulated using LMS Algorithm. The effects of the filter length and step size parameters have been analyzed to reveal the behavior of the two algorithms. On comparison of LMS with RLS, the adaptation rate is Equal. RLS has fast convergence rate and infinite memory and high complexity. The LMS algorithm has produced good results for noise cancellation problem. LMS Algorithm is easy to implement, simple and it has a fast convergence rates. The Least Mean Square (LMS) algorithm is known for its simplification, low computational complexity, and better performance in different running environment. When compared to other algorithms used for implementing adaptive filters, the LMS algorithm is seen to perform very well in terms of the number of iterations required for convergence.

REFERENCES:

1. S. Haykin, *Adaptive Filter Theory*, 3rd ed., Upper Saddle River, New Jersey : Prentice Hall ,1996.
2. S. M. Kuo, and B. H. Lee, *Real-Time Digital Signal Processing*, Chichester, New York: John Wiley & Sons, 2001.pp.359-364.

3. B. Widrow , J. Glover , J. R. , J. McCool , J. Kaunitz , C. Williams , R. Hearn , J. Zeidler , J. Eugene Dong , and R. Goodlin .
“Adaptive noise cancelling: Principles and applications.” Proc.IEEE, 63, pp.1692 – 1716 , Dec.1975 .
4. Tian Lan, Jinlin Zhang, “FPGA Implementation of an Adaptive Noise Canceller,” Proc.Int.Symp.Information Processing(ISIP08), pp.553– 558, May.2008.
5. A. B. Diggikar, and S.S.Ardhapurkar, “Design and Implementation of Adaptive filtering algorithm for Noise Cancellation in speech signal on FPGA,” Proc.Int.Conf.Computing,Electronics and Electrical Technologies [ICCEET],pp.766-771, 2012.
6. B.Dukel, M.E.Rizkalla, and P.Salama, “Implementation of Pipelined LMS Adaptive Filter for Low-Power Applications,” Proc.45th IEEE Int. Midwest Symp.Circuits and Systems, Tulsa, Vol.2, 2002, pp. 533-536.
7. Simon Haykin, *Least-Mean-Square Adaptive Filters*, John Wiley & Sons, 2003, ch.1., pp.1-12.
8. Cristian Contan, Marcus Zeller, Walter Kellermann, and Marina Topal, “Excitation-Dependent Stepsize Control Of Adaptive Volterra Filters For Acoustic Echo Cancellation,” Proc.20th European Signal Processing Conference(EUSIPCO2012),pp.604-608, Aug,2012.
9. Markus Rupp, “The LMS Algorithm Under Arbitrary Linearly Filtered Processes,” Proc.19th European Signal Processing Conf.(EUSIPCO2011),pp.126-130, 2011.
10. Md. Zameari Islam, G.M. Sabil Sajjad, Md. Hamidur Rahman, Ajoy Kumar Dey, “ Performance Comparison of Modified LMS and RLS Algorithms in Denoising of ECG Signals” ,International Journal of Engineering and Technology Volume 2 No. 3, March, 2012
11. D.C. Dhubkarya , Aastha Katara , “Comparative Performance Analysis of Adaptive Algorithms for Simulation & Hardware Implementation of an ECG Signal”,*International Journal of Electronics and Computer Science Engineering ...*,ISSN- 2277-1956.
12. Pranjali M. Awachat, S.S.Godbole , “A Design Approach For Noise Cancellation In Adaptive LMS Predictor Using MATLAB ”. (IJERA) ISSN: 2248-9622 Vol. 2, Issue4, July-august 2012, pp.2388-2391
13. Jyoti dhiman¹, shadab ahmad², kuldeep gulia , “Comparison between Adaptive filter Algorithms (LMS, NLMS and RLS)” ISSN: 2278 – 7798 (IJSETR)..; Volume 2, Issue 5, May 2013

Design and Analysis of Welding Fixture for Fuel Tank Mounting Bracket

Prof. A. A. Karad^[1], Brijeshwar Wagh^[2], Ajay Shukla^[3], Niladhari Pyata^[4], Chetan Gujar^[5]

[1] Associate professor, Department of Mechanical Engineering, K.V.N. Naik Institute of Engineering Education and Research, Nashik

[2], [3], [4], [5] Students of B.E. [Mechanical], Department of Mechanical Engineering, K.V.N. Naik Institute of Engineering Education and Research, Nashik

[1] avinash.karad1974@gmail.com, 9860288527

[2] brijeshwarwagh000@gmail.com, 7588844767

Abstract— this paper deals with the design and analysis of the welding fixture for the fuel tank mounting bracket. A fixture is a work holding or support device used in manufacturing industries. Fixture are used for supporting and holding the work ensuring that all parts produced using the fixture will maintain conformity and interchangeability. Locating and supporting areas must be large and stiff enough to accommodate welding operation, strong clamps are also requirement. Thus, pneumatic clamps are used. Pneumatic clamps allow the automatic clamping. Since the fuel tank mounting bracket consist of number of child parts which have to be welded to each other with a specified tolerance and weld quality. The material used for the mounting bracket is mild steel which is commonly used in fabrication. The deformation on mounting bracket due to clamping and of rotating disc due to loading of all parts have been found using FEA by using ANSYS software. Finally the deformation results are presented in this document.

Keywords — Fixture, Design, Pneumatic clamp, clamping force, ANSYS

1. INTRODUCTION

A fixture is a device for locating, holding and supporting a work piece during a manufacturing operation. Fixtures are essential elements of production processes as they are required in most of the automated manufacturing, inspection, and assembly operations. Fixtures must correctly locate a work piece in a given orientation with respect to a cutting tool or measuring device, or with respect to another component, as for instance in assembly or welding. Such location must be invariant in the sense that the devices must clamp and secure the work piece in that location for the particular processing Operation. Fixtures are normally designed for a definite operation to process a specific work piece and are designed and manufactured individually.

The correct relationship and alignment between the components to be assembled must be maintained in the welding fixture. To do this, a fixture is designed and built to hold, support and locate work piece to ensure that each component is joined within the specified limits. A fixture should be securely and rigidly clamp the component against the rest pads and locator upon which the work is done.

Fixtures vary in design from relatively simple tools to expensive, complicated devices. Fixtures also help to simplify metalworking operations performed on special equipments. Fixtures play an important role on reducing production cycle time and ensuring production quality, by proper locating and balanced clamping methods .Therefore to reduce production cost, fixture design, fabrication and its testing is critical.

2. INTRODUCTION TO FUEL TANK MOUNTING BRACKET

Fuel tank mounting bracket is a frame which consists of number of child parts which needs to weld with specified tolerance and weld quality. The function of bracket is to hold and support the fuel tank of respected vehicle. The bracket is of Mahindra's bolero maxi truck. The bracket is made of material of mild steel which is commonly use by industries for manufacturing.

Table No. 1 Child Part of bracket

Component	Quantity	Material
L Channel	1	Mild Steel
L Rib	1	Mild Steel
Rib	2	Mild Steel
C Channel	1	Mild Steel
Strip	1	Mild Steel

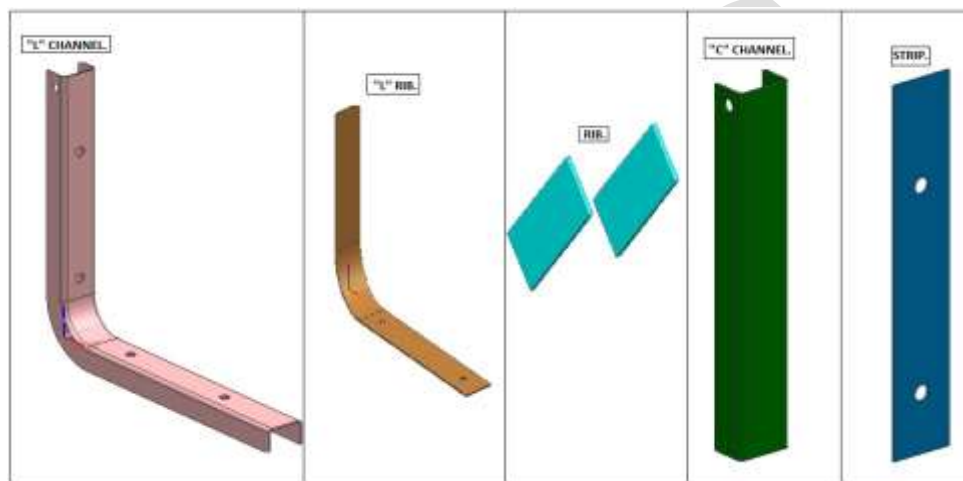


Figure No.1 Child parts of Bracket

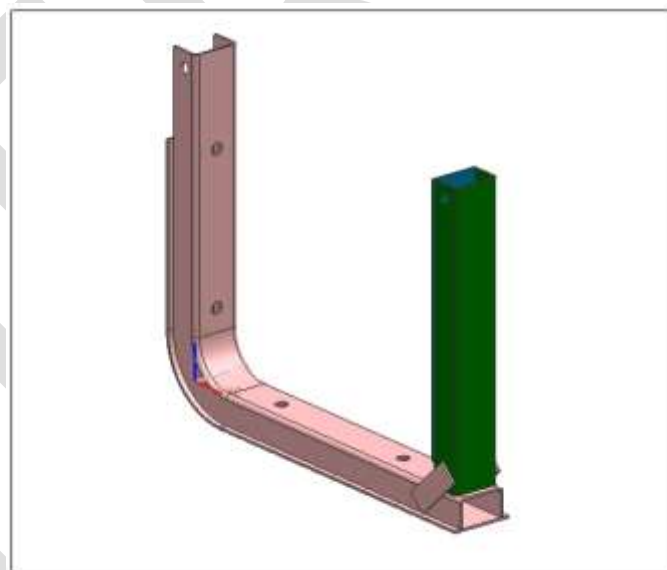


Figure No. 2 Assembled bracket

3. FIXTURE SETUP

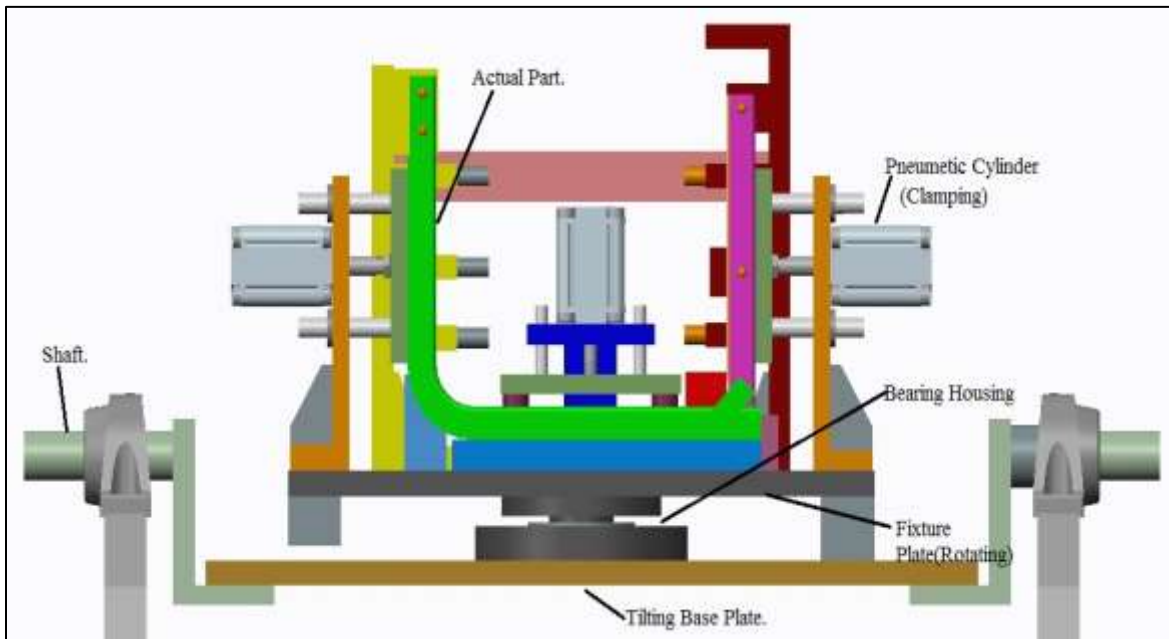


Figure No. 3 Welding Fixture setup

As fig. shows the assembly of welding fixture with fuel tank mounting bracket mounted. This welding fixture is specially design for this component to produce mass production and to reduce time consume.

This welding fixture is having 3 pneumatic cylinders to clamp the component by force actuating mechanism which exerted force on the component to hold it. Here are locaters are also provided to locate the holes. It is supported on rotating plate which is on work table or trolley for mounting of fixture.

Basically this fixture is work as to reduce welder fatigue and to obtain the mass production. As shown in fig the main component is hold and supported in between the locaters and clampers. The rotating plate is mounted in plumber block to till the whole assembly of fixture is rotate up to 45°. There is a bearing housing on the rotating plate on which fixture rotating plate is mounted. That fixture rotating plate is rotate about 180° horizontally. Which reduce the time required to weld as compare to manual welding? Here is the distance is very important thing that should be as the distance is not maintain by the operator or by any technical reason the locaters locate that distance and it should not be accurate and alarm will be generated and the operator got an idea about that there is any misalignment in the component. same way the holes are presented for mounted that fuel tank on it if that holes are not present their or not made by the operator then the alarm will be generated an the operator get an idea that there is anything wrong and had to be solve and any misalignment is present in the fixture the whole system is stop and do not start welding on the component means the welding electrode is not come out from the welding arm.

4. LOCATION AND CLAMPING CONSIDERATION

It is very important to understand the meaning of location before understanding about fixtures. The basic principles of locating and holding that apply to the machining fixtures can also be applied to welding fixtures. The locating arrangement should be decided after studying the type of work, type of operation, degree of accuracy required. Before deciding the locating points it is necessary to find out the all possible degrees of freedom of the work piece. Then some of the degrees of freedom or all of them are restrained by making suitable arrangements usually the locaters are used to restrict the degrees of freedom. Usually 3 2 1 locating principle is used for locating a work piece.

A clamping device holds the work piece securely in a fixture against the forces applied over it during on operation. Provide clamps that are quick acting, easy to use and economical. Clamps should be integral part of fixture. In case of welding fixtures the Clamps used must hold the parts in the proper position and prevent their movement due to alternate heating and cooling. Clamping pressure should not deform the parts to be joined.

Considering the locating and clamping factors, the locating is accomplished by using 14 locating pins. Clamping is accomplished by using pneumatic cylinder. The complete fixture assembly weighs 98 kg excluding component weight. Pneumatic clamping allows automatic clamping for the bracket. The pneumatic cylinder is of A63 050 040 O-M of Janatics.

5. ANALYSIS

Analysis has been carried out by using finite analysis method with help of ANSYS software. The analysis of clamping component and rotating disc has been carried out.

5.1 ANALYSIS OF CLAMPING COMPONENT

Since the bracket consists of number of thin part thus the clamping force considered should not deform it. Thus the analysis of clamping component was carried out and a proper required clamping force was selected.

As per the design consideration clamping force is applied on three faces for suitable clamping. The solid model of the component is selected and geometric conditions are selected, direction of the force is selected and clamping load of 120 N is given and results are evaluated using the software.

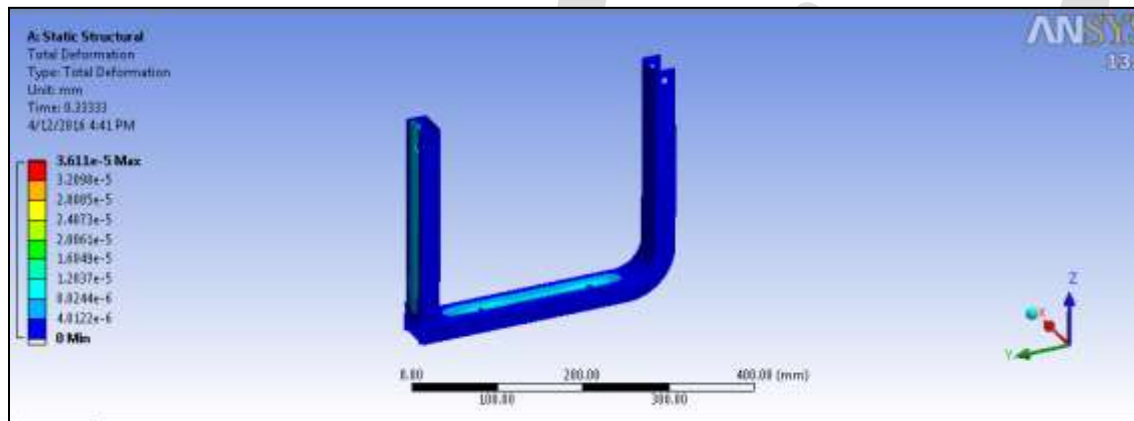
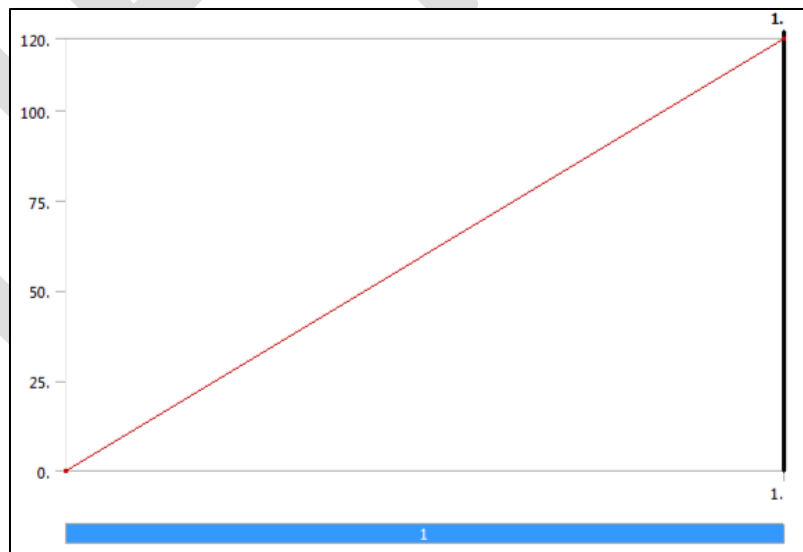
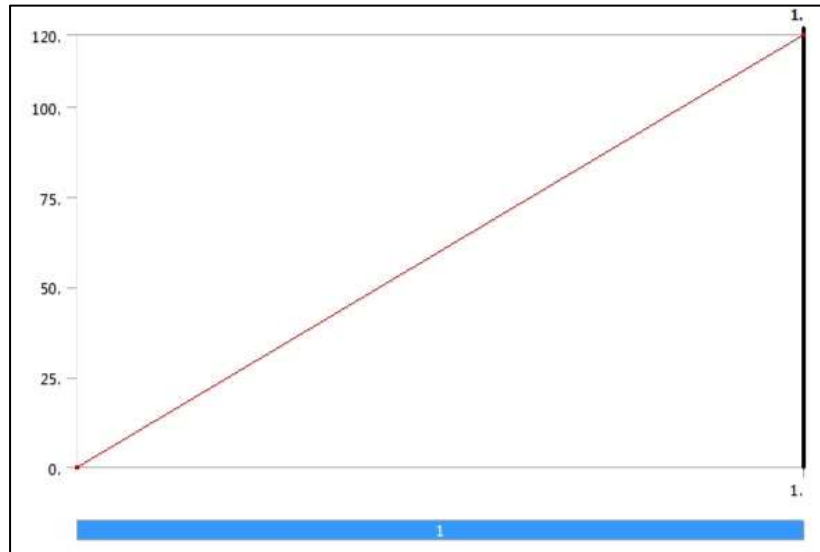


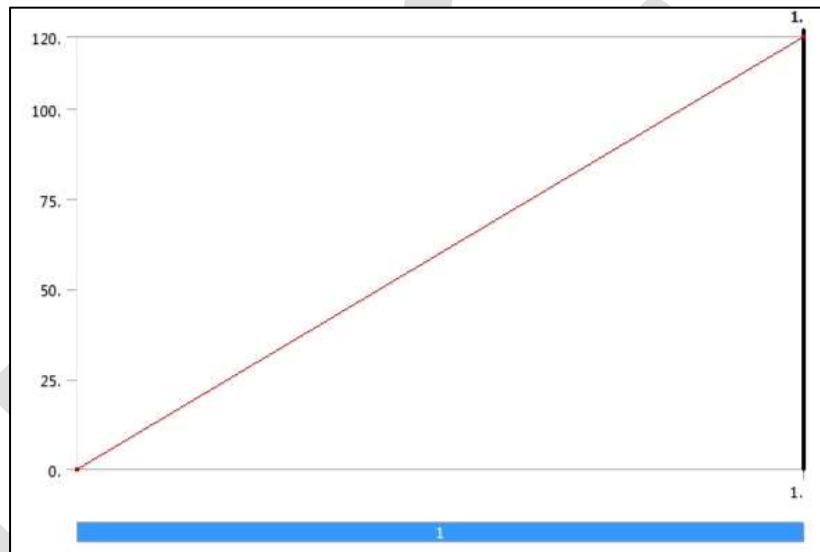
Figure No .4. Total deformation of bracket due to clamping load



Graph No. 1 Force Vs Deformation for surface 1



Graph No. 2 Force Vs Deformation for surface 2



Graph No. 3 Force Vs Deformation for surface 3

From the above graphs it can be seen that as the force applied increases the deformation also increases that is force is directly proportional to deformation this result is achieved for the maximum force applied. Thus the pneumatic clamp of less than 120N force needs to be selected.

5.2 ANALYSIS OF ROTATING DISC

Rotating disc is designed to achieve 180 degree rotation of the base plate. It was designed to bear the load and produce a proper rotation of the base plate constituting all elements. It bears the load of all the components fastened on the disc. It bears the load about 100Kg.

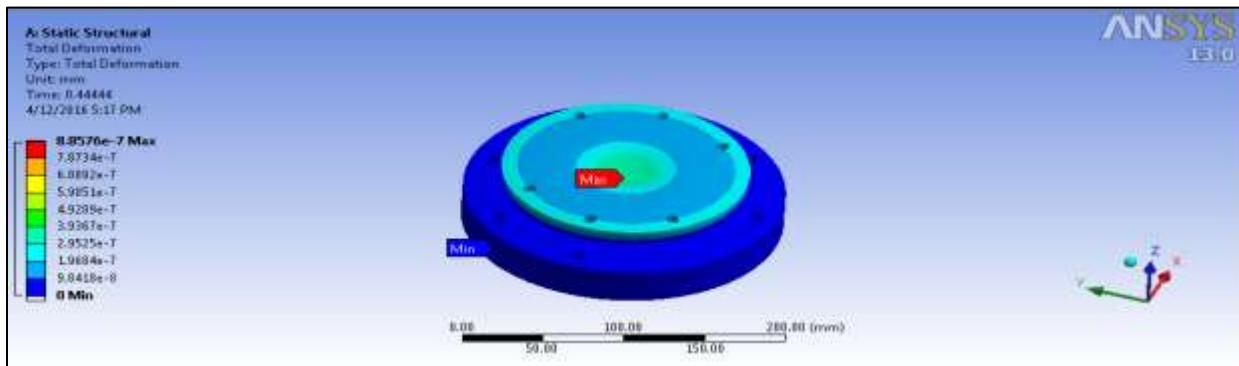
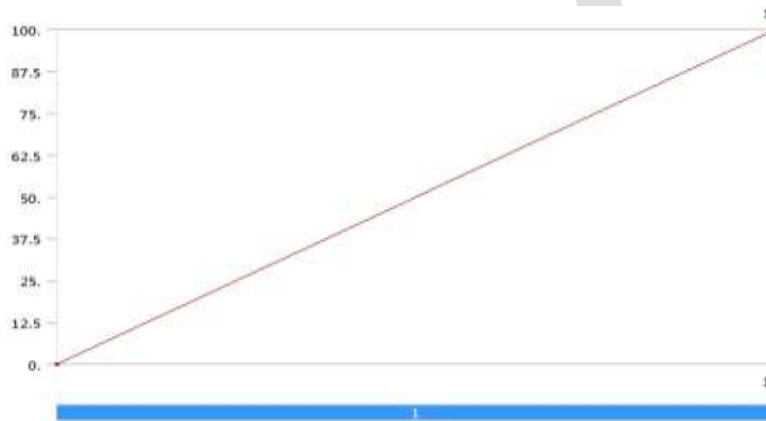


Figure No .5. Total deformation of rotating disc.



Graph No. 4 Load Vs Deformation.

Thus the rotating disc of selected dimension was found within permissible limit.

6. CONCLUSION

In this paper, the design and analysis of welding fixture for Fuel tank mounting bracket is performed successfully and in this process of designing. The analysis is done by ANSYS 13.0 WORKBENCH. This paper addresses the fixture design verification issue. In this paper, the work piece deformation in the component due to clamping load is taken into account.

REFERENCES:

- [1] Shailesh S. Pachbhai, Laukik P. Raut, "A Review on Design of Fixtures," International Journal of Engineering Research and General Science, Volume 2, Issue 2, Feb-Mar 2014.
- [2] Naveen A M , V A Girisha, Pruthvi H M "Design And Analysis Of Welding Fixture For Motor Case Assembly " in the International journal of mechanical and production engineering ISSN:2320-2092, VOLUME-2, Pg no 54-59, 2014.
- [3] Hui Wang, Yiming (Kevin) Rong, " Case based reasoning method for computer aided welding fixture design", Polytechnic Institute, Worcester: May, 2005.
- [4] Rong, Y and Zhu, Y, 1999; "Computer-Aided Fixture Design", Marcel Dekker Inc. NY; 1999.
- [5] Iain Boyle , Yiming Rong , David C. Brown "A Review and Analysis of Current Computer-aided Fixture Design Approaches", ELSEVIER, Robotics and Computer –Integrated Manufacturing 27 (2011)

STEPPER MOTOR DRIVEN THREE AXIS ROBOT USING PLC

Kanchan Pandita¹, Yamini Sharma², Vijaykumar Kamble³

Savitribai Phule Pune University, India,

Department of Electrical, AISSMS's Institute of Information Technology, Pune, India, 8796641497

kanchan_pandita@yahoo.com, yaminisharma93@gmail.com, vskamble76@gmail.com

Abstract— The subject of control system design is usually approached from two distinct perspectives: development of general principles such as mathematically or experimentally derived theory, and case studies which describe instances of specific applications in practice. This paper fills the gap between these two approaches for a particular topic, application of PLCs to robotic workcells. Specifically, the subject of interest is organization of PLC program. Robotic workcells are custom built. Despite that, it is possible to discern common physical features and operating characteristics among robotic workcells. As a good design practice, these common traits are used, on an individual device or axis of motion basis, to generate typical portion of code. Similarly, on equipment, workcell or global level, typical organization of code is developed with a standardized program format, order and naming conventions. A library of code segments can be developed for specific sensors, actuators, axis of motion arrangements, robot and workcell configurations. This library can then be used for mix and match software development without sacrificing flexibility to customize or refine programs. Since the structure of the code is standardized and known ahead, the benefits of this approach extend beyond the code development stage to the program debugging and the life of product maintenance and repair troubleshooting of equipment.

Keywords— Stepper Motor, PLC, Custom built, Flexibility, Work cell, Standardize, Three Axis Robot.

INTRODUCTION

Robots are the integral part of manufacturing industry which largely depends upon its productivity for profit. The manufacturing industry may be automotive, textile, good packaging etc. Till date the industrial robot available in the market are microcontroller based for their robotic operation and path calculation. The work cell of the robot is controlled by industrial programmable logic controller. As we are using stepper motor as a drive for axis because no feedback path element is required such as encoder, resolver. As the robot manipulator has three axes so, the work envelope is a cube. Till date there are microcontrollers for the path calculation and PLC for the specific applications. But in this project we are now proposing PLC as an integrated robot architecture. [1]

Even in a typical robotics system, the PLC controls the entire operation of the cell. However, robot operations and path planning are done on a different controls platform that is proprietary to the robot manufacturer. As with any proprietary system, robots require specially trained professionals to program, control and interface them with the PLC for major operational commands. These specially trained technicians are in high demand but short supply, especially when needed unexpectedly for emergency repairs or adjustments. Even qualified robot technicians are usually familiar with only one or two – of many – brands of robots, and not necessarily the ones that you have. This specialization contributes to the technical skills scarcity and related delays and downtime. In most cases, manufacturers rely on their systems integration house or the robot manufacturer for troubleshooting, service and support. This reliance on outside resources is the reason robot “ownership” has been a myth. [1]

In comparison to the scarcity and specialization of robot experts, PLC experts are much more accessible because the programming concepts and foundations remain the same no matter what brand of PLC is being used. Insofar as most machinery in a plant runs on a PLC, there are naturally more PLC experts than robot experts. Also, PLC programming is commonly taught in technical schools, while robot programming is not. To solve this problem, manufacturers and industrial and process engineers sought a way for robots to be programmed and controlled entirely through a PLC. Their work led to the development and implementation of the PLC-integrated robot control concept, also known as Unified Controls Architecture. [5][2]

UNIFIED CONTROLS ARCHITECTURE

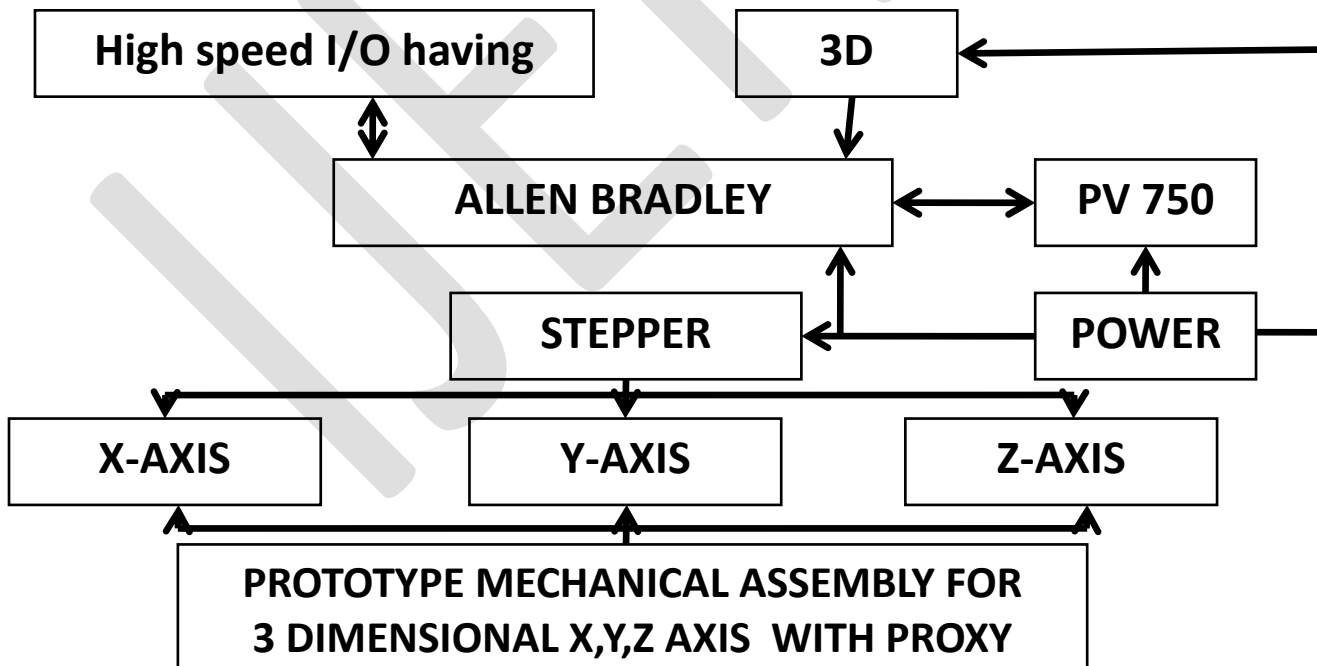
The definition of Unified Controls Architecture changes based on the usage context. In production and packaging systems, we define Unified Controls Architecture as a single unified primary controls platform for the entire workcell, so that the programming, diagnosis and troubleshooting is done in a single place. Unifying controls simplifies the system design because it decreases the number of cables, communication nodes and controls that are necessary in a traditional system's architecture. A reduction in components leads to a reduced number of failure points and spare parts required. The Unified Controls Architecture approach promotes greater interoperability among components and systems, both upstream and downstream in the packaging line. Unified controls make the system more user-friendly because there is only one programming language to learn and maintain throughout the manufacturing plant. Robots become more maintenance staff -friendly as troubleshooting of the entire system happens in one place, in one language. Multiple programming languages are no longer required. With the advent of smart sensors such as vision systems, the unified architecture makes it simple to integrate sensor guidance and line tracking options that may be required for packaging applications.[1]

The Unified Controls Architecture benefits the end users of the automation by providing maintenance-friendly systems. And it offers tremendous advantages to system integration houses, since programming the robots and all of the peripheral equipment happens in one place. Additionally, a single person can usually both program and debug the systems. This approach makes the system development more efficient in comparison to a traditional approach. Another key benefit that Unified Controls Architecture offers is the ability to redeploy assets with your own maintenance staff. As the robots in this architecture are programmed, taught and controlled entirely through a PLC, your resident experts could easily redeploy them into another application or perform required upgrades as needed. Therefore, a Unified Control Architecture makes robotics system ownership a practical reality.[2]

OBJECTIVE

The main objective of this project is to prepare a PLC programme such that it will calculate path coordinates also at the same time it will drive a stepper motor accordingly. Also to prepare the HMI program to allow user to interface the robot program through appropriate screens. We are going to prepare such a program which allows user to program the robot path manually using joystick at first teaching and then the robot will perform the same function automatically afterwards with desired accuracy

PROPOSED MODEL



Proposed model enlightens the following areas

Electrical and electronics, Mechanical, Programming

Electrical and electronics consists of stepper motor and stepper motor driver. The stepper motor driver drives the stepper motor. Mechanical consists of lead screw, nuts and bolts, coupler etc. The whole mechanical assembly runs over the track because of the rotation of stepper motor. Programming mainly is the ladder logic programming of Allen and Bradley. Hybrid stepper motor is used because of its high torque, greater inertia. DM320C is used as the stepper motor driver because of its great compatibility with the stepper motor. The lead screw is made up of stainless steel because of its non- rusty nature. PLC used is Micrologix 500 of ALLEN & BRADLEY mainly because of numerous instructions available in the kit like PTO.[4]

PROBLEM STATEMENT

Restricted authorization to user: - Because of the use of embedded microcontroller in robotics, the users are restricted to a certain level. Use of such system results in low capital cost but high running cost involved in service and troubleshooting. Existing robots need skilled labours to troubleshoot the problem.

Solution: - To solve this problem we will programme a PLC such that it will perform robotic calculations such as calculating path coordinates and will drive the stepper motor in conjunction with each other by using high speed input-output of ALLEN BRADLEY Micrologix 1400 PLC & PV750 plus HMI for user interface.

METHODOLOGY

Robot will have three axis namely x, y, z in both the positive and negative directions so, the work envelope will be a cube having coordinates of the origin as (0, 0, 0). For better accuracy, high resolution stepper motor will be used as an open loop system. As being a open loop position control system we need to check whether the given electrical command (pulses) has successfully converted into desired mechanical movement, a position check must be incorporated using proxy sensor. These sensors will check the positioning operation of the overall system through every cycle.



Fig. 1. Lead screw



Micrologix 1400



Fig. 3. Hybrid stepper motor

SPECIFICATIONS OF HYBRID STEPPER MOTOR

Step angle(deg)	1.8	Rated voltage(v)	12
Temperature rise(deg-c)	80 max	Rated current(A)	0.9
No. of phases	2	Resistance per phase	38.5
Insulation resistance	100M Ohm	Inductance per phase	21
Insulation class	Class B	Holding torque(kg-cm)	1.6
Max. radial force(N)	28	Detain torque(g-cm)	120
Max. axial force(N)	10	Rotor inertia(g-cm)	35

CONCLUSION

The robot manipulator will have position accuracy of about $\pm 2\%$. Robots can be used for variety of applications like pick and place, palletizing in an array form or drawing a circle, square etc.

REFERENCES:

- [1] Zein El Din, A.S. ; Electr. Eng. Dept., Menoufia Univ., Egypt “High performance PLC controlled stepper motor in robot manipulator” Industrial Electronics, 1996. ISIE '96. Proceedings of the IEEE International Symposium on (Volume: 2)
- [2] Gary Dunning, “Introduction to Programmable Logic Controllers”, Thomson, 2nd Edition
- [3] John R. Hackworth, Frederick D., Hackworth Jr., “Programmable Logic Controllers Programming Methods and Applications”
- [4] John W. Webb, Ronald A. Reis, “Programmable Logic Controllers: Principles and Application”, 5th Edition
- [5] PLC AS A DRIVER FOR STEPPER MOTOR CONTROL Laurean BOGDAN University “Lucian Blaga” of Sibiu, e-mail: laurean.bogdan@ulbsibiu.ro
- [6] PLC-controlled stepper motor drive for NC positioning system Hussein Sarhan Faculty of Engineering Technology, Amman, Jordan E-mail: Hussein_74707@hotmail.com
- [7] PLC-Based Robotic Controls versus OEM Robotic Controls What’s the Best Choice for Your Application? By Matt Wicks, VP Systems Engineering, Intelligrated.
- [8] Boczkaj, B.F. ;Irvine, CA, USA, “Software aspects of PLC’s application in robotic work cells” Industry applications conference, 1996.thirty-first IAS annual meeting, IAS '96., conference record of the 1996 IEEE (volume3)
- [9] 3D stepper motor system and its GUI design. Meng Lian , M.A Abidi Imaging, Robotics, and Intelligent Systems Laboratory Dept. of Electrical and Computer Engineering. The University of Tennessee Email: mlian@utk.edu
- [10] Micrologix 1400 programmable logic controller Publication 1766-RM001F-EN-P - May 2014 634 Supersedes Publication 1766-RM001E-EN-P - May 2012

Design and Implementation of Binary Motion Vector technique with Pruning DWT for Video Compression

Megha S.Gaoture

Asst.Prof. (ETC Department,GHRIETW,Nagpur)

meghgaoture@gmail.com,9096043304

Abstract— Now days, video quality is a very important factor in entertainment world. A movie could be interesting only because of its quality and its graphics. To send and store these videos, we have to compress them, rejecting part of the unneeded data to reduce the video capacity. Video Compression algorithms combine Spatial image compression and Temporal motion compression. The sequence of frames contains Spatial and Temporal redundancies that Video Compression algorithms attempt to eliminate or code in smaller size. In this paper, We presented a design of Binary motion vector technique with Pruning Discrete Wavelet Transform for the compression of AVI video. Here, Binary motion vector technique used for searching the Best matching block. This technique requires less candidates block than other motion vector technique. Pruning based DWT uses thresholding which enhanced the compression ratio with desirable Peak Signal to Noise ratio. This algorithm has simulated on Xilinx ISE13.1 and Model Sim 6.2c and implemented on SPARTEN3 FPGA. Hardware implementation of algorithm consumes 15% of slices on Xilinx SPARTEN3 FPGA with maximum operating speed of 198MHz.

Keywords— Video compression, Binary motion vector algorithm, Block Matching, Pruning DWT, MATLAB, Compression ratio, FPGA

I. INTRODUCTION

Video is an illusion that makes use of the properties of eye. Eye has a peculiar property that image sensed by eye persists for 1/30th of a second and video clips are made up of sequences of individual images, or "frames." Video compression is essential for developers of embedded systems, processors, and tools targeting video applications. In order to achieve compression of video signals, motion estimation between the successive frames is performed which contributes significant bit saving by transmitting only the motion vectors. This is the most computationally intensive operation in the coding and transmitting of video signals. For this, Block Matching is the most preferred Motion Estimation technique. BM divides the video frames into $N \times N$ pixel blocks and tries to find the block from the reference frame in a given search range that best matches the current block. Sum of Absolute Differences (SAD) is the most preferred block matching criterion because of its low computational cost. The block with minimum SAD is then taken as Best reference block. Among the BM algorithm, Full search algorithm achieves the best performance since it searches all search locations in the given search range. But, its computational complexity is very high, it requires huge hardware and large candidate blocks [1]. Many Frequency based techniques are also used which uses Fourier Transform. But if we compare Fourier Transform with DWT, then, DWT is effective because it has multiresolution capability. Wavelets are signals which are local in time and scale and generally have an irregular shape. The wavelet transform can be seen as a decomposition of a signal in the time-scale plane. Once this is done the coefficients of the wavelets can be decimated to remove some of the details. Wavelets have the great advantage of being able to separate the fine details in a signal. Different types of wavelets also present which has different features. One particular wavelet may generate a more sparse representation of a signal than another. So, we are using here Binary Motion Vector technique with Pruning DWT.

The binary motion vector technique classifies each block to a class, in which each pixel is given a value of "0", "1", "2", "3", depending on the pixel value after the Frequency transformation. When the reference block has the same class of the current block, this reference block is considered a candidate block, and otherwise the reference block is rejected. Then after adding the 64 pixels of the block, this block is classified as one of 8 classes. This algorithm will be implemented on FPGA.

II. PREVIOUS WORK

Many algorithms are proposed in the literature for the Video compression which requires less computational complexity. Fast search methods such as three step search, square search, diamond search and hexagon search can be used instead of FS algorithm [6]. Square and diamond search is used to determine the BRF of the current block, and this BRF is searched using FS algorithm in literature. In the literature [5], Arithmetic encoding and Run length encoding algorithm is implemented. Here, Discrete cosine transform is used to convert each pixel value into frequency domain. RLE algorithm is easy to implement but not gives high compression ratio. In the literature [1], Multiple reference frame motion estimation is used. This algorithm uses number of reference frames for each macro block and early termination. This hardware has less energy consumption.

III. PROPOSED WORK

We are using Binary Motion vector technique with Pruning DWT and then the algorithm will be implemented on Xilinx Spartan3 FPGA. First, input to the DWT is given in form of frames. For this, Video is divided into Frames using MATLAB tool. We are taking the Video of different format. The flowchart of algorithm is given in the following figure 1.

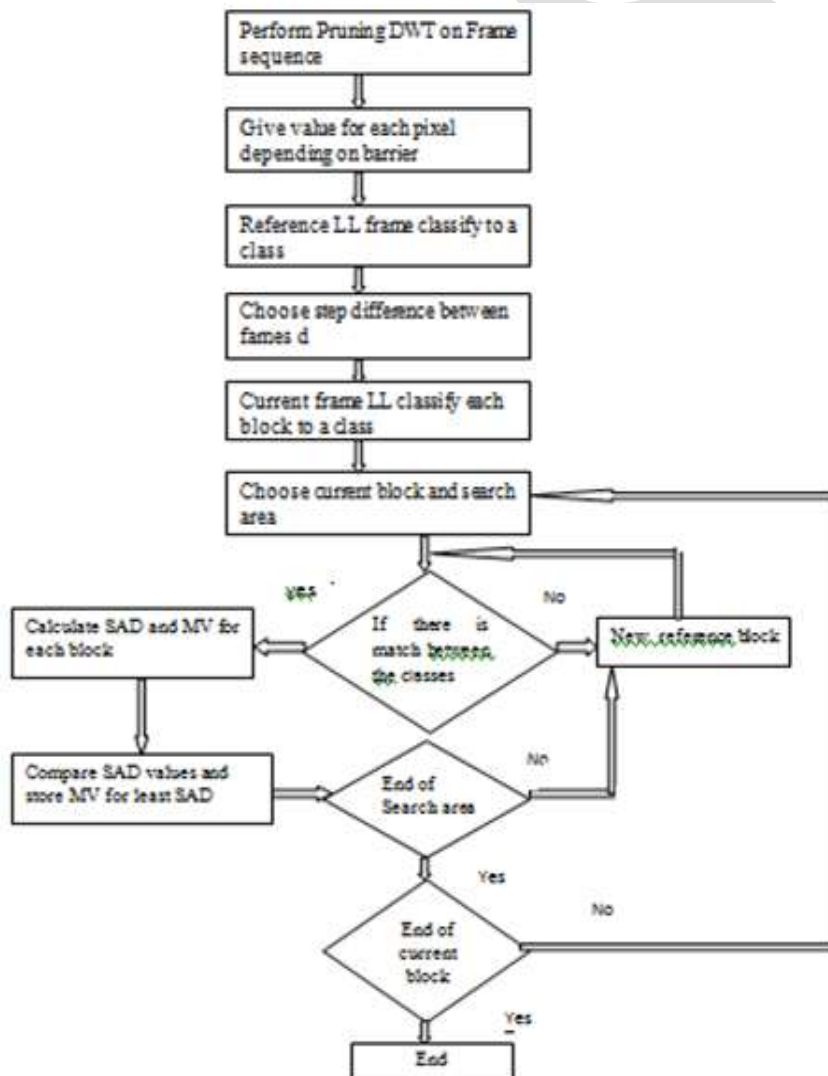


Figure 1: Flowchart of algorithm

A] Pruning based DWT

Due to a wavelet transform, a signal can be decomposed into many shifted and scaled representation of original mother wavelet. Many wavelets display a property ideal for compact signal representation: orthogonality.

This property ensures that data is not over represented.

A wavelet function $\Psi(t)$ has two main properties,

$$\int_{-\infty}^0 \Psi(t) dt = 0;$$

That is, the function is oscillatory or has wavy appearance,

$$\int_{-\infty}^0 |\Psi(t)|^2 dt < \infty;$$

That is, the most of the energy in $\Psi(t)$ is confined to a finite duration.

the proposed compression technique with pruning proposal based on discrete wavelet transform (DWT) first decomposes an image into coefficients called sub-bands and then the resulting coefficients are compared with a threshold. Coefficients below the threshold are then taken as zero and coefficients above the threshold value are encoded.

B] Proposed algorithm

Architecture of proposed algorithm is shown in the figure 2. It consists of main blocks such as block creator unit, accumulator unit, class unit, SAD unit and comparator unit. Here, step difference is taken as distance between the reference frame and current frame. If step difference is 4 then it takes 4 reference frames. In DWT, each frame is divided into four quarters, Low Low (LL) coefficients having the image information, High Low (HL) coefficients, Low High coefficients (LH) and High High (HH) coefficients having only the sharp edges of the image. After transformation, LL coefficients are used in the process while LH, HL and HH coefficients are sent to the decoder to be used in retrieving the frames. After retrieving these frames, these frames are used as reference frames. After transformation, LL quarter is divided into 8x8 pixel blocks, each pixel is given a number depending on its value. We then add all the values of all pixels, then the block is classified into a class of 8 classes. Compare the current block to the corresponding block in the reference frame; in addition to all the blocks in a search area. Where the search area is a square area of 7 blocks above the corresponding block in the reference frame, 7 blocks below, 7 blocks right and 7 blocks. Candidate blocks are selected if having the same class, a higher class or a lower class. Calculate the Sum of Absolute Differences (SAD) between the candidate block and the current block, the block with the least SAD is the best matching one. MV is calculated for the best matching block. MV and residuals are sent, this method is applied for all blocks in the current frame.

In the architecture of algorithm, there is a control unit that controls the entrance of frames at the DWT unit where each pixel coefficient is transformed into Discrete wavelet coefficients. We only take the LL coefficients by the help of the control unit. After transformation, each pixel coefficient is divided by 2, in order to operate on 8 bits instead of 9 bits. Then coefficients will be taken to the block creator unit where coefficients will be put in matrix form. In this way one by one all frames enter and are stored in the RAM. When each frame is transformed, the control unit orders the RAM to save data in its place. At the same time, after filling the matrix in the block creator unit, the control unit controls the process of releasing each coefficient to the class stage, in a block manner. A simple 2 counters in the control unit manage this process, each coefficient in the block takes a value of "0" or "1" or "2" or "3" or "4" depending on the number of frames. and then flows to the accumulator block, where summation of the pixel coefficients takes place. then the summation flows to the class look-up table to classify the block to a class number. The class will be saved in the RAM in an address after the block addresses. To save data in the RAM, RAM is divided into the number of stages depending on the number of frames entering.

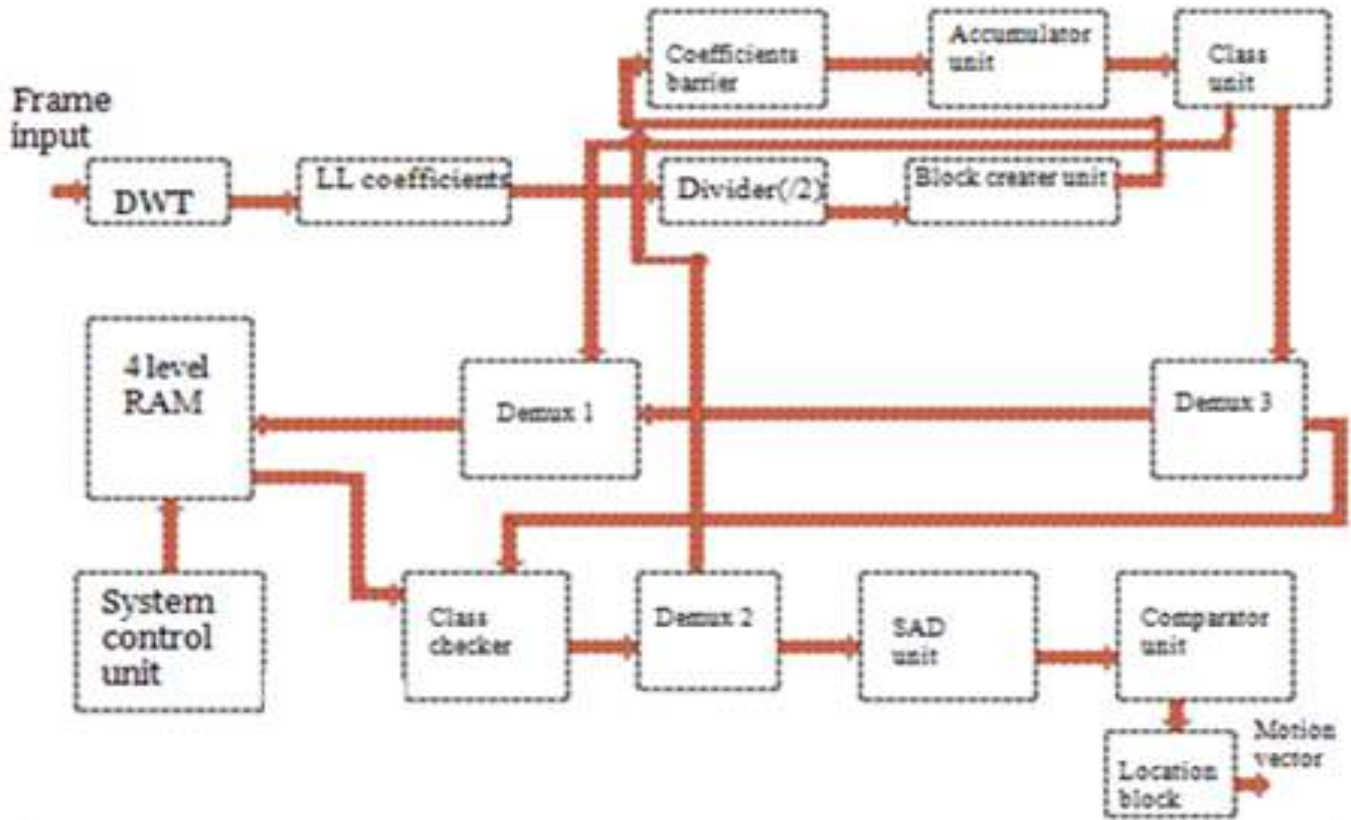


Figure2: Proposed algorithm design

For the current block, we have to calculate motion vectors. The control unit calls the 1st main block to the class checker unit, where it will pass normally as its class is calculated, then to Demux 2 where the control unit makes it pass to the SAD block. The control unit calls for blocks in search area.

The control unit produces a number called the location number which is number of candidate block in the search area. The class checker then calls for each candidate block, if the class was calculated. Then it will go to the SAD unit. Demux 2 allows this block to flow back to the class stage, in order to calculate the candidate block class, in case the block is an overlapping not a main block. The main block is the block that when the frame is divided regularly to blocks, these blocks are main ones, but that doesn't mean that the frame doesn't have any other blocks than these. There can be overlapping blocks. So the possibility that the best matching candidate block in the overlapping blocks is much more than the main blocks. Demux 3 is to send the data back to the class checker where it makes sure if the class is calculated. The candidate block data flows through DEMUX 2 to the SAD unit. Now two blocks are in the SAD block, the SAD value is calculated. Then SAD values will go to the comparator unit where it compares two values till we get least SAD values. After that block with least SAD value is taken as best matching block. Finally, its location number flows to the location block where the MV is calculated. This process is then done for all blocks of the current frame of video.

IV. RESULTS

The proposed architectures of algorithm has simulated using VHDL language using Xilinx 13.1 ISE. It has been implemented on Xilinx 13.1 ISE, SPARTAN 3 FPGA. We have taken three videos of AVI, 3GP, FLV and retrieved frames for each video. For each video, Performance is measured in the form of parameters like Compression rate, PSNR ratio. Results of three videos are shown below



Figure 3: Original frame



Figure 4: Retrieved frame

Video	Original file size (KB)	Compressed file size (KB)	Compression rate(%)	PSNR(db)
1	2310	769	3	30



Figure 5: Original frame



Figure 6: Retrieved frame

Video	Original file size (KB)	Compressed file size (KB)	Compression rate(%)	PSNR(db)
2	2310	769	3	33

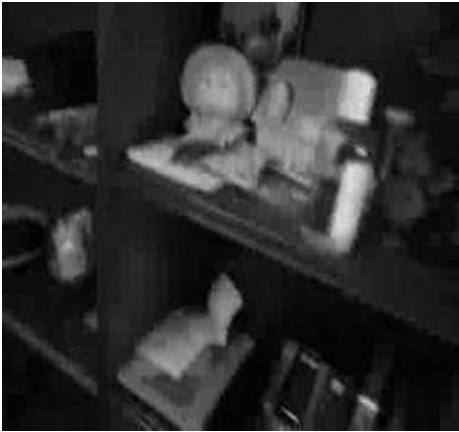


Figure 7: Original frame



Figure 8: Retrieved frame

Video	Original file size (KB)	Compressed file size (KB)	Compression rate(%)	PSNR(db)
3	3850	769	5	38

Performance of Proposed algorithm and area utilization on Xilinx Spartan 3 FPGA

Video	Original file size(KB)	Compressed file size (KB)	Maximum frequency (MHz)	Used no. of slices	Compression	No. of LUT's used
1	38500	769	198	15%	50%	20

V. CONCLUSION

In this paper, We proposed Binary Motion vector algorithm architecture which improves the video quality and compression ratio. Also, Pruning DWT is applied on the frames of video to store the image in few coefficients which is useful for compression of video. In comparison of DCT, DWT has many advantages like multi resolution. It improves compression. Here, SAD parameter is used as measuring parameter for best matching block. It requires less computational complexity and easy to implement. Our proposed algorithm consumes 15% of slices on Xilinx SPARATEN3 FPGA with maximum operating speed of 198MHz.

REFERENCES:

- [1] Aydin Aysu, Gokhan Sayilar, and Ilker Hamzaoglu, "A Low Energy Adaptive Hardware for H.264 Multiple Reference Frame Motion Estimation", IEEE Transactions on Consumer Electronics, Vol. 57, No. 3, August 2011
- [2] S.Anantha Padmanabhan, S.Chandramathi, "A Proficient Video Encoding System through a Novel Motion Estimation Algorithm" IEEE-ICoAC,978-1-4673-0671-3/11, 2011
- [3] Ahtsham Ali, Nadeem A. Khan, "A Spatio-temporal Recursive search based prediction scheme for efficient multi-frame and bidirectional motion estimation" IEEE International conference on Acoustics speech and signal processing(ICASSP),ISSN 1520-6149 ,pages 1209-1212, 25-30 March, 2012.
- [4] M. Abomhara, O.O.Khalifa, O.zakaria, A.A.Zaidan, B.B.Zaidan and A.Rame, "Video Compression techniques: An Overview", Journal of Applied Sciences, Vol.10, No.16, pp.1834-1840, 2010.

- [5] Mozammil, S. M. Zakariya and M. Inamullah, "Analysis of Video Compression Algorithms on Different Video Files" IEEE Fourth International Conference on Computational Intelligence and Communication Networks, 2012.
- [6] Jafari, A. and Rezvan, M. and Shahbahrami, A.: 'A Comparison Between Arithmetic and Huffman Coding Algorithms' The 6th Iranian Machine Vision and Image Processing Conference, pp: 248-254, October, 2010
- [7] Sharma, M, "Compression Using Huffman Coding", International Journal of Computer Science and Network Security, VOL.10 No.5, May 2010.
- [8] S. R. Kodituwakku and U.S. Amara singhe, "Comparison of Lossless Data compression Algorithms for text data", Indian Journal of Computer Science and Engineering ,Volume 1 (No4) pp. 416 - 425, 2010
- [9] Ajnadeen Khalil, "Matching Binary Motion Estimation Algorithm Based on Discrete Wavelet Transform of Video Sequences" June 2008.
- [10] C.W. Ting, L. M. Po, and C. H. Cheung, "Center-biased frame selection algorithms for fast multi-frame motion estimation in H.264," IEEE International Conference on Neural Networks and Signal Processing, pp. 1258–1261, December 2003.
- [11] K. Anil Jain, "Fundamentals of Digital Image Processing", Chapter 11 3 October 1988.
- [12] Lai-Man Po, Wing-Chung Ma "A Novel Four Step Search Algorithm for Fast Block Motion Estimation" IEEE Transactions on Circuits and Systems for Video Technology, vol. 6, no.3, pp 313-7, June 1996.

Design and analysis of dedicated machining fixture hook for cylinder block to operate by overhead crane

Rohit Gokarn Jadhav (M.E Design)¹, Prof.Aldar.B.D (Head of Mechanical Engineering)²

Email Jadhav.rohit37@gmail.com and contact no 9767897918

Abstract— Work gives conceptual model and mechanical design of special application fixture hook made for crane which is to be used overhead material handling application in component machining automation. Cylinder block is to be machined for drilling operation executes in line on bottom face of the component so this hook gives perfect fixturing with full proof poka yoke to move on overhead sliding panel provided in shop floor. Design and product development considered with the manufacturability and practical feasibility. Structural weldment is the out coming function for this work of innovation .Boundary conditions are examined and applied for analysis on actual behavior of the structure in working conditions. Loads are calculating by considering input parameters. Structural behavior analysis formed in ansys tool to prove its workability.

Keywords— Design and Analysis , Fixture hook ,Cylinder Block , Modeling , Ansys.

INTRODUCTION

Casted cylinder block is to be machined on its bottom face for drilling operation to be carried out at height of 2.2 m from ground level. Dedicated Hook will catch the component from powerised conveyor and pick and place operation will be there but the operation will not end till drilling and tapping get finished ,In assembly line this crank shaft is required to be drilled before shaft ending plate is assembled with it. For this requirement we want this production rate to be cover 12 components in every hour. Existing system is giving manually operating process with average 7 components processed in one hour.

Crane used to make hook as handler:

A **lifting hook** is a device for grabbing and lifting loads by means of a device such as a [hoist](#) or [crane](#). A lifting hook is usually equipped with a safety latch to prevent the disengagement of the lifting wire rope sling, chain or rope to which the load is attached. A hook may have one or more built-in [pulleys](#) to amplify the lifting force. Crane & Overhead Lifting Applications Bullivants prides itself on setting the highest standards for quality and safety with all of Crane and Overhead Lifting Devices. For Lifting applications Crane and Overhead Lifting Products are designed and manufactured in accordance with all relevant Standards and are guaranteed to meet all criteria necessary to proper usage. custom design, re-certify, manufacture and repair virtually any type of lifting device used in industrial applications. standard range offers versatility across a variety of applications. Lifting & Rigging Equipment fully tested chain slings and hardware with fabricated lifting product as a complete unit so that everything is ready to go when it gets to site.

Lifting Beams

35 Tonne Container Lifting Beam • 90° maximum sling angle • Heavy duty. • Approved, tested and certified with WLL clearly marked. • Engraved ID tag • Powder coated safety yellow

Input :

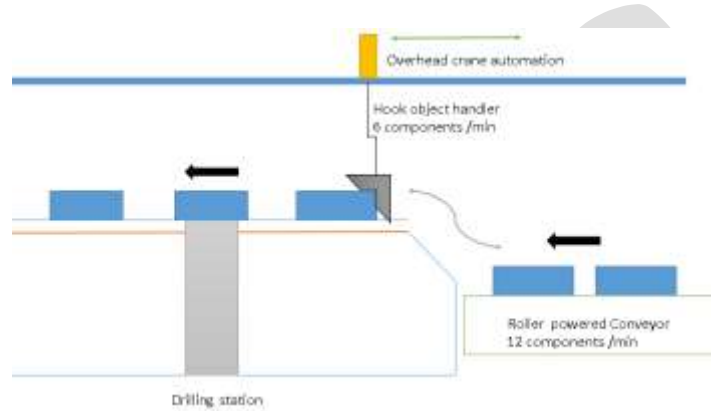
4 Cylinder block

Weight: 94 kg.

Drilling operation to be perform on bottom side ,

No of holes and size : M10 x12

Working layout:



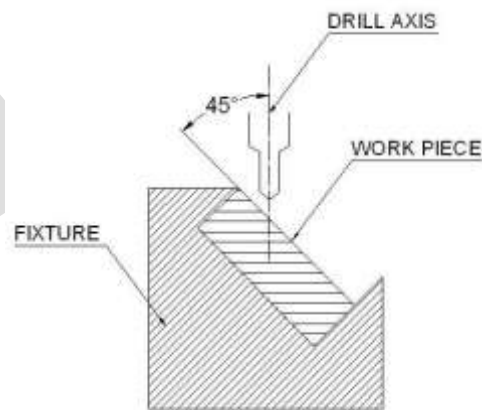
Methodology:-

Methodology for working system building:

We have a drill machine and want to make a 10mm diameter hole at the point of intersection of the two diagonals of a square plate. The hole should be inclined at 45 degree angle with the surface.

This arrangement is a simple drilling fixture.

3-2-1 Principle of Fixture Design



Sample drilling fixture

Rest the work piece on three non-collinear points of the bottom surface (XY), and you will be able to fix the +Z, CROT-X, ACROT-X, CROT-Y and ACROT-Y degrees of freedom. Now, rest the work piece at two points of side surface (XZ), and you

will be able to fix the +Y and ACROT-Z degrees of freedom. Now, rest the work piece at one point of the adjacent surface (YZ), and you will be able to fix the +X and CROT-Z degrees of freedom. So, you can successfully fixate 9 required degrees of freedom by using the 3-2-1 principle of fixture design.

Design and Development

1. Preliminary CAD model :

1. LOCATOR PIN

Locator Pin used here to restrict DOF in linear and rotational X direction i.e. to restrict 4 DOF Viz. Linear +X,-X, and rotational clockwise X, anticlockwise X. This pin plays the role for reference point also which delivers the exact position. The component having hole at bottom side which get locate with this pin at two position as shown in fixture view. Pin is designed as a dowel pin which get mount In this fixture there are total two Locator pins are used and material of construction is AISI 304

2. LOCK PAD

Lock Pad is used here to restrict DOF in Linear Z direction i.e., +Z, -Z, and Rotational clockwise Z, anticlockwise Z as shown in fixture arrangement.

MOC: UHMW

3. TROLLEY STRUCTURE

Trolley structure made up of steel flats is the platform Made for locating and Assembled the entire Fixture elements.

MOC: AISI304

4. LOCKING PAD

These pads are avoiding Metal to metal contact between fixturing and components. Pad are bolted and rested to talk the position on trolley structure.

M.O.C.:UHMW

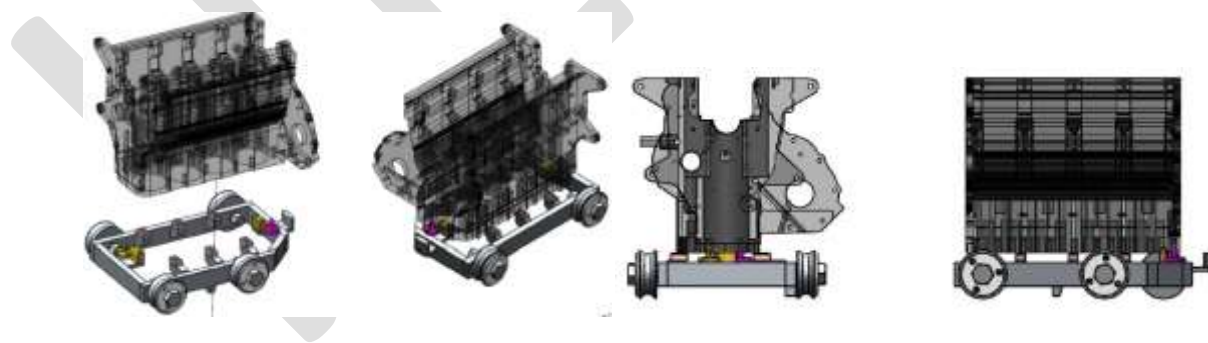


Fig: Various views of moving fixture trolley .

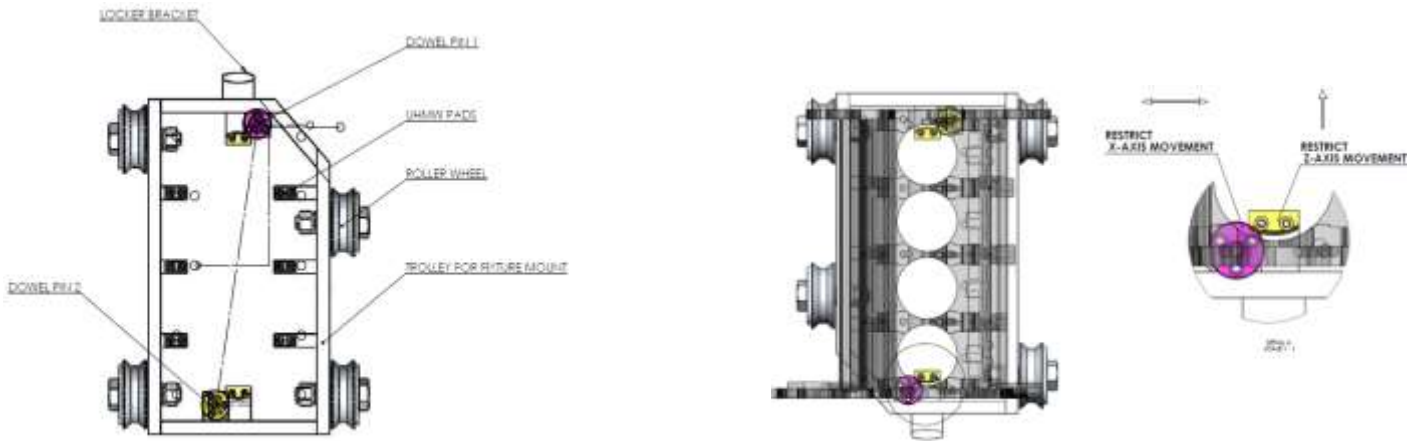


Fig. 3-2-1 principle restrictions

1. Design of Dedicated lifting hook

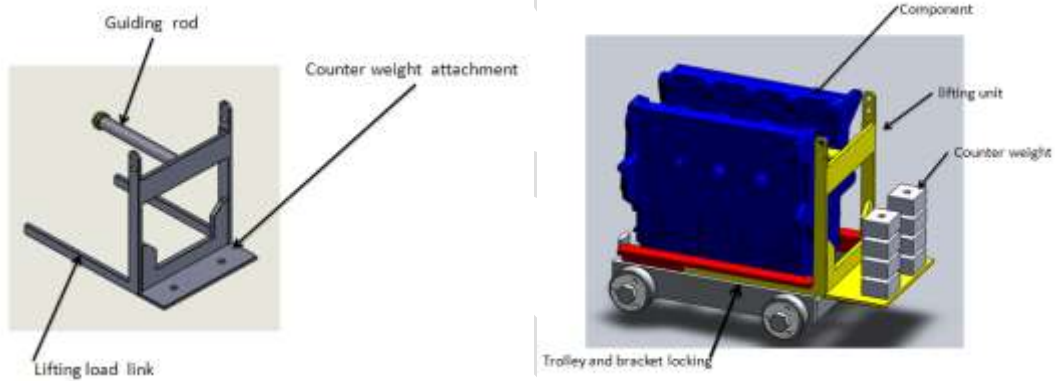
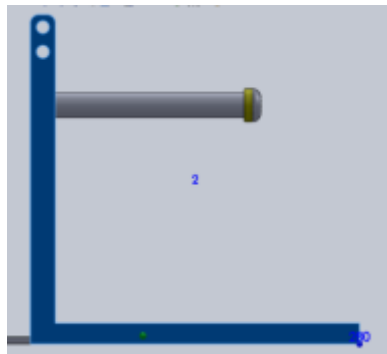


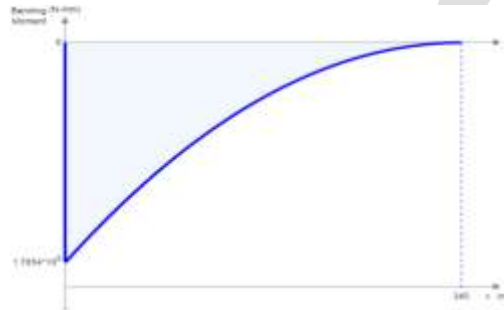
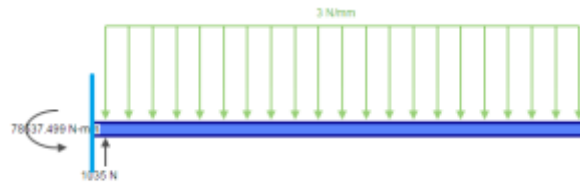
Fig : Ready Lifting unit

Design valuation:

Shear Force and Bending Moment Diagram



The maximum load on the bracket is distributed load of 2.75N/mm. Let the Maximum load equals to 3N/mm. The SFD and BMD are as shown.



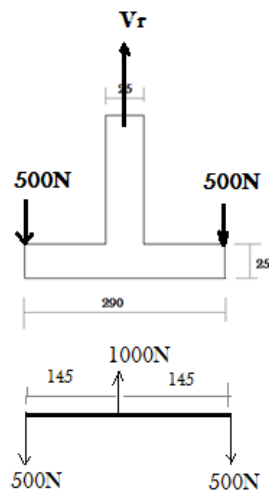
From SFD and BMD

Maximum Shear force = 1035 N

Maximum Bending Moment, $M = 1.7854 \times 10^4$ N-mm.

Hook and hanging behavior

The free body diagram of the bracket is as shown in fig.



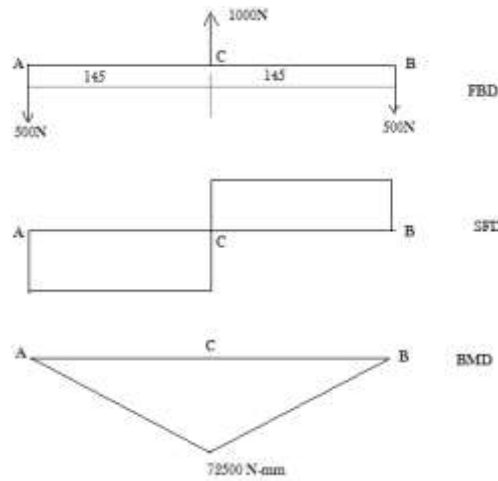
Bending moment about A = 0

Bending moment about B = 0

Bending moment about C = $-500 \times 145 = -72500$ N-mm

Maximum Bending moment occurs at c , $M = 72500 \text{ N-mm}$.

SFD And BMD Are as shown in following figure



The cross section of the bracket is as shown in fig.



We know,

$$y = \frac{\sum AY}{\sum A} = \frac{A_1y_1 + A_2y_2}{A_1 + A_2}$$

$$y = 157.5 \text{ mm}$$

Moment of Inertia,

$$I = \sum (I_x + A(Y - y)^2)$$

$$I = 20.84 \times 10^6 \text{ mm}^4$$

As the hogging moment is there, $y = y_c$

$$\text{Hence, } y_t = 315 - 157.5 \text{ mm} = 157.5 \text{ mm}$$

We have from Flexure formula,

$$\frac{M}{I} = \frac{\sigma}{y}$$

Hence,

$$\frac{72500}{20.84 \times 10^6} = \frac{\sigma}{157.5}$$

$$\sigma = 0.5 \text{ N/mm}^2$$

CAE validation :

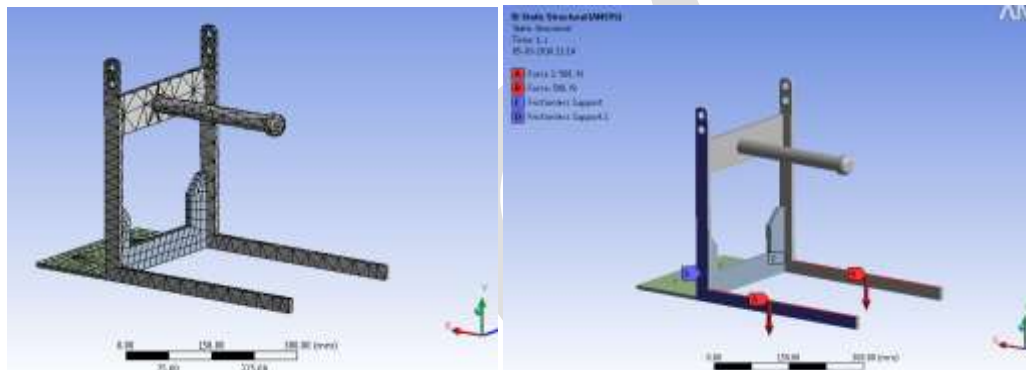
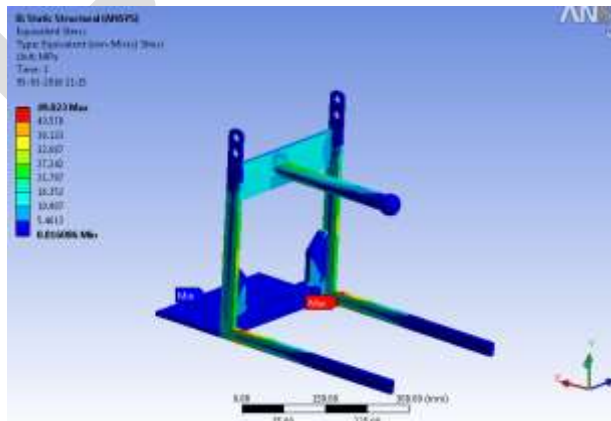
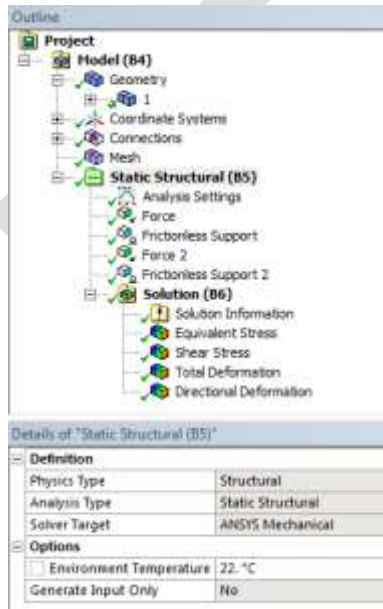
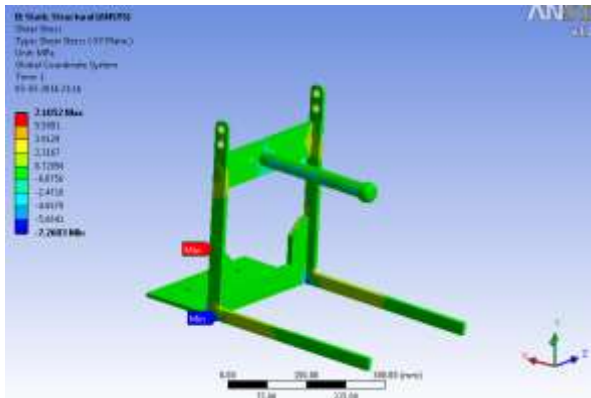


Fig: Weldment Hook Meshing Model

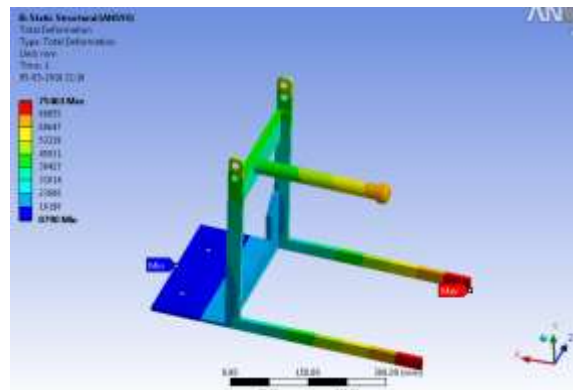
Loading conditions
 Outlines of validation :



Equivalent (von-Miss) Stress



Shear Stress (XY Plane)



Total Deformation

ACKNOWLEDGMENT

I feel immense pleasure in expressing our deep sense of gratitude to Prof.Aldar.B.D my guide & Head of Mechanical Engineering Department for his excellent guidance, continuous encouragement and providing his valuable advice whenever the need arouses during the completion of seminar work.

I thanks to all those who help intellectually and materially in completion of seminar report. I would like to express my appreciation and thanks to all my friends who knowingly or unknowingly have assisted and encouraged us.

CONCLUSION

Working of hanging conveying handler is feasible found here with full proof mechanism and mounting with production requirement process feasibility.

It's found specific tool for handler only for cylinder block, for other standard components all the assembly structure will change with its shape, size and volume.

REFERENCES:

Reference Books:

- [1] V.B.Bhandari, Design of Machine Elements, (TATA Mc-GRAW-Hill Publication).
- [2] Erik K. Henriksen, Jig and Fixture Design Manual, (Industrial press inc. New York, 1902).

Papers from Journal or Transactions :

- [1] Y.S.Kapnichor, V.V.Patil, P.D.Shinde "Design of Automated Rotary Cage Type Fixture For Cylinder Block" Journal of Engineering Research and application ISSN: 2248-9622 Vol . 4, Issue 8 (Version 3), August 2014.
- [2] V.S.Jakukore, L.B.Raut"Combined load analysis of rotary cage fixture by FEA and Experimental approach", International Journal of Innovative Research in Advanced Engineering ISSN: 2349-2163 Volume1 Issue, September 2014.
- [3] L.B.Raut , V.S.Jakukore "Cylinder Block Fixture For Mistake Proofing", American Journal of Engineering Resarch e-ISSN : 2320-0847 p-ISSN: 2320-0936 Volume-03 , Issue -10,pp-145-150.2014
- [4] V.S.Jakukore , L.B.Raut "Combined load analysis of rotary cage fixture by FEA andExperimental approach"International Journal of Innovative Research in Advanced Engineering (IJIRAE) ISSN: 2349-2163Volume 1 Issue 8 (September 2014)

Internet

- [1] http://www.shoho-g.co.jp/en/items/processing_assembling_jigs/,
- [2] <http://www.makino.com/resources/case-studies/parallel-processing-for-engine-blocks/157/>
- [3] <http://www.industrial-lasers.com/articles/print/volume-26/issue-3/features/laser-cladding-of-worn-cylinder-boxes.html>

Improving Power Quality Performance in Distributed Power Generation (Smart Grid)

Rejani R. J
P G scholar

Thejus Engineering College
rejani01@gmail.com
9745265618

Nivya M. R
P G scholar

Thejus Engineering College
ramvasniv97@gmail.com
8129393524

Mohammed Reneesh
PG Scholar

Thejus Engineering College
reneesh4u@gmail.com
9656036227

Jaison Joy
Asst. Prof

Thejus Engineering College
Jaisonjoy2007@gmail.com

Abstract — The voltage sag, swell, harmonics are the major power quality issues produced by the wind and solar system. In a distributed power system the focusing is on the improvements of these power quality issues. This can be achieved by the modified design of PI controller. The structure of designed controller consists of voltage control loop, current control loop, power control loop in dq0 reference frame. The operation of the controller is investigated for varying power demand with linear and non-linear loads from customer side and for varying smart grid impedance along with varying distributed generation source voltage. An increase in reactive demand at PCC (Point of Common coupling) would affect the system power factor at PCC. The conventional type PI controller for such change in consumer load and variation of the smart grid impedance do not exhibit a dynamic behaviour. Alternatively, the proposed controller simultaneously compute current dynamics and harmonics of the parameter for the generating control reference value to meet the additional reactive power requirement with reduced total harmonic distortion used as new reactive power reference value for the power controller. The design and modelling of photovoltaic cell, MPPT, DC/DC converter and inverter connected to the grid are done. The simulation for the proposed system is carried out using MATLAB 2010 Simulink software.

Keywords - smart grid connected inverter, distributed generation, harmonic control, dq0 reference frame, PI controller, power control loop, voltage and current control loop

I INTRODUCTION

The combined solar and wind energy generation are several advantages for used as the distributed energy resource. In earlier days some drawbacks are there. This can be avoided by using the inverter and its controller circuit for PV based DG units. During the day and night times for improving the reactive power compensation and harmonic elimination on its neighbouring DG units and the grid by proper exchange of reactive power between the sources. For this approach the existing developed linear controller are PI and predictive control method. These two methods are more dominant in current error compensation. But in the case of conventional type PI controller normally do not have appropriate compensation from the inverter for grid connected application. The existing predictive control method is not superior for PV based DG units without dc-dc converter. This can be eliminated in SVPWM based PI controller. But this controller is insensitive to the system parameter since the algorithm does not include the system model. However the result is in the power imbalance between the generated power and load power due to grid impedance variation and can damage the capacitor and predictive device. The DVR with novel detection method [4] can compensate the voltage sag or interruption within 2-ms delay but this method additionally requires super capacitor and power additional electronic devices. The existing control method are mainly focusing on voltage sag compensation and interruption at PCC. In this project a novel control strategy in dq0 frame with communication interface is attempted to compensate

II. BLOCK SCHEMATIC OF THE PROPOSED SYSTEM

The proposed model consists of two different Distributed generating units (DG) comprises of PV array and wind power resource integrated to the grid through VSI and filter and control blocks as indicated in Fig. (1). The consumer loads are connected at PCC. The control block consists of abc – dq0 conversion block and voltage, current and power control blocks. Measuring instruments (voltage and current transformers are connected at the point of common coupling) to measure the currents flow through the VSI, induction generator, grid, customer demand.

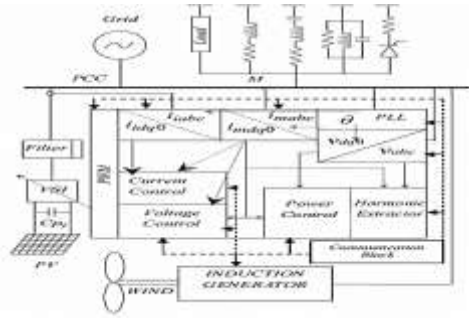


Fig 1: block diagram

This two units are supply's the local load and the surplus power is injected to the grid simultaneously PV sourced VSI is used for reactive compensation at PCC for avoid the voltage swell and sag. In order for communication between measured units and DG control units through DSC, embedded kit is used.

III . MODELING OF 3Ø SELF EXCITED INDUCTION GENERATOR

The d-q axes equivalent circuits of an induction generator (IG) in synchronously rotating reference frame are shown in Fig. 2. The complete dynamic equations of IG, taking saturation into account, in synchronously rotating reference frame [2], [3] are represented in matrix form as follows

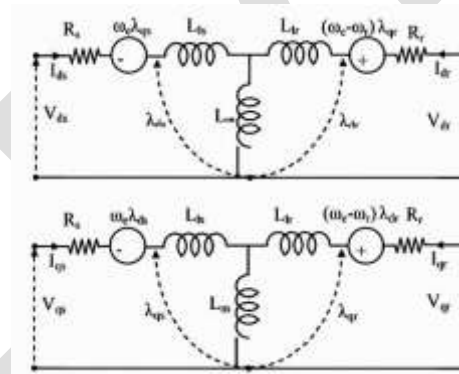


Fig.2- Equivalent circuit of IG - d-q model (a) d-axis (b) q-axis

These are represented in matrix form as follows

$$\frac{d}{dt} \begin{bmatrix} \lambda_{ds} \\ \lambda_{qs} \end{bmatrix} = \begin{bmatrix} V_{ds} \\ V_{qs} \end{bmatrix} - R_s \begin{bmatrix} i_{ds} \\ i_{qs} \end{bmatrix} - \omega \begin{bmatrix} 0 & -1 \\ 1 & 0 \end{bmatrix} \begin{bmatrix} \lambda_{ds} \\ \lambda_{qs} \end{bmatrix}$$

$$\frac{d}{dt} \begin{bmatrix} \lambda_{dr} \\ \lambda_{qr} \end{bmatrix} = \begin{bmatrix} V_{dr} \\ V_{qr} \end{bmatrix} - R_r \begin{bmatrix} i_{dr} \\ i_{qr} \end{bmatrix} - (\omega - \omega_r) \begin{bmatrix} 0 & -1 \\ 1 & 0 \end{bmatrix} \begin{bmatrix} \lambda_{dr} \\ \lambda_{qr} \end{bmatrix}$$

Where,

R_s = Per-phase stator resistance

R_r = Per-phase rotor resistance referred to stator

i_{qs} = Stator q-axis current, i_{ds} = Stator d-axis current

i_{qr} = Rotor q-axis current, i_{dr} = Rotor d-axis current

Y_{qs} = Stator q-axis voltage, Y_{ds} = Stator d-axis voltage

V_{qr} = Rotor q-axis voltage, V_{dr} = Rotor d-axis voltage

ω_e = Arbitrary reference frame speed

ω_r = Rotor speed in rad/sec

λ_{qs} = Flux linkages of stator in q -axis

λ_{ds} = Flux linkages of stator in d- axis

λ_{qr} = Flux linkages of rotor in q-axis

λ_{dr} = Flux linkages of rotor in d-axis

L_s = Stator Leakage reactance

L_r = Rotor Leakage reactance

L_m = Magnetizing inductance of inductance generator

IV . MATHEMATICAL MODELLING OF THE PROPOSED SCHEME

In grid connected mode, both DGs are utilized for supplying pre specified power to load to minimize the power import from the grid. The simplified equivalent circuit of VSI integrated to grid in current control mode is indicated in Fig.3.

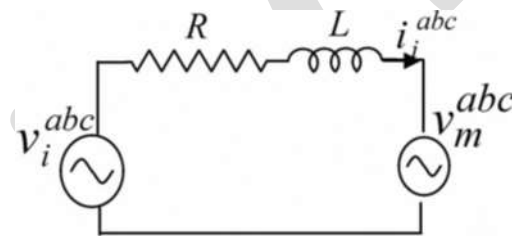


Fig 3: Simplified equivalent model of current control scheme for proposed system

The V_{ma} , V_{mb} , V_{mc} & V_{ia} , V_{ib} , V_{ic} are the three phase ac voltage at the point of common coupling and voltage on inverter side, the subscripts m and i denote at the point of common coupling and inverter. The input to the inverter is a three phase voltage and is given by

$$V_{ia} = V_{max} \sin \omega t \quad (1)$$

$$V_{ib} = V_{max} \sin \omega t - \frac{2\pi}{3} \quad (2)$$

$$V_{ic} = V_{max} \sin \omega t + \frac{2\pi}{3} \quad (3)$$

Where V_{max} and ω are the maximum phase voltage and angular frequency of the inverter respectively.

The voltage and current control model of the grid connected are implemented in [4] [5] for voltage and power controls. This developed controller model mostly concentrates only voltage sag and voltage interruption because the system model is not included in the controller. Accordingly the inverter output voltage is obtained as in eqn. (4)

$$\frac{d}{dt} \begin{bmatrix} i_{id} \\ i_{iq} \end{bmatrix} = \frac{1}{L} \begin{bmatrix} -R & \omega L \\ \omega L & -R \end{bmatrix} \begin{bmatrix} i_{id} \\ i_{iq} \end{bmatrix} + \begin{bmatrix} v_{id} \\ v_{iq} \end{bmatrix} - \begin{bmatrix} v_{md} \\ v_{mq} \end{bmatrix} \quad (4)$$

The injected active and reactive power components, p and q, can be represented in terms of the d- and q-axis components of the supply voltage at the Point of Common Coupling and the injected currents as follows:

$$p_{inv} = \frac{3}{2}(v_{id}i_{id} + v_{iq}i_{iq})$$

$$q_{inv} = \frac{3}{2}(v_{iq}i_{id} - v_{id}i_{iq})$$

To compensate for this filter-capacitor current component and the inductor current references are calculated by adding a simple feed-forward compensation term as follows in this proposed model

V. CONTROL FUNCTION

One of the main objectives of the voltage controller is to achieve fast and accurate generation of the reactive current reference for regulating the voltage at PCC. To achieve this objective, the principle of voltage sag and swell mitigations along with harmonic reduction of DG sourced voltage source inverters are to inject a current into the PCC in order to keep the load voltage at its rated value. Using the voltage-oriented control, the active and reactive power injection can be controlled via a current-controlled VSI.

5.1 POWER CONTROL LOOP

$$Q_s(v) = Q_0\left(\frac{v}{v_0}\right)^{\beta_s} \quad (5)$$

$$P_t(v) = P_0\left(\frac{v}{v_0}\right)^{\alpha_t} \quad (6)$$

$$Q_t(v) = Q_0\left(\frac{v}{v_0}\right)^{\beta_t} \quad (7)$$

With this arrangement, the dynamics of the system changes rapidly in the case of instantaneous load varying situations. A flexible control strategy is required to be developed to handle this dynamics. The proposed multilevel controller comprises of power control loop (external level control), voltage control loop (middle level control) and inner or current control loop. Outer loop creates reference for inner loop as indicated in Fig.4..

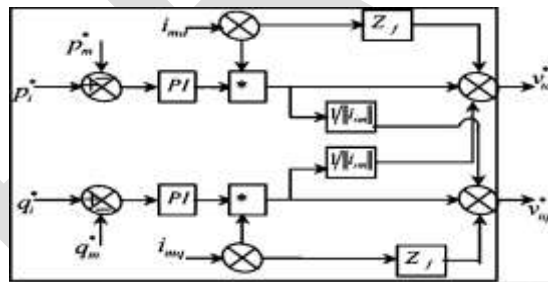


Fig 4: power control loop

$$\begin{bmatrix} L_s + \frac{K^2}{c_s} & \omega_0 L_s \\ \omega_0 L_s & L_s \end{bmatrix} \begin{bmatrix} i_{pn}(s) \\ i_{rn}(s) \end{bmatrix} = \begin{bmatrix} v_{pn}(s) \\ v_{rn}(s) \end{bmatrix} \quad (8)$$

$$v_{pn}(t) = v_n \cos(n-1)t\omega_0 t \quad (9)$$

$$v_{rn}(t) = -v_n \sin(n-1)t\omega_0 t \quad (10)$$

$$\left(L_s + \frac{K^2}{c_s}\right) i_{pn}(s) + i_{rn}(s)\omega_0 L_s = V_{pn}(s) \quad (11)$$

$-\omega_0 i_{pn}(s) + L_s i_{rn}(s) = V_{rn}(s)$ for harmonic analysis.

$$i_{rn}(t) = v_n A \sin(n-1)\omega_0 t \quad (12)$$

$$i_{pn}(t) = v_n B \cos(n-1)\omega_0 t \quad (13)$$

$$A = -\frac{n-1}{D}, B = \frac{1}{D} \left[(n-2) - \frac{\omega_n^2}{\omega_0^2(n-1)} \right]$$

$$D = X_L \left[\frac{\omega_r^2}{\omega_0} - n(n-2) \right];$$

$$X_L = \omega_0 L, \omega_r = \frac{K^2}{LC}, K = \frac{\sqrt{6}}{\pi}$$

5.2 VOLTAGE AND CURRENT CONTROL LOOP

The inverter terminal voltage V_i is calculated and compared to V_i^* . An error signal is produced and then fed to a PI controller. The instantaneous values of the three-phase ac bus voltages in the dq0 reference frame permits to design a simpler control system than using abc components. The current control loop following the voltage control loop and this loop controls the real and reactive power independently and good response of the system dynamics and harmonics are ensured due to the inclusion of system modelling and inclusion of instantaneous grid impedance variation due to load variation.

One is active power control mode (P-CM) and the voltage control mode (Q-CM) and reduce the harmonic at PCC. In this paper voltage mode control is employed. In this mode, the current reactive power value is measured at point (qm) in this value of qm is compared with qi and error value is fed to the PI control for error minimization and the output of this controller gives dq0 voltage reference value (V_{id}^* , V_{iq}^*). These variables are fed to the voltage controller for generation of current reference. The change of reactive power requirement with respect to change of grid impedance value and local loads results in voltage drop across the filter.

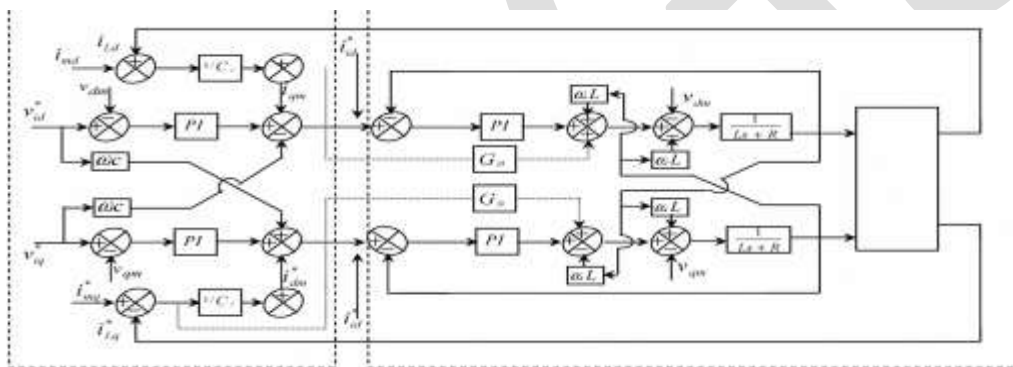


Fig 5: voltage and current control loop

V. OPERATION THEORY OF PROPOSED CONTROLLER

This paper focuses on the control of reactive power for maintaining the rated voltage at PCC. The principles of voltage swell and sag mitigation during the change of local or grid impedance variation is identified by measuring the value of reactive power flow at PCC (qm). This amount of reactive power requirement is compared with the reactive power from the inverter (qi) and the error is used by the controller to balance the present reactive power requirement at PCC for voltage swell and sag. The conventional controllers mostly concentrate on voltage sag and interruption but the proposed controller also compensates the voltage swell by absorbing the Var during this period real power supplied by the inverter is affected by small value absorbing and reduce the values by extracting the harmonics but the power factor is maintained unity at PCC.

ACKNOWLEDGEMENT

I thank **ALMIGHTY GOD**, who laid the foundation for knowledge and wisdom and has always been the source of my strength, inspiration who guides me throughout. I would like to thank my guide, Mr JAISON JOY, assistant professor, for his judicious and important piece of information, expert suggestion, guidance and support during every stage of this work. I express my sincere thanks to all the teachers in the EEE department for providing me with valuable guidance and encouragement throughout the work.

CONCLUSION

This report presents analysis and improvement of power quality (voltage sag, swell and harmonics) performance of smart grid connected inverter used in distributed generation. The developed controller controls the real and reactive power supplied by the DGs at the PCC. The controller is designed to deliver current at unity power factor at PCC. An increase in reactive power demand and harmonics at PCC due to change of load and grid impedance variation, would affect the system voltage at PCC. To study the dynamic behaviour of the proposed scheme, the state space model in dq reference frame has been developed for the entire hybrid scheme with the controller for validating the proposed with existing conventional SVPWM PI controller through simulation. The developed controller has been designed with outer power control loop, middle voltage control loop and inner current control loop. The performance of the developed controller model is evaluated through MATLAB/Simpower platform .Simulation have been carried out and the results are presented for both varying local power demand and grid impedance variation to evaluate the performance the proposed controller.

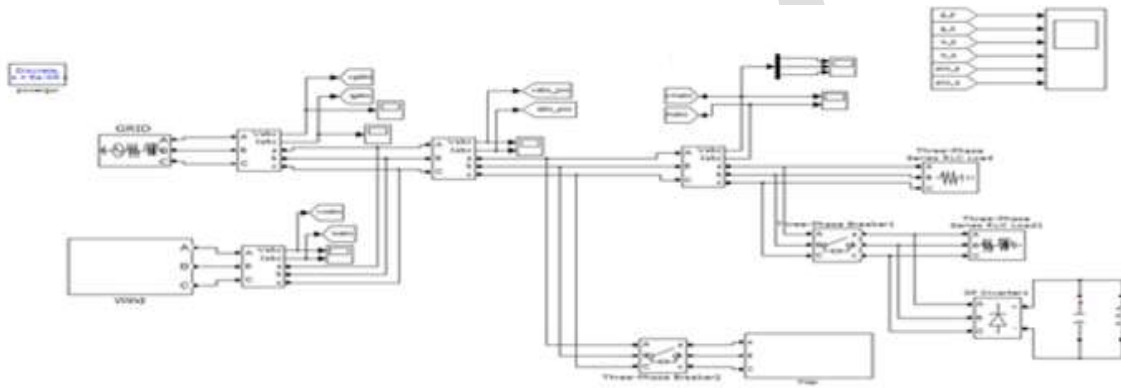


Fig 6: simulation diagram

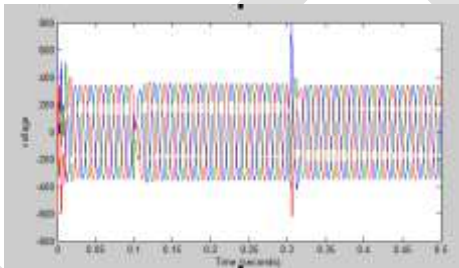


Fig 7 : Grid voltage

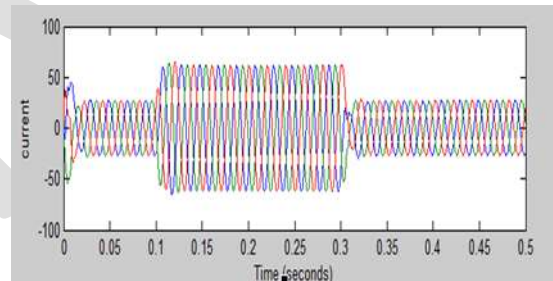


Fig 8: Grid current

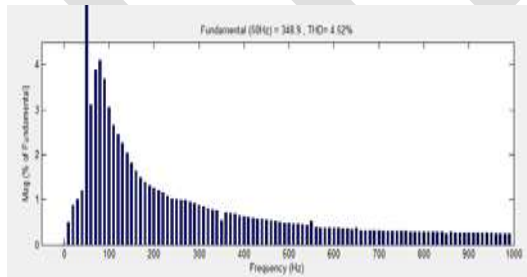


Fig 9: THD calculation of input voltage.

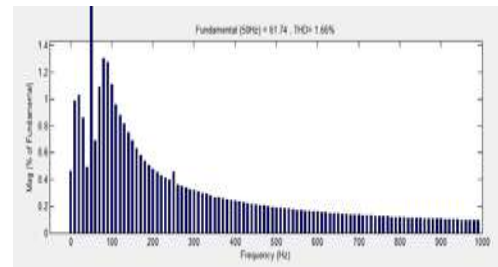


Fig 10:THD calculation of input current.

REFERENCES:

- [1] Muralekrishnen R, Mr.Sivakumar .P , “Improving The Power Quality Performance For Distributed Power Generation” 2012 International Conference on Computing, Electronics and Electrical Technologies [ICCEET]

- [2] N. Hamrouni-, M. Jraidi, A. Cherif "New control strategy for 2- stage grid-connected photovoltaic power system," Renewable Energy 33 (2008) 2212-2221
- [3] Habbati Bellia, Ramdani Youcef, Moulay Fatima," A detailed modelling of photovoltaic module using MATLAB", NRIAG Journal of Astronomy and Geophysics (2014) 3, 53–61
- [4] Freed Blaabjerg,remus Teodorescu,Adrian V.Timbus, "Overview of control and grid synchronization for distributed power generation systems",IEEE Transactions on Industrial Electronics Vol.53.NO.5.OCT.2006.
- [5] Marian p, Kazmierkowski, Fellow, IEEE, and Luigi Malesani, Fellow, IEEE, "Current Control Techniques for Three-Phase Voltage-Source PWM Converters: A Survey"IEEE Transactions on Industrial Electronics, Vol. 45, NO. 5, OCTOBER 1998.
- [6] Qingrong Zeng and Liuchen Chang, IEEE Senior Member, "Study of Advanced Current Control Strategies for Three-Phase Grid-Connected PWM Inverters for Distributed Generation" Proceedings of the 2005 IEEE Conference on Control Applications Toronto, Canada, August 28-31, 2005,
- [7] Qingrong Zeng and Liuchen Chang, IEEE Senior Memb" Study of Advanced Current Control Strategies for Three-Phase Grid-Connected PWM Inverters for Distributed Generation"
- [8] K.J.P. Macken Katholieke Universiteit Leuven , " Control of inverter based distributed generation used (0 provide premium power quality" 2004351h Annual IEEE Power Ektrcnics Specialisrs Conference
- [9] Trishan Efram, Student Member, IEEE, and Patrick L. Chapman, Senior Member, IEEE, "Comparison of Photovoltaic Array Maximum Power Point Tracking Techniques," IEEE Transactions on Energy Conversion, Vol. 22, NO. 2, JUNE 2007
- [10] Jain\$, Fellow, IEEE "A Nonlinear Approach to Control Instantaneous Power for Single-Phase Grid-Connected Photovoltaic Systems," 978-1-4244-2893- 9/09/\$25.00 ©2009 IEEE
- [11] Muralidhar Killi, and Susovon Samanta, Member, IEEE" Modified Perturb and Observe MPPT Algorithm for Drift Avoidance in Photovoltaic "10.1109/TIE.2015.2407854, IEEE Transactions on Industrial Electronics.
- [12] Dr. Recayi Pecan, Dr. MD Salim, & Dr. Marc Timmerman. A Hybrid Solar-Wind Power Generation System as an Instructional Resource for Industrial Technology Students. Volume 16, Number 3 - May 2000 to July 2000

ANALYSIS OF MALWARES FOR ANDROID APK

Mr. Akash J. Wadate, ME 2nd year, CSE department , G.H.Raisoni COE&M, Amravati, Maharashtra,India,

akashwadate007@gmail.com

Prof. N. R. Chopde,Assistant Professor,CSE Dept.,G.H .Raisoni COE&M,Amravati,Maharashtra,India

Nitin.chopde@raisoni.net

Prof.D.R.Datar, Assistant Professor,CSE Dept.,G.H. Raisoni COE&M,Amravati,Maharashtra,India

Dinesh.datar@raisoni.net

ABSTRACT: The aim of this work is to check whether an android application is having malware or not. Day by day malwares are spreading very fast. Malwares are dangerous to any system. By this work user will be able to verify the presence of malwares in apk file, based on that he can avoid installing it in his mobile and thus can be protected from malware attacks. Here cloud computing is used to provide portability and other features.

Keywords: malwares, apk , cloud computing, android application.

1. Introduction

The increasing ability of attacks to avoid traditional security systems and remain undetectable was a prediction we got right five years ago, but we have seen only the early stages of this phenomenon. Malware is still very popular and growing, but the past year has marked the beginnings of a significant shift toward new threats that are more difficult to detect, including fileless attacks, exploits of remote shell and remote control protocols, encrypted infiltrations, and credential theft[1].

As endpoint, perimeter, and gateway security systems got better at inspecting and convicting malicious executables, attackers moved to other file types. Now they are experimenting with infections that do not use a file. Leveraging vulnerabilities in BIOS, drivers, and other firmware, they are evading defenses by injecting commands straight into memory, or manipulating functions in memory to install an infection or exfiltrate data[1]. These attacks are not easy to execute and are not as interchangeable as some of the most popular malware, so the number of known attacks is currently quite small. However, like other techniques, they will get simpler and commoditized over time, broadening their accessibility and fueling their growth. The security industry is developing active memory protection and scanning technology that detects memory not linked to a specific file, but we expect to see an escalation in this type of attack until these defenses are commonly deployed[1].

The merging of cybercrime and APT has emboldened financially motivated criminals who have gracefully transitioned from attacking end users to going after the financial institutions themselves. The past year has seen plenty of examples of attacks on point-of-sale systems and

ATM s, not to mention the daring Carbanak heist that pilfered hundreds of millions of dollars[2]. In the same vein, we expect cybercriminals to set their sights on novelties like alternate payment systems (ApplePay and AndroidPay) whose increasing rate of adoption should offer a new means of immediate monetization. Another inevitable point of interest is stock exchanges, the true mother lode. While frontal attacks may yield quick payoffs, we mustn't overlook the possibility of more subtle means of interference, such as going after the black-box algorithms employed in high-frequency trading to ensure prolonged gains with a lower likelihood of getting caught[2].

2. Literature Survey

Android is covering most of market today. There are millions of clients are available for android today. That's why attackers are targeting towards android more than other platforms. Malwares are the biggest threat to mobile applications as they get directly spread from internet or application stores. There are various reasons behind spread of malwares through application store. Some includes that the one who develops any application is not properly authorized before that application is uploaded in app store. Another reason includes that there are no signature testing included before uploading any application over through application market. Simply any attacker can develop an application and can upload it, where because there is no proper security checks are performed ,it get directly deployed in market and any normal user only see the fake purpose of whose from end shows different thing and at the back side it does malicious work.

Jianlin Xu[3] has worked on this and in his work, based on home-brewed cloud computing platform and data mining, they proposed a methodology to evaluate mobile apps for improving current security status of mobile apps, MobSafe, a demo and prototype system, is also proposed to identify the mobile app's virulence or benignancy. MobSafe combines the dynamic and static analysis methods to comprehensively evaluate an Android app, and reduce the total analyse time to an acceptable level. In the implementation, they adopted the two representatives dynamic and static analysis methods, i.e. Android Security Evaluation Framework (ASEF) and Static Android Analysis Framework (SAAF) to evaluate the Android apps and estimate the total time needed to evaluate all the apps stored in one mobile app market, which provide useful reference for a mobile app market owner to filter out the mobile malwares[3].

3. Proposed Work

In this work an analysis system is proposed which will scan th given apk first, give its analysis report and based on that user can install it or can avoid it. For analysis it uses two techniques SAAF and ASEF, which are two framework . After applying this over the application, the results are taken out in form of percentages. There are three categories of analysis malware , spyware ad safe. The user will be given output divided into three categories and highest percentage result will be considered as an output , based on what user can accept or reject that particular application. The analysis application is basically divided into two phases-training and testing. The flowchart of training phase is given as follows.

By this training part, the developer will upload an apk file to record the byte codes of that apk for doing further analysis. The procedure of selecting that that particular apk for reference is omitted here as that work include the process of installing the newly launched apk over various devices and doing observation over number of days.

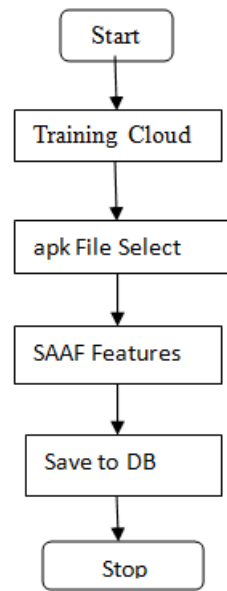


Fig. 1: Training phase

The testing phase of the system is shown in the fig.2, where apk file will be selected for analysis. From that apk again with the application of SAAF , features are extracted then are compared with the stored pattern of apk's , ASEF analysis is performed over that and the data mining technique Top-K rules are applied over that in order to get the best matching features. Finally the result is displayed. The time needed to do the analysis is also displayed in training and testing phase. This procedure is also depicted with the percentage analysis, the percentage of each category of type is displayed i.e. as in training there are following categories – malware, spyware , safe , so the percentage of these categories are displayed. Four kinds of output get displayed: safe or unsafe status, time analysis, path of that selected apk, percentage analysis.

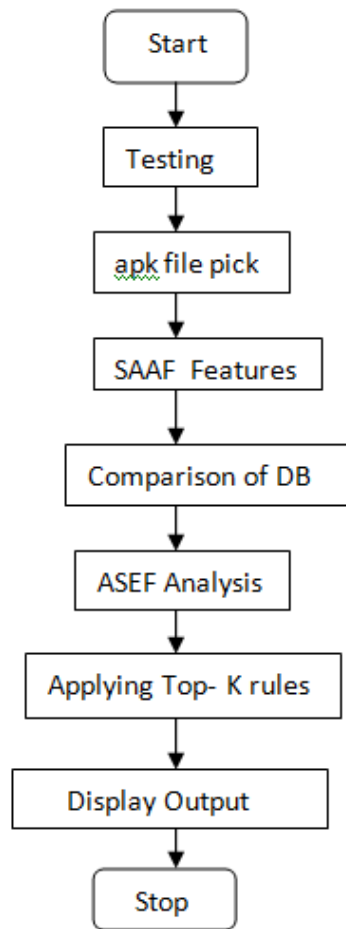


Fig. 2: Testing phase

4. Conclusion and Future Scope

By this work Security status of the application is analyzed in terms of malware, spyware and safe and the user will be notified and prevented from use of such applications having presence of malware and spyware. Here the total time needed to evaluate a mobile app is estimated. Here the apk is analyzed and percentage of features get displayed based on three types and based on that the one having highest percentage from three types will be declared as the result of analysis.

As the future perspective some web mining and more advanced data mining techniques will be implemented to get more optimized outputs. Machine learning is the issue which will be in the future work of this system. The system can be extended to include the facility of providing the user security by which the user will be notified about the safe and unsafe contacts numbers and generate the report of one user.

REFERENCES:

1. McAfee Labs Report 2016 Threats Predictions, 7 April 2016.
2. Kaspersky Security Bulletin 2015 2016 PREDICTIONS: IT'S THE END OF THE WORLD FOR APTs AS WE KNOW THEM, 10 April 2016.

3. MobSafe: Cloud Computing Based Forensic Analysis for Massive Mobile Applications Using Data Mining Jianlin Xu, Yifan Yu, Zhen Chen, Bin Cao, Wenyu Dong, Yu Guo, and Junwei Cao TSINGHUA SCIENCE AND TECHNOLOGY ISSN11007-0214110/1011pp418-427 Volume 18, Number 4, August 2013

IJERGS

Fully Reconfigured VLSI architecture of FM0, Manchester and Miller Encoder for DSRC Applications

Ms. Jomcy Rani Xavier¹, Dr. U. A.Kshirsagar²

¹PG student, ECE Dept., HVPM's CoET, M.S, India

²HoD.of Electronics & Telecommunication, HVPM's CoET, M.S, India
jomcyranixavier@yahoo.com, phone: 08554858859

Abstract- Intelligent transportation system (ITS) aim to provide innovative services at different modes of transport and traffic management. Dedicated short range communication (DSRC) is a new technique to promote the intelligent transportation into our daily life. DSRC standard generally use FM0 and Manchester codes for encoding. These codes enhance the signal reliability with dc balance. The coding diversity between FM0 and Manchester codes limits the potential to design a fully reused VLSI architecture for both codes. This project proposes a fully reused VLSI architecture design by using SOLS (similarity oriented logic simplification) technique. This technique overcome the coding diversity between FM0 and Manchester and Miller encoding for DSRC application. The SOLS technique eliminates the limitation on hardware utilization by two core techniques: area compact retiming and balance logic-operation sharing. The area-compact retiming relocates the hardware resource to reduce the number of transistors. This project is mainly motivated by the desire to implement the intelligent transportation system concept to the real world because of the key benefits in safety and travelling ease in a low cost manner. Here in this project we are using FM0, Manchester and Miller encoding techniques to reach dc balance and enhancing the signal reliability. The SOLS technique improves the hardware utilization rate to 100%. The encoding capability of this paper fully support the DSRC standards of America, Europe, and Japan. This paper not only develops a fully reconfigured VLSI architecture, but also exhibits a competitive performance compared with the existing works. All the codes for the processor design are written in Verilog HDL.

Keywords: Dedicated short-range communication (DSRC), FM0 encoder, Manchester encoder, Miller encoder, SOLS technique, VLSI, FPGA

1. INTRODUCTION

Today, automobile industries are paving a way for intelligent transportation. Google driverless cars are the state of art in this direction. DSRC system plays an important role in modern automobile industry. DSRC is an emerging technique, it is one way or two way short to medium range wireless communication. It enables different users to be better informed, make safer, more coordinated and advanced use of transportation networks. The DSRC standards have been established by several organisation in different countries.

DSRC can be classified into two categories. These are automobile to automobile and automobile to roadside. In automobile to automobile, the DSRC provides the message sending and broadcasting for safety issues public information announcement. It mainly deals with the collision alarms, hard break warnings etc. In automobile to roadside, the DSRC enables the intelligent transportation services such as ETC (Electronic Toll Collection), highway rail intersection warning, in vehicle signing etc.

System architecture of DSRC transceiver consists of three modules namely; base band processors, RF front end and the microprocessors. The microprocessor is used to transfer the instruction to the baseband processing and RF frontend. The RF frontend is used to transmit and receive the wireless signals using the antenna. The baseband processing is responsible for modulation, error correction, encoding and synchronization.

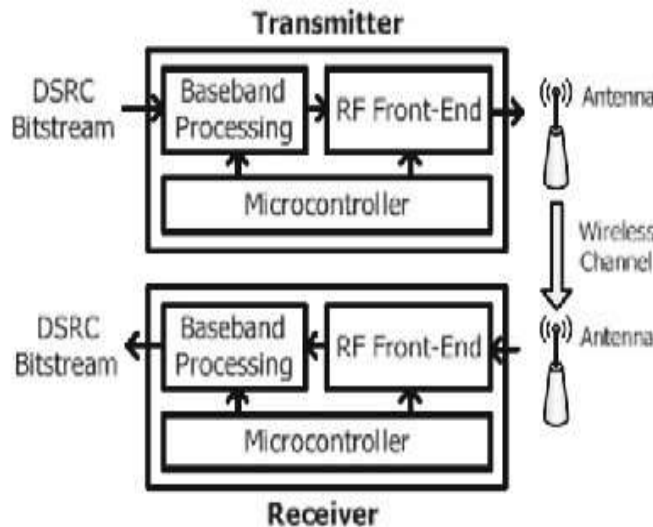


Fig. 1. System architecture of DSRC transceiver

2. LITERATURE REVIEW

An accountable work is being done in this field of intelligent transportation and modern automobile industries are devoting considerable amount of resources for research in this field. Because in day to day life the intelligent transportation system has its own advantages like smooth traffic control, vehicular safety etc. The following section will point out the evolution of the proposed project's work and research till date.

P. Benabes, A. Gauthier, and J. Oksman implemented a Manchester code generator running at 1 GHz. This literature [4] proposed a VLSI architecture of Manchester encoder for the use of optical communication. This design used the CMOS inverter and the gated inverter as the switch for the construction of Manchester encoder. It was executed by 0.35- μm CMOS technology and its operation frequency is 1 GHz. (P. Benabes, A. Gauthier, and J. Oksman 2003)

M. A. Khan, M. Sharma, and P. R. Brahmanandha presented FSM based Manchester encoder for UHF RFID tag emulator. This literature [5] also proposed a Manchester encoding architecture for ultrahigh frequency (UHF) RFID tag emulator. This hardware architecture is operated by the FSM (finite state machine) of Manchester code, and is performed by FPGA (field-programmable gate array) prototyping system. The maximum operation frequency of this architecture is about 256 MHz. (M. A. Khan, M. Sharma, and P. R. Brahmanandha 2008)

Karagounis, A. Polyzos, B. Kotsos, and N. Assimakis implemented a 90nm Manchester code generator with CMOS switches running at 2.4 GHz and 5 GHz. This literature [3] later replaced the architecture of switch in [5] by the NMOS device. It is performed in 90nm CMOS technology, and the maximum operation frequency is higher than 5 GHz. (A. Karagounis, A. Polyzos, B. Kotsos, and N. Assimakis 2009)

Y.C. Hung, M. M. Kuo, C.-K. Tung, and S.H. Shieh presented a High-speed CMOS chip design for Manchester and Miller encoder. This literature [2] evolved a high-speed VLSI architecture relatively fully reused with Manchester and Miller encodings for RFID applications. This architecture was performed in 0.35- μm CMOS technology and the maximum operation frequency is 200 MHz. (Y.C. Hung, M.M. Kuo, C.K. Tung, and S.H. Shieh 2009)

The new methodology presented by Yu Hsuan Lee and Cheng Wei Pan. They implemented a fully reused VLSI Architecture of FM0/Manchester encoding using SOLS technique for DSRC applications. This paper [1] is the inspiration for this project. It proposed a promising solution for high performance fully reused VLSI architecture of FM0/Manchester encoding using similarity oriented logic simplification (SOLS) technique for dedicated short range communication. The SOLS technique improves the hardware utilization rate from 57.14% to 100% for both FM0 and Manchester encodings. (Yu-Hsuan Lee and Cheng-Wei Pan 2014)

3. CODING PRINCIPLES OF FM0, MANCHESTER AND MILLER ENCODER

3.1. FM0 ENCODING

For each input data, the FM0 code consists of two parts: one for former half cycle of clock signal, A, and the other one for later half cycle of clock signal, B. The coding principle of FM0 encoder is given below:

- 1) If input data is logic-0, the FM0 code must show a transition between A and B.
- 2) If input data is logic-1, no transition is allowed between A and B.
- 3) There is a transition is allocated among each FM0 code no matter what the X is.

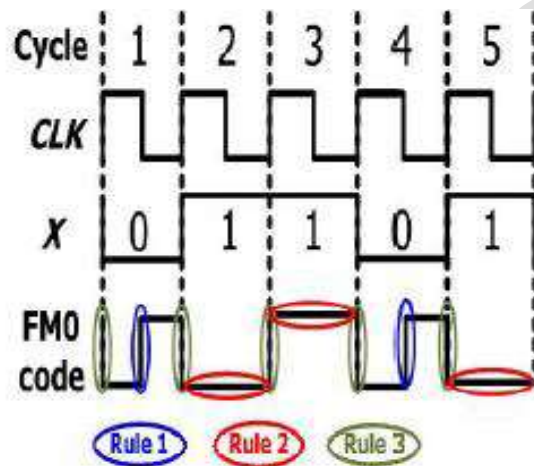


Fig.2. Example for FM0 coding

3.2. MANCHESTER ENCODING

The Manchester encoding is realized with XOR operation between clock and input signal. Manchester encoder always produces a transition between the center of each cycle. The Manchester coding example is shown in Figure. 3.

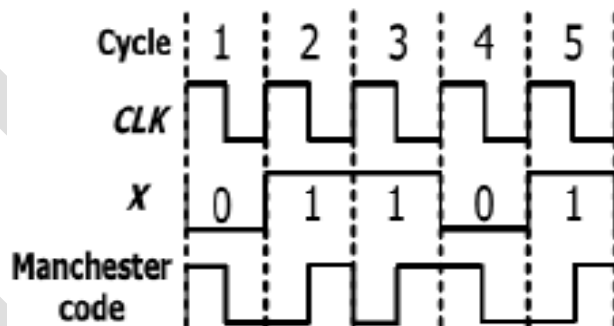


Fig. 3. Example for Manchester encoding

3.3. MILLER ENCODER

Miller encoding is also known as delay encoding. It can be used for higher operating frequency and it is similar to Manchester encoding except that the transition occurs in the middle of an interval when the bit is 1. While using the Miller delay, noise interference can be reduced.

The block diagram of Miller encoder consists of a D flip flop, T flip flop, NOT gate and XOR gate. Here the input is A and CLK. For example, if the input is 0 and the clock, given the XOR operation has done in between A and CLK, therefore 0 plus a positive edge

clock produces the output as 0. Given it to D flip flop, the clock has inverted, and after that output is given to T flip which is 0. Then the TFF is toggle FF, which produces the Miller output as 1.

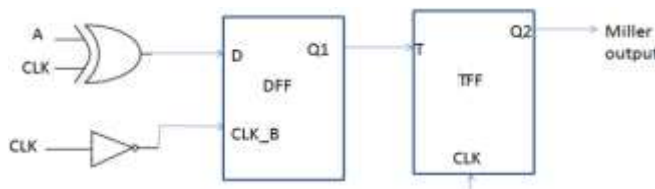


Fig.4. Block diagram of Miller encoder

4. SOLS TECHNIQUE

DSRC encoders make use of FM0, Manchester and Miller encoding techniques. Hence these encoders can be combined together to form a reusable encoder. The final circuit obtained is an integrated architecture of FM0, Manchester and Miller encoding to overcome various drawbacks of traditional method. Such a reusable encoder of FM0 and Manchester encoder can be illustrated as shown in the figure 5.

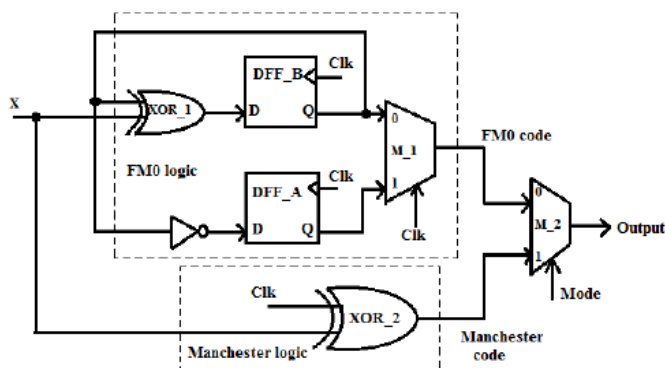


Fig.5. Hardware architecture of FM0 and Manchester encoder

The reason why FM0 encoding dissipates more power than Manchester encoding is explained as follows: The dynamic power can be given as

$$P = \gamma f CV^2$$

Where γ , f , C , and V denote the switching-activity, operation frequency, equivalent capacitance of circuitry node, and supply voltage, respectively.

In existing works the coding diversity between the FM0 and Manchester encoders limits the potential to design a fully reconfigured VLSI architecture. To rectify these problems, the FM0 and Manchester and Miller encoders are designed with area compact retiming and balance logic operation sharing techniques, and if this project is implemented, it will construct a fully reused VLSI architecture with high speed and reliability for DSRC application systems.

5. IMPLEMENTATION OF THE ENCODING TECHNIQUES

To implement the project, we need two core concepts to design a fully reused VLSI architecture for FM0 and Manchester codes. These two core concepts are area-compact retiming and balance logic-operation sharing techniques. The area compact retiming relocates the hardware resource and to reduce the number of transistors. The balance logic operation sharing will efficiently combines FM0 and Manchester encodings with the fully reused VLSI architecture. Each part is individually described as follows.

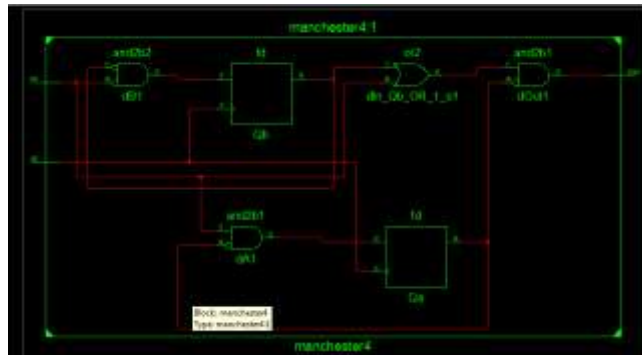


Fig.8. RTL schematic of Manchester encoder

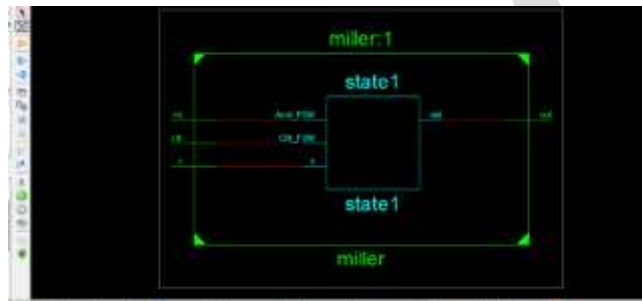


Fig.9. RTL schematic of Miller encoder

This paper adopts the proposed SOLS technique to construct a fully reused VLSI architecture for FM0, Manchester and Miller encodings. Every logic component of this design is utilized in FM0, Manchester and Miller encodings. None of them is wasted in either encoding function; therefore, the HUR of the proposed VLSI architecture is as high as 100%. The performance evaluation classifies the electrical characteristics into the operation frequency, the power consumption, and the area.

The SOLS technique integrates Manchester, FM0 and Miller encodings into a fully reused hardware architecture. Obviously, the coding procedure of FM0 is more complex than that of Manchester. The data path of Manchester encoding restricted to that of FM0 encoding. Then, the operation frequency of Manchester encoding is also limited by that of FM0 encoding. Our work targets at an efficient integration of hardware devices for Manchester, Miller and FM0 encoding instead of operation frequency and power consumption. Generally, more coding methods a hardware architecture can support, more hardware devices it requires. A performance evaluation is given under identical conditions for a more objective evaluation. A building block that can perform FM0, Manchester and Miller encodings is considered an evaluation platform.

PERFORMANCE EVALUATION ON FM0, MANCHESTER AND MILLER ENCODINGS

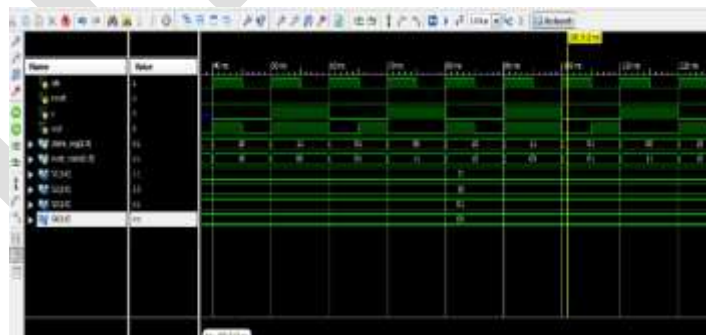


Fig.10. Simulation results for FM0 encoding

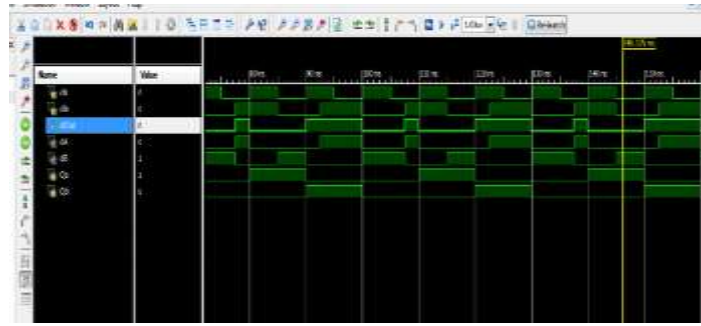


Fig.11. Simulation results for Manchester encoding

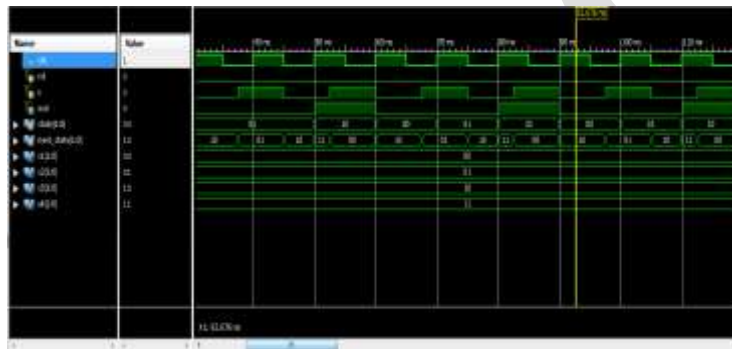


Fig.12. Simulation results for Miller encoding

The simulation result for FM0 encoding is shown in Figure 10. When the input X is 0, and the CLK is given as a rising edge which produces a transition in middle of that FM0 cycle. When the input X is 1, there is no transition in the FM0 cycle. Also there is a transition in among each FM0 code. The simulation result for Manchester encoding is shown in Fig 11. The Manchester encoding is realized with a XOR operation for CLK and X. The clock always has a transition within one cycle, and so does the Manchester code no matter what the X is. The simulation results for Miller encoding is shown in Figure 12. The input X plus a positive edge clock produces the output as 0 .

5. CONCLUSION

The coding diversity between FM0, Manchester and Miller codes causes the limitation on designing VLSI architecture. Hence, the fully reused VLSI architecture using area compact retiming and balance logic operation sharing technique for both FM0 and Manchester encodings is adapted. The realization of this project will solve most of the difficulties discussed above and in the problem definition section. This project will have following results:

1. Improved hardware utilization rate (HUR)
2. Area optimization
3. reduced power consumption
4. Lower latency

The coding diversity between FM0, Manchester and Miller encodings causes the limitation on hardware utilization of VLSI architecture design. The area compact retiming and balance logic operation sharing techniques eliminates the limitation on hardware utilization. Area compact retiming concept relocates the hardware resource and to reduce the number of transistors effectively. The Balance Logic operation sharing technique combines FM0 and Manchester encodings with the identical logic components to produce balanced computation time. Every component is active in both FM0 and Manchester encodings and it will greatly improve the

hardware utilization rate to 100% and reduce the power consumption. The FM0 and Manchester encoders are designed with these techniques to achieve high speed and fully reconfigured VLSI architecture for application system. In future the design can be implemented using high performance FPGA devices.

REFERENCES:

- [1] Yu-Hsuan Lee and Cheng-Wei Pan, "Fully Reused VLSI Architecture of FM0/Manchester Encoding Using SOLS Technique for DSRC Applications," *Member, IEEE, IEEE trans. in Very Large Scale Integr. (VLSI) Syst., vol. pp, issue 99, Feb 2014.*
- [2] Y.C. Hung, M.-M. Kuo, C.-K. Tung, and S.-H. Shieh, "High-speed CMOS chip design for Manchester and Miller encoder" in *Proc. Intell. Inf. Hiding Multimedia Signal Process., Sep. 2009, pp. 538–541*
- [3] A. Karagounis, A. Polyzos, B. Kotsos, and N. Assimakis, "90nm Manchester code generator with CMOS switches running at 2.4 GHz and 5 GHz" in *Proc. 16th Int. Conf. Syst., Signals Image Process., Jun. 2009, pp. 1–4*
- [4] P. Benabes, A. Gauthier, and J. Oksman, "A Manchester code generator running at 1 GHz," in *Proc. IEEE, Int. Conf. Electron., Circuits Syst., vol. 3. Dec. 2003, pp. 1156–1159.*
- [5] M. A. Khan, M. Sharma, and P. R. Brahmanandha, "FSM based Manchester encoder for UHF RFID tag emulator," in *Proc. Int. Conf. Comput., Commun. Netw., Dec. 2008, pp.1–6*
- [6] Mohanraj S. and Dr. Sudha S, Professor, "Low Power VLSI Architecture of Encoder for Downlink Applications," *Aust. J. Basic & Appl. Sci., 9(15): 43-51, 2015.*
- [7] Daniel Jiang, Vikas Taliwal, Andreas Meier, Wieland Holfelder, Ralf Herrtwich, "Design of 5.9GHz DSRC based Vehicular Safety Communication," *DaimlerChrysler Research and Technology North America, Inc.*
- [8] F. Ahmed-Zaid, F. Bai, S. Bai, C. Basnayake, B. Bellur, S. Brovold, *et al.*, "Vehicle safety communications—Applications (VSC-A) final report," *U.S. Dept. Trans., Nat. Highway Traffic Safety Admin., Washington, DC, USA, Rep. DOT HS 810 591, Sep. 2011.*
- [9] J. B. Kenney, "Dedicated short-range communications (DSRC) standards in the United States," *Proc. IEEE, vol. 99, no. 7, pp. 1162–1182, Jul. 2011.*
- [10] M. A. Khan, M. Sharma, and P. R. Brahmanandha, "FSM based FM0 and Miller encoder for UHF RFID tag emulator," in *Proc. IEEE Adv. Comput. Conf., Mar. 2009, pp. 1317–1322.*
- [11] J. Daniel, V. Taliwal, A. Meier, W. Holfelder, and R. Herrtwich, "Design of 5.9 GHz DSRC-based vehicular safety communication," *IEEE Wireless Commun. Mag., vol. 13, no. 5, pp. 36–43, Oct. 2006.*
- [12] J.-H. Deng, F.-C. Hsiao, and Y.-H. Lin, "Top down design of joint MODEM and CODEC detection schemes for DSRC coded-FSK systems over high mobility fading channels," in *Proc. Adv. Commun. Technol. Jan. 2013, pp. 98–103.*
- [13] I.-M. Liu, T.-H. Liu, H. Zhou, and A. Aziz, "Simultaneous PTL buffer insertion and sizing for minimizing Elmore delay," in *Proc. Int. Workshop Logic Synth., May 1998, pp. 162–168.*

Available Transfer Capacity with Renewable Energy

¹Haris K V, ¹Hrudhya Kurian C

¹PG Scholar Thejus engineering college, Thrissur

hariskv.kv@gmail.com, hrudhyakurianc888@gmail.com

Abstract- Electric utility around the world is facing with restructuring, deregulation and privatization. And transmission network tend to be heavily loaded and transmission services become one of the most critical element. Power system transfer capability indicates how much inter area power transfers can be increased without compromising system security. For both planning and operation of the bulk power market, accurate identification of this capability is very important. Available transfer capacity (ATC) as the amount of transfer capacity that is available at a certain time for purchase or sale in the electric power market under different system conditions. The computation of ATC is very important to keep reliability and security of deregulated power system. An accurate ATC computation is also very important to the transmission system. If the computed ATC is less than the ATC of the system, the transmission of power will not be efficient economically, if the computed ATC is more than the ATC of the system, the transmission will be operating in a dangerous state and any power increased will stand a chance to collapse the whole system and the result of that is disastrous. The computation of real time ATC value is very important sine it is not fixed for a line. The value of ATC for a transmission line will vary with many cases. This project also focuses on the variation of ATC value with varying renewable energy sources, with increasing load demand and with incorporation of UPFC controllers.

Keywords- ATC, UPFC, TTC, ETC, PTDF, etc

I. INTRODUCTION

Nowadays the demand and of non renewable energy is increasing day by day. To overcome this issue we go for renewable energy sources. So a new method is implementing ATC with renewable energy. The commonly used renewable energy sources are wind, tide, solar, fuel cell, geothermal, etc. Here we are choosing the renewable energy source as solar energy. To calculate the available transfer capacity of six bus system following steps are (a) to study the impact of renewable energy variation on ATC value. (b) To study the variation of ATC with load demand. (c) To calculate ATC of the proposed six bus system with the incorporation of UPFC controller [1].

II. AVAILABLE TRANSFER CAPABILITY

Available Transfer Capability (ATC) is a measure of the transfer capability remaining in the physical transmission network for further commercial activity over and above already committed uses [2]. Mathematically, ATC is defined as the Total Transfer Capability (TTC) less the Transmission Reliability Margin (TRM), less the sum of Existing Transmission Commitment (ETC) (which includes retail customer service) and the Capacity benefit Margin (CBM). ATC can be expressed as:

$$ATC = TTC - TRM - CBM - ETC$$

Where, TTC=Total transfer capability, TRM=Transmission reliability margin, CBM=Capacity benefit margin, ETC=Existing transmission commitments etc.

A. Transfer capability

Transfer capability is the measure of the ability of interconnected electric systems to reliably move or transfer power from one area to another over all transmission lines (or paths) between those areas under specified system conditions. The units of transfer capability are in terms of electric power, generally expressed in megawatts (MW).

B. Transmission reliability margin (trm)

Transmission Reliability Margin (TRM) is defined as that amount of transmission transfer capability necessary to ensure that the interconnected transmission network is secure under a reasonable range of uncertainties in system conditions.

C. Capacity benefit margin

Capacity Benefit Margin (CBM) is defined as that amount of transmission transfer capability reserved by load serving entities to ensure access to generation from interconnected systems to meet generation reliability requirements.

D. Limits to transfer capability

The ability of interconnected transmission networks to reliably transfer electric power may be limited by the physical and electrical characteristics of the systems including any one or more of the following:

1. Thermal Limits — Thermal limits establish the maximum amount of electrical current that a transmission line or electrical facility can conduct over a specified time period before it sustains permanent damage by overheating.
2. Voltage Limits — System voltages and changes in voltages must be maintained within the range of acceptable minimum and maximum limits.
3. Stability Limits — the transmission network must be capable of surviving disturbances through the transient and dynamic time periods following the disturbance.

Therefore, the TTC becomes:

TTC = Minimum of {Thermal Limit, Voltage Limit, Stability Limit}

III. METHODS OF ATC CALCULATION

A. Continuation power flow method (cpf)

Continuation Power Flow (CPF) is first introduced for determining the maximum load ability however; it is adaptable for other applications including ATC computation without changing its principle. CPF method is based on full AC power flow solution to incorporate the effects of reactive power flows, voltage limits and voltage collapse as well as thermal loading effects [3]. But the use of CPF in determining ATC is complex and the computational time increases when the contingency analyses are introduced for all possible cases. Consequently, it is not suitable for on-line applications in its present form. The CPF algorithm effectively increases the controlling parameter in discrete steps and solves the resulting power flow problem at each step. The procedure is continued until a given condition or physical limit preventing further increase is reached. Hence, the speed of proposed method is very slow. Consequently, it is not suitable for online applications in its present form [4].

B. Optimal power flow method (opf)

Optimal Power Flow approach is another approach used to calculate ATC. The main idea is to formulate an optimization problem such that the dominant elements are the equality and inequality constraints of power flow. But solution of optimization problem for large systems becomes very time consuming and hence this approach cannot be applied in real-time for large systems. OPF methods are widely used to determine ATC in power corridors of the system. However these optimization methods are suitable in case of open access system where there is a possibility of power transactions occurring from any point to any point.

C. Repeated power flow method (rpf)

Repeated power flow method was proposed to explore its computational advantage. This approach starts from a base case, and repeatedly solves the power flow equations each time increasing the power transfer by a small increment until an operation limit is reached. The advantage of this approach is its simple implementation and the ease to take security constraints into consideration but takes long time for iteration.

D. Sensitivity based power flow method

Sensitivity based power flow methods have been proposed for fast computation of ATC. This method is based on power transfer distribution factors (PTDFs) using DC and AC load flow approach. DC power transfer distribution factors (DCPTDF) based method is reported for fast calculation of ATC. But this method has a poor accuracy when X/R ratio is low due to assumptions involved. This is

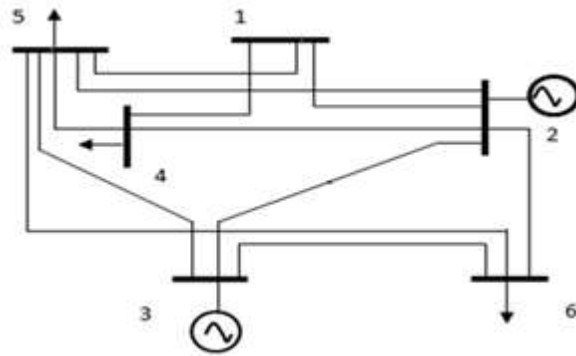
very useful due to its simplicity in calculation and speedy outcomes [5]. The DC load flow based approaches are fast using assumptions for DC load flow. Many researchers have presented more accurate methods considering reactive power flow based on AC load flow formulation for ATC calculation using the sensitivity factors. These sensitivity factors are based on linear incremental power flow, which are very simple to define and calculate [7]. In ACPTDF method, a sequential full ac power flow is not required and hence has a high calculation speed. Studies have indicated that CPF and OPF based methods are accurate but very time consuming, especially for large systems [6]. Among the existing methods of ATC calculation, PTDF based methods are fastest.

III. SIMULATION

The software used in this paper to calculate ATC is MATLAB and the results are tested using MATLAB programming in the version MATLAB2 R2013b. MATLAB is widely used in academic and research institutions as well as industrial enterprises. The MATLAB application is built around the MATLAB language, and most use of MATLAB involves typing MATLAB code into the Command Window or executing text files containing MATLAB code, including scripts and/or functions.

A. Proposed 6 bus system

The 6-bus test system is considered here to demonstrate the calculations of ATC using proposed method. Bus 1 is the swing bus, bus 2 and 3 are generator buses whereas bus 4, 5 and 6 are load buses. Code 0, Code 1, Code 2 for the load buses, the slack bus and the voltage controlled buses, respectively. The figure below shows the one-line diagram of 6 bus system [8].



B. Line data for the 6 bus system

From	To	R(p.u)	X(p.u)	Thermal limit
1	2	0.1	0.2	40
1	4	0.05	0.2	80
1	5	0.08	0.3	60
2	3	0.05	0.25	40
2	4	0.05	0.10	60
2	5	0.1	0.3	30
2	6	0.07	0.20	90
3	5	0.12	0.26	70
3	6	0.02	0.10	100
4	5	0.1	0.40	20
5	6	0.1	0.30	40

Bus No.	Bus Code.	Voltage magnitude(V)	Angle (degree)	Load (MW)	Load (Mvar)	Generator (MW)	Generator (Mvar)
1	1	1.0	0.0	0	0	0.0	0.0
2	2	1.05	0.0	0	0	69.36	0.0
3	2	1.07	0.0	0	0	77.47	0.0
4	0	1.0	0.0	70	70	0.0	0.0
5	0	1.0	0.0	70	70	0	0.0
6	0	1.0	0.0	70	70	0	0.0

Bus data for the proposed system

V. SIMULATION RESULTS

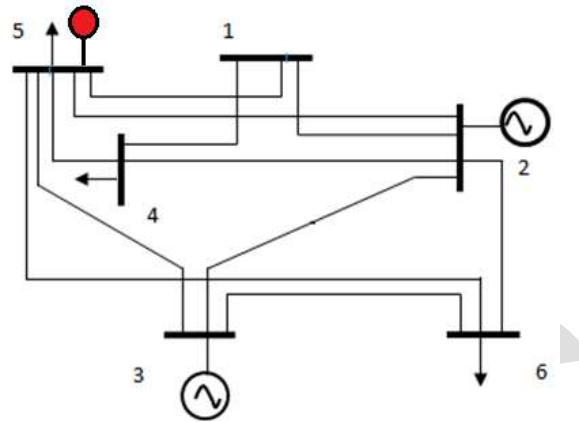
Renewable energy power generation can reduce human dependence on fossil fuels and environment and climate issues. It is an important part of the world power industry development to vigorously promote the new energy power generation. Solar power represents one of the new energy power generation industry developed rapidly [9]. With the development of renewable energy power generation technology and increase of power load demand, renewable energy power generation can not only service specific users outside power grid,

but also can massively incorporate into the power grid. Here we study the variation of ATC value with some connected solar energy sources. Since the solar power output is not fixed we imaging an upper and lower limit for the solar power output in MW [10].

In order to make comparable research, 2 kinds of penetration level of renewable energy power generation are set as:

Penetration level 1: No solar source is added.

Penetration level 2: A solar source having an out 20 to 25 MW power is connected in bus five as shown in the figure below. The output is also given below.



Line No	Sending bus	Receiving bus	ATC in MW Without renewable	ATC in Mw with renewable 20- 25MW
1	1	2	0.3635	0.4311-0.4478
2	1	4	0.5609	0.6956-0.7291
3	1	5	0.4509	0.5051-0.5186
4	2	3	0.1911	0.2331-0.2546
5	2	4	0.4052	0.5567-0.5936
6	2	5	0.2166	0.3896-0.4794
7	2	6	1.6251	1.6307-1.7042
8	3	5	0.9912	0.9958-0.9970
9	3	6	0.2435	0.2595-0.2676
10	4	5	0.3319	0.4734-0.5549
11	5	6	1.3462	1.6933-1.8701

CONCLUSION

An accurate ATC computation is also very important to the transmission system. If the computed ATC is less than the ATC of the system, the transmission of power will not be efficient economically, if the computed ATC is more than the ATC of the system, the transmission will be operating in a dangerous state and any power increased will stand a chance to collapse the whole system and the result of that is disastrous. In this project we use a simple and efficient method for determining the available transfer capability of the system and studying its variation by renewable energy, varying load demands and with connected UPFC controllers. The MATLAB programs for all ATC calculations are done and the results presented in a tabular data for each section.

REFERENCES:

1. A. Khairuddin, ; N. A. Bakar "ATC Determination Incorporating Wind Generation" 2013 IEEE 7th International Power Engineering and Optimization Conference (PEOCO2013), Langkawi, Malaysia. 3-4 June.
2. Anup Kumar and Mukesh Kumar "Available Transfer Capability Determination Using Power Transfer Distribution Factors", International Journal of Information and Computation Technology, Volume 3,(2013).
3. M. Y. Patel and A. A. Girgis "New Iterative Method for Available Transfer Capability Calculation", 2011 IEEE.
4. G. Hamoud, "Assessment of available transfer capability of transmission systems", IEEE Transactions on Power systems 15 (1) (2000) 27-32.

5. G.C. Ejebe, J. Tong, J.G. Waight, J.G. Flame, X. Wang, W.F. Tinney, "Available Transfer Capability Calculations", IEEE Transactions on Power Systems, Vol. 13, No. 4, November 1998.
6. Nirmal Solanki , Mr. U. L. Makwana "Calculation of Available Transfer Capability Using AC Load Flow Method", International Journal for Scientific Research & Development Vol. 2, Issue 01, 2014.
7. Poornima Pankajam T, J Srinivasa Rao, J Amarnath "ATC Enhancement with FACTS Devices Considering Reactive Power Flows Using PTDF", International Journal of Electrical and Computer Engineering (IJECE) Vol. 3, No. 6, December 2013, pp. 741~750.
8. Rajnikant H. Bhesdadiya, Dr. Rajesh M. Patel "Available Transfer Capability Calculation Methods: A Review", International Journal of Advanced Research in Electrical, Electronics and Instrumentation Engineering, Vol. 3, Issue 1, January 2014.
9. Luis Luna, Jorge Martínez Carlos, Valero Pacual and Vanesa Valiño "impact of wind power generation on the atc value", 17th Power Systems Computation Conference Stockholm Sweden - August 22-26, 2011.
10. Mojgan Hojabri and Hashim Hizam "Available Transfer Capability Calculation", Applications of MATLAB in Science and Engineering.

SURVEY ON SECURE AND DISTRIBUTED DATA DISCOVERY AND DISSEMINATION IN WSN

B.Gouthami

M. Tech Student (GNITS, Hyderabad), gouthamichinni.01743@gmail.com, 9440022281.

A.Naveena

Assistant Professor(GNITS, Hyderabad), ambidinaveena@yahoo.com,9866937347

Abstract — Dissemination is a basic sensor network protocol. The ability to reliably deliver a piece of data to every node allows administrators to reconfigure, query, and reprogram a network. Data Discovery and Dissemination Protocol is responsible for updating the configuration small commands, parameters, queries, variables. Dissemination protocols have self-organizing capabilities because WSNs are deployed in critical environments and remote areas where manual reprogramming of nodes are difficult. All existing data discovery and dissemination protocols suffer from two drawbacks. First, they are based on centralized approach and second, they were not designed with security in mind and hence adversaries can easily launch attacks. This paper proposes DiDrip protocol. This is the first secure and distribute Data discovery and dissemination protocol.

Keywords—Data Discovery, Data dissemination, wireless sensor networks, reprogramming, Trickle, tuples, security

INTRODUCTION

A wireless sensor network (WSN) is made of a group of nodes and is used for monitoring and analysis purposes. Wireless sensor networks mainly use broadcast communication. In comparison with wired systems, wireless sensor networks have their own special features and limitations. Wireless sensor networks are limited by sensors limited power, energy and computational capability. The evolving conditions and environment can change application requirements. This requires altering the behavior of the network by introducing new code or updates. This can be achieved by data discovery and dissemination protocol, which facilitates a source to inject small programs, commands, queries, and configuration parameters to sensor Nodes [1]. Unlike flooding protocols, which are discrete efforts that terminate, possibly not delivering the data to some nodes, dissemination achieves reliability by using a continuous approach that can detect when a node is missing the data. Reliability is important because it makes the operation robust to temporary disconnections or high packet loss.

Some WSNs do not have any base station at all. For example, for a WSN monitoring human trafficking in a country's border or a WSN deployed in a remote area to monitor crop cultivation, a base station becomes an attractive target to be attacked. For such networks, data dissemination is better to be carried out by authorized network users in a distributed manner.

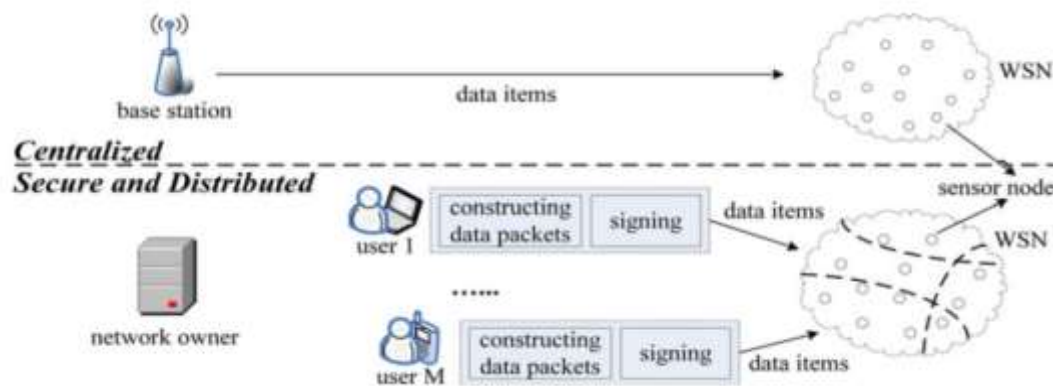


Figure 1: shows the difference between centralized and distributed dissemination of data packets.

Fig.1, data items can only be disseminated by the base station. Unfortunately, this approach suffers from the single point of failure as dissemination is impossible when the base station is not functioning or when the connection between the base station and a node is broken. In addition, the centralized approach is inefficient, non-scalable, and vulnerable to security attacks that can be launched anywhere along the communication path. Even worse, some WSNs do not have any base station at all. For example, for a WSN monitoring human trafficking in a country's border or a WSN deployed in a remote area to monitor illicit crop cultivation, a base station becomes an attractive target to be attacked. For such networks, data dissemination is better to be carried out by authorized network users in a distributed manner.

The primary challenge of providing security functions in WSNs is the limited capabilities of sensor nodes in terms of computation, energy and storage.

LITERATURE SURVEY:

1. TRICKLE: A Self Regulating Algorithm

Propagating code is costly; learning when to propagate code is even more so. Motes must [1] periodically communicate to learn when there is new code. To reduce energy costs, motes can transmit metadata to determine when code is needed. Trickle, an algorithm for propagating and maintaining code updates in wireless sensor networks. It is based on "Polite Gossip".

Each node only gossip about new things that it has heard from its neighbors, but it won't repeat gossip it has already heard, as that would be rude. Each mote periodically broadcasts metadata describing what code it has. However, if a mote hears gossip about identical metadata to its own, it stays quiet. When a mote hears old gossip, it triggers a code update, so the gossipier can be brought up to date. To achieve both rapid propagation and a low maintenance overhead, motes adjust the length of their gossiping attention spans, communicating more often when there is new code.

For example, if mote A broadcasts that it has code ϕ_x , but B has code ϕ_{x+1} , then B knows that A needs an update. Similarly, if B broadcasts that it has ϕ_{x+1} , A knows that it needs an update. If B broadcasts updates, then all of its neighbors can receive them without having to advertise their need. Some of these recipients might not even have heard A's transmission. In this example, it does not matter who first transmits, A or B; either case will detect the inconsistency. [2] All that matters is that some motes communicate with one another at some nonzero rate; we will informally call this the "communication rate." As long as the network is connected and there is some minimum communication rate for each mote, everyone will stay up to date. The fact that communication can be either transmission or reception enables Trickle to operate in sparse as well as dense networks.

Each mote maintains a counter c , a threshold k , and a timer t in the range $[0, T]$. K is a small, fixed integer and T is a time constant. When a mote hears metadata identical to its own, it increments c . At time t , the mote broadcasts its metadata if $c < k$. When the interval of size T completes, c is reset to zero and t is reset to a new random value in the range $[0, T]$. Scaling logarithmically with density, it can be used effectively in a wide range of networks [2]. One limitation of Trickle is that it currently assumes motes are always on. To conserve energy, long-term mote deployments often have very low duty cycles (e.g., 1%). Correspondingly, motes are rarely awake, and rarely able to receive messages.

Advantages:

- i. Can be used effectively in wide range of networks.
- ii. Trickle can scale to very dense networks.

Limitations:

- i. Sensor nodes are always on
- ii. Overhead increases with number of data items

2 DRIP

SNMS [4], a Sensor Network Management System. SNMS is designed to be simple and have minimal impact on memory and network traffic, while remaining open and flexible. The system is evaluated in light of issues derived from real deployment experiences. In

contrast, wireless sensor networks act in aggregate, and thus, a wireless sensor network management system must be able to manage in the aggregate. Aggregate management requires a dissemination protocol that can deliver messages reliably to a set of nodes within a sensor network. The underlying algorithm used by our dissemination layer is the Trickle algorithm.

Trickle [2] uses periodic retransmissions to ensure eventual delivery of the message to every node in the network. To minimize the number of required messages, retransmissions can be suppressed by prior transmissions of similar messages, and randomization is used to prevent permanent suppression. [4] The dissemination layer takes the Trickle retransmission algorithm and builds a transport-layer interface atop it. The SNMS dissemination protocol, named Drip, provides a transport layer interface to multiple channels of reliable message dissemination. Drip provides a standard message reception interface. Each component wishing to use Drip registers a specific identifier, which represents a reliable dissemination channel. Messages received on that channel will be delivered directly to the component. Each node is responsible for caching the data extracted from the most recent message received on each channel to which it subscribes, and returning it in response to periodic rebroadcast requests. Drip avoids redundant transmission and achieves greater efficiency.

Advantages:

- i. Avoids redundant transmission and greater efficiency.
- ii. Gives information about health of nodes.

Limitations:

- i. Centralized method.
- ii. Security is not provided for data.

3 DIP

DIP, a data discovery and dissemination protocol for wireless networks [5]. Prior approaches, such as trickle or [3] SPIN, have overheads that scale linearly with the number of data items. For T items, DIP can identify new items with $O(\log(T))$ packets while maintaining an $O(1)$ detection latency.

DIP is a hybrid data detection and dissemination protocol. It separates this into two parts: detecting that a difference occurs, and identifying which data item is different. DIP dynamically uses a combination of searching and scanning based on network and version metadata conditions. [5] To aid its decisions, DIP continually estimates the probability that a data item is different. DIP maintains these estimates through message exchanges. When probabilities reach 100%, DIP exchanges the actual data items. It is an eventual consistency protocol in that when data items are not changing, all nodes will eventually see a consistent set of data items.

DIP stores a version number for each data item. DIP periodically broadcast a summary message containing hashes of its keys and versions. Hash-tree based algorithm detects if there is an update. If a node hears a hash that differs from its own, it knows that a difference exists. On receiving a data message whose version number is newer than its own, DIP installs the new item. DIP improves searching performance by combining hashes over ranges of the key space with a bloom filter. The overhead problem is reduced and this protocol sends 20-60% fewer packets than previous protocols.

Advantages:

- i. Overhead decreases.
- ii. Sends 20-60% fewer packets than existing protocols.

Limitations:

- i. No security system.
- ii. Centralized system.

3 DHV

It is a code consistency maintenance protocol (Difference detection, Horizontal search, and Vertical search). The main objective is to overcome the disadvantages of previous protocols like DRIP [4] and DIP [5] by reducing the complexity. Here data items are represented as tuples (key, version). If two versions are different; they may only differ in a few least significant bits of their version number rather than in all their bits.

DHV [6] includes two important phases: Detection phase and Identification phase. In detection, each node will broadcast a hash of all its versions in SUMMARY message. In identification, the horizontal search and vertical search steps are used. In horizontal search, a node broadcasts a checksum of all versions, called a HSUM message. In vertical search, the node broadcasts a bit slice, starting at the least significant bit of all versions, called a VBIT message. After identifying this, the node broadcasts those (key, version) tuples in a VECTOR message.

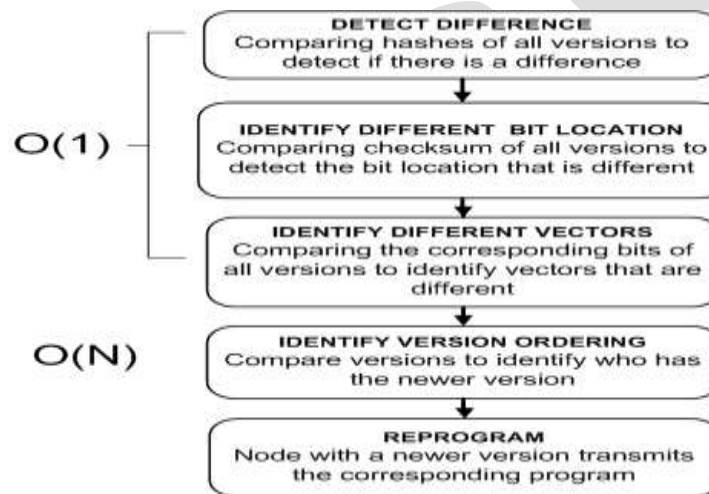


Figure 2: Main steps in the DHV protocol

Advantages:

- i. DHV reduces the number of transmitted bytes.
- ii. DHV performs at least twice better than DIP protocol.

Limitations:

- i. Centralized approach.
- ii. Chance for DOS attack.

5 Code drip

Code Drip [7] utilizes Network Coding to improve energy efficiency, reliability, and speed of dissemination. Network coding allows recovery of lost packets by combining the received packets thereby making dissemination robust to packet losses. Code Drip uses Network Coding to improve the efficiency of dissemination in Wireless Sensor Networks. Network Coding is a technique that combines packets in the network thereby increasing the throughput, decreasing energy consumption, and reducing the number of messages that are transmitted. Dropped packets are recovered using re-transmissions. By combining packets using network coding, it is possible to re-cover the transmitted information without needing to retransmit all the lost packets to all the nodes.

Network Coding allows packets to be combined using a XOR logic operator. Like Drip, Code Drip uses the Trickle timer [2] to time the message transmissions with the goal that the data will eventually arrive at all the nodes in the network. The unmodified Drip message has

only one identifier and its payload is the data to be disseminated. A combined message has two or more identifiers corresponding to the packets that were combined.

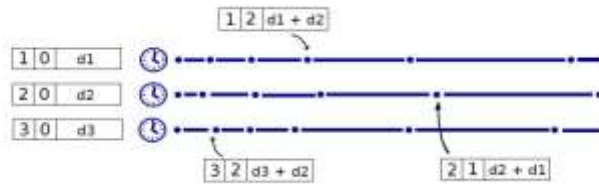


Figure 3: Code Drip example. There are three values to be disseminated. Each value has an associated Trickle timer. Each packet transmission might combine the packets.

Code Drip is faster than Drip, DIP and DHV protocols to disseminate information. It also requires less ROM memory than Drip, DHV and DIP. Code Drip is faster, smaller and sends fewer messages than Drip, DHV and DIP protocols.

Advantages:

- i. Applying Network Coding reduces the dissemination time.
- ii. Packet loss is reduced.

Limitations:

- i. Centralized method.
- ii. Need maximum buffer size.

6 DiDrip

DiDrip consists of four phases, system initialization, user joining, and packet pre-processing and packet verification. For our basic protocol, in system initialization phase, the network owner creates its public and private keys, and then loads the public parameters on each node before the network deployment. In user joining phase, a user gets the dissemination privilege through registering to the network owner. In packet pre-processing phase, if a user enters to the network and wants to disseminate some data items, he/she will need to construct the data dissemination packets and then send them to the nodes. In packet verification phase, a node verifies each received packet. If the result is positive, it updates the data according to the received packet. Based on the design objectives, they propose DiDrip. It is the first distributed data discovery and dissemination protocol, which allows network owners and authorized users to disseminate data items into WSNs without relying on the base station.

CONCLUSION

In this paper, a survey has been done on various existing dissemination protocols for wireless sensor networks. We have seen the architecture and security considerations on each protocol. In wireless sensor networks, security is the key objective in dissemination of data. Therefore in this paper, a secure and distributed data discovery and dissemination protocol named DiDrip has been proposed. DiDrip protocol addresses many of the drawbacks and limitations of the previous dissemination protocols like security, distributed approach, multi owner-multi user capabilities but its efficiency and security is tested under limited parameters.

REFERENCES:

- [1] J. W. Hui and D. Culler, "The dynamic behavior of a data dissemination protocol for network programming at scale," in Proc. 2nd Int. Conf. Embedded Netw. Sensor Syst., 2004, pp. 81–94.
- [2] P. Levis, N. Patel, D. Culler, and S. Shankar. "Trickle: A self-regulating algorithm for code maintenance and propagation in wireless sensor networks." In First USENIX/ACM Symposium on Network Systems Design and Implementation (NSDI), 2004

- [3] I.F. Akyildiz, W. Su, Y. Sankarasubramanian, and Erdal Cayirci, "A Survey on Sensor Networks", IEEE Communications Magazine, November 7, 2002, pp. 102-114, vol. 40(8).
- [4] G.Tolle, D.Culler "Design of an application-cooperative management system for wireless sensor networks". In: Proceedings of the 2005 International Conference on Information Processing in Sensor Networks (IPSN 2008), IEEE Computer Society (2005) 121 - 132.
- [5] Lin, K., Levis, P.: "Data discovery and dissemination with dip". In: Proceedings of the 2008 International Conference on Information Processing in Sensor Networks (IPSN 2008), Washington, DC, USA, IEEE Computer Society (2008) 433-444.
- [6] T.Dang, N. Bulusu, W. Feng, and S. Park, "DHV: A code consistency maintenance protocol for multi-hop wireless sensor networks," in Proc. 6th Eur. Conf. Wireless Sensor Netw., 2009, pp. 327-342.
- [7] Nildo Ribeiro Junior, Marcos A. M. Vieira, Luiz F. M. Vieira, and Omprakash Gnawali, "CodeDrip: Data Dissemination Protocol with Network Coding for Wireless Sensor Networks", in Proceedings of the 11th European conference on Wireless sensor networks (EWSN 2014), Feb. 2014

FPGA Implementation of Safe Mode Detection and Sun Acquisition Logic in a Satellite

Dhanyashree T S¹, Mrs. Sangeetha B G, Mrs. Gayatri Malhotra

¹Post-graduate Student at RNSIT Bangalore India, dhanz1ec@gmail.com, +919482153794

Abstract— Satellite/spacecraft enter into Safe Mode in case of contingency when the solar panel is not rotated towards Sun in order to provide full solar array power. The transition from safe mode to sun pointing mode, carried out automatically by Sun acquisition logic. In sun acquisition logic selected yaw and roll errors are used as inputs to controller whose outputs are routed to thruster selection logic. On Safe Mode enable condition, based on the safe mode pulse from on board computer (OBC) thruster block reconfiguration is done. This initiates thruster selection logic (TSL), whose outputs are routed to thruster drivers to fire the thrusters in satellites/spacecraft to change the spacecraft orientation. The eclipse condition is also detected from 4PI pitch output on safe mode.

Keywords— Pitch, yaw, roll, safe mode detection, loop-on pulse generation, long pulse detection, thruster selection, sun pointing mode .

INTRODUCTION

Communications satellite or a weather forecasting satellite or even a remote sensing satellite, irrespective of the intended application, all the satellites have several things in common. They have a metal or composite frame and body, usually known as the bus, a source of power (usually solar cells) and batteries for storage, a radio system and antenna for Telemetry, tracking and command (TT&C), an attitude control system and an onboard computer system to control and monitor the different systems[1].

The purpose of On Board Computer (OBC) system is to integrate and miniaturize Spacecraft Electronics to match the global trend and meet the requirements of Autonomous spacecraft operations. Cost-effective spacecraft engineering is achieved by integrating the various elements of the spacecraft bus that realize the functions of command processing, Data acquisition and processing, Attitude and Orbit control, Telemetry and Housekeeping and Thermal Management into a single OBC. The MIL STD 1553B protocol is used for interfacing with various sub-systems of the spacecraft. The OBC interfaces with sensors (attitude and temperature), actuators, power, thermal control elements like heaters and Solar Array Drive Assembly through special interfaces, TTC (RF) for command and housekeeping TM[2][3]. For all these operations a functionally redundant OBC is present. In case of failure or contingency in main and redundant OBC, a separate package is configured, which houses 4Pi Sun Sensor based Hardware based Safe Mode detection and Sun Acquisition and Contingency Telemetry logics.

This paper describes the implementation of this package on a FPGA. The design implemented is synthesized and simulated, where simulation results show the detection of safe mode and thruster controls for sun acquisition.

METHODOLOGY

A. Terminology

Safe mode is an operating mode of a modern spacecraft during which all non-essential systems such as science instruments are shut down and only essential functions such as thermal management, radio reception and attitude control are active. Safe mode is entered automatically upon the detection of sun absence. The spacecraft attempts to maintain orientation with respect to the Sun for illumination of solar panels and for thermal management. The spacecraft then awaits radio commands from its mission control center monitoring for signals on its low-gain omnidirectional antenna[4].

This system uses coordinates that maintain their orientation relative to the earth as spacecraft moves in orbit. These coordinates are known as roll, pitch, and yaw or RPY, and are illustrated in figure 1. In this system, the yaw axis is directed toward the nadir (i.e., toward the center of the Earth), the pitch axis is directed toward the negative orbit normal, and the roll axis is perpendicular to the other. Thus, in a circular orbit, the roll axis will be along the velocity vector[6].



Fig 1. Satellite's position w.r.t.to the Earth and the Sun

B. Implementation overview

Safe mode detection, Sun acquisition and telemetry interfacing are the three basic logics designed and implemented as shown in figure 2. Safe mode detection logic produces safe mode initiation status. After which thrusters are controlled by sun acquisition logic. The status of the signals used and manipulated in these two logics is sent to telemetry(TM) subsystem after interfacing with TM interface logic.

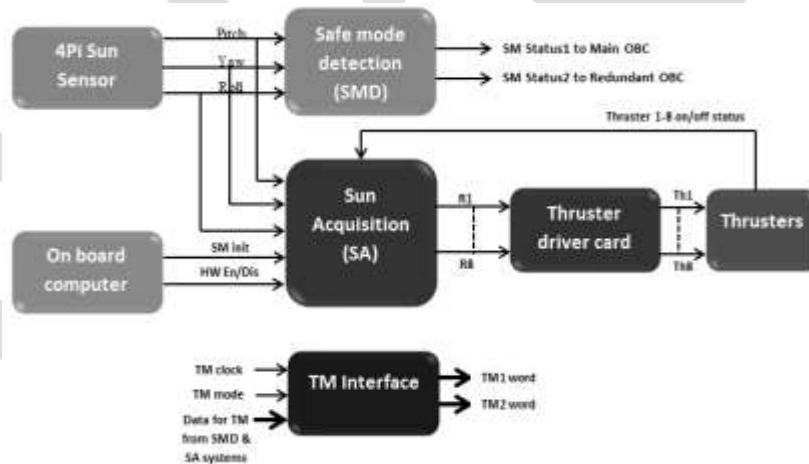


Fig 2. Package overview

C. Safe mode detection

Safe mode detection logic shown in figure 3 is based on 4Pi sun sensors pitch, yaw and roll signals errors. Selected sensor outputs are compared with respect to threshold set to detect errors in sensors signals. The Sun will be on negative pitch axis, when the solar panels are normal to the Sun. The 4pi pitch output magnitude will be high when the Sun is directly looking at the pitch cells. So when the Sun is on negative pitch side, the pitch output will be -5.0 volts that is high in magnitude[5].

The presence of error is verified by the following conditions.

1. If 4pi pitch output greater than the threshold (for example, 1.5 volts is greater than 1.0 volts). This check is to say that the Sun is away from the body negative pitch axis.
2. If absolute values of 4pi yaw or roll outputs (magnitudes alone) are beyond certain threshold (say, 1.5 volts). This check is to ensure that the Sun is beyond the cone of 45° about the negative pitch axis.

The second condition supports the 4pi pitch output checking. The check also supports logic validity during eclipse. Checking could

have been either yaw or roll, but checking together may be more robust.

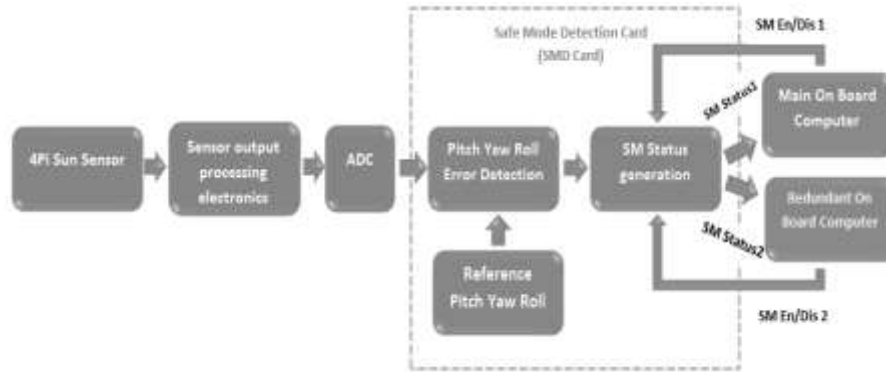


Fig 3. Safe Mode Detection System

D. Sun Acquisition

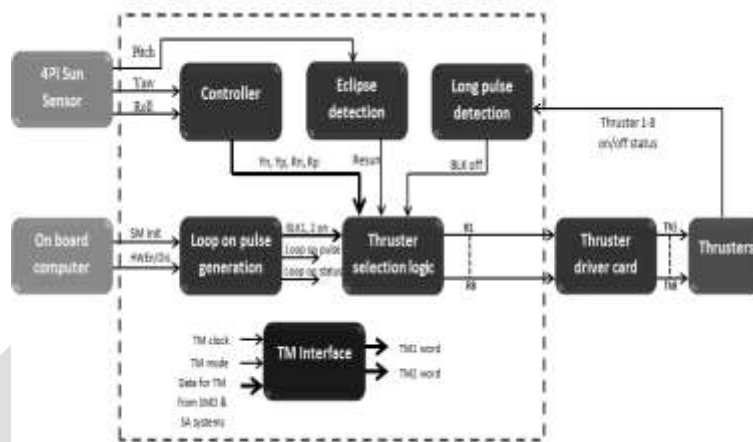


Fig 4. Sun Acquisition system

In sun acquisition logic selected pitch, yaw and roll errors are used as inputs to controller whose outputs are routed to thruster selection logic. The sun acquisition system is shown in figure 4. On Safe Mode enable condition, the SM pulse from OBC initiates a 400sec timer whose outputs do thruster block reconfiguration. Thruster selection logic (TSL) is initiated after obtaining assertions from block reconfiguration logic. The TSL outputs are routed to thruster drivers. The thruster outputs in turn change the spacecraft orientation. The sensor data will sense it and controller (closed loop) will change the thruster firing duration accordingly. The eclipse condition is detected from 4PI pitch on safe mode condition. If eclipse is detected, sun acquisition is initiated on end of eclipse. The duration of eclipse is based on mission / orbit. Long pulse detection logic makes thrusters block off, if any of the thrusters is firing for more than 96 sec. The flow diagram depicting the operation sequence of safe mode detection and sun acquisition is shown in figure 5.

E. TM Interface

When in Safe mode, the satellites rejects on-board stored commands and relies on the ground for the transition back to normal mode. To support ground investigation and recovery actions, the observability is ensured through telemetry, which provides sensors acquisition data, status of essential signals of safe mode detection and sun acquisition logics.

The TM word to be sent is provided by TM interface logic. The operational sequence of this logic is represented in figure 6. The clock rate at which TM interface is done is 40Khz. With the telemetry mode pulse, status of signals is latched into an 8 bit register and is serially interfaced to TM subsystem.

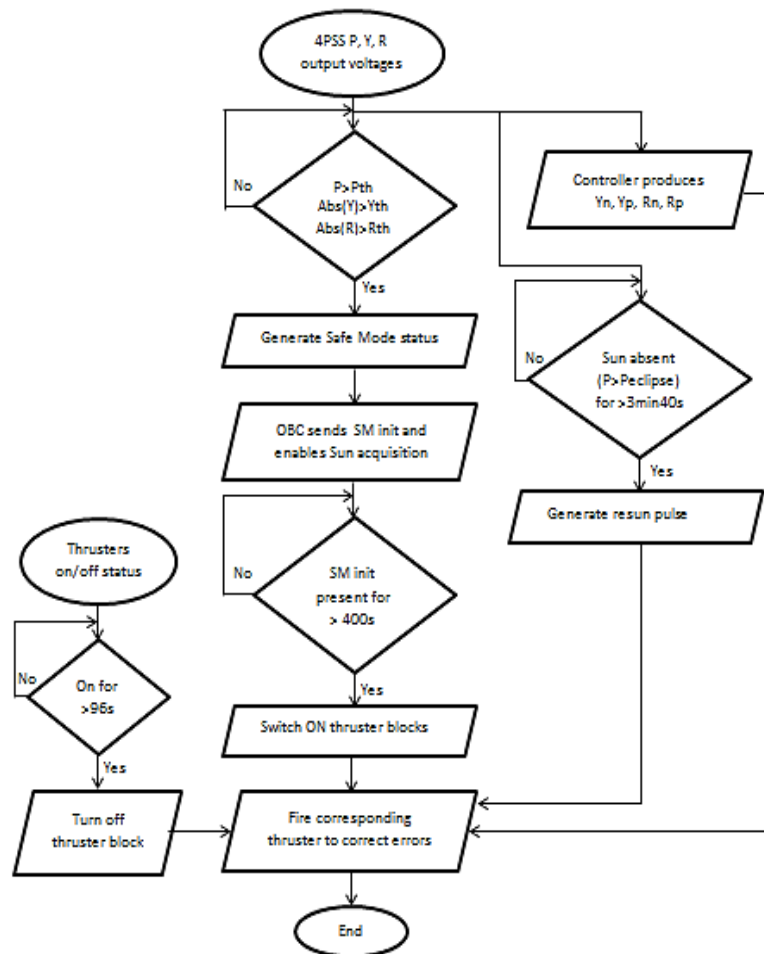


Fig 5. Flowchart depicting the operation in Safe mode detection and Sun acquisition logics

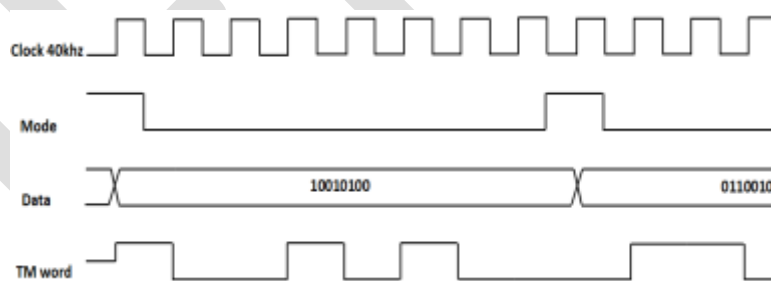


Fig 6. TM interface operational sequence

F. Testing

The design is implemented on Spartan family FPGA. Xilinx ISE design suite software tool is used for synthesis on FPGA and analysis of HDL designs. For testing purpose the outputs of 4Pi sun sensor are provided using voltage sources. These analog outputs are fed to ADC to get the digitized values before inputting to FPGA. ADC used for testing purpose is of Analog device's AD7891 family ADC. Possible range of pitch, yaw and roll voltages are fed to verify the correctness of design. The signals from OBC to be used in the design are given externally by a voltage source for testing.

SIMULATION RESULTS

The Safe mode detection and Sun acquisition logic is designed using VHDL code and is synthesized on Spartan family FPGA[7][8]. The synthesized design is simulated for different test cases. The design coded using editor in Xilinx ISE design suite is simulated

using the Xilinx ISE simulator (version 12.1). The results of the simulation are shown in the waveform.

Simulation results of Safe Mode Detection logic is shown in figure 7. For given pitch, yaw and roll voltage, as the error is present, the design detects the error and safe mode is initiated by SM Status signal transition from low to high logic. This shows that SM detection logic detects the sun absence.

Simulation results also show the loop on pulse and status generated for the test values. The results show whether the thruster blocks will be turned on or off with the BLK on signals. As one of the thruster statuses is held high for more than 96s for testing purpose, the BLK off pulse is generated, as seen on simulation waveform.

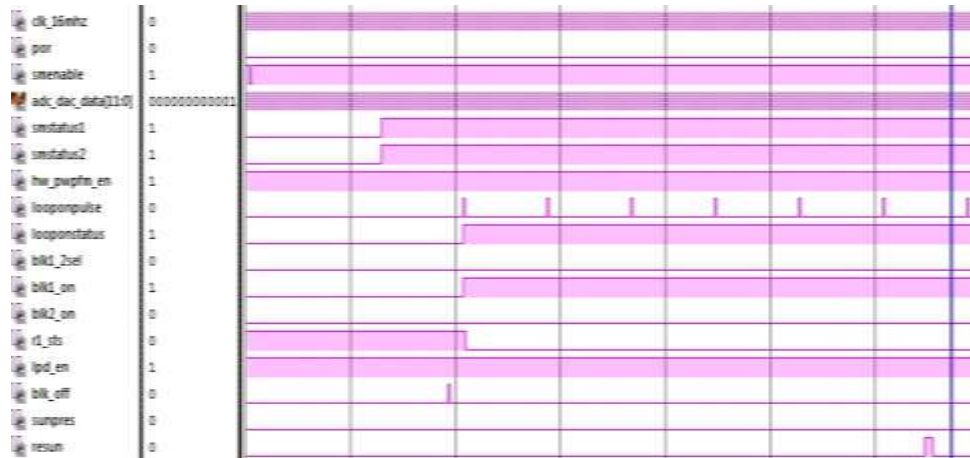


Fig 7. Simulation waveform of safe mode detection logic, loop on pulse generation, long pulse detection and eclipse detection logic

Figure 8 shows the outputs of thruster selection logic, where firing pulses are continuously given to thruster 4, based on the yp, yn, rp, rn signals. Pulse width increase and thruster 3 turning on along with thruster 4 can be seen when resun pulse is generated detecting eclipse.



Fig 8. Simulation waveform of thruster selection logic

Simulation result of TM interface logic is shown in figure 9, where the operational sequence is simulated and TM data words are serially transmitted.

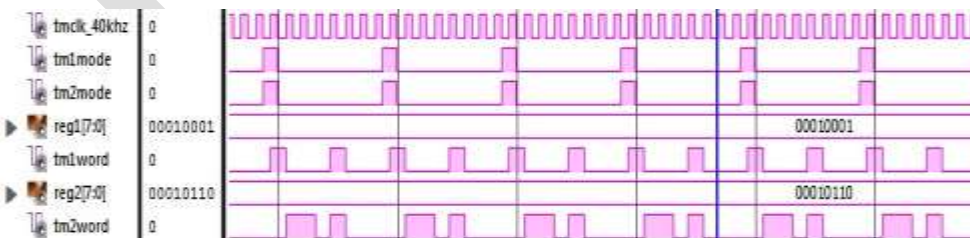


Fig 9. Simulation waveform of TM interface logic

CONCLUSION

Through this work, the architecture and function of the package consisting safe mode detection, Sun acquisition and TM interfacing, have been implemented on FPGA. Safe mode is detected based on the 4Pi sun sensor outputs, which indicates the loss of sun presence. This is followed by transition, from safe mode to sun pointing mode, carried out by sun acquisition logic which controls thrusters to orient solar arrays to point to sun. The scope of the future development is since the design is implemented using VHDL code, it is easy to add new features and design is target independent. The design can be targeted on to any family of FPGA/ASIC.

REFERENCES:

- [1] Anil K. Maini, Varsha Agrawal-“Satellite technology: Principles & applications”, John Wiley & Sons Ltd., Publication
- [2] Preliminary design review document of on board computer for CARTOSAT-2C, ISRO
- [3] Comprehensive design document on spacecraft bus management unit(hardware) of CARTOSAT-2/2A/2B, ISRO
- [4] Vinod Kumar, A.K.Kulkarni, K.Parameshwaran, R. Pandiyan and N.K.Malik, “On-Board Autonomy For ISRO Geosynchronous Spacecraft”, IAA-AAS-DyCoSS1-01-10
- [5] Yasir, M.; Grillmayer, G.; Roeser, H.-P. "Development of a safe mode attitude control for a FPGA based micro satellite", Multitopic Conference, 2008. INMIC 2008. IEEE International, On page(s): 42 - 46
- [6] Marcel J. Sidi, “Spacecraft dynamics and control: a practical engineering approach”, Press Syndicate of the University of Cambridge publication
- [7] Andrew Rushton, “VHDL for Logic Synthesis”, John Wiley & Sons, Ltd. Publication, 2011
- [8] Peter J. Ashenden, “The Designer’s Guide to VHDL”, Elsevier Inc publication, 2008

A survey on image based steganography framework to enhance quality of payload object

Monika Er. Mohinder Singh
(Pursuing M. Tech, CSE) (Assistant Professor, CSE)
Maharishi Ved Vyas Engineering College, Kurukshetra University

monika66.sharma@gmail.com, +91-9034183367

Abstract— Numeric description of a two dimensional image is known as digital image. Steganography is an elderly technique of invisible communication. The past form of Steganography has been outline by the Chinese as the confidential message was written in very fine paper, and then rolled it into a ball and covered with wax. The communicator would either devour the ball or hide it in his parts. The method used to retain the contents of a message secret is known as steganography. Cryptography is necessary for secure communications. Encryption makes the communication unsure by scrambling the data. Other third party can see the two parties communicating in confidential and can certainly make some procedure to unscramble the code. In this paper we improve the quality of image by using 12 bits instead of 8 bits.

Keywords— Least significant bit, Joint photographic experts group, Peak signal to noise ratio, moving pictures expert group, bitmap, graphic interchange format, human vision system.

Introduction

The vital progress took place in the field of information technology has create many issues related to data security. The application areas which circulate around data security are: confidentiality of business transactions, payments in personal communication and password protection. Cryptography is necessary for secure communications. Encryption makes the communication unsure by scrambling the data. Other third party can see the two parties communicating in confidential and can certainly make some procedure to unscramble the code. The method used to retain the contents of a message secret is known as steganography. The aim of steganography is to keep the actuality of a message secret. Steganography is concealed writing and is the method of hiding secret data within a cover media such that it doesn't draw the attention of an unauthorized person. The hidden secret information can be removed by recovering algorithm. Procedure of the digital file apperence can be used for steganography. Image steganography is concealed communication technique that uses an image as the cover to conceal the truth from potential attackers. The image is first transformed in transformed domain based steganography and in the image then the message is insert. MPEG or JPEG is used as common image compression format in DCT, wherein, the LSBs of the DCT coefficients of the cover image are replaced by the MSBs of the payload in transfer domain . Internet has lead the way to sharing of information earthly. When problem of ownership is introduced the people can simply copy information and its their. Thus there elevate the need for the technique which can provide defence against detection and removal. Using watermarking we can be provided defence against removal. Steganography and watermarking conduct a diversity of techniques to hide urgent information in an invisible and procedure in audio and video data. Invisible mark placed is an a watermark on an image that can be recognize when the image is contrast with the original. Steganaography is the medium for secret communication. The "Steganography" acquires by Greek .Not visible communication middle two parties is the method of steganography and it is across from cryptography. Its main idea is to hide the content of a message. Steganography uses a media like a images, video, audio or text file to confidential information in it in such a method that it doesn't attract any attention and looks like an innocent medium. images are the most accepted cover files used for steganography. Many different image file formats exist in image steganography. Different steganographic algorithms are there for different image file format. There are two category of compression: Lossy and Lossless. These two methods save storage space, but the process are dissimilar. Smaller files are created by Lossy compression by disposing excess image data from the original image. It deletes feature there are two small for the human eye to discriminate. Close approximations of the original image are made as a result, but not an precise duplicate. This compression technique JPEG is an example of image format whereas Lossless method conceal messages in incredible section of the cover image, that is long-lasting(robust). For image steganography lossless image formats are most suitable. Image steganography uses image as the cover files to conceal the confidential data. Images are most widely used cover files as they contented many redundancy. redundancy data can be expressed as the bits of an object that provide accuracy more greater than

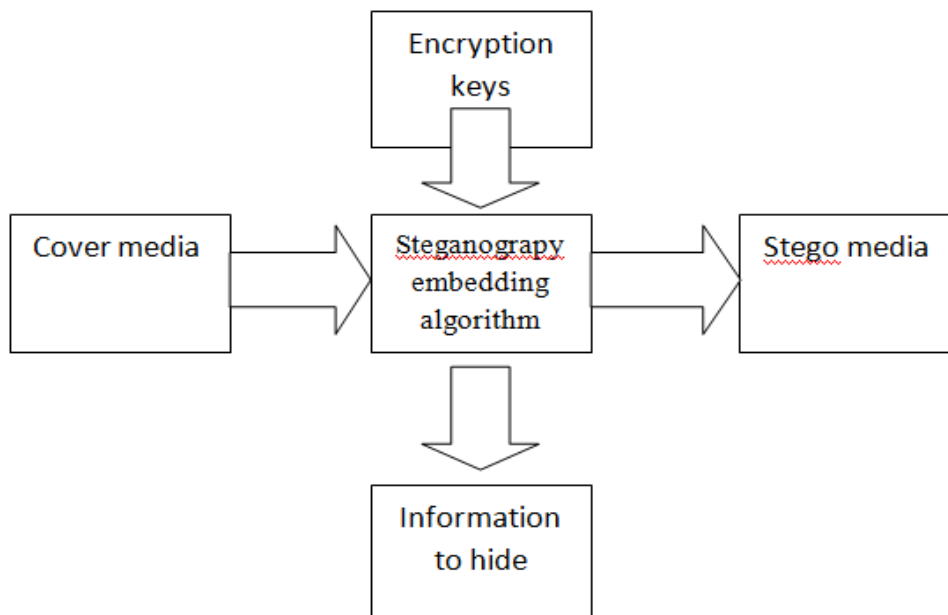
mandatory for the objects use and display. The redundant bits of an object are those bits that can be modify without the variations reality recognized clearly.

Evolution of Steganography

Steganography is an elderly technique of invisible communication. The past form of Steganography has been outline by the Chinese as the confidential message was written in very fine paper, and then rolled it into a ball and covered with wax. The communicator would either devour the ball or hide it in his parts. Herodotus “the father of history” has disclosed in one of his seminal works of history, about the heritage of confidential writing. He has disclosed about the conflicts between Greece and Persia. A king “Histiaeus” stimulate the Aristagoras of Miletus to rebel against the Persian king. He used to shave the head of his most believable servants and tattooed the scalps with confidential message and waited for the hair to get taller. The servants could proceed between the borders directly. At the reception end his head would be shaved again and the message will be transport. During the World War II, the Germans originate the use of microdots. For image steganography there are many methods and techniques. We can use any of them according to our necessity. Least significant bit insertion technique is most frequently used method to confidential the data in images and audio files. In spite of all still there is need of enhancement in steganographic systems. Because we have also robust steganalysis algorithms which reclaims the confidential messages very easily.

steganography over [cryptography](#) comfort is that the knowing confidential message does not attract observations to itself as an object of inspection. Plainly observable encrypted messages—no matter how resistant—arouse interest, and may in themselves be compromise in countries where enoding is unlawful. Thus, whereas cryptography is the implementation of safeguard the contents of a message alone, steganography is disturbed with concealing the fact that a confidential message is being sent, as well as hide the contents of the message.

Steganography comprise the beating of information inside computer files. Electronic communications may incorporate steganographic coding interior of a transport layer, namely a document file, image file, program or protocol in digital steganography. Media files are perfect for steganographic transmission because of their large area. For example, a sender might start with an harmless image file and adjust the color of every 100th [pixel](#) to correlate to a letter in the alphabet, a change so narrow that someone not specifically looking for it is unexpected to attention it.



Symmetric key algorithm and public key algorithm are systemize as cryptographic algorithms . The same key for encryption and decoding utilize by symmetric key algorithm, and in other case public key algorithm uses dissimilar keys for encryption and decryption. Steganography system can be executed using two techniques. Firstly, the spatial domain based steganography, where the LSB of the cover object is substitute by the secret message bits and the second is the transform domain based steganography; in this

case, the confidential message is embedded with the coefficient of the cover object. The most familiar transform domains are discrete Fourier transform and discrete wavelet transform. To enhance the reliability of the transmission system; cryptography and steganography can be integrate to implement a long-lasting and assured system; in this case, the encryption and hiding are attain in the transmitter, while the removal and decryption are attain in the receiver. There are some concerned that should be addressed in the intriguing of a steganography system:

a) *Invisibility*: In this invisibility the stego image should not be observed by human.

b) *Security*: The steganography process should provide elevated level of safety, therefore, the stego image should be very adjacent to the actual cover image, and the striker could not recognize the concealed information. PSNR is recruit to evaluate the difference between the cover image and the stego image.

Challenges

The prime provocation of steganography are:

- 1) Security of concealed Communication: The concealed contents must be unseeable both perceptually and statistically so as to avoid the suspicions of eavesdroppers.
- 2) area of Payload: Steganography requires abundant embedding capacity. Necessity for higher payload and secure communication are often conflicting.

Techniques

Physical

Steganography has been generally used, including in recent former times and the present day. Some examples are:

- concealed messages within wax tablet—in past Greece, people wrote messages on wood and covered it with wax that drill an innocent covering message.
- concealed messages on messenger's body—also used in past Greece. Herodotus notify the story of a message tattooed on the shaved head of a slave of Histiaeus, concealed by the hair that eventually grew over it, and reveal by shaving the head. The message reputedly carried a warning to Greece about Persian appropriation plans. This method has obvious disadvantage, such as delayed transmission while waiting for the slave's hair to grow, and reductions on the number and area of messages that can be encoded on one person's scalp.

Digital messages

Modern steganography invade the world in 1985 with the arrival of personal computers being applied to plain steganography problems. Development backing that was very slowgoing, but has since taken off, going by the vast number of steganography software accessible:

- Direct messages within the little bits of rowdy images or sound files.
- Direct data inside encrypted data or within unplanned data. The message to dissemble is encrypted, then used to overwrite part of a much huge block of encrypted data or a block of unplanned
- Scrape and separate.
- Mock functions transform one file to have the statistical profile of another.

Digital text

- Production text the same color as the framework in word processor charter, e-mails, and seminar posts.
- Using Unicode characters that look like the standard ASCII character set. On many systems, there is no optical difference from typical text. Some structure may exhibit the fonts differently, and the additional statistics would then be simply brindle.

- Using invisible characters, and unnecessary use of markup (e.g., empty bold, underline or italics) to implant information within hyper text markup language, which is observable by inspect the document origin.

Need of Image Compression

The alter from the cine film to digital techniques of image interchange and archival is essentially stimulated by the facility and plasticity of lifting digital image information alternative of the film media. While constructing this step and expanding standards for digital image communication, one has to make perfectly sure that also the image standard of coronary angiograms and ventriculograms is retained or upgraded. Similar essential exist also in echocardiography. Regarding image standard, the most disparaging step in going from the analog to the digital is the digitization of the signals. For this stride, the basic essential of keeping image standard is easily converted into two basic quantitative parameters:

- the rate of digital image data convey or **data rate** (Megabit per second or Mb/s)
- and the whole volume of digital storage need or **data capacity** (Megabyte or MByte).

LITERATURE REVIEW

Mridul Kumar Mathur.et.al(2012) A picture's value more than thousand words "is a common saying. What a image can interface can not be along via words. Images play an essential role in representing crucial information and needs to be saved for further use or can be transferred over a way. In order to have well organized utilization of disk space and transmission rate, images need to be flate standard. Image flatten is the technique of diminish the file size of a image without compromising with the image at a satisfactory level. This reduction in file size saves disk/memory space and allows faster transference of images over a way. Image compression is been used from a long time and many algorithms have been devised. In this paper the author have converted an image into an array using Delphi image control tool. Image control can be used to show a graphical image - Icon (ICO), BMP, Metafile (WMF), GIF, JPEG, etc, then an algorithm is produced in Delphi to instrument Huffman coding method that removes redundant codes from the image and flatten a BMP Resemblance file and it is successfully recreated. This recreated image is an exact presentation of the original because it is lossless compression method. This Program can also be appeal on other somewhat of RGB resemblance(BMP, JPEF, Gif, and tiff) but it dispense some color quality loss after recreated .Compression ratio for grayscale image is superior as compared to other standard methods.

Gowtham Dhanarasi .et.al(2012) A block convolution investigation for alter domain image stegonagraphy is confirmed in this paper. The algorithm advanced here works on the wavelet transform coefficients which embedded the confidential data into the original image. The technique executed which are capable of constructing a confidential-embedded image that is alike from the original image to human eye. This can be attained by keeping integrity of the wavelet coefficients at high capacity embedding. This refinement to capacity-quality trading –off interrelation is examined in detailed and experimentally illustrated in the paper.

Inderjeet Kaur.et.al(2013) Confidential communication and copyright defence are the two principal matter of modern communication system. The research done so far shows a variation of techniques to communicate confidentially. The technique executed in this paper is a merger of steganography and watermarking which produced copyright protection to the information being transmitted confidentiality. The proposed aptness is a transform domain based system with the intervention of segmentation and watermarking (TDSSW). It is discovered that the advanced technique comes up with good PSNR (Peak Signal to Noise Ratio) and enhanced confidentiality.

Sneha Arora.et.al(2013) This paper advanced a new technique for image steganography that are utilizing edge detection for RGB images. There are lots of algorithms to confidential data with exactness level but they are also reducing the quality of the image. In this advanced study, edges of an RGB image will be observed by scanning method that are utilizing 3x3 window, and then text will be inserted in to the edges of the color image. Not only high inserting volume will be attained but also the quality of the stego image also magnifies from the HVS.

Pallavi Hemant Dixit.et.al(2013) Network security and protection of data have been of significant treat and a subject of investigation over the years. There are many different configuration of steganography mechanisms like LSB, filtering and masking and Transform techniques. All of them have particular strong and weak points. The Least Significant Bit (LSB) embedding Technique recommends that data can be confidential in the least significant bits of the cover image and the human eye would be ineffective to perception the confidential image in the cover file. This technique can be used for beating images in 24-Bit, 8-Bit, Gray scale format. This paper narrate the LSB inserting technique and Presents the estimation for different file Formats. In a network, the victory of the algorithm depends on beating technique used to reserve information into the image. This paper is formed on the learning of steganography with its LSB algorithm. Human biometrics like fingerprint, iris, and face are the individual things for human. That's why the author advance a individual authentication and encryption ability using IRIS biometric motif of a person. Text message encrypted by cryptographic key which is produced by iris image. Then operate LSB algorithm this encrypted text message conceal into the iris image. LSB algorithm is executed in ARM7 LPC2148.

Saleh Saraireh.et.al(2013) The information safety has become one of the most remarkable problems in data communication. So it becomes an inextricable part of data communication. In order to address this issue, cryptography and steganography can be integrate. This paper advances a fixed communication system. It recruits cryptographic algorithm together with steganography. The carve of these techniques dispense a long-lasting and strong communication order that expert to confront against strikesrs. In paper, the filter bank cipher is used to encrypt the confidential text message, it provide high level of certainty, scalability and pace and then a discrete wavelet transforms (DWT) based steganography is recruited to conceal the encrypted message in the cover image by altering the wavelet coefficients. The presentation of the advanced system is assessed using PSNR and histogram survey. The simulation results show that, the advanced system produce high level of certainty.

Rahna E.et.al(2013) Steganography is a process of dispatch dissemble transmission in such a method that no one, apart from the sender and intentional recipient, thinks the existant of the message. There prevail many techniques for digital image steganography. But most of the existing methods are based on lossy approach and the vital provocation of steganography are certainty of concealed transmission and in an image sector of message can be embedded. So, this paper is intentional to advance an image steganography technique based on contest between cover image and confidential data. This advanced method retained the cover image as such and has limitless volume of payload.

H.B.Kekre.et.al(2014) A number of techniques are attainable in literature to provide pledge to digital images, these potential give their terminal to Information beating, Image Scrambling and Image Encryption. In paper the author have advanced a hybrid Approach to confidential digital images. The advanced framework is a merger of Information Hiding and Image Encryption. In Information beating there are four different techniques of many LSB's Algorithm are used and assessed. A number of parameters are also used to assess the advanced framework. Experimental results show a good performance.

S.Shanmugasundaram.et.al(2014) Steganography is the art of beating the existing of data in another transference medium i.e. image, audio, video files to attain confidential communication. It does not substitute cryptography but rather raise the certainty using its unimportance features. Cryptography and Steganography are advanced methods. The exclusive communication is first encrypted using RSA and then using OAEP randomized. This encoded message is then implant in the bitmap cover image using frequency domain approach. For inserting the encrypted message, originally skin tone regions of the cover image are observed using HSV (Hue, Saturation, Value) model. afterwards, a section from skin observed area is choosed, which is known as the cropped region. In this cropped region confidential message is inserting using DD-DWT (stands for Double Density Discrete Wavelet Transform). DD-DWT defeat the interlace imperfections of DWT. Hence the image acquired after inserting confidential message (i.e. Stego image) is far more fixed and has an satisfactory range of PSNR. The expression of PSNR and robustness against different sounds (like Poisson, Gaussian, salt and pepper, rotation, translation etc.).

Mazhar Tayel.et.al(2014) Data certainty has become an main issue in the communication systems. Steganography is used to conceal extent of a confidential message. In this thing a altered Steganography algorithm will be advanced depending on decay principle of both confidential message and cover-image. A fuzzification is advanced in the confidential message to optimize the decay coefficients before inserting in the cover image to acquire a Stego Image. The conventional metrics (Cor., MSE, PSNR, and Entropy) were used to assess the altered algorithm. Also, a trade-off factor was established to regulate an optimum value for the inserting strength factor to get an reasonable degradation. Moreover to evaluate the modified algorithm and any other Steganography algorithms, a new histogram metrics are advanced which represents the relative frequency incident of the different images.

CONCLUSION OF SURVEY

In the following Table, carry all the steganography methods that are described formerly

METHOD	AUTHOR AND YEAR	FEATURES
Transform domain image steganography	Gowtham Dhanarasi (2012)	The technique which are capable of producing a secret-embedded image are executed that is alike from the native image to human eye.
Merger Of Steganography and Water Marking	Inderjeet Kaur (2013)	The technique advanced in this paper is a merger of steganography and watermarking which produced copyright conservation to the statistics being transfered confidentially.
Edge Detection For RGB Images	Sneha Arora (2013)	Boundary of an RGB image will be observed by scanning method using 3x3 window, and then text will be inserted in to the boundary of the color image.
Reliable Communication System	Saleh Saraireh (2013)	It recruits cryptographic algorithm jointly with steganography. The carve of these methods produced a long-lasting and strong communication system that expert to resist against strikers. In this paper, the filter bank cipher is used to encrypt the confidential text message, it produced high level of certainty, scalability and speed.

CONCLUSION

In this paper we are study the digital image and its application, steganography and its techniques. In this a message is hide by the use of digital image. The technique which are capable of producing a secret-embedded image are executed that is alike from the native image to human eye. In this paper we are study the merger of steganography and watermarking which produced copyright conservation to the statistics being transfered confidentially. It recruits cryptographic algorithm jointly with steganography. The carve of these methods produced a long-lasting and strong communication system that expert to resist against strikers. In this paper, the filter

bank cipher is used to encrypt the confidential text message, it produced high level of certainty, scalability and speed. We can use these techniques for security of the message.

REFERENCES:

1. ventriculograms H.B.Kekre, Tanuja Sarode and Pallavi Halarnkar “A Hybrid Approach for Information Hiding and Encryption using Multiple LSB’s Algorithms” International Journal of Application or Innovation in Engineering & Management (IJAIEM) Volume 3, Issue 6, June 2014 ISSN 2319 – 4847.
- 2.Mridul Kumar Mathur, Seema Loonker, Dr. Dheeraj Saxena “ LOSSLESS HUFFMAN CODING TECHNIQUE FOR IMAGE COMPRESSION AND RECONSTRUCTION USING BINARY TREES” IJCTA | JAN-FEB 2012 ISSN:2229-6093.
3. Gowtham Dhanarasi,,Dr.A. Mallikarjuna Prasad “IMAGE STEGANOGRAPHY USING BLOCK COMPLEXITY ANALYSIS” International Journal of Engineering Science and Technology (IJEST).
4. Inderjeet Kaur, Rohini Sharma, Deepak Sharma” TRANSFORM DOMAIN BASED STEGANOGRAPHY USING SEGMENTATION AND WATERMARKING” ISSN (Online) : 2229-6166 Volume 4 Issue 1 January 2013.
5. Sneha Arora, Sanyam Anand” A New Approach for Image Steganography using Edge Detection Method” International Journal of Innovative Research in Computer and Communication Engineering Vol. 1, Issue 3, May 2013.
6. Pallavi Hemant Dixit, Uttam L. Bombale “Arm Implementation of LSB Algorithm of Steganography” International Journal of Engineering and Advanced Technology (IJEAT) ISSN: 2249 – 8958, Volume-2, Issue-3, February 2013.
7. Rahna E. and V. K. Govindan” A Novel Technique for Secure, Lossless Steganography with Unlimited Payload” International Journal of Future Computer and Communication, Vol. 2, No. 6, December 2013.
- 8.Saleh Saraireh “A SECURE DATA COMMUNICATION SYSTEM USING CRYPTOGRAPHY AND STEGANOGRAPHY” International Journal of Computer Networks & Communications (IJCNC) Vol.5, No.3, May 2013
- 9.S.Shanmugasundaram “ A Highly Secure Skin Tone Based Optimal ParityAssignment Steganographic Scheme Using DoubleDensity Discrete Wavelet Transform” International Journal of Scientific and Research Publications, Volume 4, Issue 3, March 2014 1 ISSN 2250-3153
10. Mazhar Tayel, Hamed Shawky “A Proposed Assessment Metrics for Image Steganography” International Journal on Cryptography and Information Security (IJCIS), Vol. 4, No. 1, March 2014

An Unmanned Ground Vehicle-aided Task Exchange System Of Small Air Vehicles For Remote Surveillance Missions

Serkan ÇAŞKA¹, Ahmet GAYRETLİ²

¹ Mechatronic Engineering Department, Afyon Kocatepe University, serkancaska@aku.edu.tr

² Mechatronic Engineering Department, Afyon Kocatepe University, agayretli@aku.edu.tr

Abstract— Small/portable unmanned air vehicles which supply their energy from electric batteries have been successfully used in applications of intelligence, surveillance and reconnaissance-based missions gradually. Despite their increasing usage, studies which focus on S-UAVs limited battery capacities has not been completely dealt in the literature. This obstructs the usage of small unmanned air vehicles in long range and unremitting mission scenarios. In addition, small unmanned air vehicles have been supported with unmanned ground vehicles to carry out surveillance-based missions efficiently in recent researches. However, studies including collaborative teams with unmanned air and ground vehicle are limited in literature. In this paper, a surveillance system that is based on collaboration of two small unmanned air vehicles and a transporter unmanned ground vehicle was proposed. In order to provide the continuity of surveillance mission, an assigning and directing algorithm that considers battery charge level of the small unmanned air vehicles was developed within the proposed system. Developed algorithm assigns tasks to unmanned air vehicles and changes their role in surveillance mission by checking their battery levels. The proposed system was examined with tests in simulation and outdoor environment in a specified range and unmanned air vehicles completed surveillance mission by making a successful task exchange during their mission.

Keywords— Unmanned Ground vehicle, Unmanned Air vehicle, Multi Robot Collaboration, Missions Of Intelligence Surveillance And Reconnaissance, Battery Limitations Of Small Unmanned Air Vehicle, Proportional Navigation, PID Controller

INTRODUCTION

Small unmanned air vehicles (S-UAV) have become one of the most preferred air platform for intelligence, surveillance and reconnaissance (ISR)-based missions in recent years. A small UAV is an unmanned air platform that is enough to be transportable. S-UAV-based unmanned systems have been used for information gathering in various applications that are carried out in border security, environment mapping and so on [1], [2]. ISR can be defined as information gathering from something or somewhere for human operators [3]. By using multiple S-UAVs, the time that is spent to carry out ISR-based missions can be minimized [4]. S-UAVs have been successfully used in applications of ISR-based missions gradually. [5] proposed a prototype of an autonomous helicopter that offers a cheap platform for ISR based missions. [6] presented a study of multiple S-UAVs performed for an ISR-based task that aims to guarantee to visit all the parts of a the target area continuously. In addition to increasing S-UAV usage, recently, there have been various research that were carried out by combining S-UAVs and unmanned ground vehicles (UGV) to perform ISR-based missions. [7] presented an advanced framework of crowd control that is carried out with S-UAVs and UGVs. [8] proposed a communication and control method for ISR-based missions including UGVs and S-UAVs. [9] proposed a system that is carried out with the collaboration of UGV and S-UAV. Proposed system performs the mission of periodical surveillance in an indoor test area. [10] presented two cooperation methods between a S-UAV and UGV. Developed two methods proposed practical advices to coordinate S-UAVs and UGVs on an outdoor test environment where a chemical substance spread is simulated within an exercise of train accident scenario. [11] introduced a visual based method that will be used in coordination of a S-UAV and an UGV to perform an ISR-based mission. S-UAV tracks and also carry out auto-landing on a moving UGV. [12] presented an experimental collaborative study including a S-UAV and UGVs. The experiment demonstrated that detection of pedestrians and vehicles is possible by using an autonomous unmanned vehicle based system under real dynamic environment conditions. [13] presented an ISR-based system of UGVs and S-UAVs that is developed to detect the location of the victims of a possible earthquake. [14] introduced a method for multi-target tracking by using S-UAVs. The proposed method tries to eliminate tracking interruptions because of obstacles and other S-UAVs in test area. Figure 1 shows data that was obtained from web of science database and demonstrates number of the studies including UAVs (TS1), UGVs (TS2) and cooperation between UAVs and UGVs (TS3). It is clear that the number of studies including only UAVs and UGVs have showed a big increase in recent years. However number of studies including cooperation of UAVs and UGVs has remained limited [15].

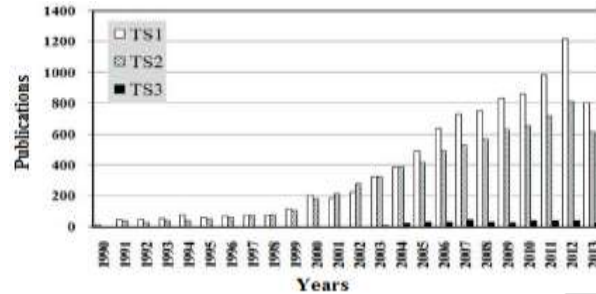


Figure 1: Web of Science data that shows the number of publications including unmanned vehicles in recent years [15]

In literature, despite various studies focused on ISR-based missions with teams including S-UAVs and UGVs, few of them consider battery limitations of S-UAVs and persistence of the mission. Furthermore, carrying the S-UAVs to mission areas by using unmanned ground vehicles is still a new study field for researchers. Unlike the many of the studies in related literature, the proposed system takes into account the energy limitations of batteries replaced on S-UAVs. Required energy for S-UAVs is generally provided from batteries that has Li-Po (lithium polymer) structure. S-UAVs can fly and communicate several minutes via consuming their Li-Po batteries. When an S-UAV consumes its battery charge in an ISR-based mission, in order to continue its fly, a new battery with complete charge must be provided. However, recharge or swapping operation of a S-UAV batteries need several minutes. Therefore, an auxiliary S-UAV must be ready to assist the other one in target mission area. For this reason, the presented system in this paper was developed to carry out ISR-based missions by using two S-UAVs that were assigned to help each other.

By using our proposed system, an efficient surveillance can be performed in mission areas with insecure conditions for a human. Besides, our proposed system will give a new perspective to ISR-based unmanned system developers to design more effective systems for the scenarios that require long time. The developed system can be implemented in mission areas as a quick and a low budget surveillance method. Our proposed system is suitable to implement in surveillance of power production centers, surroundings of military zones, and so on. S-UAV cooperation method of our proposed system can be used not only with unmanned ground systems but also with manned ground vehicles. However, in order to demonstrate the collaboration capacity of the proposed system, S-UAVs were used in cooperation with an unmanned ground vehicle. In this work, the authors focused on the cooperation of unmanned air and ground vehicles while air vehicles are carrying out a continuous ISR-based mission. However, in literature, various studies were executed on automatic swap and recharge systems for batteries of S-UAVs [16], [17]. It shows that a battery recharge or a battery swapping system can be used to provide the continuity of our proposed system. Design and implementation of a battery swapping mechanism to our proposed system was decided to realize in future project.

S-UAVs that can take off and land vertically do not need a runway and this makes them one of the most preferred air platforms for ISR-based missions. In our study, unmanned air platforms were designed as quad-copters and unmanned ground platform was designed as a differential drive robot. Ground robot was developed as a transporter vehicle for two quad-copters where a take-off and landing platform was placed on it.

THE PROPOSED SYSTEM

The proposed system consists of two quad-copter S-UAVs, a transporter UGV, a central computer, S-UAV assigning/directing algorithm that run in central computer, a human operator who watches data of unmanned vehicles and also sends his commands to the vehicles. General structure of the proposed system is as shown in Figure 2.



Figure 2: General structure of the proposed system

The proposed system was composed in both simulation and real environment and also was implemented within a sample application. This application is implemented through exchanging the tasks of two S-UAVs. An UAD (UAV assigning and directing) algorithm developed and run on Matlab software guides S-UAVs during their mission. In sample application, one of the S-UAV (assigned S-UAV) was directed manually by a human operator. When battery charge of the assigned S-UAV exceeded a pre-defined level, the auxiliary S-UAV was sent to take on the task from the assigned S-UAV. Sample application demonstrated that the proposed system is proper for the applications which the S-UAVs are directed manually. Since controlling a S-UAV can include unpredictable and dynamic movements of S-UAVs, our proposed system can be used within the dynamic applications such as target tracking, formation flight and so forth.

According to the sample application of the proposed system, after stopping the transporter UGV on a proper mission point in a mission area, one of the S-UAV takes off and is directed with manual commands of a human operator. If battery level of the assigned S-UAV exceeds a pre-defined TEDL (task exchange demand level) during its movement, the UAD algorithm directs the auxiliary S-UAV to a location that was specified by considering current position of the assigned S-UAV. In order to not to cause a collision of S-UAVs, the UAD algorithm indicates the target position of auxiliary S-UAV as the position that is three meters far to current position of the assigned S-UAV in z axis. Furthermore, two meters error margin was specified for the target position of the auxiliary S-UAV. Therefore, the UAD algorithm assumes that the auxiliary S-UAV reached its target point when it becomes closer than two meters to the target point. The assigned S-UAV is sent onto the transporter UGV when the auxiliary S-UAV arrives the target coordinates. In addition, the assigned S-UAV's battery level exceeds a specified ERL (emergency return level) before the auxiliary S-UAV arrives the target position, the assigned S-UAV urgently returns to the transporter UGV without regarding the current position of the auxiliary S-UAV.

The position of the assigned S-UAV (tracked or target S-UAV) is defined as $U_T \in \mathbb{R}^3$. The auxiliary S-UAV's position is defined as $U \in \mathbb{R}^3$. The position error between the auxiliary S-UAV with respect to and the target position can be defined as in Equation (1).

$$Ue = \sqrt{(U_Tx - Ux)^2 + (U_Ty - Uy)^2} \quad (1)$$

If PID method is used in tracking of the assigned S-UAV, it will try to decrease the error between the auxiliary S-UAV's position and the target. However, in this study, our aim is to make the auxiliary S-UAV catch the assigned S-UAV as quickly as possible. Tracking a moving target with PID method is not the best approach for our purpose. Thus, a PN (proportional navigation) strategy that was inspired from Realistic True Proportional Navigation (RTPN) method was developed. RTPN method is proper for the quad-copter's lateral navigation and our RTPN-based method was developed for the guidance of the auxiliary S-UAV [18]. In developed PN strategy, the additional distances for meeting (adm) were specified for x and y directions to guarantee the intersection of S-UAVs. In Equation (2) and Equation (3), adm values were defined respectively in x and y directions.

$$x^{adm} = (U_Tx - U_Tx)\lambda \quad (2)$$

$$y^{adm} = (U_Ty - U_Ty)\lambda \quad (3)$$

In Equation (2) and Equation (3), adm values of x and y directions are calculated by multiplying λ that is the navigation coefficient and the absolute value of the position difference between the auxiliary S-UAV and the assigned S-UAV.

In order to guarantee the intersection of S-UAVs, estimated meeting positions were defined. In Equation (4) and Equation (5), estimated meeting positions of S-UAVs were calculated by adding adm values to current position of the assigned S-UAV.

$$U_T^{emp}x = U_Tx + x^{adm} \quad (4)$$

$$U_T^{emp}y = U_Ty + y^{adm} \quad (5)$$

Parameters of adm and emp that were calculated within PN method are shown in Figure 3.



Figure 3: PN method for tracking of the assigned S-UAV

The auxiliary S-UAV tries to reduce the difference between its altitude and altitude of the assigned S-UAV and also tries to equalize its yaw angle to yaw angle of the assigned S-UAV. In proposed system, tracking of the auxiliary S-UAV's altitude and yaw angle were performed by using traditional PID method.

In sample application, a parameter of mr (mission range) that represents the furthest reachable distance for S-UAVs was defined. The value of mr should be defined by the human operator by taking account S-UAV battery capacities. The worst situation for the assigned S-UAV is to exceed a specified IRL when it is on the furthest point from the transporter UGV. Therefore, in order to guarantee return of S-UAVs to transporter UGV safely, mr should be regarded in calculation of ERL. The auxiliary S-UAV tries to equalize its yaw angle to yaw angle of the assigned S-UAV while it is reaching *sepat* (start/end point for attitude tracking). The auxiliary S-UAV turns into the new assigned S-UAV when it arrives the target point and the old assigned S-UAV turns into the transporter UGV by visiting *sepat*. During the tracking process, the assigned S-UAV might exhibit quick and varying movement, therefore the time will pass for meeting of S-UAVs can not be predicted exactly. Thus, TEDL also can not be defined exactly and was regarded as twice ERL. During the assigned S-UAV tracking process of the auxiliary S-UAV, if the charge level of the returning assigned S-UAV's battery exceeds ERL, the UAD algorithm urgently directs the assigned S-UAV onto the transporter UGV. In this situation, when charge level of the assigned S-UAV exceeds ERL, the UAD algorithm registers the latest recorded coordinates of the returning assigned S-UAV and takes into account it as the target position for the auxiliary S-UAV. When the charge level of the assigned S-UAV's battery exceeds TEDL, at first the UAD algorithm directs the auxiliary S-UAV to the *sepat* and then directs it to the current position of the assigned S-UAV. Similarly, the assigned S-UAV visits *sepat* before it is directed to land on the transporter UGV. If the altitude of *sepat* is high to neglect, it must be taken into account in calculation of TEDL. TEDL and ERL are expressed as in Equation (6) and Equation (7) respectively.

$$TEDL = (mr + \text{altitude of sepat}) * 2 * cf \quad (6)$$

$$ERL = (mr + \text{altitude of sepat}) * cf \quad (7)$$

In sample application, after the assigned S-UAV lands on the transporter UGV, it becomes the new auxiliary S-UAV.

In literature, studies that were executed on consumption of electrical batteries include approximate models and there is not a common consumption formulation for batteries of S-UAVs [19]. Therefore, power consumption of S-UAVs was generated with experiments that were carried out in real flight tests. Power consumption experiments of S-UAVs were executed in windless environment. After power consumption experiments, it was detected that a quad-copter S-UAV consumes 0.093% of its battery charge, while it is passing each meter during its vertical and horizontal movements. This detected consumption value was considered as consumption factor (cf) in this study. This means that a quad-copter S-UAV used in our system can move 1080 meters approximately in each direction with a completely charged battery (2200 mAh battery with lithium polymer structure). The consumption factor might be changed by human operator depending on the loads of S-UAVS and the weather conditions. In our study, a simple approach was used in define power consumption and TEDL and ERL of S-UAVs. However, detailed consumption approaches with various parameters might be used within the proposed system.

DYNAMIC MODELS OF UNMANNED VEHICLES

Dynamic models of quad-copter S-UAVs and UGV were obtained to simulate the proposed system. Then the vehicle models were formed in Matlab-Simulink. Finally, sample application that was carried out with the proposed system was visualized by using 3D VRML builder software that can connect to Simulink models of the quad-copter S-UAVs and UGV.

In this study, quad-copter was used as S-UAV. As illustrated in Figure 4, quad-copter is an air vehicle with four rotors. By changing angular velocities of rotors, movements of throttle, roll, pitch and yaw are obtained [20].

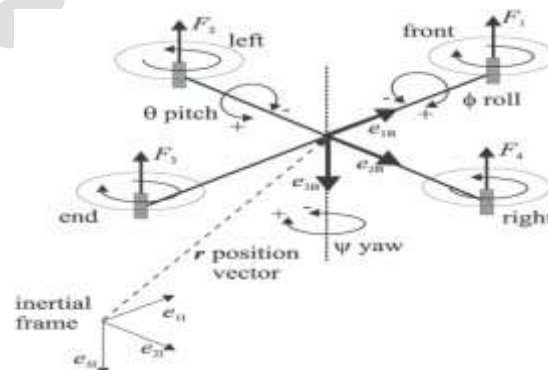


Figure 4: Configuration and structure of a quad-copter [20]

In order to derive the quad-copter's dynamic model, the inertial frame must be considered as showed in Figure 4. The vector of $\Omega^T = (\phi, \theta, \psi)$ that represents the quad-copter's orientation is obtained by using Euler angles which are ϕ (roll angle), θ (pitch angle) and ψ (yaw angle). $r^T = (x, y, z)$ is the vector that represents the position of quad-copter in the inertial frame. R that was given in Equation (8) is the rotation matrix that provides the transformation of the vectors from the body frame of the quad-copter to inertial frame. In representation of R , for instance, $c\phi$ indicates $\cos\phi$ and $s\theta$ indicates $\sin\theta$ [21].

$$R = \begin{pmatrix} c\psi c\theta & c\psi s\theta s\phi - s\psi c\phi & c\psi s\theta c\phi + s\psi s\phi \\ s\psi c\theta & s\psi s\theta s\phi + c\psi c\phi & s\psi s\theta c\phi - c\psi s\phi \\ -s\theta & c\theta s\phi & c\theta c\phi \end{pmatrix} \quad (8)$$

If we define the forces of the propellers, the thrust force is equal to $F_i = b.\omega_i^2$ and it is obtained from i^{th} ($i=1,2,3,4$) rotor. In this representation, b is the thrust factor and ω_i is i^{th} rotor's the rotational speed. The total thrust force generated by the four rotors is written as in Equation (9).

$$T = \sum_{i=1}^4 |F_i| = b \sum_{i=1}^4 \omega_i^2 \quad (9)$$

By using T , differential equations that represent the quad-copter's acceleration are written as in Equation (10).

$$\begin{pmatrix} \ddot{x} \\ \ddot{y} \\ \ddot{z} \end{pmatrix} = g \begin{pmatrix} 0 \\ 0 \\ 1 \end{pmatrix} - R \frac{T}{m} \begin{pmatrix} 0 \\ 0 \\ 1 \end{pmatrix} \quad (10)$$

Another differential equation are written as in Equation (11) by using the matrix I which is diagonal matrix including the inertias of x , y , z axis and M that represents the torque implemented to the quad-copter's body and M_G that represents the gyroscopic torques.

$$I\dot{\Omega} = -(\dot{\Omega} \times I\dot{\Omega}) - M_G - M \quad (11)$$

M can be represented as in Equation (12).

$$M = \begin{pmatrix} Lb(\omega_1^2 - \omega_3^2) \\ Lb(\omega_2^2 - \omega_4^2) \\ d(\omega_1^2 + \omega_3^2 - \omega_2^2 - \omega_4^2) \end{pmatrix} \quad (12)$$

In representation of the M , d defines the drag factor and L represents distance between the propellers and center of the quad-copter. The gyroscopic torques that are generated by rotations of the vehicle are written as in Equation (13).

$$M_G = I_R \left(\dot{\Omega} \times \begin{pmatrix} 0 \\ 0 \\ 1 \end{pmatrix} \right) (\omega_1 - \omega_2 + \omega_3 - \omega_4) \quad (13)$$

The real input variables of the quad-copter are ω_i of each rotor. However, transforming the real inputs to artificial inputs is more convenient. Artificial inputs are defined as in Equation (14) to Equation (17).

$$u_1 = (\omega_1^2 + \omega_2^2 + \omega_3^2 + \omega_4^2) \quad (14)$$

$$u_2 = (\omega_1^2 - \omega_3^2) \quad (15)$$

$$u_3 = (\omega_2^2 - \omega_4^2) \quad (16)$$

$$u_4 = (\omega_1^2 - \omega_2^2 + \omega_3^2 - \omega_4^2) \quad (17)$$

In Equation (14) to Equation (17), u_1 is the total thrust force; u_2 is the force that generates roll torque; u_3 is the force that generates pitch torque and u_4 is the force that generates yaw torque. In addition, gyroscopic torques that were given in Equation (13) depend on the rotational speeds of the rotors and also depend on the vector of the artificial inputs that is defined as $u^T = (u_1, u_2, u_3, u_4)$.

$$g(u) = \omega_1 - \omega_2 + \omega_3 - \omega_4 \quad (18)$$

Complete model of a quad-copter is obtained in Equation (19) to Equation (24) through evaluating Equation (10) and Equation (11):

$$\ddot{x} = -(\cos\psi\sin\theta\cos\phi + \sin\psi\sin\phi)\frac{u1}{m} \quad (19)$$

$$\ddot{y} = -(\cos\psi\sin\theta\sin\phi - \cos\psi\sin\phi)\frac{u1}{m} \quad (20)$$

$$\ddot{z} = g - \cos\theta\cos\phi\frac{u1}{m} \quad (21)$$

$$\ddot{\phi} = \dot{\theta}\dot{\psi}\left(\frac{I_y - I_z}{I_x}\right) - \frac{I_R}{I_x}\dot{\theta}g(u) + \frac{L}{I_x}u2 \quad (22)$$

$$\ddot{\theta} = \dot{\phi}\dot{\psi}\left(\frac{I_z - I_x}{I_y}\right) + \frac{I_R}{I_y}\dot{\phi}g(u) + \frac{L}{I_y}u3 \quad (23)$$

$$\ddot{\psi} = \dot{\theta}\dot{\phi}\left(\frac{I_x - I_y}{I_z}\right) + \frac{1}{I_z}u4 \quad (24)$$

Six controllers were used to completely control a quad-copter S-UAVs. The inner controllers of the quad-copter are Z, Phi, Theta and Psi controllers. The outer controllers are X and Y controllers. By generating pitch and roll angles for inner controllers, outer controllers provide the quad-copter's navigation to desired positions. Controllers of the quad-copter UAVs are shown in Figure 5.

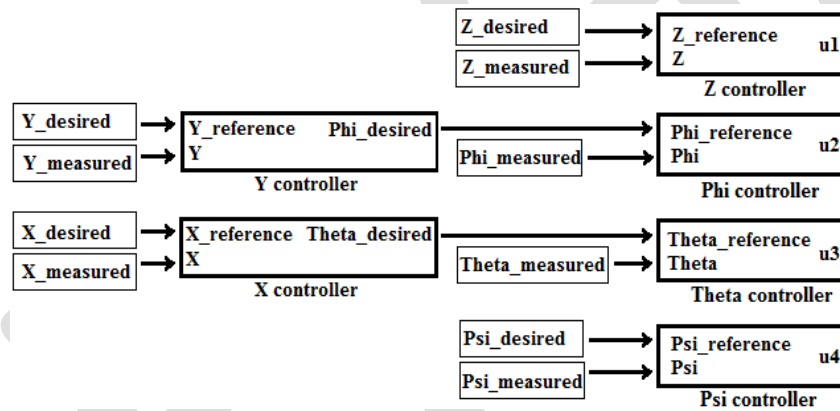


Figure 5: Controllers of the quad-copter

The controllers of the quad-copters were designed by using conventional PID (proportional integral derivative) method [22]. Parameters of controllers were defined with Hand-Tuning procedure that is based on tuning P, I and D parameters respectively and is a convenient method for tuning PID parameters of quad-copters.

In proposed system, transporter vehicle was a differential drive UGV that has two independent wheels which were controlled by using electrical motors. As can be seen in Figure 6, a represents the distance between two wheels, and r represents the radius of each wheel.

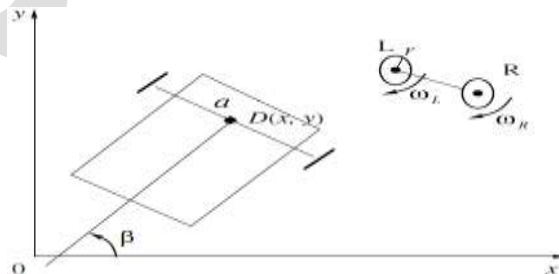


Figure 6: Configuration of differential drive vehicle [23]

In mathematical presentation of movement of a differential drive UGV, firstly Equation 25 to Equation 27 should be written.

$$\dot{x} = V\cos\beta \quad (25)$$

$$\dot{y} = V \sin \beta \tag{26}$$

$$\dot{\beta} = \omega \tag{27}$$

In Equation 25 and Equation 26, V represents UGV's linear velocity, ω represents UGV's angular velocity and β represents the UGV's orientation. Angular and linear velocities of UGV are derived with angular velocities of left (ω_L) and right (ω_R) wheels in Equation 28 and Equation 29.

$$\omega = \frac{r}{a} (\omega_R - \omega_L) \tag{28}$$

$$V = \frac{r}{2} (\omega_R + \omega_L) \tag{29}$$

Equation 30, Equation 31 and Equation 32 are derived, if we apply Equation 28 and Equation 29 into Equation 25 to Equation 27.

$$\dot{x} = \frac{r}{2} (\omega_R + \omega_L) \cos \beta \tag{30}$$

$$\dot{y} = \frac{r}{2} (\omega_R + \omega_L) \sin \beta \tag{31}$$

$$\dot{\beta} = \frac{r}{a} (\omega_R - \omega_L) \tag{32}$$

In our sample application, the role of the transporter UGV was limited to transport the quad-copter S-UAVs to target mission area. The obtained mathematical model that was derived by considering kinematic constraints was used to represent the movement of the transporter UGV. In sample application, a human operator directed the transporter UGV with manually. Commands of human operator were converted to desired angular velocities for the wheels of transporter UGV.

SIMULATION TEST FRAME OF THE DEVELOPED SYSTEM

Simulation of the proposed system was achieved within Matlab/Simulink software by using mathematical models of the unmanned vehicles. Our sample application was visualized via VRML builder software.

In simulation of our developed system, an operator directs one of the S-UAVs with manual commands. Directing of S-UAV is performed by considering mr. The auxiliary S-UAV is directed to take on the task of the assigned S-UAV when battery charge level of the assigned S-UAV exceeds TEDL. Figure 7 indicates the connections among Simulink models of unmanned vehicles, UAD algorithm, VRML builder and Graphical user interface.

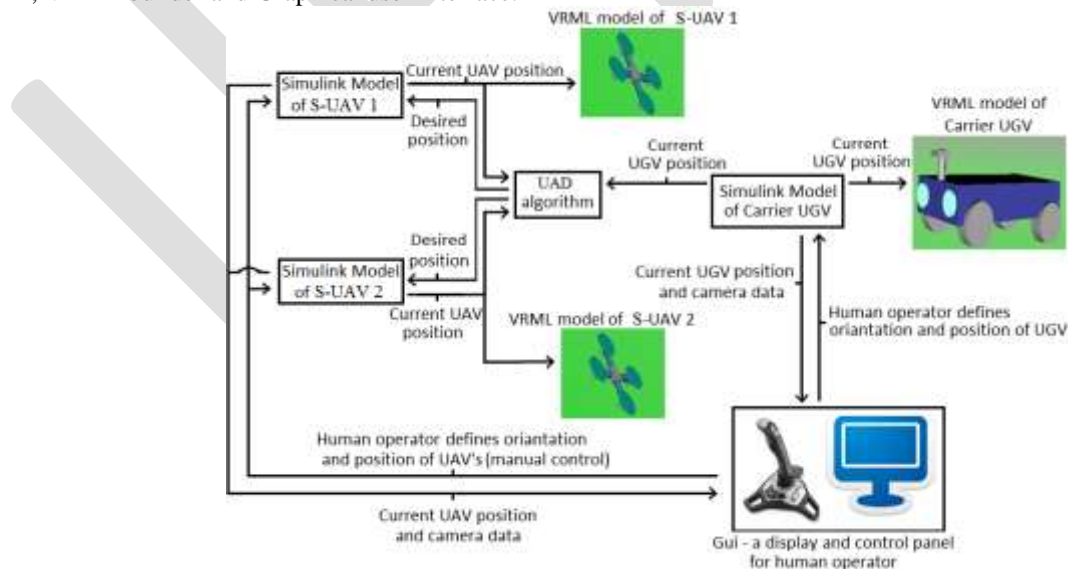


Figure 7: Simulation configuration of the proposed system

Since the proposed system is developed as a visual ISR-based mission, virtual camera objects were integrated to the S-UAVs and the transporter UGV. Figure 8 indicates unmanned vehicles created in VRML builder software.

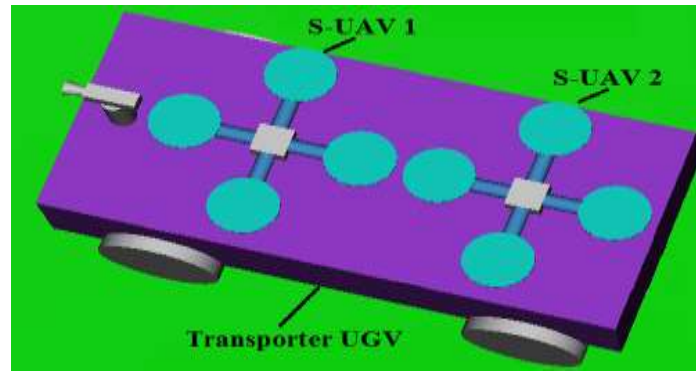


Figure 8: Virtual unmanned vehicles created in VRML builder

EXPERIMENTAL TEST FRAME OF THE DEVELOPED SYSTEM

In experimental tests of our developed system, ArduCopter autopilot boards were used to control the S-UAVs and ArduRover boards was used to control the transporter UGV.

In order to display data of the unmanned vehicles and to send the commands of UAD algorithm and human operator, Mission Planner that is an open source ground station software developed for unmanned air and ground vehicles was used.

Experimental tests of our developed system were achieved via a computer where the Mission Planner and Matlab programs run, APM control boards and sensors that were placed on unmanned vehicles and wireless communication devices.

Central computer was used as a ground station that operates Mission Planner and Matlab software and provides the connection between these programs. Human operator watches onboard cameras and access sensor data of the unmanned vehicles and send his commands to vehicles by using a graphical user interface in central computer. In experimental tests, human operator directs one of the quad-copter S-UAVs with manual commands. S-UAVs are directed within mr. While the assigned S-UAV is directed by the human operator, the assigned S-UAV sends the charge level of its battery to Mission Planner that it is in connection. Mission Planner writes the current position of the assigned S-UAV into a txt file. Mission Planner of the assigned S-UAV writes its battery charge level into another txt file. The UAD algorithm that is running on Matlab reads the charge level of the assigned S-UAV's battery and sends the take-off command to the auxiliary S-UAV that is on the transporter UGV when the charge level of the assigned S-UAV' battery exceeds TEDL. Then, the auxiliary S-UAV is assigned by the UAD algorithm to take on the task of the assigned S-UAV when the auxiliary S-UAV reaches sepat. By regarding the task take on command, the auxiliary S-UAV starts to track the assigned S-UAV. When the S-UAVs meets in air, the assigned S-UAV is directed to sepat and then onto the transporter UGV respectively. After the S-UAVs meets in air, the auxiliary S-UAV turn into the new assigned S-UAV. After the assigned S-UAV lands on the transporter UGV, it turns into the new auxiliary S-UAV and waits for the take-off command from the UAD algorithm that checks battery charge level of the current assigned S-UAV. The task take on process of S-UAVs is achieved continually with this method.

APM board is an autopilot was designed to use in unmanned surface, aerial and ground vehicles. In the proposed system, S-UAVs was controlled with APM flight controller that has an external compass and GPS, an internal barometer, a gyroscope with 3 axis, and an accelerometer. Communication between APM controllers and the central computer is achieved with radio telemetry devices. CCD cameras were integrated to S-UAVs and the transporter UGV to obtain the view of the mission area. Analog video receiver and transmitter kits were used to transfer onboard camera image to the central computer. Onboard camera image were transformed to digital signal in order to input them into the central computer. On board camera image were displayed by using software of the analog to digital transformer equipment. Equipment on unmanned vehicles are given in Table 1.

Table 1: Main equipment on unmanned vehicles.

Flight Controller	GPS and Compass	Gyroscope and Accelerometer	Frame	Radio telemetry
APM 2.6	3DR u-blox	MPU - 6000	F 450 quad-copter	3 DR 915 MHz

frame

Experimental test configuration of the developed system is illustrated in Figure 9.

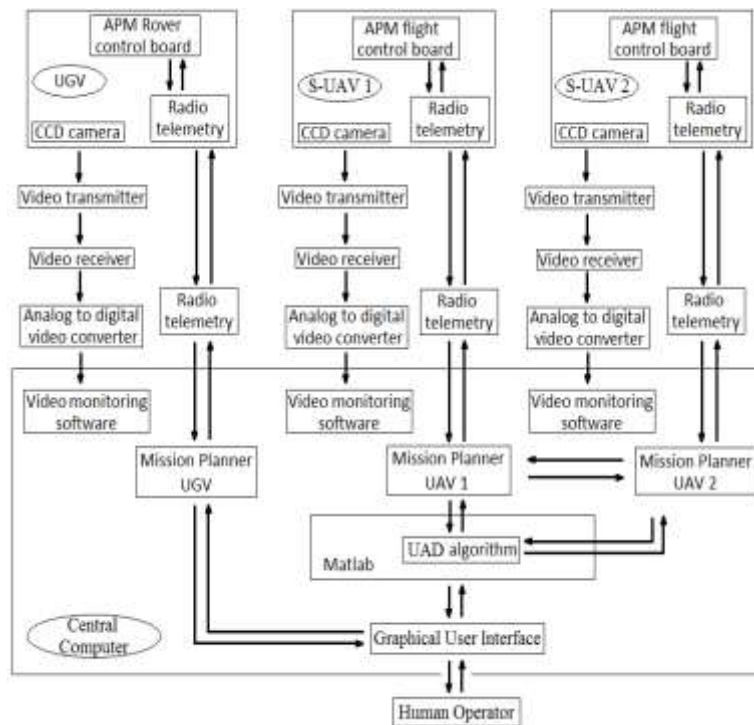


Figure 9: Configuration of the experimental tests of the developed system

Transporter UGV is a differential drive vehicle whose movement is provided with two separate wheels. Desired linear and angular velocity of the transporter UGV might be obtained by changing the rotational speeds of the wheels. Two free wheels were integrated to vehicle chassis to balance the robot. Landing and take-off of S-UAVs were achieved on the separate parts of a platform that was integrated on the transporter UGV. The experimental configuration of our proposed system is given in Figure 10.



Figure 10: Experimental configuration of the proposed system

RESULTS

A sample application was performed in experimental and simulation tests, and the results of the tests were presented under this section. In sample application, a human operator manually steered the transporter UGV with two quad-copter S-UAVs to a pmp. After the transporter UGV reached to selected pmp, S-UAVs started to perform the surveillance mission.

In simulation of sample application, mr was defined as 200 meters and $sepat$ was defined as 20 meters. By placing mr and $sepat$ in Eq. 3 and in Eq. 4, TEDL and ERL were obtained as 40.92 and 20.46 respectively. In this situation, the auxiliary S-UAV should take off when the assigned S-UAV's battery level exceeds 40.92% and the assigned S-UAV urgently returns to the transporter UGV when

its battery charge level exceeds 20.46%. In sample application, it was accepted that pmp of the transporter UGV as the origin. Human operator started to direct the assigned S-UAV that has maximum speed of 3 m/s in x, y and z directions. When the assigned S-UAV's battery level exceeds 40.92%, the auxiliary S-UAV took off. The auxiliary S-UAV equalized its yaw angle to the yaw angle of the assigned S-UAV while it was moving to sepat. When the auxiliary S-UAV arrived to sepat, the assigned S-UAV was at coordinates of X=60 m, Y=100 m, Z= 25 m. When auxiliary S-UAV reached to sepat, it started to track the assigned S-UAV and arrived to the position of its target. The auxiliary S-UAV met the assigned S-UAV within 56.4 seconds. The auxiliary S-UAV passed 189 meters to meet the assigned S-UAV. Battery charge level of the assigned S-UAV was at 9.28% when it landed its platform on the transporter UGV. In experimental tests of sample application, human operator started to direct the assigned S-UAV that has maximum speed of 3 m/s in x, y and z directions. When the assigned S-UAV's battery level exceeds 40.92%, the auxiliary S-UAV took off. The auxiliary S-UAV equalized its yaw angle to the yaw angle of the assigned S-UAV while it was moving to sepat. When the auxiliary S-UAV arrived to sepat, the assigned S-UAV was at coordinates of X=60 m, Y=100 m, Z= 25 m. When the auxiliary S-UAV reached to sepat, it started to track the assigned S-UAV and arrived to the position of its target. The auxiliary S-UAV met the assigned S-UAV within 59.7 seconds. The auxiliary S-UAV passed 198 meters to meet the assigned S-UAV. Battery charge level of the old assigned S-UAV was at 7.73%, when it landed its platform on the transporter UGV. Difference between the simulation and experimental tests occurred because of non-ideal conditions of real test environment. Navigation parameters and variables of S-UAVs during tracking process carried out in experimental test of the sample application are given in Table 2.

Table 2: Navigation parameters during tracking.

UAV	Start Position	Time passed during tracking	Distance passed during tracking	Remained battery charge level(at meeting position)
Assigned S-UAV	x=60, y=100	59.7 sec	166 meters	24.96%
Auxiliary S-UAV	x=0, y=0	59.7 sec	198 meters	81.55%

Figure 11 illustrates the path of the auxiliary S-UAV and the assigned S-UAV while the PN-based tracking was carried out within experimental tests.

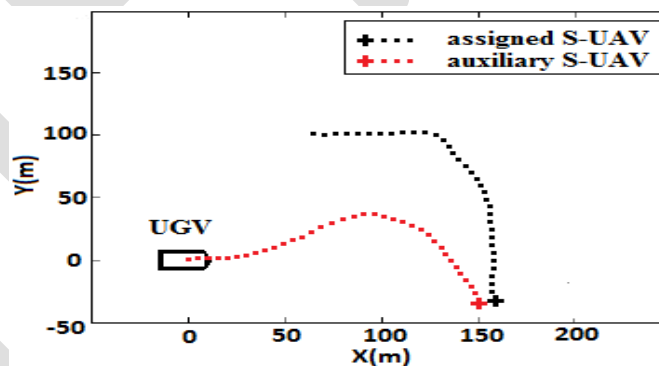


Figure 11: Path of the auxiliary and the assigned S-UAVs

CONCLUSION AND FUTURE WORK

In this study, a cooperative ISR-based system of unmanned ground and aerial vehicles that is proper to use for remote surveillance of hazardous conditions for humans was proposed. The proposed system was tested with a sample application including a surveillance mission that was carried out in simulation and real experimental environment. The S-UAVs completed the mission without encountering running out of their battery charge during their mission. This demonstrates the validity of the approach that we used to define battery consumption of the S-UAVs.

S-UAVs access position of the transporter UGV via the connection that was established between Mission Planner programs in central computer. Therefore S-UAVs can move to the transporter UGV but cannot land on their platform automatically because their GPS are not precise enough. It is clear that a sub-system that will provide a precise auto landing should be integrated to the S-UAVs of the proposed system. Auto landing sub-system was not integrated in current status of our proposed system. Therefore landing of the S-UAVs was carried out via remote controllers by the human operator. It is hard and time-consuming method to carry out precise landing of the S-UAVs onto their marked part of the take-off/landing platform by directing them only according to onboard camera view. If the proposed system is carried out in a large target area, our proposed system that includes two S-UAVs might not perform an efficient surveillance on such a large mission area. To overcome this, quantity of unmanned vehicles should be increased. The previous work of the authors that is based on dividing the mission to balanced parts might be used to obtain the minimum number of required unmanned vehicles [24].

In proposed system, ranges of video transfer system and radio telemetry were 300 meters and 1000 meters respectively. Thus, when the surveillance mission was carried out in limits of the video transfer and telemetry devices, problems that were related with video signal and flight data transfer were occurred. This prevents to apply the proposed system in long range tests. In order to overcome this problem and guarantee a success communication, more advanced communication approaches such as GSM communication and long range video transfer devices should be integrated to the proposed system.

In this paper, the consumption of electrical batteries of the S-UAVs was defined with a predictive and approximate approach. Therefore results that were obtained while dynamic tracking process of S-UAVs might change according to variables that were not considered in our work such as agility of the assigned S-UAVs movement, wind direction and speed, and so on. A more certain consumption formulation for batteries of S-UAVs should be developed to obtain more precise results.

Authors will focus to design an auto landing system and to design a battery swapping mechanism for S-UAVs. The planned auto landing sub-system will be designed by using ultrasonic sensors and image processing methods that will use onboard camera view. Implementation of a battery swapping mechanism for S-UAVs is a hard work. However, swapping the battery of S-UAVs is a very proper solution when a surveillance mission requires quick actions.

REFERENCES:

- [1] Caska S, Gayretli A. "A Survey of UAV/UGV Collaborative Systems". *CIE44 & IMSS'14 Conference*, Istanbul, Turkey, 14-16 October 2014.
- [2] Ercan C, Gencer C. "Literature Review of Dynamic Unmanned Aerial System Routing Problems and Proposals For Future Studies of UASs". *Pamukkale University Journal of Engineering Science*, 19(2), 104-111, 2013.
- [3] Bürkle A, Segor F, Kollmann M. "Towards Autonomous Micro UAV Swarms". *Journal of Intelligent and Robotic Systems*, 61, 339-353, 2011.
- [4] Oh S, Suk J. "Evolutionary controller design for area search using multiple UAVs with minimum altitude maneuver". *Journal of Mechanical Science and Technology*, 27(2), 541-548, 2013.
- [5] Frontoni E, Mancini A, Caponetti F, Zingaretti P, Longhi S. "Prototype UAV helicopter working in cooperative environments". *IEEE/ASME international conference on Advanced intelligent mechatronics*, Zurich, Switzerland, 4-7 September 2007.
- [6] Nigam N, Bieniawski S, Kroo I, Vian J. "Control of Multiple UAVs for Persistent Surveillance: Algorithm and Flight Test Results". *IEEE Transactions on control systems technology*, 20(5), 1236-1251, 2012.
- [7] Wang Z, Mingyang L, Khaleghi A, Xu D, Lobos A, Vo C, Lien J, Liu J, Son Y. "DDDAMS-based Crowd Control via UAVs and UGVs". *2013 International Conference on Computational Science, Procedia Computer Science*, 18, 2028-2035, 2013.
- [8] Tripathi B, Mishra S, Garg S, Kumar A. "An RF Relay Based Control and Communication System for Unmanned Ground Vehicle and Micro Air Vehicle". *2nd International Conference on Computing for Sustainable Global Development*, New Delhi, India, 11-13 March 2015.
- [9] Saska M, Krajnik T, Pireucil L. "Cooperative μ UAV-UGV autonomous indoor surveillance". *9th International Multi-Conference on Systems, Signals and Devices*, Chemnitz, Germany, 20-23 March 2012.
- [10] Perkins T, Murphy R. "Active and Mediated Opportunistic Cooperation Between an Unmanned Aerial Vehicle and an Unmanned Ground Vehicle". *IEEE International Symposium on Safety, Security, and Rescue Robotics (SSRR)*, Linköping, Sweden, 21-26 October 2013.
- [11] Hui C, Yousheng C, Xiaokun L, Shing W. "Autonomous takeoff, tracking and landing of a UAV on a moving UGV using onboard monocular vision". *32nd Chinese Control Conference*, Xi'an, China, 26-28 July 2013.
- [12] Langerwisch M, Wittmann T, Thamke S, Remmersmann T, Tiderko A, Wagner B. "Heterogeneous Teams of Unmanned Ground and Aerial Robots for Reconnaissance and Surveillance - A Field Experiment". *11th IEEE International Symposium on Safety, Security, and Rescue Robotics (SSRR)*, Linköping, Sweden, 21-26 October 2013.
- [13] Kruijff G, Tretyakov V, Linder T, Pirri F. "Rescue Robots at Earthquake-Hit Mirandola, Italy: a Field Report". *11th IEEE International Symposium on Safety, Security, and Rescue Robotics (SSRR)*, Texas, USA, 5-8 November 2012.

- [14] Capitan J, Merino L, Ollero A. "Cooperative Decision-Making Under Uncertainties for Multi-Target Surveillance with Multiples UAVs", *Journal of Intelligent and Robotic Systems*, 61, 1-16, 2011.
- [15] Chen J, Zhang X, Xin B, Fang H. "Coordination Between Unmanned Aerial and Ground Vehicles: A Taxonomy and Optimization Perspective". *IEEE Transactions on Cybernetics*, 99, 1, 2015.
- [16] Fujii K, Higuchi K, Rekimoto J. "Endless Flyer: A Continuous Flying Drone with Automatic Battery Replacement". *IEEE 10th International Conference on Ubiquitous Intelligence & Computing and 2013 IEEE 10th International Conference on Autonomic & Trusted Computing*, Salerno, Italy, 18-21 December 2013.
- [17] Suzuki K, Filho P, Morrison J. "Automatic Battery Replacement System for UAVs: Analysis and Design". *Journal of Intelligent and Robotic Systems*, 65, 563-586, 2012.
- [18] Tan R, Kumar M. "Tracking of Ground Mobile Targets by Quadrotor Unmanned Aerial Vehicles". *Unmanned Systems*, 2(2), 157-173, 2014.
- [19] Chi Q, Bole B, Hogge E, Vazquez S, Daigle M, Celaya J, Weber A, Goebel K. "Battery Charge Depletion Prediction on an Electric Aircraft". *Annual Conference of the Prognostics and Health Management Society*, New Orleans, USA, 14-17 October 2013.
- [20] Voos H. "Nonlinear Control of a Quadrotor Micro-UAV Using Feedback-Linearization". *IEEE International Conference on Mechatronics*, Malaga, Spain, 14-17 April 2009.
- [21] Tayebi A, McGilvray S. "Attitude stabilization of a four-rotor aerial robot". *43rd IEEE Conference on Decision and Control*, Paradise Island, Bahamas, 14-17 December 2004.
- [22] Mazumder S., Dutta S. "Analytical study and Designing of a I-PD controller (a practical Modified PID controller) for a third order system using MATLAB simulation". *International Journal of Engineering Research and General Science*, 3(1), 976-980, 2015
- [23] Evgrafov V, Pavlovsky V, Pavlovsky V E. "Dynamics, Control, and Simulation of Robots with Differential Drive". *Journal of Computer and Systems Sciences International*, 46(5), 836-841, 2007.
- [24] Caska S, Gayretli A. "An Algorithm for Collaborative Patrolling Systems with Unmanned Air Vehicles and Unmanned Ground Vehicles". *7th International Conference on Recent Advances in Space Technologies (RAST)*, Istanbul, Turkey, 16-19 June 2015

SUBJECTIVE ANALYSIS OF NOISE LEVELS AND ITS POSSIBLE EFFECTS ON WORKERS AND THEIR ENVIRONMENT IN IKOT UDUAK TIMBER MARKET, CALABAR, CROSS RIVER STATE, NIGERIA

Okoro, R.C., Umunnah, R.A. & Bassey D.E.
Electronics and Computer Technology Unit,
Department of Physics,
University of Calabar, Calabar.
(asomech461@yahoo.com, +2348038744144)

ABSTRACT: This research measures the social and attitudinal responses to noise by the workers and the business populace in Ikot Uduak timber market, in Calabar, Cross River State, Nigeria. This social survey and attitudinal response to the industrial noise were determined by means of questionnaires. The subjective results showed that over 200 respondents out of 320 responses work for 8 hours and above in a day, which represents 63 percent of the results obtained. 205 of 270 respondents representing 76 percent of the respondents, work for 6 days per week while 155 of 270, which is 57 percent of the respondents, have worked for over 10 years now. From this, and also from the data already gotten from objective analysis of the noise levels in the market, the Occupational Safety and Health Act (OSHA) permissible level of 90dBA for 8-hour day and 5 days a week has been exceeded and this could lead to noise related ailments. The subjective assessment also showed that 98 percent of the respondents agitated that the noise should be controlled.

Key words: Timber market, Social survey, Attitudinal response, Subjective results, Objective analysis, Questionnaire, Noise related ailments.

1. INTRODUCTION:

Noise has been defined as unpredictable sound, especially loud ones, which upset people or make it hard for them to hear 'desired' sound (EPA, 2009). In industries generally, noise is one of the most undesired and unavoidable by-products of modern mechanical operations and a prolonged exposure to it of 85dB (which is the threshold for dangerous levels of noise, based on the stipulations of the Academy of Pediatrics and the National Campaign for Hearing and Health) and above, can lead to hearing impairments, hypertension, ischemic heart diseases, annoyance, and sleep disturbance (Field, 1993).

Noise quantification is very difficult due to the subjective contents involved. Annoyance, for example, as an effect of noise is extremely difficult to quantify, since the decibel level that can cause annoyance to one person may not have the same effect on another person within the same environment or community. In this research work, emphasis was on the whole residents or community, rather than on individuals or small groups.

The machines available in the timber market were identified through a field survey. They are (with their machine code): Band saw (IUM1), Table saw (IUM2), Plainer (IUM3), Spindle/Curving machine (IUM4) and the Drilling machine (IUM5). The subjective assessments of the noise were carried out through the use of questionnaires distributed to respondents around each of the machines listed above. The respondents were asked to respond on how he or she is affected by the closest machine.

2. MATERIALS AND METHODS:

This research was carried out with three hundred and fifty (350) copies of a self-study questionnaire which has twenty-eight items. (See appendix 1). The questionnaires were distributed to workers who operate the machines at the designated locations in the timber market as well as the business men and women who are directly influenced by the noise from the machines, and it was tailored towards obtaining information about the effects of the timber market noise on the workers and their environment. The questionnaire was designed to have five degrees of response as summarized below:

- i Very High (VH) = 5 points
- ii High (H) = 4 points
- iii Moderate (M) = 3 points
- iv Low (L) = 2 points
- v Very Low (VL) = 1 point

The questionnaires were distributed to respondents from ages 20 years to 55 years and above. Out of a total of three hundred and fifty (350) copies that were distributed, the valid responses received were three hundred and twenty-five (325), representing 93 percent.

The assessment questionnaire was sub-divided into three major sections; A, B and C. Questions 1 to 4 in section A provides information on easy sorting. Question 5 to 13 in section B was the demographic information section. In this section, respondents answered questions about age, marital status, sex, area of residence, number of years of residence in that area, and educational qualification, if any. Section C contains questions 15 to 28 which was based on general feeling on the effect of woodworking noise such as communication disruption, annoyance rating, likeness rating, who should control noise, and the effects like sleeplessness, headache, hearing loss, fatigue, and adaptation, as the case may be.

3. RESULTS AND DISCUSSION:

Tables 1, 2 and 3 show the hourly response of respondents to timber market noise, daily exposure to the noise and respondents' yearly exposure to the timber market noise. It can be observed from Table 1 that 200 out of 320 workers, which is about 63 percent of the respondents, work for 9 hours and above in a day, while Table 2 shows that 205 out of 270 workers, representing about 76 percent of the respondents, work for 6 days and above in a week. Fifty-seven percent of the respondents, that is, a total of 155 out of 270 respondents, have been exposed to the noise for more than ten years, as can be seen from Table 3.

It can be seen also from the clustered column chart of Fig. 1, that headache and irritation of the ear, represented by 107 and 132 respectively, out of a total of 321 respondents are the most common effects of noise as expressed by the respondents while the least is annoyance, represented by only 10 respondents. Fig. 2 is a line graph that shows the respondents' reaction to timber market

noise pollution control. A total of 285 respondents out of 291, representing 98 per cent, were of the opinion that timber market machines noise should be controlled.

TABLE 1

Hourly exposure of respondents to the timber market noise

Location code	Exposure time (Hours)				Total
	3-5	6-8	9-12	Above 12	
IUM1	10	25	55	0	90
IUM2	6	10	40	0	56
IUM3	5	30	50	0	85
IUM4	5	15	39	0	59
IUM5	4	10	16	0	30
Total	30	90	200	0	320

TABLE 2

Daily exposure of respondents to the timber market noise

Location code	Exposure time (Days)						Total
	2	3	4	5	6	7	
IUM1	0	0	0	15	40	0	55
IUM2	0	0	0	10	40	2	52
IUM3	0	0	0	20	50	0	70
IUM4	0	0	0	15	40	0	55
IUM5	0	0	0	5	30	3	38
Total	0	0	0	65	200	5	270

TABLE 3

Yearly exposure of respondents to the timber market noise

Location code	Exposure time (Years)						Total
	1-5	6-10	11-15	16-20	21-25	26-30	
IUM1	7	15	30	8	3	1	64
IUM2	5	25	15	7	1	1	54
IUM3	8	10	30	5	2	1	56
IUM4	10	20	25	3	2	1	61
IUM5	5	10	15	2	2	1	35
Total	35	80	115	25	10	5	270

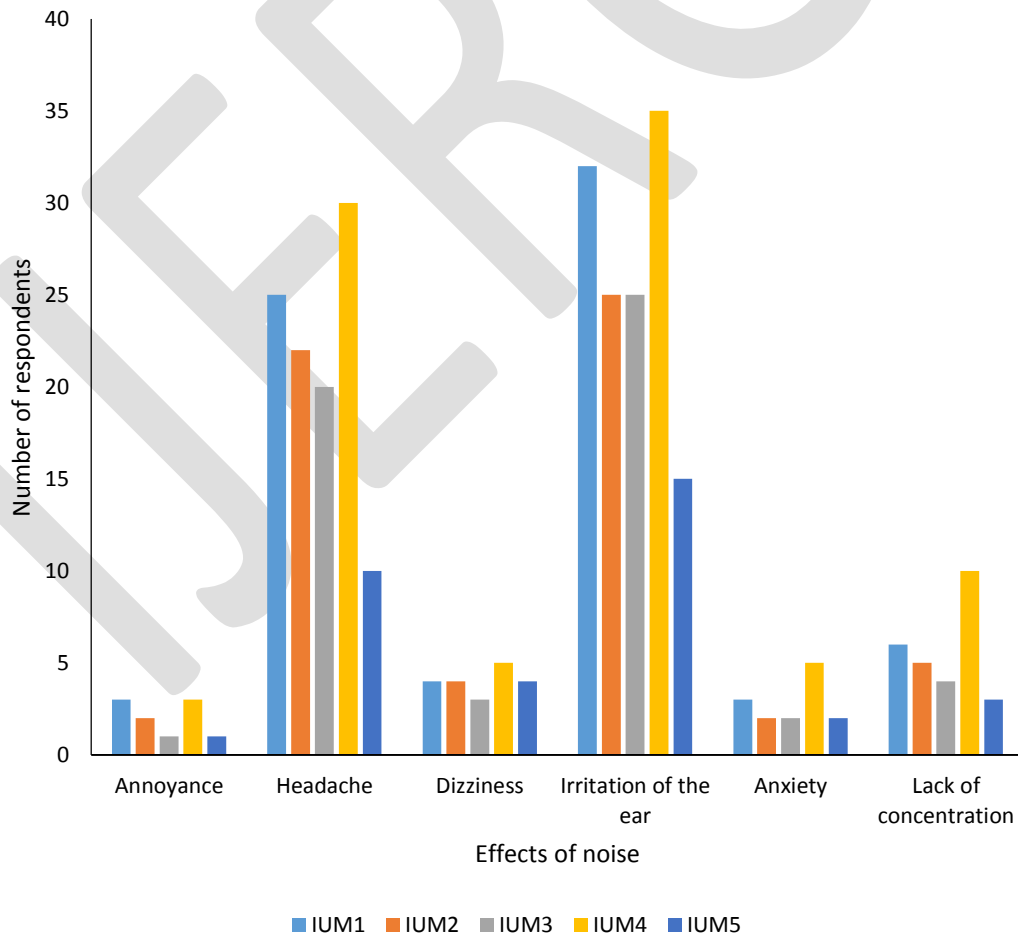


FIG. 1: Respondents' reaction to the effects of noise

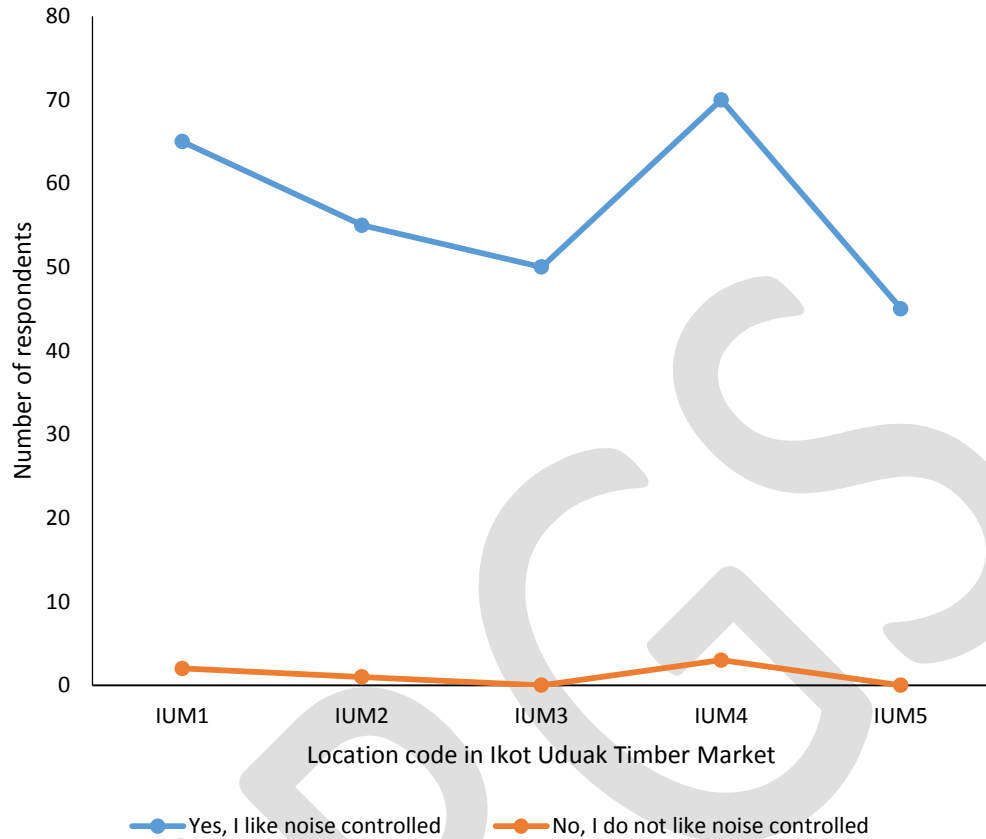


FIG. 2: Respondents' reaction to the timber market pollution control

In order to discover how the subjective responses obtained by making use of questionnaires as a study instrument are related to the objective responses got by the use of the sound level meter (from the work done by Okoro et al 2016, in the same market), the coefficient of correlation was deduced using the standard expression. Correlation coefficient is a rough calculation of the extent of the relationship that exists between two variants and this estimate is only valid when the sample is randomly drawn from the population. The numbers 5, 4, 3, 2 and 1 represent "very high", "high", "moderate", "low," and "very low" respectively, as shown on tables 5 and 6. The corresponding weighted ratings, as shown on table 4, are obtained by finding the product of the numbers and their corresponding frequency of responses. The ratio of the weighted ratings to their separate total responses for each location gives the overall average scale values for each machine (Molino, 1979). These general mean scale values for machines in the markets represent the overall industrial noise rating for that specific industry.

The objective responses determined by the use of the level meter, shown on table 4, represents the x-variants while the subjective responses are shown by the equivalent scale value as y - variants. Table 6 shows the correlation between objective and subjective responses in the market. The correlation coefficient is given by:

$$r = \frac{\{n\sum xy - \sum x \sum y\}}{\sqrt{\{[n\sum x^2 - (\sum x)^2][n\sum y^2 - (\sum y)^2]\}}} \text{---3.1}$$

The correlation coefficient between objective and subjective measures was calculated 0.99. This shows that there is a good correlation between the objective measurements of the noise and the attitudinal responses of the workers to the noise. This is not unrelated to the fact that Ikot Uduak timber market is located in residential environment where residential buildings, hotels and churches are located. This situation had made the workers and the people around to react adversely to any increases in noise level. They are thus poorly adapted to the noise from the machines and as such could easily decipher any slight effect the noise had on them.

TABLE 4
 Relationship between sound pressure level and the working condition of the machines

Machine code	Average sound level when there is no load (dBA)	Average sound level when loaded (dBA)
IUM1	98.0	100.5
IUM2	86.0	98.5
IUM3	96.0	98.2
IUM4	95.5	101.5
IUM5	82.5	90.5

Source: Okoro et al 2016

TABLE 5
 Summary of respondents' timber market noise rating

Location code	Noise rating					Response per location (n)	Weighting rating (nx)	Average value per location (nx/n)=y
	Very high (5)	High (4)	Moderate (3)	Low (2)	Very low (1)			
IUM1	40	25	5	0	0	70	315	4.50
IUM2	35	15	10	0	0	60	265	4.42
IUM3	30	20	5	0	0	55	245	4.45
IUM4	50	23	7	0	0	80	363	4.54
IUM5	25	20	15	0	0	60	250	4.17

TABLE 6
www.ijergs.org

Correlation between objective and subjective responses

S/N	Location code	Mean value, loaded -state, A-weighted SPL ± 0.5 dBA (x_i)	Mean value per location (y_i)	$x_i y_i$	x_i^2	y_i^2	Correlation coefficient (r)
1	IUM1	100.5	4.50	452.25	10,100.25	20.25	0.99
2	IUM2	98.5	4.42	435.37	9,702.25	19.54	
3		98.2	4.45	436.99	9,643.24	19.80	
4	IUM3	101.5	4.54	460.81	10,302.25	20.61	
5	IUM4	90.5	4.17	377.39	8,190.25	17.39	
	IUM5						
	Total	489.2	22.08	2,162.81	47,938.24	97.59	

4. SUMMARY/CONCLUSION:

Generally, the subjective results in the industry under survey show that over 200 respondents out of a total of 320 results received work for 8 hours and above in a day, and this represents 63 per cent of the results obtained. Two hundred and five out of 270, which is about 76 percent of the respondents work 6 days per week while a total of 155 of 270 respondents representing 57 percent of the respondents have worked for 10 years and above. These values exceed the recommendation of the Occupational Safety and Health Act (OSHA) of 1970 which permits noise level of 90 (dBA) for a daily exposure time of 8 hours and 5 days per week. Hence, the workers exposed to such noise levels are assumed to have hearing impairment and other noise related ailments.

REFERENCES:

- [1] Akpan, E. R., Offem, J. O. & Nya, A. E. (2006). *Baseline ecological studies of the Great Kwa River, Nigeria I: Physio-chemical studies*. Ecoserve. Retrieved 2011-09-08.
- [2] American Academy of Paediatrics, Committee on Environmental Health (1997). *Noise: a hazard to the fetus and newborn. Pediatrics*. 100:724-727.
- [3] Eja, E. I.; Inah, S. A.; Yaro, M. A. & Inyang, I. O. (2011). The consequences of rapid population growth on housing in Calabar Metropolis. *African Journal of Social Sciences*, 1 (2): 84-94.
- [4] Field, J. M. (1993). Effect of personal and situational variables upon noise annoyance in residential areas. *Journal of the Acoustical Society of America*, 93: 2753-2763.
- [5] Gerges, S. N. Y. (1992). *Ruído: Fundamentos e controle*. Santa Catarina: Universidade Federal de Santa Catarina, 600.
- [6] Houghton Mifflin Company (HMC) (2000). *The American Heritage Dictionary of the English Language* (4th ed.). Archived from the original on June 25, 2008. Retrieved May 20, 2010.

- [7] International Electrotechnical Commission (IEC) (2003). International standard 61672-2:2003. Sound level meters – Part 2: Pattern evaluation tests. Retrieved August 9, 2011 from <http://www.cirrusresearch.co.uk/blog/2012/07/iec-61672-a-standard-for-sound-level-meters-in-three-parts/>
- [8] International Standards Organization (ISO) (2010). ISO 3746:2010. Acoustics -- Determination of sound power levels and sound energy levels of noise sources using sound pressure -- Survey method using an enveloping measurement surface over a reflecting plane. Retrieved August 21, 2011 from <https://www.iso.org/obp/ui/#iso:std:iso:3746:ed-3:v1:en>
- [9] Mbian, A. B., (2009). Measurement and analysis of electricity generator plant noise and impact on residents in Calabar, Nigeria. Unpublished M.Sc. thesis, University of Calabar, Nigeria.
- [10] Molino, J. A. (1979). Annoyance and noise. In C. M. Harris (Ed.), *Handbook of noise control* (2nd ed.). New York: McGraw-Hill.
- [11] **Occupational Safety and Health Administration (OSHA) (1970). General industry standard. Table G-16, 29 CFR 1910.95.**
- [12] Okoro, R.C., Bassey D.E. & Umunnah, R.A. (2016). Sound Levels and Its Possible Effects On the Workers and Their Environment in Ikot Uduak (MCC) Timber Market, Calabar, Cross River State. Unpublished Research Work, University of Calabar, Nigeria.
- [13] Onuu, M. U. (2000). Noise levels and anti-noise laws. *The Guardian*. July 4, 16.
- [14] Onuu, M. U. & Menkiti, A. I. (1996). Analysis of Nigerian community response to road traffic noise. *Journal of Science Engineering and Technology*, 3: 536-547.
- [15] Optiz, H. (1968). A discussion on the origin and treatment of noise in industrial environment noise gears. *Proceedings of the Royal Society*, 12: 369-380.
- [16] **Rosen, S. & Olin, P. (1965). Hearing Loss and Coronary Heart Disease. Archives of Otolaryngology, 82:236.**
- [17] Sehrndt, G. A., Parthey, W. & Gerges, S. N. Y. (2006). *Noise sources*. Retrieved August 3, 2012 from http://www.who.int/occupational_health/publications/noise5.pdf
- [18] Umunnah, R. A. & Okon, B. E. (2015). A Survey of the Noise Generated by Timber Market Machines and Its Health Implications On the Workers and Their Environment, In Calabar, Cross River State. *International Journal of Science and Engineering Research*, 6 (5), 1713-1721.
- [19] United States Environmental Protection Agency (EPA) (2009). *Noise Pollution*. Revised Regulation for the Labeling of Hearing Protection Devices (HPD) Proposed. Retrieved 2013-09-24.
- [20] United States Environmental Protection Agency (EPA) (1978). *Noise: A health problem*. Washington DC: Office of Noise Abatement and Control, 22.
- [21] Western Electric Company (WEC) (1969). *Fundamentals of Telephone Communication Systems*. p. 2.1.

**D & R
I & A**



Publication

International Journal of Engineering Research and general science is an open access peer review publication which is established for publishing the latest trends in engineering and give priority to quality papers which emphasis on basic and important concept through which there would be remarkable contribution to the research arena and also publish the genuine research work in the field of science, engineering and technologies

**International Journal Of Engineering Research and
General Science**

ISSN 2091 - 2730